Alexander Altland and Ben Simons

Condensed Matter Field Theory

SECOND EDITION

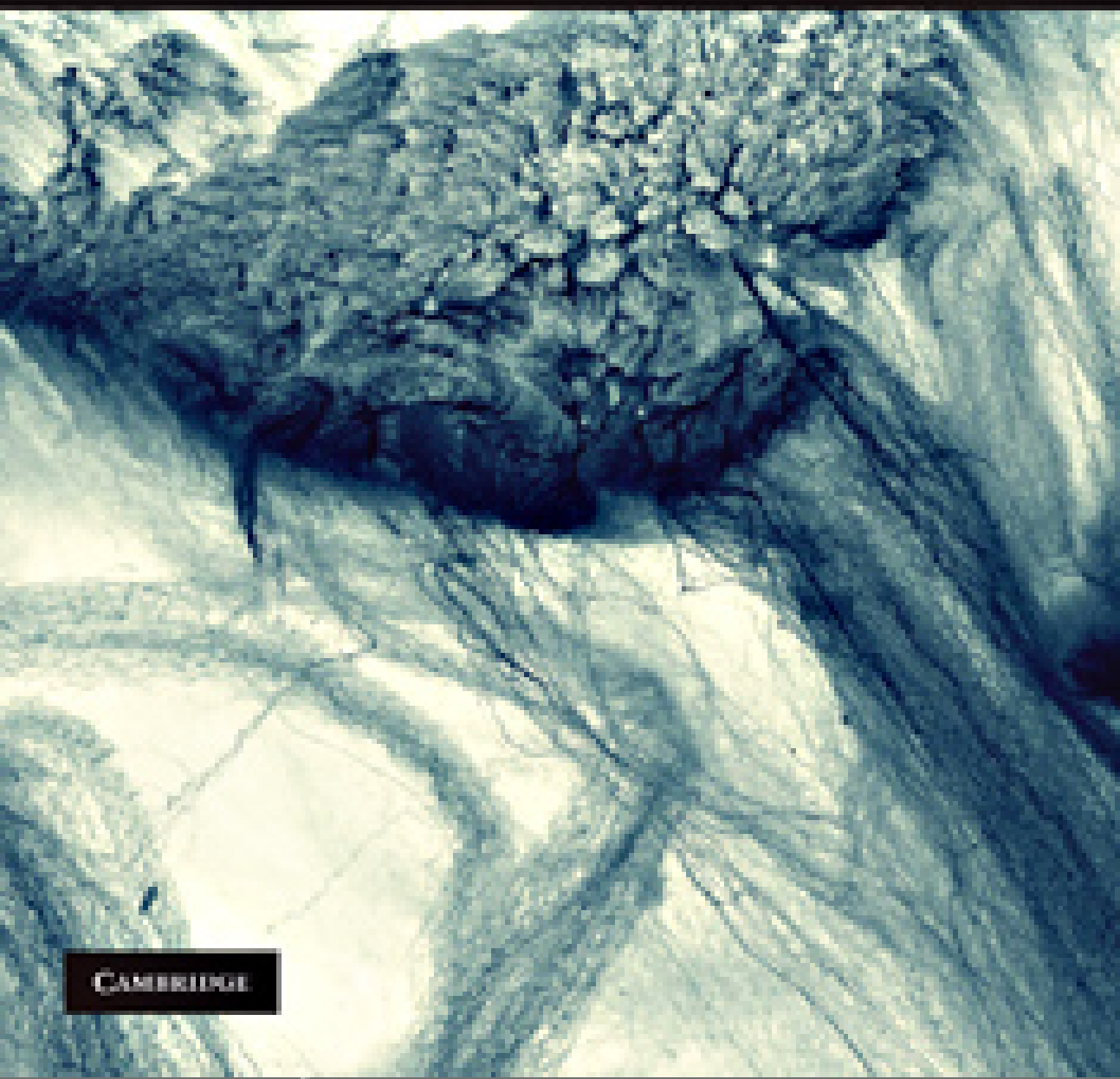

CAMBRIDGE

CAMBRIDGE www.cambridge.org/9780521769754

This page intentionally left blank

Condensed Matter Field Theory

Second edition

Modern experimental developments in condensed matter and ultracold atom physics present formidable challenges to theorists. This book provides a pedagogical introduction to quantum field theory in many particle physics, emphasizing the applicability of the formalism to concrete problems.

This second edition contains two new chapters developing path integral approaches to classical and quantum nonequilibrium phenomena. Other chapters cover a range of topics, from the introduction of many-body techniques and functional integration, to renormalization group methods, the theory of response functions, and topology. Conceptual aspects and formal methodology are emphasized, but the discussion focuses on practical experimental applications drawn largely from condensed matter physics and neighboring fields.

Extended and challenging problems with fully–worked solutions provide a bridge between formal manipulations and research-oriented thinking. Aimed at elevating graduate students to a level where they can engage in independent research, this book complements graduate level courses on many particle theory.

Alexander Altland is Professor of Theoretical Condensed Matter Physics at the Institute of Theoretical Physics, University of Köln. His main areas of research include mesoscopic physics, the physics of interacting many particle systems, and quantum nonlinear dynamics.

Benjamin D. Simons is Professor of Theoretical Condensed Matter Physics at the Cavendish Laboratory, University of Cambridge. His main areas of research include strongly correlated condensed matter systems, mesoscopic and ultracold atom physics.

Condensed Matter Field Theory

Second edition

Alexander Altland and Ben Simons

CAMBRIDGE
UNIVERSITY PRESS

CAMBRIDGE UNIVERSITY PRESS
Cambridge, New York, Melbourne, Madrid, Cape Town, Singapore,
São Paulo, Delhi, Dubai, Tokyo

Cambridge University Press
The Edinburgh Building, Cambridge CB2 8RU, UK

Published in the United States of America by Cambridge University Press, New York

www.cambridge.org
Information on this title: www.cambridge.org/9780521769754

First published in print format 2010

ISBN-13 978-0-511-78928-1 eBook (NetLibrary)

ISBN-13 978-0-521-76975-4 Hardback

Contents

Preface

In the past few decades, the field of quantum condensed matter physics has seen rapid and, at times, almost revolutionary development. Undoubtedly, the success of the field owes much to ground-breaking advances in experiment: already the controlled fabrication of phase coherent electron devices on the nanoscale is commonplace (if not yet routine), while the realization of ultra–cold atomic gases presents a new arena in which to explore strong interaction and condensation phenomena in Fermi and Bose systems. These, along with many other examples, have opened entirely new perspectives on the quantum physics of many-particle systems. Yet, important as it is, experimental progress alone does not, perhaps, fully explain the appeal of modern condensed matter physics. Indeed, in concert with these experimental developments, there has been a "quiet revolution" in condensed matter theory, which has seen phenomena in seemingly quite different systems united by common physical mechanisms. This relentless "unification" of condensed matter theory, which has drawn increasingly on the language of low-energy quantum field theory, betrays the astonishing degree of *universality*, not fully appreciated in the early literature.

On a truly microscopic level, all forms of quantum matter can be formulated as a many-body Hamiltonian encoding the fundamental interactions of the constituent particles. However, in contrast with many other areas of physics, in practically all cases of interest in condensed matter the structure of this operator conveys as much information about the properties of the system as, say, the knowledge of the basic chemical constituents tells us about the behavior of a living organism! Rather, in the condensed matter environment, it has been a long-standing tenet that the degrees of freedom relevant to the low-energy properties of a system are very often not the microscopic. Although, in earlier times, the passage between the microscopic degrees of freedom and the relevant low-energy degrees of freedom has remained more or less transparent, in recent years this situation has changed profoundly. It is a hallmark of many "deep" problems of modern condensed matter physics that the connection between the two levels involves complex and, at times, even controversial mappings. To understand why, it is helpful to place these ideas on a firmer footing.

Historically, the development of modern condensed matter physics has, to a large extent, hinged on the "unreasonable" success and "notorious" failures of *non-interacting* theories. The apparent impotency of interactions observed in a wide range of physical systems can be attributed to a deep and far-reaching principle of *adiabatic continuity*: the

quantum numbers that characterize a many-body system are determined by fundamental symmetries (translation, rotation, particle exchange, etc.). Providing that the integrity of the symmetries is maintained, the elementary "quasi-particle" excitations of an interacting system can be usually traced back "adiabatically" to those of the bare particle excitations present in the non-interacting system. Formally, one can say that the radius of convergence of perturbation theory extends beyond the region in which the perturbation is small. For example, this *quasi-particle correspondence*, embodied in Landau's Fermi-liquid theory, has provided a reliable platform for the investigation of the wide range of Fermi systems from conventional metals to ^{3}helium fluids and cold atomic Fermi gases.

However, being contingent on symmetry, the principle of adiabatic continuity and, with it, the quasi-particle correspondence, must be abandoned at a *phase transition*. Here, interactions typically effect a substantial rearrangement of the many-body ground state. In the symmetry-broken phase, a system may – and frequently does – exhibit elementary excitations very different from those of the parent non-interacting phase. These elementary excitations may be classified as new species of quasi-particle with their own characteristic quantum numbers, or they may represent a new kind of excitation – *a collective mode* – engaging the cooperative motion of many bare particles. Many familiar examples fall into this category: when ions or electrons condense from a liquid into a solid phase, translational symmetry is broken and the elementary excitations – phonons – involve the motion of many individual bare particles. Less mundane, at certain field strengths, the effective low-energy degrees of freedom of a two-dimensional electron gas subject to a magnetic field (the quantum Hall system) appear as quasi-particles carrying a rational *fraction* (!) of the elementary electron charge – an effect manifestly non-perturbative in character.

This reorganization lends itself to a hierarchical perspective of condensed matter already familiar in the realm of particle physics. Each phase of matter is associated with a unique "non-interacting" reference state with its own characteristic quasi-particle excitations – a product only of the fundamental symmetries that classify the phase. While one stays within a given phase, one may draw on the principle of continuity to infer the influence of interactions. Yet this hierarchical picture delivers two profound implications. Firstly, within the quasi-particle framework, the underlying "bare" or elementary particles remain invisible (witness the fractionally charged quasi-particle excitations of the fractional quantum Hall fluid!). (To quote from P. W. Anderson's now famous article "More is different," (*Science* **177** (1972), 393–6), "the ability to reduce everything to simple fundamental laws does not imply the ability to start from those laws and reconstruct the universe.") Secondly, while the capacity to conceive of new types of interaction is almost unbounded (arguably the most attractive feature of the condensed matter environment!), the freedom to identify non-interacting or free theories is strongly limited, constrained by the space of fundamental symmetries. When this is combined with the principle of continuity, the origin of the observed "universality" in condensed matter is revealed. Although the principles of adiabatic continuity, universality, and the importance of symmetries have been anticipated and emphasized long ago by visionary theorists, it is perhaps not until relatively recently that their mainstream consequences have become visible.

How can these concepts be embedded into a theoretical framework? At first sight, the many-body problem seems overwhelmingly daunting. In a typical system, there exist some 10^{23} particles interacting strongly with their neighbors. Monitoring the collective dynamics, even in a classical system, is evidently a hopeless enterprise. Yet, from our discussion above, it is clear that, by focussing on the coordinates of the collective degrees of freedom, one may develop a manageable theory involving only a restricted set of excitations. The success of quantum field theory in describing low-energy theories of particle physics as a successive hierarchy of broken symmetries makes its application in the present context quite natural. As well as presenting a convenient and efficient microscopic formulation of the many-body problem, the quantum field theory description provides a vehicle to systematically identify, isolate, and develop a low-energy theory of the collective field. Moreover, when cast as a field integral, the quantum field theory affords a classification of interacting systems into a small number of universality classes defined by their fundamental symmetries (a phenomenon not confined by the boundaries of condensed matter – many concepts originally developed in medium- or high-energy physics afford a seamless application in condensed matter). This phenomenon has triggered a massive trend of unification in modern theoretical physics. Indeed, by now, several sub-fields of theoretical physics have emerged (such as conformal field theory, random matrix theory, etc.) that define themselves not so much through any specific application as by a certain conceptual or methodological framework.

In deference to the importance attached to the subject, in recent years a number of texts have been written on the subject of quantum field theory within condensed matter. It is, therefore, pertinent for a reader to question the motivation for the present text. Firstly, the principal role of this text is as a primer aimed at elevating graduate students to a level where they can engage in independent research. Secondly, while the discussion of conceptual aspects takes priority over the exposure to the gamut of condensed matter applications, we have endeavored to keep the text firmly rooted in practical experimental application. Thirdly, as well as routine exercises, the present text includes extended problems which are designed to provide a bridge from formal manipulations to research-oriented thinking. Indeed, in this context, readers may note that some of the "answered" problems are deliberately designed to challenge: it is, after all, important to develop a certain degree of *intuitive* understanding of formal structures and, sadly, this can be acquired only by persistent and, at times, even frustrating training!

With this background, let us now discuss in more detail the organization of the text. To prepare for the discussion of field theory and functional integral techniques we begin in Chapter 1 by introducing the notion of a classical and a quantum field. Here we focus on the problem of lattice vibrations in the discrete harmonic chain, and its "ancestor" in the problem of classical and quantum electrodynamics. The development of field integral methods for the many-body system relies on the formulation of quantum mechanical theories in the framework of the second quantization. In Chapter 2 we present a formal and detailed introduction to the general methodology. To assimilate this technique, and motivate some of the examples discussed later in the text, a number of separate and substantial applications are explored in this chapter. In the first of these, we present (in second-quantized form) a somewhat cursory survey of the classification of metals and insulators, identifying a

canonical set of model Hamiltonians, some of which form source material for later chapters. In the case of the one-dimensional system, we will show how the spectrum of elementary collective excitations can be inferred using purely operator methods within the framework of the bosonization scheme. Finally, to close the chapter, we will discuss the application of the second quantization to the low-energy dynamics of quantum mechanical spin systems. As a final basic ingredient in the development of the quantum field theory, in Chapter 3 we introduce the Feynman path integral for the single-particle system. As well as representing a prototype for higher-dimensional field theories, the path integral method provides a valuable and recurring computational tool. This being so, we have included in this chapter a pedagogical discussion of a number of rich and instructive applications which range from the canonical example of a particle confined to a single or double quantum well, to the tunneling of extended objects (quantum fields), quantum dissipation, and the path integral formulation of spin.

Having accumulated all of the necessary background, in Chapter 4 we turn to the formulation and development of the field integral of the quantum many-particle system. Beginning with a discussion of coherent states for Fermi and Bose systems, we develop the many-body path integral from first principles. Although the emphasis in the present text is on the field integral formulation, the majority of early and seminal works in the many-body literature were developed in the framework of diagrammatic perturbation theory. To make contact with this important class of approximation schemes, in Chapter 5 we explore the way diagrammatic perturbation series expansions can be developed systematically from the field integral. Employing the ϕ^4-theory as a canonical example, we describe how to explore the properties of a system in a high order of perturbation theory around a known reference state. To cement these ideas, we apply these techniques to the problem of the weakly interacting electron gas.

Although the field integral formulation provides a convenient means to organize perturbative approximation schemes as a diagrammatic series expansion, its real power lies in its ability to identify non-trivial reference ground states, or "mean-fields," and to provide a framework in which low-energy theories of collective excitations can be developed. In Chapter 6, a fusion of perturbative and mean-field methods is used to develop analytical machinery powerful enough to address a spectrum of rich applications ranging from metallic magnetism and superconductivity to superfluidity. To bridge the gap between the (often abstract) formalism of the field integral, and the arena of practical application, it is necessary to infer the behavior of correlation functions. Beginning with a brief survey of concepts and techniques of experimental condensed matter physics, in Chapter 7 we highlight the importance of correlation functions and explore their connection with the theoretical formalism developed in previous chapters. In particular, we discuss how the response of many-body systems to various types of electromagnetic perturbation can be described in terms of correlation functions and how these functions can be computed by field theoretical means.

Although the field integral is usually simple to formulate, its properties are not always easy to uncover. Amongst the armory of tools available to the theorist, perhaps the most adaptable and versatile is the method of the renormalization group. Motivating

our discussion with two introductory examples drawn from a classical and a quantum theory, in Chapter 8 we become acquainted with the renormalization group method as a concept whereby nonlinear theories can be analyzed beyond the level of plain perturbation theory. With this background, we then proceed to discuss renormalization methods in more rigorous and general terms, introducing the notion of scaling, dimensional analysis, and the connection to the general theory of phase transitions and critical phenomena. To conclude this chapter, we visit a number of concrete implementations of the renormalization group scheme introduced and exemplified on a number of canonical applications.

In Chapter 9, we turn our attention to low-energy theories with non–trivial forms of long-range order. Specifically, we will learn how to detect and classify topologically non-trivial structures, and to understand their physical consequences. Specifically, we explore the impact of topological terms (i.e. θ-terms, Wess–Zumino terms, and Chern–Simons terms) on the behavior of low-energy field theories solely through the topology of the underlying field configurations. Applications discussed in this chapter include persistent currents, 't Hooft's θ-vacua, quantum spin chains, and the quantum Hall effects.

So far, our development of field theoretic methodologies has been tailored to the consideration of single-particle quantum systems, or many-body systems in thermal equilibrium. However, studies of classical nonequilibrium systems have a long and illustrious history, dating back to the earliest studies of thermodynamics, and these days include a range of applications from soft matter physics to population dynamics and ecology. At the same time, the control afforded by modern mesoscopic semiconducting and metallic devices, quantum optics, as well as ultracold atom physics now allow controlled access to quantum systems driven far from equilibrium. For such systems, traditional quantum field theoretical methodologies are inappropriate.

Starting with the foundations of non-equilibrium statistical mechanics, from simple one-step processes, to reaction–diffusion type systems, in Chapter 10 we begin by developing Langevin and Fokker–Planck theory, from which we establish classical Boltzmann transport equations. We then show how these techniques can be formulated in the language of the functional integral developing the Doi–Peliti and Martin–Siggia–Rose techniques. We conclude our discussion with applications to nonequilibrium phase transitions and driven lattice gases. These studies of the classical nonequilibrium system provide a platform to explore the quantum system. In Chapter 11, we develop the Keldysh approach to quantum non-equilibrium systems based, again, on the functional integral technique. In particular, we emphasize and exploit the close connections to classical nonequilibrium field theory, and present applications to problems from the arena of quantum transport.

To focus and limit our discussion, we have endeavored to distill material considered "essential" from the "merely interesting" or "background." To formally acknowledge and identify this classification, we have frequently included reference to material which we believe may be of interest to the reader in placing the discussion in context, but which can be skipped without losing the essential thread of the text. These intermissions are signaled in the text as "Info" blocks.

At the end of each chapter, we have collected a number of pedagogical and instructive problems. In some cases, the problems expand on some aspect of the main text requiring only

an extension, or straightforward generalization, of a concept raised in the chapter. In other cases, the problems rather complement the main text, visiting fresh applications of the same qualitative material. Such problems take the form of case studies in which both the theory and the setting chart new territory. The latter provide a vehicle to introduce some core areas of physics not encountered in the main text, and allow the reader to assess the degree to which the ideas in the chapter have been assimilated. With both types of questions to make the problems more inclusive and useful as a reference, we have included (sometimes abridged, and sometimes lengthy) answers. In this context, Section 6.5 assumes a somewhat special role: the problem of phase coherent electron transport in weakly disordered media provides a number of profoundly important problems of great theoretical and practical significance. In preparing this section, it became apparent that the quantum disorder problem presents an ideal environment in which many of the theoretical concepts introduced in the previous chapters can be practiced and applied – to wit diagrammatic perturbation theory and series expansions, mean-field theory and collective mode expansions, correlation functions and linear response, and topology. We have therefore organized this material in the form of an extended problem set in Chapter 6.

This concludes our introduction to the text. Throughout, we have tried to limit the range of physical applications to examples which are rooted in experimental fact. We have resisted the temptation to venture into more speculative areas of theoretical condensed matter at the expense of excluding many modern and more-circumspect ideas which pervade the condensed matter literature. Moreover, since the applications are intended to help motivate and support the field theoretical techniques, their discussion is, at times, necessarily superficial. (For example, the hundreds pages of text in this volume could have been invested in their entirety in the subject of superconductivity!) Therefore, where appropriate, we have tried to direct interested readers to the more specialist literature.

In closing, we would like to express our gratitude to Jakob Müller-Hill, Tobias Micklitz, Jan Müller, Natalja Strelkova, Franjo-Frankopan Velic, Andrea Wolff, and Markus Zowislok for their invaluable assistance in the proofreading of the text. Moreover, we would also like to thank Julia Meyer for her help in drafting problems. Finally we would like to acknowledge Sasha Abanov for his advice and guidance in the drafting of the chapter on Topology.

As well as including additional material on the formulation of functional field integral methods to classical and quantum nonequilibrium physics in Chapters 10 and 11, in preparing the second edition of the text, we have endeavored to remove some of the typographical errors that crept into the first edition. Although it seems inevitable that some errors will still have escaped identification, it is clear that many many more would have been missed were it not for the vigilance of many friends and colleagues. In this context, we would particularly like to acknowledge the input of Piet Brouwer, Christoph Bruder, Chung-Pin Chou, Jan von Delft, Karin Everschor, Andrej Fischer, Alex Gezerlis, Sven Gnutzmann, Colin Kiegel, Tobias Lück, Patrick Neven, Achim Rosch, Max Schäfer, Matthias Sitte, Nobuhiko Taniguchi, and Matthias Vojta.

1

From particles to fields

To introduce some fundamental concepts of field theory, we begin by considering two simple model systems – a one-dimensional "caricature" of a solid, and a freely propagating electromagnetic wave. As well as exemplifying the transition from discrete to continuous degrees of freedom, these examples introduce the basic formalism of classical and quantum field theory, the notion of elementary excitations, collective modes, symmetries, and universality – concepts which will pervade the rest of the text.

One of the more remarkable facts about condensed matter physics is that phenomenology of fantastic complexity is born out of a Hamiltonian of comparative simplicity. Indeed, it is not difficult to construct microscopic "condensed matter Hamiltonians" of reasonable generality. For example, a prototypical metal or insulator might be described by the many-particle Hamiltonian, $H = H_{\rm e} + H_{\rm i} + H_{\rm ei}$ where

$$\left.\begin{aligned} H_{\rm e} &= \textstyle\sum_i \dfrac{\mathbf{p}_i^2}{2m} + \sum_{i<j} V_{\rm ee}(\mathbf{r}_i - \mathbf{r}_j), \\ H_{\rm i} &= \textstyle\sum_I \dfrac{\mathbf{P}_I^2}{2M} + \sum_{I<J} V_{\rm ii}(\mathbf{R}_I - \mathbf{R}_J), \\ H_{\rm ei} &= \textstyle\sum_{iI} V_{\rm ei}(\mathbf{R}_I - \mathbf{r}_i). \end{aligned}\right\} \tag{1.1}$$

Here, $\mathbf{r}_i$ ($\mathbf{R}_I$) denote the coordinates of the valence electrons (ion cores) and $H_{\rm e}, H_{\rm i}$, and $H_{\rm ei}$ describe the dynamics of electrons, ions and the interaction of electrons and ions, respectively (see Fig. 1.1). Of course, the Hamiltonian Eq. (1.1) can be made "more realistic," for example by remembering that electrons and ions carry spin, adding disorder, or introducing host lattices with multi-atomic unit-cells. However, for developing our present line of thought the prototype H will suffice.

The fact that a seemingly innocuous Hamiltonian like Eq. (1.1) is capable of generating the vast panopticon of metallic phenomenology can be read in reverse order: one will normally not be able to make theoretical progress by approaching the problem in an "*ab initio*" manner, i.e. by an approach that treats all microscopic constituents as equally relevant degrees of freedom.

How then can successful analytical approaches be developed? The answer to this question lies in a number of basic principles inherent in generic condensed matter systems.

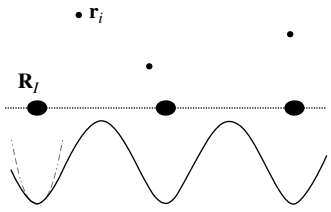

Figure 1.1 A one-dimensional cartoon of a (metallic) solid. Positively charged ions located at positions $\mathbf{R}_I$ are surrounded by a conduction electron cloud (electron coordinates denoted by $\mathbf{r}_i$). While the motion of the ions is massively constrained by the lattice potential $V_{\rm ii}$ (indicated by the solid line and its harmonic approximation shown dashed), t he dynamics of the electrons is affected by their mutual interaction ($V_{\rm ee}$) and their interaction with the core ions ($V_{\rm ei}$).

1. **Structural reducibility**: Not all components of the Hamiltonian (1.1) need to be treated simultaneously. For example, when the interest is foremost in the vibrational motion of the ion lattice, the dynamics of the electron system can often be neglected or, at least, be treated in a simplistic manner. Similarly, much of the character of the dynamics of the electrons is independent of the ion lattice, etc.
2. In the majority of condensed matter applications, one is interested not so much in the full profile of a given system, but rather in its energetically low-lying dynamics. This is motivated partly by practical aspects (in daily life, iron is normally encountered at room temperature and not at its melting point), and partly by the tendency of large systems to behave in a "universal" manner at low temperatures. Here **universality** implies that systems differing in microscopic detail (e.g. different types of interaction potentials, ion species, etc.) exhibit common collective behavior. As a physicist, one will normally seek for unifying principles in collective phenomena rather than to describe the peculiarities of individual species. However, universality is equally important in the *practice* of condensed matter theory. It implies, for example, that, at low temperatures, details of the functional form of microscopic interaction potentials are of secondary importance, i.e. that one may employ *simple* model Hamiltonians.
3. For most systems of interest, the number of degrees of freedom is formidably large with $N = \mathcal{O}(10^{23})$. However, contrary to first impressions, the magnitude of this figure is rather an advantage. The reason is that in addressing condensed matter problems we may make use of the **concepts of statistics** and that (precisely due to the largeness of N) statistical errors tend to be negligibly small.[1]
4. Finally, condensed matter systems typically possess a number of intrinsic **symmetries**. For example, our prototype Hamiltonian above is invariant under simultaneous translation and rotation of all coordinates, which expresses the global Galilean invariance of the system (a continuous set of symmetries). Spin rotation invariance (continuous) and

[1] The importance of this point is illustrated by the empirical observation that the most challenging systems in physical sciences are of *medium* (and not large) scale, e.g., metallic clusters, medium-sized nuclei or large atoms consist of $\mathcal{O}(10^1$–$10^2)$ fundamental constituents. Such problems are well beyond the reach of few-body quantum mechanics while not yet accessible to reliable statistical modeling. Often the only viable path to approaching systems of this type is massive use of phenomenology.

time-reversal invariance (discrete) are other examples of frequently encountered symmetries. The general importance of symmetries cannot be over emphasized: symmetries entail the conservation laws that simplify any problem. Yet in condensed matter physics, symmetries are "even more" important. A conserved observable is generally tied to an energetically low-lying excitation. In the universal low-temperature regimes in which we will typically be interested, it is precisely the dynamics of these low-level excitations that governs the gross behavior of the system. In subsequent sections, the sequence "symmetry $\mapsto$ conservation law $\mapsto$ low-lying excitations" will be encountered time and again. At any rate, identification of the fundamental symmetries will typically be the first step in the analysis of a solid state system.

To understand how these basic principles can be used to formulate and explore "effective low-energy" field theories of solid state systems we will begin our discussion by focussing on the harmonic chain; a collection of atoms bound by a harmonic potential. In doing so, we will observe that the universal characteristics encapsulated by the low-energy dynamics[2] of large systems relate naturally to concepts of **field theory**.

1.1 Classical harmonic chain: phonons

Returning to the prototype Hamiltonian (1.1) discussed earlier, let us focus on the dynamical properties of the positively charged *core ions* that constitute the host lattice of a crystal. For the moment, let us neglect the fact that atoms are quantum objects and treat the ions as *classical* entities. To further simplify the problem, let us consider an atomic chain rather than a generic d-dimensional solid. In this case, the positions of the ions can be specified by a sequence of coordinates with an average lattice spacing a. Relying on the reduction principle (1) we will first argue that, to understand the behavior of the ions, the dynamics of the conduction electrons are of secondary importance, i.e. we will set $H_{\rm e} = H_{\rm ei} = 0$.

At strictly zero temperature, the system of ions will be frozen out, i.e. the one-dimensional ion coordinates $R_I \equiv \bar{R}_I = Ia$ settle into a regularly spaced array. Any deviation from a perfectly regular configuration has to be paid for by a price in potential energy. For low enough temperatures (principle 2), this energy will be approximately quadratic in the small deviation from the equilibrium position. The reduced low-energy **Hamiltonian** of our system then reads

$$H = \sum_{I=1}^{N} \left[\frac{P_I^2}{2M} + \frac{k_{\rm s}}{2}(R_{I+1} - R_I - a)^2 \right], \tag{1.2}$$

where the coefficient $k_{\rm s}$ determines the steepness of the lattice potential. Notice that H can be interpreted as the Hamiltonian of N point-like particles of mass M elastically connected by springs with spring constant $k_{\rm s}$ (see Fig. 1.2).

[2] In this text, we will focus on the *dynamical* behavior of large systems, as opposed to their *static* structural properties. In particular, we will not address questions related to the formation of definite crystallographic structures in solid state systems.

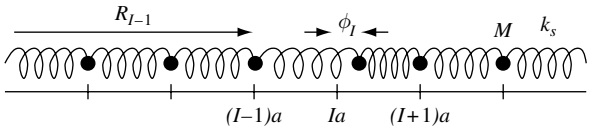

Figure 1.2 Toy model of a one-dimensional solid; a chain of elastically bound massive point particles.

Lagrangian formulation and equations of motion

Joseph–Louis Lagrange 1736–1813

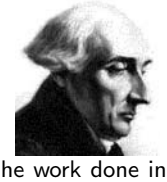

A mathematician who excelled in all fields of analysis, number theory, and celestial mechanics. In 1788 he published *Mécanique Analytique*, which summarised all the work done in the field of mechanics since the time of Newton, and is notable for its use of the theory of differential equations. In it he transformed mechanics into a branch of mathematical analysis.

What are the elementary low-energy excitations of the system? To answer this question we might, in principle, attempt to solve Hamilton's equations of motion. Indeed, since H is quadratic in all coordinates, such a program is, in this case, feasible. However, we must bear in mind that few of the problems encountered in general solid state physics enjoy this property. Further, it seems unlikely that the low-energy dynamics of a macroscopically large chain – which we know from our experience will be governed by *large-scale* wave-like excitations – is adequately described in terms of an "atomistic" language; the relevant degrees of freedom will be of a different type. We should, rather, draw on the basic principles 1–4 set out above. Notably, we have so far paid attention neither to the intrinsic symmetry of the problem nor to the fact that N is large.

Crucially, to reduce a microscopic model to an effective low-energy theory, the Hamiltonian is often not a very convenient starting point. Usually, it is more efficient to start out from an *action*. In the present case, the **Lagrangian action** corresponding to a time interval $[0, t_0]$ is defined as $S = \int_0^{t_0} dt\ L(R, \dot{R})$, where $(R, \dot{R}) \equiv \{R_I, \dot{R}_I\}$ symbolically represents the set of all coordinates and their time derivatives. The **Lagrangian** L related to the Hamiltonian (1.2) is given by

$$L = T - U = \sum_{I=1}^{N} \left[\frac{M\dot{R}_I^2}{2} - \frac{k_s}{2}(R_{I+1} - R_I - a)^2 \right], \tag{1.3}$$

where T and U denote respectively the kinetic and potential energy.

Since we are interested in the properties of the large-N system, we can expect boundary effects to be negligible. This being so, we are at liberty to impose on our atomic chain the topology of a circle, i.e. we adopt periodic boundary conditions identifying $R_{N+1} = R_1$. Further, anticipating that the effect of lattice vibrations on the solid is weak (i.e. long-range atomic order is maintained) we may assume that the deviation of the ions from their

equilibrium position is small ($|R_I(t) - \bar{R}_I| \ll a$), and the integrity of the solid is maintained. With $R_I(t) = \bar{R}_I + \phi_I(t)$ ($\phi_{N+1} = \phi_1$) the Lagrangian (1.3) assumes the simplified form

$$L = \sum_{I=1}^{N} \left[\frac{M}{2} \dot{\phi}_I^2 - \frac{k_\mathrm{s}}{2} \left(\phi_{I+1} - \phi_I \right)^2 \right].$$

To make further progress, we will now make use of the fact that we are not concerned with the behavior of our system on "atomic" scales. (In any case, for such purposes a modeling like the one above would be much too primitive!) Rather, we are interested in experimentally observable behavior that manifests itself on macroscopic length scales (principle 2). For example, one might wish to study the specific heat of the solid in the limit of infinitely many atoms (or at least a macroscopically large number, $\mathcal{O}(10^{23})$). Under these conditions, microscopic models can usually be substantially simplified (principle 3). In particular, it is often permissible to subject a discrete lattice model to a so-called **continuum limit**, i.e. to neglect the discreteness of the microscopic entities and to describe the system in terms of effective continuum degrees of freedom.

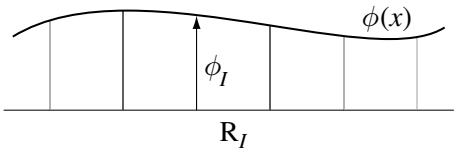

In the present case, taking a continuum limit amounts to describing the lattice fluctuations ϕ_I in terms of smooth functions of a continuous variable x (see the figure where the [horizontal] displacement of the point particles has been plotted along the vertical). Clearly such a description makes sense only if relative fluctuations on atomic scales are weak (for otherwise the smoothness condition would be violated). However, if this condition is met – as it will be for sufficiently large values of the stiffness constant k_s – the continuum description is much more powerful than the discrete encoding in terms of the "vector" $\{\phi_I\}$. All steps that we will need to take to go from the Lagrangian to concrete physical predictions will be much easier to formulate.

Introducing continuum degrees of freedom $\phi(x)$, and applying a first-order Taylor expansion,[3] let us define

$$\phi_I \to a^{1/2} \phi(x)\Big|_{x=Ia}, \quad \phi_{I+1} - \phi_I \to a^{3/2} \partial_x \phi(x)\Big|_{x=Ia}, \quad \sum_{I=1}^{N} \to \frac{1}{a} \int_0^L dx,$$

where $L = Na$. Note that, as defined, the functions $\phi(x,t)$ have dimensionality $[\text{length}]^{1/2}$. Expressed in terms of the new degrees of freedom, the continuum limit of the Lagrangian then reads

$$L[\phi] = \int_0^L dx \; \mathcal{L}(\phi, \partial_x \phi, \dot{\phi}), \quad \mathcal{L}(\phi, \partial_x \phi, \dot{\phi}) = \frac{m}{2} \dot{\phi}^2 - \frac{k_\mathrm{s} a^2}{2} (\partial_x \phi)^2, \tag{1.4}$$

[3] Indeed, for reasons that will become clear, higher-order contributions to the Taylor expansion are immaterial in the long-range continuum limit.

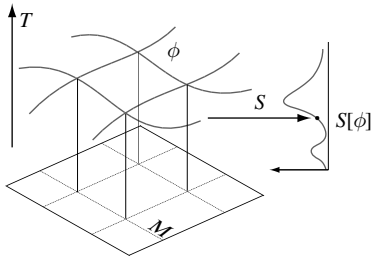

Figure 1.3 Schematic visualization of a field: a mapping ϕ from a base manifold M into a target space T (in this case, T are the real numbers; but, in general, T can be more complicated). A functional assigns to each ϕ a real number $S[\phi]$. The grid embedded into M indicates that fields in condensed matter physics arise as continuum limits of discrete mappings.

where the **Lagrangian density** $\mathcal{L}$ has dimensionality [energy]/[length] and we have designated the particle mass by the more common symbol $m \equiv M$. Similarly, the classical action assumes the continuum form

$$\boxed{S[\phi] = \int dt\ L[\phi] = \int dt \int_0^L dx\ \mathcal{L}(\phi, \partial_x\phi, \dot{\phi}).} \tag{1.5}$$

We have thus succeeded in abandoning the N-point particle description in favor of one involving *continuous* degrees of freedom, a **(classical) field**. The dynamics of the latter are specified by the **functionals** L and S, which represent the continuum generalizations of the discrete classical Lagrangian and action, respectively.

INFO The continuum variable ϕ is our first encounter with a **field**. Before proceeding with our example, let us pause to make some preliminary remarks on the general definition of these objects. This will help to place the subsequent discussion of the atomic chain into a broader context. Formally, a field is a smooth mapping

$$\begin{aligned} \phi: \quad M &\to T, \\ z &\mapsto \phi(z), \end{aligned}$$

from a certain manifold M,[4] often called the "base manifold," into a "target" or "field manifold" T (see Fig. 1.3).[5] In our present example, $M = [0, L] \times [0, t] \subset \mathbb{R}^2$ is the product of intervals in space and time, and $T = \mathbb{R}$. In fact, the factorization $M \subset \mathcal{R} \times \mathcal{T}$ into a space-like manifold $\mathcal{R}$ multiplied by a one-dimensional time-like manifold $\mathcal{T}$ is inherent in most applications of condensed matter physics.[6]

[4] If you are unfamiliar with the notion of manifolds (for a crash course, see page 537), think of M and T as subsets of some vector space. For the moment, this limitation won't do any harm.

[5] In some (rare) cases it becomes necessary to define fields in a more general sense (e.g. as sections of mathematical objects known as fiber bundles). However, in practically all condensed matter applications the more restrictive definition above will suffice.

[6] By contrast, the condition of Lorentz invariance implies the absence of such factorizations in relativistic field theory. In classical statistical field theories, i.e. theories probing the thermodynamic behavior of large systems, M is just space-like.

However, the individual factors $\mathcal{R}$ and $\mathcal{T}$ may, of course, be more complex than in our prototypical problem above. As to the target manifold, not much can be said in general; depending on the application, the realizations of T range from real or complex numbers over vector spaces and groups to the "fanciest objects" of mathematical physics.

In applied field theory, fields appear not as final objects but rather as input to *functionals* (see Fig. 1.3). Mathematically, a functional $S : \phi \mapsto S[\phi] \in \mathbb{R}$ is a mapping that takes a field as its argument and maps it into the real numbers. The functional profile $S[\phi]$ essentially determines the character of a field theory. Notice that the argument of a functional is commonly indicated in square brackets [ ].

While these formulations may appear unnecessarily abstract, remembering the mathematical backbone of the theory often helps to avoid confusion. At any rate, it takes some time and practice to get used to the concept of fields and functionals. Conceptual difficulties in handling these objects can be overcome by remembering that any field in condensed matter physics arises as the limit of a *discrete* mapping. In the present example, the field $\phi(x)$ is obtained as a continuum approximation of the discrete vector $\{\phi_I\} \in \mathbb{R}^N$; the functional $L[\phi]$ is the continuum limit of the function $L : \mathbb{R}^N \to \mathbb{R}$, etc. While in practical calculations fields are usually easier to handle than their discrete analogs, it is sometimes helpful to think about problems of field theory in a discrete language. Within the discrete picture, the mathematical apparatus of field theory reduces to finite-dimensional calculus.

Although Eq. (1.4) contains the full information about the model, we have not yet learned much about its actual behavior. To extract concrete physical information from Eq. (1.4) we need to derive **equations of motion**. At first sight, it may not be entirely clear what is meant by the term "equations of motion" in the context of an infinite-dimensional model: the equations of motion relevant for the present problem are obtained as the generalization of the conventional Lagrange equations of N-particle classical mechanics to a model with infinitely many degrees of freedom. To derive these equations we need to generalize Hamilton's extremal principle (i.e. the route from an action to the associated equations of motion) to infinite dimensions. As a warm-up, let us briefly recapitulate how the extremal principle works for a system with one degree of freedom.

Suppose the dynamics of a classical *point* particle with coordinate $x(t)$ is described by the classical Lagrangian $L(x, \dot{x})$, and action $S[x] = \int dt\ L(x, \dot{x})$. **Hamilton's extremal principle** states that the configurations $x(t)$ that are *actually realized* are those that extremize the action, $\delta S[x] = 0$. This means (for a substantiated discussion, see Section 1.2 below) that, for any smooth curve $t \mapsto y(t)$,

$$\lim_{\epsilon \to 0} \frac{1}{\epsilon} (S[x + \epsilon y] - S[x]) = 0. \tag{1.6}$$

To first order in ϵ, the action has to remain invariant. Applying this condition, one finds that it is fulfilled if and only if x satisfies **Lagrange's equation of motion**

$$\boxed{\frac{d}{dt}(\partial_{\dot{x}} L) - \partial_x L = 0.} \tag{1.7}$$

EXERCISE Recapitulate the derivation of (1.7) from the classical action.

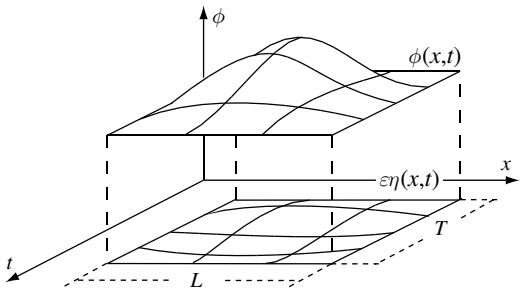

Figure 1.4 Schematic showing the variation of the field associated with the action functional. Notice that the variation $\epsilon\eta$ is supposed to vanish on the boundaries of the base $M = [0, L] \times [0, t]$.

In Eq. (1.5) we are dealing with a system of infinitely many degrees of freedom, $\phi(x, t)$. Yet Hamilton's principle is general and we may see what happens if Eq. (1.5) is subjected to an extremal principle analogous to Eq. (1.6). To do so, we substitute $\phi(x, t) \to \phi(x, t) + \epsilon\eta(x, t)$ into Eq. (1.5) and require vanishing of the first-order contribution to an expansion in ϵ (see Fig. 1.4). When applied to the specific Lagrangian (1.4), substituting the "varied" field leads to

$$S[\phi + \epsilon\eta] = S[\phi] + \epsilon \int dt \int_0^L dx \left(m\dot{\phi}\dot{\eta} - k_{\mathrm{s}} a^2 \partial_x \phi \partial_x \eta \right) + \mathcal{O}(\epsilon^2).$$

Integrating by parts and requiring that the contribution linear in ϵ vanishes, one obtains

$$\lim_{\epsilon \to 0} \frac{1}{\epsilon} \left(S[\phi + \epsilon\eta] - S[\phi] \right) = - \int dt \int_0^L dx \left(m\ddot{\phi} - k_{\mathrm{s}} a^2 \partial_x^2 \phi \right) \eta \stackrel{!}{=} 0.$$

(Notice that the boundary terms vanish identically.) Now, since η was defined to be an arbitrary smooth function, the integral above can vanish only if the factor in parentheses is globally vanishing. Thus the equation of motion takes the form of a **wave equation**

$$\boxed{\left(m\partial_t^2 - k_{\mathrm{s}} a^2 \partial_x^2 \right) \phi = 0.} \tag{1.8}$$

The solutions of Eq. (1.8) have the general form $\phi_+(x - vt) + \phi_-(x + vt)$ where $v = a\sqrt{k_{\mathrm{s}}/m}$, and $\phi_\pm$ are arbitrary smooth functions of the argument. From this we can deduce that the basic low-energy **elementary excitations** of our model are lattice vibrations propagating as **sound waves** to the left or right at a constant velocity v (see the figure).[7] The trivial behavior of our model is of course a direct consequence of its simplistic definition – no dissipation, dispersion, or other non-trivial ingredients. Adding these refinements leads to the general classical theory of lattice vibrations (such as that described in the text by Ashcroft and Mermin[8]). Finally, notice that

[7] Strictly speaking, the modeling of our system enforces a periodicity constraint $\phi_\pm(x + L) = \phi_\pm(x)$. However, in the limit of a large system, this aspect becomes inessential.

[8] N. W. Ashcroft and N. D. Mermin, *Solid State Physics* (Holt–Saunders International, 1983).

the elementary excitations of the chain have little in common with its "microscopic" constituents (the atomic oscillators). Rather they are **collective excitations**, i.e. elementary excitations comprising a macroscopically large number of microscopic degrees of freedom.

INFO The "relevant" **excitations of a condensed matter system** can, but need not, be of collective type. For example, the interacting electron gas (a system to be discussed in detail below) supports microscopic excitations – charged quasi-particles standing in 1:1 correspondence with the electrons of the original microscopic system – while the collective excitations are plasmon modes of large wavelength and engaging many electrons. Typically, the nature of the fundamental excitations cannot be straightforwardly inferred from the microscopic definition of a model. Indeed, the mere *identification* of the relevant excitations often represents the most important step in the solution of a condensed matter problem.

Hamiltonian formulation

Sir William Rowan Hamilton 1805–65
A mathematician credited with the discovery of quaternions, the first non-commutative algebra to be studied. He also invented important new methods in mechanics. (Image from W. R. Hamilton, *Collected Papers*, vol. II, Cambridge University Press, 1940.

An important characteristic of any excitation is its *energy*. How much energy is stored in the sound waves of the harmonic chain? To address this question, we need to switch back to a Hamiltonian formulation. Once again, this is achieved by generalizing standard manipulations from point mechanics to the continuum. Remembering that, for a Lagrangian of a point particle, $p \equiv \partial_{\dot{x}} L$ is the momentum conjugate to the coordinate x, let us consider the Lagrangian *density* and define[9]

$$\pi(x) \equiv \frac{\partial \mathcal{L}(\phi, \partial_x \phi, \dot{\phi})}{\partial \dot{\phi}(x)}, \tag{1.9}$$

as the **canonical momentum** associated with ϕ (at the point x). In common with ϕ, the momentum π is a continuum degree of freedom. At each space point it may take an independent value. Notice that $\pi(x)$ is nothing but the continuum generalization of the lattice momentum P_I of Eq. (1.2). (Applied to P_I, a continuum approximation like $\phi_I \to \phi(x)$ would produce $\pi(x)$.) The **Hamiltonian density** is then defined as usual through the Legendre transformation,

$$\mathcal{H}(\phi, \partial_x \phi, \pi) = \left(\pi \dot{\phi} - \mathcal{L}(\phi, \partial_x \phi, \dot{\phi}) \right) \Big|_{\dot{\phi} = \dot{\phi}(\phi, \pi)}, \tag{1.10}$$

[9] In field theory literature it is popular to denote the momentum by a Greek letter.

from where the full Hamiltonian is obtained as $H = \int_0^L dx\, \mathcal{H}$.

EXERCISE Verify that the transition $L \to H$ is a straightforward continuum generalization of the Legendre transformation of the N-particle Lagrangian $L(\{\phi_I\}, \{\phi_I\})$.

Having introduced a Hamiltonian, we are in a position to determine the energy of the sound waves. Application of Eq. (1.9) and (1.10) to the Lagrangian of the atomic chain yields $\pi(x,t) = m\dot{\phi}(x,t)$ and

$$H[\pi,\phi] = \int dx \left(\frac{\pi^2}{2m} + \frac{k_{\rm s} a^2}{2} (\partial_x \phi)^2 \right). \tag{1.11}$$

Considering, say, a right-moving sound-wave excitation, $\phi(x,t) = \phi_+(x - vt)$, we find that $\pi(x,t) = -mv\partial_x \phi_+(x - vt)$ and $H[\pi,\phi] = k_{\rm s} a^2 \int dx [\partial_x \phi_+(x - vt)]^2 = k_{\rm s} a^2 \int dx\, [\partial_x \phi_+(x)]^2$, i.e. a positive definite, time-independent expression, as one would expect.

Before proceeding, let us note an interesting feature of the energy functional: in the limit of an infinitely shallow excitation, $\partial_x \phi_+ \to 0$, the energy vanishes. This sets the stage for the last of the principles (4) hitherto unconsidered, **symmetry**. The Hamiltonian of an atomic chain is invariant under simultaneous translation of all atom coordinates by a fixed increment: $\phi_I \to \phi_I + \delta$, where δ is constant. This expresses the fact that a global translation of the solid as a whole does not affect the internal energy. Now, the ground state of any specific realization of the solid will be defined through a static array of atoms, each located at a fixed coordinate $R_I = Ia \Rightarrow \phi_I = 0$. We say that the translational symmetry is "spontaneously broken," i.e. the solid has to decide where exactly it wants to rest. However, spontaneous breakdown of a symmetry does not imply that the symmetry disappeared. On the contrary, infinite-wavelength deviations from the pre-assigned ground state come close to global translations of (macroscopically large portions of) the solid and, therefore, cost a vanishingly small amount of energy. This is the reason for the vanishing of the sound wave energy in the limit $\partial_x \phi \to 0$. It is also our first encounter with the aforementioned phenomenon that symmetries lead to the formation of soft, i.e. low-energy, excitations. A much more systematic exposition of these connections will be given in Chapter 6.

Ludwig Boltzmann 1844–1906
A physicist whose greatest achievement was in the development of statistical mechanics, which explains and predicts how the properties of atoms (such as mass, charge, and structure) determine the visible properties of matter (such as viscosity, thermal conductivity, and diffusion).

To conclude our discussion of the classical harmonic chain, let us consider the **specific heat**, a quantity directly accessible in experiment. A rough estimate of this quantity can be readily obtained from the microscopic harmonic Hamiltonian (1.2). According to the principles of statistical mechanics, the thermodynamic energy density is given by

$$u = \frac{1}{L} \frac{\int d\Gamma\; e^{-\beta H} H}{\int d\Gamma\; e^{-\beta H}} = -\frac{1}{L} \partial_\beta \ln \int d\Gamma\; e^{-\beta H},$$

where $\beta = 1/k_{\rm B}T$, $\mathcal{Z} \equiv \int d\Gamma e^{-\beta H}$ is the **Boltzmann partition function** and the phase space volume element $d\Gamma = \prod_{I=1}^{N} dR_I dP_I$. We will set $k_{\rm B} = 1$ throughout. The specific heat

is then obtained as $c = \partial_T u$. To determine the temperature dependence of this quantity, we make use of the fact that, upon rescaling of integration variables, $R_I \to \beta^{-1/2} X_I$, $P_I \to \beta^{-1/2} Y_I$, the exponent $\beta H(R,P) \to H(X,Y)$ becomes independent of temperature (a property that relies on the quadratic dependence of H on both R and P). The integration measure transforms as $d\Gamma \to \beta^{-N} \prod_{I=1}^{N} dX_I \; dY_I \equiv \beta^{-N} d\Gamma'$. Expressed in terms of the rescaled variables, one obtains the energy density

$$u = -\frac{1}{L} \partial_\beta \ln \left(\beta^{-N} K \right) = \rho T,$$

where $\rho = N/L$ is the density of atoms, and we have made use of the fact that the constant $K \equiv \int d\Gamma' \; e^{-H(X,Y)}$ is independent of temperature. We thus find a temperature independent specific heat $c = \rho$. Notice that c is fully universal, i.e. independent of the material constants M and $k_{\rm s}$ determining H. (In fact, we could have anticipated this result from the equipartition theorem of classical mechanics, i.e. the law that in a system with N degrees of freedom, the energy scales as $U = NT$.)

How do these findings compare with experiment? Figure 1.5 shows the specific heat of the insulating compound $EuCoO_3$.[10] For large temperatures, the specific heat approaches a constant value, in accord with our analysis. However, for lower temperatures, substantial deviations from $c = \text{const.}$ appear. Yet, this strong temperature dependence does not reflect a failure of the simplistic microscopic modeling. Rather, the deviation is indicative of a **quantum phenomenon**. Indeed, we have so far totally neglected the quantum nature of the atomic oscillators. In the next chapter we will rectify this deficiency and discuss how the effective low-energy theory of the harmonic chain can be promoted to a quantum field theory. However, before proceeding with the development of the theory let us pause to introduce a number of mathematical concepts that surfaced above, in a way that survives generalization to richer problems.

1.2 Functional analysis and variational principles

Let us revisit the derivation of the equations of motion associated with the harmonic chain, Eq. (1.8). Although straightforward, neither was the calculation efficient, nor did it reveal general structures. In fact, what we did – expanding explicitly to first order in the variational parameter ϵ – had the same status as evaluating derivatives by explicitly taking limits: $f'(x) = \lim_{\epsilon \to 0} \left((f(x+\epsilon) - f(x))/\epsilon \right)$. Moreover, the derivation made explicit use of the particular form of the Lagrangian, thereby being of limited use with regard to a general understanding of the construction scheme. Given the importance attached to extremal principles in all of field theory, it is worthwhile investing some effort in constructing a more efficient scheme for the general variational analysis of continuum theories. In order to carry out this program we first need to introduce a mathematical tool of functional analysis, namely the concept of **functional differentiation**.

[10] In metals, the specific heat due to lattice vibrations exceeds the specific heat of the free conduction electrons for temperatures larger than a few degrees kelvin.

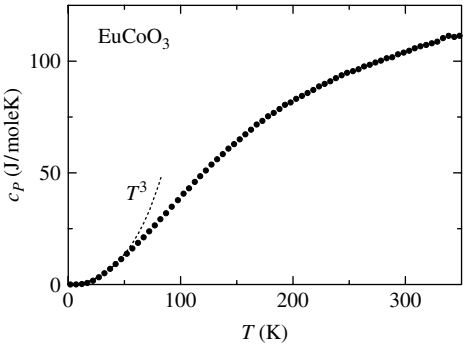

Figure 1.5 Specific heat c_p of the insulator $EuCoO_3$. At large temperatures, the specific heat starts to approach a constant value, as predicted by the analysis of the classical harmonic chain. However, for small temperatures, deviations from $c_p = \text{const.}$ are substantial. Such deviations can be ascribed to quantum mechanical effects. (Courtesy of M. Kriener, A. Reichl, T. Lorenz, and A. Freimuth.)

In working with functionals, one is often concerned with how a given functional behaves under (small) variations of its argument function. In particular, given a certain function f, suspected to make a functional $F[f]$ stationary, one would like to find out whether, indeed, the functional remains invariant under variations $f \to f+h$, where h is an "infinitely small" increment function. In ordinary analysis, questions of this type are commonly addressed by exploring *derivatives*, i.e. we need to generalize the concept of a derivative to functionals. This is achieved by the following definition: a functional F is called differentiable if

$$F[f + \epsilon g] - F[f] = \epsilon \cdot DF_f[g] + \mathcal{O}(\epsilon^2),$$

where the **differential** DF_f is a linear functional (i.e. one with $DF_f[g_1 + g_2] = DF_f[g_1] + DF_f[g_2]$), ϵ is a small parameter, and g is an arbitrary function. The subscript indicates that the differential generally depends on the "base argument" f. A functional F is said to be **stationary** on f, if and only if $DF_f = 0$.

In principle, the definition above answers our question concerning a stationarity condition. However, to make use of the definition, we still need to know how to compute the differential DF and how to relate the differentiability criterion to the concepts of ordinary calculus. In order to understand how answers to these questions can be systematically found, it is helpful to return temporarily to a discrete way of thinking, i.e. to interpret the argument f of a functional $F[f]$ as the limit $N \to \infty$ of a discrete vector $\mathbf{f} = \{f_n \equiv f(x_n), n = 1, \ldots, N\}$, where $\{x_n\}$ denotes a discretization of the support of f (cf. the harmonic chain, $\phi \leftrightarrow f$). Prior to taking the continuum limit, $N \to \infty$, $\mathbf{f}$ has the status of an N-dimensional vector and $F(\mathbf{f})$ is a function defined over N-dimensional space. After the continuum limit, $\mathbf{f} \to f$ becomes a function itself and $F(\mathbf{f}) \to F[f]$ becomes a functional.

Now, within the discrete picture, it is clear how the variational behavior of functions is to be analyzed. For example, the condition that, for all ϵ and all vectors $\mathbf{g}$, the linear expansion of $F(\mathbf{f} + \epsilon\mathbf{g})$ ought to vanish is simply to say that the ordinary differential, $dF_{\mathbf{f}}$, defined

through

$$F(\mathbf{f}+\epsilon\mathbf{g}) - F(\mathbf{f}) = \epsilon \cdot dF_{\mathbf{f}}(\mathbf{g}) + \mathcal{O}(\epsilon^2),$$

must be zero. In practice, one often expresses conditions of this type in terms of a certain basis. In a Cartesian basis of N unit vectors, $\mathbf{e}_n$, $n = 1, \ldots, N$, $dF_{\mathbf{f}}(\mathbf{g}) \equiv \langle \nabla F_{\mathbf{f}}, \mathbf{g}\rangle$, where $\langle \mathbf{f}, \mathbf{g}\rangle \equiv \sum_{n=1}^{N} f_n g_n$ denotes the standard scalar product, $\nabla F_{\mathbf{f}} = \{\partial_{f_n} F\}$ represents the gradient with the partial derivative defined as

$$\partial_{f_n} F(\mathbf{f}) \equiv \lim_{\epsilon\to 0} \frac{1}{\epsilon} \left[F(\mathbf{f}+\epsilon\mathbf{e}_n) - F(\mathbf{f})\right]. \tag{1.12}$$

From these identities, the differential is identified as

$$dF_{\mathbf{f}}(\mathbf{g}) = \sum_n \partial_{f_n} F(\mathbf{f}) g_n. \tag{1.13}$$

The vanishing of the differential amounts to vanishing of all partial derivatives $\partial_{f_n} F = 0$.

Equations (1.12) and (1.13) can now be straightforwardly generalized to the continuum limit whereupon the summation defining the finite-dimensional scalar product translates to an integral,

$$\langle \mathbf{f}, \mathbf{g}\rangle = \sum_{n=1}^{N} f_n g_n \to \langle f, g\rangle = \int dx\ f(x) g(x).$$

The analog of the nth unit vector is a δ-distribution, $\mathbf{e}_n \to \delta_x$, where $\delta_x(x') \equiv \delta(x - x')$, as can be seen from the following correspondence:

$$f_n \overset{!}{=} \langle \mathbf{f}, \mathbf{e}_n\rangle = \sum_m f_m (e_n)_m \to f(x) \overset{!}{=} \langle f, \delta_x\rangle = \int dx'\ f(x')\delta_x(x').$$

Here $(e_n)_m = \delta_{nm}$ denotes the mth component of the nth unit vector. The correspondence (unit vector $\leftrightarrow$ δ-distribution) is easy to memorize: while the components of $\mathbf{e}_n$ vanish, save for the nth component, that equals unity, δ_x is a function that vanishes everywhere, save for x where it is *infinite*. That a unit component is replaced by "infinity" reflects the fact that the support of the δ-distribution is infinitely narrow; to obtain a unit-normalized integral $\int \delta_x$, the function must be singular.

As a consequence of these identities, Eq. (1.13) translates to the continuum differential,

$$DF_f[g] = \int dx\ \frac{\delta F[f]}{\delta f(x)} g(x), \tag{1.14}$$

where the generalization of the partial derivative,

$$\frac{\delta F[f]}{\delta f(x)} \equiv \lim_{\epsilon\to 0} \frac{1}{\epsilon} \left(F[f + \epsilon\delta_x] - F[f]\right), \tag{1.15}$$

is commonly denoted by "δ" instead of "∂." Equations (1.14) and (1.15) establish the conceptual connection between ordinary and functional differentiation. Notice that we have not yet learned how to calculate the differential practically, i.e. to evaluate expressions like Eq. (1.15) for concrete functionals. Nevertheless, the identities above are very useful, enabling us to generalize more-complex derivative operations of ordinary calculus by

Table 1.1 *Summary of basic definitions of discrete and continuum calculus.*

Entity	Discrete	Continuum
Argument	vector $\mathbf{f}$	function f
Function(al)	multidimensional function $F(\mathbf{f})$	functional $F[f]$
Differential	$dF_{\mathbf{f}}(\mathbf{g})$	$DF_f[g]$
Cartesian basis	$\mathbf{e}_n$	δ_x
Scalar product $\langle\,,\,\rangle$	$\sum_n f_n g_n$	$\int dx\; f(x)g(x)$
"Partial derivative"	$\partial_{f_n} F(\mathbf{f})$	$\frac{\delta F[f]}{\delta f(x)}$

straightforward transcription. For example, the generalization of the standard **chain rule**, $\partial_{f_n} F(\mathbf{g}(\mathbf{f})) = \sum_m \partial_{g_m} F(\mathbf{g})\,\big|_{\mathbf{g}=\mathbf{g}(\mathbf{f})}\, \partial_{f_n} g_m(\mathbf{f})$ reads

$$\frac{\delta F[g[f]]}{\delta f(x)} = \int dy\; \frac{\delta F[g]}{\delta g(y)}\bigg|_{g=g[f]} \frac{\delta g(y)[f]}{\delta f(x)}.$$

Here $g[f]$ is the continuum generalization of an $\mathbb{R}^m$-valued function, $\mathbf{g} : \mathbb{R}^n \to \mathbb{R}^m$, a function whose components $g(y)[f]$ are functionals by themselves. Furthermore, given some functional $F[f]$, we can construct its **Taylor expansion** as

$$F[f] = F[0] + \int dx_1\; \frac{\delta F[f]}{\delta f(x_1)}\bigg|_{f=0} f(x_1) + \frac{1}{2}\;\int dx_1\; dx_2\; \frac{\delta^2 F[f]}{\delta f(x_2)\delta f(x_1)}\bigg|_{f=0} f(x_1)f(x_2) + \cdots,$$

where (exercise)

$$\frac{\delta^2 F[f]}{\delta f(x_2)\delta f(x_1)} = \lim_{\epsilon_{1,2}\to 0} \frac{1}{\epsilon_1\epsilon_2}\left(F[f + \epsilon_1\delta_{x_1} + \epsilon_2\delta_{x_2}] - F[f + \epsilon_1\delta_{x_1}] - F[f + \epsilon_2\delta_{x_2}] + F[f]\right)$$

generalizes a two-fold partial derivative. The validity of these identities can be made plausible by applying the transcription, Table 1.1, to the corresponding relations of standard calculus. To actually verify the formulae, one has to take the continuum limit of each step taken in the discrete variant of the corresponding proofs. At any rate, experience shows that it takes some time to get used to the concept of functional differentiation. However, after some practice it will become clear that this operation is not only extremely useful but also as easy to handle as conventional partial differentiation.

We finally address the question how to compute functional derivatives in practice. In doing so, we will make use of the fact that, in all but a few cases, the functionals encountered in field theory are of the structure

$$\boxed{S[\phi] = \int_M d^m x\, \mathcal{L}(\phi^i, \partial_\mu \phi^i).} \tag{1.16}$$

Here, we assume the base manifold M to be parameterized by an m-dimensional coordinate vector $x = \{x_\mu\}$. (In most practical applications, $m = d + 1$, and $x = (x_0, x_1, \ldots, x_d)$

contains one time-like component $x_0 = t$ and d space-like components $x_k, k = 1, \ldots, d$.[11]) We further assume that the field manifold has dimensionality n and that ϕ^i, $i = 1, \ldots, n$, are the coordinates of the field.

What makes the functional $S[\phi]$ easy to handle is that all of its information is stored in the *function* $\mathcal{L}$. Owing to this simplification, the functional derivative can be related to an ordinary derivative of $\mathcal{L}$. To see this, all that we have to do is to evaluate the general definition Eq. (1.14) on the functional S:

$$S[\phi + \epsilon\theta] - S[\phi] = \int_M d^m x \, [\mathcal{L}(\phi + \epsilon\theta, \partial_\mu \phi + \epsilon \partial_\mu \theta) - \mathcal{L}(\phi, \partial_\mu \phi)]$$
$$= \int_M d^m x \left[\frac{\partial \mathcal{L}}{\partial \phi^i} \theta^i + \frac{\partial \mathcal{L}}{\partial \partial_\mu \phi^i} \partial_\mu \theta^i \right] \epsilon + O(\epsilon^2) = \int_M d^m x \left[\frac{\partial \mathcal{L}}{\partial \phi^i} - \partial_\mu \frac{\partial \mathcal{L}}{\partial \partial_\mu \phi^i} \right] \theta^i \epsilon + O(\epsilon^2),$$

where in the last line we have assumed that the field variation vanishes on the boundary of the base manifold, $\theta\,|_{\partial M} = 0$. Comparison with Eq. (1.14) identifies the functional derivative as

$$\frac{\delta S[\phi]}{\delta \phi^i(x)} = \frac{\partial \mathcal{L}}{\partial \phi^i(x)} - \partial_\mu \frac{\partial \mathcal{L}}{\partial (\partial_\mu \phi^i(x))}.$$

We conclude that **stationarity of the functional** (1.16) is equivalent to the condition

$$\boxed{\forall x, i : \frac{\partial \mathcal{L}}{\partial \phi^i(x)} - \partial_\mu \frac{\partial \mathcal{L}}{\partial \partial_\mu \phi^i(x)} = 0.} \tag{1.17}$$

Equation (1.17) is known as the **Euler–Lagrange equation** of field theory. In fact, for $d = 0$ and $x_0 = t$, Eq. (1.17) reduces to the familiar Euler–Lagrange equation of a point particle in n-dimensional space. For $d = 1$ and $(x_0, x_1) = (t, x)$ we get back to the stationarity equations discussed in the previous section. In the next section we will apply the formalism to a higher-dimensional problem.

1.3 Maxwell's equations as a variational principle

As a second example, let us consider *the* archetype of classical field theory, classical electrodynamics. Indeed, as well as exemplifying the application of continuum variational principles on a problem with which we are all acquainted, this example illustrates the unifying potential of the approach: that problems as different as the low-lying vibrational modes of a crystalline solid, and electrodynamics can be described by almost identical language indicates that we are dealing with a useful formalism. Specifically, our aim will be to explore how the equations of motion of electrodynamics, the inhomogeneous **Maxwell** equations,

$$\nabla \cdot \mathbf{E} = \rho, \qquad \nabla \times \mathbf{B} - \partial_t \mathbf{E} = \mathbf{j}, \tag{1.18}$$

[11] Following standard conventions we denote space-like components by small Latin indices $k = 1, \ldots, d$. In contrast, space-time indices are denoted by Greek indices $\mu = 0, \ldots, d$.

can be obtained from variational principles. (For simplicity, we restrict ourselves to a vacuum theory, i.e. $\mathbf{E} = \mathbf{D}$ and $\mathbf{B} = \mathbf{H}$. Further, we have set the velocity of light to unity, $c = 1$. Within the framework of the variational principle, the homogeneous equations,

$$\nabla \times \mathbf{E} + \partial_t \mathbf{B} = 0, \qquad \nabla \cdot \mathbf{B} = 0, \tag{1.19}$$

are regarded as *ab initio* constraints imposed on the "degrees of freedom" $\mathbf{E}$ and $\mathbf{B}$.)

James Clerk Maxwell 1831–79

Scottish theoretical physicist and mathematician. Amongst many other achievements, he is credited with the formulation of the theory of electromagnetism, synthesizing all previous unrelated experiments and equations of electricity, magnetism and optics into a consistent theory. (He is also known for creating the first true color photograph in 1861.)

To formulate Maxwell's theory as a variational principle we require (1) a field formulated in a set of suitable "generalized coordinates," and (2) its action. As to coordinates, the natural choice will be the coefficients of the electromagnetic (EM) 4-potential, $A_\mu = (\phi, -\mathbf{A})$, where ϕ is the scalar and $\mathbf{A}$ is the vector potential. The potential A is unconstrained and uniquely determines the fields $\mathbf{E}$ and $\mathbf{B}$ through the standard equations $\mathbf{E} = -\nabla\phi - \partial_t \mathbf{A}$ and $\mathbf{B} = \nabla \times \mathbf{A}$. (In fact, the set of coordinates A_μ is "overly free" in the sense that gauge transformations $A_\mu \to A_\mu + \partial_\mu \Gamma$, where Γ is an arbitrary function, leave the physical fields invariant. Later we will comment explicitly on this point.) The connection between A and the physical fields can be expressed in a more symmetric way by introducing the EM field tensor,

$$F = \{F_{\mu\nu}\} = \begin{bmatrix} 0 & E_1 & E_2 & E_3 \\ -E_1 & 0 & -B_3 & B_2 \\ -E_2 & B_3 & 0 & -B_1 \\ -E_3 & -B_2 & B_1 & 0 \end{bmatrix}. \tag{1.20}$$

The relation between fields and potential now reads $F_{\mu\nu} = \partial_\mu A_\nu - \partial_\nu A_\mu$ where $x_\mu = (t, -\mathbf{x})$ and $\partial_\mu = (\partial_t, \nabla)$.

EXERCISE Confirm that this connection follows from the definition of the vector potential. To verify that the constraint (1.19) is automatically included in the definition (1.20), compute the construct $\partial\ F_\mu\ + \partial_\mu F\ \ + \partial\ F\ _\mu$, where $(\lambda\nu\mu)$ represent arbitrary but *di erent* indices. This produces four different terms, identified as the left-hand side of Eq. (1.19). Evaluation of the same construct on $F_\mu\ \equiv \partial_\mu A\ \ - \partial\ A_\mu$ produces zero by the symmetry of the right-hand side.

Hendrik Antoon Lorentz 1853–1928

1902 Nobel Laureate in Physics (with Pieter Zeeman) in recognition of the extraordinary service they rendered by their researches into the influence of magnetism upon radiation phenomena. Lorentz derived the transformation equations subsequently used by Albert Einstein to describe space and time.

As to the structure of the action $S[A]$ we can proceed in different ways. One option would be to regard Maxwell's equations as fundamental, i.e. to construct an action that produces these equations upon variation (by analogy with the situation in classical mechanics where the action functional was designed so as to reproduce Newton's equations). However, we can also be a little bit more ambitious and ask whether the structure of the action can be motivated independently of Maxwell's equations. In fact, there is just one principle in electrodynamics as "fundamental" as Maxwell's equations: **symmetry**. A theory of electromagnetism must be Lorentz invariant, i.e. invariant under relativistic coordinate transformations.

INFO Let us briefly recapitulate the notion of **Lorentz invariance**. Suppose we are given a 4-vector X_μ. A linear coordinate transformation $X_\mu \to X'_\mu \equiv T_\mu{}^\nu X^\nu$ is a Lorentz transformation if it leaves the 4-metric

$$g = \{g^\mu{}_\nu\} = \begin{matrix} 1 & & & \\ & -1 & & \\ & & -1 & \\ & & & -1 \end{matrix}, \tag{1.21}$$

invariant: $T^T g T = g$. To concisely formulate the invariance properties of relativistic theories, it is common to introduce the notion of raised and lowered indices. Defining $X^\mu \equiv g^\mu{}_\nu X^\nu$, Lorentz invariance is expressed as $X^\mu X_\mu = X'^\mu X'_\mu$.

Aided by the symmetry criterion, we can attempt to conjecture the structure of the action from three basic assumptions, all independent of Maxwell's equations: the action should be invariant under (a) Lorentz transformations and (b) gauge transformations, and (c) it should be simple! The most elementary choice compatible with these conditions is

$$S[A] = \int d^4x \, (c_1 \, F_{\mu\nu} F^{\mu\nu} + c_2 \, A_\mu j^\mu) \,, \tag{1.22}$$

where $d^4x = \prod_\mu dx_\mu = dt \; dx_1 \; dx_2 \; dx_3$ denotes the measure, $j_\mu = (\rho, -\mathbf{j})$ the 4-current, and $c_{1,2}$ are undetermined constants. Up to quadratic order in A, Eq. (1.22) in fact defines the only possible structure consistent with gauge and Lorentz invariance.

EXERCISE Using the continuity equation $\partial_\mu j^\mu = 0$, verify that the Aj-coupling is gauge invariant. (Hint: Integrate by parts.) Verify that a contribution like $\int A_\mu A^\mu$ would *not* be gauge invariant.

Having defined a trial action, we can apply the variational principle Eq. (1.17) to compute equations of motion. In the present context, the role of the field ϕ is taken by the four components of A. Variation of the action with respect to A_μ gives four equations of motion,

$$\frac{\partial \mathcal{L}}{\partial A_\mu} - \partial_\nu \frac{\partial \mathcal{L}}{\partial(\partial_\nu A_\mu)} = 0, \quad \mu = 0, \ldots, 3, \tag{1.23}$$

where the Lagrangian density is defined by $S = \int d^4x\ \mathcal{L}$. With the specific form of $\mathcal{L}$, it is straightforward to verify that $\partial_{A_\mu}\mathcal{L} = c_2 j^\mu$ and $\partial_{\partial_\nu A_\mu}\mathcal{L} = -4c_1 F^{\mu\nu}$. Substitution of these building blocks into the equations of motion finally yields $4c_1\partial^\nu F_{\nu\mu} = c_2 j_\mu$. Comparing this with the definition of the field tensor (1.20), and setting $c_1/c_2 = 1/4$, we arrive at Maxwell's equations (1.18). We finally fix the overall multiplicative constant c_1 ($= c_2/4$) by requiring that the Hamiltonian density associated with the Lagrangian density $\mathcal{L}$ reproduce the known energy density of the EM field (see Problem 1.8). This leads to $c_1 = -1/4$, so that we have identified

$$\boxed{\mathcal{L}(A_\mu, \partial_\nu A_\mu) = -\frac{1}{4}F_{\mu\nu}F^{\mu\nu} + A_\mu j^\mu,} \tag{1.24}$$

as the **Lagrangian density of the electromagnetic field**. The corresponding action is given by $S[A] = \int d^4x\ \mathcal{L}(A_\mu, \partial_\nu A_\mu)$.

At first sight, this result does not look particularly surprising. After all, Maxwell's equations can be found on the first page of most textbooks on electrodynamics. However, further reflection will show that our achievement is actually quite remarkable. By invoking only symmetry, the algebraic structure of Maxwell's equations has been established unambiguously. We have thus proven that Maxwell's equations are relativistically invariant, a fact not obvious from the equations themselves. Further, we have shown that Eq. (1.18) are the *only* equations of motion linear in the current–density distribution and consistent with the invariance principle. One might object that, in addition to symmetry, we have also imposed an ad hoc "simplicity" criterion on the action $S[A]$. However, later we will see that this was motivated by more than mere aesthetic principles.

Finally, we note that the symmetry-oriented modeling that led to Eq. (1.22) is illustrative of a popular construction scheme in modern field theory. The symmetry-oriented approach stands complementary to the "microscopic" formulation exemplified in Section 1.1. Crudely speaking, these are the two principal approaches to constructing effective low-energy field theories:

- ▷ **Microscopic analysis**: Starting from a microscopically defined system, one projects onto those degrees of freedom that one believes are relevant for the low-energy dynamics. Ideally, this "belief" is backed up by a small expansion parameter stabilizing the mathematical parts of the analysis. *Advantages:* The method is rigorous and fixes the resulting field theory completely. *Disadvantages:* The method is time-consuming and, for sufficiently complex systems, not even viable.
- ▷ **Symmetry considerations**: One infers an effective low-energy theory on the basis of only fundamental symmetries of the physical system. *Advantages:* The method is fast and

elegant. *Disadvantages:* It is less explicit than the microscopic approach. Most importantly, it does not fix the coefficients of the different contributions to the action.

Thus far, we have introduced some basic concepts of field theoretical modeling in condensed matter physics. Starting from a microscopic model Hamiltonian, we have illustrated how principles of universality and symmetry can be applied to distill effective continuum field theories capturing the low-energy content of the system. We have formulated such theories in the language of Lagrangian and Hamiltonian continuum mechanics, respectively, and shown how variational principles can be applied to extract concrete physical information. Finally, we have seen that field theory provides a unifying framework whereby analogies between seemingly different physical systems can be uncovered. In the next section we discuss how the formalism of classical field theory can be elevated to the quantum level.

1.4 Quantum chain

Earlier we saw that, at low temperatures, the excitation profile of the classical atomic chain differs drastically from that observed in experiment. Generally, in condensed matter physics, low-energy phenomena with pronounced temperature sensitivity are indicative of a quantum mechanism at work. To introduce and exemplify a general procedure whereby quantum mechanics can be incorporated into continuum models, we next consider the low-energy physics of the quantum mechanical atomic chain.

The first question to ask is conceptual: how can a model like Eq. (1.4) be quantized in general? Indeed, there exists a standard procedure for quantizing continuum theories, which closely resembles the quantization of Hamiltonian point mechanics. Consider the defining Eq. (1.9) and (1.10) for the canonical momentum and the Hamiltonian, respectively. Classically, the momentum $\pi(x)$ and the coordinate $\phi(x)$ are canonically conjugate variables: $\{\pi(x), \phi(x')\} = -\delta(x-x')$ where $\{,\}$ is the Poisson bracket and the δ-function arises through continuum generalization of the discrete identity $\{P_I, R_{I'}\} = -\delta_{II'}$, $I, I' = 1, \ldots, N$. The theory is quantized by generalization of the canonical quantization procedure for the discrete pair of conjugate coordinates (R_I, P_I) to the continuum: (i) promote $\phi(x)$ and $\pi(x)$ to operators, $\phi \mapsto \hat{\phi}$, $\pi \mapsto \hat{\pi}$, and (ii) generalize the canonical commutation relation $[P_I, R_{I'}] = -i\hbar\delta_{II'}$ to[12]

$$\boxed{[\hat{\pi}(x), \hat{\phi}(x')] = -i\hbar\delta(x - x').} \tag{1.25}$$

Operator-valued functions like $\hat{\phi}$ and $\hat{\pi}$ are generally referred to as **quantum fields**. For clarity, the relevant relations between canonically conjugate classical and quantum fields are summarized in Table 1.2.

INFO By introducing quantum fields, we have departed from the conceptual framework laid out on page 6: being operator-valued, the quantized field no longer represents a mapping into an

[12] Note that the dimensionality of both the quantum and the classical continuum field is compatible with the dimensionality of the Dirac δ-function, $[\delta(x - x')] = [\text{length}]^{-1}$, i.e. $[\phi(x)] = [\phi_I] \cdot [\text{length}]^{-1/2}$ and similarly for π.

Table 1.2 *Relations between discrete and continuum canonically conjugate variables/operators.*

	Classical	Quantum
Discrete	$\{P_I, R_{I'}\} = -\delta_{II'}$	$[\hat{P}_I, \hat{R}_{I'}] = -i\hbar\delta_{II'}$
Continuum	$\{\pi(x), \phi(x')\} = -\delta(x - x')$	$[\hat{\pi}(x), \hat{\phi}(x')] = -i\hbar\delta(x - x')$

ordinary differentiable manifold.[13] It is thus legitimate to ask why we bothered to give a lengthy exposition of fields as "ordinary" functions. The reason is that, in the not too distant future, after the framework of functional field integration has been introduced, we will return to the comfortable ground of the definition of page 6.

Employing these definitions, the classical Hamiltonian density (1.10) becomes the quantum operator

$$\hat{\mathcal{H}}(\hat{\phi}, \hat{\pi}) = \frac{1}{2m}\hat{\pi}^2 + \frac{k_{\rm s}a^2}{2}(\partial_x\hat{\phi})^2. \tag{1.26}$$

The Hamiltonian above represents a quantum field theoretical *formulation* of the problem but not yet a solution. In fact, the development of a spectrum of methods for the analysis of quantum field theoretical models will represent a major part of this text. At this point the objective is merely to exemplify the way physical information can be extracted from models like Eq. (1.26). As a word of caution, let us mention that the following manipulations, while mathematically straightforward, are conceptually deep. To disentangle different aspects of the problem, we will first concentrate on plain operational aspects. Later, in Section 1.4, we will reflect on "what has really happened."

As with any function, operator-valued functions can be represented in a variety of different ways. In particular, they can be subjected to Fourier transformation,

$$\begin{Bmatrix} \hat{\phi}_k \\ \hat{\pi}_k \end{Bmatrix} \equiv \frac{1}{L^{1/2}} \int_0^L dx\, e^{\{\ ikx} \begin{Bmatrix} \hat{\phi}(x) \\ \hat{\pi}(x) \end{Bmatrix}, \quad \begin{Bmatrix} \hat{\phi}(x) \\ \hat{\pi}(x) \end{Bmatrix} = \frac{1}{L^{1/2}} \sum_k e^{\{\pm ikx} \begin{Bmatrix} \hat{\phi}_k \\ \hat{\pi}_k \end{Bmatrix}, \tag{1.27}$$

where $\sum_k$ represents the sum over all Fourier coefficients indexed by quantized momenta $k = 2\pi m/L$, $m \in \mathbb{Z}$ (not to be confused with the "operator momentum" $\hat{\pi}$!). Note that the *real* classical field $\phi(x)$ quantizes to a *Hermitian* quantum field $\hat{\phi}(x)$, implying that $\hat{\phi}_k = \hat{\phi}^\dagger_{-k}$ (and similarly for $\hat{\pi}_k$). The corresponding Fourier representation of the canonical commutation relations reads (exercise)

$$[\hat{\pi}_k, \hat{\phi}_{k'}] = -i\hbar\delta_{kk'}. \tag{1.28}$$

[13] At least if we ignore the mathematical subtlety that a linear operator can also be interpreted as an element of a certain manifold.

When expressed in the Fourier representation, making use of the identity

$$\int dx\,(\partial_x\hat{\phi})^2 = \sum_{k,k'}(-ik\hat{\phi}_k)(-ik'\hat{\phi}_{k'})\overbrace{\frac{1}{L}\int dx\,e^{-i(k+k')x}}^{\delta_{k+k',0}} = \sum_k k^2\hat{\phi}_k\hat{\phi}_{-k} = \sum_k k^2|\hat{\phi}_k|^2$$

together with a similar relation for $\int \mathrm{d}x\ \hat{\pi}^2$, the Hamiltonian $\hat{H} = \int \mathrm{d}x\ \mathcal{H}(\hat{\phi},\hat{\pi})$ assumes the near diagonal form

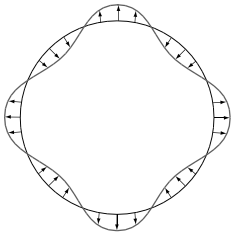

$$\hat{H} = \sum_k \left[\frac{1}{2m}\hat{\pi}_k\hat{\pi}_{-k} + \frac{m\omega_k^2}{2}\hat{\phi}_k\hat{\phi}_{-k}\right], \tag{1.29}$$

where $\omega_k = v|k|$ and $v = a\sqrt{k_\mathrm{s}/m}$ denotes the classical sound wave velocity. In this form, the Hamiltonian can be identified as nothing but a superposition of independent **harmonic oscillators**.[14] This result is actually not difficult to understand (see figure): Classically, the system supports a discrete set of wave excitations, each indexed by a wave number $k = 2\pi m/L$. (In fact, we could have performed a Fourier transformation of the classical fields $\phi(x)$ and $\pi(x)$ to represent the Hamiltonian function as a superposition of classical harmonic oscillators.) Within the quantum picture, each of these excitations is described by an oscillator Hamiltonian operator with a k-dependent frequency. However, it is important not to confuse the atomic constituents, also oscillators (albeit coupled), with the independent *collective* oscillator modes described by $\hat{H}$.

The description above, albeit perfectly valid, still suffers from a deficiency: our analysis amounts to explicitly describing the effective low-energy excitations of the system (the waves) in terms of their microscopic constituents (the atoms). Indeed the different contributions to $\hat{H}$ keep track of details of the microscopic oscillator dynamics of individual k-modes. However, it would be much more desirable to develop a picture where the relevant excitations of the system, the waves, appear as fundamental units, without explicit account of underlying microscopic details. (As with hydrodynamics, information is encoded in terms of collective density variables rather than through individual molecules.) As preparation for the construction of this improved formulation of the system, let us temporarily focus on a single oscillator mode.

Revision of the quantum harmonic oscillator

Consider a standard harmonic oscillator (HO) Hamiltonian

$$\hat{H} = \frac{\hat{p}^2}{2m} + \frac{m\omega^2}{2}\hat{x}^2.$$

[14] The only difference between Eq. (1.29) and the canonical form of an oscillator Hamiltonian $\hat{H} = \hat{p}^2/(2m) + m\omega^2\hat{x}^2/2$ is the presence of the sub-indices k and $-k$ (a consequence of $\hat{\phi}_k^\dagger = \hat{\phi}_{-k}$). As we will show shortly, this difference is inessential.

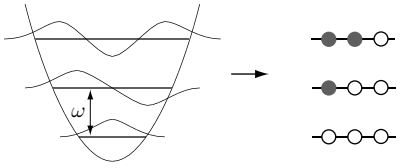

Figure 1.6 Low-lying energy levels/states of the harmonic oscillator.

The first few energy levels $\epsilon_n = \omega\left(n + \frac{1}{2}\right)$ and the associated Hermite polynomial eigenfunctions are displayed schematically in Fig. 1.6. (To simplify the notation we henceforth set $\hbar = 1$.)

The HO has, of course, the status of a single-particle problem. However, the equidistance of its energy levels suggests an alternative interpretation. One can think of a given energy state ϵ_n as an accumulation of n elementary entities, or **quasi-particles**, each having energy ω. What can be said about the features of these new objects? First, they are structureless, i.e. the only "quantum number" identifying the quasi-particles is their energy ω (otherwise n-particle states formed of the quasi-particles would not be equidistant). This implies that the quasi-particles must be *bosons*. (The same state ω can be occupied by more than one particle, see Fig. 1.6.)

This idea can be formulated in quantitative terms by employing the formalism of ladder operators in which the operators $\hat{p}$ and $\hat{x}$ are traded for the pair of Hermitian adjoint operators $\hat{a} \equiv \sqrt{\frac{m\omega}{2}}(\hat{x} + \frac{i}{m\omega}\hat{p})$, $\hat{a}^\dagger \equiv \sqrt{\frac{m\omega}{2}}(\hat{x} - \frac{i}{m\omega}\hat{p})$. Up to a factor of i, the transformation $(\hat{x}, \hat{p}) \to (\hat{a}, \hat{a}^\dagger)$ is canonical, i.e. the new operators obey the canonical commutation relation

$$[\hat{a}, \hat{a}^\dagger] = 1. \tag{1.30}$$

More importantly, the a-representation of the Hamiltonian is very simple, namely

$$\hat{H} = \omega\left(\hat{a}^\dagger\hat{a} + \frac{1}{2}\right), \tag{1.31}$$

as can be checked by direct substitution. Suppose, now, we had been given a zero eigenvalue state $|0\rangle$ of the operator $\hat{a}$: $\hat{a}|0\rangle = 0$. As a direct consequence, $\hat{H}|0\rangle = (\omega/2)|0\rangle$, i.e. $|0\rangle$ is identified as the ground state of the oscillator.[15] The complete hierarchy of higher energy states can now be generated by setting $|n\rangle \equiv (n!)^{-1/2}\,(\hat{a}^\dagger)^n|0\rangle$.

EXERCISE Using the canonical commutation relation, verify that $\hat{H}|n\rangle = \omega(n + 1/2)|n\rangle$ and $\langle n|n\rangle = 1$.

Formally, the construction above represents yet another way of constructing eigenstates of the quantum HO. However, its "real" advantage is that it naturally affords a many-particle interpretation. To this end, let us *declare* $|0\rangle$ to represent a "vacuum" state, i.e. a state with zero particles present. Next, imagine that $\hat{a}^\dagger|0\rangle$ is a state with a single featureless particle

[15] This can be verified by explicit construction. Switching to a real-space representation, the solution of the equation $[x + \partial_x/(m\omega)]\langle x|0\rangle = 0$ obtains the familiar ground state wavefunction $\langle x|0\rangle = \sqrt{m\omega/2\pi}e^{-m\omega x^2/2}$.

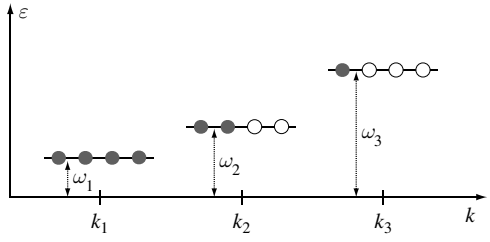

Figure 1.7 Diagram visualizing an excited state of the chain. Here, the number of quasi-particles decreases with increasing energy ω_k.

(the operator $\hat{a}^\dagger$ does not carry any quantum number labels) of energy ω. Similarly, $(\hat{a}^\dagger)^n|0\rangle$ is considered as a many-body state with n particles, i.e. within the new picture, $\hat{a}^\dagger$ is an operator that creates particles. The total energy of these states is given by $\omega \times$ (occupation number). Indeed, it is straightforward to verify (see exercise above) that $\hat{a}^\dagger\hat{a}|n\rangle = n|n\rangle$, i.e. the Hamiltonian basically counts the number of particles. While, at first sight, this may look unfamiliar, the new interpretation is internally consistent. Moreover, it achieves what we had asked for above, i.e. it allows an interpretation of the HO states as a superposition of independent structureless entities.

INFO The representation above illustrates the capacity to think about individual quantum problems in **complementary pictures**. This principle finds innumerable applications in modern condensed matter physics. The existence of different interpretations of a given system is by no means heretical but, rather, reflects a principle of quantum mechanics: there is no "absolute" system that underpins the phenomenology. The only thing that matters is observable phenomena. For example, we will see later that the "fictitious" quasi-particle states of oscillator systems *behave* as "real" particles, i.e. they have dynamics, can interact, be detected experimentally, etc. From a quantum point of view these object are, then, real particles.

Quasi-particle interpretation of the quantum chain

Returning to the oscillator chain, one can transform the Hamiltonian (1.29) to a form analogous to (1.31) by defining the ladder operators[16]

$$\hat{a}_k \equiv \sqrt{\frac{m\omega_k}{2}}\left(\hat{\phi}_k + \frac{i}{m\omega_k}\hat{\pi}_{-k}\right), \quad \hat{a}_k^\dagger \equiv \sqrt{\frac{m\omega_k}{2}}\left(\hat{\phi}_{-k} - \frac{i}{m\omega_k}\hat{\pi}_k\right). \tag{1.32}$$

With this definition, applying the commutation relations Eq, (1.28), one finds that the ladder operators obey commutation relations generalizing Eq. (1.30):

$$\left[\hat{a}_k, \hat{a}_{k'}^\dagger\right] = \delta_{kk'}, \quad [\hat{a}_k, \hat{a}_{k'}] = \left[\hat{a}_k^\dagger, \hat{a}_{k'}^\dagger\right] = 0. \tag{1.33}$$

[16] As to the consistency of these definitions, recall that $\hat{\phi}_k^\dagger = \hat{\phi}_{-k}$ and $\hat{\pi}_k^\dagger = \hat{\pi}_{-k}$. Under these conditions the second of the definitions following in the text follows from the first upon taking the Hermitian adjoint.

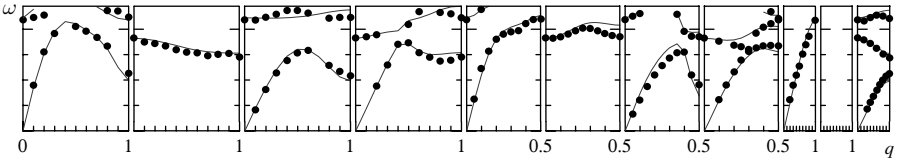

Figure 1.8 Phonon spectra of the transition metal oxide Sr_2RuO_4 measured along different axes in momentum space. Notice the approximate linearity of the low-energy branches (acoustic phonons) at small momenta. Superimposed at high frequencies are various branches of optical phonons. (Source: Courtesy of M. Braden, II. Physikalisches Institut, Universität zu Köln.)

Expressing the operators $(\hat{\phi}_k, \hat{\pi}_k)$ in terms of $(\hat{a}_k, \hat{a}_k^\dagger)$, it is now straightforward to bring the Hamiltonian into the quasi-particle oscillator form (exercise)

$$\hat{H} = \sum_k \omega_k \left(\hat{a}_k^\dagger \hat{a}_k + \frac{1}{2} \right). \tag{1.34}$$

Equations (1.34) and (1.33) represent the final result of our analysis. The Hamiltonian $\hat{H}$ takes the form of a sum of harmonic oscillators with characteristic frequencies ω_k. In the limit $k \to 0$ (i.e. long wavelength), one finds $\omega_k \to 0$; excitations with this property are said to be **massless**.

An excited state of the system is indexed by a set $\{n_k\} = (n_1, n_2, \dots)$ of quasi-particles with energy $\{\omega_k\}$ (see Fig. 1.7). Physically, the quasi-particles of the harmonic chain are identified with the **phonon modes** of the solid. A comparison with measured phonon spectra (Fig. 1.8) reveals that, at low momenta, $\omega_k \sim |k|$ in agreement with our simplistic model (even in spite of the fact that the spectrum was recorded for a three-dimensional solid with non-trivial unit cell – universality!). While the linear dispersion was already a feature of the classical sound wave spectrum, the low-temperature specific heat reflected non-classical behavior. It is left as an exercise (problem 1.8) to verify that the quantum nature of the phonons resolves the problem with the low-temperature specific heat discussed in Section 1.1. (For further discussion of phonon modes in atomic lattices we refer to Chapter 2 of the text by Kittel.[17])

1.5 Quantum electrodynamics

The generality of the procedure outlined above suggests that the quantization of the EM field Eq. (1.24) proceeds in a manner analogous to the phonon system. However, there are a number of practical differences that make quantization of the EM field a harder (but also more interesting!) enterprise. Firstly, the vectorial character of the vector potential, in combination with the condition of relativistic covariance, gives the problem a non-trivial internal geometry. Closely related, the gauge freedom of the vector potential introduces redundant degrees of freedom whose removal on the quantum level is not easily achieved. For

[17] C. Kittel, *Quantum Theory of Solids*, 2nd edition (Wiley, 1987).

example, quantization in a setting where only physical degrees of freedom are kept – i.e. the two polarization directions of the transverse photon field – is technically cumbersome, the reason being that the relevant gauge condition is not relativistically covariant. In contrast, a manifestly covariant scheme, while technically more convenient, introduces spurious "ghost degrees of freedom" that are difficult to remove. To circumvent a discussion of these issues, we will not discuss the problem of EM field quantization in full detail.[18] On the other hand, the photon field plays a much too important role in condensed matter physics for us to drop the problem altogether. We will therefore aim at an intermediate exposition, largely insensitive to the problems outlined above but sufficiently general to illustrate the main principles.

Field quantization

Consider the Lagrangian of the matter-free EM field, $L = -\frac{1}{4}\int d^3x\ F_{\mu\nu}F^{\mu\nu}$. As a first step towards quantization of this system we fix a gauge. In the absence of charge, a particularly convenient choice is the **Coulomb gauge**, $\nabla \cdot \mathbf{A} = 0$, with the scalar component $\phi = 0$. (Keep in mind that, once a gauge has been set, we cannot expect further results to display "gauge invariance.") Using the gauge conditions, one may verify that the Lagrangian assumes the form

$$L = \frac{1}{2}\int d^3x \left[(\partial_t \mathbf{A})^2 - (\nabla \times \mathbf{A})^2\right]. \tag{1.35}$$

By analogy with our discussion of the atomic chain, we would now proceed to "decouple" the theory by expanding the action in terms of eigenfunctions of the Laplace operator. The difference with our previous discussion is that we are dealing (i) with the full three-dimensional Laplacian (instead of a simple second derivative) acting on (ii) the vectorial quantity $\mathbf{A}$ that is (iii) subject to the constraint $\nabla \cdot \mathbf{A} = 0$. It is these aspects which lead to the complications outlined above.

We can circumvent these difficulties by considering cases where the geometry of the system reduces the complexity of the eigenvalue problem. This restriction is less artificial than it might appear. For example, in anisotropic electromagnetic waveguides, the solutions of the eigenvalue equation can be formulated as[19]

$$-\nabla^2 \mathbf{R}_k(\mathbf{x}) = \lambda_k \mathbf{R}_k(\mathbf{x}), \tag{1.36}$$

where $k \in \mathbb{R}$ is a *one-dimensional* index and the vector-valued functions $\mathbf{R}_k$ are real and orthonormalized, $\int \mathbf{R}_k \cdot \mathbf{R}_{k'} = \delta_{kk'}$. The dependence of the eigenvalues λ_k on k depends on details of the geometry (see Eq. (1.38) below) and need not be specified for the moment.

INFO An **electrodynamic waveguide** is a quasi-one-dimensional cavity with metallic boundaries (see Fig. 1.9). The practical advantage of waveguides is that they are good at confining EM

[18] Readers interested in learning more about EM field quantization are referred to, e.g., L. H. Ryder, *Quantum Field Theory* (Cambridge University Press, 1996).

[19] More precisely, one should say that Eq. (1.36) defines the set of eigenfunctions relevant for the low-energy dynamics of the waveguide. More-complex eigenfunctions of the Laplace operator exist but they carry much higher energy.

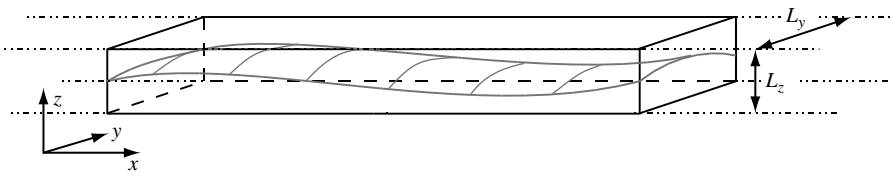

Figure 1.9 EM waveguide with rectangular cross-section. The structure of the eigenmodes of the EM field is determined by boundary conditions at the walls of the cavity.

waves. At large frequencies, where the wavelengths are of order meters or less, radiation loss in conventional conductors is high. In these frequency domains, hollow conductors provide the only practical way of transmitting radiation.

EM field propagation inside a waveguide is constrained by boundary conditions. Assuming the walls of the system to be perfectly conducting,

$$\mathbf{E}_{\parallel}(\mathbf{x}_{\rm b}) = 0, \qquad \mathbf{B}_{\perp}(\mathbf{x}_{\rm b}) = 0, \tag{1.37}$$

where $\mathbf{x}_{\rm b}$ is a point at the system boundary and $\mathbf{E}_{\parallel}$ ($\mathbf{B}_{\perp}$) is the parallel (perpendicular) component of the electric (magnetic) field.

For concreteness, returning to the problem of field quantization, let us consider a cavity with uniform rectangular cross-section $L_y \times L_z$. To conveniently represent the Lagrangian of the system, we wish to express the vector potential in terms of eigenfunctions $\mathbf{R}_{\mathbf{k}}$ that are consistent with the boundary conditions (1.37). A complete set of functions fulfilling this condition is given by

$$\mathbf{R}_{\mathbf{k}} = \mathcal{N}_k \begin{pmatrix} c_1 \cos(k_x x)\sin(k_y y)\sin(k_z z) \\ c_2 \sin(k_x x)\cos(k_y y)\sin(k_z z) \\ c_3 \sin(k_x x)\sin(k_y y)\cos(k_z z) \end{pmatrix}.$$

Here, $k_i = n_i \pi / L_i$, $n_i \in \mathbb{N}$, $i = x, y, z$, $\mathcal{N}_k$ is a factor normalizing $\mathbf{R}_{\mathbf{k}}$ to unit modulus, and the coefficients c_i are subject to the condition $c_1 k_x + c_2 k_y + c_3 k_z = 0$. Indeed, it is straightforward to verify that a general superposition of the type $\mathbf{A}(\mathbf{x}, t) \equiv \sum_{\mathbf{k}} \alpha_{\mathbf{k}}(t) \mathbf{R}_{\mathbf{k}}(\mathbf{x})$, $\alpha_{\mathbf{k}}(t) \in \mathbb{R}$, is divergenceless, and generates an EM field compatible with (1.37). Substitution of $\mathbf{R}_{\mathbf{k}}$ into Eq. (1.36) identifies the eigenvalues as $\lambda_{\mathbf{k}} = k_x^2 + k_y^2 + k_z^2$. In the physics and electronic engineering literature, eigenfunctions of the Laplace operator in a quasi-one-dimensional geometry are commonly described as **modes**. As we will see shortly, the energy of a mode (i.e. the Hamiltonian evaluated on a specific mode configuration) grows with $|\lambda_{\mathbf{k}}|$. In cases where one is interested in the low-energy dynamics of the EM field, only configurations with small $|\lambda_{\mathbf{k}}|$ are relevant. For example, let us consider a massively anisotropic waveguide with $L_z < L_y \ll L_x$. In this case the modes with smallest $|\lambda_k|$ are those with $k_z = 0$, $k_y = \pi / L_y$, and $k_x \equiv k \ll L_{z,y}^{-1}$. (Why is it not possible to set both k_y and k_z to zero?) With this choice,

$$\lambda_k = k^2 + \left(\frac{\pi}{L_y}\right)^2, \tag{1.38}$$

and a scalar index k suffices to label both eigenvalues and eigenfunctions $\mathbf{R}_k$. A caricature of the spatial structure of the functions $\mathbf{R}_k$ is shown in Fig. 1.9. The dynamical properties of these configurations will be discussed in the text.

Returning to the problem posed by Eq. (1.35) and (1.36), one can expand the vector potential in terms of eigenfunctions $\mathbf{R}_k$ as $\mathbf{A}(\mathbf{x},t) = \sum_k \alpha_k(t)\mathbf{R}_k(\mathbf{x})$, where the sum runs over all allowed values of the index parameter k. (In a waveguide, $k = \pi n/L$, $n \in \mathbb{N}$, where L is the length of the guide.) Substituting this expansion into Eq. (1.35) and using the normalization properties of $\mathbf{R}_k$, we obtain $L = \frac{1}{2}\sum_k \left(\dot{\alpha}_k^2 - \lambda_k \alpha_k^2\right)$, i.e. a decoupled representation where the system is described in terms of independent dynamical systems with coordinates α_k. From this point on, quantization proceeds along the lines of the standard algorithm. Firstly, define momenta through the relation $\pi_k = \partial_{\dot{\alpha}_k} L = \dot{\alpha}_k$. This produces the Hamiltonian $H = \frac{1}{2}\sum_k (\pi_k \pi_k + \lambda_k \alpha_k \alpha_k)$. Next quantize the theory by promoting fields to operators $\alpha_k \to \hat{\alpha}_k$ and $\pi_k \to \hat{\pi}_k$, and declaring $[\hat{\pi}_k, \hat{\alpha}_{k'}] = -i\delta_{kk'}$. The quantum Hamiltonian operator, again of harmonic oscillator type, then reads

$$\hat{H} = \frac{1}{2}\sum_k \left(\hat{\pi}_k \hat{\pi}_k + \omega_k^2 \hat{\alpha}_k \hat{\alpha}_k\right),$$

where $\omega_k^2 = \lambda_k$. Following the same logic as marshaled in Section 1.4, we then define ladder operators $a_k \equiv \sqrt{\frac{\omega_k}{2}}(\hat{\alpha}_k + \frac{i}{\omega_k}\hat{\pi}_k)$, $a_k^\dagger \equiv \sqrt{\frac{\omega_k}{2}}(\hat{\alpha}_k - \frac{i}{\omega_k}\hat{\pi}_k)$, whereupon the Hamiltonian assumes the now familiar form

$$\hat{H} = \sum_k \omega_k \left(a_k^\dagger a_k + \frac{1}{2}\right). \tag{1.39}$$

For the specific problem of the first excited mode in a waveguide of width L_y, $\omega_k = \left[k^2 + (\pi/L_y)^2\right]^{1/2}$. Equation (1.39) represents our final result for the quantum Hamiltonian of the EM waveguide. Before concluding this section let us make a few comments on the structure of the result:

- ▷ Firstly, notice that the construction above almost completely paralleled our previous discussion of the harmonic chain.[20] The structural similarity between the two systems finds its origin in the fact that the free field Lagrangian (1.35) is quadratic and, therefore, bound to map onto an oscillator-type Hamiltonian. That we obtained a simple *one-dimensional* superposition of oscillators is due to the boundary conditions specific to a narrow waveguide. For less restrictive geometries, e.g. free space, a more complex superposition of vectorial degrees of freedom in three-dimensional space would have been obtained. However, the principal mapping of the free EM field onto a superposition of oscillators is independent of geometry.
- ▷ Physically, the quantum excitations described by Eq. (1.39) are, of course, the **photons** of the EM field. The unfamiliar appearance of the dispersion relation ω_k is again a peculiarity of the waveguide. However, in the limit of large longitudinal wave numbers $k \gg L_y^{-1}$, the dispersion approaches $\omega_k \sim |k|$, i.e. the relativistic dispersion of the photon field. Also notice that, due to the equality of the Hamiltonians (1.34) and (1.39), all that has been said about the behavior of the phonon modes of the atomic chain carries over to the photon modes of the waveguide.

[20] Technically, the only difference is that instead of index pairs $(k, -k)$ all indices (k, k) are equal and positive. This can be traced back to the fact that we have expanded in terms of the real eigenfunctions of the closed waveguide instead of the complex eigenfunctions of the circular oscillator chain.

▷ As with their phononic analogue, the oscillators described by Eq. (1.39) exhibit zero-point fluctuations. It is a fascinating aspect of quantum electrodynamics that these oscillations, caused by quantization of *the* most relativistic field, surface at various points of non-relativistic physics. In the section below two prominent manifestations of zero-point fluctuations in condensed matter physics will be briefly discussed.

Vacuum fluctuations in matter

The quantum oscillation of the electromagnetic field manifests itself in a multitude of physical phenomena. In the following, we shall briefly discuss some of the more prominent effects caused by the dynamics of the **quantum vacuum**.

One of the most important phenomena induced by vacuum fluctuations is the **Casimir effect**:[21] two parallel conducting plates embedded into the vacuum exert an attractive force on each other. This phenomenon is not only of conceptual importance – better than anything else it demonstrates that the vacuum is "alive" – but also of applied relevance. For example, the force balance of hydrophobic suspensions of particles of size 0.1–1 μm in electrolytes is believed to be strongly influenced by Casimir forces. At least it is applications in colloidal chemistry which prompted Casimir to his famous analysis of the idealized vacuum problem. Qualitatively, the origin of the Casimir force is readily understood. Like their classical analog, quantum photons exert a certain radiation pressure on macroscopic media. The difference with the classical case is that, due to zero-point oscillations, even the quantum vacuum is capable of creating radiation pressure. For a single conducting body embedded into the infinite vacuum, the net pressure vanishes by symmetry. However, for two parallel plates, the situation is different. Mode quantization arguments similar to the ones used in the previous section show that the density of quantum modes between the plates is lower than in the semi-infinite outer spaces. Hence, the force (density) created by outer space exceeds the counter-pressure from the inside; the plates "attract" each other. The unambiguous measurement of the Casimir force required advanced nano-technological instrumentation and has succeeded only recently.[22]

A second important phenomenon where vacuum fluctuations play a role is **van der Waals forces**: atoms or molecules attract each other by a potential that, at small separation r, scales as r^{-6}. Early attempts to explain classically the phenomenon produced results for the force that, in conflict with experimental findings, were strongly temperature dependent. It was considered a major breakthrough of the new quantum mechanics when London proposed a model whereby a temperature-independent r^{-6} law was obtained. The essence of London's

[21] H. B. G. Casimir and D. Polder, The influence of retardation on the London–van der Waals forces, *Phys. Rev.* **73**, 360–72 (1948); H. B. G. Casimir, On the attraction between two perfectly conducting plates, *Proc. Kon. Nederland. Akad. Wetensch.* **51**, 793–6 (1948).

[22] S. K. Lamoreaux, Demonstration of the Casimir force in the 0.6 to 6 m Range, *Phys. Rev. Lett.* **78**, 5–9 (1997); G. Bressi *et al.*, Measurement of the Casimir force between parallel metallic surfaces, *Phys. Rev. Lett.* **88**, 41804–9 (2002). For a review on recent developments see M. Bordag *et al.*, New developments in the Casimir effect, *Phys. Rep.* **353**, 1–205 (2001).

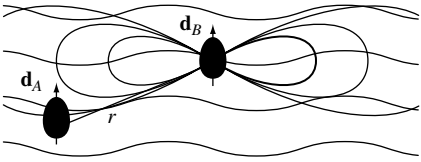

Figure 1.10 On the creation of van der Waals forces by EM vacuum fluctuations. An atom or molecule B is exposed to fluctuations of the EM quantum vacuum (depicted by wavy lines). This leads to the creation of a dipole element $\mathbf{d}_B$. A nearby partner atom A sees both the vacuum amplitude and the dipole field created by $\mathbf{d}_B$. The cooperation of the two field strengths leads to a net lowering of the energy of A.

idea is easily explained: imagine each of the atoms/molecules as an oscillator. The zero-point motion of these oscillators, measured in terms of some coordinate x, creates a dipole moment of strength $\sim x$. At close distances, the systems interact through a dipole–dipole interaction.[23] Writing down coupled oscillator equations (see Problem 1.8), one readily obtains a lowering of the ground state energy by a contribution $V(r) \sim r^{-6}$.

Johannes Diderik van der Waals
1837–1923

1910 Nobel Laureate in physics in recognition of his work on the state equation of non-ideal gases. Van der Waals was one of the first to postulate inter-molecular forces, at a time when the existence of atoms and molecules was still disputed. Other important work includes the derivation of first variants of thermodynamic scaling relations.

However, there is a subtle point about the seemingly innocuous coupling of the *quantum* oscillator to the *classical* Coulomb potential. Close inspection (see Milonni's text for details[24]) shows that, to maintain the quantum commutation relations of the oscillator degrees of freedom, the EM field must not be assumed entirely classical. In fact, once the quantum nature of the EM field has entered the stage, it becomes possible to explain the force without need for phenomenological introduction of atomic oscillator degrees of freedom.

Consider an atom A exposed to an electric field $\mathbf{E}$ (see Fig. 1.10). The field gives rise to the atomic **Stark** effect, i.e. a level shift of order $W \sim \alpha \langle \mathbf{E}^2(\mathbf{x}_A) \rangle$, where α is the atomic polarizability, $\mathbf{E} = \partial_t \mathbf{A}$ is the *operator* representing the EM field, and $\langle \ldots \rangle$ a quantum expectation value. For an atom in empty space, $\mathbf{E}(\mathbf{x}_A) \equiv \mathbf{E}_0(\mathbf{x}_A)$ is an operator measuring the vacuum fluctuations of the free field. However, in the neighborhood of a second atom B, an induced dipole contribution adds to $\mathbf{E}_0$. The point is that the zero-point amplitude $\mathbf{E}_0$ induces a dipole element $\mathbf{d}_B \propto \alpha \mathbf{E}_0(\mathbf{x}_B)$ which, in turn, creates a dipole field $\mathbf{E}_B$

[23] In passing, we mention that various animal species benefit from the short-distance efficiency of the van der Waals force. For instance, **geckos** and **spiders** owe their ability to climb up planar surfaces of basically any material to the presence of bushels of ultra-fine hair (about three orders of magnitude thinner than human hair) on their feet. The tips of these hairs come close enough to the atoms of the substrate material to make the van der Waals force sizeable. Impressively, this mechanism provides a force of about two orders of magnitude larger than that required to support a spider's full body weight. Both spiders and geckos have to "roll" their feet off the surface to prevent getting stuck by the enormous power of the forces acting on their many body hairs!

[24] P. W. Milonni, *The Quantum Vacuum* (Academic Press, 1994).

contributing to the total field amplitude felt by atom A: $\mathbf{E}(\mathbf{x}_A) = (\mathbf{E}_0 + \mathbf{E}_B)(\mathbf{x}_A)$ (see Fig. 1.10). The dominant contribution to the level shift due to the proximity of B is then given by

$$V = W - \alpha\langle \mathbf{E}_0^2(\mathbf{x}_A)\rangle \sim \alpha\langle \mathbf{E}_0(\mathbf{x}_A)\cdot\mathbf{E}_B(\mathbf{x}_A)\rangle \sim \alpha^2\langle \mathbf{E}_0^T(\mathbf{x}_A)K(\mathbf{x}_A-\mathbf{x}_B)\mathbf{E}(\mathbf{x}_B)\rangle, \quad (1.40)$$

where K is a matrix kernel describing the geometric details of the dipole interaction. (Here, we have subtracted the vacuum level shift because it represents an undetectable offset.) Notice that Eq. (1.40) predicts the van der Waals interaction to be proportional to the square of the zero-point field amplitude.

Unfortunately, the quantitative evaluation of the matrix element, involving a geometric average over all polarization directions of the quantum field amplitude, is somewhat involved. As a final result of a calculation[25] one obtains

$$V(\mathbf{r}) = -\frac{3\omega_0\alpha^2}{4r^6}, \quad (1.41)$$

Johannes Stark 1874–1957

Nobel laureate 1919 for his discovery of the Stark effect in 1913. Later, Stark became infamous for the role he played during the third Reich. He attacked theoretical physics as "Jewish" and stressed that scientific positions in Nazi Germany should only be held by pure-blooded Germans. Image ©The Nobel Foundation

where $r = |\mathbf{x}_A - \mathbf{x}_B|$ is the distance between the atoms and ω_0 is the transition frequency between the ground state and the first excited state of the atom. (This parameter enters the result through the dependence of the microscopic polarizability on the transition frequencies.)

1.6 Noether's theorem

According to a basic paradigm of physics every continuous symmetry of a system entails a conservation law.[26] Conservation laws, in turn, greatly simplify the solution of any problem which is why one gets acquainted with the correspondence (symmetry $\leftrightarrow$ conservation law) at a very early stage of the physics curriculum, e.g. the connection between rotational symmetry and the conservation of angular momentum. However, it is not all that trivial to see (at least within the framework of Newtonian mechanics) that the former entails the latter. One needs to know what to look for (angular momentum) to identify the conserved quantity corresponding to rotational invariance. It is one of the major advantages of Lagrangian over Newtonian mechanics that it provides one with a tool – Noether's theorem – to automatically identify the conservation laws generated by the symmetries of classical mechanics.

[25] Detailed, e.g., in Milonni, *The Quantum Vacuum*, Section 3.11.

[26] Before exploring the ramifications of symmetries and conservation laws for fields, it may be instructive to recapitulate Noether's theorem in the context of classical point-particle mechanics – see, e.g., L. D. Landau and E. M. Lifshitz, *Classical Mechanics* (Pergamon, 1960).

Amalie E. Noether 1882–1935

German mathematician known for her groundbreaking contributions to abstract algebra and theoretical physics. Alive at a time when women were not supposed to attend college preparatory schools, she was often forbidden from lecturing under her own name. Despite these obstacles, Noether became one of the greatest algebraists of the century. Described by Albert Einstein as the most significant creative mathematical genius thus far produced since the higher education of women began, she revolutionized the theories of rings, fields, and algebras. In physics, Noether's theorem explains the fundamental connection between symmetry and conservation laws. In 1933, she lost her teaching position due to being a Jew and a woman, and was forced out of Germany by the Nazis.

What happens when one advances from point to continuum mechanics?[27] Clearly, multidimensional continuum theories leave more room for the emergence of complex symmetries; even more so than in classical mechanics, we are in need of a tool identifying the corresponding conservation laws. Fortunately, it turns out that Noether's theorem of point mechanics affords a more or less straightforward generalization to higher dimensions. Starting from the general form of the action of a continuum system, Eq. (1.16), the continuum version of Noether's theorem will be derived below. In not referring to a specific physical problem, our discussion will be somewhat dry. This lack of physical context is, however, more than outweighed by the general applicability of the result: the generalized form of Noether's theorem can be – without much further thought – applied to generate the conservation laws of practically any physical symmetry. In this section, we will illustrate the application of the formalism on the simple (yet important) example of space–time translational invariance. A much more intriguing case study will be presented in Section 4.3 after some further background of quantum field theory has been introduced.

Symmetry transformations

The symmetries of a physical system manifest themselves in the invariance of its action under certain transformations. Mathematically, symmetry transformations are described by two pieces of input data: firstly, a mapping $M \to M$, $x \mapsto x'(x)$ that assigns to any point of the base manifold some "transformed" point; secondly, the field configurations themselves may undergo some change, i.e. there may be a mapping $(\phi : M \to T) \mapsto (\phi' : M \to T)$ that defines transformed values $\phi'(x') = F[\{\phi(x)\}]$ in terms of the "old" field. It is important to understand that these two operations may, in general, be independent of each other.

[27] Later on we shall see that all we are discussing here carries over to the quantum level.

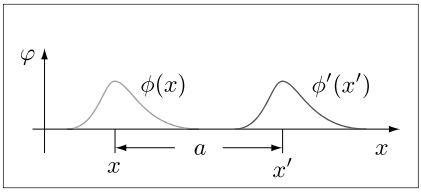

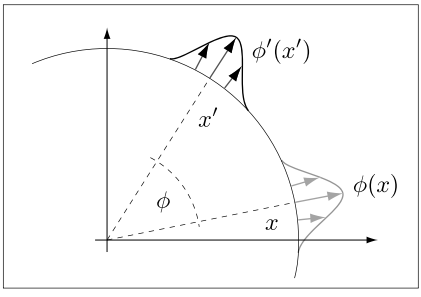

For example, suppose we want to explore the invariance properties of a theory under translations in space–time. In this case, we can consider a mapping $x' = x + a$, $a \in \mathbb{R}^m$, $\phi'(x') = \phi(x)$. This describes the translation of a field by a fixed offset a in space–time (see figure). The system is translationally invariant if and only if $S[\phi] = S[\phi']$. As a second example, let us probe rotational symmetry: $x' = Rx$, where $R \in \mathrm{O}(m)$ is a rotation of Euclidean space–time. In this case it would, in general, be unphysical to define $\phi'(x') = \phi(x)$. To illustrate this point, consider the example of a vector field in two dimensions $n = m = 2$ (see the figure.) A properly rotated field configuration is defined by $\phi'(x') = R\phi(x)$, i.e. the field amplitude actively participates in the operation. In fact, one often considers symmetry operations where only the fields are transformed while the base manifold is left untouched.[28] For example, the intrinsic[29] rotational invariance of a magnet is probed by $x' = x$, $m'(x) = R \cdot m(x)$, where the vector field m describes the local magnetization.

To understand the impact of a symmetry transformation, it is fully sufficient to consider its infinitesimal version. (Any finite transformation can be generated by successive application of infinitesimal ones.) Consider, thus, the two mappings

$$\begin{aligned} x_\mu \to x'_\mu \quad &= x_\mu + \left.\frac{\partial x_\mu}{\partial \omega_a}\right|_{\omega=0} \omega_a(x), \\ \phi^i(x) \to \phi'^i(x') \quad &= \phi^i(x) + \omega_a(x) F^i_a[\phi], \end{aligned} \tag{1.42}$$

expressing the change of both fields and coordinates to linear order in a set of parameter functions $\{\omega_a\}$ characterizing the transformation. (For a three-dimensional rotation, $(\omega_1, \omega_2, \omega_3) = (\phi, \theta, \psi)$ would be the rotation angles, etc.) The functionals $\{F^i_a\}$ – which need not depend linearly on the field ϕ, and may explicitly depend on the coordinate x – *define* the incremental change $\phi'(x') - \phi(x)$.

We now ask how the action Eq. (1.16) changes under the transformation Eq. (1.42), i.e. we wish to compute the difference

$$\Delta S = \int d^m x' \; \mathcal{L}(\phi'^i(x'), \partial_{x'_\mu} \phi'^i(x')) - \int d^m x \; \mathcal{L}(\phi^i(x), \partial_{x_\mu} \phi^i(x)).$$

[28] For example, the standard symmetry transformations of classical mechanics, $q(t) \to q'(t)$, belong to this class: the coordinate vector of a point particle, q (a "field" in $0+1$ space–time dimensions) changes while the "base" (time t) does not transform.

[29] "Intrinsic" means that we rotate just the spins but not the entire magnet (as in our second example).

Inserting Eq. (1.42), using the fact that $\partial x'_\mu/\partial x_\nu = \delta_{\mu\nu} + (\partial/\partial x_\nu)\,(\omega_a \partial x_\mu/\partial\omega_a)$, together with[30] $\left|\partial x'_\mu/\partial x_\nu\right| \simeq 1 + (\partial/\partial x_\mu)\,(\omega_a \partial x_\mu/\partial\omega_a)$, one obtains

$$\begin{aligned}\Delta S \;\simeq\; & \int d^m x\,(1+\partial_{x_\mu}(\omega_a\partial_{\omega_a}x_\mu))\mathcal{L}(\phi^i + F^i_a\omega_a, (\delta_{\mu\nu} - \partial_{x_\mu}(\omega_a\partial_{\omega_a}x_\nu))\partial_{x_\nu}(\phi^i + F^i_a\omega_a)) \\ & - \int d^m x\,\mathcal{L}(\phi^i(x), \partial_{x_\mu}\phi^i(x)).\end{aligned}$$

So far, we did not use the fact that the transformation was actually meant to be a symmetry transformation. By definition, we are dealing with a symmetry if, for constant parameters ω_a – a uniform rotation, global translation, etc. – the action difference ΔS vanishes. In other words, the leading contribution to the action difference of a symmetry transformation must be linear in the derivatives $\partial_\mu\omega_a$. A straightforward expansion of the formula above for ΔS shows that these terms are given by

$$\Delta S \overset{\text{sym.}}{=} -\int d^m x\; j^a_\mu(x)\partial_\mu\omega_a,$$

where the so-called **Noether current** is given by

$$\boxed{j^a_\mu = \left(\frac{\partial\mathcal{L}}{\partial(\partial_\mu\phi^i)}\partial_\nu\phi^i - \mathcal{L}\delta_{\mu\nu}\right)\frac{\partial x_\nu}{\partial\omega_a}\bigg|_{\omega=0} - \frac{\partial\mathcal{L}}{\partial(\partial_\mu\phi^i)}F^i_a.} \tag{1.43}$$

For a completely general field configuration, there is not much can be said about the Noether current (whether or not the theory possesses the symmetry). However, if the field ϕ obeys the classical equations of motion *and* the theory is symmetric, the Noether current is locally conserved, $\partial_\mu j^a_\mu = 0$. This follows from the fact that, for a solution ϕ of the Euler–Lagrange equations, the linear variation of the action in any parameter must vanish. Specifically, the vanishing of $\Delta S[\phi]$ for arbitrary symmetry transformations $\{\omega_a\}$ enforces the condition $\partial_\mu j^a_\mu = 0$. (But keep in mind the fact that the conservation law holds only on the classical level!) Therefore, in summary, we have Noether's theorem:

A continuous symmetry entails a classically conserved current.

The local conservation of the current entails the existence of a globally conserved "charge." For example, for a base manifold $x = (x_0, x_1, \ldots, x_d)$ in Euclidean $(1+d)$-dimensional space–time, integration over the space–like directions, and application of Stokes' theorem, gives $\partial_0 Q^a = 0$, where[31]

$$Q^a \equiv \int d^d x\; j^a_0, \tag{1.44}$$

is the **conserved charge** and we have assumed that the current density vanishes at spatial infinity.

[30] This follows from $\frac{x'_\mu}{x_\nu} = \det\frac{x'_\mu}{x_\nu} = \exp\mathrm{tr}\,\ln\frac{x'_\mu}{x_\nu} \simeq \exp\left(\frac{}{x_\mu}\left(\omega_a\frac{x_\mu}{\omega_a}\right)\right) \simeq 1 + \frac{}{x_\mu}\left(\omega_a\frac{x_\mu}{\omega_a}\right)$.
(Exercise: Show that $\det A = \exp\mathrm{tr}\,\ln A$, where A is a linear operator. Hint: Use the eigenbasis.)

[31] Notice that the integral involved in the definition of Q runs only over spatial coordinates.

Notice that nowhere in the discussion above have we made assumptions about the internal structure of the Lagrangian. In particular, all results apply equally to the Minkowskian and the Euclidean formulation of the theory.

Example: translational invariance

As an example that is as elementary as it is important, we consider the case of space–time translational invariance. The corresponding symmetry transformation is defined by $x'_\mu = x_\mu + a_\mu$, $\phi'(x') = \phi(x)$. The infinitesimal version of this transformation reads as $x'_\mu = x_\mu + \omega_\mu$ where we have identified the parameter index a with the space–time index μ. Noether's current, which in the case of translational invariance is called the **energy–momentum tensor**, is given by T^ν_μ:

$$T^\nu_\mu(x) = \frac{\partial \mathcal{L}}{\partial(\partial_\mu \phi^i)} \partial_\nu \phi^i - \delta_{\mu\nu} \mathcal{L}.$$

The conserved "charges" corresponding to this quantity are

$$P^\nu \equiv \int d^d x \left(\frac{\partial \mathcal{L}}{\partial(\partial_0 \phi^i)} \partial_\nu \phi^i - \delta_{\nu 0} \mathcal{L} \right).$$

Specifically, P^0 is the energy and $P^l, l = 1, \ldots, d$ the total momentum carried by the system.

EXERCISE Consider the one-dimensional elastic chain discussed in Section 1.1. Convince yourself that the continuity equation of the system assumes the form $\partial_t \int_{x_1}^{x_2} dx \rho(x,t) = \partial_t(\phi(x_2,t) - \phi(x_1,t))$, where $\rho(x,t)$ is the local density of the medium. Use this result to show that $\rho = \partial_x \phi$. Show that the momentum $\int dx$ (particle density) $\times$ (velocity) $= \int dx \rho \partial_t \phi$ carried by the system coincides with the Noether momentum.

EXERCISE Compute the energy-momentum tensor for the Lagrangian of the free electromagnetic field. Derive the corresponding energy–momentum vector and convince yourself that you obtain results familiar from electrodynamics.

Admittedly, translational invariance is not a particularly exciting symmetry and, if this were the only example of relevance, the general discussion above would not have been worth the effort. However, later in the text, we shall exemplify (see, for example, Section 4.3) how concepts hinging on Noether's theorem can be applied to obtain far-reaching results that are not readily accessible by different means.

1.7 Summary and outlook

In this chapter we have introduced the general procedure whereby classical continuum theories are quantized. Employing the elementary harmonic oscillator as a example, we have seen that the Hilbert spaces of these theories afford different interpretations. Of particular use was a quasi-particle picture whereby the collective excitations of the continuum theories acquired the status of elementary particles.

Suspiciously, both examples discussed in this text, the harmonic quantum chain and free quantum electrodynamics, led to exactly solvable **free field theories**. However, it takes only little imagination to foresee that only few continuum theories will be as simple. Indeed, the exact solvability of the atomic chain would have been lost had we included higher-order contributions in the expansion in powers of the lattice displacement. Such terms would hinder the free wave-like propagation of the phonon modes. Put differently, phonons would begin to scatter off each other (i.e. interact). Similarly, the free status of electrodynamics is lost once the EM field is allowed to interact with a matter field. Needless to say, **interacting field theories** are infinitely more complex, but also more interesting, than the systems considered so far.

Technically, we have seen that the phonon/photon interpretation of the field theories discussed in this chapter could conveniently be formulated in terms of ladder operators. However, the applications discussed so far provide only a glimpse of the advantages of this language. In fact, the formalism of ladder operators, commonly described as "second quantization," represents a central, and historically the oldest, element of quantum field theory. The next chapter is devoted to a more comprehensive discussion of both the formal aspects and applications of this formulation.

1.8 Problems

Electrodynamics from a variational principle

Choosing the Lorentz-gauged components of the vector potential as generalized coordinates, the aim of this problem is to show how the wave equations of electrodynamics can be obtained as a variational principle.

Electrodynamics can be described by Maxwell's equations or, equivalently, by wave-like equations for the vector potential. Working in the **Lorentz gauge**, $\partial_t \phi = \nabla \cdot \mathbf{A}$, these equations read $\left(\partial_t^2 - \nabla^2\right)\phi = \rho, \left(\partial_t^2 - \nabla^2\right)\mathbf{A} = \mathbf{j}$. Using relativistically covariant notation, the form of the equations can be compressed further to $\partial_\mu \partial^\mu A^\nu = j^\nu$. Starting from the Lagrangian action, $S[A] = -\int d^4x \left(\frac{1}{4} F_{\mu\nu} F^{\mu\nu} + A_\mu j^\mu\right)$, obtain these equations by applying the variational principle. Compare the Lorentz gauge representation of the action of the field with the action of the elastic chain. What are the differences/parallels?

Answer:
Using the definition of the electromagnetic field tensor $F_{\mu\nu} = \partial_\mu A_\nu - \partial_\nu A_\mu$, and integrating by parts, the action assumes the form

$$S[A] = -\int d^4x \left(-\frac{1}{2} A_\nu \left[\partial_\mu \partial^\mu A^\nu - \partial_\mu \partial^\nu A^\mu\right] + j_\mu A^\mu\right).$$

Owing to the Lorentz gauge condition, the second contribution in the square brackets vanishes and we obtain $S[A] = -\int d^4x \left(\frac{1}{2} \partial_\mu A_\nu \partial^\mu A^\nu + j_\mu A^\mu\right)$, where we have again integrated by parts. Applying the general variational Eq. (1.17) one finally obtains the wave equation.

Hamiltonian of electromagnetic field

Here it is shown that the Hamiltonian canonically conjugate to the Lagrangian of the electromagnetic field indeed coincides with the energy density familiar from elementary electrodynamics.

Consider the electromagnetic field in the absence of matter, $j = 0$. Verify that the total energy stored in the field is given by $H \equiv \int d^3x\, \mathcal{H}(\mathbf{x})$ where $\mathcal{H}(\mathbf{x}) = \mathbf{E}^2(\mathbf{x}) + \mathbf{B}^2(\mathbf{x})$ is the familiar expression for the EM energy density. (Hint: Use the vacuum form of Maxwell's equations and the fact that, for an infinite system, the energy is defined only up to surface terms.)

Answer:
Following the canonical prescription, let us first consider the Lagrangian density,

$$\mathcal{L} = -\frac{1}{4}F_{\mu\nu}F^{\mu\nu} = \frac{1}{2}\sum_{i=1}^{3}(\partial_0 A_i - \partial_i A_0)(\partial_0 A_i - \partial_i A_0) - \frac{1}{4}\sum_{i,j=1}^{3}(\partial_i A_j - \partial_j A_i)(\partial_i A_j - \partial_j A_i).$$

We next determine the components of the canonical momentum through the relation $\pi_\mu = \partial_{\partial_0 A_\mu}\mathcal{L} : \pi_0 = 0$, $\pi_i = \partial_0 A_i - \partial_i A_0 = E_i$. Using the fact that $\partial_i A_j - \partial_j A_i$ is a component of the magnetic field, the Hamiltonian density can now be written as

$$\begin{aligned}\mathcal{H} &= \pi_\mu \partial_0 A_\mu - \mathcal{L} = \frac{1}{2}(2\mathbf{E}\cdot\partial_0\mathbf{A} - \mathbf{E}^2 + \mathbf{B}^2) \overset{(1)}{=} \frac{1}{2}(2\mathbf{E}\cdot\nabla\phi + \mathbf{E}^2 + \mathbf{B}^2)\\ &\overset{(2)}{=} \frac{1}{2}(2\nabla\cdot(\mathbf{E}\phi) + \mathbf{E}^2 + \mathbf{B}^2),\end{aligned}$$

where (1) is based on addition and subtraction of a term $2\mathbf{E}\cdot\nabla\phi$, and (2) on $\nabla\cdot\mathbf{E} = 0$ combined with the identity $\nabla\cdot(\mathbf{a}f) = \nabla\cdot\mathbf{a}f + \mathbf{a}\cdot\nabla f$ (valid for general vector [scalar] functions $\mathbf{a}(f)$). Substitution of this expression into the definition of the Hamiltonian yields

$$H = \frac{1}{2}\int d^3x \left(2\nabla\cdot(\mathbf{E}\phi) + \mathbf{E}^2 + \mathbf{B}^2\right) = \frac{1}{2}\int d^3x \left(\mathbf{E}^2 + \mathbf{B}^2\right),$$

where we have used the fact that the contribution $\nabla\cdot(\mathbf{E}\phi)$ is a surface term that vanishes upon integration by parts.

Phonon specific heat

In the text, we have stated that the mode quantization of elastic media manifests itself in low-temperature anomalies of the specific heat. In this problem, concepts of elementary quantum statistical mechanics are applied to determine the temperature profile of the specific heat.

Compute the energy density $u = -(1/L)\partial_\beta \ln \mathcal{Z}$ of one-dimensional longitudinal phonons with dispersion $\omega_k = v|k|$, where $\mathcal{Z} = \operatorname{tr} e^{-\beta\hat{H}}$ denotes the quantum partition function. As an intermediate result, show that the thermal expectation value of the energy density of the system can be represented as

$$u = \frac{1}{L}\sum_k \left(\frac{\omega_k}{2} + \omega_k n_{\mathrm{B}}(\omega_k)\right), \tag{1.45}$$

where $n_{\rm B}(\epsilon) = \left(e^{\beta\epsilon} - 1\right)^{-1}$ is the Bose–Einstein distribution function. Approximate the sum over k by an integral and show that $c_v \sim T$. At what temperature $T_{\rm cl}$ does the specific heat cross over to the classical result $c_v = \text{const}$? (Remember that the linear dispersion $\omega_k = v|k|$ is based on a quadratic approximation to the Hamiltonian of the system and, therefore, holds only for $|k| < \Lambda$, where Λ is some cutoff momentum.) Reiterate the discussion of Section 1.4 for a d-dimensional isotropic solid of volume L^d (i.e. assume that the atomic exchange constants remain the same in all directions). Show that the dispersion generalizes to $\omega_{\mathbf{k}} = v|\mathbf{k}|$, where $\mathbf{k} = (n_1, \ldots, n_d)2\pi/L$ and $n_i \in \mathbb{Z}$. Show that the specific heat shows the temperature dependence $c_v \sim T^d$.

Answer:
As discussed in the text, the quantum eigenstates of the system are given by $|n_1, n_2, \ldots\rangle$, where n_m is the number of phonons of wavenumber $k_m = 2\pi m/L$, $E_{|n_1,n_2,\ldots\rangle} = \sum_m \omega_{k_m}(n_m + 1/2) \equiv \sum_m \epsilon_m^{n_m}$ the eigenenergy, and $\omega_m = v|k_m|$. In the energy representation, the quantum partition function then takes the form

$$\mathcal{Z} = \operatorname{tr} e^{-\beta\hat{H}} = \sum_{\text{states}} e^{-\beta E_{\text{state}}} = \prod_{m=1,2,\ldots} \sum_{n_m=0}^{\infty} e^{-\beta\omega_m(n_m+1/2)} = \prod_{m=1,2,\ldots} \frac{e^{-\beta\omega_m/2}}{1 - e^{-\beta\omega_m}},$$

where n_m is the occupation number of the state with wavenumber k_m. Hence,

$$\ln \mathcal{Z} = -\sum_m \left[\beta\frac{\omega_m}{2} + \ln\left(1 - e^{-\beta\omega_m}\right)\right].$$

Differentiation with respect to β yields Eq. (1.45) and, replacing $\sum_m \to (L/2\pi)\int dk$, we arrive at

$$u = C_1 + \frac{1}{2\pi}\int_{|k|<\Lambda} dk\ \frac{v|k|}{e^{\beta v|k|} - 1} = C_1 + \beta^{-2}C_2.$$

Here, C_1 is the temperature-independent constant accounting for the "zero-point energies" $\omega_m/2$. In the second equality, we have scaled $k \to \beta k$. This produces a prefactor β^{-2} multiplied by a temperature-independent (up to the temperature dependence of the boundaries $\Lambda \to \beta\Lambda$) integral that we denoted by C_2. Differentiation with respect to T then leads to the relation $c_v = \partial_T u \sim T$. However, for temperatures $T > v\Lambda$ higher than the highest frequencies stored in the phonon modes, the procedure above no longer makes sense (formally, due to the now non-negligible temperature dependence of the boundaries). Yet in this regime we may expand $e^{\beta v|k|} - 1 \simeq \beta v|k|$, which brings us back to the classical result $c_v = \text{const}$.

Consider now a d-dimensional solid with "isotropic" exchange coupling $\left(\frac{k_{\rm s}}{2}\right)\sum_{i=1}^{d}(\phi_{\mathbf{R}+\mathbf{e}_i} - \phi_{\mathbf{R}})^2$ ($\mathbf{e}_i$: unit vector in the i-direction). Taking a continuum limit leads to a contribution $(k_{\rm s}a^2/2)(\nabla\phi(\mathbf{x}))^2$. Proceeding along the lines of the text, we find that the relevant excitations are now waves with wave vector $\mathbf{k} = 2\pi(n_1, \ldots, n_d)/L$ and energy $\omega_{\mathbf{k}} = |\mathbf{k}|v$. Accordingly, the sum in our formula for the specific heat becomes $\sum_{\mathbf{k}} \sim \int d^dk$. Scaling $k_i \to \beta k_i$ then generates a prefactor β^{-d-1} and we arrive at the relation $c_v \sim T^d$.

Van der Waals force

We here discuss a semi-phenomenological approach to the van der Waals force: modelling the constituents participating in the interaction as quantum oscillators, we find that the ground state energy of the ensuing two-body system is lower than that of the isolated compounds.

London's phenomenological approach to explaining the van der Waals force starts out from the Hamiltonian

$$\hat{H} = \frac{\hat{p}_1^2}{2m} + \frac{\hat{p}_2^2}{2m} + \frac{m\omega_o^2}{2}\left(\hat{x}_1^2 + \hat{x}_2^2\right) + mK\hat{x}_1\hat{x}_2,$$

where $\hat{x}_i$ is the coordinate of an oscillator phenomenologically representing one of two atoms $i = 1, 2$. The atoms are coupled through a dipole–dipole interaction, where the dipole operators are proportional to $\hat{x}_i$ and $K(r) = qe^2/(mr^3)$ encapsulates the details of the interaction. Here r denotes the distance between the atoms and q is a dipole–dipole orientation factor.

Compute the spectrum of the two-particle system described by $\hat{H}$ and verify that the dipole coupling leads to a lowering of the ground state energy by an amount $V(r) = K^2/8\omega_o^3$. Using the fact that the classical polarizability of an oscillator is given by $\alpha = e^2/m\omega_o^2$ this becomes $V = q^2\omega_o\alpha^2/8r^6$. Finally, using the fact that the directional average of the geometric factor q^2 equals 2, and multiplying by three to take account of the three-dimensional character of a "real" atomic oscillator, we recover the result Eq. (1.41).

Answer:
We begin by formulating the potential $\hat{U}$ of the oscillator system in a matrix notation, $\hat{U} = \hat{\mathbf{x}}^T A\hat{\mathbf{x}}$, where $\hat{\mathbf{x}}^T = (\hat{x}_1, \hat{x}_2)^T$ and

$$A = \frac{m}{2}\begin{pmatrix} \omega^2 & K \\ K & \omega^2 \end{pmatrix}.$$

Diagonalizing the matrix, $A = UDU^T$, and transforming coordinates, $\mathbf{x} \to U^T\mathbf{x} = \mathbf{x}'$, the system decouples into two independent oscillators,

$$\hat{H} = \sum_{i=1,2}\left(\frac{\hat{p}_i'^2}{2m} + \frac{m\omega_i^2}{2}\hat{x}_i'^2\right),$$

where the new characteristic frequencies $\omega_{1/2} = \left(\omega_o^2 \pm K\right)^{1/2}$ are determined by the eigenvalues of the matrix A. The ground state of this system is given by $E_0 = (\omega_1 + \omega_2)/2 \approx \omega_o - K^2/8\omega_o^3$, which lies by an amount $V = -K^2/\left(8\omega_o^3\right)$ lower than the energy of the isolated atoms.

2

Second quantization

The purpose of this chapter is to introduce and apply the method of second quantization, a technique that underpins the formulation of quantum many-particle theories. The first part of the chapter focuses on methodology and notation, while the remainder is devoted to the development of applications designed to engender familiarity with and fluency in the technique. Specifically, we will investigate the physics of the interacting electron gas, charge density wave propagation in one-dimensional quantum wires, and spin waves in a quantum Heisenberg (anti)ferromagnet. Indeed, many of these examples and their descendants will reappear as applications in our discussion of methods of quantum field theory in subsequent chapters.

In the previous chapter we encountered two field theories that could conveniently be represented in the language of "second quantization," i.e. a formulation based on the algebra of certain ladder operators $\hat{a}_k$.[1] There were two remarkable facts about this formulation: firstly, second quantization provides a compact way of representing the many-body space of excitations; secondly, the properties of the ladder operators were encoded in a simple set of commutation relations (cf. Eq. (1.33)) rather than in some explicit Hilbert space representation.

Apart from a certain aesthetic appeal, these observations would not be of much relevance if it were not for the fact that the formulation can be generalized to a comprehensive and highly efficient formulation of many-body quantum mechanics in general. In fact, second quantization can be considered the first major cornerstone on which the theoretical framework of quantum field theory was built. This being so, extensive introductions to the concept can be found throughout the literature. We will therefore not develop the formalism in full mathematical rigor but rather proceed pragmatically by first motivating and introducing its basic elements, followed by a discussion of the "second quantized" version of standard operations of quantum mechanics (taking matrix elements, changing bases, representing operators, etc.). The second part of the chapter is concerned with developing fluency in the method by addressing a number of applications. Readers familiar with the formalism may therefore proceed directly to these sections.

[1] The term "second quantization" is unfortunate. Historically, this terminology was motivated by the observation that the ladder operator algebra fosters an interpretation of quantum excitations as discrete "quantized" units. Fundamentally, however, there is nothing like "two" superimposed quantization steps in single- or many-particle quantum mechanics. Rather, one is dealing with a particular representation of the "first and only quantized" theory tailored to the particular problem at hand.

2.1 Introduction to second quantization

Motivation

We begin our discussion by recapitulating some fundamental notions of many-body quantum mechanics, as formulated in the traditional language of symmetrized/anti-symmetrized wavefunctions. Consider the (normalized) set of wavefunctions $|\lambda\rangle$ of some single-particle Hamiltonian $\hat{H}$: $\hat{H}|\lambda\rangle = \epsilon_\lambda|\lambda\rangle$, where ϵ_λ are the eigenvalues. With this definition, the normalized two-particle wavefunction $\psi_{\rm F}(\psi_{\rm B})$ of two fermions (bosons) populating levels λ_1 and λ_2 is given by the anti-symmetrized (symmetrized) product

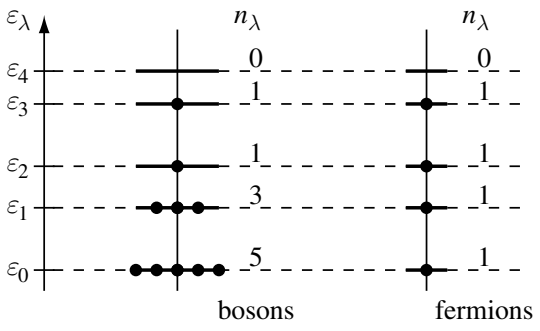

$$\begin{aligned}\psi_{\rm F}(x_1,x_2) &= \frac{1}{\sqrt{2}}\left(\langle x_1|\lambda_1\rangle\langle x_2|\lambda_2\rangle - \langle x_1|\lambda_2\rangle\langle x_2|\lambda_1\rangle\right),\\ \psi_{\rm B}(x_1,x_2) &= \frac{1}{\sqrt{2}}\left(\langle x_1|\lambda_1\rangle\langle x_2|\lambda_2\rangle + \langle x_1|\lambda_2\rangle\langle x_2|\lambda_1\rangle\right).\end{aligned}$$

In the Dirac bracket representation, the two-body states $|\lambda_1,\lambda_2\rangle_{\rm F(B)}$ corresponding to the wave functions $\psi_{\rm F(B)}(x_1,x_2) = \left(\langle x_1|\otimes\langle x_2|\right)|\lambda_1,\lambda_2\rangle_{\rm F(B)}$ above can be presented as

$$|\lambda_1,\lambda_2\rangle_{\rm F(B)} \equiv \frac{1}{\sqrt{2}}\left(|\lambda_1\rangle\otimes|\lambda_2\rangle + \zeta|\lambda_2\rangle\otimes|\lambda_1\rangle\right),$$

where $\zeta = -1$ for fermions while $\zeta = 1$ for bosons.

Note that the explicit symmetrization of the wavefunctions is necessitated by quantum mechanical **indistinguishability**: for fermions (bosons) the wave function has to be anti-symmetric (symmetric) under particle exchange.[2] More generally, an appropriately symmetrized N-particle wavefunction can be expressed in the form

Enrico Fermi 1901–54
Nobel Laureate in Physics in 1938 for his demonstrations of the existence of new radioactive elements produced by neutron irradiation, and for his related discovery of nuclear reactions brought about by slow neutrons. (Image © The Nobel Foundation.)

$$|\lambda_1,\lambda_2,\ldots,\lambda_N\rangle \equiv \frac{1}{\sqrt{N!\prod_{\lambda=0}^{\infty}(n_\lambda!)}}\sum_{\mathcal{P}}\zeta^{(1-\mathrm{sgn}\,\mathcal{P})/2}|\lambda_{\mathcal{P}1}\rangle\otimes|\lambda_{\mathcal{P}2}\rangle\otimes\cdots\otimes|\lambda_{\mathcal{P}N}\rangle, \quad (2.1)$$

[2] Notice, however, that in two-dimensional systems the standard doctrine of fully symmetric/anti-symmetric many particle wave functions is too narrow and more general types of exchange statistics can be realized, cf. our discussion on page 41.

where n_λ represents the total number of particles in state λ (for fermions, Pauli exclusion enforces the constraint $n_\lambda \leq 1$) – see the schematic figure above. The summation runs over all $N!$ permutations of the set of quantum numbers $\{\lambda_1, \ldots, \lambda_N\}$, and $\operatorname{sgn}\mathcal{P}$ denotes the sign of the permutation $\mathcal{P}$. ($\operatorname{sgn}\mathcal{P} = 1\,[-1]$ if the number of transpositions of two elements which brings the permutation $(\mathcal{P}_1, \mathcal{P}_2, \ldots, \mathcal{P}_N)$ back to its original form $(1, 2, \ldots, N)$ is even [odd].) The prefactor $1/\sqrt{N! \prod_\lambda (n_\lambda!)}$ normalizes the many-body wavefunction. In the fermionic case, wave functions corresponding to the states above are known as **Slater determinants**.

Finally, notice that it will be useful to assume that the quantum numbers $\{\lambda_i\}$ defining the state $|\lambda_1, \lambda_2, \ldots, \lambda_N\rangle$ are ordered according to some convention. (For example, for $\lambda_i = x_i$ a one-dimensional coordinate representation, we might order according to the rule $x_1 \leq x_2 \leq \cdots \leq x_N$.) Once an ordered sequence of states has been fixed we may – for notational convenience – label our quantum states by integers, $\lambda_i = 1, 2, \ldots$. Any initially non-ordered state (e.g. $|2, 1, 3\rangle$) can be brought into an ordered form ($|1, 2, 3\rangle$) at the cost of, at most, a change of sign.

David Hilbert 1862–1943

He contributed to many branches of mathematics, including invariants, algebraic number fields, functional analysis, integral equations, mathematical physics, and the calculus of variations. His work in geometry had the greatest influence in that area after Euclid. A systematic study of the axioms of Euclidean geometry led Hilbert to propose twenty one such axioms and he analyzed their significance.

INFO For the sake of completeness, let us spell out the connection between the **permutation group and many-body quantum mechanics** in a more mathematical language. The basic arena wherein N-body quantum mechanics takes place is the product space,

$$\mathcal{H}^N \equiv \underbrace{\mathcal{H} \quad \cdots \quad \mathcal{H}}_{N \text{ copies}},$$

of N single-particle Hilbert spaces. In this space, we have a linear representation of the permutation group, S^N,[3] assigning to each $\mathcal{P} \in S^N$ the permutation (no ordering of the λs implied at this stage),

$$\mathcal{P} : \mathcal{H}^N \quad \to \quad \mathcal{H}^N, \quad |\lambda_1\rangle \quad \cdots \quad |\lambda_N\rangle \mapsto |\lambda_{\mathcal{P}1}\rangle \quad \cdots \quad |\lambda_{\mathcal{P}N}\rangle.$$

[3] Recall that a **linear representation** of a group G is a mapping that assigns to each $g \in G$ a linear mapping $\rho_g : V \to V$ of some vector space V. For notational convenience one usually writes $g : V \to V$ instead of $\rho_g : V \to V$. Conceptually, however, it is often important to carefully discriminate between the abstract group elements g and the *matrices* (also g) assigned to them by a given representation. (Consider, for example the symmetry group $G = \mathrm{SU}(2)$ of quantum mechanical spin. SU(2) is the two-dimensional group of unitary matrices with determinant one. However, when acting in the Hilbert space of a quantum spin $S = 5$, say, elements of SU(2) are represented by $(2S + 1 = 11)$-dimensional matrices.) Two representations ρ and ρ' that differ only by a unitary transformation, $g \in G : \rho_g = U \rho'_g U^{-1}$, are called unitary equivalent. If a transformation U can be found such that all representation matrices ρ_g assume a block structure, the representation is called reducible, and otherwise **irreducible**. Notice that the different sub-blocks of a reducible representation by themselves form irreducible representation spaces. The identification of all distinct irreducible representations of a given group is one of the most important objectives of group theory.

The identification of all irreducible subspaces of this representation is a formidable task that, thanks to a fundamental axiom of quantum mechanics, we need not address in full. All we need to know is that S^N has two particularly simple one-dimensional irreducible representations: one wherein each $\mathcal{P} \in S^N$ acts as the identity transform $\mathcal{P}(\ ) \equiv$ and, another, the alternating representation $\mathcal{P}(\ ) = \operatorname{sgn}\mathcal{P} \cdot$. According to a basic postulate of quantum mechanics, the state vectors $\in \mathcal{H}^N$ describing bosons/fermions must transform according to the identity/alternating representation. The subset $\mathcal{F}^N \subset \mathcal{H}^N$ of all states showing this transformation behavior defines the physical N-body Hilbert space. To construct a basis of $\mathcal{F}^N$, one may apply the symmetrization operator $P^s \equiv \sum_{\mathcal{P}} \mathcal{P}$ (anti-symmetrization operator $P^a \equiv \sum_{\mathcal{P}} (\operatorname{sgn}\mathcal{P})\mathcal{P}$) to the basis vectors $|\lambda_1\rangle \quad \cdots \quad |\lambda_N\rangle$ of $\mathcal{H}^N$. Up to normalization, this operation obtains the states (2.1).

Some readers may wonder why we mention these representation-theoretic aspects. Being pragmatic, all we really need to know is the symmetrization/anti-symmetrization postulate, and its implementation through Eq. (2.1). Notice, however, that one may justly question what we actually mean when we talk about the permutation exchange of quantum numbers. For example, when we compare wavefunctions that differ by an exchange of coordinates, we should, at least in principle, be able to tell by what physical operation we effect this exchange (for, otherwise, we cannot really compare them other than in a formal and, in fact, in an ambiguous sense).

Oddly enough, decades passed before this crucial issue in quantum mechanics was critically addressed. In a now seminal work by Leinaas and Myrheim[4] it was shown that the standard paradigm of permutation exchange is far from innocent. In particular, it turned out that its applicability is tied to the dimensionality of space! Specifically, in two-dimensional spaces (in a sense, also in $d = 1$) a more elaborate scheme is needed. (Still one may use representation-theoretic concepts to describe particle exchange. However, the relevant group – the **braid group** – now differs from the permutation group.) Physically, these phenomena manifest themselves in the emergence of quantum particles different from both bosons and fermions. For a further discussion of these "**anyons**" we refer to Chapter 9.

While representations like Eq. (2.1) *can* be used to represent the full Hilbert space of many-body quantum mechanics, a moment's thought shows that this formulation is not at all convenient:

- ▷ It takes little imagination to anticipate that practical computation in the language of Eq. (2.1) will be cumbersome. For example, to compute the overlap of two wavefunctions one needs to form no less than $(N!)^2$ different products.
- ▷ The representation is tailor-made for problems with fixed particle number N. However, we know from statistical mechanics that for $N = \mathcal{O}(10^{23})$ it is much more convenient to work in a grand canonical formulation where N is allowed to fluctuate.
- ▷ Closely related to the above, in applications one will often ask questions such as, "What is the amplitude for injection of a particle into the system at a certain space-time coordinate (x_1, t_1) followed by annihilation at some later time (x_2, t_2)?" Ideally, one would work with a representation that supports the intuition afforded by thinking in terms of such

[4] J. M. Leinaas and J. Myrheim, On the theory of identical particles, Il *Nuovo Cimento* B **37** (1977), 1–23.

processes: i.e. a representation where the quantum numbers of individual quasi-particles rather than the entangled set of quantum numbers of all constituents are fundamental.

The "second quantized" formulation of many-body quantum mechanics, as introduced in the next subsection, will remove all these difficulties in an elegant and efficient manner.

The apparatus of second quantization

Occupation number representation and Fock space

Some of the disadvantages of the representation (2.1) can be avoided with relatively little effort. In our present notation, quantum states are represented by "N-letter words" of the form $|1,1,1,1,2,2,3,3,3,4,6,6,\ldots\rangle$. Obviously, this notation contains a lot of redundancy. A more efficient encoding of the state above might read $|4,2,3,1,0,2,\ldots\rangle$, where the ith number signals how many particles occupy state number i; no more information is needed to characterize a symmetrized state. (For fermions, these occupation numbers take a value of either zero or one.) This defines the "**occupation number representation**." In the new representation, the basis states of $\mathcal{F}^N$ are specified by $|n_1,n_2,\ldots\rangle$, where $\sum_i n_i = N$. Any state $|\Psi\rangle$ in $\mathcal{F}^N$ can be obtained by a linear superposition

$$|\Psi\rangle = \sum_{\substack{n_1,n_2,\ldots,\\ \sum n_i = N}} c_{n_1,n_2,\ldots}|n_1,n_2,\ldots\rangle.$$

As pointed out above, eventually we will want to emancipate ourselves from the condition of a fixed particle number N. A Hilbert space large enough to accommodate a state with an undetermined number of particles is given by

$$\mathcal{F} \equiv \bigoplus_{N=0}^{\infty} \mathcal{F}^N. \tag{2.2}$$

Notice that the direct sum contains a curious contribution $\mathcal{F}^0$, the "vacuum space." This is a one-dimensional Hilbert space which describes the sector of the theory with no particles present. Its single normalized basis state, the **vacuum state**, is denoted by $|0\rangle$. We will soon see why it is convenient to add this strange animal to our family of basis states. The space $\mathcal{F}$ is called **Fock space** and it defines the principal arena of quantum many-body theory.

Vladimir Aleksandrovich Fock
1898–1974

One of the main participants in the history of the general theory of relativity in Russia. His groundbreaking contributions to many-body theory include the introduction of Fock space and the development of perhaps the most important many-particle approximation scheme, the Hartree-Fock approximation (see Chapter 5).

To obtain a basis of $\mathcal{F}$, we need only take the totality of our previous basis states $\{|n_1,n_2,\ldots\rangle\}$, and drop the condition $\sum_i n_i = N$ on the occupation numbers. A general many-body state $|\Psi\rangle$ can then be represented by a linear superposition $|\Psi\rangle =$

$\sum_{n_1,n_2,\ldots} c_{n_1,n_2,\ldots}|n_1,n_2,\ldots\rangle$. Notice that states of different particle numbers may contribute to the linear superposition forming $|\Psi\rangle$. We shall see that such mixtures play an important role, for example in the theory of superconductivity.

Foundations of second quantization

The occupation number representation introduced above provides a step in the right direction, but it does not yet solve our main problem, the need for explicit symmetrization/antisymmetrization of a large number of states in each quantum operation.

As a first step towards the construction of a more powerful representation, let us recall an elementary fact of linear algebra: a linear map $A : V \to V$ of a vector space into itself is fully determined by defining the images $w_i \equiv Av_i$ of the action of A on a basis $\{v_i\}$. Now let us use this scheme to introduce a set of linear operators acting in Fock space. For every $i = 1, 2, \ldots$, we define operators $a_i^\dagger : \mathcal{F} \to \mathcal{F}$ through

$$a_i^\dagger|n_1,\ldots,n_i,\ldots\rangle \equiv (n_i+1)^{1/2}\zeta^{s_i}|n_1,\ldots,n_i+1,\ldots\rangle, \tag{2.3}$$

where $s_i = \sum_{j=1}^{i-1} n_j$. In the fermionic case, the occupation numbers n_i have to be understood mod 2. Specifically, $(1+1) = 0 \bmod 2$, i.e. the application of $a_i^\dagger$ to a state with $n_i = 1$ annihilates this state.

Notice that by virtue of this definition we are able to generate every basis state of $\mathcal{F}$ by repeated application of $a_i^\dagger$s to the vacuum state. (From a formal point of view, this fact alone is motivation enough to add the vacuum space to the definition of Fock space.) Indeed, repeated application of Eq. (2.3) leads to the important relation

$$\boxed{|n_1,n_2,\ldots\rangle = \prod_i \frac{1}{(n_i!)^{1/2}}(a_i^\dagger)^{n_i}|0\rangle.} \tag{2.4}$$

Notice that Eq. (2.4) presents a strong statement: the complicated permutation "entanglement" implied in the definition (2.1) of the Fock states can be generated by straightforward application of a set of linear operators to a single reference state. Physically, N-fold application of operators $a^\dagger$ to the empty vacuum state generates an N-particle state, which is why the $a^\dagger$s are commonly called **creation operators**. Of course, the introduction of creation operators might still turn out to be useless, i.e. consistency with the properties of the Fock states (such as the fact that, in the fermionic case, the numbers $n_i = 0, 1$ are defined only mod 2), might invalidate the simple relation (2.3) with its (n_i-independent!) operator $a_i^\dagger$. However, as we shall demonstrate below, this is not the case.

Consider two operators $a_i^\dagger$ and $a_j^\dagger$ for $i \neq j$. From the definition (2.3), one may readily verify that $(a_i^\dagger a_j^\dagger - \zeta a_j^\dagger a_i^\dagger)|n_1,n_2,\ldots\rangle = 0$. Holding for every basis vector, this relation implies that $[a_i^\dagger, a_j^\dagger]_\zeta = 0$, where

$$[\hat{A},\hat{B}]_\zeta \equiv \hat{A}\hat{B} - \zeta\hat{B}\hat{A},$$

i.e. $[\,,\,]_{\zeta=1} \equiv [\,,\,]$ is the commutator and $[\,,\,]_{\zeta=-1} \equiv \{\,,\,\} \equiv [\,,\,]_+$ the anti-commutator. Turning to the case $i = j$, we note that, for fermions, the two-fold application of $a_i^\dagger$ to any state leads to its annihilation. Thus, $a_i^{\dagger 2} = 0$ is nilpotent, a fact that can be formulated as

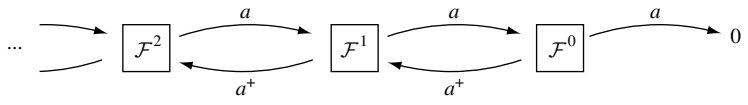

Figure 2.1 Visualization of the generation of the Fock subspaces $\mathcal{F}^N$ by repeated action of creation operators on the vacuum space $\mathcal{F}^0$.

$[a_i^\dagger, a_i^\dagger]_+ = 0$. For bosons we have, of course, $[a_i^\dagger, a_i^\dagger] = 0$ (identical operators commute!). Summarizing, we have found that the creation operators obey the commutation relation

$$\forall i,j: \quad \left[a_i^\dagger, a_j^\dagger\right]_\zeta = 0. \tag{2.5}$$

Now, quantum mechanics is a unitary theory so, whenever one meets a new operator $\hat{A}$, one should determine its Hermitian adjoint $\hat{A}^\dagger$. To understand the action of the Hermitian adjoints $\left(a_i^\dagger\right)^\dagger = a_i$ of the creation operators we may take the complex conjugates of all basis matrix elements of Eq. (2.3):

$$\begin{aligned} & \langle n_1, \ldots, n_i, \ldots | a_i^\dagger | n_1', \ldots, n_i', \ldots \rangle &&= \left(n_i'+1\right)^{1/2} \zeta^{s_i'} \delta_{n_1, n_1'} \ldots \delta_{n_i, n_i'+1} \ldots \\ \Rightarrow \quad & \langle n_1', \ldots, n_i', \ldots | a_i | n_1, \ldots, n_i, \ldots \rangle^* &&= n_i^{1/2} \zeta^{s_i} \delta_{n_1', n_1} \ldots \delta_{n_i', n_i - 1} \ldots \end{aligned}$$

Holding for every bra $\langle n_1', \ldots, n_i', \ldots |$, the last line tells us that

$$a_i | n_1, \ldots, n_i, \ldots \rangle = n_i^{1/2} \zeta^{s_i} | n_1, \ldots, n_i - 1, \ldots \rangle, \tag{2.6}$$

a relation that identifies a_i as an operator that "annihilates" particles. The action of creation and **annihilation operators** in Fock space is illustrated in Fig. 2.1. Creation operators $a^\dagger : \mathcal{F}^N \to \mathcal{F}^{N+1}$ increase the particle number by one, while annihilation operators $a : \mathcal{F}^N \to \mathcal{F}^{N-1}$ lower it by one; the application of an annihilation operator to the vacuum state, $a_i|0\rangle = 0$, annihilates it. (Do not confuse the vector $|0\rangle$ with the number zero.)

Taking the Hermitian adjoint of Eq. (2.5) we obtain $[a_i, a_j]_\zeta = 0$. Further, a straightforward calculation based on the definitions (2.3) and (2.6) shows that $[a_i, a_j^\dagger]_\zeta = \delta_{ij}$. Altogether, we have shown that the creation and annihilation operators satisfy the algebraic closure relation

$$\boxed{[a_i, a_j^\dagger]_\zeta = \delta_{ij}, \quad [a_i, a_j]_\zeta = 0, \quad [a_i^\dagger, a_j^\dagger]_\zeta = 0.} \tag{2.7}$$

Given that the full complexity of Fock space is generated by application of $a_i^\dagger$s to a single reference state, the simplicity of the relations obeyed by these operators seems remarkable and surprising.

INFO Perhaps less surprising is that, behind this phenomenon, there lingers some mathematical structure. Suppose we are given an abstract algebra $\mathcal{A}$ of objects $a_i, a_i^\dagger$ satisfying the relation (2.7). (Recall that an algebra is a vector space whose elements can be multiplied by each other.) Further suppose that $\mathcal{A}$ is irreducibly represented in some vector space V, i.e. that there is a mapping assigning to each $a_i \in \mathcal{A}$ a linear mapping $a_i : V \to V$, such that every vector $|v\rangle \in V$ can be reached from any other $|w\rangle \in V$ by (possibly iterated) application of operators a_i and $a_i^\dagger$

(irreducibility).[5] According to the **Stone–von Neumann theorem** (a) such a representation is unique (up to unitary equivalence), and (b) there is a unique state $|0\rangle \in V$ that is annihilated by every a_i. All other states can then be reached by repeated application of $a_i^\dagger$s. The precise formulation of this theorem, and its proof – a good practical exercise in working with creation/annihilation operators – are left as Problem 2.4. From the Stone–von Neumann theorem, we can infer that the Fock space basis could have been constructed in reverse. Not knowing the basis $\{|n_1, n_2, \ldots\rangle\}$, we could have started from a set of operators obeying the commutation relations (2.7) acting in some a priori unknown space $\mathcal{F}$. Outgoing from the unique state $|0\rangle$, the prescription (2.4) would then have yielded an equally unique basis of the entire space $\mathcal{F}$ (up to unitary transformations). In other words, the algebra (2.7) fully characterizes the operator action and provides information equivalent to the definitions (2.3) and (2.6).

Practical aspects

Our next task will be to promote the characterization of Fock space bases introduced above to a full reformulation of many-body quantum mechanics. To this end, we need to find out how changes from one single-particle basis $\{|\lambda\rangle\}$ to another $\{|\tilde{\lambda}\rangle\}$ affect the operator algebra $\{a_\lambda\}$. (In this section we shall no longer use integers to identify different elements of a given single-particle basis. Rather, we use Greek labels λ, i.e. $a_\lambda^\dagger$ creates a particle in state λ.) Equally important, we need to understand in what way generic operators acting in many-particle Hilbert spaces can be represented in terms of creation and annihilation operators.

▷ **Change of basis:** Using the resolution of identity $\mathrm{id} = \sum_{\lambda=0}^{\infty} |\lambda\rangle\langle\lambda|$, the relations $|\tilde{\lambda}\rangle = \sum_\lambda |\lambda\rangle\langle\lambda|\tilde{\lambda}\rangle$, $|\lambda\rangle \equiv a_\lambda^\dagger|0\rangle$, and $|\tilde{\lambda}\rangle \equiv a_{\tilde{\lambda}}^\dagger|0\rangle$ immediately give rise to the transformation law

$$\boxed{a_{\tilde{\lambda}}^\dagger = \sum_\lambda \langle\lambda|\tilde{\lambda}\rangle a_\lambda^\dagger, \qquad a_{\tilde{\lambda}} = \sum_\lambda \langle\tilde{\lambda}|\lambda\rangle a_\lambda.} \tag{2.8}$$

In many applications, we will be dealing with continuous sets of quantum numbers (such as position coordinates). In these cases, the quantum numbers are commonly denoted by a bracket notation $a_\lambda \to a(x) = \sum_\lambda \langle x|\lambda\rangle a_\lambda$ and the summations appearing in the transformation formula above translate to integrals: $a_\lambda = \int dx \langle\lambda|x\rangle a(x)$.

EXERCISE The transformation from the coordinate to the Fourier momentum representation in a finite one-dimensional system of length L would read

$$a_k = \int_0^L dx\, \langle k|x\rangle a(x), \qquad a(x) = \sum_k \langle x|k\rangle a_k, \tag{2.9}$$

where $\langle k|x\rangle \equiv \langle x|k\rangle^* = e^{-ikx}/\sqrt{L}$.

[5] To appropriately characterize the representation, we need to be a bit more precise. Within $\mathcal{A}$, a_i and $a_i^\dagger$ are independent objects, i.e. in general there exists no notion of Hermitian adjointness in $\mathcal{A}$. We require, though, that the representation assigns to $a_i^\dagger$ the Hermitian adjoint (in V) of the image of a_i. Also, we have to require that $[a_i, a_j^\dagger] \in \mathcal{A}$ be mapped onto $[a_i, a_j^\dagger] : V \to V$ where, in the latter expression, the commutator involves the ordinary product of matrices $a_i, a_j^\dagger : V \to V$.

▷ **Representation of operators (one-body):** Single-particle or one-body operators $\hat{\mathcal{O}}_1$ acting in the N-particle Hilbert space $\mathcal{F}^N$ generally take the form $\hat{\mathcal{O}}_1 = \sum_{n=1}^{N} \hat{o}_n$, where $\hat{o}_n$ is an ordinary single-particle operator acting on the nth particle. A typical example is the kinetic energy operator $\hat{T} = \sum_n \hat{p}_n^2/2m$, where $\hat{p}_n$ is the momentum operator acting on the nth particle. Other examples include the one-particle potential operator $\hat{V} = \sum_n V(\hat{x}_n)$, where $V(x)$ is a scalar potential, the total spin operator $\sum_n \hat{\mathbf{S}}_n$, etc. Since we have seen that, by applying field operators to the vacuum space, we can generate the Fock space in general and any N-particle Hilbert space in particular, it must be possible to represent any operator $\hat{\mathcal{O}}_1$ in an a-representation.

Now, although the representation of n-body operators is, after all, quite straightforward, the construction can, at first sight, seem daunting. A convenient way of finding such a representation is to express the operator in terms of a basis in which it is diagonal, and only later transform to an arbitrary basis. For this purpose it is useful to define the **occupation number operator**

$$\boxed{\hat{n}_\lambda = a_\lambda^\dagger a_\lambda}, \tag{2.10}$$

with the property that, for bosons or fermions (exercise), $\hat{n}_\lambda \left(a_\lambda^\dagger\right)^n |0\rangle = n\left(a_\lambda^\dagger\right)^n |0\rangle$. Since $\hat{n}_\lambda$ commutes with all $a_{\lambda' \neq \lambda}^\dagger$, Eq. (2.4) readily implies that $\hat{n}_{\lambda_j} |n_{\lambda_1}, n_{\lambda_2}, \ldots\rangle = n_{\lambda_j} |n_{\lambda_1}, n_{\lambda_2}, \ldots\rangle$, i.e., $\hat{n}_\lambda$ simply counts the number of particles in state λ (hence the name "occupation number operator"). Let us now consider a one-body operator, $\hat{\mathcal{O}}_1$, which is diagonal in the basis $|\lambda\rangle$, with $\hat{o} = \sum_i o_{\lambda_i} |\lambda_i\rangle\langle\lambda_i|$, $o_{\lambda_i} = \langle\lambda_i|\hat{o}|\lambda_i\rangle$. With this definition, one finds that

$$\begin{aligned} \langle n'_{\lambda_1}, n'_{\lambda_2}, \ldots | \hat{\mathcal{O}}_1 | n_{\lambda_1}, n_{\lambda_2}, \ldots\rangle &= \sum_i o_{\lambda_i} n_{\lambda_i} \langle n'_{\lambda_1}, n'_{\lambda_2}, \ldots | n_{\lambda_1}, n_{\lambda_2}, \ldots\rangle \\ &= \langle n'_{\lambda_1}, n'_{\lambda_2}, \ldots | \sum_i o_{\lambda_i} \hat{n}_{\lambda_i} | n_{\lambda_1}, n_{\lambda_2}, \ldots\rangle. \end{aligned}$$

Since this equality holds for any set of states, one can infer the second quantized representation of the operator $\hat{\mathcal{O}}_1$,

$$\hat{\mathcal{O}}_1 = \sum_{\lambda=0}^{\infty} o_\lambda \hat{n}_\lambda = \sum_{\lambda=0}^{\infty} \langle\lambda|\hat{o}|\lambda\rangle a_\lambda^\dagger a_\lambda.$$

The result is straightforward: a one-body operator engages a single particle at a time – the others are just spectators. In the diagonal representation, one simply counts the number of particles in a state λ and multiplies by the corresponding eigenvalue of the one-body operator. Finally, by transforming from the diagonal representation to a general basis, one obtains the general result,

$$\boxed{\hat{\mathcal{O}}_1 = \sum_{\mu\nu} \langle\mu|\hat{o}|\nu\rangle a_\mu^\dagger a_\nu.} \tag{2.11}$$

To cement these ideas, let us consider some specific examples: representing the matrix elements of the single-particle spin operator as $(S_i)_{\alpha\alpha'} = \frac{1}{2}(\sigma_i)_{\alpha\alpha'}$, where α, α' is a two-component spin index and σ_i are the Pauli spin matrices

$$\sigma_1 = \begin{pmatrix} 0 & 1 \\ 1 & 0 \end{pmatrix}, \quad \sigma_2 = \begin{pmatrix} 0 & -i \\ i & 0 \end{pmatrix}, \quad \sigma_3 = \begin{pmatrix} 1 & 0 \\ 0 & -1 \end{pmatrix}, \tag{2.12}$$

the **spin operator** of a many-body system assumes the form

$$\hat{\mathbf{S}} = \sum_{\lambda} a^{\dagger}_{\lambda\alpha'} \mathbf{S}_{\alpha'\alpha} a_{\lambda\alpha}. \tag{2.13}$$

(Here, λ denotes the set of additional quantum numbers, e.g. a lattice site index.) When second quantized in the position representation, one can show that the **one-body Hamiltonian** for a free particle is given as a sum of kinetic and potential energy as

Wolfgang Ernst Pauli 1900–58
Nobel Laureate in Physics in 1945 "for the discovery of the Exclusion Principle, also called the Pauli Principle." The exclusion principle crystallized the existing knowledge of atomic structure at the time it was postulated and it led to the recognition of the two-valued variable required to characterize the state of an electron. Pauli was the first to recognize the existence of the neutrino. (Image © The Nobel Foundation.)

$$\boxed{\hat{H} = \int d^d r \; a^{\dagger}(\mathbf{r}) \left[\frac{\hat{\mathbf{p}}^2}{2m} + V(\mathbf{r}) \right] a(\mathbf{r}),} \tag{2.14}$$

where $\hat{\mathbf{p}} = -i\hbar\partial$.

EXERCISE Starting with momentum representation (in which the kinetic energy is diagonal), transform to the position representation and thereby establish Eq. (2.14).

The **local density operator** $\hat{\rho}(\mathbf{r})$, measuring the particle density at a certain coordinate $\mathbf{r}$, is simply given by

$$\hat{\rho}(\mathbf{r}) = a^{\dagger}(\mathbf{r}) a(\mathbf{r}). \tag{2.15}$$

Finally, the **total occupation number operator**, obtained by integrating over the particle density, is defined by $\hat{N} = \int d^d r \; a^{\dagger}(\mathbf{r}) a(\mathbf{r})$. In a theory with discrete quantum numbers, this operator assumes the form $\hat{N} = \sum_{\lambda} a^{\dagger}_{\lambda} a_{\lambda}$.

▷ **Representation of operators (two-body):** Two-body operators $\hat{\mathcal{O}}_2$ are needed to describe pairwise interactions between particles. Although pair-interaction potentials are straightforwardly included in classical many-body theories, their embedding into conventional many-body quantum mechanics is made cumbersome by particle indistinguishability. The formulation of interaction processes within the language of second quantization is considerably more straightforward:

Initially, let us consider particles subject to the symmetric two-body potential $V(\mathbf{r}_m, \mathbf{r}_n) \equiv V(\mathbf{r}_n, \mathbf{r}_m)$ between two particles at position $\mathbf{r}_m$ and $\mathbf{r}_n$. Our aim is to find an operator $\hat{V}$ in second quantized form whose action on a many-body state gives

(presently, it is more convenient to use the original representation Eq. (2.1) rather than the occupation number representation)

$$\hat{V}|\mathbf{r}_1, \mathbf{r}_2, \dots \mathbf{r}_N\rangle = \sum_{n<m}^{N} V(\mathbf{r}_n, \mathbf{r}_m)|\mathbf{r}_1, \mathbf{r}_2, \dots \mathbf{r}_N\rangle = \frac{1}{2}\sum_{n\neq m}^{N} V(\mathbf{r}_n, \mathbf{r}_m)|\mathbf{r}_1, \mathbf{r}_2, \dots \mathbf{r}_N\rangle.$$

When this is compared with the one-point function, one might immediately guess that

$$\hat{V} = \frac{1}{2}\int d^d r \int d^d r' a^\dagger(\mathbf{r}) a^\dagger(\mathbf{r}') V(\mathbf{r}, \mathbf{r}') a(\mathbf{r}') a(\mathbf{r}).$$

That this is the correct answer can be confirmed by applying the operator to a many-body state:

$$\begin{aligned}
a^\dagger(\mathbf{r})a^\dagger(\mathbf{r}')a(\mathbf{r}')a(\mathbf{r})|\mathbf{r}_1, \mathbf{r}_2, \dots, \mathbf{r}_N\rangle &= a^\dagger(\mathbf{r})a^\dagger(\mathbf{r}')a(\mathbf{r}')a(\mathbf{r})a^\dagger(\mathbf{r}_1)\cdots a^\dagger(\mathbf{r}_N)|0\rangle \\
&= \sum_{n=1}^{N} \zeta^{n-1}\delta(\mathbf{r}-\mathbf{r}_n)a^\dagger(\mathbf{r}_n)\overbrace{a^\dagger(\mathbf{r}')a(\mathbf{r}')}^{\hat{\rho}(\mathbf{r}')} a^\dagger(\mathbf{r}_1)\cdots a^\dagger(\mathbf{r}_{n-1})a^\dagger(\mathbf{r}_{n+1})\cdots a^\dagger(\mathbf{r}_N)|0\rangle \\
&= \sum_{n=1}^{N} \zeta^{n-1}\delta(\mathbf{r}-\mathbf{r}_n)\sum_{m(\neq n)}^{N} \delta(\mathbf{r}'-\mathbf{r}_m)a^\dagger(\mathbf{r}_n)a^\dagger(\mathbf{r}_1)\cdots a^\dagger(\mathbf{r}_{n-1})a^\dagger(\mathbf{r}_{n+1})\cdots a^\dagger(\mathbf{r}_N)|0\rangle \\
&= \sum_{n,m\neq n}^{N} \delta(\mathbf{r}-\mathbf{r}_n)\delta(\mathbf{r}'-\mathbf{r}_m)|\mathbf{r}_1, \mathbf{r}_2, \cdots \mathbf{r}_N\rangle.
\end{aligned}$$

Multiplying by $V(\mathbf{r}, \mathbf{r}')/2$, and integrating over $\mathbf{r}$ and $\mathbf{r}'$, one confirms the validity of the expression. It is left as an exercise to confirm that the naive expression $\frac{1}{2}\int d^d r \int d^d r' V(\mathbf{r}, \mathbf{r}')\hat{\rho}(\mathbf{r})\hat{\rho}(\mathbf{r}')$ does not reproduce the two-body operator. More generally, turning to a non-diagonal basis, it is straightforward to confirm that a general two-body operator can be expressed in the form

$$\boxed{\hat{\mathcal{O}}_2 = \sum_{\lambda\lambda'\mu\mu'} \mathcal{O}_{\mu,\mu',\lambda,\lambda'} a^\dagger_\mu a^\dagger_{\mu'} a_\lambda a_{\lambda'}}, \tag{2.16}$$

where $\mathcal{O}_{\mu,\mu',\lambda,\lambda'} \equiv \langle \mu, \mu'|\hat{\mathcal{O}}_2|\lambda, \lambda'\rangle$.

As well as the pairwise **Coulomb interaction** formulated above, another important interaction, frequently encountered in problems of quantum magnetism, is the **spin–spin interaction**. From our discussion of the second-quantized representation of spin $\hat{\mathbf{S}}$ above, we can infer that the general spin–spin interaction can be presented in second-quantized form as

$$\hat{V} = \frac{1}{2}\int d^d r \int d^d r' \sum_{\alpha\alpha'\beta\beta'} J(\mathbf{r}, \mathbf{r}')\mathbf{S}_{\alpha\beta}\cdot\mathbf{S}_{\alpha'\beta'} a^\dagger_\alpha(\mathbf{r}) a^\dagger_{\alpha'}(\mathbf{r}') a_{\beta'}(\mathbf{r}') a_\beta(\mathbf{r}),$$

where $J(\mathbf{r}, \mathbf{r}')$ denotes the exchange interaction.

In principle, one may proceed in the same manner and represent general n-body interactions in terms of second-quantized operators. However, as $n > 2$ interactions appear infrequently, we refer to the literature for discussion.

This completes our formal introduction to the method of second quantization. To develop fluency in the operation of the method, we will continue by addressing a number of problems chosen from the realm of condensed matter. In doing so, we will see that second quantization often leads to considerable simplification of the analysis of many-particle systems. The effective model Hamiltonians that appear below provide the input for subsequent applications considered in this text. Readers not wishing to get distracted from our main focus – the development of modern methods of quantum field theory in the condensed matter setting – may safely skip the next sections and turn directly to Chapter 3 below. It is worthwhile keeping in mind, however, that the physical motivation for the study of various prototypical model systems considered later in the text is given in Section 2.2.

2.2 Applications of second quantization

Starting from the prototype Hamiltonian (1.1) introduced in Chapter 1, we have already explored generic aspects of lattice dynamics in condensed matter systems. In much of the remaining text we will explore examples from the complementary sector focusing on the electronic degrees of freedom. Drawing on the first of the principles discussed in Chapter 1, we will begin our discussion by reducing the full Hamiltonian to a form that contains the essential elements of the electron dynamics. As well as the pure electron sub-Hamiltonian $H_{\rm e}$, the reduced Hamiltonian will involve the interaction between the electrons and the positively charged ionic background lattice. However, typically, lattice distortions due to both the motion of the ions and the ion–ion interaction couple only indirectly. (Exercise: Try to think of a prominent example where the electron sector is crucially influenced by the dynamics of the host lattice.) To a first approximation, we may, therefore, describe the electron system through the simplified Hamiltonian, $\hat{H} = \hat{H}_0 + \hat{V}_{\rm ee}$, where

$$\left.\begin{aligned} \hat{H}_0 &= \int d^d r\, a^\dagger_\sigma(\mathbf{r}) \left[\frac{\hat{\mathbf{p}}^2}{2m} + V(\mathbf{r})\right] a_\sigma(\mathbf{r}) \\ \hat{V}_{\rm ee} &= \frac{1}{2}\int d^d r \int d^d r'\, V_{\rm ee}(\mathbf{r}-\mathbf{r}') a^\dagger_\sigma(\mathbf{r}) a^\dagger_{\sigma'}(\mathbf{r}') a_{\sigma'}(\mathbf{r}') a_\sigma(\mathbf{r}), \end{aligned}\right\} \tag{2.17}$$

$V(\mathbf{r}) = \sum_I V_{\rm ei}(\mathbf{R}_I - \mathbf{r})$ denotes the lattice potential experienced by the electrons, and the coordinates of the lattice ions $\mathbf{R}_I$ are assumed fixed. For completeness, we have also endowed the electrons with a spin index, $\sigma = \uparrow / \downarrow$. The Hamiltonian defines the problem of the interacting electron gas embedded in a solid state system.

Despite its seemingly innocuous structure, the interacting electron Hamiltonian (2.17) accommodates a wide variety of electron phases from metals and magnets to insulators. To classify the phase behavior of the model, it is helpful to divide our considerations, focusing first on the properties of the non-interacting single-particle system $\hat{H}_0$ and then, later, restoring the electron interaction $V_{\rm ee}$.

Electrons in a periodic potential

Felix Bloch 1905–83
Nobel Laureate in Physics in 1952 "for the development [with Edward M. Purcell] of new methods for nuclear magnetic precision measurements and discoveries in connection therewith." (Image © The Nobel Foundation.)

As we know from Bloch's theorem, eigenstates of a periodic Hamiltonian can be presented in the form of Bloch waves[6] $\psi_{\mathbf{k}n}(\mathbf{r}) = e^{i\mathbf{k}\cdot\mathbf{r}}u_{\mathbf{k}n}(\mathbf{r})$, where the components of the crystal momentum $\mathbf{k}$ take values inside the Brillouin zone, $k_i \in [-\pi/a, \pi/a]$, and we have assumed that the periodicity of the lattice potential is the same in all directions, i.e. $V(\mathbf{r} + a\mathbf{e}_i) = V(\mathbf{r})$. The index n labels the separate energy bands of the solid, and the functions $u_{\mathbf{k}n}(\mathbf{r} + a\mathbf{e}_i) = u_{\mathbf{k}n}(\mathbf{r})$ are periodic on the lattice. Now, depending on the nature of the bonding, there are two complementary classes of materials where the general structure of the Bloch functions can be simplified significantly.

Nearly free electron systems

For certain materials, notably the elemental metals drawn from groups I–IV of the periodic table, the outermost itinerant conduction electrons behave as if they were "nearly free," i.e. their dynamic is largely oblivious to both the Coulomb potential created by the positively charged ion background and their mutual interaction.

INFO Loosely speaking, Pauli exclusion of the bound state inner core electrons prevents the conduction electrons from exploring the region close to the ion core, thereby effectively screening the nuclear charge. In practice, the conduction electrons experience a renormalized **pseudopotential**, which accommodates the effect of the lattice ions and core electrons. Moreover, the high mobility of the conduction electrons provides an efficient method of screening their own mutual Coulomb interaction. In nearly free electron compounds, complete neglect of the lattice potential is usually a good approximation (as long as one considers crystal momenta remote from the boundaries of the Brillouin zone, $k_i = \pm\pi/a$).

In practice, this means that we are at liberty to set the Bloch function to unity, $u_{\mathbf{k}n} = 1$, and regard the eigenstates of the non-interacting Hamiltonian as plane waves. This in turn motivates the representation of the field operators in momentum space Eq. (2.9), whereupon the non-interacting part of the Hamiltonian assumes the free particle form (once again, we have set $\hbar = 1$)

$$\hat{H}_0 = \sum_{\mathbf{k}} \frac{\mathbf{k}^2}{2m} a^\dagger_{\mathbf{k}\sigma} a_{\mathbf{k}\sigma}, \tag{2.18}$$

[6] For a more detailed discussion one may refer to one of the many texts on the basic elements of solid state physics, e.g., Ashcroft and Mermin, *Solid State Physics* (Holt-Saunders International, 1995).

where the sum extends over all wavevectors $\mathbf{k}$ and, as usual, summation convention of the spin indices is assumed. Turning to the Coulomb potential between conduction electrons, in the Fourier representation, the two-body interaction takes the form

$$\hat{V}_{\rm ee} = \frac{1}{2L^d} \sum_{\mathbf{k},\mathbf{k}',\mathbf{q}} V_{\rm ee}(\mathbf{q}) a^\dagger_{\mathbf{k}-\mathbf{q}\sigma} a^\dagger_{\mathbf{k}'+\mathbf{q}\sigma'} a_{\mathbf{k}'\sigma'} a_{\mathbf{k}\sigma}, \tag{2.19}$$

where (choosing units such that $4\pi\epsilon = 1$), $V_{\rm ee}(\mathbf{q}) = e^2/q^2$ represents the Fourier transform of the Coulomb interaction potential $V_{\rm ee}(\mathbf{r}) = e^2/|\mathbf{r}|$. Now, as written, this expression neglects the fact that, in ionized solids, the negative charge density of the electron cloud will be compensated by the charge density of the positively ionized background. The latter can be incorporated into Eq. (2.19) by placing on the sum over $\mathbf{q}$ the restriction that $\mathbf{q} \neq 0$ (exercise). Taken together, the free electron Hamiltonian $\hat{H}_0$ and the Coulomb interaction potential $\hat{V}_{\rm ee}$ are known as the **Jellium model**.

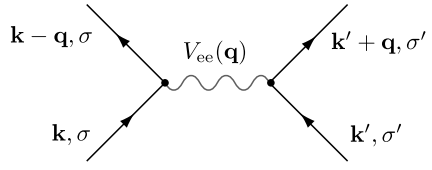

The interaction described by Eq. (2.19) can be illustrated graphically, as shown in the figure (for a more elaborate discussion of such diagrams, see Chapter 5): an electron of momentum $\mathbf{k}$ is scattered into a new momentum state $\mathbf{k}-\mathbf{q}$ while another electron is scattered from $\mathbf{k}' \to \mathbf{k}' + \mathbf{q}$.

Niels Henrik David Bohr 1885–1962
Recipient of the 1922 Nobel Prize in Physics "for his services in the investigation of the structure of atoms and of the radiation emanating from them." (Image © The Nobel Foundation.)

In concrete applications of low-temperature condensed matter physics, one will typically consider low excitation energies. The solution of such problems is naturally organized around the zero-temperature ground state as a reference platform. However, the accurate calculation of the ground state energy of the system is a complicated problem of many-body physics that cannot be solved in closed form. Therefore, assuming that interactions will not substantially alter the ground state of the free particle problem Eq. (2.18) – which is often not the case! – one usually uses the ground state of the latter as a reference state.

INFO Deferring a more qualified discussion to later, a preliminary justification for this assumption can be given as follows. Suppose that the density of the electron gas is such that each of its N constituent particles occupies an average volume of $\mathcal{O}(a^d)$. The average kinetic energy per particle is then estimated to be $T \sim 1/ma^2$, while the Coulomb interaction potential will scale as $V \sim e^2/a$. Thus, for a much smaller than the **Bohr radius** $a_0 = 1/e^2 m$, the interaction contribution is much smaller than the average kinetic energy. In other words, for the dense electron gas, the interaction energy can indeed be treated as a perturbation. Unfortunately, for most metals one finds that $a \sim a_0$ and neither high- nor low- density approximations are strictly justified.

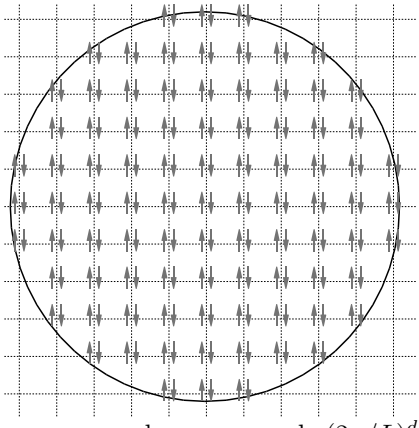

The ground state of the system occupied by N non-interacting particles can be readily inferred from Eq. (2.18). The Pauli principle implies that all energy states $\epsilon_{\mathbf{k}} = k^2/2m$ will be uniformly occupied up to a cutoff **Fermi energy**, $E_{\rm F}$. Specifically, for a system of size L, allowed momentum states $\mathbf{k}$ have components $k_i = 2\pi n_i/L$, $n_i \in \mathbb{Z}$. The summation extends up to momenta with $|\mathbf{k}| \leq k_{\rm F}$, where the **Fermi momentum** $k_{\rm F}$ is defined through the relation $k_{\rm F}^2/2m = E_{\rm F}$ (see figure at right). The relation between the Fermi momentum and the occupation number can be established by dividing the volume of the **Fermi sphere** $\sim k_{\rm F}^d$ by the momentum space volume per mode $(2\pi/L)^d$, viz. $N = C(k_{\rm F}L)^d$ where C denotes a dimensionless geometry-dependent constant.

In the language of second quantization, the ground state can now be represented as

$$|\Omega\rangle \equiv \mathcal{N} \prod_{|\mathbf{k}| \ \ k_{\rm F},\sigma} a^\dagger_{\mathbf{k}\sigma}|0\rangle\,, \tag{2.20}$$

where $|0\rangle$ denotes the state with zero electrons present. When the interaction is weak, one may anticipate that low-temperature properties will be governed by energetically low-lying excitations superimposed upon the state $|\Omega\rangle$. Therefore, remembering the philosophy whereby excitations rather than microscopic constituents play a prime role, one would like to declare the filled Fermi sea, $|\Omega\rangle$ (rather than the empty state $|0\rangle$), to be the "physical vacuum" of the theory. To make this compatible with the language of second quantization, we need to identify a new operator algebra $c_{\mathbf{k}\sigma}, c^\dagger_{\mathbf{k}\sigma}$ such that the new operators $c_{\mathbf{k}\sigma}$ annihilate the Fermi sea. This can be easily engineered by defining

$$c^\dagger_{\mathbf{k}\sigma} = \begin{array}{ll} a^\dagger_{\mathbf{k}\sigma}, & k > k_{\rm F}, \\ a_{\mathbf{k}\sigma}, & k \leq k_{\rm F}, \end{array} \qquad c_{\mathbf{k}\sigma} = \begin{array}{ll} a_{\mathbf{k}\sigma}, & k > k_{\rm F}, \\ a^\dagger_{\mathbf{k}\sigma}, & k \leq k_{\rm F}. \end{array} \tag{2.21}$$

It is then a straightforward matter to verify that $c_{\mathbf{k}\sigma}|\Omega\rangle = 0$, and that the canonical commutation relations are preserved.

The Hamiltonian defined through Eq. (2.18) and (2.19), represented in terms of the operator algebra (2.21) and the vacuum (2.20), forms the basis of the theory of interactions in highly mobile electron compounds. The investigation of the role of Coulomb interactions in such systems will provide a useful arena to apply the methods of quantum field theory formulated in subsequent chapters. Following our classification of electron systems, let us now turn our attention to a complementary class of materials where the lattice potential presents a strong perturbation on the conduction electrons. In such situations, realized, for example, in transition metal oxides, a description based on "almost localized" electron states will be used to represent the Hamiltonian (2.17).

Tight–binding systems

Let us consider a "rarefied" lattice in which the constituent ion cores are separated by a distance in excess of the typical Bohr radius of the valence band electrons. In this "**atomic limit**" the weight of the electron wavefunctions is "tightly bound" to the lattice centers. Here, to formulate a microscopic theory of interactions, it is convenient to expand the Hamiltonian in a local basis that reflects the atomic orbital states of the isolated ion. Such a representation is presented by the basis of **Wannier states** defined by

$$|\psi_{\mathbf{R}n}\rangle \equiv \frac{1}{\sqrt{N}} \sum_{\mathbf{k}}^{\text{B.Z.}} e^{-i\mathbf{k}\cdot\mathbf{R}} |\psi_{\mathbf{k}n}\rangle, \qquad |\psi_{\mathbf{k}n}\rangle = \frac{1}{\sqrt{N}} \sum_{\mathbf{R}} e^{i\mathbf{k}\cdot\mathbf{R}} |\psi_{\mathbf{R}n}\rangle, \tag{2.22}$$

where $\mathbf{R}$ denote the coordinates of the lattice centers, and $\sum_{\mathbf{k}}^{\text{B.Z.}}$ represents a summation over all momenta $\mathbf{k}$ in the first Brillouin zone. For a system with a vanishingly weak interatomic overlap, i.e. a lattice where V approaches a superposition of independent atomic potentials, the Wannier function $\psi_{\mathbf{R}n}(\mathbf{r}) \equiv \langle \mathbf{r}|\psi_{\mathbf{R}n}\rangle$ converges on the nth orbital of an isolated atom centered at coordinate $\mathbf{R}$. However, when the interatomic coupling is non-zero, i.e. in a "real" solid, the N formerly degenerate states labeled by n split to form an energy band (see figure below). Here, the Wannier functions (which, note, are not eigenfunctions of the Hamiltonian) differ from those of the atomic orbitals through residual oscillations in the region of overlap to ensure orthogonality of the basis. Significantly, in cases where the Fermi energy lies between two energetically separated bands, the system presents **insulating** behavior. Conversely, when the Fermi energy is located within a band, one may expect **metallic** behavior. Ignoring the complications that arise when bands begin to overlap, we will henceforth focus on metallic systems where the Fermi energy is located within a definite band n_0.

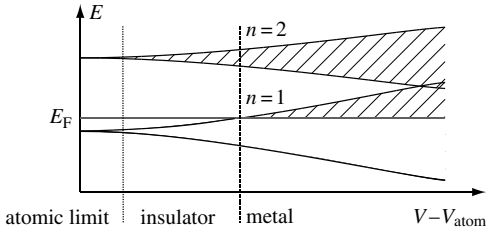

How can the Wannier basis be exploited to obtain a simplified representation of the general Hamiltonian (2.17)? The first thing to notice is that the Wannier states $\{|\psi_{\mathbf{R}n}\rangle\}$ form an orthonormal basis of the single-particle Hilbert space, i.e. the transformation between the real space and the Wannier representation is unitary, $|\mathbf{r}\rangle = \sum_{\mathbf{R}} |\psi_{\mathbf{R}}\rangle\langle\psi_{\mathbf{R}}|\mathbf{r}\rangle = \sum_{\mathbf{R}} \psi^*_{\mathbf{R}}(\mathbf{r})|\psi_{\mathbf{R}}\rangle$. (Here, since we are interested only in contributions arising from the particular "metallic" band n_0 in which the Fermi energy lies, we have dropped the remaining set of bands $n \neq n_0$ and, with them, reference to the specific band index.) (Exercise: By focusing on just a single band n_0, in what sense is the Wannier basis now complete?) As such, it induces a transformation

$$a^\dagger_\sigma(\mathbf{r}) = \sum_{\mathbf{R}} \psi^*_{\mathbf{R}}(\mathbf{r}) a^\dagger_{\mathbf{R}\sigma} \equiv \sum_i \psi^*_{\mathbf{R}_i}(\mathbf{r}) a^\dagger_{i\sigma}, \tag{2.23}$$

between the real space and the Wannier space operator basis, respectively. In the second representation, following a convention commonly used in the literature, we have labeled the lattice center coordinates $\mathbf{R} \equiv \mathbf{R}_i$ by a counting index $i = 1, \ldots, N$. Similarly, the

unitary transformation between Bloch and Wannier states Eq. (2.22) induces an operator transformation

$$a^\dagger_{\mathbf{k}\sigma} = \frac{1}{\sqrt{N}} \sum_i e^{i\mathbf{k}\cdot\mathbf{R}_i} a^\dagger_{i\sigma}, \qquad a^\dagger_{i\sigma} = \frac{1}{\sqrt{N}} \sum_{\mathbf{k}}^{\text{B.Z.}} e^{-i\mathbf{k}\cdot\mathbf{R}_i} a^\dagger_{\mathbf{k}\sigma}. \tag{2.24}$$

We can now use the transformation formulae (2.23) and (2.24) to formulate a Wannier representation of the Hamiltonian (2.17). Using the fact that the Bloch states diagonalize the single-particle component $\hat{H}_0$, we obtain

$$\hat{H}_0 = \sum_{\mathbf{k}} \epsilon_k a^\dagger_{\mathbf{k}\sigma} a_{\mathbf{k}\sigma} \overset{(2.24)}{=} \frac{1}{N} \sum_{ii'} \sum_{\mathbf{k}} e^{i\mathbf{k}(\mathbf{R}_i - \mathbf{R}_{i'})} \epsilon_k a^\dagger_{i\sigma} a_{i'\sigma} \equiv \sum_{ii'} a^\dagger_{i\sigma}\, t_{ii'}\, a_{i'\sigma},$$

where we have defined $t_{ii'} = N^{-1} \sum_{\mathbf{k}} e^{i\mathbf{k}\cdot(\mathbf{R}_i - \mathbf{R}_{i'})} \epsilon_k$. The new representation of $\hat{H}_0$ describes electrons hopping from one lattice center i' to another, i. The strength of the hopping matrix element $t_{ii'}$ is controlled by the effective overlap of neighboring atoms. In the extreme atomic limit, where the levels $\epsilon_k = \text{const.}$ are degenerate, $t_{ii'} \propto \delta_{ii'}$ and no inter-atomic transport is possible. The tight-binding representation becomes useful when $t_{i\neq i'}$ is non-vanishing, but the orbital overlap is so weak that only nearest neighbor hopping effectively contributes.

EXERCISE Taking a square lattice geometry, and setting $t_{ii'} = -t$ for i, i' nearest neighbors and zero otherwise, diagonalize the two-dimensional tight-binding Hamiltonian $\hat{H}_0$. Show that the eigenvalues are given by $\epsilon_{\mathbf{k}} = -2t(\cos(k_x a) + \cos(k_y a))$. Sketch contours of constant energy in the Brillouin zone and note the geometry at half-filling.

To assess the potency of the tight-binding approximation, let us consider its application to two prominent realizations of carbon-based lattice systems, graphene and carbon nanotubes.

INFO **Graphene** is a single layer of graphite: a planar hexagonal lattice of sp^2-hybridized[7] carbon atoms connected by strong covalent bonds of their three planar σ-orbitals. (See the Fig. 2.2 and figure overleaf for a schematic.) The remaining p_z orbitals – oriented vertically to the lattice plane – overlap weakly to form a band of mobile electrons. For a long time, it was thought that graphene sheets in isolation will inevitably be destabilized by thermal fluctuations; only layered stacks of graphene would mutually stabilize to form a stable compound – graphite. It thus came as a surprise when in 2004 a team of researchers[8] succeeded in the isolation of large (micron-sized) graphene flakes on an SiO_2 substrate. (Meanwhile, the isolation of even free standing graphene layers has become possible. In fact, our whole conception of the stability of the compound has changed. It is now believed that whenever you draw a pencil line, a trail of graphene flakes will be left behind.)

Immediately after its discovery, it became clear that graphene possesses unconventional conduction properties. Nominally a gapless semiconductor, it has an electron mobility $\sim 2 \times 10^5 \text{cm}^2/\text{Vs}$, by far more than that of even the purest silicon based semiconductors; it shows manifestations of the integer quantum Hall effect qualitatively different from those of conventional two-dimensional electron compounds (cf. Chapter 9 for a general discussion of the quantum Hall

[7] Although this will not be necessary to follow the text, readers may find it rewarding to recapitulate the quantum chemistry of sp^2-hybridized carbon and its covalent bonds.

[8] K. S. Novoselov, *et al.*, Electric field effect in atomically thin carbon films, *Science* **306** (2004), 666–9.

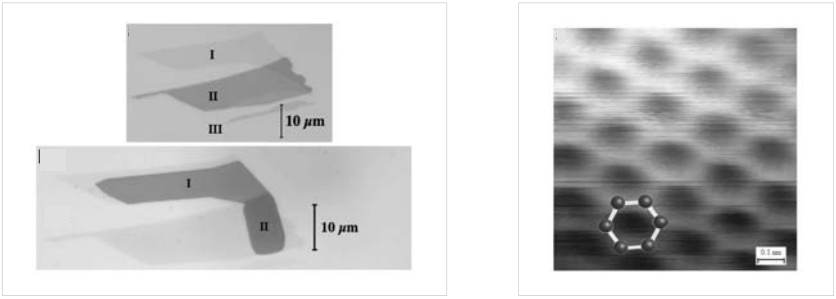

Figure 2.2 Left: optical microscopy image of graphene flakes. Regions labeled by I' define monolayer graphene sheets. Right: STM image of the graphene samples shown in the left part. Images taken from E. Stolyarova *et al.*, High-resolution scanning tunneling microscopy imaging of mesoscopic graphene sheets on an insulating surface, *PNAS* **104** (2007), 9210–12.

effect), etc. Although an in-depth discussion of graphene is beyond the scope of this text, we note that it owes most of its fascinating properties to its band structure: electrons in graphene show a linear dispersion and behave like two-dimensional Dirac fermions! By way of an illustration of the concepts discussed above, we here derive this unconventional band dispersion from a tight binding formulation of the system.

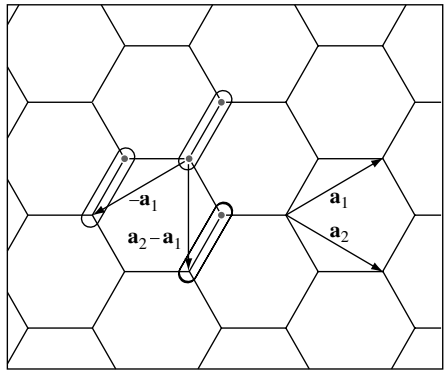

To a first approximation, graphene's π-electron system can be modeled as a tight-binding Hamiltonian characterized by a single hopping matrix element between neighboring atoms $-t$, and the energy offset ϵ of the p-electron states. To determine the spectrum of the system, one may introduce a system of bi-atomic unit cells (see the ovals in the schematic figure right) and two (non-orthogonal) unit vectors of the hexagonal lattice $\mathbf{a}_1 = (\sqrt{3}, 1)a/2$ and $\mathbf{a}_2 = (\sqrt{3}, -1)a/2$, where $a = |\mathbf{a}_1| = |\mathbf{a}_2| \simeq 2.46\,A$ denotes the lattice constant. The tight-binding Hamiltonian can then be represented in the form $\hat{H} = -\sum_{\langle \mathbf{r},\mathbf{r}' \rangle} (t a_1^\dagger(\mathbf{r}) a_2(\mathbf{r}') + \text{h.c.})$, where the sum runs over all nearest neighbor basis vectors of the unit cells (the coordinate vectors of the bottom left atom) and $a_{1(2)}^\dagger(\mathbf{r})$ creates a state in the first (second) atom of the cell at vector $\mathbf{r}$. Switching to a Fourier representation, the Hamiltonian assumes the form

$$\hat{H} = \sum_{\mathbf{k}\sigma} \begin{pmatrix} a_{1\sigma}^\dagger & a_{2\sigma}^\dagger \end{pmatrix} \begin{pmatrix} 0 & -tf(\mathbf{k}) \\ -tf^*(\mathbf{k}) & 0 \end{pmatrix} \begin{pmatrix} a_{1\sigma} \\ a_{2\sigma} \end{pmatrix}, \tag{2.25}$$

where $f(\mathbf{k}) = 1 + e^{-ik_1 a} + e^{i(-k_1+k_2)a}$.

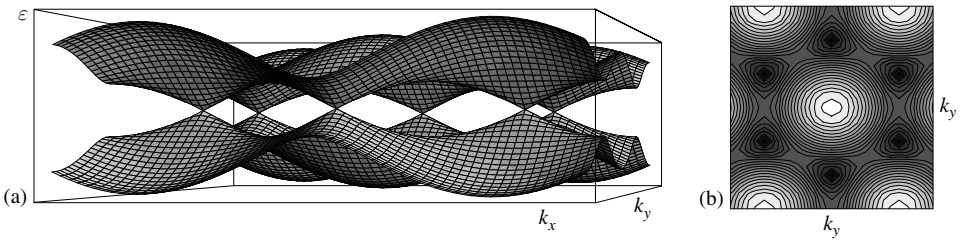

Figure 2.3 (a) Spectrum of the tight-binding Hamiltonian (2.24) showing the point-like structure of the Fermi surface when $E_F = 0$. (b) A contour plot of the same.

EXERCISE (Recall the concept of the reciprocal lattice in solid state theory.) To derive the Fourier representation above, show that a system of two reciprocal lattice vectors conjugate to the unit vectors above is given by $\mathbf{G}_{1/2} = \frac{2\pi}{\sqrt{3}a}(1, \pm\sqrt{3})$. Next, show that the Fourier decomposition of a field operator reads as $a_a(\mathbf{r}) = \frac{1}{\sqrt{N}} \sum_{\mathbf{k}} e^{-i\frac{a}{2\pi}(k_1\mathbf{G}_1 + k_2\mathbf{G}_2)\cdot\mathbf{r}} a_{a,\mathbf{k}}$, where $k_i \in [0, 2\pi/a]$ is quantized in units $2\pi/L_i$. (L_i is the extension of the system in the direction of $\mathbf{a}_i$ and N its total number of unit cells.) Substitute this decomposition into the real space representation of the Hamiltonian to arrive at the Fourier representation.

Diagonalizing the Hamiltonian, one obtains the dispersion relation,[9]

$$\epsilon_{\mathbf{k}} = \pm t|f(\mathbf{k})| = \pm t\sqrt{3 + 2\cos(k_1 a) + 2\cos((k_1 - k_2)a) + 2\cos(k_2 a)}. \tag{2.26}$$

Here, in contrast to the square lattice tight-binding Hamiltonian, the half-filled system is characterized by a point-like Fermi surface (see Figure 2.3). When lightly doped away from half-filling, the spectrum divides into Dirac-like spectra with a linear dispersion. Fig. 2.3 shows the full spectrum of the tight binding Hamiltonian. Notice that of the six Dirac points displayed in the figure only two are independent. The complementary four can be reached from those two points by addition of a reciprocal lattice vector and, therefore, do not represent independent states.

EXERCISE Derive an explicit representation of the **Dirac-Hamiltonian** describing the low-energy physics of the system. To this end, choose two inequivalent (not connected by reciprocal lattice vectors) zero-energy points $\mathbf{k}_{1,2}$ in the Brillouin zone. Expand the Hamiltonian (2.25) around these two points in small momentum deviations $\mathbf{q} \equiv \mathbf{k} - \mathbf{k}_{1,2}$ up to linear order. Show that in this approximation, $\hat{H}$ reduces to the sum of two two-dimensional Dirac Hamiltonians.

Now, against this background, let us consider the **carbon nanotube** system. A single-wall nanotube describes a one-dimensional structure involving a graphene sheet rolled into a cylinder (see Fig 2.4 for an STM image of a carbon nanotube). Tubes of comparatively simple structure are obtained by rolling the hexagonal pattern of the sheet along one of its two axes of symmetry: along the $\mathbf{a}_1$-direction one obtains a **zig-zag tube** and along the

[9] P. R. Wallace, The band theory of graphite, *Phys. Rev.* **71** (1947), 622–34.

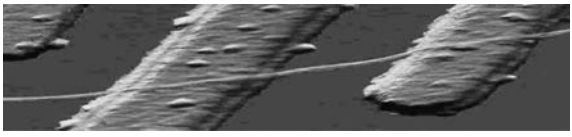

Figure 2.4 STM image of a carbon nanotube contacted with Pt electrodes. (Source: Courtesy of C. Dekker.)

$(\mathbf{a}_1 + \mathbf{a}_2)$-direction an **armchair tube** (Exercise: Where do you see an armchair?). More complex, "chiral" structures involve twists along the circumference of the tube.

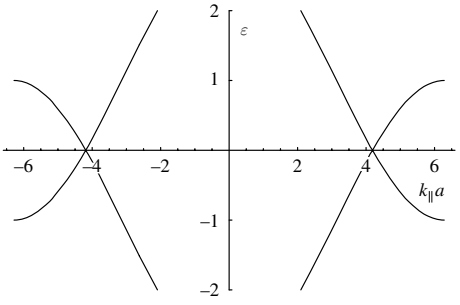

By knowing the band structure of graphene, the dispersion of the nanotube system can be straightforwardly inferred. The situation is most easily visualized for the achiral geometries. Essentially a graphene sheet with periodic boundary conditions and length L in the direction transverse to the length of the tube, the quasi-one-dimensional system has a spectrum that obtains by projection of the two-dimensional dispersion onto lines indexed by the discrete values $k_\perp$ along the compact axis. For example, the dispersion of lowest transverse harmonic, $k_\perp = 0$, of the armchair tube is given by (see the figure)

$$\epsilon_{k_\parallel} = \pm t\sqrt{3 + 4\cos(k_\parallel a/2) + 2\cos(k_\parallel a)}.$$

Notice the presence of two nodal points in the spectrum. Electrons with longitudinal momentum close to one of these two "hot spots" propagate with approximately linear dispersion. The physics of effectively one-dimensional electron systems of this type will be discussed in Section 2.2 below.

EXERCISE Verify the one-dimensional dispersion relation $\epsilon_{k_\parallel}$ above. To this end, notice that the single-electron wave functions of the system must obey periodic boundary conditions $\psi(\mathbf{r} + N(\mathbf{a}_1 + \mathbf{a}_2)) = \psi(\mathbf{r})$, where N is the number of cells in the transverse direction (i.e. $L_\perp \equiv N|\mathbf{a}_1 + \mathbf{a}_2| = Na\sqrt{3}$ is the circumference of the tube). Use this condition to obtain the quantization rule $k_1 + k_2 = 2\pi\sqrt{3}m/L_\perp$, where m is integer. When evaluated for the lowest harmonic, $m = 0$, the dispersion relation (2.26) collapses to $\epsilon_{k_\parallel}$ (where $k_\parallel = k_1 - k_2$ is the momentum in the longitudinal direction). Show that the zig-zag tube supports zero-energy excitations only for specific values of the transverse lattice spacings N. In general, it is insulating with a band gap of ca. 0.5 eV. In the case of the chiral tubes, it may be shown that a third of the tubes are semi-metallic while all others are insulating.[10]

[10] For futher details on the electronic structure of carbon nanotubes, we refer to the text *Physical Properties of Carbon Nanotubes* by R. Saito, G. Dresselhaus, and M. S. Dresselhaus (Imperial College Press, 1998).

Interaction effects in the tight-binding system

Although the pseudopotential of the *nearly free electron system* accommodates the effects of Coulomb interaction between the conduction and valence band electrons, the mutual Coulomb interaction between the conduction electrons themselves may lead to new physical phenomena. These effects can substantially alter the material parameters (e.g. effective masses), however, they neither change the nature of the ground state, nor that of the elementary quasi-particle excitations in any fundamental way – this is the content of Fermi-liquid theory, and a matter to which we will return. By contrast even weak interaction effects significantly influence the physics of the *tight-binding system*. Here, commensurability effects combined with interaction may drive the system towards a correlated magnetic state or an insulating phase.

To understand why, let us re-express the interaction in field operators associated with the Wannier states. Once again, to keep our discussion simple (yet generic in scope), let us focus attention on a single sub-band and drop reference to the band index. Then, applied to the Coulomb interaction, the transformation (2.23) leads to the expansion $\hat{V}_{\rm ee} = \sum_{ii'jj'} U_{ii'jj'} a^\dagger_{i\sigma} a^\dagger_{i'\sigma'} a_{j\sigma} a_{j'\sigma'}$ where

$$U_{ii'jj'} = \frac{1}{2} \int d^d r \int d^d r' \, \psi^*_{\mathbf{R}_i}(\mathbf{r}) \psi_{\mathbf{R}_j}(\mathbf{r}) V(\mathbf{r}-\mathbf{r}') \psi^*_{\mathbf{R}_{i'}}(\mathbf{r}') \psi_{\mathbf{R}_{j'}}(\mathbf{r}'). \tag{2.27}$$

Taken together, the combination of the contributions $\hat{H}_0$ and $\hat{V}_{\rm ee}$,

$$\boxed{\hat{H} = \sum_{ii'} a^\dagger_{i\sigma} t_{ii'} a_{i'\sigma} + \sum_{ii'jj'} U_{ii'jj'} a^\dagger_{i\sigma} a^\dagger_{i'\sigma'} a_{j'\sigma'} a_{j\sigma},} \tag{2.28}$$

where the sum of repeated spin indices is implied, defines the **tight-binding representation** of the interaction Hamiltonian. Apart from the neglect of the neighboring sub-bands, the Hamiltonian is exact. Yet, to assimilate the effects of the interaction, it is useful to assess the relative importance of the different matrix elements drawing on the nature of the atomic limit that justified the tight-binding description. We will thus focus on contributions to $U_{ii'jj'}$ where the indices are either equal or, at most, nearest neighbors. Focusing on the most relevant of these matrix elements, a number of physically different contributions can be identified:

- ▷ The **direct terms** $U_{ii'ii'} \equiv V_{ii'}$ involve integrals over square moduli of Wannier functions and couple *density "uctuations* at neighboring sites, $\sum_{i \neq i'} V_{ii'} \hat{n}_i \hat{n}_{i'}$, where $\hat{n}_i = \sum_\sigma a^\dagger_{i\sigma} a_{i\sigma}$. This contribution accounts for the – essentially classical – interaction between charges localized at neighboring sites (see Fig. 2.5). In certain materials, interactions of this type have the capacity to induce global instabilities in the charge distribution known as **charge density wave** instabilities.
- ▷ A second important contribution derives from the **exchange coupling**, which induces magnetic correlations among the electron spins. Setting $J^{\rm F}_{ij} \equiv U_{ijji}$, and making use of

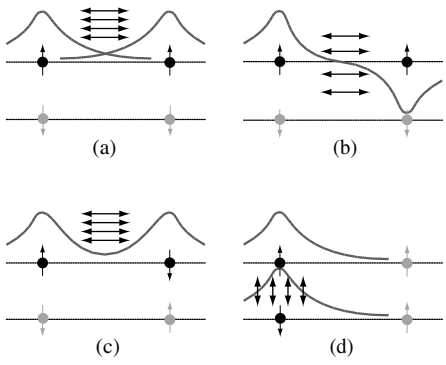

Figure 2.5 Different types of interaction mechanism induced by the tight-binding interaction $V_{\rm ee}$. The curves symbolically indicate wavefunction envelopes. (a) Direct Coulomb interaction between neighboring sites. Taking account of the exchange interaction, parallel alignment of spins (b) is preferred since it enforces anti-symmetry of the spatial wave function. By contrast, for anti-parallel spin configurations (c) the wave function amplitude in the repulsion zone is enhanced. (d) Coulomb interaction between electrons of opposite spin populating the same site.

Pauli matrix identities (see below), one obtains

$$\sum_{i\neq j} U_{ijji} a^\dagger_{i\sigma} a^\dagger_{j\sigma'} a_{i\sigma'} a_{j\sigma} = -2 \sum_{i\neq j} J^{\rm F}_{ij} \left(\hat{\mathbf{S}}_i \cdot \hat{\mathbf{S}}_j + \frac{1}{4} \hat{n}_i \hat{n}_j \right).$$

Such contributions tend to induce weak **ferromagnetic coupling** of neighboring spins (i.e. $J^{\rm F} > 0$). The fact that an effective *magnetic* coupling is born out of the *electrostatic* interaction between quantum particles is easily understood. Consider two electrons inhabiting neighboring sites. The Coulomb repulsion between the particles is minimized if the orbital two-particle wave function is anti-symmetric and, therefore, has low amplitude in the interaction zone between the particles. Since the overall wavefunction must be anti-symmetric, the energetically favored real-space configuration enforces a symmetric alignment of the two spins. Such a mechanism is familiar from atomic physics where it is manifested as **Hund's rule**. In general, magnetic interactions in solids are usually generated as an indirect manifestation of the much stronger Coulomb interaction.

EXERCISE Making use of the Pauli matrix identity $\sigma_{\alpha\beta} \cdot \sigma_{\gamma\delta} = 2\delta_{\alpha\delta}\delta_{\beta\gamma} - \delta_{\alpha\beta}\delta_{\gamma\delta}$, show that $\hat{\mathbf{S}}_i \cdot \hat{\mathbf{S}}_j = -a^\dagger_{i\alpha} a^\dagger_{j\beta} a_{i\beta} a_{j\alpha}/2 - \hat{n}_i \hat{n}_j/4$ where, as usual, $\hat{\mathbf{S}}_i = a^\dagger_{i\alpha} \sigma_{\alpha\beta} a_{i\beta}/2$ denotes the operator for spin 1/2, and the lattice sites i and j are assumed distinct.

▷ Finally, far into the atomic limit, where the atoms are very well separated, and the overlap between neighboring orbitals is weak, the matrix elements t_{ij} and $J^{\rm F}_{ij}$ are exponentially small in the interatomic separation. In this limit, the "on-site" Coulomb or **Hubbard interaction**, $U_{iiii} \equiv U/2$, $\sum_{i\sigma\sigma'} U_{iiii} a^\dagger_{i\sigma} a^\dagger_{i\sigma'} a_{i\sigma'} a_{i\sigma} = \sum_i U \hat{n}_{i\uparrow} \hat{n}_{i\downarrow}$, generates the dominant interaction mechanism. Taking only the nearest neighbor contribution to the hopping matrix elements, and neglecting the energy offset due to the diagonal term, the effective

Hamiltonian takes a simplified form known as the **Hubbard model**,

$$\hat{H} = -t \sum_{\langle ij \rangle} a^{\dagger}_{i\sigma} a_{j\sigma} + U \sum_{i} \hat{n}_{i\uparrow} \hat{n}_{i\downarrow}, \tag{2.29}$$

where $\langle ij \rangle$ is a shorthand used to denote neighboring lattice sites. In hindsight, a model of this structure could have been proposed from the outset on purely phenomenological grounds: electrons tunnel between atomic orbitals localized on individual lattice sites while double occupancy of a lattice site incurs an energetic penalty associated with the mutual Coulomb interaction.

Mott–Hubbard transition and the magnetic state

Deceptive in its simplicity, the Hubbard model is acknowledged as a paradigm of strong electron correlation in condensed matter. Yet, after 40 years of intense investigation, the properties of this seemingly simple model system – the character of the ground state and nature of the quasi-particle excitations – are still the subject of controversy (at least in dimensions higher than one – see below). Nevertheless, given the importance attached to this system, we will close this section with a brief discussion of the remarkable phenomenology that is believed to characterize the Hubbard system.

As well as dimensionality, the phase behavior of the Hubbard Hamiltonian is characterized by three dimensionless parameters: the ratio of the Coulomb interaction scale to the bandwidth U/t, the particle density or filling fraction n (i.e. the average number of electrons per site), and the (dimensionless) temperature, T/t. The symmetry of the Hamiltonian under particle–hole interchange (exercise) allows one to limit consideration to densities in the range $0 \leq n \leq 1$ while densities $1 < n \leq 2$ can be inferred by "reflection."

Focusing first on the low temperature system, in the dilute limit $n \ll 1$, the typical electron wavelength is greatly in excess of the site separation and the dynamics are free. Here the local interaction presents only a weak perturbation and one can expect the properties of the Hubbard system to mirror those of the weakly interacting nearly free electron system. While the interaction remains weak one expects a metallic behavior to persist.

Sir Neville Francis Mott 1905–96
Nobel Laureate in Physics in 1977, with Philip W. Anderson and John H. van Vleck, for their "fundamental theoretical investigations of the electronic structure of magnetic and disordered systems." Amongst his contributions to science, Mott provided a theoretical basis to understand the transition of materials from metallic to nonmetallic states (the Mott transition). (Image © The Nobel Foundation.)

By contrast, let us consider the half-filled system where the average site occupancy is unity. Here, if the interaction is weak, $U/t \ll 1$, one may again expect properties reminiscent

of the weakly interacting electron system.[11] If, on the other hand, the interaction is very strong, $U/t \gg 1$, site double occupancy is inhibited and electrons in the half-filled system become "jammed": migration of an electron to a neighboring lattice site necessitates site double occupancy incurring an energy cost U. Here, in this strongly correlated state, the mutual Coulomb interaction between the electrons drives the system from a metallic to an insulating phase with properties very different from those of a conventional band insulator.

INFO Despite the ubiquity of the experimental phenomenon (first predicted in a celebrated work by Mott) the nature of the **Mott–Hubbard transition** from the metallic to the insulating phase in the half-filled system has been the subject of considerable discussion and debate. In the original formulation, following a suggestion of Peierls, Mott conceived of an insulator characterized by two "Hubbard bands" with a bandwidth $\sim t$ separated by a charge gap U.[12] States of the upper band engage site double occupancy while those states that make up the lower band do not. The transition between the metallic and the insulating phase was predicted to occur when the interaction was sufficiently strong that a charge gap develops between the bands. Later, starting from the weakly interacting Fermi-liquid, Brinkman and Rice[13] proposed that the transition was associated with the localization of quasi-particles created by an interaction driven renormalization of the effective mass. Finally, a third school considers the transition to the Mott insulating phase as inexorably linked to the development of magnetic correlations in the weak coupling system – the Slater instability.

In fact, the characterizations of the transition above are not mutually exclusive. Indeed, in the experimental system, one finds that all three possibilities are, in a sense, realized. In particular, a transition between the Mott insulating phase and an itinerant electron phase can be realized in two ways. In the first case, one can reduce the interaction strength U/t while, in the second, one can introduce charge carriers (or vacancies) into the half-filled system. Experimentally, the characteristic strength of the interaction is usually tuned by changing the bandwidth t through external pressure (see Fig. 2.6), while a system may be doped away from half-filling by chemical substitution. Remarkably, by focusing on the scaling behavior close to the critical end-point, researchers have been able to show that the Mott transition in this system belongs to the universality class of the three-dimensional Ising model (see the discussion of critical phenomena in Chapter 8). Lowering the temperature, both the Mott insulating phase and the strongly correlated metallic phase exhibit a transition to a magnetic phase where the local moments order antiferromagnetically (for the explanation of this phenomenon, see below).

Experimentally, it is often found that the low-temperature phase of the Mott insulator is accompanied by the **anti-ferromagnetic ordering** of the local moments. The origin of these magnetic correlations can be traced to a mechanism known as superexchange and can be understood straightforwardly within the framework of the Hubbard model system.

[11] In fact, one has to exercise some caution since the commensurability of the Fermi wavelength with the lattice can initiate a transition to an insulating **spin density wave** state characterized by a small quasi-particle energy gap. In later chapters, we will discuss the nature of this **Slater instability** (J. C. Slater, Magnetic effects and the Hartree–Fock equation, *Phys. Rev.* **82** (1951), 538–41) within the framework of the quantum field integral.

[12] N. F. Mott, The basis of the electron theory of metals with special reference to the transition metals, *Proc. Roy. Soc. A* **62** (1949), 416–22 – for a review see, e.g., N. F. Mott, Metal–insulator transition, *Rev. Mod. Phys.* **40** (1968), 677–83, or N. F. Mott, *Metal–Insulator Transitions*, 2nd ed. (Taylor and Francis, 1990).

[13] W. Brinkman and T. M. Rice, Application of Gutzwiller's variational method to the metal–insulator transition, *Phys. Rev. B* **2** (1970), 4302–4.

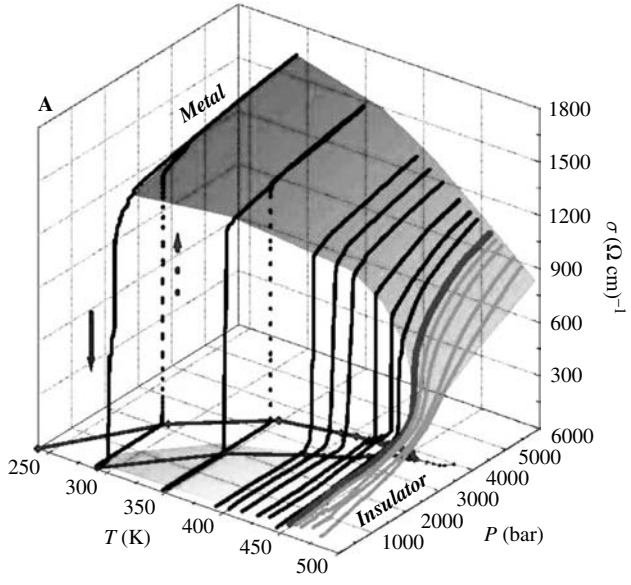

Figure 2.6 Conductivity of Cr-doped V_2O_3 as a function of decreasing pressure and temperature. At temperatures below the Mott–Hubbard transition point ($P_c = 3738\,\text{bar}$, $T_c = 457.5\,\text{K}$) the conductivity reveals hysteretic behavior characteristic of a first-order transition. (Reprinted from P. Limelette, A. Georges, D. Jérome, *et al.*, Universality and critical behavior at the Mott transition, *Science* **302** (2003), 89–92. Copyright 2003 AAAS.)

To this end, one may consider a simple "two-site" system from which the characteristics of the infinite lattice system can be inferred. For the two-site system, at half-filling (i.e. with just two electrons to share between the two sites), one can identify a total of six basis states: two spin-polarized states $a^\dagger_{1\uparrow}a^\dagger_{2\uparrow}|\Omega\rangle$, $a^\dagger_{1\downarrow}a^\dagger_{2\downarrow}|\Omega\rangle$, and four states with $S^z_{\text{total}} = 0$: $|s_1\rangle = a^\dagger_{1\uparrow}a^\dagger_{2\downarrow}|\Omega\rangle$, $|s_2\rangle = a^\dagger_{2\uparrow}a^\dagger_{1\downarrow}|\Omega\rangle$, $|d_1\rangle = a^\dagger_{1\uparrow}a^\dagger_{1\downarrow}|\Omega\rangle$, and $|d_2\rangle = a^\dagger_{2\uparrow}a^\dagger_{2\downarrow}|\Omega\rangle$. Recalling the constraints imposed by the Pauli principle, it is evident that the fully spin polarized states are eigenstates of the Hubbard Hamiltonian with zero energy, while the remaining eigenstates involve superpositions of the basis states $|s_i\rangle$ and $|d_i\rangle$. In the strong coupling limit $U/t \gg 1$, the ground state will be composed predominantly of states with no double occupancy, $|s_i\rangle$. To determine the precise structure of the ground state, we could simply diagonalize the 4×4 Hamiltonian exactly – a procedure evidently infeasible in the large lattice system. Instead, to gain some intuition for the extended system, we will effect a perturbation theory which projects the insulating system onto a low-energy effective spin Hamiltonian. Specifically, we will treat the hopping part of the Hamiltonian $\hat{H}_t$ as a weak perturbation of the Hubbard interaction $\hat{H}_U$.

To implement the perturbation theory, it is helpful to invoke a canonical transformation of the Hamiltonian, namely

$$\hat{H} \mapsto \hat{H}' \equiv e^{-t\hat{O}}\hat{H}e^{t\hat{O}} = e^{-t[\hat{O},\,]}\hat{H} \equiv \hat{H} - t[\hat{O},\hat{H}] + \frac{t^2}{2!}[\hat{O},[\hat{O},\hat{H}]] + \cdots , \tag{2.30}$$

where the exponentiated commutator is defined by the series expansion on the right.

EXERCISE Prove the second equality. (Hint: Consider the derivative of $\hat{H}'$ with respect to t.)

By choosing the operator $\hat{O}$ such that $\hat{H}_t + t[\hat{H}_U, \hat{O}] = 0$, all terms at first order in t can be eliminated from the transformed Hamiltonian. As a result, the effective Hamiltonian is brought to the form

$$\hat{H}' = \hat{H}_U + \frac{t}{2}[\hat{H}_t, \hat{O}] + \mathcal{O}(t^3). \tag{2.31}$$

Applying the ansatz, $t\hat{O} = [\hat{P}_\mathrm{s}\hat{H}_t\hat{P}_\mathrm{d} - \hat{P}_\mathrm{d}\hat{H}_t\hat{P}_\mathrm{s}]/U$, where $\hat{P}_\mathrm{s}$ and $\hat{P}_\mathrm{d}$ are operators that project onto the singly and doubly occupied subspaces respectively, the first-order cancellation is assured.

EXERCISE To verify this statement, take the matrix elements of the first-order equation with the basis states. Alternatively, it can be confirmed by inspection, noting that $\hat{P}_\mathrm{s}\hat{P}_\mathrm{d} = 0$, $\hat{H}_U\hat{P}_\mathrm{s} = 0$, and, in the present case, $\hat{P}_\mathrm{s}\hat{H}_t\hat{P}_\mathrm{s} = \hat{P}_\mathrm{d}\hat{H}_t\hat{P}_\mathrm{d} = 0$.

Substituting this result into Eq. (2.31) and projecting onto the singly occupied subspace one obtains

$$\hat{P}_\mathrm{s}\hat{H}'\hat{P}_\mathrm{s} = -\frac{1}{U}\hat{P}_\mathrm{s}\hat{H}_t\hat{P}_\mathrm{d}\hat{H}_t\hat{P}_\mathrm{s} = -2\frac{t^2}{U}\hat{P}_\mathrm{s}\left(1 + a^\dagger_{1\sigma}a^\dagger_{2\sigma'}a_{1\sigma'}a_{2\sigma}\right)\hat{P}_\mathrm{s} = J\left(\hat{\mathbf{S}}_1 \cdot \hat{\mathbf{S}}_2 - \frac{1}{4}\right),$$

where $J = 4t^2/U$ denotes the strength of the **anti-ferromagnetic** exchange interaction that couples the spins on neighboring sites.

EXERCISE Remembering the anti-commutation relations of the electron operators, find the matrix elements of the Hubbard Hamiltonian on the four basis states $|s_i\rangle$ and $|d_i\rangle$. Diagonalizing the 4×4 matrix Hamiltonian, obtain the eigenstates of the system. In the strong coupling system $U/t \gg 1$, determine the spin and energy dependence of the ground state.

Philip W. Anderson 1923–

Nobel Laureate in Physics in 1977, with Sir Neville Mott and John H. van Vleck, for their "fundamental theoretical investigations of the electronic structure of magnetic and disordered systems." Anderson made numerous contributions to theoretical physics from theories of localization and antiferromagnetism to superconductivity. (Image © The Nobel Foundation.)

The perturbation theory above shows that electrons subject to a strong local repulsive Coulomb interaction have a tendency to adopt an antiparallel or antiferromagnetic spin configuration between neighboring sites. This observation has a simple physical interpretation. Anti-parallel spins can take advantage of the hybridization (however small) and reduce their kinetic energy by hopping to a neighboring site (see Fig. 2.7). Parallel spins on the other hand are restricted from participating in this virtual process by the Pauli principle. This mechanism, which involves a two-step process, was first formulated by Anderson[14] and is known as **superexchange**.

[14] P. W. Anderson, Antiferromagnetism. Theory of superexchange interaction, *Phys. Rev.* **79** (1950) 350–6.

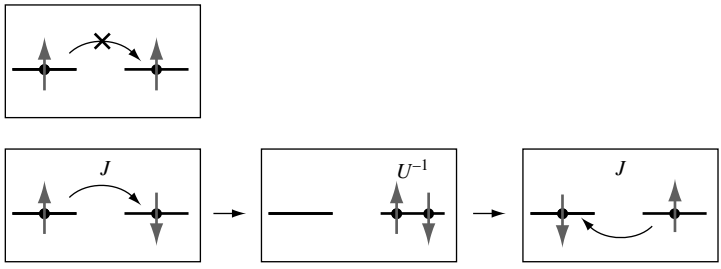

Figure 2.7 Top: hybridization of spin polarized states is forbidden by Pauli exclusion. Bottom: superexchange mechanism by which two antiparallel spins can lower their energy by a virtual process in which the upper Hubbard band is occupied.

The calculation presented above is easily generalized to an extended lattice system. Once again, projecting onto a basis in which all sites are singly occupied, virtual exchange processes favor an antiferromagnetic arrangement of neighboring spins. Such a correlated magnetic insulator is described by the quantum spin-(1/2) **Heisenberg Hamiltonian**

$$\boxed{\hat{H} = J \sum_{\langle mn \rangle} \hat{\mathbf{S}}_m \cdot \hat{\mathbf{S}}_n,} \tag{2.32}$$

where, as usual, $\langle mn \rangle$ denotes a sum of neighboring spins on the lattice and the positive exchange constant $J \sim t^2/U$. While, in the insulating magnetic phase, the charge degrees of freedom remain "quenched," spin fluctuations can freely propagate.

When doped away from half-filling, the behavior of the Hubbard model is notoriously difficult to resolve. The removal of electrons from the half-filled system introduces vacancies into the "lower Hubbard band" that may propagate through the lattice. For a low concentration of holes, the strong coupling Hubbard system may be described by the effective **t–J Hamiltonian**,

$$\boxed{\hat{H}_{t-J} = -t \sum_{\langle mn \rangle} \hat{P}_s a^\dagger_{m\sigma} a_{n\sigma} \hat{P}_s + J \sum_{\langle mn \rangle} \hat{\mathbf{S}}_m \cdot \hat{\mathbf{S}}_n.}$$

However, the passage of vacancies is frustrated by the antiferromagnetic spin correlations of the background. Here transport depends sensitively on the competition between the exchange energy of the spins and the kinetic energy of the holes. Oddly, at $J = 0$ (i.e. $U = \infty$), the ground state spin configuration is known to be driven ferromagnetic by a *single* hole while, for $J > 0$, it is generally accepted that a critical concentration of holes is required to destabilize antiferromagnetic order.

EXERCISE At $U = \infty$, all 2^N states of the half-filled Hubbard model are degenerate – each site is occupied by a single electron of arbitrary spin. This degeneracy is lifted by the removal of a single electron from the lower Hubbard band. In such a case, there is a theorem due to

Nagaoka[15] that, on a bipartite lattice (i.e. one in which the neighbors of one sublattice belong to the other sublattice), the ground state is ferromagnetic. For a four-site "plaquette" with three electrons determine the eigenspectrum of the Hubbard system with $U = \infty$ within the manifold (a) $S^z_{\text{total}} = 3/2$, and (b) $S^z_{\text{total}} = 1/2$. In each case, determine the total spin of the ground state. (Hint: In (b) there are a total of 12 basis states – here it useful to arrange these states in the order in which they are generated by application of the Hamiltonian.)

INFO The rich behavior of the Mott–Hubbard system is nowhere more exemplified than in the **ceramic cuprate system** – the basic material class of the high-temperature superconductors. Cuprates are built of layers of CuO_2 separated by heavy rare earth ions such as lanthanum. Here, the copper ions adopt a square lattice configuration separated by oxygen ions. At half-filling, electrons in the outermost occupied shell of the copper sites in the plane adopt a partially filled $3\,d^9$ configuration, while the oxygen sites are completely filled. Elevated in energy by a frozen lattice distortion, the Fermi energy lies in the $d_{x^2-y^2}$ orbital of copper. According to a simple band picture, the single band is exactly half-filled (one electron per Cu site) and, therefore, according to the standard band picture, should be metallic. However, strong electron interaction drives the cuprate system into an insulating antiferromagnetic Mott–Hubbard phase.

When doped away from half-filling (by, for example, replacing the rare earth atoms by others with a different stoichiometry; see the figure, where the phase diagram of $La_{2-x}Sr_xCuO_4$ is shown as a function of the concentration x of Sr atoms replacing La atoms and temperature), charge carriers are introduced into the "lower Hubbard band." However, in this case, the collapse of the Hubbard gap and loss of antiferromagnetic (AF) order is accompanied by the development of a high-temperature unconventional superconducting (SC) phase whose mechanism is believed to be rooted in the exchange of antiferromagnetic spin fluctuations. Whether the rich phenomenology of the cuprate system is captured by the Hubbard model remains a subject of great interest and speculation.

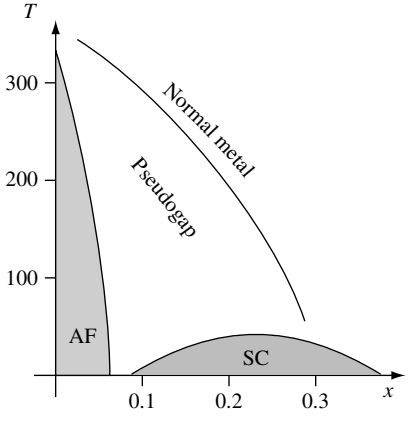

This concludes our preliminary survey of the rich phenomenology of the interacting electron system. Notice that, so far, we have merely discussed ways to distill a reduced model from the original microscopic many-body Hamiltonian (2.17). However, save for the two examples of free field theories analyzed in Chapter 1, we have not yet learned how methods of second quantization can be applied to actually solve problems. To this end, in the following section we will illustrate the application of the method on a prominent *strongly* interacting problem.

[15] Y. Nagaoka, Ferromagnetism in a narrow, almost half-filled s-band, *Phys. Rev.* **147** (1966), 392–405.

Interacting fermions in one dimension

Within the context of many-body physics, a theory is termed **free** if the Hamiltonian is bilinear in creation and annihilation operators, i.e. $\hat{H} \sim \sum_{\mu\nu} a_\mu^\dagger H_{\mu\nu} a_\nu$, where H may be a finite- or infinite-dimensional matrix.[16] Such models are "solvable" in the sense that the solution of the problem simply amounts to a diagonalization of the matrix $H_{\mu\nu}$ (subject to the preservation of the commutation relations of the operators a and $a^\dagger$). However, only a few models of interest belong to this category. In general, interaction contributions typically quartic in the field operators are present and complete analytical solutions are out of reach.

Yet there are a few precious examples of genuinely interacting systems that are amenable to (nearly) exact solution. In this section we will address an important representative of this class, namely the one-dimensional interacting electron gas. Not only is the analysis of this system physically interesting but, in addition, it provides an opportunity to practice working with the second quantized operator formalism on a deeper level.

Qualitative discussion

Consider the nearly free electron Hamiltonian (2.18) and (2.19) reduced to a one-dimensional environment. Absorbing the chemical potential E_F into the definition of the Hamiltonian, and neglecting spin degrees of freedom (e.g. one might consider a fully spin polarized band),

$$\hat{H} = \sum_k a_k^\dagger \left(\frac{k^2}{2m} - E_\mathrm{F} \right) a_k + \frac{1}{2L} \sum_{kk',q\neq 0} V(q) a_{k-q}^\dagger a_{k'+q}^\dagger a_{k'} a_k. \tag{2.33}$$

INFO At first sight, the treatment of a one-dimensional electron system may seem an academic exercise. However, effective one-dimensional interacting fermion systems are realized in a surprisingly rich spectrum of materials. We have already met with **carbon nanotubes** above. A nanotube is surrounded by clouds of mobile electrons (see earlier discussion in section 2.2). With the latter, confinement of the circumferential direction divides the system into a series of one-dimensional bands, each classified by a sub-band index and a wavenumber k. At low temperatures, the Fermi surface typically intersects a single sub-band, allowing attention to be drawn to a strictly one-dimensional system. A similar mechanism renders certain **organic molecules** (such as the Bechgaard salt $(\mathrm{TMTSF})_2\mathrm{PF}_6$, where TMTSF stands for the tetramethyl-tetraselenafulvalene) one-dimensional conductors.

A third, solid state, realization is presented by artificial low-dimensional structures fabricated from semiconducting devices. Redistribution of electron charge at the interface of a GaAs/AlGaAs heterostructure results in the formation of a two-dimensional electron gas. By applying external gates, it is possible to fabricate quasi-one-dimensional **semiconductor quantum wires** in which electron motion in the transverse direction is impeded by a large potential gradient (Fig. 2.8 (a)). At sufficiently low Fermi energies, only the lowest eigenstate of the transverse Schrödinger equation (the lowest "quantum mode") is populated and one is left with a strictly one-dimensional electron system. There are other realizations, such as edge modes in **quantum Hall systems**, "**stripe phases**" in high-tempterature superconductors, or certain **inorganic crystals**, but we shall not discuss these here explicitly.

[16] More generally, a free Hamiltonian may also contain contributions $\sim a_\mu a_\nu$ and $a_\mu^\dagger a_\nu^\dagger$.

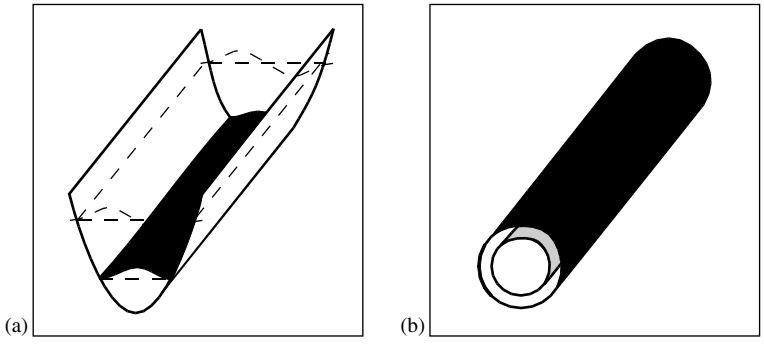

Figure 2.8 Different realizations of one-dimensional electron systems. (a) Steep potential well (realizable in, e.g., gated two-dimensional electron systems). (b) (Approximately) cylindrical quantum system (carbon nanotubes, quasi-one-dimensional molecules, etc.). In both cases, the single-particle spectrum is subject to mechanisms of size quantization. This leads to the formation of "minibands" (indicated by shaded areas in the figure), structureless in the transverse direction and extended in the longitudinal direction.

The one-dimensional fermion system exhibits a number of features not shared by higher-dimensional systems. The origin of these peculiarities can be easily understood from a simple qualitative picture. Consider an array of interacting fermions confined to a line. To optimize their energy the electrons can merely "push" each other around, thereby creating density fluctuations. By contrast, in higher-dimensional systems, electrons are free to avoid contact by moving around each other. A slightly different formulation of the same picture can be given in momentum space. The Fermi "sphere" of the one-dimensional system is defined through the interval $[-k_{\rm F}, k_{\rm F}]$ of filled momentum states. The Fermi "surface" consists of two isolated points, $\{k_{\rm F}, -k_{\rm F}\}$ (see the figure below). By contrast, higher-dimensional systems typically exhibit continuous and simply connected Fermi surfaces. It takes little imagination to anticipate that an extended Fermi sphere provides more phase space to two-particle interaction processes than the two isolated Fermi energy sectors of the one-dimensional system. The one-dimensional electron system represents a rare exception of an interacting system that can be solved under no more than a few, physically weak, simplifying assumptions. This makes it a precious test system on which non-perturbative quantum manifestations of many-body interactions can be explored.

Quantitative analysis

We now proceed to develop a quantitative picture of the charge density excitations of the one-dimensional electron system. Anticipating that, at low temperatures, the relevant dynamics will take place in the vicinity of the two Fermi points $\{k_{\rm F}, -k_{\rm F}\}$, the Hamiltonian (2.33) can be reduced further to an effective model describing the propagation of left and right moving excitations. To this end, we first introduce the notation that the subscripts R/L indicate that an operator $a^{\dagger}_{(+/-)k_{\rm F}+q}$ creates an electron that moves to the right/left with velocity $\simeq v_{\rm F} \equiv k_{\rm F}/m$.

We next observe (see the figure below) that, in the immediate vicinity of the Fermi points, the dispersion relation is approximately linear, implying that the non-interacting part of

the Hamiltonian can be represented as (exercise)

$$\hat{H}_0 \simeq \sum_{s=\mathrm{R,L}} \sum_q a^\dagger_{sq} \sigma_s v_\mathrm{F} q \, a_{sq}, \tag{2.34}$$

where $\sigma_s = (+/-)$ for $s = \mathrm{R/L}$ and the summation over q is restricted by some momentum

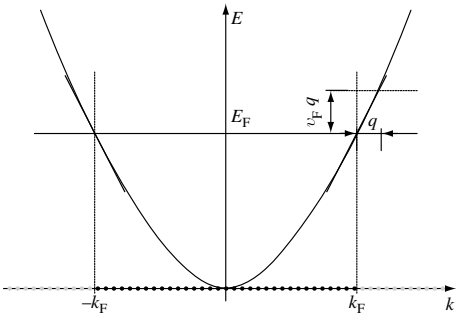

cut–off $|q| < \Gamma$ beyond which the linearization of the dispersion is invalid. (Throughout this section, all momentum summations will be subject to this constraint.) Turning to the interacting part of the Hamiltonian, let us first define the operator

$$\hat{\rho}_{sq} = \sum_k a^\dagger_{sk+q} a_{sk}. \tag{2.35}$$

Crucially, the definition of these operators is not just motivated by notational convenience. It is straightforward to verify (exercise) that $\hat{\rho}_s(q)$ is obtained from the Fourier transform of the local density operator $\hat{\rho}(x)$. In other words, $\hat{\rho}_{sq}$ measures density fluctuations of characteristic wavelength q^{-1} supported by electron excitations with characteristic momentum $\pm k_\mathrm{F}$ (see Fig. 2.9 (a)). From our heuristic argument above, suggesting charge density modulations to be the basic excitations of the system, we expect the operators $\hat{\rho}_{sq}$ to represent the central degrees of freedom of the theory.

Represented in terms of the density operators, the interaction contribution to the Hamiltonian may be recast as

$$\hat{V}_\mathrm{ee} = \frac{1}{2L} \sum_{kk'q} V_\mathrm{ee}(q) \, a^\dagger_{k-q} a^\dagger_{k'+q} a_{k'} a_k \equiv \frac{1}{2L} \sum_{qs} \left[g_4 \hat{\rho}_{sq} \hat{\rho}_{s-q} + g_2 \hat{\rho}_{sq} \hat{\rho}_{\bar{s}-q} \right], \tag{2.36}$$

where $\bar{s} = \mathrm{L/R}$ denotes the complement of $s = \mathrm{R/L}$, and the constants g_2 and g_4 measure the strength of the interaction in the vicinity of the Fermi points, i.e. where $q \simeq 0$ and $q \simeq 2k_\mathrm{F}$. (With the notation $g_{2,4}$ we follow a common convention in the literature.)

EXERCISE Explore the relation between the coupling constants g_2, g_4 and the Fourier transform of V_ee. Show that to the summation $\sum_{kk'q}$, not only terms with $(k, k', q) \simeq (\pm k_\mathrm{F}, \pm k_\mathrm{F}, 0)$, but also terms with $(k, k', q) \simeq (\pm k_\mathrm{F}, \mp k_\mathrm{F}, 2k_\mathrm{F})$ contribute. When adequately ordered (do it!), these contributions can be arranged into the form of the right-hand side of Eq. (2.36). (For a detailed discussion see, e.g., T. Giamarchi, *Quantum Physics in One Dimension* (Oxford University Press, 2004) or G. Mahan, *Many Particle Physics* (Plenum Press, 1981)). At any rate, the only point that matters for our present discussion is that the interaction *can* be represented through density operators with positive constants $g_{2,4}$ determined by the interaction strength.

INFO Working with second quantized theories, one frequently needs to compute commutators of operators $\hat{A}(a, a^\dagger)$ polynomial in the elementary boson/fermion operators of the theory (e.g. $\hat{A} = aa^\dagger$, $\hat{A} = aaa^\dagger a^\dagger$, etc. where we have omitted the quantum number subscripts generally carried by a and $a^\dagger$). Such types of operation are made easier by a number of operations of elementary

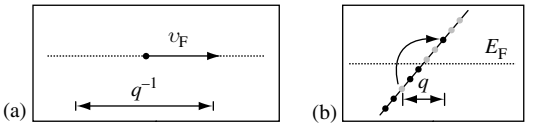

Figure 2.9 Two different interpretations of the excitations created by the density operators $\hat{\rho}_{sq}$. (a) Real space; $\hat{\rho}_{sq}$ creates density modulations of characteristic wavelength q^{-1} and characteristic velocity v_F. (b) Momentum space; application of $\hat{\rho}_{sq}$ to the ground state excites electrons from states k to $k+q$. This creates particle–hole excitations of energy $\epsilon_{k+q} - \epsilon_k = v_F q$ independent of the particle/hole momentum k. Both particles and holes forming the excitation travel with the same velocity v_F, implying that the excitation does not disperse (i.e. decay).

commutator algebra. The most basic identity, from which all sorts of other formulae can be generated recursively, is the following:

$$\boxed{[\hat{A}, \hat{B}\hat{C}]_{\pm} = [\hat{A}, \hat{B}]_{\pm}\hat{C} \mp \hat{B}[\hat{A}, \hat{C}]_{-}.} \tag{2.37}$$

Iteration of this equation for boson operators $a, a^\dagger$ shows that

$$[a^\dagger, a^n] = -n a^{n-1}. \tag{2.38}$$

(Due to the fact that $a^2 = 0$ in the fermionic case, there is no fermion analog of this equation.) Taylor expansion then shows that, for any analytic function $F(a)$, $[a^\dagger, F(a)] = -F'(a)$. Similarly, another useful formula which follows from the above is the relation $a^\dagger F(aa^\dagger) = F(a^\dagger a)a^\dagger$, which is also verified by series expansion.

So far, we have merely rewritten parts of the Hamiltonian in terms of density operators. Ultimately, however, we wish to arrive at a representation whereby these operators, instead of the original electron operators, represent the fundamental degrees of freedom of the theory. Since the definition of the operators ρ involves the squares of two Fermi operators, we expect the density operators to resemble bosonic excitations. Thus, as a first and essential step towards the construction of the new picture, we explore the commutation relations between the operators $\hat{\rho}_{sq}$.

From the definition (2.35) and the auxiliary identity (2.37) it is straightforward to verify the commutation relation $[\hat{\rho}_{sq}, \hat{\rho}_{s'q'}] = \delta_{ss'} \sum_k (a^\dagger_{sk+q} a_{sk-q'} - a^\dagger_{sk+q+q'} a_{sk})$. As it stands, this relation is certainly not of much practical use. To make further progress, we must resort to a (not very restrictive) approximation. Ultimately we will want to compute some observables involving quantum averages taken on the ground state of the theory, $\langle\Omega| \ldots |\Omega\rangle$. To simplify the structure of the theory, we may thus replace the right-hand side of the relation by its ground state expectation value:

$$[\hat{\rho}_{sq}, \hat{\rho}_{s'q'}] \approx \delta_{ss'} \sum_k \langle\Omega| a^\dagger_{sk+q} a_{sk-q'} - a^\dagger_{sk+q+q'} a_{sk} |\Omega\rangle = \delta_{ss'}\delta_{q,-q'} \sum_k \langle\Omega|(\hat{n}_{sk+q} - \hat{n}_{sk})|\Omega\rangle\,,$$

where, as usual, $\hat{n}_{sk} = a^\dagger_{sk} a_{sk}$, and we have made use of the fact that $\langle\Omega| a^\dagger_{sk} a_{sk'} |\Omega\rangle = \delta_{kk'}$. Although this is an uncontrolled approximation, it is expected to become better the closer we stay to the zero-temperature ground state $|\Omega\rangle$ of the theory (i.e. at low excitation energies).

EXERCISE Try to critically assess the validity of the approximation. (For a comprehensive discussion, see the text by Giamarchi.[17])

At first glance, it would seem that the right-hand side of our simplified commutator relation actually vanishes. A simple shift of the summation index, $\sum_k \langle\Omega|\hat{n}_{sk+q}|\Omega\rangle \stackrel{?}{=} \sum_k \langle\Omega|\hat{n}_{sk}|\Omega\rangle$ indicates that the two terms contributing to the sum cancel. However, this argument is certainly too naive. It ignores the fact that our summation is limited by a cut-off momentum Γ. Since the shift $k \to k - q$ changes the cut-off, the interpretation above is invalid.

To obtain a more accurate result, let us consider the case $s = R$ and $q > 0$. We know that, in the ground state, all states with momentum $k < 0$ are occupied while all states with $k \geq 0$ are empty. This implies that

$$\begin{aligned}\sum_k \langle\Omega|(\hat{n}_{Rk+q} - \hat{n}_{Rk})|\Omega\rangle &= \sum_{-\Gamma<k\ -q} + \sum_{-q<k\ 0} + \sum_{0<k<\Gamma} \langle\Omega|(\hat{n}_{Rk+q} - \hat{n}_{Rk})|\Omega\rangle \\ &= \sum_{-q\ k\ 0} \langle\Omega|(\hat{n}_{Rk+q} - \hat{n}_{Rk})|\Omega\rangle = -\frac{qL}{2\pi}\,,\end{aligned}$$

where, with the last equality, we have used the fact that a momentum interval of size q contains $q/(2\pi/L)$ quantized momentum states. Similar reasoning for $s = L$ shows that the effective form of the commutator relation reads

$$[\hat{\rho}_{sq}, \hat{\rho}_{s'q'}] = -\delta_{ss'}\delta_{q,-q'}\sigma_s \frac{qL}{2\pi}. \tag{2.39}$$

Now, if it were not for the q-dependence of the right-hand side of this relation, we would indeed have found (approximate) bosonic commutation relations. Therefore, to make the connection to bosons explicit, let us define

$$\left.\begin{aligned} b_q &\equiv n_q\,\hat{\rho}_{\mathrm{L}q}, \qquad b_q^\dagger \equiv n_q \hat{\rho}_{\mathrm{L}(-q)}, \\ b_{-q} &\equiv n_q \hat{\rho}_{\mathrm{R}(-q)}, \quad b_{-q}^\dagger \equiv n_q \hat{\rho}_{\mathrm{R}q}, \end{aligned}\right\} \tag{2.40}$$

where $q > 0$ and $n_q \equiv (2\pi/Lq)^{1/2}$. It is easily confirmed that the newly defined operators b_q obey canonical commutation relations (exercise), i.e. we have indeed found that, apart from the scaling factors n_q, the density excitations of the system behave as bosonic "particles."

Expressed in terms of the operators b, the interaction part of the Hamiltonian takes the form (exercise)

$$V_{\mathrm{ee}} = \frac{1}{2\pi}\sum_{q>0} q\,(b_q \quad b_{-q}^\dagger)\begin{pmatrix} g_4 & g_2 \\ g_2 & g_4 \end{pmatrix}\begin{pmatrix} b_q^\dagger \\ b_{-q} \end{pmatrix}.$$

Notice that we have succeeded in representing a genuine two-body interaction, a contribution that usually renders a model unsolvable, in terms of a quadratic representation. However,

[17] T. Giamarchi, *Quantum Physics in One Dimension* (Oxford University Press, 2004).

the free boson representation of the interaction term will be of little use until the **kinetic part of the Hamiltonian** $\hat{H}_0$ is represented in terms of the b operators. There are various ways of achieving this goal. The most straightforward route, a direct construction of a representation of $\hat{H}_0$ in terms of the Bose operators, is cumbersome in practice. However, there exists a more efficient way that is based on indirect reasoning. As follows from the discussion of Section 2.1, the properties of second quantized operators are fixed by their commutation relations.[18] So what we are going to do is search for an operator $\hat{H}_0'(b, b^\dagger)$ that has the same commutation relations with the boson operators $(b, b^\dagger)$ as the original kinetic energy operator $\hat{H}_0(a, a^\dagger)$. Using Eq. (2.34), the definition (2.35), and the auxiliary identity (2.37), it is straightforward to verify that $[\hat{H}_0, \hat{\rho}_{sq}] = q v_{\mathrm{F}} \sigma_s \hat{\rho}_{sq}$. On the other hand, using Eq. (2.39) one finds that the same commutation relations hold with the operator

$$\hat{H}_0' = \frac{2\pi v_F}{L} \sum_{qs} \hat{\rho}_{sq} \hat{\rho}_{s-q} \,,$$

i.e. $[\hat{H}_0', \hat{\rho}_{sq}] = q v_{\mathrm{F}} \sigma_s \hat{\rho}_{sq}$. Following the logic of our argument we thus identify $\hat{H}_0 = \hat{H}_0'$ (up to inessential constants) and substitute $\hat{H}_0'$ for the non-interacting Hamiltonian.

EXERCISE To gain some confidence in the identification $\hat{H}_0 = \hat{H}_0' + \text{const.}$, and to show that the undetermined constant actually equals zero, compute the energy expectation value of the state $|\ _{sq}\rangle \equiv \hat{\rho}_{sq} |\ \rangle$ both as $\langle\ _{sq} | \hat{H}_0 |\ _{sq}\rangle$ and as $\langle\ _{sq} | \hat{H}_0' |\ _{sq}\rangle$. Confirm that the two expressions coincide.

Finally, using Eq. (2.40) and adding the interaction contribution V_{ee} we arrive at the effective Hamiltonian

$$\hat{H} = \sum_{q>0} q \begin{pmatrix} b_q & b_{-q}^\dagger \end{pmatrix} \begin{pmatrix} v_{\mathrm{F}} + \frac{g_4}{2\pi} & \frac{g_2}{2\pi} \\ \frac{g_2}{2\pi} & v_{\mathrm{F}} + \frac{g_4}{2\pi} \end{pmatrix} \begin{pmatrix} b_q^\dagger \\ b_{-q} \end{pmatrix} . \tag{2.41}$$

We have thus succeeded in mapping the full interacting problem onto a *free* bosonic theory. The mapping $a \to \hat{\rho} \to b$ is our first example of a technique known as **bosonization**. Such techniques play an important role in 2(= 1 space + 1 time)-dimensional field theory in general. More sophisticated bosonization schemes will be discussed in Sections 4.3 and 9.4.4. Conversely, it is sometimes useful to represent a boson problem in terms of fermions via **fermionization**. One may wonder why it is indeed possible to effortlessly represent the low-lying excitations of a gas of fermions in terms of bosons. **Fermi–Bose transmutability** is indeed a peculiarity of one-dimensional quantum systems. Particles confined to a line cannot pass "around" each other. That means that the whole issue of sign factors arising from the interchange of particle coordinates does not arise, and much of the exclusion-type

[18] This argument can be made quantitative by group theoretical reasoning: Eq. (2.4) and (2.7) define the irreducible representation of an operator algebra – an *algebra* because [,] defines a product in the space of generators $\{a_\lambda, a_\lambda^\dagger\}$, a *representation* because the operators act in a vector space (namely Fock space $\mathcal{F}$), which is *irreducible* because all states $|\lambda_1, \ldots, \lambda_N\rangle \in \mathcal{F}$ can be reached by iterative application of operators onto a unique reference state (e.g. $|\Omega\rangle$). Under these conditions, Schur's lemma – to be discussed in more detail in Chapter 4 – states that two operators $\hat{A}_1$ and $\hat{A}_2$ having identical commutation relations with all $\{a_\lambda, a_\lambda^\dagger\}$ are equal up to a constant.

characteristics of the Fermi system are inactivated. A more systematic formulation of Fermi $\leftrightarrow$ Bose transformations will be discussed in Chapter 4.

Now, there is one last problem that needs to be overcome to actually solve the interacting problem. In Chapter 1, we learned how to interpret Hamiltonians of the structure $\sum_q b_q^\dagger b_q$ as superpositions of harmonic oscillators. However, in our present problem, terms of the type $b_q b_{-q}$ and $b_{-q}^\dagger b_q^\dagger$ appear. To return to familiar terrain, we need to eliminate these terms. However, before doing so, it is instructive to discuss the physical meaning of the problem.

Firstly, let us recall that the total number operator of a theory described by operators $b_\lambda^\dagger, b_\lambda$ is given by $\hat{N} = \sum_\lambda b_\lambda^\dagger b_\lambda$. Now, if the Hamiltonian has the form $\hat{H} = \sum_{\mu\nu} b_\mu^\dagger H_{\mu\nu} b_\nu$, the total number operator commutes with $\hat{H}$, i.e. $[\hat{N}, \hat{H}] = 0$ (exercise). This means that $\hat{H}$ and $\hat{N}$ can be simultaneously diagonalized, or, in more physical terms, that the Hamiltonian enjoys the feature of **particle number conservation**. More generally, any Hamiltonian in which operators appear as polynomials containing equal numbers of creation and annihilation operators (e.g. $b^\dagger b^\dagger b b, b^\dagger b^\dagger b^\dagger b b b$, etc.) has this property. This is because any operator of this structure creates as many particles as it annihilates. In problems where the total number of particles is conserved (e.g. the theory of interacting electrons in an isolated piece of metal), the Hamiltonian is bound to have this structure. Conversely, in situations where the number of excitations is not fixed (e.g. a theory of photons or phonons) particle number violating terms like bb or $b^\dagger b^\dagger$ can appear. Such a situation is realized in our present problem; the number of density excitations in an electron system is certainly not a conserved quantity which explains why contributions like $b_q b_{-q}$ appear in $\hat{H}$.

To eliminate the non-particle-number-conserving contributions we should, somehow, transform the matrix

$$K \equiv \begin{pmatrix} v_\mathrm{F} + \frac{g_4}{2\pi} & \frac{g_2}{2\pi} \\ \frac{g_2}{2\pi} & v_\mathrm{F} + \frac{g_4}{2\pi} \end{pmatrix},$$

to a diagonal structure. Transformations of K can be generated by transforming the operators b_q and $b_q^\dagger$ to a different representation. Specifically, with $\Psi_q \equiv (b_q^\dagger, b_{-q})^T$, we may define $\Psi'_q \equiv T^{-1}\Psi_q$, where T is a 2×2 matrix acting on the two components of Ψ. (Since K does not depend on q, T can be chosen to have the same property.) After the transformation, the Hamiltonian will have the form

$$H = \sum_{q>0} q\, \Psi_q^\dagger K \Psi_q \to \sum_{q>0} q\, \Psi_q'^\dagger \underbrace{T^\dagger K T}_{K'} \Psi'_q\,, \tag{2.42}$$

with a new matrix $K' \equiv T^\dagger K T$. We will seek for a transformation T that makes K' diagonal. However, an important point to be kept in mind is that not all 2×2 matrices T qualify as transformations. We must ensure that the transformed "vector" again has the structure $\Psi'_q \equiv \left(b_q'^\dagger, b'_{-q}\right)^T$, with a boson creation/annihilation operator in the first/second component – i.e. the commutation relations of the operators must be conserved by the transformation. Remembering that the algebraic properties of the operators b are specified through commutation relations, this condition can be cast in mathematical form by requiring that the commutator $\left[\Psi_{qi}, \Psi_{qj}^\dagger\right] = (-\sigma_3)_{ij} \stackrel{!}{=} \left[\Psi'_{qi}, \Psi_{qj}'^\dagger\right]$ be invariant under the transformation. Using the fact that $\Psi' = T^{-1}\Psi$, this condition is seen to be equivalent to the pseudo-unitarity condition, $T^\dagger \sigma_3 T \stackrel{!}{=} \sigma_3$.

With this background, we are now in a position to find a transformation that brings the matrix K' to a 2×2 diagonal form. Multiplication of the definition $K' = T^\dagger K T$ by σ_3 leads to

$$T^\dagger K T = K' \qquad \underbrace{\sigma_3 T^\dagger \sigma_3}_{T^{-1}} \sigma_3 K T = \sigma_3 K'.$$

This means that the matrix $\sigma_3 K'$ is obtained by a *similarity* transformation $T^{-1}(\cdots)T$ from the matrix $\sigma_3 K$, or, in other words, that the matrix $\sigma_3 K'$ contains the eigenvalues $\pm u$ of $\sigma_3 K$ on its diagonal. (That the eigenvalues sum to 0 follows from the fact that the trace vanishes, $\mathrm{tr}(\sigma_3 K) = 0$.) However, the eigenvalues of $\sigma_3 K$ are readily computed as

$$v_\rho = \frac{1}{2\pi}\left[(2\pi v_\mathrm{F} + g_4)^2 - g_2^2\right]^{1/2}. \tag{2.43}$$

Thus, with $\sigma_3 K' = \sigma_3 v_\rho$ we arrive at $K' = v_\rho \cdot \mathrm{id.}$, where "id." stands for the unit matrix.[19] Substitution of this result into Eq. (2.42) finally leads to the diagonal Hamiltonian $\hat{H} = v_\rho \sum_{q>0} q\, \Psi_q'^\dagger \Psi_q'$, or equivalently, making use of the identity $\Psi_q'^\dagger \Psi_q' = b_q^\dagger b_q + b_{-q}^\dagger b_{-q} + 1$,

$$\hat{H} = v_\rho \sum_q |q| b_q^\dagger b_q. \tag{2.44}$$

Here we have ignored an overall constant and omitted the prime on our new Bose operators.

Nicolai Nikolaevich Bogoliubov 1909–92
A theoretical physicist acclaimed for his works in nonlinear mechanics, statistical physics, theory of superfluidity and superconductivity, quantum field theory, renormalization group theory, proof of dispersion relations, and elementary particle theory.

In the literature, the transformation procedure outlined above is known as a **Bogoliubov transformation**. Transformations of this type are frequently applied in quantum magnetism (see below), superconductivity, or, more generally, all problems where the particle number is not conserved. Notice that the possibility to transform to a representation $\sim b^\dagger b$ does not imply that miraculously the theory has become particle number conserving. The new "quasi-particle" operators b are related to the original Bose operators through a transformation that mixes b and $b^\dagger$. While the quasi-particle number is conserved, the number of original density excitations is not.

Equations (2.43) and (2.44) represent our final solution of the problem of spinless interacting fermions in one dimension. We have suceeded in mapping the problem onto a form analogous to our previous results (1.34) and (1.39) for the phonon and the photon system, respectively. Indeed, all that has been said about those Hamiltonians applies equally to Eq. (2.44): the basic elementary excitations of the one-dimensional fermion system are waves, i.e. excitations with linear dispersion $\omega = v_\rho |q|$. In the present context, they are

[19] Explicit knowledge of the transformation matrix T, i.e. knowledge of the relation between the operators b and b', is not needed for our construction. However, for the sake of completeness, we mention that

$$T = \begin{matrix} \cosh\theta_k & \sinh\theta_k \\ \sinh\theta_k & \cosh\theta_k \end{matrix}$$

with $\tanh(2\theta) = -g_2/(2\pi v_\mathrm{F} + g_4)$ represents a suitable parameterization.

termed **charge density waves (CDW)**. The Bose creation operators describing these excitations are, up to the Bogoliubov transformation, and a momentum dependent scaling factor $(2\pi/Lq)^{1/2}$, equivalent to the density operators of the electron gas. For a non-interacting system, $g_2 = g_4 = 0$, and the CDW propagates with the velocity of the free Fermi particles, $v_{\rm F}$. A fictitious interaction that does not couple particles of opposite Fermi momentum, $g_2 = 0$, $g_4 \neq 0$, speeds up the CDW. Heuristically, this can be interpreted as an "acceleration process" whereby a CDW pushes its own charge front. By contrast, interactions between left and right movers, $g_2 \neq 0$, diminish the velocity, i.e. due to the Coulomb interaction it is difficult for distortions of opposite velocities to penetrate each other. (Notice that, for a theory with $g_2 = 0$, no Bogoliubov transformation would be needed to diagonalize the Hamiltonian, i.e. in this case, undisturbed left- and right-moving waves would be the basic excitations of the theory.)

Our discussion above neglected the spin carried by the conduction electrons. Had we included the electron spin, the following picture would have emerged (see Problem 2.4): the long-range dynamics of the electron gas is governed by two independently propagating wave modes, the charge density wave discussed above, and a **spin density wave** (SDW).[20] The SDW carries a **spin current**, but is electrically neutral. As with the CDW, its dispersion is linear with an interaction-renormalized velocity, $v_{\rm s}$ (which, however, is generally larger than the velocity v_ρ of the CDW). To understand the consequences of this phenomenon, imagine an electron had been thrown into the system (e.g. by attaching a tunnel contact somewhere along the wire). As discussed above, a single electron does not represent a stable excitation of the one-dimensional electron gas. What will happen is that the spectral weight of the particle[21] disintegrates into a collective charge excitation and a spin excitation. The newly excited waves then propagate into the bulk of the system at different velocities $\pm v_\rho$ and $\pm v_{\rm s}$. In other words, the charge and the spin of the electron effectively "disintegrate" into two separate excitations, a phenomenon known as **spin–charge separation**. Spin–charge separation in one-dimensional metals exemplifies a mechanism frequently observed in condensed matter systems: the set of quantum numbers carried by elementary particles may get effectively absorbed by different excitation channels. One of the more spectacular manifestations of this effect is the appearance of fractionally charged excitations in quantum Hall systems, to be discussed in more detail in Chapter 9.

The theory of spin and charge density waves in one-dimensional conductors has a long history spanning four decades. However, despite the rigor of the theory its experimental verification has proved excruciatingly difficult! While various experiments are consistent with theory (for a review, see Ref.[17]), only recently have signatures of spin and charge density wave excitations been experimentally observed.

[20] One may think of the charge density of the electron gas $\rho = \rho_\uparrow + \rho_\downarrow$ as the sum of the densities of the spin up and spin down populations, respectively. The local spin density is then given by $\rho_{\rm s} \equiv \rho_\uparrow - \rho_\downarrow$. After what has been said above, it is perhaps not too surprising that fluctuations of these two quantities represent the dominant excitations of the electron gas. What *is* surprising, though, is that these two excitations do not interact with each other.

[21] For a precise definition of this term, see Chapter 7.

Quantum spin chains

In the previous section, the emphasis was placed on charging effects generated by Coulomb interaction. However, as we have seen in Section 2.2, Coulomb interaction may also lead to the indirect generation of magnetic interactions. In one dimension, one can account for these mechanisms by adding to our previously structureless electrons a spin degree of freedom. This leads to the **Tomonaga–Luttinger liquid**, a system governed by the coexistence of collective spin and charge excitations. However, to introduce the phenomena brought about by quantum magnetic correlations, it is best to first consider systems where the charge degrees of freedom are frozen and only spin excitations remain. Such systems are realized, for example, in Mott insulators where interaction between the spins of localized electrons is mediated by virtual exchange processes between neighboring electrons. One can describe these correlations through models of localized quantum spins – either in chains or, more generally, in higher-dimensional quantum spin lattices. We begin our discussion with the ferromagnetic spin chain.

Werner Heisenberg 1901–76

Nobel Laureate in Physics in 1932 "for the creation of quantum mechanics, the application of which has, inter alia, led to the discovery of the allotropic forms of hydrogen." In 1927 he published his uncertainty principle, for which he is perhaps best known. He also made important contributions to the theories of hydrodynamics of turbulent flows, ferromagnetism, cosmic rays, and subatomic particles, and he was instrumental in planning the first West German nuclear reactor at Karlsruhe, together with a research reactor in Munich, in 1957. (Image © The Nobel Foundation.)

Quantum ferromagnet

The quantum Heisenberg ferromagnet is specified by the Hamiltonian

$$\boxed{\hat{H} = -J \sum_{\langle mn \rangle} \hat{\mathbf{S}}_m \cdot \hat{\mathbf{S}}_n}, \tag{2.45}$$

where $J > 0$, $\hat{\mathbf{S}}_m$ represents the quantum mechanical spin operator at lattice site m, and, as before, $\langle mn \rangle$ denotes summation over neighboring sites. In Section 2.1 (see Eq. (2.13)) the quantum mechanical spin was represented through an electron basis. However, one can conceive of situations where the spin sitting at site m is carried by a different object (e.g. an atom with non-vanishing magnetic moment). At any rate, for the purposes of our present discussion, we need not specify the microscopic origin of the spin. All we need to know is (i) that the lattice operators $\hat{S}^i_m$ obey the SU(2) commutator algebra,

$$\left[\hat{S}^i_m, \hat{S}^j_n\right] = i\delta_{mn}\epsilon^{ijk}\hat{S}^k_n, \tag{2.46}$$

characteristic of quantum spins, and (ii) the total spin at each lattice site is S.[22]

[22] Remember that the finite-dimensional representations of the spin operator are of dimension $2S + 1$ where S may be integer or half integer. While a single electron has spin $S = 1/2$, the total magnetic moment of electrons bound to an atom may be much larger.

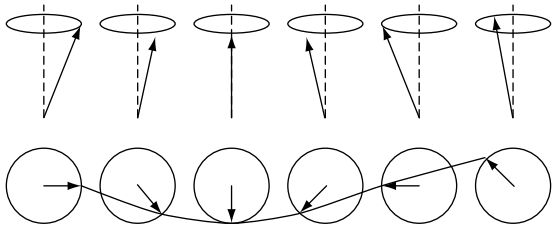

Figure 2.10 Showing the spin configuration of an elementary spin-wave excitation from the spin polarized ground state.

Now, due to the positivity of the coupling constant J, the Hamiltonian favors configurations where the spins at neighboring sites are aligned in the same direction (cf. Fig. 2.10). A ground state of the system is given by $|\Omega\rangle \equiv \quad_m |S_m\rangle$, where $|S_m\rangle$ represents a state with maximal spin-z component: $S^z_m|S_m\rangle = S|S_m\rangle$. We have written "a" ground state instead of "the" ground state because the system is highly degenerate: a simultaneous change of the orientation of all spins does not change the ground state energy, i.e. the system possesses a global rotation symmetry.

EXERCISE Compute the energy expectation value of the state $|\ \rangle$. Defining *global* spin operators through $\hat{S}^i \equiv \sum_m \hat{S}^i_m$, consider the state $|\alpha\rangle \equiv \exp(i\alpha\cdot\hat{\mathbf{S}})|\ \rangle$. Verify that the state α is degenerate with $|\ \rangle$. Explicitly compute the state $|(\pi/2, 0, 0)\rangle$. Convince yourself that, for general α, $|\alpha\rangle$ can be interpreted as a state with rotated quantization axis.

As with our previous examples, we expect that a global continuous symmetry will involve the presence of energetically low-lying excitations. Indeed, it is obvious that, in the limit of long wavelength λ, a weak distortion of a ground state configuration (see Fig. 2.10) will cost vanishingly small energy. To quantitatively explore the physics of these **spin waves**, we adopt a "semiclassical" picture, where the spin $S \gg 1$ is assumed to be large. In this limit, the rotation of the spins around the ground state configuration becomes similar to the rotation of a classical magnetic moment.

INFO To better understand the mechanism behind the **semi-classical approximation**, consider the Heisenberg uncertainty relation, $\Delta S^i\ \Delta S^j \sim |\langle[\hat{S}^i, \hat{S}^j]\rangle| = \epsilon^{ijk}|\langle\hat{S}^k\rangle|$, where ΔS^i is the root mean square of the quantum uncertainty of spin component i. Using the fact that $|\langle\hat{S}^k\rangle| \quad S$, we obtain for the relative uncertainty, $\Delta S^i/S$,

$$\frac{\Delta S^i}{S}\frac{\Delta S^j}{S} \sim \frac{S}{S^2} \xrightarrow{S\ \to\ \infty} 0.$$

I.e., for $S \gg 1$, quantum fluctuations of the spin become less important.

In the limit of large spin S, and at low excitation energies, it is natural to describe the ordered phase in terms of small fluctuations of the spins around their expectation values (cf. the description of the ordered phase of a crystal in terms of small fluctuations of the atoms around the ordered lattice sites). These fluctuations are conveniently represented in

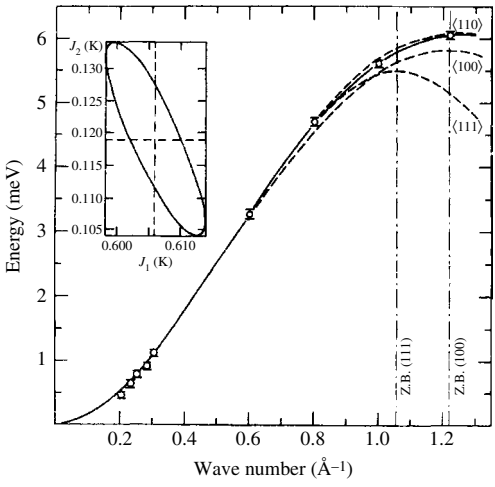

Figure 2.11 Spin-wave spectrum of europium oxide as measured by inelastic neutron scattering at a reference temperature of 5.5 K. Note that, at low values of momenta q, the dispersion is quadratic, in agreement with the low-energy theory. (Exercise: A closer inspection of the data shows the existence of a small gap in the spectrum at $\mathbf{q} = 0$. To what may this gap be attributed?) Figure reprinted with permission from L. Passell, O. W. Dietrich, and J. Als-Nielser, Neutron scattering from the Heisenberg ferromagnets EuO and EuS I: the exchange interaction, *Phys. Rev. B* **14** (1976), 4897–907. Copyright (1976) by the American Physical Society.

terms of spin raising and lowering operators: with $\hat{S}^{\pm}_m \equiv S^1_m \pm iS^2_m$, it is straightforward to verify that

$$\left[\hat{S}^z_m, \hat{S}^{\pm}_n\right] = \pm\delta_{mn} S^{\pm}_m, \qquad \left[\hat{S}^+_m, \hat{S}^-_n\right] = 2\delta_{mn} S^z_m. \tag{2.47}$$

Application of $\hat{S}^{-(+)}_m$ lowers (raises) the z-component of the spin at site m by one. To actually make use of the fact that deviations around $|\Omega\rangle$ are small, a representation known as the **Holstein–Primakoff transformation**[23] was introduced in which the spin operators $\hat{S}^{\pm}, \hat{S}$ are specified in terms of bosonic creation and annihilation operators $a^\dagger$ and a:

$$\hat{S}^-_m = a^\dagger_m \left(2S - a^\dagger_m a_m\right)^{1/2}, \quad \hat{S}^+_m = \left(2S - a^\dagger_m a_m\right)^{1/2} a_m, \quad \hat{S}^z_m = S - a^\dagger_m a_m.$$

EXERCISE Confirm that the spin operators satisfy the commutation relations (2.47).

The utility of this representation is clear. When the spin is large, $S \gg 1$, an expansion in powers of $1/S$ gives $\hat{S}^z_m = S - a^\dagger_m a_m$, $\hat{S}^-_m \simeq (2S)^{1/2} a^\dagger_m$, and $\hat{S}^+_m \simeq (2S)^{1/2} a_m$. In this

[23] T. Holstein and H. Primakoff, Field dependence of the intrinsic domain magnetisation of a ferromagnet, *Phys. Rev.* **58** (1940), 1098–113.

approximation, the one-dimensional Heisenberg Hamiltonian takes the form

$$\begin{aligned}\hat{H} &= -J\sum_m \hat{S}^z_m\hat{S}^z_{m+1} + \frac{1}{2}\left(\hat{S}^+_m\hat{S}^-_{m+1} + \hat{S}^-_m\hat{S}^+_{m+1}\right)\\ &= -JNS^2 - JS\sum_m -2a^\dagger_m a_m + \left(a^\dagger_m a_{m+1} + \text{h.c.}\right) + \mathcal{O}(S^0)\\ &= -JNS^2 + JS\sum_m (a^\dagger_{m+1} - a^\dagger_m)(a_{m+1} - a_m) + \mathcal{O}(S^0).\end{aligned}$$

Keeping fluctuations at leading order in S, the quadratic Hamiltonian can be diagonalized by Fourier transformation. In this case, it is convenient to impose periodic boundary conditions: $\hat{S}_{m+N} = \hat{S}_m$, and $a_{m+N} = a_m$, where N denotes the total number of lattice sites. Defining

$$a_k = \frac{1}{\sqrt{N}}\sum_{m=1}^{N} e^{ikm}a_m, \quad a_m = \frac{1}{\sqrt{N}}\sum_k^{\text{B.Z.}} e^{-ikm}a_k, \quad \left[a_k, a^\dagger_{k'}\right] = \delta_{kk'},$$

where the summation over k runs over the Brillouin zone, the Hamiltonian for the one-dimensional lattice system takes the form (exercise)

$$\boxed{\hat{H} = -JNS^2 + \sum_k^{\text{B.Z.}} \hbar\omega_k a^\dagger_k a_k + \mathcal{O}(S^0).} \tag{2.48}$$

Here $\hbar\omega_k = 2JS(1-\cos k) = 4JS\sin^2(k/2)$ represents the dispersion relation of the spin excitations. In particular, in the limit $k \to 0$, the energy of the elementary excitations vanishes, $\hbar\omega_k \to JSk^2$. These massless low-energy excitations, known as **magnons**, describe the elementary spin-wave excitations of the ferromagnet. Taking into account terms at higher order in the parameter $1/S$, one finds interactions between the magnons. A comparison of these theoretical predictions and experiment is shown in Fig. 2.11.

Quantum antiferromagnet

Having explored the elementary excitation spectrum of the ferromagnet, we now turn to the discussion of the spin S Heisenberg antiferromagnetic Hamiltonian

$$\boxed{\hat{H} = J\sum_{\langle mn\rangle} \hat{\mathbf{S}}_m \cdot \hat{\mathbf{S}}_n,}$$

where, once again, $J > 0$. As we have seen above, such antiferromagnetic systems occur

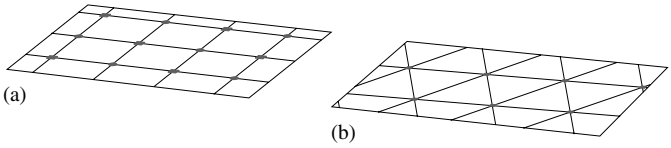

Figure 2.12 (a) Example of a two-dimensional bipartite lattice. (b) Example of a non-bipartite lattice. Notice that, with the latter, no antiferromagnetic arrangement of the spins can be made that recovers the maximum exchange energy from each and every bond.

Louis Néel 1904–2000

Nobel Laureate in Physics in 1970, shared with Hannes Olof Gösta Alfvén, for his "fundamental work and discoveries concerning antiferromagnetism and ferrimagnetism that have led to important applications in solid state physics." (Image © The Nobel Foundation.)

in the arena of strongly correlated electron compounds. Although the Hamiltonian differs from its ferromagnetic relative "only" by a change of sign, the differences in the physics are drastic. Firstly, the phenomenology displayed by the antiferromagnetic Hamiltonian $\hat{H}$ depend sensitively on the morphology of the underlying lattice. For a **bipartite lattice**, i.e. one in which the neighbors of one sublattice A belong to the other sublattice B (see Fig. 2.12(a)), the ground states of the Heisenberg antiferromagnet are close[24] to a staggered spin configuration, known as a **Néel state**, where all neighboring spins are antiparallel (see Fig. 2.12). Again the ground state is degenerate, i.e. a global rotation of all spins by the same amount does not change the energy. By contrast, on non-bipartite lattices such as the triangular lattice shown in Fig. 2.12(b), no spin arrangement can be found wherein each bond recovers the full exchange energy J. Spin models of this kind are said to be **frustrated**.

EXERCISE Engaging only symmetry considerations, try to identify a possible classical ground state of the triangular lattice Heisenberg antiferromagnet. (Hint: Construct the classical ground state of a three-site plaquette and then develop the periodic continuation.) Show that the classical antiferromagnetic ground state of the Kagomé lattice – a periodic array of corner-sharing "stars of David" – has a continuous spin degeneracy generated by *local* spin rotations. How might the degeneracy affect the transition to an ordered phase?

Returning to the one-dimensional system, we first note that a chain is trivially bipartite. As before, our strategy will be to expand the Hamiltonian in terms of bosonic operators. However, before doing so, it is convenient to apply a canonical transformation to the Hamiltonian in which the spins on one sublattice, say B, are rotated through 180° about the

[24] It is straightforward to verify that the classical ground state – the Néel state – is now not an exact eigenstate of the quantum Hamiltonian. The true ground state exhibits zero-point fluctuations reminiscent of the quantum harmonic oscillator or atomic chain. However, when $S \gg 1$, it serves as a useful reference state from which fluctuations can be examined.

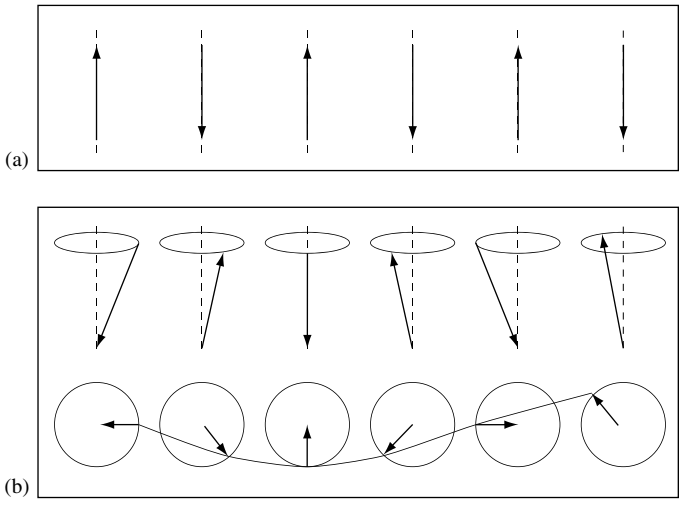

Figure 2.13 (a) Néel state configuration of the spin chain. (b) Cartoon of an antiferromagnetic spin wave.

x-axis, i.e. $S_B^x \to \widetilde{S}_B^x = S_B^x$, $S_B^y \to \widetilde{S}_B^y = -S_B^y$, and $S_B^z \to \widetilde{S}_B^z = -S_B^z$. That is, when represented in terms of the new operators, the Néel ground state looks like a ferromagnetic state, with all spins aligned. We expect that a gradual distortion of this state will produce the antiferromagnetic analog of the spin waves discussed in the previous section (see Fig. 2.11).

Represented in terms of the transformed operators, the Hamiltonian takes the form

$$\hat{H} = -J \sum_m \left[S_m^z \widetilde{S}_{m+1}^z - \frac{1}{2} \left(S_m^+ \widetilde{S}_{m+1}^+ + S_m^- \widetilde{S}_{m+1}^- \right) \right].$$

Once again, applying an expansion of the Holstein–Primakoff representation, $S_m^- \simeq (2S)^{1/2} a_m^\dagger$, etc., one obtains the Hamiltonian

$$\hat{H} = -NJS^2 + JS \sum_m \left[a_m^\dagger a_m + a_{m+1}^\dagger a_{m+1} + a_m a_{m+1} + a_m^\dagger a_{m+1}^\dagger \right] + \mathcal{O}(S^0).$$

At first sight the structure of this Hamiltonian, albeit quadratic in the Bose operators, looks awkward. However, after Fourier transformation, $a_m = N^{-1/2} \sum_k e^{-ikm} a_k$ it assumes the more accessible form

$$\hat{H} = -NJS(S+1) + JS \sum_k \begin{pmatrix} a_k^\dagger & a_{-k} \end{pmatrix} \begin{pmatrix} 1 & \gamma_k \\ \gamma_k & 1 \end{pmatrix} \begin{pmatrix} a_k \\ a_{-k}^\dagger \end{pmatrix} + \mathcal{O}(S^0),$$

where $\gamma_k = \cos k$. Apart from the definition of the matrix kernel between the Bose operators, $\hat{H}$ is equivalent to the Hamiltonian (2.41) discussed in connection with the charge density wave. Performing the same steps as before, the non-particle-number-conserving con-

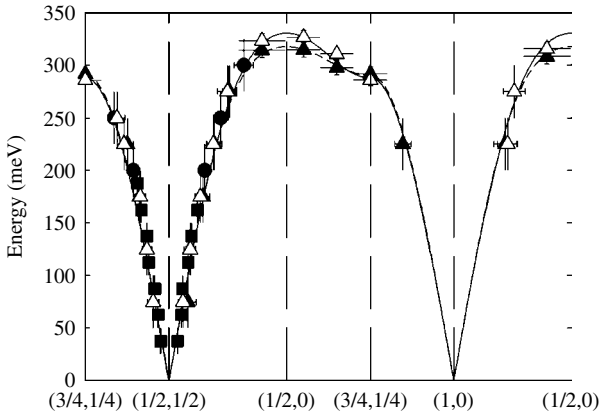

Figure 2.14 Experimentally obtained spin-wave dispersion of the high-T_c parent compound $LaCuO_4$ – a prominent spin 1/2 antiferromagnet. Reprinted with permission from R. Coldea S. M. Hayder, G. Aeppli, *et al.*, Spin waves and electronic excitations in La_2CuO_4, *Phys. Rev. Lett.* **86** (2001), 5377–80. Copyright (2001) by the American Physical Society.

tributions $a^\dagger a^\dagger$ can be removed by Bogoliubov transformation. As a result, the transformed Hamiltonian assumes the diagonal form

$$\boxed{\hat{H} = -NJS^2 + 2JS\sum_k |\sin k| \left[\alpha_k^\dagger \alpha_k + \frac{1}{2}\right].} \tag{2.49}$$

Thus, in contrast to the ferromagnet, the spin-wave excitations of the antiferromagnet (Fig. 2.14) display a *linear spectrum* in the limit $k \to 0$. Surprisingly, although developed in the limit of large spin, experiment shows that even for $S = 1/2$ spin chains, the integrity of the linear dispersion is maintained (see Fig. 2.14).

More generally, it turns out that, for chains of arbitrary half integer spin $S = 1/2, 3/2, 5/2, \ldots$, the low-energy spectrum is linear, in agreement with the results of the harmonic approximation. In contrast, for chains of integer spin $S = 1, 2, 3 \ldots$, the low-energy spectrum contains a gap, i.e. these systems do not support long-range excitations. As a rule, the sensitivity of a physical phenomenon to the characteristics of a sequence of *numbers* – such as half integer vs. integer – signals the presence of a mechanism of topological origin.[25] At the same time, the formation of a gap (observed for integer chains) represents an interaction effect; at orders beyond the harmonic approximation, spin waves begin to interact nonlinearly with each other, a mechanism that may (S integer) but need not (S half integer) destroy the-wave like nature of low-energy excitations. In Section 9.3.3 – in a chapter devoted to a general discussion of the intriguing condensed matter phenom-

[25] Specifically, the topological signature of a spin field configuration will turn out to be the number of times the classical analog of a spin (a vector on the unit sphere) will wrap around the sphere in $(1+1)$-dimensional space time.

ena generated by the conspiracy of global (topological) structures with local interaction mechanisms – we will discuss these phenomena on a deeper level.

2.3 Summary and outlook

This concludes our preliminary discussion of applications of the second quantization. Additional examples can be found in the problems. In this chapter, we have introduced second quantization as a tool whereby problems of many-body quantum mechanics can be addressed more efficiently than by the traditional language of symmetrized many-body wave functions. We have discussed how the two approaches are related to each other and how the standard operations of quantum mechanics can be performed by second quantized methods.

One may note that, beyond qualitative discussions, the list of concrete applications encountered in this chapter involved problems that either were non-interacting from the outset, or could be reduced to a quadratic operator structure by a number of suitable manipulations. However, we carefully avoided dealing with interacting problems where no such reductions are possible – the majority by far of the problems encountered in condensed matter physics. What can be done in situations where interactions, i.e. operator contributions of fourth or higher order, are present and no tricks like bosonization can be played? Generically, either interacting problems of many-body physics are fundamentally inaccessible to perturbation theory, or they necessitate perturbative analyses of *infinite* order in the interaction contribution. Situations where a satisfactory result can be obtained by first- or second-order perturbation theory are exceptional. Within second quantization, large-order perturbative expansions in interaction operators lead to complex polynomials of creation and annihilation operators. Quantum expectation values taken over such structures can be computed by a reductive algorithm, known as **Wick's theorem**. However, from a modern perspective, the formulation of perturbation theory in this way is not very efficient. More importantly, problems that are principally non-perturbative have emerged as the focus of interest.

To understand the language of modern condensed matter physics, we thus need to develop another layer of theory, known as **field integration**. In essence, the latter is a concept generalizing the effective action approach of Chapter 1 to the quantum level. However, before discussing quantum field theory, we should understand how the concept works in principle, i.e. on the level of single particle quantum mechanics. This will be the subject of the next chapter.

2.4 Problems

Stone–von Neumann theorem

In the text we introduced creation and annihilation operators in a constructive manner, i.e. by specifying their action on a fixed Fock space state. We saw that this definition implied remarkably simple algebraic relations between the newly introduced operators – the Heisenberg algebra (2.7). In this problem we explore the mathematical structure behind this observation. (The problem has been included for the

benefit of the more mathematically inclined. Readers primarily interested in the practical aspects of second quantization may safely skip it.)

Let us define an abstract algebra of objects a_λ and $\tilde{a}_\lambda$ by

$$[a_\lambda, \tilde{a}_\mu]_\zeta = \delta_{\lambda\mu}, \quad [a_\lambda, a_\mu]_\zeta = [\tilde{a}_\lambda, \tilde{a}_\mu]_\zeta = 0.$$

Further, let us assume that this algebra is unitarily represented in some vector space $\mathcal{F}$. This means that (i) to every a_λ and $\tilde{a}_\lambda$ we assign a linear map $T_{a_\lambda} : \mathcal{F} \to \mathcal{F}$ such that (ii) $T_{[a_\lambda, \tilde{a}_\mu]_\zeta} = [T_{a_\lambda}, T_{\tilde{a}_\mu}]_\zeta$, and (iii) $T_{\tilde{a}_\lambda} = T^\dagger_{a_\lambda}$. To keep the notation simple, we will denote T_{a_λ} by a_λ (now regarded as a linear map $\mathcal{F} \to \mathcal{F}$) and $T_{\tilde{a}_\lambda}$ by $a^\dagger_\lambda$.

The Stone–von Neumann theorem states that the representation above is unique, i.e. that, up to unitary transformations of basis, there is only one such representation. The statement is proven by explicit construction of a basis on which the operators act in a specific and well-defined way. We will see that this action is given by Eq. (2.6), i.e. the reference basis is but the Fock space basis used in the text. This proves that the Heisenberg algebra encapsulates the full mathematical structure of the formalism of second quantization.

(a) We begin by noting that the operators $\hat{n}_\lambda \equiv a^\dagger_\lambda a_\lambda$ are Hermitian and commute with each other, i.e. they can be simultaneously diagonalized. Let $|n_{\lambda_1}, n_{\lambda_2}, \ldots\rangle$ be an orthonormalized eigenbasis of the operators $\{\hat{n}_\lambda\}$, i.e. $\hat{n}_{\lambda_i}|n_{\lambda_1}, n_{\lambda_2}, \ldots\rangle = n_{\lambda_i}|n_{\lambda_1}, n_{\lambda_2}, \ldots\rangle$. Show that, up to unit-modular factors, this basis is unique. (Hint: Use the irreducibility of the transformation.)

(b) Show that $a_{\lambda_i}|n_{\lambda_1}, n_{\lambda_2}, \ldots\rangle$ is an eigenstate of $\hat{n}_{\lambda_i}$ with eigenvalue $n_{\lambda_i} - 1$. Use this information to show that all eigenvalues n_{λ_i} are positive integers. (Hint: note positivity of the scalar norm.) Show that the explicit representation of the basis is given by

$$|n_{\lambda_1}, n_{\lambda_2}, \ldots\rangle = \prod_i \frac{a^{\dagger n_{\lambda_i}}_{\lambda_i}}{\sqrt{n_{\lambda_i}!}}|0\rangle, \tag{2.50}$$

where $|0\rangle$ is the unique state which has eigenvalue 0 for all $\hat{n}_i$. Comparison with Eq. (2.4) shows that the basis constructed above indeed coincides with the Fock space basis considered in the text.

Answer:

(a) Suppose we had identified two bases $\{|n_{\lambda_1}, n_{\lambda_2}, \ldots\rangle\}$ and $\{|n_{\lambda_1}, n_{\lambda_2}, \ldots\rangle'\}$ on which all operators $\hat{n}_i$ assumed equal eigenvalues. The irreducibility of the representation implies the existence of some polynomial $P(\{a_{\mu_i}, a^\dagger_{\mu_i}\})$ such that $|n_{\lambda_1}, n_{\lambda_2}, \ldots\rangle = P(\{a_{\mu_i}, a^\dagger_{\mu_i}\})|n_{\lambda_1}, n_{\lambda_2}, \ldots\rangle'$. Now, the action of P must not change any of the eigenvalues of $\hat{n}_i$, which means that P contains the operators a_μ and $a^\dagger_\mu$ in equal numbers. Reordering operators, we may thus bring P into the form $P(\{a_{\mu_i}, a^\dagger_{\mu_i}\}) = \tilde{P}(\{\hat{n}_{\mu_i}\})$. However, the action of this latter expression on $|n_{\lambda_1}, n_{\lambda_2}, \ldots\rangle'$ just produces a number, i.e. the bases are equivalent.

(b) For a given state $|n\rangle$, (concentrating on a fixed element of the single-particle basis, we suppress the subscript λ_i throughout), let us choose an integer q such that $\hat{n}a^{q-1}|n\rangle = (n-q+1)a^{q-1}|n\rangle$ with $n-q+1>0$ while $n-q\leq 0$. We then obtain

$$0 \geq (n-q)\langle n|a^{\dagger q}a^q|n\rangle = \langle n|a^{\dagger q}\hat{n}a^q|n\rangle = \langle n|(a^\dagger)^{q+1}a^{q+1}|n\rangle \geq 0.$$

The only way to satisfy this sequence of inequalities is to require that $\langle n|a^{\dagger q+1}|a^{q+1}|n\rangle = 0$ and $n-q=0$. The last equation implies the "integer-valuedness" of n. (In principle, we ought to prove that a zero-eigenvalue state $|0\rangle$ exists. To show this, take any reference state $|n_{\lambda_1}, n_{\lambda_2}, \ldots\rangle$ and apply operators a_{λ_i} as long as it takes to lower all eigenvalues n_{λ_i} to zero.) Using the commutation relations, it is then straightforward to verify that the r.h.s. of Eq. (2.50) (a) is unit normalized and (b) has eigenvalue n_{λ_i} for each $\hat{n}_{\lambda_i}$.

Semiclassical spin waves

In Chapter 1, the development of a theory of lattice vibrations in the harmonic atom chain was motivated by the quantization of the continuum classical theory. The latter provided insight into the nature of the elementary collective excitations. Here we will employ the semiclassical theory of spin dynamics to explore the nature of elementary spin-wave excitations.

(a) Making use of the spin commutation relation, $[\hat{S}_i^\alpha, \hat{S}_j^\beta] = i\delta_{ij}\epsilon^{\alpha\beta\gamma}\hat{S}_i^\gamma$, apply the operator identity $i\dot{\hat{\mathbf{S}}}_i = [\mathbf{S_i}, \mathbf{H}]$ to express the equation of motion of a spin in a nearest neighbor spin-S one-dimensional Heisenberg ferromagnet as a difference equation (N.B. $\hbar = 1$).

(b) Interpreting the spins as classical vectors, and taking the continuum limit, show that the equation of motion of the hydrodynamic modes takes the form $\dot{\mathbf{S}} = J\mathbf{S}\times\partial^2\mathbf{S}$ where we have assumed a unit lattice spacing. (Hint: In taking the continuum limit, apply a Taylor expansion to the spins i.e. $S_{i+1} = S_i + \partial S_i + \cdots$.) Find and sketch a wave-like solution describing small angle precession around a globally magnetized state $\mathbf{S}_i = S\mathbf{e}_z$ (i.e. a solution as shown in Fig. 2.10).

Answer:

(a) Making use of the equation of motion, and the commutation relation, substitution of the Heisenberg ferromagnetic Hamiltonian gives the difference equation

$$\dot{\hat{\mathbf{S}}}_i = J\hat{\mathbf{S}}_i \times (\hat{\mathbf{S}}_{i+1} + \hat{\mathbf{S}}_{i-1}).$$

(b) Interpreting the spins as classical vectors, and applying the Taylor expansion $\mathbf{S}_{i+1} \mapsto \mathbf{S}(x+1) = \mathbf{S} + \partial\mathbf{S} + \partial^2\mathbf{S}/2 + \cdots$, one obtains the classical equation of motion shown. Making the ansatz $\mathbf{S} = (c\cos(kx-\omega t), c\sin(kx-\omega t), \sqrt{S^2-c^2})$ one may confirm that the equation of motion is satisfied if $\omega = Jk^2$.

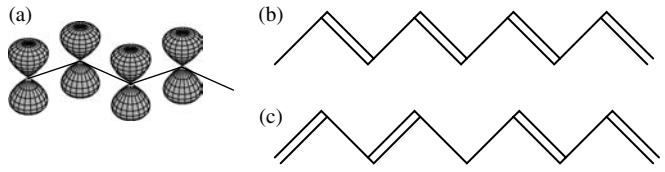

Figure 2.15 (a) An sp^2-hybridized polymer chain. (b) One of the configurations of the Peierls distorted chain. The double bonds represent the short links of the lattice. (c) A topological defect separating two domains of the ordered phase.

Su–Shrieffer–Heeger model of a conducting polymer chain

Polyacetylene consists of bonded CH groups forming an isomeric long-chain polymer. According to molecular orbital theory, the carbon atoms are expected to be sp^2-hybridized suggesting a planar configuration of the molecule. An unpaired electron is expected to occupy a single π-orbital which is oriented perpendicular to the plane. The weak overlap of the π-orbitals delocalizes the electrons into a narrow conduction band. According to the nearly free electron theory, one might expect the half-filled conduction band of a polyacetylene chain to be metallic. However, the energy of a half-filled band of a one-dimensional system can always be lowered by imposing a periodic lattice distortion known as a **Peierls instability** (see Fig. 2.15). The aim of this problem is to explore the instability.

(a) At its simplest level, the conduction band of polyacetylene can be modeled by a simple (arguably over-simplified) microscopic Hamiltonian, due to Su, Shrieffer, and Heeger,[26] in which the hopping matrix elements of the electrons are modulated by the lattice distortion of the atoms. By taking the displacement of the atomic sites to be u_n, and treating their dynamics as classical, the effective Hamiltonian can be cast in the form

$$\hat{H} = -t \sum_{n=1}^{N} (1 + u_n) \left[c^{\dagger}_{n\sigma} c_{n+1\sigma} + \text{h.c.} \right] + \sum_{n=1}^{N} \frac{k_{\text{s}}}{2} (u_{n+1} - u_n)^2 ,$$

where, for simplicity, the boundary conditions are taken to be periodic, and summation over the spins σ is assumed. The first term describes the hopping of electrons between neighboring sites with a matrix element modulated by the periodic distortion of the bond-length, while the last term represents the associated increase in the elastic energy. Taking the lattice distortion to be periodic, $u_n = (-1)^n \alpha$, and the number of sites to be even, bring the Hamiltonian to diagonal form. (Hint: Note that the lattice distortion lowers the symmetry of the lattice. The Hamiltonian is most easily diagonalized by distinguishing the two sites of the sublattice – i.e. doubling the size of the elementary unit cell.) Show that the Peierls distortion of the lattice opens a gap in the spectrum at the Fermi level of the half-filled system.

(b) By estimating the total electronic and elastic energy of the half-filled band (i.e. an average of one electron per lattice site), show that the one-dimensional system is always unstable towards the Peierls distortion. To complete this calculation, you will need

[26] W. P. Su, J. R. Schrieffer, and A. J. Heeger, Solitons in polyacetylene, *Phys. Rev. Lett.* **42** (1979), 1698–701.

the approximate formula for the (elliptic) integral, $\int_{-\pi/2}^{\pi/2} dk \left(1-\left(1-\alpha^2\right)\sin^2 k\right)^{1/2} \simeq 2+(a_1-b_1\ln\alpha^2)\alpha^2+\mathcal{O}(\alpha^2\ln\alpha^2)$, where a_1 and b_1 are (unspecified) numerical constants.

(c) For an even number of sites, the Peierls instability has two degenerate configurations (see Fig. 2.15(a)) – ABABAB... and BABABA... Comment on the qualitative form of the ground state lattice configuration if the number of sites is odd (see Fig. 2.15(b)). Explain why such configurations give rise to mid-gap states.

Answer:

(a) Since each unit cell is of twice the dimension of the original lattice, we begin by recasting the Hamiltonian in a sublattice form

$$\hat{H} = -t \sum_{m=1,\sigma}^{N/2} (1+\alpha)\left[a^\dagger_{m\sigma} b_{m\sigma} + \text{h.c.}\right] + (1-\alpha)\left[b^\dagger_{m\sigma} a_{m+1\sigma} + \text{h.c.}\right] \quad + 2Nk_s\alpha^2,$$

where the creation operators $a^\dagger_m$ and $b^\dagger_m$ act on the two sites of the elemental unit cell of the distorted lattice. Switching to the Fourier basis, $a_m = \sqrt{2/N}\sum_k e^{2ikm} a_k$ (similarly b_m), where k takes $N/2$ values uniformly on the interval $[-\pi/2, \pi/2]$ and the lattice spacing of the undistorted system is taken to be unity, the Hamiltonian takes the form

$$\hat{H} = 2Nk_s\alpha^2 - t\sum_k \left(a^\dagger_{k\sigma}, b^\dagger_{k\sigma}\right) \begin{pmatrix} 0 & (1+\alpha)+(1-\alpha)e^{2ik} \\ (1+\alpha)+(1-\alpha)e^{-2ik} & 0 \end{pmatrix} \begin{pmatrix} a_{k\sigma} \\ b_{k\sigma} \end{pmatrix}.$$

Diagonalizing the 2×2 matrix , one obtains $\epsilon(k) = \pm 2t\left[1+(\alpha^2-1)\sin^2 k\right]^{1/2}$. Reassuringly, in the limit $\alpha \to 0$, one recovers the cosine spectrum characteristic of the undistorted tight-binding problem while, in the limit $\alpha \to 1$, pairs of monomers become decoupled and we obtain a massively degenerate bonding and antibonding spectrum.

(b) According to the formula given in the text, the total shift in energy is given by $\delta\epsilon = -4t(a_1 - b_1\ln\alpha^2)\alpha^2 + 2k_s\alpha^2$. Maximizing the energy gain with respect to α, one finds that the stable configuration is found when $\alpha^2 = \exp[\frac{a_1}{b_1} - 1 - \frac{k_s\alpha}{2tb_1}]$.

(c) If the number of sites is odd, the Peierls distortion is inevitably frustrated. The result is that the polymer chain must accommodate a **topological excitation**. The excitation is said to be topological because the defect cannot be removed by a smooth continuous deformation. Its effect on the spectrum of the model is to introduce a state that lies within the band gap of the material. The consideration of an odd number of sites forces a topological defect into the system. However, even if the number of sites is even, one can create low energy topological excitations of the system either by doping (see Fig. 2.15(b)), or by the creation of **excitons**, particle–hole excitations of the system. Indeed, such topological excitations can dominate the transport properties of the system.

Schwinger boson representation

As with the Holstein–Primakoff representation, the Schwinger boson provides another representation of quantum mechanical spin. The aim of this problem is to confirm the validity of the representation. For practical purposes, the value of the particular representation depends on its application.

In the **Schwinger boson representation**, the quantum mechanical spin is expressed in terms of two bosonic operators a and b in the form

$$\hat{S}^+ = a^\dagger b, \quad \hat{S}^- = (\hat{S}^+)^\dagger,$$
$$\hat{S}^z = \frac{1}{2}\left(a^\dagger a - b^\dagger b\right).$$

Julian Schwinger 1918–1994
Nobel Laureate in Physics with Sin-Itiro Tomonaga and Richard P. Feynman, for their fundamental work in quantum electrodynamics, with far-reaching consequences for the physics of elementary particles. (Image © The Nobel Foundation.)

(a) Show that this definition is consistent with the commutation relations for spin: $[\hat{S}^+, \hat{S}^-] = 2\hat{S}^z$.
(b) Using the bosonic commutation relations, show that

$$|S, m\rangle = \frac{(a^\dagger)^{S+m}}{\sqrt{(S+m)!}} \frac{(b^\dagger)^{S-m}}{\sqrt{(S-m)!}} |\Omega\rangle,$$

is compatible with the definition of an eigenstate of the total spin operator $\mathbf{S}^2$ and S^z. Here $|\Omega\rangle$ denotes the vacuum of the Schwinger bosons, and the total spin S defines the physical subspace $\{|n_a, n_b\rangle | n_a + n_b = 2S\}$.

Answer:

(a) Using the commutation relation for bosons, one finds $[\hat{S}^+, \hat{S}^-] = a^\dagger b\ b^\dagger a - b^\dagger a\ a^\dagger b = a^\dagger a - b^\dagger b = 2\hat{S}^z$, as required.
(b) Using the identity $\hat{\mathbf{S}}^2 = (\hat{S}^z)^2 + \frac{1}{2}(\hat{S}^+\hat{S}^- + \hat{S}^-\hat{S}^+) = \frac{1}{4}(\hat{n}_a - \hat{n}_b)^2 + \hat{n}_a\hat{n}_b + \frac{1}{2}(\hat{n}_a + \hat{n}_b)$ one finds that $\hat{\mathbf{S}}^2|S, m\rangle = \left[m^2 + (S+m)(S-m) + S\right]|S, m\rangle = S(S+1)|S, m\rangle$, as required. Similarly, one finds $\hat{S}^z|S, m\rangle = \frac{1}{2}(n_a - n_b)|n_a = S+m, n_b = S-m\rangle = m|S, m\rangle$ showing $|S, m\rangle$ to be an eigenstate of the operator $\hat{S}^z$ with eigenvalue m.

Jordan–Wigner transformation

So far we have shown how the algebra of quantum mechanical spin can be expressed using boson operators – cf. the Holstein–Primakoff transformation and the Schwinger boson representation. In this problem we show that a representation for spin-(1/2) can be obtained in terms of Fermion operators.

Let us represent an up spin as a particle and a down spin as the vacuum, i.e. $|\uparrow\rangle \equiv |1\rangle = f^\dagger|0\rangle, |\downarrow\rangle \equiv |0\rangle = f|1\rangle$. In this representation the spin raising and lowering operators are expressed in the forms $\hat{S}^+ = f^\dagger$ and $\hat{S}^- = f$, while $\hat{S}^z = f^\dagger f - 1/2$.

(a) With this definition, confirm that the spins obey the algebra $[\hat{S}^+, \hat{S}^-] = 2\hat{S}^z$.

However, there is a problem: spins on different sites commute while fermion operators anticommute, e.g. $S_i^+ S_j^+ = S_j^+ S_i^+$, but $f_i^\dagger f_j^\dagger = -f_j^\dagger f_i^\dagger$. To obtain a faithful spin representation, it is necessary to cancel this unwanted sign. Although a general procedure is hard to formulate, in one dimension this can be achieved by a nonlinear transformation, namely

$$\hat{S}_l^+ = f_l^\dagger e^{i\pi \sum_{j<l} \hat{n}_j}, \qquad \hat{S}_l^- = e^{-i\pi \sum_{j<l} \hat{n}_j} f_l, \qquad \hat{S}_l^z = f_l^\dagger f_l - \frac{1}{2}.$$

Operationally, this seemingly complicated transformation is straightforward: in one dimension, the particles can be ordered on the line. By counting the number of particles "to the left" we can assign an overall sign of $+1$ or -1 to a given configuration and thereby transmute the particles into fermions. (Put differently, the exchange of two fermions induces a sign change that is compensated by the factor arising from the phase – the "Jordan–Wigner string.")

(b) Using the Jordan–Wigner representation, show that $\hat{S}_m^+ \hat{S}_{m+1}^- = f_m^\dagger f_{m+1}$.

(c) For the spin-(1/2) anisotropic quantum Heisenberg spin chain, the spin Hamiltonian assumes the form $\hat{H} = -\sum_n \left[J_z \hat{S}_n^z \hat{S}_{n+1}^z + \frac{J_\perp}{2} \left(\hat{S}_n^+ \hat{S}_{n+1}^- + \hat{S}_n^- \hat{S}_{n+1}^+ \right) \right]$. Turning to the Jordan–Wigner representation, show that the Hamiltonian can be cast in the form

$$\hat{H} = -\sum_n \left[\frac{J_\perp}{2} \left(f_n^\dagger f_{n+1} + \text{h.c.} \right) + J_z \left(\frac{1}{4} - f_n^\dagger f_n + f_n^\dagger f_n f_{n+1}^\dagger f_{n+1} \right) \right].$$

(d) The mapping above shows that the one-dimensional quantum spin-(1/2) XY-model (i.e. $J_z = 0$) can be diagonalized as a non-interacting theory of spinless fermions. In this case, show that the spectrum assumes the form $\epsilon(k) = -J_\perp \cos ka$.

Answer:

(a) Using the fermionic anti-commutation relations, one finds $[\hat{S}^+, \hat{S}^-]_- = [f^\dagger, f]_- = f^\dagger f - f f^\dagger = 2f^\dagger f - 1 = 2\hat{S}^z$.

(b) Using the fact that the number operators on different sites commute, one finds $\hat{S}_m^+ \hat{S}_{m+1}^- = f_m^\dagger e^{i\pi \sum_{j<m} n_j} e^{-i\pi \sum_{l<m+1} n_l} f_{m+1} = f_m^\dagger e^{-i\pi n_m} f_{m+1} = f_m^\dagger f_{m+1}$, where we have made use of the fact that, for fermionic particles, $f_m^\dagger e^{-i\pi n_m} \equiv f_m^\dagger$.

(c) The fermion representation is simply obtained by substitution.

(d) With $J_z = 0$, the spin Hamiltonian assumes the form of a non-interacting tight-binding Hamiltonian $\hat{H} = \frac{J_\perp}{2} \sum_n (f_n^\dagger f_{n+1} + \text{h.c.})$. This Hamiltonian, which has been encountered previously, is diagonalized in the Fourier space, after which one obtains the cosine band dispersion.

Spin–charge separation in one-dimension

In Section 2.2 a free theory of interacting spinless fermions was developed in one dimension making use of the bosonization formalism. This analysis showed that the low-energy degrees of freedom were described by hydrodynamic charge (i.e. density) fluctuations that propagated with a linear dispersion. However, as well as charge, the electron degrees of freedom carry spin. The aim of this problem is to explore the fate of the spin degrees of freedom in a one-dimensional environment.

As a first step, we introduce operators (cf. Eq. (2.35)) $\hat{\rho}_{sq\alpha} = \sum_k a^\dagger_{s(k+q)\alpha} a_{sk\alpha}, \alpha = \uparrow, \downarrow$ generalizing the previously introduced density operators for the presence of spin. Similarly, the bosonic degrees of freedom of the theory (cf. Eq. (2.40)) now carry a spin index, $b_q \to b_{q\alpha}$. One aspect that makes the problem more difficult to tackle than the previously explored spinless case is that the $2k_{\rm F}$-momentum transfer interaction $|k_{\rm F}+q+q_1,\uparrow; k_{\rm F}+q-q_1,\downarrow\rangle \to |-k_{\rm F}+q+q_2,\uparrow; -k_{\rm F}+q-q_2,\downarrow\rangle$ in which a right-moving spin up electron is scattered to a left-moving spin up electron cannot be expressed in terms of slowly fluctuating density operators. (If you don't believe this, try!) However, using the renormalisation group methods introduced in Chapter 8, it can be shown that this type of interaction is physically largely irrelevant and can be neglected from the outset.

Concentrating on the low-momentum-transfer interaction, the effective bosonic Hamiltonian assumes the form (exercise)

$$\hat{H} = \sum_{q>0,s,\alpha} v_{\rm F} q b^\dagger_{sq\alpha} b_{sq\alpha} + \sum_{q>0,s,\alpha,\alpha'} |q| \left[\frac{g_2}{2\pi} \left(b^\dagger_{sq\alpha} b^\dagger_{\bar{s}q\alpha'} + \text{h.c.} \right) + \frac{g_4}{2\pi} b^\dagger_{sq\alpha} b_{sq\alpha'} \right].$$

Introducing operators that create charge (ρ) and spin (σ) fluctuations, $b_{sq\rho} = \frac{1}{\sqrt{2}}(b_{sq\uparrow} + b_{sq\downarrow}), b_{sq\sigma} = \frac{1}{\sqrt{2}}(b_{sq\uparrow} - b_{sq\downarrow})$, rearrange the Hamiltonian, and thereby show that it assumes a diagonal form with the spin and charge degrees of freedom exhibiting different velocities. This is a manifestation of **spin–charge separation**: even without the introduction of spin-dependent forces, the spin and charge degrees of freedom of the electron in the metallic conductor separate and propagate at different velocities. In this sense, there is no way to adiabatically continue from non-interacting electrons to the collective charge and spin excitations of the system.

Despite the "fragility" of the electron, and the apparent ubiquity of this phenomenon, the **observation of spin–charge separation in one-dimensional conductors** has presented a significant challenge to experimentalists. The reason is subtle. The completion of an electrical circuit necessarily requires contact of the quantum wire with bulk leads. The leads involve a reservoir of electrons with conventional Fermi-liquid character. Electrical transport requires the recombination of the collective charge (holon) and spin (spinon) degrees of freedom at the contact to reconstitute physical electrons. It is an exasperating fact that this reconstitution of the physical electron "masks" the character of spin–charge separation. Instead, the phenomenon of spin–charge separation has been inferred indirectly through spectroscopic techniques.

Answer:

Motivated by the separation into spin and charge degrees of freedom, a rearrangement of

the Hamiltonian gives

$$\hat{H} = \sum_{q>0,s} v_{\rm F} q \left(b^\dagger_{sq\rho} b_{sq\rho} + b^\dagger_{sq\sigma} b_{sq\sigma} \right) + |q| \left[\frac{g_2}{\pi} \left(b^\dagger_{sq\rho} b^\dagger_{\bar{s}q\rho} + \text{h.c.} \right) + \frac{g_4}{\pi} b^\dagger_{sq\rho} b_{sq\rho} \right] \quad .$$

Once again, applying a Bogoliubov transformation, the Hamiltonian is brought to the diagonal form

$$\hat{H} = \sum_{q>0,s} \left[|q| \sqrt{(v_{\rm F} + g_4/\pi)^2 - (g_2/\pi)^2} \alpha^\dagger_{sq\rho} \alpha_{sq\rho} + |q| v_{\rm F} \alpha^\dagger_{sq\sigma} \alpha_{sq\sigma} \right] + \text{const.}.$$

The Kondo problem

Historically, the Kondo problem has assumed a place of great significance in the development of the field of strongly correlated quantum systems. It represents perhaps the simplest example of a phenomenon driven by strong electron interaction and, unusually for this arena of physics, admits a detailed theoretical understanding. Further, in respect of the principles established in Chapter 1, it exemplifies a number of important ideas from the concept of reducibility – the collective properties of the system may be captured by a simplified effective Hamiltonian which includes only the relevant low-energy degrees of freedom – and the renormalization group. In the following problem, we will seek to develop the low-energy theory of the "Kondo impurity system" leaving the discussion of its phenomenology to Problems 5.5 and 8.8.5 in subsequent chapters.

The Kondo effect is rooted in the experimental observation that, when small amounts of magnetic ion impurities are embedded in a metallic host (such as manganese in copper, or iron in CuAu alloys), a pronounced minimum develops in the temperature dependence of the resistivity. Although the phenomenon was discovered experimentally in 1934,[27] it was not until 1964 that a firm understanding of the phenomenon was developed by Kondo.[28] Historically, the first step towards the resolution of this phenomenon came with a suggestion by Anderson that the system could be modeled as an itinerant band of electron states interacting with local dilute magnetic moments associated with the ion impurities.[29] Anderson proposed that the integrity of the local moment was protected by a large local Coulomb repulsion which inhibited multiple occupancy of the orbital state – a relative of the Hubbard U-interaction. Such behavior is encoded in the **Anderson impurity Hamiltonian**

$$\hat{H} = \sum_{\mathbf{k}\sigma} \left[\epsilon_{\mathbf{k}} c^\dagger_{\mathbf{k}\sigma} c_{\mathbf{k}\sigma} + \left(V_{\mathbf{k}} d^\dagger_\sigma c_{\mathbf{k}\sigma} + \text{h.c.} \right) \right] + \sum_\sigma \epsilon_d n_{d\sigma} + U n_{d\uparrow} n_{d\downarrow},$$

where the operators $c^\dagger_{\mathbf{k}\sigma}$ create itinerant electrons of spin σ and $\epsilon_{\mathbf{k}}$ in the metallic host while the operators $d^\dagger_\sigma$ create electrons of spin σ on the local impurity at position $\mathbf{r} = 0$. Here we have used $n_{d\sigma} = d^\dagger_\sigma d_\sigma$ to denote the number operator. While electrons in the band

[27] de Haas, de Boer, and van den Berg, The electrical resistance of gold, copper, and lead at low temperatures, *Physica* **1** (1934), 1115.
[28] J. Kondo, Resistance minimum in dilute magnetic alloys, *Prog. Theor. Phys.* **32** (1964), 37–69.
[29] P. W. Anderson, Localized magnetic states in metals, *Phys. Rev.* **124** (1961), 41–53.

are assumed to be characterized by a Fermi-liquid-like behavior, those associated with the impurity state experience an on-site Coulomb interaction of a strength characterized by a Hubbard energy U.

According to the experimental phenomenology, the Fermi level $\epsilon_{\rm F}$ is assumed to lie somewhere in between the single-particle impurity level ϵ_d and $\epsilon_d + U$ so that, on average, the site occupancy of the impurity is unity. Nevertheless, the matrix element coupling the local moment to the itinerant electron states $V_{\mathbf{k}} = L^{-d/2} \int d\mathbf{r}\, V(\mathbf{r}) e^{i\mathbf{k}\cdot\mathbf{r}}$ admits the existence of virtual processes in which the site occupancy can fluctuate between zero and two. These virtual fluctuations allow the spin on the impurity site to flip through exchange.

The discussion of the half-filled Hubbard system in Section 2.2 suggests that it will be helpful to transform the Anderson impurity Hamiltonian to an effective theory which exposes the low-energy content of the system. To this end, let us express the total wavefunction of the many-body Hamiltonian $|\psi\rangle$ as the sum of terms $|\psi_0\rangle$, $|\psi_1\rangle$, and $|\psi_2\rangle$, where the subscript denotes the occupancy of the impurity site. With this decomposition, the Schrödinger equation for the Hamiltonian can be cast in matrix form, $\sum_{n=0}^{2} \hat{H}_{mn}|\psi_n\rangle = E|\psi_m\rangle$, where $\hat{H}_{mn} = \hat{P}_m \hat{H} \hat{P}_n$, and the operators $\hat{P}_m$ project onto the subspace with m electrons on the impurity (i.e. $\hat{P}_0 = \prod_\sigma (1 - n_{d\sigma})$, etc.).

(a) Construct the operators $\hat{H}_{mn}$ explicitly and explain why $\hat{H}_{20} = \hat{H}_{02} = 0$.

(b) Since we are interested in the effect of virtual excitations from the $|\psi_1\rangle$ subspace, we may proceed by formally eliminating $|\psi_0\rangle$ and $|\psi_2\rangle$ from the Schrödinger equation. Doing so, show that the equation for $|\psi_1\rangle$ can be written as

$$\left[\hat{H}_{10} \frac{1}{E - \hat{H}_{00}} \hat{H}_{01} + \hat{H}_{11} + \hat{H}_{12} \frac{1}{E - \hat{H}_{22}} \hat{H}_{21} \right] |\psi_1\rangle = E|\psi_1\rangle.$$

(c) At this stage, the equation for $|\psi_1\rangle$ is exact. Show that, when substituted into this expression, an expansion to leading order in $1/U$ and $1/\epsilon_d$ leads to the expression

$$\hat{H}_{12} \frac{1}{E - \hat{H}_{22}} \hat{H}_{21} + \hat{H}_{10} \frac{1}{E - \hat{H}_{00}} \hat{H}_{01} \simeq - \sum_{\mathbf{k}\mathbf{k}'\sigma\sigma'} V_{\mathbf{k}} V^*_{\mathbf{k}'} \left(\frac{c^\dagger_{\mathbf{k}\sigma} c_{\mathbf{k}'\sigma'} d_\sigma d^\dagger_{\sigma'}}{U + \epsilon_d - \epsilon_{\mathbf{k}'}} + \frac{c_{\mathbf{k}'\sigma'} c^\dagger_{\mathbf{k}\sigma} d^\dagger_{\sigma'} d_\sigma}{\epsilon_{\mathbf{k}} - \epsilon_d} \right).$$

To obtain the first term in the expression, consider the commutation of $(E - \hat{H}_{22})^{-1}$ with $\hat{H}_{21}$ and make use of the fact that the total operator acts upon the singly occupied subspace. A similar line of reasoning will lead to the second term in the expression. Here $U + \epsilon_d - \epsilon_{\mathbf{k}'}$ and $\epsilon_d - \epsilon_{\mathbf{k}}$ denote the respective excitation energies of the virtual states.

Making use of the Pauli matrix identity, $\boldsymbol{\sigma}_{\alpha\beta} \cdot \boldsymbol{\sigma}_{\gamma\delta} = 2\delta_{\alpha\delta}\delta_{\beta\gamma} - \delta_{\alpha\beta}\delta_{\gamma\delta}$, it follows that (exercise)

$$\sum_{\sigma\sigma'} c^\dagger_{\mathbf{k}\sigma} c_{\mathbf{k}'\sigma'} d^\dagger_{\sigma'} d_\sigma = 2\hat{\mathbf{s}}_{\mathbf{k}\mathbf{k}'} \cdot \hat{\mathbf{S}}_d + \frac{1}{2} \sum_{\sigma\sigma'} c^\dagger_{\mathbf{k}\sigma} c_{\mathbf{k}'\sigma} n_{d\sigma'},$$

where $\hat{\mathbf{S}}_d = \sum_{\alpha\beta} d^\dagger_\alpha \boldsymbol{\sigma}_{\alpha\beta} d_\beta / 2$ denotes the impurity spin 1/2 degree of freedom associated with the impurity and $\hat{\mathbf{s}}_{\mathbf{k}\mathbf{k}'} = \sum_{\alpha\beta} c^\dagger_{\mathbf{k}\alpha} \boldsymbol{\sigma}_{\alpha\beta} c_{\mathbf{k}'\beta} / 2$. Combining this result with that

obtained above, up to an irrelevant constant, the total effective Hamiltonian (including $\hat{H}_{11}$) acting in the projected subspace, $|\psi_1\rangle$ is given by

$$\hat{H}_{\rm sd} = \sum_{\mathbf{k}\sigma} \epsilon_{\mathbf{k}} c^\dagger_{\mathbf{k}\sigma} c_{\mathbf{k}\sigma} + \sum_{\mathbf{k}\mathbf{k}'} \left[2J_{\mathbf{k},\mathbf{k}'}\, \hat{\mathbf{s}}_{\mathbf{k}\mathbf{k}'} \cdot \hat{\mathbf{S}}_d + K_{\mathbf{k},\mathbf{k}'} \sum_\sigma c^\dagger_{\mathbf{k}\sigma} c_{\mathbf{k}'\sigma} \right],$$

where

$$J_{\mathbf{k},\mathbf{k}'} = V^*_{\mathbf{k}'} V_{\mathbf{k}} \left[\frac{1}{U + \epsilon_d - \epsilon_{\mathbf{k}'}} + \frac{1}{\epsilon_{\mathbf{k}} - \epsilon_d} \right],$$
$$K_{\mathbf{k},\mathbf{k}'} = \frac{V^*_{\mathbf{k}'} V_{\mathbf{k}}}{2} \left[\frac{1}{\epsilon_{\mathbf{k}} - \epsilon_d} - \frac{1}{U + \epsilon_d - \epsilon_{\mathbf{k}'}} \right].$$

With both $U + \epsilon_d$ and ϵ_d greatly in excess of the typical excitation energy scales, one may safely neglect the particular energy dependence of the parameters $J_{\mathbf{k},\mathbf{k}'}$ and $K_{\mathbf{k},\mathbf{k}'}$. In this case, the exchange interaction $J_{\mathbf{k},\mathbf{k}'}$ can be treated as local, the scattering term $K_{\mathbf{k},\mathbf{k}'}$ can be absorbed into a shift of the single-particle energy of the itinerant band, and the positive (i.e. antiferromagnetic) exchange coupling can be accommodated through the effective **sd-Hamiltonian**

$$\boxed{\hat{H}_{\rm sd} = \sum_{\mathbf{k}\sigma} \epsilon_{\mathbf{k}} c^\dagger_{\mathbf{k}\sigma} c_{\mathbf{k}\sigma} + 2J \hat{\mathbf{S}}_d \cdot \hat{\mathbf{s}}(\mathbf{r} = 0),} \tag{2.51}$$

where $\hat{\mathbf{s}}(\mathbf{r} = 0) = \sum_{\mathbf{k}\mathbf{k}'\sigma\sigma'} c^\dagger_{\mathbf{k}\sigma} \sigma_{\sigma\sigma'} c_{\mathbf{k}'\sigma'}/2$ denotes the spin density of the itinerant electron band at the impurity site. To understand how the magnetic impurity affects the low-temperature transport, we refer to Problem 5.5, where the sd-Hamiltonian is explored in the framework of a diagrammatic perturbation theory in the spin interaction.

Answer:

(a) Since the diagonal elements $\hat{H}_{mm}$ leave the occupation number fixed, they may be identified with the diagonal elements of the microscopic Hamiltonian, i.e.

$$\hat{H}_{00} = \sum_{\mathbf{k}} \epsilon_{\mathbf{k}} c^\dagger_{\mathbf{k}\sigma} c_{\mathbf{k}\sigma}, \qquad \hat{H}_{11} = \sum_{\mathbf{k}} \epsilon_{\mathbf{k}} c^\dagger_{\mathbf{k}\sigma} c_{\mathbf{k}\sigma} + \epsilon_d, \qquad \hat{H}_{22} = \sum_{\mathbf{k}} \epsilon_{\mathbf{k}} c^\dagger_{\mathbf{k}\sigma} c_{\mathbf{k}\sigma} + 2\epsilon_d + U.$$

The off-diagonal terms arise from the hybridization between the free electron states and the impurity. Since the coupling involves only the transfer of single electrons, $\hat{H}_{02} = \hat{H}_{20} = 0$ and

$$\hat{H}_{10} = \sum_{\mathbf{k}\sigma} V_{\mathbf{k}} d^\dagger_\sigma (1 - n_{d\bar{\sigma}}) c_{\mathbf{k}\sigma}, \qquad \hat{H}_{21} = \sum_{\mathbf{k}\sigma} V_{\mathbf{k}} d^\dagger_\sigma n_{d\bar{\sigma}} c_{\mathbf{k}\sigma},$$

where $\bar{\sigma} = \uparrow$ for $\sigma = \downarrow$ and vice versa, $\hat{H}_{01} = \hat{H}^\dagger_{10}$ and $\hat{H}_{12} = \hat{H}^\dagger_{21}$.

(b) Using the fact that $\hat{H}_{00}|\psi_0\rangle + \hat{H}_{01}|\psi_1\rangle = E|\psi_0\rangle$, one may set $|\psi_0\rangle = (E - \hat{H}_{00})^{-1}\hat{H}_{01}|\psi_1\rangle$ and, similarly, $|\psi_2\rangle = (E - \hat{H}_{22})^{-1}\hat{H}_{21}|\psi_1\rangle$. Then, substituting into the equation for $|\psi_1\rangle$, one obtains the required expression.

(c) Making use of the expressions from part (a), we have

$$\hat{H}_{12}\frac{1}{E-\hat{H}_{22}}\hat{H}_{21} = \sum_{\mathbf{k}\mathbf{k}'\sigma\sigma'} V_{\mathbf{k}}V^*_{\mathbf{k}'}\, c^\dagger_{\mathbf{k}\sigma} n_{d\bar{\sigma}} d_\sigma \frac{1}{E-\hat{H}_{22}} d^\dagger_{\sigma'} n_{d\bar{\sigma}'} c_{\mathbf{k}'\sigma'},$$
$$\hat{H}_{10}\frac{1}{E-\hat{H}_{00}}\hat{H}_{01} = \sum_{\mathbf{k}\mathbf{k}'\sigma\sigma'} V_{\mathbf{k}}V^*_{\mathbf{k}'}\, d^\dagger_{\sigma}(1-n_{d\bar{\sigma}}) c_{\mathbf{k}\sigma} \frac{1}{E-\hat{H}_{00}} c^\dagger_{\mathbf{k}'\sigma'}(1-n_{d\bar{\sigma}'}) d_{\sigma'}.$$

Then, substituting for $\hat{H}_{22}$ and $\hat{H}_{00}$ from (a), and commuting operators, we have

$$\frac{1}{E-\hat{H}_{22}} d^\dagger_{\sigma'} n_{d\bar{\sigma}'} c_{\mathbf{k}'\sigma'} = -\frac{d^\dagger_{\sigma'} n_{d\bar{\sigma}'} c_{\mathbf{k}'\sigma'}}{U+\epsilon_d-\epsilon_{\mathbf{k}'}} \left[1 - \frac{E-\epsilon_d-\hat{H}_{00}}{U+\epsilon_d-\epsilon_{\mathbf{k}'}}\right]^{-1},$$
$$\frac{1}{E-\hat{H}_{00}} c^\dagger_{\mathbf{k}'\sigma'}(1-n_{d\bar{\sigma}'}) d_{\sigma'} = -\frac{c^\dagger_{\mathbf{k}'\sigma'}(1-n_{d\bar{\sigma}'}) d_{\sigma'}}{\epsilon_{\mathbf{k}'}-\epsilon_d} \left[1 - \frac{E-\epsilon_d-\hat{H}_{00}}{\epsilon_{\mathbf{k}'}-\epsilon_d}\right]^{-1}.$$

Then expanding in large U and ϵ_d, to leading order we obtain

$$\hat{H}_{12}\frac{1}{E-\hat{H}_{22}}\hat{H}_{21} + \hat{H}_{10}\frac{1}{E-\hat{H}_{00}}\hat{H}_{01} \simeq$$
$$-\sum_{\mathbf{k}\mathbf{k}'\sigma\sigma'} V_{\mathbf{k}}V^*_{\mathbf{k}'} \left(\frac{c^\dagger_{\mathbf{k}\sigma} n_{d,\bar{\sigma}} d_\sigma d^\dagger_{\sigma'} n_{d\bar{\sigma}'} c_{\mathbf{k}'\sigma'}}{U+\epsilon_d-\epsilon_{\mathbf{k}'}} + \frac{d^\dagger_\sigma (1-n_{d,\bar{\sigma}}) c_{\mathbf{k}\sigma} c^\dagger_{\mathbf{k}'\sigma'}(1-n_{d\bar{\sigma}'}) d_{\sigma'}}{\epsilon_{\mathbf{k}'}-\epsilon_d} \right).$$

Finally, noting that this operator acts upon the singly-occupied subspace spanned by $|\psi_1\rangle$, we see that the factors involving $n_{d\sigma}$ are redundant and can be dropped. As a result, swapping the momentum and spin indices in the second part of the expression, we obtain the required expression.

3

Feynman path integral

The aim of this chapter is to introduce the concept of the Feynman path integral. As well as developing the general construction scheme, particular emphasis is placed on establishing the interconnections between the quantum mechanical path integral, classical Hamiltonian mechanics, and classical statistical mechanics. The practice of path integration is discussed in the context of several pedagogical applications. As well as the canonical examples of a quantum particle in a single and a double potential well, we discuss the generalization of the path integral scheme to tunneling of extended objects (quantum fields), dissipative and thermally assisted quantum tunneling, and the quantum mechanical spin.

In this chapter we temporarily leave the arena of many-body physics and second quantization and, at least superficially, return to single-particle quantum mechanics. By establishing the path integral approach for ordinary quantum mechanics, we will set the stage for the introduction of field integral methods for many-body theories explored in the next chapter. We will see that the path integral not only represents a gateway to higher-dimensional functional integral methods but, when viewed from an appropriate perspective, already represents a field theoretical approach in its own right. Exploiting this connection, various concepts of field theory, namely stationary phase analysis, the Euclidean formulation of field theory, instanton techniques, and the role of topology in field theory, are introduced in this chapter.

3.1 The path integral: general formalism

Broadly speaking, there are two approaches to the formulation of quantum mechanics: the "operator approach" based on the canonical quantization of physical observables and the associated operator algebra, and the Feynman path integral.[1] Whereas canonical quantization is usually taught first in elementary courses on quantum mechanics, path integrals seem to have acquired the reputation of being a sophisticated concept that is better reserved for

[1] For a more extensive introduction to the Feynman path integral, one can refer to one of the many standard texts including R. P. Feynman and A. R. Hibbs, *Quantum Mechanics and Path Integrals* (McGraw-Hill, 1965), J. W. Negele and H. Orland, *Quantum Many Particle Systems* (Addison-Wesley, 1988), and L. S. Schulman, *Techniques and Applications of Path Integration* (Wiley, 1981). Alternatively, one may turn to the original paper, R. P. Feynman, Space-time approach to non-relativistic quantum mechanics, *Rev. Mod. Phys.* **20** (1948), 362–87. Historically, Feynman's development of the path integral was motivated by earlier work by Dirac on the connection between classical and quantum mechanics, P. A. M. Dirac, On the analogy between classical and quantum mechanics, *Rev. Mod. Phys.* **17** (1945), 195–9.

advanced courses. Yet this treatment is hardly justified! In fact, the path integral formulation has many advantages, most of which explicitly support an intuitive understanding of quantum mechanics. Moreover, integrals – even the infinite-dimensional ones encountered below – are hardly more abstract than infinite-dimensional linear operators. Further merits of the path integral include the following:

Richard P. Feynman 1918–88

Nobel Laureate in Physics in 1965 (with Sin-Itiro Tomonaga, and Julian Schwinger) for "fundamental work in quantum electrodynamics, with far-reaching consequences for the physics of elementary particles." He was also well known for his unusual life style and for his popular books and lectures on mathematics and physics. (Image © The Nobel Foundation.)

- ▷ Whereas the classical limit is not always easy to retrieve within the canonical formulation of quantum mechanics, it constantly remains visible in the path integral approach. The latter makes explicit use of classical mechanics as a "platform" on which to construct a theory of quantum fluctuations. The classical solutions of Hamilton's equation of motion always remain a central ingredient of the formalism.[2]
- ▷ Path integrals allow for an efficient formulation of *non-perturbative* approaches to the solution of quantum mechanical problems. Examples include the "instanton" formulation of quantum tunneling discussed below. The extension of such methods to continuum theories has led to some of the most powerful concepts of quantum field theory.
- ▷ The Feynman path integral represents a prototype of the higher-dimensional field integrals to be introduced in the next chapter. However, even the basic "zero-dimensional" path integral is of relevance to applications in many-body physics. Very often, one encounters environments such as the superconductor, superfluid, or strongly correlated few-electron devices where a macroscopically large number of degrees of freedom "lock" to form a single collective variable. (For example, to a first approximation, the phase information carried by the order parameter field in moderately large superconducting grains can often be described in terms of a *single* phase degree of freedom, i.e. a "quantum particle" living on the unit circle.) Path integral techniques have proven ideally suited to the analysis of such systems.

What then is the basic idea of the path integral approach? More than any other formulation of quantum mechanics, the path integral formalism is based on connections to classical mechanics. The variational approach employed in Chapter 1 relied on the fact that classically allowed trajectories in configuration space extremize an action functional. A principal constraint to be imposed on any such trajectory is energy conservation. By contrast, quantum particles have a little bit more freedom than their classical counterparts. In particular, by the Uncertainty Principle, energy conservation can be violated by an amount ΔE over a time $\sim \hbar/\Delta E$ (here, and throughout this chapter, we will use $\hbar$ for clarity). The connection

[2] For this reason, path integration has turned out to be an indispensable tool in fields such as **quantum chaos** where the quantum manifestations of classically non-trivial behavior are investigated – for more details, see Section 3.3.

to action principles of classical mechanics becomes particularly apparent in problems of quantum tunneling: a particle of energy E may tunnel through a potential barrier of height $V > E$. However, this process is penalized by a damping factor $\sim \exp(i \int_{\text{barrier}} dx\, p/\hbar)$, where $p = \sqrt{2m(E-V)}$, i.e. the exponent of the (imaginary) action associated with the classically forbidden path.

These observations motivate the idea of a new formulation of quantum propagation: could it be that, as in classical mechanics, the quantum amplitude A for propagation between any two points in coordinate space is again controlled by the action functional – controlled in a relaxed sense where not just a single extremal path $x_{\text{cl}}(t)$, but an entire manifold of neighboring paths contribute? More specifically, one might speculate that the quantum amplitude is obtained as $A \sim \sum_{x(t)} \exp(iS[x]/\hbar)$, where $\sum_{x(t)}$ symbolically stands for a summation over all paths compatible with the initial conditions of the problem, and S denotes the *classical* action. Although, at this stage, no formal justification for the path integral has been presented, with this ansatz some features of quantum mechanics would obviously be borne out correctly. Specifically, in the classical limit ($\hbar \to 0$), the quantum mechanical amplitude would become increasingly dominated by the contribution to the sum from the classical path $x_{\text{cl}}(t)$. This is because non-extremal configurations would be weighted by a rapidly oscillating amplitude associated with the large phase $S/\hbar$ and would, therefore, average to zero.[3] Secondly, quantum mechanical tunneling would be a natural element of the theory; non-classical paths do contribute to the net amplitude, but at the cost of a damping factor specified by the imaginary action (as in the traditional formulation).

Fortunately, no fundamentally novel "picture" of quantum mechanics needs to be declared to promote the idea of the path "integral" $\sum_{x(t)} \exp(iS[x]/\hbar)$ to a working theory. As we will see in the next section, the new formulation can be developed from the established principles of canonical quantization.

3.2 Construction of the path integral

All information about an autonomous[4] quantum system is contained in its time evolution operator. A formal integration of the time-dependent Schrödinger equation $i\hbar\partial_t|\Psi\rangle = \hat{H}|\Psi\rangle$ gives the time evolution operator

$$|\Psi(t')\rangle = \hat{U}(t',t)|\Psi(t)\rangle, \quad \hat{U}(t',t) = e^{-\frac{i}{\hbar}\hat{H}(t'-t)}\Theta(t'-t). \tag{3.1}$$

The operator $\hat{U}(t',t)$ describes dynamical evolution under the influence of the Hamiltonian from a time t to time t'. Causality implies that $t' > t$, as indicated by the step or Heaviside Θ-function. In the real space representation we can write

$$\Psi(q',t') = \langle q'|\Psi(t')\rangle = \langle q'|\hat{U}(t',t)\Psi(t)\rangle = \int dq\; U(q',t';q,t)\Psi(q,t),$$

[3] More precisely, in the limit of small $\hbar$, the path sum can be evaluated by saddle-point methods, as detailed below.

[4] A system is classified as **autonomous** if its Hamiltonian does not explicitly depend on time. Actually the construction of the path integral can be straightforwardly extended so as to include time-dependent problems. However, in order to keep the introductory discussion as simple as possible, here we assume time independence.

where $U(q',t';q,t) = \langle q'|e^{-\frac{i}{\hbar}\hat{H}(t'-t)}|q\rangle\Theta(t'-t)$ defines the (q',q)-component of the time evolution operator. As the matrix element expresses the probability amplitude for a particle to propagate between points q and q' in a time $t'-t$, it is sometimes known as the **propagator** of the theory.

The basic idea behind Feynman's path integral approach is easy to formulate. Rather than attacking the Schrödinger equation governing the time evolution for general times t, one may first attempt to solve the much simpler problem of describing the time evolution for infinitesimally small times Δt. In order to formulate this idea one must first divide the time evolution into $N \gg 1$ time steps,

$$e^{-i\hat{H}t/\hbar} = \left[e^{-i\hat{H}\Delta t/\hbar}\right]^N, \tag{3.2}$$

where $\Delta t = t/N$. Albeit nothing more than a formal rewriting of Eq. (3.1), the representation (3.2) has the advantage that the factors $e^{-i\hat{H}\Delta t/\hbar}$ (or, rather, their expectation values) are small. (More precisely, if Δt is much smaller than the [reciprocal of the] eigenvalues of the Hamiltonian in the regime of physical interest, the exponents are small in comparison with unity and, as such, can be treated perturbatively.) A first simplification arising from this fact is that the exponentials can be factorized into two pieces, each of which can be readily diagonalized. To achieve this factorization, we make use of the identity

$$e^{-i\hat{H}\Delta t/\hbar} = e^{-i\hat{T}\Delta t/\hbar}e^{-i\hat{V}\Delta t/\hbar} + O(\Delta t^2),$$

where the Hamiltonian $\hat{H} = \hat{T} + \hat{V}$ is the sum of a kinetic energy $\hat{T} = \hat{p}^2/2m$, and some potential energy operator $\hat{V}$.[5] (The following analysis, restricted for simplicity to a one-dimensional Hamiltonian, is easily generalized to arbitrary spatial dimension.) The advantage of this factorization is that the eigenstates of each factor $e^{-i\hat{T}\Delta t/\hbar}$ and $e^{-i\hat{V}\Delta t/\hbar}$ are known independently. To exploit this fact we consider the time evolution operator factorized as a product,

$$\langle q_\mathrm{f}|\left[e^{-i\hat{H}\Delta t/\hbar}\right]^N|q_\mathrm{i}\rangle \simeq \langle q_\mathrm{f}| \wedge e^{-i\hat{T}\Delta t/\hbar}e^{-i\hat{V}\Delta t/\hbar} \wedge \cdots \wedge e^{-i\hat{T}\Delta t/\hbar}e^{-i\hat{V}\Delta t/\hbar}|q_\mathrm{i}\rangle, \tag{3.3}$$

and insert at each of the positions indicated by the symbol "$\wedge$" the resolution of identity

$$\mathrm{id} = \int dq_n \int dp_n \; |q_n\rangle\langle q_n|p_n\rangle\langle p_n|. \tag{3.4}$$

Here $|q_n\rangle$ and $|p_n\rangle$ represent a complete set of position and momentum eigenstates respectively, and $n = 1, \ldots, N$ serves as an index keeping track of the time steps at which the unit operator is inserted. The rationale behind the particular choice (3.4) is clear. The unit operator is arranged in such a way that both $\hat{T}$ and $\hat{V}$ act on the corresponding

[5] Although this ansatz covers a wide class of quantum problems, many applications (e.g. Hamiltonians involving spin or magnetic fields) do not fit into this framework. For a detailed exposition covering its realm of applicability, we refer to the specialist literature such as, e.g., Schulman[1].

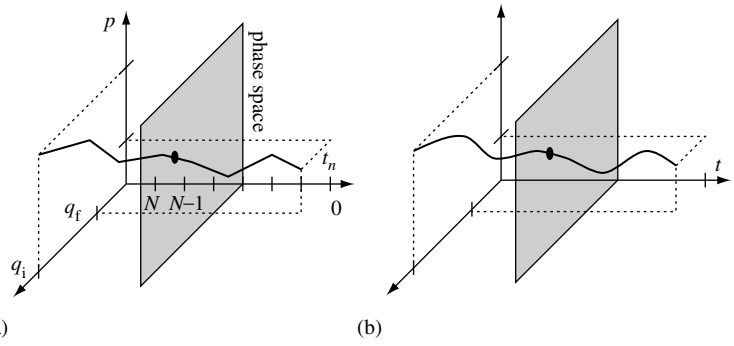

Figure 3.1 (a) Visualization of a set of phase space points contributing to the discrete time configuration integral (3.5). (b) In the continuum limit, the set of points becomes a smooth curve.

eigenstates. Inserting Eq. (3.4) into (3.3), and making use of the identity $\langle q|p\rangle = \langle p|q\rangle^* = e^{iqp/\hbar}/(2\pi\hbar)^{1/2}$, one obtains

$$\langle q_{\rm f}|e^{-i\hat{H}t/\hbar}|q_{\rm i}\rangle \simeq \int \prod_{\substack{n=1 \\ q_N=q_{\rm f}, q_0=q_{\rm i}}}^{N-1} dq_n \prod_{n=1}^{N} \frac{dp_n}{2\pi\hbar} e^{-i\frac{t}{\hbar}\sum_{n=0}^{N-1}\left(V(q_n)+T(p_{n+1})-p_{n+1}\frac{q_{n+1}-q_n}{t}\right)}. \quad (3.5)$$

Thus, the matrix element of the time evolution operator has been expressed as a $(2N-1)$-dimensional integral over eigenvalues. Up to corrections of higher order in $V\Delta t/\hbar$ and $T\Delta t/\hbar$, the expression (3.5) is exact. At each "time step" $t_n = n\Delta t$, $n = 1, \ldots, N$, we are integrating over a pair of coordinates $x_n \equiv (q_n, p_n)$ parameterizing the **classical phase space**. Taken together, the points $\{x_n\}$ form an N-point discretization of a path in this space (see Fig. 3.1).

To make further progress, we need to develop some intuition for the behavior of the integral (3.5). We first notice that rapid fluctuations of the integration arguments x_n as a function of the index n are strongly inhibited by the structure of the integrand. When taken together, contributions for which $(q_{n+1} - q_n)p_{n+1} > O(\hbar)$ (i.e. when the phase of the exponential exceeds 2π) tend to lead to a "random phase cancellation." In the language of wave mechanics, the superposition of partial waves of erratically different phases destructively interferes. The *smooth* variation of the paths that contribute significantly motivates the application of a continuum limit analogous to that employed in Chapter 1.

To be specific, sending $N \to \infty$ whilst keeping $t = N\Delta t$ fixed, the formerly discrete set $t_n = n\Delta t, n = 1, \ldots, N$, becomes dense on the time interval $[0, t]$, and the set of phase space points $\{x_n\}$ becomes a continuous curve $x(t)$. In the same limit,

$$\Delta t \sum_{n=0}^{N-1} \mapsto \int_0^t dt', \quad \frac{q_{n+1} - q_n}{\Delta t} \mapsto \partial_{t'} q\,|_{t'=t_n} \equiv \dot{q}|_{t'=t_n},$$

while $[V(q_n) + T(p_{n+1})] \mapsto [T(p|_{t'=t_n}) + V(q|_{t'=t_n})] \equiv H(x|_{t'=t_n})$ denotes the classical Hamiltonian. In the limit $N \to \infty$, the fact that kinetic and potential energies are evaluated

at neighboring time slices, n and $n+1$, becomes irrelevant.[6] Finally,

$$\lim_{N\to\infty}\int \prod_{\substack{n=1\\ q_N=q_\mathrm{f},\,q_0=q_\mathrm{i}}}^{N-1} dq_n \prod_{n=1}^{N}\frac{dp_n}{2\pi\hbar} \equiv \int_{\substack{q(t)=q_\mathrm{f}\\ q(0)=q_\mathrm{i}}} Dx,$$

defines the integration measure of the integral.

INFO Integrals extending over infinite-dimensional integration measures like $D(q,p)$ are generally called **functional integrals** (recall our discussion of functionals in Chapter 1). The question of the way functional integration can be rigorously defined is far from innocent and represents a subject of current, and partly controversial, mathematical research. In this book – as in most applications in physics – we take a pragmatic point of view and deal with the infinite-dimensional integration naively unless mathematical problems arise (which actually will not be the case!).

Then, applying these conventions to Eq. (3.5), one finally obtains

$$\boxed{\langle q_\mathrm{f}|e^{-i\hat{H}t/\hbar}|q_\mathrm{i}\rangle = \int_{\substack{q(t)=q_\mathrm{f}\\ q(0)=q_\mathrm{i}}} Dx\, \exp\left[\frac{i}{\hbar}\int_0^t dt'\,(p\dot{q}-H(p,q))\right].} \tag{3.6}$$

Equation (3.6) represents the **Hamiltonian formulation of the path integral**. The integration extends over all possible paths through the classical phase space of the system which begin and end at the same *configuration* points q_i and q_f respectively (cf. Fig. 3.1). The contribution of each path is weighted by its Hamiltonian action.

INFO Remembering the connection of the Hamiltonian to the Lagrangian through the Legendre transform, $H(p,q) = pq - L(p,q)$, the **classical action** of a trajectory $t \mapsto q(t)$ is given by $S[p,q] = \int_0^t dt'\, L(q,q) = \int_0^t dt'\,[pq - H(p,q)]$.

Before we turn to the discussion of the path integral (3.6), it is useful to recast the integral in an alternative form which will be both convenient in applications and physically instructive. The search for an alternative formulation is motivated by the resemblance of Eq. (3.6) to the Hamiltonian formulation of classical mechanics. Given that, classically, Hamiltonian and Lagrangian mechanics can be equally employed to describe dynamical evolution, it is natural to seek a Lagrangian analog of Eq. (3.6). Focusing on Hamiltonians for which the kinetic energy $T(p)$ is quadratic in p, the Lagrangian form of the path integral can indeed be inferred from Eq. (3.6) by straightforward Gaussian integration.

[6] To see this formally, one may Taylor expand $T(p_{n+1}) = T(p(t'+\Delta t))|_{t'=n\ \ t}$ around $p(t')$. For smooth $p(t')$, all but the zeroth-order contribution $T(p(t'))$ scale with powers of Δt, thereby becoming irrelevant. Note, however, that all of these arguments are based on the assertion that the dominant contributions to the path integral are smooth in the sense $q_{n+1}-q_n \sim O(\Delta t)$. A closer inspection, however, shows that in fact $q_{n+1}-q_n \sim O(\sqrt{\Delta t})$ (see Schulman[1].) In some cases, the most prominent one being the quantum mechanics of a particle in a magnetic field, the lowered power of Δt spoils the naive form of the continuity argument above, and more care must be applied in taking the continuum limit. In cases where a "new" path integral description of a quantum mechanical problem is developed, it is imperative to delay taking the continuum limit until the fluctuation behavior of the discrete integral across individual time slices has been thoroughly examined.

To make this point clear, let us rewrite the integral in a way that emphasizes its dependence on the momentum variable p:

$$\langle q_{\rm f}|e^{-i\hat{H}t/\hbar}|q_{\rm i}\rangle = \int_{\substack{q(t)=q_{\rm f}\\ q(0)=q_{\rm i}}} Dq\; e^{-\frac{i}{\hbar}\int_0^t dt' V(q)} \int Dp\; e^{-\frac{i}{\hbar}\int_0^t dt' \left(\frac{p^2}{2m} - p\dot{q}\right)}. \tag{3.7}$$

The exponent is quadratic in p which means that we are dealing with the continuum generalization of a Gaussian integral. Carrying out the integration by means of Eq. (3.13) below, one obtains

$$\boxed{\langle q_{\rm f}|e^{-i\hat{H}t/\hbar}|q_{\rm i}\rangle = \int_{\substack{q(t)=q_{\rm f}\\ q(0)=q_{\rm i}}} Dq\, \exp\left[\frac{i}{\hbar}\int_0^t dt' L(q,\dot{q})\right],} \tag{3.8}$$

where $Dq = \lim_{N\to\infty}\left(\frac{Nm}{it2\pi\hbar}\right)^{N/2}\prod_{n=1}^{N-1} dq_n$ denotes the functional measure of the remaining q-integration, and $L(q,\dot{q}) = m\dot{q}^2/2 - V(q)$ represents the classical Lagrangian. Strictly speaking, the (finite-dimensional) integral formula (3.13) is not directly applicable to the infinite-dimensional Gaussian integral (3.7). This, however, does not represent a substantial problem as we can always rediscretize the integral (3.7), apply Eq. (3.13), and reinstate the continuum limit after integration (exercise).

Together Eq. (3.6) and (3.8) represent the central results of this section. A quantum mechanical transition amplitude has been expressed in terms of an infinite-dimensional integral extending over paths through phase space, Eq. (3.6), or coordinate space, Eq. (3.8).

All paths begin (end) at the initial (final) coordinate of the matrix element. Each path is weighted by its *classical* action. Notice in particular that the quantum transition amplitude has been cast in a form that does not contain quantum mechanical operators. Nonetheless, quantum mechanics is still fully present! The point is that the integration extends over all paths and not just the subset of solutions of the classical equations of motion. (The distinguished role classical paths play in the path integral will be discussed below in Section 3.2.) The two forms of the path integral, Eq. (3.6) and Eq. (3.8), represent the formal implementation of the "alternative picture" of quantum mechanics proposed heuristically at the beginning of the chapter.

Johann Carl Friedrich Gauss
1777–1855

Worked in a wide variety of fields in both mathematics and physics including number theory, analysis, differential geometry, geodesy, magnetism, astronomy, and optics. As well as several books, Gauss published a number of memoirs (reports of his experiences), mainly in the journal of the Royal Society of Göttingen. However, in general, he was unwilling to publish anything that could be regarded as controversial and, as a result, some of his most brilliant work was found only after his death.

INFO **Gaussian integration**: Apart from a few rare exceptions, all integrals encountered in this book will be of Gaussian form. In most cases the dimension of the integrals will be large if not infinite. Yet, after a bit of practice, it will become clear that high-dimensional representatives of Gaussian integrals are no more difficult to handle than their one-dimensional counterparts.

Therefore, considering the important role played by Gaussian integration in field theory, we will here derive the principal formulae once and for all. Our starting point is the one-dimensional integral (both real and complex). The ideas underlying the proofs of the one-dimensional formulae will provide the key to the derivation of more complex functional identities that will be used liberally throughout the remainder of the text.

One-dimensional Gaussian integral: The basic ancestor of all Gaussian integrals is the identity

$$\boxed{\int_{-\infty}^{\infty} dx\; e^{-\frac{a}{2}x^2} = \sqrt{\frac{2\pi}{a}},\ \mathrm{Re}\ a > 0.} \tag{3.9}$$

In the following we will need various generalizations of Eq. (3.9). Firstly, we have $\int_{-\infty}^{\infty} dx\, e^{-ax^2/2}x^2 = \sqrt{2\pi/a^3}$, a result established either by substituting $a \to a+\epsilon$ in Eq. (3.9) and expanding both the left and the right side of the equation to leading order in ϵ, or by differentiating Eq. (3.9). Often one encounters integrals where the exponent is not purely quadratic from the outset but rather contains both quadratic and linear pieces. The generalization of Eq. (3.9) to this case reads

$$\int_{-\infty}^{\infty} dx\; e^{-\frac{a}{2}x^2+bx} = \sqrt{\frac{2\pi}{a}} e^{\frac{b^2}{2a}}. \tag{3.10}$$

To prove this identity, one simply eliminates the linear term by means of the change of variables $x \to x + b/a$ which transforms the exponent $-ax^2/2 + bx \to -ax^2/2 + b^2/2a$. The constant factor scales out and we are left with Eq. (3.9). Note that Eq. (3.10) holds even for complex b. The reason is that as a result of shifting the integration contour into the complex plane no singularities are encountered, i.e. the integral remains invariant.

Later, we will be concerned with the generalization of the Gaussian integral to complex arguments. The extension of Eq. (3.9) to this case reads

$$\int d(\bar{z}, z)\; e^{-\bar{z}wz} = \frac{\pi}{w}, \quad \mathrm{Re}\ w > 0,$$

where $\bar{z}$ represents the complex conjugate of z. Here, $\int d(\bar{z}, z) \equiv \int_{-\infty}^{\infty} dx\; dy$ represents the independent integration over the real and imaginary parts of $z = x + iy$. The identity is easy to prove: owing to the fact that $\bar{z}z = x^2 + y^2$, the integral factorizes into two pieces, each of which is equivalent to Eq. (3.9) with $a = w$. Similarly, it may be checked that the complex generalization of Eq. (3.10) is given by

$$\int d(\bar{z}, z)\, e^{-\bar{z}wz+\bar{u}z+\bar{z}v} = \frac{\pi}{w} e^{\frac{\bar{u}v}{w}}, \quad \mathrm{Re}\, w > 0. \tag{3.11}$$

More importantly $\bar{u}$ and v may be independent complex numbers; they need not be related to each other by complex conjugation (exercise).

Gaussian integration in more than one dimension: All of the integrals above have higher-dimensional counterparts. Although the real and complex versions of the N-dimensional integral formulae can be derived in a perfectly analogous manner, it is better to discuss them separately in order not to confuse the notation.

(a) **Real case**: The multi-dimensional generalization of the prototype integral (3.9) reads

$$\int d\mathbf{v}\; e^{-\frac{1}{2}\mathbf{v}^T\mathbf{A}\mathbf{v}} = (2\pi)^{N/2} \det \mathbf{A}^{-1/2}, \tag{3.12}$$

where $\mathbf{A}$ is a positive definite real symmetric N-dimensional matrix and $\mathbf{v}$ is an N-component real vector. The proof makes use of the fact that $\mathbf{A}$ (by virtue of being symmetric) can be diagonalized by orthogonal transformation, $\mathbf{A} = \mathbf{O}^T\mathbf{D}\mathbf{O}$, where the matrix $\mathbf{O}$ is orthogonal, and all elements of the diagonal matrix $\mathbf{D}$ are positive. The matrix $\mathbf{O}$ can be absorbed into the integration vector by means of the variable transformation, $\mathbf{v} \mapsto \mathbf{O}\mathbf{v}$, which has unit Jacobian, $\det \mathbf{O} = 1$. As a result, we are left with a Gaussian integral with exponent $-\mathbf{v}^T\mathbf{D}\mathbf{v}/2$. Due to the diagonality of $\mathbf{D}$, the integral factorizes into N independent Gaussian integrals, each of which contributes a factor $\sqrt{2\pi/d_i}$, where $d_i, i = 1, \ldots, N$, is the ith entry of the matrix $\mathbf{D}$. Noting that $\prod_{i=1}^{N} d_i = \det \mathbf{D} = \det \mathbf{A}$, Eq. (3.12) is derived.
The multi-dimensional generalization of Eq. (3.10) reads

$$\boxed{\int d\mathbf{v}\; e^{-\frac{1}{2}\mathbf{v}^T\mathbf{A}\mathbf{v}+\mathbf{j}^T\cdot\mathbf{v}} = (2\pi)^{N/2}\det \mathbf{A}^{-1/2} e^{\frac{1}{2}\mathbf{j}^T\mathbf{A}^{-1}\mathbf{j}},} \tag{3.13}$$

where $\mathbf{j}$ is an arbitrary N-component vector. Equation (3.13) is proven by analogy with Eq. (3.10), i.e. by shifting the integration vector according to $\mathbf{v} \to \mathbf{v} + \mathbf{A}^{-1}\mathbf{j}$, which does not change the value of the integral but removes the linear term from the exponent, $-\frac{1}{2}\mathbf{v}^T\mathbf{A}\mathbf{v} + \mathbf{j}^T\cdot\mathbf{v} \to -\frac{1}{2}\mathbf{v}^T\mathbf{A}\mathbf{v} + \frac{1}{2}\mathbf{j}^T\mathbf{A}^{-1}\mathbf{j}$. The resulting integral is of the type (3.12), and we arrive at Eq. (3.13).
The integral (3.13) not only is of importance in its own right, but also serves as a "generator" of other useful integral identities. Applying the differentiation operation $\partial^2_{j_m j_n}|_{\mathbf{j}=0}$ to the left- and the right-hand side of Eq. (3.13), one obtains the identity[7] $\int d\mathbf{v}\; e^{-\frac{1}{2}\mathbf{v}^T\mathbf{A}\mathbf{v}} v_m v_n = (2\pi)^{N/2}\det \mathbf{A}^{-1/2} A^{-1}_{mn}$. This result can be more compactly formulated as

$$\langle v_m v_n \rangle = A^{-1}_{mn}, \tag{3.14}$$

where we have introduced the shorthand notation

$$\langle \cdots \rangle \equiv (2\pi)^{-N/2}\det \mathbf{A}^{1/2} \int d\mathbf{v}\; e^{-\frac{1}{2}\mathbf{v}^T\mathbf{A}\mathbf{v}} (\cdots), \tag{3.15}$$

suggesting an interpretation of the Gaussian weight as a probability distribution.
Indeed, the differentiation operation leading to Eq. (3.14) can be iterated. Differentiating four times, one obtains $\langle v_m v_n v_q v_p \rangle = A^{-1}_{mn}A^{-1}_{qp} + A^{-1}_{mq}A^{-1}_{np} + A^{-1}_{mp}A^{-1}_{nq}$. One way of memorizing the structure of this – important – identity is that the Gaussian "expectation" value $\langle v_m v_n v_p v_q \rangle$ is given by all "pairings" of type (3.14) that can be formed from the four components v_m. This rule generalizes to expectation values of arbitrary order: $2n$-fold differentiation of Eq. (3.13) yields

$$\boxed{\langle v_{i_1} v_{i_2} \ldots v_{i_{2n}} \rangle = \sum_{\substack{\text{pairings of} \\ \{i_1,\ldots,i_{2n}\}}} A^{-1}_{i_{k_1} i_{k_2}} \ldots A^{-1}_{i_{k_{2n-1}} i_{k_{2n}}}.} \tag{3.16}$$

This result is the mathematical identity underlying **Wick s theorem** (for real bosonic fields), to be discussed in more physical terms below.

[7] Note that the notation A^{-1}_{mn} refers to the mn-element of the matrix $\mathbf{A}^{-1}$.

(b) **Complex case**: The results above are straightforwardly extended to multi-dimensional complex Gaussian integrals. The complex version of Eq. (3.12) is given by

$$\int d(\mathbf{v}^\dagger, \mathbf{v})\; e^{-\mathbf{v}^\dagger \mathbf{A} \mathbf{v}} = \pi^N \det \mathbf{A}^{-1}, \tag{3.17}$$

where $\mathbf{v}$ is a complex N-component vector, $d(\mathbf{v}^\dagger, \mathbf{v}) \equiv \prod_{i=1}^{N} d\,\mathrm{Re}\; v_i\; d\,\mathrm{Im}\; v_i$, and $\mathbf{A}$ is a complex matrix with positive definite Hermitian part. (Remember that every matrix can be decomposed into a Hermitian and an anti-Hermitian component, $\mathbf{A} = \frac{1}{2}(\mathbf{A} + \mathbf{A}^\dagger) + \frac{1}{2}(\mathbf{A} - \mathbf{A}^\dagger)$.) For Hermitian $\mathbf{A}$, the proof of Eq. (3.17) is analogous to that of Eq. (3.12), i.e. $\mathbf{A}$ is unitarily diagonalizable, $\mathbf{A} = \mathbf{U}^\dagger \mathbf{A} \mathbf{U}$, the matrices $\mathbf{U}$ can be transformed into $\mathbf{v}$, the resulting integral factorizes, etc. For non-Hermitian $\mathbf{A}$ the proof is more elaborate, if unedifying, and we refer to the literature for details. The generalization of Eq. (3.17) to exponents with linear contributions reads

$$\boxed{\int d(\mathbf{v}^\dagger, \mathbf{v})\; e^{-\mathbf{v}^\dagger \mathbf{A} \mathbf{v} + \mathbf{w}^\dagger \cdot \mathbf{v} + \mathbf{v}^\dagger \cdot \mathbf{w}'} = \pi^N \det \mathbf{A}^{-1} e^{\mathbf{w}^\dagger \mathbf{A}^{-1} \mathbf{w}'}.} \tag{3.18}$$

Note that $\mathbf{w}$ and $\mathbf{w}'$ may be independent complex vectors. The proof of this identity mirrors that of Eq. (3.13), i.e. by effecting the shift $\mathbf{v}^\dagger \to \mathbf{v}^\dagger + \mathbf{w}^\dagger$, $\mathbf{v} \to \mathbf{v} + \mathbf{w}'$.[8] As with Eq. (3.13), Eq. (3.18) may also serve as a generator of integral identities. Differentiating the integral twice according to $\partial^2_{w'_m, \bar{w}_n}|_{\mathbf{w}=\mathbf{w}'=0}$ gives

$$\langle \bar{v}_m v_n \rangle = A^{-1}_{nm},$$

where $\langle \cdots \rangle \equiv \pi^{-N} \det \mathbf{A} \int d(\mathbf{v}^\dagger, \mathbf{v})\; e^{-\mathbf{v}^\dagger \mathbf{A} \mathbf{v}} (\cdots)$. The iteration to more than two derivatives gives $\langle \bar{v}_n \bar{v}_m v_p v_q \rangle = A^{-1}_{pm} A^{-1}_{qn} + A^{-1}_{pn} A^{-1}_{qm}$ and, eventually,

$$\boxed{\langle \bar{v}_{i_1} \bar{v}_{i_2} \cdots \bar{v}_{i_n} v_{j_1} v_{j_2} \cdots v_{j_n} \rangle = \sum_P A^{-1}_{j_1 i_{P1}} \cdots A^{-1}_{j_n i_{Pn}},}$$

where $\sum_P$ represents for the sum over all permutations of n integers.

Gaussian functional integration: With this preparation, we are in a position to investigate the main practice of quantum and statistical field theory – the method of Gaussian functional integration. Turning to Eq. (3.13), let us suppose that the components of the vector $\mathbf{v}$ parameterize the weight of a real scalar field on the sites of a one-dimensional lattice. In the continuum limit, the set $\{v_i\}$ translates to a function $v(x)$, and the matrix A_{ij} is replaced by an **operator** kernel or **propagator** $A(x, x')$. In this limit, the natural generalization of Eq. (3.13) is

$$\begin{aligned} \int Dv(x)\; \exp\left[-\frac{1}{2} \int dx\; dx'\; v(x) A(x, x') v(x') + \int dx\; j(x) v(x) \right] \\ \propto (\det A)^{-1/2} \exp\left[\frac{1}{2} \int dx\; dx'\; j(x) A^{-1}(x, x') j(x') \right], \end{aligned} \tag{3.19}$$

[8] For an explanation of why $\mathbf{v}$ and $\mathbf{v}^\dagger$ may be shifted independently of each other, cf. the analyticity remarks made in connection with Eq. (3.11).

where the inverse kernel $A^{-1}(x,x')$ satisfies the equation

$$\boxed{\int dx'\ A(x,x')A^{-1}(x',x'') = \delta(x-x''),} \tag{3.20}$$

i.e. $A^{-1}(x,x')$ can be interpreted as the **Green function** of the operator $A(x,x')$. The notation $Dv(x)$ is used to denote the measure of the functional integral. Although the constant of proportionality, $(2\pi)^N$, left out of Eq. (3.19) is formally divergent in the thermodynamic limit $N \to \infty$, it does not affect averages that are obtained from derivatives of such integrals. For example, for Gaussian distributed functions, Eq. (3.14) has the generalization

$$\boxed{\langle v(x)v(x')\rangle = A^{-1}(x,x').}$$

Accordingly, Eq. (3.16) assumes the form

$$\boxed{\langle v(x_1)v(x_2)\cdots v(x_{2n})\rangle = \sum_{\substack{\text{pairings of}\\ \{x_1,\ldots,x_{2n}\}}} A^{-1}(x_{k_1},x_{k_2})\cdots A^{-1}(x_{k_{2n-1}},x_{k_{2n}}).} \tag{3.21}$$

The generalization of the other Gaussian averaging formulae discussed above should be obvious.

To make sense of Eq. (3.19) one must interpret the meaning of the determinant, $\det A$. When the variables entering the Gaussian integral were discrete, the integral simply represented the determinant of the (real symmetric) matrix. In the present case, one must interpret A as a Hermitian operator having an infinite set of eigenvalues. The determinant simply represents the product over this infinite set (see, e.g., Section 3.3).

Before turning to specific applications of the Feynman path integral, let us stay with the general structure of the formalism and identify two fundamental connections of the path integral to *classical point mechanics* and *classical and quantum statistical mechanics*.

Path integral and statistical mechanics

The path integral reveals a connection between quantum mechanics and classical (and quantum) statistical mechanics whose importance to all areas of field theory and statistical physics can hardly be exaggerated. To reveal this link, let us for a moment forget about quantum mechanics and consider, by way of an example, a perfectly classical, one-dimensional continuum model describing a "flexible string." We assume that our string is held under constant tension, and confined to a "gutter-like potential" (as shown in Fig. 3.2). For simplicity, we also assume that the mass density of the string is pretty high, so that its fluctuations are "asymptotically slow" (the kinetic contribution to its energy is negligible). Transverse fluctuations of the string are then penalized by its line tension, and by the external potential.

Assuming that the transverse displacement of the string $u(x)$ is small, the potential energy stored in the string separates into two parts. The first arises from the line tension stored in the string, and the second comes from the external potential. Starting with the former, a transverse fluctuation of a line segment of length dx by an amount du leads to a potential

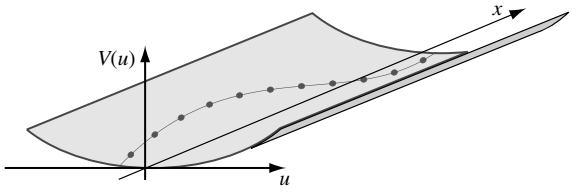

Figure 3.2 A string held under tension and confined to a potential well V.

energy of magnitude $\delta V_{\rm tension} = \sigma[(dx^2+du^2)^{1/2}-dx] \simeq \sigma dx\ (\partial_x u)^2/2$, where σ denotes the tension. Integrating over the length of the string, one obtains $V_{\rm tension}[\partial_x u] \equiv \int \delta V_{\rm tension} = \frac{1}{2}\int_0^L dx\ \sigma(\partial_x u(x))^2$. The second contribution, arising from the external potential, is given by $V_{\rm external}[u] \equiv \int_0^L dx\, V(u(x))$. Adding the two contributions, we find that the total energy of the string is given by $V = V_{\rm tension} + V_{\rm external} = \int_0^L dx\ [\frac{\sigma}{2}(\partial_x u)^2 + V(u)]$.

EXERCISE Find an expression for the kinetic energy contribution assuming that the string has a mass per unit length of m. How does this model compare to the continuum model of lattice vibrations discussed in Chapter 1? Convince yourself that in the limit $m \to \infty$, the kinetic contribution to the partition function $\mathcal{Z} = {\rm tr}\left[e^{-\beta H}\right]$ is inessential.

According to the general principles of statistical mechanics, the equilibrium properties of a system are encoded in the partition function $\mathcal{Z} = {\rm tr}\left[e^{-\beta V}\right]$, where "tr" denotes a summation over all possible configurations of the system and V is the total potential energy functional. Applied to the present case, ${\rm tr} \to \int Du$, where $\int Du$ stands for the functional integration over all configurations of the string $u(x)$, $x \in [0, L]$. Thus, the partition function of the string is given by

$$\mathcal{Z} = \int Du\, \exp\left[-\beta \int_0^L dx \left(\frac{\sigma}{2}(\partial_x u)^2 + V(u)\right)\right]. \tag{3.22}$$

A comparison of this result with Eq. (3.8) shows that the partition function of the *classical* system coincides with the *quantum mechanical* amplitude

$$\boxed{\mathcal{Z} = \int dq\ \langle q|e^{-it\hat{H}/\hbar}|q\rangle\Big|_{\substack{\hbar=1/\beta,\\ t=-iL}}},$$

evaluated at an imaginary "time" $t \to -i\tau \equiv -iL$, where $\hat{H} = \hat{p}^2/2\sigma + V(q)$, and Planck's constant is identified with the "temperature," $\hbar = 1/\beta$. (Here we have assumed that our string is subject to periodic boundary conditions.)

To see this explicitly, let us assume that we had reason to consider quantum propagation in imaginary time, i.e. $e^{-it\hat{H}/\hbar} \to e^{-\tau\hat{H}/\hbar}$, or $t \to -i\tau$. Assuming convergence (i.e. positivity of the eigenvalues of $\hat{H}$), a construction scheme perfectly analogous to the one outlined in Section 3.1 would have led to a path integral formula of the structure (3.8). Formally, the only differences would be (a) that the Lagrangian would be integrated along the imaginary time axis $t' \to -i\tau' \in [0, -i\tau]$ and (b) that there would be a change of the sign of the kinetic

energy term, i.e. $(\partial_{t'} q)^2 \to -(\partial_{\tau'} q)^2$. After a suitable exchange of variables, $\tau \to L, \hbar \to 1/\beta$, the coincidence of the resulting expression with the partition function (3.22) is clear.

The connection between quantum mechanics and classical statistical mechanics outlined above generalizes to **higher dimensions**. There are close analogies between quantum field theories in d dimensions and classical statistical mechanics in $d+1$. (The equality of the path integral above with the one-dimensional statistical model is merely the $d = 0$ version of this connection.) In fact, this connection turned out to be one of the major driving forces behind the success of path integral techniques in modern field theory/statistical mechanics. It offered, for the first time, a possibility to draw connections between systems that had seemed unrelated.

However, the concept of imaginary times not only provides a bridge between quantum and classical statistical mechanics, but also plays a role within a purely quantum mechanical context. Consider the partition function of a *single-particle* quantum mechanical system,

$$\boxed{\mathcal{Z} = \mathrm{tr}[e^{-\beta \hat{H}}] = \int dq \ \langle q|e^{-\beta \hat{H}}|q\rangle.}$$

The partition function can be interpreted as a trace over the transition amplitude $\langle q|e^{-i\hat{H}t/\hbar}|q\rangle$ evaluated at an imaginary time $t = -i\hbar\beta$. Thus, real time dynamics and quantum statistical mechanics can be treated on the same footing, provided that we allow for the appearance of imaginary times.

Later we will see that the concept of imaginary or even generalized complex times plays an important role in all of field theory. There is even some nomenclature regarding imaginary times. The transformation $t \to -i\tau$ is described as a **Wick rotation** (alluding to the fact that a multiplication by the imaginary unit can be interpreted as a $(\pi/2)$-rotation in the complex plane). Imaginary time representations of Lagrangian actions are termed **Euclidean**, whereas the real time forms are called **Minkowski actions**.

INFO The origin of this terminology can be understood by considering the structure of the action of, say, the phonon model (1.4). Forgetting for a moment about the magnitude of the coupling constants, we see that the action has the bilinear structure $\sim x_\mu g^\mu \ x$, where $\mu = 0, 1$, the vector $x_\mu = \partial_\mu \phi$, and the diagonal matrix $g = \mathrm{diag}(-1, 1)$ is the two-dimensional version of a Minkowski metric. (In three spatial dimensions, g would take the form of the standard Minkowski metric of special relativity.) On Wick rotation of the time variable, the factor -1 in the metric changes sign to $+1$, and g becomes a positive definite Euclidean metric. The nature of this transformation motivates the notation above.

Once one has grown accustomed to the idea that the interpretation of time as an imaginary quantity can be useful, yet more general concepts can be conceived. For example, one may contemplate propagation along temporal contours that are neither purely real nor purely imaginary but rather are generally complex. Indeed, it has turned out that path integrals with curvilinear integration contours in the complex "time plane" find numerous applications in statistical and quantum field theory.

Semiclassics from the path integral

In deriving the two path integral representations (3.6) and (3.8) no approximations were made. Yet the vast majority of quantum mechanical problems are unsolvable in closed form, and it would be hoping for too much to expect that within the path integral approach this situation would be any different. In fact no more than the path integrals of problems with a quadratic Hamiltonian – corresponding to the quantum mechanical harmonic oscillator and generalizations thereof – can be carried out in closed form. Yet what counts more than the (rare) availability of exact solutions is the flexibility with which approximation schemes can be developed. As to the path integral formulation, it is particularly strong in cases where **semiclassical limits of quantum theories** are explored. Here, by "semiclassical," we mean the limit $\hbar \to 0$, i.e. the case where the theory is expected to be largely governed by classical structures with quantum fluctuations superimposed.

To see more formally how classical structures enter the path integral approach, let us explore Eq. (3.6) and (3.8) in the limit of small $\hbar$. In this case the path integrals are dominated by path configurations with stationary action. (Non-stationary contributions to the integral imply massive phase fluctuations that largely average to zero.) Now, since the exponents of the two path integrals (3.6) and (3.8) involve the classical action functionals in their Hamiltonian and Lagrangian forms respectively, the extremal path configurations are simply the solutions of the classical equations of motion, namely,

$$\begin{aligned} \text{Hamiltonian}\colon \delta S[x] = 0 \Rightarrow d_t x = \{H(x), x\} \equiv \partial_p H \; \partial_q x - \partial_q H \; \partial_p x, \\ \text{Lagrangian}\colon \delta S[q] = 0 \Rightarrow (d_t \partial_{\dot q} - \partial_q)\, L(q, \dot q) = 0. \end{aligned} \tag{3.23}$$

These equations are to be solved subject to the boundary conditions $q(0) = q_{\rm i}$ and $q(t) = q_{\rm f}$. (Note that these boundary conditions do not uniquely specify a solution, i.e. in general there are many solutions to the equations (3.23). As an exercise, one may try to invent examples!)

Now the very fact that the stationary phase configurations are classical does not imply that quantum mechanics has disappeared completely. As with saddle-point approximations in general, it is not just the saddle-point itself that matters but also the fluctuations around it. At least it is necessary to integrate out Gaussian (quadratic) fluctuations around the point of stationary phase. In the case of the path integral, fluctuations of the action around the stationary phase configurations involve non-classical (in that they do not solve the classical equations of motion) trajectories through phase or coordinate space. Before exploring how this mechanism works in detail, let us consider the stationary phase analysis of functional integrals in general.

INFO **Stationary phase approximation**: Consider a general functional integral $\int Dx\; e^{-F[x]}$ where $Dx = \lim_{N\to\infty} \prod_{n=1}^{N} dx_n$ represents a functional measure resulting from taking the continuum limit of some finite-dimensional integration space, and the "action" $F\,[x]$ may be an arbitrary complex functional of x (leading to convergence of the integral). The function resulting from taking the limit of infinitely many discretization points, $\{x_n\}$, is denoted by $x : t \mapsto x(t)$ (where t plays the role of the formerly discrete index n). Evaluating the integral above within a stationary phase approximation amounts to performing the following steps:

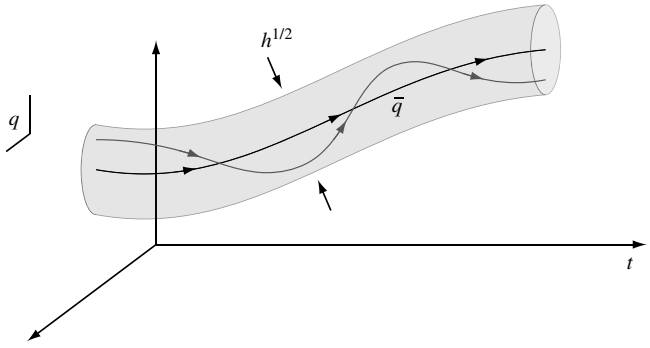

Figure 3.3 Quantum fluctuations around a classical path in coordinate space (here we assume a set of two-dimensional coordinates). Non-classical paths q fluctuating around a classical solution $q_{\rm cl}$ typically extend a distance $O(h^{1/2})$. All paths begin and end at $q_{\rm i}$ and $q_{\rm f}$, respectively.

1. Firstly, find the "points" of stationary phase, i.e. configurations $\bar{x}$ qualified by the condition of vanishing functional derivative (cf. Section 1.2),

$$DF_x = 0 \Leftrightarrow \forall t : \left.\frac{\delta F\,[x]}{\delta x(t)}\right|_{x=\bar{x}} = 0.$$

   Although there may, in principle, be one or many solutions, for clarity we first discuss the case in which the stationary phase configuration $\bar{x}$ is unique.
2. Secondly, Taylor expand the functional to second order around $\bar{x}$, i.e.

$$F\,[x] = F\,[\bar{x}+y] = F\,[\bar{x}] + \frac{1}{2}\int dt \int dt'\; y(t')A(t,t')y(t) + \cdots, \tag{3.24}$$

   where $A(t,t') = \frac{\delta^2 F[x]}{\delta x(t)\;\delta x(t')}\big|_{x=\bar{x}}$ denotes the second functional derivative. Due to the stationarity of $\bar{x}$, no first-order contribution can appear.
3. Thirdly, check that the operator $\hat{A} \equiv \{A(t,t')\}$ is positive definite. If it is not, there is a problem – the integration over the Gaussian fluctuations y diverges. (In practice, where the analysis is rooted in a physical context, such eventualities arise only rarely. In situations where problems do occur, the resolution can usually be found in a judicious rotation of the integration contour.) For positive definite $\hat{A}$, however, the functional integral over y can be performed, after which one obtains $\int Dx\; e^{-F[x]} \simeq e^{-F[\bar{x}]}\det(\frac{\hat{A}}{2\pi})^{-1/2}$, (cf. the discussion of Gaussian integrals above and, in particular, Eq. (3.19)).
4. Finally, if there are many stationary phase configurations, $\bar{x}_i$, the individual contributions have to be added:

$$\int Dx\; e^{-F[x]} \simeq \sum_i e^{-F[\bar{x}_i]}\det\left(\frac{\hat{A}_i}{2\pi}\right)^{-1/2}. \tag{3.25}$$

Equation (3.25) represents the most general form of the stationary phase evaluation of a (real) functional integral.

EXERCISE Applied to the Gamma function, $\Gamma(z+1) = \int_0^\infty dx\; x^z e^{-x}$, with z complex, show that the stationary phase approximation is consistent with Stirling's approximation, i.e. $\Gamma(s+1) = \sqrt{2\pi s}e^{s(\ln s - 1)}$.

Applied to the Lagrangian form of the Feynman path integral, this program can be implemented directly. In this case, the extremal field configuration $\bar{q}(t)$ is identified as the classical solution associated with the Lagrangian, i.e. $\bar{q}(t) \equiv q_{\rm cl}(t)$. Defining $r(t) = q(t) - q_{\rm cl}(t)$ as the deviation of a general path, $q(t)$, from a nearby classical path, $q_{\rm cl}(t)$ (see Fig. 3.3), and assuming for simplicity that there exists only one classical solution connecting $q_{\rm i}$ with $q_{\rm f}$ in a time t, a stationary phase analysis obtains

$$\langle q_{\rm f}|e^{-i\hat{H}t/\hbar}|q_{\rm i}\rangle \simeq e^{iS[q_{\rm cl}]/\hbar} \int_{r(0)=r(t)=0} Dr\, \exp\left[\frac{i}{2\hbar}\int_0^t dt' \int dt'' r(t')\, \frac{\delta^2 S[q]}{\delta q(t')\, \delta q(t'')}\bigg|_{q=q_{\rm cl}} r(t'')\right], \tag{3.26}$$

as the Gaussian approximation to the path integral (cf. Eq. (3.24)). For free Lagrangians of the form $L(q,\dot{q}) = m\dot{q}^2/2 - V(q)$, the second functional derivative of the action can be straightforwardly computed by means of the rules of functional differentiation formulated in Chapter 1. Alternatively, one can obtain this result by simply expanding the action as a Taylor series in the deviation $r(t)$. As a result, one obtains (exercise)

$$\frac{1}{2}\int_0^t dt \int dt'\; r(t)\, \frac{\delta^2 S[q]}{\delta q(t)\, \delta q(t')}\bigg|_{q=q_{\rm cl}} r(t') = -\frac{1}{2}\int dt\; r(t)\left[m\partial_t^2 + V''(q_{\rm cl}(t))\right] r(t), \tag{3.27}$$

where $V''(q_{\rm cl}(t)) \equiv \partial_q^2 V(q)|_{q=q_{\rm cl}}$ represents an ordinary derivative of the potential function. Thus, the Gaussian integration over r yields the square root of the determinant of the operator $m\partial_t^2 + V''(q_{\rm cl}(t))$ – interpreted as an operator acting in the space of functions $r(t)$ with boundary conditions $r(0) = r(t) = 0$. (Note that, as we are dealing with a differential operator, the issue of boundary conditions is crucial.)

INFO More generally, Gaussian integration over fluctuations around the stationary phase configuration obtains the formal expression

$$\langle q_f|e^{-i\hat{H}t/\hbar}|q_i\rangle \simeq \det\left(\frac{i}{2\pi\hbar}\frac{\partial^2 S[q_{\rm cl}]}{\partial q_{\rm i}\, \partial q_{\rm f}}\right)^{1/2} e^{\frac{i}{\hbar}S[q_{\rm cl}]}, \tag{3.28}$$

as the final result for the **transition amplitude evaluated in the semiclassical approximation**. (In cases where there is more than one classical solution, the individual contributions have to be added.) To derive this expression, one shows that the operator controlling the quadratic action (3.27) fulfils some differential relations which can again be related back to the classical action. While a detailed formulation of this calculation[9] is beyond the scope of the present text, the heuristic interpretation of the result is straightforward, as detailed below.

According to the rules of quantum mechanics $P(q_{\rm f}, q_{\rm i}, t) = |\langle q_{\rm f}|e^{-i\hat{H}t/\hbar}|q_{\rm i}\rangle|^2$ defines the probability density function for a particle injected at coordinate $q_{\rm i}$ to arrive at coordinate $q_{\rm f}$ after a time t. In the semiclassical approximation, the probability density function assumes the form $P(q_{\rm f}, q_{\rm i}, t) = |\det(\frac{1}{2\pi\hbar}\frac{\partial^2 S[q_{\rm cl}]}{\partial q_{\rm i}\partial q_{\rm f}})|$. We can gain some physical insight into this expression from the following consideration: for a fixed initial coordinate $q_{\rm i}$, the final coordinate $q_{\rm f}(q_{\rm i}, p_{\rm i})$ becomes a function of the initial momentum $p_{\rm i}$. The classical probability density function $P(q_{\rm i}, q_{\rm f})$ can

[9] See, e.g., Schulman[1].

then be related to the probability density function $P(q_\mathrm{i}, p_\mathrm{i})$ for a particle to leave from the initial phase space coordinate $(q_\mathrm{i}, p_\mathrm{i})$ according to

$$P(q_\mathrm{i}, q_\mathrm{f})dq_\mathrm{i}dq_\mathrm{f} = P(q_\mathrm{i}, q_\mathrm{f}(q_i, p_i))\left|\det\left(\frac{\partial q_\mathrm{f}}{\partial p_\mathrm{i}}\right)\right| dq_\mathrm{i}dp_\mathrm{i} = P(q_\mathrm{i}, p_\mathrm{i})dq_\mathrm{i}dp_\mathrm{i}.$$

Now, if we say that our particle actually left at the phase space coordinate $(q_\mathrm{i}, p_\mathrm{i})$, P must be singular at $(q_\mathrm{i}, p_\mathrm{i})$ while being zero everywhere else. In quantum mechanics, however, all we can say is that our particle was initially confined to a *Planck cell* centered around $(q_\mathrm{i}, p_\mathrm{i})$: $P(q_\mathrm{i}, p_\mathrm{i}) = 1/(2\pi\hbar)^d$. We thus conclude that $P(q_\mathrm{i}, q_\mathrm{f}) = |\det(\partial p_\mathrm{i}/\partial q_\mathrm{f})|(2\pi\hbar)^{-d}$. Finally, noticing that $p_\mathrm{i} = -\partial_{q_\mathrm{i}} S$ we arrive at the result of the semiclassical analysis above.

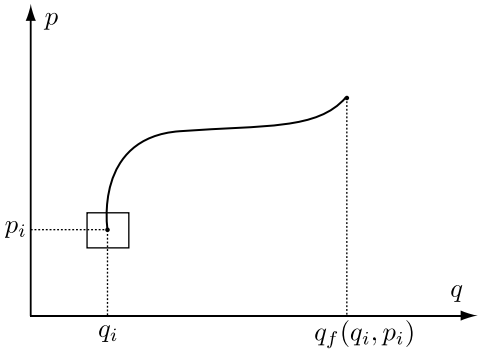

In deriving Eq. (3.28) we have restricted ourselves to the consideration of quadratic fluctuations around the classical paths. Under what conditions is this semiclassical approximation justified? Unfortunately there is no rigorous and generally applicable answer to this question. For finite $\hbar$, the quality of the approximation depends largely on the sensitivity of the action to path variations. Whether or not the approximation is legitimate is a question that has to be judged from case to case. However, the *asymptotic* stability of the semiclassical approximation in the limit $\hbar \to 0$ can be deduced simply from power counting. From the structure of Eq. (3.28) it is clear that the typical magnitude of fluctuations $r(t)$ scales as $r \sim (\hbar/\delta_q^2 S)^{1/2}$, where $\delta_q^2 S$ is a symbolic shorthand for the functional variation of the action. (Variations larger than that lead to phase fluctuations $> 2\pi$, thereby being negligible.) Non-Gaussian contributions to the action would have the structure $\sim \hbar^{-1} r^n \delta_q^n S$, $n > 2$. For a typical r, this is of the order $\sim \delta_q^n S/(\delta_q^2 S)^{n/2} \times \hbar^{n/2-1}$. Since the S-dependent factors are classical ($\hbar$-independent), these contributions scale to zero as $\hbar \to 0$.

This concludes the conceptual part of the chapter. Before turning to the discussion of applications of the path integral, let us first briefly summarize the main steps taken in its construction.

Construction recipe of the path integral

Consider a general quantum transition amplitude $\langle\psi|e^{-i\hat{H}t/\hbar}|\psi'\rangle$, where t may be real, purely imaginary, or generally complex. To construct a functional integral representation of the amplitude:

1. Partition the time interval into $N \gg 1$ steps,

$$e^{-i\hat{H}t/\hbar} = \left[e^{-i\hat{H}\Delta t/\hbar}\right]^N, \quad \Delta t = t/N.$$

2. Regroup the operator content appearing in the expansion of each factor $e^{-i\hat{H}\Delta t/\hbar}$ according to the relation

$$e^{-i\hat{H}\Delta t/\hbar} = 1 + \Delta t \sum_{mn} c_{mn} \hat{A}^m \hat{B}^n + O(\Delta t^2),$$

where the eigenstates $|a\rangle, |b\rangle$ of $\hat{A}, \hat{B}$ are known and the coefficients c_{mn} are c-numbers. (In the quantum mechanical application above $\hat{A} = \hat{p}, \hat{B} = \hat{q}$.) This "normal ordering" procedure emphasizes that distinct quantum mechanical systems may be associated with the same classical action.

3. Insert resolutions of identity according to

$$\begin{aligned} e^{-i\hat{H}\Delta t/\hbar} &= \sum_{a,b} |a\rangle\langle a| \left(1 + \Delta t \sum_{mn} c_{mn} \hat{A}^m \hat{B}^n + O(\Delta t^2)\right) |b\rangle\langle b| \\ &= \sum_{a,b} |a\rangle\langle a| e^{-iH(a,b)\Delta t/\hbar} |b\rangle\langle b| + O(\Delta t^2), \end{aligned}$$

where $H(a,b)$ is the Hamiltonian evaluated at the eigenvalues of $\hat{A}$ and $\hat{B}$.

4. Regroup terms in the exponent: due to the "mismatch" of the eigenstates at neighboring time slices n and $n+1$, not only the Hamiltonians $H(a,b)$, but also sums over differences of eigenvalues, appear (cf. the last term in the action (3.5)).
5. Take the continuum limit.

3.3 Applications of the Feynman path integral

Having introduced the general machinery of path integration we now turn to the discussion of specific applications. Our starting point will be an investigation of a low-energy quantum particle confined to a single potential well, and the phenomenon of tunneling in a double well. With the latter, we become acquainted with instanton techniques and the role of topology in field theory. The ideas developed in this section are generalized further in the investigation of quantum mechanical decay and quantum dissipation. Finally, we turn our attention to the development of the path integral for quantum mechanical spin and, as a case study, explore the semiclassical trace formulae for quantum chaos.

The simplest example of a quantum mechanical problem is that of a **free particle** ($\hat{H} = \hat{p}^2/2m$). Yet, within the framework of the path integral, this example, which can be dealt with straightforwardly by elementary means, is far from trivial: the Gaussian functional integral engaged in its construction involves divergences which must be regularized by rediscretizing the path integral. Nevertheless, its knowledge will be useful as a means to normalize the path integral in the applications below. Therefore, we leave it as an exercise to show[10]

$$\boxed{G_{\rm free}(q_{\rm f}, q_{\rm i}; t) \equiv \langle q_{\rm f}| e^{-\frac{i}{\hbar}\frac{p^2}{2m}t} |q_{\rm i}\rangle \Theta(t) = \left(\frac{m}{2\pi i\hbar t}\right)^{1/2} e^{\frac{i}{\hbar}\frac{m}{2t}(q_{\rm f}-q_{\rm i})^2} \Theta(t),} \tag{3.29}$$

[10] Compare this result with the solution of a classical diffusion equation.

where the Heaviside Θ-function reflects causality.[11]

EXERCISE Derive Eq. (3.29) by the standard methodology of quantum mechanics. (Hint: Insert a resolution of identity and perform a Gaussian integral.)

EXERCISE Using the path integral, obtain a perturbative expansion for the scattering amplitude $\langle \mathbf{p}'|U(t \to \infty, t' \to -\infty)|\mathbf{p}\rangle$ of a free particle from a short-range central potential $V(r)$. In particular, show that the first-order term in the expansion recovers the Born scattering amplitude $-i\hbar e^{-i(t-t')E(p)/\hbar}\delta(E(p) - E(p'))\langle \mathbf{p}'|V|\mathbf{p}\rangle$.

Quantum particle in a well

As a first application of the path integral, let us consider the problem of a quantum particle in a one-dimensional potential well (see figure). The discussion of this example illustrates how the semiclassical evaluation scheme discussed above works in practice. For simplicity we assume the potential to be symmetric, $V(q) = V(-q)$ with $V(0) = 0$. The quantity we wish to compute is the probability amplitude that a particle injected at $q = 0$ returns after a time t, i.e. with $\hat{H} = \hat{p}^2/2m + V(\hat{q})$, $G(0,0;t) \equiv \langle q_\mathrm{f} = 0|e^{-i\hat{H}t/\hbar}|q_\mathrm{i} = 0\rangle\Theta(t)$. Drawing on our previous discussion, the path integral representation of the transition amplitude is given by

$$G(0,0;t) = \int\limits_{q(t)=q(0)=0} Dq\, \exp\left[\frac{i}{\hbar}\int_0^t dt'\; L(q,\dot{q})\right],$$

where $L = m\dot{q}^2/2 - V(q)$ represents the corresponding Lagrangian.

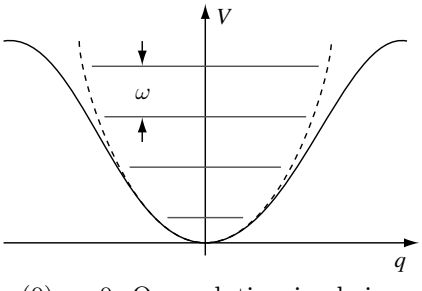

Now, for a generic potential $V(q)$, the path integral cannot be evaluated exactly. Instead, we wish to invoke the semiclassical analysis outlined above. Accordingly, we must first find solutions to the classical equation of motion. Minimizing the action with respect to variations of $q(t)$, one obtains the Euler–Lagrange equation of motion $m\ddot{q} = -V'(q)$. According to the Feynman path integral, this equation must be solved subject to the boundary conditions $q(t) = q(0) = 0$. One solution is obvious, namely $q_\mathrm{cl}(t) = 0$. Assuming that this is in fact the only solution,[12] we obtain (cf. Eq. (3.26)

[11] Motivated by its interpretation as a Green function, in the following we refer to the quantum transition probability amplitude by the symbol G (as opposed to U used above).

[12] In general, this assumption is wrong. For smooth potentials $V(q)$, a Taylor expansion of V at small q obtains the harmonic oscillator potential, $V(q) = V_0 + m\omega^2 q^2/2 + \cdots$. For times t that are commensurate with π/ω, one has periodic solutions, $q_\mathrm{cl}(t) \propto \sin(\omega t)$ that start out from the origin at time $t = 0$ and revisit it at just the right time t. In the next section we will see why the restriction to just the trivial solution was nonetheless legitimate (for arbitrary times t).

and (3.27))

$$G(0,0;t) \simeq \int\limits_{r(0)=r(t)=0} Dr\, \exp\left[-\frac{i}{\hbar}\int_0^t dt' r(t')\frac{m}{2}\left(\partial_{t'}^2+\omega^2\right) r(t')\right],$$

where, by definition, $m\omega^2 \equiv V''(0)$ is the second derivative of the potential at the origin.[13] Note that, in this case, the contribution to the action from the stationary phase field configuration vanishes: $S[q_{\rm cl}] = 0$. Following the discussion of Section 3.2, Gaussian functional integration over r then leads to the semiclassical expansion

$$G(0,0;t) \simeq J \det\left(-m(\partial_t^2+\omega^2)/2\right)^{-1/2}, \tag{3.30}$$

where the prefactor J absorbs various constant prefactors.

Operator determinants are usually most conveniently obtained by presenting them as a product over eigenvalues. In the present case, the eigenvalues ϵ_n are determined by the equation

$$-\frac{m}{2}\left(\partial_t^2+\omega^2\right) r_n = \epsilon_n r_n,$$

which is to be solved subject to the boundary condition $r_n(t) = r_n(0) = 0$. A complete set of solutions to this equation is given by,[14] $r_n(t') = \sin(n\pi t'/t)$, $n = 1, 2, \ldots$, with eigenvalues $\epsilon_n = m[(n\pi/t)^2 - \omega^2]/2$. Applying this to the determinant, one finds

$$\det\left(-m(\partial_t^2+\omega^2)/2\right)^{-1/2} = \prod_{n=1}^{\infty}\left[\frac{m}{2}\left(\left(\frac{n\pi}{t}\right)^2-\omega^2\right)\right]^{-1/2}.$$

To interpret this result, one must make sense of the infinite product (which even seems divergent for times commensurate with π/ω). Moreover the value of the constant J has yet to be determined. To resolve these difficulties, one may exploit the facts that (a) we do know the transition amplitude Eq. (3.29) of the *free* particle system, and (b) the latter coincides with the transition amplitude G in the special case where the potential $V \equiv 0$. In other words, had we computed $G_{\rm free}$ via the path integral, we would have obtained the same constant J and, more importantly, an infinite product like the one above, but with $\omega = 0$. This allows the transition amplitude to be regularized as

$$G(0,0;t) \equiv \frac{G(0,0;t)}{G_{\rm free}(0,0;t)} G_{\rm free}(0,0;t) = \prod_{n=1}^{\infty}\left[1-\left(\frac{\omega t}{n\pi}\right)^2\right]^{-1/2}\left(\frac{m}{2\pi i\hbar t}\right)^{1/2}\Theta(t).$$

Then, with the help of the identity $\prod_{n=1}^{\infty}[1-(x/n\pi)^2]^{-1} = x/\sin x$, one finally arrives at the result

$$G(0,0;t) \simeq \sqrt{\frac{m\omega}{2\pi i\hbar\sin(\omega t)}}\Theta(t). \tag{3.31}$$

[13] Those who are uncomfortable with functional differentiation can arrive at the same expression simply by substituting $q(t) = q_{\rm cl}(t) + r(t)$ into the action and expanding in r.

[14] To find the solutions of this equation, recall the structure of the Schrödinger equation of a particle in a one-dimensional box of width $L = t$.

In the case of the harmonic oscillator, the expansion of the potential necessarily truncates at quadratic order and, in this case, the expression above is exact. (For a more wide-ranging discussion of the path integral for the quantum harmonic oscillator system, see Problem 3.5.) For a general potential, the semiclassical approximation effectively involves the replacement of $V(q)$ by a quadratic potential with the same curvature. The calculation above also illustrates how coordinate space fluctuations around a completely static solution may reinstate the zero-point fluctuations characteristic of quantum mechanical bound states.

Double well potential: tunneling and instantons

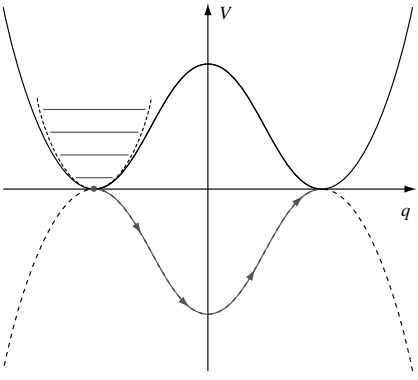

As a second application of the path integral let us now consider the motion of a particle in a double well potential (see figure). Our aim will be to estimate the quantum probability amplitude for a particle either to stay at the bottom of one of the local minima or to go from one minimum to the other. In doing so, it is understood that the energy range accessible to the particle (i.e. $\Delta E \sim \hbar/t$) is well below the potential barrier height, i.e. quantum mechanical transfer between minima is by **tunneling**. Here, in contrast to the single well system, it is far from clear what kind of classical stationary phase solutions may serve as a basis for a description of the quantum dynamics; there appear to be no classical paths connecting the two minima. Of course one may think of particles "rolling" over the potential hill. Yet, these are singular and, by assumption, energetically inaccessible.

The key to resolving these difficulties is an observation, already made above, that the time argument appearing in the path integral should be considered as a general complex quantity that can (according to convenience) be set to any value in the complex plane. In the present case, a Wick rotation to imaginary times will reveal a stationary point of the action. At the end of the calculation, the real time amplitudes we seek can be obtained by analytic continuation.

INFO The mechanism of quantum double (or multiple) well tunneling plays a role in a number of problems of condensed matter physics. A prominent example is in the physics of amorphous solids such as **glasses**.

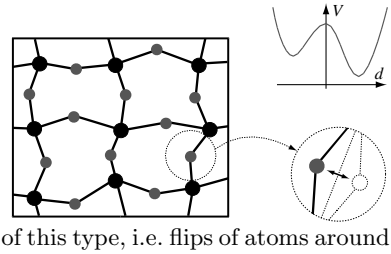

A caricature of a glass is shown in the figure. The absence of long-range order in the system implies that individual chemical bonds cannot assume their optimal binding lengths. For understretched bonds this leads to the formation of two approximately equal metastable minima around the ideal binding axis (see the inset). The energetically lowest excitations of the system are transitions of individual atoms between nearly degenerate minima of this type, i.e. flips of atoms around

the binding axis. A prominent phenomenological model[15] describes the system by an ensemble of quantum double wells of random center height and width. This model effortlessly explains the existence of a vast system of metastable points in the landscape of low-energy configurations of glassy systems.

To be specific, let us consider the imaginary time transition amplitudes

$$G_E(a, \pm a; \tau) \equiv \left\langle a \right| \exp\left(-\frac{\tau}{\hbar}\hat{H}\right) \left| \pm a \right\rangle = G_E(-a, \mp a; \tau), \tag{3.32}$$

where the coordinates $\pm a$ coincide with the two minima of the potential. From Eq. (3.32) the real time amplitudes $G(a, \pm a; t) = G_E(a, \pm a; \tau \to it)$ can be recovered by the analytic continuation $\tau \to it$. According to Section 3.2, the **Euclidean path integral** formulation of the transition amplitudes is given by

$$\boxed{G_E(a, \pm a; \tau) = \int\limits_{q(0)=\pm a, q(\tau)=a} Dq \, \exp\left[-\frac{1}{\hbar}\int_0^\tau d\tau' \left(\frac{m}{2}\dot{q}^2 + V(q)\right)\right],} \tag{3.33}$$

where the function q now depends on imaginary time. From Eq. (3.33) we obtain the stationary phase (or saddle-point) equations

$$-m\ddot{q} + V'(q) = 0. \tag{3.34}$$

From this result, one can infer that, as a consequence of the Wick rotation, there is an effective *inversion* of the potential, $V \to -V$ (shown dashed in the figure on page 115). The crucial point is that, within the inverted potential landscape, the barrier has become a sink, i.e. within the new formulation, there *are* classical solutions connecting the two points, $\pm a$. More precisely, there are three different types of classical solution that fulfill the condition to be at coordinates $\pm a$ at times 0 and/or τ: (a) the solution wherein the particle rests permanently at a;[16] (b) the corresponding solution staying at $-a$; and, most importantly, (c) the solution in which the particle leaves its initial position at $\pm a$, accelerates through the minimum at 0 and eventually reaches the final position $\mp a$ at time τ. In computing the transition amplitudes, all three types of path have to be taken into account. As to (a) and (b), by computing quantum fluctuations around these solutions, one can recover the physics of the zero-point motion described in Section 3.3 for each well individually. (Exercise: Convince yourself that this is true!) Now let us see what happens if the paths connecting the two coordinates are added to this picture.

[15] P. W. Anderson, B. I. Halperin, and C. M. Varma, Anomalous low-temperature thermal properties of glasses and spin glasses, *Phil. Mag.* **25** (1972), 1–9.

[16] Note that the potential inversion answers a question that arose above, i.e. whether or not the classical solution staying at the bottom of the single well was actually the only one to be considered. As with the double well, we could have treated the single well within an imaginary time representation, whereupon the well would have become a hill. Clearly, the boundary condition requires the particle to start and finish at the top of the hill, i.e. the solution that stays there forever. By formulating the semiclassical expansion around that path, we would have obtained Eq. (3.31) with $t \to -\mathrm{i}\tau$, which, upon analytic continuation, would have led back to the real time result.

The instanton gas

The classical solution of the Euclidean equation of motion that connects the two potential maxima is called an **instanton solution** while a solution traversing the same path but in the opposite direction ("$-a \to a$" $\to$ "$a \to -a$") is called an anti-instanton. The name "instanton" was invented by 't Hooft with the idea that these objects are very similar in their mathematical structure to "solitons," particle-like solutions of classical field theories. However, unlike solitons, they are structures in time (albeit Euclidean time); thus the "instant-." As another etymological remark, note that the syllable "-on" in "instanton" hints at an interpretation of these states as a kind of particle. The background is that, as a function of the time coordinate, instantons are almost everywhere constant save for a short region of variation (see below). Alluding to the interpretation of time as something akin to a spatial dimension, these states can be interpreted as a well-localized excitation or, according to standard field theoretical practice, a *particle*.[17]

Gerardus t Hooft 1946–
Nobel Laureate in Physics in 1999, with Martinus J. G. Veltman, "for elucidating the quantum structure of electroweak interactions in physics." Together, they were able to identify the properties of the W and Z particles. The 't Hooft–Veltman model allowed scientists to calculate the physical properties of other particles, including the mass of the top quark, which was directly observed in 1995. (Image © The Nobel Foundation.)

To proceed, we must first compute the classical action associated with a single-instanton solution. Multiplying Eq. (3.34) by $\dot{q}_{\rm cl}$, integrating over time (i.e. performing the first integral of the equation of motion), and using the fact that, at $q_{\rm cl} = \pm a$, $\partial_\tau q_{\rm cl} = V = 0$, one finds that

$$\frac{m}{2}\dot{q}_{\rm cl}^2 = V(q_{\rm cl}). \tag{3.35}$$

With this result, one obtains the instanton action

$$S_{\rm inst} = \int_0^\tau d\tau' \overbrace{\left(\frac{m}{2}\dot{q}_{\rm cl}^2 + V(q_{\rm cl})\right)}^{m\dot{q}_{\rm cl}^2} = \int d\tau' \, \frac{dq_{\rm cl}}{d\tau'}(m\dot{q}_{\rm cl}) = \int_{-a}^{a} dq \, (2mV(q))^{1/2}. \tag{3.36}$$

Notice that $S_{\rm inst}$ is determined solely by the functional profile of the potential V (i.e. does not depend on the structure of the solution $q_{\rm cl}$).

Secondly, let us explore the structure of the instanton as a function of time. Defining the second derivative of the potential at $\pm a$ by $V''(\pm a) = m\omega^2$, Eq. (3.35) implies that, for large times (where the particle is close to the right maximum), $\dot{q}_{\rm cl} = -\omega(q_{\rm cl} - a)$, which integrates to $q_{\rm cl}(\tau) \overset{\tau\to\infty}{\longrightarrow} a - e^{-\tau\omega}$. Thus the temporal extension of the instanton is set by the oscillator frequencies of the local potential minima (the maxima of the inverted potential) and, in

[17] In addition to the original literature, the importance that has been attached to the instanton method has inspired a variety of excellent and pedagogical reviews of the field. Of these, the following are highly recommended: A. M. Polyakov, Quark confinement and topology of gauge theories, *Nucl. Phys.* **B120** (1977), 429–58 – see also A. M. Polyakov, *Gauge Fields and Strings* (Harwood, 1987); S. Coleman, *Aspects of Symmetry – Selected Erice Lectures* (Cambridge University Press, 1985), Chapter 7.

cases where tunneling takes place on time scales much larger than that, can be regarded as short (see Fig. 3.4).

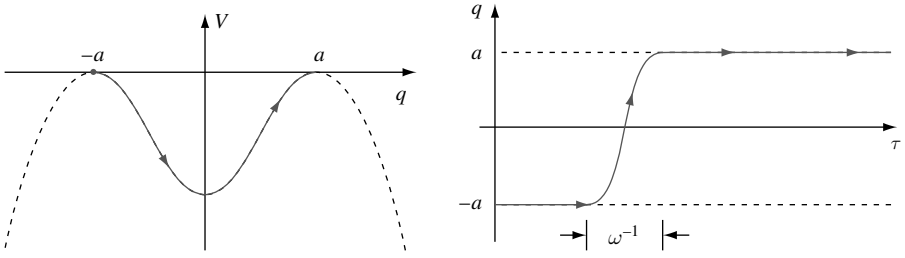

Figure 3.4 Single-instanton configuration.

The confinement of the instanton configuration to a narrow interval of time has an important implication – there must exist *approximate* solutions of the stationary equation involving further anti-instanton/instanton pairs (physically, the particle repeatedly bouncing to and fro in the inverted potential). According to the general philosophy of the saddle-point scheme, the path integral is obtained by summing over all solutions of the saddle-point equations and hence over all instanton configurations. The summation over multi-instanton configurations – termed the "**instanton gas**" – is substantially simplified by the fact that individual instantons have short temporal support (events of overlapping configurations are rare) and that not too many instantons can be accommodated in a finite time interval (the instanton gas is dilute). The actual density is dictated by the competition between the configurational "entropy" (favoring high density), and the "energetics," the exponential weight implied by the action (favoring low density) – see the estimate below.

In practice, multi-instanton configurations imply a transition amplitude

$$G(a,\pm a;\tau) \simeq \sum_{n \text{ even/odd}} K^n \int_0^\tau d\tau_1 \int_0^{\tau_1} d\tau_2 \ldots \int_0^{\tau_{n-1}} d\tau_n \; A_n(\tau_1,\ldots,\tau_n), \tag{3.37}$$

where A_n denotes the amplitude associated with n instantons, and we have taken into account the fact that, in order to connect a with $\pm a$, the number of instantons must be even/odd. The n instanton bounces contributing to each A_n can take place at arbitrary times $\tau_i \in [0,\tau], i = 1,\ldots,n$, and all these possibilities have to be added (i.e. integrated). Here K denotes a (dimensionful) constant absorbing the temporal dimension $[\text{time}]^n$ introduced by the time integrations, and $A_n(\tau_1,\ldots,\tau_n)$ is the transition amplitude, evaluated within the semiclassical approximation around a configuration of n instanton bounces at times $0 \le \tau_n \le \tau_{n-1} \le \cdots \le \tau_1 \le \tau$ (see Fig. 3.5). In the following, we first focus on the transition amplitude A_n, which controls the exponential dependence of the tunneling amplitude, returning later to consider the prefactor K.

According to the general semiclassical principle, each amplitude $A_n = A_{n,\text{cl}} \times A_{n,\text{qu}}$ factorizes into two parts: a classical contribution $A_{n,\text{cl}}$ accounting for the action of the instanton configuration; and a quantum contribution $A_{n,\text{qu}}$ resulting from quadratic fluctuations around the classical path. Focusing initially on $A_{n,\text{cl}}$ we note that, at intermediate times, $\tau_i \ll \tau' \ll \tau_{i+1}$, where the particle rests on top of either of the maxima at $\pm a$, no

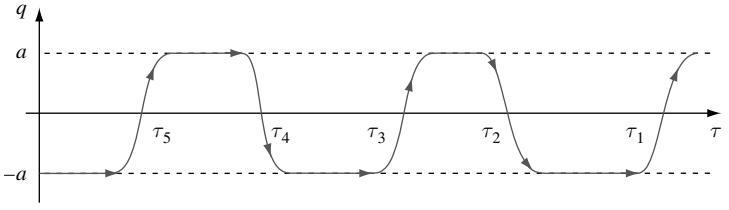

Figure 3.5 Dilute instanton gas configuration.

action accumulates (cf. the previous section). However, each instanton bounce has a finite action $S_{\rm inst}$ (see Eq. (3.36)) and these contributions add up to give the full classical action,

$$A_{n,\rm cl}(\tau_1,\ldots,\tau_n) = e^{-nS_{\rm inst}/\hbar}, \tag{3.38}$$

which is independent of the time coordinates τ_i. (The individual instantons "do not know of each other"; their action is independent of their relative position.)

As to the quantum factor $A_{n,\rm qu}$, there are, in principle, two contributions. Whilst the particle rests on either of the hills (the straight segments in Fig. 3.5), quadratic fluctuations around the classical (i.e. spatially constant) configuration play the same role as the quantum fluctuations considered in the previous section, the only difference being that we are working in a Wick rotated picture. There it was found that quantum fluctuations around a classical configuration which stays for a (real) time t at the bottom of the well result in a factor $\sqrt{1/\sin(\omega t)}$ (the remaining constants being absorbed into the prefactor K^n). Rotating to imaginary times, $t \to -{\rm i}\tau$, one can infer that the quantum fluctuation accumulated during the stationary time $\tau_{i+1} - \tau_i$ is given by

$$\sqrt{\frac{1}{\sin(-i\omega(\tau_{i+1}-\tau_i))}} \sim e^{-\omega(\tau_{i+1}-\tau_i)/2},$$

where we have used the fact that, for the dilute configuration, the typical separation times between bounces are much larger than the inverse of the characteristic oscillator scales of each of the minima. (It takes the particle much longer to tunnel through a high barrier than to oscillate in either of the wells of the *real* potential.)

Now, in principle, there are also fluctuations around the "bouncing" segments of the path. However, due to the fact that a bounce takes a time of $O(\omega^{-1}) \ll \Delta\tau$, where $\Delta\tau$ represents the typical time between bounces, one can neglect these contributions (which is to say that they can be absorbed into the prefactor K without explicit calculation). Within this approximation, setting $\tau_0 \equiv 0, \tau_{n+1} \equiv \tau$, the overall quantum fluctuation correction is given by

$$A_{n,\rm qu}(\tau_1,\ldots,\tau_n) = \prod_{i=0}^{n} e^{-\omega(\tau_{i+1}-\tau_i)/2} = e^{-\omega\tau/2}, \tag{3.39}$$

again independent of the particular spacing configuration $\{\tau_i\}$. Combining Eq. (3.38) and (3.39), one finds that

$$\begin{aligned} G(a,\pm a;\tau) &\simeq \sum_{n \text{ even/odd}}^{\infty} K^n e^{-nS_{\rm inst}/\hbar} e^{-\omega\tau/2} \overbrace{\int_0^\tau d\tau_1 \int_0^{\tau_1} d\tau_2 \ldots \int_0^{\tau_{n-1}} d\tau_n}^{\tau^n/n!} \\ &= e^{-\omega\tau/2} \sum_{n \text{ even/odd}} \frac{1}{n!} \left(\tau K e^{-S_{\rm inst}/\hbar}\right)^n . \end{aligned} \tag{3.40}$$

Finally, performing the summation, one obtains the transition amplitude

$$G(a,\pm a;\tau) \simeq C e^{-\omega\tau/2} \quad \begin{matrix} \cosh\left(\tau K e^{-S_{\rm inst}/\hbar}\right), \\ \sinh\left(\tau K e^{-S_{\rm inst}/\hbar}\right) \end{matrix} \tag{3.41}$$

where C is some factor that depends in a non-exponential way on the transition time.

Before we turn to a discussion of the physical content of this result, let us check the self-consistency of our central working hypothesis – the diluteness of the instanton gas. To this end, consider the representation of G in terms of the partial amplitudes (3.40). To determine the typical number of instantons contributing to the sum, one may make use of the fact that, for a general sum $\sum_n c_n$ of positive quantities $c_n > 0$, the "typical" value of the summation index can be estimated as $\langle n\rangle \equiv \sum_n c_n n / \sum_n c_n$. With the abbreviation $X \equiv \tau K e^{-S_{\rm inst}/\hbar}$ the application of this estimate to our current sum yields

$$\langle n\rangle \equiv \frac{\sum_n n X^n/n!}{\sum_n X^n/n!} = X,$$

where we have used the fact that, as long as $\langle n\rangle \gg 1$, the even/odd distinction in the sum is irrelevant. Thus, we can infer that the average instanton density, $\langle n\rangle/\tau = K e^{-S_{\rm inst}/\hbar}$, is both exponentially small in the instanton action $S_{\rm inst}$, and independent of τ, confirming the validity of our diluteness assumptions above.

Finally, let us discuss how the form of the transition amplitude (3.41) can be understood in physical terms. To this end, let us reconsider the basic structure of the problem we are dealing with (see Fig. 3.6). While there is no coupling across the barrier, the Hamiltonian has two independent, oscillator-like sets of low-lying eigenstates sitting in the two local minima. Allowing for a weak inter-barrier coupling, the oscillator ground states (like all higher states) split into a doublet of a symmetric and an antisymmetric eigenstate, $|S\rangle$ and $|A\rangle$ with energies ϵ_A and ϵ_S, respectively. Focusing on the low-energy sector formed by the ground state doublet, we can express the transition amplitudes (3.32) as

$$G(a,\pm a;\tau) \simeq \langle a| \left(|S\rangle e^{-\epsilon_S\tau/\hbar}\langle S| + |A\rangle e^{-\epsilon_A\tau/\hbar}\langle A|\right) |\pm a\rangle.$$

Setting $\epsilon_{A/S} = \hbar\omega/2 \pm \Delta\epsilon/2$, where $\Delta\epsilon$ represents the tunnel-splitting, the symmetry properties $|\langle a|S\rangle|^2 = |\langle -a|S\rangle|^2 = C/2$ and $\langle a|A\rangle\langle A|-a\rangle = -|\langle a|A\rangle|^2 = -C/2$ imply that

$$G(a,\pm a;\tau) \simeq \frac{C}{2}\left(e^{-(\hbar\omega-\Delta\epsilon)\tau/2\hbar} \pm e^{-(\hbar\omega+\Delta\epsilon)\tau/2\hbar}\right) = C e^{-\omega\tau/2} \quad \begin{matrix} \cosh(\Delta\epsilon\tau/\hbar), \\ \sinh(\Delta\epsilon\tau/\hbar). \end{matrix}$$

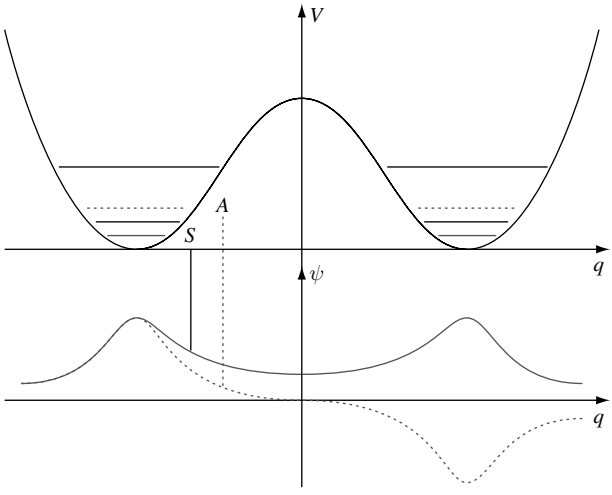

Figure 3.6 Quantum states of the double well. The thick lines indicate energy levels of harmonic oscillator states; the thin and dotted lines indicate exact symmetric (S) and antisymmetric (A) eigenstates.

Comparing this expression with Eq. (3.41) the interpretation of the instanton calculation becomes clear: at long times, the transition amplitude engages the two lowest states – the symmetric and anti-symmetric combinations of the two oscillator ground states. The energy splitting $\Delta\epsilon$ accommodates the energy shift due to the tunneling between the two wells. Remarkably, the effect of tunneling was obtained from a purely classical picture (formulated in imaginary time!). The instanton calculation also produced a prediction for the tunnel splitting of the energies, namely

$$\Delta\epsilon = \hbar K \, \exp(-S_{\rm inst}/\hbar),$$

which, up to the prefactor, agrees with the result of a WKB-type analysis of the tunnel process.

Before leaving this section, some general remarks on instantons are in order:

- ▷ In hindsight, was the approximation scheme used above consistent? In particular, terms at second order in $\hbar$ were neglected, while terms non-perturbative in $\hbar$ (the instanton) were kept. Yet, the former typically give rise to a larger correction to the energy than the latter. However, the large perturbative shift affects the energies of the symmetric and antisymmetric states equally. The instanton contribution gives the *leading* correction to the splitting of the levels. It is the latter that is likely to be of more physical significance.
- ▷ Secondly, it may – legitimately – appear as though the development of the machinery above was a bit of an "overkill" for describing a simple tunneling process. As a matter of fact, the basic result Eq. (3.41) could have been obtained in a simpler way by more elementary means (using, for example, the WKB method). Why then did we discuss instantons at such length? One reason is that, even within a purely quantum mechanical framework, the instanton formulation of tunneling is much stronger than WKB. The

latter represents, by and large, an uncontrolled approximation. In general it is hard to tell whether WKB results are accurate or not. In contrast, the instanton approximation to the path integral is controlled by a number of well-defined expansion parameters. For example, by going beyond the semiclassical approximation and/or softening the diluteness assumption, the calculation of the transition amplitudes can, in principle, be driven to arbitrary accuracy.

▷ A second and, for our purposes, more important motivation is that instanton techniques are of crucial importance within higher-dimensional field theories (here we regard the path integral formulation of quantum mechanics as a (0 space + 1 time) = 1-dimensional field theory). The reason is that instantons are intrinsically non-perturbative objects, which is to say that instanton solutions to stationary phase equations describe a type of physics that cannot be obtained by a perturbative expansion around a non-instanton sector of the theory. (For example, the bouncing orbits in the example above cannot be incorporated into the analysis by doing a kind of perturbative expansion around a trivial orbit.) This non-perturbative nature of instantons can be understood by topological reasoning.

Relatedly, one of the features of the instanton analysis above was that the *number* of instantons involved was a stable quantity; "stable" in the sense that by including perturbative fluctuations around the n-instanton sector, say, one does not connect with the $n+2$ sector. Although no rigorous proof of this statement has been given, it should be heuristically clear: a trajectory involving n bounces between the hills of the inverted potential cannot be smoothly connected with one of a different number. Suppose for instance we should forcibly attempt to interpolate between two paths with different bounce numbers. Inevitably, some of the intermediate configurations would be charged with actions that are far apart from any stationary phase-like value. Thus, the different instanton sectors are separated by an energetic barrier that cannot be penetrated by smooth interpolation and, in this sense, they are **topologically distinct**.

INFO **Fluctuation determinant**: Our analysis above provided a method to extract the tunneling rate between the quantum wells to a level of exponential accuracy. However, in some applications, it is useful to compute the exponential prefactor K. Although such a computation follows the general principles outlined above and implemented explicitly for the single well, there are some idiosyncrasies in the tunneling system that warrant discussion.

According to the general principles outlined in Section 3.2, integrating over Gaussian fluctuations around the saddle-point field configurations, the contribution to the transition amplitude from the n-instanton sector is given by

$$G_n = J \det \ \left[-m\partial_\tau^2 + V''(q_{\mathrm{cl},n})\right] \ e^{-nS_{\mathrm{inst}}},$$

where $q_{\mathrm{cl},n}(\tau)$ represents an n-instanton configuration and J the normalization. Now, in the zero-instanton sector, the evaluation of the functional determinant recovers the familiar harmonic oscillator result, $G(a,a,\tau) = (m\omega/\pi\hbar)^{\frac{1}{2}} \ \exp[-\omega\tau/2]$. Let us now consider the one-instanton sector of the theory. To evaluate the functional determinant, one must consider the spectrum of the operator $-m\partial_\tau^2 + V''(q_{\mathrm{cl},1})$. Differentiating the defining equation for $q_{\mathrm{cl},1}$ Eq. (3.34), one may confirm that

$$\left[-m\partial_\tau^2 + V''(q_{\mathrm{cl},1})\right] \ \partial_\tau q_{\mathrm{cl},1} = 0,$$

i.e. the function $\partial_\tau q_{\mathrm{cl},1}$ presents a zero mode of the operator! Physically, the origin of the zero mode is elucidated by noting that a translation of the instanton along the time axis, $q_{\mathrm{cl},1}(\tau) \to q_{\mathrm{cl},1}(\tau+\delta\tau)$, should leave the action approximately invariant. However, for small $\delta\tau$, $q_{\mathrm{cl},1}(\tau+\delta\tau) \simeq q_{\mathrm{cl},1}(\tau) + \delta\tau\partial_\tau q_{\mathrm{cl},1}$, i.e. to first order, the addition of the increment function $\partial_\tau q_{\mathrm{cl},1}$ leaves the action invariant, and $\delta\tau$ is a "zero mode coordinate."

With this interpretation, it becomes clear how to repair the formula for the fluctuation determinant. While the Gaussian integral over fluctuations is controlled for the non-zero eigenvalues, its execution for the zero mode must be rethought. Indeed, by integrating over the coordinate of the instanton, that is $\int_0^\tau d\tau_0 = \tau$, one finds that the contribution to the transition amplitude in the one-instanton sector is given by

$$J\tau \quad \overline{\frac{S_{\mathrm{inst}}}{2\pi\hbar}}\det{}'\left[-m\partial_\tau^2 + V''(q_{\mathrm{cl},1})\right]^{-1/2} e^{-S_{\mathrm{inst}}},$$

where the prime indicates the exclusion of the zero mode from the determinant, and the factor $\sqrt{S_{\mathrm{inst}}/2\pi\hbar}$ reflects the Jacobian associated with the change to a new set of integration variables which contains the zero mode coordinate τ as one of its elements.[18] To fix the, as yet, undetermined coupling constant J, we normalize by the fluctuation determinant of the (imaginary time) harmonic oscillator, i.e. we use the fact that (cf. Section 3.3), for the harmonic oscillator, the return amplitude evaluates to $G(a,a,\tau) = J\det(m(-\partial_\tau^2+\omega^2)/2)^{-1/2} = (m\omega/\pi\hbar)^{1/2}\, e^{-\omega\tau/2}$, where the first/second representation is the imaginary time variant of Eq. (3.30)/Eq.(3.31). Using this result, and noting that the zero mode analysis above generalizes to the n-instanton sector, we find that the pre-exponential constant K used in our analysis of the double-well problem above affords the explicit representation

$$K = \omega \quad \overline{\frac{S_{\mathrm{inst}}}{2\pi\hbar}} \quad \frac{m\omega^2\det{}'\left[-m\partial_\tau^2 + V''(q_{\mathrm{cl},1})\right]}{\det\left[-m\partial_\tau^2 + m\omega^2\right]} \quad^{-1/2}.$$

Naturally, the instanton determinant depends sensitively on the particular nature of the potential $V(q)$. For the quartic potential $V(q) = m\omega^2(x^2-a^2)^2/8a^2$, it may be confirmed that

$$\frac{m\omega^2\det{}'\left[-m\partial_\tau^2 + V''(q_{\mathrm{cl},1})\right]}{\det\left[-m\partial_\tau^2 + m\omega^2\right]} = \frac{1}{12},$$

while $S_{\mathrm{inst}} = (2/3)m\omega a^2$. For further details of the calculation, we refer to, e.g., Zinn-Justin (1993).[18]

Escape from a metastable minimum: bounces

The instanton gas approximation for the double-well system can be easily adapted to explore the problem of quantum mechanical tunneling from a metastable state such as that presented by an unstable nucleus. In particular, suppose one wishes to estimate the "survival probability" of a particle captured in a metastable minimum of a one-dimensional potential such as that shown in Fig. 3.7.

According to the path integral scheme, the survival probability, defined by the probability amplitude of remaining at the potential minimum q_{m}, i.e. the propagator $G(q_{\mathrm{m}}, q_{\mathrm{m}}; t)$, can

[18] See J. Zinn-Justin, *Quantum Field Theory and Critical Phenomena* (Oxford University Press, 1993) for an explicit calculation of this Jacobian.

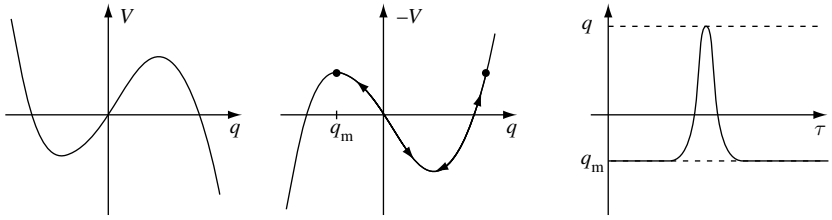

Figure 3.7 Effective potential showing a metastable minimum together with the inverted potential and a sketch of a bounce solution. To obtain the tunneling rate it is necessary to sum over a dilute gas of bounce trajectories.

be evaluated by making use of the Euclidean time formulation of the Feynman path integral. As with the double well, in the Euclidean time formalism the dominant contribution to the transition probability arises from the classical path minimizing the action corresponding to the inverted potential (see Fig. 3.7). However, in contrast to the double-well potential, the classical solution takes the form of a "**bounce**" (i.e. the particle spends only a short time away from the potential minimum – there is only one metastable minimum of the potential). As with the double well, one can expect multiple bounce trajectories to present a significant contribution. Summing over all bounce trajectories (note that in this case we have an exponential series – no even/odd parity effect), one obtains the survival probability

$$G(q_{\rm m}, q_{\rm m}; \tau) = Ce^{-\omega\tau/2} \exp\left[\tau K e^{-S_{\rm bounce}/\hbar}\right].$$

Applying an analytic continuation to real time, one finds $G(q_m, q_m; t) = Ce^{-i\omega t/2} \exp[-\frac{\Gamma}{2}t]$, where the decay rate is given by $\Gamma/2 = |K|e^{-S_{\rm bounce}/\hbar}$. (Note that on physical grounds we can see that K must be imaginary.[19])

EXERCISE Consider a heavy nucleus having a finite rate of α-decay. The nuclear forces can be considered very short-range so that the rate of α particle emission is controlled by tunneling under a Coulomb barrier. Taking the effective potential to be spherically symmetric with a deep minimum core of radius r_0 beyond which it decays as $U(r) = 2(Z-1)e^2/r$ where Z is the nuclear charge, find the temperature of the nuclei above which α-decay will be thermally assisted if the energy of the emitted particles is E_0. Estimate the mean energy of the α particles as a function of temperature.

EXERCISE A uniform electric field E is applied perpendicular to the surface of a metal with work function W. Assuming that the electrons in the metal describe a Fermi gas of density n, with exponential accuracy, find the tunneling current at zero temperature ("cold emission"). Show that, effectively, only electrons with energy near the Fermi level are tunneling. With the same accuracy, find the current at finite temperature ("hot emission"). What is the most probable energy of tunneling electrons as a function of temperature?

[19] In fact, a more careful analysis shows that this estimate of the decay rate is too large by a factor of 2 (for further details see, e.g., the discussion in Coleman.[17]

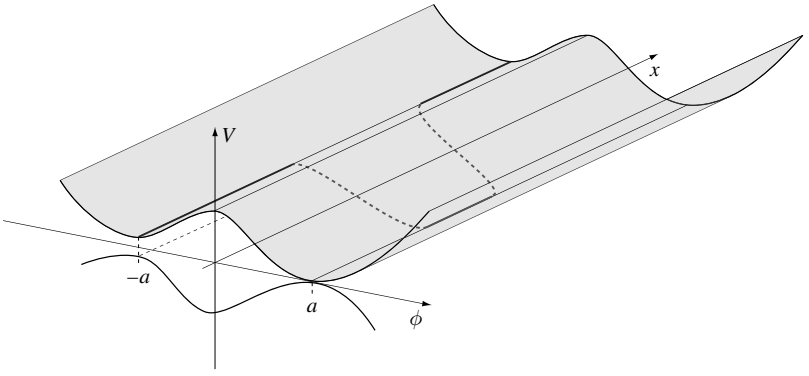

Figure 3.8 Snapshot of a field configuration $\phi(x, t = \text{const.})$ in a potential landscape with two nearly degenerate minima. For further discussion, see the text.

Tunneling of quantum fields: "fate of the false vacuum"

Hitherto we have focused on applications of the Feynman path integral to the quantum mechanics of isolated point-like particles. In this setting, the merit of the path integral scheme over, say, standard perturbative methods or the "WKB" approach is perhaps not compelling. Therefore, by way of motivation, let us present an example that builds on the structures elucidated above and illustrates the power of the path integral method.

To this end, let us consider a theory involving a continuous classical field that can adopt two homogeneous equilibrium states with different energy densities. To be concrete, one may consider a harmonic chain confined to one or other minimum of an asymmetric quasi-one-dimensional "gutter-like" double-well potential (see Fig. 3.8). When quantized, the state of higher energy density becomes unstable through barrier penetration – it is said to be a "**false vacuum**".[20] Specifically, drawing on our discussion of the harmonic chain in Chapter 1, let us consider a quantum system specified by the Hamiltonian density

$$\hat{\mathcal{H}} = \frac{\hat{\pi}^2}{2m} + \frac{k_{\rm s} a^2}{2}(\partial_x \hat{\phi})^2 + V(\hat{\phi}), \tag{3.42}$$

where $[\hat{\pi}(x), \hat{\phi}(x')] = -i\hbar\delta(x - x')$. Here we have included a potential $V(\phi)$ which, in the present case, assumes the form of a double well. The inclusion of a weak bias $-f\phi$ in $V(\phi)$ identifies a stable and a metastable potential minimum. Previously, we have seen that, in the absence of the confining potential, the quantum string exhibits low-energy collective wave-like excitations – phonons. In the confining potential, these harmonic fluctuations are rendered massive. However, drawing on the quantum mechanical principles established in the single-particle system, one might assume that the string tunnels freely between the two potential minima. To explore the capacity of the system to tunnel, let us suppose that, at

[20] For a detailed discussion of the history and ramifications of this idea, we refer to the original insightful paper by Sidney Coleman, Fate of the false vacuum: semiclassical theory, *Phys. Rev. D* **15** (1977), 2929–36. In fact, many of the ideas developed in this work were anticipated in an earlier analysis of metastability in the context of classical field theories by J. S. Langer, Theory of the condensation point, *Ann. Phys. (NY)* **41** (1967), 108–57.

some time $t = 0$, the system adopts a field configuration in which the string is located in the (metastable) minimum of the potential at, say, $\phi = -a$. What is the probability that the *entire* string of length L will tunnel across the barrier into the potential minimum at $\phi = a$ in a time t?

INFO The tunneling of fields between nearly degenerate ground states plays a role in numerous physical contexts. By way of example, consider a **superheated liquid**. In this context, the "false" vacuum is the liquid state, the true one the gaseous phase. The role of the field is taken by the local density distribution in the liquid. Thermodynamic fluctuations trigger the continuous appearance of vapor bubbles in the liquid. For bubbles of too small a diameter, the gain in volume energy is outweighed by the surface energy cost – the bubble will collapse. However, for bubbles beyond a certain critical size, the energy balance is positive. The bubble will grow and, eventually, swallow the entire mass density of the system; the liquid has vaporized or, more formally, the density field tunneled[21] from the false ground state into the true one.

More speculative (but also potentially more damaging) manifestations of the phenomenon have been suggested in the context of **cosmology**:[22] what if the big bang released our universe not into its true vacuum configuration but into a state separated by a huge barrier from a more favorable sector of the energy landscape. In this case, everything would depend on the tunneling rate:

> If this time scale is of the order of milliseconds, the universe is still hot when the false vacuum decays... if this time is of the order of years, the decay will lead to a sort of secondary big bang with interesting cosmological consequences. If this time is of the order of 10^9 years, we have occasion for anxiety.
>
> (S. Coleman)

Previously, for the point-particle system, we have seen that the transition probability between the minima of the double well is most easily accessed by exploring the classical field configurations of the Euclidean time action. In the present case, anticipating to some extent our discussion of the quantum field integral in the next chapter, the Euclidean time action associated with the Hamiltonian density (3.42) assumes the form[23]

$$S[\phi] = \int_0^T d\tau \int_0^L dx \left[\frac{m}{2} (\partial_\tau \phi)^2 + \frac{k_s a^2}{2} (\partial_x \phi)^2 + V(\phi) \right],$$

where the time integral runs over the interval $[0, T = it]$. Here, for simplicity, let us assume that the string obeys periodic boundary conditions in space, namely $\phi(x+L, \tau) \equiv \phi(x, \tau)$. To estimate the tunneling amplitude, we will explore the survival probability of the metastable state, imposing the boundary conditions $\phi(x, \tau = 0) = \phi(x, \tau = T) = -a$ on the path integral. Once again, when the potential barrier is high, and the time T is long, one may assume that the path integral is dominated by the saddle-point field configuration of the

[21] At this point, readers should no longer be confused regarding the mentioning of "tunneling" in the context of a classical system. Within the framework of the path integral, the classical partition sum maps onto the path integral of a fictitious quantum system. It is this tunneling that we have in mind.

[22] See note 25.

[23] Those readers who wish to develop a more rigorous formulation of the path integral for the string may either turn to the discussion of the field integral in the next chapter or, alternatively, may satisfy themselves of the validity of the Euclidean action by (re-)discretizing the harmonic chain, presenting the transition amplitude as a series of Feynman path integrals for each element of the string and, finally, taking the continuum limit.

Euclidean action. In this case, varying the action with respect to the field $\phi(x,\tau)$, one obtains the classical equation of motion

$$m\partial_\tau^2\phi + k_s a^2 \partial_x^2 \phi = \partial_\phi V(\phi),$$

which must be solved subject to the boundary conditions above.

Now, motivated by our consideration of the point-particle problem, one might seek a solution in which the string tunnels as a single rigid entity without "flexing." However, it is evident from the spatial translational invariance of the system that the instanton action would scale with the system size L. In the infinite system $L \to \infty$, such a trajectory would therefore not contribute significantly to the tunneling amplitude. Instead, one must consider a different type of field configuration in which the transfer of the chain is by degree. In this,

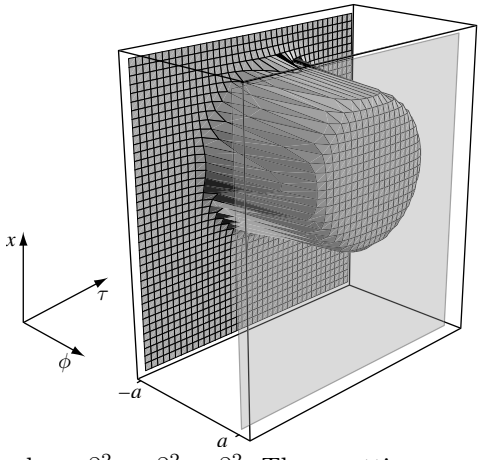

elements of the string cross the barrier in a consecutive sequence as two outwardly propagating "domain walls" (see the figure, where the emergence of such a double-kink configuration is shown as a function of space and time; notice the circular shape of the resulting space-time droplet – a consequence of the rotational symmetry of the rescaled problem). Such a field configuration can be motivated from symmetry considerations by noting that, after rescaling $x \mapsto v_s x$ (where $v_s = \sqrt{k_s a^2/m}$ denotes the classical sound wave velocity), the saddle-point equation assumes the isotropic form $m\partial^2\phi = \partial_\phi V(\phi)$, where $\partial^2 = \partial_\tau^2 + \partial_x^2$. Then, setting $r = \sqrt{x^2 + (\tau - T/2)^2}$, and sending $(T, L) \to \infty$, the space-time rotational symmetry suggests a solution of the form $\phi = \phi(r)$, where $\phi(r)$ obeys the radial diffusion equation

$$m\partial_r^2\phi + \frac{m}{r}\partial_r\phi = \partial_\phi V,$$

with the boundary condition $\lim_{r\to\infty}\phi(r) = -a$. This equation describes the one-dimensional motion of a particle in a potential $-V$ and subject to a strange "friction force" $-mr^{-1}\partial_r\phi$ whose strength is inversely proportional to "time" r.

To understand the profile of the **bounce solution**, suppose that at time $r = 0$ the particle has been released from rest at a position slightly to the left of the (inverted) potential maximum at a. After rolling through the potential minimum it will climb the potential hill at $-a$. Now, the initial position may be fine-tuned in such a way that the viscous damping of the particle compensates for the excess potential energy (which would otherwise make the particle overshoot and disappear to infinity): there exists a solution where the particle starts close to $\phi = a$ and eventually winds up at $\phi = -a$, in accord with the imposed boundary conditions. In general, the analytical solution for the bounce depends sensitively on the form of the confining potential. However, while we assume that the well asymmetry imposed by external potential $-f\phi$ is small, the radial equation may be considerably simplified. In this limit, one may invoke a "thin-wall" approximation in which one assumes that the bounce

configuration is described by a domain wall of thickness Δr, at a radius $r_0 \gg \Delta r$ separating an inner region where $\phi(r < r_0) = a$ from the outer region where $\phi(r > r_0) = -a$. In this case, and to lowest order in an expansion in f, the action of the friction force is immaterial, i.e. we may set $m\partial_r^2\phi = \partial_\phi V$ – the very instanton equation formulated earlier for the point-particle system!

Then, substituting back into S, one finds that the bounce (or kink-like) solution is characterized by the Euclidean action

$$S = v_{\rm s}\left[2\pi r_0 S_{\rm inst} - \pi r_0^2 2af\right],$$

where $S_{\rm inst}$ denotes the action of the instanton associated with the point-particle system Eq. (3.36), and the last term accommodates the effect of the potential bias on the field configuration. Crucially, one may note that the instanton contribution to the action scales with the circumference of the domain wall in the space-time, while that of the potential bias scales with the area of the domain. From this scaling dependence, it is evident that, however small the external force f, at large enough r_0 the contribution of the second term will always outweigh the first and the string will tunnel from the metastable minimum to the global minimum of the potential. More precisely, the optimal size of domain is found by minimizing the action with respect to r_0. In doing so, one finds that $r_0 = S_{\rm inst}/2af$. Then, substituting back into the action, one obtains the tunneling rate

$$\Gamma \sim \ \exp\left[-\frac{1}{\hbar}\frac{\pi v_{\rm s} S_{\rm inst}^2}{2af}\right].$$

From this result, one can conclude that, in the absence of an external force f, the tunneling of the string across the barrier is *completely quenched*! In the zero-temperature unbiased system, the symmetry of the quantum Hamiltonian is broken: the ground state exhibits a two-fold degeneracy in which the string is confined to one potential minimum or another.

The ramifications of the tunneling amplitude suppression can be traced to the statistical mechanics of the corresponding classical system. As emphasized in Section 3.2, any Euclidean time path integral of a d-dimensional system can be identified with the statistical mechanics of a classical system $(d+1)$-dimensional problem. In the double-well system, the Euclidean time action of the point-particle quantum system is isomorphic to the one-dimensional realization of the classical Ising ferromagnet, namely

$$\beta H_{\rm Ising} = \int_0^L dx \left[\frac{t}{2}m^2 + um^4 + \frac{K}{2}(\nabla m)^2\right]. \tag{3.43}$$

Translated into this context, the saddle-point (or mean-field) analysis suggests that the system will exhibit a spontaneous symmetry breaking to an ordered phase ($m \neq 0$) when the parameter t (the reduced temperature) becomes negative. However, drawing on our analysis of the quantum point-particle system, in the thermodynamic limit, we see that fluctuations (non-perturbative in temperature) associated with instanton field configurations of the Hamiltonian $m(x)$ may restore the symmetry of the system and destroy long-range order at any finite temperature $1/\beta$. Whether this happens or not depends on the competition between the energy cost of instanton creation and the entropy gained by integrating over the instanton zero-mode coordinates. It turns out that, in $d = 1$, the latter wins, i.e.

the system is "disordered" at any finite temperature. In contrast, for $d \geq 2$, the creation of instantons is too costly, i.e. the system will remain in its energetically preferred ground state. For further discussion of these issues, we refer to the Info block in Section 8.1.1.

Tunneling in a dissipative environment

In the condensed matter context it is, of course, infeasible to completely divorce a system from its environment. Indeed, in addition to the dephasing effect of thermal fluctuations, the realization of quantum mechanical phenomena depends sensitively on the strength and nature of the coupling to the external degrees of freedom. For example, the tunneling of an atom from one interstitial site in a crystal to another is likely to be heavily influenced by its coupling to the phonon degrees of freedom that characterize the crystal lattice. By exchanging energy with the phonons, which act in the system as an external bath, a quantum particle can lose its phase coherence and with it, its quantum mechanical character. Beginning with the seminal work of Caldeira and Leggett,[24] there have been numerous theoretical investigations of the effect of an environment on the quantum mechanical properties of a system. Such effects are particularly acute in systems where the quantum mechanical degree of freedom is *macroscopic*, such as the magnetic flux trapped in a superconducting quantum interference device (SQUID). In the following, we show that the Feynman path integral provides a natural (and almost unique) setting in which the effects of the environment on a microscopic or macroscopic quantum mechanical degree of freedom can be explored. For further discussion of the response of quantum wave coherence to environmental coupling, we refer to Chapter 11.

Before we begin, let us note that the phenomenon of macroscopic quantum tunneling represents an extensive and still active area of research recently reinvigorated by the burgeoning field of quantum computation. By contrast, our discussion here will be necessarily limited in scope, targeting a particular illustrative application, and highlighting only the guiding principles. For a more thorough and detailed discussion, we refer the reader to one of the many comprehensive reviews.[25]

Caldeira–Leggett model

Previously, we have discussed the ability of the Feynman path integral to describe quantum mechanical tunneling of a particle q across a potential barrier $V(q)$. In the following, we will invoke the path integral to explore the capacity for quantum mechanical tunneling when the particle is coupled to degrees of freedom of an external environment. Following Caldeira and

[24] A. O. Caldeira and A. J. Leggett, Influence of dissipation on quantum tunneling in macroscopic systems, *Phys. Rev. Lett.* **46** (1981), 211–14.

[25] See, e.g., A. J. Leggett *et al.*, Dynamics of the dissipative two-state system, *Rev. Mod. Phys* **59** (1976), 1–85, and U. Weiss, *Quantum Dissipative Systems* (World Scientific Publishing, 1993).

Leggett's original formulation, let us represent the environment by a **bath of quantum harmonic oscillators** characterized by a set of frequencies $\{\omega_\alpha\}$,

$$\hat{H}_{\rm bath}[q_\alpha] = \sum_\alpha^N \left[\frac{\hat{p}_\alpha^2}{2m_\alpha} + \frac{m_\alpha}{2}\omega_\alpha^2 q_\alpha^2\right],$$

where N is the number of bath-oscillators. For simplicity, let us suppose that, in the leading approximation, the particle–bath coupling is linear in the bath coordinates and such that $\hat{H}_{\rm c}[q,q_\alpha] = -\sum_\alpha^N f_\alpha[q]q_\alpha$, where $f_\alpha[q]$ represents some function of the particle coordinate q. Expressed as a Feynman path integral, the survival probability of a particle confined to a metastable minimum at a position $q=a$, and coupled to an external environment, can then be expressed as ($\hbar=1$)

$$\langle a|e^{-i\hat{H}t/\hbar}|a\rangle = \int\limits_{q(0)=q(t)=a} Dq\; e^{iS_{\rm part.}[q]} \int Dq_\alpha\; e^{iS_{\rm bath}[q_\alpha]+iS_{\rm c}[q,q_\alpha]},$$

where $\hat{H} = \hat{H}_{\rm part} + \hat{H}_{\rm bath} + \hat{H}_{\rm c}$ denotes the total Hamiltonian of the system,

$$S_{\rm part}[q] = \int_0^t dt' \left[\frac{m}{2}\dot{q}^2 - V(q)\right], \quad S_{\rm bath}[q_\alpha] = \int_0^t dt' \sum_\alpha \frac{m_\alpha}{2}\left[\dot{q}_\alpha^2 - \omega_\alpha^2 q_\alpha^2\right],$$

denote, respectively, the actions of the particle and bath, while

$$S_{\rm c}[q,q_\alpha] = -\int_0^t dt' \left(\sum_\alpha f_\alpha[q]q_\alpha + \sum_a \frac{f_\alpha[q]^2}{2m_a\omega_a^2}\right)$$

represents their coupling.[26] Here we assume that the functional integral over $q_\alpha(t)$ is taken over all field configurations of the bath while, as before, the path integral on $q(t)$ is subject to the boundary conditions $q(0)=q(t)=a$.

To reveal the effect of the bath on the capacity for tunneling of the particle, it is instructive to integrate out fluctuations q_α and thereby obtain an effective action for q. Being Gaussian in the coordinates q_α, the integration can be performed straightforwardly. Although not crucial, since we are dealing with quantum mechanical tunneling, it is useful to transfer to the Euclidean time representation. Taking the boundary conditions on the fields $q_\alpha(\tau)$ to be periodic on the interval $[0, T^{-1}\equiv\beta]$, it may be confirmed that the Gaussian functional integral over q_α induces a time non-local interaction of the particle (exercise) $\langle a|e^{-i\hat{H}t/\hbar}|a\rangle = \int Dq\; e^{-S_{\rm eff}[q]}$ where a constant of integration has been absorbed into the measure and

$$S_{\rm eff}[q] = S_{\rm part}[q] + \frac{1}{2T}\sum_{\omega_n,\alpha} \frac{\omega_n^2 f_\alpha[q(\omega_n)]f_\alpha[q(-\omega_n)]}{m_\alpha\omega_\alpha^2(\omega_\alpha^2+\omega_n^2)}.$$

[26] The second term in the coupling action has been added to keep the effect of the environment minimally invasive (purely dissipative). If it were not present, the coupling to the oscillator degrees of freedom would effectively shift the extremum of the particle potential, i.e. change its potential landscape. (Exercise: Substitute the solutions of the Euler–Lagrange equations $\delta_{q_\alpha} S[q,q_\alpha]=0$ [computed for a fixed realization of q] into the action to obtain the said shift.)

Here, the sum $\sum_{\omega_n}$ runs over the discrete set of Fourier frequencies $\omega_n = 2\pi n T$ with n integer.[27] By integrating out of the bath degrees of freedom, the particle action acquires an induced contribution. To explore its effect on dissipation and tunneling, it is necessary to specialize our discussion to a particular form of coupling.

In the particular case that the coupling to the bath is linear, i.e. $f_\alpha[q(\tau)] = c_\alpha q(\tau)$, the effective action assumes the form (exercise)

$$\boxed{S_{\rm eff}[q] = S_{\rm part}[q] - T\int_0^\beta d\tau\ d\tau'\ K(\tau-\tau')q(\tau)q(\tau'),}$$

where $K(\tau) = \int_0^\infty \frac{d\omega}{\pi} J(\omega) D_\omega(\tau)$, $J(\omega) = \frac{\pi}{2}\sum_\alpha \frac{c_\alpha^2}{m_\alpha \omega_\alpha}\delta(\omega-\omega_\alpha)$ and

$$D_\omega(\tau) = -\sum_{\omega_n} \frac{\omega_n^2}{\omega(\omega^2+\omega_n^2)} e^{i\omega_n \tau},$$

resembles the Green function of a boson with energy $\hbar\omega$. Physically, the non-locality of the action is easily understood. By exchanging fluctuations with the external bath, a particle can effect a self-interaction, retarded in time. Taken as a whole, the particle and the bath maintain quantum phase coherence. However, when projected onto the particle degree of freedom, the total energy of the system appears to fluctuate and the phase coherence of the particle transport is diminished. To explore the properties of the dissipative action, it is helpful to separate the non-local interaction according to the identity $q(\tau)q(\tau') = [q^2(\tau)+q^2(\tau')]/2 - [q(\tau)-q(\tau')]^2/2$. The first square-bracketed contribution presents an innocuous renormalization of the potential $V(q)$ and, applying equally to the classically allowed motion and quantum tunneling, presents an unobservable perturbation. Therefore, we will suppose that its effect has been absorbed into a redefinition of the particle potential $V(q)$. By contrast, the remaining contribution is always positive.

Either the particular form of the "spectral function" $J(\omega)$ may be obtained from an *a priori* knowledge of the microscopic interactions of the bath or, phenomenologically, it can be inferred from the structure of the classical damped equations of motion. For example, for a system subject to an "ohmic" dissipation (where, in real time, the classical equations of motion obtain a dissipative term $-\eta\dot{q}$ with a "friction coefficient" η), one has $J(\omega) = \eta|\omega|$ for all frequencies smaller than some characteristic cut-off (at the scale of the inverse Drude relaxation time of the environment). By contrast, for a defect in a three-dimensional crystal, interaction with acoustic phonons presents a frequency dependence of ω^3 or ω^5 depending on whether ω is below or above the Debye frequency.

INFO Consider, for example, the coupling of a particle to a continuum of bosonic modes whose spectral density $J(\omega) = \eta\omega$ grows linearly with frequency. In this case,

$$K(\omega_n) = \frac{\omega_n^2}{\pi}\int_0^\infty d\omega\ \frac{J(\omega)}{\omega(\omega^2+\omega_n^2)} = \frac{\eta}{2}|\omega_n|,$$

[27] More precisely, anticipating our discussion of the Matsubara frequency representation, we have defined the Fourier decomposition on the Euclidean time interval T, namely $q(\tau) = \sum_m q_m e^{i\omega_m\tau}$, $q_m = T\int_0^\beta d\tau\ q(\tau)e^{-i\omega_m\tau}$, where $\omega_m = 2\pi m/\beta$ with m integer.

describes **Ohmic dissipation** of the particle. Fourier transforming this expression we obtain

$$K(\tau) = \frac{\pi T \eta}{2} \frac{1}{\sin^2(\pi T \tau)} \overset{\tau \ll T^{-1}}{\simeq} \frac{\eta}{2\pi T} \frac{1}{\tau^2}, \tag{3.44}$$

i.e. a strongly time non-local "self-interaction" of the particle.

Disssipative quantum tunneling

To return to the particular problem at hand, previously we have seen that the tunneling rate of a particle from a metastable potential minimum can be inferred from the extremal field configurations of the Euclidean action: the bounce trajectory. To explore the effect of the dissipative coupling, it is necessary to understand how it revises the structure of the bounce solution. Now, in general, the non-local character of the interaction inhibits access to an exact solution of the classical equation of motion. In such cases, the effect of the dissipative coupling can be explored perturbatively or with the assistance of the renormalization group (see the discussion in Section 8.2). However, by tailoring our choice of potential $V(q)$, we can gain some intuition about the more general situation.

To this end, let us consider a particle of mass m confined in a metastable minimum by a (semi-infinite) harmonic potential trap (see figure),

$$V(q) = \begin{cases} m\omega_c^2 q^2/2, & 0 < |q| \leq a, \\ -\infty, & |q| > a. \end{cases}$$

Further, let us assume that the environment imparts an ohmic dissipation with a damping or viscosity η. To keep our discussion general, let us consider the combined impact of dissipation and temperature on the rate of tunneling from the potential trap. To do so, following Langer[28] it is natural to investigate the "quasi-equilibrium" quantum partition function $\mathcal{Z}$ of the combined system. In this case, the tunneling rate appears as an imaginary contribution to the free energy $F = -T \ln \mathcal{Z}$, namely $\Gamma = -(2/\hbar)\mathrm{Im}\, F$.

By drawing on the path integral, the quantum partition function of the system can be presented as a functional integral $\mathcal{Z} = \int_{q(\beta)=q(0)} Dq\, e^{-S_{\rm eff}/\hbar}$ where, as we have seen above, for ohmic coupling, the Euclidean action assumes the form

$$\begin{aligned} S_{\rm eff}[q] &= \int_0^\beta d\tau \left(\frac{m}{2}\dot{q}^2 + V(q) \right) \\ &\quad + \frac{\eta}{4\pi} \int_0^\beta d\tau\, d\tau' \left(\frac{q(\tau) - q(\tau')}{\tau - \tau'} \right)^2. \end{aligned}$$

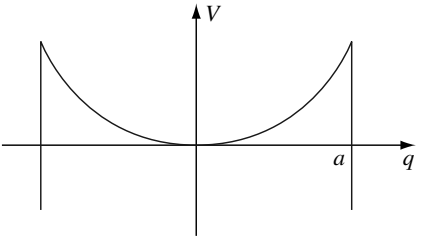

Once again, to estimate the tunneling rate, we will suppose that the barrier is high and the temperature is low, so that the path integral is dominated by stationary configurations of the action. In this case, one may identify three distinct solutions. In the first place, the particle may

[28] J. S. Langer, Theory of the condensation point, *Ann. Phys. (NY)* **41** (1967), 108–57.

remain at $q = 0$ poised precariously on the maximum of the inverted harmonic potential. Contributions from this solution and the associated harmonic fluctuations reproduce terms in the quantum partition function associated with states of the *closed* harmonic potential trap. Secondly, there exists a singular solution in which the particle remains at the minimum of the inverted potential, i.e. perched on the potential barrier. The latter presents a negligible contribution to the quantum partition function and can be neglected. Finally, there exists a bounce solution in which the particle injected at a position q inside the well accelerates down the inverted potential gradient, is reflected from the potential barrier, and returns to the initial position q in a time β. While, in the limit $\beta \to \infty$, the path integral singles out the boundary condition $q(0) = q(\beta) \to 0$, at finite β the boundary condition will depart from 0 in a manner that depends non-trivially on the temperature. It is this general bounce solution that governs the decay rate.

Since, in the inverted potential, the classical bounce trajectory stays within the interval over which the potential is quadratic, a variation of the Euclidean action with respect to $q(\tau)$ obtains the classical equation of motion

$$-m\ddot{q} + m\omega_c^2 q + \frac{\eta}{\pi}\int_0^\beta d\tau' \, \frac{q(\tau) - q(\tau')}{(\tau - \tau')^2} = A\delta(\tau - \beta/2),$$

where the term on the right-hand side of the equation imparts an impulse that changes discontinuously the velocity of the particle, while the coefficient A is chosen to ensure symmetry of the bounce solution on the Euclidean time interval. Turning to the Fourier representation, the solution of the saddle-point equation then assumes the form

$$q_n = ATe^{-i\omega_n\beta/2}g(\omega_n), \quad g(\omega_n) \equiv [m(\omega_n^2 + \omega_c^2) + \eta|\omega_n|]^{-1}. \tag{3.45}$$

Imposing the condition that $q(\tau = \beta/2) = a$, one finds that $A = a/f$ where $f \equiv T\sum_n g(\omega_n)$. Finally, the action of the bounce is given by

$$S_{\text{bounce}} = \frac{1}{2T}\sum_n (m(\omega_n^2 + \omega_c^2) + \eta|\omega_m|)|q_n|^2 = \frac{a^2}{2f}. \tag{3.46}$$

1. To make sense of these expressions, as a point of reference, let us first determine the **zero-temperature tunneling rate in the absence of dissipation**, that is $\eta \to 0$ and $\beta \to \infty$. In this case, the (Matsubara) frequency summation translates to the continuous integral, $f = \int_{-\infty}^{\infty}(d\omega/2\pi)g(\omega) = (2m\omega_c)^{-1}$. Using this result, the bounce action (3.46) takes the form $S_{\text{bounce}} = m\omega_c a^2$. As one would expect, the tunneling rate $\Gamma \sim e^{-S_{\text{bounce}}}$ is controlled by the ratio of the potential barrier height $m\omega_c^2 a^2/2$ to the attempt frequency ω_c. Also notice that the bounce trajectory is given by

$$q(\tau) = \frac{a}{f}\int_{-\infty}^{\infty}\frac{d\omega}{2\pi}\, e^{i\omega(\tau-\beta/2)}g(\omega) = a\, e^{-\omega_c|\tau-\beta/2|},$$

   i.e., as expected from our discussion in section 3.3, the particle spends only a time $1/\omega_c$ in the under-barrier region.
2. Now, restricting attention to the zero-temperature limit, let us consider the **influence of dissipation** on the nature of the bounce solution and the capacity for tunneling. Focusing on the limit in which the dynamics of the particle is overdamped, $\eta \gg m\omega_c$,

$f = \int_{-\infty}^{\infty} d\omega g(\omega) \simeq (2/\pi\eta) \ln(\eta/m\omega_c)$, which implies $S_{\text{bounce}} = \pi\eta a^2/(4\ln[\eta/(m\omega_c)])$. In particular, this result shows that, in the limit $\eta \to \infty$, the coupling of the particle to the ohmic bath leads to an *exponential* suppression of the tunneling rate while only a weak dependence on the jump frequency persists. Physically, this result is easy to rationalize: under-barrier tunneling is a feature of the quantum mechanical system. In the transfer of energy to and from the external bath, the phase coherence of the particle is lost. At zero temperature, the tunneling rate becomes suppressed and the particle confined.

3. Let us now consider the **influence of temperature on the tunneling rate when the dissipative coupling is inactive**, $\eta \to 0$. In this case, the discrete frequency summation takes the form[29] $f = T\sum_n g(\omega_n) = (\coth(\beta\omega_c/2)/2\omega_c m)$. Using this result, one obtains the action $S_{\text{bounce}} = m\omega_c a^2 \tanh(\beta\omega_c/2)$. In the low temperature limit $\beta \to \infty$, $S_{\text{bounce}} = m\omega_c a^2$ as discussed above. At high temperatures $\beta \to 0$, as expected, one recovers a classical activated dependence of the escape rate, namely $S_{\text{bounce}} \simeq \beta m\omega_c^2 a^2/2$.
4. Finally, let us briefly remark on the **interplay of thermal activation with ohmic dissipation**. Applying the the Euler–Maclaurin formula $\sum_{m=0}^{\infty} f(m) = \int_0^{\infty} dx\, f(x) + \frac{f(0)}{2} - \frac{f'(0)}{12} + \cdots$ to relate discrete sums over Matsubara frequencies to their zero-temperature integral limits, one finds that $S_{\text{bounce}}(T) - S_{\text{bounce}}(T=0) \propto \eta T^2$. This shows that, in the dissipative regime, an increase in temperature diminishes the tunneling rate with a scale proportion to the damping.

This concludes our cursory discussion of the application of the Feynman path integral to dissipative quantum tunneling. As mentioned above, our brief survey was able only to touch upon the broad field of research. Those interested in learning more about the field of macroscopic quantum tunneling are referred to the wider literature. To close this chapter, we turn now to our penultimate application of the path integral – quantum mechanical spin.

Path integral for spin

The quantum mechanics of a spin-(1/2) particle is a standard example in introductory courses. Indeed, there is hardly any other system whose quantum mechanics is as easy to formulate. Given that, it is perhaps surprising that for a long time the spin problem defied all attempts to cast it in path integral form: Feynman, the architect of the path integral, did not succeed in incorporating spin into the new formalism. It took several decades to fill this gap (for a review of the early history up to 1980, see Schulman's text[1]), and a fully satisfactory formulation of the subject was obtained no earlier than 1988. (The present exposition follows closely the lines of the review by Michael Stone.[30])

Why then is it so difficult to find a path integral of spin? In hindsight it turns out that the spin path integral is in fact no more complex than any other path integral, it merely appears to be a bit unfamiliar. The reason is that, on the one hand, the integrand of the path integral is essentially the exponentiated classical action whilst, on the other, the **classical**

[29] For details on how to implement the discrete frequency summation, see the Info block on page 170 below.
[30] M. Stone, Supersymmetry and the quantum mechanics of spin, *Nucl. Phys B* **314** (1989), 577–86.

mechanics of spin is a subject that is not standard in introductory or even advanced courses. In other words, the path integral approach must, by necessity, lead to an unusual object. The fact that the classical mechanics of spin is hardly ever mentioned is related not only to the common view that spin is something "fundamentally quantum" but also to the fact that the mechanics of a classical spin (see below) cannot be expressed within the standard formulation of Hamiltonian mechanics, i.e. there is no formulation in terms of a set of globally defined coordinates and equally many global momenta. It is therefore inevitable that one must resort to the (less widely applied) symplectic formulation of Hamiltonian mechanics.[31] However, as we will see below, the classical mechanics of spin can nevertheless be quite easily understood physically.

Besides attempting to elucidate the connections between quantum and classical mechanics of spin, there is yet another motivation for discussing the spin path integral. Pretending that we have forgotten essential quantum mechanics, we will formulate the path integral ignoring the fact that spin quantum numbers are half integer or integer. The quantization of spin will then be derived in hindsight, by way of a geometric consideration. In other words, the path integral formulation demonstrates how quantum mechanical results can be obtained by geometric rather than standard algebraic reasoning. Finally, the path integral of spin will serve as a basic platform on which our analysis of higher-dimensional spin systems below will be based.

A reminder of finite-dimensional SU(2)*-representation theory*

In order to formulate the spin path integral, it is necessary to recapitulate some facts regarding the role of SU(2) in quantum mechanics. The **special unitary group in two dimensions**, SU(2), is defined by $\mathrm{SU}(2) = \{g \in \mathrm{Mat}(2\times 2, \mathbb{C}) | g^\dagger g = \mathbf{1}_2, \det g = 1\}$, where $\mathbf{1}_2$ is the two-dimensional unit matrix. Counting independent components one finds that the group has three free real parameters or, equivalently, that its Lie algebra, su(2), is three-dimensional. As we have seen, the basis vectors of the algebra – the group generators – $\hat{S}^i, i = x, y, z$, satisfy the closure relation $[\hat{S}^i, \hat{S}^j] = i\epsilon_{ijk}\hat{S}^k$, where ϵ_{ijk} is the familiar fully antisymmetric tensor. Another useful basis representation of su(2) is given by the spin **raising and lowering operators**, $\hat{S}^\pm = \hat{S}^x \pm i\hat{S}^y$. Again, as we have seen earlier, the algebra $\{\hat{S}^+, \hat{S}^-, \hat{S}^z\}$ is defined by the commutation relations $[\hat{S}^+, \hat{S}^-] = 2\hat{S}^z$, $[\hat{S}^z, \hat{S}^\pm] = \pm\hat{S}^\pm$.

Each group element can be uniquely parameterized in terms of the exponentiated algebra. For example, in the **Euler angle representation**, the group is represented as

$$\mathrm{SU}(2) = \quad g(\phi,\theta,\psi) = e^{-i\phi\hat{S}_3}e^{-i\theta\hat{S}_2}e^{-i\psi\hat{S}_3}\Big|\, \phi,\psi \in [0,2\pi], \theta \in [0,\pi] \quad .$$

The Hilbert spaces $\mathcal{H}_S$ of quantum spin are irreducible representation spaces of SU(2). Within the spaces $\mathcal{H}_S$, SU(2) acts in terms of representation matrices (which will be denoted by g) and the matrix representations of its generators $\hat{S}_i$. The index S is the so-called weight

[31] Within this formulation, the phase space is regarded as a differential manifold with a symplectic structure (cf. Arnold's text on classical mechanics: V. I. Arnold, *Mathematical Methods of Classical Mechanics* [Springer-Verlag, 1978]). In the case of spin, this manifold is the 2-sphere S^2.

of the representation (physically: the total spin).[32] Within each $\mathcal{H}_S$, there is a distinguished state, a state of highest weight $|\uparrow\rangle$, which is defined as the (normalized) eigenstate of $\hat{S}^z$ with maximum eigenvalue, S (physically: a spin state polarized in the 3-direction). Owing to the irreducibility of the representation, each (normalized) state of the Hilbert space $\mathcal{H}_S$ can be obtained by applying the Euler-angle-parameterized elements of the representation to the maximum weight state.

Being a compact group, SU(2) can be integrated over, i.e. it makes sense to define objects like $\int_{\mathrm{SU}(2)} dg\, f(g)$, where f is some function of g and dg is a realization of a group measure.[33] Among the variety of measures that can be defined in principle, the (unique) **Haar measure** plays a distinguished role. It has the convenient property that it is invariant under left and right multiplication of g by fixed group elements, i.e.

$$\forall h \in \mathrm{SU}(2) : \int dg\ f(gh) = \int dg\ f(hg) = \int dg\ f(g),$$

where, for notational simplicity, we have omitted the subscript in $\int_{\mathrm{SU}(2)}$.

Construction of the path integral

With this background, we are now in a position to formulate the Feynman path integral. To be specific, let us consider a particle of spin S subject to the Hamiltonian

$$\hat{H} = \mathbf{B} \cdot \hat{\mathbf{S}},$$

where $\mathbf{B}$ is a magnetic field and $\hat{\mathbf{S}} \equiv (\hat{S}_1, \hat{S}_2, \hat{S}_3)$ is a vector of spin operators in the spin-S representation. Our aim is to calculate the imaginary time path integral representation of the partition function $\mathcal{Z} \equiv \operatorname{tr} e^{-\beta \hat{H}}$. In constructing the path integral we will follow the general strategy outlined at the end of Section 3.2, i.e. the first step is to represent $\mathcal{Z}$ as $\mathcal{Z} = \operatorname{tr}\,(e^{-\epsilon \hat{H}})^N$, where $\epsilon = \beta/N$. Next, we have – the most important step in the construction – to insert a suitably chosen resolution of identity between each of the factors $e^{-\epsilon \hat{H}}$. A representation that will lead us directly to the final form of the path integral is specified by

$$\mathrm{id} = C \int dg\ |g\rangle\langle g|, \tag{3.47}$$

where "id" represents the unit operator in $\mathcal{H}_S$, $\int dg$ is a group integral over the Haar measure, C is some constant, and $|g\rangle \equiv g|\uparrow\rangle$ is the state obtained by letting the representation matrix g act on the maximum weight state $|\uparrow\rangle$ (cf. the glossary of SU(2) representation theory above).

Of course it remains to be verified that the integral (3.47) is indeed proportional to the unit operator. That this is so follows from **Schur's lemma**, which states that, if, and only if, an operator $\hat{A}$ commutes with all representation matrices of an irreducible group

[32] The index S is defined in terms of the eigenvalues of the Casimir operator (physically: the total angular momentum operator) $\hat{\mathbf{S}}^2 \equiv \sum_i \hat{\mathbf{S}}_i^2$ according to the relation $|s\rangle \in \mathcal{H}_S : \hat{\mathbf{S}}^2 |s\rangle = S(S+1)|s\rangle$.

[33] To define group measures in a mathematically clean way, one makes use of the fact that (as a Lie group) SU(2) is a three-dimensional differentiable manifold. Group measures can then be defined in terms of the associated volume form (see the primer in differential geometry on page 537).

representation (in our case the gs acting in the Hilbert space $\mathcal{H}_S$), $\hat{A}$ is proportional to the unit matrix. That the group above integral fulfills the global commutativity criterion follows from the properties of the Haar measure: $\forall h \in \mathrm{SU}(2)$:

$$h \int dg\ |g\rangle\langle g| = \int dg\ |hg\rangle\langle g| \overset{\text{Haar}}{=} \int dg\ |hh^{-1}g\rangle\langle h^{-1}g| = \int dg\ |g\rangle\langle g|h.$$

Thus, $\int dg\ |g\rangle\langle g|$ is, indeed, proportional to the unit operator. The proportionality constant appearing in Eq. (3.47) will not be of any concern to us – apart from the fact that it is non-zero.[34]

Substituting the resolution of identity into the time-sliced partition function and making use of the fact that

$$\begin{aligned}\langle g_{i+1}|e^{-\epsilon \mathbf{B}\cdot\hat{\mathbf{S}}}|g_i\rangle &\simeq \langle g_{i+1}|g_i\rangle - \epsilon\langle g_{i+1}|\mathbf{B}\cdot\hat{\mathbf{S}}|g_i\rangle \overset{\langle g_i|g_i\rangle=1}{=} 1 - \langle g_i|g_i\rangle + \langle g_{i+1}|g_i\rangle - \epsilon\langle g_{i+1}|\mathbf{B}\cdot\hat{\mathbf{S}}|g_i\rangle \\ &\simeq \exp\Big(\langle g_{i+1}|g_i\rangle - \langle g_i|g_i\rangle - \epsilon\langle g_{i+1}|\mathbf{B}\cdot\hat{\mathbf{S}}|g_i\rangle\Big),\end{aligned}$$

one obtains

$$\mathcal{Z} = \lim_{N\to\infty} \int_{g_N=g_0} \prod_{i=0}^{N} dg_i\ \exp\left[-\epsilon \sum_{i=0}^{N-1}\left(-\frac{\langle g_{i+1}|g_i\rangle - \langle g_i|g_i\rangle}{\epsilon} + \langle g_{i+1}|\mathbf{B}\cdot\hat{\mathbf{S}}|g_i\rangle\right)\right].$$

By taking the limit $N \to \infty$, this can be cast in path integral form,

$$\boxed{\mathcal{Z} = \int Dg\ \exp\left[-\int_0^\beta d\tau\left(-\langle\partial_\tau g|g\rangle + \langle g|\mathbf{B}\cdot\hat{\mathbf{S}}|g\rangle\right)\right],} \tag{3.48}$$

where the $\mathcal{H}_S$-valued function $|g(\tau)\rangle$ is the continuum limit of $|g_i\rangle$. Equation (3.48) is our final, albeit somewhat over-compact, representation of the path integral. In order to give this expression physical interpretation, we need to examine more thoroughly the meaning of the states $|g\rangle$.

In the literature, the states $|g\rangle$ expressed in the Euler-angle representation

$$\boxed{|\widetilde{g}(\phi,\theta,\psi)\rangle \equiv e^{-i\phi\hat{S}_3}e^{-i\theta\hat{S}_2}e^{-i\psi\hat{S}_3}|\uparrow\rangle},$$

are referred to as **spin coherent states**. Before discussing the origin of this terminology, it is useful to explore the algebraic structure of these states. Firstly, note that the maximum weight state $|\uparrow\rangle$ is, by definition, an eigenstate of $\hat{S}_3$ with maximum eigenvalue S. Thus, $|\widetilde{g}(\phi,\theta,\psi)\rangle \equiv e^{-i\phi\hat{S}_3}e^{-i\theta\hat{S}_2}|\uparrow\rangle e^{-i\psi S}$ and the angle ψ enters the coherent state merely as a phase or gauge factor. By contrast, the two remaining angles θ and ϕ act through true rotations. Now, the angular variables $\phi \in [0, 2\pi)$ and $\theta \in [0, \pi)$ define a standard representation of the 2-sphere. In view of the fact that the states $|\tilde{g}(\phi,\theta,\psi)\rangle$ cover the entire Hilbert space

[34] Actually, the constant C can be straightforwardly computed by taking the trace of Eq. (3.47), which leads to $C =$ (dimension of the representation space)/(volume of the group).

$\mathcal{H}_S$, we are led to suspect that the latter bears similarity with a sphere.[35] To substantiate this view, let us compute the expectation values

$$n_i \equiv \langle \tilde{g}(\phi,\theta,\psi)|\hat{S}_i|\tilde{g}(\phi,\theta,\psi)\rangle, \quad i=1,2,3. \tag{3.49}$$

To this end, we first derive an auxiliary identity which will spare us much of the trouble that will arise in expanding the exponentials appearing in the definition of $|\widetilde{g}\rangle$. By making use of the identity ($i \neq j$)

$$e^{-i\phi\hat{S}_i}\hat{S}_j e^{i\phi\hat{S}_i} = e^{-i\phi[\hat{S}_i,\,]}\ \hat{S}_j = \hat{S}_j\cos\phi + \epsilon_{ijk}\hat{S}_k\sin\phi, \tag{3.50}$$

where the last equality follows from the fact that $\cos x$ ($\sin x$) contain x in even (odd) orders and $[\hat{S}_j,\,]^2\hat{S}_i = \hat{S}_i$, it is straightforward to obtain (exercise) $\mathbf{n} = S(\sin\theta\cos\phi, \sin\theta\sin\phi, \cos\theta)$, i.e. $\mathbf{n}$ is the product of S and a unit vector parameterized in terms of spherical coordinates.

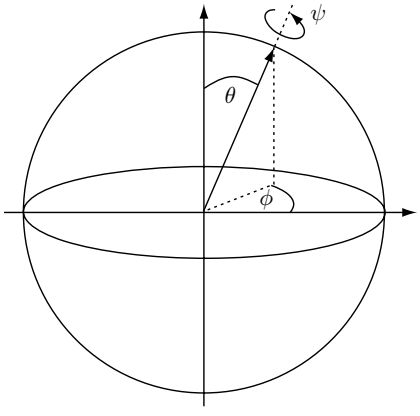

This is the key to understanding the terminology "spin coherent states." The vectors $|\widetilde{g}(\phi,\theta,\psi)\rangle$ represent the closest approximation of a classical angular momentum state one can formulate in Hilbert space (see figure).

Let us now see what happens if we employ the **Euler angle representation in formulating the path integral**. A first and important observation is that the path integral is gauge invariant – in the sense that it does not depend on the U(1)-phase, ψ. As to the **B**-dependent part of the action, the gauge invariance is manifest: Eq. (3.49) implies that

$$S_B[\phi,\theta] \equiv \int_0^\beta d\tau\ \langle\tilde{g}|\mathbf{B}\cdot\hat{\mathbf{S}}|\tilde{g}\rangle = \int_0^\beta d\tau\ \langle g|\mathbf{B}\cdot\hat{\mathbf{S}}|g\rangle = S\int_0^\beta d\tau\ \mathbf{n}\cdot\mathbf{B} = SB\int_0^\beta d\tau\ \cos\theta.$$

Here, we have introduced the gauge-independent part $|g\rangle$ of the state vector by setting $|\widetilde{g}\rangle \equiv |g\rangle\,\exp(-iS\psi)$ or, equivalently, $|g(\phi,\theta)\rangle \equiv e^{-i\phi\hat{S}_3}e^{-i\theta\hat{S}_2}|\uparrow\rangle$. Substituting this representation into the first term of the action of Eq. (3.48), one obtains

$$\begin{aligned} S_{\rm top}[\phi,\theta] &\equiv -\int_0^\beta d\tau\ \langle\partial_\tau\tilde{g}|\tilde{g}\rangle = -\int_0^\beta d\tau\ \langle\partial_\tau e^{-iS\psi}g|ge^{-iS\psi}\rangle \\ &= -\int_0^\beta d\tau\,(\langle\partial_\tau g|g\rangle - iS\partial_\tau\psi\langle g|g\rangle) = -\int_0^\beta d\tau\ \langle\partial_\tau g|g\rangle, \end{aligned} \tag{3.51}$$

where the last equality holds because $\langle g|g\rangle = 1$ is constant and ψ is periodic in β. We thus conclude that the path integral does not depend on the gauge phase, i.e. it effectively extends over paths living on the 2-sphere (rather than the entire group manifold SU(2)). This finding is reassuring in the sense that a degree of freedom living on a sphere comes

[35] There is a group theoretical identity behind this observation, namely the isomorphism $\mathrm{SU}(2) \cong S^2 \times \mathrm{U}(1)$, where U(1) is the "gauge" subgroup contained in SU(2).

close to what one might intuitively expect to be the classical counterpart of a quantum particle of definite angular momentum.

Let us now proceed by exploring the action of the path integral. By using the auxiliary identity (3.50) it is a straightforward matter to show that

$$S_{\rm top}[\phi,\theta] = -\int_0^\beta d\tau\ \langle \partial_\tau g|g\rangle = -iS\int_0^\beta d\tau\ \partial_\tau\phi\cos\theta = iS\int_0^\beta d\tau\ \partial_\tau\phi(1-\cos\theta). \quad (3.52)$$

Combining this with the **B**-dependent term discussed above, one obtains

$$\boxed{S[\theta,\phi] = S_B[\phi,\theta] + S_{\rm top}[\phi,\theta] = S\int_0^\beta d\tau\,[B\cos\theta + i(1-\cos\theta)\partial_\tau\phi]}\,, \quad (3.53)$$

for the action of the path integral for spin.

EXERCISE Derive the Euler–Lagrange equations associated with this action. Show that they are equivalent to the **Bloch equations** $i\partial_\tau \mathbf{n} = \mathbf{B}\times\mathbf{n}$ of a spin with expectation value $\langle\mathbf{S}\rangle = S\mathbf{n}$ subject to a magnetic field. Here, $\mathbf{n}(\phi,\theta)\in S^2$ is the unit vector defined by the two angles ϕ,θ.

Analysis of the action

To formulate the second term in the action (3.53) in a more illuminating way, we note that the velocity of the point **n** moving on the unit sphere is given by $\dot{\mathbf{n}} = \dot\theta\hat{\mathbf{e}}_\theta + \dot\phi\sin\theta\,\hat{\mathbf{e}}_\phi$, where $(\hat{\mathbf{e}}_r,\hat{\mathbf{e}}_\theta,\hat{\mathbf{e}}_\phi)$ form a spherical orthonormal system. We can thus rewrite Eq. (3.52) as

$$S_{\rm top}[\phi,\theta] = iS\int_0^\beta d\tau\ \dot{\mathbf{n}}\cdot\mathbf{A} = iS\oint_\gamma d\mathbf{n}\cdot\mathbf{A}, \quad (3.54)$$

where

$$\mathbf{A} = \frac{1-\cos\theta}{\sin\theta}\hat{\mathbf{e}}_\phi. \quad (3.55)$$

Notice that, in spite of its compact appearance, Eq. (3.54) does not represent a coordinate invariant formulation of the action $S_{\rm top}$. (The field $\mathbf{A}(\phi,\theta)$ explicitly depends on the coordinates (ϕ,θ).) In fact, we will see in Chapter 9 that the action $S_{\rm top}$ *cannot* be expressed in a coordinate invariant manner, for reasons deeply rooted in the topology of the 2-sphere.

A second observation is that Eq. (3.54) can be read as the (Euclidean time) action of a particle of charge S moving under the influence of a vector potential **A**.[36] Using standard formulae of vector calculus[37] one finds $\mathbf{B}_{\rm m}\equiv\nabla\times\mathbf{A} = \mathbf{e}_r$, i.e. our particle moves in a radial magnetic field of constant strength unity. Put differently, the particle experiences the field of a magnetic "charge" of strength 4π centered at the origin of the sphere.

INFO If you find this statement difficult to reconcile with the Maxwell equation $\nabla\cdot\mathbf{B} = 0$ $\int_S \mathbf{B}\cdot d\mathbf{S} = 0$ for any closed surface S, notice that $\nabla\cdot\mathbf{B} = \nabla\cdot(\nabla\times\mathbf{A}) = 0$ holds only if **A** is non-singular. However, the vector potential Eq. (3.55) is manifestly singular along the line

[36] See, e.g., H. Goldstein, *Classical Mechanics* (Addison-Wesley, 1981).
[37] See, e.g., J. D. Jackson, *Classical Electrodynamics* (Wiley, 1975).

$(r, \theta = \pi)$ through the south pole of the sphere. The physical picture behind this singularity is as follows: imagine an infinitely thin solenoid running from $r = \infty$ through the south pole of the sphere to its center. Assuming that the solenoid contains a magnetic flux 4π, the center of the sphere becomes a source of magnetic flux, the so-called **Dirac monopole**. This picture is consistent with the presence of a field $\mathbf{B} = \mathbf{e}_r$. It also explains the singularity of $\mathbf{A}$ along the string. (Of course, the solenoidal construction does not lead to the prediction of a genuine monopole potential: somewhere, at $r = \infty$, our auxiliary magnetic coil has to end, and this is where the flux lines emanating from the point $r = 0$ terminate.) The postulate of a flux line at the singularity of $\mathbf{A}$ merely helps to reconcile the presence of a radial magnetic field with the principles of electrodynamics. However, as far as our present discussion goes, this extra structure is not essential, i.e. we may simply interpret $r = 0$ as the position of a magnetic "charge."

To explore the consequences of this phenomenon, we apply Stokes' theorem to write

$$S_{\rm top}[\mathbf{n}] \;=\; iS \oint_\gamma d\mathbf{n}\cdot\mathbf{A} = iS\int_{A_{\gamma,n}} dS\cdot(\nabla\times\mathbf{A}) = iS\int_{A_{\gamma,n}} dS\cdot\mathbf{e}_r = iSA_{\gamma,n}. \quad (3.56)$$

Here, $A_{\gamma,n}$ is the domain on the 2-sphere which (a) has the curve γ as its boundary, and (b) contains the north pole (see figure on next page). The integral produces the area of this surface which we again denote by $A_{\gamma,n}$. Curiously, the action $S_{\rm top}$ is but a measure of the area bounded by the curve $\gamma : \tau \mapsto \mathbf{n}(\tau)$. However, simple as it is, this result should raise some suspicion: by assigning a designated role to the *northern* hemisphere of the sphere some symmetry breaking, not present in the original problem, has been introduced. Indeed, we might have defined our action by $S_{\rm top}[\phi,\theta] = iS\oint_\gamma d\mathbf{n}\cdot\mathbf{A}'$ where $\mathbf{A}' = -\frac{1+\cos\theta}{\sin\theta}\hat{e}_\phi = \mathbf{A} - 2\nabla\phi$ differs from $\mathbf{A}$ only by a gauge transformation.[38] The newly defined vector potential is non-singular in the *southern* hemisphere, so that application of Stokes' theorem leads to the conclusion $S_{\rm top}[\mathbf{n}] = -iS\int_{A_{\gamma,s}} dS\cdot\mathbf{B}_m = -iSA_{\gamma,s}$. Here, $A_{\gamma,s}$ is the area of a surface bounded by γ but covering the south pole of the sphere. The absolute minus sign is due to the outward orientation of the surface $A_{\gamma,s}$.

Sir George Gabriel Stokes 1819–1903

As Lucasian Professor of Mathematics at Cambridge, Stokes established the science of hydrodynamics with his law of viscosity (1851), describing the velocity of a small sphere through a viscous fluid. Furthermore, he investigated the wave theory of light, named and explained the phenomenon of fluorescence, and theorized an explanation of the Fraunhofer lines in the solar spectrum. (Figure reproduced from Sir George Gabriel Stokes *Memoirs* presented to the Cambridge Philosophical Society on the occasion of the Jubilee of Stokes volume XVIII of the *Transactions of the Cambridge Philosophical Society*, Cambridge University Press, 1900.)

[38] You may, with some justification, feel uneasy about the fact that ϕ is not a true "function" on the sphere (or, alternatively, about the fact that $\int d\mathbf{n}\cdot\quad\phi = \phi(\beta) - \phi(0)$ may be a non-vanishing multiple of 2π). We will return to the discussion of this ambiguity shortly. (Notice that a similarly hazardous manipulation is performed in the last equality of Eq. (3.52).)

One has to concede that the result obtained for the action $S_{\rm top}$ depends on the chosen gauge of the monopole vector potential! The difference between the northern and the southern variant of our analysis is given by

$$iS\int_{A_{\gamma,n}} dS\cdot\mathbf{B}_m + iS\int_{A_{\gamma,s}} dS\cdot\mathbf{B}_m = iS\int_{S^2} dS\cdot\mathbf{e}_r = 4\pi iS,$$

where we have made use of the fact that $A_{\gamma,n}\cup A_{\gamma,s} = S^2$ is the full sphere. At first sight,

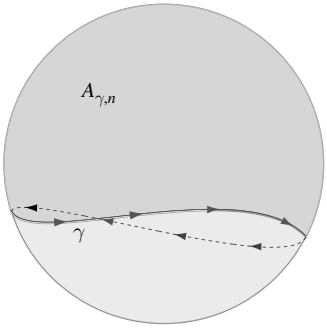

it looks as if our analysis has led us to a gauge-dependent, and therefore pathological, result. Let us recall, however, that physical quantities are determined by the exponentiated action $\exp(-S[\mathbf{n}])$ and not by the action itself. Now, S is either integer or half integer, which implies the factor $\exp(4\pi iS) = 1$ is irrelevant. In the operator representation of the theory, **spin quantization** follows from the representation theory of the algebra su(2). It is a "non-local" feature, in the sense that the action of the spin operators on all eigenstates has to be considered to fix the dimensionality $2S+1$ of $\mathcal{H}_S$. In hindsight, it is thus not too surprising that the same information is encapsulated in a "global" condition (gauge invariance) imposed on the action of the path integral.

Summarizing, we have found that the classical dynamics of a spin is that of a massless point particle on a sphere coupled to a monopole field $\mathbf{B}_m$. We have seen that the vector potential of the field cannot be globally continuous on the full sphere. More generally, the phase space S^2 cannot be represented in terms of a global system of "coordinates and momenta" which places it outside the scope of traditional treatments of classical mechanics. This probably explains the failure of early attempts to describe the spin in terms of a path integral or, equivalently, in terms of a Hamiltonian action.

In Chapter 9 we will use the path action (3.53) as a building block for our construction of the field theory of higher-dimensional spin systems. However, before concluding this section, let us make some more remarks on the curious properties of the monopole action $S_{\rm top}$. Unlike all other Euclidean actions encountered thus far, the action (3.54) is imaginary. In fact, it will stay imaginary upon Wick rotation $\tau \to it$ back to real times. More generally, $S_{\rm top}$ is invariant under the rescaling $\tau \to c\tau$, and invariant even under arbitrary reparameterizations $\tau \to g(\tau) \equiv \tau'$. This invariance is a hallmark of a **topological term**. Loosely speaking (see Chapter 9 for a deeper discussion), a topological term is a contribution to the action of a field theory that depends on the global geometry of a field configuration rather than on its local structure. In contrast, "conventional" operators in field theoretical actions measure the energy cost of dynamical or spatial field fluctuations. In doing so they must relate to a specific spatio-temporal reference frame, i.e. they cannot be invariant under reparameterization.

Summarizing our results, we have found that:

1. The classical action of a spin is one of a massless particle (there is no standard kinetic energy term in Eq. (3.48)) moving on a unit sphere. The particle carries a magnetic moment of magnitude S. It is coupled (a) to a conventional magnetic field via its magnetic moment, and (b) to a monopole field via its orbital motion. Note that we have come, finally, to a position which hints at the difficulties plaguing attempts to formulate a classical mechanics of spin. The vector potential of a monopole, $\mathbf{A}$, cannot be globally defined on the entire sphere. The underlying physical reason is that, by the very nature of the monopole (flux going radially outwards everywhere), the associated vector potential must be singular at one point of the surface.[39] As a consequence, the classical phase space of the system, the sphere, cannot be covered by a global choice of coordinate system. (Unlike most standard problems of classical mechanics there is no system of globally defined "p"s and "q"s.) This fact largely spoils a description within the standard – coordinate-oriented – formulation of Hamiltonian mechanics (cf. the discussion in the article by Stone[40]).
2. Terms akin to the monopole contribution to the spin action appear quite frequently within path integral formulations of systems with non-trivial topology (like the two-sphere above). Depending on the particular context under consideration, one distinguishes between **Wess–Zumino–Witten (WZW) terms, θ-terms, Chern–Simons terms** and a few other terms of topological origin. What makes these contributions generally important is that the value taken by these terms depends *only* on the topology of a field configuration but not on structural details. For further discussion of phenomena driven by non-trivial topological structures we refer to Chapter 9 below.

Trace formulae and quantum chaos

As a final application of the path integral, we turn now to the consideration of problems in which the dynamics of the classical system is, itself, non-trivial. Introductory courses on classical mechanics usually convey the impression that dynamical systems behave in a regular and, at least in principle, mathematically predictable way. However, experience shows that the majority of dynamical processes in nature do not conform to this picture. Partly, or even fully, chaotic motion (i.e. motion that depends in a singular and, thereby, in an essentially unpredictable way on initial conditions) is the rule rather than the exception. In view of the drastic differences in the observable behavior of classically integrable and chaotic systems, an obvious question arises: in what way does the *quantum* phenomenology of chaotic systems differ from that associated with integrable dynamics? This question defines the field of **quantum chaos**.

[39] To better understand this point, consider the integral of $\mathbf{A}$ along an infinitesimal closed curve γ on the sphere. *If* $\mathbf{A}$ were globally continuous, we would have two choices to transform the integral into a surface integral over $\mathbf{B}$: an integral over the "large" or the "small" surface area bounded by γ. The monopole nature of $\mathbf{B}$ would demand that both integrals are proportional to the respective areas of the integration domain which, by assumption, are different, contradiction. The resolution of this paradox is that $\mathbf{A}$ must be discontinuous at one point on the sphere, i.e. we cannot globally set $\mathbf{B} = \times \mathbf{A}$, and the choice of the integration area is prescribed by the condition that it must not encompass the singular point.

[40] M. Stone, Supersymmetry and the quantum mechanics of spin, *Nucl. Phys. B* **314** (1986), 557–86.

Understanding signatures of classically chaotic motion in quantum mechanics is an issue not only of conceptual, but also of great practical relevance, impinging on areas such as quantum electron transport in condensed matter systems. The inevitable presence of impurities and imperfections in any macroscopic solid renders the long-time dynamics of electronic charge carriers chaotic. Relying on a loose interpretation of the Heisenberg principle, $\Delta t \sim \hbar/\Delta E$, i.e. the relation between long-time dynamical behavior and small-scale structures in energy, one would expect that signatures of chaotic quantum dynamics are especially important in the low-energy response in which one is usually interested. This expectation has been confirmed for innumerable observables related to low-temperature electronic transport in solid state systems.

Disordered conducting media represent but one example of a wide class of dynamical systems with long-time chaotic dynamics. Indeed, recent experimental advances have made it possible to realize a plethora of effectively *non-disordered* chaotic dynamical systems in condensed matter devices. For example, by employing modern semiconductor device technology, it has become possible to manufacture small two-dimensional conducting systems, of a size $\mathcal{O}(< 1\,\mu\mathrm{m})$ and of almost any geometric shape. Here, the number of imperfections can be reduced to a negligible minimum, i.e. electrons propagate ballistically along straight trajectories, as with a billiard system. The smallness of the devices further implies that the ratio between Fermi wavelength and system size is of $\mathcal{O}(10^{-1}$–$10^{-3})$, so, while semiclassical concepts will surely be applicable, the wave aspects of quantum propagation remain visible. In recent years, the experimental and theoretical study of electron transport in such **quantum billiards** has emerged as a field in its own right.

How then can signatures of chaotic dynamics in quantum systems be sought? The most fundamental characteristic of a quantum system is its spectrum. Although not a direct observable, it determines the majority of properties accessible to measurement. On the other hand, it is clear that the manifestations of chaos we are looking for must relate back to the classical dynamical properties of the system. The question then is, *how can a link between classical mechanics and quantum spectra be drawn?* This problem is tailor-made for analysis by path integral techniques.

Semiclassical approximation to the density of states

The close connection between the path integral and classical mechanics should be evident from the previous sections. However, to address the problem raised above, we still need to understand how the path integral can be employed to analyze the spectrum of a quantum system. The latter is described by the (single-particle) **density of states**

$$\rho(\epsilon) = \mathrm{tr}\,\delta(\epsilon - \hat{H}) = \sum_a \delta(\epsilon - \epsilon_a), \tag{3.57}$$

where $\{\epsilon_a\}$ represents the complete set of energy levels. To compute the sum, one commonly employs a trick based on the **Dirac identity**,

$$\lim_{\delta \searrow 0} \frac{1}{x + i\delta} = -i\pi\delta(x) + \mathcal{P}\frac{1}{x}, \tag{3.58}$$

where $\mathcal{P}(1/x)$ denotes the principal part of $1/x$. By taking the imaginary part of Eq. (3.58), Eq. (3.57) can be represented as $\rho(\epsilon) = -\frac{1}{\pi}\,\mathrm{Im}\sum_a \frac{1}{\epsilon^+-\epsilon_a} = -\frac{1}{\pi}\,\mathrm{Im\ tr}\,(\frac{1}{\epsilon^+-\hat{H}})$, where $\epsilon^+ \equiv \epsilon + i\delta$ and the limit $\lim_{\delta\searrow 0}$ is implicit. Using the identity $1/x^+ = -i\int_0^\infty dt\, e^{ix^+t}$, and representing the trace $\mathrm{tr}\,\hat{A} = \int dq\ \langle q|\hat{A}|q\rangle$ as a real space integral,

$$\rho(\epsilon) = \frac{1}{\pi\hbar}\int_0^\infty dt\ \mathrm{Re\ tr}(e^{i(\epsilon^+-\hat{H})t/\hbar}) = \frac{1}{\pi\hbar}\mathrm{Re}\int_0^\infty dt\, e^{i\epsilon^+t/\hbar}\int dq\langle q|e^{-i\hat{H}t/\hbar}|q\rangle, \qquad (3.59)$$

we have made the connection between the density of states and the quantum propagation amplitude explicit.

Without going into full mathematical detail (see, for example, the work by Haake,[41] for a modern discourse) we now outline how this integral is evaluated by path integral techniques within the semiclassical approximation. Although, for brevity, some of the more tricky steps of the calculation are swept under the carpet, the sketch will be accurate enough to make manifest some aesthetic connections between the spectral theory of chaotic quantum systems and classically chaotic dynamics. (For a more formal and thorough discussion, we refer to Haake[41] and Gutzwiller.[42])

Making use of the semiclassical approximation (3.28) established earlier, and substituting into Eq. (3.59), one obtains $\rho(\epsilon) \simeq \frac{1}{\pi\hbar}\,\mathrm{Re}\int_0^\infty dt\, e^{i\epsilon^+t/\hbar}\int dq\, A[q_{\rm cl}]e^{\frac{i}{\hbar}S[q_{\rm cl}]}$, where, following our discussion in Section 3.2, we have defined $A[q_{\rm cl}] \equiv \det\left(\frac{i}{2\pi\hbar}\frac{\partial^2 S[q_{\rm cl}]}{\partial q(0)\ \partial q(t)}\right)^{1/2}$ and $q_{\rm cl}$ represents a closed classical path that begins at q at time zero and ends at the same coordinate at time t. Again relying on the semiclassical condition $S[q_{\rm cl}] \gg \hbar$, the integrals over q and t can be performed in a stationary phase approximation. Beginning with the time integral, and noticing that $\partial_t S[q_{\rm cl}] = -\epsilon_{q_{\rm cl}}$ is the (conserved) energy of the path $q_{\rm cl}$, we obtain the saddle-point condition $\epsilon \stackrel{!}{=} \epsilon_{q_{\rm cl}}$ and

$$\rho(\epsilon) \simeq \frac{1}{\pi\hbar}\mathrm{Re}\int dq\ A[q_{{\rm cl},\epsilon}]e^{\frac{i}{\hbar}S[q_{\rm cl},\ ]},$$

where the symbol $q_{{\rm cl},\epsilon}$ indicates that only paths $q \to q$ of energy ϵ are taken into account, and the contribution coming from the quadratic integration around the saddle-point has been absorbed into a redefinition of $A[q_{{\rm cl},\epsilon}]$.

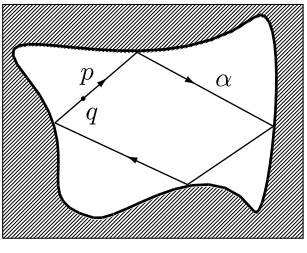

Turning to the q-integration, making use of the fact that $\partial_{q_{\rm i}} S[q_{\rm cl}] = -p_{\rm i}, \partial_{q_{\rm f}} S[q_{\rm cl}] = p_{\rm f}$, where $q_{\rm i,f}$ are the initial and final coordinates of a path $q_{\rm cl}$, and $p_{\rm i,f}$ are the initial and final momentum, the stationary phase condition assumes the form $0 \stackrel{!}{=} d_q S[q_{{\rm cl},\epsilon}] = (\partial_{q_{\rm i}} + \partial_{q_{\rm f}})\, S[q_{{\rm cl},\epsilon}]|_{q_{\rm i}=q_{\rm f}=q} = p_{\rm f} - p_{\rm i}$, i.e. the stationarity of the integrand under the q-integration requires that the initial and final momentum of the path $q_{{\rm cl},\epsilon}$ be identical. We thus find that the paths contributing to the integrated transition amplitude are periodic not only in coordinate space but even in phase space. Such paths are called **periodic**

[41] F. Haake, *Quantum Signatures of Chaos* (Springer-Verlag, 2001).
[42] M. C. Gutzwiller, *Chaos in Classical and Quantum Mechanics* (Springer-NY, 1991), and Haake, *Quantum Signatures of Chaos*.

orbits –"periodic" because the path comes back to its initial phase space coordinate after a certain revolution time. As such, the orbit will be traversed repeatedly as time goes by (see the figure, where a periodic orbit α with initial coordinates $x = (p, q)$ is shown).

According to our analysis above, each coordinate point q lying on a periodic orbit is a stationary phase point of the q-integral. The stationary phase approximation of the integral can thus be formulated as

$$\rho(\epsilon) \simeq \frac{1}{\pi\hbar}\mathrm{Re}\sum_{n=1}^{\infty}\sum_{\alpha}\int_{\alpha} dq\, A_\alpha e^{\frac{i}{\hbar}nS_\alpha},$$

where $\sum_\alpha$ stands for a sum over all periodic orbits (of energy ϵ) and S_α is the action corresponding to one traversal of the orbit (all at fixed energy ϵ). The index n accounts for the fact that, owing to its periodicity, the orbit can be traversed repeatedly, with total action nS_α. Furthermore, $\int_\alpha dq$ is an integral over all coordinates lying on the orbit and we have again absorbed a contribution coming from the quadratic integration around the stationary phase points in the pre-exponential amplitude A_α.

Finally, noting that $\int_\alpha dq \propto T_\alpha$, where T_α is the period of one traversal of the orbit α (at energy ϵ), we arrive at the result

$$\boxed{\rho(\epsilon) \simeq \frac{1}{\pi\hbar}\mathrm{Re}\sum_{n=1}^{\infty}\sum_{\alpha} T_\alpha A_\alpha e^{\frac{i}{\hbar}nS_\alpha}.} \tag{3.60}$$

This is a (simplified, see info block below) representation of the famous **Gutzwiller trace formula**. The result is actually quite remarkable: the density of states, an observable of quantum mechanical significance, has been expressed entirely in terms of classical quantities.

EXERCISE Making use of the Feynman path integral, show that the propagator for a particle of mass m confined by a square well potential of infinite strength is given by

$$G(q_\mathrm{f}, q_\mathrm{i}; t) = \sqrt{\frac{m}{2\pi i\hbar t}}\sum_{n=-\infty}^{\infty} \exp\left[\frac{im(q_\mathrm{f} - q_\mathrm{i} + 2na)^2}{2\hbar t}\right] - \exp\left[\frac{im(q_\mathrm{f} + q_\mathrm{i} + 2na)^2}{2\hbar t}\right] .$$

INFO Had we carefully kept track of all determinants arising from the stationary phase integrals, the prefactor A_α would have read

$$A_\alpha = \frac{1}{\hbar}\frac{e^{i\frac{\pi}{2}\ \alpha}}{|\mathrm{det}M_\alpha^r - 1|^{\frac{1}{2}}},$$

where ν_α is known as the **Maslov index** (an integer-valued factor associated with the singular points on the orbit, i.e. the classical turning points). The meaning of this object can be understood, e.g., by applying the path integral to the problem of a quantum particle in a box. To correctly reproduce the spectrum, the contribution of each path must be weighted by $(-)^n = \exp(i\pi n)$, where n is the number of its turning points in the box potential), and M_α represents the **monodromy matrix**. To understand the meaning of this object, notice that a phase space point $\bar{x}$ on a periodic orbit can be interpreted as a fixed point of the *classical* time evolution

operator $U(T_\alpha)$: $U(T_\alpha, \bar{x}) = \bar{x}$, which is just to say that the orbit is periodic. As with any other smooth mapping, U can be linearized in the vicinity of its fixed points, $U(T_\alpha, \bar{x} + y) = \bar{x} + M_\alpha y$, where the linear operator M_α is the monodromy matrix. Evidently, M_α determines the stability of the orbit under small distortions, which makes it plausible that it appears as a controlling prefactor of the stationary phase approximation to the density of states.

3.4 Summary and outlook

In this chapter we have introduced the path integral formulation of quantum mechanics, an approach independent of, yet (modulo certain mathematical imponderabilities related to continuum functional integration) equivalent to, the standard route of canonical operator quantization. While a few precious exactly solvable quantum problems (e.g. the evolution of a free particle, the harmonic oscillator, and, perhaps intriguingly, quantum mechanical spin) are more efficiently formulated by the standard approach, a spectrum of unique features makes the path integral an indispensable tool of modern quantum mechanics. The path integral approach is highly intuitive, powerful in the treatment of non-perturbative problems, and tailor-made to formulation of semiclassical limits. Perhaps most importantly, we have seen that it provides a unifying link whereby quantum problems can be related to classical statistical mechanics. Indeed, we have found that the path integral of a quantum point particle is, in many respects, equivalent to the partition function of a classical one-dimensional continuum system. We have hinted at a generalization of this principle, i.e. an equivalence principle relating d-dimensional quantum *field* theory to $(d+1)$-dimensional statistical mechanics. However, before exploring this bridge further, we first need to generalize the concept of path integration to problems involving quantum fields. This will be the subject of the next chapter.

3.5 Problems

Quantum harmonic oscillator

As emphasized in the main text, the quantum harmonic oscillator provides a valuable environment in which to explore the Feynman path integral and methods of functional integration. In this, along with a small number of other precious examples, the path integral may be computed exactly, and the Feynman propagator explored rigorously.

(a) Starting with the Feynman path integral, show that the propagator for the one-dimensional quantum harmonic oscillator, $\hat{H} = \hat{p}^2/2m + m\omega^2\hat{q}^2/2$, takes the form

$$\langle q_\mathrm{f}|e^{-i\hat{H}t/\hbar}|q_\mathrm{i}\rangle = \left(\frac{m\omega}{2\pi i\hbar \sin\omega t}\right)^{1/2} \exp\left[\frac{i}{2\hbar} m\omega \left(\left[q_\mathrm{i}^2 + q_\mathrm{f}^2\right]\cot\omega t - \frac{2q_\mathrm{i}q_\mathrm{f}}{\sin\omega t}\right)\right].$$

Suggest why the propagator varies periodically on the time interval t, and explain the origin of the singularities at $t = n\pi/\omega, n = 1, 2, \ldots$ Taking the frequency $\omega \to 0$, show that the propagator for the free particle is recovered.

(b) Show that the wavepacket $\psi(q, t = 0) = (2\pi a)^{-1/4} \exp[-q^2/4a]$ remains Gaussian at all subsequent times. Obtain the width $a(t)$ as a function of time.

(c) Semiclassical limit: Taking the initial wavepacket to be of the form

$$\psi(q, t = 0) = (2\pi a)^{-1/4} \exp\left[\frac{i}{\hbar} mvq - \frac{1}{4a} q^2\right],$$

(which corresponds to a wavepacket centered at an initial position $q = 0$ with a velocity v), find the wavepacket at times $t > 0$, and determine the mean position, mean velocity, and mean width as functions of time.

Answer:

(a) Making use of the Feynman path integral, the propagator can be expressed as the functional integral,

$$\langle q_{\rm f}|e^{-i\hat{H}t/\hbar}|q_{\rm i}\rangle = \int_{q(0)=q_{\rm i}}^{q(t)=q_{\rm f}} Dq\; e^{iS[q]/\hbar}, \qquad S[q] = \int_0^t dt'\; \frac{m}{2}\left(\dot{q}^2 - \omega^2 q^2\right).$$

The evaluation of the functional integral over field configurations $q(t')$ is facilitated by parameterizing the path in terms of fluctuations around the classical trajectory. Setting $q(t') = q_{\rm cl}(t') + r(t')$ where $q_{\rm cl}(t')$ satisfies the classical equation of motion $m\ddot{q}_{\rm cl} = -m\omega^2 q_{\rm cl}$, and applying the boundary conditions, one obtains the solution $q_{\rm cl}(t') = A\sin(\omega t') + B\cos(\omega t')$, with the coefficients $B = q_{\rm i}$ and $A = q_{\rm f}/\sin(\omega t) - q_{\rm i}\cot(\omega t)$. Being Gaussian in q, the action separates as $S[q] = S[q_{\rm cl}] + S[r]$, where

$$\begin{aligned} S[q_{\rm cl}] &= \frac{m\omega^2}{2}\left[(A^2 - B^2)\frac{\sin(2\omega t)}{2\omega} + 2AB\frac{\cos(2\omega t) - 1}{2\omega}\right] \\ &= \frac{m\omega}{2}\left[(q_{\rm i}^2 + q_{\rm f}^2)\cot(\omega t) - \frac{2q_{\rm i}q_{\rm f}}{\sin(\omega t)}\right]. \end{aligned}$$

Finally, integrating over the fluctuations and applying the identity

$$z/\sin z = \prod_{n=1}^{\infty}(1 - z^2/\pi^2 n^2)^{-1},$$

one obtains the required result, periodic in t with frequency ω, and singular at $t = n\pi/\omega$. In particular, a careful regularization of the expression for the path integral shows that

$$\langle q_{\rm f}|e^{-i\hat{H}t/\hbar}|q_{\rm i}\rangle \mapsto \begin{cases} \delta(q_{\rm f} - q_{\rm i}), & t = 2\pi n/\omega, \\ \delta(q_{\rm f} + q_{\rm i}), & t = \pi(2n+1)/\omega. \end{cases}$$

Physically, the origin of the singularity is clear. The harmonic oscillator is peculiar in having a spectrum with energies uniformly spaced in units of $\hbar\omega$. Noting the eigenfunction expansion $\langle q_{\rm f}|e^{-i\hat{H}t/\hbar}|q_{\rm i}\rangle = \sum_n \langle q_{\rm f}|n\rangle\langle n|q_{\rm i}\rangle e^{-i\omega n t}$, this means that when $\hbar\omega \times t/\hbar = 2\pi \times$ integer there is a coherent superposition of the states and the initial state is recovered. Furthermore, since the ground state and its even integer descendants are symmetric

while the odd states are antisymmetric, it is straightforward to prove the identity for the odd periods (exercise).

(b) Given the initial condition $\psi(q,t=0)$, the time evolution of the wavepacket can be determined from the propagator as $\psi(q,t)=\int_{-\infty}^{\infty}dq'\ \langle q|e^{-i\hat{H}t/\hbar}|q'\rangle\psi(q',0)$, from which one obtains

$$\psi(q,t)=J(t)\int_{-\infty}^{\infty}dq'\ \frac{1}{(2\pi a)^{1/4}}e^{-q'^2/4a}e^{\frac{i}{\hbar}\frac{m\omega}{2}\left([q^2+q'^2]\cot(\omega t)-\frac{2qq'}{\sin(\omega t)}\right)},$$

where $J(t)$ represents the time-dependent contribution arising from the fluctuations around the classical trajectory. Being Gaussian in q', the integral can be performed explicitly. Setting $\alpha=1/2a-im\omega\cot(\omega t)/\hbar$, $\beta=im\omega q/(\hbar\sin(\omega t))$, and performing the Gaussian integral over q', one obtains

$$\psi(q,t)=J(t)\frac{1}{(2\pi a)^{1/4}}\sqrt{\frac{2\pi}{\alpha}}e^{\beta^2/2\alpha}\ \exp\left[\frac{i}{2\hbar}m\omega q^2\cot(\omega t)\right],$$

where $\beta^2/2\alpha=-(1+i\kappa\cot(\omega t))q^2/4a(t)$. Rearranging terms, it is straightforward to show that $\psi(q,t)=(2\pi a(t))^{-1/4}\ \exp\left[-\frac{q^2}{4a(t)}\right]e^{i\varphi(q,t)}$, where $a(t)=a[\cos^2(\omega t)+\kappa^{-2}\sin^2(\omega t)]$, $\kappa=2am\omega/\hbar$, and $\varphi(q,t)$ represents a pure phase.[43] As required, under the action of the propagator the normalization of the wavepacket is preserved. (A graphical representation of the time evolution is shown in Fig. 3.9(a).) Note that, if $a=\hbar/2m\omega$ (i.e. $\kappa=1$), $a(t)=a$ for all times – i.e. it is a pure eigenstate.

(c) Still of a Gaussian form, the integration can again be performed explicitly for the new initial condition. In this case, we obtain an expression of the form above but with $\beta=\frac{i}{\hbar}\frac{m\omega}{\sin(\omega t)}\times(q-\frac{v}{\omega}\sin(\omega t))$. Reading off the coefficients, we find that the position and velocity of the wavepacket have the forms $q_0(t)=(v/\omega)\sin(\omega t)$, $v(t)=v\cos(\omega t)$, coinciding with those of classical dynamics. Note that, as above, the width $a(t)$ of the wavepacket oscillates at frequency ω. (A graphical representation of the time evolution is shown in Fig. 3.9(b).)

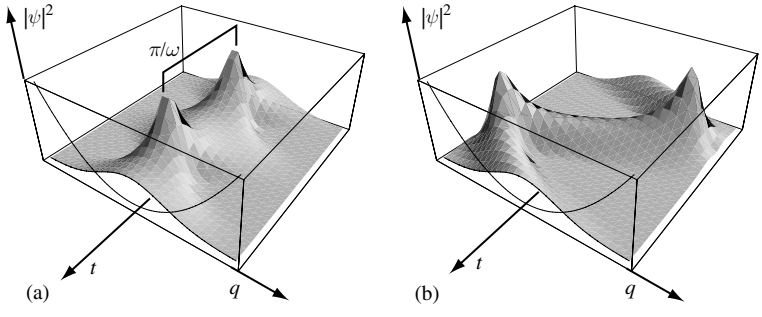

Figure 3.9 (a) Variation of a "stationary" Gaussian wavepacket in the harmonic oscillator taken from the solution, and (b) variation of the moving wavepacket.

[43] For completeness, we note that $\varphi(q,t)=-\frac{1}{2}\tan^{-1}(\frac{1}{\kappa}\cot(\omega t))-\frac{\kappa q^2}{4a}\cot(\omega t)(\frac{a}{a(t)}-1)$.

Density matrix

Using the results derived in the previous section as an example, we explore how real-time dynamical information can be converted into quantum statistical information.

Using the results of the previous question, obtain the density matrix $\rho(q,q') = \langle q|e^{-\beta\hat{H}}|q'\rangle$ for the harmonic oscillator at finite temperature, $\beta = 1/T$ ($k_{\rm B} = 1$). Obtain and comment on the asymptotics: (i) $T \ll \hbar\omega$ and (ii) $T \gg \hbar\omega$. (Hint: In the high-temperature case, be sure to carry out the expansion in $\hbar\omega/T$ to second order.)

Answer:
The density matrix can be deduced from the general solution of the previous question. Turning to the Euclidean time formulation,

$$\begin{aligned}\rho(q,q') &= \langle q|e^{-\beta H}|q'\rangle = \langle q|e^{-(i/\hbar)H(\hbar\beta/i)}|q'\rangle \\ &= \left(\frac{m\omega}{2\pi\hbar\sinh(\beta\hbar\omega)}\right)^{1/2} \exp\left[-\frac{m\omega}{2\hbar}\left((q^2+q'^2)\coth(\beta\hbar\omega) - \frac{2qq'}{\sinh(\beta\hbar\omega)}\right)\right].\end{aligned}$$

(i) In the low-temperature limit $T \ll \hbar\omega$ ($\beta\hbar\omega \gg 1$), $\coth(\beta\hbar\omega) \to 1, \sinh(\beta\hbar\omega) \to e^{\beta\hbar\omega}/2$, and

$$\rho(q,q') \simeq \left(\frac{m\omega}{\pi\hbar e^{\beta\hbar\omega}}\right)^{1/2} \exp\left[-\frac{m\omega}{2\hbar}(q^2+q'^2)\right] = \langle q|n=0\rangle\, e^{-\beta E_0}\, \langle n=0|q'\rangle\,.$$

(ii) Using the relations $\coth(x) \overset{x\ll 1}{=} 1/x + x/3 + \cdots$ and $1/\sinh(x) \overset{x\ll 1}{=} 1/x - x/6 + \cdots$, the high-temperature expansion ($T \gg \hbar\omega$) of the density operator gives

$$\begin{aligned}\rho(q,q') &\simeq \left(\frac{m}{2\pi\beta\hbar^2}\right)^{1/2} e^{-m(q-q')^2/2\beta\hbar^2} \exp\left[-\frac{\hbar\beta m\omega^2}{6\hbar}(q^2+q'^2+qq')\right] \\ &\simeq \delta(q-q')e^{-\frac{\beta m\omega^2 q^2}{2}},\end{aligned}$$

i.e. one recovers the classical Maxwell–Boltzmann distribution!

Depinning transition and bubble nucleation

In Section 3.3 we explored the capacity for a quantum field to tunnel from the metastable minimum of a potential, the "false vacuum." Yet, prior to the early work of Coleman on the quantum mechanical problem, similar ideas had been developed by Langer in the context of classical bubble nucleation. The following problem is an attempt to draw the connections between the classical and the quantum problem. As posed, the quantum formulation describes the depinning of a flux line in a superconductor from a columnar defect.

Consider a quantum elastic string embedded in a three-dimensional space and "pinned" by a columnar defect potential V oriented parallel to the z-axis. The corresponding Euclidean time action is given by

$$S[\mathbf{u}] = \int d\tau \int dz \left(\frac{1}{2}\rho \dot{\mathbf{u}}^2 + \frac{1}{2}\sigma(\partial_z \mathbf{u})^2 + V(|\mathbf{u}|) \right),$$

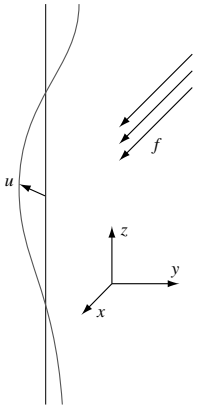

where the two-dimensional vector field $\mathbf{u}(z,\tau)$ denotes the string displacement within the xy-plane, ρ represents the density per unit length, and σ defines the tension in the string. On this system (See figure), let us suppose that an external in-plane field f is imposed along the x-direction, $S_{\text{ext}} = -f \int d\tau \int dz\, \mathbf{u}\cdot\mathbf{e}_{\mathbf{x}}$. Following the steps below, determine the probability (per unit time and per unit length) for the string to detach from the defect:

(a) Derive a saddle-point equation in the two-dimensional $z\tau$-space. Rescaling the coordinates, transform the equation of motion to a problem with circular symmetry.
(b) If the field is weak, one can invoke a "thin-wall" or "bubble" approximation to describe the saddle-point solution $\mathbf{u}(z,t)$ by specifying two regions of space-time, where the string is free, or is completely locked to the defect, respectively. In this approximation, find $\mathbf{u}(z,t)$. (Hint: Use the fact that, in either case, complete locking or complete freedom, the potential does not exert a net force on the string.)
(c) With exponential accuracy, determine the detaching probability. You may assume that, for all values of u_x obtained in (b), $V(|u|) \simeq V_0 = \text{const}$.

(Exercise: Think how the quantum model can be related to the classical system.)

Answer:

(a) Varying the action with respect to u_x, the saddle-point equation assumes the form $\rho\ddot{u}_x + \sigma\partial^2 u_x = -f + V'(u)(u_x/u)$, where $u = |\mathbf{u}|$. Applying the rescaling $\tau = (\rho/\sigma)^{1/4}\widetilde{\tau}$ and $z = (\sigma/\rho)^{1/4}\widetilde{z}$, the equation takes the symmetrized form $\sqrt{\sigma\rho}\partial^2 u_x = -f + V'(u)(u_x/u)$, where $\partial^2 = \partial_\tau^2 + \partial_z^2$ and boundary conditions

$$u_x(r) = \begin{cases} 0, & r > R, \\ g(r), & r < R, \end{cases}$$

on the radial coordinate $(\widetilde{\tau},\widetilde{z}) \mapsto (r,\phi)$ are imposed.
(b) In the thin-wall approximation, the potential gradient can be neglected. In this case the saddle-point equation assumes the form $\nabla^2 g = -f/\sqrt{\sigma\rho}$, with the solution $g = (R^2 - r^2)f/\sqrt{4\sigma\rho}$.
(c) With the result, the tunneling rate can be estimated from the saddle-point action

$$S_{\text{bubble}} = \int^R d\mathbf{r} \left(\frac{\sqrt{\sigma\rho}}{2}(\widetilde{\partial} g)^2 + V_0 - fg \right) = -\pi R^2 \left(\frac{3f^2R^2}{16(\sigma\rho)^{1/2}} - V_0 \right).$$

Minimizing over R, one obtains the optimal radius $R_*^2 = \frac{8V_0\sqrt{\sigma\rho}}{3f^2}$. As a result, we obtain the estimate for the tunneling rate $W \propto e^{-S(R_*)} = \exp\left[-\frac{4\pi V_0^2\sqrt{\sigma\rho}}{3f^2}\right]$.

Tunneling in a dissipative environment

In Section 3.3 we considered the impact of dissipation on the action of a point-particle in a quantum well. There a model was chosen in which the degrees of freedom of the environment were represented phenomenologically by a bath of harmonic oscillators. In the following we will explore a model in which the particle is coupled to the fluctuations of a quantum mechanical "string." Later, in Section 8.2, we will see that this model provides a description of tunneling through a single impurity in a Luttinger liquid.

(a) A quantum particle of mass m is confined by a sinusoidal potential $U(q) = 2g\sin^2(\pi q/q_0)$. Employing the Euclidean (imaginary time) Feynman path integral ($\hbar = 1$),

$$\mathcal{Z} = \int Dq(\tau)\; e^{-S_{\rm part}[q(\tau)]}, \qquad S_{\rm part}[q(\tau)] = \int_{-\infty}^{\infty} d\tau \left[\frac{m}{2}\dot{q}^2 + U(q)\right],$$

confirm by direct substitution that the extremal contribution to the propagator connecting two neighboring degenerate minima ($q(\tau = -\infty) = 0$ and $q(\tau = \infty) = q_0$) is given by the instanton trajectory $q_{\rm cl}(\tau) = (2q_0/\pi)\arctan\left(\exp\left[\omega_0\tau\right]\right)$, where $\omega_0 = (2\pi/q_0)\sqrt{g/m}$. Show that $S[q_{\rm cl}] = (2/\pi^2)mq_0^2\omega_0$. (Note: Although the equation of motion associated with the minimum of the Euclidean path integral is nonlinear, the solution above is exact. It is known in the literature as a **soliton** configuration.)

(b) If the quantum particle is coupled at one point to an infinite "string," the path integral is given by

$$\mathcal{Z} = \int Du(x,\tau) \int Dq(\tau)\; \delta\left(q(\tau) - u(\tau, x = 0)\right) e^{-S_{\rm string}[u(x,\tau)] - S_{\rm part}[q(\tau)]},$$

where the classical action of the string is given by (cf. the action functional for phonons discussed in Section 1.1)

$$S_{\rm string}[u(x,\tau)] = \int_{-\infty}^{\infty} d\tau \int_{-\infty}^{\infty} dx \left[\frac{\rho}{2}\dot{u}^2 + \frac{\sigma}{2}\left(\frac{\partial u}{\partial x}\right)^2\right].$$

Here $\delta(q(\tau) - u(\tau, x = 0))$ represents a functional δ-function which enforces the condition $q(\tau) = u(\tau, x = 0)$ for all times τ. Operationally, it can be understood from the discretized form $\prod_n \delta(q(\tau_n) - u(\tau_n, x = 0))$. By representing the functional δ-function as the functional integral

$$\delta(q(\tau) - u(\tau, 0)) = \int Df(\tau)\; \exp\left[i\int_{-\infty}^{\infty} d\tau\; f(\tau)(q(\tau) - u(\tau, 0))\right],$$

and integrating over the fluctuations of the string, show that the dynamics of the particle is governed by the effective action $S_{\rm eff}[q] = S_{\rm part}[q] + (\eta/2)\int (d\omega/2\pi)|\omega\; q(\omega)|^2$,

where $\eta = \sqrt{\rho\sigma}$. How does this result compare with the dissipative action discussed in Section 3.3?

(c) Treating the correction to the particle action as a perturbation, use your result from (a) to show that the effective action for an instanton–anti-instanton pair $q(\tau) = q_{\rm cl}(\tau + \bar\tau/2) - q_{\rm cl}(\tau - \bar\tau/2)$, where $\omega_0\bar\tau \gg 1$, is given approximately by

$$S_{\rm eff}[q] = 2S_{\rm part}[q_{\rm cl}] - \frac{\eta q_0^2}{\pi}\ln(\omega_0\bar\tau)\,.$$

(Hint: Note that, in finding the Fourier decomposition of $q_{\rm cl}(\tau)$, a crude estimate is sufficient.)

(d) Using this result, estimate the typical separation of the pair (i.e. interpret the overall action as an effective probability distribution function for $\bar\tau$, and evaluate $\langle\bar\tau\rangle = \int d\bar\tau\ \bar\tau e^{-S_{\rm eff}}$). Comment on the implications of your result for the nature of the tunneling probability.

Answer:

(a) Varying the Euclidean time path integral with respect to $q(\tau)$ one finds that the extremal field configuration obeys the classical **sine–Gordon equation**

$$m\ddot q - \frac{2\pi g}{q_0}\sin\left(\frac{2\pi q}{q_0}\right) = 0.$$

Applying the trial solution, one finds that the equation of motion is satisfied if $\omega_0 = (2\pi/q_0)\sqrt{g/m}$. From this result one obtains the classical action

$$S[q_{\rm cl}] = \int_0^\infty d\tau\,\left[\frac{m}{2}\dot q_{\rm cl}^2 + U(q_{\rm cl})\right] = \int_0^\infty d\tau\ m\dot q_{\rm cl}^2 = m\int_0^{q_0} dq\ \dot q_{\rm cl} = 2\frac{mq_0^2}{\pi^2}\omega_0.$$

(b) In Fourier space, the action of the classical string takes the form

$$S_{\rm string} = \int_{-\infty}^{\infty}\frac{d\omega}{2\pi}\int_{-\infty}^{\infty}\frac{dk}{2\pi}\frac{\rho\omega^2+\sigma k^2}{2}|u(\omega,k)|^2.$$

Representing the functional δ-function as the functional integral

$$\int Df\ \exp\left[i\int_{-\infty}^{\infty}\frac{d\omega}{2\pi}f(\omega)\left(q(-\omega) - \int_{-\infty}^{\infty}\frac{dk}{2\pi}u(-\omega,-k)\right)\right],$$

and performing the integral over the degrees of freedom of the string, one obtains

$$\int Du\ e^{-S_{\rm string} - i\int d\tau\ f(\tau)u(\tau,0)} \propto\ \exp\left[-\int_{-\infty}^{\infty}\frac{d\omega}{2\pi}\int_{-\infty}^{\infty}\frac{dk}{2\pi}\frac{1}{2}\frac{1}{(\rho\omega^2+\sigma k^2)}|f(\omega)|^2\right].$$

Integrating over k, and performing the Gaussian functional integral over the Lagrange multiplier field $f(\omega)$, one obtains the effective action as required.

(c) Approximating the instanton/anti-instanton pair $q(\tau) = q_{\rm cl}(\tau+\bar\tau) - q_{\rm cl}(\tau-\bar\tau)$ by a "top-hat" function, one finds that $q(\omega) = \int_{-\bar\tau/2}^{\bar\tau/2} d\tau\ q_0 e^{i\omega\tau} = q_0\bar\tau \sin(\omega\bar\tau/2)/(\omega\bar\tau/2)$. Treating the dissipative term as a perturbation, the action then takes the form

$$S_{\rm eff} - 2S_{\rm part} = \frac{\eta}{2}\int_0^{\omega_0} \frac{d\omega}{2\pi}|\omega|(q_0\bar\tau)^2 \frac{\sin^2(\omega\bar\tau/2)}{(\omega\bar\tau/2)^2} \simeq \frac{q_0^2}{\pi}\eta\ln(\omega_0\bar\tau),$$

where ω_0 serves as a high-frequency cut-off.

(d) Interpreted as a probability distribution for the instanton separation, one finds

$$\langle\bar\tau\rangle = \int d\bar\tau\ \bar\tau\ \exp\left[-\frac{q_0^2}{\pi}\eta\ln(\omega_0\bar\tau)\right] \sim \int^{\infty} d\bar\tau\ \bar\tau^{1-q_0^2\eta/\pi}.$$

The divergence of the integral shows that, for $\eta > 2\pi/q_0^2$, instanton–anti-instanton pairs are confined and particle tunneling is deactivated. Later, in Chapter 8 we revisit the dissipative phase transition from the standpoint of the renormalization group.

Winding numbers

In the main text, we considered the application of the Feynman path integral to model systems where trajectories could be parameterized in terms of their harmonic (Fourier) expansion. However, very often, one is interested in applications of the path integral to spaces that are not simply connected. In this case, one must include classes of trajectories which cannot be simply continued. Rather, trajectories are classified by their "winding number" on the space. To illustrate the point, let us consider the application of the path integral to a particle on a ring.

(a) Starting with the Hamiltonian $\hat H = -(1/2I)(\partial^2/\partial\theta^2)$, where θ denotes an angle variable, show from first principles that the quantum partition function $\mathcal{Z} = {\rm tr} e^{-\beta\hat H}$ is given by

$$\mathcal{Z} = \sum_{n=-\infty}^{\infty} \exp\left[-\beta\frac{n^2}{2I}\right]. \tag{3.61}$$

(b) Formulated as a Feynman path integral, show that the quantum partition function can be cast in the form

$$\mathcal{Z} = \int_0^{2\pi} d\theta \sum_{m=-\infty}^{\infty} \int_{(\beta)=\ ^{(0)=}_{(0)+2\pi m}} D\theta(\tau)\ \exp\left[-\frac{I}{2}\int_0^\beta d\tau\ \dot\theta^2\right].$$

(c) Varying the Euclidean action with respect to θ, show that the path integral is minimized by the classical trajectories $\bar\theta(\tau) = \theta + 2\pi m\tau/\beta$. Parameterizing a general path as $\theta(\tau) = \bar\theta(\tau) + \eta(\tau)$, where $\eta(\tau)$ is a path with no net winding, show that

$$\mathcal{Z} = \mathcal{Z}_0 \sum_{m=-\infty}^{\infty} \exp\left[-\frac{I}{2}\frac{(2\pi m)^2}{\beta}\right], \tag{3.62}$$

where $\mathcal{Z}_0$ represents the quantum partition function for a free particle with open boundary conditions. Making use of the free particle propagator, show that $\mathcal{Z}_0 = \sqrt{I/2\pi\beta}$.

(d) Finally, making use of Poisson's summation formula, $\sum_m h(m) = \sum_n \int_{-\infty}^{\infty} d\phi\, h(\phi) e^{2\pi i n\phi}$, show that Eq. (3.62) coincides with Eq. (3.61).

Answer:

(a) Solving the Schrödinger equation, the wavefunctions obeying periodic boundary conditions take the form $\psi_n = e^{in\theta}/\sqrt{2\pi}, n$ integer, and the eigenvalues are given by $E_n = n^2/2I$. Cast in the eigenbasis representation, the partition function assumes the form Eq. (3.61).

(b) Interpreted as a Feynman path integral, the quantum partition function takes the form of a propagator with

$$\mathcal{Z} = \int_0^{2\pi} d\theta\ \langle\theta|e^{-\beta\hat{H}}|\theta\rangle = \int_0^{2\pi} d\theta \int_{\theta(\beta)=\theta(0)=\theta} D\theta(\tau)\ \exp\left[-\int_0^{\beta} d\tau\ \frac{I}{2}\dot{\theta}^2\right].$$

The trace implies that paths $\theta(\tau)$ must start and finish at the same point. However, to accommodate the invariance of the field configuration θ under translation by 2π we must impose the boundary conditions shown in the question.

(c) Varying the action with respect to θ we obtain the classical equation $I\ddot{\theta} = 0$. Solving this equation subject to the boundary conditions, we obtain the solution given in the question. Evaluating the Euclidean action, we find that

$$\int_0^{\beta} (\partial_\tau\theta)^2 d\tau = \int_0^{\beta} d\tau \left[\frac{2\pi m}{\beta} + \partial_\tau\eta\right]^2 = \beta\left(\frac{2\pi m}{\beta}\right)^2 + \int_0^{\beta} d\tau(\partial_\tau\eta)^2.$$

Thus, we obtain the partition function (3.62), where

$$\mathcal{Z}_0 = \int D\eta(\tau)\ \exp\left[-\frac{I}{2}\int_0^{\beta} d\tau(\partial_\tau\eta)^2\right] = \sqrt{\frac{I}{2\pi\beta}},$$

denotes the free particle partition function. This can be obtained from direct evaluation of the free particle propagator.

(d) Applying the Poisson summation formula with $h(x) = \exp[-\frac{(2\pi)^2 I}{2\beta}x^2]$, one finds that

$$\sum_{m=-\infty}^{\infty} e^{-\frac{(2\pi)^2 I m^2}{2\beta}} = \sum_{n=-\infty}^{\infty}\int_{-\infty}^{\infty} d\phi\ e^{-\frac{(2\pi)^2 I}{2\beta}\phi^2 + 2\pi i n\phi} = \sqrt{\frac{\beta}{2\pi I}}\sum_{n=-\infty}^{\infty} e^{-\frac{\beta}{2I}n^2}.$$

Multiplication by $\mathcal{Z}_0$ obtains the result.

Particle in a periodic potential

In Section 3.3 it was shown that the quantum probability amplitude for quantum mechanical tunneling can be expressed as a sum over instanton field configurations of the Euclidean action. By generalizing this approach, the aim of the present problem is to explore quantum mechanical tunneling in a periodic potential. Such an analysis allows us to draw a connection to the problem of the Bloch spectrum.

(a) A quantum mechanical particle moves in a periodic lattice potential V with period a. Taking the Euclidean action for the instanton connecting two neighboring minima to be $S_{\rm inst}$, express the Euclidean time propagator $G(ma, na; \tau)$, with m and n integer, as a sum over instanton and anti-instanton field configurations.

(b) Making use of the identity $\delta_{qq'} = \int_0^{2\pi} d\theta \; e^{i(q-q')\theta}/(2\pi)$ show that

$$G(ma, na; \tau) \sim e^{-\omega\tau/2} \int_0^{2\pi} \frac{d\theta}{2\pi} e^{-i(n-m)\theta} \; \exp\left[\frac{\Delta\epsilon\tau}{\hbar} 2\cos\theta\right],$$

where our notation is taken from Section 3.3.

(c) Keeping in mind that, in the periodic system, the eigenfunctions are Bloch states $\psi_{p\alpha}(q) = e^{ipq} u_{p\alpha}(q)$ where $u_{p\alpha}(q + ma) \equiv u_{p\alpha}(q)$ denotes the periodic part of the Bloch function, show that the propagator is compatible with a spectrum of the lowest band $\alpha = 0, \epsilon_p = \hbar\omega/2 - 2\Delta\epsilon \; \cos(pa)$.

Answer:

(a) In the double-well potential, the extremal field configurations of the Euclidean action involve consecutive sequences of instanton–anti-instanton pairs. However, in the periodic potential, the q instantons and q' anti-instantons can appear in any sequence provided only that $q - q' = m - n$. In this case, the Feynman amplitude takes the form

$$G(ma, na; \tau) \sim \sum_{q=0}^{\infty} \sum_{q'=0}^{\infty} \frac{\delta_{q-q',n-m}}{q!\; q'!} (\tau K e^{-S_{\rm inst}/\hbar})^{q+q'} e^{-\omega\tau/2}.$$

(b) To evaluate the instanton summation, we can make use of the identity $\delta_{q-q',n-m} = \int_0^{2\pi} d\theta \; e^{i(q-q'-n+m)\theta}/(2\pi)$. As a result, we obtain

$$\begin{aligned} G(ma, na; \tau) &\sim e^{-\omega\tau/2} \int_0^{2\pi} \frac{d\theta}{2\pi} e^{-i(n-m)\theta} \sum_{q=0}^{\infty} \frac{(\tau K e^{i\theta} e^{-S_{\rm inst}/\hbar})^q}{q!} \sum_{q'=0}^{\infty} \frac{(\tau K e^{-i\theta} e^{-S_{\rm inst}/\hbar})^{q'}}{q'!} \\ &\sim e^{-\omega\tau/2} \int_0^{2\pi} \frac{d\theta}{2\pi} e^{-i(n-m)\theta} \; \exp\left[\frac{\Delta\epsilon\tau}{\hbar} e^{i\theta}\right] \; \exp\left[\frac{\Delta\epsilon\tau}{\hbar} e^{-i\theta}\right], \end{aligned}$$

from which can be obtained the required result.

(c) Expanded in terms of the Bloch states of the lowest band of the periodic potential $\alpha = 0$, one obtains

$$G(ma, na; \tau) = \sum_p \psi_p^*(ma) \psi_p(na) e^{-\epsilon_p\tau/\hbar} = \sum_p |u_p(0)|^2 e^{ip(n-m)a} e^{-\epsilon_p\tau/\hbar}.$$

Interpreting $\theta = pa$, and taking $|u_p(0)|^2 =$ const. independent of p, we can draw the correspondence $\epsilon_p = \hbar\omega/2 - 2\Delta\epsilon \cos(pa)$.

4

Functional field integral

In this chapter, the concept of path integration is generalized to integration over quantum fields. Specifically we will develop an approach to quantum field theory that takes as its starting point an integration over all configurations of a given field, weighted by an appropriate action. To emphasize the importance of the formulation that, methodologically, represents the backbone of the remainder of the text, we have pruned the discussion to focus only on the essential elements. This being so, conceptual aspects stand in the foreground and the discussion of applications is postponed to the following chapters.

In this chapter, the concept of path integration is extended from quantum mechanics to quantum field theory. Our starting point is a situation very much analogous to that outlined at the beginning of the previous chapter. Just as there are two different approaches to quantum mechanics, quantum field theory can also be formulated in two different ways: the formalism of canonically quantized field operators, and functional integration. As to the former, although much of the technology needed to efficiently implement this framework – essentially Feynman diagrams – originated in high-energy physics, it was with the development of condensed matter physics through the 1950s, 1960s, and 1970s that this approach was driven to unprecedented sophistication. The reason is that, almost as a rule, problems in condensed matter investigated at that time necessitated perturbative summations to infinite order in the non-trivial content of the theory (typically interactions). This requirement led to the development of advanced techniques to sum perturbation series in many-body interaction operators to infinite order.

In the 1970s, however, essentially non-perturbative problems began to attract more and more attention – a still prevailing trend – and it turned out that the formalism of canonically quantized operators was not tailored to this type of physics. By contrast, the alternative approach to many-body problems, functional integration, is ideally suited! The situation is similar to the one described in the last chapter, where we saw that the Feynman path integral provided a spectrum of novel routes to approaching quantum mechanical problems (controlled semiclassical limits, analogies to classical mechanics, statistical mechanics, concepts of topology and geometry, etc.). Similarly, the introduction of field integration into many-body physics spawned new theoretical developments, many of which went beyond perturbation theory. In fact, the advantage of the path integral approach in many-body physics is more pronounced than in single-particle quantum mechanics: higher dimensionality introduces more complex fields, and the concept of field integration is ideally suited to explore the ensuing structures. Also, the connections to classical statistical mechanics

play a more important role than in single-particle quantum mechanics. All of these concepts will begin to play a role in subsequent chapters when applications of the field integral are discussed.

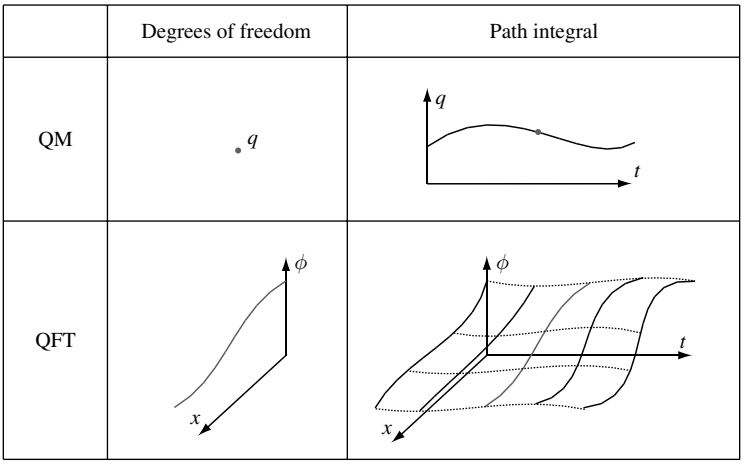

Figure 4.1 The concept of field integration. Upper panels: path integral of quantum mechanics – integration over all time-dependent configurations of a point particle degree of freedom leads to integrals over curves. Lower panels: field integral – integration over time-dependent configurations of d-dimensional continuum mappings (fields) leads to integrals over generalized $(d+1)$-dimensional surfaces.

Before embarking on the quantitative construction of the field integral – the subject of the following sections – let us anticipate the kind of structures that one should expect. In quantum mechanics, we were starting from a single point particle degree of freedom, characterized by some coordinate $\mathbf{q}$ (or some other quantum numbers for that matter). Path integration then meant integration over all time-dependent configurations $\mathbf{q}(t)$, i.e. a set of curves $t \mapsto \mathbf{q}(t)$ (see Fig. 4.1, upper panel). By contrast, the degrees of freedom of field theory are continuous objects $\phi(x)$ by themselves, where x parameterizes some d-dimensional base manifold and ϕ takes values in some target manifold (Fig. 4.1, lower panel). The natural generalization of a "path" integral then implies integration over a single copy of these objects at each instant of time, i.e. we shall have to integrate over generalized surfaces, mappings from $(d+1)$-dimensional space-time into the field manifold, $(x,t) \mapsto \phi(x,t)$. While this notion may sound worrying, it is important to realize that, conceptually, nothing much changes in comparison with the path integral: instead of a one-dimensional manifold – a curve – our object of integration will be a $(d+1)$-dimensional manifold.

We now proceed to formulate these ideas in quantitative terms.

EXERCISE If necessary, recapitulate the general construction scheme of path integrals (Section 3.2) and the connection between quantum fields and second quantized operators.

4.1 Construction of the many-body path integral

The construction of a path integral for field operators follows the general scheme outlined at the end of Section 3.2. The basic idea is to segment the time evolution of a quantum (many-body) Hamiltonian into infinitesimal time slices and to absorb as much as possible of the quantum dynamical phase accumulated during the short-time propagation into a set of suitably chosen eigenstates. But how should these eigenstates be chosen? In the context of single-particle quantum mechanics, the structure of the Hamiltonian suggested a representation in terms of coordinate and momentum eigenstates. Now, given that many-particle Hamiltonians are conveniently expressed in terms of creation/annihilation operators, an obvious idea would be to search for eigenstates of *these* operators. Such states indeed exist and are called **coherent states**.

Coherent states (bosons)

Our goal is, therefore, to find eigenstates of the (non-Hermitian) Fock space operators $a^\dagger$ and a. Although the general form of these states will turn out to be the same for bosons and fermions, there are major differences regarding their algebraic structure. The point is that the anti-commutation relations of fermions require that the eigenvalues of an annihilation operator themselves anti-commute, i.e. they *cannot* be ordinary numbers. Postponing the introduction of the unfamiliar concept of anti-commuting "numbers" to the next section, we first concentrate on the bosonic case where problems of this kind do not arise.

So what form do the eigenstates $|\phi\rangle$ of the bosonic Fock space operators a and $a^\dagger$ take? Being a state of the Fock space, an eigenstate $|\phi\rangle$ can be expanded as

$$|\phi\rangle = \sum_{n_1,n_2,\ldots} C_{n_1,n_2,\ldots}|n_1,n_2,\ldots\rangle, \quad |n_1,n_2,\ldots\rangle = \frac{(a_1^\dagger)^{n_1}}{\sqrt{n_1!}}\frac{(a_2^\dagger)^{n_2}}{\sqrt{n_2!}}\ldots|0\rangle,$$

where $a_i^\dagger$ creates a boson in state i, $C_{n_1,n_2,\ldots}$ represents a set of expansion coefficients, and $|0\rangle$ represents the vacuum. Here, for reasons of clarity, it is convenient to adopt this convention for the vacuum as opposed to the notation $|\Omega\rangle$ used previously. Furthermore, the many-body state $|n_1,n_2,\ldots\rangle$ is indexed by a set of occupation numbers: n_1 in state $|1\rangle$, n_2 in state $|2\rangle$, and so on. Importantly, the state $|\phi\rangle$ can, in principle (and will in practice) contain a superposition of basis states which have different numbers of particles. Now, if the minimum number of particles in state $|\phi\rangle$ is n_0, the minimum of $a_i^\dagger|\phi\rangle$ must be n_0+1. Clearly the creation operators $a_i^\dagger$ themselves cannot possess eigenstates.

However, with annihilation operators this problem does not arise. Indeed, the annihilation operators do possess eigenstates, known as **boson coherent states**,

$$\boxed{|\phi\rangle \equiv \exp\Big(\sum_i \phi_i a_i^\dagger\Big)|0\rangle,} \tag{4.1}$$

where the elements of $\phi = \{\phi_i\}$ represent a set of complex numbers. The states $|\phi\rangle$ are eigenstates in the sense that, for all i,

$$\boxed{a_i|\phi\rangle = \phi_i|\phi\rangle,} \tag{4.2}$$

i.e. they simultaneously diagonalize all annihilation operators. Noting that a_i and $a_j^\dagger$, with $j \neq i$, commute, Eq. (4.2) can be verified by showing that $a\exp(\phi a^\dagger)|0\rangle = \phi\exp(\phi a^\dagger)|0\rangle$.[1] Although not crucial to the practice of field integration, in the construction of the path integral it will be useful to assimilate some further properties of coherent states:

▷ By taking the Hermitian conjugate of Eq. (4.2), we find that the "bra" associated with the "ket" $|\phi\rangle$ is a left eigenstate of the set of creation operators, i.e. for all i,

$$\langle\phi|a_i^\dagger = \langle\phi|\bar{\phi}_i, \tag{4.3}$$

where $\bar{\phi}_i$ is the complex conjugate of ϕ_i, and $\langle\phi| = \langle 0|\exp[\sum_i \bar{\phi}_i a_i]$.

▷ It is a straightforward matter – e.g. by a Taylor expansion of Eq. (4.1) – to show that the action of a creation operator on a coherent state yields the identity

$$a_i^\dagger|\phi\rangle = \partial_{\phi_i}|\phi\rangle. \tag{4.4}$$

Reassuringly, it may be confirmed that Eq. (4.4) and (4.2) are consistent with the commutation relations $[a_i, a_j^\dagger] = \delta_{ij}$: $[a_i, a_j^\dagger]|\phi\rangle = (\partial_{\phi_j}\phi_i - \phi_i\partial_{\phi_j})|\phi\rangle = \delta_{ij}|\phi\rangle$.

▷ Making use of the relation $\langle\theta|\phi\rangle = \langle 0|e^{\sum_i \bar{\theta}_i a_i}|\phi\rangle = e^{\sum_i \bar{\theta}_i\phi_i}\langle 0|\phi\rangle$, one finds that the overlap between two coherent states is given by

$$\langle\theta|\phi\rangle = \exp\Big(\sum_i \bar{\theta}_i\phi_i\Big). \tag{4.5}$$

▷ From this result, one can infer that the norm of a coherent state is given by

$$\langle\phi|\phi\rangle = \exp\Big(\sum_i \bar{\phi}_i\phi_i\Big). \tag{4.6}$$

▷ Most importantly, the coherent states form a complete – in fact an overcomplete – set of states in Fock space:

$$\boxed{\int \prod_i \frac{d\bar{\phi}_i d\phi_i}{\pi} e^{-\sum_i \bar{\phi}_i\phi_i}|\phi\rangle\langle\phi| = \mathbf{1}_{\mathcal{F}},} \tag{4.7}$$

where $d\bar{\phi}_i d\phi_i = d\,\mathrm{Re}\,\phi_i\, d\,\mathrm{Im}\,\phi_i$, and $\mathbf{1}_{\mathcal{F}}$ represents the unit operator or identity in the Fock space.

[1] Using the result $[a, (a^\dagger)^n] = n(a^\dagger)^{n-1}$ (cf. Eq. (2.38)) a Taylor expansion shows $a\exp(\phi a^\dagger)|0\rangle = [a, \exp(\phi a^\dagger)]|0\rangle = \sum_{n=0}^\infty \frac{\phi^n}{n!}[a, (a^\dagger)^n]|0\rangle = \sum_{n=1}^\infty \frac{n\phi^n}{n!}(a^\dagger)^{n-1}|0\rangle = \phi\sum_{n=1}^\infty \frac{\phi^{n-1}}{(n-1)!}(a^\dagger)^{n-1}|0\rangle = \phi\exp(\phi a^\dagger)|0\rangle$.

INFO The proof of Eq. (4.7) proceeds by application of Schur's lemma (cf. our discussion of the completeness of the spin coherent states in the previous chapter). The operator family $\{a_i\}$, $\{a_i^\dagger\}$ acts irreducibly in Fock space. According to Schur's lemma, the proportionality of the left-hand side of Eq. (4.7) to the unit operator is, therefore, equivalent to its commutativity with all creation and annihilation operators. Indeed, this property is easily confirmed:

$$\begin{aligned} a_i \int d(\bar{\phi},\phi)\; e^{-\sum_i \bar{\phi}_i\phi_i}|\phi\rangle\langle\phi| \quad &= \quad \int d(\bar{\phi},\phi)\; e^{-\sum_i \bar{\phi}_i\phi_i}\phi_i|\phi\rangle\langle\phi| \\ &= \quad -\int d(\bar{\phi},\phi)\;\; \partial_{\bar{\phi}_i} e^{-\sum_i \bar{\phi}_i\phi_i} \;\; |\phi\rangle\langle\phi| \\ &\overset{\text{by parts}}{=} \quad \int d(\bar{\phi},\phi)\; e^{-\sum_i \bar{\phi}_i\phi_i}|\phi\rangle \;\; \partial_{\bar{\phi}_i}\langle\phi| \\ &= \quad \int d(\bar{\phi},\phi)\; e^{-\sum_i \bar{\phi}_i\phi_i}|\phi\rangle\langle\phi|a_i, \end{aligned} \tag{4.8}$$

where, for brevity, we have set $d(\bar{\phi},\phi) \equiv \prod_i d\bar{\phi}_i\, d\phi_i/\pi$. Taking the adjoint of Eq. (4.8), one may further check that the left-hand side of Eq. (4.7) commutes with the set of creation operators, i.e. it must be proportional to the unit operator. To fix the constant of proportionality, one may simply take the overlap with the vacuum:

$$\int d(\bar{\phi},\phi)\; e^{-\sum_i \bar{\phi}_i\phi_i}\langle 0|\phi\rangle\langle\phi|0\rangle = \int d(\bar{\phi},\phi)\; e^{-\sum_i \bar{\phi}_i\phi_i} = 1. \tag{4.9}$$

Taken together, Eq. (4.8) and (4.9) prove (4.7). Note that the coherent states are overcomplete in the sense that they are not pairwise orthogonal (see Eq. (4.5)). The exponential weight $e^{-\sum_i \bar{\phi}_i\phi_i}$ appearing in the resolution of the identity compensates for the overcounting achieved by integrating over the whole set of coherent states.

With these definitions we have all that we need to construct the path integral for the bosonic system. However, before doing so, we will first introduce the fermionic version of the coherent state. This will allow us to construct the path integrals for bosons and fermions simultaneously, thereby emphasizing the similarity of their structure.

Coherent states (fermions)

Much of the formalism above generalizes to the fermionic case: as before, it is evident that creation operators cannot possess eigenstates. Following the bosonic system, let us suppose that the annihilation operators are characterized by a set of coherent states such that, for all i,

$$\boxed{a_i|\eta\rangle = \eta_i|\eta\rangle,} \tag{4.10}$$

where η_i is the eigenvalue. Although the structure of this equation appears to be equivalent to its bosonic counterpart Eq. (4.2) it has one frustrating feature: anti-commutativity of the fermionic operators, $[a_i, a_j]_+ = 0$, where $i \neq j$, implies that the eigenvalues η_i also have to anti-commute,

$$\boxed{\eta_i\eta_j = -\eta_j\eta_i.} \tag{4.11}$$

Clearly, these objects cannot be ordinary numbers. In order to define a fermionic version of coherent states, we now have two choices: we may (a) accept Eq. (4.11) as a working definition and pragmatically explore its consequences, or (b) first try to remove any mystery from the definitions (4.10) and (4.11). This latter task is tackled in the Info block below where objects $\{\eta_i\}$ with the desired properties are defined in a mathematically clean way. Readers wishing to proceed in a maximally streamlined manner may skip this exposition and directly turn to the more praxis-oriented discussion below.

Hermann Gnther Grassmann 1809–77

Credited with inventing what is now called exterior algebra.(Figure reproduced from Hermann Grassmann, *Gesamnelte Mathematische and Physikalische Werke* (Druck and Verlag von B. G. Teubner, 1894).)

INFO There is a mathematical structure ideally suited to generalize the concept of ordinary number (fields), namely **algebras**. An algebra $\mathcal{A}$ is a vector space endowed with a multiplication rule $\mathcal{A}\times\mathcal{A}\to\mathcal{A}$. So let us *construct* an algebra $\mathcal{A}$ by starting out from a set of elements, or generators, $\eta_i\in\mathcal{A}, i=1,\ldots,N$, and imposing the rules:

(i) The elements η_i can be added and multiplied by complex numbers, i.e.

$$c_0+c_i\eta_i+c_j\eta_j\in\mathcal{A},\quad c_0,c_i,c_j\in\mathbb{C}, \tag{4.12}$$

i.e. $\mathcal{A}$ is a complex vector space.

(ii) The product, $\mathcal{A}\times\mathcal{A}\to\mathcal{A}, (\eta_i,\eta_j)\mapsto\eta_i\eta_j$, is associative and anti-commutative, i.e. it obeys the anti-commutation relation (4.11). Because of the associativity of this operation, there is no ambiguity when it comes to forming products of higher order, i.e. $(\eta_i\eta_j)\eta_k=\eta_i(\eta_j\eta_k)\equiv\eta_i\eta_j\eta_k$. The definition requires that products of odd order in the number of generators anti-commute, while (even, even) and (even, odd) combinations commute (exercise).

By virtue of (i) and (ii), the set $\mathcal{A}$ of all linear combinations

$$c_0+\sum_{n=1}^{\infty}\sum_{i_1,\ldots i_n=1}^{N}c_{i_1,\ldots,i_n}\eta_{i_1}\ldots\eta_{i_n},\qquad c_0,c_{i_1,\ldots,i_n}\in\mathbb{C},$$

spans a finite-dimensional associative algebra $\mathcal{A}$,[2] known as the **Grassmann algebra** (and sometimes also the **exterior algebra**). For completeness we mention that Grassmann algebras find a number of realizations in mathematics, the most basic being exterior multiplication in linear algebra. Given an N-dimensional vector space V, let V^* be the dual space, i.e. the space of all linear mappings, or "forms" $\Lambda: V\to\mathbb{C}, v\mapsto\Lambda(v)$, where $v\in V$. (Like V, V^* is a vector space of dimension N.) Next, define exterior multiplication through $(\Lambda,\Lambda')\to\Lambda\ \ \Lambda'$, where $\Lambda\ \ \Lambda'$ is the mapping

$$\begin{aligned}\Lambda\ \ \Lambda' : V\times V &\to \mathbb{C}\\ (v,v') &\mapsto \Lambda(v)\Lambda'(v')-\Lambda(v')\Lambda'(v).\end{aligned}$$

[2] Whose dimension can be shown to be 2^N (exercise).

This operation is manifestly anti-commutative: $\Lambda \quad \Lambda' = -\Lambda' \quad \Lambda$. Identifying the N linear basis forms $\Lambda_i \quad \eta_i$ with generators and with the product, we see that the space of exterior forms defines a Grassmann algebra.

Apart from their anomalous commutation properties, the generators $\{\eta_i\}$, and their product generalizations $\{\eta_i\eta_j, \eta_i\eta_j\eta_k, \ldots\}$, resemble ordinary, albeit anti-commutative, numbers. (In practice, the algebraic structure underlying their definition can safely be ignored. All we will need to work with these objects is the basic rule Eq. (4.11) and the property Eq. (4.12).) We emphasize that $\mathcal{A}$ contains not only anti-commuting but also commuting elements, i.e. linear combinations of an even number of Grassmann numbers η_i are overall commutative. (This mimics the behavior of the Fock space algebra: products of an even number of annihilation operators $a_i a_j \ldots$ commute with all other linear combinations of operators a_i. In spite of this similarity, the "numbers" η_i must not be confused with the Fock space operators; there is nothing on which they act.)

To make practical use of the new concept, we need to go beyond the level of pure arithmetic. Specifically, we need to introduce functions of anti-commuting numbers, and elements of calculus. Remarkably, not only do most of the concepts of calculus – differentiation, integration, etc. – naturally generalize to anti-commuting number fields, but, contrary to what one might expect, they turn out to be *simpler* than in ordinary calculus.

▷ Functions of Grassmann numbers are defined via their Taylor expansion:

$$f(\xi_1, \ldots, \xi_k) = \sum_{n=0}^{\infty} \sum_{i_1,\ldots,i_n=1}^{k} \frac{1}{n!} \frac{\partial^n f}{\partial\xi_{i_1} \cdots \partial\xi_{i_n}}\bigg|_{\xi=0} \xi_{i_n} \cdots \xi_{i_1}, \quad \xi_1, \ldots, \xi_k \in \mathcal{A}, \tag{4.13}$$

where f is an analytic function. Note that the anti-commutation properties of the algebra imply that the series terminates after a finite number of terms. For example, in the simple case where η is first-order in the generators of the algebra, $N = 1$, and $f(\eta) = f(0)+f'(0)\eta$ (since $\eta^2 = 0$) – functions of Grassmann variables are fully characterized by a finite number of Taylor coefficients!

▷ Differentiation with respect to Grassmann numbers is defined by

$$\boxed{\partial_{\eta_i}\eta_j = \delta_{ij}.} \tag{4.14}$$

Note that, in order to be consistent with the commutation relations, the differential operator ∂_{η_i} must itself be anti-commutative. In particular, $\partial_{\eta_i}\eta_j\eta_i \overset{i\neq j}{=} -\eta_j$.

▷ Integration over Grassmann variables is defined by

$$\boxed{\int d\eta_i = 0, \quad \int d\eta_i \ \eta_i = 1.} \tag{4.15}$$

Note that the definitions (4.13), (4.14), and (4.15) imply that the actions of *Grassmann di erentiation and integration are e ectively identical*, that is

$$\int d\eta \ f(\eta) = \int d\eta \ (f(0) + f'(0)\eta) = f'(0) = \partial_\eta f(\eta).$$

With this background, let us now proceed to apply the Grassmann algebra to the construction of fermion coherent states. To this end we need to enlarge the algebra so as to allow for a multiplication of Grassmann numbers by fermion operators. In order to be consistent with the anti-commutation relations, we need to require that fermion operators and Grassmann generators anti-commute,

$$[\eta_i, a_j]_+ = 0. \tag{4.16}$$

It then becomes a straightforward matter to demonstrate that **fermionic coherent states** are defined by

$$\boxed{|\eta\rangle = \exp\Big(-\sum_i \eta_i a_i^\dagger\Big)|0\rangle,} \tag{4.17}$$

i.e. by a structure perfectly analogous to the bosonic states (4.1).[3] It is a straightforward matter – and also a good exercise – to demonstrate that the properties (4.3), (4.4), (4.5), (4.6), and, most importantly, (4.7) carry over to the fermionic case. One merely has to identify a_i with a fermionic operator and replace the complex variables ϕ_i by $\eta_i \in \mathcal{A}$. Apart from a few sign changes and the $\mathcal{A}$-valued arguments, the fermionic coherent states differ only in two respects from their bosonic counterpart: firstly, the Grassmann variables $\bar\eta_i$ appearing in the adjoint of a fermion coherent state,

$$\boxed{\langle\eta| = \langle 0|\exp\Big(-\sum_i a_i\bar\eta_i\Big) = \langle 0|\exp\Big(\sum_i \bar\eta_i a_i\Big),}$$

are not related to the η_is of the state $|\eta\rangle$ via some kind of complex conjugation. Rather η_i and $\bar\eta_i$ are strictly independent variables.[4] Secondly, the Grassmann version of a Gaussian integral (exercise), $\int d\bar\eta\; d\eta\; e^{-\bar\eta\eta} = 1$ does not contain the factors of π characteristic of standard Gaussian integrals. Thus, the measure of the fermionic analog of Eq. (4.7) does not contain a π in the denominator.

For the sake of future reference, the most important properties of Fock space coherent states are summarized in Table 4.1.

[3] To prove that the states (4.17) indeed fulfill the defining relation (4.10), we note that $a_i\exp(-\eta_i a_i^\dagger)|0\rangle \overset{(4.13)}{=} a_i(1-\eta_i a_i^\dagger)|0\rangle \overset{(4.16)}{=} \eta_i a_i a_i^\dagger|0\rangle = \eta_i|0\rangle = \eta_i(1-\eta_i a_i^\dagger)|0\rangle = \eta_i\exp(-\eta_i a_i^\dagger)|0\rangle$. This, in combination with the fact that a_i and $\eta_j a_j^\dagger$ $(i \neq j)$ commute, proves Eq. (4.10). Note that the proof has actually been simpler than in the bosonic case. The fermionic Taylor series terminates after the first contribution. This observation is representative of a general rule: Grassmann calculus is simpler than standard calculus – all series are finite, integrals always converge, etc.

[4] In the literature, complex conjugation of Grassmann variables is sometimes defined. Although appealing from an aesthetic point of view – symmetry between bosons and fermions – this concept is problematic. The difficulties become apparent when **supersymmetric theories** are considered, i.e. theories where operator algebras contain both bosons and fermions (the so-called super-algebras). It is not possible to introduce a complex conjugation that leads to compatibility with the commutation relations of a super-algebra. It therefore seems to be better to abandon the concept of Grassmann complex conjugation altogether. (Unlike with the bosonic case where complex conjugation is inevitable in order to define convergent Gaussian integrals, no such need arises in the fermionic case.)

Table 4.1 *Basic properties of coherent states for bosons ($\zeta = 1$, $\psi_i \in \mathbb{C}$) and fermions ($\zeta = -1$, $\psi_i \in \mathcal{A}$). In the last line, the integration measure is defined as* $d(\bar{\psi}, \psi) \equiv \prod_i \frac{d\bar{\psi}_i \, d\psi_i}{\pi^{(1+\zeta)/2}}$.

Definition	$\|\psi\rangle = \exp\ \zeta \sum_i \psi_i a_i^\dagger\ \|0\rangle$
Action of a_i	$a_i\|\psi\rangle = \psi_i\|\psi\rangle, \quad \langle\psi\|a_i = \partial^{-}{}_{i}\langle\psi\|$
Action of $a_i^\dagger$	$a_i^\dagger\|\psi\rangle = \zeta\partial\ {}_i\|\psi\rangle, \quad \langle\psi\|a_i^\dagger = \langle\psi\|\bar{\psi}_i$
Overlap	$\langle\psi'\|\psi\rangle = \exp\ \sum_{i} \bar{\psi}'_i\psi_i$
Completeness	$\int d(\bar{\psi}, \psi)\ e^{-\sum_i \ {}_i\ {}^i}\|\psi\rangle\langle\psi\| = \mathbf{1}_{\mathcal{F}}$

INFO **Grassmann Gaussian integration**: Finally, before turning to the development of the field integral, it is useful to digress on the generalization of Gaussian integrals for Grassmann variables. The prototype of all Grassmann Gaussian integration formulae is the identity

$$\boxed{\int d\bar{\eta}\ d\eta\ e^{-\bar{}\,a}\ = a,} \tag{4.18}$$

where $a \in \mathbb{C}$ takes arbitrary values. Equation (4.18) is derived by a first-order Taylor expansion of the exponential and application of Eq. (4.15). The multi-dimensional generalization of Eq. (4.18) is given by

$$\int d(\bar{\phi}, \phi)\ e^{-\bar{\phi}^T \mathbf{A}\phi} = \det \mathbf{A}, \tag{4.19}$$

where $\bar{\phi}$ and ϕ are N-component vectors of Grassmann variables, the measure $d(\bar{\phi}, \phi) \equiv \prod_{i=1}^{N} d\bar{\phi}_i \, d\phi_i$, and $\mathbf{A}$ may be an *arbitrary* complex matrix. For matrices that are unitarily diagonalizable, $\mathbf{A} = \mathbf{U}^\dagger\mathbf{D}\mathbf{U}$, with $\mathbf{U}$ unitary, and $\mathbf{D}$ diagonal, Eq. (4.19) is proven in the same way as its complex counterpart (3.17): one changes variables $\phi \to \mathbf{U}^\dagger\phi$, $\bar{\phi} \to \mathbf{U}^T\bar{\phi}$. Since $\det \mathbf{U} = 1$, the transform leaves the measure invariant (see below) and leaves us with N decoupled integrals of the type Eq. (4.18). The resulting product of N eigenvalues is just the determinant of $\mathbf{A}$ (cf. the later discussion of the partition function of the non-interacting gas). For general (non-diagonalizable) $\mathbf{A}$, the identity is established by a straightforward expansion of the exponent. The expansion terminates at Nth order and, by commuting through integration variables, it may be shown that the resulting Nth-order polynomial of matrix elements of $\mathbf{A}$ is the determinant.[5]

[5] As with ordinary integrals, Grassmann integrals can also be subjected to **variable transforms**. Suppose we are given an integral $\int d(\bar{\phi}, \phi)\ f(\bar{\phi}, \phi)$ and wish to change variables according to

$$\bar{\nu} = \mathbf{M}\bar{\phi}, \nu = \mathbf{M}'\phi, \tag{4.20}$$

where, for simplicity, $\mathbf{M}$ and $\mathbf{M}'$ are complex matrices (i.e. we here restrict ourselves to linear transforms). One can show that

$$\bar{\nu}_1 \cdots \bar{\nu}_N = (\det \mathbf{M})\bar{\phi}_1 \cdots \bar{\phi}_N, \quad \nu_1 \cdots \nu_N = (\det \mathbf{M}')\phi_1 \cdots \phi_N. \tag{4.21}$$

(There are different ways to prove this identity. The most straightforward is by explicitly expanding Eq. (4.20) in components and commuting all Grassmann variables to the right. A more elegant way is to argue that the coefficient relating the right- and left-hand sides of Eq. (4.21) must be an Nth-order polynomial of matrix

Keeping the analogy with ordinary commuting variables, the Grassmann version of Eq. (3.18) reads

$$\int d(\bar{\phi},\phi)\; e^{-\bar{\phi}^T \mathbf{A}\phi + {}^{-T}\cdot\phi + \bar{\phi}^T\cdot} = \det \mathbf{A}\; e^{{}^{-T}\mathbf{A}^{-1}} \quad . \tag{4.22}$$

To prove the latter, we note that $\int d\eta\; f(\eta) = \int d\eta\; f(\eta+\nu)$, i.e. in Grassmann integration one can shift variables as in the ordinary case. The proof of the Gaussian relation above thus proceeds in complete analogy to the complex case. As with Eq. (3.18), Eq. (4.22) can also be employed to generate further integration formulae. Defining $\langle\cdots\rangle \equiv \det \mathbf{A}^{-1} \int d(\bar{\phi},\phi)\; e^{-\bar{\phi}^T\mathbf{A}\phi}(\cdots)$, and expanding both the left-and the right-hand side of Eq. (4.22) to leading order in the "monomial" $\bar{\nu}_j\nu_i$, one obtains $\langle\phi_j\bar{\phi}_i\rangle = A^{-1}_{ji}$. The N-fold iteration of this procedure gives

$$\boxed{\langle\phi_{j_1}\phi_{j_2}\cdots\phi_{j_n}\bar{\phi}_{i_n}\cdots\bar{\phi}_{i_2}\bar{\phi}_{i_1}\rangle = \sum_P (\mathrm{sgn}P) A^{-1}_{j_1 i_{P1}}\cdots A^{-1}_{j_n i_{Pn}},}$$

where the sign of the permutation accounts for the sign changes accompanying the interchange of Grassmann variables. Finally, as with Gaussian integration over commuting variables, by taking $N\to\infty$ the Grassmann integration can be translated to a Gaussian functional integral.

4.2 Field integral for the quantum partition function

Having introduced the coherent states, the construction of path integrals for many-body systems no longer presents substantial difficulties. However, before proceeding, we should address the question: what does the phrase "path integral for many-body systems" actually mean? In the next chapter we will see that much of the information on quantum many-particle systems is encoded in expectation values of products of creation and annihilation operators, i.e. expressions of the structure $\langle a^\dagger a\cdots\rangle$. By an analogy to be explained then, objects of this type are generally called **correlation functions**. More important for our present discussion, at any finite temperature, the average $\langle\cdots\rangle$ entering the definition of the

Josiah Willard Gibbs 1839–1903
Credited with the development of chemical thermodynamics, he introduced concepts of free energy and chemical potential. (Figure reproduced from *The Collected Works of J. Willard Gibbs*, vol. I (Longmans, Green and Co., 1928).)

elements of $\mathbf{M}$. In order to be consistent with the anti-commutation behavior of Grassmann variables, the polynomial must obey commutation relations which uniquely characterize a determinant. Exercise: Check the relation for $N = 2$.) On the other hand, the integral of the new variables must obey the defining relation, $\int d\bar{\nu}\;\bar{\nu}_1\cdots\bar{\nu}_N = \int d\nu\nu_1\cdots\nu_N = (-)^{N(N-1)/2}$, where $d\bar{\nu} = \prod_{i=1}^N d\bar{\nu}_i$ and the sign on the right-hand side is attributed to ordering of the integrand, i.e. $\int d\nu_1\; d\nu_2\;\nu_1\nu_2 = -\int d\nu_1\;\nu_1\int d\nu_2\;\nu_2 = -1$. Together Eq. (4.21) and (4.20) enforce the identities $d\bar{\nu} = (\det\mathbf{M})^{-1}d\bar{\phi}$, $d\nu = (\det\mathbf{M}')^{-1}d\phi$, which combine to give

$$d(\bar{\phi},\phi)\; f(\bar{\phi},\phi) = \det(\mathbf{M}\mathbf{M}') \qquad d(\bar{\nu},\nu)\; f(\bar{\phi}(\bar{\nu}),\phi(\nu)).$$

correlation function runs over the quantum Gibbs distribution $\hat{\rho} \equiv e^{-\beta(\hat{H}-\mu\hat{N})}/\mathcal{Z}$, where, as usual,

$$\mathcal{Z} = \mathrm{tr}\, e^{-\beta(\hat{H}-\mu\hat{N})} = \sum_n \langle n|e^{-\beta(\hat{H}-\mu\hat{N})}|n\rangle, \tag{4.23}$$

is the quantum partition function, $\beta \equiv 1/T$, μ denotes the chemical potential, and the sum extends over a complete set of Fock space states $\{|n\rangle\}$. (For the time being we specify neither the statistics of the system – bosonic or fermionic – nor the structure of the Hamiltonian.)

Ultimately, we will want to construct the path integral representations of correlation functions. Later we will see that all of these representations can be derived by a few straightforward manipulations from a prototypical path integral, namely that for $\mathcal{Z}$. Further, the (path integral of the) partition function is of importance in its own right, as it contains much of the information needed to characterize the thermodynamic properties of a many-body quantum system.[6] We thus begin our journey into many-body field theory with a construction of the path integral for $\mathcal{Z}$.

To prepare the representation of the partition function (4.23) in terms of coherent states, one must insert the resolution of identity

$$\mathcal{Z} = \int d(\bar{\psi},\psi)\, e^{-\sum_i \bar{\psi}_i\psi_i} \sum_n \langle n|\psi\rangle\langle\psi|e^{-\beta(\hat{H}-\mu\hat{N})}|n\rangle. \tag{4.24}$$

We now wish to get rid of the – now redundant – Fock space summation over $|n\rangle$ (another resolution of identity). To bring the summation to the form $\sum_n |n\rangle\langle n| = \mathbf{1}_{\mathcal{F}}$, one must commute the factor $\langle n|\psi\rangle$ to the right-hand side. However, in performing this operation, we must be careful not to miss a sign change whose presence will have important consequences for the structure of the fermionic path integral. Indeed, it may be checked that, whilst for bosons $\langle n|\psi\rangle\langle\psi|n\rangle = \langle\psi|n\rangle\langle n|\psi\rangle$, the fermionic coherent states change sign upon permutation, $\langle n|\psi\rangle\langle\psi|n\rangle = \langle -\psi|n\rangle\langle n|\psi\rangle$ (i.e. $\langle -\psi| \equiv \langle 0|\exp\big(-\sum_i \bar{\psi}_i a_i\big)$). The presence of the sign is a direct consequence of the anti-commutation relations between Grassmann variables and Fock space operators (exercise). Note that, as both $\hat{H}$ and $\hat{N}$ contain elements even in the creation/annihilation operators, the sign is insensitive to the presence of the Boltzmann factor in Eq. (4.24). Making use of the sign factor ζ, the result of the interchange can be formulated as the general expression

$$\begin{aligned} \mathcal{Z} &= \int d(\bar{\psi},\psi)\; e^{-\sum_i \bar{\psi}_i\psi_i} \sum_n \langle\zeta\psi|e^{-\beta(\hat{H}-\mu\hat{N})}|n\rangle\langle n|\psi\rangle \\ &= \int d(\bar{\psi},\psi)\; e^{-\sum_i \bar{\psi}_i\psi_i} \langle\zeta\psi|e^{-\beta(\hat{H}-\mu\hat{N})}|\psi\rangle. \end{aligned} \tag{4.25}$$

[6] In fact, the statement above is not entirely correct. Strictly speaking, thermodynamic properties involve the **thermodynamic potential** $\Omega = -T\ln\mathcal{Z}$ rather than the partition function itself. At first sight it seems that the difference between the two is artificial – one might first calculate $\mathcal{Z}$ and then take the logarithm. However, typically, one is unable to determine $\mathcal{Z}$ in closed form, but rather one has to perform a perturbative expansion, i.e. the result of a calculation of $\mathcal{Z}$ will take the form of a series in some small parameter ϵ. Now a problem arises when the logarithm of the series is taken. In particular, the Taylor series expansion of $\mathcal{Z}$ to a given order in ϵ does not automatically determine the expansion of Ω to the same order. Fortunately, the situation is not all that bad. As we will see in the next chapter, the logarithm essentially rearranges the perturbation series in an order known as a **cumulant expansion**.

Equation (4.25) can now be directly subjected to the general construction scheme of the path integral. To be concrete, let us assume that the Hamiltonian is limited to a maximum of two-body interactions (see Eq. (2.11) and (2.16)),

$$\hat{H}(a^\dagger, a) = \sum_{ij} h_{ij} a_i^\dagger a_j + \sum_{ijkl} V_{ijkl} a_i^\dagger a_j^\dagger a_k a_l. \tag{4.26}$$

Note that we have arranged for all of the annihilation operators to stand to the right of the creation operators. Fock space operators of this structure are said to be **normal ordered**.[7] The reason for emphasizing normal ordering is that such an operator can be readily diagonalized by means of coherent states. Dividing the "time interval" β into N segments and inserting coherent state resolutions of identity (steps 1, 2, and 3 of the general scheme), Eq. (4.25) assumes the form

$$\mathcal{Z} = \int_{\substack{-0=\zeta \\ 0=\zeta}}^{-N \quad N} \prod_{n=1}^{N} d(\bar{\psi}^n, \psi^n)\; e^{-\delta \sum_{n=0}^{N-1} \left[\delta^{-1}(\bar{\psi}^n - \bar{\psi}^{n+1})\cdot\psi^n + H(\bar{\psi}^{n+1}, \psi^n) - \mu N(\bar{\psi}^{n+1}, \psi^n)\right]}, \tag{4.27}$$

where $\delta = \beta/N$ and $\frac{\langle\psi|\hat{H}(a^\dagger,a)|\psi'\rangle}{\langle\psi|\psi'\rangle} = \sum_{ij} h_{ij}\bar{\psi}_i\psi'_j + \sum_{ijkl} V_{ijkl}\bar{\psi}_i\bar{\psi}_j\psi'_k\psi'_l \equiv H(\bar{\psi}, \psi')$ (similarly $N(\bar{\psi}, \psi')$) and we have adopted the shorthand $\psi^n = \{\psi_i^n\}$, etc. Finally, sending $N \to \infty$ and taking limits analogous to those leading from Eq. (3.5) to (3.6) we obtain the continuum version of the path integral,[8]

$$\boxed{\mathcal{Z} = \int D(\bar{\psi}, \psi)\; e^{-S[\bar{\psi},\psi]}, \quad S[\bar{\psi}, \psi] = \int_0^\beta d\tau \left[\bar{\psi}\partial_\tau\psi + H(\bar{\psi}, \psi) - \mu N(\bar{\psi}, \psi)\right],} \tag{4.28}$$

where $D(\bar{\psi}, \psi) = \lim_{N\to\infty} \prod_{n=1}^{N} d(\bar{\psi}^n, \psi^n)$, and the fields satisfy the boundary condition

$$\bar{\psi}(0) = \zeta\bar{\psi}(\beta), \quad \psi(0) = \zeta\psi(\beta). \tag{4.29}$$

Written in a more explicit form, the action associated with the general pair-interaction Hamiltonian (4.26) can be cast in the form

$$S = \int_0^\beta d\tau \left[\sum_{ij} \bar{\psi}_i(\tau)\left[(\partial_\tau - \mu)\delta_{ij} + h_{ij}\right]\psi_j(\tau) + \sum_{ijkl} V_{ijkl}\bar{\psi}_i(\tau)\bar{\psi}_j(\tau)\psi_k(\tau)\psi_l(\tau)\right]. \tag{4.30}$$

Notice that the structure of the action fits nicely into the general scheme discussed in the previous chapter. By analogy, one would expect that the exponent of the many-body

[7] More generally, an operator is defined to be "normal ordered" with respect to a given vacuum state $|0\rangle$ if, and only if, it annihilates $|0\rangle$. Note that the vacuum need not necessarily be defined as a zero-particle state. If the vacuum contains particles, normal ordering need not lead to a representation where all annihilators stand to the right. If, for whatever reason, one is given a Hamiltonian whose structure differs from Eq. (4.26), one can always effect a normal ordered form at the expense of introducing commutator terms. For example, normal ordering the quartic term leads to the appearance of a quadratic contribution that can be absorbed into $h_{\alpha\beta}$.

[8] Whereas the bosonic continuum limit is indeed perfectly equivalent to the one taken in constructing the quantum mechanical path integral ($\lim_{\delta\to 0} \delta^{-1}(\bar{\psi}^{n+1} - \bar{\psi}^n) = \partial_\tau|_{\tau=n\delta}\bar{\psi}(\tau)$ gives an ordinary derivative, etc.), a novelty arises in the fermionic case. The notion of replacing differences by derivatives is purely symbolic for Grassmann variables. There is no sense in which $\bar{\psi}^{n+1} - \bar{\psi}^n$ is small. The symbol $\partial_\tau\bar{\psi}$ rather denotes the formal (and well-defined expression) $\lim_{\delta\to 0} \delta^{-1}(\bar{\psi}^{n+1} - \bar{\psi}^n)$.

path integral carries the significance of the Hamiltonian action, $S \sim \int d(p\dot{q} - H)$, where (q, p) symbolically stands for a set of generalized coordinates and momenta. In the present case, the natural pair of canonically conjugate operators is $(a, a^\dagger)$. One would then interpret the eigenvalues $(\psi, \bar{\psi})$ as "coordinates" (much as (q, p) are the eigenvalues of the operators $(\hat{q}, \hat{p})$). Adopting this interpretation, we see that the exponent of the path integral indeed has the canonical form of a Hamiltonian action and, therefore, is easy to memorize.

Equations (4.28) and (4.30) define the **functional integral in the time representation** (in the sense that the fields are functions of a time variable). In practice we shall mostly find it useful to represent the action in an alternative, Fourier conjugate representation. To this end, note that, due to the boundary conditions (4.29), the functions $\psi(\tau)$ can be interpreted as functions on the entire Euclidean time axis that are periodic/antiperiodic on the interval $[0, \beta]$. As such, they can be represented in terms of a Fourier series,

$$\psi(\tau) = \frac{1}{\sqrt{\beta}} \sum_{\omega_n} \psi_n e^{-i\omega_n \tau}, \quad \psi_n = \frac{1}{\sqrt{\beta}} \int_0^\beta d\tau \; \psi(\tau) e^{i\omega_n \tau},$$

where

$$\omega_n = \begin{array}{ll} 2n\pi T, & \text{bosons}, \\ (2n+1)\pi T, & \text{fermions}, \end{array} \qquad n \in \mathbb{Z}, \tag{4.31}$$

are known as **Matsubara frequencies**. Substituting this representation into Eq. (4.28) and (4.30), we obtain $\mathcal{Z} = \int D(\bar{\psi}, \psi) \; e^{-S[\bar{\psi}, \psi]}$, where $D(\bar{\psi}, \psi) = \prod_n d(\bar{\psi}_n, \psi_n)$ defines the measure (for each Matsubara index n we have an integration over a coherent state basis $\{|\psi_n\rangle\}$),[9] and the action takes the form

$$S[\bar{\psi}, \psi] = \sum_{ij,n} \bar{\psi}_{in} \left[(-i\omega_n - \mu)\, \delta_{ij} + h_{ij} \right] \psi_{jn} + \frac{1}{\beta} \sum_{ijkl, n_i} V_{ijkl} \bar{\psi}_{in_1} \bar{\psi}_{jn_2} \psi_{kn_3} \psi_{ln_4} \delta_{n_1 + n_2, n_3 + n_4}. \tag{4.32}$$

Here we have used the identity $\int_0^\beta d\tau \; e^{-i\omega_n \tau} = \beta \delta_{\omega_n 0}$. Equation (4.32) defines the **frequency representation of the action**.[10]

INFO In performing calculations in the Matsubara representation, one sometimes runs into convergence problems (which will manifest themselves in the form of ill-convergent Matsubara frequency summations). In such cases it will be important to remember that Eq. (4.32) does not actually represent the precise form of the action. What is missing is a convergence generating factor whose presence follows from the way in which the integral was constructed, and which will save us in cases of non-convergent sums (except, of course, in cases where divergences have a physical origin). More precisely, since the fields $\bar{\psi}$ are evaluated infinitesimally later than the fields ψ (cf. Eq. (4.27)), the h- and μ-dependent contributions to the action acquire a factor

[9] Notice, however, that the fields ψ_n carry dimension $[\text{energy}]^{-1/2}$, i.e. the frequency coherent state integral is normalized as $\int d(\bar{\psi}_n, \psi_n) \; e^{-\bar{\ }_n \quad n} = (\beta\epsilon)^{-\zeta}$.

[10] As to the signs of the Matsubara indices appearing in Eq. (4.32), note that the Fourier representation of $\bar{\psi}$ is defined as $\bar{\psi}(\tau) = \frac{1}{\beta} \sum_n \bar{\psi}_n e^{+i\omega_n \tau}$, $\bar{\psi}_n = \frac{1}{\beta} \int_0^\beta d\tau \; \bar{\psi}(\tau) e^{-i\omega_n \tau}$. In the bosonic case, this sign convention is motivated by $\bar{\psi}$ being the complex conjugate of ψ. For reasons of notational symmetry, this convention is also adopted in the fermionic case.

$\exp(-i\omega_n\delta)$, δ infinitesimal. Similarly, the V contribution acquires a factor $\exp(-i(\omega_{n_1}+\omega_{n2})\delta)$. In cases where the convergence is not critical, we will omit these contributions. However, once in a while it is necessary to remember their presence.

Partition function of non-interacting gas

As a first exercise, let us consider the quantum partition function of the non-interacting gas. (Later, this object will prove to be a "reference" in the development of weakly interacting theories.) In some sense, the field integral formulation of the non-interacting partition function has a status similar to that of the path integral for the quantum harmonic oscillator: the direct quantum mechanical solution of the problem is straightforward and application of the full artillery of the field integral seems somewhat ludicrous. From a pedagogical point of view, however, the free partition function is a good problem; it provides us with the welcome opportunity to introduce a number of practical concepts of field integration within a comparatively simple setting. Also, the field integral representation of the free partition function will be an important operational building block for our subsequent analysis of interacting problems.

Consider, then, the partition function (4.28) with $H_0(\bar\psi,\psi)=\sum_{ij}\bar\psi_i H_{0,ij}\psi_j$. Diagonalizing H_0 by a unitary transformation U, $H_0=UDU^\dagger$, and transforming integration variables, $U^\dagger\psi\equiv\phi$, the action assumes the form $S=\sum_a\sum_{\omega_n}\bar\phi_{an}(-i\omega_n+\xi_a)\phi_{an}$, where $\xi_a\equiv\epsilon_a-\mu$ and ϵ_a are the single-particle eigenvalues. Remembering that the fields $\phi_a(\tau)$ are independent integration variables (Exercise: Why does the transformation $\psi\to\phi$ have a Jacobian of unity?), we find that the partition function decouples, $\mathcal{Z}=\prod_a\mathcal{Z}_a$, where

$$\mathcal{Z}_a=\int D(\bar\phi_a,\phi_a)\; e^{-\sum_n\bar\phi_{an}(-i\omega_n+\xi_a)\phi_{an}}=\prod_n[\beta(-i\omega_n+\xi_a)]^{-\zeta}, \tag{4.33}$$

and the last equality follows from the fact that the integrals over ϕ_{an} are one-dimensional complex or Grassmann Gaussian integrals. Here, let us recall our convention defining $\zeta=1$ (-1) for bosonic (fermionic) fields. At this stage, we have left all aspects of field integration behind us and reduced the problem to one of computing an infinite product over factors $i\omega_n-\xi_a$. Since products are usually more difficult to get under control than sums, we take the logarithm of $\mathcal{Z}$ to obtain the free energy

$$F=-T\ln\mathcal{Z}=T\zeta\sum_{an}\ln[\beta(-i\omega_n+\xi_a)]. \tag{4.34}$$

INFO Before proceeding with this expression, let us take a second look at the intermediate identity (4.33). Our calculation showed the partition function to be the product over all eigenvalues of the operator $-i\hat\omega+\hat H-\mu\hat N$ defining the action of the non-interacting system (here, $\hat\omega=\{\omega_n\delta_{nn'}\}$). As such, it can be written compactly as:

$$\boxed{\mathcal{Z}=\det\left[\beta(-i\hat\omega+\hat H-\mu\hat N)\right]^{-}\quad.} \tag{4.35}$$

This result was derived by first converting to an eigenvalue integration and then performing the one-dimensional integrals over "eigencomponents" ϕ_{an}. While technically straightforward, that – explicitly representation-dependent – procedure is not well suited to generalization to

more complex problems. (Keep in mind that later on we will want to embed the free action of the non-interacting problem into the more general framework of an interacting theory.)

Indeed, it is not necessary to refer to an eigenbasis at all. In the bosonic case, Eq. (3.17) tells us that Gaussian integration over a bilinear $\sim \bar{\phi}\hat{X}\phi$ generates the inverse determinant of $\hat{X}$. Similarly, as we have seen, Gaussian integration extends to the Grassmann case with the determinants appearing in the numerator rather than in the denominator (as exemplified by Eq. (4.35)). (As a matter of fact, Eq. (4.33) is already a proof of this relation.)

We now have to face up to a technical problem: how do we compute Matsubara sums of the form $\sum_n \ln(i\omega_n - x)$? Indeed, it takes little imagination to foresee that sums of the type $\sum_{n_1,n_2,\ldots} X(\omega_{n_1}, \omega_{n_2}, \ldots)$, where X symbolically stands for some function, will be a recurrent structure in the analysis of functional integrals. A good ansatz would be to argue that, for sufficiently low temperatures (i.e. temperatures smaller than any other characteristic energy scale in the problem), the sum can be traded for an integral, specifically $T\sum_n \to \int d\omega/(2\pi)$. However, this approximation is too crude to capture much of the characteristic temperature dependence in which one is usually interested. Yet there exists an alternative, and much more accurate, way of computing sums over Matsubara frequencies (see Info below).

INFO Consider a single **Matsubara frequency summation**,

$$S \equiv \sum_n h(\omega_n), \tag{4.36}$$

where h is some function and ω_n may be either bosonic or fermionic (cf. Eq. (4.31)). The basic idea behind the standard scheme of evaluating sums of this type is to introduce a complex auxiliary function $g(z)$ that has simple poles at $z = i\omega_n$. The sum S then emerges as the sum of residues obtained by integrating the product gh along a suitably chosen path in the complex plane. Typical choices of g include

$$g(z) = \begin{cases} \frac{\beta}{\exp(\beta z)-1}, & \text{bosons,} \\ \frac{\beta}{\exp(\beta z)+1}, & \text{fermions,} \end{cases} \quad \text{or } g(z) = \begin{cases} \frac{\beta}{2}\coth(\beta z/2), & \text{bosons,} \\ \frac{\beta}{2}\tanh(\beta z/2), & \text{fermions,} \end{cases} \tag{4.37}$$

where, in much of this section, we will employ the functions of the first column. (Notice the similarity between these functions and the familiar Fermi and Bose distribution functions.) In practice, the choice of the counting function is mostly a matter of taste, save for some cases where one of the two options is dictated by convergence criteria.

Integration over the path shown in the left part of Fig. 4.2 then produces

$$\frac{\zeta}{2\pi i}\oint dz\; g(z)h(-iz) = \zeta\sum_n \mathrm{Res}(g(z)h(-iz))|_{z=i\omega_n} = \sum_n h(\omega_n) = S,$$

where, in the third identity, we have used the fact that the "counting functions" g are chosen so as to have residue ζ and it is assumed that the integration contour closes at $z \to \pm i\infty$. (The difference between using the first and the second column of Eq. (4.37) lies in the value of the residue. In the latter case, it is equal to unity rather than ζ.) Now, the integral along a contour in the immediate vicinity of the poles of g is usually intractable. However, as long as we are careful not to cross any singularities of g or the function $h(-iz)$ (symbolically indicated

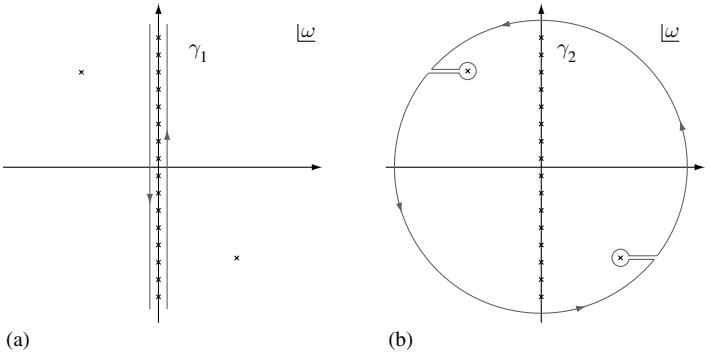

Figure 4.2 (a) The integration contour employed in calculating the sum (4.36). (b) The deformed integration contour.

by isolated crosses in Fig. 4.2[11]) we are free to distort the integration path, ideally to a contour along which the integral *can* be done. Finding a suitable contour is not always straightforward. If the product hg decays sufficiently fast as $|z| \to \infty$ (i.e. faster than z^{-1}), one will usually try to "inflate" the original contour to an infinitely large circle (Fig. 4.2(b)).[12] The integral along the outer perimeter of the contour then vanishes and one is left with the integral around the singularities of the function h. In the simple case where $h(-iz)$ possesses a number of isolated singularities at $\{z_k\}$ (i.e. the situation indicated in the figure) we thus obtain

$$S = \frac{\zeta}{2\pi i} \oint dz\; h(-iz)g(z) = -\zeta \sum_k \text{Res}\; h(-iz)g(z)\big|_{z=z_k}\,, \tag{4.38}$$

where the contour integral encircles the singularities of $h(-iz)$ in clockwise direction. The computation of the infinite sum S has been now been reduced to the evaluation of a finite number of residues – a task that is always possible!

To illustrate the procedure on a simple example, let us consider the function

$$h(\omega_n) = -\frac{\zeta T}{i\omega_n e^{-i\omega_n \delta} - \xi}\,,$$

where δ is a positive infinitesimal.[13] To evaluate the sum $S = \sum_n h(\omega_n)$, we first observe that the product $h(-iz)g(z)$ has benign convergence properties. Further, the function $h(-iz)$ has a

[11] Remember that a function that is bounded and analytic in the entire complex plane is constant, i.e. every "interesting" function will have singularities.

[12] Notice that the condition $\lim_{|z|\to\infty} |hg| < z^{-1}$ is not as restrictive as it may seem. The reason is that the function h will be mostly related to physical observables that approach some limit (or vanish) for large excitation energies. This implies vanishing in at least portions of the complex plane. The convergence properties of g depend on the concrete choice of the counting function. (Exercise: Explore the convergence properties of the functions shown in Eq. (4.37).)

[13] In fact, this choice of h is actually not as artificial as it may seem. The expectation value of the **number of particles** in the grand canonical ensemble is defined through the identity $N \equiv -\partial F/\partial\mu$ where F is the free energy. In the non-interacting case, F is given by Eq. (4.34) and, remembering that $\xi_a = \epsilon_a - \mu$, one obtains $N \approx \zeta T \sum_{an} \frac{1}{-i\omega_n + \xi_a}$. Now, why did we write "$\approx$" instead of "$=$"? The reason is that the right-hand side, obtained by naive differentiation of Eq. (4.34), is ill-convergent. (The sum $\sum_{n=-\infty}^{\infty} \frac{1}{n+x}$, x arbitrary, does not exist!) At this point we have to remember the remark made on page 168, i.e., had we carefully treated the discretization of the field integral, both the logarithm of the free energy and $\partial_\mu F$ would have acquired infinitesimal phases $\exp(-i\omega_n\delta)$. As an exercise, try to keep track of the discretization of the field integral from

simple pole that, in the limit $\delta \to 0$, lies on the real axis at $z = \xi$. This leads to the result

$$\sum_n h(\omega_n) = -\zeta \operatorname{Res} g(z) h(-iz)|_{z=\xi} = \frac{1}{e^{\beta\xi} - \zeta} \,.$$

We have thus arrived at the important identity

$$\boxed{-\zeta T \sum_n \frac{1}{i\omega_n - \xi_a} = \begin{cases} n_{\rm B}(\epsilon_a), & \text{bosons}, \\ n_{\rm F}(\epsilon_a), & \text{fermions}, \end{cases}} \tag{4.39}$$

where

$$n_{\rm F}(\epsilon) = \frac{1}{\exp(\epsilon - \mu) + 1}, \quad n_{\rm B}(\epsilon) = \frac{1}{\exp(\epsilon - \mu) - 1}, \tag{4.40}$$

are the Fermi/Bose distribution functions. As a corollary we note that the expectation value for the number of particles in a non-interacting quantum gas assumes the familiar form $N = \sum_a n_{\rm F/B}(\epsilon_a)$.

Before returning to our discussion of the partition function, let us note that life is not always as simple as the example above. More often than not, the function h contains not only isolated singularities but also cuts or worse singularities. In such circumstances, finding a good choice of the integration contour can be far from straightforward!

Returning to the problem of computing the sum (4.34), consider for a moment a fixed eigenvalue $\xi_a \equiv \epsilon_a - \mu$. In this case, we need to evaluate the sum $S \equiv \sum_n h(\omega_n)$, where $h(\omega_n) \equiv \zeta T \ln[\beta(-i\omega_n + \xi)] = \zeta T \ln[\beta(i\omega_n - \xi)] + C$ and C is an inessential constant. As discussed before, the sum can be represented as $S = \frac{\zeta}{2\pi i} \oint dz\, g(z) h(-iz)$, where $g(z) = \beta(e^{\beta z} - \zeta)^{-1}$ is (β times) the distribution function and the contour encircles the poles of g as in Fig. 4.2(a). Now, there is an essential difference from the example discussed previously, i.e. the function $h(-iz) = \zeta T \ln(z - \xi) + C$ has a branch cut along the real axis, $z \in (-\infty, \xi)$ (see the figure). To avoid contact with this singularity one must distort the integration contour as shown in the figure. Noticing that the (suitably regularized, cf. our previous discussion of the particle number N) integral along the perimeter vanishes, we conclude that

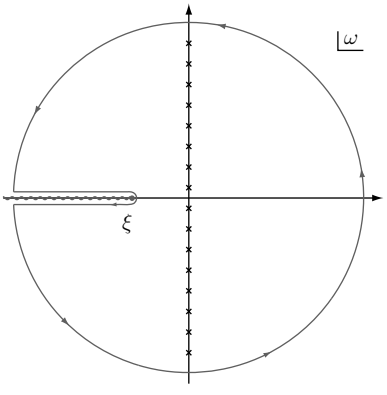

$$S = \frac{T}{2\pi i} \int_{-\infty}^{\infty} d\epsilon\, g(\epsilon) \left(\ln(\epsilon^+ - \xi) - \ln(\epsilon^- - \xi) \right),$$

its definition to Eq. (4.34) to show that the accurate expression for N reads

$$N = \zeta T \sum_{an} \frac{1}{-i\omega_n e^{-i\omega_n \delta} + \xi_a} = \sum_a \sum_n h(\omega_n)|_{\xi=\xi_a} \,,$$

where h is the function introduced above. (Note that the necessity to keep track of the lifebuoy $e^{-i\delta\omega_n}$ does not arise too often. Most Matsubara sums of physical interest relate to functions f that decay faster than z^{-1}.)

where $\epsilon^{\pm} = \epsilon \pm i\eta$, η is a positive infinitesimal, and we have used the fact that $g(\epsilon^{\pm}) \simeq g(\epsilon)$ is continuous across the cut. (Also, without changing the value of the integral (exercise: why?), we have enlarged the integration interval from $(-\infty, \xi]$ to $(-\infty, \infty)$.) To evaluate the integral, we observe that $g(\epsilon) = \zeta \partial_\epsilon \ln\left(1 - \zeta e^{-\beta\epsilon}\right)$ and integrate by parts:

$$S = -\frac{\zeta T}{2\pi i} \int d\epsilon \ln\left(1 - \zeta e^{-\beta\epsilon}\right) \left(\frac{1}{\epsilon^+ - \xi} - \frac{1}{\epsilon^- - \xi} \right) \overset{(3.58)}{=} \zeta T \ln\left(1 - \zeta e^{-\beta\xi}\right).$$

Insertion of this result into Eq. (4.34) finally gives the familiar expression

$$F = \zeta T \sum_a \ln\left(1 - \zeta e^{-\beta(\epsilon_a - \mu)}\right), \tag{4.41}$$

for the free energy of the non-interacting Fermi/Bose gas. While this result could have been obtained much more straightforwardly by the methods of quantum statistical mechanics, we will shortly see how powerful a tool the methods discussed in this section are when it comes to the analysis of less elementary problems!

4.3 Field theoretical bosonization: a case study

The field integral (4.28) provides an exact representation of the quantum partition function; it contains the full information on the microscopic Hamiltonian operator. However, what we are actually interested in is the universal large-scale behavior of a quantum system. To extract this information from the field integral we will need to identify the relevant long-range degrees of freedom and to dispense with the abundance of microscopic data controlling the short-range behavior. In other words, we will have to pass from the microscopic field theory to some effective long-range theory.

In Chapter 1 we saw that there are usually two principal strategies to obtain effective long range theories of microscopic systems: explicit construction – the subject of the next two chapters – and more phenomenological approaches based on consistency considerations and symmetry arguments. Besides a certain lack of rigor, the principal disadvantage of the second route is the lack of quantitative control of the results (which implies susceptibility to mistakes). On the other hand, the phenomenological approach is far less laborious and involves a minimal amount of technical preparation. Often, the phenomenological deduction of a low-energy field theory precedes its rigorous construction (sometimes by years). In fact, there are cases where phenomenology is the only viable route.

Below we will illustrate the power of the phenomenological approach on the example of the interacting one-dimensional electron gas. We will map the microscopic partition function of the system onto a free (and thus exactly solvable) bosonic theory.[14] In this section the emphasis is placed on purely methodological aspects, i.e. we will derive an effective theory, but will not do anything with it. (Nonetheless, the derivation is instructive and helps us to understand the essential physics of the system!) In later chapters, the field theory derived

[14] A preliminary account of the ideas underlying this mapping has already been given in Section 2.2.

below will then serve as the starting point for the discussion of a number of interesting applications.

One-dimensional electron gas (fermionic theory)

Non-interacting system

Let us begin by considering the action of a non-interacting one-dimensional electron gas

$$S_0[\psi^\dagger,\psi] = \sum_{s=\pm 1} \int dx d\tau \; \psi_s^\dagger \left(-isv_{\rm F}\partial_x + \partial_\tau\right) \psi_s,$$

where $\psi_{+/-}$ are the right-/left-moving fermions and we have denoted the Grassmann field conjugate to ψ by $\psi^\dagger$.[15] For later reference we recall that the left-/right-moving fermion operators are projections of the global momentum-dependent fermion operator to the vicinity of the left/right Fermi point, i.e. $\psi_+^\dagger(q) = \psi_{k_{\rm F}+q}^\dagger, \psi_-^\dagger(q) = \psi_{-k_{\rm F}+q}^\dagger$, where $|q| \ll k_{\rm F}$. Fourier transforming this expression we obtain the approximate decomposition

$$\psi(x) = e^{ik_{\rm F}x}\psi_+(x) + e^{-ik_{\rm F}x}\psi_-(x). \tag{4.42}$$

Before proceeding, let us rewrite the action in a form that emphasizes the symmetries of the problem:

$$S_0[\psi^\dagger,\psi] = \int d^2x\, \psi^\dagger \left(\sigma_0\partial_{x_0} + i\sigma_3\partial_{x_1}\right)\psi = \int d^2x \bar\psi \left(\sigma_1\partial_{x_0} + \sigma_2\partial_{x_1}\right)\psi, \tag{4.43}$$

where we have set $v_{\rm F} = 1$ for notational simplicity. Here, $\psi = (\psi_+,\psi_-)^T$ is a two-component field comprising left- and right-moving fermions, $x = (x_0,x_1) = (\tau,x)$ parameterizes $(1+1)$-dimensional space-time, and $\bar\psi \equiv \psi^\dagger\sigma_1$. The second equality identifies the action of the free one-dimensional fermion with that of a $(1+1)$-dimensional Dirac particle.[16]

We next turn to the discussion of the **symmetries of the problem**. For one thing, the action is clearly invariant under the transformation, $\psi \to e^{i\phi_{\rm v}}\psi$, where $\phi_{\rm v} = {\rm const.}$ What is the resulting conserved current? The infinitesimal variant of this transformation is described by $\psi \to \psi + (i\delta\phi_{\rm v})\psi$ or, in a notation adapted to Eq. (1.42), $\psi \leftrightarrow \phi^i$, $\omega^{\rm a} \leftrightarrow i\phi_{\rm v}$, $F_{\rm a}^i = \mathbf{1}$. Equation (1.43) then gives the conserved current $j_{\nu,\mu} = \frac{\partial\mathcal{L}}{\partial(\partial_\mu\psi)}\psi = \bar\psi\gamma_\mu\psi$. For later reference, we mention that, under a rotation of space-time, $x_\mu \to (R\cdot x)_\mu$, the components of $j_{\rm v}$ transform like a vector, $j_\mu \to (R\cdot j)_\mu$. In relativistic field theory, $j_{\rm v}$ is therefore usually called a **vector current**.

Notice that the two components of the vector, $j_0 = \psi^\dagger\psi = \psi_+^\dagger\psi_+ + \psi_-^\dagger\psi_- \equiv \rho$ and $j_1 = i\psi^\dagger\sigma_3\psi = i\left(\psi_+^\dagger\psi_+ - \psi_-^\dagger\psi_-\right) \equiv ij$, are the charge density, ρ, of the system and (i times)

[15] Following the remarks earlier, this represents an abuse of notation; there is no Grassmann complex conjugation! However, within the context of relativistic fermions our standard symbol $\bar\psi$ is reserved for another object (see below).

[16] For a review of the theory of the standard four-dimensional massless Dirac equation $\gamma_\mu\partial_\mu\psi = 0$, see, e.g., L. H. Ryder, *Quantum Field Theory* (Cambridge University Press, 1996). The Dirac equation affords a natural generalization to any even-dimensional space. Specifically, for $d = 2$, the algebra of Dirac γ-matrices, $\{\gamma_\mu,\gamma_\nu\} = 2\delta_{\mu\nu}$, $\mu,\nu = 0,1,5$, is satisfied by $\gamma_0 \equiv \sigma_1$, $\gamma_1 \equiv \sigma_2$, $\gamma_5 \equiv -i\gamma_0\gamma_1 = \sigma_3$.

the current density, j, respectively.[17] Thus, the equation $-i\partial_\mu j_\mu = -i\partial_\tau \rho + \partial_x j = 0$ simply expresses the conservation of particle current.

INFO A particular example of the general fact that the U(1)-symmetry of quantum mechanics (the freedom to multiply wave functions or operators of a second quantized approach by a constant phase $e^{i\phi}$) implies the **conservation of particle current.**

EXERCISE Subject the action of the general field integral (4.28) to the transformation $\psi \to e^{i\phi}\psi$, $\bar\psi \to \bar\psi e^{-i\phi}$ and compute the resulting Noether current. Convince yourself that the components of the current are the coherent state representation of the standard density/current operator of quantum mechanics.

Now, the action (4.43) possesses a somewhat less obvious second symmetry: it remains invariant under the transformation $\psi \to e^{i\phi_a\sigma_3}\psi$, $\bar\psi \to \bar\psi e^{i\phi_a\sigma_3}$. (Notice that this is not a unitary symmetry, i.e. the matrices transforming ψ and $\bar\psi$ are not inverse to each other.) Indeed, one may note that $(\bar\psi e^{i\phi_a\sigma_3})\sigma_\mu\partial_\mu(e^{i\phi_a\sigma_3}\psi) \overset{[\sigma_3,\sigma_\mu]_+=0}{=} \bar\psi\sigma_\mu\partial_\mu\psi$. A straightforward application of Noether's theorem based on the infinitesimal variant $\psi \to \psi + (i\phi_a)\sigma_3\psi$ gives the conserved current $j_{a,\mu} = i\bar\psi\sigma_\mu\sigma_3\psi = \epsilon_{\mu\nu}\bar\psi\sigma_\nu\psi$. Introducing a unit vector e_2 pointing into a fictitious third dimension perpendicular to the space-time plane, the current can be written as $j_a = e_2 \times j_v$. This representation shows that, under rotations, j_a transforms like an axial vector (similar to, say, a magnetic field). For this reason, j_a is commonly called an **axial current**.

INFO The axial symmetry of the relativistic electron gas is a prominent example of symmetry that does not pervade to the quantum level. I.e. the conservation of the axial current breaks down once quantum fluctuations are taken into account, a phenomenon known as the **chiral** or **axial anomaly**.[18] Although we will meet with various manifestations of the chiral anomaly, a thorough discussion of all its implications is beyond the scope of this text. (However, most textbooks on particle physics contain an extensive coverage of anomalies.)

Finally, notice that the existence of two distinct symmetries, vectorial and axial, affords a simple interpretation in the original representation of the theory (the first equality in Eq. (4.43)). All it means is that the left- and right-moving fermion states do not couple, i.e. that the left- and the right-moving fermion particle currents are separately conserved. (Compute the corresponding Noether currents!)

Given that we are dealing with but the simplest one-dimensional theory one can imagine, the formal discussion of symmetries may seem to be a bit of an overkill. However, we shall see in a moment that the effort was well invested: as soon as we switch on interactions, the fermionic theory ceases to be exactly solvable. It turns out, however, that our symmetry discussion above provides the key to a bosonic reformulation of the problem which *does* enjoy exact solvability. Yet, before turning to the bosonic approach, let us briefly recapitulate how interactions couple to the model.

[17] Notice that, for a one-dimensional Fermi system with uniform Fermi velocity $v_F = 1$, the current density is equal to the density of right movers minus that of the left movers.

[18] In field theory, the quantum violation of a classical conservation law is generally called an **anomaly**.

Interacting case

As in Section 2.2 we assume a short-range interaction between the left- and right-moving densities. Quantitatively, this is described by the coherent state representation of the second quantized Hamiltonian (2.36), i.e.

$$S_{\rm int}[\psi^\dagger,\psi] = \frac{1}{2}\sum_s \int dx d\tau\ (g_2\hat\rho_s\hat\rho_{\bar s} + g_4\hat\rho_s\hat\rho_s), \tag{4.44}$$

where $\hat\rho_s \equiv \psi_s^\dagger\psi_s$. Notice that the interaction term leaves the vectorial/axial symmetry of the system intact (why?). But what else can we say about the interacting system? In fact, we have seen in Section 2.2 that it is difficult to understand the physics of the system in the microscopic language of interacting fermion states. Rather, one should turn to a formulation in terms of the effective long-range degrees of freedom of the model – non-dispersive charge density fluctuations. In the next section, we will formulate the dynamics of these excitations in a field theoretical language. Remarkably, it will turn out that all we need to extract this formulation from the microscopic model is a minimal investment of phenomenological input plus symmetry considerations.

One-dimensional electron gas (bosonic theory)

We have seen in Section 2.2 that the one-dimensional fermion system supports collective bosonic excitations. In this section, we apply phenomenological and symmetry arguments to construct a field theory of these excitations.[19] Consider the electron operators $c^\dagger(x)$ of a one-dimensional system. As seen in Chapter 2, the operators $c^\dagger$ afford a representation in terms of bosons – the Jordan–Wigner transformation. As we are after an effective bosonic theory, it is certainly a good idea to switch to this Bose representation right from the outset. Expressed in terms of Jordan–Wigner bosons, $c^\dagger(x) = e^{i\pi\int_{x'<x} dx'\, b^\dagger(x')b(x')}b^\dagger(x)$, where $b^\dagger(x)$ creates a (bosonic) unit-charge excitation at x and the "Jordan–Wigner string" $\sim \int_{x'<x} dx'\, b^\dagger(x')b(x')$ implements the fermionic exchange statistics of the cs in terms of Bose operators. Now, we have seen in Section 2.2 that the dominant excitations of the (spinless) system are charge-density fluctuations. Thus, our next step is to switch to a representation that separately treats density and phase degrees of freedom. To this end, we define charge and phase operators through

$$b(x) \equiv \left(\frac{k_{\rm F}}{\pi} + \hat\rho(x)\right)^{1/2} e^{i\hat\phi(x)}, \quad b^\dagger(x) \equiv e^{-i\hat\phi(x)}\left(\frac{k_{\rm F}}{\pi} + \hat\rho(x)\right)^{1/2}, \tag{4.45}$$

where $k_{\rm F}/\pi$ is the average background density of the system, $\hat\rho$ describes density fluctuations, and $\hat\phi$ describes the phase of the Bose excitations.

INFO **Charge-density representations** of this type are frequently employed in bosonic theories. Importantly, the transformation $(b, b^\dagger) \to (\hat\rho, \hat\phi)$ is canonical, i.e. the density and the phase

[19] For a detailed account of the rigorous construction (elements of which have been used in Section 2.2) we refer to H. Schöller and J. von Delft, Bosonization for beginners – refermionization for experts, *Ann. Phys.* **7** (1998), 225–305.

of a bosonic excitation form a canonically conjugate pair, $[\hat{\rho}(x), \hat{\phi}(x')] = i\delta(x - x')$.[20] To check this assertion, let us temporarily shift the density operator $\hat{\rho} \to \hat{\rho} + k_F/\pi$, so that $\hat{\rho}$ now describes the total density of the system. (Of course, the shift by a number does not alter the commutation relations.) We thus write $b = \hat{\rho}^{1/2}\exp(i\hat{\phi})$ and $b^\dagger = \exp(-i\hat{\phi})\hat{\rho}^{1/2}$, where the position index has been dropped for notational transparency, and check that $[b, b^\dagger] = 1$ indeed requires $[\hat{\rho}, \hat{\phi}] = i$:

$$\begin{aligned}[b, b^\dagger] &= \left[\hat{\rho}^{1/2}e^{i\hat{\phi}}, e^{-i\hat{\phi}}\hat{\rho}^{1/2}\right] = \hat{\rho} - e^{-i\hat{\phi}}\hat{\rho}e^{i\hat{\phi}} \\ &= \hat{\rho} - e^{-i[\hat{\phi},\,]}\hat{\rho} = \hat{\rho} - \hat{\rho} + i[\hat{\phi}, \hat{\rho}] - \frac{1}{2}[\hat{\phi}, [\hat{\phi}, \hat{\rho}]] + \cdots \overset{[\hat{\,},\hat{\phi}]=i}{=} 1,\end{aligned}$$

as required. (In the last line we have used the general operator identity $e^{\hat{A}}\hat{B}e^{-\hat{A}} = e^{[\hat{A},.]}\hat{B}$.)

To represent the fermions in terms of bosonic degrees of freedom we might now substitute the charge/phase decomposition directly into our expression for the Jordan–Wigner transformed fermion. It turns out, however, that the resulting representation – though perfectly valid – is not quite what we want. To obtain a representation better adjusted to the present problem, let us, rather, construct a fermion "from scratch." To this end, let us think of the fermion as a structureless charge endowed with fermionic exchange statistics. The charge is created by application of $e^{i\hat{\phi}}$,[21] while the fermionic exchange statistics are then generated in a second step through multiplication by a Jordan–Wigner string. In fact, there is a certain ambiguity in the definition of the string variable: defining $\hat{\theta}(x) \equiv \pi \int_{-\infty}^{x} dx'\ \hat{\rho}(x')$, it is straightforward to show that for m, m' odd integers

$$\left[e^{im\hat{\theta}(x)}e^{i\hat{\phi}(x)}, e^{im'\hat{\theta}(x')}e^{i\hat{\phi}(x')}\right]_+ \propto e^{i\pi m'\ \ (x'-x)} + e^{i\pi m\ \ (x-x')} = 0,$$

which implies that the most general representation of the fermion operator reads as,[22] $c^\dagger(x) = \Gamma \sum_{m=\pm 1} e^{im(k_F x + \hat{\theta}(x)/\pi)}e^{i\hat{\phi}(x)}$. Here we have introduced a scalar prefactor Γ whose presence is needed to regularize the right-hand side of the equation in the limit of vanishing lattice spacing (the short distance cutoff of the theory, see the problem set). We have also reinstalled the constant shift, $\hat{\rho} \to \hat{\rho} + k_F/\pi \Rightarrow \hat{\theta} \to \hat{\theta} + k_F x$.

EXERCISE Verify the commutator identity above. (Hint: Use the general identities $e^{\hat{A}}\hat{B}e^{-\hat{A}} = e^{[\hat{A},]}\hat{B}$ and $e^{\hat{A}}e^{\hat{B}}e^{-\hat{A}} = e^{e^{A}\hat{B}e^{-A}}$.)

For most purposes, it is sufficient to keep the lowest two contributions to the harmonic expansion of the fermion operator: $c^\dagger(x) = \Gamma \sum_{s=\pm 1} e^{is(k_F x + \hat{\theta}(x)/\pi)}e^{i\hat{\phi}(x)}$. Comparison with Eq. (4.42) then leads to the tentative identification

$$c_s^\dagger(x) = \Gamma e^{is\hat{\theta}(x)}e^{i\hat{\phi}(x)}. \tag{4.46}$$

[20] This implies, in particular, that the corresponding field integral transformation $(\psi, \bar{\psi}) \to (\rho, \phi)$ from complex integration variables to the two real variables (ρ, ϕ) has a unit Jacobian (check this!).

[21] Notice that $\hat{\phi}$ is the "momentum" conjugate to $\hat{\rho}$, i.e. the "translation operator" $e^{i\phi(x)}$ increases the charge at x by unity.

[22] To obtain the correct normalization of the anti-commutator at coinciding arguments $x = x'$, all expansion coefficients have to be equal to each other.

Finally, one may notice that the two fields $\hat{\theta}$ and $\hat{\phi}$ – our principal degrees of freedom throughout – are characterized by the commutation relations

$$\boxed{[\hat{\phi}(x), \hat{\theta}(x')] = i\pi\Theta(x' - x).} \tag{4.47}$$

At first sight, the results derived above may look strange: we have traded our simple fermion operator for a nonlinear representation in terms of bosonic degrees of freedom – but why? The point is that we are usually interested not in expressions linear in the fermion operators but in fermion bilinears (currents, densities, etc.). In contrast to the case of a single fermion, fermion bilinears have very simple expressions in terms of bosons. In particular, the Hamiltonian operator of the interacting system becomes quadratic (manifestly solvable) when expressed in terms of bosons. This aspect of the theory – undoubtedly the prime motivation behind the method of **bosonization** – will be explored next.

Non-interacting system

We now apply a combination of symmetry and dynamical arguments to identify the Hamiltonian of the non-interacting system. The fermionic prototype action is invariant under global rotations of space-time, $x \to x' = R \cdot x, \psi'(x') = \psi(x)$. This symmetry must pertain to the bosonic description of the theory. Turning to the system's "intrinsic" **symmetries**, we notice that the vectorial and axial symmetry operations considered in the previous section act on the left-/right-moving fermion states as $\psi_s \to e^{i\phi_{\rm v}}\psi_s$ and $\psi_s \to e^{is\phi_{\rm a}}\psi_{\rm s}$, respectively. Of course, these transformations must continue to be symmetries no matter which representation of the theory (bosonic, fermionic, or whatever) is chosen. A glance at Eq. (4.46) shows that the symmetry transformation acts on the bosonic variables by a simple shift operation, *vectorial*: $(\phi, \theta) \to (\phi + \phi_{\rm v}, \theta)$, *axial*: $(\phi, \theta) \to (\phi, \theta + \phi_{\rm a})$. For $\phi_{\rm a,v} = \text{const.}$, these transformations must not change the action, which excludes the presence of non-derivative terms. (For example, a contribution such as $\sim \int \theta^2$ would not be invariant under a uniform axial transformation, etc.)

Of course, symmetries alone do not suffice to fix the action of the system. What we need, in addition, is a minimal amount of **dynamical input**. More specifically, what we shall build on is the fact that the creation of a density distortion $\rho = \partial_x\theta/\pi$ in the system costs a certain amount of energy U. Assuming that $U \sim \rho^2$ (i.e. that screening has rendered the Coulomb interaction effectively short-range), the Lagrangian action of the charge displacement field θ will contain a term $\sim (\partial_x\theta)^2$. However, this expression lacks rotational invariance. Its canonical rotationally invariant extension reads $(\partial_x\theta)^2 + (\partial_\tau\theta)^2$. Thus, up to second order in derivatives, the Lagrangian action is given by $S_0[\theta] = \frac{c}{2}\int dx\, d\tau\, [(\partial_x\theta)^2 + (\partial_\tau\theta)^2]$, where the coupling constant c needs to be specified. This expression tells us that the field θ has a linear dispersion and propagates at constant velocity (recall our discussion of, e.g., the phonon action in Chapter 1). Recalling that $\partial_x\theta \sim \rho$, this confirms our results regarding the behavior of density distortions in one-dimensional electron systems derived in Section 2.2.

To fix the value of the coupling constant c, we must compute the "correlation function"[23]

$$C(x,\tau) \equiv \langle (\psi_+^\dagger \psi_-)(x,\tau)(\psi_-^\dagger \psi_+)(0,0)\rangle_\psi, \tag{4.48}$$

first in the fermionic, then in the bosonic, language, and require coinciding answers. Referring for a detailed discussion to the problem set, we here merely note that the result obtained for the free fermion action Eq. (4.43) reads $C(x,\tau) = (4\pi^2(x^2+\tau^2))^{-1}$. The bosonic variant $C(x,\tau) = \Gamma^4 \left\langle e^{2i\theta(x,\tau)} e^{-2i\theta(0,0)} \right\rangle_\theta$ leads to the same expression provided that we set $c = 1/\pi$ and $\Gamma = 1/(2\pi a)^{1/2}$.

Thus, our final result for the Lagrangian of the non-interacting system reads

$$S[\theta] = \frac{1}{2\pi} \int dx\, d\tau\, [(\partial_x\theta)^2 + (\partial_\tau\theta)^2].$$

Before proceeding to include interactions, let us turn from the Lagrangian to the Hamiltonian formulation. Using the fact that the canonical momentum corresponding to θ is $\pi_\theta = \partial_{\partial_\tau\theta}\mathcal{L} = \partial_\tau\theta/\pi$, we obtain the Hamiltonian density $\frac{1}{2\pi}\left[(\partial_x\theta)^2 + \pi^2\pi_\theta^2\right]$ and the action

$$S[\theta,\pi_\theta] = \frac{1}{2}\int dx\, d\tau \left(\frac{1}{\pi}(\partial_x\theta)^2 + \pi\pi_\theta^2 + 2i\partial_\tau\theta\pi_\theta\right).$$

At the same time, the relation (4.47) identifies the canonical momentum as $\pi_\theta = \partial_x\phi/\pi$. Expressed in terms of the two fundamental degrees of freedom of the theory, the Hamiltonian action thus reads

$$S[\theta,\phi] = \frac{1}{2\pi}\int dx\, d\tau \left((\partial_x\theta)^2 + (\partial_x\phi)^2 + 2i\partial_\tau\theta\partial_x\phi\right). \tag{4.49}$$

It is instructive to inspect the Noether current corresponding to the vectorial symmetry in the bosonic language. A straightforward application of Noether's theorem to the transformation $\phi \to \phi + \phi_\mathrm{v}$ obtains $\partial_\mu j_{\mathrm{v},\mu} = 0$, where $j_{\mathrm{v},0} \overset{\text{p. 174}}{=} \rho = \partial_x\theta/\pi$ and $j_{\mathrm{v},1} \overset{\text{p. 174}}{=} ij = -i\partial_x\phi/\pi$.[24] While the first of these relations merely reiterates the definition of the displacement field, the second contains new information. Remembering that $\rho = \rho_+ + \rho_-$ and $j = \rho_+ - \rho_-$, we obtain the important identification

$$\boxed{\rho_\pm = \frac{1}{2\pi}\left[\partial_x\theta \mp \partial_x\phi\right]}, \tag{4.50}$$

of the left- and right-moving densities in terms of the Bose field.

EXERCISE Compute the bosonic representation of the axial Noether current.

[23] The function C describes the correlation of the bilinear $\bar\psi_+\psi_-$ with itself measured at different values of space and time. We have more to say on the subject of correlation functions in the next chapter.

[24] The (arbitrary) normalization constant π^{-1} has been chosen to obtain consistency with previous definitions, see below.

Interacting system

We are now in a position to turn to the interacting case. In fact, all the hard work necessary to get the interacting problem under control has already been done! We simply substitute the bosonic representation Eq. (4.50) into the Coulomb action Eq. (4.44) and obtain

$$\begin{aligned} S_{\rm int} &= \frac{1}{8\pi^2}\sum_s \int dx\, d\tau\, [g_2 \partial_x(\theta - s\phi)\partial_x(\theta + s\phi) + g_4 \partial_x(\theta - s\phi)\partial_x(\theta - s\phi)] \\ &= \frac{1}{4\pi^2}\int dx\, d\tau\, \left[(g_2+g_4)(\partial_x\theta)^2 + (g_4 - g_2)(\partial_x\phi)^2\right], \end{aligned}$$

i.e. an action that is still quadratic and, thus, exactly solvable.

INFO In the field theoretical literature (especially the literature on conformal field theory), interactions of this type are commonly referred to as **current–current interactions**. This is because $S_{\rm int}$ can be expressed as a bilinear form in the Noether currents generated by the symmetries of the system.

Adding $S_{\rm int}$ to the action of the non-interacting action Eq. (4.49), we arrive at the final expression

$$\boxed{S[\theta,\phi] = \frac{1}{2\pi}\int dx\, d\tau \left(g^{-1} v (\partial_x\theta)^2 + g v (\partial_x\phi)^2 + 2i\partial_\tau\theta\partial_x\phi\right),} \tag{4.51}$$

where we have introduced the parameters

$$v \equiv \left[\left(v_{\rm F} + \frac{g_4}{2\pi}\right)^2 - \left(\frac{g_2}{2\pi}\right)\right]^{\frac{1}{2}}, \quad g \equiv \left[\frac{v_{\rm F} + \frac{g_4 - g_2}{2\pi}}{v_{\rm F} + \frac{g_4+g_2}{2\pi}}\right]^{\frac{1}{2}}, \tag{4.52}$$

and have reinstated $v_{\rm F}$. Comparison with the results of Section 2.2 identifies v as the effective velocity of the charge-density wave excitations of the system.[25] Equation (4.51) represents the main result of our analysis. We have succeeded in mapping a non-linear (i.e. interacting) problem onto a linear bosonic field theory. Critical readers may justly object that this result does not contain much new information. After all, a (second quantized) representation of the theory in terms of free bosons has been derived previously in Section 2.2. Nonetheless, the analysis of this section is very valuable from both a methodological and a conceptual point of view. Methodologically, it turns out that the field integral formulation $\int D(\theta,\phi)\exp(-S[\theta,\phi])$ is very convenient for calculation. Many intriguing phenomena displayed by one-dimensional electron systems (we will meet some examples) can straightforwardly be addressed in this language. From a conceptual point of view, it is quite remarkable that no "microscopic" calculations had to be performed to determine the effective field theory above. "All" we had to invest was symmetry arguments, a minimal amount of phenomenological input, and a number of consistency checks. In Chapter 9 we will meet a related problem – the low-energy field theory of quantum spin chains – where

[25] Of course, we do not need to resort to the results of Section 2.2 to draw this conclusion: the structure of Eq. (4.51) by itself determines the interpretation of v as an effective velocity. To see this, one may integrate over ϕ to arrive at an effective wave-type Lagrangian for θ whose characteristic velocity is set by v (exercise).

a microscopic construction scheme for the effective field theory is not known at all. In this case a (suitably generalized) version of the symmetry analysis above will represent the *only* viable route towards the solution of the problem.

4.4 Summary and outlook

This concludes our preliminary introduction to the field integral. We have learned how to represent the partition function of a quantum many-body system in terms of a generalized path integral. The field integral representation of the partition function will be the basic platform on which all our further developments will be based. In fact, we are now in a position to face up to the main problem addressed in this text: practically none of the "non-trivial" field integrals in which one might be interested can be executed in closed form. This reflects the fact that, save for a few exceptions (such as the one considered in Section 4.3 above), interacting many-body problems do not admit closed solutions. Before employing the field integral to solve serious problems, we need to develop a spectrum of approximation strategies – perturbation theory, linear response theory, mean-field methods, instanton techniques and the like. The construction and application of such methods will be the subject of the following chapters.

4.5 Problems

Exercises on fermion coherent states

To practice the coherent state method, we begin with a few simple exercises on the fermionic coherent state which complement the structures discussed in the main text.

Considering a fermionic coherent state $|\eta\rangle$, verify the following identities: (a) $\langle\eta|a_i^\dagger = \langle\eta|\bar\eta_i$, (b) $a_i^\dagger|\eta\rangle = -\partial_{\eta_i}|\eta\rangle$ and $\langle\eta|a_i = \partial_{\bar\eta_i}\langle\eta|$, (c) $\langle\eta|\nu\rangle = \exp\big(\sum_i \bar\eta_i\nu_i\big)$, and (d) $\int d(\bar\eta,\eta)\; d\eta_i\; e^{-\sum_i \bar\eta_i\eta_i}|\eta\rangle\langle\eta| = \mathbf{1}_{\mathcal{F}}$, where $d(\bar\eta,\eta) \equiv \prod_i d\bar\eta_i\; d\eta_i$. Finally, (e) show that $\langle n|\psi\rangle\langle\psi|n\rangle = \langle\zeta\psi|n\rangle\langle n|\psi\rangle$, where $|n\rangle$ is an n-particle state in Fock space while $|\psi\rangle$ is a coherent state.

Answer:
Making use of the rules of Grassmann algebra,

$$\begin{aligned}
\text{(a)}\quad \langle\eta|a_i^\dagger &= \langle 0|\exp\Big(-\sum_j a_j\bar\eta_j\Big)a_i^\dagger = \langle 0|\prod_j(1-a_j\bar\eta_j)a_i^\dagger = \langle 0|(1-a_i\bar\eta_i)a_i^\dagger\prod_{j\neq i}(1-a_j\bar\eta_j)\\
&= \underbrace{\langle 0|a_ia_i^\dagger}_{=\langle 0|[a_i,a_i^\dagger]_+=\langle 0|}\bar\eta_i\prod_{j\neq i}(1-a_j\bar\eta_j) = \langle 0|\prod_j(1-a_j\bar\eta_j)\bar\eta_i = \langle\eta|\bar\eta_i.\\
\text{(b)}\quad a_i^\dagger|\eta\rangle &= \underbrace{a_i^\dagger(1-\eta_ia_i^\dagger)}_{=a_i^\dagger=\partial_{\eta_i}\eta_ia_i^\dagger=-\partial_{\eta_i}(1-\eta_ia_i^\dagger)}\prod_{j\neq i}(1-\eta_ja_j^\dagger)|0\rangle = -\partial_{\eta_i}\prod_j(1-\eta_ja_j^\dagger)|0\rangle = -\partial_{\eta_i}|\eta\rangle,\\
\langle\eta|a_i &= \langle 0|\prod_{j\neq i}(1-a_j\bar\eta_j)\underbrace{(1-a_i\bar\eta_i)a_i}_{=a_i=-\partial_{\eta_i}a_i\bar\eta_i=\partial_{\eta_i}(1-a_i\bar\eta_i)} = \partial_{\bar\eta_i}\langle 0|\prod_j(1-a_j\bar\eta_j) = \partial_{\bar\eta_i}\langle\eta|.
\end{aligned}$$

(c) $\langle\eta|\nu\rangle = \langle\eta|\prod_i \underbrace{(1-\nu_i a_i^\dagger)}_{(1+a_i^\dagger\nu_i)}|0\rangle = \langle\eta|\prod_i \underbrace{(1+\bar\eta_i\nu_i)}_{\exp[\sum_i \bar\eta_i\nu_i]}|0\rangle = \exp\Big(\sum_i \bar\eta_i\nu_i\Big)$.

(d) To prove the completeness of fermion coherent states, we apply Schur's lemma, i.e. we need to show that $[a_j^{(\dagger)}, \int d(\bar\eta,\eta)e^{-\sum_i\bar\eta_i\eta_i}|\eta\rangle\langle\eta|] = 0$.

$$\begin{aligned}
a_j^\dagger \int d(\bar\eta,\eta)\; e^{-\sum_i\bar\eta_i\eta_i}|\eta\rangle\langle\eta| &= -\int d(\bar\eta,\eta)\; e^{-\sum_i\bar\eta_i\eta_i}\partial_{\eta_j}|\eta\rangle\langle\eta| \\
= \int d(\bar\eta,\eta)\underbrace{\partial_{\eta_j}\Big(e^{-\sum_i\bar\eta_i\eta_i}\Big)}_{=\bar\eta_j e^{-\sum_i \bar{}_i\ {}_i}}|\eta\rangle\langle\eta| &= \int d(\bar\eta,\eta)\; e^{-\sum_i\bar\eta_i\eta_i}|\eta\rangle\langle\eta|a_j^\dagger, \\
a_j \int d(\bar\eta,\eta)\; e^{-\sum_i\bar\eta_i\eta_i}|\eta\rangle\langle\eta| &= \int d(\bar\eta,\eta)\;\underbrace{e^{-\sum_i\bar\eta_i\eta_i}\eta_j}_{=-\partial_{\bar{}_j}\left(e^{-\sum_i \bar{}_i\ {}_i}\right)}|\eta\rangle\langle\eta| \\
= \int d(\bar\eta,\eta)\; e^{-\sum_i\bar\eta_i\eta_i}|\eta\rangle\partial_{\bar\eta_j}\langle\eta| &= \int d(\bar\eta,\eta)\; e^{-\sum_i\bar\eta_i\eta_i}|\eta\rangle\langle\eta|a_j.
\end{aligned}$$

The constant of proportionality is fixed by taking the expectation value with the vacuum.

$$\langle 0|\int d(\bar\eta,\eta)e^{-\sum_i\bar\eta_i\eta_i}|\eta\rangle\langle\eta|0\rangle = \int d(\bar\eta,\eta)\; e^{-\sum_i\bar\eta_i\eta_i} = 1.$$

(e) A general n-particle state is given as $|n\rangle = a_1^\dagger\dots a_n^\dagger|0\rangle$, $\langle n| = \langle 0|a_n\dots a_1$, where we neglected a normalization factor. The matrix element $\langle n|\psi\rangle$, thus, reads

$$\langle n|\psi\rangle = \langle 0|a_n\dots a_1|\psi\rangle = \langle 0|\psi_n\dots\psi_1|\psi\rangle = \psi_n\dots\psi_1.$$

Similarly, we obtain $\langle\psi|n\rangle = \bar\psi_1\dots\bar\psi_n$. Using these results,

$$\begin{aligned}
\langle n|\psi\rangle\langle\psi|n\rangle &= \psi_n\dots\psi_1\bar\psi_1\dots\bar\psi_n = \psi_1\bar\psi_1\dots\psi_n\bar\psi_n \\
&= (\zeta\bar\psi_1\psi_1)\dots(\zeta\bar\psi_n\psi_n) = (\zeta\bar\psi_1)\dots(\zeta\bar\psi_n)\psi_n\dots\psi_1 = \langle\zeta\psi|n\rangle\langle n|\psi\rangle.
\end{aligned}$$

Feynman path integral from the functional field integral

The abstraction of the coherent state representation betrays the close similarity between the Feynman and coherent state path integrals. To help elucidate the connection, the goal of the present problem is to confirm that the Feynman path integral of the quantum harmonic oscillator follows from the coherent state path integral.

Consider the simplest bosonic many-body Hamiltonian, $\hat H = \hbar\omega(a^\dagger a + \frac{1}{2})$, where $a^\dagger$ creates "structureless" particles, i.e. states in a one-dimensional Hilbert space. Note that $\hat H$ can be interpreted as the Hamiltonian of a single oscillator degree of freedom. Show that the field integral for the partition function $\mathcal{Z} = \mathrm{tr}[\exp(-\beta\hat H)]$ can be mapped onto the (imaginary-time) path integral of a harmonic oscillator by a suitable variable transformation. (Hint: Let yourself be guided by the fact that the conjugate operator pair $(a, a^\dagger)$ is related to the momentum and coordinate operators $(\hat p, \hat q)$ through a canonical transformation.)

Answer:
In the coherent state representation, the quantum partition function of the oscillator Hamiltonian is expressed in terms of the path integral ($\hbar = 1$):

$$\mathcal{Z} = \int D(\bar{\phi}, \phi) \, \exp\left[- \int_0^\beta d\tau \left(\bar{\phi} \partial_\tau \phi + \omega \bar{\phi} \phi \right) \right], \tag{4.53}$$

where $\phi(\tau)$ denotes a complex scalar field, the constant factor $e^{-\beta\omega/2}$ has been absorbed into the measure of the functional integral $D(\bar{\phi}, \phi)$, and we have set the chemical potential $\mu = 0$. The connection between the coherent state and Feynman integral is established by the change of field variables, $\phi(\tau) = (m\omega/2)^{1/2} \left(q(\tau) + ip(\tau)/m\omega \right)$, where $p(\tau)$ and $q(\tau)$ represent real fields. Substituting this representation in Eq. (4.53), and rearranging some terms by integrating by parts, the connection is established: $\mathcal{Z} = \int D(p,q) \, \exp\left[- \int_0^\beta d\tau \left(-ip\dot{q} + \frac{p^2}{2m} + \frac{m\omega^2}{2} q^2 \right) \right]$. (Of course, the "absorption" of the constant $\hbar\omega/2$ in the Hamiltonian into the measure has been a bit of cheating. In operator quantum mechanics, the correspondence between the (q,p) and the $(a, a^\dagger)$ representation of the Hamiltonian includes that constant. Keeping in mind that the constant reflects the non-commutativity of operators, think how it might be recovered within the path integral formalism. Hint: it is best to consider the mapping between representations within a time-slice discretized setting.)

Quantum partition function of the harmonic oscillator

The following involves a practice exercise on elementary field integral manipulations, and infinite products.

Compute the partition function of the harmonic oscillator Hamiltonian in the field integral formulation. To evaluate the resulting infinite product over Matsubara frequencies apply the formula $x/\sin x = \prod_{n=1}^\infty \left(1 - x^2/(\pi n)^2 \right)^{-1}$. (Hint: The normalization of the result can be fixed by requiring that, in the zero-temperature limit, the oscillator occupy its ground state.) Finally, compute the partition function by elementary means and check your result. As an additional exercise, repeat the same steps for the "fermionic oscillator," i.e. with $a, a^\dagger$ fermion operators. Here you will need the auxiliary identity $\cos x = \prod_{n=1}^\infty \left(1 - \frac{x^2}{(\pi(n+1/2))^2} \right)$.

Answer:
Making use of the Gaussian functional integral for complex fields, one obtains from Eq. (4.53) ($\hbar = 1$)

$$\begin{aligned} \mathcal{Z}_{\rm B} &\sim \det(\partial_\tau + \omega)^{-1} \sim \prod_{\omega_n} (-i\omega_n + \omega)^{-1} \sim \prod_{n=1}^\infty \left[\left(\frac{2n\pi}{\beta} \right)^2 + \omega^2 \right]^{-1} \\ &\sim \prod_{n=1}^\infty \left[1 + \left(\frac{\beta\omega}{2\pi n} \right)^2 \right]^{-1} \sim \frac{1}{\sinh(\beta\omega/2)}. \end{aligned}$$

Now, in the limit of small temperatures, the partition function is dominated by the ground state, $\lim_{\beta\to\infty} \mathcal{Z}_{\rm B} = \exp[-\beta\omega/2]$, which fixes the constant of proportionality. Thus, $\mathcal{Z}_{\rm B} = [2\sinh(\beta\hbar\omega/2)]^{-1}$.

In the fermionic case, the Gaussian integration gives a product over eigenvalues in the numerator and we have to use fermionic Matsubara frequencies, $\omega_n = (2n+1)\pi/\beta$:

$$\mathcal{Z}_{\rm F} \sim \det(\partial_\tau + \omega) \sim \prod_{\omega_n} (-i\omega_n + \omega) \sim \prod_{n=1}^{\infty} \left[\left(\frac{(2n+1)\pi}{\beta} \right)^2 + \omega^2 \right]$$
$$\sim \prod_{n=1}^{\infty} \left[1 + \left(\frac{\beta\omega}{(2n+1)\pi} \right)^2 \right] \sim \cosh(\beta\omega/2).$$

Fixing the normalization, one obtains $\mathcal{Z}_{\rm F} = 2e^{-\beta\omega}\cosh(\beta\omega/2)$. Taken together, these results are easily confirmed by direct computation, viz.

$$\mathcal{Z}_{\rm B} = e^{-\beta\omega/2} \sum_{n=0}^{\infty} e^{-n\beta\omega} = \frac{e^{-\beta\omega/2}}{1-e^{-\beta\omega}} = \frac{1}{2\sinh(\beta\omega/2)},$$
$$\mathcal{Z}_{\rm F} = e^{-\beta\omega/2} \sum_{n=0}^{1} e^{-n\beta\omega} = e^{-\beta\omega/2}(1+e^{-\beta\omega}) = 2e^{-\beta\omega}\cosh(\beta\omega/2).$$

Boson–fermion duality

The equivalence of the bosonic and the fermionic representation of the one-dimensional electron gas is exemplified by computation of the correlation function Eq. (4.48) considered in the main text.

(a) Employ the free fermion field integral with action (4.43) to compute the zero-temperature limit of the correlation function (4.48) considered in the text (assume $x > 0$).
(b) Considering a free scalar bosonic field θ with action $S[\theta] = \frac{1}{2c}\int dx\, d\tau\, [(\partial_\tau\theta)^2 + (\partial_x\theta)^2]$, compute the correlation function $K(x,\tau) \equiv \langle \theta(x,\tau)\theta(0,0) - \theta(0,0)\theta(0,0)\rangle$ for $x > 0$.
(c) Compute the correlation function $C(x,\tau) = \gamma^2 \langle \exp[2i\theta(x,\tau)]\, \exp[-2i\theta(0,0)]\rangle$.

Answer:

(a) Setting $v_{\rm F} = 1$ and defining $\mathcal{Z}_\pm \equiv \int D(\bar\psi,\psi)\, \exp\left(-S_\pm[\bar\psi,\psi]\right)$, where $S_\pm[\bar\psi,\psi] = \int dx\, d\tau\, \bar\psi(\partial_\tau \mp i\partial_x)\psi$, we obtain

$$G_\pm(x,\tau) = \mathcal{Z}_\pm^{-1} \int D(\bar\psi,\psi)\, \bar\psi(x,\tau)\, \psi(0,0) e^{-S_\pm[\bar\psi,\psi]} = -(\partial_{\tau'} \mp i\partial_{x'})^{-1}_{(x,\tau;0,0)}$$
$$= -\frac{T}{L} \sum_{p,\omega_n} \frac{1}{-i\omega_n \mp p} e^{-ipx - i\omega_n\tau}.$$

Assuming for definiteness that $x > 0$ and integrating over momenta, we arrive at

$$G_{\pm}(x,\tau) = \mp iT \sum_n \Theta(\pm n) e^{\omega_n(\ x - i\tau)} \simeq \frac{1}{2\pi} \frac{1}{\pm ix - \tau},$$

where in the last equality we have approximated the frequency sum by an integral. Thus, the correlation function (4.48) is given by $C(x,\tau) = G_+(x,\tau)G_-(-x,\tau) = \frac{1}{(2\pi)^2}\frac{1}{x^2+\tau^2}$.

(b) Expressed in a frequency/momentum Fourier representation, $S[\theta] = \frac{L}{2cT}\sum_{q,n} |\theta_{q,n}|^2(q^2 + \omega_n^2)$. Performing the Gaussian integral over θ, we obtain

$$\begin{aligned} K(x,\tau) &= \frac{cT}{L}\sum_{q,n} \frac{e^{iqx+i\omega_n\tau}}{q^2+\omega_n^2} - 1 \simeq \frac{cT}{2}\sum_n \frac{e^{-|\omega_n|x+i\omega_n\tau}-1}{|\omega_n|} \\ &\simeq \frac{c}{4\pi}\int_0^{a^{-1}} d\omega\ \frac{e^{-\omega(x-i\tau)}-1}{\omega} + \text{c.c.} \overset{x,\tau\gg a}{\simeq} -\frac{c}{4\pi}\ln((x^2+\tau^2)/a^2), \end{aligned}$$

where we have approximated the momentum sum by an integral and the frequency sum by an integral, cut off at large frequencies by $E_{\rm F} \simeq v_{\rm F}a^{-1} \overset{v_{\rm F}=1}{=} a^{-1}$.

(c) Using the results derived in (b),

$$\begin{aligned} C(x,\tau) &= \gamma^2\ \ e^{2i(\theta(x,\tau)-\theta(0,0))} = \gamma^2 e^{-2\langle(\theta(x,\tau)-\theta(0,0))^2\rangle} \\ &= \gamma^2 \exp\left(-\frac{c}{\pi}\ln\left(\frac{x^2+\tau^2}{a^2}\right)\right) = \gamma^2\left[\frac{a^2}{x^2+\tau^2}\right]^{\frac{c}{\pi}}. \end{aligned}$$

Setting $c = \pi$ and $\Gamma = 1/2\pi a$, we obtain equivalence to the fermionic representation of the correlation function considered in (a).

Frequency summations

Using the frequency summation techniques developed in the text, this problem involves the computation of two basic correlation functions central to the theory of the interacting Fermi gas.

(a) The **pair correlation function** $\chi^{\rm c}_{n,\mathbf{q}}$ is an important building block entering the calculation of the Cooper pair propagator in superconductors (see Section 6.4). It is given by

$$\chi^{\rm c}_{n,\mathbf{q}} \equiv -\frac{T}{L^d}\sum_{m,\mathbf{p}} G_0(\mathbf{p}, i\omega_m) G_0(-\mathbf{p}+\mathbf{q}, -i\omega_m + i\omega_n) = \frac{1}{L^d}\sum_{\mathbf{p}} \frac{1 - n_{\rm F}(\xi_{\mathbf{p}}) - n_{\rm F}(\xi_{-\mathbf{p}+\mathbf{q}})}{i\omega_n - \xi_{\mathbf{p}} - \xi_{-\mathbf{p}+\mathbf{q}}},$$

where $G_0(\mathbf{p}, i\omega_m) = 1/(i\omega_m - \xi_{\mathbf{p}})$. Verify the second equality. (Note that $\omega_m = (2m+1)\pi\beta$ are fermionic Matsubara frequencies, while $\omega_n = 2\pi nT$ is a bosonic Matsubara frequency.)

(b) Another correlation function central to the theory of the interacting Fermi gas (see Section 5.2), the so-called **density–density response function**, is given by

$$\chi^{\rm d}_{\mathbf{q},\omega_n} \equiv -\frac{T}{L^d}\sum_{\mathbf{p},\omega_m} G_0(\mathbf{p}, i\omega_m) G_0(\mathbf{p}+\mathbf{q}, i\omega_m + i\omega_n) = -\frac{1}{L^d}\sum_{\mathbf{p}} \frac{n_{\rm F}(\xi_{\mathbf{p}}) - n_{\rm F}(\xi_{\mathbf{p}+\mathbf{q}})}{i\omega_n + \xi_{\mathbf{p}} - \xi_{\mathbf{p}+\mathbf{q}}}.$$

Again verify the second equality.

Answer:

(a) To evaluate a sum over fermionic frequencies ω_m, we employ the Fermi function $\beta n_{\rm F}(z) = \beta(e^{\beta z}+1)^{-1}$ defined in the left column of Eq. (4.37). Noting that the function $G_0(\mathbf{p}_1, z)G_0(\mathbf{p}_2, z+i\omega_n)$ has simple poles at $z = \xi_{\mathbf{p}_1}$ and $z = i\omega_n - \xi_{\mathbf{p}_2}$, and applying Eq. (4.38) (with the identification $S = \sum h$ and $h = G_0G_0$), we obtain $S = \frac{-n_{\rm F}(\xi_{\mathbf{p}_1})+n_{\rm F}(\xi_{-\mathbf{p}_2}+i\omega_n)}{i\omega_n-\xi_{\mathbf{p}_1}-\xi_{\mathbf{p}_2}}$. Using the fact that $n_{\rm F}(x+i\omega_n) = n_{\rm F}(x)$ and $n_{\rm F}(-x) = 1 - n_{\rm F}(x)$ we arrive at the result.
(b) One may proceed as in part (a).

Pauli paramagnetism

There are several mechanisms whereby a Fermi gas subject to an external magnetic field responds to the perturbation. One of these, the phenomenon of Pauli paramagnetism, is purely quantum mechanical in nature. Its origin lies in the energy balance of spinful fermions rearranging at the Fermi surface in response to the field. We explore the resulting contribution to the magnetic susceptibility of the electron gas.

Fermions couple to a magnetic field by their orbital momentum as well as by their spin. Concentrating on the latter mechanism, consider the Hamiltonian

$$\hat{H}_z = -\mu_0 \mathbf{B}\cdot\hat{\mathbf{S}}, \quad \hat{\mathbf{S}} = \frac{1}{2} a^\dagger_{\alpha\sigma}\sigma_{\sigma\sigma'}\, a_{\alpha\sigma'},$$

where $\sigma = (\sigma_x, \sigma_y, \sigma_z)^T$ is a vector of Pauli matrices, α an orbital quantum number, and

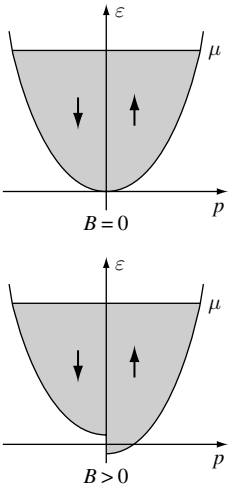

$\mu_0 = e/(2m)$ the Bohr magneton. It turns out that the presence of $\hat{H}_z$ in the energy balance leads to the generation of a net paramagnetic response of purely quantum mechanical origin. To understand the origin of the effect, consider a two-fold (spin!) degenerate single-particle band of free electrons states (see the figure). Both bands are filled up to a certain chemical potential μ. Upon the switching on of an external field, the degeneracy is lifted and the two bands shift in opposite directions by an amount $\sim \mu_0 B$. While, deep in the bands, the Pauli principle forbids a rearrangement of spin configurations, up at the Fermi energy, $\downarrow$ states can turn to energetically more favorable $\uparrow$ states. More precisely, for bands shifted by an amount $\sim \mu_0 B$, a number $\sim \mu_0 B\rho(\mu)$ of states may change their spin direction, which leads to a total energy change of $\Delta E \sim -\mu_0^2 B^2 \rho(\mu)$. Differentiating twice with respect to the magnetic field gives a positive contribution $\chi \sim -\partial_B^2 \Delta E \sim \mu_0^2 \rho(\mu)$ to the magnetic susceptibility of the system.

(a) To convert the qualitative estimate above into a quantitative result, write down the coherent state action of the full Hamiltonian $\hat{H} = \hat{H}_0 + \hat{H}_z$, where $\hat{H}_0 = \sum_{\alpha,\sigma} a^\dagger_{\alpha\sigma}\epsilon_\alpha a_{\alpha\sigma}$

is the non-magnetic part of the Hamiltonian. Integrate out the Grassmann fields to obtain the free energy F as a sum over frequencies.

(b) Show that, at low temperatures, the spin contribution to the magnetic susceptibility $\chi \equiv -\partial_B^2\big|_{B=0} F$ is given by

$$\boxed{\chi \overset{T\to 0}{\longrightarrow} \frac{\mu_0^2}{2}\rho(\mu),} \tag{4.54}$$

where $\rho(\epsilon) = \sum_\alpha \delta(\epsilon - \epsilon_\alpha)$ denotes the single-particle density of states. (Hint: It is convenient to perform the field derivatives prior to the frequency summation.)

Answer:

(a) Choosing the quantization axis parallel to the magnetic field the Hamiltonian assumes a diagonal form $\hat{H} = \sum_{\alpha\sigma} a^\dagger_{\alpha\sigma}\big[\epsilon_\alpha - \frac{\mu_0 B}{2}(\sigma_z)_{\sigma\sigma}\big]a_{\alpha\sigma}$ and the (frequency representation of the) action reads $S[\bar\psi,\psi] = \sum_{\alpha\sigma n}\bar\psi_{\alpha\sigma n}(-i\omega_n + \xi_\alpha - \frac{\mu_0 B}{2}(\sigma_z)_{\sigma\sigma})\psi_{\alpha\sigma n}$. Integrating over ψ, we obtain the partition function $\mathcal{Z} = \prod_{\alpha;n}\beta^2\left((-i\omega_n+\xi_\alpha)^2 - \frac{1}{4}(\mu_0 B)^2\right)$ and

$$F = -T\ln\mathcal{Z} = -T\sum_{\alpha;n}\ln\left[\beta^2\left((-i\omega_n+\xi_\alpha)^2 - \frac{1}{4}(\mu_0 B)^2\right)\right].$$

(b) Differentiating the free energy twice with respect to B, we obtain $\chi = -\frac{1}{2}\mu_0^2 T\sum_{\alpha\omega_n}(-i\omega_n+\xi_\alpha)^{-2}$. Defining $\chi = \sum_{n\alpha} h_\alpha(\omega_n)$, where $h_\alpha(\omega_n) = \frac{1}{2}\mu_0^2 T(-i\omega_n+\xi_\alpha)^{-2}$, Eq. (4.38) can be applied to perform the frequency sum. Noting that the function $h(-iz)$ has poles of *second* order at $z=\xi_\alpha$, i.e. $\mathrm{Res}[h(-iz)g(z)]|_{z=\xi_\alpha} = g'(\xi_\alpha)$, we obtain

$$\chi = -\frac{\mu_0^2}{2}\sum_\alpha n_{\mathrm{F}}'(\xi_\alpha) = -\frac{\mu_0^2}{2}\int_{-\infty}^{\infty} d\epsilon\ \rho(\epsilon)n_{\mathrm{F}}'(\epsilon-\mu).$$

At low temperatures, $T\to 0$, the Fermi distribution function approaches a step function, $n_{\mathrm{F}}(\epsilon)\to\theta(-\epsilon)$, i.e. $n_{\mathrm{F}}'(\epsilon) = -\delta(\epsilon)$ and our result reduces to Eq. (4.54).

Electron–phonon coupling

As follows from the structure of our prototypical condensed matter "master Hamiltonian" (1.1), mobile electrons in solids are susceptible to the vibrations of the host ions, the phonons. This coupling mechanism generates a net attractive interaction between the electrons. Referring for a qualitative discussion of this interaction mechanism to page 266 below, it is the purpose of this problem to quantitatively explore the profile of the phonon mediated electron–electron interaction. In Section 6.4 we will see that this interaction lies at the root of conventional BCS superconductivity.

Consider the three-dimensional variant of the phonon Hamiltonian (1.34),

$$\hat{H}_{\mathrm{ph}} = \sum_{\mathbf{q},j}\omega_q a^\dagger_{\mathbf{q},j}a_{\mathbf{q},j} + \text{const.},$$

where ω_q is the phonon dispersion (here assumed to depend only on the modulus of the momentum, $|\mathbf{q}| = q$) and the index $j = 1, 2, 3$ accounts for the fact that the lattice ions can oscillate in three directions in space (i.e. there are three linearly independent oscillator modes[26]). Electrons in the medium sense the induced charge $\rho_{\rm ind} \sim \nabla \cdot \mathbf{P}$, where $\mathbf{P} \sim \mathbf{u}$ is the polarization generated by the local distortion $\mathbf{u}$ of the lattice ($\mathbf{u}(\mathbf{r})$ is the three-dimensional generalization of the displacement field $\phi(r)$ considered in Chapter 1). Expressed in terms of phonon creation and annihilation operators (cf. Eq. (1.32)), $\mathbf{u_q} = \mathbf{e}_j(a_{\mathbf{q},j} + a^\dagger_{-\mathbf{q},j})/(2m\omega_q)^{1/2}$, where $\mathbf{e}_j$ is the unit vector in the j-direction,[26] and we conclude that the electron–phonon Hamiltonian reads

$$\hat{H}_{\rm el-ph} = \gamma \int d^d r \hat{n}\,(\mathbf{r}) \nabla \cdot \mathbf{u}(\mathbf{r}) = \gamma \sum_{\mathbf{k},\mathbf{q},j} \frac{iq_j}{(2m\omega_q)^{1/2}} \hat{n}_{\mathbf{q}} (a_{\mathbf{q},j} + a^\dagger_{-\mathbf{q},j}).$$

Here, $\hat{n}_{\mathbf{q}} \equiv \sum_{\mathbf{k}} c^\dagger_{\mathbf{k}+\mathbf{q}} c_{\mathbf{k}}$ denotes the electronic density expressed in terms of fermion creation and annihilation operators, and the electron spin has been neglected for simplicity.

(a) Formulate the coherent state action of the electron–phonon system.
(b) Integrate out the phonon fields, and show that an attractive interaction between electrons is generated.

Answer:

(a) Introducing a Grassmann field ψ (a complex field ϕ) to represent the electron (phonon) operators, one obtains the coherent state field integral

$$\mathcal{Z} = \int D[\bar{\psi}, \psi] \int D[\bar{\phi}, \phi]\; e^{-S_{\rm el}[\bar{\psi},\psi] - S_{\rm ph}[\bar{\phi},\phi] - S_{\rm el-ph}[\bar{\psi},\psi,\bar{\phi},\phi]},$$

where

$$\begin{aligned} S_{\rm ph}[\bar{\phi}, \phi] &= \sum_{q,j} \bar{\phi}_{qj}(-i\omega_n + \omega_q)\phi_{qj}, \\ S_{\rm el-ph}[\bar{\psi}, \psi, \bar{\phi}, \phi] &= \gamma \sum_{q,j} \frac{iq_j}{(2m\omega_q)^{1/2}}\, \rho_q(\phi_{qj} + \bar{\phi}_{-qj}), \end{aligned}$$

$\rho_q = \sum_k \bar{\psi}_{k+q}\psi_k$, and the electron action need not be specified explicitly. Here we have adopted a short-hand convention setting $q = (\omega_n, \mathbf{q})$.[27]

[26] For more details see N. W. Ashcroft and N. D. Mermin, *Solid State Physics* (Holt-Saunders International, 1983).
[27] Do not confuse the 4-momentum q with the modulus $|\mathbf{q}| = q$.

(b) We next perform the Gaussian integration over the phonon fields to obtain the effective electron action

$$\begin{aligned} S_{\rm eff}[\bar\psi,\psi] &= S_{\rm el}[\bar\psi,\psi] - \ln\left(\int D[\bar\phi,\phi]\; e^{-(S_{\rm ph}[\bar\phi,\phi]+S_{\rm el-ph})[\bar\psi,\psi,\bar\phi,\phi]}\right) \\ &= S_{\rm el}[\bar\psi,\psi] - \frac{\gamma}{2m}\sum_q \frac{q^2}{\omega_n^2+\omega_q^2}\rho_q\rho_{-q}. \end{aligned}$$

Sloppily transforming from Matsubara to real frequencies, $\omega_n \to -i\omega$, we notice that, for every momentum mode $\mathbf{q}$, the interaction is attractive at low frequencies, $\omega < \omega_q$.

Disordered quantum wires

In this problem, we consider a one-dimensional interacting Fermi system – a "quantum wire" – in the presence of impurities. Building on the results obtained in Section 4.3, we derive an effective low-energy action of this system. (The actual analysis of the large-scale behavior of the disordered quantum wire necessitates the application of renormalization group methods and is postponed to Chapter 8.)

In Sections 2.2 and 4.3 we discussed the physics of interacting fermions in one dimension. We saw that, unlike in a Fermi liquid, the fundamental excitations of the system are charge (and spin) density waves – collective excitations describing the wave-like propagation of spin and charge degrees of freedom, respectively. Going beyond the level of an idealized translationally invariant environment, the question we wish to address currently is to what extent the propagation of these modes will be hampered by the presence of spatially localized imperfections. This problem is of considerable practical relevance. All physical realizations of one-dimensional conductive systems – semiconductor quantum wires, conducting polymers, carbon nanotubes, quantum Hall edges, etc. – generally contain imperfections. Further, and unlike systems of higher dimensionality, a spin/charge degree of freedom propagating down a one-dimensional channel will inevitably hit any impurity blocking its way. We thus expect that impurity scattering has a stronger impact on the transport coefficients than in higher dimensions.

However, there is a second and less obvious mechanism behind the strong impact of

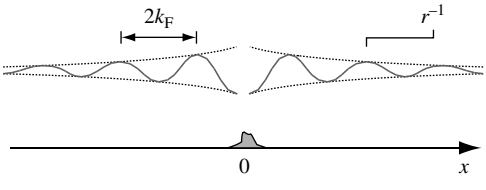

disorder scattering on the conduction behavior of one-dimensional quantum wires: imagine a wavepacket of characteristic momentum $k_{\rm F}$ colliding with an impurity at position $x = 0$ (see figure). The total wave amplitude to the left of the impurity, $\psi(x) \sim \exp(ik_{\rm F}x) + r\exp(-ik_{\rm F}x)$ will be a linear superposition of the incoming amplitude $\sim \exp(ik_{\rm F}x)$ and the reflected outgoing amplitude $\sim r\exp(-ik_{\rm F}x)$, where r is the reflection coefficient. Thus, the electronic density profile is given by $\rho(x) = |\psi(x)|^2 \sim 1 + |r|^2 + 2{\rm Re}\left(re^{-2ik_{\rm F}x}\right)$, which contains an oscillatory contribution known as a **Friedel oscillation**. Moreover, a closer analysis (see exercise below) shows that, in one dimension, the amplitude of these oscillations decays rather slowly, varying as $\sim |x|^{-1}$. The key point is that, in the presence of electron–electron

interactions, other particles approaching the impurity will notice, not only the impurity itself, but also the charged density pattern of the Friedel oscillation. The additional scattering potential then creates a secondary Friedel oscillation, etc. We thus expect that even a weak imperfection in a Luttinger liquid acts as a "catalyst" for the recursive accumulation of a *strong* potential. In this problem, we will derive the effective low-energy action describing the interplay of interaction and impurity scattering. The actual catalytic amplification mechanism outlined above is then explored in Chapter 8 by renormalization group methods.

EXERCISE To explore the **Friedel oscillatory response of the one-dimensional electron gas** to a local perturbation, consider the connected density–density correlation function

$$(x,t) = \langle\hat{\rho}(x,t)\hat{\rho}(0,0)\rangle - \langle\hat{\rho}(x,t)\rangle\langle\hat{\rho}(0,0)\rangle,$$

where $\langle\cdots\rangle$ denotes the ground state expectation value, $\hat{\rho} = a^\dagger a$ and $a(x) = e^{ik_\mathrm{F}x}a_+(x) + e^{-ik_\mathrm{F}x}a_-(x)$ splits into a left- and a right-moving part as usual. Using the fact that $\hat{H} = \sum_{q,s} v_\mathrm{F}(p_\mathrm{F} + sq)a^\dagger_{sq}a_{sq}$ and the von Neumann equation $a_{sq} = i[\hat{H}, a_{sq}]$, show that the time-dependence of the annihilation operators is given by $a_{sq}(t) = e^{-iv_\mathrm{F}(p_\mathrm{F}+sq)t}a_{sq}$. Use this result, the canonical operator commutation relations, and the ground state property $a_{\pm,q}|\ \rangle = 0$ for $\pm q > 0$ to show that

$$(x,t) = \frac{1}{4\pi^2}\left(\frac{1}{(x - v_\mathrm{F}t)^2} + \frac{1}{(x + v_\mathrm{F}t)^2} + \frac{2\cos(2p_\mathrm{F}x)}{x^2 - (v_\mathrm{F}t)^2}\right).$$

Use this result to argue why the *static* response to an impurity potential decays as $\sim |x|^{-1}$.

Consider the one-dimensional quantum wire, as described by the actions Eq. (4.43) and (4.44). Further, assume that, at $x = 0$, the system contains an imperfection or impurity. Within the effective action approach, this is described by

$$S_\mathrm{imp}[\psi^\dagger,\psi] = \int d\tau \left[v_+\psi^\dagger_+\psi_+ + v_-\psi^\dagger_+\psi_+ + v\psi^\dagger_+\psi_- + \bar{v}\psi^\dagger_-\psi_+\right],$$

where all field amplitudes are evaluated at $x = 0$ and the constants $v_\pm \in \mathbb{R}$ and $v \in \mathbb{C}$ describe the amplitudes of forward and backward scattering, respectively.

(a) Show that the forward scattering contributions can be removed by a gauge transformation. This demonstrates that forward scattering is inessential as long as only gauge invariant observables are considered. What is the reason for the insignificance of forward scattering?

We next reformulate the problem in a bosonic language. While the clean system is described by Eq. (4.51), substitution of (4.46) into the impurity action gives $S_\mathrm{imp}[\theta] = \gamma\int d\tau\cos(2\theta(\tau))$, where $\gamma = 2v\Gamma^2$ and we have assumed the backward scattering amplitude to be real. (Any phase carried by the scattering amplitude can be removed by a global gauge transformation of the fields $\psi_\pm$. How?) Notice the independence of S_imp on the field ϕ.

(b) Integrate out the Gaussian field ϕ to obtain the Lagrangian formulation of the action,

$$S[\theta] = \frac{1}{2\pi g}\int dx d\tau \left[v(\partial_x\theta)^2 + v^{-1}(\partial_\tau\theta)^2\right] + S_{\rm imp}[\theta].$$

The formulation of the problem derived in (b) still contains redundancy. The point is that, everywhere except for $x = 0$, the action is Gaussian. This observation suggests that one may integrate out all field degrees of freedom $\theta(x \neq 0)$, thus reducing the problem to one that is local in space (though, as we shall see, non-local in time). To this end, we reformulate the field integral as $\mathcal{Z} = \int D\tilde{\theta}\exp(-S[\tilde{\theta}])$, where

$$\exp(-S[\tilde{\theta}]) = \int D\theta \left(\prod_\tau \delta(\tilde{\theta}(\tau) - \theta(0,\tau))\right)\exp(-S[\theta]),$$

is the action integrated over all field amplitudes save for $\theta(0,\tau)$ and $\prod_\tau \delta(\tilde{\theta}(\tau)-\theta(0,\tau))$ is a product of δ-functions (one for each time slice) imposing the constraints $\theta(0,\tau) = \tilde{\theta}(\tau)$. We next represent these δ- functions as $\delta(\tilde{\theta} - \theta(0,\tau)) = \frac{1}{2\pi}\int dk(\tau)\,\exp(ik(\tau)(\tilde{\theta}(\tau) - \theta(0,\tau)))$ to obtain

$$\begin{aligned}\exp(-S[\tilde{\theta}]) &= \int D\theta\ Dk\ \exp\left[-S[\theta] + i\int d\tau\, k(\tau)(\tilde{\theta}(\tau) - \theta(0,\tau))\right] \\ &= \int D\theta Dk \exp\left[-\int dx d\tau \left(\frac{1}{2\pi g}\left[v(\partial_x\theta)^2 + v^{-1}(\partial_\tau\theta)^2\right] + (c\cos(2\tilde{\theta}) + ik(\tilde{\theta}-\theta))\delta(x)\right)\right].\end{aligned}$$

The advantage gained by this representation is that it permits us to replace $\cos(2\theta(0,\tau)) \to \cos(2\tilde{\theta}(\tau))$, whereupon the θ-dependence of the action becomes purely quadratic.

(c) Integrate out the field $\theta(x,\tau)$ to obtain the representation $\mathcal{Z} = \int D\theta\ e^{-S[\theta]}$,

$$\boxed{S_{\rm eff}[\theta] = \frac{1}{\pi T g}\sum_n \theta_n|\omega_n|\theta_{-n} + \gamma\int d\tau\cos(2\theta(\tau)),} \tag{4.55}$$

entirely in terms of a single time-dependent degree of freedom $\theta(\tau)$.

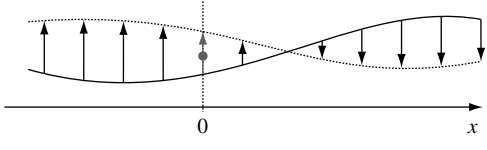

Notice that the entire effect of the bulk of the electron gas at $x \neq 0$ went into the first, dissipative term. We have, thus, reduced the problem to one involving a single time-dependent degree of freedom subject to a dissipative damping mechanism and a periodic potential (cf. our discussion of this problem in Problem 3.5 above).

INFO To understand the **physical origin of the dissipative damping mechanism** notice that, in the absence of the impurity, the system is described by a set of harmonic oscillators. We can thus think of the degree of freedom $\theta(0,\tau)$ as the coordinate of a "bead" embedded into an infinitely extended harmonic chain. From the point of view of this bead, the neighboring degrees of freedom hamper its free kinematic motion, i.e., in order to move, the bead has to drag an

entire "string" of oscillators behind. In other words, a local excitation of the $x = 0$ oscillator will lead to the dissipation of kinetic energy into the continuum of neighboring oscillators. Clearly, the rate of dissipation will increase with both the stiffness of the oscillator chain (g^{-1}) and the frequency of the excitation (ω_n), as described by the first term in the last operator in Eq. (4.55).

Answer:

(a) Consider the gauge transformation $\psi_+(x,\tau) \to e^{-iv_{\rm F}^{-1}v_+\theta(x)}$. While $S_{\rm int}$ and $S_{\rm imp}$ are gauge invariant and do not change, substitution of the transformed field into the non-interacting action leads to

$$S_0[\psi^\dagger,\psi] \to S_0[\psi^\dagger,\psi] - v_+ \int d\tau\, \psi_+^\dagger \psi_+.$$

The induced term cancels against the v_+ contribution to $S_{\rm imp}$. A similar transformation removes the v_- contribution. The physical reason for the insignificance of the forward scattering operators is that they describe the scattering of states $|\pm k_{\rm F}\rangle$ into the same states $|\pm k_{\rm F}\rangle$. The optional phase shift picked up in these processes is removed by the transformation above.

(b) This involves an elementary Gaussian integral.

(c) Expressed in momentum space, the effective action assumes the form

$$\begin{aligned} e^{-S[\tilde\theta]} &= \int D\theta\; Dk\; \exp\Big[-\frac{T}{L}\sum_{q,\omega_n}\Big[\frac{1}{2\pi g}\left(vq^2+v^{-1}\omega_n^2\right)|\theta_{q,n}|^2 + ik_n\theta_{q,-n}\Big] \\ &\qquad\qquad -ik_n\tilde\theta_{-n} - S_{\rm imp}[\tilde\theta]\Big] \\ &= \int Dk\; \exp\left[-\frac{\pi g T}{2L}\sum_{q,\omega_n} k_n (vq^2+v^{-1}\omega_n^2)^{-1}k_{-n} - ik_n\tilde\theta_{-n} - S_{\rm imp}[\tilde\theta]\right] \\ &= \mathcal{N}\int Dk\; \exp\left[-\frac{\pi T g}{4}\sum_{\omega_n} k_n|\omega_n|^{-1}k_{-n} - ik_n\tilde\theta_{-n} - S_{\rm imp}[\tilde\theta]\right] \\ &= \exp\left[-\frac{1}{\pi T g}\sum_n \tilde\theta_n|\omega_n|\tilde\theta_{-n} - S_{\rm imp}[\tilde\theta]\right]. \end{aligned}$$

Denoting $\tilde\theta(\tau)$ by $\theta(\tau)$, we obtain the effective action Eq. (4.55).

5

Perturbation theory

In this chapter, we introduce the analytical machinery to investigate the properties of many-body systems perturbatively. Specifically, employing the "ϕ^4-theory" as an example, we learn how to describe systems that are not too far from a known reference state by perturbative means. Diagrammatic methods are introduced as a tool to e ciently implement perturbation theory at large orders. The new concepts are then applied to the analysis of various properties of the weakly interacting electron gas.

In previous chapters we have emphasized repeatedly that the majority of many-particle problems cannot be solved in closed form. Therefore, in general, one is compelled to think about approximation strategies. One promising *ansatz* leans on the fact that, when approaching the low-temperature physics of a many-particle system, we often have some idea, however vague, of its preferred states and/or its low-energy excitations. One may then set out to explore the system by using these prospective ground state configurations as a working platform. For example, one might expand the Hamiltonian in the vicinity of the reference state and check that, indeed, the residual "perturbations" acting in the low-energy sector of the Hilbert space are weak and can be dealt with by some kind of approximate expansion. Consider, for example, the quantum Heisenberg magnet. In dimensions higher than one, an exact solution of this system is out of the question. However, we know (or, more conservatively, "expect") that, at zero temperature, the spins will be frozen into configurations aligned along some (domain-wise) constant magnetisation axes. Residual fluctuations around these configurations, described by the Holstein–Primakoff boson excitations, or spin waves, discussed before can be described in terms of a controlled expansion scheme. Similar programs work for countless other physical systems.

These considerations dictate much of our further strategy. We will need to construct methods to identify and describe the lowest-energy configurations of many-particle systems – often called "mean-fields" – and learn how to implement perturbation theory around them. In essence, the first part of that program amounts to solving a variational problem, a relatively straightforward task. However, the formulation of perturbation strategies requires some preparation and, equally important, a good deal of critical caution (because many systems notoriously defy perturbative assaults – a fact easily overlooked or misjudged!). We thus turn the logical sequence of the two steps upside down and devote *this* chapter to an introduction to many-body perturbation theory. This will include a number of applications, i.e. problems where the mean-field is trivial and perturbation theory on its own suffices to

produce meaningful results. Perturbation theory superimposed on non-trivial mean-fields will then be the subject of the next chapter.

5.1 General structures and low-order expansions

As with any other perturbative approach, many-body perturbation theory amounts to an expansion of observables in powers of some parameter – typically the coupling strength of an interaction operator. However, before discussion of how this program is implemented in practice, it is imperative to develop some understanding of the mathematical status of such "series expansions." (To motivate the point: it may, and often *does*, happen that the infinite-order expansion in the "small parameter" of the problem does not exist in a mathematical sense!) This can be achieved by considering the following.

An instructive integral

Consider the integral

$$I(g) = \int_{-\infty}^{\infty} \frac{dx}{\sqrt{2\pi}} \exp\left[-\frac{1}{2}x^2 - gx^4\right]. \tag{5.1}$$

This can be regarded as a caricature of a particle subject to some harmonic potential (x^2) together with an "interaction" (x^4). For small $g \ll 1$, it seems natural to treat the interaction perturbatively, i.e. to develop the expansion $I(g) \approx \sum_n g^n I_n$, where, applying Stirling's approximation, $n! \overset{n\gg 1}{\sim} n^n e^{-n}$,

$$g^n I_n = \frac{(-g)^n}{n!} \int_{-\infty}^{\infty} \frac{dx}{\sqrt{2\pi}} e^{-\frac{1}{2}x^2} x^{4n} = (-g)^n \frac{(4n-1)!!}{n!} \overset{n\gg 1}{\sim} \left(-\frac{gn}{e}\right)^n.$$

This estimate should alarm us: strictly speaking, it states that a series expansion in the "small parameter" g does not exist. No matter how small g, at roughly the $(1/g)$th order in the perturbative expansion the series begins to diverge. In fact, it is easy to predict this breakdown on qualitative grounds: for $g > 0$ ($g < 0$), the integral (5.1) is convergent (divergent). This implies that the series expansion of the function $I(g)$ around $g = 0$ must have zero radius of convergence.

However, there is also a more "physical" way of understanding the phenomenon. Consider a one-dimensional version of Eq. (3.16), where the 'Gaussian average' is given by Eq. (3.15):

$$\int_{-\infty}^{\infty} \frac{dx}{\sqrt{2\pi}} e^{-\frac{1}{2}x^2} x^{4n} = \sum_{\substack{\text{all possible} \\ \text{pairings of } 4n \text{ objects}}} 1 = (4n-1)!!.$$

The factor $(4n-1)!!$ measures the combinatorial freedom to pair up $4n$ objects. This suggests an interpretation of the breakdown of the perturbative expansion as the result of a competition between the smallness of the expansion parameter g and the combinatorial proliferation of equivalent contributions, or "pairings," to the Gaussian integral. Physically, the combinatorial factor can be interpreted as the number of different "partial amplitudes" contributing to the net result at any given order of perturbation theory. Eventually, the

exponential growth of this figure overpowers the smallness of the expansion parameter, which is when perturbation theory breaks down. (Oddly the existence of this rather general mechanism is usually not mentioned in textbook treatments of quantum perturbation theory!)

Does the ill-convergence of the series imply that perturbative approaches to problems of the structure of Eq. (5.1) are doomed to fail? Fortunately, this is not the case. While the infinite series $\sum_{n=0}^{\infty} g^n I_n$ is divergent, a partial resummation $\sum_{n=0}^{n_{\max}} g^n I_n$ can yield excellent approximations to the exact result $I(g)$. To see this, let us use the fact that $|e^{-gx^4} - \sum_{n=0}^{n_{\max}} \frac{(-gx^4)^n}{n!}| \leq \frac{(gx^4)^{n_{\max}+1}}{(n_{\max}+1)!}$ to estimate the error

$$\left| I(g) - \sum_{n=0}^{n_{\max}} g^n I_n \right| \leq g^{n_{\max}+1} |I_{n_{\max}+1}| \overset{n_{\max}\gg 1}{\sim} \left(\frac{g n_{\max}}{e}\right)^{n_{\max}}.$$

Variation with respect to $n_{\max}$ shows that the error reaches its minimum when $n_{\max} \sim g^{-1}$ where it scales like $e^{-1/g}$. (Notice the exponential dependence of the error on the coupling g – e.g. for a small coupling $g \approx 0.01$, the 100th order of the perturbation theory would lead to an approximation of astronomic absolute precision e^{-100}.) By contrast, for $g \approx 0.3$, perturbation theory becomes poor after the third order!

Summarizing, the moral to be taken from the analysis of the integral (5.1) (and its generalizations to theories of a more complex structure) is that perturbative expansions should not be confused with rigorous Taylor expansions. Rather they represent **asymptotic expansions**, in the sense that, for weaker and weaker coupling, a *partial* resummation of the perturbation series leads to an ever more precise approximation to the exact result. For weak enough coupling the distinction between Taylor expansion and asymptotic expansion becomes academic (at least for physicists). However, for intermediate or strong coupling theories, the asymptotic character of perturbation theory must be kept in mind.

ϕ^4-theory

While the ordinary integral discussed in the previous section conveyed something of the general status of perturbation theory, we need to proceed to the level of functional integrals to learn more about the practical implementation of perturbative methods. The simplest interacting field theory displaying all relevant structures is defined through the field integral

$$\mathcal{Z} \equiv \int D\phi\, e^{-S[\phi]}, \quad S[\phi] \equiv \int d^d x \left(\frac{1}{2}(\partial\phi)^2 + \frac{r}{2}\phi^2 + g\phi^4\right), \tag{5.2}$$

where ϕ is a scalar bosonic field. Owing to the structure of the interaction, this model is often referred to as the ϕ^4**-theory**. The ϕ^4-model not only provides a prototypical environment in which features of interacting field theories can be explored, but also appears in numerous applications. For example, close to its critical point, the d-dimensional Ising model is described by the ϕ^4-action (see Info below). More generally, it can be shown that the long-range behavior of classical statistical systems with a single order parameter (e.g.

the density of a fluid, uniaxial magnetization, etc.) is described by the ϕ^4-action.[1] Within the context of statistical mechanics, $S[\phi]$ is known as the **Ginzburg–Landau free energy functional** (and less frequently also as the **Landau–Wilson model**).

INFO The d-dimensional **Ising model** describes the classical magnetism of a lattice of magnetic moments $S_i \in \{1, -1\}$ that can take only two values ± 1. It is defined through the Hamiltonian

$$H_{\text{Ising}} = \sum_{ij} S_i C_{ij} S_j - H \sum_i S_i, \tag{5.3}$$

where $C_{ij} = C(|i-j|)$ is a (translationally invariant) correlation matrix describing the mutual interaction of the spins, H is an external magnetic field, and the sums run over the sites of a d-dimensional lattice (assumed hypercubic for simplicity). The Ising model represents the simplest Hamiltonian describing classical magnetism. In low dimensions $d = 1, 2$, it can be solved exactly, i.e. the partition function and all observables depending on it can be computed rigorously (see our discussion in Chapter 8). However, for higher dimensions, no closed solutions exist and one has to resort to approximation strategies to analyze the properties of the partition function. Below we will show that the long-range physics of the system is described by ϕ^4-theory. Notice that (save for the exceptional case $d = 1$ discussed in Section 8.1) the system is expected to display a magnetic phase transition. As a corollary this implies that the ϕ^4-model must exhibit much more interesting behavior than its innocent appearance suggests!

Consider the classical partition function

$$\mathcal{Z} = \sum_{\{S_i\}} e^{\sum_{ij} S_i K_{ij} S_j + \sum_i h_i S_i}, \tag{5.4}$$

where $K \equiv -\beta C$, and $h_i \equiv \beta H_i$, and we have generalized Eq. (**??**) to the case of a spatially varying magnetic field, H_i. The feature that prevents us from rigorously computing the configurational sum is, of course, the interaction between the spins. However, at a price, the interaction can be removed: let us consider the "fat unity," $1 = \mathcal{N} \int D\psi \, e^{-\frac{1}{4} \sum_{ij} \ i(K^{-1})_{ij} \ j}$, where $D\psi \equiv \ _i d\psi_i$, K^{-1} is the inverse of the correlation matrix, and $\mathcal{N} = 1/\sqrt{\det(4\pi K)}$ is a factor normalizing the integral to unity. A shift of the integration variables, $\psi_i \to \psi_i - 2\sum_j K_{ij} \mathbf{S}_j$, brings the integral into the form

$$1 = \mathcal{N} \int D\psi \, e^{-\frac{1}{4} \sum_{ij} \ i(K^{-1})_{ij} \ j + \sum_i S_i \ i - \sum_{ij} S_i K_{ij} S_j}.$$

Incorporating the fat unity under the spin sum in the partition function, one obtains

$$\mathcal{Z} = \mathcal{N} \int D\psi \sum_{\{S_i\}} e^{-\frac{1}{4} \sum_{ij} \ i(K^{-1})_{ij} \ j + \sum_i S_i(\ i + h_i)}. \tag{5.5}$$

Thus, we have removed the interaction between the spin variables at the expense of introducing a new continuous field $\{\psi_i\}$. Why should one do this? A multi-dimensional integral $\int D\psi$ is usually easier to work with than a multi-dimensional sum $\sum_{\{S_i\}}$ over discrete objects. Moreover, the new representation may provide a more convenient platform for approximation strategies. The

[1] Heuristically, this is explained by the fact that $S[\phi]$ is the simplest interacting (i.e. non-Gaussian) model action invariant under inversion $\phi \to -\phi$. (The action of a uniaxial magnet should depend on the value of the local magnetization, but not on its sign.) A purely Gaussian theory might describe wave-like fluctuations of the magnetization, but not the "critical" phenomenon of a magnetic transition. One thus needs, at least, a ϕ^4-interaction term. Later on we will see that more complex monomials of ϕ, such as ϕ^6 or $(\partial\phi)^4$, are inessential in the long-range limit.

transformation leading from Eq. (5.4) to (5.5) is our first example of a **Hubbard–Stratonovich transformation**. The interaction of one field is decoupled at the expense of the introduction of another. Notice that, in spite of the somewhat high-minded designation, the transformation is tantamount to a simple shift of a Gaussian integration variable, a feature shared by all Hubbard–Stratonovich transformations!

The summation $\sum_{\{S_i\}} = \quad_i \sum_{S_i}$ can now be trivially performed:

$$\begin{aligned} \mathcal{Z} &= \mathcal{N} \int D\psi \, e^{-\frac{1}{4}\sum_{ij} \quad i(K^{-1})_{ij} \quad j} \prod_i (2\cosh(\psi_i + h_i)) \\ &= \mathcal{N} \int D\psi \, e^{-\frac{1}{4}\sum_{ij}(\quad i - h_i)(K^{-1})_{ij}(\quad j - h_j) + \sum_i \ln(\cosh \quad i)}, \end{aligned}$$

where we have absorbed the inessential factor $\quad_i 2$ into a redefinition of the normalization $\mathcal{N}$. Finally, changing integration variables from ψ_i to $\phi_i \equiv \frac{1}{2}\sum_j [K^{-1}]_{ij}\psi_j$, one arrives at the intermediate result

$$\mathcal{Z} = \mathcal{N} \int D\phi \, e^{-\sum_{ij} \phi_i K_{ij} \phi_j + \sum_i \phi_i h_i + \sum_i \ln\cosh(2\sum_j K_{ij}\phi_j)}.$$

This representation of the problem still does not look very inviting. To bring it into a form amenable to further analytical evaluation, we need to make the simplifying assumption that we are working at low temperatures such that the exponential weight $K_{ij} = \beta C(|i-j|)$ inhibits strong fluctuations of the field ϕ. More precisely, we assume that $|\phi_i| \ll 1$ and that the spatial profile of the field is smooth. To make use of these conditions, we switch to a Fourier representation, $\phi_i = \frac{1}{\sqrt{N}}\sum_{\mathbf{k}} e^{-i\mathbf{k}\cdot\mathbf{r}_i}\phi(\mathbf{k})$, $K_{ij} = \frac{1}{N}\sum_{\mathbf{k}} e^{-i\mathbf{k}\cdot(\mathbf{r}_i - \mathbf{r}_j)}K(\mathbf{k})$, and expand $\ln\cosh(x) = \frac{1}{2}x^2 - \frac{1}{12}x^4 + \cdots$. Noting that $(K\phi)(\mathbf{k}) = K(\mathbf{k})\phi(\mathbf{k}) = K(0)\phi(\mathbf{k}) + \frac{1}{2}\mathbf{k}^2 K''(0)\phi(\mathbf{k}) + \mathcal{O}(\mathbf{k}^4)$, we conclude that the low-temperature expansion of the action has the general structure

$$\begin{aligned} S[\phi] &= \sum_{\mathbf{k}} [\phi_{\mathbf{k}}(c_1 + c_2\mathbf{k}\cdot\mathbf{k})\phi_{-\mathbf{k}} + c_3\phi_{\mathbf{k}}h_{-\mathbf{k}}] \\ &\quad + \frac{c_4}{N}\sum_{\mathbf{k}_1,\ldots,\mathbf{k}_4} \phi_{\mathbf{k}_1}\phi_{\mathbf{k}_2}\phi_{\mathbf{k}_3}\phi_{\mathbf{k}_4}\delta_{\mathbf{k}_1+\mathbf{k}_2+\mathbf{k}_3+\mathbf{k}_4,\mathbf{0}} + \mathcal{O}(\mathbf{k}^4, h^2, \phi^6). \end{aligned}$$

EXERCISE Show that the coefficients c_i are given by $c_1 = K(0)(1-2K(0))$, $c_2 = \frac{1}{2}K''(0)(1-4K(0))$, $c_3 = 1$, $c_4 = \frac{4K(0)^4}{3}$.

Switching back to a real space representation and taking a continuum limit, $S[\phi]$ assumes the form of a prototypical ϕ^4-action

$$S[\phi] = \int d^d x \quad c_2(\partial\phi)^2 + c_1\phi^2 + c_3\phi h + c_4\phi^4 \quad .$$

A rescaling of variables $\phi \to \frac{1}{\sqrt{2c_2}}\phi$ finally brings the action into the form Eq. (5.2) with coefficients $r = c_1/c_2$ and $g = c_4/(2c_2)$.[2]

We have thus succeeded in describing the low-temperature phase of the Ising model in terms of a ϕ^4-model. While the structure of the action could have been guessed on symmetry grounds, the "microscopic" derivation has the advantage that it yields explicit expressions for the coupling constants. There is actually one interesting aspect of the dependence of these constants on the

[2] The only difference is that the magnetic ϕ^4-action contains a term linear in ϕ and h. The reason is that, in the presence of a finite magnetic field, the action is no longer invariant under inversion $\phi \to -\phi$.

parameters of the microscopic model. Consider the constant c_1 controlling the **k**-independent contribution to the Gaussian action: $c_1 \propto K(0)(1-2K(0)) \propto (1-2\beta C(0))$. Since $C(0)$ must be positive to ensure the overall stability of the model (exercise: why?) the constant c_1 will change sign at a certain "critical temperature" β^*. For temperatures lower than β^*, the Gaussian action is unstable (i.e. fluctuations with low wavevector become unbound) and the anharmonic term ϕ^4 alone controls the stability of the model. Clearly, the behavior of the system will change drastically at this point. Indeed, the critical temperature $c_1(\beta^*) = 0$ marks the position of the magnetic phase transition, a point to be discussed in more detail below.

Let us begin our primer of perturbation theory by introducing some nomenclature.[3] For simplicity, let us first define the notation

$$\langle \cdots \rangle \equiv \frac{\int D\phi\, e^{-S[\phi]}(\cdots)}{\int D\phi\, e^{-S[\phi]}}, \tag{5.6}$$

for the functional integral, weighted by the action S, of any expression $(\cdots)$. Due to the structural similarity to thermal averages of statistical mechanics, $\langle \cdots \rangle$ is sometimes called a **functional average** or **functional expectation value**. Similarly, let us define

$$\langle \cdots \rangle_0 \equiv \frac{\int D\phi\, e^{-S_0[\phi]}(\cdots)}{\int D\phi\, e^{-S_0[\phi]}}, \tag{5.7}$$

for the functional average over the Gaussian action $S_0 \equiv S|_{g=0}$. The average over a product of field variables,

$$C_n(\mathbf{x}_1, \mathbf{x}_2, \ldots, \mathbf{x}_n) \equiv \langle \phi(\mathbf{x}_1)\phi(\mathbf{x}_2)\cdots\phi(\mathbf{x}_n)\rangle, \tag{5.8}$$

is known as an **n-point correlation function** or, for brevity, just the **n-point function**.[4]

George Green 1793–1841
His only schooling consisted of four terms in 1801/1802. He owned and worked a Nottingham windmill. Green made major contributions to potential theory although where he learnt his mathematical skills is a mystery. The inventor of Green functions, he used the method of sources and sinks in potential flows. He published only ten mathematical works, the first and most important being published at his own expense in 1828, "An essay on the application of mathematical analysis to the theories of electricity and magnetism." He left his mill and became an undergraduate at Cambridge in 1833 at the age of 40, then a Fellow of Gonville and Caius College in 1839.

The one-point function $C_1(\mathbf{x}) = \langle \phi(\mathbf{x})\rangle$ simply measures the expectation value of the field amplitude. For the particular case of the ϕ^4-problem above the phase transition and, more generally, the majority of field theories with an action even in the field amplitudes, $C_1 = 0$ and the first non-vanishing correlation function is the two-point function

$$G(\mathbf{x}_1 - \mathbf{x}_2) \equiv C_2(\mathbf{x}_1, \mathbf{x}_2). \tag{5.9}$$

(Why does C_2 depend only on the *di erence* of its arguments?) The two-point function is sometimes also called the **propagator** of the theory, the **Green function** or, especially in the more formal literature, the **resolvent operator**.

[3] Needless to say, the jargon introduced below is not restricted to the ϕ^4 example!
[4] Notice that, depending on the context and/or scientific community, the phrase "n-point function" sometimes refers to C_{2n} instead of C_n.

The existence of different names suggests that we have met with an important object. Indeed, we will shortly see that the Green function not only represents a central building block of the theory but also carries profound physical significance.

INFO To develop some understanding of the **physical meaning of the correlation function**, let us recall that the average of a linear field amplitude, $\langle\phi(\mathbf{0})\rangle$, vanishes. (See the figure, where a diagram of a few "typical" field configurations is sketched as functions of a coordinate.)

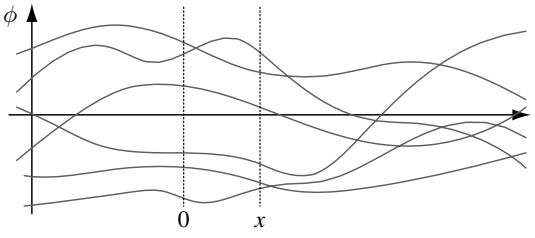

However, the average of the squared amplitude $(\phi(\mathbf{0}))^2$ is certainly non-vanishing simply because we are integrating over a positive object. Now, what happens if we split our single observation point into two, $\langle\phi^2(\mathbf{0})\rangle_0 \to \langle\phi(\mathbf{0})\phi(\mathbf{x})\rangle_0 = G(\mathbf{x})$? For asymptotically large values of $\mathbf{x}$, it is likely that the two amplitudes fluctuate independently of each other, i.e. $G(\mathbf{x}) \overset{|\mathbf{x}|\to\infty}{\longrightarrow} 0$. However, this decoupling will not happen locally. The reason is that the field amplitudes are correlated over a certain range in space. For example, if $\phi(\mathbf{0}) > 0$, the field amplitude will, on average, stay positive in an entire neighborhood of $\mathbf{0}$ since rapid fluctuations of the field are energetically costly (i.e. due to the gradient term in the action!). The spatial correlation profile of the field is described by the function $G(\mathbf{x})$.

How does the correlation behavior of the field relate to the basic parameters of the action? A quick answer can be given by **dimensional analysis**. The action of the theory must be dimensionless (because it appears as the argument of an exponential). Denoting the dimension of any quantity X by $[X]$, and using the fact that $\left[\int d^dx\right] = L^d$, $[\partial] = L^{-1}$, inspection of Eq. (5.2) obtains the set of relations

$$L^{d-2}[\phi]^2 = 1, \quad L^d[r][\phi]^2 = 1, \quad L^d[g][\phi]^4 = 1,$$

from which it follows that $[\phi] = L^{-(d-2)/2}$, $[r] = L^{-2}$, $[g] = L^{d-4}$. In general, both system parameters, g and r, carry a non-zero length-dimension. However, temporarily concentrating on the non-interacting sector, $g = 0$, the only parameter of the theory, r, has dimensionality L^{-2}. Arguing in reverse, we conclude that any intrinsic length scale produced by the theory (e.g. the range over which the fields are correlated), must scale as $\sim r^{-1/2}$.

A more quantitative description can be obtained by considering the **free propagator** of the theory,

$$G_0(\mathbf{x}) \equiv \langle\phi(\mathbf{0})\phi(\mathbf{x})\rangle_0. \tag{5.10}$$

Since the momentum representation of the Gaussian action is simply given by $S_0[\phi] = \frac{1}{2}\sum_{\mathbf{p}} \phi_{\mathbf{p}}(p^2 + r)\phi_{-\mathbf{p}}$, it is convenient to first compute G_0 in reciprocal space: $G_{0,\mathbf{p}} \equiv \int d^dx\, e^{i\mathbf{p}\cdot\mathbf{x}} G_0(\mathbf{x}) = \sum_{\mathbf{p}'}\langle\phi_{\mathbf{p}}\phi_{\mathbf{p}'}\rangle_0$. Using the Gaussian contraction rule Eq. (3.14), the free functional average takes the form $\langle\phi_{\mathbf{p}}\phi_{\mathbf{p}'}\rangle_0 = \delta_{\mathbf{p}+\mathbf{p}',0}(p^2 + r)^{-1}$, i.e.[5]

$$G_{0,\mathbf{p}} = \langle\phi_{\mathbf{p}}\phi_{-\mathbf{p}}\rangle_0 = \frac{1}{p^2 + r}. \tag{5.11}$$

[5] The result $G_{0,\mathbf{p}} = (p^2 + r)^{-1}$ clarifies why G is referred to as a "Green function." Indeed, $G_{0,\mathbf{p}}$ is (the Fourier representation of the) Green function of the differential equation $(-\partial_{\mathbf{r}}^2 + r)G(\mathbf{r}, \mathbf{r}') = \delta(\mathbf{r} - \mathbf{r}')$.

To obtain $G(\mathbf{x})$, we need to compute the inverse transform

$$G_0(\mathbf{x}) = \frac{1}{L^d}\sum_{\mathbf{p}} e^{-i\mathbf{p}\cdot\mathbf{x}} G_{0,\mathbf{p}} \approx \int \frac{d^d p}{(2\pi)^d}\frac{e^{-i\mathbf{p}\cdot\mathbf{x}}}{p^2+r}, \tag{5.12}$$

where we have assumed that the system is large, i.e. the sum over momenta can be exchanged for an integral.

For simplicity, let us compute the integral for a one-dimensional system. (For the two- and three-dimensional cases see exercise below.) Setting $p^2 + r = (p + ir^{1/2})(p - ir^{1/2})$, we note that the (complex extension of the) p integral has simple poles at $\pm ir^{1/2}$. For x smaller (larger) than zero, the integrand is analytic in the upper (lower) complex p-plane and closure of the integration contour to a semicircle of infinite radius gives

$$G_0(x) = \int \frac{dp}{2\pi}\frac{e^{-ipx}}{(p+ir^{1/2})(p-ir^{1/2})} = \frac{e^{-r^{1/2}|x|}}{2r^{1/2}}. \tag{5.13}$$

This result conveys an interesting observation: typically, correlations decay exponentially, at a rate set by the **correlation length** $\xi \equiv r^{-1/2}$. However, as r approaches 0, the system becomes long-range correlated. The origin of this phenomenon can be understood by inspecting the structure of the Gaussian contribution to the action (5.2). For $r \to 0$ (and still neglecting the ϕ^4 contribution) nothing prevents the constant field mode $\phi(\mathbf{x}) = \phi_0 = \text{const.}$ from becoming infinitely large, i.e. the fluctuating contribution to the field becomes relatively less important than the constant offset. The increasing "stiffness" of the field in turn manifests itself in a growth of spatial correlations (cf. the figure on page 201). Notice that this dovetails with our previous statement that $r = 0$ marks the position of a phase transition. Indeed, the build-up of infinitely long-range spatial correlations is known to be a hallmark of second-order phase transitions (see Chapter 8).

EXERCISE Referring to Eq. (5.12), show that, in dimensions $d = 2$ and $d = 3$,

$$G_0(\mathbf{x}) \overset{d=2}{=} \int \frac{d^2k}{(2\pi)^2}\frac{e^{-i\mathbf{k}\cdot\mathbf{x}}}{k^2+r} = \frac{1}{2\pi}K_0(\sqrt{r}|\mathbf{x}|) = \begin{cases} -\frac{1}{2\pi}\ln\frac{\sqrt{r}|\mathbf{x}|}{2}, & |\mathbf{x}| \ll 1/\sqrt{r}, \\ \frac{1}{2}(2\pi\sqrt{r}|\mathbf{x}|)^{-\frac{1}{2}}e^{-\sqrt{r}|\mathbf{x}|}, & |\mathbf{x}| \gg 1/\sqrt{r}, \end{cases}$$

$$G_0(\mathbf{x}) \overset{d=3}{=} \int \frac{d^3k}{(2\pi)^3}\frac{e^{-i\mathbf{k}\cdot\mathbf{x}}}{k^2+r} = \frac{e^{-\sqrt{r}|\mathbf{x}|}}{4\pi|\mathbf{x}|}.$$

Notice that, in both cases, the Green function diverges in the limit $|\mathbf{x}| \to 0$ and decays exponentially (at a rate $\sim r^{-1/2}$) for $|\mathbf{x}| \gg r^{-1/2}$.

Perturbation theory at low orders

Having discussed the general structure of the theory and of its free propagator, let us turn our attention to the role of the interaction contribution to the action,

$$S_{\text{int}}[\phi] \equiv g\int d^d x\, \phi^4.$$

Within the jargon of field theory, an integrated monomial of a field variable (like ϕ^4) is commonly called an **(interaction) operator** or a **vertex (operator)**. Keeping in mind the words of caution given in Section 5.1, we wish to explore perturbatively how the interaction

vertex affects the functional expectation value of any given field observable, i.e. we wish to analyze expansions of the type

$$\langle X[\phi]\rangle \approx \frac{\sum_{n=0}^{\cdots} \frac{(-g)^n}{n!}\langle X[\phi](\int d^dx\,\phi^4)^n\rangle_0}{\sum_{n=0}^{\cdots} \frac{(-g)^n}{n!}\langle (\int d^dx\,\phi^4)^n\rangle_0} \approx \sum_{n=0}^{n_{\max}} X^{(n)}, \tag{5.14}$$

where X may be any observable and $X^{(n)}$ denotes the contribution of nth order to the expansion in g. The limits on the summation in the numerator and denominator are symbolic because, as explained above, we will need to terminate the total perturbative expansion at a certain finite order $n_{\max}$.

EXERCISE To navigate the following section, it is helpful to recapitulate Section 3.2 on continuum Gaussian integration.

To keep the discussion concrete, let us focus on the perturbative expansion of the propagator in the coupling constant, g. (A physical application relating to this expansion will be discussed below.) The zeroth-order contribution $G^{(0)} = G_0$ has been discussed before, so the first non-trivial term we have to explore is $G^{(1)}$:

$$G^{(1)}(\mathbf{x},\mathbf{x}') = -g\Big(\phi(\mathbf{x})\int d^dy\,\phi(\mathbf{y})^4\phi(\mathbf{x}')\Big\rangle_0 - \phi(\mathbf{x})\phi(\mathbf{x}')\Big\rangle_0 \int d^dy\,\phi(\mathbf{y})^4\Big\rangle_0\Big). \tag{5.15}$$

Since the functional average is now over a Gaussian action, this expression can be evaluated by Wick's theorem, Eq. (3.21). For example, the functional average of the first of the two terms leads to (integral signs and constants stripped off for clarity)

$$\begin{aligned}\big\langle \phi(\mathbf{x})\phi(\mathbf{y})^4\phi(\mathbf{x}')\big\rangle_0 &= 3\langle\phi(\mathbf{x})\phi(\mathbf{x}')\rangle_0\,[\langle\phi(\mathbf{y})\phi(\mathbf{y})\rangle_0]^2 \\ &\quad +12\langle\phi(\mathbf{x})\phi(\mathbf{y})\rangle_0\langle\phi(\mathbf{y})\phi(\mathbf{y})\rangle_0\langle\phi(\mathbf{y})\phi(\mathbf{x}')\rangle_0 \\ &= 3G_0(\mathbf{x}-\mathbf{x}')G_0(\mathbf{0})^2 + 12G_0(\mathbf{x}-\mathbf{y})G_0(\mathbf{0})G_0(\mathbf{y}-\mathbf{x}'),\end{aligned} \tag{5.16}$$

where we have used the fact that the operator inverse of the Gaussian action is, by definition, the free Green function (cf. Eq. (5.10)). Further, notice that the total number of terms appearing on the right-hand side is equal to $15 = (6-1)!!$ which is just the number of distinct pairings of six objects (cf. Eq. (3.21) and with our discussion of Section 5.1). Similarly, the second contribution to $G^{(1)}$ leads to

$$\langle\phi(\mathbf{x})\phi(\mathbf{x}')\rangle_0\langle\phi(\mathbf{y})^4\rangle_0 = 3\langle\phi(\mathbf{x})\phi(\mathbf{x}')\rangle_0[\langle\phi(\mathbf{y})^2\rangle_0]^2 = 3G_0(\mathbf{x}-\mathbf{x}')G_0(\mathbf{0})^2.$$

Before analyzing these structures in more detail, let us make some general observations. The first-order expansion of G contains a number of factors of $G_0(\mathbf{0})$, the free Green function evaluated at coinciding points. This bears disturbing consequences. To see this, consider $G_0(\mathbf{0})$ evaluated in momentum space:

$$G_0(\mathbf{0}) = \int \frac{d^dp}{(2\pi)^d}\frac{1}{p^2+r}. \tag{5.17}$$

For dimensions $d > 1$, the integral is divergent at large momenta or short wavelengths; we have met with an **ultraviolet (UV) divergence**. Physically, the divergence implies that,

already at first order, our expansion runs into a difficulty that is obviously related to the short-distance structure of the system. How can this problem be overcome? One way out is to remember that field theories like the ϕ^4-model represent effective low-temperature, or long-wavelength, approximations to more microscopic models. The range of applicability of the action must be limited to wavelengths in excess of some microscopic lattice cutoff a (e.g. the lattice spacing), or momenta $k < a^{-1}$. It seems that, once that cutoff has been built in, the convergence problem is solved. However, there is something unsatisfactory in this argument. All our perturbative corrections, and therefore the final result of the analysis, exhibit sensitivity to the microscopic cutoff parameter. But this is not what we expect of a sensible low-energy theory (cf. the discussion of Chapter 1)! The UV problem signals that something more interesting is going on than a naive cutoff regularization has the capacity to describe. We discuss this point extensively in Chapter 8.

However, even if we temporarily close our eyes to the UV-phenomenon, there is another problem. For dimensions $d \leq 2$, and in the limit $r \to 0$, $G_0(\mathbf{0})$ also diverges at **small momenta**, an **infrared (IR) divergence**. Being related to structures at large wavelengths, this type of singularity should attract our attention even more than the UV-divergence mentioned above. Indeed, it is intimately related to the accumulation of long-range correlations in the limit $r \to 0$ (cf. the structure of the integral (5.12)). We come back to the discussion of the IR singularities, and their connection to the UV phenomenon, in Chapter 8.

The considerations above show that the perturbative analysis of functional integrals will be accompanied by all sorts of divergences. Moreover, there is another, less fundamental, but also important, point: referring to Eq. (5.16), we have to concede that the expression does not look particularly inviting. To emphasize the point, let us consider the core contribution to the expansion at second order in g.

EXERCISE Show that the 10th-order contraction leads to the 945=(10-1)!! terms

$$\begin{aligned}
&\left\langle \phi(\mathbf{x})\phi(\mathbf{y})^4\phi(\mathbf{y}')^4\phi(\mathbf{x}')\right\rangle_0 = 9G_0(\mathbf{x}-\mathbf{x}')G_0(\mathbf{0})^4 + 72G_0(\mathbf{x}-\mathbf{x}')G_0(\mathbf{y}-\mathbf{y}')^2G_0(\mathbf{0})^2 \\
&+24G_0(\mathbf{x}-\mathbf{x}')G_0(\mathbf{y}-\mathbf{y}')^4 + \big[36G_0(\mathbf{x}-\mathbf{y})G_0(\mathbf{x}'-\mathbf{y})G_0(\mathbf{0})^3 \\
&+144(G_0(\mathbf{x}-\mathbf{y})G_0(\mathbf{x}'-\mathbf{y})G_0(\mathbf{y}-\mathbf{y}')^2G_0(\mathbf{0}) + G_0(\mathbf{x}-\mathbf{y})G_0(\mathbf{x}'-\mathbf{y}')G_0(\mathbf{0})^2G_0(\mathbf{y}-\mathbf{y}')) \\
&+96G_0(\mathbf{x}-\mathbf{y})G_0(\mathbf{x}'-\mathbf{y}')G_0(\mathbf{y}'-\mathbf{y})^3 + (\mathbf{y} \quad \mathbf{y}')\big] . \qquad (5.18)
\end{aligned}$$

Note: Our further discussion will not rely on this result. It only serves an illustrative purpose.

Clearly Eq. (5.18) is highly opaque. There are eight groups of different terms, but it is not obvious how to attribute any meaning to these contributions. Further, should we consider the full second-order Green function $G^{(2)}$, i.e. take account of the expansion of both numerator and denominator in Eq. (5.14), we would find that some contributions cancel (see Problem 5.5). Clearly, the situation will not improve at third and higher orders in g.

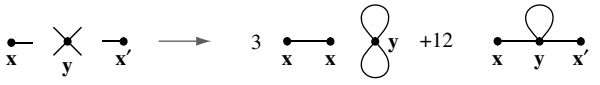

Figure 5.1 Graphical representation of a first-order-in-g contraction contributing to the expansion of the Green function.

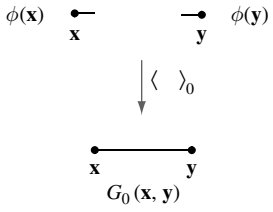

To efficiently apply perturbative concepts beyond lowest orders, a more efficient formulation of the expansion is needed. The key to the construction of a better language lies in the observation that our previous notation is full of redundancy, i.e. in the full contraction of a perturbative contribution, we represent our fields by $\phi(\mathbf{x})$. A more compact way of keeping track of the presence of that field is shown in the upper portion of the figure to the right. Draw a point (with an optional "$\mathbf{x}$" labeling its position) and attach a little leg to it. The leg indicates that the fields are sociable objects, i.e. they need to find a partner with which to pair. After the contraction, a pair $\langle\phi(\mathbf{x})\phi(\mathbf{y})\rangle \to G_0(\mathbf{x}-\mathbf{y})$ becomes a free Green function. Graphically, this information can be represented by a pairwise connection of the legs of the field symbols to lines, where each line is identified with a Green function connecting the two terminating points. The full contraction of a free correlation function $\langle\phi(\mathbf{x}_1)\phi(\mathbf{x}_2)\cdots\phi(\mathbf{x}_{2n})\rangle_0$ is represented by the set of all distinct diagrams formed by pairwise connection of the field vertices.

Figure 5.1 shows the graphical representation of the contraction of Eq. (5.16). (The cross appearing on the left-hand side represents four field operators sitting at the same point $\mathbf{y}$.) According to our rule formulated above, each of the two diagrams on the right-hand side represents the product of three Green functions, taken between the specified coordinates. Further, each contribution is weighted by a combinatorial factor, i.e. the number of identical diagrams of that structure. Consider, for example, the second contribution on the right-hand side. It is formed by connecting the "external" field vertex at $\mathbf{x}$ to any of the legs of the internal vertex at $\mathbf{y}$: four possibilities. Next, the vertex at $\mathbf{x}'$ is connected with one of the remaining three unsaturated vertices at $\mathbf{y}$: three possibilities. The last contraction $\mathbf{y} \leftrightarrow \mathbf{y}$ is fixed, i.e. we obtain altogether $3 \times 4 = 12$ equivalent diagrams – "equivalent" in that each of these represents the same configuration of Green functions.

EXERCISE Verify that the graphical representation of the second-order contraction Eq. (5.18) is as shown in Fig. 5.2.[6] Associate the diagrams with individual contributions appearing in Eq. (5.18) and try to reproduce the combinatorial factors. (For more details, see Problem 5.5.)

The graphical representation of the contractions shown in Fig. 5.1 and 5.2 provides us with sufficient background to list some general aspects of the diagrammatic approach:

[6] In the figure, the coordinates carried by the field vertices have been dropped for notational simplicity. To restore the full information carried by any of these "naked" graphs one attaches coordinates $\mathbf{x}$ and $\mathbf{x}'$ to the external field vertices and integration coordinates $\mathbf{y}_i$ to each of the i nodes that do not connect to an external field vertex. Since no information is lost, diagrams are often represented without explicit reference to coordinates.

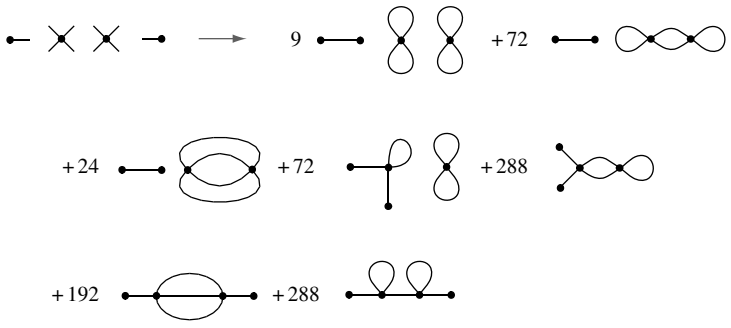

Figure 5.2 Graphical representation of the second-order correction to the Green function. In the main text, the seven types of diagram contributing to the contraction will be referred to (in the order they appear above) as diagrams 1 to 7.

- ▷ Firstly, diagrammatic methods help to efficiently *represent* the perturbative expansion. However, we are still left with the problem (see the discussion above) of *computing* the analytical expressions corresponding to individual diagrams. To go back from an nth-order graph to its analytical representation one (i) attaches coordinates to all field vertices, (ii) identifies lines between points with Green functions, (iii) multiplies the graph by the overall constant $g^n/n!$, and (iv) integrates over all of the internal coordinates. When one encounters expressions like $G^{(n)}$ = "sum of graphs," the operations (i)–(iv) are implicit.
- ▷ As should be clear from the formulation of our basic rules, there is no fixed rule as to how to represent a diagram. As long as no lines are cut, any kind of reshaping, twisting, rotating, etc. of the diagram leaves its content invariant. (At large orders of perturbation theory, it often takes a second look to identify two diagrams as equivalent.)
- ▷ From the assembly of diagrams contributing to any given order, a number of internal structures common to the series expansion become apparent. For example, looking at the diagrams shown in Fig. 5.2, we notice that some are connected, and some are not. Among the set of **connected diagrams** (nos. 5, 6, 7) there are some whose "core portion," i.e. the content of the diagram after the legs connecting to the external vertices have been removed, can be cut into two pieces just by cutting one more line (no. 7). Diagrams of this type are called **one-particle reducible** while the others are termed one-particle irreducible. More generally, a diagram whose core region can be cut by severing n lines is called **n-particle reducible**. (For example, no. 6 is three-particle reducible, no. 7 one-particle reducible, etc.) One can also attach a **loop order** to a diagram, i.e. the number of inequivalent loops formed by segments of Green functions (for Fig. 5.2: 4, 3, 3, 3, 2, 2, 2, in that order). One (correctly) expects that these structures, which are difficult to discern from the equivalent analytical representation, will reflect themselves in the mathematics of the perturbative expansion. We return to the discussion of this point below.
- ▷ Then there is the issue of **combinatorics**. The diagrammatic representation simplifies the determination of the combinatorial factors appearing in the expansion. However, the problem of getting the combinatorics right remains non-trivial. (If you are not impressed with the factors entering the second-order expansion, consider the $(14-1)!! = 135135$

terms contributing at third order!) In some sub-disciplines of theoretical physics, the art of identifying the full set of combinatorial coefficients at large orders of perturbation theory has been developed to a high degree of sophistication. Indeed, one can set up refined sets of diagrammatic construction rules which to a considerable extent automate the combinatorics. Pedagogical discussions of these rules can be found, for example, in the textbooks by Negele and Orland, and Ryder.[7] However, as we will see shortly, the need to explicitly carry out a large-order expansion, with account of all diagrammatic sub-processes, rarely arises in modern condensed matter physics; mostly one is interested in subclasses of diagrams, for which the combinatorics is less problematic. For this reason, the present text does not contain a state-of-the-art exposition of all diagrammatic tools and interested readers are referred to the literature.

▷ Finally, and perhaps most importantly, the diagrammatic representation of a given contribution to the perturbative expansion often suggests a **physical interpretation** of the corresponding physical process. (After all, any term contributing to the expansion of a physical observable must correspond to some "real" physical process.) Unfortunately, the ϕ^4-theory is not well suited to illustrate this aspect, i.e., being void of any dynamical content, it is a little bit too simple. However, the possibility of "reading" individual diagrams will become evident in the next section when we discuss an application to the interacting electron gas.

Above we have introduced the diagrammatic approach on the example of field expectation values $\langle\phi(\mathbf{x})(\phi(\mathbf{y})^4)^n\phi(\mathbf{x}')\rangle_0$. However, to obtain the Green function to any given order in perturbation theory, we need to add to these expressions the contributions emanating from the expansion of the denominator of the functional average (cf. Eq. (5.14) and (5.15)). While, at first sight, the need to keep track of even more terms seems to complicate matters, we will see that, in fact, quite the opposite is true! The combined expansion of numerator and denominator leads to a miraculous "cancellation mechanism" that greatly simplifies the analysis.

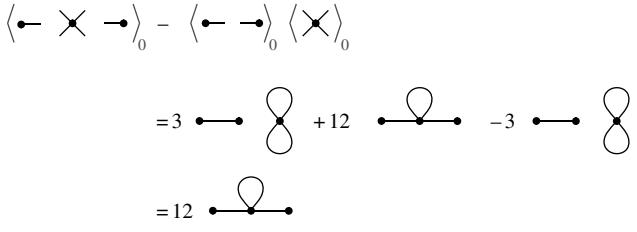

Figure 5.3 Graphical representation of the first-order correction to the Green function: vacuum graphs cancel out.

Let us exemplify the mechanism of cancellation on $G^{(1)}$. The three diagrams corresponding to the contractions of Eq. (5.15) are shown in Fig. 5.3, where integral signs and coordinates are dropped for simplicity. On the left-hand side of the equation, the brackets $\langle\cdots\rangle_0$

[7] J. W. Negele and H. Orland, *Quantum Many Particle Systems* (Addison-Wesley, 1988); L. H. Ryder, *Quantum Field Theory* (Cambridge University Press, 1996).

indicate that the second contribution comes from the expansion of the denominator. The point to be noticed is that the graph produced by the contraction of that term cancels against a contribution arising from the numerator. One further observes that the canceled graph is of a special type: it contains an interaction vertex that does not connect to any of the external vertices. Diagrams with that property are commonly termed **vacuum graphs**.[8]

EXERCISE Construct the diagrammatic representation of $G^{(2)}$ and verify that the expansion of the denominator eliminates all vacuum graphs of the numerator. In particular, show that $G^{(2)}$ is given by the sum of connected diagrams shown in Fig. 5.4. (For more details, see Problem 5.5.)

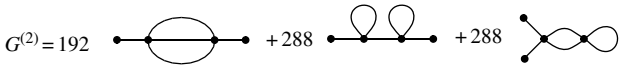

Figure 5.4 Graphical representation of the second-order contribution to the Green function.

Indeed, the cancellation of vacuum graphs pertains to higher-order correlation functions and to all orders of the expansion:

> The contribution to a correlation function $C^{(2n)}(\mathbf{x}_1, \ldots, \mathbf{x}_{2n})$ at lth order of perturbation theory is given by the sum of all graphs, excluding vacuum graphs.

For example, the first-order expansion of the four-point function $C^{(4)}(\mathbf{x}_1, \ldots \mathbf{x}_4)$ is shown in the figure, where coordinates $\mathbf{x}_i \leftrightarrow i$ are abbreviated by indices and "+ perm." stands for the six permutations obtained by interchanging arguments. In the literature, the statement of vacuum graph cancellation is sometimes referred to as the **linked cluster theorem**. Notice that the linked cluster feature takes care of two problems: firstly we are relieved of the burden of a double expansion of numerator and denominator, and secondly only non-vacuum contributions to the expansion of the former need to be kept.

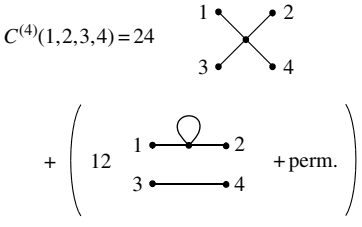

INFO The **proof of the linked cluster theorem** is straightforward. Consider a contribution of nth order to the expansion of the numerator of Eq. (5.14): $\frac{(-g)^n}{n!} \left\langle X[\phi] (\int d_x^d \phi^4)^n \right\rangle_0$. The contraction of this expression will lead to a sum of vacuum graphs of pth-order and non-vacuum graphs of $(n-p)$th-order, where p runs from 0 to n. The pth-order contribution is given by

$$\frac{1}{n!} \binom{n}{p} \left\langle X[\phi] \left(\int \phi^4 \right)^{n-p} \right\rangle_0^{\text{n.v.}} \left\langle \left(\int \phi^4 \right)^p \right\rangle_0 ,$$

where the superscript $\langle \cdots \rangle^{\text{n.v.}}$ indicates that the contraction excludes vacuum graphs and the combinatorial coefficient counts the number of possibilities to choose p vertices ϕ^4 of a total of n

[8] The term "vacuum graph" has its origin in the diagrammatic methods invented in the 1950s in the context of particle theory. Instead of thermal averages $\langle \cdots \rangle_0$, one considered matrix elements $\langle \Omega | \cdots | \Omega \rangle$ taken on the ground state or "vacuum" of the field theory. This caused matrix elements $\langle \Omega | (S_{\text{int}}[\phi])^n | \Omega \rangle$ not containing an external field vertex to be dubbed "vacuum graphs."

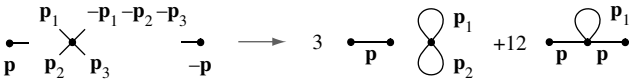

Figure 5.5 Momentum space representation of a first-order contribution to the Green function. Internal momenta $\mathbf{p}_i$ are integrated over.

vertices to form a vacuum graph. Summing over p, we find that the expansion of the numerator, split into vacuum and non-vacuum contributions, reads

$$\sum_{n=0}^{\infty}\sum_{p=0}^{n}\frac{(-g)^n}{(n-p)!\,p!}\left\langle X[\phi]\left(\int,\phi^4\right)^{n-p}\right\rangle_0^{\text{n.v.}}\left\langle\left(\int,\phi^4\right)^{p}\right\rangle_0 .$$

By a straightforward rearrangement of the summations, this can be rewritten as

$$\sum_{n=0}^{\infty}\frac{(-g)^n}{n!}\left\langle X[\phi]\left(\int,\phi^4\right)^{n}\right\rangle_0^{\text{n.v.}}\sum_{p=0}^{\infty}\frac{(-g)^p}{p!}\left\langle\left(\int,\phi^4\right)^{p}\right\rangle_0 .$$

The p-summation recovers exactly the expansion of the denominator, so we are left with the sum over all non-vacuum contractions.

Before concluding this section, let us discuss one last technical point. The translational invariance of the ϕ^4-action suggests a representation of the theory in reciprocal space. Indeed, the **momentum space representation** of the propagator Eq. (5.11) is much simpler than the real space form, and the subsequent analytical evaluation of diagrams will be formulated in momentum space anyway (cf. the prototypical expression (5.17)).

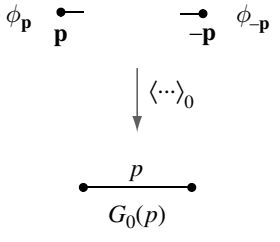

The diagrammatic formulation of the theory in momentum space is straightforward. All we need to do is to slightly adjust the graphical code. Inspection of Eq. (5.11) shows that the elementary contraction should now be formulated as indicated in the figure. Only fields with opposite momentum can be contracted; the line carries this momenta as a label. Notice that the momentum representation of the field vertex $\phi^4(\mathbf{x})$ is **not** given by $\phi^4_{\mathbf{p}}$. Rather, Fourier transformation of the vertex leads to the three-fold convolution

$$\int d^dx\,\phi^4(\mathbf{x}) \to \frac{1}{L^d}\sum_{\mathbf{p}_1,\dots,\mathbf{p}_4}\phi_{\mathbf{p}_1}\phi_{\mathbf{p}_2}\phi_{\mathbf{p}_3}\phi_{\mathbf{p}_4}\delta_{\mathbf{p}_1+\mathbf{p}_2+\mathbf{p}_3+\mathbf{p}_4}.$$

The graphical representation of the first-order correction to the Green function (i.e. the momentum space analog of Fig. 5.3) is shown in Fig. 5.5. It is useful to think about the vertices of the momentum-space diagrammatic language in the spirit of "Kirchhoff laws": the sum of all momenta flowing into a vertex is equal to zero. Consequently (exercise) the total sum of all momenta "flowing" into a diagram from external field vertices must also equal zero: $\langle\phi_{\mathbf{p}_1}\phi_{\mathbf{p}_2}\cdots\phi_{\mathbf{p}_n}\rangle_0 \to \delta_{\sum_{i=1}^n\mathbf{p}_i,\mathbf{0}}(\cdots)$. This fact expresses the conservation of the total momentum characteristic for theories with global momentum conservation.

EXERCISE Represent the diagrams of the second-order contraction shown in Fig. 5.2 in momentum space. Convince yourself that the "Kirchhoff law" suffices to fix the result. Observe that the number of summations over internal momenta is equal to the number of loops.

This concludes the first part of our introduction to the formal elements of perturbation theory. Critical readers will object that, while we undertook some efforts to efficiently represent the perturbative expansion, we have not in the least addressed the question of how interactions will actually modify the results of the free theory. Indeed, we are not yet in a position to quantitatively address this problem, the reason being that we first need to better understand the origin and remedy of the UV/IR divergences observed above.

However, temporarily ignoring the presence of this roadblock, let us try to outline what kind of information can be extracted from perturbative analyses, in principle. One important point to be noted is that, in condensed matter physics,[9] low-order perturbation theory is usually not enough to obtain quantitative results. The fact that the "perturbation" couples to a macroscopic number of degrees of freedom[10] usually necessitates summation of infinite (sub)series of a perturbative expansion or even the application of non-perturbative methods. This, however, does not mean that the tools developed above are useless: given a system subject to unfamiliar interactions, low-order perturbation theory will usually be applied as a first step to qualitatively explore the situation. For example, a malign divergence of the expansion in the interaction operator may signal the presence of an instability towards the formation of a different phase. Or it may turn out that certain contributions to the expansion are "physically more relevant" than others. Technically, such contributions usually correspond to diagrams of a regular graphical structure. If so, a summation over all "relevant processes" may be in reach. In either case, low-order expansions provide vital hints as to the appropriate strategy of further analysis. In the following we discuss two examples that may help to make these remarks more transparent.

5.2 Ground state energy of the interacting electron gas

In Section 2.2 we began to consider the physics of highly mobile electron compounds. We argued that such a system can be described in terms of the free particle Hamiltonian (2.18) together with the interaction operator (2.19). While we have reviewed the physics of the non-interacting system, nothing has hitherto been said about the role of electron–electron interactions. Yet by now we have developed enough analytical machinery to begin to address this problem. Below we will apply concepts of perturbation theory to estimate the contribution of electronic correlations to the ground state energy of a Fermi system. However, before plunging into the technicalities of this analysis, it is worthwhile discussing some qualitative aspects of the problem.

[9] There are subdisciplines of physics where the situation is different. For example, consider the high-precision scattering experiments of atomic and sub-atomic physics. In these areas, the power of a theory to quantitatively predict the dependence of scattering rates on the strength of the projectile/target interaction (the "perturbation") is a measure of its quality. Such tests involve large-order expansions in the physical coupling parameters.

[10] In contrast, low-order expansions in the *external* perturbation (e.g. experimentally applied electric or magnetic fields) are usually secure; see Chapter 7.

Qualitative aspects

A principal question that we will need to address is under what physical conditions are interactions "weak" (in comparison to the kinetic energy), i.e. when does a perturbative approach with the interacting electron system make sense at all? To estimate the relative magnitude of the two contributions to the energy, let us assume that each electron occupies an average volume r_0^3. According to the uncertainty relation, the minimum kinetic energy per particle will be of order $\mathcal{O}(\hbar^2/mr_0^2)$. On the other hand, assuming that each particle interacts predominantly with its nearest neighbors, the Coulomb energy is of order $\mathcal{O}(e^2/r_0)$. The ratio of the two energy scales defines the **dimensionless density parameter** (see figure)

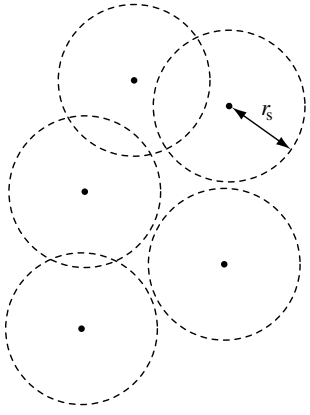

$$\frac{e^2}{r_0}\frac{mr_0^2}{\hbar^2} = \frac{r_0}{a_0} \equiv r_s,$$

where $a_0 = \hbar^2/e^2m$ denotes the Bohr radius.[11] Physically, r_s is the radius of the spherical volume containing one electron on average; for the Coulomb interaction, the denser the electron gas, the smaller r_s. We have thus identified the electron density as the relevant parameter controlling the relative strength of electron–electron interactions.

Eugene P. Wigner 1902–95
Nobel Laureate in Physics in 1963 "for his contributions to the theory of the atomic nucleus and the elementary particles, particularly through the discovery and application of fundamental symmetry principles." (Image © The Nobel Foundation.)

Below, we will be concerned with the regime of high density, $r_s \ll 1$, or weak Coulomb interaction. In the opposite limit, $r_s \gg 1$, properties become increasingly dominated by electronic correlations. Ultimately, for sufficiently large r_s (low density) it is believed that the electron gas undergoes a (first order) transition to a condensed phase known as a **Wigner crystal**. Although Wigner crystals have never been unambiguously observed, several experiments performed on low-density electron gases are consistent with a Wigner crystal ground state. Monte Carlo simulation suggests that Wigner crystallization may occur for densities with $r_s > 35$ in the two-dimensional electron gas and $r_s > 106$ in three.[12] (Note that this scenario relies on being at low temperature,

[11] Notice that the estimate of the relative magnitude of energy scales mimics Bohr's famous qualitative discussion of the average size of the hydrogen atom.

[12] With the earliest reference to electron crystallization appearing in E. Wigner, On the interaction of electrons in metals, *Phys. Rev.* **46** (1934), 1002–11, a discussion of the results of quantum Monte Carlo simulations in three-dimensions can be found in the following papers: D. M. Ceperley and B. J. Alder, Ground state of the electron gas by a stochastic method, *Phys. Rev. Lett.* **45** (1980), 566–569 and N. D. Drummond, Z. Radnai, J. R. Train, M. D. Towler, and R. J. Needs, Diffusion quantum Monte Carlo study of three-dimensional Wigner crystals, *Phys. Rev. B* **69** (2004), 085116, and in two-dimensions in B. Tanatar and D. M. Ceperley, Ground state of the two-dimensional electron gas, *Phys. Rev. B* **39** (1989) 5005-5016. For a further discussion of the subtleties of the transition in two-dimensions, we refer to B. Spivak and S. A. Kivelson, Phases intermediate between a two-dimensional electron liquid and Wigner crystal, Phys. Rev. B **70** (2004), 155114.

Table 5.1 *Density parameters of a number of metals.*

Metal	r_s	Metal	r_s	Metal	r_s	Metal	r_s
Li	3.2	Be	1.9	Na	3.9	Al	2.1
K	4.9	Sn	2.2	Cu	2.7	Pb	2.3

Source: Data taken from Ashcroft and Mermin, *Solid State Physics*.[a]

[a] N. W. Ashcroft and N. D. Mermin, *Solid State Physics* (Holt-Saunders International, 1983).

and on the long-range nature of the Coulomb interaction. In particular, if the Coulomb interaction is subject to some screening mechanism, $V(r) \sim e^{-r/\lambda}$, $r_s \sim (r_0/a_0)e^{-r_0/\lambda}$, and the influence of Coulomb interaction at low densities becomes diminished.)

For $r_s \sim O(1)$, the potential and kinetic energies are comparable. This regime of intermediate coupling is notoriously difficult to describe quantitatively. Yet most metals lie in a regime of intermediate coupling $2 < r_s < 6$ (see Table 5.1). Fortunately, there is overwhelming evidence to suggest that a weak coupling description holds even well outside the regime over which the microscopic theory can be justified. The phenomenology of the intermediate coupling regime is the realm of Landau's **Fermi liquid Theory**.[13]

The fundamental principle underlying the Fermi liquid theory is one of "adiabatic continuity":[14] in the absence of an electronic phase transition (such as Wigner crystallization), a non-interacting ground state evolves smoothly or adiabatically into the interacting ground state as the strength of interaction is increased.[15] An elementary excitation of the non-interacting system represents an "approximate excitation" of the interacting system (i.e. its "lifetime" is long). Excitations are quasi-particles (and quasi-holes) above a sharply defined Fermi surface.

Lev D. Landau 1908–68

Nobel Laureate in Physics in 1962 "for his pioneering theories for condensed matter, especially liquid helium." Landau's work covers all branches of theoretical physics, ranging from fluid mechanics to quantum field theory. A large portion of his papers refer to the theory of the condensed state. They started in 1936 with a formulation of a general thermodynamical theory of the phase transitions of the second order. After P.L. Kapitsa's discovery, in 1938, of the superfluidity of liquid helium, Landau began extensive research which led him to the construction of the complete theory of the "quantum liquids" at very low temperatures. (Image © The Nobel Foundation.)

[13] L. D. Landau, The theory of a Fermi liquid, *Sov. Phys. JETP* **3** (1956), 920.

[14] P. W. Anderson, *Basic Notions in Condensed Matter Physics* (Benjamin, 1984).

[15] 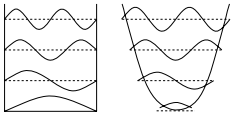

As a simple non-interacting example, consider the adiabatic evolution of the bound states of a quantum particle as the confining potential is changed from a box to a harmonic potential well (see figure). While the wavefunctions and energies evolve, the topological characteristics of the wavefunctions, i.e. the number of the nodes, and therefore the assignment of the corresponding quantum numbers, remain unchanged.

The starting point of Fermi liquid theory is a few phenomenological assumptions, all rooted in the adiabaticity principle. For example, it is postulated that the density of quasiparticles can be described in terms of a momentum-dependent density distribution $n(\mathbf{p})$ which, in the limit of zero interaction, evolves into the familiar Fermi distribution. From this assumption (and a few more postulates) a broad spectrum of observables can be analyzed without further "microscopic" calculation. Its remarkable success (as well as the few notorious failures) has made Landau Fermi liquid theory a powerful tool in the development of modern condensed matter physics but one which we are not going to explore in detail.[16] Instead, motivated in part by the phenomenological success of the "adiabatic continuity," we will continue with the development of a microscopic theory of the weakly interacting three-dimensional electron gas, with $r_{\rm s} \ll 1$.

Perturbative approach

The starting point of the perturbative analysis is the functional representation of the free energy $F = -T \ln \mathcal{Z}$ through the quantum partition function. (Here, as usual, we set $k_{\rm B} = 1$.) Expressed as a coherent state path integral, $\mathcal{Z} = \int D(\bar\psi, \psi)\; e^{-S[\bar\psi,\psi]}$, where

$$S[\psi,\bar\psi] = \sum_{p} \bar\psi_{p\sigma} \left(-i\omega_n + \frac{\mathbf{p}^2}{2m} - \mu \right) \psi_{p\sigma} + \frac{T}{2L^3} \sum_{pp'q} \bar\psi_{p+q\sigma} \bar\psi_{p'-q\sigma'} V(\mathbf{q}) \psi_{p'\sigma'} \psi_{p\sigma}.$$

Here, for brevity, we have introduced the "**4-momentum**" $p \equiv (\mathbf{p}, \omega_n)$ comprising both frequency and momentum.[17] As with the Green function discussed in the previous section, the free energy can be expanded in terms of an interaction parameter. To fix a reference scale against which to compare the correlation energies, let us begin by computing the free energy Eq. (4.41) of the non-interacting electron gas:

$$F^{(0)} = -T \sum_{\mathbf{p}\sigma} \ln \left(1 + e^{-\beta(\mathbf{p}^2/2m - \mu)} \right) \stackrel{T\to 0}{\longrightarrow} \sum_{\mathbf{p}^2/2m<\mu,\sigma} \left(\frac{\mathbf{p}^2}{2m} - \mu \right) \simeq -\frac{2}{5} N\mu, \qquad (5.19)$$

where $\mu \equiv p_{\rm F}^2/2m$, $N = (2^{3/2}/3\pi^2) m^{3/2} L^3 \mu^{3/2}$ is the number of particles, and the last estimate is obtained by replacing the sum over momenta by an integral. According to Eq. (5.19), the average kinetic energy per particle is equal to 3/5 of the Fermi energy. To relate this scale to the density parameter $r_{\rm s}$, we choose to measure all energies in units of the Rydberg energy (alias the ionization energy of hydrogen), $E_{\rm Ry} = me^4/2\hbar^2 = 13.6\,{\rm eV}$,

$$\frac{F^{(0)}}{E_{\rm Ry}} \sim \frac{N}{r_{\rm s}^2}. \qquad (5.20)$$

[16] Interested readers are referred to one of several excellent reviews, e.g. P. W. Anderson, *Basic Notions in Condensed Matter Physics* (Benjamin, 1984).

[17] Notice that "4-momentum" p and the modulus of the "3-momentum", $p = |\mathbf{p}|$, are denoted by the same symbol (standard notation!). However, in its context, this should not cause confusion.

If we turn now to the discussion of interactions, a formal expansion of F to first order in V gives

$$F^{(1)} = \frac{T^2}{2L^3} \sum_{pp'q} \bar{\psi}_{p+q\sigma}\bar{\psi}_{p'-q\sigma'}V(\mathbf{q})\psi_{p'\sigma'}\psi_{p\sigma}\Big\rangle_0 , \tag{5.21}$$

where $\langle\cdots\rangle_0$ denotes the functional average with respect to the non-interacting action. The two[18] diagrams contributing to this expression are shown in the figure overleaf. To account for the specifics of the electron gas, we are using a diagrammatic code slightly different from that of the previous section:

- ▷ The Coulomb interaction is represented by a wavy line labeled by the momentum argument $\mathbf{q}$.
- ▷ A contraction $\langle\psi_{p\sigma}\bar{\psi}_{p\sigma}\rangle_0$ is indicated by a solid arrow representing the **free Green function of the electron gas**,

$$G_p \equiv \frac{1}{-i\omega_n + \frac{\mathbf{p}^2}{2m} - \mu}, \tag{5.22}$$

  i.e. the inverse of the free action. The labeling of the contraction by an arrow (instead of a unidirectional line as in ϕ^4-theory) is motivated by two considerations: firstly, the mnemonic has the effect of indicating that a contraction $\langle\psi_\eta\bar{\psi}_\lambda\rangle_0$ describing the creation of an electron with quantum numbers λ, followed by the annihilation of an electron at η, is a directed process; secondly, there are situations (e.g. when a magnetic field is present) where $\langle\psi_{n\sigma}(\mathbf{r})\bar{\psi}_{n\sigma}(\mathbf{r}')\rangle_0 \neq \langle\psi_{n\sigma}(\mathbf{r}')\bar{\psi}_{n\sigma}(\mathbf{r})\rangle_0$.
- ▷ The sum of all 4-momenta emanating from an interaction vertex formed by a wavy line and two electron field lines is equal to zero (exercise) – the "Kirchhoff law."
- ▷ Finally, we have to be careful about **sign factors** arising when Grassmann variables are interchanged. However, the anti-commutativity of the fields merely leads to an overall factor $(-)^{N_\mathrm{l}}$, where N_l is the number of loops of a diagram. (To verify this claim, one may notice that a loop is formed by a "ringwise contraction" $\langle\bar{\psi}_1\psi_2\bar{\psi}_3\ldots\psi_N\rangle_0, (2\to3)(4\to5)\ldots((N-2)\to(N-1))(N\to1)$. The last contraction introduces the minus sign.)

First-order perturbation theory

Turning to the discussion of the specific diagrams shown in the figure below, we notice that the first, generally known as a **Hartree contribution**, vanishes. Technically, this is a consequence of the fact that the interaction line connecting the two loops carries zero momentum. However, as discussed in Section 2.2, $V(\mathbf{q}=0)=0$. Physically, the vanishing of the Hartree contribution is a consequence of charge neutrality.

Douglas R. Hartree, 1897–1958
Originally appointed as a professor of applied mathematics he became one of the first "computational physicists." He developed methods for numerically solving the Schrödinger equation, among them the celebrated "Hartree approximation."

[18] Remember that, in a theory with complex or Grassmann fields, only contractions $\sim\langle\bar{\psi}\psi\rangle_0$ exist, i.e. there is a total of $n!$ distinct contributions to a contraction $\langle\bar{\psi}\psi\ldots\psi\rangle_0$ of $2n$ field operators.

Indeed, the two Green function loops $\sum_p G_p$ measure the local particle density of the electron gas (cf. the discussion on page 171). Global charge neutrality requires that the electronic density cancels against the density of the ionic background. However, notice that this cancellation mechanism relies on our assumption of overall spatial homogeneity.

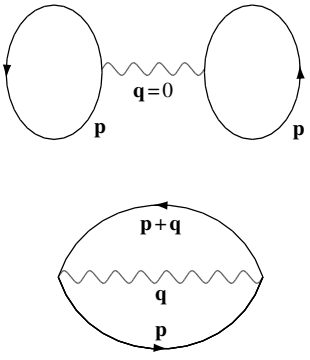

Only in a spatially uniform system does the density of the electron gas locally compensate the positive counter-density. In realistic metals, the inevitable presence of impurities breaks translational invariance and there is no reason for the Hartree contribution to vanish. Indeed, the analysis of Hartree-type contributions to the correlation energy in disordered electronic media is a subject of ongoing research.

While the Hartree term describes the classical interaction of charge densities through the Coulomb potential, the second diagram shown in the figure, known as a **Fock contribution**, is quantum. Translating the diagrammatic language back into Green functions, we obtain

$$\begin{aligned} F^{(1)} &= -\frac{T^2}{L^3}\sum_{p,p'} G_p G_{p'} V(\mathbf{p}-\mathbf{p}') \\ &= -\frac{1}{L^3}\sum_{\mathbf{p},\mathbf{p}'} n_{\mathrm{F}}(\epsilon_{\mathbf{p}}) n_{\mathrm{F}}(\epsilon_{\mathbf{p}'}) \frac{e^2}{|\mathbf{p}-\mathbf{p}'|^2} \\ &\overset{T\to 0}{=} -\frac{1}{L^3}\sum_{\epsilon_{\mathbf{p}},\epsilon_{\mathbf{p}'}<\mu} \frac{e^2}{|\mathbf{p}-\mathbf{p}'|^2} = -\frac{e^2 L^3 p_{\mathrm{F}}^4}{(2\pi)^4}. \end{aligned} \tag{5.23}$$

Here, the sign factor in the first equality is due to the odd number of fermion loops, and the evaluation of the last sum, which can be found, for example, in the text by Kittel,[19] is left as an exercise. (Up to numerical factors, the result follows from dimensional considerations. We are integrating the inverse square of the distance in momentum space ($[\text{momentum}]^{-2}$) over two Fermi spheres ($[\text{momentum}]^6$). Since the integral is convergent at low momenta, it must scale as the fourth power of the upper cutoff $\sim p_{\mathrm{F}}^4$.) Division by the Rydberg energy leads to the scaling

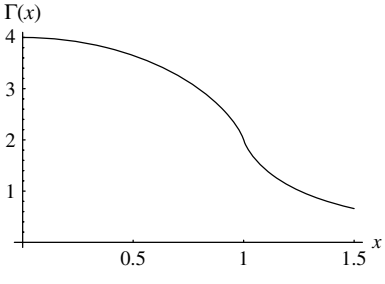

$$\frac{F^{(1)}}{E_{\mathrm{Ry}}} = \text{const.} \cdot \frac{N}{r_{\mathrm{s}}}, \tag{5.24}$$

where the constant is of order unity. This result conforms with our previous estimate of the density dependence of correlation energies.

[19] C. Kittel, *Quantum Theory of Solids* (Wiley, 1963).

INFO A closer analysis shows that other predictions following from Eq. (5.23) are less sensible. To understand **what goes wrong**, let us rewrite the sum of $F^{(0)}$ and $F^{(1)}$ as

$$F^{(0)} + F^{(1)} = \sum_{|\mathbf{p}|<p_\mathrm{F}} \left(\frac{\mathbf{p}^2}{2m} - \mu - \frac{1}{L^3} \sum_{\mathbf{p}'<\mu} \frac{e^2}{|\mathbf{p}-\mathbf{p}'|^2} \right).$$

This way of writing suggests that the interaction of an electron of momentum $\mathbf{p}$ with all partner electrons of momentum $\mathbf{p}'$ leads to a reduction[20] of the single particle energy by an amount $L^{-3}\sum_{\mathbf{p}'<\mu} e^2/|\mathbf{p}-\mathbf{p}'|^2$.

Evaluation of the internal sum (exercise) leads to[21]

$$F^{(0)} + F^{(1)} = \sum_{|\mathbf{p}|<p_\mathrm{F}} \left(\frac{\mathbf{p}^2}{2m} - \mu - \frac{e^2 p_\mathrm{F}}{2\pi} \Gamma(|\mathbf{p}|/p_\mathrm{F}) \right),$$

where the function $\Gamma(x) = 2 + \frac{1-x^2}{x} \ln\left|\frac{1+x}{1-x}\right|$ is shown in the figure. The most important characteristic of the scaling function Γ is a logarithmically diverging derivative at $x = 1$ (exercise). To appreciate the consequences of this feature, let us consider the single particle **density of states** $\rho(\epsilon) = \sum_{\mathbf{p}\sigma} \delta(\epsilon - \epsilon_p)$, where $\epsilon_p = \frac{p^2}{2m} - \frac{e^2 p_\mathrm{F}}{2\pi}\Gamma(p/p_\mathrm{F})$ is the first-order Fock single-particle energy. Approximating the sum by an integral, we obtain

$$\rho(\epsilon) = \frac{L^3}{\pi^2} \int_0^\infty p^2 dp\, \delta(\epsilon - \epsilon_p) = \frac{L^3 p^2}{\pi^2} \left(\frac{d\epsilon_p}{dp} \right)^{-1},$$

where p is defined through $\epsilon_p = \epsilon$. The singularity of the derivative of $\Gamma(p/p_\mathrm{F})$ at $p = p_\mathrm{F}$ implies that the density of states is predicted to vanish as ϵ approaches the Fermi energy, clearly a nonsensical result.[22] The origin of this pathological divergence can be traced back to the long-range ($|\mathbf{r}|^{-1} \to |\mathbf{q}|^{-2}$) decay of the Coulomb potential (cf. Eq. (5.21)). Yet we know that, in systems with mobile charge carriers, electrostatic forces are screened, i.e. they decay exponentially. Microscopically, screening is due to the polarization of a medium in response to an applied electric field. This by itself is an interaction effect, albeit one of "higher order" in the Coulomb interaction, i.e. if we ever want to observe signatures of the screening mechanism, we need to advance to higher orders in the expansion in V.

Second-order perturbation theory

Let us then consider the second-order contribution

$$F^{(2)} = -\frac{T}{2} \left(\frac{T}{2L^3} \right)^2 \sum_{pp'q} \bar{\psi}_{p+q\sigma} \bar{\psi}_{p'-q\sigma'} V(\mathbf{q}) \psi_{p'\sigma'} \psi_{p\sigma} \Big|_0^{2\ \mathrm{c}},$$

where the superscript indicates that only connected diagrams contribute.

[20] Why a reduction? Charge neutrality implies that the classical correlation energy vanishes. However, being fermionic in nature, electrons tend to avoid each other even more than classical particles, i.e. quantum statistics leads to a lowering of the correlation energy below the classical value of zero.

[21] See, e.g., J. Hubbard, The description of collective motion in terms of many-body perturbation theory, *Proc. Roy. Soc. (London)* **A243** (1957), 336.

[22] The majority of transport observables in metals are proportional to the density of states at the Fermi energy, i.e. $\rho(\mu) = 0$ would entail the vanishing of almost all transport coefficients!

EXERCISE Using the field integral representation of $\mathcal{Z}$, show that second-order expansion of $F = -T \ln \mathcal{Z}$ in the interaction operator $S_{\rm int}$ leads to $F^{(2)} = -(T/2)\left[\langle S_{\rm int}^2 \rangle_0 - \left[\langle S_{\rm int} \rangle_0\right]^2\right]$. Convince yourself that the second term cancels disconnected diagrams. Apply arguments similar to those involved in the proof of the linked cluster theorem to verify that the cancellation of disconnected graphs pertains to all orders in the expansion of F. I.e. the free energy can be obtained by expanding the partition function $\mathcal{Z}$ (not its logarithm) and keeping only connected diagrams; dropping disconnected contributions is equivalent to taking the logarithm.

Connected contraction of the eight field operators leads to four distinct types of diagram (exercise) of which two are of Hartree type (i.e. contain a zero-momentum interaction line $V(\mathbf{q} = \mathbf{0})$). The non-vanishing diagrams $F^{(2),1}$ and $F^{(2),2}$ are shown in the figure below.[23] Translating these diagrams to momentum summations over Green functions, one obtains (exercise)

$$\begin{aligned} F^{(2),1} &= -\frac{T^3}{L^6} \sum_{p_1,p_2,q} G_{p_1} G_{p_1+q} G_{p_2} G_{p_2+q} V(\mathbf{q})^2, \\ F^{(2),2} &= \frac{1}{2}\frac{T^3}{L^6} \sum_{p,q_1,q_2} G_p G_{p-q_1} G_{p-q_1-q_2} G_{p-q_2} V(\mathbf{q}_1) V(\mathbf{q}_2). \end{aligned} \tag{5.25}$$

While, at first sight, these expressions do not look very illuminating, closer inspection reveals some structure. Reflecting the fact that electronic transport in solids is carried by excitations at the Fermi energy, the electron Green function (5.22) assumes large values for momenta $\mathbf{p} \simeq p_{\rm F}$. This implies that only configurations where all momentum arguments carried by the Green function are close to the Fermi surface contributes significantly to the sums (5.25). Considering the first sum, we see that, for small $|\mathbf{q}|$ and $|\mathbf{p}_i| \simeq p_{\rm F}$, this condition is met, i.e. there are two unbound summations over momentum shells around the Fermi surface. However, with the second sum, the situation is less favourable. For fixed $|\mathbf{p}_1| \simeq p_{\rm F}$, fine-tuning of both $\mathbf{q}_1$ and $\mathbf{q}_2$ is necessary to bring all momenta close to $p_{\rm F}$, i.e. effectively one momentum summation is frozen out. There is no need to enter into detailed calculations to predict that, due to the relatively larger "phase volume," $F^{(2),1}/F^{(2),2} \gg 1$, where the ratio will be proportional to the area of the Fermi surface which, in turn, is proportional to the density of the electron gas. For large densities, the second Fock diagram can be neglected in comparison with the first.

[23] In fact, one more non-vanishing contribution is obtained by drawing a single "ring" of Green functions containing two non-crossing interaction lines. This diagram, and its obvious generalization to higher order processes containing sequential "self–interactions" of a single Green function do not play an essential role (in the present context.) The reasons why will become clear in section 5.3 when we introduce the notion of self-energies.

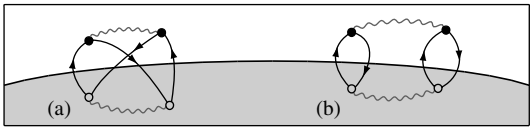

Figure 5.6 Diagram of second-order Fock contributions to the free energy of the electron gas. (a) Interaction process involving a single electron–hole pair. An electron is virtually excited above the Fermi energy, and subsequently recombines with a hole state left behind by a second electron excitation which then jumps into the hole created by the initial excitation. (b) Virtual excitation of independent electron–hole pairs.

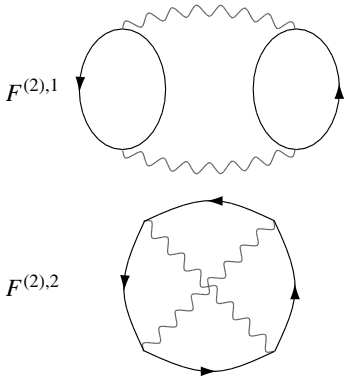

Of course, there must be a 'more physical' way of understanding this observation. The Green function lines in the diagrams $F^{(2),i}$ describe the propagation of quasi-particles and quasi-holes[24] on the background of the interacting medium. Now, the diagram $F^{(2),2}$ contains a simply connected propagator line: a single particle–hole excitation undergoes a second-order interaction process with itself (see Fig. 5.6(a)). By contrast, the first diagram $F^{(2),1}$ involves two independent electron–hole excitations, as shown in Fig. 5.6(b). Since, in a dense electron gas, a second-order interaction process will more likely involve different particles, this type of contribution is more important. Notice that the process shown in Fig. 5.6(b) can be interpreted as a "polarization" of the medium due to the excitation of electron–hole pairs.

Higher orders in perturbation theory

The picture above readily generalizes to interaction processes of higher order. In the high-density limit, dominant contributions to the free energy should contain one free integration over the Fermi momentum per interaction process. A moment's thought shows that only diagrams of "ring graph" structure (see the figure) meet this condition. Expanding the free energy functional to nth order in the interaction operator, and retaining only diagrams of that structure, one obtains

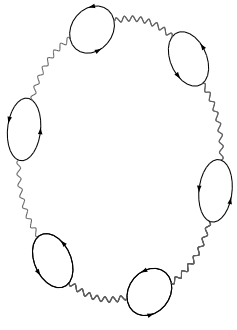

$$F^{(n)}_{\mathrm{RPA}} = -\frac{T}{2n}\sum_{q}\left(\frac{2T}{L^3}V(\mathbf{q})\sum_{p}G_pG_{p+q}\right)^n . \qquad (5.26)$$

(To understand the origin of the multiplicative factor $1/n$, notice that $F^{(n)}$ results from the connected contraction of an operator $\sim$

[24] In principle, the system consists of physical electrons immersed into a globally positive background. However (cf. the discussion of Section 2.2), keeping in mind that at low temperatures dynamical processes take place in the immediate vicinity of the Fermi surface, a more problem-oriented way of thinking about states is in terms of quasi-particles and quasi-holes, i.e. electronic states immediately above and below the Fermi surface.

$(n!)^{-1}\langle (S_{\rm int}[\bar\psi,\psi])^n\rangle_0^{\rm c}$. There are $(n-1)!$ different ways of arranging the interaction operators $S_{\rm int}$ in a ring-shaped structure, i.e. the diagram carries a global factor $(n-1)!/n! = 1/n$.)

In Eq. (5.26) the subscript "RPA" stands for **random phase approximation**.[25] However, more important than the designation are the facts: (a) we have managed to identify a particularly relevant subclass of diagrams contributing to the plethora of interaction processes; (b) there is a physical parameter controlling the dominance of these diagrams; and (c) we are apparently able to sum up the entire series of nth-order RPA-interaction contributions. Indeed, summation over n leads to the simple result

$$F_{\rm RPA} \equiv \sum_n F_{\rm RPA}^{(n)} = \frac{T}{2}\sum_q \ln\left(1 - V(\mathbf{q})\Pi_q\right), \tag{5.27}$$

where we have introduced the **polarization operator**,[26]

$$\boxed{\Pi_q \equiv \frac{2T}{L^3}\sum_p G_p G_{p+q}.} \tag{5.28}$$

Equation (5.27) represents our first example of an infinite-order expansion. However, before turning to the discussion of further aspects of infinite-order perturbation theory, let us stay for a moment with the RPA free energy. Specifically, let us investigate whether the RPA repairs the pathology in the Fermi surface density of states observed above.

The last unknown we need to compute before turning to the discussion of the RPA free energy is the polarization operator. Drawing on the frequency summation in Problem 4.5, the polarization operator can be written explicitly as

$$\Pi_q = \frac{2T}{L^3}\sum_p \frac{1}{-i\omega_n + \xi_{\mathbf{p}}}\frac{1}{-i\omega_{n+m} + \xi_{\mathbf{p}+\mathbf{q}}} = \frac{2}{L^3}\sum_{\mathbf{p}} \frac{n_{\rm F}(\epsilon_{\mathbf{p}+\mathbf{q}}) - n_{\rm F}(\epsilon_{\mathbf{p}})}{i\omega_m + \xi_{\mathbf{p}+\mathbf{q}} - \xi_{\mathbf{p}}}. \tag{5.29}$$

The evaluation of the momentum sum is straightforward if a bit tedious. As a result of the calculation outlined in the Info block below one obtains

$$\boxed{\Pi_{\mathbf{q},\omega_m} = -\nu_0\left[1 - \frac{i\omega_m}{2v_{\rm F}q}\ln\left(\frac{i\omega_m + v_{\rm F}q}{i\omega_m - v_{\rm F}q}\right)\right],} \tag{5.30}$$

where

$$\nu_0 \equiv \frac{1}{L^d}\sum_{\mathbf{p},\sigma}\delta(\mu - \epsilon_p) = 2\int\frac{d^3p}{(2\pi)^3}\delta(\epsilon_p - \mu) = \frac{mp_{\rm F}}{\pi^2}, \tag{5.31}$$

[25] The attribute "random phase" seems to allude to the fact that the quantum mechanical phase carried by the particle–hole excitations stirred up by interactions gets lost after each elementary polarization process. This contrasts with more-generic contributions to F where quantum phases may survive more complex interaction processes. Also notice that more than one approximation scheme in statistical physics has been dubbed "random phase."

[26] The definition (5.28) applies to the specific case of a three-dimensional translationally invariant system. More generally, the polarization operator is defined as the frequency/momentum Fourier transform of the connected average

$$\langle\bar\psi(\mathbf{x},\tau)\psi(\mathbf{x},\tau)\bar\psi(\mathbf{x}',\tau')\psi(\mathbf{x}',\tau')\rangle_{\rm c}.$$

is the density of states per volume of non-interacting electrons at the Fermi surface.

INFO For an isotropic three-dimensional system at zero temperature, the polarization operator (5.29) becomes a function of $|\mathbf{q}|$ and ω_n, known as the **Lindhard function**. The evaluation of the momentum sum is greatly simplified by noting that, due to the difference of the Fermi functions, only momenta with $|\mathbf{p}| \simeq p_{\rm F}$ significantly contribute. Assuming that $|\mathbf{q}| \ll p_{\rm F}$, we may thus effect the linearization $\xi_{\mathbf{p}+\mathbf{q}} - \xi_{\mathbf{p}} = (1/m)\mathbf{p}\cdot\mathbf{q} + \mathcal{O}(q^2)$, where the term of $\mathcal{O}(q^2)$ is negligibly small. Similarly, $n_{\rm F}(\epsilon_{\mathbf{p}+\mathbf{q}}) - n_{\rm F}(\epsilon_{\mathbf{p}}) \simeq \partial_{\,p} n_{\rm F}(\epsilon_p)(1/m)\mathbf{p}\cdot\mathbf{q} \simeq -\delta(\epsilon_p - \mu)(1/m)\mathbf{p}\cdot\mathbf{q}$, where, in the zero-temperature limit, the last equality becomes exact. Converting the momentum sum into an integral, we thus obtain

$$\Pi_{\mathbf{q},\omega_m} = -2\int \frac{d^3p}{(2\pi)^3}\delta(\epsilon_p - \mu)\frac{\frac{1}{m}\mathbf{p}\cdot\mathbf{q}}{i\omega_m + \frac{1}{m}\mathbf{p}\cdot\mathbf{q}}.$$

Setting $1/(2\pi)^3 \int d^3p = 1/(2\pi)^3 \int dp\, p^2 \int d\,\Omega$, where $\int d\,\Omega$ is the integral over the three-dimensional unit sphere, and $\mathbf{p} = p\mathbf{n}$, with $|\mathbf{n}| = 1$, the integral can be evaluated, thus:

$$\begin{aligned}
\Pi_{\mathbf{q},\omega_m} &= -\frac{2}{(2\pi)^3}\int dp\, p^2 \int d\,\Omega\ \delta(\epsilon_p - \mu)\frac{v_{\rm F}\mathbf{n}\cdot\mathbf{q}}{i\omega_m + v_{\rm F}\mathbf{n}\cdot\mathbf{q}} \\
&= -\underbrace{\frac{2}{(2\pi)^3}\int dp\, p^2 \int d\,\Omega\ \delta(\epsilon_p - \mu)}_{\nu_0}\frac{1}{\int d\,\Omega}\int d\,\Omega\ \frac{v_{\rm F}\mathbf{n}\cdot\mathbf{q}}{i\omega_m + v_{\rm F}\mathbf{n}\cdot\mathbf{q}} \\
&= -\frac{\nu_0}{2}\int_{-1}^{1} dx\ \frac{v_{\rm F}xq}{i\omega_m + v_{\rm F}xq} = -\nu_0\left[1 - \frac{i\omega_m}{2v_{\rm F}q}\ln\left(\frac{i\omega_m + v_{\rm F}q}{i\omega_m - v_{\rm F}q}\right)\right].
\end{aligned}$$

Murray Gell-Mann 1929–
Nobel Laureate in Physics in 1969 "for his contributions and discoveries concerning the classification of elementary particles and their interactions." Among his many accomplishments, he formulated the quark model of hadronic resonances, and identified the SU(3) flavor symmetry of the light quarks, extending isospin to include strangeness, which he also discovered. (Image © The Nobel Foundation.)

To obtain the free energy, we need to substitute the Lindhard function into Eq. (5.27) and sum over $q = \{\mathbf{q}, \omega_m\}$. Yet, due to the complicated dependence of the function $\Pi_{\mathbf{q},\omega_m}$ on its arguments, this final part of the calculation is far from trivial. An asymptotic expression for the high-density expansion of the RPA approximation to F was first obtained in a famous study by Gell-Mann and Brueckner.[27] Measuring in atomic units, they obtained the free energy per particle of

$$\frac{F_{\rm RPA}}{E_{\rm Ry}N} = -0.142 + 0.0622\ln r_{\rm s}. \tag{5.32}$$

For a derivation of this result we refer the interested reader to the literature. (In the late 1950s, motivated largely by applications to the physics of heavy nuclei, the perturbative calculation of ground state energies had become an industry. A comprehensive discussion of

[27] M. Gell-Mann and K. Brueckner, Correlation energy of an electron gas at high density, *Phys. Rev.* **106** (1957), 364–8. To explore this and related literature, it is useful to refer to D. Pines, *The Many-Body Problem* (Benjamin, 1962) where the important reprints are collected.

the subject, and details of the asymptotic r_s- expansion of $F_{\rm RPA}$ can be found, for example, in Mahan.[28]) When added to the kinetic energy Eq. (5.20) and the first-order correlation energy Eq. (5.24), the structure of the density expansion of the free energy becomes clear: the sum over all RPA diagrams yields the coefficient of $\mathcal{O}(r_s^0)$ in the expansion in r_s.[29]

More important for our present discussion is the conceptual meaning of the RPA, notably the connection to screening. To this end, let us temporarily consider the expectation value of the particle number $N = -\partial_\mu F$, rather than the free energy itself. Specifically, we wish to compare the first order correction (with the non-interacting result) $N^{(1)} = -\partial_\mu F$ to the RPA, $N_{\rm RPA} = -\partial_\mu F_{\rm RPA}$. Noting that $\partial_\mu G_p = -(G_p)^2$ we readily find (cf. Eq. (5.23))

$$N^{(1)} = -\frac{2T^2}{L^3}\sum_{p,q}(G_p)^2 G_{p+q} V(\mathbf{q}).$$

After a second differentiation, $\rho^{(1)} = \partial_\mu N^{(1)}$, this expression would lead to the pathological density of states, a consequence of the unscreened interaction line. (The diagrammatic visualization of $N^{(1)}$ is shown in Fig. 5.7(a).) Now, consider the μ-derivative of $F_{\rm RPA}$, Eq. (5.27):

$$\begin{aligned} N_{\rm RPA} &= \frac{T}{2}\sum_q \frac{V(\mathbf{q})\partial_\mu \Pi_q}{1 - V(\mathbf{q})\Pi_q} = -\frac{T^2}{L^3}\sum_q \frac{V(\mathbf{q})}{1 - V(\mathbf{q})\Pi_q}\left[\sum_p G_{p+q}(G_p)^2 + (q \leftrightarrow -q)\right] \\ &= -\frac{2T^2}{L^3}\sum_q \frac{V(\mathbf{q})}{1 - V(\mathbf{q})\Pi_q}\sum_p G_{p+q}(G_p)^2 = -\frac{2T^2}{L^3}\sum_q V_{\rm eff}(q)\sum_p G_{p+q}(G_p)^2, \end{aligned} \quad (5.33)$$

where we have defined the "effective" interaction

$$V_{\rm eff}(q) \equiv \frac{1}{V(\mathbf{q})^{-1} - \Pi_q} \equiv \frac{V(\mathbf{q})}{\epsilon(q)}, \quad (5.34)$$

with the generalized **dielectric function**

$$\boxed{\epsilon(q) \equiv 1 - V(\mathbf{q})\Pi_q.} \quad (5.35)$$

Structurally, the expression for $N_{\rm RPA}$ resembles the first-order expression $N^{(1)}$, only with the "bare" Coulomb interaction replaced by the effective interaction $V_{\rm eff}$. From its definition, it is clear that $V_{\rm eff}$ represents a geometric series over polarization bubbles, augmented by bare interaction lines. This is visualized in Fig. 5.7(b), where the fat line is defined in the bottom part of the figure. In fact, we do not need to stare at the analytical expression (5.33) to understand its origin. The μ-differentiation acting on $F_{\rm RPA}$ may pick any of the n rings contributing to $F_{\rm RPA}^{(n)}$ in Eq. (5.26). The "differentiated ring" becomes the bubble in Fig. 5.7, while all other rings conspire to form the $(n-1)$th-order contribution to the effective interaction line.

[28] G. Mahan, *Many Particle Physics* (Plenum Press, 1981).

[29] Here we follow a convention (used mostly in the older literature) where the RPA starts from the *second*-order ring diagram $F^{(2),1}$. However, henceforth we will refer to the "RPA" as the sum over all ring diagrams, including the first, $F^{(1)}$.

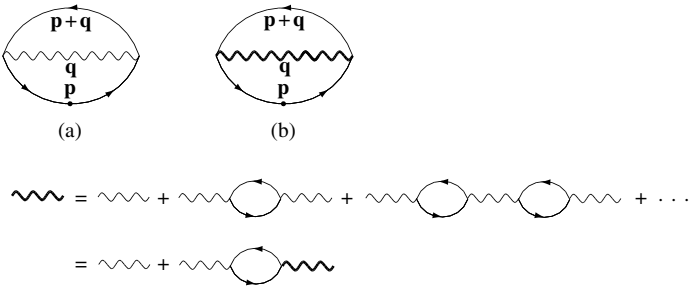

Figure 5.7 Diagrammatic visualization of expectation value of the particle number. (a) First-order Fock correction and (b) the RPA approximation, where the definition of the RPA interaction line is shown in the bottom part of the figure.

At this stage, the connection between RPA and the collective electromagnetic response of the charged system becomes discernible. We remember that the electric field $\mathbf{E}$ in a medium is related to the vacuum field $\mathbf{D}$ through the relation $\mathbf{D}(\mathbf{q},\omega) = \epsilon(\mathbf{q},\omega)\mathbf{E}(\mathbf{q},\omega)$, where the dielectric function $\epsilon(\mathbf{q},\omega) = 1+4\pi\chi(\mathbf{q},\omega)$ is determined by the **electromagnetic susceptibility**, i.e. a function that measures the tendency of the medium to "respond" or adjust to an external electromagnetic perturbation. Identifying $\mathbf{E}(\mathbf{D})$ with the gradient of the "dressed" potential V_{eff} (the "bare" potential V), we conclude that, on the level of the microscopic theory, $4\pi\chi(\mathbf{q},\omega) = -V(\mathbf{q})\Pi_{\mathbf{q},\omega_n}$, i.e. the susceptibility is proportional to the polarization operator Π_q. These connections motivate the introduction of the dielectric function as in Eq. (5.35) above.

The full complexity of the polarization of the dense homogeneous electron gas is encoded by the Lindhard function (5.30). However, there are some interesting limiting cases, where the situation simplifies. Inspection of Eq. (5.30) shows that the Lindhard function depends on the dimensionless ratio between two characteristic length scales: the "wavelength" q^{-1}, and the distance v_{F}/ω an excitation propagating with Fermi velocity travels during the time ω^{-1}. For small frequencies, $v_{\text{F}}/\omega \gg q^{-1}$, the electron gas has enough time to optimally adjust to the spatial variation $\sim q^{-1}$ of the potential, i.e. to screen out electro-neutrality violating potential fluctuations. In this **static limit**, we may expand $\Pi_{\mathbf{q},\omega_m} \overset{\omega\ll qv_{\text{F}}}{=} -\nu_0 + \mathcal{O}(\omega/v_{\text{F}}q)$. In this case, the electron gas interacts through the effective potential,

$$V_{\text{eff}}(q) \overset{\omega\ll qv_{\text{F}}}{=} \frac{1}{V(\mathbf{q})^{-1}+\nu_0} = \frac{4\pi e^2}{q^2+4\pi e^2\nu_0} \equiv \frac{4\pi e^2}{q^2+\lambda^{-2}},$$

where the constant $\lambda \equiv \left(4\pi e^2\nu_0\right)^{-1/2}$ is known as the **Thomas–Fermi screening** length. Indeed, it is straightforward to verify that the inverse Fourier transform leads to an effective interaction potential

$$\boxed{V_{\text{eff}}(\mathbf{r}) = e^2\frac{e^{-|\mathbf{r}|/\lambda}}{|\mathbf{r}|},} \tag{5.36}$$

i.e. the potential is exponentially supressed, or screened, on length scales $|\mathbf{r}| > \lambda$.

EXERCISE To verify Eq. (5.36), introduce polar coordinates $\mathbf{q} = (q, \theta, \phi)$ in $\mathbf{q}$-space and perform first the elementary integrations over ϕ and θ. It is then straightforward to complete the remaining q-integration over the radial coordinate by analogy to the contour integral (5.13).

INFO Let us briefly recapitulate the **heuristic interpretation of Thomas–Fermi screening**. Imagine a test charge e has been immersed in an electron gas. The host system will respond to this perturbation by a local distortion of its density. To compute the distortion, we note that the effective potential $V_{\rm eff}(\mathbf{r})$ created by the test charge changes the electronic energy levels according to $\epsilon_p \to \epsilon_p - V_{\rm eff}$. (Here, we assume that the external perturbation changes so slowly that the simultaneous usage of momentum and coordinate quantum numbers is not in conflict with the uncertainty relation.) The induced charge density thus reads as

$$\begin{aligned}\rho_{\rm ind}(\mathbf{r}) &= -e\int \frac{d^3p}{(2\pi)^3}\left[n_{\rm F}(\epsilon_p - V_{\rm eff}(\mathbf{r})) - n_{\rm F}(\epsilon_p)\right] \approx eV_{\rm eff}(\mathbf{r})\int \frac{d^3p}{(2\pi)^3}\,\partial\, n_{\rm F}(\epsilon_p)\\ &\overset{T\to 0}{\simeq} -eV_{\rm eff}(\mathbf{r})\int d\epsilon \underbrace{\int \frac{d^3p}{(2\pi)^3}\delta(\epsilon-\epsilon_p)}_{(\,)}\delta(\epsilon-\mu) = -eV_{\rm eff}(\mathbf{r})\nu_0,\end{aligned}$$

where in the second equality we assumed weakness of the induced potential and in the third equality used the low-temperature approximation $\partial\, n_{\rm F}(\epsilon) \simeq -\delta(\epsilon-\mu)$. A substitution of this result into the Fourier transform of the Poisson equation $\nabla^2 V_{\rm eff}(\mathbf{r}) = -4\pi e\rho(\mathbf{r}) = -4\pi e(e\delta(\mathbf{r}) + \rho_{\rm ind}(\mathbf{r}))$ gives

$$V_{\rm eff}(\mathbf{q}) = \frac{4\pi e^2}{q^2 + 4\pi e^2\nu_0}.$$

We also note that Thomas–Fermi screening repairs our problem with the density of states. The pathology discussed on page 213 found its origin in the $(1/q^2)$-singularity of the unscreened potential. This IR singularity is now cut off at momenta $q \sim \lambda^{-1}$, implying benign behavior of the density of states. Using the fact that the density parameter $r_{\rm s}$ scales with the Fermi energy as (exercise) $r_{\rm s} \sim \mu^{-1/2}$, and differentiating $\rho = \partial_\mu^2 F$, it is indeed straightforward to verify that the RPA expansion of F no longer leads to singular behavior of ρ at the Fermi energy.

It is also interesting to consider the limit $v_{\rm F}/\omega \ll q^{-1}$ of essentially **dynamic polarization**. Expansion of $\Pi_{\mathbf{q},\omega_m}$ in Eq. (5.30) to first order in $v_{\rm F}q/\omega \ll 1$ leads to the expression

$$V_{\rm eff}(\mathbf{q},\omega_m) = \frac{4\pi e^2}{q^2}\frac{1}{1+\frac{4\pi\nu_0 e^2 v_{\rm F}^2}{3\omega_{\rm m}^2}} = \frac{4\pi e^2}{q^2}\frac{1}{1-\frac{\omega_{\rm p}^2}{\omega^2}},$$

where $\omega_{\rm p} \equiv (4\pi n e^2/m)^{1/2}$ denotes the **plasma frequency** and we have used the fact that (exercise) the particle density $n \equiv N/L^3 = 2k_F^3/6\pi^2$. In fact, the form of the denominator hints at a collective instability of the electron gas at frequencies $\sim \omega_{\rm p}$. Referring for a more rigorous discussion to the next chapter, one can understand the origin of the instability by another heuristic argument. What we need to remember is that the current formalism is

developed for imaginary times τ. Eventually we will be interested in real-time dynamics, i.e. we need to analytically continue back to $t \sim -i\tau$. In the language of frequencies, this amounts to an analytic continuation process from Matsubara frequencies to real frequencies, $i\omega_m \to \omega$. Sloppily substituting a real frequency into the potential, we obtain $V_{\text{eff}}(\mathbf{q}, \omega_m \to -i\omega) \propto \left(1 - \omega_p^2/\omega^2\right)^{-2}$, i.e. the system seems to respond singularly to excitations with frequency $\omega \sim \omega_p$. The cause of this instability is the well-known plasmon mode of the electron gas.

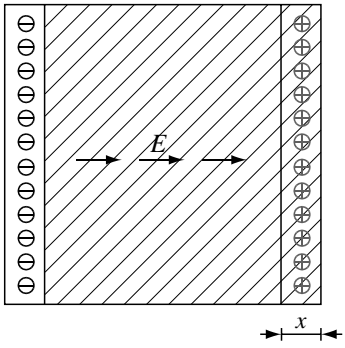

INFO The physics of the **plasmon mode** can be understood as follows. Imagine the electron gas uniformly displaced by a distance x against the positively charged background (see figure). This will lead to the formation of oppositely charged surface layers at the two ends of the system. The surface charge densities $\rho_\pm = \pm exn$ lead to an electric field $E = 4\pi enx$ directed opposite to the displacement vector. Mobile charge carriers inside the system are thus subject to a force $-4\pi e^2 nx$. The solution of the equation of motion $m\ddot{x} = -4\pi e^2 nx$ oscillates at a frequency $\omega_{\text{p}} = (4\pi e^2 n/m)^{1/2}$, the plasma frequency. Since the motion of the charge carriers is in turn responsible for the accumulation of the charged surface layers, we conclude that the system performs a collective oscillatory motion, known as the plasmon excitation.

At this point we conclude our preliminary discussion of the electron gas. We have seen that large-order perturbation theory can be applied to successfully explain various features of the interacting system: energetic lowering due to quantum correlation, screening, and even collective instabilities.

The interacting electron gas is but one example of the many applications of the diagrammatic perturbation theory. After the full potential of the approach had become evident – in the late 1950s and early 1960s – diagrammatic techniques of great sophistication were developed, and applied to a plethora of many-body problems. Indeed, more than two decades passed before large-order perturbation theory eventually ceased to be *the* most important tool of theoretical condensed matter physics. Reflecting the great practical relevance of the approach, there is a huge body of textbook literature concentrating on perturbative methods.[30] Although it would make little sense to develop the field in its full depth once again, a few generally important concepts of diagrammatic perturbation theory are summarized in the next section.

[30] See, e.g., A. A. Abrikosov, L. P. Gorkov, and I. E. Dzyaloshinkii, *Methods of Quantum Field Theory in Statistical Physics* (Dover Publications, Inc., 1975), A. Fetter and J. D. Walecka, *Quantum Theory of Many-Particle Systems* (McGraw-Hill, 1971), D. Pines and P. Nozières, *The Theory of Quantum Liquids – Normal Fermi Liquids* (Addison-Wesley, 1989), and S. Doniach and E. H. Sondheimer, *Green Functions for Solid State Physicists* (Benjamin/Cummings, 1974).

5.3 Infinite-order expansions

Turning back to the prototypical ϕ^4-model, it is the purpose of the present section to introduce a number of general concepts of infinite-order perturbative summations. As should be clear from the discussion above, a meaningful summation over an infinite set of diagrams necessitates the existence of a class of perturbative corrections that is "more important" than others. In practice, what we need is a small parameter that discriminates between diagrams of different structure. In our example above, this parameter was the effective density $r_{\rm s}$ of the electron gas. However, in other settings, the control parameter N may be defined quite differently: large values of a spin, S, the number of colors, $N_{\rm c}$, in QCD, the number of spatial dimensions, d, the number of modes of an optical wave guide, etc. Unfortunately, in most physical contexts, these parameters are typically far from large, $S = 1/2$, $d = N_c = 3$, etc. So we have to resort to a "poor man's" strategy where we develop a controlled and self-consistent theory in the limit of asymptotically large control parameters and hope that some fragments of truth survive the limit down to more mundane values of N. Perhaps unexpectedly, this strategy often works astonishingly well down to values $N = \mathcal{O}(1)$.

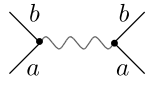

So let us, then, begin by introducing a large control parameter into a ϕ^4-type theory. This can be achieved by promoting ϕ from a scalar to an N-component vector field $\phi = \{\phi^a\}$, $a = 1, \ldots, N$. The self-interaction of the field is modeled as $g \int d^dx\, \phi^a \phi^a \phi^b \phi^b$, i.e. an expression that is "rotationally" invariant in ϕ-space. The action of our modified theory is thus given by

$$S[\phi] \equiv \int d^dx \left(\frac{1}{2} \partial\phi \cdot \partial\phi + \frac{r}{2} \phi \cdot \phi + \frac{g}{4N} (\phi \cdot \phi)^2 \right), \tag{5.37}$$

where the factor $1/N$ in front of the interaction constant has been introduced for later convenience.

As before, we shall concentrate on the Green function $G^{ab}(\mathbf{x} - \mathbf{y}) = \langle \phi^a(\mathbf{x}) \phi^b(\mathbf{y}) \rangle$ as a "test observable." Denoting the Green function by a bold line, the free Green function $G_0 \equiv \langle \phi^a(\mathbf{x}) \phi^b(\mathbf{y}) \rangle_0 \propto \delta^{ab}$ by a thin line, and the interaction operator by a wavy line,[31] the structure of the first- and second-order expansion of the Green function is shown in the upper portion of Fig. 5.8. For simplicity, the combinatorial factors weighting individual diagrams have been omitted.

Self-energy operator

Even without resorting to the large-N structure of the theory, it is possible to bring some order in the spaghetti of diagrams contributing to the expansion. Indeed, there are two distinct subclasses of diagrams: diagrams that are one-particle reducible (i.e. can be cut into two halves by cutting a single internal line, see the classification on page 204) and those that are not. This observation motivates the collection of all one-particle irreducible

[31] Since the four field vertices entering the interaction are no longer indiscriminate, the interaction "point" representation of Section 5.1 is no longer suitable.

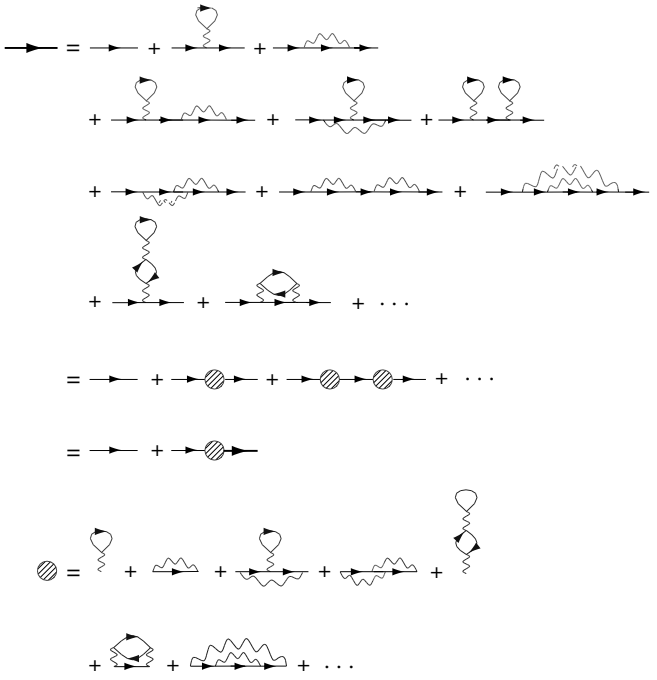

Figure 5.8 Expansion of the Green function of ϕ^4-theory. Bottom: expansion of the self-energy operator.

subportions of the diagrammatic expansion into a structural unit. In Fig. 5.8 this entity, which is commonly called the **self-energy operator**, and sometimes also the **effective mass operator**, is denoted by a hatched circle. The first- and second-order expansion of the self-energy is shown in the bottom part of the figure.

With that definition, the Green function becomes a "chain" of self-energy operators, separated by free Green function lines, as shown in the second equality of the figure. A convenient representation of the expansion is shown in the third equality. An insertion of the full Green function after the first self-energy correction recursively generates the full series. Let us translate these statements into the language

Freeman Dyson, 1923–

Trained as a mathematician, Dyson turned to physics in the 1940s. His work in condensed matter physics, statistical mechanics, and several other areas has had lasting influence on the development of modern theoretical physics. Beyond his professional work in physics, Dyson has written several books on the social implications of modern science. (Photo by Randall Hagadorn. Courtesy of the Institute of Advanced Study.)

of formulae. Denoting the set of all self-energy diagrams by $\hat{\Sigma} = \{\Sigma^{ab}(\mathbf{x}-\mathbf{y})\}$,[32] the expansion of the Green function assumes the form

$$\hat{G} = \hat{G}_0 + \hat{G}_0\hat{\Sigma}\hat{G}_0 + \hat{G}_0\hat{\Sigma}\hat{G}_0\hat{\Sigma}\hat{G}_0 + \cdots = \hat{G}_0 + \hat{G}_0\hat{\Sigma}\hat{G}. \tag{5.38}$$

Here, the operator products involve summation over coordinates and internal indices, i.e $(\hat{A}\hat{B})^{ab}(\mathbf{x}-\mathbf{y}) = \int d^dz\, A^{ac}(\mathbf{x}-\mathbf{z})B^{cb}(\mathbf{z}-\mathbf{y})$. Recursion relations of this type are commonly referred to as **Dyson equations**. The Dyson equation states that the problem of calculating $\hat{G}$ is essentially tantamount to that of analyzing the self-energy. To make this point more explicit, let us reformulate the Dyson equation in momentum space:

$$\hat{G}_{\mathbf{p}} = \hat{G}_{0,\mathbf{p}} + \hat{G}_{0,\mathbf{p}}\hat{\Sigma}_{\mathbf{p}}\hat{G}_{\mathbf{p}} \qquad [\mathbf{1} - \hat{G}_{0,\mathbf{p}}\hat{\Sigma}_{\mathbf{p}}]\hat{G}_{\mathbf{p}} = \hat{G}_{0,\mathbf{p}}.$$

Here we have used the convolution theorem or, more physically, the fact that all scattering processes lumped into the self-energy conserve momentum separately. Matrix multiplication of this identity from the right by $[\mathbf{1} - \hat{G}_{0,\mathbf{p}}\hat{\Sigma}_{\mathbf{p}}]^{-1}$ leads to the expression

$$\hat{G}_{\mathbf{p}} = [\mathbf{1} - \hat{G}_{0,\mathbf{p}}\hat{\Sigma}_{\mathbf{p}}]^{-1}\hat{G}_{0,\mathbf{p}} = \left[\hat{G}_{0,\mathbf{p}}^{-1} - \hat{\Sigma}_{\mathbf{p}}\right]^{-1}.$$

Finally, using the fact that $\left[\hat{G}_{0,\mathbf{p}}^{-1}\right]^{ab} = (p^2 + r)\delta^{ab}$, we arrive at the formal solution

$$\boxed{G_p^{ab} = \left[(p^2 + r - \hat{\Sigma}_p)^{-1}\right]^{ab}.} \tag{5.39}$$

This equation provides two lessons: firstly, the full information about the Green function is indeed stored in the self-energy; secondly, the self-energy somehow "adds" to the arguments p^2 and r entering the quadratic action, a point to be discussed in more detail below.

But how then do we compute the self-energy operator? In fact, the construction recipe follows from what has been said above. By definition, the nth-order contributions to the self-energy are generated by a connected and one-particle irreducible contraction of n interaction operators (weighted with the appropriate combinatorial factor $1/n!$). Two field vertices stay uncontracted as connectors to the free Green function lines contacting the self-energy. For example, the first-order contribution is given by (exercise)

$$\left[\Sigma_{\mathbf{p}}^{(1)}\right]^{ab} = -\delta^{ab}\frac{g}{L^d} \quad \frac{1}{N}\sum_{\mathbf{p}'} G_{0,\mathbf{p}'} + \sum_{\mathbf{p}'} G_{0,\mathbf{p}-\mathbf{p}'} \quad ,$$

where the first (second) contribution corresponds to the first (second) diagram in the self-energy expansion of Fig. 5.8.

EXERCISE Represent the second-order contribution $\Sigma^{(2)}$ in terms of Green functions.

Once the self-energy has been computed to any desired order, the result is substituted into Eq. (5.39) and one obtains the Green function.

[32] The conservation of global momentum of the theory implies (exercise: think about it!) that, like the Green function, the self-energy depends only on the difference of its coordinate arguments.

INFO The critical reader will note that there are some problems with the line of argument above. Firstly, we have tacitly ignored the issue of combinatorics. (How do we know that once we have plugged the expansion of the self-energy into the Dyson equation we get the same result as a brute-force direct expansion of the Green function would have obtained?) To understand that the two-step program – "first compute the self-energy, and then substitute into the Dyson series" – indeed produces correct results, let us consider the nth-order contribution to the expansion of the Green function with its overall combinatorial factor $1/n!$. Now imagine that we want to distribute those diagrams that contain, say, one free internal Green function over two self-energy operators according to the expression $G_0\Sigma G_0\Sigma G_0$. Assuming that the first self-energy operator is of order $m < n$ and the second one of order $n - m$, we notice that there are $\binom{n}{m}$ possibilities to distribute the interaction vertices over the two self-energies. That means that we obtain an overall combinatorial factor of $\frac{1}{n!}\binom{n}{m} = \frac{1}{m!\,(n-m)!}$. But $1/m!$ and $1/(n-m)!$ are precisely the combinatorial factors that appear in the definition of an mth- and an $(n-m)$th-order self-energy operator, respectively. Arguing in reverse, we conclude that the prescription above indeed produces the correct combinatorics.

A second objection concerns the consistency of the expansion, i.e. the nth-order expansion of the self-energy is, of course, by no means equivalent to nth-order expansion of the Green function, nor to any specific order of the expansion. Indeed, when working with the concept of a self-energy, structuring the expansion according to its order in the interaction operator does not make much sense. We should rather focus on the summation of specific infinite-order diagram classes as exemplified in the previous section and discussed in more general terms below.

Large-N expansion

So far we have not made reference to the N-component structure of the theory. However, let us now assume that N is very large, i.e. that we may be content with an expansion of the Green function to leading order in $1/N$. This condition can be made explicit by sending $N \to \infty$ and declaring $\lim_{N\to\infty} G^{aa}_{\mathbf{p}}$ to be our observable of interest.

The limit of large N entails a drastic simplification of the diagrammatic expansion. Each interaction vertex comes with an overall factor of $1/N$ which must be compensated by a summation over field components to produce a contribution that survives the limit $N \to \infty$. This condition removes numerous diagrams contributing to the series. For example, in the Green function expansion of Fig. 5.8 only the first, third, eighth and ninth diagrams survive the limit. In all other contributions, interaction and Green function lines are interwoven in a way that does not leave room for one field-index summation per interaction vertex.

Max Born, 1882–1970

Worked on the mathematical basis of quantum mechanics. Amongst his major contributions was the interpretation of the absolute square of the wave function as a measure of the probability of finding the particle at a given location. Born shared the 1954 Nobel Prize in Physics with Walter Bothe for "for his fundamental research in quantum mechanics, especially for his statistical interpretation of the wavefunction." (Image © The Nobel Foundation.)

Inspection of the series shows that only diagrams void of crossing interaction lines (cf. the figure on the right) survive the limit of large N. The approximation – indeed in the limit of infinite N it becomes exact – that retains only these contributions is commonly called the **non-crossing approximation (NCA)**. More poetically, the diagrams contributing to the reduced expansion are sometimes called "rainbow diagrams."

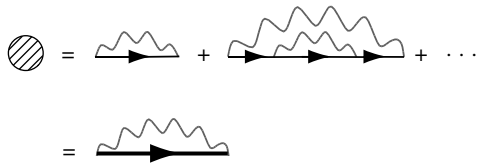

Importantly, the NCA self-energy can be computed in closed form. All one has to realize is that the summation over all rainbow diagrams amounts to substitution of the full NCA Green function under a single interaction line (exercise). Using the fact that in the NCA the self-energy is proportional to unity in the field-index space, we can express this fact through the formula

$$\hat{\Sigma}_{\mathbf{p}} \overset{\text{NCA}}{=} -gL^{-d}\sum_{\mathbf{p}'} G_{\mathbf{p}'} = -gL^{-d}\sum_{\mathbf{p}'} \left(p'^2 + r - \Sigma_{\mathbf{p}'}\right)^{-1}. \tag{5.40}$$

In the literature, this equation goes under the name **self-consistent Born approximation**. It is a "Born approximation" because, formally, it resembles a first-order perturbative correction (the overall factor of g). The approximation is "self-consistent" because the self-energy recursively appears on the right-hand side of the equation again, i.e. the equation is in fact not of first but of infinite order.

INFO Although the objective of the present section is to expose general structures, let us briefly review the **solution of a Born equation**. To keep things simple, let us assume that we are dealing with the low-energy approximation to some microscopic model, i.e. that the momentum summations must be cut off at some upper limit Λ. We further make the assumption (to be checked self-consistently) that the solution for the self-energy operator will turn out to be momentum-independent: $\Sigma_{\mathbf{p}} = \Sigma$. This leads to the expression

$$\Sigma \approx -g\int^{\Lambda} \frac{d^d p}{(2\pi)^d}\frac{1}{p^2 + r - \Sigma}.$$

The evaluation of the integral depends on dimensionality and on the analytical structure of the energy denominator. For example, taking $d = 2$ and assuming that the parameter r is much smaller than the self-energy induced by scattering – an assumption also to be checked self-consistently later on – we obtain

$$\Sigma \approx -\frac{g}{4\pi}\int_0^{\Lambda^2} d(p^2)\frac{1}{p^2 - \Sigma} \simeq -\frac{g}{4\pi}\ln\left(-\frac{\Lambda^2}{\Sigma}\right).$$

A solution $\Sigma(g, \Lambda)$ can now be sought by approximate analytical methods, or graphically. (One plots both sides of the equation as functions of Σ and seeks a crossing point.)

However, for our present discussion, more important than the detailed dependence of Σ on the input parameters g and Λ is the principal meaning of the self-energy: apparently, Σ adds to the parameter r of the naked Green function. (Notice that the solution of the equation determining Σ will be negative.) Remembering that $r \sim \xi^{-1/2}$, one concludes that the interaction operator lowers the spatial correlation of the system. This is indeed what one should expect intuitively: scattering due to interactions acts as a source of "disorder" inside the system.

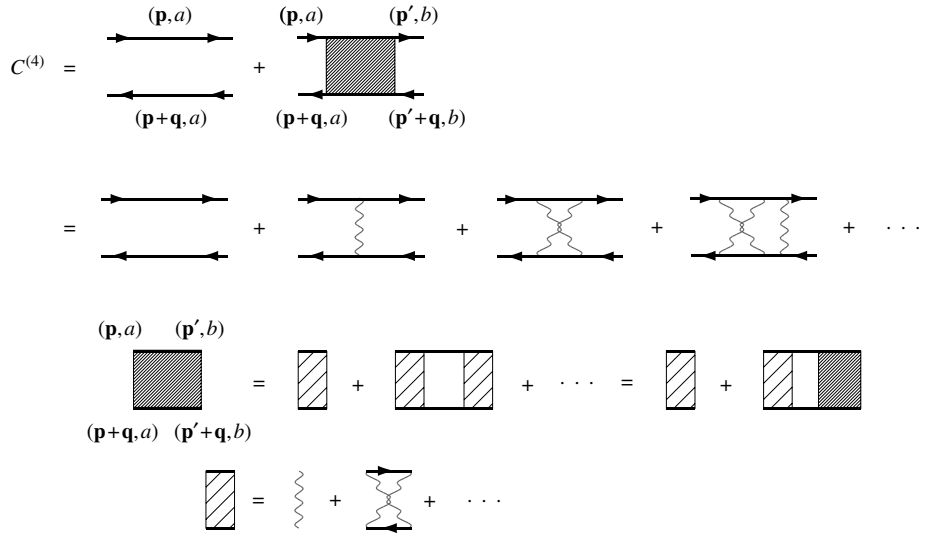

Figure 5.9 Expansion of the four-point function. Notice that the arrows represent the full Green function, i.e. all diagrams "renormalizing" the two-particle subunits of the diagram are automatically included.

At this stage, it is worthwhile to take a step back and see what we have achieved. We have managed to compute the Green function to infinite order in an expansion in the set of "relevant" diagrams. How does that fit together with what has been said in Section 5.1 about the "asymptotic" nature of perturbative series? In fact, the exponential proliferation of the number of diagrams, i.e. the mechanism that led to the eventual breakdown of the perturbative expansion, is blocked by the limit $N \to \infty$. Only subclasses of diagrams, with far fewer members, contribute and the series remains summable.

The large-N principle is actually not limited to the expansion of the Green function. To illustrate the point, let us briefly consider the expansion of the **four-point correlation function**

$$C^{(4)}_{\mathbf{q}} = \frac{1}{N}\sum_{ab}\frac{1}{L^{2d}}\sum_{\mathbf{p},\mathbf{p}'}\langle\phi^a_{\mathbf{p}}\phi^a_{-\mathbf{p}-\mathbf{q}}\phi^b_{-\mathbf{p}'}\phi^b_{\mathbf{p}'+\mathbf{q}}\rangle. \tag{5.41}$$

In the next chapter we will see that objects of this architecture represent the most important information carriers of the theory. Unlike the Green function discussed previously, they relate directly to observable quantities. In the many-body literature, the *four*-point function is described as a **two-particle propagator**, indicating that it describes the joint propagation of two particles. Leaving a more substantial discussion of the meaning of this object to the next chapter, we concentrate here on the formal aspects of its perturbative expansion.

The structure of the expansion of the four-point function is shown in Fig. 5.9 where, for simplicity, momentum/component-indices are indicated only once. The simplest diagram contributing to the expansion consists of just two Green functions. It encapsulates all disconnected contractions, i.e. $\left\langle\phi^a_{\mathbf{p}}\phi^b_{-\mathbf{p}'}\right\rangle\left\langle\phi^a_{-\mathbf{p}-\mathbf{q}}\phi^b_{\mathbf{p}'+\mathbf{q}}\right\rangle \sim \delta^{ab}\delta_{\mathbf{p}\mathbf{p}'}$ contributing to $C^{(4)}$. All

other contractions simultaneously involve all four field operators, i.e. they contain interaction lines between the Green functions. The sum of all these contributions is represented by the diagram containing the hatched surface. A few low-order contributions to the expansion are explicitly shown in the second line. Notice that all arrows appearing in these diagrams are fat. This means that diagrams "dressing" the two-particle sub-units of the expansion are automatically included. For example, the second contribution, containing just a single interaction line between the two-particle propagators, in fact represents an entire series of diagrams obtained by substituting the expansion of Fig. 5.8 for the full Green function. (In an analytical calculation, one will take account of these contributions simply by substitution of the self-energy renormalized Green function for each arrow.)

EXERCISE Write down the analytical expressions contributing to the low-order diagrams shown in the first and second lines of the figure.

All diagrams involving interactions between the two Green functions have the common factor that they contain four external "legs," i.e. the Green function connectors to the external field operators. If you imagine these legs removed, you end up with a "core contribution" often called the **vertex**. (The designation is motivated by the fact that the first contribution to the vertex is, indeed, the contracted interaction vertex of the action; see diagram no. 2.) In Fig. 5.9, the vertex is denoted by a tightly hatched area.

As with the Green function, the expansion of the vertex can be given some structure. To this end, notice that some of the diagrams contributing to the vertex (e.g. the second diagram in the second line with external legs removed) can be cut into two just by cutting two internal Green function lines. Vertex diagrams of this type are called **two-particle reducible**, by analogy with the "one-particle reducible" contributions to the expansion of the Green function. As with the expansion of the latter, one can lump all irreducible contributions to the vertex (e.g. the last diagram in the first line, or the first diagram in the second line, external legs removed) into a structural subunit called the **irreducible vertex**. In Fig. 5.9, that unit is denoted by a lightly hatched area. The first two diagrams contributing to the irreducible vertex are shown in the fourth line of the figure. Here, one can see that the irreducible vertex plays a role similar to the self-energy of the Green function. Expressed in terms of the irreducible vertex, the expansion assumes the regular form shown in the third line.

To represent these graphical relations in analytical form, we denote the full vertex by the symbol $\hat{\Gamma} = \{\Gamma^{aa',bb'}_{\mathbf{p},\mathbf{p}',\mathbf{q}}\}$ and the irreducible vertex by $\hat{\Gamma}_0 = \{\Gamma^{aa',bb'}_{0,\mathbf{p},\mathbf{p}',\mathbf{q}}\}$ where the indices a, a', b, b' keep track of the index labels carried by the four Green functions entering the vertex. (Although we have defined our correlation function in such a way that $a = a'$, $b = b'$, a generalization

Hans Albrecht Bethe, 1906–2005

Nobel Laureate in physics in 1967 for his "contributions to the theory of nuclear reactions, especially his discoveries concerning the energy production in stars." As well as nuclear matter, he has also contributed substantially to atomic and condensed matter physics." (Image © The Nobel Foundation.)

to a four-fold index label is necessary to formulate the recursion Eq. (5.42).) The three momentum arguments represent the momenta of the Green functions connecting to the vertex operators, as indicated explicitly in the first line of the figure. (Remember that the theory has overall momentum conservation, i.e. three momentum arguments suffice to unambiguously fix the momentum dependence of Γ and $C^{(4)}$.) The content of the third line of the figure can then be expressed in terms of a closed recursion relation:

$$\Gamma^{aa',bb'}_{\mathbf{p},\mathbf{p}',\mathbf{q}} = \Gamma^{aa',bb'}_{0,\mathbf{q},\mathbf{p}',\mathbf{p}} + \frac{1}{L^d} \sum_{c,c',\mathbf{p}''} \Gamma^{aa',cc'}_{0,\mathbf{p},\mathbf{p}'',\mathbf{q}} G^{c}_{\mathbf{p}''} G^{c'}_{\mathbf{p}''+\mathbf{q}} \Gamma^{cc',bb'}_{\mathbf{p}'',\mathbf{p}',\mathbf{q}}. \tag{5.42}$$

Equations of this type are (often) called **Bethe–Salpeter equations**. Comparison with Eq. (5.38) shows that this equation appears to be conceptually similar to the Dyson equation for the one-particle Green function.[33] Indeed, the principle behind most recursion relations of perturbation theory is a structure like

$$\boxed{\hat{X} = \hat{X}_0 + \hat{X}_0 * \hat{Z} * \hat{X},} \tag{5.43}$$

where $\hat{X}$ is our object of interest (e.g. $\hat{\Gamma}$), $\hat{X}_0$ its "free" version, $\hat{Z}$ a subunit that is, in some sense, "irreducible" ($\hat{\Sigma}$ or $\hat{\Gamma}_0 GG$), and $*$ some generalized matrix convolution.

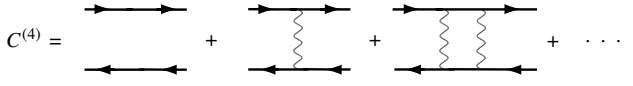

Figure 5.10 Large-N expansion of the two-particle correlation function into a "ladder structure".

Owing to the importance of the two-particle propagator, the solution of Bethe–Salpeter type equations is a central issue of many areas of many-body physics. In most cases only approximate solutions can be obtained. With our present example, "approximate" means that one sends N to large values and seeks a solution to leading order in N^{-1}. In that limit, the only surviving contribution to the irreducible vertex is the first, i.e. a plain interaction line (see Fig. 5.10). As with the self-energy operator discussed in the previous section, all diagrams with "entangled" interaction lines are frustrated in the sense that we do not have as many index summations as interaction constants $\sim g/N$. Such contributions vanish in the limit of large N. We thus conclude that the Bethe–Salpeter equation assumes the simple form

$$\Gamma^{ab}_{\mathbf{p},\mathbf{p}',\mathbf{q}} = -\frac{g}{NL^d} - \frac{g}{N}\frac{1}{L^d} \sum_{c,\mathbf{p}''} G^{a}_{\mathbf{p}''} G^{c}_{\mathbf{p}''+\mathbf{q}} \Gamma^{cb}_{\mathbf{p}'',\mathbf{p}',\mathbf{q}},$$

[33] We can make the analogy perfect by defining a "one-particle vertex" $\hat{\Gamma}^{(1)} = \hat{G}^{(0)-1}[\hat{G} - \hat{G}^{(0)}]\hat{G}^{(0)-1}$. Inspection of the second equality of Fig. 5.8 shows that the expansion of $\Gamma^{(1)}$ starts and ends with a self-energy operator, i.e. the first free Green function line G_0 is removed, and so are the two external G_0s connecting to the self-energy operator. In direct analogy to Eq. (5.42), the analytical formula for $\Gamma^{(1)}$ then reads $\hat{\Gamma}^{(1)} = \Sigma + \Sigma G_0 \hat{\Gamma}^{(1)}$.

where $\Gamma^{ab} \equiv \Gamma^{aa',bb'}\delta^{aa'}\delta^{bb'}$.[34] This equation can be simplified even further by making the *ansatz* $\Gamma^{ab}_{\mathbf{p},\mathbf{p}',\mathbf{q}} = \Gamma_{\mathbf{q}}$, where Γ is independent of discrete indices and input momenta $\mathbf{p}$ and $\mathbf{p}'$. (When solving a perturbative recursion relation, it is always a good idea to try an *ansatz* of maximal simplicity, i.e. one that is no more complex than the constituting elements of the equation.) Then,

$$\Gamma_{\mathbf{q}} = -\frac{g}{NL^d} - gP_{\mathbf{q}}\Gamma_{\mathbf{q}} \Rightarrow \Gamma_{\mathbf{q}} = -\frac{g}{NL^d}\frac{1}{1+gP_{\mathbf{q}}}, \tag{5.44}$$

where we have introduced the abbreviation $P_{\mathbf{q}} = \frac{1}{L^d}\sum_{\mathbf{p}} G_{\mathbf{p}}G_{\mathbf{p}+\mathbf{q}}$. In principle, one may now proceed by substituting the large-N expansion of the Green function (5.39) and computing the function $P_{\mathbf{q}}$ by integration over $\mathbf{p}$. This would produce a closed expression for Γ and, by virtue of the relation

$$C^{(4)}_{\mathbf{q}} = P_{\mathbf{q}}\left[\frac{1}{L^d} + N\Gamma_{\mathbf{q}}P_{\mathbf{q}}\right],$$

our correlation function. Since the emphasis in this section is on conceptual aspects of perturbation theory, we will not pursue the analysis to its very end. (For an analysis of the Bethe–Salpeter equation in a context more interesting than ϕ^4-theory, see the discussion of the quantum disorder problem in the next chapter.) Yet there is one aspect of the expression for $\Gamma_{\mathbf{q}}$ worth noticing. Consider $P_{\mathbf{q}}$ expanded as a Taylor series in $\mathbf{q}$ and focus on the zeroth-order contribution, P_0. From the definition of the Green function (5.39) we have

$$P_0 = \frac{1}{L^d}\sum_{\mathbf{p}} G^2_{\mathbf{p}} = \partial_\Sigma \frac{1}{L^d}\sum_{\mathbf{p}} G_{\mathbf{p}} \overset{(5.40)}{=} -g^{-1}\partial_\Sigma\Sigma = -g^{-1}. \tag{5.45}$$

When substituted into the formula for Γ, this shows that for small momenta the expansion of the numerator of the vertex starts with a power of $\mathbf{q}$. (By symmetry, the first non-vanishing contribution will be of $\mathcal{O}(q^2)$.) This means that both the vertex and the four-point correlation function are long-ranged objects, i.e. unlike the Green function, they decay not exponentially, but as a power law. The long-range character of the four-point function has observable consequences, as discussed in the next chapter.

Summarizing, our discussion of the two- and four-point functions, and of the RPA theory of the interacting electron gas has shown that, if a large parameter is present, (a) relevant subclasses of perturbative contributions can be identified and (b) they can be summed to infinite order. As a matter of fact, there are not too many of these summable diagram classes: ring-diagrams, rainbow-diagrams and ladder-diagrams nearly exhaust the set of "friendly" corrections, amenable to analytical summation. Notice that, so far, we have largely restricted ourselves to the discussion of abstract summation schemes; i.e. we still need to learn more about the way intermediate results like Eq. (5.39) or (5.44) can be translated into concrete physical information. These aspects are discussed – on applications more rewarding than

[34] Here we have used the fact that the large-N approximation of the irreducible vertex forces the two input indices a, a' to be equal (and the same for the output indices). As a word of caution, strictly speaking, our large-N approximation of the irreducible vertex explicitly uses the fact that the input/output indices entering our definition of the vertex are equal, i.e. should we compute a correlation function where the two input/output indices are different (a rare occurrence in realistic applications), the large-N approximation of the four-point functions would no longer assume the simple form of a regular ladder.

plain ϕ^4-theory – a little later. However, at this point we leave the discussion of formal perturbation theory. While a state-of-the-art exposition of the subject would require much more space – for pedagogical and condensed-matter-oriented texts on perturbative methods, see Pines and Nozières, and Schulman[35] – the material introduced in this section suffices for nearly all purposes of the present text.

Turning back to our prototypical problem of the interacting electron gas, in the next chapter we extend the purely diagrammatic methods discussed above to a more powerful hybrid approach comprising perturbative concepts in combination with functional methods.

5.4 Summary and outlook

This concludes our preliminary introduction to the concepts of perturbation theory. We have seen that general perturbative expansions mostly have the status of "asymptotic" rather than convergent series. We have learned how to efficiently encode perturbative series by graphical methods and how to assess the "importance" of individual contributions. Further, we have seen how the presence of a large parameter can be utilized to firmly establish infinite-order expansions. A number of recursive techniques have been introduced to sum up diagram sequences of infinite order.

However, a second look at the discussion of the previous sections shows that the central tool, the functional integral, did not play much of a role. All it did was to provide the combinatorial framework of the perturbative expansion of correlation functions. However, for that we hardly need the full machinery of functional integration. Indeed, the foundations of the perturbative approach were laid down in the 1950s, long before people even began to think about the conventional path integral. (For a pure operator construction of the perturbative expansion, see the problem set.)

More importantly, the analysis so far has a serious methodological weakness: all subclasses of relevant diagrams had the common feature that they contained certain "sub-units," more structured than the elementary propagator or the interaction line. For example, the RPA diagrams were organized in terms of polarization bubbles, the NCA diagrams had their rainbows, and the ladder diagrams their rungs. Within the diagrammatic approach, in each diagram these units are reconstructed "from scratch," i.e. in terms of elementary propagators and interaction lines. However, taking seriously the general philosophy on information reduction declared at the beginning of the text, we should strive to make the "important" structural elements of an expansion our *elementary* degrees of freedom. This program is hardly feasible within purely diagrammatic theory. However, the functional integral is ideally suited to introducing degrees of freedom hierarchically, i.e. trading microscopic objects for entities of higher complexity. The combination of functional integral techniques with perturbation theory presents a powerful theoretical machinery which is the subject of the next chapter.

[35] See D. Pines and P. Nozières, *The Theory of Quantum Liquids Normal Fermi Liquids* (Addison-Wesley, 1989), and L. S. Schulman, *Techniques and Applications of Path Integration* (Wiley, 1981).

5.5 Problems

Technical aspects of diagrammatic perturbation theory

Taking the second-order expansion of the ϕ^4 Green function as an example, it is the purpose of this problem to discuss a number of technical aspects relating to the classification and the combinatorics of diagrams.

(a) Show that the full contraction of $\langle \phi(\mathbf{x})\phi^4(\mathbf{y})\phi^4(\mathbf{y}')\phi(\mathbf{x}')\rangle$ generates the 945 terms

$$\begin{aligned}
&\underbrace{9G_0(\mathbf{x}-\mathbf{x}')G_0^4(\mathbf{0})}_{1} + \underbrace{72G_0(\mathbf{x}-\mathbf{x}')G_0^2(\mathbf{y}-\mathbf{y}')G_0^2(\mathbf{0})}_{2} + \underbrace{24G_0(\mathbf{x}-\mathbf{x}')G_0^4(\mathbf{y}-\mathbf{y}')}_{3} \\
&+\Bigg[\underbrace{36G_0(\mathbf{x}-\mathbf{y})G_0(\mathbf{x}'-\mathbf{y})G_0^3(\mathbf{0})}_{4} + \underbrace{144G_0(\mathbf{x}-\mathbf{y})G_0(\mathbf{x}'-\mathbf{y})G_0^2(\mathbf{y}-\mathbf{y}')G_0(\mathbf{0})}_{5} \\
&+\underbrace{96G_0(\mathbf{x}-\mathbf{y})G_0(\mathbf{x}'-\mathbf{y}')G_0^3(\mathbf{y}-\mathbf{y}')}_{6} \\
&+\underbrace{144G_0(\mathbf{x}-\mathbf{y})G_0(\mathbf{x}'-\mathbf{y}')G_0(\mathbf{y}-\mathbf{y}')G_0^2(\mathbf{0})}_{7} \\
&+(\mathbf{y} \quad \to \mathbf{y}').\Bigg]
\end{aligned} \tag{5.46}$$

Try to reproduce the combinatorial prefactors.

(b) Check explicitly that the disconnected terms cancel against the "vacuum loops" from the expansion of the denominator.

(c) Represent the corresponding diagrams in momentum space. Convince yourself that the "Kirchhoff law" discussed in the main text suffices to unambiguously fix the result.

Answer:

(a) The seven distinct pairings of the ten ϕ-fields are shown in Fig. 5.2 (and referred to here as diagrams 1–7 in the order in which they appear in the figure). By way of example, let us consider the combinatorial factor of diagram 2. There are $3 \cdot 2 = 6$ ways to pair two fields $\phi(\mathbf{y})$ and the same for $\phi(\mathbf{y}')$. From these two contractions, we obtain a factor $(6G(\mathbf{0}))^2$. Then, there are two possible ways of pairing the two remaining $\phi(\mathbf{y})$ with the two remaining $\phi(\mathbf{y}')$ leading to a factor $2G_0^2(\mathbf{y}-\mathbf{y}')$. Finally, the pairing of $\phi(\mathbf{x})$ with $\phi(\mathbf{x}')$ obtains a single factor $G_0(\mathbf{x}-\mathbf{x}')$. Multiplying all contributions, we obtain term 2.

(b) To obtain all terms contributing to $G^{(2)}$, both numerator and denominator of Eq. (5.14) have to be expanded to second order (where the identification $X[\phi] = \phi(\mathbf{x})\phi(\mathbf{x}')$ is understood). In symbolic notation,

$$\frac{N_0 + N_1 + \frac{1}{2}N_2 + \cdots}{1 + D_1 + \frac{1}{2}D_2 + \cdots} \simeq N_0 + \underbrace{N_1 - N_0 D_1}_{G^{(1)}} + \underbrace{\frac{1}{2}N_2 - N_1 D_1 + N_0 D_1^2 - \frac{1}{2}N_0 D_2}_{G^{(2)}}.$$

The expression for N_2 is given by formula (5.46). From the main text, we know that $N_1 = 3G_0(\mathbf{x}-\mathbf{x}')G_0^2(\mathbf{0}) + 12G_0(\mathbf{x}-\mathbf{y})G_0(\mathbf{0})G_0(\mathbf{y}-\mathbf{x}')$ and $D_1 = 3G_0^2(\mathbf{0})$. Further, $N_0 = G_0(\mathbf{x}-\mathbf{x}')$. Finally, D_2 reads

$$\left\langle \phi^4(\mathbf{y})\phi^4(\mathbf{y}')\right\rangle = 9G_0^4(\mathbf{0}) + 72G_0^2(\mathbf{0})G_0^2(\mathbf{y}-\mathbf{y}') + 24G_0^4(\mathbf{y}-\mathbf{y}').$$

Collecting all the terms, we obtain

$$\begin{aligned} N_2 \quad - \quad & 18G_0(\mathbf{x}-\mathbf{x}')G_0^4(\mathbf{0}) \underbrace{-72G_0(\mathbf{x}-\mathbf{y})G_0^3(\mathbf{0})G_0(\mathbf{y}-\mathbf{x}')}_{-(4+\mathbf{y}\quad\mathbf{y}')} + 18G_0(\mathbf{x}-\mathbf{x}')G_0^4(\mathbf{0}) \\ & \underbrace{-9G_0(\mathbf{x}-\mathbf{x}')G_0^4(\mathbf{0})}_{-1} \underbrace{-72G_0(\mathbf{x}-\mathbf{x}')G_0^2(\mathbf{0})G_0^2(\mathbf{y}-\mathbf{y}')}_{-2} \\ & \underbrace{-24G_0(\mathbf{x}-\mathbf{x}')G_0^4(\mathbf{y}-\mathbf{y}')}_{-3} \\ = \quad & \underbrace{144G_0(\mathbf{x}-\mathbf{y})G_0(\mathbf{x}'-\mathbf{y})G_0^2(\mathbf{y}-\mathbf{y}')G_0(\mathbf{0})}_{5} \\ & + \underbrace{144G_0(\mathbf{x}-\mathbf{y})G_0(\mathbf{x}'-\mathbf{y}')G_0(\mathbf{y}-\mathbf{y}')G_0^2(\mathbf{0})}_{6} \\ & + \underbrace{96G_0(\mathbf{x}-\mathbf{y})G_0(\mathbf{x}'-\mathbf{y}')G_0^3(\mathbf{y}-\mathbf{y}')}_{7} \\ & + (\mathbf{y} \quad \to \mathbf{y}'), \end{aligned}$$

i.e. the set of connected diagrams shown in Fig. 5.4.

(c) This translates to a straightforward exercise in Fourier transformation.

Self-consistent T-matrix approximation

As well as scattering from lattice vibrations and other electrons, the low-temperature conductivity of a metal is heavily influenced by defects or impurities. The general role of weak impurity scattering is discussed in some detail in Section 6.5. As a warm-up to our more comprehensive discussion below, the aim of the present problem is to determine the scattering rate imposed by a collection of isolated impurities using diagrammatic perturbation theory.

Consider a system of spinless electrons subject to a random pattern of $N_{\rm imp}$ non-magnetic scattering impurities and described by the Hamiltonian $\hat{H} = \hat{H}_0 + \hat{H}_{\rm imp}$, where $\hat{H}_0 = \sum_{\mathbf{k}} \epsilon_{\mathbf{k}} c_{\mathbf{k}}^\dagger c_{\mathbf{k}}$,

$$\hat{H}_{\rm imp} = v_0 a^d \int d^d r \sum_{i=1}^{N_{\rm imp}} \delta(\mathbf{r}-\mathbf{R}_i) c^\dagger(\mathbf{r}) c(\mathbf{r}) = v_0 a^d \sum_{i=1}^{N_{\rm imp}} c^\dagger(\mathbf{R}_i) c(\mathbf{R}_i),$$

and we have assumed that an impurity at position $\mathbf{R}_i$ creates a local potential $v_0 a^d \delta(\mathbf{r}-\mathbf{R}_i)$. (Here a is a constant, of dimensionality [length], identified roughly with the extension of the impurity.)

Our aim is to compute the single-particle Green function $G_n(\mathbf{r}-\mathbf{r}') \equiv \langle\langle c_n^\dagger(\mathbf{r}) c_n(\mathbf{r}')\rangle\rangle_{\rm imp}$ where n is a Matsubara frequency index and the configurational average $\langle\ldots\rangle_{\rm imp} \equiv L^{-dN_{\rm imp}} \prod_i \int d^dR_i$ is defined by integration over all impurity coordinates.

(a) To begin, let us consider scattering from a single impurity (i.e. $N_{\rm imp} = 1$). By developing a perturbative expansion in the impurity potential, show that the Green function can be written as $\hat{G}_n = \hat{G}_{0,n} + \hat{G}_{0,n}\hat{T}_n\hat{G}_{0,n}$, where

$$\hat{T}_n = \langle \hat{H}_{\rm imp} + \hat{H}_{\rm imp}\hat{G}_{0,n}\hat{H}_{\rm imp} + \hat{H}_{\rm imp}\hat{G}_{0,n}\hat{H}_{\rm imp}\hat{G}_{0,n}\hat{H}_{\rm imp} + \cdots\rangle_{\rm imp}, \tag{5.47}$$

denotes the **T-matrix**,[36] and $\hat{G}_n = \{G_n(\mathbf{r}-\mathbf{r}')\}$. Show that the T-matrix equation is solved by $T_n(\mathbf{r},\mathbf{r}') = \delta(\mathbf{r}-\mathbf{r}')L^{-d}\left((v_0a^d)^{-1} - G_{0,n}(0)\right)^{-1}$.

(b) For a collection of random impurities, the capacity for multiple scattering makes the concept of the T-matrix defined for the full operator $\hat{H}_{\rm imp}$ unilluminating. Instead, one would like to find an expression for the configurational average of the Green function involving the T-matrix of a single isolated impurity. Presenting the Green function as a series expansion in the impurity potential v, enumerate and classify the contributions entering the configurational average up to third order in v. Organising the series at this order in a diagrammatic expansion, show that a subset (all but one) of the diagrams can be incorporated into a Dyson series expansion, $G_k = G_{0,k} + G_{0,k}\Sigma_k G_k$, where $G_k \equiv G_{n,\mathbf{k}}$ denotes the Green function in a four-momentum representation, $\Sigma_k = N_{\rm imp}\langle\mathbf{k}|\hat{T}_n|\mathbf{k}\rangle$ is the self-energy and $\hat{T}_n$ represents the T-matrix for a single isolated impurity.

The Dyson series expansion can be inverted to give $G_k = (i\omega_n - \xi_k - \Sigma_k)^{-1}$. When Fourier transformed back to time/space, one may note that the imaginary part of the self-energy can be associated with (one half of) the scattering rate, ${\rm Im}\Sigma_k = -\frac{1}{2\tau}{\rm sgn}(n)$ (cf. the Info block on page 379 for further discussion of this point). To understand the sign factor ${\rm sgn}(n)$, notice that the imaginary part of T_n is determined by the imaginary part of $G_{0,n}$. However, it is straightforward to verify that ${\rm sgn}({\rm Im}G_{0,n}) \propto {\rm sgn}n$. (For a comprehensive discussion of the analyticity properties of the self-energy, we refer to Chapter 7.)

(c) Sometimes, one is interested in the T-matrix for a fixed (unaveraged) pattern of dilute impurities. In this case, the single-impurity T-matrix is given by the right hand side of Eq. (5.47), without the averaging brackets; it is no longer diagonal in momentum space, i.e. $\hat{T}_n = \{\langle\mathbf{k}|\hat{T}_n|\mathbf{k}'\rangle\} = \{T_{n,\mathbf{k}\mathbf{k}'}\}$.

Making use of the operator identity $(\mathbf{1}-\hat{O}_2)^{-1} - (\mathbf{1}-\hat{O}_1)^{-1} = (\mathbf{1}-\hat{O}_2)^{-1}(\hat{O}_2-\hat{O}_1)(\mathbf{1}-\hat{O}_1)^{-1}$, and defining the real-frequency analytical continuation $\hat{T}^\pm(\epsilon) \equiv \hat{T}(i\omega_n \to \epsilon \pm i\delta)$ (the same for $\hat{G}$) show that

$$\hat{T}^+(\epsilon) - \hat{T}^-(\epsilon) = \hat{T}^-(\epsilon)(\hat{G}_0^+(\epsilon) - \hat{G}_0^-(\epsilon))\hat{T}^+(\epsilon). \tag{5.48}$$

Using this result, show that the scattering rate is given by

$$\frac{1}{2\tau} \equiv {\rm Im}\ \Sigma(\epsilon = \epsilon_{\mathbf{k}} + i0) = \pi \sum_{\mathbf{k}'} |\langle\mathbf{k}'|\hat{T}^+(\epsilon_{\mathbf{k}})|\mathbf{k}\rangle|^2\, \delta(\epsilon_{\mathbf{k}} - \epsilon_{\mathbf{k}'}). \tag{5.49}$$

[36] For a discussion of the physical content of the T-matrix and its connection to the scattering matrix, we refer to any elementary text on scattering theory.

Answer:

(a) Representing the Green function as a coherent state path integral and performing the Gaussian integral over the Grassmann field, we obtain the formal result $\hat{G}_n = (i\omega_n - \hat{H}_0 - \hat{H}_{\rm imp})^{-1}$. We next expand $\hat{G}_n$ in $\hat{H}_{\rm imp}$ and compare with the definition of the T-matrix to identify the series in Eq. (5.47). Substitution of $\hat{H}_{\rm imp} = v_0 a^d \delta(\mathbf{r}-\mathbf{R})$, where $\mathbf{R}$ is the impurity position, we obtain $\hat{T} = \langle \delta(\mathbf{r}-\mathbf{R})\delta(\mathbf{r}'-\mathbf{R})\rangle_{\rm imp} v_0 a^d (1 - v_0 a^d G_{0,n}(0,0))^{-1}$. Performing the average and rearranging terms we arrive at the result (see Fig. 5.11).

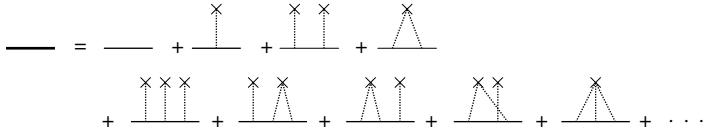

Figure 5.11 Diagrammatic series expansion of the impurity averaged Green function (for a discussion, see the main text).

(b) Presented as a series expansion in the random potential,

$$\hat{G}_n = \langle \hat{G}_{0,n} + \hat{G}_{0,n}\hat{H}_{\rm imp}\hat{G}_{0,n} + \hat{G}_{0,n}\hat{H}_{\rm imp}\hat{G}_{0,n}\hat{H}_{\rm imp}\hat{G}_{0,n} + \cdots \rangle_{\rm imp}.$$

Turning to a momentum space representation and using the fact that $\langle \mathbf{k}|\hat{H}_{\rm imp}|\mathbf{k}'\rangle = v_0 (a/L)^d \sum_i e^{i\mathbf{R}_i(\mathbf{k}-\mathbf{k}')}$, the first term in the series assumes the form

$$G^{(1)}_{k,k'} = G_{0,k} v_0 \left(\frac{a}{L}\right)^d \sum_i \langle e^{i\mathbf{R}_i(\mathbf{k}-\mathbf{k}')}\rangle_{\rm imp} G_{0,k'} = G_{0,k} v_0 N_{\rm imp} \left(\frac{a}{L}\right)^d G_{0,k}\delta_{kk'}.$$

At second order, we obtain

$$\begin{aligned} G^{(2)}_{k,k'} &= G_{0,k} v_0^2 \left(\frac{a}{L}\right)^{2d} \sum_{\mathbf{k}''} \sum_{i,i'} \langle e^{i\mathbf{R}_i(\mathbf{k}-\mathbf{k}'')} G_{0,k''} e^{i\mathbf{R}_{i'}(\mathbf{k}''-\mathbf{k}')}\rangle_{\rm imp} G_{0,k'} \\ &= G_{0,k} v_0^2 \left(\frac{a}{L}\right)^{2d} \left(N_{\rm imp} \sum_{\mathbf{k}''} G_{0,k''} + N^2_{\rm imp} G_{0,k} \right) G_{0,k}\delta_{kk'}, \end{aligned}$$

where the first (second) contribution describes the two-fold scattering off a single (one-fold scattering off two different) impurities. Notice that, upon averaging, both types of scattering conserve momentum, i.e. $G_{kk'} \propto \delta_{kk'}$. A graphical representation of the two processes is shown in the first line of Fig. 5.11 where crosses represent individual impurities (averaging over position understood) while the dashed lines denote scattering events. At third order in v, one may identify contributions from where all three impurities are distinct, where only two are distinct, and where the scattering occurs at the same impurity (see the bottom line of the figure). Of these terms, one may note that the penultimate diagram is special as it involves a "crossing" of the impurity (i.e. the dotted) lines. Later, in the discussion of the weakly disordered system, we show that such contributions enter with a suppression factor of $1/k_{\rm F}\ell \ll 1$, where $\ell = v_{\rm F}\tau$ is the elastic mean free path, $k_{\rm F}$ the Fermi wavevector, and the inequality holds in all but the dirtiest metals. Physically, diagrams with crossed lines represent processes wherein an

electron alternately scatters off different impurities. Clearly, such events become highly improbable in the limit of a low impurity concentration.

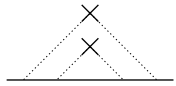

Since impurity averages engaging a single impurity involve zero momentum transfer, one may note that the remaining series can be organised into the form of the required Dyson series expansion. Here, since the blocks entering the series do not correlate different impurities, the self-energy may be identified as $N_{\rm imp}$ times the single-impurity T-matrix; the approximation neglecting crossed lines is called the **T-matrix approximation**.

Now, when pursuing to fourth order and higher, one may note the existence of a second class of "rainbow" diagrams which (a) do not involve crossed impurity lines and (b) are not included in the Dyson series (see the figure above.) These contributions can be incorporated by replacing the bare Green function $\hat{G}_{0,k}$ by the impurity averaged Green $\hat{G}_k$ in the T-matrix expansion Eq. (5.47), an exercise that can be performed only self-consistently. Such a scheme is known as the **self-consistent T-matrix approximation (SCTA)**.

(c) Noting that $\hat{T}^{\pm}(\epsilon) = \hat{H}_{\rm imp}(\mathbf{1} - \hat{G}_0^{\pm}(\epsilon)\hat{H}_{\rm imp})^{-1}$, a straightforward application of the given identity gives the required expression. Now, applying this result to the self-energy, substituting $\epsilon = \epsilon_{\mathbf{k}}$ for the energy arguments of the Green functions, and noting that $\mathrm{Im}\,\langle \mathbf{k}'|\hat{G}_0^{+}(\epsilon_{\mathbf{k}})|\mathbf{k}'\rangle = \pi\delta(\epsilon_{\mathbf{k}} - \epsilon_{\mathbf{k}'})$, one obtains Eq. (5.49), a manifestation of the "Golden Rule."

Kondo effect: perturbation theory

In Problem 2.4, we introduced the Kondo effect, describing the interaction of a local impurity with an itinerant band of carriers. (Those unfamiliar with the physical context and background to the problem are referred back to that section.) There we determined an effective Hamiltonian for the coupled system, describing the spin exchange interaction that acts between the local moment of the impurity state and the itinerant band. In the following, motivated by the seminal work of Kondo, we employ methods of perturbation theory to explore the impact of magnetic fluctuations on transport. In doing so, we elucidate the mechanism responsible for the observed minimum of electrical resistance found in magnetic impurity systems.

The perturbation theory of the Kondo effect is one of those problems where the traditional formalism of second quantized operators is superior to the field integral (the reason being that perturbative manipulations on quantum spins are di cult to formulate in a field integral language). More specifically, the method of choice would be second quantized perturbation theory formulated in the interaction picture, a concept discussed in great detail in practically any textbook on many-body perturbation theory, but not in this text. For this reason, the solution scheme discussed below is somewhat awkward and surely not very e cient (yet fully su cient for understanding the essence of the phenomenon).

Although the phenomenology of the Kondo system can be explored in several different ways ranging from the exact analytical solution of the Kondo Hamiltonian system[37] to a variational analysis of the Anderson impurity Hamiltonian,[38] in the following we focus on the perturbative scheme developed in the original work of Kondo. Later, in Problem 8.8.5, we will introduce a more advanced approach based on the renormalization group. The starting point of the analysis is the effective sd–Hamiltonian (2.51) introduced in Problem 2.4. Setting $\hat{H}_{\rm sd} = \hat{H}_0 + \hat{H}_{\rm imp}$ where

$$\hat{H}_0 = \sum_{\mathbf{k}\sigma} \epsilon_{\mathbf{k}} c^\dagger_{\mathbf{k}\sigma} c_{\mathbf{k}\sigma}, \quad \hat{H}_{\rm imp} = 2J\hat{\mathbf{S}} \cdot \hat{\mathbf{s}}(\mathbf{r}=0),$$

and $\hat{\mathbf{s}}(0) = \frac{1}{2}\sum_{\mathbf{k}\mathbf{k}'\sigma\sigma'} c^\dagger_{\mathbf{k}\sigma} \boldsymbol{\sigma}_{\sigma\sigma'} c_{\mathbf{k}'\sigma'}$, our aim here is to develop a perturbative expansion in J to explore the scattering properties of the model. Here we have assumed that the exchange constant J is characterized by a single parameter, positive in sign (i.e. antiferromagnetic).

In Problem 5.5, we have seen that the scattering rate associated with a system of impurities is specified by the T-matrix:

$$\frac{1}{2\tau} = \pi N_{\rm imp} \sum_{\mathbf{k}',\sigma'} \left\langle |\langle \mathbf{k},\sigma|T^+(\epsilon)|\mathbf{k}',\sigma'\rangle|^2 \right\rangle_{\rm S} \delta(\epsilon_{\mathbf{k}} - \epsilon_{\mathbf{k}'}),$$

where the symbol $\langle \cdots \rangle_{\rm S} \equiv {\rm tr}_{\rm S}(\cdots)/{\rm tr}_{\rm S}(\mathbf{1})$ indicates that the calculation of the electron self-energy implies an average over all configurations of the impurity spin. (Indeed, it is the presence of an internal impurity degree of freedom which makes the problem distinct from conventional disorder scattering.) Via the Drude formula, $\rho = m/e^2 n\tau$ (n is the electron density), the scattering time can be used to estimate the effect of the impurities on the electric resistivity ρ of the system.[39]

(a) Show that to leading order in the exchange constant J the scattering rate is given by

$$\frac{1}{2\tau(\epsilon_F)} = \pi c_{\rm imp} \nu J^2 S(S+1),$$

where ν denotes the density of states at the Fermi level. From this result, one can infer a resistivity $\rho_{\rm imp} \sim (m/e^2\epsilon_{\rm F}) c_{\rm imp} J^2 S(S+1)$, independent of temperature. Taken at this order, scattering off magnetic impurities clearly does not explain the existence of a resistance minimum.

(b) At second order in the expansion in $\hat{H}_{\rm imp}$, the T-matrix assumes the form $\hat{T}^{(2)} = \hat{H}_{\rm imp}(\epsilon^+ - \hat{H}_0)^{-1}\hat{H}_{\rm imp}$. Assuming for simplicity that we are working at zero temperature, $|\mathbf{k},\sigma\rangle = c^\dagger_{\mathbf{k}\sigma}|\Omega\rangle$ is a configuration where a single particle with momentum $\mathbf{k}$, $|\mathbf{k}| > p_{\rm F}$, and spin σ is superimposed on the filled Fermi sphere. Convince yourself that the state $\hat{H}_{\rm imp}|\mathbf{k},\sigma\rangle$ is a linear combination of a single-particle state and a two-particle–one-hole

[37] N. Andrei, Diagonalization of the Kondo Hamiltonian, *Phys. Rev. Lett.* **45** (1980), 379–82, P. B. Wiegmann, Exact solution of the s–d exchange model (Kondo problem), *J. Phys. C.* **14** (1981), 1463–78.

[38] C. M. Varma and Y. Yafet, Magnetic susceptibility of mixed-valence rare-earth compounds, *Phys. Rev. B* **13** (1976), 2950–4.

[39] Notice that, besides magnetic impurities, the system will typically contain non-magnetic scattering centers, i.e. $\rho_{\rm total} = \rho_0 + \delta\rho$, where ρ_0 is the resistivity due to conventional disorder and we used the fact that the inverse scattering times corresponding to different types of disorder add independently, $\tau^{-1}_{\rm total} = \tau_0^{-1} + \tau^{-1}$.

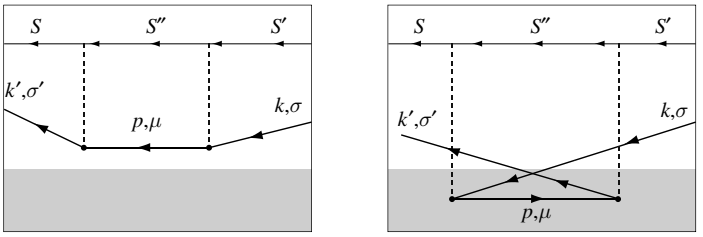

Figure 5.12 The two spin-scattering processes contributing to the electron T-matrix at second-order perturbation theory. The second process involves a two-particle–one-hole configuration as an intermediate state.

state (see Fig. 5.12). Determine the excitation energies of the two configurations. Use this result to compute $(\epsilon^+_{\mathbf{k}} - \hat{H}_0)^{-1}\hat{H}_{\rm imp}|\mathbf{k},\sigma\rangle$. Then show that the real part of the second-order matrix element is given by

$$\text{Re}\ \langle \mathbf{k}',\sigma'|\hat{T}^{(2)}|\mathbf{k},\sigma\rangle = J^2 \sum_{\mathbf{p}} \frac{1}{\xi_{\mathbf{k}} - \xi_{\mathbf{p}}} \left[S(S+1) - \mathbf{S}\cdot\sigma_{\sigma\sigma'}(\Theta(\xi_{\mathbf{p}}) - \Theta(-\xi_{\mathbf{p}}))\right]. \quad (5.50)$$

(Hint: (i) In deriving this result, all "vacuum contributions" have to be discarded [for they cancel against the partition function denominator of the properly normalized perturbation series]. The defining property of a vacuum contribution is that it factorizes into two independent ground state matrix elements. For example, $\langle\Omega|c_{\mathbf{k}\sigma}\hat{H}_{\rm imp}(\epsilon^+ - \hat{H}_0)^{-1}c^\dagger_{\mathbf{k}'\sigma'}|\Omega\rangle \cdot \langle\Omega|\hat{H}_{\rm imp}|\Omega\rangle$ is of this type. (ii) Note that $(\hat{\mathbf{S}}\cdot\sigma)^2 = \hat{\mathbf{S}}^2 - \sigma\cdot\hat{\mathbf{S}}$. (iii) Taking the real part of the T- matrix amounts to omitting the infinitesimal imaginary increment in the energy denominators.)
At finite temperature, the Pauli blocking factors $\Theta(\epsilon) \to (1-n_{\rm F}(\epsilon))$ and $\Theta(-\epsilon) \to n_{\rm F}(\epsilon)$ generalize to Fermi functions and we obtain

$$\text{Re}\langle \mathbf{k}',\sigma'|\hat{T}^{(2)}|\mathbf{k},\sigma\rangle = J^2 \sum_{\mathbf{p}} \frac{1}{\xi_{\mathbf{k}} - \xi_{\mathbf{p}}} \left[S(S+1)\delta_{\sigma'\sigma} + (2n_{\rm F}(\xi_{\mathbf{p}}) - 1)\hat{\mathbf{S}}\cdot\sigma_{\sigma'\sigma}\right]. \quad (5.51)$$

Neglecting the first (non-singular, why?) contribution, one may note that the second can be absorbed into a renormalization of the term first-order in J derived above, viz. $\frac{1}{2\tau} = \pi\nu c_{\rm imp}J^2_{\rm eff}S(S+1)$, where $J_{\rm eff} = J(1+2Jg(\epsilon,T))$ and the function $g(\epsilon,T) = \frac{\nu}{2}\mathcal{P}\int_{-D}^{D} d\xi\ \frac{\tanh(\beta\xi/2)}{\xi-\epsilon}$ depends sensitively on the bandwidth $2D$ of the itinerant electrons and on the energy $\epsilon \equiv \epsilon_{\mathbf{k}}$ of the reference state. Noting that

$$\lim_{\epsilon\to 0} g(\epsilon,0) = \nu \ln\left|\frac{D}{\epsilon}\right|, \quad \lim_{T\to 0} g(0,T) = \nu\ln\left|\frac{D}{k_{\rm B}T}\right|,$$

the effective exchange constant can be written as

$$J_{\rm eff} = J\left(1 + 2\nu(\epsilon_F)J\ln\left|\frac{D}{\max(\epsilon,T)}\right|\right).$$

On substituting into the expression for the scattering rate, one finds that the resistivity diverges logarithmically with temperature,

$$\rho(T) \simeq \rho(0) \left[1 - 4\nu J \ln\left(\frac{T}{D}\right)\right].$$

Finally, on combining with the effect of electron scattering from phonons, which provides a contribution to the resistivity that scales as T^5, one may confirm that the resistance develops a shallow minimum.

Although the perturbation theory suggests a divergence of the resistivity with temperature, the result remains valid only up to the characteristic **Kondo temperature** scale,

$$T_{\mathrm{K}} = D \exp\left[-\frac{1}{2\nu J}\right],$$

i.e. a temperature where the logarithmic correction becomes of the order of the first-order term. Experimentally, it is found that, at temperatures $T \ll T_{\mathrm{K}}$, the resistance saturates. In fact, the low-energy physics can be reconciled through the formation of a resonance in which an electron in the itinerant band combines with the electron on the impurity site to form a singlet bound state effectively screening the magnetic impurity. Formally, one can explore the formation of the resonance state by developing a variational analysis based on the trial wavefunction $|\psi\rangle = \left[\alpha_0 + \sum_{\mathbf{k}\sigma} \alpha_\alpha d_\sigma^\dagger c_{\mathbf{k}\sigma}\right] |\Omega\rangle$, where $|\Omega\rangle$ represents a filled Fermi sea. In doing so, one may confirm that a bound state develops with a binding energy $\Delta_{\mathrm{K}} = T_{\mathrm{K}}$ set by the Kondo temperature.

INFO Although it was originally conceived for the problem of magnetic impurities in metals, lately the effects of **Kondo resonance formation** have been observed in artificial **quantum dot** structures.[40] Here a microscopic quantum dot (with dimensions of ca. $1\,\mu$m) is sandwiched between two metallic leads. In the so-called Coulomb blockade regime (see Problem 6.7), the charging energy of the dot plays the role of the local Hubbard interaction while the leads act as the Fermi sea. The development of a Kondo resonance below T_{K} appears as a signature in the quantum transport through the dot. In particular, for temperatures $T < T_{\mathrm{K}}$, the differential conductance dI/dV shows a peak corresponding to the suppression of scattering off the impurity state.

[40] D. Goldhaber-Gordon, H. Shtrikman, D. Mahalu, *et al.*, Kondo effect in a single-electron transistor, *Nature* **391** (1998), 156–9.

Answer:

(a) To leading order in $\hat{H}_{\rm imp}$, the T-matrix is given by $\hat{T} \simeq \hat{T}^{(1)} = \hat{H}_{\rm imp}$. Using the fact that $\langle \mathbf{k}', \sigma' | \hat{H}_{\rm imp} | \mathbf{k}, \sigma \rangle = JL^{-d} \langle \sigma | \mathbf{S} \cdot \sigma | \sigma' \rangle$ we then obtain

$$\begin{aligned}
\frac{1}{2\tau} &\simeq \pi N_{\rm imp} \sum_{\mathbf{k}',\sigma'} |\langle \mathbf{k}, \sigma | \hat{H}_{\rm imp} | \mathbf{k}', \sigma' \rangle|^2 \; {}_{\rm S}\, \delta(\epsilon_{\mathbf{k}} - \epsilon_{\mathbf{k}'}) \\
&= \pi c_{\rm imp} J^2 L^{-d} \sum_{\sigma'} \langle \langle \sigma | \mathbf{S} \cdot \sigma | \sigma' \rangle \langle \sigma' | \mathbf{S} \cdot \sigma | \sigma \rangle \rangle_{\rm S} \sum_{\mathbf{k}} \delta(\epsilon_{\mathbf{k}} - \epsilon_{\mathbf{k}'}) \\
&= \pi c_{\rm imp} \nu J^2 \langle \langle \sigma | \mathbf{S} \cdot \sigma \mathbf{S} \cdot \sigma | \sigma \rangle \rangle_{\rm S} = \pi J^2 S(S+1) c_{\rm imp} \nu,
\end{aligned}$$

where in the last line we have used the fact that $\sum_{\mathbf{k}} \delta(\epsilon_{\mathbf{k}} - \epsilon_{\mathbf{k}'}) = L^d \nu$ and $\langle (\mathbf{S} \cdot \sigma)(\mathbf{S} \cdot \sigma) \rangle_{\rm S} = S(S+1) \cdot \mathbf{1}$.

(b) Substituting the explicit form of $\hat{H}_{\rm imp}$ and using the anti-commutation relations of fermions, we obtain (summation convention)

$$\begin{aligned}
\hat{H}_{\rm imp} | \mathbf{k}', \sigma' \rangle &= J \sum_{\mathbf{p}_1 \mathbf{p}_2} c^\dagger_{\mathbf{p}_1 \mu_1} (\mathbf{S} \cdot \sigma_{\mu_1 \mu_2}) c_{\mathbf{p}_2 \mu_2} c^\dagger_{\mathbf{k}',\sigma'} |\Omega\rangle \\
&= J \sum_{\mathbf{p}_1} (\mathbf{S} \cdot \sigma_{\mu_1 \sigma'}) c^\dagger_{\mathbf{p}_1 \mu_1} |\Omega\rangle - J \sum_{\mathbf{p}_1 \mathbf{p}_2} (\mathbf{S} \cdot \sigma_{\mu_1 \mu_2}) c^\dagger_{\mathbf{p}_1 \mu_1} c^\dagger_{\mathbf{k}' \sigma'} c_{\mathbf{p}_2 \mu_2} |\Omega\rangle,
\end{aligned}$$

i.e. a linear combination of a one-particle state and a two-particle–one-hole state. Noting that the energies of the two contributions are given by $\epsilon_{\mathbf{p}_1}$ and $\epsilon_{\mathbf{p}_1} + \epsilon_{\mathbf{k}'} - \epsilon_{\mathbf{p}_2}$, respectively, multiplying by the "bra" $\langle \mathbf{k}, \sigma | \hat{H}_{\rm imp}$, and observing that the overlap between a one-particle state and a two-particle–one-hole state vanishes, we obtain

$$\begin{aligned}
{\rm Re} \langle \mathbf{k}, \sigma | \hat{T}^{(2)} | \mathbf{k}', \sigma' \rangle &= J^2 (\mathbf{S} \cdot \sigma_{\sigma \mu_1'}) (\mathbf{S} \cdot \sigma_{\mu_1 \sigma'}) \sum_{\mathbf{p}_1 \mathbf{p}_1'} \frac{\langle \;\; | c_{\mathbf{p}_1' \mu_1'} c^\dagger_{\mathbf{p}_1 \mu_1} | \;\; \rangle}{\epsilon_{\mathbf{k}} - \epsilon_{\mathbf{p}_1}} \\
&\quad + J^2 (\mathbf{S} \cdot \sigma_{\mu_2' \mu_1'}) (\mathbf{S} \cdot \sigma_{\mu_1 \mu_2}) \sum_{\mathbf{p}_1 \mathbf{p}_2 \mathbf{p}_1' \mathbf{p}_2'} \frac{\langle \;\; | c^\dagger_{\mathbf{p}_2' \mu_2'} c_{\mathbf{k} \sigma} c_{\mathbf{p}_1' \mu_1'} c^\dagger_{\mathbf{p}_1 \mu_1} c^\dagger_{\mathbf{k}' \sigma'} c_{\mathbf{p}_2 \mu_2} | \;\; \rangle}{\epsilon_{\mathbf{k}} - \epsilon_{\mathbf{p}_1} - \epsilon_{\mathbf{k}'} + \epsilon_{\mathbf{p}_2}} \\
&\quad \to J^2 (\mathbf{S} \cdot \sigma_{\sigma \mu}) (\mathbf{S} \cdot \sigma_{\mu \sigma'}) \sum_{\mathbf{p}} \frac{\Theta(\xi_{\mathbf{p}})}{\epsilon_{\mathbf{k}} - \epsilon_{\mathbf{p}}} + J^2 (\mathbf{S} \cdot \sigma_{\mu \sigma'}) (\mathbf{S} \cdot \sigma_{\sigma \mu}) \sum_{\mathbf{p}} \frac{\Theta(-\xi_{\mathbf{p}})}{\epsilon_{\mathbf{k}} - \epsilon_{\mathbf{p}}},
\end{aligned}$$

where the arrow indicates that vacuum contributions have been discarded. Application of the spin identity then leads directly to Eq. (5.50).

6

Broken symmetry and collective phenomena

Previously, we have seen how the field integral method can be deployed to formulate perturbative approximation schemes to explore weakly interacting theories. In this chapter, we will learn how elements of the perturbative approach can be formulated more e ciently by staying firmly within the framework of the field integral. More importantly, in doing so, we will see how the field integral provides a method for identifying and exploring non-trivial reference ground states – "mean-fields." A fusion of perturbative and mean-field methods will provide us with analytical machinery powerful enough to address a spectrum of rich applications ranging from superfluidity and superconductivity to metallic magnetism and the interacting electron gas.

As mentioned in Chapter 5, the perturbative machinery is but one part of a larger framework. In fact, the diagrammatic series already contained hints indicating that a straightforward expansion of a theory in the interaction operator might not always be an optimal strategy: all previous examples that contained a large parameter "N" – and usually it is only problems of this type that are amenable to controlled analytical analysis – shared the property that the diagrammatic analysis bore structures of "higher complexity." (For example, series of polarization operators appeared rather than series of the elementary Green functions, etc.) This phenomenon suggests that large-N problems should qualify for a more efficient and, indeed, a more physical formulation.

While these remarks appear to be largely methodological, the rationale behind searching for an improved theoretical formulation is, in fact, much deeper. With our previous examples, the perturbative expansion was benign. However, we already saw some glimpses indicating that more drastic things may happen. For example, for frequencies approaching the plasma frequency, the polarization operator of the weakly interacting electron gas developed an instability. The appearance of such instabilities usually indicates that one is formulating a theory around the "wrong" reference state (in that case, the uniformly filled Fermi sphere of the non-interacting electron gas). Thus, what we would like to develop is a theoretical framework (a) that is capable of detecting the "right" reference states, or "mean-fields" of a system, and that enables us (b) to efficiently apply perturbative methods around these states and, finally, (c) to do this in a language that draws upon the "physical" rather than the plain microscopic degrees of freedom as the fundamental units.

To this end, in the following sections we develop a functional-integral-based approach that meets these criteria. In contrast to the previous chapters, the discussion here is decidedly biased towards concrete application to physically motivated problems. After the formulation

of the general strategy of field-integral-based mean-field methods, the next section addresses a problem that we have encountered before, the weakly interacting electron gas. The exemplification of the new concepts on a known problem enables us to better understand the intimate connection between the mean-field approach and straightforward perturbation theory. In subsequent sections we then turn to the discussion of problems that lie firmly outside the range of direct perturbative summation, superfluidity and superconductivity.

6.1 Mean-field theory

Roughly speaking, the functional approach to problems with a large parameter proceeds according to the following program:

1. In the first place, one must identify the relevant structural units of the theory. (That part of the program *can* be efficiently carried out by the straightforward methods discussed above.)
2. Secondly, it is necessary to introduce a new field – let us call it ϕ for concreteness – that encapsulates the relevant degrees of freedom of the low-energy theory.
3. With this in hand, one can then trade integration over the "microscopic fields" for an integration over ϕ, a step often effected by an operation known as the Hubbard–Stratonovich transformation.
4. The low-energy content of the theory can often be explored by subjecting the resulting action $S[\phi]$ to a stationary phase analysis. (The justification for applying stationary phase methods is provided by the existence of a large parameter $N \gg 1$.) Often, at this stage, instabilities in the theory show up – an indication of a physically interesting problem!
5. Finally, the nature of the elementary (collective) excitations above the ground state can be explored by expanding the functional integral around the solution of the stationary phase equations – the "mean-field." From this low-energy effective action, one can compute physical observables.

In the next section, we will illustrate how such a program can be implemented on a specific example, studied earlier by diagrammatic means.

6.2 Plasma theory of the interacting electron gas

To begin, let us return to the field theory of the interacting electron gas (see the action defined in section 5.2),

$$S[\psi,\bar{\psi}] = \sum_p \bar{\psi}_{p\sigma}\left(-i\omega_n + \frac{\mathbf{p}^2}{2m} - \mu\right)\psi_{p\sigma} + \frac{T}{2L^3}\sum_{pp'q}\bar{\psi}_{p+q\sigma}\bar{\psi}_{p'-q\sigma'}V(\mathbf{q})\psi_{p'\sigma'}\psi_{p\sigma},$$

where the pairwise Coulomb interaction assumes the form $V(\mathbf{q}) = 4\pi e^2/|\mathbf{q}|^2$. Here the summation runs over the 4-momenta $k = (\omega_n, \mathbf{k})$ comprising Matsubara and momentum components and summation over repeated spin indices is implied. Being quartic in the fields ψ_σ, the Coulomb interaction prevents an explicit computation of the ψ-integral along the

lines of the free fermion integrals discussed in the previous chapter. However, it is actually a straightforward matter to reduce, or "decouple," the interaction operator, bringing it to a form quadratic in the fields ψ. Let us multiply the functional integral by the "fat unity"

$$1 \equiv \int D\phi \exp\left[-\frac{e^2\beta}{2L^d}\sum_q \phi_q V^{-1}(\mathbf{q})\phi_{-q}\right],$$

where ϕ represents a real bosonic field variable, and a normalization constant has been absorbed in the definition of the functional measure $D\phi$. Notice that the summation runs over a 4-momentum $q = (\omega_m, \mathbf{q})$ comprising a vectorial momentum and a *bosonic* Matsubara frequency. Employing the variable shift $\phi_q \to \phi_q + ie^{-1}V(\mathbf{q})\rho_q/\beta$, where $\rho_q \equiv \sum_p \bar{\psi}_{p\sigma}\psi_{p+q\sigma}$ (summation on σ implied), one obtains

$$1 = \int D\phi \exp\left[\frac{1}{L^d}\sum_q \left(-\frac{e^2\beta}{2}\phi_q V^{-1}(\mathbf{q})\phi_{-q} + ie\rho_q\phi_{-q} + \frac{1}{2\beta}\rho_q V(\mathbf{q})\rho_{-q}\right)\right].$$

The rationale behind this exercise can be seen in the last contribution to the exponent: this term is equivalent to the quartic interaction contribution to the fermionic path integral, albeit with opposite sign. Therefore, multiplication of our unity by $\mathcal{Z}$ leads to the field integral $\mathcal{Z} = \int D\phi \int D(\bar{\psi}_\sigma, \psi_\sigma)\; e^{-S[\phi,\bar{\psi}_\sigma,\psi_\sigma]}$, where

$$S[\phi,\bar{\psi}_\sigma,\psi_\sigma] = \frac{\beta}{8\pi L^d}\sum_q \phi_q \mathbf{q}^2 \phi_{-q} + \sum_{pp'}\bar{\psi}_{p\sigma}\left[\left(-i\omega_n + \frac{\mathbf{p}^2}{2m} - \mu\right)\delta_{pp'} + \frac{ie}{L^d}\phi_{p'-p}\right]\psi_{p'\sigma}, \quad (6.1)$$

denotes the action, i.e. an expression that is free of quartic field interactions of ψ_σ. Before proceeding, to acquire some intuition for the nature of the action it is helpful to rewrite S in a real space representation. With $\phi_q = T\int_0^\beta d\tau \int d^dr\; e^{-i\mathbf{q}\cdot\mathbf{r}+i\omega\tau}\phi(\mathbf{r},\tau)$, one may confirm that (exercise)

$$S[\phi,\bar{\psi},\psi] = \int d\tau \int d^dr \quad \frac{1}{8\pi}(\partial\phi)^2 + \bar{\psi}_\sigma\left[\partial_\tau - \frac{\partial^2}{2m} - \mu + \frac{ie}{L^d}\phi\right]\psi_\sigma \quad .$$

Physically, ϕ couples to the electron degrees of freedom as a space/time-dependent (imaginary) potential, while the first term reflects the Lagrangian energy density associated with the electric component of the electromagnetic field. Before proceeding, let us step back and discuss the general philosophy of the manipulations that led from the original partition function to the two-field representation Eq. (6.1).

INFO The sequence of manipulations developed above, i.e. the "decoupling" of a quartic interaction through an auxiliary field, is known more generally as a **Hubbard–Stratonovich transformation** (see our discussion of the Ising model on page 196). The essence of the transformation is a straightforward manipulation of a Gaussian integral. To make this point more transparent, let us reformulate the Hubbard–Stratonovich transformation in a notation that is not burdened by the presence of model-specific constants. Consider an interaction operator of the form $S_{\rm int} = V_{\alpha\beta\gamma\delta}\bar{\psi}_\alpha\psi_\beta\bar{\psi}_\gamma\psi_\delta$ (summation convention implied), where $\bar{\psi}$ and ψ may be either bosonic or fermionic field variables, the indices $\alpha, \beta, \ldots$ refer to an unspecified set of quantum numbers, Matsubara frequencies, etc., and $V_{\alpha\beta\gamma\delta}$ is an interaction matrix element. Now, let us introduce composite operators $\hat{\rho}_{\alpha\beta} \equiv \bar{\psi}_\alpha\psi_\beta$ to rewrite the interaction as $S_{\rm int} = V_{\alpha\beta\gamma\delta}\,\hat{\rho}_{\alpha\beta}\hat{\rho}_{\gamma\delta}$. The notation

can be simplified still further by introducing composite indices $m \equiv (\alpha\beta)$, $n \equiv (\gamma\delta)$, whereupon the action $S_{\rm int} = \hat\rho_m V_{mn} \hat\rho_n$ acquires the structure of a generalized bilinear form. To reduce the action to a form quadratic in the ψs, one may simply multiply the exponentiated action by unity, i.e.

$$e^{-\hat{}_m V_{mn} \hat{}_n} = \underbrace{\int D\phi \; e^{-\frac{1}{4}\phi_m V^{-1}_{mn}\phi_n}}_{1} e^{-\hat{}_m V_{mn} \hat{}_n},$$

where ϕ is bosonic. (Notice that here V^{-1}_{mn} represents the matrix elements of the inverse and not the inverse $(V_{mn})^{-1}$ of individual matrix elements.) Finally, applying the variable change $\phi_m \to \phi_m + 2i(V\hat\rho)_m$, where the notation $(V\hat\rho)$ is shorthand for $V_{mn}\hat\rho_n$, one obtains

$$\boxed{\exp\left[-\hat\rho_m V_{mn}\hat\rho_n\right] = \int D\phi \exp\left[-\frac{1}{4}\phi_m V^{-1}_{mn}\phi_n - i\phi_m\hat\rho_m\right],}$$

i.e. the term quadratic in $\hat\rho$ is cancelled.[1] This completes the formulation of the Hubbard–Stratonovich transformation. The interaction operator has been traded for (a) an integration over an auxiliary field (b) coupled to a ψ-bilinear (the operator $\phi_m\hat\rho_m$).

In essence, the Hubbard–Stratonovich transformation is tantamount to the Gaussian integral identity Eq. (3.13) but read in reverse. An exponentiated square is removed in exchange for a linear coupling. (In (3.13) we showed how terms linear in the integration variable can be removed.)

To make the skeleton outlined above a well-defined prescription, one has to be more specific about the meaning of the Gaussian integration over the kernel $\phi_m V^{-1}_{mn}\phi_n$, i.e. the integration variables can be real or complex, and V must be a positive matrix (which is usually the case on physical grounds).

There is some freedom as to the choice of the integration variable. For example, the factor of $1/4$ in front of the Gaussian weight $\phi_m V^{-1}_{mn}\phi_n$ was introduced for mere convenience (i.e. to generate a coupling $\phi_m\hat\rho_m$ free of numerical factors). If one does not like to invert the matrix kernel V_{mn}, one can scale $\phi_m \to (V\phi)_m$, whereupon the key formula reads

$$e^{-\hat{}_m V_{mn} \hat{}_n} = \int D\phi \; e^{-\frac{1}{4}\phi_m V_{mn}\phi_n - i\phi_m V_{mn}\hat{}_n}.$$

EXERCISE Show that the passage from the Lagrangian to the Hamiltonian formulation of the Feynman path integral can be interpreted as a Hubbard–Stratonovich transformation.

As defined, the Hubbard–Stratonovich transformation is exact. However, to make it a meaningful operation, it must be motivated by some physical considerations. In our discussion above, we split up the interaction by choosing $\hat\rho_{\alpha\beta}$ as a composite operator. However, there is clearly some arbitrariness with this choice. Why not, for example, pair the fermion-bilinears according to $(\bar\psi_\alpha\psi_\beta)(\bar\psi_\gamma\psi_\delta)$, or otherwise? The three inequivalent choices of pairing up operators are shown in Fig. 6.1 where, as usual, the wavy line with attached field vertices represents the interaction, and the dashed ovals indicate how the field operators are paired.

[1] Here we have assumed that the matrix V is symmetric. If it is not, we can apply the relation $\hat\rho_m V_{mn}\hat\rho_n \equiv \hat\rho^T V\hat\rho = \frac{1}{2}\;\hat\rho^T(V+V^T)\hat\rho$ to symmetrize the interaction.

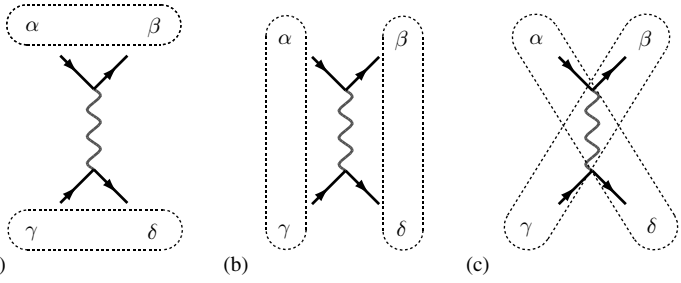

Figure 6.1 On the different channels of decoupling an interaction by Hubbard–Stratonovich transformation. (a) Decoupling in the "density" channel; (b) decoupling in the "pairing" or "Cooper" channel; and (c) decoupling in the "exchange" channel.

The version of the transformation discussed above corresponds to Fig. 6.1(a). That type of pairing is sometimes referred to as decoupling in the **direct channel**. The designation becomes more transparent if we consider the example of the spinful electron–electron interaction,

$$S_{\rm int} = \frac{1}{2}\int d\tau \int d^d r\, d^d r'\ \bar{\psi}_\sigma(\mathbf{r},\tau)\bar{\psi}_{\sigma'}(\mathbf{r}',\tau)V(\mathbf{r}-\mathbf{r}')\psi_{\sigma'}(\mathbf{r}',\tau)\psi_\sigma(\mathbf{r},\tau),$$

i.e. here $\alpha = \beta = (\mathbf{r},\tau,\sigma)$, $\gamma = \delta = (\mathbf{r}',\tau,\sigma')$, and $V_{\alpha\beta\gamma\delta} = V(\mathbf{r}-\mathbf{r}')$. The "direct" decoupling proceeds via the most obvious choice, i.e. the density operator $\hat{\rho}(\mathbf{r},\tau) = \bar{\psi}_\sigma(\mathbf{r},\tau)\psi_\sigma(\mathbf{r},\tau)$. One speaks about decoupling in a "channel" because, as will be elucidated below, the propagator of the decoupling field can be interpreted in terms of two Green function lines tied together by multiple interactions, a sequential object reminiscent of a "channel."

However, more important than the terminology is the fact that there are other choices for ρ. Decoupling in the **exchange channel** (Fig. 6.1(c)) is generated by the choice $\hat{\rho}_{\alpha\delta} \sim \bar{\psi}_\alpha\psi_\delta$ where, in the context of the Coulomb interaction, the reversed pairing of field operators is reminiscent of the exchange contraction generating Fock-type contributions. Finally, one may decouple in the **Cooper channel** (Fig. 6.1(b)) $\hat{\rho}_{\alpha\gamma} = \bar{\psi}_\alpha\bar{\psi}_\gamma$, $\hat{\rho}_{\beta\gamma} = \hat{\rho}^\dagger_{\gamma\beta}$. Here, the pairing field is conjugate to two creation operators. Below we will see that this type of decoupling is tailored to problems involving superconductivity.

The remarks above may convey the impression of a certain arbitrariness inherent in the Hubbard–Stratonovich scheme. Indeed, the "correct" choice of decoupling can be motivated only by physical reasoning, not by plain mathematics. Put differently, the transformation as such is exact, no matter what channel we choose. However, later on we will want to derive an effective low-energy theory based on the decoupling field. In cases where one has accidentally decoupled in an "unphysical" channel, it will be difficult, if not impossible, to distill a meaningful low-energy theory for the field ϕ conjugate to ρ. Although the initial model still contains the full microscopic information (by virtue of the exactness of the transformation) it is not amenable to further approximation schemes.

In fact, one is frequently confronted with situations where more than one Hubbard–Stratonovich field is needed to capture the full physics of the problem. To appreciate this point, consider the Coulomb interaction in momentum space.

$$S_{\rm int}[\bar{\psi},\psi] = \frac{1}{2}\sum_{p_1,\ldots,p_4} \bar{\psi}_{\sigma p_1}\bar{\psi}_{\sigma' p_3}V(\mathbf{p}_1-\mathbf{p}_2)\psi_{\sigma' p_4}\psi_{\sigma p_2}\delta_{p_1-p_2+p_3-p_4}. \tag{6.2}$$

In principle, we can decouple this interaction in any one of the three channels discussed above. However, "interesting" physics is usually generated by processes where one of the three unbounded momenta entering the interaction vertex is small. Only these interaction processes have a chance to accumulate an overall collective excitation of low energy (see our previous discussion of the RPA, the interacting electron gas, and many of the examples to follow). It may be instructive to imagine the situation geometrically: in the three-dimensional Cartesian space of free momentum coordinates (p_1, p_2, p_3) entering the vertex, there are three thin layers, where one of the momenta is small, (q, p_2, p_3), (p_1, q, p_3), (p_1, p_2, q), $|q| \ll |p_i|$. (Why not make all momenta small? Because that would be in conflict with the condition that the Green functions connecting to the vertex be close to the Fermi surface.) One will thus often choose to break down the full momentum summation to a restricted summation over the small-momentum sublayers:

$$S_{\rm int}[\bar\psi,\psi] \simeq \frac{1}{2}\sum_{p,p',q} \bar\psi_{\sigma p}\psi_{\sigma p+q}V(\mathbf{q})\bar\psi_{\sigma' p'}\psi_{\sigma' p'-q} - \bar\psi_{\sigma p}\psi_{\sigma' p+q}V(\mathbf{p}'-\mathbf{p})\bar\psi_{\sigma' p'+q}\psi_{\sigma p'} - \bar\psi_{\sigma p}\bar\psi_{\sigma' -p+q}V(\mathbf{p}'-\mathbf{p})\psi_{\sigma p'}\psi_{\sigma' -p'+q} \quad .$$

Now, each of these three contributions has its own predestined choice of a slow decoupling field. The first term should be decoupled in the direct channel $\hat\rho_{{\rm d},q} \sim \sum_p \bar\psi_{\sigma p}\psi_{\sigma p+q}$, the second in the exchange channel $\hat\rho_{{\rm x},\sigma\sigma' q} \sim \sum_p \bar\psi_{\sigma p}\psi_{\sigma' p+q}$, and the third in the Cooper channel $\hat\rho_{{\rm c},\sigma\sigma' q} \sim \sum_p \bar\psi_{\sigma p}\bar\psi_{\sigma' -p+q}$. One thus winds up with an effective theory that contains three independent slow Hubbard–Stratonovich fields. (Notice that the decoupling fields in the exchange and in the Cooper channel explicitly carry a spin structure.)

In our discussion of the high-density limit of the electron gas above, we effected a decoupling in the direct channel. That choice is made because, drawing on our previous discussion, we already know in advance that relevant contributions to the free energy of the system are generated by RPA-type contraction of operators $\hat\rho_{{\rm d},q} \sim \sum_p \bar\psi_{\sigma p}\psi_{\sigma p+q}$, where q is small. If we had not known, a more careful three-fold Hubbard–Stratonovich decoupling, followed (see below) by a careful analysis of the decoupled action, would have identified the density channel as relevant. More generally, if in doubt, one should decouple in all available channels, and let the mean-field analysis discriminate between the relevant fields.

After this digression on the principles of the Hubbard–Stratonovich transformation, let us now return to the discussion of the electron gas.

At the expense of introducing a second field, the Hubbard–Stratonovich transformation provides an action quadratic in the fermion fields. In this case, the fermion integration can be undertaken exactly. Making use of the Gaussian functional integral Eq. (4.19), one obtains

$$\mathcal{Z} = \int D\phi\; e^{-\frac{\beta}{8\pi L^3}\sum_q \phi_q \mathbf{q}^2 \phi_{-q}} \det\left[-i\hat\omega + \frac{\hat{\mathbf{p}}^2}{2m} - \mu + \frac{ie}{L^d}\hat\phi\right],$$

where, as usual, the circumflexes appearing in the argument of the determinant indicate that symbols have to be interpreted as operators (acting in the space of Matsubara and Hilbert space components).

The standard procedure to deal with the determinants generated at intermediate stages of the manipulation of a field integral is to simply re-exponentiate them. This is achieved

by virtue of the identity

$$\boxed{\ln\det\hat{A} = \mathrm{tr}\ln\hat{A},} \tag{6.3}$$

valid for arbitrary (non-singular) operators $\hat{A}$.[2] Thus, the quantum partition function takes the form $\mathcal{Z} = \int D\phi\; e^{-S[\phi]}$, where

$$S[\phi] = \frac{\beta}{8\pi L^d}\sum_q \phi_q \mathbf{q}^2 \phi_{-q} - \mathrm{tr}\ln\left[-i\hat{\omega} + \frac{\hat{\mathbf{p}}^2}{2m} - \mu + \frac{ie}{L^d}\hat{\phi}\right]. \tag{6.4}$$

This is as far as purely formal exact manipulations can carry us. We have managed to trade the integration over the interacting Grassmann field ψ_σ for an integration over an auxiliary field ϕ; a field that we believe encapsulates the relevant degrees of freedom of the model. This completes steps 1, 2, and 3 of the general program outlined above.

The next step in the program is to subject the action to a stationary phase analysis, i.e. to seek solutions of the set of saddle-point equations such that

$$\forall q = (\mathbf{q} \neq 0, \omega):\ \frac{\delta S[\phi]}{\delta \phi_q} \stackrel{!}{=} 0.$$

The solution $\phi(\mathbf{x}, t) \leftrightarrow \phi_q$ is commonly referred to as the **mean-field**. This terminology can be understood by inspection of the argument of the "tr ln" above. The structure $\hat{\mathbf{p}}^2/2m - \mu + ie\phi/L^d$, where ϕ is a fixed configuration (to be determined by solving the saddle-point equations), resembles the Hamiltonian operator of particles subject to some background potential, or "mean" field. The notation on the left-hand side of the saddle-point equations indicates that our original interaction $V(\mathbf{q})$ and, therefore, the decoupling field ϕ do not possess a zero-momentum mode (a consequence of charge neutrality).

The concrete evaluation of the functional derivative $\delta S/\delta\phi$ leads us to question how one differentiates the trace of the logarithm of the operator,

$$\hat{G}^{-1}[\phi] = i\hat{\omega} - \frac{\hat{\mathbf{p}}^2}{2m} + \mu - \frac{ie}{L^d}\hat{\phi},$$

with respect to its argument. (The notation $\hat{G}^{-1}$ is motivated by its structural similarity to an inverse Green function.) Owing to the presence of the trace, the differentiation can be carried out as if $\hat{G}$ were a function:[3] $(\delta/\delta\phi_q)\mathrm{tr}\ln(\hat{G}^{-1}) = \mathrm{tr}(\hat{G}(\delta/\delta\phi_q)\hat{G}^{-1})$, where we

[2] Equation (6.3) is readily established by switching to an eigenbasis, whereupon one obtains $\ln\det\hat{A} = \sum_a \ln\epsilon_a = \mathrm{tr}\ln\hat{A}$, where ϵ_a are the eigenvalues of $\hat{A}$ and we have used the fact that the eigenvalues of $\ln\hat{A}$ are $\ln\epsilon_a$.

[3] Consider an operator $\hat{A}(x)$ depending on some parameter x. Let $f(\hat{A})$ be an arbitrary function ($f(\hat{A}) = \ln\hat{A}$ in the present application). Then

$$\begin{aligned}\partial_x \mathrm{tr}(f(\hat{A})) &= \partial_x \sum_n \frac{f^{(n)}(0)}{n!}\mathrm{tr}(\hat{A}^n) = \sum_n \frac{f^{(n)}(0)}{n!}\mathrm{tr}((\partial_x\hat{A})\hat{A}^{n-1} + \hat{A}(\partial_x\hat{A})\hat{A}^{n-2} + \cdots + \hat{A}^{n-1}\partial_x\hat{A}) \\ &= \sum_n \frac{n}{n!} f^{(n)}(0)\mathrm{tr}(\hat{A}^{n-1}(\partial_x\hat{A})) = \mathrm{tr}(f'(\hat{A})\partial_x\hat{A}),\end{aligned}$$

where, in the third equality, we have used the cyclic invariance of the trace.

omitted the argument $[\phi]$ for notational clarity. Then, making use of the identity

$$\mathrm{tr}\left[\hat{G}\frac{\delta}{\delta\phi_q}\hat{G}^{-1}\right] = 2\sum_{q_1 q_2}\hat{G}_{q_1 q_2}\left(\frac{\delta}{\delta\phi_q}\hat{G}^{-1}\right)_{q_2 q_1} = -\frac{2ie}{L^d}\sum_{q_1 q_2}\hat{G}_{q_1 q_2}\delta_{q_1-q_2,q},$$

the saddle-point equation assumes the form

$$\frac{\delta}{\delta\phi_q}S[\phi] = \frac{\beta}{4\pi L^d}\mathbf{q}^2\phi_{-q} + \frac{2ie}{L^d}\sum_{q_1}\hat{G}_{q_1,q_1-q} \stackrel{!}{=} 0. \tag{6.5}$$

Here, the factor of two appearing in front of the double summation accounts for the electron spin. Further, we have used the fact that $\hat{G}^{-1}$ is linear in its argument ϕ and that, following the rules of functional differentiation, $(\delta_{\phi_q}\hat{\phi})_{q_1 q_2} = \delta_{q_1-q_2,q}$. In fact (owing to the discreteness of the momentum) we are not even differentiating functionals: $\hat{\phi}$ is a matrix in momentum space. Its matrix elements are given by components ϕ_q: $(\hat{\phi})_{q_1,q_2} = \phi_{q_1-q_2}$. Differentiation of this matrix with respect to ϕ_q then produces another matrix with matrix elements one for $q_1 - q_2 = q$ and zero otherwise. (Admittedly, it takes some time to get used to differentiation formulae of this type.)

Equations of this form are solved not from scratch, but by making a physically motivated *ansatz*, i.e. by guessing the solution! Naturally, the first guess is a homogeneous solution, $\phi(\mathbf{r},t) \equiv \bar{\phi} = \text{const.}$, i.e. one relies on the picture that a spatially and temporarily varying field configuration is energetically more costly than a constant one, and therefore cannot provide a stable extremum.

INFO Be aware that there exist translationally invariant problems with inhomogeneous mean-fields; or a homogeneous solution exists, but it is energetically inferior to a textured field configuration. Indeed, there may be sets of degenerate solutions, etc. Often, when new theories describing an unknown territory have been developed, the search for the "correct" mean-field turns out to be a matter of long, and sometimes controversial, research.

In the present context, spatial and temporal homogeneity translates to the solution $\phi_{\mathbf{q},\omega} = 0$ if either ω or $\mathbf{q}$ is non-zero. Indeed, such an *ansatz* solves the mean-field equation: assuming that all fluctuating components of ϕ are switched off, the Green function operator becomes diagonal in momentum space, $(\hat{G}[\phi])_{q_1,q_2} \propto \delta_{q_1,q_2}$. We thus see that, for non-vanishing q, both terms in the equation vanish. Moreover, since charge neutrality requires $\phi_{q=0} = 0$ one may identify $\hat{\phi} = 0$ as the solution of the mean-field equation, settling step 4 of the general program.

We now proceed to expand the functional in fluctuations around $\phi = 0$. Since the mean-field solution vanishes, it makes no sense to introduce new notation, i.e. we will denote the fluctuations again by the symbol ϕ. As regards the first term in the action (6.4), it already has a quadratic form. The logarithmic contribution can be expanded as if we were dealing with a function (again, a consequence of the trace), i.e.

$$\mathrm{tr}\ln\hat{G}^{-1} = \mathrm{tr}\ln\hat{G}_0^{-1} + \frac{ie}{L^d}\mathrm{tr}(\hat{G}_0\hat{\phi}) + \frac{1}{2}\left(\frac{e}{L^d}\right)^2\mathrm{tr}(\hat{G}_0\hat{\phi}\hat{G}_0\hat{\phi}) + \cdots,$$

where $\hat{G}_0^{-1} \equiv i\hat{\omega} - \frac{\hat{\mathbf{p}}^2}{2m} + \mu$ is the momentum and frequency diagonal operator whose matrix elements give the free Green function of the electron gas. Now, let us discuss the terms

appearing on the right-hand side in turn. Being ϕ-independent, the first term generates an overall constant multiplying the functional integral, i.e. a constant that must describe the non-interacting content of the theory. Indeed, one may note that $e^{\mathrm{tr}\ln\hat{G}_0^{-1}} = e^{-\mathrm{tr}\ln\hat{G}_0} = \det\hat{G}_0^{-1} \equiv \mathcal{Z}_0$ is just the partition function of the non-interacting electron gas. Linear in $\hat{\phi}$, the second term of the expansion must, by virtue of the mean-field analysis, vanish after all. (We are expanding around an extremum! Exercise: Write out the momentum representation of the first-order contribution to confirm that it vanishes identically.) The third term is the interesting one. Remembering that $\hat{\phi}$ couples to the theory as a voltage, this term describes the way potential fluctuations are affected by the presence of the electron gas, i.e. it must encode screening.

To resolve this connection, let us make the momentum dependence of the second-order term explicit (exercise):

$$\frac{1}{2}\left(\frac{e}{L^d}\right)^2 \mathrm{tr}(\hat{G}_0\hat{\phi}\hat{G}_0\hat{\phi}) = \left(\frac{e}{L^d}\right)^2 \sum_{p,q} G_{0,p}\phi_q G_{0,p+q}\phi_{-q} = \frac{e^2}{2TL^d}\sum_q \Pi_q\phi_q\phi_{-q},$$

where, once again, we encounter the polarization operator (5.28). Combining with the first term in the action, one finally obtains

$$S_{\mathrm{eff}}[\phi] = \frac{1}{2TL^3}\sum_q \phi_q\left(\frac{\mathbf{q}^2}{4\pi} - e^2\Pi_q\right)\phi_{-q} + \mathcal{O}(\phi^4), \tag{6.6}$$

where we note that odd powers of ϕ vanish by the symmetry of the problem (exercise). Indeed, the form of the effective action (6.6) is suggestive. Ignoring the coupling to the electron gas, ϕ represents a field with bare "propagator" $\sim \mathbf{q}^{-2}$, i.e. the long-range correlation mediated by the electric field in vacuum. Coupling the field to a medium leads to the appearence of a "self-energy" $\sim \Pi_q$. As we saw above, the self-energy converts the long-range power law correlation into something exponential – screening. The form of the screened propagator exactly coinicides with the effective RPA interaction (5.34) derived diagrammatically above. In passing we note that the structures emerging in the functional integral analysis support a unified way of "reading" the theory: there appear "propagators," "self-energies," etc. irrespective of the concrete context, i.e. irrespective of whether we are dealing with a fermionic field (ψ) or a bosonic field (ϕ).

From here it is a one-line calculation to reproduce the result for the RPA free energy of the electron gas discussed previously. Gaussian integration over the field ϕ (step 5 of the program) leads to the expression $\mathcal{Z}_{\mathrm{RPA}} = \mathcal{Z}_0\prod_q(1-\frac{4\pi e^2}{\mathbf{q}^2}\Pi_q)^{-1/2}$, where we have noted that the ϕ-integration was normalized to unity, i.e. for $\Pi = 0$, the integral collapses to unity. Taking the logarithm, we obtain the free energy

$$F_{\mathrm{RPA}} = -T(\ln\mathcal{Z} - \ln\mathcal{Z}_0) = \frac{T}{2}\sum_q \ln\left(1 - \frac{4\pi e^2}{\mathbf{q}^2}\Pi_q\right),$$

in agreement with Eq. (5.27).

At this point, it is instructive to pause and compare the two approaches to the problem: diagrammatics and field integration. We first note that the functional integral formulation indeed leads to the "reduced" description we sought: the minimal degree of freedom (ϕ)

directly couples to the physically relevant entities of the theory (Π_q). The downside is that, to formulate the approach, we had to go through some preparatory analysis, notably work that required prior physical insight into the problem (i.e. the correct choice of the Hubbard–Stratonovich decoupling). However, this turned out to be an effort well invested. After the identification of ϕ as the "appropriate" field, the further construction of the theory proceeded along the lines of a largely "automated program" (seeking saddle-points, expanding, etc.). In particular, there was no need to do battle with combinatorial problems. Further, in functional integral approaches, the risk of missing relevant contributions, or diagrams, in the expansion of the theory is far less pronounced than in direct diagrammatic expansions. But undoubtedly the most important advantage of the functional integral route is its extensibility. For example, an expansion of the theory to higher orders in ϕ would have generated an interacting theory of voltage fluctuations. Correlations on the level of that theory correspond to diagrams beyond the RPA level, i.e. diagrams whose direct and error-free summation would require more refined skills, a program beyond the scope of the present text.

The mean-field optimizing the problem above was particularly simple with $\phi = 0$. More-interesting situations arise when one encounters non-vanishing mean-field configurations, i.e. the perturbation theory has to be organized around a state different from the trivial vacuum of the theory. Referring to Problem 6.7, we will discuss how, under certain circumstances, Coulomb interaction can favor an itinerant magnetic state.

6.3 Bose–Einstein condensation and superfluidity

Previously, we have considered the influence of weak Coulomb interaction on the properties of the electron gas. In the following, our goal will be to consider the phases realized by a weakly interacting Bose gas. To this end, let us introduce the quantum partition function $\mathcal{Z} = \int D(\bar{\psi}, \psi)\, e^{-S[\bar{\psi},\psi]}$, where

$$S[\bar{\psi}, \psi] = \int d^d r \int d\tau \left[\bar{\psi}(\mathbf{r}, \tau)(\partial_\tau + \hat{H}_0 - \mu)\psi(\mathbf{r}, \tau) + \frac{g}{2}(\bar{\psi}(\mathbf{r}, \tau)\psi(\mathbf{r}, \tau))^2 \right]. \tag{6.7}$$

Here ψ represents a complex field subject to the periodic boundary condition $\psi(\mathbf{r}, \beta) = \psi(\mathbf{r}, 0)$. The functional integral $\mathcal{Z}$ describes the physics of a system of bosonic particles in d dimensions subject to a repulsive contact interaction of strength $g > 0$. For the moment the specific structure of the one-body operator $\hat{H}_0$ need not be specified. The most remarkable phenomena displayed by systems of this type are Bose–Einstein condensation and superfluidity. However, contrary to a widespread belief, these two effects

Satyendranath Bose 1894–1974

He undertook important work in quantum theory, in particular on Planck's black body radiation law. His work was enthusiastically endorsed by Einstein. He also published on statistical mechanics, leading most famously to the concept of Bose-Einstein statistics. Dirac coined the term "boson" for particles obeying such statistics.

do not depend on each other: superfluidity can arise without condensation and vice versa. We begin our discussion with the more elementary of the two phenomena.

Bose–Einstein condensation

As may be recalled from elementary statistical mechanics, at sufficiently low temperatures the ground state of a bosonic system can involve the condensation of a macroscopic fraction of particles into a single state. This phenomenon, predicted in a celebrated work by Einstein, is known as Bose–Einstein condensation. To see how this phenomenon is born out of the functional integral formalism, let us temporarily switch off the interaction and turn to the basis in which the one-particle Hamiltonian is diagonal. Expressed in the frequency representation, the partition function of the non-interacting system is given by

Albert Einstein 1879–1955
Nobel Laureate in Physics in 1921 "for his services to theoretical physics, and especially for his discovery of the law of the photoelectric effect." He is perhaps best known for his theory of relativity and specifically mass–energy equivalence, expressed by the equation $E = mc^2$. His work on the low-temperature behavior of the bosonic quantum gas is published in A. Einstein, Quantentheorie des einatomigen idealen Gases, *Sitzungsber. Preuss. Akad. Wiss.* (1925), 261-7. (Image © The Nobel Foundation.)

$$\mathcal{Z}_0 \equiv \mathcal{Z}|_{g=0} = \int D(\bar{\psi},\psi)\, \exp\left[-\sum_{an} \bar{\psi}_{an}\left(-i\omega_n + \epsilon_a - \mu\right)\psi_{an}\right].$$

Without loss of generality, we may assume that the eigenvalues $\epsilon_a \geq 0$ are positive with a ground state $\epsilon_0 = 0$.[4] (In contrast to the fermionic systems discussed above, we should not have in mind low-energy excitations superimposed on high-energy microscopic degrees of freedom. Here, everything will take place in the vicinity of the ground state of the microscopic single-particle Hamiltonian.) Further, we note that, to ensure stability, the chemical potential determining the number of particles in the system must be negative for, otherwise, the Gaussian weight corresponding to the low-lying states $\epsilon_a < -\mu$ would change sign, resulting in an ill-defined theory.

From our discussion of Section 4.2 we recall that the number of particles in the system is set by the relation

$$N(\mu) = -\partial_\mu F = T\sum_{na} \frac{1}{i\omega_n - \epsilon_a + \mu} = \sum_a n_{\rm B}(\epsilon_a),$$

[4] The chemical potential μ can always be adjusted so as to meet this condition.

where, as usual, $n_{\rm B}(\epsilon) = (e^{\beta(\epsilon-\mu)}-1)^{-1}$ denotes the Bose distribution. For a given number of particles, this equation determines the temperature dependence of the chemical potential, $\mu(T)$. As the temperature is reduced, the distribution function controlling the population of individual states decreases. Since the number of particles must be kept constant, this scaling must be counter-balanced by a corresponding increase in the chemical potential.

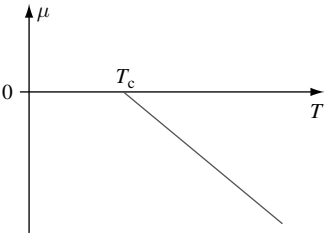

Below a certain critical temperature T_c, even the maximum value of the chemical potential, $\mu = 0$, will not suffice to keep the distribution function $n_{\rm B}(\epsilon_{a\neq 0})$ large enough to accommodate all particles in the states of non-vanishing energy, i.e. $\sum_{a>0} n_{\rm B}(\epsilon_a)|_{\mu=0} \overset{T<T_c}{\equiv} N_1 < N$. I.e. below the critical temperature, the chemical potential stays constant at $\mu = 0$ (see the figure). As a result, a macroscopic number of particles, $N - N_1$, must accumulate in the single-particle ground state: **Bose–Einstein condensation**.

EXERCISE For a three-dimensional free particle spectrum, $\epsilon_k = \hbar^2 k^2/2m$, show that the critical temperature is set by $T_c = c_0\hbar^2/ma^2$, where $a = \rho^{-1/3}$ is the average inter-particle spacing, and c_0 is a constant of order unity. Show that for temperatures $T < T_c$, the density of particles in the condensate ($\mathbf{k} = 0$) is given by $\rho_0(T) = \rho[1 - (T/T_c)^{3/2}]$.

Since its prediction in the early 1920s, the phenomenon of Bose–Einstein condensation has been a standard component of undergraduate texts. However, it took some seven decades before the condensation of bosonic particles was directly[5] observed in experiment. The reason for this delay is that the critical condensation temperature of particles (atoms) that are comfortably accessible to experiment is absurdly low.

Eric A. Cornell 1961– (left), Wolfgang Ketterle 1957– (center), and Carl E. Wieman 1951– (right) Joint recipients of the 2001 Nobel Prize in Physics "for the achievement of Bose-Einstein condensation in dilute gases of alkali atoms, and for early fundamental studies of the properties of the condensates." (Images © The Nobel Foundation.)

INFO In 1995 the groups of Cornell and Wieman at Colorado University and, soon after, Ketterle at MIT succeeded in cooling a system of rubidium atoms down to temperatures of 20 billionths(!) of a kelvin.[6] To reach these temperatures, a gas of rubidium atoms was caught in a magnetic

[5] Here, by "direct" we refer to the controlled preparation of a state of condensed massive bosonic particles. There are numerous "indirect" manifestations of condensed states, e.g. the anomalous properties of the helium liquids at low temperatures, or of Cooper-pair condensates in superconductors.

[6] M. H. Anderson, J.R. Ensher, M.R. Matthews, C.E. Wieman, and E. A. Cornell, Observation of Bose–Einstein condensation in a dilute atomic vapor, *Science* **269** (1995), 198-201.

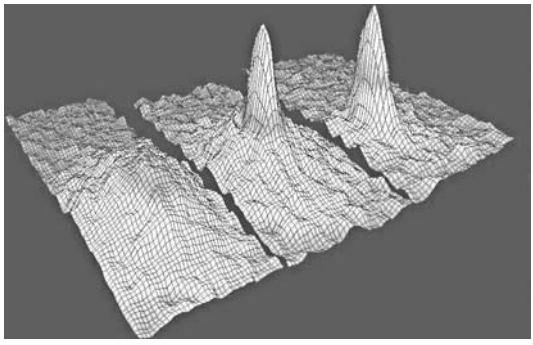

Figure 6.2 Spectroscopic images of the Bose–Einstein condensation process for three values of temperature (400 nK, 200 nK, and 50 nK from left to right). (Figure courtesy of the JILA Institute, University of Colorado.)

trap, i.e. a configuration of magnetic field gradients that couple to the magnetic moments of the atoms so as to keep the system spatially localized.

The gas of atoms was then brought to a temperature of $\mathcal{O}(10^{-5})\,\mathrm{K}$ – still much too hot to condense – by "laser cooling": crudely speaking, a technique where atoms, subjected to a suitably adjusted ray of monochromatic light, may transmit more of their kinetic energy to the photons than they get back. To lower the temperature still further, the principle of "evaporative cooling" was applied: by lowering the potential well of the trap, a fraction of the atoms, namely those with large kinetic energy, is allowed to escape. The remaining atoms have a low kinetic energy and, therefore, a low temperature. What sounds like a simple recipe actually represents a most delicate experimental procedure. (For example, if the trap potential is lowered too strongly, all atoms escape and there is nothing left to condense. If, on the other hand, trapping is too strong, the atoms remain too hot, etc.) However, after more than a decade of intensive experimental preparation, the required temperatures have been reached.

Spectroscopic images of the Bose–Einstein condensation process are shown in Fig. 6.2 at three temperatures. The peak in the density distribution signals the onset of condensation. On lowering the temperature, one may observe the transition to a condensed phase by monitoring the formation of a peak in the density distribution. The preparation of a Bose-Einstein condensed state of matter was recognized with the award of the 2001 Nobel prize in physics. Since 1995, research on atomic condensates has blossomed into a broad arena of research. Already, it is possible to prepare complex states of Bose condensed matter such as atomic vortices in rotating Bose–Einstein condensates, condensates in different dimensionalities, or even an artificial crystalline state of matter (see Fig. 6.3). Regrettably, a detailed discussion of these interesting developments is beyond the scope of the present text. Those interested in learning more about this area are referred to the many reviews of the field.

With this background, let us now try to understand how the phenomenon of Bose–Einstein condensation can be implemented in the functional integral representation. Evidently, the characteristics of the condensate will be described by the zero field component $\psi_0(\tau)$. The problem with this zero mode is that, below the condensation transition, its action appears to be unbounded: both the chemical potential and the eigenvalue are zero. This means that the action of the zero Matsubara component $\psi_{0,0}$ vanishes. We will deal with this difficulty

in a pragmatic way. That is, we will treat $\psi_0(\tau)$ not as an integration variable but rather as a time-independent Lagrange multiplier to be used to fix the number of particles below the transition. More precisely, we introduce a reduced action of the form

$$S_0[\bar{\psi},\psi] = -\bar{\psi}_0\beta\mu\psi_0 + \sum_{a\neq 0,n} \bar{\psi}_{an}\left(-i\omega_n + \epsilon_a - \mu\right)\psi_{an},$$

where we did not yet set $\mu = 0$ (since we still need μ as a differentiation variable). To understand the rationale behind this simplification one may note that

$$N = -\partial_\mu F_0|_{\mu=0^-} = T\partial_\mu \ln \mathcal{Z}_0|_{\mu=0^-} = \bar{\psi}_0\psi_0 + T\sum_{a\neq 0,n} \frac{1}{i\omega_n - \epsilon_a} = \bar{\psi}_0\psi_0 + N_1, \qquad (6.8)$$

determines the number of particles. According to this expression, $\bar{\psi}_0\psi_0 = N_0$ sets the number of particles in the condensate. Now, what enables us to regard ψ_0 as a time-independent field? Remembering the construction of the path integral, we note that the introduction of time-dependent fields, or "time slicing," was necessitated by the fact that the operators appearing in the Hamiltonian of a quantum theory do not, in general, commute. (Otherwise we could have decoupled the expression $\mathrm{tr}(e^{-\beta(\hat{H}-\mu\hat{N})(a^\dagger,a)}) \simeq \int d(\bar{\psi},\psi)\ e^{-\beta(\hat{H}-\mu\hat{N})(\bar{\psi},\psi)}$ in terms of a single coherent state resolution, i.e. a "static" configuration.) Reading this observation in reverse, we conclude that the dynamic content of the field integral represents the quantum character of a theory. (Alluding to this fact, the temporal fluctuations of field variables are often referred to as **quantum fluctuations**.) Conversely,

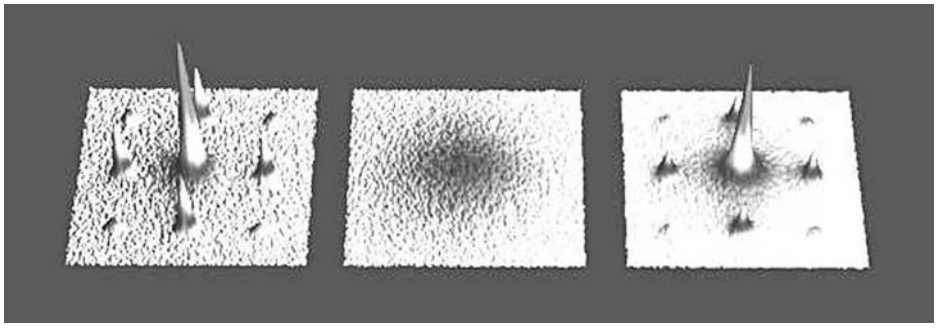

Figure 6.3 The creation of an artificial mono-atomic crystal from a Bose–Einstein condensate. A system of bosons in a condensed state – the state signaled by the pronounced coherent intensity peaks in the left portion of the figure – is exposed to a "grid" formed by two crossing fields of intense laser radiation. For strong enough field amplitudes, the electromagnetic radiation interferes, presenting a periodic lattice of deep potential minima. These minima become occupied by one atom each. The result is an artificial mono-atomic crystal, characterized by the absence of coherent superposition of atomic wavefunction amplitudes, i.e. an equilibrated density profile (middle). If the laser intensity is lowered, the atoms re-arrange to the characteristic density distribution of the condensate (right). (Source: Courtesy of Max-Planck-Institut für Quantenoptik, Garching, Germany.)

> A static approximation in a field integral $\psi(\tau) = \psi_0 = \text{const.}$ amounts to replacing a quantum degree of freedom by its classical approximation.

(In order to distinguish them from quantum, fluctuations in the "classical" static sector of the theory are called **thermal fluctuations**.) To justify the approximation of $a_0 \leftrightarrow \psi_0$ by a classical object, notice that, upon condensation, $N_0 = \langle a_0^\dagger a_0 \rangle$ will assume "macroscopically large" values. On the other hand, the commutator $[a_0, a_0^\dagger] = 1$ continues to be of $\mathcal{O}(1)$. It thus seems to be legitimate to neglect all commutators of the zero operator a_0 in comparison with its expectation value – a classical approximation.[7]

Now, we are still left with the problem that the ψ_0-integration appears to be undefined. The way out is to remember that the partition function should extend over those states that contain an average number N of particles. That is, Eq. (6.8) has to be interpreted as a relation that fixes the modulus $\bar{\psi}_0\psi_0$ so as to adjust the appropriate value of N.[8]

The weakly interacting Bose gas

Now, with this background, let us restore the interactions focusing on a small but non-zero coupling constant g. To keep the discussion concrete, we specialize to the case of a free single-particle system, $\hat{H}_0 = \hat{\mathbf{p}}^2/2m$. (Notice that the ground state wavefunction of this system is described by a spatially constant zero-momentum state.) By adiabatic continuity we expect that much of the picture developed above will survive generalization to non-zero interaction strengths. In particular, the ground state, which in the case under consideration corresponds to a temporally and spatially constant mode ψ_0, will continue to be macroscopically occupied. In these circumstances, the dominant contribution to the action will again come from the classical ψ_0 sector:

$$TS[\bar{\psi}_0, \psi_0] = -\mu\bar{\psi}_0\psi_0 + \frac{g}{2L^d}(\bar{\psi}_0\psi_0)^2. \tag{6.9}$$

(Notice the similarity of the action to the integrand of the toy problem discussed in Section 5.1.) Crucially, the stability of the action is now guaranteed by the interaction vertex, no matter how small is $g > 0$ (see the schematic plot of the action in the figure on page 263). Accordingly, we will treat ψ_0 no longer as a fixed parameter but rather as an ordinary integration variable. Integration over all field components will produce a partition function $\mathcal{Z}(\mu)$ that depends parametrically on the chemical potential. As usual in statistical physics, the function can then be employed to fix the particle number. (Notice that, vis-à-vis aspects

[7] Notice the similarity of that reasoning to the arguments employed in connection with the semi-classical treatment of spin systems in the limit of large S (Section 2.2). Unfortunately, the actual state of affairs with the classical treatment of the condensate is somewhat more complex than the simple argument above suggests. (For a good discussion, see A. A. Abrikosov, L. P. Gorkov, and I. E. Dzyaloshinskii, *Methods of Quantum Field Theory in Statistical Physics* [Dover Publications, 1975]) However, the net result of a more thorough analysis, i.e. an integration over all dynamically fluctuating components $\psi_{0,n=0}$, shows that the treatment of ψ_0 as classical represents a legitimate approximation.

[8] For a more rigorous discussion of the choice of the thermodynamic variables in the present context, we again refer to Abrikosov *et al.*, *ibid.*

of thermodynamics, the interacting system appears to behave more "naturally" than its ideal, non-interacting approximation. This reflects a general feature of bosonic systems: interactions "regularize" a number of pathological features of the ideal gas.)

Returning to the ψ_0-integration, we observe that, for low enough temperatures, the problem is an ideal candidate for saddle-point analysis. Variation of the action with respect to ψ_0 gives

$$\bar{\psi}_0 \left(-\mu + \frac{g}{L^d} \bar{\psi}_0 \psi_0 \right) = 0.$$

This equation is solved by any constant complex field configuration ψ_0 with modulus $|\psi_0| = \sqrt{\mu L^d / g} \equiv \gamma$. In spite of its innocent appearance, this equation reveals much about the nature of the system:

- ▷ For $\mu < 0$ (i.e. above the condensation threshold of the non-interacting system), the equation exhibits only the trivial solution $\psi_0 = 0$. This means that no stable condensate amplitude exists.
- ▷ Below the condensation threshold (i.e. for $\mu \geq 0$),[9] the equation is solved by any configuration with $|\psi_0| = \gamma \equiv \sqrt{\mu L^d / g}$. (Notice that $\bar{\psi}_0 \psi_0 \propto L^d$, reflecting the macroscopic population of the ground state.)
- ▷ The equation couples only to the modulus of ψ_0. That is, the solution of the stationary phase equation is continuously degenerate: each configuration $\psi_0 = \gamma \exp(i\phi), \phi \in [0, 2\pi]$, is a solution.

For our present discussion, the last of the three aspects mentioned above is the most important. It raises the question of which configuration $\psi_0 = \gamma \exp(i\phi)$ is the "right" one?

Without loss of generality, we may choose $\psi_0 = \gamma \in \mathbb{R}$ as a reference configuration for our theory. This choice amounts to selecting a particular minimum lying in the "Mexican hat" profile of the action shown above. However, it is clear that an expansion of the action around that minimum will be singular: fluctuations $\psi_0 \to \psi_0 + \delta\psi$ that do not leave the azimuthally symmetric well of degenerate minima do not change the action and, therefore, have vanishing expansion coefficients. As a result, in the present situation, we will not be able to implement a simple scheme, i.e. "saddle-point plus quadratic fluctuations"; there is nothing that constrains the deviations $\delta\psi$ to be small. In the next section, we discuss the general principles behind this phenomenon. In section 6.3, we then continue to explore its ramifications in the physics of the Bose system.

Spontaneous symmetry breaking

The mechanism encountered here is one of **spontaneous symmetry breaking**. To understand the general principle, consider an action $S[\psi]$ with a global continuous symmetry under some transformation g (not to be confused with the aforementioned coupling constant of the Bose gas): specifically, the action remains invariant under a global transformation of

[9] Owing to the stabilization of the zero mode integration by the interaction constant, $\mu \quad 0$ is no longer a strict condition.

the fields such that $\forall i \in M$: $\psi_i \to g\psi_i$, where M is the base manifold, i.e. $S[\psi] = S[g\psi]$. The transformation is "continuous" in the sense that g takes values in some manifold, typically a group G.

Examples: The action of a Heisenberg ferromagnet is invariant under **rotation** of all spins simultaneously by the same amount, $\mathbf{S}_i \to g\mathbf{S}_i$. In this case, $g \in G = \mathrm{O}(3)$, the three-dimensional group of rotations (g not to be confused with the coupling constant of the interaction). The action of the displacement fields $\mathbf{u}$ describing elastic deformations of a solid (phonons) is invariant under simultaneous **translation** of all displacements $\mathbf{u}_i \to \mathbf{u}_i + \mathbf{a}$, i.e. the symmetry manifold is the d-dimensional translation group $G \cong \mathbb{R}^d$. In the example above, we encountered a U(1) symmetry under phase multiplication $\psi_0 \to e^{i\phi}\psi_0$. This phase freedom expresses the **global gauge symmetry** of quantum mechanics under transformation by a phase, a point we discuss in more detail below.

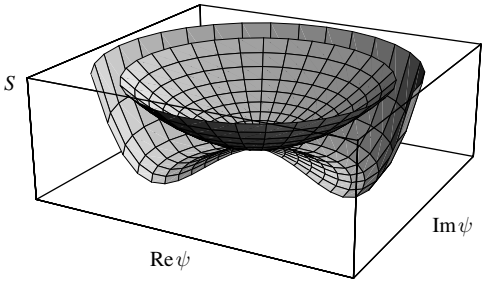

Now, given a theory with globally G invariant action, two scenarios are conceivable: either the ground states share the invariance properties of the action or they do not. The two alternatives are illustrated in the figure for the example of the Bose system. For $\mu < 0$, the action $S[\bar{\psi}_0, \psi_0]$ has a single ground state at $\psi_0 = 0$. This state is trivially symmetric under the action of $G = \mathrm{U}(1)$. However, for positive μ, i.e. in the situation discussed above, there is an entire manifold of degenerate ground states, defined through the relation $|\psi_0| = \gamma$. These ground states transform into each other under the action of the gauge group. However, none of them is individually invariant.

With the other examples mentioned above, the situation is similar. For symmetry groups more complex than the one-dimensional manifold U(1), the ground states will, in general, be invariant under transformation by the elements of a certain subgroup $H \subseteq G$ (that includes the two extremes $H = \{\mathbf{1}\}$ and $H = G$). For example, below the transition temperature, the ground state of the Heisenberg magnet will be given by (domain-wise) aligned configurations of spins. Assuming that the spins are oriented along the z-direction, the ground state is invariant under the abelian subgroup $H \subset \mathrm{O}(3)$ containing all rotations around the z-axis. However, invariance under the full rotation group is manifestly broken. Solids represent states where the translation symmetry is fully broken, i.e. all atoms collectively occupy a fixed pattern of spatial positions in space, $H = \{\mathbf{1}\}$, etc.

In spite of the undeniable existence of solids, magnets, and Bose-Einstein condensates of definite phase, the notion of a ground state that does not share the full symmetry of the theory may appear paradoxical, or at least "unnatural." For example, even if any particular ground state of the "Mexican hat" potential shown in the figure above "breaks" the rotational symmetry, should not all these states enter the partition sum with equal statistical weight, such that the net outcome of the theory is again fully symmetric?

To understand why symmetry breaking is a "natural" and observable phenomenon, it is instructive to perform a gedankenexperiment. To this end, consider the partition function

of a classical[10] ferromagnet,

$$\mathcal{Z} = \mathrm{tr}\left(e^{-\beta(H-\mathbf{h}\cdot\sum_i \mathbf{S}_i)}\right),$$

where H is the rotationally invariant part of the energy functional and $\mathbf{h}$ represents a weak external field. (Alternatively, we can think of $\mathbf{h}$ as an internal field, caused by a slight structural imperfection of the system.) In the limit of vanishing field strength, the theory becomes manifestly symmetric. Symbolically,

$$\lim_{N\to\infty}\lim_{h\to 0}\mathcal{Z} \longrightarrow \text{rot. sym.},$$

where the limit $N \to \infty$ serves as a mnemonic indicating that we consider systems of macroscopic size. However, keeping in mind the fact that the model ought to describe a physical magnetic system, the order of limits taken above appears questionable. Since the external perturbation couples to a macroscopic number of spins, a more natural description of an "almost" symmetric situation would be

$$\lim_{h\to 0}\lim_{N\to\infty}\mathcal{Z} \longrightarrow ?$$

The point is that the two orders of limits lead to different results. In this case, for any $\mathbf{h}$, the $N \to \infty$ system is described by an explicitly symmetry broken action. No matter how small the magnetic field, the energetic cost to rotate $N \to \infty$ spins against the field is too high, i.e. the ground state $|\mathbf{S}\rangle$ below the transition temperature will be uniquely aligned, $\mathbf{S}_i \quad \mathbf{h}$. When we then send $\mathbf{h} \to 0$ in a subsequent step, that particular state will remain the observable reference state of the system. Although, formally, a spontaneous thermal fluctuation rotating all spins by the same amount $|\mathbf{S}\rangle \to |g\mathbf{S}\rangle$ would not cost energy, that fluctuation can be excluded by entropic reasoning.[11] (By analogy, one rarely observes kettles crashing into the kitchen wall as a consequence of a concerted thermal fluctuation of the water molecules!)

However, the appearance of non-trivial ground states is just one manifestation of spontaneous symmetry breaking. Equally important, residual fluctuations around the ground state lead to the formation of **soft modes** (sometimes known as **massless modes**), i.e. field configurations $\phi_{\mathbf{q}}$ whose action $S[\phi]$ vanishes in the limit of long wavelengths, $\mathbf{q} \to 0$. Specifically, the soft modes formed on top of a symmetry broken ground state are called **Goldstone modes**. As a rule, the presence of soft modes in a continuum theory has important phenomenological consequences. To understand this point, notice that the general structure of a soft mode action is given by

$$S[\phi] = \sum_{\mathbf{q},i} \phi_{\mathbf{q}}\left[c_1^i|q_i| + c_2^i q_i^2\right]\phi_{-\mathbf{q}} + \mathcal{O}(\phi^4, q^3), \tag{6.10}$$

where $c_{1,2}^i$ are coefficients. As discussed in Section 5.1, the absence of a constant contribution to the action (i.e. a contribution that does not vanish in the limit $q \to 0$) signals the existence of long-range power-law correlations in the system. As we will see shortly, the vanishing of

[10] The same argument can be formulated for the quantum magnet.

[11] In Chapter 8, we show that this (overly) simple picture in fact breaks down in dimensions $d \quad 2$.

the action in the long-wavelength limit $q \to 0$ further implies that the contribution of the soft modes dominates practically all observable properties of the system.

EXERCISE Explore the structure of the propagator $G(\mathbf{q}) \equiv \langle \phi_{\mathbf{q}} \phi_{-\mathbf{q}} \rangle$ associated with $S[\phi]$ and convince yourself that the arguments formulated for the specific case of the ϕ^4-theory are of general validity. To this end, notice that, for small $\mathbf{q}$, $G(\mathbf{q}) \sim |\mathbf{q}|^{-n}$, where n denotes the index of the first non-vanishing coefficient $c_1, c_2, \ldots$, i.e. the propagator is dominated by the smallest $\mathbf{q}$-power appearing in the action. The power-law behavior of the correlation function implies a homogeneity relation $G(\mathbf{q}/\lambda) = \lambda^n G(\mathbf{q})$. Show that this scaling relation implies that the Fourier transform $G(r \equiv |\mathbf{r}|) = \langle \phi(\mathbf{r})\phi(\mathbf{0}) \rangle$ obeys the "scaling law" $G(\lambda \mathbf{r}) = \lambda^{-d+n} G(\mathbf{r})$. This, in turn, implies that the real space correlation function also decays as a power law, namely $G(\mathbf{r}) \sim |\mathbf{r}|^{-d+n}$, i.e. in a "long-range" manner. Explore the breakdown of the argument for an action with a finite mass term. Convince yourself that, in this case, the decay would be exponential, i.e. "short-range."

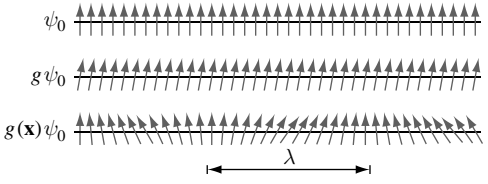

What, then, are the origin and nature of the soft Goldstone modes caused by the spontaneous breakdown of a symmetry? To address this point let us consider the action of a symmetry group element g on a (symmetry broken) ground state ψ_0 (cf. the middle row of the figure). By definition, $S[g\psi_0] = S[\psi_0]$ still assumes its extremal value. Assuming that g is close to the group identity, we may express $g = \exp[\sum_a \phi_a T_a]$, where the $\{T_a\}$ are generators living in the Lie algebra of the group and ϕ_a are some expansion coefficients.[12] Expressing fluctuations around ψ_0 in terms of the "coordinates" ϕ_a, we conclude that the action $S[\phi] = 0$. However, if we promote the global transformation to one with a weakly fluctuating spatial profile, $g \to g(\mathbf{r})$, $\psi_0 \to g(\mathbf{r})\psi_0$ (bottom row of the figure), some price must be paid. That is, for a spatially fluctuating coordinate profile $\{\phi_a(\mathbf{r})\}$, $S[\phi] \neq 0$, where the energy cost depends inversely on the fluctuation rate λ of the field ϕ. The expansion of S in terms of gradients of ϕ is thus bound to lead to a soft mode action of the type Eq. (6.10).

In view of their physical significance, it is important to ask how many independent soft modes exist. The answer can be straightforwardly given on the basis of the geometric picture developed above. Suppose our symmetry group G has dimension r, i.e. its Lie algebra is spanned by r linearly independent generators $T_a, a = 1, \ldots, r$. If the subgroup $H \subset G$ has dimension $s < r$, s of these generators can be chosen so as to leave the ground state invariant. On the other hand, the remaining $p \equiv r - s$ generators inevitably create Goldstone modes. In the language of group theory, these generators span the coset space G/H. For example, for the ferromagnet, $H = \mathrm{O}(2)$ is the one-dimensional subgroup of rotations around the quantization axis (e.g. the z-axis). Since the rotation group has dimension 3, there must be two independent Goldstone modes. These can be generated by the action of the rotation, or angular momentum generators $J_{x,y}$ acting on the z-aligned ground state. The coset space

[12] Here we have used the fact that, for any reasonable model, G will be a Lie group, i.e. a group with the structure of a differentiable manifold.

O(3)/O(2) can be shown to be isomorphic to the 2-sphere, i.e. the sphere traced out by the spins as they fluctuate around the ground state.

Finally, you may ask why we bothered to formulate these concepts in the abstract language of Lie groups and generators, etc. The reason is that the connection between the coordinates parameterizing the Goldstone modes $\phi_i, i = 1, \ldots, p$, residual "massive modes" $\kappa_j, j = 1, \ldots, n-p$, and the original coordinates $\psi_i, i = 1, \ldots, n$, of the problem, respectively, is usually nonlinear and sometimes not even very transparent. With problems more complex than the three prototypical examples mentioned above, it is usually profitable to first develop a good understanding of the geometry of the problem before specific coordinate systems are introduced.

After these general considerations it is time to get back to the Bose system and to explore the physical consequences of Goldstone mode formation on the level of a concrete example!

Superfluidity

The theory of the weakly interacting superfluid to be discussed below was originally conceived by Bogoliubov, then in the language of second quantization.[13] We will reformulate the theory in the language of the field integrals starting with the action of the weakly interacting Bose gas (6.7). Focussing on temperatures below T_c ($\mu > 0$), let us expand the theory around the particular mean-field ground state $\bar{\psi}_0 = \psi_0 = (\mu L^d/g)^{1/2} = \gamma$. (Of course, any other state lying in the "Mexican hat" minimum of the action would be just as good.) Notice that the quantum ground state corresponding to the configuration ψ_0 is unconventional in the sense that it cannot have a definite particle number. The reason is that, according to the correspondence $\psi \leftrightarrow a$ between coherent states and operators, respectively, a non-vanishing functional expectation value of ψ_0 is equivalent to a non-vanishing quantum expectation value $\langle a_0 \rangle$. Assuming that, at low temperatures, the thermal average $\langle \ldots \rangle$ will project onto the ground state $|\Omega\rangle$, we conclude that $\langle \Omega | a_0 | \Omega \rangle \neq 0$, i.e. $|\Omega\rangle$ cannot be a state with a definite number of particles.[14]

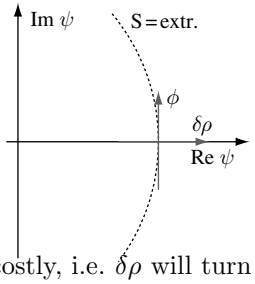

The symmetry group U(1) acts on this state by multiplication, $\psi_0 \to e^{i\phi}\psi_0$ and $\bar{\psi}_0 \to e^{-i\phi}\bar{\psi}_0$. Knowing that the action of a weakly modulated field $\phi(\mathbf{r}, \tau)$ will be massless, let us introduce coordinates

$$\psi(\mathbf{r}, \tau) = \rho^{1/2}(\mathbf{r}, \tau) e^{i\phi(\mathbf{r},\tau)}, \qquad \bar{\psi}(\mathbf{r}, \tau) = \rho^{1/2}(\mathbf{r}, \tau) e^{-i\phi(\mathbf{r},\tau)},$$

where $\rho(\mathbf{r}, \tau) = \rho_0 + \delta\rho(\mathbf{r}, \tau)$ and $\rho_0 = \bar{\psi}_0\psi_0/L^d$ is the condensate density. Evidently, the variable $\delta\rho$ parametrizes deviations of the field $\psi(\mathbf{r}, \tau)$ from the extremum. These excursions are energetically costly, i.e. $\delta\rho$ will turn out to be a massive mode. Also notice that the transformation of coordinates $(\bar{\psi}, \psi) \to (\rho, \phi)$, viewed as a change of integration variables, has a Jacobian of unity.

[13] N. N. Bogoliubov, On the theory of superfluidity, *J. Phys. (USSR)* **11**, 23-32 (1947) (reprinted in D. Pines, *The Many-Body Problem*, [Benjamin, 1961]).

[14] However, as usual with grand canonical descriptions, in the thermodynamic limit the relative uncertainty in the number of particles, $(\langle \hat{N}^2 \rangle - \langle \hat{N} \rangle^2)/\langle \hat{N} \rangle^2$, will become vanishingly small.

INFO As we are dealing with a (functional) integral, there is a lot of freedom as to the choice of integration parameters. (I.e., in contrast to the operator formulation, there is no *a priori* constraint for a transform to be "canonical.") However, physically meaningful changes of representation will usually be **canonical transformations**, in the sense that the corresponding transformations of operators would conserve the commutation relations. Indeed, as we have seen in the info block starting on page 176, the operator transformation $a(\mathbf{r}) \equiv \hat{\rho}(\mathbf{r})^{1/2}\, e^{i\hat{\phi}(\mathbf{r})}, a^\dagger(\mathbf{r}) \equiv e^{-i\hat{\phi}(\mathbf{r})}\, \hat{\rho}(\mathbf{r})^{1/2}$, fulfills this criterion.

We next substitute the density–phase relation into the action and expand to second order around the reference mean-field. Ignoring gradients acting on the density field (in comparison with the "potential" cost of these fluctuations), we obtain

$$S[\rho,\phi] \approx \int d\tau \int d^d r \left[i\delta\rho\partial_\tau\phi + \frac{\rho_0}{2m}(\nabla\phi)^2 + \frac{g\rho^2}{2} \right]. \tag{6.11}$$

The first term of the action has the canonical structure "momentum $\times\, \partial_\tau$(coordinate)" indicative of a canonically conjugate pair. The second term measures the energy cost of spatially varying phase fluctuations. Notice that fluctuations with $\phi(\mathbf{r},\tau) = $ const. do not incur an energy cost – ϕ is a Goldstone mode. Finally, the third term records the energy cost of massive fluctuations from the potential minimum. Equation (6.11) represents the Hamiltonian version of the action, i.e. an action comprising coordinates ϕ and momenta ρ. Gaussian integration over the field $\delta\rho$ leads us to the Lagrangian form of the action (exercise):

$$S[\phi] \approx \frac{1}{2}\int d\tau \int d^d r \left[\frac{1}{g}(\partial_\tau\phi)^2 + \frac{\rho_0}{m}(\nabla\phi)^2 \right]. \tag{6.12}$$

Comparison with Eq. (1.4) identifies this action as the familiar d-dimensional oscillator. Drawing on the results of Chapter 1 (see, e.g., Eq. (1.29)), we find that the energy $\omega_{\mathbf{k}}$ carried by elementary excitations of the system scales linearly with momentum, $\omega_{\mathbf{k}} = |\mathbf{k}|(g\rho_0/m)^{1/2}$.

Let us now discuss the physical ramifications of these results. The actions (6.11) and (6.12) describe the phenomenon of superfluidity. To make the connection between the fundamental degree of freedom of a superfluid system, the **supercurrent**, and the phase field explicit, let us consider the quantum mechanical current operator

$$\begin{aligned} \hat{\mathbf{j}}(\mathbf{r},\tau) \quad &= \quad \frac{i}{2m}\left[(\nabla a^\dagger(\mathbf{r},\tau))a(\mathbf{r},\tau) - a^\dagger(\mathbf{r},\tau)\nabla a(\mathbf{r},\tau) \right] \\ &\overset{\text{fun. int.}}{\longrightarrow} \quad \frac{i}{2m}\left[(\nabla\bar{\psi}(\mathbf{r},\tau))\psi(\mathbf{r},\tau) - \bar{\psi}(\mathbf{r},\tau)\nabla\psi(\mathbf{r},\tau) \right] \approx \frac{\rho_0}{m}\nabla\phi(\mathbf{r},\tau), \end{aligned} \tag{6.13}$$

where the arrow indicates the functional integral correspondence of the operator description and we have neglected all contributions arising from spatial fluctuations of the density profile. (Indeed, these – massive – fluctuations describe the "normal" contribution to the current flow.)

INFO **Superfluidity** is one of the most counterintuitive and fascinating phenomena displayed by condensed matter systems. Experimentally, the most straightforward access to superfluid states of matter is provided by the helium liquids. Representative of many other effects displayed by

superfluid states of helium, we mention the capability of thin films to flow up the walls of a vessel (if the reward is that on the outer side of the container a low-lying basin can be reached – the fountain experiment) or to effortlessly propagate through porous media that no normal fluid may penetrate. Readers interested in learning more about the phenomenology of superfluid states of matter may refer to the seminal text by Pines and Nozières.[15]

The gradient of the phase variable is therefore a measure of the (super)current flow in the system. The behavior of that degree of freedom can be understood by inspection of the stationary phase equations – a.k.a. the Hamilton or Lagrange equations of motion – associated with the action (6.11) or (6.12). Turning to the Hamiltonian formulation, one obtains (exercise)

$$i\partial_\tau \phi = -g\rho + \mu, \quad i\partial_\tau \rho = \frac{\rho_0}{m}\nabla^2\phi = \nabla\cdot\mathbf{j}.$$

The second of these equations represents (the Euclidean time version of) a continuity equation. A current flow with non-vanishing divergence is accompanied by dynamical distortions in the density profile. The first equation tells us that the system adjusts to spatial fluctuations of the density by a dynamical phase fluctuation. The most remarkable feature of these equations is that they possess steady state solutions with non-vanishing current flow. Setting $\partial_\tau\phi = \partial_\tau\rho = 0$, we obtain the conditions $\delta\rho = 0$ and $\nabla\cdot\mathbf{j} = 0$, i.e. below the condensation temperature, a configuration with a uniform density profile can support a steady state divergenceless (super)current. Notice that a "mass term" in the ϕ-action would spoil this property, i.e., within our present approach, the phenomenon of supercurrent flow is intimately linked to the Goldstone mode character of the ϕ field.

EXERCISE Add a fictitious mass term to the ϕ-action and explore its consequences. How do the features discussed above present themselves in the Lagrange picture?

It is very instructive to interpret the phenomenology of supercurrent flow from a different, more microscopic perspective. Steady state current flow in normal environments is prevented by the mechanism of **energy dissipation**, i.e. particles constituting the current flow scatter off imperfections inside the system, thereby converting part of their energy into the creation of elementary excitations. (Macroscopically, the conversion of kinetic energy into the creation of excitations manifests itself as heat production.) Apparently, this mechanism is inactivated in superfluid states of matter, i.e. the current flow is dissipationless.

How can the dissipative loss of energy be avoided? Trivially, no energy can be exchanged if there are no elementary excitations to create. In reality, this means that the excitations of the system are energetically so high-lying that the kinetic energy stored in the current-carrying particles is insufficient to create them. But this is not the situation that we encounter in the superfluid! As we saw above, there is no energy gap separating the quasi-particle excitations of the system from the ground state. Rather, the dispersion $\omega(\mathbf{k})$ vanishes linearly as $\mathbf{k}\to 0$. However, there is an ingenious argument due to Landau showing that a linear excitation spectrum indeed suffices to stabilize dissipationless transport.

[15] D. Pines and P. Nozières, *The Theory of Quantum Liquids: Super uid Bose Liquids* (Addison-Wesley, 1989).

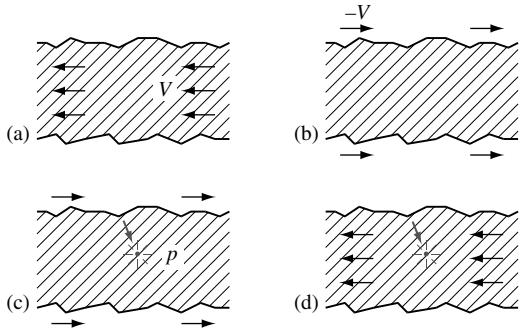

Figure 6.4 (a) Flow of a fluid through a rough pipe. (b) The same viewed from the rest frame of the fluid. (c) Dissipative creation of a (quasi-particle) excitation. (d) The same viewed from the laboratory frame.

INFO Consider the flow of some fluid through a pipe (see Fig. 6.4(a)). To be concrete, let us assume that the flow occurs at a uniform velocity $\mathbf{V}$. Taking the mass (of a certain portion of the fluid) to be M, the current carries a total kinetic energy $E_1 = M\mathbf{V}^2/2$. Now, suppose we view the situation from the point of view of the fluid, i.e. we perform a Galilean transformation into its own rest frame (Fig. 6.4(b)). From the perspective of the fluid, the walls of the pipe appear as though they were moving with velocity $-\mathbf{V}$. Now, suppose that frictional forces between fluid and the wall lead to the creation of an elementary excitation of momentum $\mathbf{p}$ and energy $\epsilon(\mathbf{p})$, i.e. the fluid is no longer at rest but carries kinetic energy (Fig. 6.4(c)). After a Galilean transformation back to the laboratory frame (Fig. 6.4(d)), one finds that the energy of the fluid after the creation of the excitation is given by (exercise)

$$E_2 = \frac{M\mathbf{V}^2}{2} + \mathbf{p}\cdot\mathbf{V} + \epsilon(\mathbf{p}).$$

Now, since all of the energy needed to manufacture the excitation must have been provided by the liquid itself, energy conservation requires that $E_1 = E_2$, or $-\mathbf{p}\cdot\mathbf{V} = \epsilon(\mathbf{p})$. Since $\mathbf{p}\cdot\mathbf{V} > -|\mathbf{p}||\mathbf{V}|$, this condition can only be met if $|\mathbf{p}||\mathbf{V}| > \epsilon(\mathbf{p})$. While systems with a "normal" gapless dispersion, $\epsilon(\mathbf{p}) \sim \mathbf{p}^2$, are compatible with this energy-balance relation (i.e. no matter how small $|\mathbf{V}|$, quasi-particles of low momentum can always be excited), both gapped dispersions $\epsilon(\mathbf{p}) \stackrel{\mathbf{p}\to 0}{\longrightarrow}$ const. and linear dispersions are incompatible if $\mathbf{V}$ becomes smaller than a certain **critical velocity** V_*. Specifically for a linear dispersion $\epsilon(\mathbf{p}) = v|\mathbf{p}|$, the critical velocity is given by $V_* = v$. For currents slower than that, the flow is necessarily dissipationless.

Let us conclude our preliminary discussion of the weakly interacting Bose gas with a very important remark. Superficially, Eq. (6.11) and (6.12) suggest that we have managed to describe the long-range behavior of the condensed matter system in terms of a free Gaussian theory. However, one must recall that ϕ is a phase field, defined only modulo 2π. (In Eq. (6.11) and (6.12) this condition is understood implicitly. At this point, it is perhaps worth reiterating that when dealing with Goldstone modes it is important to keep the underlying geometry in mind and not focus too tightly on a specific coordinate representation.) The fact that ϕ is defined only up to integer multiples of 2π manifests itself in the

formation of the most interesting excitations of the superfluid: **vortices**, i.e. phase configurations $\phi(\mathbf{r}, \tau)$ that change by a multiple of 2π as one moves around a certain reference coordinate, the vortex center. Existing in parallel with harmonic phonon-like excitations discussed above, these excitations lead to a wealth of observable phenomena, to be discussed in more detail in Chapter 8. However, for the moment let us turn to the discussion of another prominent superfluid, the condensate of Cooper pairs, more generally known as the superconductor.

6.4 Superconductivity

Kammerlingh Onnes 1853–1926
Nobel Laureate in Physics in 1913 "for his investigations on the properties of matter at low temperatures which led, inter alia to the production of liquid helium." (Image © The Nobel Foundation.)

The electrical resistivity of many metals and alloys drops abruptly to zero when the material is cooled to a sufficiently low temperature. This phenomenon, which goes by the name of **superconductivity**, was first observed by Kammerlingh Onnes in Leiden in 1911, three years after he first liquefied helium. Equally striking, a superconductor cooled below its transition temperature in a magnetic field expels all magnetic flux from its interior. (One of the more spectacular manifestations of the field-aversion of superconductors is exemplified in the figure below: a magnet levitated by a superconductor due to the expulsion of magnetic flux.) This phenomenon of **perfect diamagnetism** is known as the **Meissner effect** and is characteristic of superconductivity.

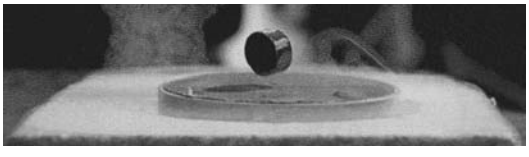

Indeed, the Meissner effect and dissipationless transport are but two of a plethora of phenomena accompanying superconductivity.[16] Along with the introduction of more advanced theoretical machinery, a variety of superconducting phenomena is discussed in the remainder of this text. The present, introductory section is devoted to the formulation of the theoretical foundations of the conventional "BCS" theory of superconductivity, cast into the language of the field integral. Although the presentation is self-contained, our focus is on the theoretical aspects. Depending on taste, some readers may find it useful to motivate their encounter with the formalism developed below by first familiarizing themselves with the basic phenomenology of the BCS superconductor.

[16] In fact, it is not even appropriate to speak about the phenomenon of "superconductivity" as deriving from the same microscopic origin: since the discovery of the class of high-temperature cuprate superconductors in 1986, it has become increasingly evident that the physical mechanisms responsible for high-temperature and "conventional" superconductivity are likely to be strikingly different.

Basic concepts of BCS theory

John Bardeen 1908–1991 (left), Leon N. Cooper 1930– (center), and John R. Schrieffer 1931– (right) Nobel Laureates in Physics in 1972 for their theory of superconductivity. (Bardeen was also awarded the 1956 Nobel Prize in Physics for his research on semiconductors and discovery of the transistor effect.) (Images © The Nobel Foundation.)

Superconductivity involves an ordered state of conduction electrons in a metal, caused by the presence of a residual attractive interaction at the Fermi surface. The nature and origin of the ordering were elucidated in a seminal work by Bardeen, Cooper, and Schrieffer – BCS theory[17] – some 50 years after its discovery! At low temperatures, an attractive pairwise interaction can induce an instability of the electron gas towards the formation of bound pairs of time-reversed states $\mathbf{k}\uparrow$ and $-\mathbf{k}\downarrow$ in the vicinity of the Fermi surface.

From where does an **attractive interaction** between charged particles appear? In conventional (BCS) superconductors, attractive correlations between electrons are due to the exchange of lattice vibrations, or phonons: The motion of an electron through a metal causes a dynamic local distortion of the ionic crystal. Crucially, this process is governed by two totally different time scales. For an electron, it takes a time $\sim E_{\mathrm{F}}^{-1}$ to traverse the immediate vicinity of a lattice ion and to trigger a distortion out of its equilibrium position into a configuration that both particles find energetically beneficial (top right panel of the figure).

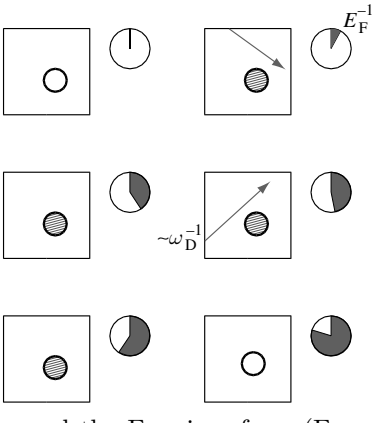

However, once the ion has been excited it needs a time of $\mathcal{O}\left(\omega_{\mathrm{D}}^{-1} \gg E_{\mathrm{F}}^{-1}\right)$ to relax back into its equilibrium position (middle left). Here, ω_{D} denotes the Debye frequency, i.e. the characteristic scale for phonon excitations. This means that, long after the first electron has passed, a second electron may benefit from the distorted ion potential (middle right). Only after the ion has been left alone for a time $> \omega_{\mathrm{D}}^{-1}$ does it relax back into its equilibrium configuration (bottom left and right). The net effect of this retardation mechanism is an attractive interaction between the two electrons. Since the maximum energy scale of ionic excitations is given by the Debye frequency, the range of the interaction is limited to energies $\sim \omega_{\mathrm{D}}$ around the Fermi surface. (For a more quantitative formulation, see Problem 4.5.) As regards the high-temperature cuprate superconductors, the particular mechanism of pair formation remains (at the time of writing) controversial, although the consensus is that its origin is rooted in spin fluctuations.

[17] J. Bardeen, L. N. Cooper, and J. R. Schrieffer, Microscopic theory of superconductivity, *Phys. Rev.* **106** (1957), 162-4; *Theory of Superconductivity*, **108** (1957), 1175-204.

Comprising two fermions, the electron–electron bound states, known as **Cooper pairs**, mimic the behavior of bosonic composite particles.[18] At low temperatures, these quasi-bosonic degrees of freedom form a condensate which is responsible for the remarkable properties of superconductors, such as perfect diamagnetism.

To appreciate the tendency to pair formation in the electron system, consider the diagram shown in the figure below. The region of attractive correlation is indicated as a shaded ring of width $\sim \omega_{\rm D}/v_{\rm F}$. Now, consider a two-electron state $|\mathbf{k}\uparrow, -\mathbf{k}\downarrow\rangle$ formed by two particles of (near) opposite momentum and opposite spin.[19] Momentum conserving scattering of the constituent particles may lead to the formation of a new state $|(\mathbf{k}+\mathbf{p})\uparrow, -(\mathbf{k}+\mathbf{p})\downarrow\rangle \equiv |\mathbf{k}'\uparrow, -\mathbf{k}'\downarrow\rangle$ of the same, opposite-momentum structure. Crucially, the momentum transfer $\mathbf{p}$ may trace out a large set of values of $\mathcal{O}(k_{\rm F}^{d-1}\omega_{\rm D}/v_{\rm F})$ without violating the condition that the final states be close to the Fermi momentum. (By contrast, if the initial state had not been formed by particles of opposite momentum, the phase space for scattering would have been greatly diminished.) Remembering our previous discussion of the RPA approximation, we recognize a familiar mechanism: an *a priori* weak interaction may amplify its effect by conspiring with a large phase space volume.

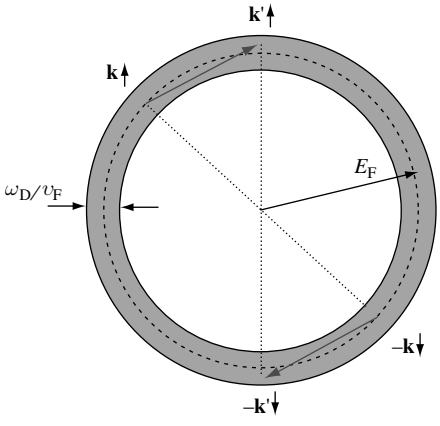

To explore this mechanism in quantitative terms, we will adopt a simplified model defined by the Hamiltonian

$$\hat{H} = \sum_{\mathbf{k}\sigma} \epsilon_{\mathbf{k}} \hat{n}_{\mathbf{k}\sigma} - \frac{g}{L^d} \sum_{\mathbf{k},\mathbf{k}',\mathbf{q}} c^\dagger_{\mathbf{k}+\mathbf{q}\uparrow} c^\dagger_{-\mathbf{k}\downarrow} c_{-\mathbf{k}'+\mathbf{q}\downarrow} c_{\mathbf{k}'\uparrow}, \tag{6.14}$$

where g represents a (positive) constant. The Hamiltonian $\hat{H}$ should be interpreted as an effective Hamiltonian describing the physics of a thin shell of states of width $\mathcal{O}(\omega_{\rm D})$ centered around the Fermi surface (i.e. the region where a net attractive interaction prevails). Although a more realistic model of attraction would involve a complicated momentum-dependent interaction such as the one obtained from the detailed consideration of the electron–phonon interaction (see Problem 4.5), the simple constant pairing interaction captures the essential physics.[20] After the trio who first explored its phenomenology, the model Hamiltonian (6.14) is commonly referred to as the **BCS Hamiltonian**.

[18] Strictly speaking, this identification deserves some qualification. In the superconducting context, Cooper pairs have a length scale (the coherence length to be introduced below) which typically exceeds the average particle spacing of the electron gas (usually by as much as three orders of magnitude). In this sense, it can be misleading to equate a pair with a single composite particle. The interpretation of the BCS state as a Bose–Einstein condensate of Cooper pairs is developed more fully in the problem set in the discussion of the BEC–BCS crossover – see Problem 6.7.

[19] Note that there are a minority of superconducting materials – the spin triplet superconductors – in which electrons of equal spin are paired.

[20] More importantly, to simplify our discussion, we will take the electrons to be otherwise non-interacting. In fact, the presence of a repulsive Coulomb interaction of the electrons plays a crucial role in controlling the properties of the superconductor. For an in-depth discussion of the role played by repulsive interactions, see A. I. Larkin and

Now the preliminary discussion above does not explain why an attractive interaction is so special. Nor does the discussion elucidate the phenomenological consequences of pair scattering at the Fermi surface. In the following we will address these issues from a number of different angles. The result will be a heuristic picture of the superconductor that will guide us in constructing the more rigorous field integral approach below. Mainly for illustrative purposes, we begin our discussion with a brief perturbative analysis of Cooper pair scattering. Proceeding in close analogy to the previous discussion of the RPA, we discover the dramatic consequences of an attractive interaction on the ground state of the system. (However, this part of the discussion is an optional (if instructive) element of the development of the theory. Readers who did not yet navigate Section 5.3 may choose to skip this part of the discussion and proceed directly to Section 6.4 where the mean-field picture of the superconductor is developed.)

Cooper instability

To explore the fate of a Cooper pair under multiple scattering, let us consider the four-point correlation function

$$C(\mathbf{q},\tau) = \frac{1}{L^{2d}} \sum_{\mathbf{k},\mathbf{k}'} \left\langle \bar{\psi}_{\mathbf{k}+\mathbf{q}\uparrow}(\tau)\bar{\psi}_{-\mathbf{k}\downarrow}(\tau)\ \psi_{\mathbf{k}'+\mathbf{q}\downarrow}(0)\psi_{-\mathbf{k}'\uparrow}(0)\right\rangle .$$

This describes the amplitude of Cooper pair propagation $|\mathbf{k}+\mathbf{q}\uparrow, -\mathbf{k}\downarrow\rangle \to |\mathbf{k}'+\mathbf{q}\uparrow, -\mathbf{k}'\downarrow\rangle$ in an imaginary time τ and averaged over all initial and final particle momenta.[21] As is usual with problems whose solution must depend only on time differences, it is convenient to switch to a frequency representation. With $C(q) \equiv C(\mathbf{q},\omega_m) = T\int_0^\beta d\tau\, e^{-i\omega_m\tau} C(\mathbf{q},\tau)$, where ω_m denotes a bosonic Matsubara frequency, it is straightforward to verify that $C(q) = \frac{T^2}{L^{2d}}\sum_{k,k'} \left\langle \bar{\psi}_{k+q\uparrow}\bar{\psi}_{-k\downarrow}\psi_{k'+q\downarrow}\psi_{-k'\uparrow}\right\rangle$.

To calculate the correlation function, let us draw on the perturbative methods introduced in Section 5.3. As with the analysis of the RPA, the density of the electron gas will play the role of a large parameter, i.e. one must expand the correlation function in pair interaction vertices g and retain only those terms that appear with one free momentum summation per interaction. Summation over these contributions leads to the ladder diagram series shown in Fig. 6.5, where the momentum labels of the Green functions are hidden for clarity. According to the definition of the correlation function, the two Green functions entering the ladder carry momenta $k+q$ and $-k$, respectively. Momentum conservation then implies that the Green functions defining each consecutive rung of the ladder also carry near opposite momenta $p+q$ and $-p$, where p is a summation variable.

A. A. Varlamov, Fluctuation phenomena in superconductors, in *Handbook on Superconductivity: Conventional and Unconventional Superconductors*, ed. K.-H. Bennemann and J. B. Ketterson (Springer-Verlag, 2002).

[21] As with applications of the path integral discussed previously, information about the real time dynamics of the pair can be extracted from the analytical continuation $\tau \to it$. Further, notice that the "center of mass" momentum $\mathbf{q}$ of a pair $\frac{1}{L^d}\sum_{\mathbf{k}} |\mathbf{k}+\mathbf{q}\uparrow, -\mathbf{k}\downarrow\rangle$ can be interpreted as a variable Fourier conjugate to the center of the pair. (Exercise: Show this by inverse Fourier transform.) An equivalent interpretation of the correlation function C is that it describes the wandering of the Cooper pair under the influence of scattering.

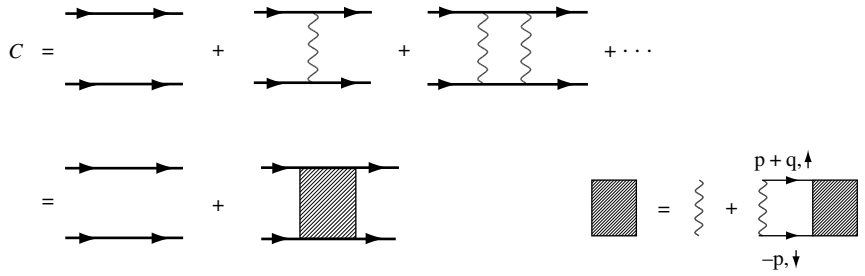

Figure 6.5 Two-particle propagator in the presence of an (attractive) interaction. The two Green function lines defining each rung of the ladder carry momenta $p+q$ and $-p$, respectively, where p is a free summation variable. The vertex of the propagator, defined through the second line, obeys the Bethe–Salpeter equation defined on the bottom right.

EXERCISE Convince yourself that the ladder diagrams shown in the figure are the only diagrams that contain one free momentum summation per interaction vertex.

As with the previous discussion in Section 5.3, the central part of the correlation function is described by a vertex Γ. The diagrammatic definition of that object is shown in the bottom right part of Fig. 6.5. Translating from diagrammatic to an algebraic formulation, one obtains the Cooper version of a Bethe–Salpeter equation $\Gamma_q = g + \frac{gT}{L^d}\sum_p G_{p+q}G_{-p}\Gamma_q$, where we have anticipated that a solution independent of the intermediate momenta can be found. Solving this equation for Γ_q, we arrive at an equation structurally similar to Eq. (5.44):

$$\Gamma_q = \frac{g}{1 - \frac{gT}{L^d}\sum_p G_{p+q}G_{-p}}. \tag{6.15}$$

Drawing on the results of Problem 4.5, the frequency part of the summation over p gives

$$\begin{aligned}\frac{T}{L^d}\sum_p G_{p+q}G_{-p} &= \frac{1}{L^d}\sum_{\mathbf{p}} \frac{1 - n_{\mathrm{F}}(\xi_{\mathbf{p}+\mathbf{q}}) - n_{\mathrm{F}}(\xi_{-\mathbf{p}})}{i\omega_m + \xi_{\mathbf{p}+\mathbf{q}} + \xi_{-\mathbf{p}}} \\ &= \frac{1}{L^d}\sum_{\mathbf{p}} \left(\frac{1}{2} - n_{\mathrm{F}}(\xi_{\mathbf{p}})\right)\left(\frac{1}{i\omega_m + \xi_{\mathbf{p}+\mathbf{q}} + \xi_{-\mathbf{p}}} + (\mathbf{q} \leftrightarrow -\mathbf{q})\right),\end{aligned}$$

where, in the last line, we have made use of the symmetry of the energy arguments, $\xi_{\mathbf{p}} = \xi_{-\mathbf{p}}$. The summation for non-zero $\mathbf{q}$ is left as an instructive exercise in Fermi-surface integration. However, for the sake of our present argument, it will be sufficient to perform the sum for zero external momentum $q = (0,0)$ (i.e. we will probe the fate of spatially homogeneous and static pair configurations). Using the identity $\frac{1}{L^d}\sum_{\mathbf{p}} F(\epsilon_{\mathbf{p}}) = \int d\epsilon\, \nu(\epsilon) F(\epsilon)$ to replace the momentum sum by an energy integral, and remembering that the pairing interaction is limited to a thin shell around the Fermi surface, we then obtain

$$\frac{T}{L^d}\sum_p G_p G_{-p} = \int_{-\omega_{\mathrm{D}}}^{\omega_{\mathrm{D}}} d\epsilon\, \nu(\epsilon)\frac{1 - 2n_{\mathrm{F}}(\epsilon)}{2\epsilon} \simeq \nu \int_T^{\omega_{\mathrm{D}}} \frac{d\epsilon}{\epsilon} = \nu \ln\left(\frac{\omega_{\mathrm{D}}}{T}\right), \tag{6.16}$$

where we have used the fact that, at energies $\epsilon \sim T$, the $1/\epsilon$ singularity of the integrand is cut off by the Fermi distribution function. Substitution of this result back into the expression for the vertex leads to the result

$$\Gamma_{(0,0)} \simeq \frac{g}{1 - g\nu \ln\left(\frac{\omega_{\rm D}}{T}\right)}.$$

From this, one can read off essential elements of the transition to the superconducting phase.

- ▷ We first note that the interaction constant appears in combination with the density of states, i.e. even a weak interaction can lead to sizeable effects if the density of states is large enough. From our previous qualitative discussion it should be clear that the scaling factor ν simply measures the number of final states accessible to the scattering mechanism depicted in the figure on page 266.
- ▷ The net strength of the Cooper pair correlation grows upon increasing the energetic range $\omega_{\rm D}$ of the attractive force or, equivalently, on lowering the temperature. Obviously, something drastic happens when $g\nu \ln\left(\frac{\omega_{\rm D}}{T}\right) = 1$, i.e. when

$$T = T_{\rm c} \equiv \omega_{\rm D} \exp\left[-\frac{1}{g\nu}\right].$$

  At this **critical temperature**, the vertex develops a singularity. Since the vertex and the correlation function are related by multiplication by a number of (non-singular) Green functions, the same is true for the correlation function itself.
- ▷ As we will soon see, $T_{\rm c}$ marks the transition temperature to the superconducting state. At and below $T_{\rm c}$ a perturbative approach based on the Fermi sea of the non-interacting system as a reference state breaks down. The Cooper instability signals that we will have to look for an alternative ground state or "mean-field," i.e. one that accounts for the strong binding of Cooper pairs.

In the next section, we explore the nature of the superconducting state from a complementary perspective.

Mean-field theory of superconductivity

The discussion of the previous section suggests that, at the transition, the system develops an instability towards pair binding, or "condensation." In the next section we build on this observation to construct a quantitative approach, based on a Hubbard–Stratonovich decoupling in the Cooper channel. However, for the moment, let us stay on a more informal level and *assume* that the ground state $|\Omega_{\rm s}\rangle$ of the theory is characterized by the presence of a macroscopic number of Cooper pairs. More specifically, let us assume that the operator $\sum_{\mathbf{k}} c_{-\mathbf{k}\downarrow} c_{\mathbf{k}\uparrow}$ acquires a non-vanishing ground state expectation value,

$$\Delta = \frac{g}{L^d} \sum_{\mathbf{k}} \langle \Omega_{\rm s} | c_{-\mathbf{k}\downarrow} c_{\mathbf{k}\uparrow} | \Omega_{\rm s} \rangle, \quad \bar{\Delta} = \frac{g}{L^d} \sum_{\mathbf{k}} \langle \Omega_{\rm s} | c^\dagger_{\mathbf{k}\uparrow} c^\dagger_{-\mathbf{k}\downarrow} | \Omega_{\rm s} \rangle, \tag{6.17}$$

where we have included the coupling constant of the theory for later convenience. The assumption that Δ assumes non-zero values (vanishes) below (above) the transition temperature T_c is tantamount to declaring Δ to be the **order parameter** of the superconducting transition. However, at the present stage, this statement has the status of a mere presumption; we will have to explore its validity below.

At any rate, the non-vanishing expectation value of Δ looks strange. It clearly implies that the fermion many-body state $|\Omega_s\rangle$ cannot have a definite number of particles (cf. the coherent states). However, a better way to think about the problem is to remember the bosonic nature of the two-fermion pair state $|\mathbf{k}\uparrow, -\mathbf{k}\downarrow\rangle$. From this perspective, $c^\dagger_{\mathbf{k}\uparrow}c^\dagger_{-\mathbf{k}\downarrow}$ appears as the operator that creates a bosonic excitation. Non-vanishing of its expectation value implies a condensation phenomenon akin to the condensates discussed in Section 6.3. Indeed, much of the remainder of this section is devoted to the (semi-phenomenological) construction of a "bosonic" mean-field picture of the superconductor.

To develop this description, let us substitute

$$\sum_{\mathbf{k}} c_{-\mathbf{k}+\mathbf{q}\downarrow}c_{\mathbf{k}\uparrow} = \frac{L^d\Delta}{g} + \underbrace{\sum_{\mathbf{k}} c_{-\mathbf{k}+\mathbf{q}\downarrow}c_{\mathbf{k}\uparrow} - \frac{\Delta L^d}{g}}_{\text{small}},$$

into the microscopic Hamiltonian and retain only those terms that appear as bilinears in the electron operators. Adding the chemical potential, and setting $\xi_{\mathbf{k}} = \epsilon_{\mathbf{k}} - \mu$, the "mean-field" Hamiltonian takes the form

$$\hat{H} - \mu\hat{N} \simeq \sum_{\mathbf{k}} \left[\xi_{\mathbf{k}} c^\dagger_{\mathbf{k}\sigma}c_{\mathbf{k}\sigma} - \left(\bar{\Delta}c_{-\mathbf{k}\downarrow}c_{\mathbf{k}\uparrow} + \Delta c^\dagger_{\mathbf{k}\uparrow}c^\dagger_{-\mathbf{k}\downarrow}\right)\right] + \frac{L^d|\Delta|^2}{g},$$

known (in the Russian literature) as the **Bogoliubov** or **Gor'kov** Hamiltonian after its authors (while the terminology **Bogoliubov–de Gennes Hamiltonian** has become more widespread in the Anglo-Saxon literature, reflecting the promotion of the mean-field description by de Gennes).

Indeed, although perfectly Hermitian, the Gor'kov Hamiltonian does not conserve particle number. Instead, pairs of particles are born out of, and annihilated into, the vacuum. To bring the mean-field Hamiltonian to a diagonal form, we proceed in a manner analogous to that of Section 2.2 (where appeared a Hamiltonian of similar structure, namely $a^\dagger a + aa + a^\dagger a^\dagger$). Specifically, let us recast the fermion operators in a two-component **Nambu spinor** representation

$$\Psi^\dagger_{\mathbf{k}} = \left(c^\dagger_{\mathbf{k}\uparrow}, c_{-\mathbf{k}\downarrow}\right), \quad \Psi_{\mathbf{k}} = \begin{pmatrix} c_{\mathbf{k}\uparrow} \\ c^\dagger_{-\mathbf{k}\downarrow} \end{pmatrix},$$

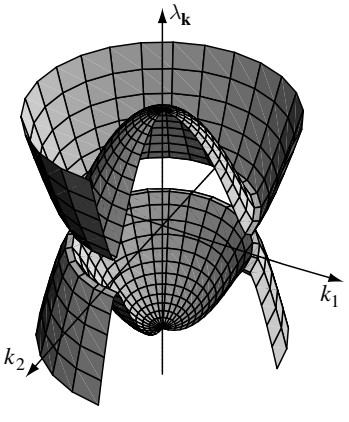

comprising ↑-creation and ↓-annihilation operators in a single object. It is then straightforward to show that the Hamiltonian assumes the bilinear form

$$\hat{H} - \mu\hat{N} = \sum_{\mathbf{k}} \Psi^\dagger_{\mathbf{k}} \begin{pmatrix} \xi_{\mathbf{k}} & -\Delta \\ -\bar{\Delta} & -\xi_{\mathbf{k}} \end{pmatrix} \Psi_{\mathbf{k}} + \sum_{\mathbf{k}} \xi_{\mathbf{k}} + \frac{L^d|\Delta|^2}{g}.$$

Now, being bilinear in the Nambu operators, the mean-field Hamiltonian can be brought to a diagonal form by employing the unitary transformation[22]

$$\chi_{\mathbf{k}} \equiv \begin{pmatrix} \alpha_{\mathbf{k}\uparrow} \\ \alpha^\dagger_{-\mathbf{k}\downarrow} \end{pmatrix} = \begin{pmatrix} \cos\theta_{\mathbf{k}} & \sin\theta_{\mathbf{k}} \\ \sin\theta_{\mathbf{k}} & -\cos\theta_{\mathbf{k}} \end{pmatrix} \begin{pmatrix} c_{\mathbf{k}\uparrow} \\ c^\dagger_{-\mathbf{k}\downarrow} \end{pmatrix} \equiv U_{\mathbf{k}} \Psi_{\mathbf{k}},$$

(under which the anti-commutation relations of the new electron operators $\alpha_{\mathbf{k}\sigma}$ are maintained – exercise). Note that the operators $\alpha^\dagger_{\mathbf{k}\uparrow}$ involve superpositions of $c^\dagger_{\mathbf{k}\uparrow}$ and $c_{-\mathbf{k}\downarrow}$, i.e. the quasi-particle states created by these operators contain linear combinations of particle and hole states. Choosing Δ to be real[23] and setting $\tan(2\theta_{\mathbf{k}}) = -\Delta/\xi_{\mathbf{k}}$, i.e. $\cos(2\theta_{\mathbf{k}}) = \xi_{\mathbf{k}}/\lambda_{\mathbf{k}}$, $\sin(2\theta_{\mathbf{k}}) = -\Delta/\lambda_{\mathbf{k}}$, where

$$\lambda_{\mathbf{k}} = (\Delta^2 + \xi^2_{\mathbf{k}})^{1/2}, \tag{6.18}$$

the transformed Hamiltonian takes the form (exercise)

$$\hat{H} - \mu\hat{N} = \sum_{\mathbf{k}\sigma} \lambda_{\mathbf{k}} \alpha^\dagger_{\mathbf{k}\sigma} \alpha_{\mathbf{k}\sigma} + \sum_{\mathbf{k}} (\xi_{\mathbf{k}} - \lambda_{\mathbf{k}}) + \frac{\Delta^2 L^d}{g}. \tag{6.19}$$

This result shows that the elementary excitations, the **Bogoliubov quasi-particles**, created by $\alpha^\dagger_{\mathbf{k}\sigma}$, have a minimum energy Δ known as the **energy gap**. The full dispersion $\pm\lambda_{\mathbf{k}}$ is shown in the figure above. Due to the energy gap separating filled from empty quasi-particle states, elementary excitations are difficult to excite at low temperatures, implying a rigidity of the ground state.

To determine the ground state wavefunction one simply has to identify the vacuum state of the algebra $\{\alpha_{\mathbf{k}}, \alpha^\dagger_{\mathbf{k}}\}$, i.e the state that is annihilated by all the quasi-particle annihilation operators $\alpha_{\mathbf{k}\sigma}$. This condition is met uniquely by the state

$$\boxed{|\Omega_s\rangle \equiv \prod_{\mathbf{k}} \alpha_{\mathbf{k}\uparrow}\alpha_{-\mathbf{k}\downarrow}|\Omega\rangle \sim \prod_{\mathbf{k}} \left(\cos\theta_{\mathbf{k}} - \sin\theta_{\mathbf{k}} c^\dagger_{\mathbf{k}\uparrow} c^\dagger_{-\mathbf{k}\downarrow}\right)|\Omega\rangle,}$$

where $|\Omega\rangle$ represents the vacuum state of the fermion operator algebra $\{c_{\mathbf{k}}, c^\dagger_{\mathbf{k}}\}$, and $\sin\theta_{\mathbf{k}} = \sqrt{(1 - \xi_{\mathbf{k}}/\lambda_{\mathbf{k}})/2}$. Since the vacuum state of any algebra of canonically conjugate operators is unique, the state $|\Omega_{\rm s}\rangle$ must, up to normalization, be *the* vacuum state. From the representation given above, it is straightforward to verify that the normalization is unity (exercise).

[22] It is instructive to compare with the previous analysis of Section 2.2 where the bosonic nature of the problem enforced diagonalization by a non-compact pseudo-unitary transformation.

[23] If $\Delta \equiv |\Delta|e^{i\phi}$ is not real, it can always be made so by the global gauge transformation $c_a \to e^{i\phi/2}c_a, c^\dagger_a \to e^{-i\phi/2}c^\dagger_a$. Notice the similarity to the gauge freedom that led to Goldstone mode formation in the previous section! Indeed, we will see momentarily that the gauge structure of the superconductor has equally far-reaching consequences.

Finally, we need to solve Eq. (6.17) self-consistently for the input parameter Δ:

$$\begin{aligned}\Delta &= \frac{g}{L^d}\sum_{\mathbf{k}}\langle\Omega_{\rm s}|c_{-\mathbf{k}\downarrow}c_{\mathbf{k}\uparrow}|\Omega_{\rm s}\rangle = -\frac{g}{L^d}\sum_{\mathbf{k}}\sin\theta_{\mathbf{k}}\cos\theta_{\mathbf{k}} = \frac{g}{2L^d}\sum_{\mathbf{k}}\frac{\Delta}{(\Delta^2+\xi_{\mathbf{k}}^2)^{1/2}} \\ &\simeq \frac{g\Delta}{2}\int_{-\omega_{\rm D}}^{\omega_{\rm D}}\frac{\nu(\xi)d\xi}{(\Delta^2+\xi^2)^{1/2}} = g\Delta\nu\sinh^{-1}(\omega_{\rm D}/\Delta), \qquad (6.20)\end{aligned}$$

where we have assumed that the pairing interaction g uniformly extends over an energy scale $\omega_{\rm D}$ (over which the density of states ν is roughly constant). Rearranging this equation for Δ, we obtain the important relation

$$\boxed{\Delta = \frac{\omega_{\rm D}}{\sinh(1/g\nu)} \overset{g\nu\ll 1}{\simeq} 2\omega_{\rm D}\exp\left(-\frac{1}{g\nu}\right).} \qquad (6.21)$$

This is the second time that we have encountered the combination of energy scales on the right-hand side of the equation. Previously we identified $T_{\rm c} = \omega_{\rm D}\exp[-(g\nu)^{-1}]$ as the transition temperature at which the Cooper instability takes place. Our current discussion indicates that $T_{\rm c}$ and the quasi-particle energy gap Δ at $T = 0$ coincide. In fact, that identification might have been anticipated from our discussion above. At temperatures $T < \Delta$, thermal fluctuations are not capable of exciting quasi-particle states above the ground state. One thus expects that $T_{\rm c} \sim \Delta$ separates a low-temperature phase, characterized by the features of the anomalous pairing ground state, from a "Fermi-liquid-like" high-temperature phase where free quasi-particle excitations prevail.

In the mean-field approximation, the ground state $|\Omega_{\rm s}\rangle$ and its quasi-particle excitations formally diagonalize the BCS Hamiltonian. Before proceeding with the further development of the theory, let us pause to discuss a number of important properties of these states.

Ground state

In the limit $\Delta \to 0$, $\sin^2\theta_{\mathbf{k}} \to \theta(\mu - \epsilon_{\mathbf{k}})$, and the ground state collapses to the filled Fermi sea with chemical potential μ. As Δ becomes non-zero, states in the vicinity of the Fermi surface rearrange themselves into a condensate of paired states. The latter involves the population of single-particle states with energy $\epsilon_{\mathbf{k}} > \mu$. (This follows simply from the energy dependence of the weight function $\sin\theta_{\mathbf{k}}$ entering the definition of the ground state – see the figure.) However, it is straightforward to show that, for any value $g > 0$, the total energy of the ground state, $E_{|\Omega_{\rm s}\rangle} \equiv \langle\Omega_{\rm s}|\hat{H} - \mu\hat{N}|\Omega_{\rm s}\rangle = \sum_{\mathbf{k}}(\xi_{\mathbf{k}} - \lambda_{\mathbf{k}}) + \Delta^2 L^d/g$, is lower than the energy $E_0 \equiv 2\sum_{|\mathbf{k}|<p_{\rm F}}\xi_{\mathbf{k}}$ of the Fermi sphere when $g = 0$:

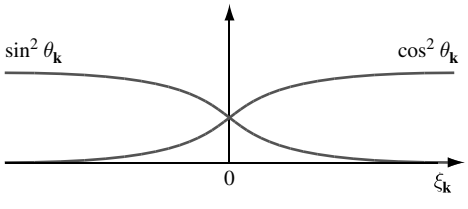

EXERCISE To show that $E_{|\Omega_{\rm s}\rangle} < E_0$, it is convenient to represent the ground state energy of the Fermi sea as $E_0 = \lim_{\Delta\to 0} E_{|\Omega_{\rm s}\rangle}$. Use this representation (and the solution of the mean-field equation) to verify that the superconductor ground state energy lies below that of the uncorrelated Fermi sea. It is also instructive to ask for the minimum value $E_{|\Omega_{\rm s}\rangle}$ may assume

upon variation of Δ for fixed g. Show that the solution of the variational equation $\partial_\Delta E_{|\Omega_s\rangle} = 0$ leads back to the mean-field equation for Δ discussed above.

Excitations

It is very important to distinguish between quasi-particle states and "excitations." Quasi-particle states are the eigenstates of the BCS Hamiltonian. Their energy–momentum relation is shown in the figure on page 271. Notice that there is a positive– and a negative–energy branch of quasi-particles. In the limit $\Delta \to 0$, the quasi-particles evolve into ordinary electrons. By contrast, the energy of *excitations* (as created by the operators $\alpha^\dagger_{\mathbf{k}}$) is always positive. An excitation can be either the creation of a quasi-particle at positive energy or the elimination of a quasi-particle (the creation of a quasi-hole) at negative energy. (In the ground state, all negative-energy quasi-particle states are filled.) As $\Delta \to 0$, the excitation operators evolve into the operator algebra introduced in Eq. (2.21). Notice that the total number of excitations is equal to the number of quasi-particle states. However, their density of states (non-vanishing for positive energies only) is twice as large. This is because the dispersion of excitations is obtained by superimposing the positive branch of the quasi-particle spectrum on the sign-inverted negative branch. For a particle–hole symmetric system, the quasi-particle spectrum is invariant under sign inversion, which implies that the two branches contribute equally to the density of excitations.

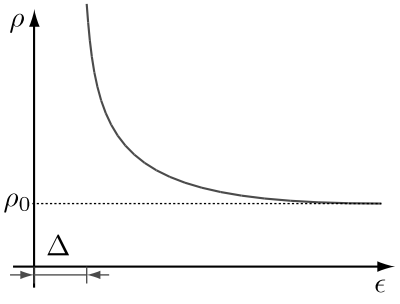

After these general remarks we turn to the specific discussion of the excitations of the BCS superconductor. According to Eq. (6.19), the excitation spectrum is gapped, i.e. it takes a minimum energy Δ to create an excitation above the BCS ground state; the formerly ($g = 0$) continuous spectrum has acquired a gap. To better understand the profile of the spectrum, let us compute the density of excitations $\rho(\epsilon)$,[24] in the vicinity of the Fermi surface, $\epsilon \approx \mu$:

$$\begin{aligned}\rho(\epsilon) &= \frac{1}{L^d}\sum_{\mathbf{k}\sigma}\delta(\epsilon-\lambda_{\mathbf{k}}) = \int d\xi \underbrace{\frac{1}{L^d}\sum_{\mathbf{k}\sigma}\delta(\xi-\xi_{\mathbf{k}})}_{\nu(\xi)}\,\delta(\epsilon-\lambda(\xi)) \\ &\approx \nu\sum_{s=\pm1}\int_0^\infty d\xi\,\frac{\delta\left(\xi - s[\epsilon^2-\Delta^2]^{1/2}\right)}{\left|\partial_\xi[\xi^2+\Delta^2]^{1/2}\right|} = 2\nu\Theta(\epsilon-\Delta)\frac{\epsilon}{(\epsilon^2-\Delta^2)^{1/2}}.\end{aligned}$$

A schematic plot of the BCS quasi-particle density of states is shown in the figure above. It is apparent that the spectral weight of the quasi-particles has been transferred from the Fermi surface to the interval $[\Delta, \infty]$. The divergence at Δ signals that the majority of quasi-particle states populate the spectral region just above the gap.

[24] To distinguish the density of states of the quasi-particles (ν) from that of the excitations, we denote the latter by ρ.

EXERCISE Integrate the result above to confirm that $\int_\Delta^E d\epsilon\, \rho(\epsilon) \stackrel{E \to \Delta}{\longrightarrow} 2E\nu$. This demonstrates that the excitation density of states is indeed twice as large as that of the quasi-particles.

The phenomenological analysis above explains important aspects of the physics of the BCS superconductor: the instability towards condensation, and the presence of a gap for quasi-particle excitations above the ground state. Indeed, it would be tempting to take the latter phenomenon as an explanation for the absence of electric resistivity below the transition temperature, i.e. if no low-lying quasi-particle excitations are available, should not external current be able to flow through the system without energy dissipation? Yet that picture neglects the most important excitation of the system, i.e. the collective phase mode. Above we made the *ad hoc* decision to set the phase of the order parameter to zero. However, as with the superfluid, the phase represents a Goldstone mode and we must expect its presence to have important consequences. Indeed, it will turn out that the phase mode of the superconductor – in contrast to its counterpart in the "neutral" superfluid – is responsible for much of the electromagnetic phenomena displayed by the superconductor.

INFO The discussion above may convey the impression that the amplitude of the superconducting order parameter is spatially uniform, with a value set by the mean field equation. It is important to realize, however, that there are superconductor species for which $|\Delta|$ exhibits strong fluctuations in space. Since it is the amplitude of the order parameter that determines the size of the quasi-particle gap, fluctuations of $|\Delta|$ lead to important phenomenological consequences, especially if there are regions for which $|\Delta| \to 0$.

Without question the most important class of superconductors with spatially varying order parameters are the **d-wave superconductors**. Firstly, practically all high temperature superconductors belong to this family, i.e. d-wave superconductivity is a field of profound interest from both a fundamental and an applied point of view. Secondly, the physical properties of the d-wave superconductor differ drastically from those of conventional superconductors. The reason is that it is "gapless" in the sense that its Brillouin zone contains four distinct points at which the order parameter vanishes. These "hot spots" are exceptional in that quasi-particles of arbitrarily low energy coexist with the order parameter condensate. The list of many exotic phenomena induced by this coexistence – for a detailed discussion of which we refer to the literature – includes unconventional heat conduction and anomalous Josephson and Meissner effects.

EXERCISE The order parameter of a lattice d-wave superconductor is given by $\Delta_{\mathbf{k}} = \Delta_0(\cos(k_x a) - \cos(k_y a))$, where $\mathbf{k} = (k_x, k_y)^T$ is a two-dimensional lattice momentum and a the lattice spacing.[25] At two lines in momentum space, $k_x = \pm k_y$, the order parameter vanishes and low-energy quasi-particles persist. Assuming that the kinetic energy of the lattice problem is given by $t_{\mathbf{k}} = -t(\cos(k_x a) + \cos(k_y a))$, compute the quasi-particle energies of the Bogoliubov Hamiltonian $\hat{H} = \sum_{\mathbf{k}} \quad {}^{\dagger}_{\mathbf{k}}((t_{\mathbf{k}} - \mu)\sigma_3 + \Delta_{\mathbf{k}}\sigma_1) \quad {}_{\mathbf{k}}$. Show that, at four points in the Brillouin zone,

[25] The origin of the designation "d-wave" is that it transforms like an $l = 2$ angular momentum state (sign change under a 90 rotation) under the action of the rotation group. On the same basis, ordinary superconductors are sometimes called s-wave superconductors. Less frequently occurring are superconductors of p-wave or other angular momentum symmetry.

$\mathbf{k} = (\pm 1, \pm 1)\pi/2a$, the quasi-particle energy vanishes. Linearize the Hamiltonian in momentum space around one of these "hot spots," say $(+1, +1)\pi/2a$, to show that it assumes the form

$$\hat{H}_{++} = \begin{pmatrix} ta(k_x + k_y) & \Delta_0 a(k_x - k_y) \\ \Delta_0 a(k_x - k_y) & -ta(k_x + k_y) \end{pmatrix}.$$

Apply a unitary transformation to bring $\hat{H}_{++}$ to the form of a **two-dimensional Dirac Hamiltonian** $\hat{H}_{++} \to k_1\sigma_1 + k_2\sigma_2$, where $k_{1/2} = k_x \mp k_y$, and we have rescaled $k_1 \to (\Delta_0/t)k_1$ and set $v_{\rm F} = 1$. Show that the quasi-particle density of states of this Hamiltonian is given by $\nu(\epsilon) \sim |\epsilon|$.

From a modern perspective, a comprehensive picture of the superconductor, encompassing the consequences of Goldstone mode formation, and the BCS structures discussed above, is most efficiently developed within the field integral approach. It is to this framework that we now turn.

Superconductivity from the field integral

To investigate the BCS transition within the framework of the coherent state path integral, we start out from a coordinate representation of the BCS Hamiltonian (6.14),

$$\hat{H}_{\rm BCS} = \int d^d r\, c^\dagger_\sigma(\mathbf{r}) \left[\frac{1}{2m}(-i\nabla - e\mathbf{A})^2 + e\phi - \mu\right] c_\sigma(\mathbf{r}) - g\int d^d r\, c^\dagger_\uparrow(\mathbf{r}) c^\dagger_\downarrow(\mathbf{r}) c_\downarrow(\mathbf{r}) c_\uparrow(\mathbf{r}),$$

where, once again, summation over repeated spin indices is implied. Anticipating the emergence of non-trivial electromagnetic phenomena, we have coupled the single-particle Hamiltonian to a vector potential $\mathbf{A}$ and a scalar potential ϕ. The origin and physical consequences of these fields are discussed somewhat later. Expressed in the form of the coherent state path integral, the corresponding quantum partition function takes the form $\mathcal{Z} = \int D(\bar\psi, \psi)\; e^{-S[\bar\psi,\psi]}$,[26]

$$S[\bar\psi, \psi] = \int_0^\beta d\tau \int d^d r \left[\bar\psi_\sigma \left(\partial_\tau + ie\phi + \frac{1}{2m}(-i\nabla - e\mathbf{A})^2 - \mu\right)\psi_\sigma - g\bar\psi_\uparrow\bar\psi_\downarrow\psi_\downarrow\psi_\uparrow\right], \tag{6.22}$$

where $\psi(\mathbf{r}, \tau)$ denote Grassmann fields.

INFO In the field theoretical literature, the substitution

$$\partial_\tau \to \partial_\tau + ie\phi, \quad -i \quad \to -i \quad - e\mathbf{A}, \tag{6.23}$$

is sometimes called a **minimal coupling** of an electromagnetic field. It is "minimal" in the sense that only orbital and potential coupling of the field are taken into account. (For example, the field–spin interaction is neglected.) At the same time, the potential–vector-potential coupling is complete enough to endow the theory with a **local gauge invariance** under U(1) transformations

$$\psi \to e^{i\ }\psi, \quad \bar\psi \to e^{-i\ }\bar\psi, \quad \phi \to \phi - e^{-1}\partial_\tau\theta, \quad \mathbf{A} \to \mathbf{A} + e^{-1}\quad\theta, \tag{6.24}$$

[26] Notice that the Eucilidean character of the imaginary time theory is responsible for the additional factor of "i," i.e. as our ϕ transforms like a time-derivative under Wick rotation, it is given by $(-i) \times$ the conventional scalar potential.

where $\theta = \theta(\tau, \mathbf{x})$ is an arbitrary space/time-dependent phase configuration. The minimal coupling introduces the general quantum electrodynamical gauge principle into the theory. This should be compared with the discussion of the neutral superfluid where only invariance under global U(1) transformations was required.

In the following, we will often use units wherein $e = 1$.

As usual the quartic interaction of the fields prevents the partition function from being evaluated explicitly. Moreover, anticipating the existence of a transition of the electron gas to a condensed phase in which electrons in the vicinity of the Fermi surface are paired, we can expect that a perturbative expansion in the coupling constant g will be inadequate. Motivated by the mean-field theory discussed above, we will instead introduce a bosonic field Δ to decouple the interaction, which will have the physical significance of the order parameter. The decoupling is arranged using a Hubbard–Stratonovich transformation in the Cooper channel (cf. the discussion on page 244)

$$\begin{aligned} &\exp\quad g\int d\tau\, d^d r\, \bar\psi_\uparrow\bar\psi_\downarrow\psi_\downarrow\psi_\uparrow \\ &\qquad = \int D(\bar\Delta,\Delta)\exp\quad -\int d\tau\, d^d r\left[\frac{1}{g}|\Delta|^2 - \left(\bar\Delta\psi_\downarrow\psi_\uparrow + \Delta\bar\psi_\uparrow\bar\psi_\downarrow\right)\right]\quad , \end{aligned}$$

where $\Delta(\mathbf{r},\tau)$ represents a dynamically fluctuating complex field. Reflecting the behavior of the bilinear $\psi_\downarrow\psi_\uparrow$, it obeys the periodic boundary condition, $\Delta(0) = \Delta(\beta)$, i.e. Δ is a bosonic field variable. Were we to take Δ to be homogeneous in space and time, the quantum Hamiltonian corresponding to the action would coincide with that of the mean-field Hamiltonian considered in the previous section. Following that analysis (but not making the *a priori* assumption $\Delta(\mathbf{r},\tau) = \text{const.}$) we turn to the **Nambu spinor** representation

$$\bar\Psi = \begin{pmatrix}\bar\psi_\uparrow & \psi_\downarrow\end{pmatrix}, \qquad \Psi = \begin{pmatrix}\psi_\uparrow \\ \bar\psi_\downarrow\end{pmatrix},$$

comprising particle and hole degrees of freedom in a single object. Expressed in terms of the Nambu spinor, the partition function takes the form

$$\mathcal{Z} = \int D(\bar\psi,\psi)\int D(\bar\Delta,\Delta)\,\exp\quad -\int d\tau\, d^d r\left[\frac{1}{g}|\Delta|^2 - \bar\Psi\hat{\mathcal{G}}^{-1}\Psi\right]\quad ,$$

where

$$\hat{\mathcal{G}}^{-1} = \begin{matrix}\left[\hat G_0^{(\mathrm{p})}\right]^{-1} & \Delta \\ \bar\Delta & \left[\hat G_0^{(\mathrm{h})}\right]^{-1}\end{matrix}\quad , \tag{6.25}$$

is known as the **Gor'kov Green function**, and $[\hat G_0^{(\mathrm{p})}]^{-1} = -\partial_\tau - ie\phi - \frac{1}{2m}(-i\nabla - e\mathbf{A})^2 + \mu$, $[\hat G_0^{(\mathrm{h})}]^{-1} = -\partial_\tau + ie\phi + \frac{1}{2m}(+i\nabla - e\mathbf{A})^2 - \mu$ represent the non-interacting Green functions of the particle and hole respectively.

INFO Computing the -representation of the action for a general single-particle Hamiltonian $\hat H$, one finds that $[\hat G_0^{(\mathrm{p})}]^{-1} = -\partial_\tau - \hat H + \mu$, $[\hat G_0^{(\mathrm{h})}]^{-1} = -\partial_\tau + \hat H^T - \mu$. (With $^T = -$, the expression above is identified as a special case of the more general form.) This representation is

actually very revealing: it tells us that the Green function of a hole is obtained from that of the electron by a sign change $\hat{H} \to -\hat{H}$ (the energy of a hole is the negative of the corresponding particle energy) followed by transposition $-\hat{H} \to -\hat{H}^T$, i.e. a quantum time reversal operation (a hole can be imagined as a particle propagating backwards in time). Noting that $\hat{\mathbf{p}}^T = -\hat{\mathbf{p}}$ and $\hat{\mathbf{x}}^T = \hat{\mathbf{x}}$, the pair of Green functions can equivalently be represented through

$$[\hat{G}_0^{(\mathrm{p})}]^{-1} = -\partial_\tau - \hat{H}(\hat{\mathbf{x}}, \hat{\mathbf{p}}) + \mu, \quad [\hat{G}_0^{(\mathrm{h})}]^{-1} = -\partial_\tau + \hat{H}(\hat{\mathbf{x}}, -\hat{\mathbf{p}}) - \mu. \tag{6.26}$$

Bilinear in Ψ, the Gaussian integration over the Grassmann fields can now be performed straightforwardly, and yields the formal expression (cf. the analogous formula (6.4) for the normal electron system)

$$\mathcal{Z} = \int D(\bar{\Delta}, \Delta)\, \exp\left[-\frac{1}{g}\int d\tau\; d^d r\; |\Delta|^2 + \ln\det \hat{\mathcal{G}}^{-1}\right]. \tag{6.27}$$

By introducing a Hubbard–Stratonovich decoupling of the local interaction, we have succeeded in expressing the quantum partition function as a path integral over an auxiliary bosonic field Δ. Further progress is possible only within some approximation.

Mean-field theory

To identify a suitable "platform" around which the action can be expanded perturbatively, we begin by identifying the mean-field configurations of Δ. A variation of the action with respect to Δ generates the mean-field equation (for the differentiation of the "tr ln" with respect to Δ we refer to the analogous calculation in Eq. (6.5)), $g^{-1}\bar{\Delta}(\tau, \mathbf{x}) - \mathrm{tr}\left[\hat{\mathcal{G}}(\tau, \mathbf{x}; \tau, \mathbf{x}) E_{12}^{\mathrm{ph}}\right] = 0$, where E_{ij}^{ph} is a 2×2 matrix in Nambu space that takes the value of unity at position (i, j) and is zero otherwise. Assuming that configurations extremizing the action will be spatially and temporally homogeneous, i.e $\Delta(\tau, \mathbf{x}) \equiv \Delta_0 = \text{const.}$, and, temporarily ignoring the dependence of the Green function on the field $(\phi, \mathbf{A})$, the equation simplifies to

$$\begin{aligned}
\frac{1}{g}\bar{\Delta}_0 &= \mathrm{tr}\left[\begin{pmatrix} -\partial_\tau + \frac{\nabla^2}{2m} + \mu & \Delta_0 \\ \bar{\Delta}_0 & -\partial_\tau - \frac{\nabla^2}{2m} - \mu \end{pmatrix}^{-1} (\tau, \mathbf{x}; \tau, \mathbf{x}) \begin{pmatrix} 0 & 1 \\ 0 & 0 \end{pmatrix}\right] \\
&= \frac{T}{L^d}\sum_{\mathbf{p}, n} \begin{pmatrix} i\omega_n - \xi_{\mathbf{p}} & \Delta_0 \\ \bar{\Delta}_0 & i\omega_n + \xi_{\mathbf{p}} \end{pmatrix}^{-1}_{21} = \frac{T}{L^d}\sum_{\mathbf{p}, n} \frac{\bar{\Delta}_0}{\omega_n^2 + \xi_{\mathbf{p}}^2 + |\Delta_0|^2},
\end{aligned}$$

where, in the second line, we have switched to a frequency–momentum representation and, as usual, $\xi_{\mathbf{p}} = \mathbf{p}^2/2m - \mu$. Rearranging the equation, we arrive at $\frac{1}{g} = \frac{T}{L^d}\sum_{\mathbf{p}, n} \frac{1}{\omega_n^2 + \lambda_{\mathbf{p}}^2}$, where $\lambda_{\mathbf{p}} = (\xi_{\mathbf{p}}^2 + \Delta_0^2)^{1/2} > 0$ (cf. Eq. (6.18)). The Matsubara summation can be performed by means of the summation techniques discussed on page 170 (see also the problem set of Chapter 4), after which one obtains,

$$\frac{1}{g} = \frac{1}{L^d}\sum_{\mathbf{p}} \frac{1 - 2n_{\mathrm{F}}(\lambda_{\mathbf{p}})}{2\lambda_{\mathbf{p}}} = \int_{-\omega_{\mathrm{D}}}^{\omega_{\mathrm{D}}} d\xi \underbrace{\frac{1}{L^d}\sum_{\mathbf{p}} \delta(\xi - \xi_{\mathbf{p}})}_{\nu(\xi)} \frac{1 - 2n_{\mathrm{F}}(\lambda(\xi))}{2\lambda(\xi)},$$

where we have taken into account the fact that the range of the attractive interaction is limited by $\omega_{\rm D}$. Noting that the integrand is even in ξ, and making use of the identity $1-2n_{\rm F}(\epsilon)=\tanh(\epsilon/2T)$, we arrive at the celebrated **BCS gap equation**

$$\frac{1}{g\nu}=\int_0^{\omega_{\rm D}} d\xi\,\frac{\tanh(\lambda(\xi)/2T)}{\lambda(\xi)}, \tag{6.28}$$

where, as usual, we have assumed that the density of states $\nu(\xi)\simeq\nu$ is specified by its value at the Fermi surface. For temperatures $T\ll\Delta_0$, we may approximate $\tanh(\lambda/2T)\simeq 1$ and we arrive back at the $T=0$ gap equation (6.20) analyzed above. However, here we wish to be more ambitious and explore the fate of the gap as the temperature is increased. Intuitively, one would expect that, for large temperatures, thermal fluctuations will eventually wash out the gap. On the other hand, we know empirically that the onset of superconductivity has the character of a second order phase transition (see Chapter 8). Since the gap parameter Δ_0 has the status of the order parameter of the transition – an identification to be substantiated shortly – we must expect that the vanishing of $\Delta_0(T)$ occurs in a singular manner (in analogy to, e.g., the magnetization of a ferromagnet at the Curie temperature). Indeed, it turns out (see Problem 6.7) that the order parameter vanishes abruptly at the **critical temperature** of the BCS transition,

$$T_{\rm c}=\text{const.}\times\omega_{\rm D}\exp\left[-\frac{1}{g\nu}\right], \tag{6.29}$$

where the numerical constant is $\mathcal{O}(1)$. Notice that this result is consistent with our perturbative analysis above. For temperatures slightly smaller than $T_{\rm c}$ (see Problem 6.7),

$$\Delta_0=\text{const.}\times\sqrt{T_{\rm c}(T_{\rm c}-T)}, \tag{6.30}$$

scales as the square root of $(T_{\rm c}-T)/T_{\rm c}$, i.e. the vanishing occurs with a diverging derivative, as is typical for second-order phase transitions. The interpolated temperature profile of the order parameter is shown in Fig. 6.6. Notice that (again, up to numerical factors) the critical temperature $T_{\rm c}$ coincides with the zero-temperature value of the gap $\Delta_0(0)$. The square-root profile of the gap function has been accurately confirmed by experiment (see Fig. 6.6).

Having explored the large-scale profile of the gap function, we next turn our attention to the vicinity of the superconductor transition, i.e. to temperature regions $\delta T=T_{\rm c}-T\ll T$.

Ginzburg–Landau theory

In the vicinity of the phase transition, the gap parameter Δ is small (in comparison with the temperature). This presents the opportunity to perturbatively expand the action (6.27) in Δ. We will see that the expansion reveals much about the character of the superconducting transition and the nature of the collective excitations. Further, the expansion will make the connection to the neutral superfluid (as well as important differences) explicit.

To keep the structure of the theory as transparent as possible, we will continue to ignore the coupling to the external field. Our task thus reduces to computing the expansion of

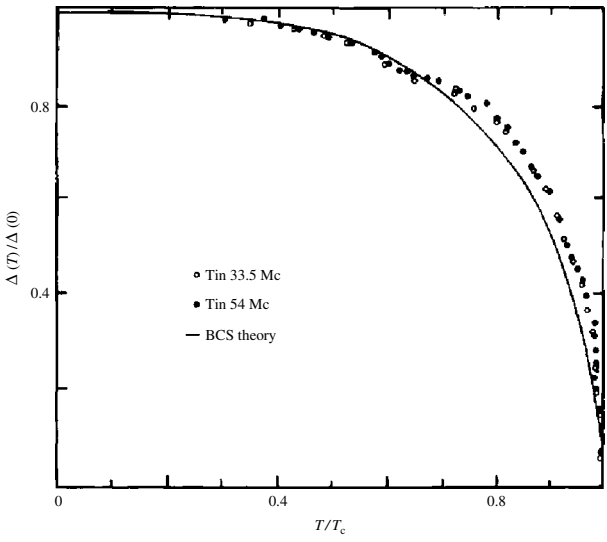

Figure 6.6 Measurements of ultrasonic attenuation in a superconductor provide access to the ratio $\Delta(T)/\Delta(0)$. The data here show the comparison of a tin alloy with the predicted square-root dependence of the mean-field theory. (Reprinted with permission from R. W. Morse and M. V. Bohm, Superconducting energy gap from ultrasonic attenuation measurements, *Phys. Rev.* **108** (1957), 1094–6. Copyright (1957) by the American Physical Society.)

$\mathrm{tr}\ln\hat{\mathcal{G}}^{-1}$ in powers of Δ. To facilitate the expansion, let us formally define $\hat{\mathcal{G}}_0^{-1} \equiv \hat{\mathcal{G}}^{-1}|_{\Delta=0}$, and set $\hat{\Delta} \equiv \begin{pmatrix} & \Delta \\ \bar{\Delta} & \end{pmatrix}$, so that

$$\mathrm{tr}\ln\hat{\mathcal{G}}^{-1} = \mathrm{tr}\ln\left[\hat{\mathcal{G}}_0^{-1}(1+\hat{\mathcal{G}}_0\hat{\Delta})\right] = \underbrace{\mathrm{tr}\ln\hat{\mathcal{G}}_0^{-1}}_{\text{const.}} + \underbrace{\mathrm{tr}\ln[1+\hat{\mathcal{G}}_0\hat{\Delta}]}_{-\sum_{n=0}^{\infty}\frac{1}{2n}\mathrm{tr}(\hat{\mathcal{G}}_0\hat{\Delta})^{2n}}.$$

Here we have used the relation $\mathrm{tr}\ln[\hat{A}\hat{B}] = \mathrm{tr}\ln\hat{A} + \mathrm{tr}\ln\hat{B}$.[27] Further, note that only even contributions in $\hat{\Delta}$ survive. The constant contribution $\mathrm{tr}\ln\hat{\mathcal{G}}_0^{-1}$ recovers the free energy of the non-interacting electron gas and, for present purposes, provides an inessential contribution to the action.

To give this formal expansion some meaning, let us consider the second-order term in more detail. By substituting the explicit form of $\hat{\mathcal{G}}_0^{-1}$ it is straightforward to verify that

$$-\frac{1}{2}\mathrm{tr}\,(\hat{\mathcal{G}}_0\hat{\Delta})^2 = -\mathrm{tr}\,\left([\hat{\mathcal{G}}_0]_{11}\Delta[\hat{\mathcal{G}}_0]_{22}\bar{\Delta}\right) = -\sum_q \underbrace{\frac{T}{L^d}\sum_p [\hat{\mathcal{G}}_{0,p}]_{11}[\hat{\mathcal{G}}_{0,p-q}]_{22}}_{-\frac{T}{L^d}\sum_p G_p G_{-p+q}}\Delta(q)\bar{\Delta}(q),$$

where we have made use of the representation of the composite Green function $\hat{\mathcal{G}}_0$ in terms of the single-particle Green function $G_p^{(\mathrm{p})} = G_p$ and the hole Green function $G_p^{(\mathrm{h})} = -G_{-p}^{(\mathrm{p})} =$

[27] Notice that the relation $\mathrm{tr}\ln[\hat{A}\hat{B}] = \mathrm{tr}\ln\hat{A} + \mathrm{tr}\ln\hat{B}$ applies to non-commutative matrices.

$-G_{-p}$ (cf. Eq. (6.26)). On combining with the first term in Eq. (6.27), we arrive at the quadratic action for the order parameter field,

$$S^{(2)}[\Delta,\bar{\Delta}] = \sum_q \Gamma_q^{-1}|\Delta(q)|^2, \quad \Gamma_q^{-1} = \frac{1}{g} - \frac{T}{L^d}\sum_p G_p G_{-p+q}. \tag{6.31}$$

This is our second encounter with the vertex function Γ_q^{-1}: in our perturbative analysis of the Cooper channel (cf. Eq. (6.15)) we had identified the same expression. To appreciate the connection we should let the dust of our current technical operations settle and revise the general philosophy of the Hubbard–Stratonovich scheme. The field Δ was introduced to decouple an attractive interaction in the Cooper channel. By analogy with the field ϕ used in the development of the RPA approximation to the direct channel, the action of the field $\Delta \sim \bar{\psi}_\uparrow\bar{\psi}_\downarrow$ can be interpreted as the "propagator" of the composite object $\bar{\psi}_\uparrow\bar{\psi}_\downarrow$, i.e. a quadratic contraction $\sim \langle\bar{\Delta}\Delta\rangle$ describes propagation in the Cooper channel $\sim \langle\bar{\psi}_\uparrow\bar{\psi}_\downarrow\psi_\downarrow\psi_\uparrow\rangle$, as described by a four-point correlation function. This connection is made explicit by comparison of the quadratic action with the direct calculation of the Cooper four-point function above.

However, in contrast to our discussion in Section 6.4 (where all we could do was to diagnose an instability as $\Gamma^{-1}_{q=0} \to 0$), we are now in a position to comprehensively explore the consequences of the symmetry breaking. Indeed, $\Gamma^{-1}_{q=0} \to 0$ corresponds to a sign change of the quadratic action of the constant order parameter mode $\Delta(q=0)$. In the vicinity of this point, the constant contribution to the action must scale as $\sim (T - T_c)$ from which one may conclude that the action assumes the form

$$S^{(2)}[\Delta,\bar{\Delta}] = \int d\tau\ d^d r\ \frac{r(T)}{2}|\Delta|^2 + \mathcal{O}(\partial\Delta, \partial_\tau\Delta),$$

where $r(T) \sim T - T_c$ and $\mathcal{O}(\partial\Delta, \partial_\tau\Delta)$ denotes temporal and spatial gradients whose role will be discussed shortly.

EXERCISE Use Eq. (6.16) and the expansion

$$n_{\rm F}(\epsilon,T) - n_{\rm F}(\epsilon,T_c) \simeq (T-T_c)\partial_T\,|_{T=T_c} n_{\rm F}(\epsilon,T) = -\partial\, n_{\rm F}(\epsilon,T_c)(T-T_c)\frac{\epsilon}{T},$$

to show that $r(T) = \nu t$ where $t = \frac{T-T_c}{T_c}$ defines the reduced temperature.

For temperatures below T_c, the quadratic action becomes unstable and – in direct analogy with our previous discussion of the superfluid condensate action – we have to turn to the fourth-order contribution, $S^{(4)}$, to ensure stability of the functional integral (see the figure below where the upper/lower surface corresponds to temperatures above/below the transition). At orders $n > 2$ of the expansion, spatial and temporal gradients can be safely

neglected (due to the smallness of $\Delta \ll T$, they will certainly be smaller than the gradient contributions to $S^{(2)}$). For $\Delta = \text{const.}$, it is straightforward to verify that

$$\begin{aligned} S^{(2n)} &= \frac{1}{2n}\mathrm{tr}\,(\hat{\mathcal{G}}_0\hat{\Delta})^{2n} = \frac{(-)^n}{2n}\sum_p \left(G_p G_{-p}\right)^n |\Delta|^{2n} \simeq \frac{\nu|\Delta|^{2n}}{2n}\sum_{\omega_l}\int_{-\omega_\mathrm{D}}^{\omega_\mathrm{D}} \frac{d\xi}{(\omega_l^2+\xi^2)^n} \\ &= \text{const.} \times \nu|\Delta|^{2n}\sum_{\omega_l}\frac{1}{\omega_l^{2n-1}} = \text{const.} \times \nu T\left(\frac{|\Delta|}{T}\right)^{2n}, \end{aligned}$$

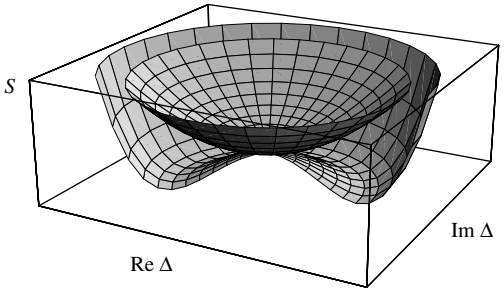

where "const." denotes only numerical constant factors. Once again, in the second equality, we have expressed the Gor'kov Green function through the respective particle and hole Green functions, and in the fourth equality we have noticed that, for $\omega_\mathrm{D} \gg T$, the integral over the energy variable is dominated by the infrared divergence at small ξ, i.e. $\int_0^{\omega_\mathrm{D}} d\xi\ (\omega_l^2+\xi^2)^{-n} \simeq \int_{\omega_l}^{\infty} d\xi\ \xi^{-2n}$. This estimate tells us that the contributions of higher order to the expansion are (i) positive and (ii) small in the parameter $|\Delta|/T \ll 1$. This being so, it is sufficient to retain only the fourth-order term (to counterbalance the unstable second-order term). We thus arrive at the effective action for the order parameter,

$$S[\Delta,\bar{\Delta}] = \int d\tau\ d^d r \left(\frac{r(T)}{2}\bar{\Delta}\Delta + u(\Delta\bar{\Delta})^2 + \mathcal{O}(\partial\Delta, \partial_\tau\Delta, |\Delta|^6)\right), \tag{6.32}$$

valid in the vicinity of the transition.[28] In particular, one may note (see the figure above) that the dependence of the action on (a constant) Δ mimics closely that of the condensate amplitude.

INFO It is straightforward to include finite spatial gradients in the derivation of the quadratic action $S^{(2)}$ (for details see Problem 6.7). The resulting action for static but spatially fluctuating configurations $\Delta(\mathbf{r})$ takes the form

$$\boxed{S_\mathrm{GL}[\Delta,\bar{\Delta}] = \beta\int d^d r \left[\frac{r}{2}|\Delta|^2 + \frac{c}{2}|\partial\Delta|^2 + u|\Delta|^4\right],} \tag{6.33}$$

where $c \sim \rho_0(v_\mathrm{F}/T)^2$. This result is known as the **(classical) Ginzburg–Landau action** of the superconductor. It is termed "classical" because (cf. our remarks on page 255) temporal fluctuations of Δ have been ignored. Notice that the form of the action might have been anticipated on symmetry grounds alone. Indeed, Eq. (6.33) was proposed by Ginzburg and Landau as an effective action for superconductivity some years before the advent of the microscopic theory.[29]

[28] Here, the coupling constant $u \sim \rho T^{-3}$ shows only a weak temperature dependence in the vicinity of the transition.

[29] V. L. Ginzburg and L. D. Landau, On the theory of superconductivity, *Zh. Eksp. Teor. Fiz.* **20** (1950), 1064–82.

A generalization of the action to include temporal fluctuations leads to the **time-dependent Ginzburg–Landau theory**, to be discussed below.

Equation (6.32) makes the connection between the superconductor and superfluid explicit (cf. the condensate action (6.9)). Above T_c, $r > 0$ and the unique mean-field configuration extremizing the action (6.32) is given by $\Delta = 0$. However, below the critical temperature, $r < 0$ and a configuration with non-vanishing Cooper pair amplitude Δ_0 is energetically favorable:

$$\left.\frac{\delta S[\Delta,\bar{\Delta}]}{\delta\Delta}\right|_{\Delta=\Delta_0} = 0 \Rightarrow \bar{\Delta}_0\left(\frac{r}{2} + 2u|\Delta_0|^2\right) = 0 \Rightarrow |\Delta_0| = \sqrt{\frac{-r}{4u}} \sim \sqrt{T_c(T_c - T)},$$

cf. the previous estimate Eq. (6.30). As with the superfluid, the mean-field equation determines only the modulus of the order parameter while the phase remains unspecified. Below the transition, the symmetry of the action will be broken by the formation of a ground state with fixed global phase, e.g. $\Delta_0 \in \mathbb{R}$. This entails the formation of a phase-like Goldstone mode θ, where configurations $\Delta = e^{2i\theta}\Delta_0$ explore deviations from the reference ground-state.[30] Pursuing further the parallels with the superfluid, it would be tempting to conjecture that these phase fluctuations have a linear dispersion, i.e. that the system supports dissipationless supercurrents of charged particles: superconductivity.

However, at this point, we have overstretched the analogies to our previous discussion. In fact, the argument above ignores the fact that the symmetry broken by the ground state of the superfluid was a global phase U(1). However, as explained on page 276, the microscopic action of the superconductor possesses a more structured local gauge U(1) symmetry. As we will discuss presently, this difference implies drastic phenomenological consequences.

Action of the Goldstone mode

The ramifications of the local gauge symmetry can only be explored in conjunction with the electromagnetic field $(\phi, \mathbf{A})$. We must, therefore, return to the ancestor action (6.27) where $\mathcal{G}$ now represents the full Gor'kov Green function (6.25). For the present, there is no need to specify the origin of the electromagnetic field; it might represent an external experimental probe, or the background electromagnetic field controlled by the vacuum action, i.e. $S_{\text{E.M.}} = \frac{1}{4}\int d\tau\ d^dr\, F_{\mu\nu}F_{\mu\nu}$, where $F_{\mu\nu} = \partial_\mu A_\nu - \partial_\nu A_\mu$ is the electromagnetic field tensor.[31] However, throughout, we will assume that the field is weak enough not to destroy the superconductivity, i.e. the mean modulus of the order parameter is still given by the value Δ_0, as described by the analysis of the previous section.

How, then, might an action describing the interplay of the phase degree of freedom and the electromagnetic field look? Below we will derive such an action explicitly by starting from the prototype Eq. (6.27). However, for the moment, let us stay on a less rigorous level

[30] The motivation for transforming by 2θ is that, under a gauge transformation $\bar{\psi} \to e^{i}\ \bar{\psi}$, the composite field $\Delta \sim \bar{\psi}\bar{\psi}$ should acquire *two* phase factors. However, the introduction of that muliplicity factor is, of course, just a matter of convention; it can always be removed by a rescaling of the field θ.

[31] Notice that we are working within the framework of imaginary (Euclidean) time field theory, i.e. the definition of the field strength tensor does not involve the Minkowski metric (cf. the discussion on page 107).

and try to determine the structure of the action by symmetry reasoning. In doing so, we will be guided by a number of principles:

- ▷ The phase θ is a Goldstone mode, i.e. the action cannot contain terms that do not vanish in the limit $\theta \to$ const.
- ▷ We will assume that gradients acting on the phase θ (but not necessarily the magnitude of the phase) and the electromagnetic potentials are small. That is, we will be content with determining the structure of the action to lowest order in these quantities.
- ▷ By symmetry, the action must not contain terms with an odd number of derivatives or mixed gradients of the type $\partial_\tau \theta \nabla \theta$. Respecting the character of the microscopic model, the action must be rotationally invariant.
- ▷ The action must be invariant under the local gauge transformation Eq. (6.24).

It may be confirmed that the first three criteria would be satisfied by the trial action

$$S[\theta] = \int d\tau d^d r \ \left[c_1 (\partial_\tau \theta)^2 + c_2 (\nabla \theta)^2 \right],$$

where c_1 and c_2 are constants. However, such an action is clearly not invariant under a gauge shift of the phase, $\theta(\tau, \mathbf{r}) \to \theta(\tau, \mathbf{r}) + \varphi(\tau, \mathbf{r})$. It can, however, be endowed with that quality by minimal substitution of the electromagnetic potential, i.e.[32]

$$\boxed{S[\theta, A] = \int d\tau \ d^d r \left[c_1 (\partial_\tau \theta + \phi)^2 + c_2 (\nabla \theta - \mathbf{A})^2 \right].} \tag{6.34}$$

To second order in gradients, this action uniquely describes the energy cost associated with phase fluctuations. When combined with the action $S_{\text{E.M.}}$ controlling fluctuations of the field $(\phi, \mathbf{A})$, it should provide a general description of the low-energy electromagnetic properties of the superconductor. Notice, however, that the present line of argument does not fix the coupling constants $c_{1,2}$. In particular, one cannot exclude the possibility that c_1 or c_2 vanishes (as would be the case, for example, in a non-superconducting system, cf. the problem set). To determine the values of $c_{1,2}$, we need either to derive the action microscopically or to invoke further phenomenological input (see the Info block below). Either way one obtains $c_2 = n_{\text{s}}/2m$ and $c_1 = \nu$, where we have defined n_{s} as the density of the Cooper pair condensate. (For a precise definition, see below.) In the following section we use the action (6.34) as a starting point to discuss the characteristic and remarkable electromagnetic phenomena displayed by superconductors.

INFO Beginning with coefficient c_2, let us briefly discuss the **phenomenological derivation** of the coupling constants. The starting point is the observation that the functional derivative, $\langle \frac{\delta S}{\delta \mathbf{A}(\tau, \mathbf{r})} \rangle = \langle \mathbf{j}(\tau, \mathbf{r}) \rangle$, generates the expectation value of the current density operator. This relation follows quite generally from the fact that a vector potential couples to the action of a system of charged particles $i = 1, \ldots, N$ through the relation

$$S_{\mathbf{A}} \equiv \int d\tau \sum_i \mathbf{r}_i \cdot \mathbf{A}(\mathbf{r}_i) = \int d\tau d^d r \sum_i \delta(\mathbf{r} - \mathbf{r}_i) \mathbf{r}_i \cdot \mathbf{A}(\tau, \mathbf{r}).$$

[32] To keep the notation simple, we will henceforth set $e = 1$.

However, $\mathbf{j} = \frac{\delta S}{\delta A(\tau,\mathbf{r})} = \sum_i \delta(\mathbf{r} - \mathbf{r}_i(\tau))\mathbf{r}_i(\tau)$ is just the definition of the total particle current density. Indeed, it is straightforward to verify that, on the microscopic level (cf., e.g., Eq. (6.22)),

$$\left\langle \frac{\delta S}{\delta \mathbf{A}} \right\rangle = -\frac{e}{2m} \left\langle \bar{\psi}_\sigma(-i \quad - \mathbf{A})\psi_\sigma + [(i \quad - \mathbf{A})\bar{\psi}_\sigma]\psi_\sigma \right\rangle \equiv \langle \mathbf{j} \rangle,$$

where $\mathbf{j}$ is the quantum current density operator. Staying for a moment on the microscopic side of the theory, let us assume that a certain fraction of the formerly uncorrelated electronic states participate in the condensate, i.e. one may write $\mathbf{j} = \mathbf{j}_{\rm n} + \mathbf{j}_{\rm s}$, where $\mathbf{j}_{\rm n}$, the current carried by the normal states of the system, will not be of further concern to us, while $\mathbf{j}_{\rm s}$ is the "supercurrent" carried by the condensate. Let us further assume that those states $\psi^{\rm s}$ participating in the condensate carry a collective' phase θ with a non-vanishing average, i.e. $\psi^{\rm s} = e^{i \ \theta}\psi^{\rm s}$, where the states $\psi^{\rm s}$ do not carry any structured phase information (the residual phase carried by the local amplitude $\psi^{\rm s}$ tends, on average, to zero). Then, concentrating on the phase information carried by the condensate and neglecting density fluctuations,

$$\left\langle \frac{\delta S}{\delta \mathbf{A}} \right\rangle \simeq \langle \mathbf{j}^{\rm s} \rangle \simeq -\frac{n_{\rm s}}{m} \langle \quad \theta - \mathbf{A} \rangle \,,$$

where $n_{\rm s} \equiv \bar{\psi}^{\rm s}\psi^{\rm s}$ is the density of the condensate.

Now, let us evaluate the fundamental relation $\left\langle \frac{\delta S}{\delta \mathbf{A}} \right\rangle = \langle \mathbf{j} \rangle$ on our trial action with its undetermined coupling constants:

$$\langle \mathbf{j} \rangle \stackrel{!}{=} \left\langle \frac{\delta S[A]}{\delta A} \right\rangle = -2c_2 \langle \quad \theta - \mathbf{A} \rangle.$$

Comparison with the phenomenological estimate for the expectation value of the (super)current operator above leads to the identification $c_2 = n_{\rm s}/2m$. Turning to the coupling constant c_1, let us assume that the electron system has been subjected to a weak external potential perturbation $\phi(\tau, \mathbf{r})$. Assuming that the potential fluctuates slowly enough to allow an adiabatic adjustment of the electron density (i.e. that it acts as a local modulation of the chemical potential), the particle density of the system would vary as

$$\delta n(\tau, \mathbf{r}) = \delta n(\mu + \phi(\tau, \mathbf{r})) \approx \frac{\partial n}{\partial \mu}\phi(\tau, \mathbf{r}) \approx \nu\phi(\tau, \mathbf{r}),$$

where we have approximately[33] identified $\partial_\mu n$ with the single-particle density of states ν. The potential energy corresponding to the charge modulation is given by $\int d^d r \ \phi(\tau, \mathbf{r})\delta n(\tau, \mathbf{r}) = \partial_\mu n \int d^d r \ \phi^2(\tau, \mathbf{r})$. Comparing this expression with our trial action – which contains the time-integrated potential – we conclude that $c_1 = \partial_\mu n = \nu$.

Despite the integrity of the phenomenological arguments given above, some may feel ill at ease with all the liberal distribution of "assumes." To complement this discussion, let us now recover the phase action using an explicit **microscopic derivation**. The construction detailed below represents a typical yet, until now, our most advanced "case study" of a low-energy quantum field theory. Although formulated for the specific example of the BCS superconductor, many of its structural sub-units appear in other applications in basically the same form. This "universality" is our prime motivation for presenting the lengthy construction of the low-energy phase action of

[33] For systems with strong inter-particle correlations, the **thermodynamic density of states** $\partial_\mu n = \frac{1}{L^d}\partial_\mu N$ may deviate significantly from the **single-particle density of states** $\nu = \frac{1}{L^d}\sum_a \delta(\epsilon_a - \mu)$.

the superconductor in some detail. Our starting point is the Gor'kov Green function appearing under the "tr ln" of the microscopic action (6.27),

$$\hat{\mathcal{G}}^{-1} = \begin{pmatrix} -\partial_\tau - i\phi - \frac{1}{2m}(-i \quad - \mathbf{A})^2 + \mu & \Delta_0 e^{2i} \\ \Delta_0 e^{-2i} & -\partial_\tau + i\phi + \frac{1}{2m}(-i \quad - \mathbf{A})^2 - \mu \end{pmatrix},$$

coupled to the full electromagnetic potential. To simplify the analysis, we have set the modulus of the order parameter to its constant mean-field value Δ_0, i.e. concentrating on the Goldstone mode, we will neglect massive fluctuations $\Delta = \Delta_0 + \delta\Delta$ around the extremum of the free energy.

We next make use of the gauge freedom inherent in the theory to remove the phase dependence of the order parameter field. To do so, we introduce the unitary matrix $\hat{U} \equiv \begin{smallmatrix} e^{-i} & \\ & e^{i} \end{smallmatrix}$, and transform the Green function as

$$\hat{\mathcal{G}}^{-1} \quad \to \quad \hat{U}\hat{\mathcal{G}}^{-1}\hat{U}^\dagger = \begin{pmatrix} -\partial_\tau - i\phi - \frac{1}{2m}(-i \quad - \mathbf{A})^2 + \mu & \Delta_0 \\ \Delta_0 & -\partial_\tau + i\phi + \frac{1}{2m}(-i \quad - \mathbf{A})^2 - \mu \end{pmatrix},$$

where the transformed electromagnetic potential is given by (exercise) $\phi = \phi + \partial_\tau\theta$, $\mathbf{A} = \mathbf{A} - \quad \theta$. (Reading the transformation in reverse, we conclude that – an important physical fact that should be remembered – *the superconductor order parameter field is a gauge non-invariant quantity.* Under gauge transformations it transforms as $\Delta \to e^{2i}\,\Delta$, as suggested by the definition of $\Delta \sim \bar{\psi}\,\bar{\psi}$ as a pairing field. This fact implies that the order parameter itself cannot be an experimentally accessible observable.[34]) Owing to the unitary invariance of the trace, $\mathrm{tr}\ln\hat{\mathcal{G}}^{-1} = \mathrm{tr}\ln(\hat{U}\hat{\mathcal{G}}^{-1}\hat{U}^\dagger)$, the gauge transformed and the original Green function, respectively, equivalently represent the theory.

Save for the neglect of massive fluctuations $\delta\Delta$, our treatment of the theory thus far has been exact. However, to make further progress, we must resort to some approximations: assuming that both the electromagnetic potential and spatio-temporal fluctuations of the phase mode are small, let us expand the action in powers of $(\phi, \mathbf{A})$. In the literature, expansions of this type are known as **gradient expansions**, i.e. we are performing an expansion where the gradients $\partial_\tau\theta$, θ and not the phase degree of freedom θ are assumed to be small. (Owing to its Goldstone mode character, θ can slide freely over the entire interval $[0, 2\pi]$.)

To facilitate the expansion, it will be useful to represent the 2×2 matrix structure of the Green function through a Pauli matrix expansion:

$$\begin{aligned} \hat{\mathcal{G}}^{-1} &= -\sigma_0\partial_\tau - \sigma_3\left(i\phi + \frac{1}{2m}(-i \quad - \mathbf{A}\sigma_3)^2 - \mu\right) + \sigma_1\Delta_0 \\ &= \underbrace{-\sigma_0\partial_\tau - \sigma_3\left(-\frac{1}{2m} \quad ^2 - \mu\right) + \sigma_1\Delta_0}_{\hat{\mathcal{G}}_0^{-1}} \underbrace{- i\sigma_3\phi + \frac{i}{2m}\sigma_0[\quad, \mathbf{A}]_+}_{\hat{\mathcal{X}}_1} \underbrace{- \sigma_3\frac{1}{2m}\mathbf{A}^2}_{\hat{\mathcal{X}}_2}, \end{aligned}$$

where we have defined $\sigma_0 \equiv \mathbf{1}$ as the unit matrix. Expressed in terms of these quantities, the expansion of the action to second order in the field A takes the form

$$\begin{aligned} S[A] &= -\mathrm{tr}\ln\ \hat{\mathcal{G}}_0^{-1} - \hat{\mathcal{X}}_1 - \hat{\mathcal{X}}_2\ = \text{const.} - \mathrm{tr}\ln\ 1 - \hat{\mathcal{G}}_0[\hat{\mathcal{X}}_1 + \hat{\mathcal{X}}_2] \\ &= \text{const.} + \underbrace{\mathrm{tr}\ \hat{\mathcal{G}}_0\hat{\mathcal{X}}_1}_{S^{(1)}[A]} + \underbrace{\mathrm{tr}\left(\hat{\mathcal{G}}_0\hat{\mathcal{X}}_2 + \frac{1}{2}\hat{\mathcal{G}}_0\hat{\mathcal{X}}_1\mathcal{G}_0\hat{\mathcal{X}}_1\right)}_{S^{(2)}[A]} + \cdots, \end{aligned} \tag{6.35}$$

[34] This follows from the fundamental doctrine of electrodynamics that gauge transformations must not cause observable effects.

where we have used the fact that $\hat{\mathcal{X}}_{1,2}$ are of first and second order in the field, respectively. (Structures of this type appear frequently in the construction of low-energy quantum field theories of many-body systems, i.e., after the introduction of some auxiliary field ϕ through a suitably devised Hubbard–Stratonovich transformation, the microscopic Bose/Fermi degrees of freedom of the theory can be integrated out and one arrives at an action $\pm\mathrm{tr}\ln(\hat{\mathcal{G}}_0^{-1}+\hat{X}[\phi])$, where $\hat{\mathcal{G}}$ is the non-interacting Green function of the problem and $\hat{X}[\phi]$ is an operator depending on the new field. An expansion of the logarithm to first and second orders in $\hat{X}$ then leads to structures similar to those given above.)

Written more explicitly, the first-order action $S^{(1)}$ takes the form (exercise)

$$S^{(1)}[A]=\frac{T}{L^d}\sum_p \mathrm{tr}\left[\hat{\mathcal{G}}_{0,p}\hat{\mathcal{X}}_1(p,p)\right]=\frac{T}{L^d}\sum_p \mathrm{tr}\left[\hat{\mathcal{G}}_{0,p}\left(i\sigma_3\phi_0+\frac{i}{m}\sigma_0\mathbf{p}\cdot\mathbf{A}_0\right)\right],$$

where the subscripts 0 refer to the zero-momentum components of the fields ϕ and $\mathbf{A}$. Since the Green function $\hat{\mathcal{G}}_0$ is even in the momentum, the second contribution $\propto\mathbf{p}$ vanishes by symmetry. Further $(\partial_\tau\theta)_0=0\cdot\theta_0=0$, i.e. $\phi_0=\phi_0$ and $S^{(1)}[A]=\frac{iT}{L^d}\sum_p\ [\hat{\mathcal{G}}_{0,p}]_{11}-[\hat{\mathcal{G}}_{0,p}]_{22}\ \ \phi_0$, where the indices refer to particle–hole space. To understand the meaning of this expression, notice that $[\hat{\mathcal{G}}_{0,p}]_{11}=\langle\bar{\psi}_{,p}\psi_{,p}\rangle_0$ gives the expectation value of the spin-up electron density operator on the background of a fixed-order parameter background. Similarly, $-[\hat{\mathcal{G}}_{0,p}]_{22}=-\langle\psi_{,p}\bar{\psi}_{,p}\rangle_0=+\langle\bar{\psi}_{,p}\psi_{,p}\rangle_0$ gives the spin-down density. Summation over frequencies and momenta recovers the full electron density: $\frac{T}{L^d}\sum_p([\hat{\mathcal{G}}_{0,p}]_{11}-[\hat{\mathcal{G}}_{0,p}]_{22})=\frac{N}{L^d}$, or

$$S^{(1)}[A]=iN\phi_0=\frac{iN}{L^d}\int d\tau\, d^dr\,\phi(\tau,\mathbf{r}).$$

Thus, the first contribution to our action simply describes the electrostatic coupling of the scalar potential to the total charge of the electron system. However, as with the Coulomb potential discussed earlier, the "correct" interpretation of this expression should rather suggest $S^{(1)}=0$. That is, the total electrostatic interaction of the potential with the electron system must be – by the overall charge neutrality of the system – compensated by an equally strong interaction with the positive counter charge of the ions (usually excluded for notational convenience).

We thus turn to the discussion of the second-order contribution to the action $S^{(2)}$. The term containing $\hat{\mathcal{X}}_2$ is reminiscent in structure to the $S^{(1)}$ contribution discussed before. Thus, replacing $\hat{\mathcal{X}}_1$ by $\hat{\mathcal{X}}_2$, we may immediately infer that

$$\mathrm{tr}(\hat{\mathcal{G}}_0\hat{\mathcal{X}}_2)=\frac{n}{2m}\int d\tau\int d^dr\,\mathbf{A}^2(\tau,\mathbf{r}),\tag{6.36}$$

where we have defined as $n\equiv N/L^d$ the total particle density. This contribution, known as the **diamagnetic term**, derives from the familiar diamagnetic contribution $\frac{1}{2m}\mathbf{A}^2$ to the electron Hamiltonian. If it were only the diamagnetic contribution, an external field would lead to an increase of the energy. However, to obtain the complete picture, we need to include the magnetic field dependence of the operator $\hat{\mathcal{X}}_1$.

Substituting for $\hat{\mathcal{X}}_1$, and noting that crossterms $\sim\phi\,\mathbf{p}\cdot\mathbf{A}$, being odd in momenta, vanish on integration, one obtains

$$\frac{1}{2}\mathrm{tr}\ \ \hat{\mathcal{G}}_0\hat{\mathcal{X}}_1\hat{\mathcal{G}}_0\hat{\mathcal{X}}_1\ \ =\frac{T}{2L^d}\sum_{p,q}\mathrm{tr}\left(-\hat{\mathcal{G}}_{0,p}\sigma_3\phi_q\hat{\mathcal{G}}_{0,p}\sigma_3\phi_{-q}+\frac{1}{m^2}\hat{\mathcal{G}}_{0,p}\sigma_0\mathbf{p}\cdot\mathbf{A}_q\hat{\mathcal{G}}_{0,p}\sigma_0\mathbf{p}\cdot\mathbf{A}_{-q}\right).$$

Here, noting that we are already working at the second order of the expansion, the residual dependence of the Green functions $\hat{\mathcal{G}}_0$ on the small momentum variable q has been neglected.[35] Alluding to its origin, i.e. the paramagnetic operator $\sim \frac{1}{2m}[\mathbf{p},\mathbf{A}]_+$ of the electron Hamiltonian, the magnetic contribution to this expression is called the **paramagnetic term**. Paramagnetic contributions to the action describe a lowering of the energy in response to external magnetic fields, i.e. the diamagnetic and the paramagnetic term act in competition.

To proceed, it is convenient to change from an explicit matrix representation of the Gor'kov Green function to an expansion in terms of Pauli matrices:[36]

$$\hat{\mathcal{G}}_{0,p} = \left[i\sigma_0\omega_n - \sigma_3\xi_{\mathbf{p}} + \sigma_1\Delta_0\right]^{-1} = \frac{1}{\omega_n^2+\xi_{\mathbf{p}}^2+\Delta_0^2}\left[-i\sigma_0\omega_n - \sigma_3\xi_{\mathbf{p}} + \sigma_1\Delta_0\right]. \tag{6.37}$$

On substituting into the equation above, noting that, for any rotationally invariant function $F(\mathbf{p}^2)$ (exercise), $\sum_{\mathbf{p}}(\mathbf{p}\cdot\mathbf{v})\,(\mathbf{p}\cdot\mathbf{v}')F(\mathbf{p}^2) = \frac{\mathbf{v}\cdot\mathbf{v}'}{d}\sum_{\mathbf{p}}\mathbf{p}^2F(\mathbf{p}^2)$, one obtains

$$\begin{aligned}&\frac{1}{2}\,\mathrm{tr}\;\;\hat{\mathcal{G}}_0\hat{\mathcal{X}}_1\hat{\mathcal{G}}_0\hat{\mathcal{X}}_1\\ &\quad= \frac{T}{L^d}\sum_{p,q}\frac{1}{(\omega_n^2+\lambda_{\mathbf{p}}^2)^2}\left(\phi_q\phi_{-q}(-\omega_n^2+\lambda_{\mathbf{p}}^2-2\Delta_0^2) - \frac{\mathbf{p}^2\mathbf{A}_q\cdot\mathbf{A}_{-q}}{3m^2}(-\omega_n^2+\lambda_{\mathbf{p}}^2)\right),\end{aligned}$$

where, as before, $\lambda_{\mathbf{p}}^2 = \xi_{\mathbf{p}}^2+\Delta_0^2$. We now substitute this result together with the diamagnetic contribution Eq. (6.36) back into the expansion (6.35), partially transform back to real space $\sum_q f_q f_{-q} = \int d\tau\; d^dr\; f^2(\tau,\mathbf{r})^2$, and arrive at the action

$$\begin{aligned}S[A] \;\;=\;\; \int d\tau\; d^dr\Big[&\underbrace{\frac{T}{L^d}\sum_p\frac{-\omega_n^2+\lambda_{\mathbf{p}}^2-2\Delta_0^2}{(\omega_n^2+\lambda_{\mathbf{p}}^2)^2}}_{c_1}\phi^2(\tau,\mathbf{r})\\ &+\underbrace{\left(\frac{n}{2m}-\frac{1}{dm^2}\frac{T}{L^d}\sum_p\frac{\mathbf{p}^2(-\omega_n^2+\lambda_{\mathbf{p}}^2)}{(\omega_n^2+\lambda_{\mathbf{p}}^2)^2}\right)}_{c_2}\mathbf{A}^2(\tau,\mathbf{r})\Big].\end{aligned}$$

This intermediate result identifies the coupling constants $c_{1,2}$. The last step of the derivation, i.e. the sum over the "fast" momenta p, is now a relatively straightforward exercise. Beginning with the frequency summations, one may note that the denominator has two isolated poles of second order at $\omega_n = \pm i\lambda_{\mathbf{p}}$. Applying the standard summation rules it is then straightforward to verify that (exercise)

$$\begin{aligned}&T\sum_n\frac{-\omega_n^2+\lambda_{\mathbf{p}}^2-2\Delta_0^2}{(\omega_n^2+\lambda_{\mathbf{p}}^2)^2} = -\frac{1}{2\lambda_{\mathbf{p}}}\left(n_{\mathrm{F}}(-\lambda_{\mathbf{p}})\left(\frac{\Delta_0}{\lambda_{\mathbf{p}}}\right)^2 + n_{\mathrm{F}}'(-\lambda_{\mathbf{p}})\frac{\xi_{\mathbf{p}}^2}{\lambda_{\mathbf{p}}}\right) + (\lambda_{\mathbf{p}} \quad -\lambda_{\mathbf{p}}) \approx -\frac{\Delta_0^2}{2\lambda_{\mathbf{p}}^3},\\ &T\sum_n\frac{-\omega_n^2+\lambda_{\mathbf{p}}^2}{(\omega_n^2+\lambda_{\mathbf{p}}^2)^2} = -\beta[n_{\mathrm{F}}(\lambda_{\mathbf{p}})(1-n_{\mathrm{F}}(\lambda_{\mathbf{p}})].\end{aligned}$$

[35] i.e. we have set $\sum_{pq}(\hat{\mathcal{G}}_p\tilde{\phi}_q\hat{\mathcal{G}}_{p+q}\tilde{\phi}_{-q}) \approx \sum_{pq}(\hat{\mathcal{G}}_p\tilde{\phi}_q\hat{\mathcal{G}}_p\tilde{\phi}_{-q})$.

[36] In working with matrix operators it is useful to keep in mind the matrix identity $[v_0\sigma_0+\mathbf{v}\cdot\sigma]^{-1} = \frac{1}{v_0^2-\mathbf{v}^2}[v_0\sigma_0-\mathbf{v}\cdot\sigma]$, where $v=(v_0,\mathbf{v})$ is a four-component vector of coefficients. Other useful identities include $(i,j=1,2,3;\mu,\nu=1,2,3,4)$ $\sigma_i^2=1, i\neq j,\ [\sigma_i,\sigma_j]_+=0,\ \sigma_i\sigma_j = i\epsilon^{ijk}\sigma_k, \mathrm{tr}\,\sigma_\mu = 2\delta_{\mu,0}$.

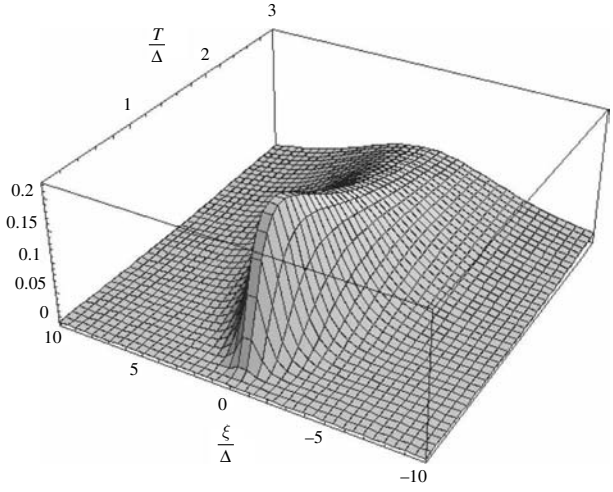

Figure 6.7 Plot of the function $\beta n_{\rm F}(\sqrt{\xi^2+\Delta_0^2})\left[1-n_{\rm F}(\sqrt{\xi^2+\Delta_0^2})\right]$ as a function of the dimensionless scales T/Δ_0 and ξ/Δ_0. For $T/\Delta_0 \to 0$, the function vanishes ($\to$ perfect diamagnetic response). For $\frac{T}{\Delta} \gg 1$, the function traces out a peak of width $\propto T$ and total weight $\int dn(1-n) = 1$ ($\to$ cancellation of diamagnetic and paramagnetic response). At intermediate temperatures, $\int dn(1-n) < 1$, resulting in a partial survival of diamagnetism.

Thus, one obtains the coupling constant of the **potential contribution**,

$$c_1 = -\frac{1}{2L^d}\sum_{\mathbf{p}} \frac{\Delta_0^2}{\lambda_{\mathbf{p}}^3} = -\frac{\nu}{2}\int d\xi \ \frac{\Delta_0^2}{(\xi^2+\Delta_0^2)^{3/2}} = -\nu,$$

in accord with the previous estimate. With the **magnetic contribution**, the situation is more interesting. Converting the momentum sum to an energy integral, one obtains

$$c_2 = \frac{n}{2m} + \frac{\nu\mu}{dm}\int d\xi\, \beta[n_{\rm F}(\lambda)(1-n_{\rm F}(\lambda)],$$

where we have noted that the integrand is strongly peaked at the Fermi surface, i.e. that the factor $\mathbf{p}^2 \approx 2m\mu$ can be removed from under the integral.

This expression illustrates the competition between the diamagnetic and paramagnetic contributions in the magnetic response of the system. At low temperatures, $T \ll \Delta_0$, the positivity of $\lambda_{\mathbf{p}} = (\Delta_0^2+\xi_{\mathbf{p}}^2)^{1/2} \geq \Delta_0$ implies that $n_{\rm F}(\lambda_{\mathbf{p}}) \approx 0$, i.e. approximate vanishing of the integral (see Fig. 6.7). Under these conditions, $c_2 \overset{T\ll\Delta_0}{\approx} \frac{n}{2m}$ is weighted by the total density of the electron gas, and the response of the system is governed by the diamagnetic term alone. Indeed, the diamagnetic response is known to be a hallmark of superconductivity; the superconductor tends to expel magnetic fields, a phenomenon that culminates in the Meissner effect to be discussed shortly.

By contrast, for high temperatures, $T \gg \Delta_0$, the integral extends over energy domains much larger than Δ_0 and we can approximate

$$-\int d\xi\, \beta[n_{\rm F}(\lambda)(1-n_{\rm F}(\lambda)] \approx -\int_0^\infty d\xi\, \beta[n_{\rm F}(\xi)(1-n_{\rm F}(\xi)] = -\int_0^\infty d\xi\; \partial_\xi n_{\rm F}(\xi) = n_{\rm F}(0) - n_{\rm F}(\infty) = 1,$$

to obtain[37] $c_2 \overset{T}{\approx}{}^{\Delta} \frac{n}{2m} - \frac{\mu}{dm} = 0$. The near[38] cancellation of dia- and paramagnetic contributions is typical for the response of normal conducting systems to external magnetic fields.

At intermediate temperatures, the integral over the Fermi functions leads to a partial cancellation of the diamagnetic response. It is common to express that fact through the notation $c_2 = \frac{n_{\rm s}}{2m}$, where the parameter

$$n_{\rm s} \equiv n + \frac{2\nu\mu}{d} \int d\xi\, \beta[n_{\rm F}(\lambda)(1-n_{\rm F}(\lambda)],$$

is known as the **superfluid density**. Historically, the concept of a "superfluid density" was introduced prior to the BCS theory, when a phenomenological model known as the **two-fluid model** presented the "state-of-the-art" understanding of superconductivity. (Remember that the experimental discovery of superconductivity preceded its microscopic description by more than four decades!) The basic picture underlying this approach was that, below the transition, a fraction of the electron system condenses into a dissipationless superfluid of density $n_{\rm s}$, while the rest of the electrons remain in the state of a "normal" Fermi liquid of density $n_{\rm n} = n - n_{\rm s}$. This simple model provided a phenomenological explanation of a large number of properties characteristic of superconductivity, prior to the development of the microscopic BCS theory.

However, notwithstanding its success and its appealing simplicity, the two-fluid notion of a complete condensation $n_{\rm s} \xrightarrow{(T\to 0)} n$ at low temperatures cannot be maintained. Indeed, we have seen that BCS superconductivity is a Fermi surface phenomenon, i.e. the bulk of the electrons are oblivious to the existence of an attraction mechanism at energies $\mu \pm \omega_{\rm D}$ and, therefore, will not enter a condensed state. Instead, our microscopic analysis produces a picture more subtle than the mere superposition of two fluids: as we saw above, the diamagnetic (paramagnetic) contribution to the response is provided by all quasi-particles (at the Fermi surface). In a normal metal, or, equivalently, a superconductor at $T \gg \Delta_0$, quasi-particle excitations at the Fermi surface conspire to cancel the diamagnetic contribution of all other quasi-particles. However, at $T \ll \Delta_0$ the existence of a quasi-particle *energy gap* at the Fermi surface blocks that compensation mechanism and a net diamagnetic signal remains. The far-reaching phenomenological consequences of the sustained diamagnetic contribution are discussed in the next section.

[37] The last equality follows straightforwardly from the two definitions

$$\begin{matrix}\nu \\ n\end{matrix} = \frac{2}{L^d}\sum_{\mathbf{p}} \begin{matrix}\delta(\mu-\xi_{\mathbf{p}}) \\ (\mu-\xi_{\mathbf{p}})\end{matrix} = \frac{2}{(2\pi)^d} \int d^d p \begin{matrix}\delta(\mu-\xi) \\ (\mu-\xi)\end{matrix} .$$

[38] Going beyond second lowest order of perturbation theory in $\mathbf{A}$, a careful analysis of the coupling of a (small) magnetic field to the orbital degrees of freedom of the Fermi gas shows that the cancellation of diamagnetic and paramagnetic contributions is not perfect. The total response of the system is described by a weak diamagnetic contribution, $_{\rm d}$, a phenomenon known as **Landau diamagnetism**. The diamagnetic orbital response is overcompensated by **Pauli paramagnetism**, i.e. the three times larger paramagnetic response of the Zeeman-coupled electron spin, $_{\rm p} = -3\ _{\rm d}$. For large magnetic fields, the situation changes totally, and more pronounced effects such as **Shubnikov de Haas oscillations** or even the **quantum Hall e ect** are observed.

Validity of the gradient expansion Before leaving this section let us discuss one last technical point. Above we have – without much of a justification – expanded the phase action up to leading order in the gradients $\partial_\tau\theta$ and θ. Indeed, why is such a truncation permissible? This question arises whenever low-energy effective theories are derived from a microscopic parent theory by expanding in slow fluctuations, and it is worthwhile to address it in a general setting. Let us suppose we had performed some kind of Hubbard–Stratonovich transformation to describe a system of interest in terms of an action $S[\phi]$. Let us further assume that the action is invariant under a shift of the field by a constant, $\phi(x) \to \phi(x) + \phi_0$, i.e. that the action depends only on gradients ϕ. (To keep the notation simple, we do not explicitly distinguish between spatial and temporal gradients.) An expansion of the action in the field gradients then leads to a series of the formal momentum-space structure

$$S \sim N \sum_q \left[(l_0 q)^2 \phi_q \phi_{-q} + (l_0 q)^4 \phi_q \phi_{-q} + \cdots \right],$$

where N represents the large parameter of the theory,[39] l_0 is some microscopic reference scale of [length] needed to make the action dimensionless, and the ellipses stand for terms of higher order in q and/or ϕ_q. Now, using the fact that only field configurations with $S \sim 1$ significantly contribute to the field integral, we obtain the estimate $\phi_q \sim \frac{1}{\sqrt{N}} \frac{1}{l_0 q}$ from the leading-order term of the action. This means that terms of higher order in the field variable, $N(l_0 q \phi_q)^{n>2} \sim N^{1-n/2}$, are small in inverse powers of the large parameter of the theory and can be neglected. Similarly, terms like $N(l_0 q)^{n>2} \phi_q \phi_{-q} \sim (l_0 q)^{n-2}$. As long as we are interested in large-scale fluctuations on scales $q^{-1} \gg l_0$, these terms, too, can be neglected.

Notice that our justification for neglecting terms of higher order relies on *two* independent parameters; large N and the smallness of the scaling factor $q l_0$. If $N = 1$ but still $q l_0 \ll 1$, terms involving two gradients but large powers of the field $\sim q^2 \phi_q^{n>2}$ are no longer negligible. Conversely, if $N \gg 1$ but one is interested in scales $q l_0 \simeq 1$, terms of second order in the field weighted by a large number of gradients $\sim q^{n>2} \phi_q^2$ must be taken into account. An incorrect treatment of this point has been the source of numerous errors in the published literature!

Meissner effect and Anderson–Higgs mechanism

If you ask a person on the street to give a one-line definition of superconductivity, the answer will probably be that superconductors are materials showing no electrical resistance. However, to a physicist, that definition should not be altogether satisfactory. It highlights only one of many remarkable features of superconductors and does not have any predictive power. A better – if for most people incomprehensible – attempt at a definition would be to say that superconductivity arises when the quantum phases of a macroscopically large number of charged particles get locked into a collective degree of freedom. Indeed, that is exactly what the action (6.34) tells us: fluctuations of the phase of the condensate are penalized by a cost that scales with the (superfluid) density of the electron gas. This is to be contrasted to the situation in a normal metal where the action – the cancellation of the

[39] In theories containing a large parameter N, that parameter mostly appears as a constant multiplying all, or at least several, operators of the action. For example, in the fermionic problems discussed above, where N was proportional to the density of states at the Fermi surface, the action contained a trace over all momentum states. The summation over these states then led to an overall factor N multiplying the action.

diamagnetic and the paramagnetic contribution! – usually does not contain the gradients of phase-like degrees of freedom. Indeed, the macroscopic phase rigidity of the BCS ground state wavefunction suffices to explain a large number of non-trivial phenomena related to superconductivity. To see this, let us consider a simplified version of the action (6.34). Specifically, let us assume (i) that the temperature is high enough to exclude quantum fluctuations of the phase, $\partial_\tau \theta = 0$, and (ii) that there are no electric fields acting on our superconductor $\phi = 0, \partial_\tau \mathbf{A} = 0$.

INFO Why do we relate the presence of **quantum fluctuations** to **temperature**? Let us reiterate (cf. the remarks made on page 255) that a temporarily constant field variable acts like a classical degree of freedom. To understand why large temperatures inhibit temporal fluctuations superimposed on the classical sector, let us take the phase action of the superconductor as an example and write

$$S[\theta] = \nu \int_0^\beta d\tau \int d^d r \, (\partial_\tau \theta)^2 + S_{\rm cl}[\theta],$$

where the first term determines the temporal fluctuation behavior of the phase field, while $S_{\rm cl}$ is the "classical" contribution to the action, i.e. the contribution independent of time derivatives. Switching to a frequency representation,

$$S[\theta] = \nu \sum_{m,\mathbf{q}} \omega_m^2 \theta_{m,\mathbf{q}} \theta_{-m,-\mathbf{q}} + S_{\rm cl}[\theta],$$

from which one can infer that quantum fluctuations, i.e. modes $\theta_{m=0}$, become inessential at large temperatures. More specifically, modes with non-vanishing Matsubara frequency can be neglected when the quantum fluctuation energy (density) $\nu\omega_m^2 \propto T^2$ exceeds the characteristic energy scales appearing in $S_{\rm cl}[\theta]$.

To understand heuristically the temperature scaling of the fluctuation energy, remember that the Bose field $\theta(\tau)$ obeys periodic boundary conditions $\theta(0) = \theta(\beta)$. Inspection of Fig. 6.8 then shows that increasing the temperature, i.e. squeezing of the imaginary time interval $[0, \beta]$, leads to a linear increase of the gradients $\partial_\tau \theta \propto T$. Accordingly, the squared gradient appearing in the action increases quadratically with T. This mechanism confirms the intuitive expectation that quantum fluctuations – i.e. fundamentally a low-energy phenomenon – should be damped out at increasing temperature.

Under these conditions, the action simplifies to

$$S[\mathbf{A}, \theta] = \frac{\beta}{2} \int d^d r \left[\frac{n_{\rm s}}{m} (\nabla\theta - \mathbf{A})^2 + (\nabla \wedge \mathbf{A})^2 \right],$$

where we have explicitly included the action $\frac{1}{4} \int d\tau \int d^d r \, F_{\mu\nu} F^{\mu\nu} \stackrel{\phi=0, \mathbf{A} \text{ static}}{=} \frac{\beta}{2} \int d^d r \, (\nabla \wedge \mathbf{A})^2 = \frac{\beta}{2} \int d^d r \mathbf{B}^2$ due to fluctuations of the magnetic field. As pointed out above, the action is invariant under the gauge transformation $\mathbf{A} \to \mathbf{A} + \nabla\phi$, $\theta \to \theta + \phi$. One thus expects that integration over all realizations of θ – a feasible task since the action is quadratic –

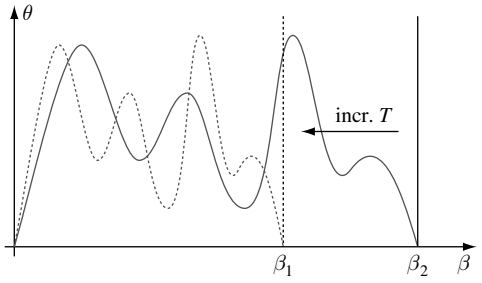

Figure 6.8 Qualitative picture behind the quadratic $\sim T^2$ energy increase of quantum fluctuations. As the temperature T is increased, the imaginary time interval $[0, \beta = T^{-1}]$ gets squeezed. The same happens to the temporal profiles of (quantum) fluctuating modes $\theta(\tau)$. Consequently, gradients $\partial_\tau \theta \propto T$ increase linearly with temperature, and the energy density $\sim (\partial_\tau \theta)^2 \propto T^2$ grows quadratically.

will produce a purely $\mathbf{A}$-dependent, and gauge invariant, action $S[\mathbf{A}]$. The integration over θ is most transparently formulated in momentum space where the action assumes the form

$$\begin{aligned} S[\mathbf{A},\theta] &= \frac{\beta}{2}\sum_{\mathbf{q}}\left(\frac{n_\mathrm{s}}{m}(i\mathbf{q}\theta_{\mathbf{q}} - \mathbf{A}_{\mathbf{q}})\cdot(-i\mathbf{q}\theta_{-\mathbf{q}} - \mathbf{A}_{-\mathbf{q}}) + (\mathbf{q}\wedge\mathbf{A}_{\mathbf{q}})\cdot(\mathbf{q}\wedge\mathbf{A}_{-\mathbf{q}})\right) \\ &= \frac{\beta}{2}\sum_{\mathbf{q}}\left(\frac{n_\mathrm{s}}{m}[\theta_{\mathbf{q}}q^2\theta_{-\mathbf{q}} - 2i\theta_{\mathbf{q}}\mathbf{q}\cdot\mathbf{A}_{-\mathbf{q}} + \mathbf{A}_{\mathbf{q}}\cdot\mathbf{A}_{-\mathbf{q}}] + (\mathbf{q}\wedge\mathbf{A}_{\mathbf{q}})\cdot(\mathbf{q}\wedge\mathbf{A}_{-\mathbf{q}})\right). \end{aligned}$$

The integration over the field components $\theta_{\mathbf{q}}$ is now straightforward and leads to an effective action for $\mathbf{A}$: $e^{-S[\mathbf{A}]} \equiv \int D\theta\; e^{-S[\mathbf{A},\theta]}$, where

$$S[\mathbf{A}] = \frac{\beta}{2}\sum_{\mathbf{q}}\left(\frac{n_\mathrm{s}}{m}\left(\mathbf{A}_{\mathbf{q}}\cdot\mathbf{A}_{-\mathbf{q}} - \frac{(\mathbf{q}\cdot\mathbf{A}_{\mathbf{q}})(\mathbf{q}\cdot\mathbf{A}_{-\mathbf{q}})}{q^2}\right) + (\mathbf{q}\wedge\mathbf{A}_{\mathbf{q}})\cdot(\mathbf{q}\wedge\mathbf{A}_{-\mathbf{q}})\right).$$

To bring this result into a more transparent form, let us split the vector potential into a longitudinal and a transverse component:

$$\mathbf{A}_{\mathbf{q}} = \underbrace{\mathbf{A}_{\mathbf{q}} - \frac{\mathbf{q}(\mathbf{q}\cdot\mathbf{A}_{\mathbf{q}})}{q^2}}_{\mathbf{A}^\perp_{\mathbf{q}}} + \underbrace{\frac{\mathbf{q}(\mathbf{q}\cdot\mathbf{A}_{\mathbf{q}})}{q^2}}_{\mathbf{A}^\parallel_{\mathbf{q}}}. \tag{6.38}$$

To motivate this decomposition, notice the following:

- ▷ The transverse component alone determines physical quantities, i.e. the magnetic field. (This follows from the relation $\mathbf{B}_{\mathbf{q}} = i\mathbf{q}\wedge\mathbf{A}_{\mathbf{q}}$ and $\mathbf{q}\wedge\mathbf{q} = 0$.)
- ▷ The transverse component is gauge invariant under transformations $\mathbf{A}_{\mathbf{q}} \to \mathbf{A}_{\mathbf{q}} + i\mathbf{q}\phi_{\mathbf{q}}$ (but $(\mathbf{q}\phi_{\mathbf{q}})^\perp = 0$). In the language of longitudinal–transverse components, the Coulomb gauge corresponds to a configuration where $\mathbf{A}^\parallel = 0$.
- ▷ The terminology "longitudinal component" emphasizes the fact that $\mathbf{F}^\parallel_{\mathbf{q}}$ is the projection of a vector field $\mathbf{F}_{\mathbf{q}}$ onto the argument vector $\mathbf{q}$. Correspondingly, the "transverse component" is the orthogonal complement of the longitudinal component.

Applying some elementary rules of vector algebra, it is straightforward to verify that the effective action can be represented in the simple form

$$S[\mathbf{A}] = \frac{\beta}{2} \sum_{\mathbf{q}} \left(\frac{n_{\mathrm{s}}}{m} + q^2 \right) \mathbf{A}^{\perp}_{\mathbf{q}} \cdot \mathbf{A}^{\perp}_{-\mathbf{q}}. \tag{6.39}$$

At this stage, it is useful to pause and review what has been achieved: (i) starting from a composite action containing the Goldstone mode θ and the gauge field $\mathbf{A}$, we have arrived at an action for the gauge field alone. In a sense, the Goldstone mode has been absorbed into (the gauge degrees of freedom of) $\mathbf{A}$. However, (ii) the coupling to the Goldstone mode has not left the gauge field unaffected. Indeed, $S[\mathbf{A}]$ has acquired a **mass** term proportional to the superfluid density, i.e., unlike the vacuum, the action of long-range field fluctuations $\mathbf{A}_{\mathbf{q}\to 0}$ no longer vanishes. That modification has serious phenomenological consequences to be discussed shortly. (iii) The action is manifestly gauge invariant.

INFO The analysis above shows that the spontaneous breaking of a global U(1) symmetry, and of a local gauge U(1) symmetry lead to very different results. In the former ($\rightarrow$ neutral superfluids), the soft action $S[\theta]$ of a phase-like Goldstone mode θ describes various long-range phenomena, such as supercurrent formation, etc. In the latter case ($\rightarrow$ superconductors or, more generally, charged superfluids), the system is described by a composite action $S[\mathbf{A}, \theta]$. The ubiquitous gauge symmetry can then be employed to absorb the Goldstone mode into the gauge field $S[\mathbf{A}, \theta] \overset{\int D}{\rightarrow} S[\mathbf{A}]$. The most important effect of the coupling $\mathbf{A}$ θ is that, after integration over the latter, the former acquires a mass term. One may say that "the photon (vector potential) field has consumed the Goldstone mode to become massive." That principal mechanism was understood in 1964 by Higgs, wherefore it is called the **Higgs mechanism** or, crediting Anderson's pioneering discussion of gauge symmetry breaking in the context of superconductivity, the **Anderson–Higgs mechanism**.

Mass generation due to spontaneous gauge symmetry breaking is a very general phenomenon, i.e. not limited to the relatively simple context of the collective phase of the superconductor. The Higgs mechanism found perhaps its most significant application in 1967 when Weinberg and Salam embedded it into their unified theory of electromagnetic and weak interactions in particle physics. Although this is not a book about elementary particles, the role of the Higgs principle in the theory of electroweak interactions is of such fundametal importance to our understanding of the microscopic world that it is irresistible to briefly discuss its implications.[40]

The **standard model of high-energy physics** describes the microscopic world in terms of a few generations of leptonic (electrons, e, electron neutrino, ν_{e}, muon, μ, etc.) and hadronic (the quarks, u, d, s, c, t, b) elementary particles that interact through the quanta of certain gauge fields. In its original formulation, the model had one severe problem, that is, it did not know how to attribute mass to these particles. However, this stands in stark contrast to any kind of experimental observation. In particular, the quanta of the gauge fields of the weak and strong interactions are known to be extremely heavy, with rest masses of $\mathcal{O}(10^2\,\mathrm{GeV}/c^2)$. In view of the much lighter masses of typical composite hadrons – the proton weighs $938\,\mathrm{MeV}/c^2$ – the mass of the gauge quanta can certainly not be explained in terms of some fictitious fine structure mechanisms superimposed on the core of the standard model, i.e. a major modification

[40] For a pedagogical and much less superficial discussion we refer, e.g., to L. H. Ryder, *Quantum Field Theory* (Cambridge University Press, 1996).

was needed. It is now widely believed that the "true" principle behind mass generation lies in the (Anderson–) Higgs mechanism, i.e. the spontaneous breakdown of a gauge symmetry.

To sketch the principal idea of Weinberg and Salam, let us concentrate on a leptonic subsector of the theory, e.g. consider the two-component object

$$\equiv \begin{pmatrix} \nu_{\mathrm{e}} \\ \mathrm{e} \end{pmatrix},$$

comprising an electron neutrino and a (left-handed[41]) electron. Involving a charged particle, the Lagrangian controlling the dynamics of will surely possess a local U(1) gauge symmetry. However, on top of that, Weinberg and Salam proposed a much more far-reaching symmetry structure. Without going into detail we just mention that, building on principles proposed earlier (1954) by Yang and Mills, transformations

$$(x) \to U(x) \quad (x), \quad U(x) \in \mathrm{SU}(2), \quad x \in \mathbb{R}^4,$$

locally mixing the two components ν_{e} and e of the "isospinor" were introduced as a symmetry of the model, i.e. in analogy to the local U(1) gauge symmetry of quantum mechanics, it was postulated that the action $S[\ ]$ possesses a local gauge symmetry under the group of SU(2) transformations. In combination with the standard U(1), the theory had thus been endowed with a composite $\mathrm{U}(1) \times \mathrm{SU}(2)$ gauge structure. Physically, declaring a symmetry between the electron – interacting through electromagnetic forces – and the neutrino – weak interactions – was tantamount to a fusion of these types of interaction, i.e. the proposal of a theory of **electroweak interactions**.

How can a theory defined through an action $S[\ ] = \int d^{d+1}x\ \mathcal{L}(\ , \partial_\mu\ )$, containing the isospinor and its derivatives, be made invariant under non-abelian SU(2) gauge transformations? Referring for a more systematic discussion to Ryder,[42] let us briefly sketch the principal idea of **non–abelian gauge theory**. We first notice that a fermion bilinear $\sim\ \bar{}\ \partial_\mu$ is generally not gauge invariant. Under a mapping $\to U$ it transforms to $\bar{}\ (\partial_\mu + U^{-1}\partial_\mu U)$. E.g. for $U = e^{i\phi} \in \mathrm{U}(1)$ a "standard" gauge transformation, the extra term $U^{-1}\partial_\mu U = i\partial_\mu\phi \in i\mathbb{R}$ would be the ordinary "derivative of a function," familiar from the gauge structure of quantum mechanics. More generally, for a non-abelian gauge transformation by an element $U \in G$ of a general group (e.g. $G = \mathrm{SU}(2)$), the gauge term $U^{-1}\partial_\mu U \in \mathrm{g}$ is an element of the Lie algebra g of the group,[43] i.e. the action picks up a matrix-valued extra contribution.

To make the theory invariant, we have to introduce a gauge field, i.e. we generalize from ∂_μ to a covariant derivative $\partial_\mu + W_\mu$, where $W_\mu \in \mathrm{g}$. For example, for $G = \mathrm{U}(1)$, $W_\mu \equiv A_\mu \in \mathbb{R}$ is the ordinary gauge field of quantum mechanics; for $G = \mathrm{SU}(2)$, $W_\mu = \sum_{a=1}^{3} \alpha_a^\mu(x)\sigma_a \in \mathrm{su}(2)$, etc. Under a gauge transformation, the field W_μ transforms as $W_\mu \to UW_\mu U^{-1} - iU^{-1}\partial_\mu U$, i.e. in a way that makes the covariant bilinear, $\bar{}\ (\partial_\mu + W_\mu)$, invariant. For $G = \mathrm{U}(1)$, $A_\mu \to UA_\mu U^{-1} - U\partial_\mu U^{-1} = A_\mu - i\partial_\mu\phi$ reduces to its familiar form. However, in the non-abelian case,

[41] When viewed as a relativistic particle, the electron field has components of left and right chirality, but we shall not need to discuss that aspect any further.

[42] Ryder, *Quantum Field Theory*.

[43] The fact that $U^{-1}\partial_\mu U \in \mathrm{g}$ takes values in the Lie algebra of the gauge group can be proven by geometric considerations (for which we refer to textbooks of group theory). By way of example, consider an SU(2)-valued field $U(x) = \exp(i\sum_{a=1}^{3} \alpha_a(x)\sigma_a)$. It is straightforward to convince oneself that $U^{-1}\partial_\mu U$ is a linear combination of Pauli matrices with real-valued coefficents, i.e. it takes values in the Lie algebra su(2).

the full structure on the right-hand side is needed to obtain invariance. The full action of the gauge theory then takes the form

$$S[\ \ ,W] = \int d^{d+1}x\ \mathcal{L}(\ \ ,(\partial_\mu - iW_\mu)\ \ ) + S[W],$$

where the Lagrangian density contains the minimally coupled gauge field, and the action $S[W]$ describes the fluctuation behavior of W_μ.[44] Within a fully quantum mechanical setting, both the "matter field" and the gauge field W_μ are quantized. The field quanta of the non-abelian gauge field are described as **vector bosons**, where the attribute "vector" (somewhat misleadingly) refers to the higher-dimensional geometry of the field, and "boson" emphasizes the generally bosonic statistic of a quantum gauge field.

We now have everything in place to turn back to the particular context of the electroweak interaction. Within the framework of the gauge theory, interactions between the particles e and ν_e are mediated by the gauge field W_μ (as with a U(1) theory where interactions between the electrons can be described in terms of a fluctuating U(1) vector potential, cf. Section 6.2). Experimental analysis of typical weak interaction processes, such as the elastic collision, $e + \nu_e \to e + \nu_e$, indicates that the weak interaction forces are extraordinarily short-range, with a decay profile $\sim \exp(-90\,\mathrm{GeV}r)$. However, according to the pure gauge theory, the propagator of W_μ should be long-range $\sim r^{-1}$. This is the most severe manifestation of the mass problem of the electroweak theory. In order to be consistent with experiment, a mechanism is needed that makes the gauge field (very) massive.

Here is where the Higgs mechanism enters the stage. To solve the mass problem, Weinberg and Salam postulated the existence of a scalar (more precisely, a two-component "iso-scalar") bosonic particle, the **Higgs boson** ϕ. The action of the Higgs particle – again a postulate – is of generalized ϕ^4 type, i.e.

$$S[\phi, W_\mu] = \int d^{d+1}x \left[\frac{1}{2}(\partial_\mu - W_\mu)\phi^\dagger(\partial_\mu - W_\mu)\phi - \frac{m^2}{2}\phi^\dagger\phi + \frac{g}{2}(\phi^\dagger\phi)^2\right],$$

where the minimal coupling to the gauge field provides the theory with local gauge invariance. The action of the Higgs has been deliberately designed so as to generate spontaneous symmetry breaking, i.e. the solution of the mean-field equations is given by $|\phi| = (\frac{m^2}{2g})^{1/2}$, with undetermined phase. In direct analogy to our discussion of the superconductor above, an integration over the phase degree of freedom (i.e. the Goldstone mode) then generates a mass term for the gauge fields. In summary, Weinberg and Salam proposed an explanation of the short-rangeness of the weak interaction through the presence of an extra particle, i.e. a particle that does not belong to the standard hadronic or leptonic generations of the standard model.

Since then, the hunt for the Higgs particle has been one of the big challenges for particle physics. In 1983 vector bosons of the predicted mass were for the first time observed in experiment[45] (see Fig. 6.9), i.e. the existence of a massive gauge structure is now out of the question. However, the detection of the Higgs turned out to be a more difficult task. In 2000 the $\mathcal{N}$-experiment installed at the LEP (Large Electron Positron Collider) at CERN reported a "shadowy" Higgs signal in the e^-e^+ scattering cross-section at the predicted energy interval. However, at that time, the designated live time of LEP had already expired and one month after

[44] Typically, $S[W]$ will be given by generalization of the field strength tensor $\int d^{d+1}x\ F_{\mu\nu}F^{\mu\nu}$ of the abelian theory, i.e. the *curvature* tensor on G.

[45] G. Arnison *et al.*, Experimental observation of isolated large transverse energy electrons with associated missing energy at $\sqrt{s} = 540\,\mathrm{GeV}$, *Phys. Lett. B* **122** (1983), 103–16.

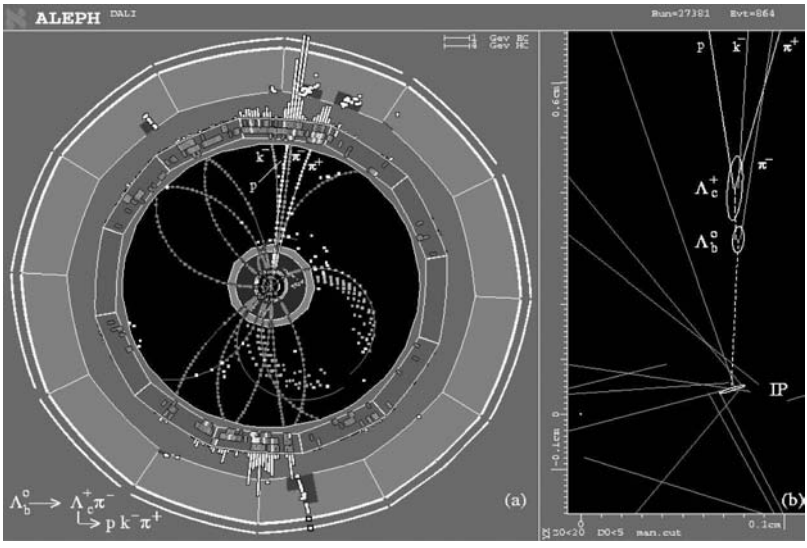

Figure 6.9 Computer-generated visualization of a scattering process recorded in the $\mathcal{N}$-experiment at CERN. Hidden somewhere in the "jet" of particles generated as a result of the collision of the scattering particles should, hopefully, be the Higgs.

the detection of the first suspicious signals the machine was indeed shut down. Unfortunately, after the closedown of LEP only a few accelerator projects offer the perspective to participate in the hunt for the Higgs. Presently, with the "Superconducting Super Collider" (SSC) disapproved by the American Congress, only the Stanford Linear Accelerator reaches the relevant energy scales. The situation may change when the Large Hadron Collider (LHC) at CERN commences its work.

In the meantime the collected data recorded at LEP over the past years have been subjected to critical review. Frustratingly, it turned out that the data reported in 2000 did not pass the test of a careful re-examination, i.e. presently (2009) there is no direct evidence for a Higgs particle. In view of the fact that the Higgs generates the mass not only of the vector bosons but of all particles known to the standard model, much indeed hinges on the question of its existence. (Some people even call the Higgs the "God particle.") If it did not exist, our understanding of the microscopic world would be turned upside down.

To conclude our discussion of BCS superconductivty, let us explore the phenomenological consequences of mass accumulation due to the Higgs mechanism. To this end, let us vary the action (6.39) with respect to $\mathbf{A}$ (keeping in mind the transversality condition $\mathbf{q}\cdot\mathbf{A}^{\perp}_{\mathbf{q}} = 0$, we henceforth drop the superscript " "), to obtain $(\frac{n_{\rm s}}{m} + q^2)A_{\mathbf{q}} = 0$, or

$$\left(\frac{n_{\rm s}}{m} - \nabla^2\right) A(\mathbf{r}) = 0. \tag{6.40}$$

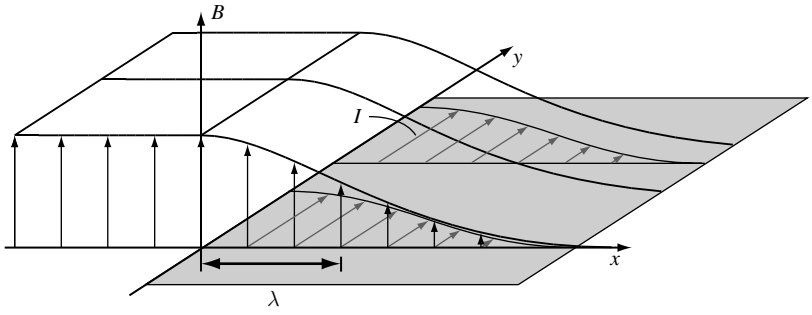

Figure 6.10 On the Meissner effect: inside a superconductor (the shaded area), magnetic fields decay exponentially. Microscopically, an external field existing outside a superconductor–vacuum interface induces diamagnetic surface currents inside the superconductor. These currents generate a counter-field that diminishes the external field.

Remembering that $\mathbf{B} = \nabla \wedge \mathbf{A}$, multiplication of this equation by $\nabla\wedge$ produces the **first London equation**

$$\boxed{\left(\frac{n_\mathrm{s}}{m} - \nabla^2\right)\mathbf{B}(\mathbf{r}) = 0.} \tag{6.41}$$

For $n_\mathrm{s} \neq 0$, this equation does not have a non-vanishing constant solution, i.e. we conclude that

A bulk superconductor cannot accommodate a magnetic field.

This phenomenon is known as the **Meissner effect**. To understand what happens at the interface between the vacuum threaded by a constant magnetic field $\mathbf{B}_0$ and a superconductor, one can solve the London equation to obtain $\mathbf{B}(x) \sim \mathbf{B}_0 \exp(-x/\lambda)$, where

$$\lambda = \sqrt{\frac{m}{n_\mathrm{s}}},$$

is known as the **penetration depth** and x is the direction perpendicular to the interface (see Fig. 6.10). The physical mechanism behind the Meissner phenomenon is as follows: above we saw that the magnetic response of a superconductor is fully diamagnetic. That is, in response to an external field, diamagnetic screening currents will be generated. The magnetic field generated by these currents counteracts the unwanted external field. To see this explicitly, we obtain the current density induced by the field by differentiating the first term of the action[46] with respect to $\mathbf{A}$:

$$\mathbf{j}(\mathbf{r}) = \frac{\delta}{\delta \mathbf{A}(\mathbf{r})} \int d^d r \; \frac{n_\mathrm{s}}{2m}\mathbf{A}^2 = \frac{n_\mathrm{s}}{m}\mathbf{A}(\mathbf{r}), \tag{6.42}$$

[46] Generally, the electrical current density induced by a field is obtained (cf. the remarks made on page 255) by differentiating the field/matter part of the action $S[\mathbf{A}]$ with respect to the vector potential, i.e. the purely field-dependent part of the action does not contribute to the current density.

i.e. the current density is directly proportional to **A**. This is the **second London equation**. Since the vector potential and the magnetic field show the same decay profile (Eq. (6.40) and (6.41)), the current density also decays exponentially inside the superconductor. However, in doing so, it annihilates the external field.

INFO To heuristically understand the **incompatibility of magnetic fields and superconductive pairing** on a still more microscopic level, consider the real space representation of a Cooper pair state, $\langle \mathbf{r}, \mathbf{r}|\mathbf{k} \quad , -\mathbf{k} \quad \rangle \sim e^{-i\mathbf{k}\mathbf{r}} e^{+i\mathbf{k}\cdot\mathbf{r}} = \text{const}$. The cancellation of the phases results from the fact that two electrons propagating with opposite momenta acquire opposite quantum phases. Thus, the pair state is a slowly fluctuating, and therefore stable, object. However, in the presence of a magnetic field, the phase factors have to be generalized to

$$\langle \mathbf{r}, \mathbf{r}|\mathbf{k} \quad , -\mathbf{k} \quad \rangle \sim e^{-i\int d\mathbf{r}\cdot(\mathbf{k}-eA)} e^{-i\int d\mathbf{r}\cdot(-\mathbf{k}-eA)} \sim e^{2ie\mathbf{A}\cdot\mathbf{r}},$$

where we assumed that the vector potential varies only slowly across our observation region of $\mathcal{O}(|\mathbf{r}|)$, i.e. the Cooper pair amplitude becomes an "incoherent" phase-dependent object. (Exercise: Employ the WKB approximation to convince yourself of the validity of this statement.) On the microscopic level, the lack of stability of the field-dependent Cooper amplitude is responsible for the aversion of the superconductor to magnetic fields.

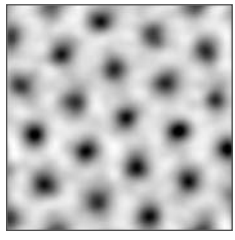

It is interesting to explore how a strong magnetic field eventually makes its way into the superconductor. To understand the **competition between superconductive ordering and magnetic field energy**, we need to go back to the Ginzburg–Landau action (6.33), i.e. to a description that involves both phase and amplitude of the order parameter (the latter detecting the presence or absence of a stable condensate). However, at the time when we derived that action, no attention had been paid to the electromagnetic properties of the system. Fortunately, after our general discussion of gauge invariance above, the minimal coupling of the system to the electromagnetic field is routine work. We simply have to remember that, under a gauge transformation, $\Delta \to \Delta e^{2i\phi}$, i.e. $\Delta \quad \bar{\Delta} \to (\quad + 2i \quad \phi)\Delta(\quad - 2i \quad \phi)\bar{\Delta}$. The gauge invariant extension of Eq. (6.33) thus reads as

$$S_{\mathrm{GL}}[\Delta, \bar{\Delta}] = \beta \int d^d r \left[\frac{r}{2}|\Delta|^2 + \frac{c}{2}|(\quad - 2i\mathbf{A})\Delta|^2 + g|\Delta|^4 \right],$$

where, as usual, **A** gauges as $\mathbf{A} \to \mathbf{A} + \quad \phi$. To monitor the fate of the order parameter as $|\mathbf{A}| \propto |\mathbf{B}|$ increases, consider the mean-field equation (exercise)

$$\left[r + c(-i \quad - 2A)^2 + 4g|\Delta|^2 \right] \Delta = 0.$$

Here we assume that we are at temperatures below the zero-field superconductor transition, i.e. $r < 0$. Superconductive ordering exists when the equation has a non-vanishing solution Δ. Now, the third contribution on the left-hand side is positive, so a solution can exist only if the first two terms add to a net negative contribution. This in turn requires the following condition on the eigenvalues of the minimally coupled operator,

$$\mathrm{EV}(-i \quad - 2\mathbf{A})^2 \overset{!}{<} \frac{|r|}{c}.$$

Formally, $(-i \quad -2\mathbf{A})^2$ is the kinetic energy operator of a particle of mass 1/2 and charge $q = 2$ in a uniform magnetic field. Its eigenvalues are the Landau levels, $\omega_{\mathrm{c}} \quad n + \frac{1}{2} \quad , n = 0, 1, \ldots$, familiar from elementary quantum mechanics. Here, ω_{c} is the cyclotron frequency, $\omega_{\mathrm{c}} = qB/m = 4B$.

Thus, a finite pairing amplitude can be obtained only if $|r|/c$ is larger than the energy of the lowest Landau level, or

$$B < B_{c2} \equiv \frac{|r|}{2c}.$$

For magnetic fields larger than this, the energy needed to expel the field is larger than the maximum gain of condensation energy $S[\Delta]$ and superconductivity breaks down. There are superconductor materials – **superconductors of type II** – where the energy criterion opts for field penetration for fields $B_{c2} > B > B_{c1}$ lower than the critical field B_{c2} specified by the mean-field criterion above. For these systems, the superconductor and the field "meet a compromise." That is, **vortex tubes** of quantized flux penetrate the superconductor for a field strength smaller than B_{c2} but larger than the critical field strength B_{c1}.[47] These **Abrikosov vortices** usually arrange into a triangular vortex lattice. The figure above (courtesy of U. Hartmann, University of Sarbrücken) shows an STM image of a vortex lattice in the type II superconductor $NbSe_2$. The distance between vortex centers is about 50 nm. Each of the vortices in a flux lattice contains magnetic flux $\Phi = \frac{n}{h}$ where $1/h$ (or e/h in units where the electron charge is kept track of) is the magnetic flux quantum. Inside the cores of the Abrikosov vortices, the superconducting order parameter is suppressed, but outside it still exists. For a discussion of the thermodynamics of superconductors not showing a mixed phase (**superconductors of type I**), we refer to the literature.[48]

To conclude this section let us discuss the most prominent superconducting phenomenon, **absence of electrical resistivity**. Assume we have chosen a gauge where an external electric field $\mathbf{E}$ is represented through $\mathbf{E} = -i\partial_\tau \mathbf{A}$ (i.e. the static component of the potential vanishes). In this case, a time differentiation of the second London equation (6.42) gives $-i\partial_\tau \mathbf{j} = -i\frac{n_s}{m}\partial_\tau \mathbf{A} = \frac{n_s}{m}\mathbf{E}$. Continuing back to real times we conclude that

$$\boxed{\partial_t \mathbf{j} = \frac{n_s}{m}\mathbf{E},}$$

i.e. in the presence of an electric field the current increases linearly at a rate inversely proportional to the carrier mass and proportional to the carrier density. The unbound increase of current is indicative of ballistic – i.e. dissipationless – motion of the condensate particles inside the superconductor. Now, an unbound increasing current is clearly unphysical, i.e. what the relation above really tells us is that a superconductor cannot maintain non-vanishing field gradients.

EXERCISE Assuming that each particle is subject to Newton's equation of motion $m\ddot{\mathbf{r}} = \mathbf{E}$, obtain the current–field relation above. How would the relation between field and current change if the equation of motion contained a friction term (modeling dissipation) $m\ddot{\mathbf{r}} = -\frac{m}{\tau}\mathbf{r} + \mathbf{E}$?

[47] A. A. Abrikosov, On the magnetic properties of superconductors of the second group, *Soviet Physics JETP* **5**, 1174-83 (1957).

[48] cf., e.g., L.D. Landau and E. M. Lifshitz, *Course of Theoretical Physics, Vol. 9 - Statistical Physics 2*, (Butterworth–Heinemann, 1981).

6.5 Field theory of the disordered electron gas

To close the chapter on broken symmetry and collective phenomena, we turn now to a final, detailed application of the field integral method involving the problem of electrons propagating in a disordered environment. As well as the importance attached to this general area in the recent literature, the quantum disorder problem presents an ideal arena in which to revise the diagrammatic and field theoretic methods developed in this and previous chapters. This being so, this section is structured in a manner that reflects the different techniques and much of our discussion is deliberately cast in the form of problem assignments. However, this section may be read equally as a complete and coherent text, depending on taste.

Disorder in metals

No semiconductor or metal of macroscopic[49] extent is ever free of imperfections and impurities. Indeed, the effect of disorder on the phenomenology of metals or semiconductors could not be more varied: in some cases, disorder plays an essential role (for example, conventional light bulbs would not function without impurity scattering!), in others the effect is parasitic (imparting only a "blurring" of otherwise structured experimental data), or it conspires to give rise to completely unexpected types of electron dynamics (as is the case in the quantum Hall transition discussed in Chapter 9).

With this in mind, a complete theory of electron transport must, by necessity, include diagnostic tools to understand whether disorder seriously affects the problem of interest. Moreover, such a theory should include some analytical machinery to deal with the cases where the answer is affirmative. What kind of criteria should a successful theory of disordered conductors meet? A fair fraction of those problems where impurity scattering plays an essential role can be addressed in terms of infinite-order perturbation theory. However, there are plenty of phenomena – Anderson localization, the quantum Hall effects, the combined theory of interactions and disorder, to mention just a few – where non-perturbative field theoretical methods are required. In this section, the foundation of a general approach to the disordered electron gas, extendable to both perturbative and non-perturbative schemes, is laid.

However, before doing this, we must first clarify what is meant by a "theory" of the disordered electron gas. Of course, while the problem may be considered formally as non-interacting, we will not be able to effect an exact diagonalization of the random Schrödinger equation for an electron in a metal for a given realization of the impurity potential. (Indeed, were such a particular solution available, it would not convey much information.) Rather, one needs to develop a statistical approach wherein the system is described in terms of a few universal characteristics of the scattering landscape – the strength of the impurity

[49] In ultraclean semiconducting devices, electrons may travel up to distances of several microns without experiencing impurity scattering. Even so, the "chaotic" scattering from the typically irregular boundaries of the system has an equally invasive effect on the charge carrier dynamics.

potential, the typical range of potential fluctuations, etc. In general, the analysis of generic properties involves averaging over microscopic realizations of the impurity potential.

INFO In situations where the system is so large that different regions behave as though they were statistically independent with respect to their microscopic impurity configuration, properties become **self–averaging**. In such cases, the configuration average can be subsumed into a volume average of the individual system. As a rule of thumb, systems which behave in a self-averaging manner must extend well beyond the phase coherence length ξ – the length scale over which the quantum propagation remains phase coherent. (A more precise characterization of ξ is given below.) Now, at low temperatures, $\xi(T)$ grows rapidly, implying that even systems of near macroscopic extent (ca. $\mathcal{O}(1\,\mu\text{m})$ and more) can behave as though they were non-self-averaging. Systems of this type are often termed **mesoscopic**,[50] where "meso-" alludes to the fact that such systems are macroscopic in extent yet microscopic in their reflection of quantum mechanical character. Mesoscopic systems manifest a multitude of unusual quantum phenomena from localization to strong sample-to-sample fluctuations, some of which will be discussed below. The experimental and theoretical study of these phenomena is the central theme of **mesoscopic physics**.

How might one set about modeling an impurity potential in statistical terms? One might, for example, propose that a single imperfection at position $\mathbf{r}_i$ creates a potential $V_{\text{imp}}(\mathbf{r}-\mathbf{r}_i)$. Assuming that all impurities are, by and large, equivalent, the total perturbation experienced by an electron at point $\mathbf{r}$ will then take the form $V(\mathbf{r}) \equiv \sum_i V_{\text{imp}}(\mathbf{r}-\mathbf{r}_i)$. Within this framework (which prevails in the older literature) the disorder average amounts to integrating over the coordinates of the impurities, i.e. $\langle\cdots\rangle_{\text{dis}} \equiv L^{-Nd}\prod_{i=1}^{N}\int d^d r_i\ (\cdots)$. The disadvantage of this scheme is that its implementation is not so straightforward, especially in functional-based approaches. In practice, it is more convenient to think of the potential V as some function whose statistical properties are described by a probability measure $P[V]$. Averages over the potential are then computed by performing the integral $\langle\cdots\rangle_{\text{dis}} = \int DV\ P[V](\cdots)$. In most[51] applications it is sufficient to implement a Gaussian distribution (unnormalized), $P[V] = \exp\left[-\frac{1}{2\gamma^2}\int d^d r\, d^d r'\, V(\mathbf{r})K^{-1}(\mathbf{r}-\mathbf{r}')V(\mathbf{r}')\right]$, where γ measures the strength of the potential and K describes its spatial correlation profile:

$$\langle V(\mathbf{r})V(\mathbf{r}')\rangle_{\text{dis}} = \gamma^2 K(\mathbf{r}-\mathbf{r}'). \tag{6.43}$$

Very often one finds that the finite spatial correlation of V is inessential, in which case one may set $K(\mathbf{r}) = \delta(\mathbf{r})$, and

$$P[V]DV = \exp\left[-\frac{1}{2\gamma^2}\int d^d r\ V^2(\mathbf{r})\right]\ DV. \tag{6.44}$$

The freedom that one can exercise in modeling the scattering potentials reflects the fact that, in a multiple scattering process, details of the potential are quickly erased. At any

[50] Note that it has, however, become fashionable to label any system of a size of $\mathcal{O}(1\,\mu\text{m})$ "mesoscopic," irrespective of whether or not its behavior is classical.

[51] An important class of exceptions is presented by bosonic problems of general type where, for stability reasons, $V(\mathbf{r}) \overset{!}{>} 0$, while Gaussian distributed potentials categorically include negative "tails."

rate, the short-range Gaussian distribution provides a convenient scheme both in purely diagrammatic perturbation theory and in functional approaches.

As discussed above, our aim is to average the quantum expectation value of a certain observable $\mathcal{O}$ over the ensemble of disorder. Let us assume that the observable $\mathcal{O}$ can be obtained by differentiation of the (functional) free energy, that is $\mathcal{O} = -\frac{\delta}{\delta J}|_{J=0} \ln \mathcal{Z}$, where J represents some source field,[52] i.e.

$$\langle \mathcal{O} \rangle_{\rm dis} = -\frac{\delta}{\delta J}\big|_{J=0} \langle \ln \mathcal{Z} \rangle_{\rm dis} \,. \tag{6.45}$$

This fundamental relation presents a technical challenge: should one first differentiate and only then average, one would need to compute integrals of the type

$$-\int DV\, P[V] \frac{1}{\mathcal{Z}[V, J=0]} \frac{\delta}{\delta J}|_{J=0}\, \mathcal{Z}[V, J].$$

Due to the appearance of the function V in both the numerator and the denominator, integrals of this type are largely intractable. The problem is particularly acute in functional approaches where one intends to take the ensemble average at an early stage of the computation.[53]

To date, three different approaches have been identified in which the problem with the denominator can be circumvented: the **supersymmetry approach**,[54] the **Keldysh technique**,[55] and the **replica trick**.[56] All of these approaches share the feature that they alter the definition of the functional partition function in such a way that (a) $\mathcal{Z}[J = 0] = 1$ (i.e. the disorder dependence of the denominator disappears), while (b) Eq. (6.45) remains valid, and (c) the algebraic structure of $\mathcal{Z}[J]$ is left largely unchanged. Since the disorder appears linearly in the Hamiltonian, point (c) implies that we need to average functionals with actions linear in the potential V, an enterprise that turns out to be quite feasible.

Let us exemplify this program on the (technically) simplest of the three approaches above, the replica trick. Consider the Rth power of the partition function, $\mathcal{Z}^R$. For integer R one may think of $\mathcal{Z}^R$ as the partition function of R identical copies of the original system (see Fig. 6.11), hence the name "replica" trick. To appreciate the merit of this procedure, one may note the formal relations

$$\langle \mathcal{O} \rangle = -\frac{\delta}{\delta J} \ln \mathcal{Z}[J] = -\frac{\delta}{\delta J} \lim_{R\to 0} \frac{1}{R} \left(e^{R \ln \mathcal{Z}} - 1 \right) = -\frac{\delta}{\delta J} \lim_{R\to 0} \frac{1}{R} \mathcal{Z}^R.$$

The last equality tells us that the expectation value of observables can be obtained by performing computations with the Rth power of $\mathcal{Z}$ (instead of its logarithm). Crucially, expressed in the coherent state representation, the expression for the replicated partition

[52] In the jargon of field theory, a **source field** represents a parameter (function) that, when linearly added to the exponent of a functional integral, can be used to generate the expectation value of observables by differentiation. For example, the parameter μ is a source generating expectation values of the particle number: $-\partial_\mu F = \langle \hat{N} \rangle$.

[53] In cases where the disorder can be treated perturbatively, one may first expand in powers of V and only then average; indeed, this is quite a viable strategy.

[54] K. B. Efetov, Supersymmetry method in localisation theory, *Sov. Phys. JETP* **55** (1982), 514-21.

[55] For a review see, e.g., A. Kamenev, Many body theory of non-equilibrium systems in *Nanophysics: Coherence and Transport* eds. H. Bouchiat *et al.* 177-246, (Elsevier, Amsterdam, 2005).

[56] S. F. Edwards and P.W. Anderson, Theory of spin glasses, *J. Phys. F* **5** (1975), 965–74.

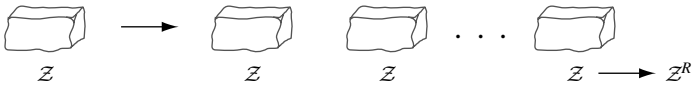

Figure 6.11 On the idea behind the replica trick; for an explanation, see the main text.

function involves an effective action which is still linear, $(e^{\int dV})^R = e^{\sum \int dV}$, i.e. $\mathcal{Z}^R$ will contain the disorder linearly in the exponent and, therefore, will be comparatively easy to average. However, the replica-averaging procedure involves one unusual feature – at the end of the calculation, one must implement the analytic continuation $R \to 0$. More precisely, we will have to compute a certain function (namely $f(R) \equiv \frac{\delta}{\delta J} R^{-1} \langle \mathcal{Z}^R \rangle_{\rm dis}$) for every integer R and then analytically continue $R \to 0$. However, there is no guarantee that $f(R)$ *is* analytic all the way down to $R = 0$.[57] In other words, the method is poorly founded, which is why it is called the "replica trick" as opposed to, say, the "replica theory." However – in view of its poorly justifiable theoretical standing, quite surprisingly – examples where the replica trick is known to fail are rare. To some extent, this success is explained by the fact that the method is exact as long as the disorder is treated perturbatively (a point to be clarified below). So long as a perturbatively accessible point in the parameter space is not too far away, the chances are that it will not fail.

INFO The applicability of **replica methods** is not limited to the theory of disordered electron systems. Replicated field theories are of potential use whenever it comes to averaging the free energy functional of a disordered classical or quantum system. The method has been proven most fruitful (at times also controversial) in the theory of conventional and spin glasses.[58]

Replica field theory

With this background, we return now to an analysis of the disordered electron system. The construction of the field integral begins with the representation of the replicated partition function as a coherent state field integral

$$\mathcal{Z}^R[J] = \int D(\bar\psi, \psi)\, \exp\left[-\sum_{a=1}^{R} S[\psi^a, \bar\psi^a, J] \right], \tag{6.46}$$

where $\psi^a, a = 1, \ldots, R$, denotes the Grassmann field representing partition function number a, $D(\bar\psi, \psi) \equiv \prod_{a=1}^{r} D(\bar\psi^a, \psi^a)$, and $S[\psi^a, \bar\psi^a, J] = S_0[\psi^a, \bar\psi^a] + S_{\rm int}[\psi^a, \bar\psi^a] + S_{\rm s}[\psi^a, \bar\psi^a, J]$. (Notice that the source J is the same for all replicas, i.e. it does not carry an index a.) Here

$$S_0[\bar\psi^a, \psi^a] = \sum_n \int d^d r\ \bar\psi_n^a(\mathbf{r}) \left(-i\omega_n - \frac{\nabla^2}{2m} - E_{\rm F} + V(\mathbf{r}) \right) \psi_n^a(\mathbf{r}), \tag{6.47}$$

[57] This uncertainty reflects disorder-generated correlations between the replicated systems. Since $\langle \mathcal{Z}^R \rangle_{\rm dis} \neq \langle \mathcal{Z} \rangle_{\rm dis}^R$, the function we wish to continue is not just a harmless power function.

[58] For a review of the industry of replica-based theoretical approaches in these fields we refer to the article by G. Parisi, Glasses, replicas and all that, in *Les Houches – Ecole d'Eté de Physique Théorique*, Vol. 77, ed. J.-L. Barrat *et al.* (Elsevier, 2004).

describes the non-interacting part of the disordered electron system (assumed, for simplicity, to be spinless), $S_{\rm int}$ specifies the bare particle interaction, and $S_{\rm s}$ is the source-dependent part of the action (whose structure we need not specify for the moment). Notice that, before averaging, the action is "replica diagonal," i.e. fields ψ^a and ψ^b, $a \neq b$, do not interact with each other.

Before proceeding with this expression, let us make one technical remark on the calculation of observables. Suppose we were interested in the expectation value of some operator which, in the non-replicated theory, assumes the form $\langle \mathcal{O} \rangle = -(\delta/\delta J) \ln \mathcal{Z}[J] = \langle \mathcal{O}(\bar{\psi}, \psi) \rangle_\psi / \langle 1 \rangle_\psi$. Here, J represents some suitably devised source and, in the last equality, $\mathcal{O}(\bar{\psi}, \psi)$ is the coherent state representation of the operator $\mathcal{O}$. The denominator $\langle 1 \rangle_\psi$ reminds us of the fact that a quantum thermal average involves an explicit normalization by the (functional) partition function. Within the replicated formalism, the same expectation value assumes the form

$$\boxed{\langle \mathcal{O} \rangle = -\lim_{R \to 0} \frac{1}{R} \frac{\delta \mathcal{Z}^R[J]}{\delta J} = \lim_{R \to 0} \frac{1}{R} \sum_{a=1}^{R} \langle \mathcal{O}(\bar{\psi}^a, \psi^a) \rangle_\psi,} \tag{6.48}$$

where the last equality follows from differentiating Eq. (6.46) with respect to the source J. Assuming that all observables are evaluated as in Eq. (6.48), we no longer need to keep an explicit reference to the source field J.

Now, let us average the functional (6.46) over the distribution (6.44). A straightforward application of the Gaussian integral formula (3.19) leads us to the result

$$\langle \mathcal{Z}^R[J] \rangle_{\rm dis} = \int D(\bar{\psi}, \psi) \, \exp \left[-\sum_{a=1}^{R} S_{\rm cl}[\psi^a, \bar{\psi}^a] - \sum_{a,b=1}^{R} S_{\rm dis}[\psi^a, \psi^b, \bar{\psi}^a, \bar{\psi}^b] \right],$$

where $S_{\rm cl} = S\big|_{V=0}$ denotes the action of the non-disordered system, and

$$S_{\rm dis}[\psi^a, \psi^b, \bar{\psi}^a, \bar{\psi}^b] \equiv -\frac{\gamma^2}{2} \sum_{mn} \int d^d r \; \bar{\psi}^a_m(\mathbf{r}) \psi^a_m(\mathbf{r}) \bar{\psi}^b_n(\mathbf{r}) \psi^b_n(\mathbf{r}), \tag{6.49}$$

represents an effective quartic interaction generated by the disorder average. Notice the superficial similarity between $S_{\rm dis}$ and an attractive short-range "interaction" term. However, in contrast to a dynamically generated interaction, (a) $S_{\rm dis}$ does not involve frequency exchanging processes (the reason being, of course, that the scattering off static impurities is energy conserving), and (b) it describes interactions between particles of a different replica index. To understand the physics behind the attractive inter-replica interaction, consider the potential landscape of a given impurity configuration (see the figure). Irrespective of their replica indices, all Feynman amplitudes will try to trace out those regions in configuration space where the potential energy is low, i.e. there will be a tendency to propagate through the same regions in the potential landscape. (Recall that all replica fields are confronted with the same potential profile.) On average, this looks as if the replica fields were subject to an attractive interaction mechanism.

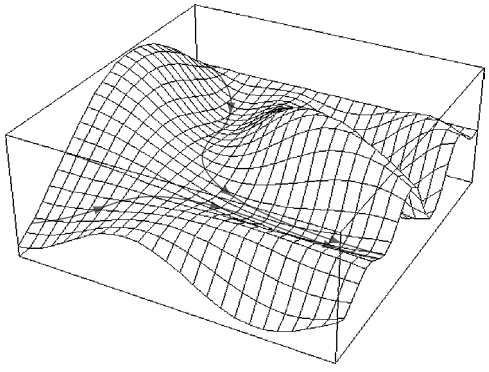

In summary, one may account for the presence of quenched or static disorder by (a) replicating the formalism, (b) representing observables as in Eq. (6.48), and (c) adding the replica non-diagonal contribution Eq. (6.49) to the action. This results in a theory wherein the disorder no longer appears explicitly. (Technically, the effective action has become translationally invariant.) The price to be paid is that the action now contains the non-linearity Eq. (6.49). This concludes our formulation of the quantum disorder problem as a functional integral. In the following section, we develop some intuition for the effects of disorder which draw on the formalism developed above.

Basic notions of impurity scattering

The most basic time scale characterizing the scattering of electrons from static impurities is the **elastic scattering time** τ. (Here the term "elastic" emphasizes that the scattering off static impurities may lead to the transfer of momentum but not of energy.) In the literature, the scattering time is often prematurely identified as the typical time of flight between neighboring impurities. However, this interpretation may be misleading. For example, a system may be (and often is) polluted by a dense accumulation of very weak scattering imperfections. In such cases, the scattering time may be parametrically larger than the time of flight. Similarly, the scattering may be from the shallow Coulomb potential created by impurities spatially separated from the conductor (a situation generically realized in semiconductor heterostructures). In such cases, impurity positions are themselves not even well-defined. How, then, can the scattering time be defined unambiguously? And how does it relate to the microscopic characteristics of the impurity potential?

To assimilate the general meaning of the scattering time, let us consider the quantum amplitude $U(\mathbf{y},\mathbf{x};t) = \langle \mathbf{y}|\exp(-i\hat{H}t)|\mathbf{x}\rangle$ for a particle to propagate from a point $\mathbf{x}$ to a point $\mathbf{y}$ in a time t for a particular realization of the disorder potential. One may think of this amplitude as the sum of all Feynman paths connecting the points $\mathbf{x}$ and $\mathbf{y}$. On its journey along each path, the particle may scatter (see Fig. 6.12), implying that the action of the path depends sensitively on the particular realization of impurities. For large separations, $|\mathbf{x}-\mathbf{y}|$, the scattering phase becomes a "quasi-random" function of the impurity configuration. The same applies, of course, to the linear superposition of all paths, the net amplitude U.

Let us now consider the impurity-averaged value of the transition amplitude $\langle U(\mathbf{x},\mathbf{y};t)\rangle_{\rm dis}$. As we are averaging over a superposition of random phases, one may expect that the disorder average will be translationally invariant and, as a result of the random phase cancellation, rapidly decaying, $\langle U(\mathbf{x},\mathbf{y};t)\rangle_{\rm dis} \sim \exp(-|\mathbf{x}-\mathbf{y}|/(2\ell))$. The decay constant ℓ of the averaged transition amplitude defines the **elastic mean free path** while the related time $\tau \equiv \ell/v_{\rm F}$ denotes the elastic scattering time. (We reiterate that only in systems of dilute strong scattering centers can this scale be identified with the average spacing between

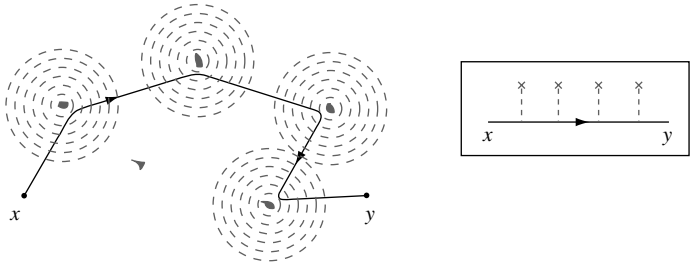

Figure 6.12 Showing the scattering of an electron off static imperfections. Inset: the corresponding Feynman diagram.

impurities.) In the following, we develop a quantitative description of this "damping" process.

Technically, it is most convenient to explore the behavior of the transition amplitude in the imaginary-time formalism. More specifically, we shall consider the imaginary-time Green function[59] $G(\mathbf{x},\mathbf{y};\tau) \equiv \langle \psi(\mathbf{x},\tau)\, \bar{\psi}(\mathbf{y},0)\rangle_\psi$, where the averaging is over the Grassmann action (6.47). (To keep the notation simple, we do not explicitly keep track of the normalizing denominator $\langle 1\rangle_\psi$ in our notation.) As usual, it will be convenient to perform the intermediate steps of the computation in frequency–momentum space. We thus represent the correlation function as

$$G(\mathbf{x},\mathbf{y};\tau) = \frac{T}{L^d} \sum_{\omega_n,\mathbf{p},\mathbf{p}'} e^{-i\omega_n\tau + i\mathbf{p}\cdot\mathbf{x} - i\mathbf{p}'\cdot\mathbf{y}} G_{\mathbf{p},\mathbf{p}';\omega_n}, \tag{6.50}$$

where ω_n is a fermionic Matsubara frequency and $G(\mathbf{p},\mathbf{p}';\omega_n) = \langle \psi_{n,\mathbf{p}} \bar{\psi}_{n\mathbf{p}'}\rangle_\psi$. (Keep in mind that, prior to the impurity average, the system lacks translational invariance, i.e. the Green function will depend on two independent momentum arguments.) Following the general prescription developed in Section 6.5, the correlation function averaged over a Gaussian disorder distribution is then given by (cf. Eq. (6.48))

$$\langle G_{\mathbf{p},\mathbf{p}',n}\rangle_{\rm dis} = \lim_{R\to 0} \frac{1}{R} \sum_{a=1}^{R} \langle \psi^a_{n,\mathbf{p}}\, \bar{\psi}^a_{n,\mathbf{p}}\rangle_\psi \delta_{\mathbf{p},\mathbf{p}'}, \tag{6.51}$$

where ψ^a is the ath component of the R-fold replicated field and $\langle\cdots\rangle_\psi$ now stands for the functional average with an action including the interaction term Eq. (6.49). (Exercise: Consider why the averaged Green function is diagonal in momentum space.) To keep the discussion simple, we shall ignore dynamical interactions (i.e. Coulomb interaction, etc.) between the particles and assume that the non-disordered part of the action $S[\psi^a,\bar{\psi}^a] = \sum_{n,\mathbf{p}} \bar{\psi}^a_{n,\mathbf{p}}(-i\omega_n + \frac{\mathbf{p}^2}{2m} - E_{\rm F})\psi^a_{n,\mathbf{p}}$ describes only free fermions.

In the remainder of this section, our objective is to explore the impact of the disorder generated interaction on the behavior of the Green function by means of diagrammatic

[59] Representing the transition amplitude for the creation of a particle at point $\mathbf{x}$ followed by an annihilation process at $\mathbf{y}$, this function generalizes the single-particle transition amplitude U to the presence of a continuum of particles; while all that has been said above about the disorder-generated attenuation remains valid.

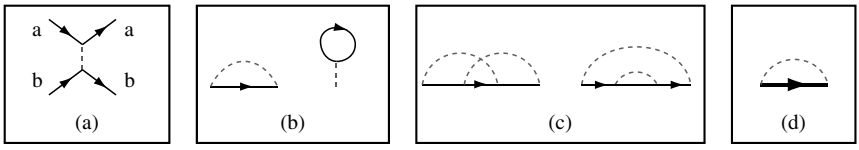

Figure 6.13 (a) Impurity scattering vertex, (b) the first-order self-energy diagrams, (c) the second-order self-energy diagrams, and (d) SCBA self-energy. With the last, the bold line represents the full Green function while the diagram states that the self-energy is computed neglecting all crossed lines (cf. the discussion in Section 5.3).

perturbation theory. As mentioned above, since the disorder problem presents a useful arena to practice the methods developed in the text we will outline the program as a sequence of assignments while the detailed solution is given below. Following the general arguments of Section 5.3, the principal object of interest is the impurity-generated self-energy operator Σ. Let us prepare the analysis of this object by introducing a bit of diagrammatic notation. We depict the impurity scattering vertex defining the action (6.49) as in Fig. 6.13(a).[60] As usual, setting $p = (\omega_n, \mathbf{p})$, the free-particle Green function $G_{0,p} \equiv (i\omega_n - \xi_{\mathbf{p}})^{-1}$ will be denoted by a fine (directed) line. Using this notation, and following the rules of diagrammatic perturbation theory developed in Chapter 5:

Q1: Consider the self-energy $\Sigma^{(1)}$ at first order in the impurity scattering (Fig. 6.13(b)). Show that the "Hartree-type" diagram (right) does not contribute (in the replica limit!). Compute the real and imaginary parts of the "Fock" (left) contribution to the self-energy. Show that, in dimensions $d \geq 2$, Re Σ actually diverges. Convince yourself (both formally and heuristically) that this divergence is an artefact of our modeling of the impurity potential by a δ-correlated function (see Eq. (6.44) and the related discussion). Consider what could be the reason for the real part of the self-energy not playing a very important role.

Q2: Turning to the second-order contribution $\Sigma^{(2)}$ (see Fig. 6.13(c)), convince yourself that, in dimensions $d > 1$, the diagram with crossed impurity lines is parametrically smaller than the second contribution. (What is the small parameter of the expansion?)

Q3: This motivates the computation of the self-energy in the self-consistent Born approximation (SCBA) (see Fig. 6.13(d)). Show that the SCBA equation can be approximately solved by the *ansatz* $\mathrm{Im}\,\Sigma(\omega_n) = -\mathrm{sgn}(\omega_n)/2\tau$, where τ is a constant. Once again, identify the small parameter of the expansion.

Q4: Put together, one thus obtains the impurity-averaged Green function $\langle G_p \rangle_{\mathrm{dis}} = (i\omega_n - \xi_{\mathbf{p}} + i\,\mathrm{sgn}(n)/2\tau)^{-1}$. Fourier transforming this result back to real time/space, justify the identification of the self-energy with (one half of) the inverse scattering time.

[60] In the diagrammatic literature, individual scattering events off the impurity potential $V(\mathbf{r})$ are traditionally depicted by dashed lines (see Fig. 6.12, inset). Once we average a product of such vertices, $V(\mathbf{r}_1)V(\mathbf{r}_2)\cdots V(\mathbf{r}_{2n})$, over the Gaussian disorder distribution (6.44), the coordinates $\{\mathbf{r}_i\}$ become pairwise identified in all possible combinations. This is usually indicated by connecting the corresponding vertex lines, i.e. a diagram with $2n$ dangling bonds becomes a sum of diagrams, each containing n interaction lines. In our pre-averaged replica field theory, we are using the corresponding interaction vertex from the outset.

Q5: Why is the replica method exact in perturbation theory?

A1: Unlike the Fock diagram, where all replica indices are locked to the index of the incoming Green functions, the Hartree diagram contains one free replica summation. This summation yields an excess factor R that, in the limit $R \to 0$, vanishes. For the same reason, all diagrams with closed fermion loops (loops connected to the external field amplitudes only by impurity lines or not at all) do not contribute to the expansion. Technically, the excluded contributions represent vacuum diagrams,[61] i.e. on the level of perturbation theory, the only[62] effect of the replica limit is the elimination of all vacuum processes. We have thus shown that the replica theory exactly simulates the effect of the normalizing partition function present in the denominator of the unreplicated theory (cf. the discussion of the linked cluster theorem in Section 5.1). This proves – all on the level of perturbation theory – the equivalence of the representations.

The representation of the disorder-generated interaction Eq. (6.49) in momentum space emphasizes the fact that the impurity scattering exchanges arbitrary momentum, but not frequency. A straightforward Wick contraction along the lines of our discussion in Section 5.3 then obtains the first-order contribution

$$\Sigma_p^{(1)} = \gamma^2 \sum_{\mathbf{p}'} G^{(0)}_{\mathbf{p}',n} \simeq \gamma^2 \int d\epsilon \, \frac{\nu(\epsilon)}{i\omega_n + E_F - \epsilon} \simeq \gamma^2 \mathrm{P} \int d\epsilon \, \frac{\nu(\epsilon)}{E_F - \epsilon} - i\pi\gamma^2 \nu \, \mathrm{sgn}\,(\omega_n),$$

where $\mathrm{P}\int$ stands for the principal value integral. For $d \geq 2$, the increase of the DoS $\nu(\epsilon)$ as a function of ϵ renders the real part of the self-energy formally divergent. This divergence is an immediate consequence of the unbounded summation over $\mathbf{p}'$ – which is an artefact of the model.[63] In any case, the real part of the self-energy is not of prime interest to us: all that $\mathrm{Re}\,\Sigma_{\mathbf{p}n} = \text{const.}$ describes is a frequency- and momentum-independent shift of the energy. This shift can be absorbed into a redefinition of the chemical potential and will not cause any observable effects. By contrast, the imaginary part $\mathrm{Im}\,\Sigma^{(1)}_{\mathbf{p},n} = -\pi\gamma^2\nu\,\mathrm{sgn}\,(\omega_n)$ describes the attenuation of the quasi-particle amplitude due to impurity scattering, a mechanism of great physical significance.

A2: The analysis of the second-order contribution $\Sigma^{(2)}$ parallels our discussion of the RPA in Chapter 5: the Green functions $G_{\mathbf{p}}$ are sharply peaked around the Fermi surface $|\mathbf{p}| = p_{\mathrm{F}}$. (Since the Matsubara index n in $p = (\mathbf{p}, n)$ is conserved in impurity scattering, we will not always write it out explicitly.) Representing the diagram with non-crossing lines in

[61] To understand this assertion, consider the non-replicated theory prior to the impurity average. Due to the absence of "real" interactions, any closed fermion loop appearing in the expansion must be a vacuum diagram. After taking the impurity average, the loop may become connected to the external amplitudes by an impurity line. However, it remains a vacuum loop and must cancel against the expansion of the normalization denominator, if we were crazy enough to formulate the numerator–denominator expansion of the theory explicitly.

[62] In a connected diagram, all replica indices are locked to the index a of the external field vertices. We thus obtain (symbolic notation) $\langle G\rangle_{\mathrm{dis}} \sim \lim_{R\to 0} \frac{1}{R} \sum_a \langle \psi^a \bar{\psi}^a \rangle \propto \lim_{R\to 0} \frac{R}{R} \times \text{const.} = \text{const.}$ where the factor of R results from the summation over a and we have used the fact that the correlation function $\langle \psi^a \bar{\psi}^a \rangle$ is independent of a (replica symmetry).

[63] In reality, the summation will be finite because either (a) there is an underlying lattice structure (i.e. the $\mathbf{p}'$-summation is limited to the Brillouin zone) or (b) the kernel $K(\mathbf{r})$ describing the profile of the impurity potential varies on scales large in comparison with the Fermi wavelength. In this latter case, its Fourier transform has to be added to the definition of the scattering vertex above. The presence of this function then limits the $\mathbf{p}'$-summation to values $|\mathbf{p}' - \mathbf{p}| < \xi^{-1} \ll p_{\mathrm{F}}$.

momentum space, one obtains $\Sigma^{(2)}_{\rm n.c.} \sim \sum_{\mathbf{p}_1,\mathbf{p}_2} [G^{(0)}_{\mathbf{p}_1}]^2 G^{(0)}_{\mathbf{p}_2}$, restricting both momenta to the Fermi surface, i.e. $|\mathbf{p}_1|, |\mathbf{p}_2| \simeq p_{\rm F}$. By contrast, the contribution with crossed lines takes the form $\Sigma^{(2)}_{\rm c.} \sim \sum_{\mathbf{p}_1,\mathbf{p}_2} G^{(0)}_{\mathbf{p}_1} G^{(0)}_{\mathbf{p}_2} G^{(0)}_{\mathbf{p}_2+\mathbf{p}-\mathbf{p}_1}$. Since all three momentum arguments have to be tuned to values close to $p_{\rm F}$, only one summation runs freely over the Fermi surface. To estimate the relative weight of the two contributions, we need to know the width of the "shell" centered around the Fermi surface in which the Green functions assume sizeable values. Since $|G| = [(E_{\rm F} - p^2/2m)^2 + ({\rm Im}\, G^{-1})^2]^{-1}$, the width of the Lorenzian profile is set by ${\rm Im}\, G^{-1}$. As long as we are working with the bare Green function, ${\rm Im}\, [G^{(0)}]^{-1} = \omega_n \propto T$ is proportional to the temperature. However, a more physical approach is to anticipate that impurity scattering will broaden the width ${\rm Im}\, [G^{(0)}]^{-1} \sim \tau^{-1}$ to a constant value (to be identified momentarily as the inverse scattering time). Then, the relative weight of the two diagrams can be estimated as $p_{\rm F}^{2(d-1)}/(p_{\rm F}(v_{\rm F}\tau)^{-1})^{d-1} = (p_{\rm F}\ell)^{d-1}$, where $\ell = v_{\rm F}\tau$ is the elastic mean-free path, and the numerator and denominator estimate the volume in momentum space accessible to the $\mathbf{p}_{1,2}$ summations in the two diagrams. The important message to be taken away from this discussion is that, for weak disorder $p_{\rm F} \gg \ell^{-1}$ (which we have assumed throughout), and in dimensions $d > 1$, scattering processes with crossed impurity lines are negligible. Under these conditions, we are entitled to evaluate the self-energy (and, for that matter, all other observables) within the self-consistent Born, or non-crossing, approximation, i.e. an approximation that neglects processes with crossed "interaction" lines.

A3: Drawing on the analogous discussion in Section 5.3, the SCBA for the self-energy is given by the diagram shown in Fig. 6.13(d). The corresponding analytical expression takes the form (cf. Eq. (5.40))

$$\Sigma_{\mathbf{p},n} = \gamma^2 L^{-d} \sum_{\mathbf{p}'} \frac{1}{i\omega_n + E_{\rm F} - p'^2/2m - \Sigma_{\mathbf{p}',n}}. \tag{6.52}$$

Guided by our results obtained in the first order of perturbation theory, we may seek a solution of (the imaginary part of) this equation by the *ansatz* ${\rm Im}\, \Sigma_{\mathbf{p},n} = -\frac{1}{2\tau}{\rm sgn}(\omega_n)$. Substitution of this expression into the SCBA equation gives

$$-\frac{1}{2\tau}{\rm sgn}(\omega_n) \simeq \gamma^2 {\rm Im} \int d\epsilon\, \frac{\nu(\epsilon)}{i\omega_n + E_{\rm F} - \epsilon + \frac{i}{2\tau}{\rm sgn}(\omega_n)} \simeq -\pi\gamma^2\nu\, {\rm sgn}\,(\omega_n),$$

where we have assumed that $E_{\rm F}\tau \gg 1$. We have thus arrived at the identification of $\tau^{-1} = 2\pi\nu\gamma^2$ as the elastic scattering rate. (In the literature, the potential strength $\gamma^2 = 1/(2\pi\nu\tau)$ is usually *defined* through the scattering time, i.e. the parameter γ^2 is expressed through τ from the outset.) Summarizing, we have obtained the important result

$$\boxed{\langle G_p \rangle_{\rm dis} = \frac{1}{i\omega_n + E_{\rm F} - \frac{p^2}{2m} + \frac{i}{2\tau}{\rm sgn}(\omega_n)}.} \tag{6.53}$$

A4: To compute the inverse Fourier transform of Eq. (6.50) one may trade the frequency summation for a complex contour integral. Taking account of the fact that the Green function has a cut along the entire real frequency axis (the non-analyticity of ${\rm sgn}(\omega_n) \to$

$\mathrm{sgn}(\mathrm{Im}\, z)$ at $\mathrm{Re}\, z = 0$), we chose the integration contour as shown in the figure. This leads us to the representation

$$\langle G(\mathbf{x},\mathbf{y};\tau)\rangle_{\mathrm{dis}} = \sum_{\mathbf{p}} \int \frac{d\epsilon}{2\pi}\, e^{-\epsilon\tau}(1-n_{\mathrm{F}}(\epsilon)) e^{i\mathbf{p}\cdot(\mathbf{x}-\mathbf{y})} \times \mathrm{Im} \frac{1}{E_{\mathrm{F}} + \epsilon - \frac{p^2}{2m} + \frac{i}{2\tau}}.$$

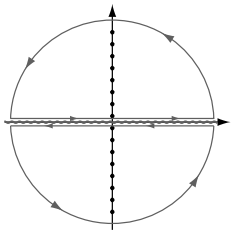

Here, we are using $1 - n_{\mathrm{F}}$ instead of n_{F} as a pole function because $e^{-z\tau}(1-n_{\mathrm{F}}(z))$ is finite for large $|z|$, whereas $e^{-z\tau}n_{\mathrm{F}}(z)$ is not. It is now a straightforward matter to compute this expression by first (a) integrating out the angular degrees of freedom of $\mathbf{p}$ followed by (b) a contour integration over p (cf. the analogous calculation of the clean Green function in the exercise at the end of section 5.1). However, as we require only the asymptotic effect of the damping, we may follow a more efficient route: the essential effect of the damping term is to shift the poles of the p-integration from the real axis into the complex plane. Equating the Green function denominator to zero and neglecting the parameter ϵ ($\epsilon \ll E_{\mathrm{F}}$ as long as the time parameter $\tau \gg E_{\mathrm{F}}^{-1}$ is not extremely small), we find that the poles are located at $p = p_{\mathrm{F}} \pm \frac{i}{2\ell}$. The essential effect of this shift is that the exponentials $\exp(ip|\mathbf{x}-\mathbf{y}|)$ have to be evaluated at the residues $\exp(ip_{\mathrm{F}}|\mathbf{x}-\mathbf{y}| - |\mathbf{x}-\mathbf{y}|/(2\ell))$. Consequently, the disorder averaged Green function is related to the Green function of the clean system G_{cl} by the exponential damping factor which we had surmised above,

$$\langle G(\mathbf{x},\mathbf{y};\tau)\rangle_{\mathrm{dis}} = G_{\mathrm{cl}}(\mathbf{x},\mathbf{y};\tau) e^{-|\mathbf{x}-\mathbf{y}|/2\ell}.$$

A5: We refer to the discussion in **A1**.

This completes our discussion of the impurity-averaged single-particle Green function $\langle G(\mathbf{x},\mathbf{y};\tau)\rangle_{\mathrm{dis}}$. The latter has been shown to be short-range on the scale of the elastic mean free path ℓ. In the following section, we shall see that, by contrast, the impurity-averaged two-particle Green function acquires long-range correlations which encode the modes of density relaxation and provide a means to explore mechanisms of quantum interference which characterize the mesoscopic regime.

Diffusion

How do local fluctuations in the electron density $\delta\hat{\rho}(\tau,\mathbf{r}) \equiv \hat{\rho}(\tau,\mathbf{r}) - \langle\hat{\tau},\rho(\mathbf{r})\rangle$ relax in a disordered environment?[64] In a classical disordered system, this relaxation mechanism would be diffusive. Below, we shall see that the same characteristic behavior survives in the quantum picture. Formally, this is achieved by exploring the correlation function $D(\tau,\mathbf{r}) \equiv$

[64] Notice that the brackets $\langle\cdots\rangle$ represent the quantum average, and not yet the disorder average.

$\langle\langle \delta\hat{\rho}(\tau,\mathbf{r})\delta\hat{\rho}(0,0)\rangle\rangle_{\rm dis}$, i.e. a function that describes how $\delta\hat{\rho}(\tau,\mathbf{r})$ changes in response to a density fluctuation at $(\mathbf{r}=0,\tau=0)$.

EXERCISE In a real time formulation, how is the correlation function D related to the quantum transmission probability density?

INFO The diffusive relaxation process described by the function D extends over distances much larger than the decay length of the average single-particle Green function, ℓ. To identify the mechanism that underlies the stability of the four-point function, think of $D(\tau,\mathbf{r}) = \langle\langle\bar{\psi}(\tau,\mathbf{r})\psi(0,0)\rangle\,\langle\psi(\tau,\mathbf{r})\bar{\psi}(0,0)\rangle\rangle_{\rm dis}$ as the product of the amplitudes for (a) the annihilation of a particle at space-time coordinate $(0,0)$ followed by particle creation at $(\tau,\mathbf{r})$ and (b) the creation of a particle at $(0,0)$ followed by its annihilation at $(\tau,\mathbf{r})$.[65] The annihilation process initiating (a) may be interpreted alternatively as the creation of a hole, i.e. the composite process D describes the joint propagation of a particle and a hole amplitude through the medium (which explains why D is sometimes called the **particle–hole propagator**).

Now, against this background, let us temporarily switch to a real time description $\tau \to it$ and draw on the intuition afforded by the consideration of Feynman amplitudes. Specifically, let us consider the particle propagator as the sum of all Feynman paths α connecting 0 and $\mathbf{r}$ (see Fig. 6.14). Similarly, the hole amplitude corresponds to a path-sum over all paths where each path β is weighted by the negative of its classical action.[66] We thus have the symbolic representation

$$D \sim \int d\epsilon\, d\epsilon' \sum_{\alpha\beta} A_\alpha A_\beta^* \exp\left[\frac{i}{\hbar}(S_\alpha(\epsilon) - S_\beta(\epsilon'))\right],$$

where the notation emphasizes that the electron and hole have different energies ϵ, ϵ'. As with the single-particle propagator, the strong sensitivity of the actions $S_{\alpha,\beta}$ on the impurity potential implies that generic contributions (α,β) to the path double sum vanish upon impurity averaging. However, the "diagonal" contribution (α,α) to the sum, $D_{\rm diag} \sim \sum_\alpha |A_\alpha|^2 \exp(\frac{i}{\hbar}(S_\alpha(\epsilon) - S_\alpha(\epsilon')))$, depends only weakly on the impurity potential, and will likely survive the averaging procedure.

A glance at Fig. 6.14 (b) suggests that the diagonal contribution to D is but an elaborate quantum description of classical diffusion: two quantum amplitudes locally tied together, and propagating in a stochastic environment, should be capable of interpretation as a classically diffusive probability density. Indeed, this interpretation is corroborated by the fact that, upon approaching the classical limit $\hbar \to 0$, the dominance of the diagonal approximation becomes more pronounced.

However, notice that, beyond the straightforward diagonal configuration, there are other contributions to the double path sum that are likely to be impervious to configurational averaging. For example, the two paths depicted in Fig. 6.14 (c) are globally different but locally paired. The former attribute tells us that we are dealing with a fundamentally non-classical contribution to the correlation function, and the latter that the action difference $S_\alpha - S_\beta$ will be small. Indeed,

[65] To understand the positioning of the quantum-thermal averaging brackets, consider the definition of D in terms of the operators $\delta\hat{\rho}$, and take into account the fact that, of the two possible Wick contractions, one gets canceled due to the subtraction of $\langle\hat{\rho}\rangle$.

[66] Heuristically, the inversion of the sign of the action accounts for the fact that a hole is a "missing" electron. More formally, it follows from the fact that the hole amplitude is obtained by complex conjugation of the particle amplitude.

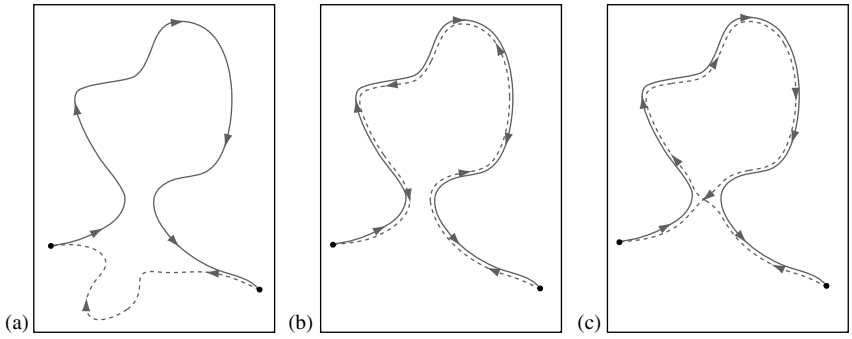

Figure 6.14 (a) A generic pair of Feynman paths contributing to the density–density correlation function prior to averaging. (b) Particle and hole propagating along the same path in configuration space – the "diffuson." (c) A non-classical contribution to the path sum.

we shall see that processes like the one shown here lie at the root of the observed quantum phenomena that characterize the physics of disordered media.

Below, we apply concepts very similar to those developed in Section 5.3 to understand the spatial long-range character of the four-point function. Further, we wish to elucidate the diffusive character of this correlation function.

Q1: Before turning to explicit computations, let us derive two exact relations obeyed by the Fourier transform $D_{\mathbf{q},\omega_m}$: Show that $\lim_{\mathbf{q}\to 0} D_{\mathbf{q},0} = L^{-d}\partial_\mu N$ and $D_{0,\omega_m} = 0$, where $N = \langle \hat{N} \rangle_\psi$ denotes the number of particles in the system and, as usual, $\mu \leftrightarrow E_{\rm F}$ represents the chemical potential. Explain the origin of these two sum rules.

Q2: Represent the four-point function in a momentum–frequency form similar in structure to that of the correlation function $C^{(4)}$ introduced in Eq. (5.41). (Hint: It is convenient to represent the correlation function as $D(x) = \delta^2_{\mu(x)\mu(0)} \langle \ln \mathcal{Z} \rangle_{\rm dis}|_{\mu(x)=\mu}$, where $x \equiv (\tau, \mathbf{r})$, and $\mu(x) = \mu(\tau, \mathbf{r})$ is the generalization of the chemical potential to a space-time-dependent source field.)

Q3: To compute the two-particle correlation function, one may apply concepts similar to those introduced in Section 5.3. In doing so, we will benefit from two major simplifications. Assuming that $(p_{\rm F}\ell)^{-1} \ll 1$, we will work to leading order in this parameter ($p_{\rm F}\ell \gg 1$ plays a role similar to that of the large parameter N in Section 5.3). Secondly, we may make use of the fact that the momentum $\mathbf{q}$ Fourier conjugate to the argument $|\mathbf{r}| \gg \ell$ is much smaller than the Fermi momentum. Show that, under these conditions, the irreducible vertex, $\Gamma_{0,q,p,p'} = (2\pi\nu\tau)^{-1}\delta_{\omega_n,\omega'_n}$, collapses to (the Fourier representation of) a single impurity vertex. (Since all field amplitudes that contribute in the replica limit carry the same replica index a, one may drop the replica structure from the notation.) Write down the Bethe–Salpeter equation for the full vertex.

Q4: Solve the Bethe–Salpeter equation to leading order in $(p_{\rm F}\ell)^{-1}$ (note $|\mathbf{q}|\ell \ll 1$). (Hint: Notice that the two cases $\omega_n \cdot \omega_{n+m} < 0$ and $\omega_n \cdot \omega_{n+m} > 0$ behave in radically differ-

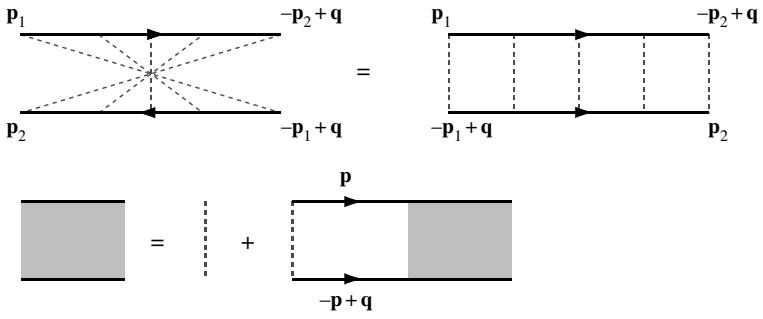

Figure 6.15 Maximally crossed contribution to the irreducible vertex. Second line: the corresponding Bethe–Salpeter equation. In all diagrams, the upper (lower) Green functions carry frequency ω_{n+m} (ω_n).

ent manners.) Use your result for the irreducible vertex to compute the density–density correlation function.

Q5: Referring to Fig. 6.14(c), the diagram suggests that a particle–hole pair propagating along the same path in a disordered medium may split up, propagate along a closed loop in opposite directions, and later recombine. Provided that the action for traversal of a scattering path in the medium does not depend on the direction of propagation, one may expect the classical action difference of the composite process to be small.[67] How would these processes – known as cooperon-modes, or just **cooperons**[68] in the literature – manifest themselves in the present formalism? The cooperon describes a process wherein the two constituent partners propagate with near opposite momenta. Indeed, it turns out that, for $\mathbf{p}_1 \simeq -\mathbf{p}_2$, the irreducible vertex contains a second contribution (besides the isolated impurity line) of more complex structure: a sum over diagrams with "maximally crossed" impurity lines (see Fig. 6.15). This diagram, too, contains one Fermi sphere summation per impurity line. The most economic way to see this is to imagine the lower of the two fermion propagators twisted by 180° (the second diagram in the figure). Superficially, it now resembles the previously explored vertex. The important difference, however, is that the arrows marking the fermion propagators now point in the same direction, i.e. as compared with the particle–hole mode discussed above, the relative sense of traversal of the impurity sequence became reversed.

Compute the cooperon contribution to the irreducible vertex. Discuss what would happen if the system was exposed to an external magnetic field. In spite of its structural similarity to the "diffuson mode" identified in Q4, why does the insertion of a single cooperon into the diffusive correlation function not give rise to a large correction?

[67] Formally, the directional invariance of the action requires that the system is invariant under **time-reversal**. Time-reversal symmetry would be lost, for example, if the system were subject to an external magnetic field. In this case, the classical probability for propagation along a path depends on the sense of traversal.

[68] The origin of the terminology "cooperon" is that these modes describe the dynamics of a two-particle process where the two constituents propagate in opposite direction (in analogy to the opposite momenta of the two electrons of a Cooper pair).

A1: The functional expectation value of the particle number is given by $\langle N\rangle = \int d\tau\, d^dr\, \langle\hat\rho(\mathbf{r},\tau)\rangle_\psi = \int d^dr\, \langle\hat\rho_{\omega_m=0}(\mathbf{r})\rangle_\psi$. Differentiating this expression with respect to μ, and noting that the chemical potential couples to the action through $\mu\int d^dr\int d\tau\hat\rho(\mathbf{r},\tau)$, one obtains[69]

$$\begin{aligned}\partial_\mu\langle N\rangle &= \int d^dr\, d^dr'\, [\langle\hat\rho_0(\mathbf{r})\hat\rho_0(\mathbf{r}')\rangle_\psi - \langle\hat\rho_0(\mathbf{r})\rangle_\psi\langle\hat\rho_0(\mathbf{r}')\rangle_\psi]\\ &= \int d^dr\, d^dr'\, D_{\omega_n=0}(\mathbf{r}-\mathbf{r}') = L^d\lim_{\mathbf{q}\to 0} D_{\mathbf{q},0}.\end{aligned}$$

Particle number conservation demands that $\int d^dr\,\langle\delta\hat\rho(\mathbf{r},\tau)\rangle_\psi = 0$ at all times. Consequently, $\int d^dr\, D(\mathbf{r},\tau) = 0$ or, equivalently, $D_{\mathbf{q}=0,\omega_m} = 0$.

A2: It is straightforward to verify that the two-fold μ-differentiation suggested above yields the correlation function D. Now, let us employ the replica formulation $\langle\ln\mathcal{Z}\rangle_{\rm dis} = \lim_{R\to 0}\frac{1}{R}\langle\mathcal{Z}^R - 1\rangle$. Differentiating the right-hand side of this equation, one obtains

$$D(x) = \lim_{R\to 0}\frac{1}{R}\langle\bar\psi^a(x)\psi^a(x)\bar\psi^b(0)\psi^b(0)\rangle_\psi.$$

To avoid the vanishing of this expression in the limit $R\to 0$, we need to connect operators $\bar\psi^a$ and ψ^b ($\bar\psi^b$ and ψ^a) by fermion lines (thus enforcing $a = b$ – otherwise the two-fold summation over a and b would produce an excessive factor R which would result in the vanishing of the expression in the replica limit). We thus obtain a structure similar to that discussed in Section 5.3 (cf. Fig. 6.16): two propagators connecting the points x and 0, where the role of the wavy interaction line of Section 5.3 is now played by the "interaction" generated by the impurity correlator $\langle VV\rangle$.

As in Section 5.3, it will be convenient to formulate the diagrammatic analysis of the correlation function in momentum space. We thus substitute the Fourier decomposition $\psi^a(x) = (T/L^d)^{1/2}\sum_p e^{-ip\cdot x}\psi^a_p$ into the definition of D, make use of the fact that $\langle\bar\psi^a_{p_1}\psi^a_{p_1+q}\bar\psi^a_{p_2+q'}\psi^a_{p_2}\rangle \propto \delta_{qq'}$ (momentum conservation in the averaged theory), and obtain $D(x) = \frac{T}{L^d}\sum_q e^{iq\cdot x}D_q$, where $D_q = \frac{T}{L^d}\lim_{R\to 0}R^{-1}\sum_{p_1p_2}\langle\bar\psi^a_{p_1}\psi^a_{p_1+q}\bar\psi^a_{p_2+q}\psi^a_{p_2}\rangle_\psi$. The impurity interaction is static, implying that the fermion frequency is conserved along each propagator: $\omega_{n'} = \omega_n$, i.e.

$$D_q = \frac{T}{L^d}\lim_{R\to 0}\frac{1}{R}\sum_{\omega_n}\sum_{\mathbf{p}_1\mathbf{p}_2}\langle\bar\psi^a_{\mathbf{p}_1,\omega_n}\psi^a_{\mathbf{p}_1+\mathbf{q},\omega_{n+m}}\bar\psi^a_{\mathbf{p}_2+\mathbf{q},\omega_{n+m}}\psi^a_{\mathbf{p}_2,\omega_n}\rangle_\psi. \tag{6.54}$$

A3: Only diagrams that contain one free summation over the Fermi surface per impurity line contribute to leading order in $(p_{\rm F}\ell)^{-1}$. (Formally, this is because each impurity line contributes a factor $\gamma^2\sim(\nu\tau)^{-1}$ and the phase volume of a momentum summation over the Fermi surface is needed to compensate the density of states factor ν in the denominator.) As in our discussion of the self-energy, this implies that diagrams with crossed impurity lines do not contribute to the irreducible vertex. (The only irreducible contribution without

[69] From the expressions above it is, in fact, not quite clear why we set first $\omega_n = 0$ and only then $\mathbf{q} = 0$. That this is the correct order of limits can be seen by generalizing $\mu\to\mu(\mathbf{r})$ to a smoothly varying static field, evaluating the corresponding functional derivatives $\delta/\delta\mu(\mathbf{r})$, and setting $\mu =$ const. at the end of the calculation.

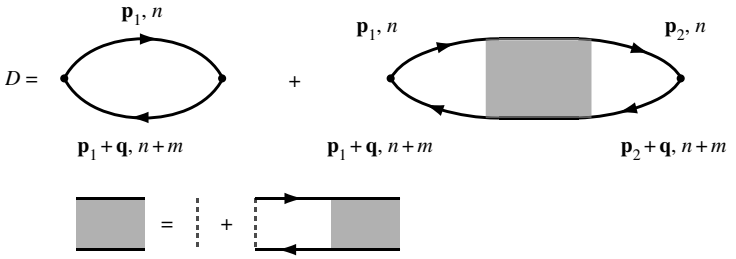

Figure 6.16 Diagrammatic expansion of the diffuson mode.

crossings is the single impurity line.) Consequently, the diagrammatic expansion of the correlation function assumes a form shown in Fig. 6.16. The Bethe–Salpeter equation for the impurity vertex (shaded in the figure) reads

$$\Gamma_{p_1,p_2,q} = \frac{1}{2\pi L^d \nu\tau} + \frac{1}{2\pi L^d \nu\tau} \sum_{\mathbf{p}} G_{\mathbf{p}+\mathbf{q},n+m} G_{\mathbf{p},n} \Gamma_{p,p_2,q}, \tag{6.55}$$

where the Gs denote the impurity-averaged single-particle Green functions evaluated in the SCBA and discussed in the previous section.

A4: The correlation function D contains a summation over frequency. Assuming that $\omega_m > 0$, let us organize the sum as $D = D^{++} + D^{+-} + D^{--}$, where D^{++}, D^{+-}, and D^{--} denote, respectively, the contributions where $\{\omega_n, \omega_{n+m}\} > 0$, $\{\omega_{n+m} > 0, \omega_n < 0\}$, and $\{\omega_n, \omega_{n+m}\} < 0$. We begin by considering the most interesting term D^{+-}. Introducing the notation $G^{\pm}_{\mathbf{p}} \equiv (E_{\mathrm{F}} - p^2/2m \pm i/2\tau)^{-1}$, one may expand the integrand appearing in the Bethe–Salpeter equation to leading order in the small[70] energies ω_n, ω_{n+m} and $\mathbf{q}\cdot\mathbf{p}/m$, and obtain

$$G_{p+q} G_p = G^+_{\mathbf{p}} G^-_{\mathbf{p}} \left(1 - iG^+_{\mathbf{p}}\omega_{n+m} - iG^-_{\mathbf{p}}\omega_n + (G^+_{\mathbf{p}}\mathbf{q}\cdot\mathbf{p}/m)^2 + \cdots\right), \tag{6.56}$$

where a term linear in $\mathbf{q}$ has been omitted as it will vanish upon integration over the angular coordinates of $\mathbf{p}$. We next make the assumption (to be checked self-consistently) that, for small $\mathbf{q}$, the vertex $\Gamma = \Gamma_q$ does not depend on the "fast" momenta $\mathbf{p}, \mathbf{p}'$. The integration over $\mathbf{p}$ – now decoupled from the vertex – can then be made with the help of two auxiliary identities:[71] $\int d^d p\, f(|\mathbf{p}|)(\mathbf{v}\cdot\mathbf{p})^2 = \frac{v^2}{d}\int d^d p\, f(|\mathbf{p}|)\mathbf{p}^2$ and

$$L^{-d} \sum_{\mathbf{p}} \left[G^+_{\mathbf{p}}\right]^{n_+ +1} \left[G^-_{\mathbf{p}}\right]^{n_- +1} = 2\pi i^{n_- - n_+} \frac{(n_+ + n_-)!}{n_+!\, n_-!} \nu\tau^{n_+ + n_- + 1}.$$

[70] The inequality $\omega_n\omega_{n+m} < 0$ implies that $|n| < |m|$. Thus $|\omega_n|, |\omega_m| \ll \tau^{-1}$, where it is assumed that the frequencies we are probing are much smaller than the scattering rate.

[71] This can be checked by writing $\mathbf{v}\cdot\mathbf{p} = v_i p_i$ and using the symmetry of the integrand under the operations $p_i \to -p_i$ and $p_i \to p_j$.

The last identity is proven by converting the momentum sum into an integral, which is then performed by contour integration (exercise). Substituting the expansion (6.56), and employing the two auxiliary identities, one arrives at the relation

$$\Gamma_q = \frac{1}{2\pi\nu\tau}\left(L^{-d} + 2\pi\nu\tau\left[1 - \tau\omega_m - q^2\frac{\tau^2 v_{\rm F}^2}{d}\right]\Gamma_q\right).$$

Solving this equation for Γ_q, we obtain our final result for the vertex,

$$\Gamma_q = \frac{1}{2\pi\nu\tau^2 L^d}\frac{1}{\omega_m + Dq^2},$$

where $D = v_{\rm F}\ell/d$ defines the **diffusion constant** of a dirty metal.

A few remarks about this result are in order. Firstly, one may note that the absence of $(\mathbf{q}, \omega_m)$-independent constants in the denominator results from a cancellation of two terms in the vertex equation. (We have met with a similar cancellation in our discussion of the vertex of the generalized ϕ^4-theory in Chapter 5.) Thanks to this cancellation, $\Gamma(\mathbf{r}, \tau)$ becomes a long-range object. Later, we will identify the absence of damping or mass-like terms in the denominator as a consequence of a fundamental symmetry in the problem. Secondly, one may note that Γ is a solution of the diffusion equation $(\partial_\tau - D\nabla^2)\Gamma(\tau, \mathbf{r}) = (2\pi L^d\tau^2)^{-1}\delta^d(\mathbf{r})\delta(\tau)$ (exercise), describing the manner in which a distribution initially centered at $\mathbf{x} = 0$ spreads out in time. Alluding to this analogy, the vertex Γ has become known as the **diffuson**. However, more important than the terminology is the fact that we have succeeded in making the connection between particle–hole propagation in a dirty medium and classical diffusive processes quantitative.

To finalize our calculation of the four-point function we need only add external Green functions to the vertex (see Fig. 6.16), add the first diagram (the empty bubble) shown in the figure, and integrate over the momenta $\mathbf{p}_1, \mathbf{p}_2$. Expanding the corresponding Green functions to zeroth order in $\mathbf{q}, \omega_n, \omega_{n+m}$ (cf. Eq. (6.56)) and using the auxiliary identity above, one obtains

$$D_q^{+-} = -T\sum_{-\omega_m < \omega_n < 0}\left(2\pi\nu\tau + \frac{(2\pi\nu\tau)^2}{2\pi\nu\tau^2}\frac{1}{\omega_m + Dq^2}\right) \simeq -\frac{\nu\omega_m}{\omega_m + Dq^2},$$

where, in the first equality, the factors $2\pi\nu\tau$ stem from the momentum integration over pairs of Green functions, and the second equality holds under the presumed conditions $\omega_m, Dq^2 \ll \tau^{-1}$. (The overall minus sign comes from the fact that we are computing a closed fermion loop.)

To complete the analysis, we need to compute the expressions $D^{++/--}$. The analysis of these objects is fairly simple inasmuch as the vertex actually collapses to a single impurity line. Since the two Green functions over which the sum in Eq. (6.55) is performed now have imaginary parts of the same sign, the contour integration over $|\mathbf{p}|$ gives zero. Similarly, the placement of the residual single-impurity line vertex into the second diagram of Fig. 6.16 leads to a vanishing contribution. Since the sum over $|\mathbf{p}_1|, |\mathbf{p}_2|$ extends over Green functions with imaginary parts of the same sign, one would be tempted to say that, for the same reasons, the empty bubble diagram ought to vanish. However, this is not the case: the tricky

point is that, with regard to the first diagram, one must keep an eye on the frequency summation. Considering D^{++}, all other diagrams correspond to frequency sums $\sum_{\omega_n>0} F(\omega_n)$, where $F(\omega_n) \overset{n\gg 1}{\sim} n^{-k}$ [4]. However, the first diagram leads to an expression with only $k = 2$. This means that, after the frequency summation, one obtains a **p**-dependent expression that does not converge quickly enough to qualify for a safe contour integration procedure.[72] To be specific:

$$\begin{aligned} D_q^{++} \simeq -\frac{T}{L^d}\sum_{\mathbf{p}}\sum_{\omega_n>0}\frac{1}{(i\omega_n - \xi_{\mathbf{p}} + \frac{i}{2\tau})^2} &= \frac{1}{2\pi i L^d}\sum_{\mathbf{p}}\int_{-\infty}^{\infty}\frac{d\epsilon\, n_{\mathrm{F}}(\epsilon)}{(\epsilon - \xi_{\mathbf{p}} + \frac{i}{2\tau})^2} \\ &\simeq -\frac{1}{2\pi i L^d}\sum_{\mathbf{p}}\frac{1}{\epsilon - \xi_{\mathbf{p}} + \frac{i}{2\tau}}, \end{aligned}$$

where, as usual, $\xi_{\mathbf{p}} = \mathbf{p}^2/2m - E_F$ and the frequency summation has been performed by integrating over the real axis and closing in the upper complex half plane, and in the last equality we have approximated $n_{\mathrm{F}}(\epsilon) \simeq \Theta(-\epsilon)$. Similarly, an analogous computation obtains $D^{--} = (D^{++})^*$, i.e.

$$D^{++} + D^{--} = \frac{i}{2\pi L^d}\sum_{\mathbf{p}}\frac{1}{\epsilon - \xi_{\mathbf{p}} + \frac{i}{2\tau}} + \text{c.c.} = -\frac{1}{\pi}\int d\epsilon\ \mathrm{Im}\frac{\nu(\epsilon)}{E_F - \epsilon + i/2\tau} \simeq \nu.$$

Combining everything, we arrive at the final result,

$$D_q = D_q^{++} + D_q^{+-} + D_q^{--} = \nu\left(1 - \frac{|\omega_m|}{|\omega_m| + Dq^2}\right) = \nu\frac{Dq^2}{|\omega_m| + Dq^2}.$$

(Here we have used the fact that the result does not change under sign inversion of ω_m. Enthusiastic readers may wish to check this claim.) Summarizing, we have thus found that the density–density correlation function assumes the form

$$D(\mathbf{r}, \tau) = \frac{T}{L^d}\sum_{\mathbf{q},\omega_m} e^{i\mathbf{q}\cdot\mathbf{r} + i\omega_m\tau}\frac{\nu D q^2}{|\omega_m| + Dq^2}.$$

This result makes the diffusive character of the density–density correlation function manifest. Notice also that D_q obeys the two limiting conditions discussed in (A1). (Indeed, for a non-interacting fermion system, $\nu = L^{-d}\partial_\mu N$.)

A5: Let us now consider the irreducible vertex in a sector in momentum space where the sum of the upper incoming momentum, $\mathbf{p}_1$, and lower incoming momentum, $-\mathbf{p}_1 + \mathbf{q}$, is small. (Momentum conservation then implies that the upper outgoing momentum, $\mathbf{p}_2$, and lower outgoing momentum, $-\mathbf{p}_2 + \mathbf{q}$, also sum to the small offset $\mathbf{q}$.) Further, let us assume that the Matsubara frequencies ω_n and ω_{n+m} carried by the upper and lower propagators are of opposite signs. Now, imagine the lower line is turned around in such a way that the diagram assumes the form of a ladder structure (still it remains "irreducible" because the notion of

[72] Indeed, the $|\mathbf{p}|$-summation only *approximately* extends over the entire real axis. We are thus well advised to do the frequency summation (which has true semi-infinite support) prior to the momentum summation.

irreducibility has been defined for fermion lines of opposite orientation). The corresponding Bethe–Salpeter equation takes the form

$$\Gamma^{\mathrm{C}}_q = \frac{1}{2\pi\nu\tau L^d} + \frac{1}{2\pi\nu\tau L^d}\sum_{\mathbf{p}} G_{-\mathbf{p}+\mathbf{q},n_1+m} G_{-\mathbf{p},n_1}\Gamma^{\mathrm{C}}_q,$$

where Γ^{C} is the cooperon contribution to the irreducible vertex, and we have assumed that, for small external momenta, Γ^{C} is independent of the "fast" momenta. In the absence of an external magnetic field, $G_{-\mathbf{p}} = G_{\mathbf{p}}$ is even, i.e. the Bethe–Salpeter equation coincides exactly with Eq. (6.55) for the diffusion mode considered above. Consequently, we may infer that

$$\Gamma^{\mathrm{C}}_{\mathbf{q},\omega_m} = \frac{1}{2\pi\nu\tau L^d}\frac{1}{|\omega_m| + Dq^2}.$$

However, in the presence of a magnetic field, the inversion symmetry is lost. Let us, for a moment, assume that the vector potential $\mathbf{A}$ representing the magnetic field depends only weakly on its spatial coordinate. Neglecting commutators between the momenta and the vector potential, and defining $G_{\mathbf{p}}(\mathbf{A}) = (i\omega_n + E_{\mathrm{F}} - (\mathbf{p}+\mathbf{A})^2/2m + i/2\tau\,\mathrm{sgn}(\omega_n))^{-1}$, ($e = c = 1$), one may then shift the fast momentum to obtain $G_{\mathbf{p}+\mathbf{q}}(\mathbf{A})G_{-\mathbf{p}}(\mathbf{A}) = G_{\mathbf{p}+\mathbf{q}}(\mathbf{A})G_{\mathbf{p}}(-\mathbf{A}) \xrightarrow{\mathbf{p}\to\mathbf{p}-\mathbf{A}} G_{\mathbf{p}+\mathbf{q}}(2\mathbf{A})G_{\mathbf{p}}(0) = G_{\mathbf{p}+\mathbf{q}-2\mathbf{A}}(0)G_{\mathbf{p}}(0)$. In this way, one may see that the magnetic field can be absorbed into a redefinition of the momentum difference $\mathbf{q}$. In the presence of an external magnetic field, the cooperon then acquires the form

$$\Gamma^{C}_{\hat{q}} = \frac{1}{2\pi\nu\tau L^d}\frac{1}{|\omega_m| + D(\mathbf{q}+2\mathbf{A})^2}.$$

The notation here emphasizes that the simplified argument above generalizes to fields with arbitrary (yet smooth on the scale of the microscopic mean free path) space dependence. In that case, Γ^{C} is defined as the solution of the equation $(|\omega_m| + D(-i\nabla_{\mathbf{r}} + 2\mathbf{A})^2)\Gamma(\mathbf{r},\omega_m) = (2\pi\nu\tau L^d)^{-1}\delta^d(\mathbf{r})$ (a formal solution of which is given by the right-hand side of the definition above). Crucially, the presence of the vector potential spoils the singularity of the cooperon mode in the limit $\mathbf{q}, \omega_m \to 0$. In other words, the magnetic field turns the cooperon into an exponentially decaying mode, as expected from our qualitative discussion above.

To conclude this section, let us discuss the role of the cooperon mode within the larger framework of the "quantum diffusive" process. Neglecting the cooperon, we had identified the density–density correlation function – formally computed as a ladder sequence where each rung was given by the trivial single impurity line irreducible vertex – with a classical diffusive process. However, we have seen that coherent loop excursions traversed in opposite directions give rise to quantum corrections to this picture. Formally, these excursions were described by maximally crossed corrections to the irreducible vertex. We saw that, in the absence of external fields, these corrections quantitatively resembled the diffusive form of the (leading-order) particle–hole mode. (This could have been anticipated from Fig. 6.14(c). Although the impurity sequence is now traversed in an opposite sense, the cooperon excursion provides a diffusive contribution.) Does this formal similarity imply that the cooperon modes give a large $\mathcal{O}(1)$ correction to the leading classical term? To understand why it

does not, we have to, once again, consider the phase space structure of the fast integration momenta.

The diffusion mode is computed for an overall conserved small momentum difference between the upper and lower momenta. On the other hand, the cooperon mode requires the momentum sum of the upper incoming and lower outgoing momenta to be small. These two conditions have to be reconciled. It is straightforward to see that this leads to the loss of Fermi-sphere integration volume. In other words, the cooperon gives rise to a singular (in $D\mathbf{q}^2 + |\omega_m|$) correction to the diffusion mode. However, this correction is weighted by a small factor $\sim (p_{\mathrm{F}}\ell)^{d-1}$.

The reader may wonder why we left the cooperon mode calculation with the semi-quantitative arguments above. The reason is that the actual embedding of the cooperon mode into the density–density correlation function, i.e. the solution of the Bethe–Salpeter equation for the full vertex in the presence of a cooperon-corrected irreducible vertex, is a tricky business. It requires a fair amount of diagrammatic skill to obtain the correct result (notably one that fulfills the conservation laws discussed in A1). In the following section, we will see that this task is much more efficiently tackled by functional methods, a feature not uncommon in the field-theoretic environment.

Further, one may wonder what happens when the external momenta are tuned to zero. Eventually, the singularity of the cooperon mode will seriously compete with its small prefactor, so that qualitative corrections to classical diffusion must be expected. Indeed, it turns out that a proliferation of cooperon corrections leads to a slowing down of the diffusive propagation of electron densities. In a way, the cooperon describes the tendency of an electron's quantum amplitude to constructively self-interfere at the point of origin of the closed loop. Through an accumulation of such processes, the electron may eventually get stuck or localized. Qualitatively, this is the origin of the phenomenon of **Anderson localization** in metals. We shall return to this phenomenon from a more field-theoretical perspective below.

Mean-field theory and spontaneous symmetry breaking

Previously, we have seen that the Green function of the disordered electron gas contains a complex self-energy describing the damping of quasi-particle amplitudes by impurity scattering. Further, we have found that the more complex four-point function is a long-range object whose behavior is governed by soft modes of density relaxation: the diffuson and cooperon modes. The existence of the latter was intimately tied to the time-reversal invariance properties of the system. In concluding, we had anticipated that a complete theory of the weakly disordered conductor should be able to describe the embedding of diffuson and cooperon modes into structures of higher complexity. It also became quite clear that the construction of a diagrammatic approach to the problem would be a formidable task; rather one should aim to find a formulation wherein the diffuson and cooperon modes (in contrast to individual fermion Green functions) appear as fundamental degrees of freedom. Such considerations call for a field-theoretical construction. In this section, we utilize the machinery of the present chapter to construct the low-energy field theory of the disordered

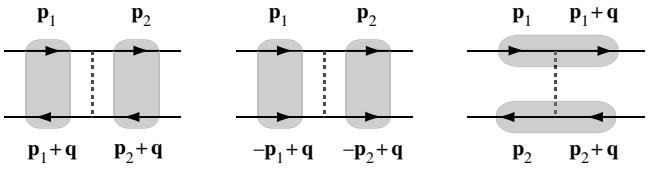

Figure 6.17 The three different low-momentum channels of the impurity vertex: exchange, Cooper, and direct.

electron gas. In doing so, we establish contact with our previous results obtained from the diagrammatic perturbation theory, and we understand the phenomenon of soft mode formation in the disordered electron system from a wider perspective.

As usual, our starting point is the replicated action of the non-interacting disordered electron gas derived in Section 6.5:

$$\begin{aligned} S[\psi,\bar\psi] &= \int d\tau\, d^d r\; \bar\psi \left(\partial_\tau - E_{\rm F} - \frac{\nabla^2}{2m} + V\right)\psi \overset{\langle\cdots\rangle_V}{\to} \int d\tau\, d^d r\; \bar\psi \left(\partial_\tau - E_{\rm F} - \frac{\nabla^2}{2m}\right)\psi \\ &\quad + \frac{1}{4\pi\nu\tau}\int d\tau\, d\tau'\, d^d r\; (\bar\psi\psi)(\tau)\,(\bar\psi\psi)(\tau'), \end{aligned} \tag{6.57}$$

where the fields $\psi = \{\psi^a\}$ carry a replica index $a = 1, \ldots, R$, and V denotes the disorder potential. The last term is generated by the ensemble averaging, where we have assumed that the potential is δ-correlated and expressed its strength through the scattering time τ. (For clarity, wherever possible, we will avoid spelling out the spatial argument $\mathbf{r}$ of the fields.) Of course, our master strategy will be to decouple the disorder-generated interaction by a Hubbard–Stratonovich transformation. However, before doing so, we need to decide which of the three low-momentum channels of the interaction vertex to keep (see Fig. 6.17).

The first contribution (termed the "exchange channel" in our general discussion in Section 6.1) appeared as a principal building block in our diagrammatic discussion of the diffuson mode above; this contribution should surely be retained. Similarly, the second diagram (the Cooper channel) played an important role in the computation of the maximally crossed diagram and must be retained. The third diagram (the "direct channel") describes the scattering off impurities at low momentum transfer. There is no reason why such processes should play a distinguished role, so we will ignore this channel.

Following the general discussion of Section 6.1, we should be prepared to introduce two different Hubbard–Stratonovich fields, one for each impurity vertex. There is, however, an ingenious trick whereby the number of required Hubbard–Stratonovich fields can be reduced to one. The idea is to exploit the fact that the diffuson and the cooperon mode are linked to each other by the symmetry operation of time-reversal. (Recall that the cooperon mode described the traversal of an impurity path in a chronologically reversed order.) In the quantum mechanics of spinless particles (for the straightforward extension of the present discussion to particles with spin, we refer to Efetov[73]) the anti-unitary operation

[73] K. B. Efetov, Supersymmetry and the theory of disordered metals, *Adv. Phys.* **32** (1983), 53–127.

of time-reversal $\mathcal{T}$ maps operators $\hat{X}$ onto their transposes $\hat{X} \to \mathcal{T}\hat{X} \equiv \hat{X}^T$.[74] Notice that $\mathcal{T}\hat{\mathbf{p}} = -\hat{\mathbf{p}}$, i.e. $\mathcal{T}$ induces the momentum reversal distinguishing the diffuson and the cooperon vertex above. This latter observation suggests that one should consider a version of the theory "symmetrized" under time-reversal. Within the symmetrized description, the diffuson and the cooperon vertex should, in some sense, merge into a unified object. The practical implementation of this idea goes as follows.

Let us return to the action prior to averaging and write

$$\begin{aligned} S[\bar{\psi},\psi] &= -\int d\tau\, d^d r\ \bar{\psi}\hat{G}^{-1}\psi = -\frac{1}{2}\int d\tau\, d^d r\ \left[\bar{\psi}\hat{G}^{-1}\psi + (\bar{\psi}\hat{G}^{-1}\psi)^T\right] \\ &= -\frac{1}{2}\int d\tau\, d^d r\ \left[\bar{\psi}\hat{G}^{-1}\psi - \psi^T\hat{G}^{-1}\,|_{\partial_\tau\to-\partial_\tau}\ \bar{\psi}^T\right] \equiv -\frac{1}{2}\int d\tau\, d^d r\ \bar{\Psi}\hat{G}^{-1}\hat{\Psi}. \end{aligned}$$

Here, $\hat{G}^{-1} = -\partial_\tau - \hat{H} + E_{\rm F}$ and, in the second equality, we have used the fact that $\bar{\psi}\hat{G}^{-1}\psi = (\bar{\psi}\hat{G}^{-1}\psi)^T$ (simply because it is a number). In the third equality, we have expressed the transpose in terms of its constituents and used the fact that $(\hat{G}^{-1})^T = \hat{G}^{-1}\,|_{\partial_\tau\to-\partial_\tau}$ (time-reversal symmetry!).[75] (The overall minus sign comes from the permutation of the Grassmann components of ψ.) Finally, we have defined

$$\Psi(\tau) \equiv \begin{pmatrix} \psi(\tau) \\ \bar{\psi}^T(-\tau) \end{pmatrix}, \quad \bar{\Psi}(\tau) \equiv (\bar{\psi}(\tau), -\psi^T(-\tau)),$$

to condense the action into a single bilinear form.[76] Notice that the enlarged fields $\bar{\Psi}$ and Ψ are no longer independent of each other; they are connected by the symmetry operation

$$\bar{\Psi}(\tau) = -\Psi^T(-\tau)(i\sigma_2^{\rm tr}), \tag{6.58}$$

where $\sigma_i^{\rm tr}$ represents Pauli matrices acting in the newly introduced "time-reversal space." Involving a transposition operation, Eq. (6.58) signals the fact that the fields Ψ and $\bar{\Psi}$ resemble "real" rather than "complex" fields (the quotes are used because we are dealing with Grassmann fields).

Being now symmetrized, an average of the field integral over the Gaussian distributed impurity potential gives

$$S[\Psi] = \frac{1}{2}\int d\tau\, d^d r\ \ \bar{\Psi}\left(\partial_\tau - E_F - \frac{\nabla^2}{2m}\right)\Psi + \frac{1}{16\pi\nu\tau}\int d\tau\, d\tau'\, d^d r\ (\bar{\Psi}\Psi)(\tau)(\bar{\Psi}\Psi)(\tau').$$

Cast in this form, we are now in a position to implement the usual programme to construct the low-energy field theory of the quantum disordered system:

Q1: Introduce a Hubbard–Stratonovich transformation to decouple the quartic interaction induced by the impurity average. Note that the corresponding Hubbard–Stratonovich field Q

[74] A more precise formulation is that there exists a representation (typically, the coordinate representation) wherein time-reversal amounts to transposition.

[75] Note that, under time-reversal, the sign of the time-derivative is reversed: $\int d\tau\ (\bar{\psi}\partial_\tau\psi)^T = -\int d\tau\ (\partial_\tau\psi^T)\bar{\psi}^T = -\int d\tau\ \psi^T(-\partial_\tau)\bar{\psi}^T$.

[76] Notice that the temporal minus sign in the fields ψ^T and $\bar{\psi}^T$ is introduced to remove the unwanted sign multiplying ∂_τ in $[\hat{G}^{-1}]^T$. Physically, it emphasizes the time-like character of the transformation.

must be matrix-valued – identify the set of indices on which the fields depend. Finally, integrate out the fermions to determine the dependence of the effective action on the field Q.

Q2: Starting with the effective action for Q, derive the corresponding mean-field equations. (Hint: You will find it convenient to switch to a frequency–momentum representation before varying the action.)

Q3: The mean-field equations can be solved by a simple matrix-diagonal *ansatz*, i.e. $Q \equiv \Lambda$. Motivate your *ansatz* and solve the equations. How does the result relate to the SCBA discussed in section 6.5?

Q4: Assuming that the frequency contribution to the action $\sim \bar{\Psi}_n \omega_n \Psi_n$ is negligibly small, identify the global continuous symmetries of the problem, i.e. explore what happens if the fermion fields are transformed as $\Psi \to T\,\Psi$, $\bar{\Psi} \to \bar{\Psi}\bar{T}$, where the matrices T and $\bar{T}$ are constant in space and must be chosen so as to respect the relation (6.58). Show that the diagonal solution of the mean-field equations derived in Q3 breaks the full symmetry of the problem. Identify the manifold of Goldstone modes of the problem.

A1: To effect a Hubbard–Stratonovich decoupling of the action, we must first isolate the Cooper and exchange contributions to the interaction vertex:

$$S_{\rm dis} \simeq \frac{1}{16\pi\nu\tau} \int d\tau\, d\tau'\, d^d r\, \Big(\bar{\Psi}^{(1)}(\tau)\Psi^{(2)}(\tau)\bar{\Psi}^{(1)}(\tau')\Psi^{(2)}(\tau') + \bar{\Psi}^{(1)}(\tau)\Psi^{(2)}(\tau)\bar{\Psi}^{(2)}(\tau')\Psi^{(1)}(\tau') \Big),$$

where the convention is that two fields carrying the same upper index form a slowly varying bilinear. Now, thanks to the symmetry Eq. (6.58), the two contributions to the action are identical. Indeed,

$$\bar{\Psi}^{(1)}\Psi^{(2)} = (\bar{\Psi}^{(1)}\Psi^{(2)})^T = -\Psi^{(2)T}\bar{\Psi}^{(1)T} = \Psi^{(2)T}(i\sigma_2^{\rm tr})\,(i\sigma_2^{\rm tr})\bar{\Psi}^{(1)T} = \bar{\Psi}^{(2)}\Psi^{(1)},$$

where in the last equality we have used the symmetry. Thus, we may focus on the decoupling of the single term $S_{\rm dis} = (8\pi\nu\tau)^{-1} \int d\tau\, d\tau'\, d^d r\ \bar{\Psi}^{(1)}(\tau)\Psi^{(2)}(\tau)\bar{\Psi}^{(2)}(\tau')\Psi^{(1)}(\tau')$. To make further progress with this expression, let us introduce a composite index $\alpha \equiv (a, \sigma)$ comprising the replica index a and an index $\sigma = 1, 2$ labeling components in time-reversal space. Using this notation,

$$\begin{aligned} S_{\rm dis} &= \frac{1}{8\pi\nu\tau} \int d\tau\, d\tau'\, d^d r\, \bar{\Psi}^{(1)\alpha}(\tau)\Psi^{(2)\alpha}(\tau)\bar{\Psi}^{(2)\beta}(\tau')\Psi^{(1)\beta}(\tau') \\ &= -\frac{1}{8\pi\nu\tau} \int d\tau\, d\tau'\, d^d r\, \Psi^{(1)\beta}(\tau')\bar{\Psi}^{(1)\alpha}(\tau)\Psi^{(2)\alpha}(\tau)\bar{\Psi}^{(2)\beta}(\tau'). \end{aligned}$$

To decouple the interaction, let us introduce an infinite-dimensional, hermitian, matrix field $Q = \{Q^{\alpha\beta}(\mathbf{r}; \tau, \tau')\}$, slowly fluctuating in space and of the same structure as the dyadic product $\Psi\bar{\Psi} \equiv \{\Psi^\alpha(\tau)\bar{\Psi}^\beta(\tau')\}$, i.e. $Q = (i\sigma_2^{\rm tr})Q^T(i\sigma_2^{\rm tr})^{-1}$. One may then multiply the action by[77] $\int DQ\, \exp[-(\pi\nu/8\tau)\int d^d r\, {\rm tr}\, Q^2]$ and perform a shift $Q \to Q + i\Psi^{(1)}\bar{\Psi}^{(1)}/\pi\nu$.

[77] Here, ${\rm tr}Q^2 \equiv \int d\tau\, d\tau'\, Q^{\alpha\beta}(\tau, \tau')Q^{*\beta\alpha}(\tau', \tau)$ and Hermiticity of Q is assumed to ensure the existence of the integral.

This generates the identity

$$e^{-S_{\rm dis}[\bar{\ },\ ]} = \int DQ\, \exp\left[-\frac{\pi\nu}{8\tau}\int d^dr\, {\rm tr}\, Q^2 - \frac{i}{4\tau}\int d^dr\, \bar\Psi Q\Psi\right],$$

where we have made use of the fact that ${\rm tr}\,(Q\Psi\bar\Psi) = -\bar\Psi Q\Psi = -\int d\tau\, d\tau'\, \bar\Psi^\alpha(\tau)\times Q^{\alpha\beta}(\tau,\tau')\Psi^\beta(\tau')$ and the superscripts (1) have been dropped. Combining terms, we arrive at the preliminary result[78]

$$\begin{aligned}\mathcal{Z} &= \int D\Psi\; DQ\, \exp\Bigg[-\frac{\pi\nu}{8\tau}\int d^dr\, {\rm tr}\, Q^2 - \frac{1}{2}\int d\tau\, d^dr\, \bar\Psi \overbrace{\left(\partial_\tau - E_{\rm F} - \frac{\nabla^2}{2m} - \frac{i}{2\tau}Q\right)}^{-\hat G^{-1}[Q]}\Psi\Bigg] \\ &= \int DQ\, \exp\left[-\frac{\pi\nu}{8\tau}\int d^dr\, {\rm tr} Q^2 + \frac{1}{2}\,{\rm tr}\ln\hat G^{-1}[Q]\right]. \end{aligned} \tag{6.59}$$

A2: Fourier transforming the field $Q(\tau,\tau')$ in its time arguments one obtains a matrix $Q = \{Q_{nn'}\}$, where n, n' index fermionic Matsubara frequencies. The frequency/momentum version of the action then assumes the form

$$S[Q] = \frac{\pi\nu L^d}{8\tau}\sum_{\mathbf q}{\rm tr}\, Q(\mathbf q)Q(-\mathbf q) - \frac{1}{2}{\rm tr}\ \ln\ \hat G^{-1}[Q],$$

where $\hat G^{-1}[Q] \equiv (i\hat\omega - \xi_{\mathbf p} + iQ/2\tau)^{-1}$, $\hat\omega$ is the diagonal operator of Matsubara frequencies and all indices (including momentum indices) not written out explicitly are traced over. Varying the action with respect to the matrix Q, i.e. $Q \to Q + \delta Q$, and requiring vanishing of contributions linear in δQ, one obtains the equation

$$\sum_{\mathbf q}{\rm tr}\left[\left(\pi\nu L^d Q(\mathbf q) - i\sum_{\mathbf p}\hat G[Q]_{\mathbf{p},\mathbf{p}+\mathbf q}\right)\delta Q(-\mathbf q)\right] = 0.$$

Holding for any matrix δQ, this equation is equivalent to the matrix mean-field equation $\pi\nu Q(\mathbf q) - \frac{i}{L^d}\sum_{\mathbf p}\hat G[Q]_{\mathbf{p},\mathbf{p}+\mathbf q} = 0$.

A3: To seek solutions of the mean-field equation, let us apply the simplest *ansatz*, $Q \equiv \Lambda$, where the Λ is diagonal in time-reversal and replica spaces, spatially uniform, and diagonal in Matsubara space. When this is substituted into the mean-field equation, the latter assumes the form

$$\pi\nu\Lambda = \frac{i}{L^d}\sum_{\mathbf p}\frac{1}{i\omega_n - \xi_{\mathbf p} + \frac{i}{2\tau}\Lambda}, \tag{6.60}$$

reminiscent of the SCBA Eq. (6.52) for the average Green function (the identification $i\Lambda/2\tau = -\Sigma$ understood). Drawing on the earlier discussion, one may identify the solution $\Lambda_n = -2i\tau\Sigma_n = {\rm sgn}(\omega_n)$ (where $\Sigma_n = -i\,{\rm sgn}(\omega_n)/2\tau$).

[78] Notice the prefactor 1/2 generated by the Grassmann integration, i.e. $\int D\quad \exp[-\frac{1}{2}\bar{\ }\hat G^{-1}\ ] \propto \det\hat G^{-1/2} = \exp[\frac{1}{2}{\rm tr}\ \ln\ \hat G^{-1}]$ arises because the components of $\bar{\ }$ and $\ $ are not independent. (To see this, assume that $\hat G$ is diagonalized and count the number of independent Grassmann integration variables.)

A4: In the mean-field approximation, $\hat{G}$ becomes equivalent to the impurity-averaged Green function discussed in Section 6.5. But, clearly, this can not be the end of the story! We have seen in Section 6.5 that impurity scattering leads to diffusive phenomena that reach far beyond the damping of single-particle amplitudes. How are such structures reflected in the field theory? To identify the diffusion modes, one must return to consider the symmetries of the theory (having in mind that symmetries tend to generate long-range low-energy excitations). We thus go back to our initial action $-\int d\bar{\Psi}\hat{G}^{-1}[V]\Psi$ and explore what happens as we transform $\Psi \to \Psi' \equiv T\,\Psi$, and $\bar{\Psi} \to \bar{\Psi}' \equiv \bar{\Psi}\bar{T}$, where T and $\bar{T}$ are matrices, constant in real space. Of course we require that the fundamental relation (6.58) be preserved under this transformation. This leads to the condition $\bar{T} = (i\sigma_2^{\rm tr})T^T(i\sigma_2^{\rm tr})^{-1}$. Moreover, T should be a symmetry of the problem, i.e. we require that $\bar{T}\hat{G}^{-1}[V]T \simeq \hat{G}^{-1}[V]\bar{T}T = G^{-1}[V]$ or $\bar{T} = T^{-1}$. Here, we have used the fact that, owing to its constancy, T commutes with the (disordered) Hamiltonian. Nevertheless, $\bar{T}G^{-1}[V] \simeq \hat{G}^{-1}[V]\bar{T}$ holds only approximately since, for a transformation $T_{nn'}$ of a general frequency structure, $[T, \hat{\omega}] \neq 0$. However, for transformations of physical interest (fluctuating slowly in time), this lack of commutativity is not of much concern. Combining the two conditions above, we find that $T = (i\sigma_2^{\rm tr})T^T(i\sigma_2^{\rm tr})^{-1}$, which is the defining relation of the unitary symplectic group $\mathrm{Sp}(2\cdot R\cdot(2M))$. Here, we have assumed that $[-\omega_{\max}, \omega_{\max}] = [-2\pi MT, 2\pi MT]$ is the range of $2M$ Matsubara frequencies over which the lack of commutativity of the symmetry group and the frequency operator can safely be neglected.

With this background, we may note that the diagonal solution of the mean-field equations breaks the symmetry above. Indeed, the fact that T is a symmetry implies that, not only Λ, but any configuration $Q \equiv T\Lambda T^{-1}$, solves the mean-field equation (6.60). The symmetry is broken, inasmuch as only a subgroup of transformations $T_0 \in K \subset \mathrm{Sp}(4RM)$, $T_0\Lambda T_0^{-1} = \Lambda$, leaves the diagonal saddle-point invariant. (It may be helpful to think of Λ as some kind of spin, $\mathrm{Sp}(4RM)$, the analog of the rotation group, and K the group of rotations around the spin axis.) The invariance group K is easily identified. Projected onto the positive/negative frequency range, the diagonal solution $\Lambda\big|_{\omega_n>/<0} \propto \pm 1$ is equal to the unit operator, i.e. transformations not mixing positive and negative frequencies will leave the saddle-point invariant. This means that the invariance subgroup is given by $\mathrm{Sp}(2RM) \times \mathrm{Sp}(2RM) \subset \mathrm{Sp}(4RM)$ where the two factors are the invariance groups of the positive/negative frequency range. Following our general line of argument on page 257 we may conclude that the Goldstone mode manifold of the present problem is the coset space $\mathrm{Sp}(4RM)/(\mathrm{Sp}(2RM) \times \mathrm{Sp}(2RM))$. The elements of this space are conveniently parameterized as $Q = T\Lambda T^{-1}$, where $T = \exp[W]$ and the generators W anti-commute with Λ, $[W, \Lambda]_+ = 0$.[79] This condition is met by setting

$$W = \begin{pmatrix} & B \\ -B^\dagger & \end{pmatrix}, \tag{6.61}$$

[79] Generators commuting with Λ need not be taken into account inasmuch as they do not affect the diagonal saddle-point (or span the group K).

where the block structure is in Matsubara frequency space (positive/negative frequencies) and B are $2MR$-dimensional matrix fields. The anti-Hermitian connection between the two blocks follows from the condition $Q^\dagger = Q \qquad W^\dagger = -W$. Notice that $(i\sigma_2^{\rm tr})\, e^W (i\sigma_2^{\rm tr})^{-1} = e^{-W}$ implies a second condition $B = (i\sigma_2^{\rm tr}) B^T (i\sigma_2^{\rm tr})^{-1}$. As one last technical remark – of crucial importance for all that follows – let us notice that the matrices Q obey the nonlinear constraint $Q^2 = \mathbf{1}$. (This follows from the fact that $Q^2 = (T\Lambda T^{-1})^2$ and $\Lambda_n^2 = {\rm sgn}^2(\omega_n) = 1$.) Field theories on manifolds with nonlinear constraints are generally called **nonlinear σ-models**.[80] In the next section, we proceed to construct the low-energy action of the nonlinear σ-model of the disordered electron gas.

Low-energy field theory

In the previous section we constructed the backbone of a field-theoretical approach to the disordered electron gas, ran into a scenario of spontaneous symmetry breaking, and identified the corresponding Goldstone mode manifold as ${\rm Sp}(4RM)/({\rm Sp}(2RM) \times {\rm Sp}(2RM))$. In the following, we now proceed to construct the low-energy action of the Goldstone mode degrees of freedom. Our second objective is to understand the connections to the diagrammatic approach introduced above. Finally, we wish to develop an efficient theoretical formalism, powerful enough to cope with the nonlinear proliferation of diffuson- and cooperon-type soft modes that govern the physics of disordered conductors at low temperatures.

Our target is a low-energy action of the elements $Q = T\Lambda T^{-1} \in {\rm Sp}(4RM)/({\rm Sp}(2RM) \times {\rm Sp}(2RM))$ of the Goldstone mode manifold. The action of this nonlinear σ-model can be constructed by substituting the slowly fluctuating matrix configuration $Q = \{Q_{nn'}^{\alpha,\alpha'}(\mathbf{r})\}$ into the action (6.59) and expanding in (a) gradients and (b) the small symmetry breaking induced by the lack of commutativity of the "rotation matrices" T and the frequency operator $\hat{\omega}$ – a program which is instructive to follow.[81] However, in the present section we shall pursue a more symmetry-oriented (but only slightly less rigorous) strategy of constructing the action.

Q1: Using only symmetry arguments, identify the minimal (lowest number of derivatives) action $S_{\rm fl}[Q]$ measuring the cost of spatial fluctuations of the Q field. What is the structure of the action $S_\omega[Q]$ accounting for the non-commutativity of Q and the frequency operator?

Q2: Our analysis so far has left the values of the two coupling constants of the theory undetermined. As we do not wish to perform an explicit gradient expansion, the only way to determine their values is to compare the predictions of the field-theoretical approach with those of another formalism. Indeed, we have seen in Section 6.5 that the long-range behavior of the density–density correlation function is governed by specific types of soft modes: diffusons and cooperons. We also saw that, at low frequency scales, these modes were prone to

[80] Other representatives of this family of field theories will be met in Chapters 8 and 9.

[81] A yet more systematic approach would be to decompose the full field manifold $Q = Q_{\rm gs} + Q_{\rm m}$ into a Goldstone mode configuration $Q_{\rm gs} = T\Lambda T^{-1}$ and a massive contribution $Q_{\rm m}$ and to integrate over the latter in the second order of perturbation theory. However, it can be shown that, in the present case, the contribution of the massive modes is inessential, i.e. we may work with the pure Goldstone theory from the outset.

"interact" with each other. (A cooperon insertion into the diffuson mode can be interpreted as some kind of "self-energy" of the diffuson propagator.) Comparing this picture with the structure of the field theory, it is evident that the elementary diffusons/cooperons must be the Goldstone modes of the σ-model. "Interactions" between diffusons and cooperons appear when we expand the theory to higher than quadratic order in the generators B.

Expand the action (6.62) to second order in the generators B defined in Eq. (6.61). Comparing the structure of the quadratic action with that of the diffuson mode, fix the ratio of the coupling constants c_{fl} and c_ω.

Q3: Having determined the ratio of the two coupling constants, one may now complete the analysis by fixing the absolute value of c_ω. We do so by introducing a source term $S[\Psi] \to S[\Psi] - \frac{1}{2L^d}\sum_{\mathbf{p},n} \bar{\Psi}_{\mathbf{p},n}\kappa_n\Psi_{\mathbf{p},n}$ such that differentiation

$$\lim_{R\to 0}\frac{1}{R}\text{Im}\frac{\delta}{\delta\kappa_n}\bigg|_{\kappa=0}\mathcal{Z}^R = \text{Im}\frac{1}{2L^d}\int d^dr\ \langle\bar{\Psi}_n\Psi_n\rangle = -\frac{1}{L^d}\text{Im}\sum_{\mathbf{p}} G_{\mathbf{p},n} = -\pi\nu\,\text{sgn}(\omega_n),$$

gives the density of states. Use the source $\hat{\kappa} = \{\kappa_n\delta_{nn'}\}$ to determine the coupling constant c_ω.

A1: As long as we ignore the symmetry breaking due to the frequency operator, the action is symmetric under transformations $Q \to \tilde{T}Q\tilde{T}^{-1}$, where $\tilde{T} \in \text{Sp}(4RM)$ is an element of the symmetry group. This requirement uniquely identifies $S_{\text{fl}}[Q] = c_{\text{fl}}\int d^dr\,\text{tr}\,(\nabla Q)^2$ as the dominant (lowest number of derivatives) contribution to the fluctuation action. The dominant operator describing the explicit breaking of the global symmetry will surely be of first order in $\hat{\omega}$: $S_\omega[Q] \sim \int d^dr\,\text{tr}(\hat{\omega}F[Q])$, where F is some function. Since $Q^2 = \mathbf{1}$, only terms linear in Q contribute to the expansion of F and we may set $S_\omega[Q] = c_\omega\int d^dr\,\text{tr}(\hat{\omega}Q)$. Summarizing, one may deduce that the soft mode action acquires the form

$$S[Q] = \int d^dr\,\text{tr}\left[c_{\text{fl}}(\nabla Q)^2 + c_\omega\,\hat{\omega}Q\right]. \tag{6.62}$$

As with other nonlinear σ-models, the innocent appearance of the action above is somewhat deceptive: we need to remember that the field $Q = e^W\Lambda e^{-W}$ is a nonlinear object. An expansion of it in terms of the generators W will generate "interaction operators" $\sim W^n$ of arbitrary (even) order in n. The analysis of these interactions is a highly non-trivial task!

A2: Substituting $Q = e^W\Lambda e^{-W} \overset{[W,\Lambda]_+=0}{=} e^{2W}\Lambda = (1 + 2W + 2W^2 + \cdots)\,\Lambda$ into the action, one obtains

$$S^{(2)}[W] = \int d^dr\,\text{tr}\left[-4c_{\text{fl}}(\nabla W)^2 + 2c_\omega\,\Lambda\hat{\omega}W^2\right].$$

One may now express the matrices W in terms of the off-diagonal blocks B and arrive at

$$\begin{aligned} S^{(2)}[B,B^\dagger] &= \int d^dr\,\text{tr}\left[8c_{\text{fl}}\partial_i B\partial_i B^\dagger - 2c_\omega\hat{\omega}(\mathcal{P}^+BB^\dagger - \mathcal{P}^-B^\dagger B)\right] \\ &= \sum_{\mathbf{q},n>0,n'<0} B^{\alpha\alpha'}_{\mathbf{q},nn'}\left(8c_{\text{fl}}q^2 - 2c_\omega|\omega_n - \omega_{n'}|\right)B^{\dagger\alpha'\alpha}_{-\mathbf{q},n'n}. \end{aligned}$$

Here, $\mathcal{P}^{+/-}$ is a projector onto the space of positive/negative Matsubara frequencies. In the second line, $\alpha = (a, \sigma)$ is the composite replica/time-reversal index introduced above. Importantly, the propagator of the B-field describes a mode of diffusive dynamics formed by the joint propagation of two states with (a) the Matsubara frequencies $\omega_n > 0$ and $\omega_{n'} < 0$ and (b) the momentum difference $\mathbf{q}$. The analogy to our previous diagrammatic analysis of such processes is made complete by choosing $8c_{\text{fl}} = cD$, $-2c_\omega = c$, or

$$S^{(2)}[B, B^\dagger] = c \sum_{\mathbf{q}, n>0, n'<0} B^{\alpha\alpha'}_{\mathbf{q},nn'} \left(Dq^2 + |\omega_n - \omega_{n'}| \right) B^{\dagger\alpha'\alpha}_{-\mathbf{q},n'n},$$

where c is an, as yet, undetermined global coupling constant.

Before continuing, it is worthwhile taking a brief look at the time-reversal structure of the theory. Recalling that $Q^{\sigma\sigma'} \sim \Psi^\sigma \bar{\Psi}^{\sigma'}$, one may conclude that Goldstone modes B with an index structure $(\sigma\sigma')$ describe the joint propagation of a fermion propagating forwards in time ($\sigma = 1$) (or time-reversed [$\sigma = 2$]) with a hole propagator moving forwards in time ($\sigma' = 1$) (or time reversed [$\sigma' = 2$]). Put differently, modes $B^{\sigma\sigma'}$ off-diagonal in time-reversal space ($\sigma \neq \sigma'$) represent cooperon modes, while modes $B^{\sigma\sigma}$ reflect the diffuson modes. In the absence of magnetic fields, the actions of these two modes are identical (rotational invariance of the action in time-reversal space). However, had we included a magnetic field, this invariance would be lost.

A3: Noting that the addition of the source to the action amounts to a shift $\hat{\omega} \to \hat{\omega} - i\hat{\kappa}/L^d$, one may conclude that the low-energy action changes to $S_\omega[Q] \to c_\omega \int d^d r \, \mathrm{tr}\, [(\hat{\omega} - i\hat{\kappa}/L^d)Q]$. Differentiation of the Q-functional thus gives

$$-\pi\nu \, \mathrm{sgn}(\omega_n) \stackrel{!}{=} \lim_{R\to 0} \frac{1}{R} \mathrm{Im} \frac{\delta}{\delta \kappa_n}\bigg|_{\kappa=0} \mathcal{Z}^R = \lim_{R\to 0} \frac{1}{R} \mathrm{Im}\, i \frac{c_\omega}{L^d} \int d^d r \langle \mathrm{tr}\, Q_{nn} \rangle = 2c_\omega \, \mathrm{sgn}(\omega_n) + \cdots,$$

where the ellipsis represents contributions arising from terms of higher order in the generators B. (In fact, one can show that all of these terms vanish in the replica limit.) Thus, $c_\omega = -\pi\nu/2$ and one obtains the low-energy action of the **nonlinear σ-model**,

$$\boxed{S[Q] = \tfrac{\pi\nu}{2} \int d^d r \, \mathrm{tr} \left[\tfrac{D}{4} (\nabla Q)^2 - \hat{\omega} Q \right].} \tag{6.63}$$

In applications, one is often interested in situations involving an **external electromagnetic field**. How would such a field affect the structure of the action (6.63)? Although this question can be answered by microscopic calculation, a more time-efficient strategy is to require that the action $S[Q]$ be gauge invariant. Under a gauge transformation, $\psi \to e^{i\phi}\psi$, the fields Ψ enlarged by a time-reversal structure transform as (exercise) $\Psi \to e^{i\Phi}\Psi$, where $\Phi = \mathrm{diag}(\phi(\tau), -\phi(-\tau))$ (matrix structure in time-reversal space). This in turn implies that the fields $Q \sim \Psi\bar{\Psi}$ transform as $Q \to e^{i\Phi} Q e^{-i\Phi}$. Invariance under such transformations is ensured (exercise) if we generalize the action according to

$$S[Q] = \frac{\pi\nu}{2} \int d^d r \, \mathrm{tr} \left[\frac{D}{4} \left((\nabla - i[\mathbf{A}, \,])Q \right)^2 - (\hat{\omega} + V)Q \right], \tag{6.64}$$

where the vector potential $\mathbf{A}$ and scalar potential V transform in the standard manner $\mathbf{A} \to \mathbf{A} + \nabla\Phi$ and $V \to V + \partial_\tau \Phi$. This way of coupling a gauge potential to an effective

action – to be discussed in more general terms in the next chapter – is known as **minimal substitution**.

6.6 Summary and outlook

This concludes our preliminary discussion of functional mean-field methods. We have learned how the integration over microscopic quantum fields can be traded for an integration over degrees of freedom adjusted to the low-energy characteristics of the system. We found that the functional dependence of the action on the new coordinates is usually highly nonlinear – the notorious "trace logarithms" – and has to be dealt with by some kind of stationary phase analysis. While a first principles solution of the mean-field equations is often not possible, all applications discussed in this chapter shared the feature that solutions could be found by an "educated guess." Importantly, we realized that these solutions did not always display the full symmetry of the action.

INFO However, it is important to realize that our discussion has excluded a number of **problem classes with complex mean-field structure**. For example, for certain lattice systems with discrete translational symmetry, the optimal mean-field solution shows **staggering**, i.e. changes sign under translation by one lattice spacing. Deceptively, these configurations usually exist in parallel to a solution that displays the full symmetry of the problem, but is of higher energy (and therefore unphysical), i.e. the "true solution" is camouflaged by the existence of an inferior but "more symmetric" solution.[82] Then, there are systems where the existence of meaningful stationary phase configurations is excluded by structural elements, such as **frustration**.

Other systems, notably **glasses** (cf. the remarks on page 115), do possess an entire continuum of mean-field configurations, i.e. there is a macroscopic number of (metastable) extremal configurations that are very close in energy space but may be very far from each other in configuration space. (For example, two such configurations may differ by a restructuring of the atomic configuration of a glass at remote places.) The dynamics of such systems is governed by the process of **aging**, i.e. transitions between different metastable extremal configurations on very long timescales (witness the apparent rigidity of window glass!). It goes without saying that the "mean-field configurations" of glassy systems are irregular and not amenable to straightforward analytic calculation.

Finally, even systems possessing a spatially homogeneous mean-field configuration may host other solutions of physical significance. Indeed, we have encountered a scenario of this type already in Chapter 3 above. Exploring quantum double-well tunneling, we observed that the imaginary time Euler–Lagrange equations of a particle in a doubly degenerate harmonic well (the "mean-field equations") had a metastable constant solution (the constant mean-field). However, in addition to that, we found **instantons**, i.e. temporally structured solutions of the mean-field equations. Superficially, it seemed that, due to their non-vanishing action, instantons are irrelevant. However, for sufficiently long times, the energetic inferiority of the single instanton was over-compensated by statistical aspects, i.e. the fact that a continuum of instantons entered the partition function with approximately equal weight. In the language of statistical mechanics:

[82] When dealing with problems whose lattice structure carries physical significance, it is therefore a good idea to try a number of different *ansätze*, i.e. trial solutions that transform differently under translation by a unit cell.

the large entropy associated with instanton configurations outweighed the finite energy (or, more precisely, action) to be paid for a single instanton. Later we will see that entropy/energy competitions of this type are realized in many other contexts of quantum and statistical field theory. For example, the phase actions of the BCS superconductor or the superfluid possess (approximate) extremal configurations wherein the phase winds around an integer multiple of 2π as a fixed reference point in space is encircled (vortices). While the energy of an individual vortex solution may be high, the entropy corresponding to the choice of its center eventually, for sufficiently large temperatures, dominates and leads to a proliferation of vortices in the system (the analog of the instanton gas). For a more qualified discussion of topologically non-trivial mean-field configurations we refer to Chapter 9.

Finally, we have explored a number of different applications showing the way low-energy effective actions describing fluctuations on top of a reference mean-field can be derived and evaluated. In cases where the mean-field breaks a continuous symmetry, these actions were partially soft, i.e. contained Goldstone modes. We saw that the presence of a Goldstone mode has a dominant effect on the observable physical properties of a system.

As exemplified above, the theoretical machinery developed thus far enables us to tackle already highly non-trivial problems. However, to make the functional integral a universally applicable tool, two important gaps have yet to be filled. Firstly, we have so far mostly been content with discussing general structures of condensed matter theory (i.e. much of the discussion has been limited to general manipulations on the level of the effective action.) However, in applications, one is typically interested in comparison with experimentally accessible data, i.e. we still need to provide links relating the field integral formalism to observables of experimental significance. Secondly, our discussion of the fluctuation behavior of field theories has been quite limited. That is, we have typically expanded an action to second order in what we believed was the "physically relevant" degree of freedom and computed the corresponding determinants. However, we also saw that some problems contain anharmonicities of profound significance. For example, the quartic term in ϕ^4-theory led to UV singularities whose nature remained largely obscure. We must, therefore, (i) develop criteria indicating in what circumstances a model can safely be limited to second order and, (ii) in cases where it cannot, learn how to deal with its anharmonic content. Beginning with the first, these two topics (which are not quite as unrelated as one might think) are discussed in Chapters 7 and 8.

6.7 Problems

Peierls instability

Previously, in Problem 2.4 we have seen that the half-filled one-dimensional lattice system is unstable towards the formation of a commensurate periodic lattice distortion. In fact, at zero temperature, a one-dimensional crystal comprising electrons and ions is always unstable against the formation of a lattice distortion which transforms the system to a dielectric. The aim of this problem is to study the nature of the lattice instability known as a Peierls distortion.

Rudolph E. Peierls 1907–95
Born in Germany, Peierls did fundamental work during the early years of quantum mechanics. He also studied the physics of lattice vibrations (phonons) and is credited with the development of the concept of the "hole" in condensed matter. In collaboration with Otto Frisch, Peierls was the first to realize that an atom bomb based on ^{235}U would be feasible, and was engaged in the Manhattan Project. (Image © University of Cambridge, Cavendish Laboratory.)

The starting point of the theory is the Euclidean action for a one-dimensional gas of electrons,

$$S_{\rm el}[\psi,\bar\psi] = \int d\tau \int dx\, \bar\psi \left(\partial_\tau - \frac{1}{2m}\partial_x^2 - \mu\right)\psi.$$

(Here, for simplicity, we take the electrons to be spinless.) Starting with a classical field theory of the lattice dynamics, the Euclidean action of the system of ions is given by

$$S_{\rm ph}[u] = \frac{\rho}{2}\int d\tau \int dx \quad (\partial_\tau u)^2 + c^2(\partial_x u)^2 \quad ,$$

where $u(\tau,x)$ denotes the scalar bosonic displacement field. Finally, to complete the theory, we suppose that the electron system is coupled to the distortion of the underlying lattice. In principle, one could try to derive a "realistic" model of the coupling. However, since we are interested in the general stability of the system, we will consider a phenomenological coupling which engages the fields in the lowest order compatible with the symmetry of the interaction (for more details, see Problem 4.5). To this end, we introduce "Fröhlich's deformation potential approximation," wherein the coupling is taken to be proportional to the gradient of the deformation $\partial_x u$,

$$S_{\rm el-ph}[\psi,\bar\psi,u] = g\int d\tau \int dx\ \bar\psi\psi\,\partial_x u.$$

The full Euclidean action $S = S_{\rm el} + S_{\rm ph} + S_{\rm el-ph}$ represents an interacting theory. As such, an explicit and exact evaluation of the coherent state path integral is not feasible. Instead, we will develop an analysis in which the coupling will be treated perturbatively. In doing so, we will be able to explore the stability of the lattice system.

(a) As a first step, integrate out the fermionic degrees of freedom ψ and thereby obtain an effective action for the displacement field u. Assuming that the electron–phonon

coupling constant g is small, expand the action up to second order in u. You will find that the coefficient of u^2 involves the density–density response function $\chi(q,\omega_m)$.

(b) In general, when seeking a saddle-point of the effective action, the first guess would be a homogeneous displacement field, $u_0(x,\tau) \equiv u_0$. Here, $u_0 = 0$ is such a solution. However, it is not necessarily the best solution. Show that the static solution $u_0(x,\tau) \equiv u_0 \cos(2k_{\rm F}x+\varphi)$ is energetically favorable (i.e. $S[u = u_0\cos(2k_{\rm F}x+\varphi)] < S[u=0]$) below a certain critical temperature $T_{\rm c}$. Thus, at low temperatures, the system is instable towards the formation of a static sinusoidal lattice distortion. Use the approximation $\chi(2k_{\rm F},0) \simeq \ln(\beta\omega_{\rm D})/4\pi v_{\rm F}$, where $\omega_{\rm D}$ is the Debye frequency, to determine the transition temperature $T_{\rm c}$.

Answer:

(a) Integrating out the electron degrees of freedom ψ, one obtains

$$\int D[\bar\psi,\psi] e^{-S_{\rm el}-S_{\rm el-ph}} = \det\left[\partial_\tau - \frac{\partial_x^2}{2m} - \mu + g(\partial_x u)\right].$$

Thus, the effective action for the displacement field u reads $S_{\rm eff}[u] = S_{\rm ph}[u] - \mathrm{tr}\ln\left[\partial_\tau - (\partial_x^2/2m) - \mu + g(\partial_x u)\right]$. While the bare phonon action is diagonal in frequency–momentum representation, the "tr ln" is not. Thus, the evaluation of the second term requires more care. Defining the bare Green function of the electron system $G_0^{-1} = \partial_\tau - \partial_x^2/2m - \mu$, an expansion up to second order in the coupling g gives $\mathrm{tr}\ln[G_0^{-1} + g(\partial_x u)] \simeq \mathrm{tr}\ln G_0^{-1} - (g^2/2)\sum_{\omega_m,q} q^2\chi(q,\omega_m)|u_{\omega_m,q}|^2$, where $\chi(q,\omega_m) = -\frac{T}{L}\sum_{p\omega_n} G_{0,p,\omega_n} G_{0,p+q,\omega_n+\omega_m}$ and we note that the linear term of the expansion vanishes by symmetry. Thus, to quadratic order in the displacement field, the effective action assumes the form

$$S_{\rm eff}[u] \simeq \sum_{q;\omega_m}\left[\frac{\rho}{2}(\omega_m^2 + c^2q^2) - \frac{g^2}{2}q^2\chi(q,\omega_m)\right]|u_{\omega_m,q}|^2.$$

(b) In the presence of the static periodic modulation, $u_{\omega_m,\mathbf{q}} = \pi u_0[e^{i\varphi}\delta(q-2k_{\rm F}) + e^{-i\varphi}\delta(q+2k_{\rm F})]\delta(\omega_m)$ the action takes the value $S_{\rm eff} = 4\pi^2 u_0^2 k_{\rm F}^2[\rho c^2 - g^2\chi(2k_{\rm F},0)]$. Thus, noting that $S[u = \text{const.}] = 0$, the transition is realized when $\rho c^2 < 4\pi^2 g^2\,\chi(2k_{\rm F},0)$. Substituting the expression for χ, one obtains the relation for the critical temperature $T_{\rm c}$: $\rho c^2 = \frac{g^2}{4\pi v_{\rm F}}\ln(\omega_{\rm D}/T_{\rm c})$ i.e. at temperatures $T < T_{\rm c} = \omega_{\rm D}\, e^{-4\pi^2 v_{\rm F}\rho c^2/g^2}$, the system becomes unstable against the formation of a periodic modulation of the lattice with a wavelength of $\pi/k_{\rm F}$.

Temperature profile of the BCS gap

The following question concerns an exploration of the functional dependence of the BCS gap on temperature. In particular, we wish to understand its singular vanishing at the transition temperature (this being a hallmark of a second-order phase transition).

Consider the BCS gap equation (6.28),

$$\frac{1}{g\nu} = \int_0^{\omega_D/2T} dx\, \frac{\tanh(x^2+\kappa^2)^{1/2}}{(x^2+\kappa^2)^{1/2}},$$

where we have introduced a dimensionless integration variable and $\kappa \equiv \Delta/2T$. In spite of its innocent appearance, the temperature dependence of this equation is not straightforward to infer. Referring for a quantitative discussion to Abrikosov *et al.*,[83] we here restrict ourselves to exploring the gap profile in the vicinity of the transition temperature.

(a) To determine the value of T_c, we proceed somewhat indirectly assuming that this is determined through the condition $\Delta(T_c) = 0$. Use this criterion to obtain Eq. (6.29) for the critical temperature. (You may assume the hierarchy of energy scales $\omega_D \gg T_c \sim \Delta_0 \gg \Delta(T \simeq T_c)$, where $\Delta_0 = \Delta(T = 0)$.)

(b) Now, let us derive the approximate profile Eq. (6.30) of the gap for temperatures T slightly smaller than T_c. To this end, add to and subtract from the right-hand side of the gap equation the integral $\int dx\, \frac{\tanh x}{x}$. Then expand to leading order in the small parameters $\delta T/T_c$ and Δ/T_c, where $\delta T = T_c - T > 0$.

Answer:

(a) For $\Delta = 0$, $\lambda(\xi) = (\xi^2+\Delta^2)^{1/2} = |\xi|$ and Eq. (6.28) assumes the form

$$\frac{1}{g\nu} = \int_0^{\omega_D/2T_c} dx\, \frac{\tanh x}{x},$$

where we have introduced $x \equiv \xi/2T_c$ as a dimensionless integration variable. The dominant contribution to the integral comes from the region $x \gg 1$, where $\tanh x \simeq 1$. As a result, one obtains $1/g\nu \simeq \ln(\omega_D/2T_c)$. Solving for T_c, we arrive at Eq. (6.29).

(b) Adding and subtracting the integral given above, we have

$$\frac{1}{g\nu} = \int_0^{\omega_D/2T} dx \left[\frac{\tanh(x^2+\kappa^2)^{1/2}}{(x^2+\kappa^2)^{1/2}} - \frac{\tanh x}{x}\right] + \int_0^{\omega_D/2T} dx\, \frac{\tanh x}{x}.$$

Arguing as in (a), the second integral can be estimated as $\ln(\omega_D/2T) \approx \ln(\omega_D/2T_c) + (\delta T/T_c) = (1/g\nu) + (\delta T/T_c)$, where we have expanded to linear order in δT. Thus,

$$-\frac{\delta T}{T_c} \approx \int_0^{\omega_D/2T} dx \left[\frac{\tanh(x^2+\kappa^2)^{1/2}}{(x^2+\kappa^2)^{1/2}} - \frac{\tanh x}{x}\right].$$

Now, the remaining integral can be split into a "low-energy region" $0 \le x \le 1$, and a "high-energy region" $1 < x < \omega_D/2T$. Using the small-x expansion, $\tanh x \simeq x - x^3/3$, we find that the first region gives a contribution $\sim \kappa^2$. With $\tanh x \overset{x>1}{\approx} 1$, the second region contributes a term $\mathcal{O}(\kappa^2)$ which, however, is approximately independent of the

[83] A. A. Abrikosov, L. P. Gorkov, and I. E. Dzyaloshinskii, *Methods of Quantum Field Theory in Statistical Physics* (Dover Publications, 1975).

large-energy cut-off $\omega_{\rm D}/2T$. Altogether, we obtain $\delta T/T_{\rm c} \approx$ const. $\times\, \kappa^2 \approx$ const. $\times$ $(\Delta_0^2/T_{\rm c}^2)$ from which one obtains Eq. (6.30).

Fluctuation contribution to the Ginzburg–Landau action of the superconductor

In this short problem we derive the energy cost corresponding to large-scale spatial fluctuations of the order parameter of a BCS superconductor. The problem mainly serves technical training purposes.

Consider the second-order contribution to the Ginzburg–Landau action of the BCS superconductor Eq. (6.31). In Problem 4.5 we have seen that the frequency summation involved in the definition of the integral kernel evaluates to

$$\chi^c(\omega_n,\mathbf{q}) \equiv -\frac{T}{L^d}\sum_{m,\mathbf{p}} G_{\mathbf{p}}(i\omega_m)G_{-\mathbf{p}+\mathbf{q}}(-i\omega_m+i\omega_n) = \frac{1}{L^d}\sum_{\mathbf{p}}\frac{1-n_{\rm F}(\xi_{\mathbf{p}})-n_{\rm F}(\xi_{-\mathbf{p}+\mathbf{q}})}{i\omega_n-\xi_{\mathbf{p}}-\xi_{-\mathbf{p}+\mathbf{q}}}.$$

Expand $\chi^c(0,\mathbf{q})$ to second order in $\mathbf{q}$. (Hints: You may trade the momentum summation for an integral, and linearize the dispersion: $\xi_{\mathbf{p}+\mathbf{q}} \simeq \xi_{\mathbf{p}}+\mathbf{p}\cdot\mathbf{q}/m$ (think why is this a permissible simplification). You may note the identity $\int d\epsilon \epsilon^{-1}\partial_\epsilon^2 n_{\rm F}(\epsilon) = cT^{-2}$ (where the numerical constant $c = 7\zeta(3)/2\pi^2$ and $\zeta(x) = \sum_{n=1}^{\infty} n^x$ defines the ζ-function).)

Answer:
Using the fact that $\xi_{\mathbf{p}} = \xi_{-\mathbf{p}}$,

$$\begin{aligned}\chi^c(0,\mathbf{q}) &= -\int\frac{d^dp}{(2\pi)^d}\frac{1-n_{\rm F}(\xi_{\mathbf{p}+\mathbf{q}/2})-n_{\rm F}(\xi_{\mathbf{p}-\mathbf{q}/2})}{\xi_{\mathbf{p}+\mathbf{q}/2}+\xi_{\mathbf{p}-\mathbf{q}/2}}\\ &\simeq -\int\frac{d^dp}{(2\pi)^d}\frac{1-2n_{\rm F}(\xi_{\mathbf{p}})-\partial_\xi^2 n_{\rm F}(\xi_{\mathbf{p}})\frac{(\mathbf{q}\cdot\mathbf{p})^2}{4m^2}}{2\xi_{\mathbf{p}}}\\ &= \chi^c(0,0)-\frac{\nu\mu\mathbf{q}^2}{12m}\int d\epsilon\;\epsilon^{-1}\partial_\epsilon^2 n_{\rm F}(\epsilon) = \chi^c(0,0)-\frac{c}{24}\frac{\nu v_F^2}{T^2}\mathbf{q}^2,\end{aligned}$$

where c is a numerical constant and in the second equality we have used the fact that, for $\xi = \mathcal{O}(T)$, $\mathbf{p}^2/2m \simeq \mu$. Substituting this expansion into the quadratic action, we obtain the gradient term in Eq. (6.33).

Coulomb blockade

Technological advances have made it possible to manufacture small metallic or semiconducting devices of extension $1\,\mu$m and less. At low temperatures, the physics of these so-called **quantum dots** is predominantly influenced by charging effects. In this problem, we explore the impact of charging on the most basic characteristic of a quantum dot, the tunneling DoS.

Consider a quantum dot weakly[84] connected to an outside environment (see Fig. 6.18 for a semiconductor realization of such a setup). The addition of an electron to, or subtrac-

[84] By "weak" we mean that the conductance of all external leads attached to the system is such that $g < g_0$, where $g_0 = e^2/h \simeq (25.8\,{\rm k}\Omega)^{-1}$ is the quantum unit of conductance.

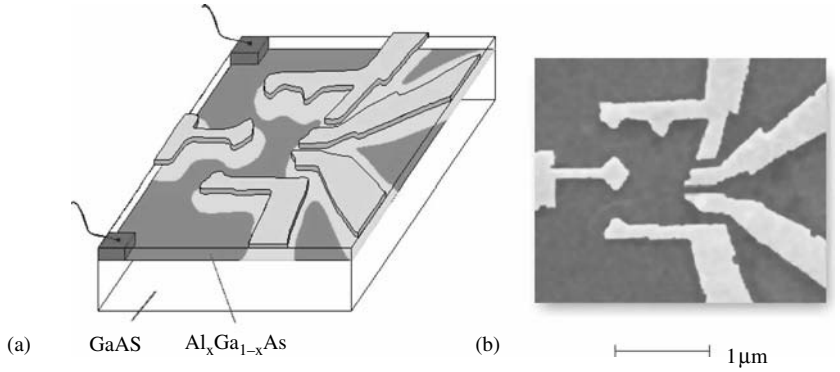

Figure 6.18 (a) Schematic picture of a confined two-dimensional electron gas (a quantum dot) formed at the interface between a GaAs and an AlGaAs layer. (b) Electron microscopic image of the "real" device. (Source: Courtesy of C. M. Marcus.)

tion of one from, the device incurs an energy cost of order $E_C = e^2/2C$, where C is the capacitance of the system. This energy cost is offset by an external gate potential. The discreteness of this **charging energy** leads to a plethora of observable physical phenomena. The most basic of these is a strong suppression of the DoS at the Fermi surface.

For a non-interacting system, the single-particle DoS is defined as $\rho(\epsilon) = \mathrm{tr}(\delta(\epsilon - \hat{H})) = -\frac{1}{\pi}\,\mathrm{Im}\,\mathrm{tr}(\hat{G}(\epsilon + i0)) = -\frac{1}{\pi}\,\mathrm{Im}\,\mathrm{tr}(\hat{G}_n)|_{i\omega_n \to \epsilon + i0}$, where $\hat{G}(z) = (z - \hat{H})^{-1}$ is the Green function. The **tunneling DoS** generalizes this definition to the interacting case: $\nu(\epsilon) = -\frac{1}{\pi}\,\mathrm{Im}\,\mathrm{tr}(\hat{G}_n)|_{i\omega_n \to \epsilon + i0}$, where the Green function $\hat{G}_n$ is defined[85] as the Fourier transform of the coherent state path integral,

$$G_{\alpha\beta}(\tau) = \mathcal{Z}^{-1} \int D(\psi, \bar{\psi})\, e^{-S[\bar{\psi},\psi]} \bar{\psi}_\beta(\tau)\psi_\alpha(0), \tag{6.65}$$

where $\mathcal{Z} = \int D(\psi, \bar{\psi})\, e^{-S[\bar{\psi},\psi]}$, and the indices α, β enumerate the eigenstates of the single-particle contribution to the Hamiltonian. Having an irregular structure, the eigenstates of the single-particle Hamiltonian are unknown. The simplest prototype Hamiltonian describing the joint effects of single particle dynamics and charging reads as $\hat{H} = \hat{H}_0 + E_C(\hat{N} - N_0)^2$, where $\hat{H}_0 = \sum_\alpha \epsilon_\alpha a_\alpha^\dagger a_\alpha$, $\hat{N} = \sum_\alpha a_\alpha^\dagger a_\alpha$ is the number operator and N_0 represents the preferred number of particles (as set by the gate voltage). The action controlling the behavior of the Green function (6.65) is thus given by

$$S[\bar{\psi}_\alpha, \psi_\alpha] = \int_0^\beta d\tau \left\{ \sum_\alpha \bar{\psi}_\alpha(\partial_\tau + \epsilon_\alpha - \mu)\psi_\alpha + E_C \left(\sum_\alpha \bar{\psi}_\alpha \psi_\alpha - N_0 \right)^2 \right\}. \tag{6.66}$$

(a) Introducing a bosonic field variable $V(\tau)$, decouple the interaction by means of a Hubbard–Stratonovich transformation. Bring the functional representation of the Green

[85] The terminology of "tunneling" DoS is motivated by the fact that $\nu(\epsilon)$ is an important building block in the calculation of tunneling currents. (Recall the "Golden Rule": tunneling rates are obtained by multiplication of transition probabilities with state densities.)

function into the form $G_\alpha(\tau) = \mathcal{Z}^{-1} \int DV\ e^{-S[V]} \mathcal{Z}^{[V]} G_\alpha^{[V]}(\tau)$, where G_α is the diagonal element of the Green function (the representation above implies that all off-diagonal elements vanish), $\mathcal{Z}^{[V]}$ is the partition function, and $G_\alpha^{[V]}$ represents the Green function of the non-interacting system subject to an imaginary time-dependent potential $iV(\tau)$.

(b) Represent the field V as a sum over Matsubara components, $V(\tau) = \sum_{\omega_m \neq 0} e^{-i\omega_m \tau} V_m + 2\pi k T + \tilde{V}_0$, where $k \in \mathbb{Z}$ and $\tilde{V}_0 \in [0, 2\pi T]$ (i.e. $2\pi k T + \tilde{V}_0$ is but a complicated representation of the zeroth Matsubara mode). Show that all but the static component $\tilde{V}_0$ can be removed from the action S by a gauge transformation. Why can not $\tilde{V}_0$ be gauged, too? Explore the transformation behavior of the Green function and integrate over the non-zero mode components $V_{m\neq 0}$.

(c) Making use of the relation $\sum_{k=1}^{\infty} \frac{\cos(kx)}{k^2} = \frac{\pi^2}{6} - \frac{\pi|x|}{2} + \frac{x^2}{4} + \cdots$, perform the Matsubara summation, $\sum_{\omega_m \neq 0}$. Show that the Green function can be expressed as $G(\tau) = F(\tau)\tilde{G}(\tau)$, where the function $F(\tau) = \exp(-E_C(\tau - \beta^{-1}\tau^2))$ is obtained by integration over the dynamical components of V, while $\tilde{G}$ is a non-interacting Green function averaged over the static component V_0.

(d) The remaining integration over the static component $\tilde{V}_0$ is achieved by the stationary phase method. Neglecting the weak dependence of the non-interacting Green function on $\tilde{V}_0$, derive and interpret the saddle-point equation. Approximate the functional by its value at the saddle-point (i.e. neglect quadratic fluctuations around the saddle-point value for $\tilde{V}_0$). As a result, obtain a representation $G(\tau) = F(\tau)G_0(\tau)$ where G_0 is a non-interacting Green function evaluated at a renormalized chemical potential.

(e) Assuming $E_C \gg T$, compute an approximation of the Fourier transform of $F(\tau)$. Use your result to obtain the zero-temperature DoS.[86] (You may approximate Matsubara sums by integrals.)

Answer:

(a) Using the identity $e^{-E_C \int d\tau \left(\sum_\alpha \bar{\psi}_\alpha \psi_\alpha - N_0\right)^2} = \int DV\ e^{-\int \left(\frac{V^2}{4E_C} - iN_0 V + i\sum_\alpha \bar{\psi}_\alpha V \psi_\alpha\right)}$, the quantum partition function takes the form

$$\mathcal{Z} = \int D(\bar{\psi}, \psi) \int DV\ e^{-S[V] - \int d\tau \sum_\alpha \bar{\psi}_\alpha (\partial_\tau + \epsilon_\alpha - \mu + iV)\psi_\alpha - S_J[\bar{\psi}, \psi]},$$

where $S[V] = \int d\tau \left(\frac{V^2}{4E_C} - iN_0 V\right)$. Thus,

$$\begin{aligned} G_\alpha(\tau) &= \mathcal{Z}^{-1} \int DV\, e^{-S[V]} \int D(\bar{\psi}, \psi)\ e^{-\int d\tau \sum_\alpha \bar{\psi}_\alpha (\partial_\tau + \epsilon_\alpha - \mu + iV)\psi_\alpha} \bar{\psi}_\alpha(\tau)\psi_\alpha(0) \\ &= \mathcal{Z}^{-1} \int DV\, e^{-S[V]} \mathcal{Z}^{[V]} G_\alpha^{[V]}(\tau), \end{aligned}$$

where $G^{[V]}$ is obtained from a non-interacting theory with action $S^{[V]} \equiv S|_{\mu \to \mu - iV}$.

[86] For a more elaborate analysis of finite-temperature corrections, we refer to A. Kamenev and Y. Gefen, Zero bias anomaly in finite-size systems, *Phys. Rev. B* **54** (1996), 5428–37.

(b) The gauge transformation removing much of the time-dependent potential from the "tr ln" is defined by

$$\bar{\psi}_\alpha(\tau) \longrightarrow \bar{\psi}_\alpha(\tau)\, e^{i\int^\tau d\tau'\,(V(\tau')-\tilde{V}_0)}; \quad \psi_\alpha(\tau) \longrightarrow\ e^{-i\int^\tau d\tau'\,(V(\tau')-\tilde{V}_0)}\psi_\alpha(\tau).$$

The zero-mode offset $\tilde{V}_0$ has to be excluded from the transformation to preserve the time periodicity of the gauge factor (i.e. to make sure that the transformed field respects the time-antiperiodicity required of a Grassmann field). Substitution of the transformed field leads to (i) removal of the dynamic V-components from the action, $S^{[V]} \to S^{[\tilde{V}_0]}$, and (ii) the appearance of a gauge factor multiplying the pre-exponential terms. We thus obtain

$$\begin{aligned} G(\tau) &= \frac{1}{\mathcal{Z}} \int DV D(\bar{\psi},\psi)\, e^{-S[V]} e^{-\int d\tau\, \sum_\alpha \bar{\psi}_\alpha[\partial_\tau - \mu + i\tilde{V}_0 + \epsilon_\alpha]\psi_\alpha} \\ &\qquad\qquad \times e^{i\int_0^\tau d\tau'\,(V(\tau')-\tilde{V}_0)} \bar{\psi}_\alpha(\tau)\psi_\alpha(0) \\ &= \frac{1}{\mathcal{Z}} \int DV\, e^{-S[V]} e^{i\int_0^\tau d\tau'\,(V(\tau')-\tilde{V}_0)}\, \mathcal{Z}^{[\tilde{V}_0]} G_\alpha^{[\tilde{V}_0]}(\tau) \\ &= \frac{F(\tau)}{\mathcal{Z}} \int d\tilde{V}_0\, e^{-\frac{\beta}{4E_C}\tilde{V}_0^2 + i\beta N_0 \tilde{V}_0}\, \mathcal{Z}^{[\tilde{V}_0]} G_\alpha^{[\tilde{V}_0]}(\tau), \end{aligned}$$

where we have omitted the $2\pi kT$ contribution to the zero mode (as it does not play much of a role in the context of this problem – for the physical meaning of the integers k see Chapter 9), the function

$$F(\tau) = \prod_{n\neq 0} \int dV_n\ e^{-\frac{\beta}{4E_C} V_n V_{-n} + \frac{V_n}{\omega_n}(\exp(i\omega_n\tau)-1)} = \prod_{n\neq 0} e^{-\frac{2E_C T}{\omega_n^2}(1-\exp(-i\omega_n\tau))},$$

and in the second equality we have performed the Gaussian integral over $V_{n\neq 0}$.

(c) Using the formulae given above, the Matsubara summation gives

$$-2E_C T \sum_{n\neq 0} \frac{1}{\omega_n^2}(1-\exp(-i\omega_n\tau)) = -E_C(|\tau| - \beta^{-1}\tau^2),$$

i.e. $F(\tau) = \exp[-E_C(|\tau| - \beta^{-1}\tau^2)]$, and $G_\alpha(\tau) = F(\tau)\tilde{G}_\alpha(\tau)$, where

$$\tilde{G}_\alpha(\tau) = \mathcal{Z}^{-1} \int d\tilde{V}_0\ e^{-\frac{\beta}{4E_C}\tilde{V}_0^2 + i\beta N_0 \tilde{V}_0}\, \mathcal{Z}^{[\tilde{V}_0]} G_\alpha^{[\tilde{V}_0]}(\tau).$$

(d) Defining a $\tilde{V}_0$-dependent free energy by $\mathcal{Z}^{[\tilde{V}_0]} = \exp(-\beta F^{[\tilde{V}_0]})$, noting that $\tilde{V}_0$ shifts the chemical potential, $F^{[\tilde{V}_0]}(\mu) = F(\mu - i\tilde{V}_0)$, and neglecting the $\tilde{V}_0$-dependence of $G^{[\tilde{V}_0]} \simeq G$, we obtain the saddle-point equation

$$0 = \frac{\partial}{\partial \tilde{V}_0}\left(\frac{1}{4E_C}\tilde{V}_0^2 - iN_0\tilde{V}_0 - F(\mu - i\tilde{V}_0)\right) = \frac{1}{2E_C}\tilde{V}_0 - iN_0 + i\langle\hat{N}\rangle_{\mu - i\tilde{V}_0},$$

where in the second equality we have used the fact that $\frac{\partial}{\partial \tilde{V}_0} F(\mu - i\tilde{V}_0) = -i\partial_\mu F(\mu - i\tilde{V}_0) = -i\langle\hat{N}\rangle_{\mu - i\tilde{V}_0}$. Substituting the solution of the saddle-point equation $\bar{V}_0 = 2iE_C(N_0 - \langle\hat{N}\rangle_{\mu - i\bar{V}_0})$ amounts to replacing the chemical potential μ by an effective chemical potential $\bar{\mu} = \mu + 2E_C(N_0 - \langle\hat{N}\rangle_{\bar{\mu}})$. As a preliminary result we thus obtain

$G_\alpha(\tau) = F(\tau)G_{0\alpha\beta}$, where the non-interacting Green function is evaluated at the renormalized chemical potential. (In passing we note that the condition for the applicability of the saddle-point approximation reads as (Exercise: Why?) $1/(2E_C) - \partial_\mu \langle \hat{N} \rangle_{\bar{\mu}} \gg \beta$.)

(e) For $E_C \gg T$, the dominant contribution to the Fourier transform of $F(\tau)$ comes from the boundary regions of the imaginary time interval, $\tau \ll \beta$ and $\beta - \tau \ll \beta$. Linearizing the exponent of F in these regions we obtain

$$F_m = \int_0^\beta d\tau\, e^{i\omega_m \tau} F(\tau) \simeq \int_0^\infty d\tau \left(e^{i\omega_m \tau} + e^{-i\omega_m \tau} \right) e^{-E_C \tau} = \frac{2E_C}{E_C^2 + \omega_m^2}.$$

Using the fact that $G_{0n\alpha} = (i\omega_n - \xi_\alpha)^{-1}$, where $\xi_\alpha = \epsilon_\alpha - \bar{\mu}$, we then obtain

$$G_{n\alpha} = T \sum_m F_m G_{0(n-m)\alpha} \simeq \frac{1}{2\pi} \int d\omega\, \frac{1}{i\omega_n - i\omega - \xi_\alpha} \frac{2E_C}{E_C^2 + \omega^2} = \frac{1}{i\omega_n - E_C\ \mathrm{sgn}(\xi_\alpha) - \xi_\alpha}.$$

From this result we obtain the DoS

$$\begin{aligned} \nu(\epsilon) &= \sum_\alpha \delta(\epsilon - E_C\ \mathrm{sgn}(\xi_\alpha) - \xi_\alpha) = \int d\omega\, \nu_0\ (\omega) \delta(\epsilon - E_C\ \mathrm{sgn}(\omega) - \omega) \\ &= \nu_0(\epsilon - E_C\ \mathrm{sgn}(\epsilon)) \Theta(|\epsilon| - E_C), \end{aligned}$$

where ν_0 is the DoS of the non-interacting systems. Due to the large charging energy, the single-particle DoS vanishes in a window of width $2E_C$ centered around the Fermi energy: the **Coulomb blockade**. Particles of energy $\epsilon > E_C$ larger than the charging threshold are free to enter the dot. However, in doing so they lose an amount E_C of (charging) energy, which explains the energy shift in the factor ν_0.

Action of a tunnel junction

In the previous problem, we considered the physics of a perfectly isolated quantum dot. However, in practice (see, e.g., the dot depicted in the last problem) the system is usually connected to an external environment by some leads. It is the purpose of this problem to derive an effective action accounting for the joint effect of charging and the coupling to an environment.

Consider a quantum dot connected to an external lead (it is straightforward to generalize to the presence of several leads). For simplicity, we model the latter as an ideal wave-guide, i.e. the eigenstates ψ_a are plane waves whose detailed structure we need not specify. The composite system is described by an action $S[\psi_\alpha, \bar{\psi}_\alpha, \psi_a, \bar{\psi}_a] = S_{\mathrm{dot}}[\psi_\alpha, \bar{\psi}_\alpha] + S_{\mathrm{lead}}[\psi_a, \bar{\psi}_a] + S_{\mathrm{T}}[\psi_\alpha, \bar{\psi}_\alpha, \psi_a, \bar{\psi}_a]$, where $S_{\mathrm{dot}}[\psi_\alpha, \bar{\psi}_\alpha]$ is given by Eq. (6.66),

$$S_{\mathrm{lead}}[\bar{\psi}_a, \psi_a] = \sum_a \int_0^\beta d\tau\, \bar{\psi}_a (\partial_\tau + \epsilon_a - \mu) \psi_a,$$

and the coupling between dot and lead is described by

$$S_{\mathrm{T}}[\psi_\alpha, \bar{\psi}_\alpha, \psi_a, \bar{\psi}_a] = \sum_{a\alpha} \int d\tau\ \bar{\psi}_\alpha T_{\alpha a} \psi_a + \mathrm{h.c.}$$

Throughout we will assume that the coupling is sufficiently weak that contributions of $\mathcal{O}(T^4)$ to the effective action are negligibly small – the "tunneling approximation."

(a) Proceeding as in the previous problem, decouple the charging interaction by a Hubbard–Stratonovich transformation. Integrate out the fermions and subject the problem to the same gauge transformation as used above to remove the dynamical contents of the Hubbard–Stratonovich field V. You will observe that the gauge phase transforms the coupling matrices T.

(b) Expand the action to leading (i.e. second) order in the coupling matrix elements $T_{\alpha a}$. (You may ignore the integration over the static component of the Hubbard–Stratonovich field; as discussed above, it leads to merely a shift of the chemical potential.) Assuming that the single-particle DoS of dot and lead do not vary significantly on the energy scales at which the field V fluctuates, determine the dependence of the tunneling term on the gauge phase $\phi(\tau) \equiv \int^\tau d\tau'(V(\tau') - \tilde{V}_0)$ and identify its coupling constant as the Golden Rule tunneling rate $4g_T$.[87] (To obtain a finite result, you will need to regularize the action by subtracting from the tunneling action $S_{\rm tun}[\phi]$ the constant $S_{\rm tun}[0]$.) Expressing the charging action $S_{\rm c}[V]$ in terms of the gauge phase $V = \dot{\phi} + \tilde{V}_0$ (and neglecting the constant offset $\tilde{V}_0$), the complete **dissipative tunneling action** takes the form

$$\boxed{S[\phi] = \int d\tau \left(\frac{\dot{\phi}^2}{4E_C} - iN_0\dot{\phi} \right) - g_T \int d\tau d\tau' \frac{\sin^2((\phi(\tau) - \phi(\tau'))/2)}{\sin^2(\pi T(\tau - \tau'))}.} \tag{6.67}$$

INFO The action (6.67) was first derived by **Ambegaokar, Eckern, and Schön**.[88] Crudely, its behavior mirrors that of the quantum dynamics of a particle on a ring with kinetic energy $\sim \phi^2/E_C$ and subject to a dissipative damping mechanism of strength $\sim g_T$. Physically, the latter describes the dissipation of the energy stored in dynamical voltage fluctuations $V \sim \phi$ into the microscopic degrees of freedom of the quasi-particle continuum.

In the absence of dissipation, the action describes the ballistic motion of a quantum point particle on a ring. The ring topology reflects the 2π-periodicity of the quantum phase, which in turn relates to the quantization of charge (recall that charge and phase are canonically conjugate). It is, thus, no surprise that the periodicity of the ϕ-dynamics is the main source of charge quantization phenomena in the AES approach. For strong ($g_T > 1$) dissipation, the particle begins to forget that it actually moves on a ring (i.e. full traversals of the ring get increasingly less likely). This damping manifests itself in a massive suppression of charge quantization phenomena. Indeed, for increasing coupling between lead and dot, the charge on the latter begins to fluctuate and is no longer effectively quantized. For a detailed account of the physical phenomena relating to the crossover from weak to strong charge quantization, we refer to one of several reviews.[89]

[87] We denote the tunneling rate by g_T because (see Problem 7.6.3) it is but (four times) the classical conductance of the tunneling barrier, measured in units of the conductance quantum e^2/h.

[88] U. Eckern, G. Schön, and V. Ambegaokar, Quantum dynamics of a superconducting tunnel junction, *Phys. Rev. B* **30** (1984), 6419–31.

[89] See, e.g., I. L. Aleiner, P. W. Brouwer, and L. I. Glazman, Quantum effects in coulomb blockade, *Phys. Rep.* **358** (2002), 309-440.

Answer:

(a) Decoupling the action and integrating over the fermionic degrees of freedom, one obtains the functional $\mathcal{Z} = \exp(-S_{\rm eff}[V])$, where

$$\begin{aligned} S_{\rm eff} &= S_{\rm c} - \mathrm{tr}\ln\begin{bmatrix} \partial_\tau - \mu + iV + \hat{\epsilon}_{\rm d} & T \\ T^\dagger & \partial_\tau - \mu + \hat{\epsilon}_{\rm l} \end{bmatrix} \\ &= S_c - \mathrm{tr}\ln\begin{bmatrix} \partial_\tau - \mu + iV_0 + \hat{\epsilon}_{\rm d} & Te^{i\phi} \\ e^{-i\phi}T^\dagger & \partial_\tau - \mu + \hat{\epsilon}_{\rm l} \end{bmatrix} \end{aligned} \tag{6.68}$$

Here, as in the previous problem, $S_{\rm c}[V] = \int d\tau(\frac{V^2}{4E_C} - iN_0V)$, $\hat{\epsilon}_d = \{\epsilon_\alpha\delta_{\alpha\alpha'}\}$ and $\epsilon_{\rm l} = \{\epsilon_a\delta_{aa'}\}$ contain the single-particle energies of dot and lead, respectively, the matrix structure is in dot/lead space, and $\phi(\tau) = \int d\tau'\,(V(\tau') - V_0)$. In passing from the first to the second equality we have subjected the argument of the "tr ln" to the unitary transformation (gauge transformation) described by the matrix $\mathrm{diag}(e^{i\phi}, 1)$ (with the block structure in dot–lead space).

(b) Expanding the "tr ln" to second order in T, and regularizing by subtracting the constant $S_{\rm tun}[0]$, we obtain

$$S_{\rm tun}[\phi] = |T|^2 \sum_{\alpha a}\sum_n \left[\sum_m G_{\alpha,n}(e^{i\phi})_m G_{a,n+m}(e^{-i\phi})_{-m} - G_{\alpha,n}G_{a,n}\right] + S_{\rm tun}[0], \tag{6.69}$$

where $G_{\alpha/a,n} = (i\omega_n - \hat{\epsilon}_{\alpha/a} + \mu)^{-1}$ are the Green functions of dot and lead, respectively, and the constant $S_{\rm tun}[0]$ will be omitted throughout. Approximating the Green functions by

$$\sum_{\alpha/a} G_{\alpha/a,n} = -\int d\epsilon\ \rho_{\rm d/l}(\epsilon+\mu)\frac{i\omega_n + \epsilon}{\omega_n^2 + \epsilon^2} \simeq -\pi i \rho_{\rm d,l}\mathrm{sgn}(\omega_n), \tag{6.70}$$

where $\rho_{\rm d,l} \equiv \rho_{\rm d,l}(\mu)$ is the density of states at energy μ, we arrive at the result

$$\begin{aligned} S_{\rm tun}[\phi] &= \frac{g_T}{2}\sum_{n,m}(-\mathrm{sgn}(\omega_n)\mathrm{sgn}(\omega_{n+m}) + 1)(e^{i\phi})_m(e^{-i\phi})_{-m} \\ &= \frac{g_T}{2\pi T}\sum_m |\omega_m|(e^{i\phi})_m(e^{-i\phi})_{-m}, \end{aligned} \tag{6.71}$$

where we note that $\sum_m (e^{i\phi})_m(e^{-i\phi})_{-m} = 1$, $g_T = 2\pi^2\rho_{\rm l}\rho_{\rm d}|T|^2$ is proportional to the Golden Rule tunneling rate between dot and lead, and the appearance of a term $\sim |\omega_m|$ is a clear signature of a dissipative damping mechanism. Using the fact that the Fourier transform of $|\omega_m|$ is given by (cf. Eq. (3.44)) $\pi T \sin^{-2}(\pi T\tau)$, the tunneling action can be cast in a time-representation as

$$\begin{aligned} S_{\rm tun}[\phi] &= -\frac{g_T}{2}\int d\tau\ d\tau' \frac{e^{i\phi(\tau) - i\phi(\tau')}}{\sin^2(\pi T(\tau - \tau'))} \\ &= g_T \int d\tau\, d\tau' \frac{\sin^2((\phi(\tau) - \phi(\tau'))/2)}{\sin^2(\pi T(\tau - \tau'))} + \text{const.} \end{aligned}$$

We finally add the charging action to obtain the result Eq. (6.67).

Josephson junction

Building on the results obtained in the previous problem, here we derive an effective action of a Josephson junction – a system comprising two superconductors separated by an insulating or normal conducting interface region. The problem includes a preliminary discussion of the physics of the Josephson junction, notably its current–voltage characteristics. In Chapter 8, renormalization group methods will be applied to explore in detail the phenomenology of the system.

Consider two superconducting quantum dots separated by a tunneling barrier. Generalizing the model discussed in the last two problems, we describe each dot by an action

$$S^i[\bar\psi^i_\alpha,\psi^i_\alpha,\phi_i]=\int_0^\beta d\tau\left\{\sum_\alpha \bar\psi^i_\alpha(\partial_\tau+\xi_{i\alpha}\sigma_3+e^{i\phi_i(\tau)\sigma_3}\Delta\sigma_1)\psi^i_\alpha \quad , \quad i=1,2,\right.$$

where $\psi^i_\alpha=(\psi^i_{\alpha\uparrow},\bar\psi^i_{\alpha\downarrow})^T$ are Nambu spinors, σ_i Pauli matrices in particle–hole space, and ϕ_i the phase of the order parameter on dot i. Noting that two dots form a capacitor, we assume the presence of a "capacitive interaction"

$$S_{\rm int}=\frac{E_C}{4}\int d\tau\ (\hat N_1-\hat N_2)^2,$$

where $\hat N_i=\sum_\alpha \bar\psi^i_\alpha\sigma_3\psi^i_\alpha$ is the charge operator on dot i, and $1/2E_C$ the capacitance of the system. Finally, the tunneling between the two dots is described by the action

$$S_{\rm T}[\psi_\alpha,\bar\psi_\alpha]=\sum_{\alpha\beta}\int d\tau\ \bar\psi^1_\alpha(T_{\alpha\beta}\sigma_3)\psi^2_\beta+{\rm h.c.},$$

where $T_{\alpha\beta}=\langle\alpha|\hat T|\beta\rangle$ denotes the tunneling matrix elements between the single-particle states $|\alpha\rangle$ and $|\beta\rangle$. Now, were it not for the presence of the superconducting order parameter, the low-energy physics of the system would again be described by the effective action (6.67).

EXERCISE Convince yourself of the validity of this statement, i.e. check that the dot–dot system can be treated along the same lines as the dot–lead system considered above and trace the phase dependence of the various contributions to the action.

(a) Turning to the superconducting case, show that, at an intermediate stage, the action is given by

$$S_{\rm eff}[V,\phi]$$
$$=S_{\rm c}[V]-{\rm tr}\ln\begin{bmatrix}\partial_\tau+(\hat\xi_1+i(\dot\phi_1+V)/2)\sigma_3+\Delta\sigma_1 & e^{-i(\phi_1-\phi_2)\sigma_3/2}T\\ T^\dagger e^{i(\phi_1-\phi_2)\sigma_3/2} & \partial_\tau+(\hat\xi_2+i(\dot\phi_2-V)/2)\sigma_3+\Delta\sigma_1\end{bmatrix},$$

where $\hat\xi_i, i=1,2$, comprise the single-particle energies of the system, and $S_{\rm c}[V]=(1/4E_C)\int d\tau\ V^2$ is the charging action. At zeroth order in T, expand the action to second order in the combinations $\dot\phi_i\pm V$. Vary your result with respect to $\dot\phi_{1,2}$ to obtain

the **Josephson condition** $\dot{\phi}_1 = -\dot{\phi}_2 \equiv -\dot{\phi}$ and $V = \dot{\phi}$. Neglecting the effect of these massive quadratic fluctuations, we will rigidly impose this condition throughout. (Hint: You may assume that the characteristic frequencies ω_m carried by both the fields ϕ_i and the voltage V are much smaller than those of the bare Green function. Use this assumption to keep your analysis on a schematic level, i.e. try to argue in general terms rather than performing the expansion in great detail.)

(b) Expanding the action to second order in T (i.e. the leading order) and using the Josephson conditions, show that $S = S_c + S_{\rm tun}$, where

$$S_{\rm tun}[\phi] = |T|^2 \sum_{\alpha\alpha'\omega_m\omega_n} \mathrm{tr}\left(G_{1,\alpha\omega_n}(e^{i\sigma_3\phi})_m G_{2,\alpha'\omega_n+\omega_m}(e^{-i\sigma_3\phi})_{-m} - (\phi \leftrightarrow 0)\right),$$

$G_{i\alpha\omega_n} = (i\omega_n - \xi_{i\alpha}\sigma_3 - \hat{\Delta}\sigma_1)^{-1}$ is the bare Gor'kov Green function, and we again regularize the tunneling action by subtracting $S_{\rm tun}[\phi = 0]$. Denoting the block diagonal/off-diagonal contributions to the Green function by $G_{i,d/o}$, respectively, the tunneling action splits into two contributions, (symbolically) $\mathrm{tr}(G_{1d}e^{i\phi\sigma_3}G_{2d}e^{-i\phi\sigma_3} + G_{1o}e^{i\phi\sigma_3}G_{2o}e^{-i\phi\sigma_3})$. Show that, up to small corrections of $\mathcal{O}(\omega_n/\Delta)$, the diagonal terms vanish and interpret this result. (Hint: Compare with the discussion of the previous problem.)

(c) Turning to the particle/hole off-diagonal sector, show that

$$S_{\rm tun}[\Delta, \phi] = \gamma \int_0^\beta d\tau \ \cos(2\phi(\tau)), \quad \gamma = |T|^2(\pi\rho)^2\Delta.$$

Combining everything, one obtains the **action of the Josephson junction**,

$$\boxed{S[\phi] = \frac{1}{4E_C}\int d\tau \ \dot{\phi}^2 + \gamma \int d\tau \ \cos(2\phi(\tau)) + \Gamma S_{\rm diss}[\phi].} \tag{6.72}$$

While our analysis above suggests that the coefficient of the dissipative term should be zero (on account of the absence of low-energy quasi-particle states which might act as a dissipative sink of energy), voltage fluctuations in "real" Josephson junctions *do* seem to be dissipatively damped, even at low fluctuation frequencies. Although there is no obvious explanation of this phenomenon, it is common to account for the empirically observed loss of energy by adding a dissipation term to the action.

(d) Finally, explore the current–voltage characteristics of the non-dissipative junction. To this end, perform a Hubbard–Stratonovich transformation on the quadratic charging interaction. What is the physical meaning of the Hubbard–Stratonovich auxiliary field? Interpret the action as the Hamiltonian action of a conjugate variable pair and compute the equations of motion. Show that the **Josephson current** flowing between the superconductors is given by

$$I = -2\gamma \sin(2\phi). \tag{6.73}$$

According to this equation, a finite-order parameter phase difference causes the flow of a static current, carried by Cooper pairs tunneling coherently across the barrier: the **DC Josephson effect**. Application of a finite voltage difference or, equivalently, the presence of a finite charging energy, render the phase $\dot{\phi} = V$ dynamical. For a static

voltage difference, ϕ increases uniformly in time and the current across the barrier behaves as time-oscillatory: the **AC Josephson effect**. Finally, if the voltage difference becomes very large, $V \gg \Delta$, the Fourier spectrum of ϕ contains frequencies $|\omega_m| > \Delta$ (think about it). At these frequencies, phase variations have the capacity to create quasi-particle excitations which in turn may tunnel incoherently across the barrier (thereby paying a price in condensate energy but benefiting from the voltage drop). The tunneling of independent quasi-particles is described by the dissipative term in the action (which, we recall, is negligible only at frequencies $|\omega_m| < \Delta$).

Answer:

(a) The given result is proven by decoupling the capacitive interaction by a field V and integrating out the fermions. We next subject the "tr ln" to the gauge transformation (symbolic notation)

$$\mathrm{tr}\ln\begin{pmatrix}\hat{G}_1^{-1} & T\\ T^\dagger & \hat{G}_2^{-1}\end{pmatrix} \to \mathrm{tr}\ln\left[\begin{pmatrix}e^{-i\phi_1\sigma_3/2} & \\ & e^{-i\phi_2\sigma_3/2}\end{pmatrix}\begin{pmatrix}\hat{G}_1^{-1} & T\\ T^\dagger & \hat{G}_2^{-1}\end{pmatrix}\begin{pmatrix}e^{i\phi_1\sigma_3/2} & \\ & e^{i\phi_2\sigma_3/2}\end{pmatrix}\right].$$

This removes the phase dependence from the order parameters of the Green functions. At the same time, the tunneling matrices become phase-dependent and the diagonal terms of the Green functions acquire a contribution $i\dot{\phi}_i$, as indicated in the formula above.

An expansion of the $T = 0$ action to second order in ϕ_i and V gives an expression of the structure

$$\begin{aligned} S[\phi_i, V] &= \sum_{i=1,2}\int d\tau\ d\tau'\ (\dot{\phi}_i - (-)^i V)(\tau)F(\tau-\tau')(\dot{\phi}_i - (-)^i V)(\tau') \\ &= C\int d\tau\ (\dot{\phi}_i - (-)^i V)^2(\tau) + \cdots, \end{aligned}$$

where the time dependence of the integral kernel F is determined by the bare Green function. Assuming that this fluctuates rapidly, we may expand as indicated in the second equality, where the ellipsis represents higher-order derivatives acting on the slow fields ϕ_i, V and the constant C must be positive on stability grounds. A straightforward variation of the quadratic integral with respect to ϕ_i and V gives the Josephson conditions.

(b) Decoupling the interaction operators by two Hubbard–Stratonovich fields $V_i = \dot{\phi}_i$ and integrating out the fermions, we obtain

$$\begin{aligned} S_{\mathrm{eff}}[\phi] &= \sum_i S_c[\phi_i] - \mathrm{tr}\ln\begin{bmatrix}\partial_\tau - (\hat{\xi}_1 - i\dot{\phi}_1)\sigma_3 - \Delta\sigma_1 & T\sigma_3\\ T^\dagger\sigma_3 & \partial_\tau - (\hat{\xi}_2 - i\dot{\phi}_2)\sigma_3 - \Delta\sigma_1\end{bmatrix} \\ &= \sum_i S_c[\phi_i] - \mathrm{tr}\ln\begin{bmatrix}\hat{G}_1^{-1} & Te^{-i\Delta\phi\sigma_3}\\ e^{i\Delta\phi\sigma_3}T^\dagger & \hat{G}_2^{-1}\end{bmatrix}, \end{aligned}$$

where $\hat{\xi}_i$ denotes the matrix of energies of the two dots. An expansion to leading order in the off-diagonal blocks obtains the preliminary action $S_{\rm tun}[\phi]$.

Substituting the diagonal contribution to the Green function $(\hat{G}_{i,d})_n = (-i\omega_n - \hat{\xi}_i\sigma_3)/(\omega_n^2 + \hat{\xi}_i^2 + \Delta^2)$ into the tunneling action and comparing with Eq. (6.69), we find that the sum Eq. (6.70) becomes replaced by

$$\sum_a (G_{i,d})_{a,\omega_n} = \int d\epsilon\, \rho_i(\epsilon+\mu) \frac{-i\omega_n - \epsilon\sigma_3}{\omega_n^2+\epsilon^2+\Delta^2} \simeq -i\pi\rho_i \frac{\omega_n}{(\omega_n^2+\Delta^2)^{1/2}}.$$

Comparing with Eq. (6.71), we obtain

$$\sum_n \left(-\frac{\omega_n}{(\omega_n^2+\Delta^2)^{1/2}} \frac{\omega_{n+m}}{(\omega_{n+m}^2+\Delta^2)^{1/2}} + 1 \right) \simeq \begin{cases} |\omega_m|/\pi T, & |\omega_m| \gg \Delta, \\ 0 + \mathcal{O}(\omega_m/\Delta), & |\omega_m| \ll \Delta, \end{cases}$$

instead of a global factor $|\omega_m|/2\pi T$. The physical interpretation of this result is that only high-frequency ($\omega > \Delta$) fluctuations of the voltage field $V = \dot{\phi}$ have the capacity to overcome the superconductor gap and dissipate their energy by creating quasi-particle excitations. In contrast, low-frequency fluctuations do not suffer from dissipative damping.

(c) Substituting the off-diagonal term $(G_{o,i})_n(\tau) = -\Delta\sigma_1/(\omega_n^2 + \hat{\xi}_i^2 + \Delta^2)$ into the tunneling action and neglecting contributions of $\mathcal{O}(|\omega_m|/\Delta)$, we find

$$\begin{aligned} S_{\rm tun}[\phi_1] &\simeq |T|^2 \sum_{n,m} \sum_{\alpha\alpha'} \frac{\Delta}{\omega_n^2+\xi_\alpha^2+\Delta^2} \frac{\Delta}{\omega_n^2+\xi_{\alpha'}^2+\Delta^2} \mathrm{tr}\left(\sigma_1 (e^{i\sigma_3\phi})_m \sigma_1 (e^{-i\sigma_3\phi})_{-m}\right) \\ &= \frac{|T|^2(\pi\rho)^2\Delta}{2T} \sum_m \mathrm{tr}\left(\sigma_1 (e^{i\sigma_3\phi})_m \sigma_1 (e^{-i\sigma_3\phi})_{-m}\right) \\ &= |T|^2(\pi\rho)^2\Delta \int d\tau \cos(2\phi(\tau)). \end{aligned}$$

(d) Think of the non-dissipative Josephson action as the action of a point particle with kinetic energy $\sim E_C^{-1}\dot{\phi}^2$ and potential energy $\cos(2\phi)$. In this language, passage to the Hubbard–Stratonovich decoupled action

$$S[\phi, N] = E_C \int d\tau\ N^2 + \gamma \int d\tau \cos(2\phi(\tau)) + i \int d\tau\ N\dot{\phi},$$

amounts to a transition from the Lagrangian to the Hamiltonian picture. The notation emphasizes that the momentum conjugate to the phase variable is the number operator of the system. (More precisely, N measures the difference of the charge carried by the two superconductors; the total charge of the system is conserved.) Varying the action, we obtain the Hamilton equations

$$\dot{\phi} = i2E_C N, \quad \dot{N} = 2i\gamma \sin(2\phi).$$

Now, $I = i\partial_\tau N$ is the current flowing from one dot to the other, i.e. the second relation gives the Josephson current Eq. (6.73). The first relation states that, for a finite charging energy, mismatches in the charge induce time variations in the phase. By virtue of the Josephson relation, such time variations are equivalent to a finite voltage drop.

Field theory of the BCS to BEC crossover

As we have seen in the main text, the formation of the superconducting and Bose–Einstein condensates – the macroscopic occupation of a single quantum state – is characterized by two paradigms.

In the BCS theory, the transition from a normal to a superconducting phase of electrons involves a pairing instability which takes place at a temperature $T_c \ll \epsilon_F$ where the Fermi energy ϵ_F sets the degeneracy scale. In particular, the formation of Cooper pairs and their condensation occur simultaneously at the transition temperature.

Similarly, the transition of a Bose gas to a Bose–Einstein condensate (BEC) phase occurs at a temperature T_c comparable to the degeneracy temperature – in the bosonic system, the temperature at which the thermal length $hv/k_B T$ becomes comparable to the typical particle separation. However, the bosonic particles participating in the condensate are invariably molecules or composites involving an even number of elementary fermionic degrees of freedom, e.g. ^{4}He, Rb atoms, etc. Usually, the corresponding dissociation temperature of the particles into their fermionic constituents T_{dis} is greatly in excess of the BEC transition temperature T_c – the condensate forms out of preformed bosons.

The separation of the energy scales T_{dis} and T_c means that systems which undergo a BCS or BEC transition can be neatly classified. However, in some systems (such as fermionic atom condensates), the transition temperature can be comparable to (or even tuned through) the molecular dissociation temperature. Such systems have the capacity to manifest a BEC to BCS crossover. The aim of this extended problem is to develop a field theory to describe the crossover.

Although the study of the BEC to BCS crossover has a long history, the modern perspective on the subject can be traced back to the seminal work[90] of Anthony Leggett. In this early work, it was shown that the smooth crossover from a BCS to a BEC state could be described within the framework of a single variational wavefunction. In the following, we will develop a field theory to explore the crossover in the framework of the original Hamiltonian considered by Leggett.[91]

Sir Anthony J. Leggett 1938– Co-recipient of the 2003 Nobel Prize in Physics (with Alexei A. Abrikosov and Vitaly L. Ginzburg) "for pioneering contributions to the theory of superconductors and superfluids." He has made important contributions to the theory of normal and superfluid helium liquids and other strongly coupled superfluids, macroscopic dissipative quantum systems, and the use of condensed systems to test the foundations of quantum mechanics. (Image © The Nobel Foundation.)

[90] See, e.g., A. J. Leggett, *Modern Trends in the Theory of Condensed Matter*, A. Pekalski and R. Przystawa, eds. (Springer-Verlag, 1980) as well as the later work by P. Nozières and S. Schmitt-Rink, *J. Low Temp. Phys.* **59** (1985), 195–211. See also the related work by Keldysh and collaborators from the 1960s on the closely related problem of exciton condensation phenomena.

[91] Our analysis will follow closely that described in M. Randeria, Crossover from BCS theory to Bose–Einstein condensation, in *Bose–Einstein Condensation*, A. Griffin, D. W. Snoke, and S. Stringari eds. (Cambridge University Press, 1985).

Consider the Hamiltonian of a three-dimensional gas of spinful fermionic particles interacting through an attractive local (i.e. contact) pairwise interaction,

$$\hat{H} - \mu\hat{N} = \sum_{\mathbf{k}\sigma} \xi_{\mathbf{k}} c^\dagger_{\mathbf{k}\sigma} c_{\mathbf{k}\sigma} - gL^3 \int d^3r \; c^\dagger_\uparrow c^\dagger_\downarrow c_\downarrow c_\uparrow,$$

where $\xi_{\mathbf{k}} = \epsilon_{\mathbf{k}} - \mu$, $\epsilon_{\mathbf{k}} = \mathbf{k}^2/2m$, and the parameter g characterizes the strength of the interaction.

(a) Starting with the coherent state path integral formulation of the quantum partition function, introduce a Hubbard–Stratonovich field, decoupling the pair interaction and, integrating out the fermionic degrees of freedom, obtain an effective action involving the pairing field Δ. (Select only the pairing channel in the decoupling.)

(b) Varying the action with respect to Δ, show that the *transition temperature* is determined by the saddle-point equation

$$\frac{1}{g} = \sum_{\mathbf{k}} \frac{\tanh(\xi_{\mathbf{k}}/2T_c)}{2\xi_{\mathbf{k}}}.$$

An inspection of the momentum summation will confirm the presence of a high-energy (UV) divergence. In the conventional BCS theory of the superconductor discussed in the main text, one may recall that this high-energy divergence was regularized by a physical cut-off derived from the pairing mechanism itself – the phonon exchange mechanism imposed a cut-off at the Debye frequency $\omega_{\rm D} \ll \mu$, the highest phonon energy allowed by the crystal lattice, which restricted the range of the momentum sum to an energy shell around the Fermi level. In the present case, the UV divergence reflects a pathology of the contact interaction. Had one chosen a more physical pair potential $g(\mathbf{r} - \mathbf{r}')$ involving both a magnitude g *and a range* b, the momentum sum would have involved a soft cut-off at the momentum scale $|\mathbf{k}| \sim 1/b$ (exercise). Equivalently, to implement the physical cut-off, one may replace the bare coupling constant g by the low-energy limit of the two-body T-matrix (in the absence of the surrounding medium). In three dimensions, this translates to the regularization[92]

$$\frac{m}{4\pi a} = -\frac{1}{g} + \sum_{\mathbf{k}} \frac{1}{2\epsilon_{\mathbf{k}}},$$

where a denotes the s-wave scattering length. As a function of the (positive) bare interaction g, $1/a$ increases monotonically from $-\infty$ for a very weak attraction to $+\infty$ for a very strong attraction. Beyond the threshold $1/a = 0$, the two-body system develops a bound state with a size a and binding energy $E_{\rm B} = 1/ma^2$. Therefore, one can identify the ratio of the typical particle separation and scattering length $1/k_{\rm F}a$ as the

[92] To understand this result, one may note that, for an isolated two-body scattering involving a potential V, the scattering T-matrix obeys the Lippmann–Schwinger equation $\hat{T} = \hat{V} + \hat{V}\hat{G}_0\hat{T}$, where $\hat{G}_0$ denotes the bare Green function of the free particles. Applied to the potential $V(\mathbf{r}) = -gL^d\delta(\mathbf{r})$, the diagonal $\mathbf{k} = 0$ component of the T-matrix, which translates to the physical scattering length a, can be obtained from the self-consistent solution of the equation as $T(0,0) = 4\pi a/m = [-(1/g) + \sum_k (1/2\epsilon_k)]^{-1}$.

dimensionless coupling constant where $k_{\rm F}$ and $\epsilon_{\rm F}$ denote the Fermi wavevector and energy of the non-interacting system.

With this interpretation, the saddle-point equation acquires the regularized form

$$-\frac{m}{4\pi a} = \sum_{\mathbf{k}} \left[\frac{\tanh(\xi_{\mathbf{k}}/2T_{\rm c})}{2\xi_{\mathbf{k}}} - \frac{1}{2\epsilon_{\mathbf{k}}} \right].$$

When combined with the equation for the particle density $n(\mu,T) = -\frac{1}{L^3}\frac{\partial F}{\partial \mu} \simeq \sum_{\mathbf{k}} [1-\tanh(\xi_{\mathbf{k}}/2T)]$, valid in the mean-field approximation, this presents an equation for $T_{\rm c}$ and μ.

(c) In the weak coupling BCS limit, $1/k_{\rm F}a \to -\infty$, show that the chemical potential is fixed by the density such that $\mu \simeq \epsilon_{\rm F}$ and, making use of the identity

$$\int_0^\infty dz\, z^{1/2} \left[\frac{\tanh((z-1)/2t)}{2(z-1)} - \frac{1}{2z} \right] = \ln\left(\frac{8\gamma}{\pi e^2 t} \right),$$

where $\gamma = e^C$ and C denotes Euler's constant, show that the saddle-point equation translates to the condition

$$T_{\rm c} = \frac{8\gamma}{\pi e^2}\epsilon_{\rm F} \exp\left[\frac{\pi}{2k_{\rm F}|a|} \right].$$

(d) In the strong coupling limit $1/k_{\rm F}a \to +\infty$, the roles of the saddle-point equation and number density are reversed. The former now fixes the chemical potential $\mu < 0$ while, superficially, the latter determines $T_{\rm c}$. In particular, making use of the identity, $\int_0^\infty dz\, z^{1/2}\left[\frac{1}{2(z+1)} - \frac{1}{2z}\right] = -\frac{\pi}{2}$, show that

$$\mu = -\frac{E_{\rm B}}{2} = \frac{1}{2ma^2}, \quad T_{\rm c} \simeq \frac{E_{\rm B}}{2\ln\left(\frac{E_{\rm B}}{\epsilon_{\rm F}}\right)^{3/2}}.$$

In fact, the apparent divergence of the transition temperature $T_{\rm c}$ in the strong coupling limit is a pathology of the mean-field analysis. The inferred value of $T_{\rm c}$ represents the dissociation energy of the pairs $T_{\rm dis}$ rather than the temperature scale at which coherence is established. To understand why, we have to turn to the analysis of fluctuations.

EXERCISE Enthusiasts may enjoy exploring the saddle-point analysis of the condensed phase at zero temperature when the order parameter Δ acquires a non-zero expectation value. These results may be compared with the variational analysis based on the ground state wavefunction $|{\rm g.s.}\rangle = \prod_k (u_{\mathbf{k}} + v_{\mathbf{k}} c^\dagger_{\mathbf{k}}\, c^\dagger_{-\mathbf{k}})|\,\rangle$ described in Leggett's original work. Note that, in the low-density limit, the variational parameter $v_{\mathbf{k}}$ describes the bound state wavefunction of a single pair.

(e) Developing the action to quartic order in Δ show that the Ginzburg–Landau expansion of the action takes the form

$$S = \frac{F_0}{T} + \sum_q \Pi(q)|\Delta(q)|^2 + \int d^d r\, \frac{u}{4}|\Delta(\mathbf{r})|^4 + \cdots,$$

where F_0 denotes the free energy of the non-interacting Fermi gas,

$$\Pi(q) = \sum_{\mathbf{k}} \left[\frac{1 - n_f(\xi_{\mathbf{k}}) - n_{\mathrm{F}}(\xi_{\mathbf{k}+\mathbf{q}})}{i\omega_m - \xi_{\mathbf{k}} - \xi_{\mathbf{k}+\mathbf{q}}} + \frac{1}{2\epsilon_{\mathbf{k}}} \right] - \frac{m}{4\pi a},$$

denotes the pairing susceptibility, and u is a positive constant. In the weak coupling limit $1/k_{\mathrm{F}}a \to -\infty$, confirm that the gradient expansion of the susceptibility leads to the Ginzburg–Landau expansion discussed in Section 6.4. Conversely, in the strong coupling limit $1/k_{\mathrm{F}}a \to +\infty$, show that

$$\Pi(q) \simeq \frac{\pi}{2} \frac{\nu(\epsilon_{\mathrm{F}})}{\sqrt{2\epsilon_{\mathrm{F}} E_{\mathrm{B}}}} \left(-i\omega_m - 2\mu + \omega_{\mathrm{B}}(\mathbf{q}) \right),$$

where $\omega_{\mathrm{B}} = -E_{\mathrm{B}} + \mathbf{q}^2/4m$. Absorbing the prefactor into an overall rescaling of the field Δ, the corresponding action can now be recognized as that of a weakly interacting Bose gas of composite particles with a mass $2 \times m$ and density $n/2$ – cf. Section 6.3. The failure of the mean-field theory to infer the correct value of T_{c} now becomes clear. In the mean-field description, it is assumed that, at temperatures $T > T_{\mathrm{c}}$, particles exist as unbound fermions. However, the action above shows that, for temperatures only slightly in excess of T_{c}, the particles already exist as bound pairs. The bulk transition takes place when these bound pairs condense.

Once identified as a weakly interacting Bose gas, one can immediately deduce that, in the strong coupling limit, T_{c} becomes independent of the scattering length and varies with density as

$$T_{\mathrm{c}} = \left(\frac{n}{2\zeta(3/2)} \right)^{2/3} \frac{\pi}{m}.$$

INFO **BEC–BCS transition in fermionic alkali atomic gases and cold exciton liquids:** As mentioned above, in the majority of condensed matter systems the dissociation energy T_{dis} is well separated from the transition temperature T_{c}, and the majority of condensates can be neatly classified as being of BCS or BEC type. However, two systems which present the opportunity to explore crossover phenomena have been the subject of considerable interest in the experimental and theoretical literature.

At low temperatures a "quasi-equilibrium" degenerate gas of electrons and holes forms a two-component plasma.[93] At low densities, the constituent electrons and holes can bind to form neutral composite objects known as excitons. Comprising an electron and hole, these objects transform as bosons and, as such, have the capacity to undergo BEC. At high densities, the electrons and holes become unbound and exist as a two-component plasma. Yet, by exploiting the Coulomb interaction, at low enough temperatures the electrons and holes can condense into a collective BCS-like phase – the *exciton insulator* in which a quasi-particle energy gap develops at the Fermi surface. Leaving aside the capacity for other phases to develop (namely electron–hole droplets or molecules), the particle density can be used as a parameter to mediate a crossover between a BEC and a BCS-like phase. (In fact, a careful study of the free energy at mean-field

[93] Here the term "quasi-equilibrium" is used to acknowledge the fact that, in a conventional direct band-gap semiconductor, an electron–hole plasma can lower its energy by recombination. If the recombination rate is slower than the equilibration time, an electron–hole plasma may, in principle, acquire a quasi-equilibrium distribution.

shows the crossover to occur via a phase transition of high order. Whether the weak transition is smeared into a crossover by thermal fluctuations remains unclear.) To date, experimentalists have been unable to defeat the problems posed by fast radiative and Auger-assisted recombination processes to unambiguously realize such a condensate.[94]

A second example of a BEC to BCS crossover is presented by the atomic condensates. As mentioned in the text, the realization of BEC in atom condensates is now almost routine. Lately, there have been considerable efforts targeted at realizing BCS-like condensates of fermionic atoms such as ^{6}Li and ^{40}K. Yet, it being charge neutral, the experimental identification of a BCS phase presents considerable difficulties – a feature shared by the electron–hole condensate. As a result experimentalists have used "*Feshbach resonance*" phenomena to tune the atomic pair interaction from weak to strong coupling, whence the atoms exist as tightly bound pairs. By monitoring the dynamics of BEC formation, attempts have been made to infer the properties of the ephemeral BCS-like phase.[95]

Answer:

(a) Referring to Section 6.4, a decoupling of the pair interaction by a field Δ gives the partition function

$$\mathcal{Z} = \int D(\bar{\Delta}, \Delta)\, \exp\left[-\frac{1}{g}\int d\tau \int d^d r\, |\Delta|^2 + \ln\det \hat{\mathcal{G}}^{-1}\right],$$

where

$$\hat{\mathcal{G}}^{-1} = \begin{pmatrix} -\partial_\tau - \xi_{\mathbf{k}} & \Delta \\ \bar{\Delta} & -\partial_\tau + \xi_{\mathbf{k}} \end{pmatrix},$$

denotes the matrix Gor'kov Green function.

(b) Once again referring to Section 6.4, a variation of the action with respect to Δ gives the saddle-point equation

$$\frac{\bar{\Delta}(\mathbf{r},\tau)}{g} - \mathrm{tr}\left[\hat{\mathcal{G}}(\mathbf{r},\tau;\mathbf{r},\tau)E_{12}^{\mathrm{ph}}\right] = 0.$$

In particular, for $\Delta \to 0$, an integration over the Matsubara frequencies leads to the required saddle-point equation.

(c) Firstly, in the weak coupling limit, we have that $T_{\mathrm{c}} \ll \mu$. Therefore, to leading order, one may note that $\mu \simeq \epsilon_{\mathrm{F}}$. Then, in this approximation, applying the regularisation procedure outlined in the question, the saddle-point equation takes the form

$$-\frac{m}{4\pi a} = \int_0^\infty d\epsilon\, \nu(\epsilon)\left[\frac{\tanh[(\epsilon-\epsilon_{\mathrm{F}})/2T_{\mathrm{c}}]}{2(\epsilon-\epsilon_{\mathrm{F}})} - \frac{1}{2\epsilon}\right],$$

[94] For a general review of the field, we refer to Griffin, Snoke, and Stringari, eds., *Bose–Einstein Condensation.*

[95] For a review of this general field, we refer to, e.g., M. Holland, S. J. J. M. F. Kokkelmans, M. L. Chiofalo, and R. Walser, Resonance superfluidity in a quantum degenerate Fermi gas, *Phys. Rev. Lett.* **87** (2001), 120406.

where $\nu(\epsilon) = m^{3/2}\sqrt{\epsilon}/\sqrt{2}\pi^2$ denotes the three-dimensional density of states. Making use of the given identity, and noting that $m/4\pi a\nu(\epsilon_{\rm F}) = \pi/2k_{\rm F}a$, one obtains the required estimate for $T_{\rm c}$.

(d) In the strong coupling limit, one expects a bound state to develop in advance of the transition. In the limit of low density $\epsilon_{\rm F} \to 0$, the appearance of the bound state is signaled by the chemical potential reversing sign. For $T_{\rm c} \ll |\mu|$, the saddle-point equation becomes largely temperature-independent and acquires the form

$$-\frac{m}{4\pi a} = \int d\epsilon\, \nu(\epsilon) \left[\frac{1}{2(\epsilon + |\mu|)} - \frac{1}{2\epsilon}\right].$$

Making use of the given identity, one obtains the required formula for the chemical potential. In the low-density limit, the latter asymptotes to (one half of) the bound state energy $E_{\rm B}$. Then, when μ is substituted into the equation for the particle number, one obtains

$$n \simeq 2\int_0^\infty d\epsilon\, \nu(\epsilon) \exp\left[-\frac{\epsilon + E_{\rm B}/2}{T}\right].$$

When equated with the expression for the number density, $n = \int_0^{\epsilon_{\rm F}} d\epsilon\, \nu(\epsilon)$, a rearrangement of the equation obtains the required estimate for $T_{\rm c}$. As mentioned in the question, here one must interpret $T_{\rm c}$ as the dissociation temperature, which may be – and, in the physical context, usually is – greatly in excess of the Bose-Einstein condensation temperature.

(e) When properly regularized, the expansion of the action to second order follows directly the procedure outlined in Section 6.4. In the weak coupling limit, the chemical potential asymptotes to the Fermi energy of the non-interacting system, $\epsilon_{\rm F}$. Here the gradient expansion of the pair susceptibility $\Pi(q)$ is strictly equivalent to that discussed in Section 6.4. By contrast, the strong coupling expansion requires further consideration. In this case, one may expect $\mu < 0$. For temperatures $T \ll |\mu|$, noting that $\xi_{\mathbf{k}+\mathbf{q}/2} + \xi_{\mathbf{k}-\mathbf{q}/2} = 2(\epsilon_{\mathbf{k}} - \mu) + \mathbf{q}^2/4m$ one obtains

$$\Pi(q) \simeq \sum_{\mathbf{k}} \left[\frac{1}{i\omega_m - 2(\epsilon_{\mathbf{k}} - \mu) - \mathbf{q}^2/4m} + \frac{1}{2\epsilon_{\mathbf{k}}}\right] - \frac{m}{4\pi a}.$$

Then, making use of the identity proposed in part (d), one obtains

$$\Pi(q) = \frac{\pi}{2}\frac{\nu(\epsilon_{\rm F})}{\sqrt{2\epsilon_{\rm F}}}\sqrt{-2\mu + \frac{\mathbf{q}^2}{4m} - i\omega_m} - \frac{m}{4\pi a}.$$

Expanding the argument of the square root in deviations from the bound state energy $E_{\rm B}$, one obtains the required gradient expansion.

Metallic magnetism

Previously we have seen that the functional field integral provides a convenient framework in which a perturbation theory of the weakly interacting electron gas can be developed. By trading the field

operators of the electrons for the dressed photon field ϕ, the diagrammatic series that comprises the RPA can be organized into a systematic expansion of the action in the charge, e. However, we have also seen that interactions can have a more striking effect on the electron liquid, initiating transitions to new electron phases. In the following, we will explore the transition of the electron gas to an itinerant magnetic phase – the **Stoner transition**.[96]

Historically, the Stoner transition has assumed a special place in the theoretical literature. Developments in statistical mechanics through the 1950s and 1960s highlighted the importance of fluctuation phenomena in the classification and phenomenology of classical phase transitions (for more details, see Chapter 8). In the vicinity of a continuous classical phase transition, the collective properties of a thermodynamic system are characterized by a set of universal critical exponents. In the quantum mechanical system, a phase transition can be tuned by a change of an external parameter even at zero temperature – a "quantum phase transition." In a seminal work, it was proposed by John Hertz[97] that the region surrounding a quantum critical point was itself characterized by **quantum critical phenomena**. In this context, the problem of metallic magnetism presents a useful prototype – and the one used by Hertz to exemplify the phenomenology of quantum criticality. Lately, the class of heavy fermion materials has provided a rich experimental arena in which quantum critical phenomena have been observed and explored. In the following, we develop a low-energy theory of the interacting electron system and discuss the nature of the mean-field transition to the itinerant ferromagnetic phase. Later, following our discussion of the renormalization group methods in Chapter 8, we use the low-energy theory as a platform to discuss the general phenomenology of quantum criticality (see Problem 8.8.2).

Our starting point is the lattice Hamiltonian for a non-interacting electron gas perturbed by a local "on-site" Hubbard interaction, $\hat{H} = \hat{H}_0 + \hat{H}_U$ where

$$\hat{H}_0 = \sum_{\mathbf{p}\sigma} \epsilon_{\mathbf{p}} c^\dagger_{\mathbf{p}\sigma} c_{\mathbf{p}\sigma}, \quad \hat{H}_U = U \sum_i^N \hat{n}_{i\uparrow}\hat{n}_{i\downarrow}.$$

Here, the sum runs over the N lattice sites i and, as usual, $\hat{n}_{i\sigma} = c^\dagger_{i\sigma} c_{i\sigma}$ denotes the number operator for spin σ on site i. The electron dispersion relation $\epsilon_{\mathbf{p}}$ (a function of the lattice geometry) as well as the dimensionality is, for the present, left unspecified.

As we have seen in Chapter 2, the phase diagram of the lattice Hubbard Hamiltonian is rich, exhibiting a range of correlated ground states depending sensitively on the density and strength of interaction. In the lattice system, commensurability effects can initiate charge or spin density wave instabilities while, at large U, the electron system can freeze into an insulating antiferromagnetic Mott–Hubbard state. Conversely, in the following, we will show that, at low densities, the system may assume an itinerant (i.e. mobile) spin-polarized phase, the Stoner ferromagnet.

The capacity of the interacting electron system to form a ferromagnetic phase reflects the competition between the kinetic and interaction potential energies. Being forbidden

[96] E. C. Stoner, Ferromagnetism, *Rep. Prog. Phys.* **11** (1947), 43-112.
[97] J. A. Hertz, Quantum critical phenomena, *Phys. Rev. B* **14** (1976), 1165–84.

by the Pauli exclusion principle to occupy the same site, electrons of the same spin can escape the local Hubbard interaction. However, the same exclusion principle requires the system to occupy higher-lying single-particle states, raising the kinetic energy. When the total reduction in potential energy outweighs the increase in kinetic energy, a transition to a spin-polarized or ferromagnetic phase is induced.

Once again, to facilitate the construction of a low-energy field theory of the magnetic transition, it is helpful to effect a Hubbard–Stratonovich decoupling of the Hubbard interaction. For this purpose it is convenient to first separate the interaction into channels sensitive to the charge and spin densities, i.e.

$$\hat{H}_U = \frac{U}{4}\sum_i (\hat{n}_{i\uparrow} + \hat{n}_{i\downarrow})^2 - \frac{U}{4}\sum_i (\hat{n}_{i\uparrow} - \hat{n}_{i\downarrow})^2.$$

Since we expect that fluctuations in the charge density channel will have little effect on the thermodynamic properties of the low-density system, we can therefore neglect their influence on the interaction, setting $\hat{H}_U \simeq -U\sum_i (\hat{S}_i^z)^2$, where $\hat{S}_i^z = (\hat{n}_{i\uparrow} - \hat{n}_{i\downarrow})/2$.

EXERCISE Here, for simplicity, we have isolated a component of the Hubbard interaction which couples to the spin degrees of freedom but violates the spin symmetry of the original interaction. How could the local interaction be recast in a manner which makes the spin symmetry explicit while isolating the coupling to the spin degrees of freedom?

(a) Making use of the coherent state path integral, express the quantum partition function of the interacting system as a functional field integral. Decoupling the local quartic interaction by the introduction of a local scalar magnetization field $m_i(\tau)$, integrate out the fermionic degrees of freedom and show that the partition function takes the form

$$\mathcal{Z} = \mathcal{Z}_0 \int Dm \exp\left\{ -\frac{U}{4}\int_0^\beta d\tau \sum_i m_i^2(\tau) + \sum_\sigma \mathrm{tr}\ln\left(1 - \frac{U}{2}\sigma_3 \hat{m}\hat{G}_0\right)\right. \quad ,$$

where $\mathcal{Z}_0$ and $G_{0,p} = (i\epsilon_n - \xi_{\mathbf{p}})^{-1}$ denote, respectively, the quantum partition function and Green function of the non-interacting electron gas, the matrix $\hat{m} = \{m_i(\tau)\delta_{ij}\delta(\tau - \tau')\}$, and σ_i are Pauli spin matrices. Left in this form, the expression for the quantum partition function is formally exact, but seemingly unmanageable.

Yet there is an expectation that the system will undergo a phase transition to a magnetic phase at some critical value of the interaction, $U = U_c$, signaled by the appearance of a non-zero expectation value of the magnetization field m_i. This being so, a mean-field description of the transition can be developed along two complementary lines. Firstly, when far below the transition, one expects that the quantum partition function is characterized by a well-developed saddle-point of the field integral. By minimizing the action with respect to m_i, the corresponding saddle-point equation can be used to track the development of magnetic order (exercise). Alternatively, if the transition to the magnetic phase is of second order (i.e. the expectation value of the magnetization field grows continously from zero as the interaction is increased through U_c), a field theory of the system near the critical point can be developed as a perturbative expansion

of the action in powers of the magnetization field. It is this program to which we now turn.

(b) Drawing on the RPA expansion of the weakly interacting electron gas discussed in the main text, expand the action to fourth order in the magnetization field. Subjecting the magnetic susceptibility to a gradient expansion, show that the action takes the general form (where $\int dx \equiv \int d\tau d^d x$)

$$S[m] = \frac{U^2\nu}{4} \sum_q \left[r + \xi^2 \mathbf{q}^2 + \frac{|\omega_n|}{v|\mathbf{q}|} \right] |m_q|^2 + \frac{uT}{4N} \int dx \; m^4(x) + \cdots ,$$

where $r = 1/(U\nu) - 1$, $v = v_{\mathrm{F}} c$, and c is some numerical constant.[98] Identify the coefficients of the expansion. (Hint: Recall the discussion of the Lindhard function on page 218; at fourth order in the expansion you will encounter the product of four fermion Green functions. Assuming that the momentum q carried by the magnetization field is much smaller than the typical momentum of the electronic single-particle states, you may approximate the product of Green functions by a constant whose value you need not specify.)

Finally, rescaling the magnetization field and u, bring the action into the form

$$\boxed{S[m] = \frac{1}{2} \sum_q \left[r + \xi^2 \mathbf{q}^2 + \frac{|\omega_n|}{v|\mathbf{q}|} \right] |m_q|^2 + \frac{u}{4} \int dx \, m^4(x).}$$

(c) In the mean-field approximation, show that the system exhibits a (Stoner) transition to a spin-polarized phase when $U_{\mathrm{c}}\nu = 1$.

INFO Although the mean-field theory provides a good qualitative understanding of the nature of the transition, the **Stoner criterion** itself is unreliable. In the lattice system, the density of states is typically set by the bandwidth, i.e. $\nu \sim 1/t$. Therefore, at the Stoner transition where $U/t \sim 1$, the system enters the strongly correlated phase where the interaction cannot be considered as a small perturbation. In this regime, the electrons experience an effective interaction renormalized by the screening effect of the charge redistribution. Following Kanamori,[99] an estimate for the effective interaction, $U_{\mathrm{eff}} \sim U/(1 + U/t)$, shows that, in the relevant regime, the Stoner criterion becomes replaced by the condition $\nu t \geq 1$. Typically, for a smoothly varying density of states, $\nu \sim 1/t$ and the inequality is difficult to satisfy. In practice, the Stoner transition to ferromagnetism tends to appear in materials where there is significant enhancement of the density of states near the Fermi energy.

[98] The validity of the gradient expansion of the action as an approximation relies on the benignancy of transverse fluctuations of the magnetization density. Recent results (D. Belitz, T. R. Kirkpatrick, and T. Vojta, Nonanalytic behavior of the spin susceptibility in clean Fermi systems, *Phys. Rev. B* **55** [1997], 9453–62) have cast some doubt on the integrity of this approximation. However, we should regard this pathology of the present scheme as an idiosyncrasy of the itinerant ferromagnetic system, while the present action provides a sound illustration of the guiding principles.

[99] J. Kanamori, Electron correlation and ferromagnetism of transition metals, *Prog. Theor. Phys.* **30** (1963), 275–89.

Answer:

(a) When cast as a field integral, the quantum partition function takes the form

$$\mathcal{Z} = \int D(\bar{\psi},\psi)\, \exp\left\{ -\int_0^\beta d\tau \left[\sum_{\mathbf{p}} \bar{\psi}_{\mathbf{p}\sigma}(\partial_\tau + \xi_{\mathbf{p}})\psi_{\mathbf{p}\sigma} - \frac{U}{4}\sum_i (\bar{\psi}_{i\sigma}\sigma^z_{\sigma\sigma'}\psi_{i\sigma'})^2 \right] \right. \quad ,$$

where the sum over repeated spin indices is assumed. In this form, the interaction may be decoupled with the introduction of a commuting scalar field conjugate to the local magnetization density,

$$\mathcal{Z} = \int \; Dm\; D(\bar{\psi},\psi) \exp\left\{ -\int d\tau \left(\frac{U}{4}\sum_i m_i^2(\tau) + \sum_{\mathbf{p}} \bar{\psi}_{\mathbf{p}\sigma}(\partial_\tau + \xi_{\mathbf{p}})\psi_{\mathbf{p}\sigma} \right.\right.$$
$$\left.\left. + \frac{U}{2}\sum_i \bar{\psi}_{i\sigma}\sigma m_i\, \psi_{i\sigma} \right) \right. \quad .$$

Finally, integrating over the fermionic degrees of freedom, one obtains the required partition function.

(b) The expansion of the action mirrors closely the RPA of the weakly interacting electron gas. Carried out to fourth order, it may be confirmed straightforwardly that terms odd in powers of m vanish identically (a property compatible with the symmetry $m \to -m$), while the even terms lead to the expression $\mathcal{Z} = \mathcal{Z}_0 \int Dm\, e^{-S[m]}$, where

$$S[m] = \frac{1}{2}\sum_q v_2(q)|m_q|^2 + \frac{T}{4N}\sum_{q_i} v_4(\{q_i\}) \prod_{i=1}^4 m_{q_i}\delta_{\sum_i q_i,0} + \cdots$$

Focusing on the second-order contribution, one finds that $v_2(q) = \frac{U}{2}(1 - U\Pi_q)$ where Π_q represents the familiar fermion bubble or Lindhard function,

$$\Pi_q = -\frac{T}{N}\sum_k G_{0,k}G_{0,k+q} = -\frac{1}{N}\sum_{\mathbf{k}} \frac{n_{\rm F}(\epsilon_{\mathbf{k}}) - n_{\rm F}(\epsilon_{\mathbf{k}+\mathbf{q}})}{i\omega_n + \xi_{\mathbf{k}} - \xi_{\mathbf{k}+\mathbf{q}}}.$$

As one would expect, the existence and nature of the magnetic instability depend sensitively on the susceptibility $v_2(q)$, which, in turn, depends on the detailed structure of the spectrum $\epsilon_{\mathbf{k}}$. The static susceptibility is dominated by contributions to the momentum sum where $\xi_{\mathbf{k}} \simeq \xi_{\mathbf{k}+\mathbf{q}}$. This involves the regions of reciprocal space where $\mathbf{q}$ is small or where, for some non-zero $\mathbf{q} = \mathbf{Q}$, $\xi_{\mathbf{k}} \simeq \xi_{\mathbf{k}+\mathbf{Q}}$ over a wide region of the Brillouin zone. The second condition reflects a **nesting symmetry** where a translation by a constant wavevector leaves the spectrum invariant. It is in this situation, where commensurability effects become significant, that magnetic or spin density waves develop. If, instead, the spectrum varies smoothly, so that nesting symmetry is absent, the susceptibility is maximized for $\mathbf{q} = 0$. Leaving the spin density wave system for "private investigation," we focus here on the channel $\mathbf{q} = 0$.

EXERCISE Explain why bipartite lattices lead naturally to nesting symmetry.

While, in general, the Lindhard function assumes a complicated structure reflecting the detailed dispersion of the non-interacting system, for the free electron system $\epsilon_{\mathbf{k}} = \mathbf{k}^2/2m$ an exact expression can be derived explicitly (see Eq. (5.30)). In particular, at frequencies $|\omega_n|/|\mathbf{q}|v_{\rm F}$ small, this expression has the expansion $\Pi_q \simeq \Pi_{0,\mathbf{q}} - \nu\frac{|\omega_n|}{v|\mathbf{q}|}$, where $v = cv_{\rm F}$ with a constant c depending on dimensionality. (In the three-dimensional system, $c = \pi/2$.) Similarly, for $\mathbf{q}$ small, one may expand the static susceptibility in gradients, i.e. $\Pi_{0,\mathbf{q}} \simeq \nu[1 - \xi^2\mathbf{q}^2 + \cdots]$ where $\xi \sim 1/k_{\rm F}$.

Turning now to the quartic interaction, the general structure of v_4 again involves a complex computation. However, since its effect near the critical point is merely to control the strength of the magnetization, in the following we may focus on the frequency- and momentum-independent contribution, setting

$$v_4(\{q_i\}) \mapsto v_4(0) \equiv u = \frac{2(U/2)^4}{\beta N}\sum_p [G_0(p)]^4 \sim U^4\nu'',$$

where $\nu'' = \partial_\epsilon^2\big|_{\epsilon=E_{\rm F}}\nu(\epsilon)$. Taken together with the quadratic interaction, the total effective action assumes the form given above.

(c) In the leading approximation, an understanding of the model can be developed by ignoring the effect of fluctuations – spatial and temporal. In such a mean-field approximation, the fields m are assumed independent of q (or x). In this case, the rescaled action takes the form

$$\frac{S[m]}{\beta N} = \frac{r}{2}m^2 + \frac{u}{4}m^4,$$

where $r = U(1 - U\nu)/2$. Minimizing the action with respect to m, one finds a Stoner transition to a spin-polarized ferromagnetic phase when $r = 0$, i.e. $U_c\nu = 1$. At values of U in excess of $U_{\rm c}$, the (oversimplified) mean-field analysis above predicts that the magnetization will grow in a continuous yet non-analytic manner, i.e. $m = \sqrt{-r/4u}$.

Functional bosonization

The techniques introduced in this chapter are engaged to develop a functional-integral-oriented scheme of bosonizing the one-dimensional electron gas.

Consider the interacting one-dimensional electron gas as described by the relativistic action Eq. (4.43) and the interaction contribution Eq. (4.44). Throughout, it will be convenient to formulate the last in a matrix representation,

$$S_{\rm int}[\psi^\dagger,\psi] = \frac{1}{2}\int d\tau\, dx\, \begin{pmatrix}\hat\rho_+ & \hat\rho_-\end{pmatrix}\begin{pmatrix} g_4 & g_2\\ g_2 & g_4\end{pmatrix}\begin{pmatrix}\hat\rho_+\\ \hat\rho_-\end{pmatrix} \equiv \frac{1}{2}\int d\tau\, dx\, \begin{pmatrix}\hat\rho_+ & \hat\rho_-\end{pmatrix}\hat g\begin{pmatrix}\hat\rho_+\\ \hat\rho_-\end{pmatrix}.$$

To probe the response of the system to external perturbations, we add to the action a source term $S_{\rm source}[\psi,\psi^\dagger,j,j^\dagger] \equiv \int d\tau\, dx\, \sum_{\rm s=\pm}(\psi^\dagger_{\rm s} j_{\rm s} + j^\dagger_{\rm s}\psi_{\rm s})$. By Grassmann differentiation with respect to the source fields j and $j^\dagger$, we may then generate any correlation function of interest.

(a) Decouple the four-fermion interaction by introducing a two-component Hubbard–Stratonovich field $\varphi^T = (\varphi_+,\varphi_-)$. Show that the action can be written as

$$S[\bar\psi,\psi,\varphi] = \frac{1}{2}\int d^2x\, \varphi^T\hat g^{-1}\varphi - \int d^2x\, \bar\psi(\partial\!\!\!/ - i\, \not\varphi)\psi, \tag{6.74}$$

where $\psi^T = (\psi_+,\psi_-)$, $\bar\psi = (\psi^\dagger_-,\psi^\dagger_+)$, and we have switched to a covariant notation: $x_1 = \tau$, $x_2 = x$, $d^2x = dx_1\, dx_2$, and $\partial\!\!\!/ = \sigma_\mu\partial_\mu$ and $\not\varphi = \sigma_\mu\varphi_\mu$. The space–time components of the interaction field are defined by $\varphi_1 = \frac{1}{2}(\varphi_+ + \varphi_-)$ and $\varphi_2 = \frac{1}{2i}(\varphi_+ - \varphi_-)$.

The interaction field φ couples to the fermion action as a two-dimensional vector potential. As with any two-component vector, the coefficients of φ can be decomposed into an irrotational and a divergenceless contribution (the Hodge decomposition): $\varphi_\mu = -(\partial_\mu\xi + i\epsilon_{\mu\nu}\partial_\nu\eta)$. This is an interesting decomposition as it suggests that the vector potential can be removed from the action by a generalized gauge transformation. Indeed, the transformation $\psi \to e^{i\xi+i\eta\sigma_3}\psi$, $\bar\psi \to \bar\psi e^{-i\xi-i\eta\sigma_3}$ naively removes the vector potential from the action (exercise: check this). A moment's thought identifies the two transformations by ξ and η as the vectorial and axial gauge transformations discussed in Section 4.3 above. It turns out, however, that the transformation by η is actually not permissible – a direct manifestation of the **chiral anomaly**.

INFO There are different ways to understand the **origin of the chiral gauge symmetry violation**. For instance, one may observe that the transformation leaves the action invariant, but not the measure $d\bar\psi\; d\psi$.[100] This means that the functional integral as a whole lacks gauge invariance. Alternatively, one may integrate out the fermions and realize that the resulting "tr ln" exhibits problematic UV behavior. Applying a UV regularization scheme – of which, due to the importance of the Dirac operator in particle physics, there are many – one observes that the chiral gauge invariance gets lost.[101]

[100] K. Fujikawa, Chiral anomaly and the Wess–Zumino condition, *Phys. Rev. D* **31** (1985), 341–51.
[101] For a detailed discussion of this point, see J. Zinn-Justin, *Quantum Field Theory and Critical Phenomena* (Oxford University Press, 1993).

Notice that both the lack of gauge invariance of the measure and the UV problems manifest themselves in an integral over (quantum) fluctuations, i.e. while the symmetry is preserved on the classical level, it gets lost in the quantum theory. This is the defining property of an anomaly.

(b) To explore the consequences of the anomaly, integrate out the fermions and expand the resulting "tr ln" to second order in the fields $\varphi_\pm$. Switching to a frequency–momentum representation and approximating the Matsubara sum by an integral, one obtains an expression that is formally UV divergent. Regularize the integral by introducing a cut-off Λ in momentum space. Show that the effective φ-action reads as

$$S[\varphi] = \frac{1}{2}\sum_{\tilde{q}} \varphi_{\tilde{q}}^T \left(\hat{g}^{-1} + \hat{\Pi}_{\tilde{q}}\right) \varphi_{-\tilde{q}}, \tag{6.75}$$

where $\tilde{q} = (\omega, q)$ and $\hat{\Pi}_{\tilde{q}} \equiv \{\frac{\delta_{ss'}}{2\pi} \frac{q}{-is\omega + q}\}$. Finally, introduce the field doublet $\Gamma^T \equiv (\xi, \eta)$ to represent the action as

$$S[\Gamma] = \frac{1}{2}\sum_{\tilde{q}} \Gamma_{\tilde{q}}^T D_{\tilde{q}}^T \left(\hat{g}^{-1} + \hat{\Pi}_{\tilde{q}}\right) D_{-\tilde{q}} \Gamma_{-\tilde{q}}, \tag{6.76}$$

where the transformation matrix

$$D_{\tilde{q}} \equiv \begin{pmatrix} q - i\omega & -q - i\omega \\ -q - i\omega & q + i\omega \end{pmatrix}$$

mediates between the field variables Γ and φ (exercise).

We next turn our attention to the source terms. The integration over the original fermion variables generates a source contribution

$$\begin{aligned} S_{\text{source}}[\psi, \psi^\dagger, j, j^\dagger] \quad &\xrightarrow{\int D\psi} S[j, j^\dagger, \Gamma] = \int d^2x\; d^2x'\; \bar{j}(x)\hat{G}^{[\Gamma]}(x, x')j(x') \\ &= \int d^2x\; d^2x'\; (\bar{j}e^{-i(\xi+\eta\sigma_3)})(x)\hat{G}(x, x')(e^{i(\xi+\eta\sigma_3)}j)(x'), \end{aligned}$$

where x are space/time indices, the superscript $[\Gamma]$ indicates that the fermion Green function depends on the Hubbard–Stratonovich interaction fields, and in the last step we have applied the generalized gauge transformation above to transfer the (ξ, η)-dependence to the source vectors j. The action above contains the free fermion Green function (a matrix in both space–time and $\pm$-space) as an integration kernel. To proceed, notice that matrix elements of the fermion Green function can be obtained as correlation functions of a free bosonic theory. This connection was introduced in Problem 4.5 on the example of a specific free fermion correlation function. Generalizing the results of that problem, one may verify that (exercise)

$$\hat{G}_{ss'}(x, x') = (2\pi a)^{-1} \langle e^{-i(\varphi + s\theta)(x)} e^{i(\varphi + s\theta)(x')} \rangle, \tag{6.77}$$

where a is the lattice spacing and the action of the bosonic doublet $\text{fl}^T \equiv (\phi, \theta)$ is given by

$$S_0[\text{fl}] = \frac{1}{2}\sum_{\tilde{q}} \text{fl}_{\tilde{q}}^T K_{\tilde{q}} \text{fl}_{-\tilde{q}}, \quad K_{\tilde{q}} \equiv \frac{1}{\pi}(q^2 - iq\omega\sigma_1) \tag{6.78}$$

i.e. a non-interacting variant of the Luttinger liquid action (cf. Eq. (4.49)).

(c) Use the Fermi–Bose correspondence to represent the generating function as a double field integral over Γ and fl. Next shift the integration variables fl to remove the field Γ from the source action and perform the quadratic integral over Γ. Show that the final form of the action is given by (4.51). Summarizing, you have rediscovered the action of the interacting Luttinger liquid, and the boson representation of fermion correlation functions (the latter obtained by differentiation with respect to the source parameters j). While the present derivation is certainly less transparent than the one discussed in Section 4.3, it has the advantage of being more "explicit" (inasmuch as we start from the standard "tr ln," which is then subjected to manipulations standard in many-body field theory. On the other hand, the authors are not aware of applications where this aspect turned out to be of much practical relevance: usually, the standard bosonization approach is just fine; and, where it is not, the formalism above would not be any better).

Answer:

(a) This is resolved by a straightforward exercise in Gaussian integration and reorganizing indices.

(b) Integrating over fermions and momentarily forgetting about the impurity, we obtain the effective action

$$\begin{aligned} S[\varphi] &= \frac{1}{2}\int d^2x\, \varphi^T \hat{g}^{-1}\varphi - \mathrm{tr}\ln(\partial\!\!\!/ - i\, A\!\!\!/) \\ &= \frac{1}{2}\int d^2x\, \varphi^T \hat{g}^{-1}\varphi - \frac{1}{2}\mathrm{tr}(\partial\!\!\!/^{-1} A\!\!\!/ \;\; \partial\!\!\!/^{-1} \;\; A\!\!\!/) + \mathcal{O}(\varphi^4) \\ &= \frac{1}{2}\sum_{\tilde{q}} \varphi_{\tilde{q},s}\left(\hat{g}^{-1}_{ss'} + \delta_{ss'}\Pi_{s,\tilde{q}}\right)\varphi_{s',-\tilde{q}} + \mathcal{O}(\varphi^4), \end{aligned}$$

where $\tilde{q} = (\omega, q)$ and $\Pi_{s,\tilde{q}} = \int d^2p\ (\epsilon + isp)^{-1}(\epsilon + \omega + is(p+q))^{-1}$. Evidently, the structure of this integral poses a problem: while all poles of the integrand appear to be on one side of the real axis (so that analyticity arguments might suggest a vanishing of the integral), the double integral is manifestly divergent. We are, thus, confronted with a $0 \cdot \infty$ conflict and a regularization scheme is called for. (At $[n > 2]$nd orders in the φ expansion, one "fast" momentum integration extends over $n > 2$ energy denominators. These terms indeed vanish by analyticity, i.e. the second-order expansion of the logarithm is, in fact, exact.) To some extent, the choice of the regularization scheme is dictated by the physical context: in particle physics, relativistic covariance is sacred, and a rotationally invariant (Euclidean formalism!) regularization is required. However, in condensed matter physics, where the effective action is obtained by linearization of some band Hamiltonian, frequency and momentum play different roles. While the integration domain of the former is infinite, the latter is bounded to values $|p| < \Lambda$, where Λ is some

cutoff. To proceed, we first integrate over frequencies and then do the finite integral over momentum:

$$\begin{aligned}\Pi_{s,\tilde{q}} &= \frac{1}{\omega+isq}\int_{-\Lambda}^{\Lambda}\frac{dp}{2\pi}\int\frac{d\epsilon}{2\pi}\left[\frac{1}{\epsilon+isp}-\frac{1}{\epsilon+\omega+is(p+q)}\right]\\ &= -\frac{1}{\omega+isq}\frac{i}{2}\int_{-\Lambda}^{\Lambda}\frac{dp}{2\pi}\left[\mathrm{sgn}(sp)-\mathrm{sgn}(s(p+q))\right]=\frac{1}{2\pi}\frac{q}{-is\omega+q}.\end{aligned}$$

(Notice that the result is actually independent of the non-universal cutoff Λ.) Substituting this result into the action, we obtain Eq. (6.75).

(c) Representing the fermion Green function as in Eq. (6.77), we obtain the local expression

$$\mathcal{Z}=\int D\mathrm{fl}\;D\Gamma\;e^{-S_0[\;]-S[\Gamma]}\exp\left(-\int d^2x\left(\bar{j}e^{-i(\xi+\phi+(\eta+\theta)\sigma_3)}+e^{i(\xi+\phi+(\eta+\theta)\sigma_3)}j\right)\right),$$

where the non-universal factor $2\pi a$ has been absorbed in the definition of the source fields. (To confirm that the fl-integral faithfully reproduces the source action, one has to take into account the fact that $\exp(i(\phi\pm\theta))\leftrightarrow\psi$ is a Gaussian correlated variable.) The structure of the source term suggests a shift $\phi\to\phi-\xi$, $\theta\to\theta-\eta$, or $\mathrm{fl}\to\mathrm{fl}-\Gamma$ for short. Denoting the now Γ-independent source contribution by $\exp(-S_{\mathrm{source}}[\mathrm{fl}])$, the partition function assumes the form $\mathcal{Z}=\int D\mathrm{fl}\;D\Gamma\,e^{-S_0[\;-\Gamma]-S[\Gamma]-S_{\mathrm{source}}[\;]}$. We further note that $K_{\tilde{q}}=-D_{\tilde{q}}^T\Pi_{\tilde{q}}D_{-\tilde{q}}$ to obtain the integral over Γ,

$$\begin{aligned}S_0[\mathrm{fl}-\Gamma]+S[\Gamma] &= \frac{1}{2}\sum_{\tilde{q}}\left[\mathrm{fl}_{\tilde{q}}^T K_{\tilde{q}}\mathrm{fl}_{-\tilde{q}}+\Gamma_{\tilde{q}}^T(D_{\tilde{q}}^T\hat{g}^{-1}D_{-\tilde{q}})\Gamma_{-\tilde{q}}\right.\\ &\qquad\left.+\mathrm{fl}_{\tilde{q}}^T K_{\tilde{q}}\Gamma_{-\tilde{q}}+\Gamma_{\tilde{q}}^T K_{\tilde{q}}\mathrm{fl}_{-\tilde{q}}\right]\\ &\xrightarrow{\int D\Gamma}\frac{1}{2}\sum_{\tilde{q}}\mathrm{fl}_{\tilde{q}}^T\left[K_{\tilde{q}}-K_{\tilde{q}}(D_{\tilde{q}}^T\hat{g}^{-1}D_{-\tilde{q}})^{-1}K_{\tilde{q}}\right]\mathrm{fl}_{-\tilde{q}}\\ &= \frac{1}{2}\sum_{\tilde{q}}\mathrm{fl}_{\tilde{q}}^T\left[K_{\tilde{q}}+2q^2(g_4-g_2\sigma_3)\right]\mathrm{fl}_{-\tilde{q}}\\ &= \frac{1}{2\pi}\sum_{\tilde{q}}(\varphi,\theta)_{\tilde{q}}\begin{pmatrix}q^2[1+2\pi(g_4-g_2)] & -iq\omega\\ -iq\omega & q^2[1+2\pi(g_4+g_2)]\end{pmatrix}\begin{pmatrix}\varphi\\ \theta\end{pmatrix}_{-\tilde{q}},\end{aligned}$$

where we have used the fact that $K_{\tilde{q}}D_{-\tilde{q}}^{-1}=-g(\mathbf{1}-i\sigma_2)$. Transforming back to real space/time, we obtain Eq. (4.51).

7

Response functions

The chapter begins with a brief survey of concepts and techniques of *experimental* condensed matter physics. It will be shown how correlation functions provide a bridge between concrete experimental data and the theoretical formalism developed in previous chapters. Specifically we discuss – an example of outstanding practical importance – how the response of many-body systems to various types of electromagnetic perturbation can be described in terms of correlation functions and how these functions can be computed by field theoretical means.

In the previous chapters we have introduced important elements of the theory of quantum many-body systems. Perhaps most importantly, we have learned how to map the basic microscopic representations of many-body systems onto effective low-energy models. However, to actually test the power of these theories, we need to understand how they can be related to experiment. This will be the principal subject of the present chapter.

Modern condensed matter physics benefits from a plethora of sophisticated and highly refined techniques of experimental analysis including the following: electric and thermal transport; neutron, electron, Raman, and X-ray scattering; calorimetric measurements; induction experiments; and many more (for a short glossary of prominent experimental techniques, see Section 7.1.2 below). While a comprehensive discussion of modern experimental condensed matter would reach well beyond the scope of the present text, it is certainly profitable to attempt an identification of some structures common to most experimental work in many-body physics. Indeed, we will need a discussion of this sort to construct meaningful links between the theoretical techniques developed above and experiment.

7.1 Crash course in modern experimental techniques

7.1.1 Basic concepts

Crudely speaking, experimental condensed matter physics can be subdivided into three[1] broad categories of analytical technique:

- ▷ experiments probing thermodynamic coefficients;
- ▷ transport experiments;
- ▷ spectroscopy.

[1] There are a few classes of experiment that do not fit comfortably into this three-fold scheme. These include scanning tunneling microscopy, a technique to be discussed in more detail below.

A summary of their utility, the basic experimental setup, the principal areas of application, and concrete realization of these families is given in the following section. (Readers who are totally unfamiliar with the basic notions of experimental many-body physics may find it useful to browse through that section before reading further.) The few occasional references to experimental data given in previous chapters were all to thermodynamic properties. The reason for this restriction was that the extraction of thermodynamic information from the theoretical formalism is relatively straightforward: one need only differentiate the partition function (alias the field integral) with respect to a few globally defined coefficients (the temperature, homogeneous magnetic field, etc.). This simplicity has advantages but also limiting aspects: thermodynamic data are highly universal[2] and, therefore, represent an important characteristic of a system. On the other hand, they contain information neither on spatial structures, nor on dynamical features. This means that thermodynamic data do not suffice to fully understand the physics of a system.

With the other two categories of experiment the situation is different. Transport and spectroscopic measurements can be used to probe both static and dynamical features of a system; further, fully angle/frequency-resolved spectroscopic data contain detailed information on the spatio-temporal structure of the dominant excitations of a system or, in other words, on their dispersion relation. It is for these reasons that the focus in the present chapter will be on the last two of the experimental classes mentioned above.

In spite of the wide diversity of present day analytical techniques, there are a few structures common to all experimental probes of condensed matter:

- ▷ Firstly, the interaction of a many-body system with its environment is almost exclusively mediated by electromagnetic forces.[3] Accordingly, most experiments subject the system under consideration to some external electromagnetic perturbation (a voltage drop, an influx of spin magnetic moments carried by a beam of neutrons, the local electric field formed at the tip of a scanning tunneling microscope, etc.). In a second step, the "response" of the system is then recorded by an appropriate detector or measuring device.

  Formally, the externally imposed perturbation is described by a (time-dependent) contribution to the Hamiltonian of the system,

$$\hat{H}_{\mathrm{F}} = \int d^d r F_i'(\mathbf{r}, t) \hat{X}_i'(\mathbf{r}). \tag{7.1}$$

  Here, the coefficients F_i', sometimes referred to as generalized "forces," represent a perturbation that couples to the system through some operators $\hat{X}'$. For example, $F_i'(\mathbf{r}, t) = \phi(\mathbf{r}, t)$ could represent a space- and time-dependent electric voltage coupling to the density of the electronic charge carriers in the system $\hat{X}_i' = \hat{\rho}$, etc.
- ▷ The use of the term "perturbation" is appropriate because the forces $\{F_i'\}$ will, in general, be much weaker than the internal correlations of the system.
- ▷ The forces perturb the system out of its $F_i' = 0$ reference state. The measurable effect of this perturbation will be that certain operators $\hat{X}_i$, whose expectation values vanish

[2] Remember that a few thermodynamic variables, i.e. numbers, suffice to unambigously characterize the state of a homogeneous system in equilibrium.

[3] An important exception involves heat conduction.

in the unperturbed state, build up non-vanishing expectation values $X_i(\mathbf{r},t) = \langle \hat{X}_i(\mathbf{r},t)\rangle$. (For example, in response to an external voltage $F_i' = \phi$, a current might begin to flow, $\hat{X}_i = \hat{j}_i$, etc.). The ultimate goal of any theory will be to understand and predict the functional dependence of the measured values of X_i on the forces F_j'.

▷ In general, there is nothing one can say about that connection other than that $X_i\left[F_j'\right]$ will be some functional of the forces. However, for a sufficiently weak force, the situation is simpler. In this case, one may expect that the functional relation between forces F_j' and the expectation values X_i is approximately linear, i.e. of the form

$$X_i(\mathbf{r},t) = \int d^d r' \int dt'\, \chi_{ij}(\mathbf{r},t;\mathbf{r}',t') F_j'(\mathbf{r}',t') + \mathcal{O}(F'^2). \tag{7.2}$$

While the quantities F_j' and $\{X_i\}$ are externally adjustable/observable – either as an experimental input/output, or as parameters in the theory – the integral kernel χ represents a purely intrinsic property of the system. It describes how the system "responds" to the application of an external probe $\{F_i'\}$ (wherefore it is commonly referred to as a **response function**) or generalized susceptibility. The functional profile of the response kernel is in turn determined by the dominant excitations of a system (notably its long-range excitations), i.e. our prime objects of interest.

These considerations show that response functions play a principal role in promoting the dialog between experiment and theory. Experimentally, they will be measured by relating the input F_j' to the response $\{X_i\}$. Theory will attempt to predict the response behavior, ideally in a way that conforms with experimental observation.

7.1.2 Experimental methods

To keep our discussion of the relation "experiment ↔ theory" less abstract, it is instructive to list a few prominent experimental techniques of condensed matter physics. Of course, the summary below can be no more than an introduction.[4] Our intention is merely to illustrate the connection (perturbation ⇝ response) through a few examples; indeed readers lacking a background in experimental many-body physics may welcome some motivation before plunging into the formalism of correlation functions and response developed below.

Thermodynamic experiments

Of the thermodynamic properties of a system that can be accessed in experiment, those most commonly investigated include the following: the **specific heat**, $c_v = \partial U/\partial T$, i.e. the rate of change of the internal energy under a change of temperature; the **magnetic susceptibility**, $\chi = \partial M/\partial H$, the change of magnetization in response to a (quasi-)static magnetic field; the **(isothermal) compressibility**, $\kappa = -V^{-1}\partial V/\partial p$, the volume change in response to

[4] For a short and pedagogical (if perhaps a bit outdated) introduction to a number of experimental approaches we refer to the classic text by N. W. Ashcroft and N. D. Mermin, *Solid State Physics* (Holt-Saunders International, 1983), while, for an up-to-date and detailed exposition of methods of spectroscopy, we refer to H. Kuzmany, *Solid State Spectroscopy* (Springer-Verlag, 1998).

the external pressure etc. Note that, strictly speaking, the magnetic susceptibility and the isothermal compressibility are both tensor quantities.

The thermodynamic response functions are highly universal. (Remember that a few thermodynamic state variables suffice to unambiguously characterize the state of a given system.) Specifically, for given values of chemical potential, magnetic field, pressure, etc., a calorimetric experiment will produce a one-dimensional function $c_v(T)$. The low-temperature profile of that function generally contains important hints as to the nature of the low-energy excitations of a system.[5] However, the universality of thermodynamic data also implies a limitation: thermodynamic coefficients contain information neither about the spatial fluctuations of a given system nor about its dynamics.

Transport experiments

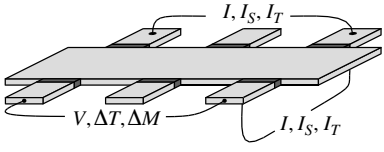

When subject to a gradient of a generalized "voltage" U, a current flows through a device (see figure). Although, typically, the voltage is electrical, $U = V$, one can apply a temperature gradient $U = \Delta T$ or even attach the sample to two "reservoirs" of different magnetizations $\mathbf{U} = \Delta\mathbf{M}$. One then records the current flow induced by U. The corresponding current can be electrical, I carried by the charge of mobile carriers, the "thermal current" I_{T} carried by their energy, or a "spin current" I_{S} carried by their magnetic moments. Also notice that the current need not neccessarily be parallel to the voltage gradient. For example, in the presence of a perpendicular magnetic field, a voltage gradient will give rise to a transverse **Hall current** $I_\perp$. The ratio of a current and a generalized voltage defines a **conductance**, $g = \frac{I}{U}$.

Conductance measurements represent the most common way to determine the transport behavior of a metal or the thermal conduction properties of insulators. A disadvantage is that conductance measurements are invasive, i.e. the system has to be attached to contacts. There are situations where the local injection process of charge carriers at the contact (rather than the bulk transport behavior in which one is interested) determines the value of the conductance. (For a further discussion of this point, we refer to Problem 7.6.1.)

Spectroscopic experiments

The general setup of a spectroscopic experiment is shown in Fig. 7.1. A beam of particles p – either massive (electrons, neutrons, muons, atoms, etc.), or the quanta of electromagnetic radiation – is generated at a source and then directed onto a sample. The kinematic information about the source beam is stored in the dispersion relation $(\mathbf{k}, \omega(\mathbf{k}))$.[6] The particles

[5] For example, the specific heat of the Fermi liquid, $c_{v,\text{Fermi liquid}} \sim T$, is linear in temperature, that of phonons, $c_{v,\text{phonon}} \sim T^3$, is cubic, while in a system without low-lying excitations, it vanishes exponentially (exercise: consider why).

[6] For some sources, e.g. a laser, the preparation of a near-monochromatic source beam is (by now) standard. For others, such as neutrons, it requires enormous experimental skills (and a lot of money!).

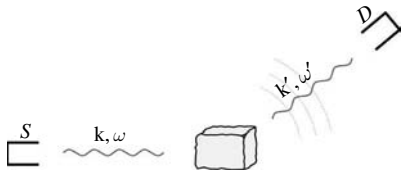

Figure 7.1 Basic setup of a spectroscopic experiment. A beam of electromagnetic radiation (or massive particles) of frequency–momentum $(\omega(\mathbf{k}), \mathbf{k})$ is emitted by some source (S) and directed onto a target sample. The sample responds by emitting radiation according to some distribution $P(\omega'(\mathbf{k}'), \mathbf{k}')$, which is, in turn, recorded by a detector (D). Notice that the emitted radiation can, but need not, contain the same type of particles as the source radiation. For example, light quanta may lead to the emission of electrons (photoemission spectroscopy).

of the source beam then interact with constituents X of the sample to generate a secondary beam of scattered particles p'. Symbolically,

$$\begin{array}{ccccccc} p & + & X & \longrightarrow & p' & + & X' \\ \updownarrow & & \updownarrow & & \updownarrow & & \updownarrow \\ \mathbf{k}, \omega(\mathbf{k}) & & \mathbf{K}, \Omega(\mathbf{K}) & & \mathbf{k}', \omega(\mathbf{k}') & & \mathbf{K}', \Omega(\mathbf{K}'), \end{array}$$

where X' represents the final state of the process inside the sample. Notice that the particles p' leaving the sample need not be identical to those incident on the sample. (For example, in photoemission spectroscopy, X-ray quanta displace electrons from the core levels of atoms in a solid. Here p represent the light quanta, and p' electrons.) Further, the dominant scattering process may be elastic (e.g. X-rays scattering off the static lattice structure) or inelastic (e.g. neutrons scattering off phononic excitations). In either case, the accessible information about the scattering process is stored in the frequency–momentum distribution $P(\omega(\mathbf{k}'), \mathbf{k}')$ of the scattered particles, as monitored by a detector.

From these data, one would like to restore the properties (i.e. the dispersion $(\Omega(\mathbf{K}), \mathbf{K})$) of the states inside the solid. This is where the detective work of spectroscopy begins. What we know is that the dispersions of the scattered particles and of the sample constituents, $(\mathbf{k}, \omega(\mathbf{k}))$ and $(\mathbf{K}, \Omega(\mathbf{k}))$, respectively, are related

Sir Chandrasekhara V. Raman 1888–1970 (left), Lord Rayleigh (John William Strutt) 1842–1919 (middle), Max von Laue 1879–1960 (right)
Raman was awarded the Nobel Prize in Physics in 1930 "for his work on the scattering of light and for the discovery of the effect named after him." Lord Rayleigh was awarded the Nobel Prize in Physics in 1904 "for his investigations of the densities of the most important gases and for his discovery of argon in connection with these studies." Laue was awarded the Nobel Prize in Physics in 1914 "for his discovery of the diffraction of X-rays by crystals." (Image © The Nobel Foundation.)

through an energy–momentum conservation law, i.e.

$$\begin{aligned} \mathbf{k}+\mathbf{K} &= \mathbf{k}'+\mathbf{K}', \\ \omega(\mathbf{k})+\Omega(\mathbf{K}) &= \omega(\mathbf{k}')+\Omega(\mathbf{K}'). \end{aligned}$$

According to this relation, a "resonant" peak in the recorded distribution $P(\omega(\mathbf{k}'),\mathbf{k}')$ signals the existence of an internal structure (for example, an excitation, or a lattice structure) of momentum $\Delta\mathbf{K} \equiv \mathbf{K}'-\mathbf{K} = \mathbf{k}-\mathbf{k}'$ and frequency $\Delta\Omega \equiv \Omega'-\Omega = \omega-\omega'$. However, what sounds like a straightforward recipe in principle may be quite involved in practice: solid state components interact almost exclusively through electromagnetic forces. When charged particles are used as scattering probes, these interactions may actually turn out to be too strong. For example, a beam of electrons may interact strongly with the surface states of a solid (rather than probing its bulk), or the scattering amplitude may be the result of a complicated process of large order in the interaction parameters, and therefore difficult to interpret. The obvious alternative – scattering of neutral particles – is met with its own problems (see below). Notwithstanding these difficulties, spectroscopy is one of the most important sources of experimental information in condensed matter physics. A number of prominent "sub-disciplines" of solid state spectroscopy are summarized below:

- ▷ **Raman spectroscopy**: The inelastic scattering of visible light can be used to explore the dispersion of optical phonons (magnons, plasmons, or other electronic excitations). Such techniques require experimental skill to discriminate the "Raman peak" from the much larger "Rayleigh peak" corresponding to the elastic scattering of light quanta.
- ▷ **Infrared spectroscopy**: The scattering of light in the infrared range can be used to explore the vibrational modes in polycrystalline solids and the band-gaps in semiconductors.
- ▷ **X-ray crystallography**: By measuring the angle-resolved intensity profile (the von Laue pattern), the elastic scattering of X-rays from the lattice ions of a solid can be used to infer the structure of a crystalline substance. (Notice that the typical wavelength of X-rays $\sim 10^{-10}\,\mathrm{m}$ is of about the size of typical interatomic spacings in solids.) Such techniques of solid state spectroscopy have already acquired a long history dating back to 1913.

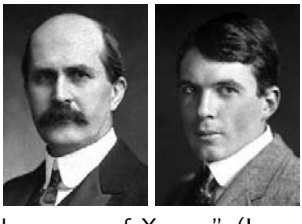

Sir William H. Bragg 1862–1942 (left) and his son Sir William Lawrence Bragg, 1890–1971 (right)
Awarded the Nobel Prize in Physics in 1915 "for their services in the analysis of crystal structure by means of X-rays." (Image © The Nobel Foundation.)

- ▷ **X-ray/electron spectroscopy**: A number of spectroscopic techniques are based on the fact that the ionization energies of atomic core levels lie in the X-ray range. In **X-ray absorption spectroscopy** the absorption of X-rays by a solid is measured as a function of the light frequency (see Fig. 7.2(a)). The absorption cross-section rises in a quasi-

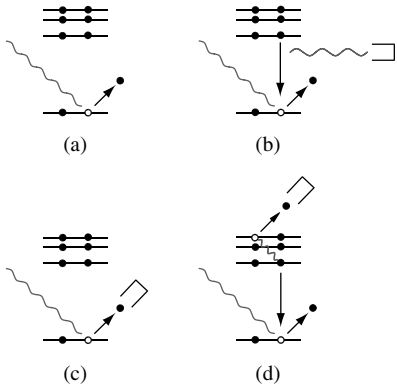

Figure 7.2 The different types of X-ray/electron spectroscopy. (a) X-ray absorption: the loss of X-ray radiation due to the ionization of core levels. (b) X-ray fluorescence: the recombination of valence electrons with previously X-ray-emptied core levels leads to the emission of radiation, which also lies in the X-ray range. The spectral analysis of this radiation contains information about the level structure of the system. (c) Photoemission spectroscopy (PES): detection of the frequency-dependence of the electrons kicked out by X-ray core level ionization. (d) Auger spectroscopy: the energy emitted by a valence electron recombining with a core level is transmitted to a second valence electron which leaves the solid as a high-energy Auger electron.

discontinuous manner whenever the energy of the X-rays becomes large enough to ionize an atomic core level of the atoms of the solid. Due to interatomic correlations, these energies differ from the ionization energies of gaseous atoms, i.e. information about solid state binding energies is revealed.

▷ In **X-ray fluorescence spectroscopy** the radiation emitted by valence electrons recombining with core holes created by incident X-ray radiation is measured (Fig. 7.2(b)). This type of spectroscopy is frequently used to chemically analyze a sample, or to detect the presence of impurity atoms, i.e. different elements have different core/valence excitation energies. Peaks in the fluorescence spectrum at frequencies characteristic of individual atoms therefore identify the presence of these atoms in the target sample. In **photoemission spectroscopy (PES)** core electrons[7] displaced by X-ray radiation are detected (Fig. 7.2(c)). The fully frequency/angle-resolved measurement of the photo-electron current, known as **angle-resolved photoemission spectroscopy (ARPES)**, is one of the most important spectroscopic techniques in the experimental analysis of band structures. **Auger spectroscopy** is based on an interaction process of higher order (Fig. 7.2(d)). In this process, a core hole is created by irradiation by either X-rays or high-energy electrons. In a secondary process, part of the energy emitted by a recombining valence electron is transferred to another valence electron, which then leaves the atom and is detected.

[7] To access valence electrons, soft X-ray radiation or hard UV radiation can be employed.

- **Neutron scattering**: Thermal neutrons are scattered elastically or inelastically by a solid state target. Being a neutral particle, the neutron interacts only weakly with solid state constituents (i.e. magnetically, through its spin) and hence penetrates deeply into the sample. Owing to its particular energy dispersion, the neutron is tailor-made to the analysis of low-lying collective excitations (phonons, magnons, etc. – for example the data shown on page 78 were obtained by neutron spectroscopy). Just as with X-ray scattering, elastic neutron scattering can be employed to obtain crystallographic information. Unfortunately, the production of thermal neutrons requires a nuclear reactor, i.e. neutron scattering is an extremely expensive experimental enterprise.

- **Magnetic resonance**: A sample containing particles of non-vanishing moment is placed into a static (in practice, a slowly varying) magnetic field, strong enough to cause complete magnetic polarization. The sample is then exposed to an AC magnetic field perpendicular to the polarizing field. If the AC field frequency is in resonance with the Zeeman energy, magnetic transitions are resonantly induced. The observable effect is a strongly enhanced radiation loss of the AC field.

- In **nuclear magnetic resonance (NMR)** the nuclear spins of the sample are polarized. In solid state physics, NMR is applied to obtain information about the magnetic properties of the electronic states of the solid. Owing to the hyperfine interaction of the electron spin and the nuclear spin, the effective magnetic field seen by the nucleus partially depends on the surrounding electron cloud. For example, in metals, the Pauli paramagnetic response of the electrons causes a characteristic shift of the spectral lines (as compared with the NMR spectra of nuclei in uncorrelated environments) known as the **Knight shift**. Analysis of this shift obtains information about the magnetic properties of the conduction electrons. Resonance spectroscopy of transitions between spin-polarized electron states, **electron spin resonance (ESR)**, is frequently used in chemical analysis and molecular physics.

For discussion of other spectroscopic techniques, e.g. **Mössbauer spectroscopy, positron–electron annihilation spectroscopy (PES), muon scattering, electron energy loss spectroscopy (EELS)**, etc., we refer to the literature.

Other experimental techniques

There are a few experimental probes of condensed matter physics that do not fit comfortably into the three-fold "transport-thermodynamics-spectroscopy" scheme discussed above. This applies, for example, to **scanning tunneling microscopy (STM)**, a technique whose development by Binnig and Rohrer in the 1980s has triggered a revolution in the area of nanotechnology.

The basic principle of STM is easily understood: a small tip, kept at a positive electrostatic potential, is brought in proximity to a surface. When the tip–surface separation becomes comparable to atomic scales, electrons begin to tunnel from the substrate onto the tip. The resulting tunnel current is fed into a piezoelectric crystal that in turn levels the height of the tip. Through this mechanism, the surface–tip separation can be kept constant, with an accuracy of fractions of typical atomic separations. A horizontal sweep of the tip then generates an accurate image of the surface profile. For example, Fig. 7.3 shows an STM image of a carbon nanotube.

Gerd Binnig 1947– and Heinrich Rohrer 1933– Awarded one half of the 1986 Nobel Prize (together with E. Ruska, the inventor of the electron microscope) for "their design of the scanning tunneling microscope." (Image © The Nobel Foundation.)

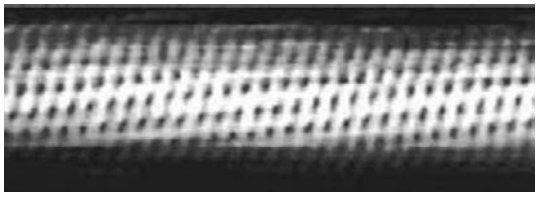

Figure 7.3 STM image of a carbon nanotube. (Figure courtesy of C. Dekker.)

7.2 Linear response theory

In the previous section, we argued that condensed matter experiments typically probe the (linear) response of a system to the application of weak perturbations F'_j . Such linear response can be cast in terms of a generalized susceptibility χ: Eq. (7.2). In the following we try to give the formal expression (7.2) a concrete meaning. Specifically,we relate the response function χ to microscopic elements of the theory familiar from previous chapters. However, before entering this discussion, let us list a few properties of χ that follow from common sense reasoning.

- ▷ **Causality**: The generalized forces $F'_j(t')$ cannot cause an effect prior to their action, i.e. $\chi_{ij}(\mathbf{r}, \mathbf{r}'; t, t') = 0, t < t'$. Formally, we say that the response is **retarded**.
- ▷ If the system Hamiltonian does not explicitly depend on time (which will usually be the case), the response depends only on the difference of the time coordinates, $\chi_{ij}(\mathbf{r}, \mathbf{r}'; t, t') = \chi_{ij}(\mathbf{r}, \mathbf{r}'; t-t')$. In this case it is convenient to Fourier transform the temporal convolution (7.2), i.e. to express the response in frequency space:

$$X_i(\mathbf{r}, \omega) = \int d^d r' \ \chi_{ij}(\mathbf{r}, \mathbf{r}'; \omega) F'_j(\mathbf{r}', \omega) + \mathcal{O}(F'^2). \tag{7.3}$$

The important statement implicit in Eq. (7.3) is that, in the linear response regime, a (near) monochromatic perturbation acting at a certain frequency ω will cause a response of the same frequency. For example, an AC voltage with frequency ω will drive an AC current of the same frequency, etc. We can read this statement in reverse to say that, if the system responds at frequencies $\neq \omega$, we have triggered a strong, nonlinear response. Indeed, it is straightforward to verify (exercise) that an expansion of the general functional $R[F']$ to nth order in F' generates a response with frequency $n\omega$.[8] According to Eq. (7.3), a peak in the response $X_i(\omega)$ at a certain frequency ω indicates a local maximum of the response function, i.e. the presence of an intrinsic excitation with characteristic frequency ω.

▷ For systems that are translationally invariant, the response function depends only on differences between spatial coordinates, $\chi_{ij}(\mathbf{r},\mathbf{r}';t-t') = \chi_{ij}(\mathbf{r}-\mathbf{r}';t-t')$. Spatial Fourier transformation then leads to the relation

$$X_i(\mathbf{q},\omega) = \chi_{ij}(\mathbf{q};\omega)F'_j(\mathbf{q},\omega) + \mathcal{O}(F'^2). \tag{7.4}$$

By analogy to what was said above about the frequency response, we conclude that a peak of the function $X_i(\mathbf{q},\omega)$ signals the presence of an excitation with frequency ω and momentum $\mathbf{q}$. We thus see that, at least in principle, linear response measurements are capable of exploring the full dispersion relation of the excitations of a system.

This is as much as one can say on general grounds. In the following we will employ the field integral formalism to relate the response function to concrete microscopic properties of the system.

EXERCISE Consider X-ray or neutron radiation probing a crystalline medium whose unit cells are spanned by vectors $\mathbf{a}_i$, $i = 1,\ldots,d$. Show that the response function χ shows this periodicity through the condition $\chi(\mathbf{k},\mathbf{k}';\omega) \propto \delta_{\mathbf{k}-\mathbf{k}'-\mathbf{G}}$, where $\mathbf{G}$ belongs to the reciprocal lattice of the system. That is, the angle-resolved scattering pattern displays the full periodicity of the reciprocal lattice and, therefore, of the original lattice. This is, in a nutshell, the main principle behind **spectroscopic crystallography**.

7.2.1 Microscopic response theory

We now set out to relate the response function to the microscopic elements of the theory. Previously we saw that, in quantum theory, the response signal $X(t)$ should be interpreted as the expectation value of some (single-particle) operator[9] $\hat{X} = \sum_{aa'} c_a^\dagger X_{aa'} c_{a'}$, where c_a

[8] While these "side bands" are usually negligible, they may become sizeable in, for example, laser-spectroscopic experiments. The field intensities reached by laser beams can be so large as to generate frequency-doubled or -tripled response signals. However, these phenomena, which belong to the realm of **nonlinear optics**, are beyond the scope of the present text.

[9] For notational clarity, the indices i and $\mathbf{r}$ labeling a multi-component set of local response quantities $X_i(\mathbf{r})$ will be dropped in this section (similarly with $F'_j(\mathbf{r}')$).

may, as appropriate, represent bosonic or fermionic operators. Within the formalism of the field integral, the expectation value at imaginary times is thus given by

$$X(\tau) = \sum_{aa'} \langle \bar{\psi}_a(\tau) X_{aa'} \psi_{a'}(\tau) \rangle, \tag{7.5}$$

where, as usual, $\langle \cdots \rangle = \mathcal{Z}^{-1} \int D(\bar{\psi}, \psi)\ (\cdots) \exp\{-S[F', \bar{\psi}, \psi]\}$ is the functional average over the action describing our system. The action of the system is given by $S[F', \bar{\psi}, \psi] = S_0[\bar{\psi}, \psi] + \delta S'[F', \bar{\psi}, \psi]$, where S_0 is the action of the unperturbed system and

$$\delta S'[F', \bar{\psi}, \psi] = \int d\tau\ \hat{H}_{F'} = \int d\tau\ F'(\tau) \sum_{aa'} \bar{\psi}_a(\tau) X'_{aa'} \psi_{a'}(\tau),$$

is the perturbation introduced by the action of the generalized force (cf. Eq. (7.1)).

In practice, it is often convenient (for a better motivation, see the next section) to represent $X(\tau)$ as a derivative of the free energy functional. To this end, let us formally couple our operator $\hat{X}$ to a second "generalized force" and define

$$\delta S[F, \bar{\psi}, \psi] \equiv \int d\tau\, F(\tau) \hat{X}(\tau) = \int d\tau\, F(\tau) \sum_{aa'} \bar{\psi}_a(\tau) X_{aa'} \psi_{a'}(\tau),$$

as a new element of our action. With $S[F, F', \bar{\psi}, \psi] = S_0[\bar{\psi}, \psi] + \delta S[F, \bar{\psi}, \psi] + \delta S'[F', \bar{\psi}, \psi]$, we then have

$$X(\tau) = -\left. \frac{\delta}{\delta F(\tau)} \right|_{F=0} \ln \mathcal{Z}[F, F'],$$

where the notation $\mathcal{Z}[F, F'] = \int \mathcal{D}(\bar{\psi}, \psi)\ e^{-S[F, F', \bar{\psi}, \psi]}$ indicates that the partition function $\mathcal{Z}$ functionally depends on the two generalized forces.

Now, if it were not for the presence of the driving force F', the expectation value X would vanish. On the other hand, we also assume that F' is weak in the sense that a linear approximation in F' satisfactorily describes the measured value of X. Noting that the formal first-order expansion of a general functional $G[F']$ is given by $G[F'] \simeq G[0] + \int d\tau'\ \frac{\delta G[F']}{\delta F'(\tau')}|_{F'=0} F'(\tau')$, we can write

$$X(\tau) \simeq -\int d\tau' \left(\left. \frac{\delta^2}{\delta F(\tau)\ \delta F'(\tau')} \right|_{F=F'=0} \ln \mathcal{Z}[F, F'] \right) F'(\tau').$$

Comparison with Eq. (7.2) then leads to the identification

$$\chi(\tau, \tau') = -\left. \frac{\delta^2}{\delta F(\tau)\ \delta F'(\tau')} \right|_{F=F'=0} \ln \mathcal{Z}[F, F'],$$

of the response kernel. Carrying out the derivatives, we find

$$\begin{aligned} \chi(\tau, \tau') = &-\mathcal{Z}^{-1} \left. \frac{\delta^2}{\delta F(\tau)\ \delta F'(\tau')} \right|_{F=F'=0} \mathcal{Z}[F, F'] \\ &+ \left(\mathcal{Z}^{-1} \left. \frac{\delta}{\delta F'(\tau')} \right|_{F'=0} \mathcal{Z}[0, F'] \right) \left(\mathcal{Z}^{-1} \left. \frac{\delta}{\delta F(\tau)} \right|_{F=0} \mathcal{Z}[F, 0] \right). \end{aligned}$$

Now, by construction, the second term in large parentheses is the functional expectation value $\langle \hat{X}(\tau)\rangle$ taken over the unperturbed action. We had assumed that this average vanishes, so that our preliminary, and still very formal, result for the response function is given by

$$\boxed{\chi(\tau,\tau') = -\mathcal{Z}^{-1}\,\frac{\delta^2}{\delta F(\tau)\;\delta F'(\tau')}\bigg|_{F=F'=0}\mathcal{Z}[F,F'].} \tag{7.6}$$

Performing the two derivatives, we obtain a more concrete representation of the response function in terms of a four-point correlation function:

$$\chi(\tau,\tau') = -\langle \hat{X}(\tau)\hat{X}'(\tau')\rangle = -\langle \sum_{ab}\bar{\psi}_a(\tau)\hat{X}_{ab}\psi_b(\tau)\sum_{a'b'}\bar{\psi}_{a'}(\tau')\hat{X}'_{a'b'}\psi_{b'}(\tau')\rangle. \tag{7.7}$$

EXERCISE Directly expand Eq. (7.5) to first order in the generalized force F to obtain this expression. As mentioned above, the usefulness of the derivative construction outlined above will become clear shortly.

INFO Equation (7.7) indicates a connection between two seemingly very different physical mechanisms. To disclose this relation, let us consider the case where the observed and the driving operator are equal: $\hat{X}' = \hat{X}$. (Shortly, we will see that the important application to the electromagnetic response of a system falls into this category.) Using the vanishing of the equilibrium expectation values, $\langle \hat{X}(\tau)\rangle = 0$, we can then rewrite (7.7) as

$$\chi(\tau,\tau') = -\langle (\hat{X}(\tau) - \langle \hat{X}(\tau)\rangle)(\hat{X}(\tau') - \langle \hat{X}(\tau')\rangle)\rangle. \tag{7.8}$$

This relation is called the **fluctuation–dissipation theorem**. Indeed, the right-hand side of the relation clearly describes the quantum thermal fluctuation behavior of (the physical observable represented through) the operator $\hat{X}$. By contrast, the left-hand side is of dissipative nature. For example, for the case $\hat{X} = \mathbf{j}$ (see below), χ relates to the conductance of the system, i.e. the way in which the kinetic energy of a charge carrier is dissipated among the intrinsic excitations of the system.

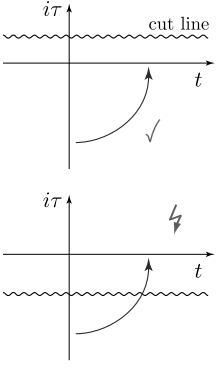

We might now proceed to evaluate this function by means of the machinery introduced in the previous chapters and that is, indeed, how the response function will be computed in practice. However, before doing this, we must face up to one more conceptual problem. What we are after is the real-time response $X(t)$ to a real-time dynamical perturbation $F'(t')$. However, our functional integral formalism produces, naturally, an imaginary-time response $\chi(\tau,\tau')$. In fact, we have frequently met with this problem before: while we are generally interested in real-time properties the formalism makes imaginary-time predictions. In previous chapters, we dealt with this problem by remembering that the imaginary-time setup could be obtained by analytical continuation $t \to -i\tau$ of the integration contour of a real-time functional integral. Reversing this "Wick rotation" we argued that a real-time response $X(t)$ can be extracted from an imaginary-time result $X(\tau)$ by substitution $\tau \to it$.

In the majority of cases, this procedure indeed leads to correct results. However, sometimes one has to be more careful and that applies, in particular, to our present linear response calculus. Indeed, the simple substitution $F(\tau) \to F(t) = F(\tau \to it)$ is a crude shortcut of what mathematically should be a decent analytical continuation. Problems with this prescription arise when the answer $F(\tau)$ generated by the functional integral contains singularities in the complex τ-plane.[10] If a fictitious contour interpolating between the limiting points τ and it inevitably crosses these singularities (see the figure), the simple substitution prescription becomes a problem. The upshot of these considerations is that, before proceeding with the construction of the linear response formalism, we need to develop a better understanding of the mathematical structure of correlation functions.

7.3 Analytic structure of correlation functions

It is the purpose of this section to clarify – at last – the connection between imaginary and real-time correlation functions. Throughout much of this section we will return to the traditional operator representation, i.e. expressions with circumflexes, $\hat{X}$, represent canonically quantized operators and $\langle \cdots \rangle = \mathcal{Z}^{-1}\mathrm{tr}(\cdots \exp\{-\beta[\hat{H} - \mu\hat{N}]\})$ represents the quantum-thermal expectation value. Restricting ourselves to correlation functions of operators taken at two different times,[11] the general definition of the **imaginary-time correlation function** reads

$$\boxed{C^{\tau}_{X_1X_2}(\tau_1 - \tau_2) \equiv -\langle T_\tau \hat{X}_1(\tau_1)\hat{X}_2(\tau_2)\rangle \equiv -\begin{cases}\langle \hat{X}_1(\tau_1)\hat{X}_2(\tau_2)\rangle, & \tau_1 \geq \tau_2,\\ \zeta_{\hat{X}}\langle \hat{X}_2(\tau_2)\hat{X}_1(\tau_1)\rangle, & \tau_2 > \tau_1,\end{cases}} \tag{7.9}$$

where $\hat{X}_i(c, c^\dagger)$ are arbitrary operators represented in terms of either boson or fermion operators $\{c, c^\dagger\}$. The time-dependence of these operators is defined through the **imaginary-time Heisenberg representation**,

$$\hat{X}(\tau) \equiv e^{\tau(\hat{H}-\mu\hat{N})}\hat{X}e^{-\tau(\hat{H}-\mu\hat{N})}, \tag{7.10}$$

i.e. the imaginary-time analog of the real-time Heisenberg representation familiar from quantum mechanics.[12] The role of the **time-ordering operator** T_τ, whose action is defined

[10] More precisely, the quantity $F(\tau)$ produced by evaluating the functional integral should be interpreted as a function defined on the imaginary axis of a complex-time domain. Analytical continuation then leads to a generalization $F(z)$, where z may take values in some two-dimensional domain of the complex plane. What we imply when we substitute $F(\tau) \to F(\tau \to it)$ is that the analyticity domain includes the real axis, and that analytical continuation amounts to a simple re-substitution of the argument. Both assumptions may happen to be violated.

[11] According to our discussion above, correlation functions of this type suffice to explore the linear response of a system. Although the situation with nonlinear response signals is more complicated, much of what we are going to say below has general validity.

[12] Within imaginary-time theory, it is customary to absorb the chemical potential into the dynamical evolution of an operator.

through the second equality,[13] is to chronologically order the two operators $\hat{X}_1(\tau_1)$ and $\hat{X}_2(\tau_2)$.

Notice that for one-body operators $\hat{X}_i = \sum_{\alpha\beta} c^\dagger_\alpha [X_i]_{\alpha\beta} c_\beta$, the definition above describes the response functions discussed in the previous section. For $\hat{X}_1 = c_\alpha, \hat{X}_2 = c^\dagger_\beta$, Eq. (7.9) coincides with the one-body imaginary-time correlation functions ("Green functions") discussed earlier in this text, i.e. Eq. (7.9) and its real time descendants to be discussed next cover most of the correlation functions of relevance in many-body physics.

INFO Although we shall postpone the discussion of the connection to the field integral formalism for a while, it is instructive to compare the definition (7.9) with the field integral correlation function (7.7) defined above. Indeed, if the quantities $\hat{X}_i(\tau_i)$ in (7.9) were to be interpreted as the functional representation of second quantized operators, $\hat{X}(a^\dagger, a) \to \hat{X}(\bar{\psi}, \psi)$, the two correlation functions would coincide. The reason is that the time-ordering operation acting on the functional representation of an operator pair is redundant, $T_\tau \hat{X}_1(\bar{\psi}(\tau_1), \psi(\tau_1)) \hat{X}_2(\bar{\psi}(\tau_2), \psi(\tau_2)) = \hat{X}_1(\bar{\psi}(\tau_1), \psi(\tau_1)) \hat{X}_2(\bar{\psi}(\tau_2), \psi(\tau_2))$ (Exercise: Try to think why). In other words, the correlation function (7.9) reduces to (7.7) when the operators are represented within the field integral formalism. (The reason why T_τ is not redundant for canonically quantized operators is that these have a non-vanishing commutator/anti-commutator at equal times.)

In a manner that is difficult to motivate in advance, we next introduce not one but three different response functions of a real-time argument. Substituting in Eq. (7.9) real-time arguments for imaginary times, $\tau \to it$, we obtain the **real-time response function**

$$\boxed{C^T_{X_1X_2}(t_1 - t_2) = -i\langle T_t \hat{X}_1(t_1) \hat{X}_2(t_2)\rangle,} \tag{7.11}$$

where the factor of i has been introduced for later convenience, T_t chronologically orders real times, and $\hat{X}(t) \equiv e^{it(\hat{H}-\mu\hat{N})} \hat{X} e^{-it(\hat{H}-\mu\hat{N})}$ are real-time Heisenberg operators. While this expression appears to be the "natural" generalization of (7.9), it is not our prime object of interest. Much more physical significance is carried by the **retarded response function**

$$\boxed{C^+_{X_1X_2}(t_1 - t_2) = -i\Theta(t_1 - t_2)\langle[\hat{X}_1(t_1), \hat{X}_2(t_2)]_{\zeta_X}\rangle,} \tag{7.12}$$

i.e. an object that exists only for times $t_1 > t_2$ (hence the attribute "retarded"). The complementary time domain, $t_1 < t_2$, is described by the **advanced response function**

$$\boxed{C^-_{X_1X_2}(t_1 - t_2) = +i\Theta(t_2 - t_1)\langle[\hat{X}_1(t_1), \hat{X}_2(t_2)]_{\zeta_X}\rangle.} \tag{7.13}$$

INFO What is the **physical meaning of the real-time retarded response function**? To address this question we need to reformulate the linear response arguments given above in the

[13] The sign factor $\zeta_X = \pm 1$ depends on the statistics of $\hat{X}_i$, i.e. $\zeta_X = 1$ if $\hat{X}_i$ are bosonic. Note that the operator $\hat{X}_i$ is bosonic if $\{c, c^\dagger\}$ are Bose operators or if it is of even order in a fermion algebra. Conversely, $\zeta_X = -1$ if they are fermionic.

language of the canonical operator formalism. What we would like to compute is the expectation value

$$X(t) = \langle \hat{X}^{F'}(t) \rangle, \tag{7.14}$$

building up in response to the presence of a weak perturbation $F'(t)\hat{X}'$ in the Hamiltonian $\hat{H} = \hat{H}_0 + F'(t)\hat{X}'$. In Eq. (7.14), the superscript "F'" indicates that the time evolution of $\hat{X}$ follows the full Hamiltonian (including the perturbation $F'(t)\hat{X}'$). In contrast, the angular brackets represent a thermal average $\langle \cdots \rangle = \mathcal{Z}^{-1}\,\mathrm{tr}[(\cdots)\exp\{-\beta\hat{H}_0\}]$ that does not include the perturbation.[14] The philosophy behind this convention is that, somewhere in the distant past, $t \to -\infty$, the system was prepared in a thermal equilibrium distribution of the unperturbed Hamiltonian $\hat{H}_0$. As time evolved, a perturbation $\propto F'(t)$ was gradually switched on until it began to affect the expectation value of the dynamically evolved operator $\hat{X}$. (One need not be irritated by the somewhat artificial definition of the **switching on procedure**; all it tells us is that $\hat{X}'$ acts on a system in thermal equilibrium, an assumption that is not problematic if the perturbation is sufficiently weak.) To compute the expectation value, it is convenient to switch to a representation wherein the evolutionary changes due to the action of the perturbation are separated:

$$X(t) = \langle (\hat{U}^{F'})^{-1}(t)\hat{X}(t)\hat{U}^{F'}(t) \rangle, \tag{7.15}$$

where $\hat{U}^{F'}(t) = \hat{U}_0^{-1}(t)\hat{U}(t)$, the evolution of $\hat{X}$ follows the standard Heisenberg dynamics $\hat{X}(t) = \hat{U}_0^{-1}(t)\hat{X}\hat{U}_0(t)$, and $\hat{U}(\hat{U}_0)$ generates the time evolution of the full (unperturbed) Hamiltonian. Using the defining equations of these evolution operators, it is straightforward to verify that $\hat{U}^{F'}$ obeys the differential equation, $d_t\hat{U}^{F'}(t) = -iF'(t)\hat{X}'(t)\hat{U}^{F'}(t)$, i.e. the time evolution of $\hat{U}^{F'}$ is controlled by the (Heisenberg representation of the) perturbation $\hat{X}'$. According to conventional time-dependent quantum mechanical perturbation theory, the solution of this differential equation (with boundary condition $\hat{U}^{F'}(t \to -\infty) \to \mathbf{1}$) is given by

$$\hat{U}^{F'}(t) = T_t \exp\left(-i\int_{-\infty}^{t} dt'\ F'(t')\hat{X}'(t')\right) \simeq \mathbf{1} - i\int_{-\infty}^{t} dt'\ F'(t')\hat{X}'(t') + \cdots$$

Substituting this result into Eq. (7.15) we obtain

$$X(t) = -i\int dt'\ \theta(t-t')F'(t')\ \ [\hat{X}(t), \hat{X}'(t')]\ \ = \int dt'\, C^{+}_{XX'}(t-t')F'(t'),$$

i.e. the retarded response function turns out to generate the linear response of $\hat{X}$ to the presence of the perturbation. In other words, the function C^+ is our prime object of interest, while all other correlation functions defined above play the (potentially important) role of supernumeraries.

We next set out to explore the connection between the different correlation functions defined above. In doing so, the principal question that should be at the back of our minds is "How do we obtain the retarded real time function C^+ provided we know the imaginary-time correlation function C^τ?" The key to the answer of this question lies in a highly formal representation of the correlation functions $C^{T,\tau,+,-}$, known as the **Lehmann representation**. This representation is obtained by representing the correlation functions in terms of an exact eigenbasis $\{|\Psi_\alpha\rangle\}$ of the system: representing the trace entering the thermal expectation values as $\mathrm{tr}(\cdots) = \sum_\alpha \langle\Psi_\alpha|\cdots|\Psi_\alpha\rangle$, and inserting a resolution of unity $\mathbf{1} = \sum_\beta |\Psi_\beta\rangle\langle\Psi_\beta|$

[14] To simplify the notation, the chemical potential has been absorbed into the definition of $\hat{H}$.

between the two operators appearing in the definition of the correlation function, it is straightforward to show that, e.g.[15]

$$C^T(t) = -i\mathcal{Z}^{-1}\sum_{\alpha\beta} X_{1\alpha\beta}X_{2\beta\alpha}e^{it\ \ _{\alpha\beta}}\left(\Theta(t)e^{-\beta\ \ _{\alpha}} + \zeta_X\Theta(-t)e^{-\beta\ \ _{\beta}}\right). \tag{7.16}$$

Here, E_α is the eigenvalue corresponding to a state Ψ_α and we have introduced the shorthand notations $\mathrm{fl}_\alpha \equiv E_\alpha - \mu N_\alpha, \mathrm{fl}_{\alpha\beta} \equiv \mathrm{fl}_\alpha - \mathrm{fl}_\beta, X_{\alpha\beta} \equiv \langle\Psi_\alpha|\hat{X}|\Psi_\beta\rangle$. We next Fourier transform C^T to find

$$C^T(\omega) = \int_{-\infty}^{\infty} dt\, C^T(t)e^{i\omega t-\eta|t|} = \mathcal{Z}^{-1}\sum_{\alpha\beta} X_{1\alpha\beta}X_{2\beta\alpha}\left[\frac{e^{-\beta\ \ _{\alpha}}}{\omega+\mathrm{fl}_{\alpha\beta}+i\eta} - \zeta_{\hat{X}}\frac{e^{-\beta\ \ _{\beta}}}{\omega+\mathrm{fl}_{\alpha\beta}-i\eta}\right],$$

where the convergence-generating factor η – which will play an important role throughout! – has been introduced to make the Fourier representation well-defined.[16]

Equation (7.16) is the Lehmann representation of the real time correlation function. What is the use of this representation? Clearly, Eq. (7.16) will be of little help for any practical purposes; the equation makes explicit reference to the exact eigenfunctions/states of the system. Should we have access to these objects, we would have a full solution of the problem anyway. Rather, the principal purpose of spectral resolutions such as (7.16) is to reveal exact connections between different types of correlation functions and the analytical structure of these objects in general. To do so, we first need to compute the Lehmann representation of the other correlation functions. Proceeding as with the real time function above, it is straightforward to show that

$$\left.\begin{matrix} C^T(\omega) \\ C^+(\omega) \\ C^-(\omega) \end{matrix}\right\} = \mathcal{Z}^{-1}\sum_{\alpha\beta} X_{1\alpha\beta}X_{2\beta\alpha}\left[\begin{matrix} \\ \dfrac{e^{-\beta\ \ _{\alpha}}}{\omega+\mathrm{fl}_{\alpha\beta}\ \left\{\begin{matrix}+\\+\\-\end{matrix}\right\} i\eta} \end{matrix} - \zeta_{\hat{X}}\frac{e^{-\beta\ \ _{\beta}}}{\omega+\mathrm{fl}_{\alpha\beta}\ \left\{\begin{matrix}-\\+\\-\end{matrix}\right\} i\eta}\right]. \tag{7.17}$$

From this result, a number of important features of the correlation functions can be readily inferred. Anticipating the analytical structures alluded to above, we should think of $C^{T,+,-}(z)$ as functions of a set of complex variables z. (The representations above apply to $C^{T,+,-}(z=\omega)$ where ω is restricted to the real axis.) This extended interpretation allows us to view $C^{T,+,-}$ as complex functions with singularities in the immediate vicinity of the real axis. More specifically:

▷ The retarded correlation function C^+ has singularities for $z = -\mathrm{fl}_{\alpha\beta} - i\eta$ slightly below the real axis. It is, however, analytic in the entire upper complex half plane $\mathrm{Im}(z) \geq 0$.

[15] Wherever no confusion may arise, we omit the operator subscript $C_{XX'}$ carried by the correlation functions.

[16] Indeed, we can attach physical significance to this factor. The switching on procedure outlined above can be implemented by attaching a small damping term $\exp(-|t|\eta)$ to an otherwise purely oscillatory force . If we absorb this factor into the definition of all Fourier integrals, $\int dt\,(F(t)e^{-t|\ \ |})e^{i\omega t}(\cdots) \to \int dt\,F(t)\,(e^{-t|\ \ |}e^{i\omega t})(\cdots)$, we arrive at the Fourier regularization mentioned above.

▷ Conversely, the advanced correlation function C^- has singularities above the real axis. It is analytic in the lower half plane $\mathrm{Im}(z) \leq 0$. Notice that C^+ and C^- are connected through complex conjugation,

$$C^+(\omega) = \left[C^-(\omega)\right]^* . \tag{7.18}$$

▷ The time-ordered correlation function has singularities on either side of the real axis (which makes it harder to analyze).

▷ The position of the singularities in the vicinity of the real axis contains important information about the fundamental excitations of the system (see Fig. 7.4). For example, consider the case where $\hat{X}_1 = c_a^\dagger$ and $\hat{X}_2 = c_b$ are one-particle creation and annihilation operators (no matter whether bosonic or fermionic). In this case, $N_\alpha - N_\beta \equiv \Delta N = 1$ (independent of the state indices α, β) and $E_\alpha - E_\beta$ is of the order of the single-particle energies of the system. (For a non-interacting system, $E_\alpha - E_\beta$ strictly coincides with the single-particle energies – exercise: why?) That is, the singularities of $C^{T,+,-}$ map out the single-particle spectrum of the system. This can be understood intuitively by remembering the meaning of the one-particle correlation function as the amplitude for creation of a state $|a\rangle$ followed by the annihilation of a state $|b\rangle$ at some later time. It is clear that the time Fourier transform of the amplitude, $|a\rangle \stackrel{t}{\to} |b\rangle$, becomes "large" when the phase ($\sim \omega t$) of the Fourier argument is in resonance with an eigenphase $\sim (E_\alpha - E_\beta)t$ supported by the system. (If you do not find this statement plausible, explore the simple example of a plane wave Hamiltonian.) Similarly, for a two-particle correlation function, $\hat{X}_1 \sim c_a^\dagger c_b$, the energies $E_\alpha - E_\beta$ describe the spectrum (the "energy cost") of two-particle excitations, etc. Notice that the single-particle spectrum can be continuous (in which case the functions $C^{T,+,-}$ have *cuts* parallel to the real axis), or discrete (isolated poles).

▷ Once one of the correlation functions is known, all others follow straightforwardly from a simple recipe: using the familiar Dirac identity,

$$\lim_{\eta \searrow 0} \frac{1}{x \pm i\eta} = \mp i\pi\delta(x) + P\frac{1}{x}, \tag{7.19}$$

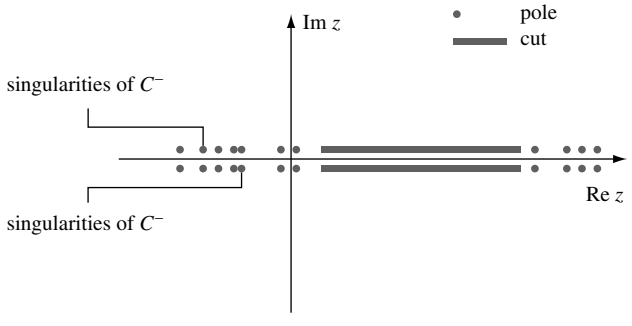

Figure 7.4 Illustrating the singularities of advanced and retarded correlation functions in the complex plane. The points denote poles and the lines branch cuts.

where P is the principal part, it is a straightforward matter to show that (exercise!)

$$\boxed{\mathrm{Re}\, C^T(\omega) = \mathrm{Re}\, C^+(\omega) = \mathrm{Re}\, C^-(\omega),} \tag{7.20}$$

and

$$\boxed{\mathrm{Im}\, C^T(\omega) = \pm \mathrm{Im}\, C^\pm(\omega) \times \begin{cases} \coth \dfrac{\beta\omega}{2}, & \text{bosons,} \\ \tanh \dfrac{\beta\omega}{2}, & \text{fermions,} \end{cases}} \tag{7.21}$$

i.e. the information stored in the three different functions is essentially equivalent.

After our discussion of the real-time correlation functions, the analysis of the imaginary-time function C^τ is straightforward. The imaginary-time analog of Eq. (7.16) reads

$$C^\tau(\tau) = -\mathcal{Z}^{-1} \sum_{\alpha\beta} X_{1\alpha\beta} X_{2\beta\alpha} e^{\ \alpha\beta\tau} \left(\Theta(\tau) e^{-\beta\ \alpha} + \zeta_{\hat{X}} \Theta(-\tau) e^{-\beta\ \beta} \right). \tag{7.22}$$

Inspection of this representation for positive and negative times shows that C^τ acquires the periodicity properties of the operators $\hat{X}_{1,2}$:

$$C^\tau(\tau) = \zeta_{\hat{X}} C^\tau(\tau + \beta), \quad \tau < 0. \tag{7.23}$$

Consequently C^τ can be expanded in a Matsubara Fourier representation just like a conventional operator, $C^\tau(i\omega_n) = \int_0^\beta d\tau C^\tau(\tau) e^{i\omega_n \tau}$, where, depending on the nature of the operators $\hat{X}_{1,2}$, ω_n may be a bosonic or a fermionic Matsubara frequency. Applying this transformation to the Lehmann representation (7.22), we obtain

$$C^\tau(i\omega_n) = \mathcal{Z}^{-1} \sum_{\alpha\beta} \frac{X_{1\alpha\beta} X_{2\beta\alpha}}{i\omega_n + \mathrm{fl}_{\alpha\beta}} \left[e^{-\beta\ \alpha} - \zeta_X e^{-\beta\ \beta} \right]. \tag{7.24}$$

Our final task is to relate the four correlation functions defined through Eq. (7.17) and (7.24) to each other. To this end, we define the "master function"

$$C(z) = \mathcal{Z}^{-1} \sum_{\alpha\beta} \frac{X_{1\alpha\beta} X_{2\beta\alpha}}{z + \mathrm{fl}_{\alpha\beta}} \left[e^{-\beta\ \alpha} - \zeta_X e^{-\beta\ \beta} \right], \tag{7.25}$$

depending on a complex argument z. When evaluated for $z = \omega^+, \omega^-, i\omega_n$, respectively, the function $C(z)$ coincides with C^+, C^-, C^τ. Further, $C(z)$ is analytic everywhere except for the real axis. This knowledge suffices to construct the relation between different correlation functions that was sought. Suppose then we had succeeded in computing $C^\tau(i\omega_n) = C(z = i\omega_n)$ for all positive Matsubara frequencies.[17] Further, let us assume that we had managed to find an analytic extension of $C(z = i\omega_n) \to C(z)$ into the entire upper complex half plane $\mathrm{Im}\, z > 0$. The evaluation of this extension on the infinitesimally shifted real axis $z = \omega + i0$ then coincides with the retarded Green function $C^+(\omega)$ (see figure below). In other words,

[17] Keep in mind that, in practical computations of this type, we will not proceed through the Lehmann representation.

To find $C^+(\omega)$ we need to (i) compute $C^\tau(i\omega_n)$ for all positive Matsubara frequencies (e.g. by means of the thermal field integral) and then (ii) continue the result down to the real axis, $i\omega_n \to \omega + i0$.

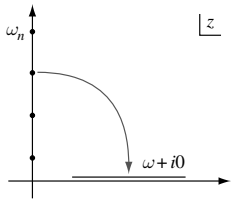

The advanced Green function C^- is obtained analogously, and by analytic extension the thermal correlation function $C^\tau(i\omega_n < 0)$, to frequencies with a negative offset, $\omega - i0$.

These statements follow from a theorem of complex function theory stating that two analytic functions $F_1(z)$ and $F_2(z)$ coincide if $F_1(z_n) = F_2(z_n)$ on a sequence $\{z_i\}$ with a limit point in the domain of analyticity. (In our case $i\omega_n \to i\infty$ is the limit point.) From inspection of (7.25) we already know that $F_1(i\omega_n) \equiv C^+(\omega \to i\omega_n)$ coincides with $F_2(i\omega_n) = C^\tau(i\omega_n)$. Thus any analytic extension of C^τ must coincide with C^+ everywhere in the upper complex half plane, including the infinitesimally shifted real axis.

EXERCISE Writing $z = \omega \pm i\eta$, transform the spectral representation (7.25) back to the time domain: $C(t) = \frac{1}{2\pi}\int d\omega\ e^{-i\omega t}C(\omega \pm i\eta)$. Convince yourself that, for $\mathrm{Im}(z)$ positive (negative), the temporal correlation function $C(t)$ contains a Θ-function $\Theta(t)$ ($\Theta(-t)$). (Hint: Make use of Cauchy's theorem.) Importantly, the presence of this constraint does not hinge on η being infinitesimal. It even survives generalization to a frequency-dependent function $\eta(\omega) > 0$. (For the physical relevance of this statement, see below.) All that matters is that, for $\eta > 0$, the function $C(\omega \pm i\eta)$ is analytic in the upper (lower) complex half plane. This observation implies a very important **connection between analyticity and causality**: temporal correlation functions whose frequency representation is analytic in the upper (lower) complex half plane are causal (anticausal). (A time-dependent function is called "(anti)causal" if it vanishes for (positive) negative times.)

How is the continuation process, required to find the retarded correlation function, carried out in practice? Basically, the answer follows from what was said above. If we know the correlation function $C^\tau(i\omega_n)$ for all positive Matsubara frequencies, and if that function remains analytic upon substitution $C^\tau(i\omega_n \to z)$ of a general element of the full complex half plane, the answer is simple: we merely have to substitute $i\omega_n \to \omega + i0$ into our result to obtain the retarded correlation function. Sometimes, however, we simply do not know $C^\tau(i\omega_n)$ for all positive frequencies. (For example, we may be working within an effective low-energy theory whose regime of validity is restricted to frequencies $\omega_n < \omega^*$ smaller than some cut-off frequency.) In this case, we are in serious trouble. Everything then hinges on finding a "meaningful" model function that can be extended to infinity and whose evaluation for small frequencies $\omega_n < \omega^*$ coincides with our result; there are no generally applicable recipes for how to deal with such situations.

INFO As a special case of great practical importance, let us briefly explore the **non-interacting single-particle Green function**, i.e. the single-particle correlation function $\hat{X}_1 = c_a$, $\hat{X}_2 = c_a^\dagger$ for a non-interacting system. (We assume that $\{|a\rangle\}$ is an eigenbasis of the one-particle Hamiltonian.) As expected, these correlation functions assume a particularly simple form. In

the non-interacting case, the eigenstates $|\alpha\rangle = |a_1, a_2, \ldots\rangle$ are symmetrical or antisymmetrical combinations of single-particle eigenstates $|a_i\rangle$. Their energy is $E_\alpha = \epsilon_{a_1} + \epsilon_{a_2} + \cdots$, where ϵ_a are the single-particle energies. Using the fact that $E_\beta = E_\alpha + \epsilon_a$ (exercise: why?) one then verifies that the correlation function acquires the simple form

$$C(z)|_{\substack{X_1=c_a \\ X_2=c_a^\dagger}} \equiv G_a(z) = \frac{1}{z - \xi_a},$$

i.e. the partition function entering the definition of the general correlation function cancels against the thermally weighted summation over $|\alpha\rangle$ (check!). Notice that the thermal version of this Green function, $G_a(i\omega_n) = (i\omega_n - \xi_a)^{-1}$, appeared previously as the fundamental building block of perturbation theory. This is, of course, no coincidence: within the formalism of the field integral, the Green function appeared as the functional expectation value $\langle \bar{\psi}_{a,n} \psi_{a,n} \rangle_0$ taken with respect to the Gaussian non-interacting action. But this object is just the functional representation of the operator correlation function considered above.

Building on this representation, it is customary to introduce a **Green function operator** through the definition

$$\hat{G}(z) \equiv \frac{1}{z + \mu - \hat{H}}.$$

By design, the eigenvalues of this operator – which are still functions of z – are given by the correlation function $G_a(z)$ above. Numerous physical observables can be compactly represented in terms of the operator Green function. For example, using Eq. (7.19), it is straightforward to verify that the single-particle density of states of a non-interacting system is obtained as

$$\boxed{\rho(\epsilon) = -\frac{1}{\pi} \text{ Im tr } \hat{G}^+(\epsilon),} \tag{7.26}$$

by taking the trace of the retarded Green function (operator).

To illustrate the procedure of analytic continuation, let us consider a few elementary examples.

1. For the single-particle Green function ($\hat{X}_1 = c_a, \hat{X}_2 = c_a^\dagger$) of an elementary excitation with energy ϵ_a, $G_a(\omega_n) = (i\omega_n - \xi_a)^{-1}$, the continuation amounts to a mere substitution,

$$G_a^+(\omega) = \frac{1}{\omega + i0 - \xi_a}.$$

2. We have seen that quasi-particle interactions lead to the appearance of a – generally complex – self-energy $\Sigma(z)$: $G_a(\omega_n) \to (i\omega_n - \xi_a - \Sigma(i\omega_n))^{-1}$, where we have simplified the notation by suppressing the potential dependence of the self-energy on the Hilbert space index a. Extension down to the real axis leads to the relation

$$G_a^+(\omega) = \frac{1}{\omega^+ - \xi_a - \Sigma(\omega^+)}, \tag{7.27}$$

where $\omega^+ \equiv \omega + i0$ and $\Sigma(\omega^+)$ is the analytic continuation of the function $\Sigma(z)$ to the real axis. Although the specific structure of the self-energy depends on the problem under

consideration, a few statements can be made in general. Specifically, decomposing the self-energy into real and imaginary parts, we have

$$\text{Re } \Sigma(\omega^+) = +\,\text{Re } \Sigma(\omega^-), \qquad \text{Im } \Sigma(\omega^+) = -\,\text{Im } \Sigma(\omega^-) < 0. \tag{7.28}$$

In words, the self-energy function has a cut on the real axis. Upon crossing the cut, its imaginary part changes sign. This important feature of the self-energy can be understood from different perspectives. Formally, it follows from Eq. (7.18) relating the retarded and advanced Green functions through complex conjugation. More intuitively, the sign dependence of the imaginary part can be understood as follows. Suppose we start from a non-interacting imaginary-time formalism and gradually switch on interactions. The (Landau) principle of adiabatic continuity implies that nowhere in this process must the Green function – alias the propagator of the theory – become singular. This implies, in particular, that the combination $i(\omega_n - \text{Im } \Sigma_{i\omega_n})$ must not become zero, lest the dangerous real axis of the energy denominator be touched. The safeguard preventing the vanishing of the imaginary part of the energy denominator is that $-\text{Im } \Sigma$ and ω_n have the opposite sign. Of course, this feature can be checked order by order in perturbation theory. Decomposing the self-energy into real and imaginary parts, $\Sigma = \Sigma' + i\Sigma''$, and transforming $G^+(\omega)$ back to the time domain we obtain

$$G^+(t) = \int \frac{d\omega}{2\pi} e^{-i\omega t} G^+(\omega) \approx e^{-it(\xi_a + \Sigma') + t\Sigma''} \Theta(t),$$

where we have made the (over)simplifying assumption that the dependence of the self-energy operator on ω is negligible: $\Sigma(\omega) \approx \Sigma$.

EXERCISE Check the second equality above.

If we interpret $G^+(t)$ as the amplitude for propagation in the state $|a\rangle$ during a time interval t, and $|G^+|^2$ as the associated probability density, we observe that the probability to stay in state $|a\rangle$ decays exponentially, $|G^+|^2 \propto e^{2t\Sigma''}$, i.e. $2\Sigma'' \equiv -\frac{1}{\tau}$ can be identified as the inverse of the **effective lifetime** τ of state $|a\rangle$. The appearence of a finite lifetime expresses the fact that, in the presence of interactions, single-particle states no longer represent stable objects, but rather tend to decay into the continuum of correlated many-body states. This picture will be substantiated in Section 7.3.1 below.

3. Let us apply Eq. (7.26) to compute the BCS quasi-particle DoS of a superconductor.
In Section 6.4 we saw that the thermal Gor'kov Green function of a superconductor with spatially constant real order parameter is given by $\hat{G}(i\omega_n) = [i\omega_n - (\hat{H} - \mu)\sigma_3 - \Delta\sigma_1]^{-1}$. Switching to an eigenrepresentation and inverting the Pauli matrix structure, we obtain

$$-\frac{1}{\pi}\text{tr } \hat{G}(i\omega_n) = \frac{1}{\pi}\sum_a \text{ tr } \left[\frac{i\omega_n + \xi_a\sigma_3 + \Delta\sigma_1}{\omega_n^2 + \xi_a^2 + \Delta^2}\right] = \frac{2i\omega_n}{\pi}\sum_a \frac{1}{\omega_n^2 + \xi_a^2 + \Delta^2}.$$

Next, performing our standard change from a summation over eigenenergies to an integral, we arrive at

$$-\frac{1}{\pi}\text{tr } \hat{G}(i\omega_n) \simeq \frac{2i\omega_n}{\pi}\nu \int d\xi \frac{1}{\omega_n^2 + \xi^2 + \Delta^2} = \frac{2i\omega_n \nu}{\sqrt{\omega_n^2 + \Delta^2}},$$

where, as usual, ν denotes the normal density of states at the Fermi level. This is the quantity we need to continue to real frequencies. To this end we adopt the standard convention whereby the cut of the square root function is on the positive real axis, i.e. $\sqrt{-r+i0} = -\sqrt{-r-i0} = i\sqrt{|r|}$ for r positive real. Then,

$$-\frac{1}{\pi}\mathrm{tr}\,\hat{G}(i\omega_n \to \epsilon^+) = \frac{2\epsilon^+\nu}{\sqrt{-\epsilon^{+2}+\Delta^2}} \simeq \frac{2\epsilon\nu}{\sqrt{-\epsilon^2 - i0\ \mathrm{sgn}\ (\epsilon)+\Delta^2}},$$

where we anticipate that the infinitesimal offset of ϵ in the numerator is irrelevant (trace its fate!) and, making use of the fact that, for ϵ approaching the real axis, only the sign of the imaginary offset matters: $(\epsilon + i0)^2 \simeq \epsilon^2 + 2i0\epsilon \simeq \epsilon^2 + 2i0\mathrm{sgn}\epsilon$. Finally, taking the imaginary part of that expression, we arrive at the standard BCS form

$$\nu(\epsilon) = \mathrm{Im}\frac{2\epsilon\nu}{\sqrt{-\epsilon^2 - i0\ \mathrm{sgn}(\epsilon)+\Delta^2}} = \begin{cases} 0, & |\epsilon| < \Delta, \\ \dfrac{2|\epsilon|\nu}{\sqrt{\epsilon^2-\Delta^2}}, & |\epsilon| > \Delta. \end{cases}$$

7.3.1 Sum rules and other exact identities

In the next section we apply the analytical structures discussed above to construct a powerful theory of real time linear response. However, before doing so, let us stay for a moment with the formal Lehmann representation to disclose a number of exact identities, or "sum rules," obeyed by the correlation functions introduced in the previous section. Admittedly, this addition to our discussion above does not directly relate to the formalism of linear response, and readers wishing to proceed in a more streamlined manner are invited to skip this section at first reading.

In fact, the formulae we are going to collect are not specific to any particular context and that is precisely their merit: identities based on the analytical structure of the Lehmann representation are exact and enjoy general applicability. They can be used (a) to obtain full knowledge of a correlation function from fragmented information – e.g. we saw in Eq. (7.20) and (7.21) how all three real time correlation functions can be deduced once any one of them is known – and, equally important, (b) to gauge the validity of approximate calculations. The violation of an exact identity within an approximate analysis is usually an indication of serious trouble, i.e. such deviations mostly lead to physically meaningless results.

The spectral (density) function

We begin by considering an object that carries profound physical significance in its own right, especially in the area of strongly correlated fermion physics, i.e. (-2 times) the imaginary part of the retarded correlation function,

$$\boxed{A(\omega) \equiv -2\mathrm{Im}C^+(\omega).} \tag{7.29}$$

Equation (7.29) defines the **spectral function** or **spectral density function**. Using Eq. (7.19) and the Lehmann representation (7.17) it is straightforward to verify that it has the spectral decomposition

$$A(\omega) = 2\pi\mathcal{Z}^{-1}\sum_{\alpha\beta} X_{1\alpha\beta}X_{2\beta\alpha}\left[e^{-\beta\ \alpha} - \zeta_{\hat{X}}e^{-\beta\ \beta}\right]\delta(\omega + \text{fl}_{\alpha\beta}). \tag{7.30}$$

INFO To understand the **physical meaning of the spectral function** let us consider the case where $\hat{X}_{1,2}$ are single-particle creation/annihilation operators, $\hat{X}_1 = c_a$, $\hat{X}_2 = c_a^\dagger$. (We assume that the non–interacting part $\hat{H}_0$ of the Hamiltonian $\hat{H}_0 + \hat{V}$ is diagonalized in the basis $\{|a\rangle\}$.) For a non-interacting problem, $\hat{V} = 0$, it is then straightforward to show that $A_a(\omega) = 2\pi\delta(\omega - \xi_a)$, i.e. the spectral function is singularly peaked at the single-particle energy (measured from the chemical potential) of the state $|a\rangle$. Here, the subscript "a" indicates that we are dealing with a spectral function defined for a pair of one-body operators $c_a, c_a^\dagger$.

Heuristically, the singular structure of $A_a(\omega)$ can be understood by observing that, in the non-interacting case, the state $c_a^\dagger|\alpha\rangle$ obtained by adding a single particle $|a\rangle$ to the many-particle state $|\alpha\rangle$ is, again, an eigenstate of the system. In particular, it is orthogonal to all states by itself, whence the eigenstate summation over $|\beta\rangle$ contains only a single non-vanishing term. We say that the "spectral weight" carried by the (unit-normalized) state $c_a^\dagger|\alpha\rangle$ is concentrated on a single eigenstate of the system.

What happens to this picture if interactions are restored? In this case, the addition $c_a^\dagger|\alpha\rangle$ of a single-particle state to a many-body eigenstate will, in general, no longer be an eigenstate of the system. In particular, there is no reason to believe that this state is orthogonal to all but one $(N+1)$ particle states $|\beta\rangle$. We have to expect that the spectral weight carried by the (still unit-normalized) state $c_a^\dagger|\alpha\rangle$ gets distributed over many, potentially a continuum, of states $|\beta\rangle$.

It is instructive to explore the consequences of this phenomenon in the representation (7.27) where the effect of interactions has been lumped into a self-energy operator Σ. Taking the imaginary part of this expression, we find

$$A_a(\omega) = -2\frac{\Sigma''(\omega)}{(\omega - \xi_a - \Sigma'(\omega))^2 + (\Sigma''(\omega))^2},$$

where Σ' and Σ'' denote the real and imaginary part of the self-energy, respectively, and we have neglected the infinitesimal imaginary offset of ω^+ in comparison with the finite imaginary contribution $i\Sigma''$. The result above suggests that the net effect of interactions is an effective shift of the single-particle energy $\epsilon_a \to \epsilon_a + \Sigma(\omega)$ by the real part of the self-energy operator; interactions lead to a distortion of the single-particle energy spectrum, an effect that follows, for example, from straightforward perturbative reasoning. More importantly, the δ-function obtained in the non-interacting case gets smeared into a Lorentzian (see Fig 7.5). In a sense, the spectral weight carried by the many-body states $C_a^+|\alpha\rangle$ is distributed over a continuum of neighboring states, wherefore the spectral function loses its singular character. The width of the smearing interval is proportional to the imaginary part of the self-energy and, therefore, to the inverse of the lifetime τ discussed in the previous section.

Notice that the smeared spectral function still obeys the normalization condition, $\int \frac{d\omega}{2\pi}A_a(\omega) = 1$, as in the non-interacting case.[18] This suggests an interpretation of A as a probability measure describing in what way the spectral weight carried by the state $c_a^\dagger|\alpha\rangle$ is spread out over the

[18] Strictly speaking, we can integrate A only if the variance of $\Sigma(\omega)$ over the interval $[\xi_a + \Sigma' - \Sigma'', \xi_a + \Sigma' + \Sigma'']$ in which the Lorentzian is peaked is negligible (but see below).

continuum of many-body states $|\beta\rangle$. To put that interpretation onto a firm basis, not bound to the self-energy representation above, we consider the spectral decomposition (7.30). The positivity of all terms contributing to the right-hand side of the equation implies that $A_a(\omega) > 0$, a condition necessarily obeyed by any probability measure. To verify the general validity of the

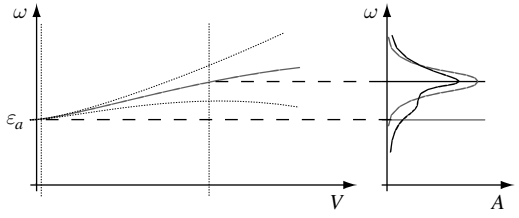

Figure 7.5 Illustrating the meaning of the spectral function. For zero interaction, $V = 0$, the spectral weight is singularly concentrated on the single particle energies of the system. As interactions are switched on, the spectral weight is distributed among a continuum of states concentrated around a shifted center point. The width of the distribution increases with growing interaction strength. Dark solid curve: (schematic) shape of the spectral function if the self-energy carries a pronounced ω dependence.

unit-normalization condition one may integrate Eq. (7.30) over ω:

$$\begin{aligned}
\int \frac{d\omega}{2\pi} A_a(\omega) &= \mathcal{Z}^{-1} \sum_{\alpha\beta} c_{a\alpha\beta} c^\dagger_{a\beta\alpha} \left[e^{-\beta\Xi_\alpha} - \zeta_c e^{-\beta\Xi_\beta} \right] \\
&= \mathcal{Z}^{-1} \left(\sum_\alpha \langle\alpha \left| c_a c_a^\dagger \right| \alpha\rangle e^{-\beta\Xi_\alpha} - \zeta_c \sum_\beta \langle\beta \left| c_a^\dagger c_a \right| \beta\rangle e^{-\beta\Xi_\beta} \right) \\
&= \mathcal{Z}^{-1} \sum_\alpha e^{-\beta\Xi_\alpha} \langle\alpha| \underbrace{c_a c_a^\dagger - \zeta_c c_a^\dagger c_a}_{[c_a, c_a^\dagger]_{\zeta_c} = 1} |\alpha\rangle = \underbrace{\mathcal{Z}^{-1} \sum_\alpha e^{-\beta\Xi_\alpha}}_{1} = 1.
\end{aligned}$$

Positivity and unit-normalization of $A_a(\omega)$ indeed suggest that this function measures the distribution of spectral weight over the many-body continuum.

To further substantiate this interpretation, consider the integral of the spectral function weighted by the Fermi- or Bose-distribution function:

$$\begin{aligned}
\int \frac{d\omega}{2\pi} n_{\mathrm{F/B}}(\omega) A_a(\omega) &= \mathcal{Z}^{-1} \sum_{\alpha\beta} c_{a\alpha\beta} c^\dagger_{a\beta\alpha} \left[e^{-\beta\Xi_\alpha} - \zeta_c e^{-\beta\Xi_\beta} \right] \int d\omega\, \delta(\omega + \Xi_{\alpha\beta}) \frac{1}{e^{\beta\omega} - \zeta_c} \\
&= \mathcal{Z}^{-1} \sum_{\alpha\beta} c_{a\alpha\beta} c^\dagger_{a\beta\alpha} e^{-\beta\Xi_\beta} \left[e^{\beta\Xi_{\beta\alpha}} - \zeta_c \right] \frac{1}{e^{\beta\Xi_{\beta\alpha}} - \zeta_c} \\
&= \mathcal{Z}^{-1} \sum_\beta e^{-\beta\Xi_\beta} \langle\beta \left| c_a^\dagger c_a \right| \beta\rangle = \langle \hat{n}_a \rangle,
\end{aligned}$$

which tells us that, if we weight the spectral density function of a single-particle state $|a\rangle$ with the thermal distribution function, and integrate over all frequencies, we obtain the total occupation of that state. The relation

$$\boxed{\int \frac{d\omega}{2\pi} n_{\mathrm{F/B}}(\omega) A_a(\omega) = \langle \hat{n}_a \rangle,} \tag{7.31}$$

indeed states that A_a is a distribution function describing in what way the spectral weight of the state $c_a^\dagger|\alpha\rangle$ spreads over the continuum of exact eigenstates.

A number of exact identities involving correlation functions are formulated in terms of the spectral function. We begin by showing that the spectral function carries the same information as the correlation function itself. (In view of the fact that A is obtained by removing the real part of C, this result might come as a surprise.) Indeed, starting from $A(\omega) = i(C^+(\omega) - C^-(\omega))$, one may confirm the relation

$$\boxed{C(z) = \int_{-\infty}^{\infty} \frac{d\omega}{2\pi} \frac{A(\omega)}{z-\omega}.} \tag{7.32}$$

Note that the first (second) term contributing to the right-hand side of the definition (a) is analytic in the upper (lower) half of the complex ω-plane and (b) decays faster than ω^{-1} for $|\omega| \to \infty$. For $\mathrm{Im}\, z > 0$, the theorem of residues then implies that the C^--term does not contribute to the integral. (Without enclosing singularities, the integration contour can be closed in the lower half plane.) As for the C^+contribution, one may integrate over an infinite semicircle γ closing in the upper half plane to obtain

$$\int_{-\infty}^{\infty} \frac{d\omega}{2\pi} \frac{A(\omega)}{z-\omega} \overset{\mathrm{Im}\, z>0}{=} -\frac{1}{2\pi i} \int_\gamma d\omega \frac{C^+(\omega)}{z-\omega} = C(z), \tag{7.33}$$

where the second identity relies on the analyticity of C^+ in the upper half plane. The case $\mathrm{Im}\, z < 0$ is treated analogously. We thus find that knowledge of the imaginary part suffices to reconstruct the full correlation function. (Notice, however, that the identity (7.32) is heavily "non-local"; i.e. we need to know the spectral function for all ω, including $\omega \to \pm\infty$, to reconstruct the correlation function at a given value of z.)

Considering the second equality in Eq. (7.33) and setting $z = \omega^+$, one obtains

$$C^+(\omega) = -\frac{1}{2\pi i} \int d\omega' \frac{C^+(\omega')}{\omega - \omega' + i0}.$$

Representing the denominator under the integral in terms of the Dirac identity (7.19), and collecting terms, the identity assumes the form

$$C^+(\omega) = \frac{1}{\pi i} \int d\omega' C^+(\omega') \mathrm{P} \frac{1}{\omega' - \omega}.$$

It is customary to consider real and imaginary parts of this relation separately, whence one arrives at the celebrated **Kramers–Kronig** or **dispersion relations**:

$$\boxed{\begin{aligned} \mathrm{Re}\, C^+(\omega) &= \frac{1}{\pi} \int d\omega'\ \mathrm{Im}\, C^+(\omega') \mathrm{P} \frac{1}{\omega' - \omega}, \\ \mathrm{Im}\, C^+(\omega) &= -\frac{1}{\pi} \int d\omega'\ \mathrm{Re}\, C^+(\omega') \mathrm{P} \frac{1}{\omega' - \omega}. \end{aligned}} \tag{7.34}$$

INFO To appreciate the **physical content of the Kramers–Kronig relations**, let us anticipate our discussion below and note that the scattering amplitude of particles incident on a medium at

energy ω is proportional to the retarded Green function $C^+(\omega)$. Taking as an example the scattering of electromagnetic radiation from a solid state sample, the Kramers–Kronig relations then tell us that the real part of the scattering amplitude – the index of refraction – is proportional to the imaginary part – the index of absorption – integrated over all energies, i.e. the Kramers–Kronig relations establish a connection between the two seemingly unrelated physical mechanisms of absorption and refraction. Other areas of application of dispersion relations include high energy physics, optics (both classical and quantum), and many more.

In the next section we discuss some concrete applications of the Kramers–Kronig relations in many-body physics.

The dielectric function: a case study

Equation (7.34) represents a "master identity" from which numerous other exact relations can be obtained. As an example of the derivation and usefulness of these identities, let us consider the frequency- and momentum-dependent **dielectric function** $\epsilon(\mathbf{q},\omega)$, i.e. *the* object describing the polarization properties of a medium in the presence of an electromagnetic field. In Section 5.2 we explored the dielectric function within the framework of the RPA approximation. However, as we are about to discuss exact relations, we should now be a bit more ambitious than that, i.e. we should base our discussion on a more generally valid representation of the dielectric function. Indeed, it is a straightforward exercise in linear response to show that (see Problem 7.6.2)

$$\epsilon(\mathbf{q},\omega) = \left[1 - \frac{V_0(\mathbf{q})}{L^d}\int d\tau\, e^{i\omega_m\tau}\langle\hat{n}(\mathbf{q},\tau)\hat{n}(-\mathbf{q},0)\rangle_{\mathrm{c}}\Big|_{i\omega_m\to\omega^+}\right]^{-1}, \tag{7.35}$$

where $V_0(\mathbf{q}) = 4\pi e^2/q^2$ is the bare Coulomb potential, $\langle\hat{n}\hat{n}\rangle_{\mathrm{c}}$ denotes the connected thermal average of two density operators $\hat{n}(\mathbf{q},\tau) = c^\dagger_{\mathbf{q}}(\tau)c_{\mathbf{q}}(\tau)$, and $i\omega_m \to \omega^+$ indicates symbolically the analytical continuation to real frequencies. Heuristically, Eq. (7.35) can be understood by noting that $1/\epsilon = V_{\mathrm{eff}}/V_0$ measures the ratio between the effective potential felt by a test charge in a medium and the vacuum potential. The difference between these two quantities is due to the polarizability of the medium which, in turn, is a measure of its inclination to build up charge distortions $\delta\langle\hat{n}\rangle$ in response to the action of the potential operator $\sim \int dV_0\hat{n}$. In linear response theory,[19] $\delta\langle\hat{n}\rangle$ is given by the kernel $\int d\langle\hat{n}\hat{n}\rangle V_0$, i.e. the second term in Eq. (7.35).

We thus observe that the (inverse of the) dielectric function is determined by the retarded correlation function $C^+(\mathbf{q},\omega)$ with $\hat{X}_1 = \hat{X}_2 = \hat{n}$. (For obvious reasons, this function is called the retarded **density–density response function**. It appears as an important building block in many areas of many-body physics.) Building on the relation

$$\epsilon(\mathbf{q},\omega)^{-1} = 1 - \frac{V_0(\mathbf{q})}{L^d}C^+(\mathbf{q},\omega), \tag{7.36}$$

[19] The linear response approximation is quite appropriate here because the standard definition of the dielectric function $\epsilon = \lim_{V_0\to 0}(V_0/V_{\mathrm{eff}})$ implies an infinitesimally weak external perturbation.

we next show how analyticity arguments and certain limit relations can be employed to derive strong test criteria for the dielectric functions. We first apply the Kramers–Kronig relation to $\epsilon^{-1} - 1 \propto C^+$ to obtain

$$\mathrm{Re}\,\epsilon(\mathbf{q},\omega)^{-1} - 1 = \frac{1}{\pi}\int_{-\infty}^{\infty} d\omega'\,\mathrm{Im}\,\epsilon\,(\mathbf{q},\omega')^{-1}\frac{1}{\omega'-\omega}.$$

Using the fact that $\mathrm{Im}\,\epsilon(\mathbf{q},\omega')^{-1} = -\mathrm{Im}\,\epsilon\,(-\mathbf{q},-\omega')^{-1} = -\mathrm{Im}\,\epsilon\,(\mathbf{q},-\omega')^{-1}$, where the first identity holds for the Fourier transform of arbitrary real-valued functions and the second follows from real space symmetry, the integral can be brought to the compact form

$$\mathrm{Re}\,\epsilon(\mathbf{q},\omega)^{-1} = 1 + \frac{2}{\pi}\int_{0}^{\infty} d\omega'\,\mathrm{Im}\,\epsilon(\mathbf{q},\omega')^{-1}\frac{\omega'}{\omega'^2-\omega^2}. \tag{7.37}$$

We next consider this relation for the special case $\omega = 0$ and $|\mathbf{q}| \to 0$. The probing of this limit is motivated by the fact that the behavior of the static dielectric function $\epsilon(\mathbf{q},\omega=0)$ is significantly more simple to analyze than that of the generic function $\epsilon(\mathbf{q},\omega)$. The reason is, of course, that a static external field does not prompt any dynamical response of the system. Indeed, one can show on general grounds (see the Info block below) that, in the static limit,

$$\epsilon(\mathbf{q},0)^{-1} = (1 + 4\pi\nu|\mathbf{q}|^{-2})^{-1} \overset{|\mathbf{q}|\to 0}{\longrightarrow} 0. \tag{7.38}$$

Substitution of this result into Eq. (7.37) then leads to the identity

$$\boxed{\lim_{\mathbf{q}\to 0}\int_0^{\infty} d\omega\,\frac{\mathrm{Im}\,\epsilon\,(\mathbf{q},\omega)^{-1}}{\omega} = -\frac{\pi}{2}.} \tag{7.39}$$

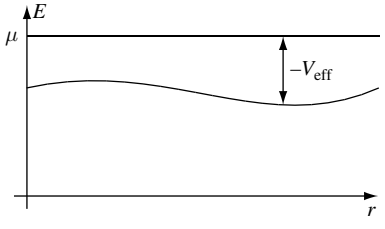

Equation (7.39) is a typical example of a **sum rule**. For the derivation of a few more sum rules to be obeyed by the dielectric function see, e.g., the text by Mahan.[20]

INFO To understand the behavior of the **dielectric function in the static limit**, imagine a system of charged particles subject to a potential $V_0(\mathbf{r})$. Since V_0 is static, it does not drive the system out of equilibrium. In particular, all fermionic quasi-particle states[21] are filled up to a uniform chemical potential μ. This, however, necessitates a redistribution of charge. The reason is that the potential shifts the energies ϵ_a of quasi-particle states $|a\rangle$ according to the relation $\epsilon_a \to \epsilon_a - V_{\mathrm{eff}}(\mathbf{r})$, where V_{eff} is the effective potential seen by the particles. (In order for this relation to make sense, the typical spatial extent of a quasi-particle must, of course, be smaller than the modulation range of $V(\mathbf{r})$.) For low temperatures, states will be filled up to an energy $\mu - V_{\mathrm{eff}}(\mathbf{r})$ (see the figure). We can make this argument quantitative by introducing a distribution function $n_{\mathrm{eff}}(\epsilon,\mathbf{r}) \equiv n_{\mathrm{F}}(\epsilon - V_{\mathrm{eff}}(\mathbf{r}))$ locally controlling the occupation of quasi-particle states. In

[20] G. Mahan, *Many Particle Physics* (Plenum Press, 1981).
[21] We assume that we are dealing with a Fermi liquid, i.e. that we can think of the constituents of the system as fermionic quasi-particles, in the spirit of Landau's theory.

a linear approximation, the induced charge density screening the external potential is then given by

$$\begin{aligned}\rho_{\rm ind}(\mathbf{r}) &= -\frac{1}{L^d}\sum_a (n_{\rm eff}(\epsilon_a,\mathbf{r}) - n_{\rm F}(\epsilon_a)) = -\nu\int_{-\infty}^{\infty} d\epsilon (n_{\rm eff}(\epsilon,\mathbf{r}) - n_{\rm F}(\epsilon)) \\ &= -\nu\int_{-\infty}^{\infty} d\epsilon (n_{\rm F}(\epsilon - V_{\rm eff}(\mathbf{r})) - n_{\rm F}(\epsilon)) \\ &\approx \nu\int_{-\infty}^{\infty} d\epsilon\, \partial\, n_{\rm F}(\epsilon) V_{\rm eff}(\mathbf{r}) = -\nu V_{\rm eff}(\mathbf{r}).\end{aligned}$$

To compute the difference between the external and the effective potential, respectively, we assume that the former had been generated through some charge density ρ_0: $-\partial^2 V_0 = 4\pi\rho_0$, or $V_0(\mathbf{q}) = 4\pi\mathbf{q}^{-2}\rho_0(\mathbf{q})$. In contrast, the full potential $V_{\rm eff}$ will be generated by a charge distribution $\rho_{\rm eff}$ comprising the external charge and the screening charge, $V_{\rm eff}(\mathbf{q}) = 4\pi\mathbf{q}^{-2}(\rho_0(\mathbf{q}) + \rho_{\rm ind}(\mathbf{q})) = V_0(\mathbf{q}) - 4\pi\nu\mathbf{q}^{-2}V_{\rm eff}(\mathbf{q})$. We thus find that

$$\epsilon(\mathbf{q},0) = \frac{V_0(\mathbf{q})}{V_{\rm eff}(\mathbf{q})} = 1 + 4\pi\nu|\mathbf{q}|^{-2},$$

as stated above. Indeed, we had obtained this result, generally known as **Thomas–Fermi screening**, long before within the more microscopic framework of the RPA. In contrast, the merit of the present argument is that it is not based on any specific approximation scheme.[22]

While Eq. (7.39) was for the specific example of the dielectric function, the general construction recipe has much wider applicability: (a) a quantity of physical interest (here, the dielectric function) is represented in terms of a retarded response function which then (b) is substituted into a Kramers–Kronig-type relation. This produces a frequency non-local connection between the response function at a given frequency to an integral ("sum") over all other frequencies. (c) This integral is evaluated for a reference frequency for which our reference quantity is generally known (here, $\omega \to 0$). This produces an integral relation which should hold under very general conditions. As mentioned at the beginning of this section, sum rules play an important role as test criteria for physical approximation schemes.

Experimental access to the spectral density function

Earlier, we have seen that the spectral density function contains highly resolved microscopic information about a many-body system. But how do we access this information other than by theoretical model calculation? Interestingly, it turns out that the spectral function is not only central to theoretical analysis, but also directly related to a key experimental observable, the **inelastic scattering cross-section.** To appreciate this connection, consider again the prototypical setup of a scattering experiment shown in Fig. 7.1. The frequency- and angle-resolved scattering cross-section is a measure of the rate of transitions from the incoming state $(\epsilon, \mathbf{k})$ into an outgoing state $(\epsilon', \mathbf{k}')$. To give the problem a quantum mechanical formulation, we first note that the full Hilbert space $\mathcal{H}$ of the system is the direct product of the Fock space, $\mathcal{F}$, of the target system and the single-particle space $\mathcal{H}_1$ of the incoming particle species, $\mathcal{H} = \mathcal{F} \otimes \mathcal{H}_1$. We assume that the interaction

[22] However, the argument is a bit phenomenological and does rely on the Fermi liquid doctrine.

between the incoming particle and the constituent particles of the system is governed by an interaction Hamiltonian whose conventional (first quantized) real space representation reads $\hat{H}_{\rm int} = \sum_i V(\hat{\mathbf{r}}_i - \hat{\mathbf{r}})$. Here, $\hat{\mathbf{r}}_i$ are the positions of the particles of the system and $\hat{\mathbf{r}}$ is the position of the incoming particle. For simplicity we assume that the interaction is point-like, i.e. $V(\hat{\mathbf{r}}-\hat{\mathbf{r}}') = C\delta(\hat{\mathbf{r}}-\hat{\mathbf{r}}')$, where C is some constant. (The generalization to more general interaction potentials is straightforward.) The second quantized representation of the interaction operator then reads

$$\hat{H}_{\rm int} = C \int d^d r \; \delta(\hat{\mathbf{r}} - \mathbf{r}) c^\dagger(\mathbf{r}) c(\mathbf{r}), \tag{7.40}$$

where $\hat{\mathbf{r}}$ retains its significance as a single-particle operator acting in the space $\mathcal{H}_1$. An alternative and, for all that follows, more convenient representation is given by

$$\hat{H}_{\rm int} = C \int d^d r \int \frac{d^d q}{(2\pi)^d} e^{i\mathbf{q}(\hat{\mathbf{r}}-\mathbf{r})} c^\dagger(\mathbf{r}) c(\mathbf{r}) = C \int \frac{d^d q}{(2\pi)^d} e^{i\mathbf{q}\cdot\hat{\mathbf{r}}} \hat{\rho}(\mathbf{q}),$$

where we have made use of a plane wave representation of the δ-function, $\delta(\mathbf{r}) = \int (d^d q/(2\pi)^d) \exp(i\mathbf{q}\cdot\mathbf{r})$, and $\hat{\rho}(\mathbf{q}) \equiv \int d\mathbf{r}\, e^{-i\mathbf{q}\cdot\mathbf{r}} c^\dagger(\mathbf{r}) c(\mathbf{r})$ describes density modulations in the target system of characteristic momentum $\mathbf{q}$. Assuming, for simplicity, that the sample is kept at zero temperature (i.e. it is in its ground state), a scattering process of first order in the interaction Hamiltonian is described by the transition amplitude $\mathcal{A}(\mathbf{q}) = \langle \beta, \mathbf{k}-\mathbf{q}|\hat{H}_{\rm int}|0,\mathbf{k}\rangle$, where $|0\rangle$ represents the ground state of the system, and $|\beta\rangle$ may be any exact eigenstate of the target system.[23] Substitution of the representation of the interaction Hamiltonian above brings the transition amplitude to the form

$$\mathcal{A}(\mathbf{q}) = \langle \beta, \mathbf{k}-\mathbf{q}|\hat{H}_{\rm int}|0,\mathbf{k}\rangle \propto \langle \beta|\hat{\rho}_{\mathbf{q}}|0\rangle. \tag{7.41}$$

A first conclusion to be drawn from Eq. (7.41) is that the scattering amplitude probes density modulations in the bulk system. According to **Fermi's Golden Rule**, the transition rate associated with the scattering amplitude $\mathcal{A}(\mathbf{q})$ is given by

$$\mathcal{P}(q) = 2\pi \sum_\beta |\langle \beta|\hat{\rho}(\mathbf{q})|0\rangle|^2 \delta(\omega - \mathrm{fl}_{\beta 0}), \tag{7.42}$$

where $\mathrm{fl}_{\beta 0} = E_\beta - E_0 > 0$ is the excitation energy of $|\beta\rangle$ above the ground state and the δ-function enforces energy conservation. The summation over β reflects the fact that only the beam of scattered particles is observed while the final state of the target remains unspecified.

[23] Using the nomenclature of Fig. 7.1, one might identify $|0\rangle$ with a ground state of zero collective momentum $\mathbf{K} = 0$ and $|\beta\rangle = |\mathbf{K}' = \mathbf{q}\rangle$ with a state that has absorbed the momentum of the scattered particle. The present discussion is more general in that it does not assume that the target eigenstates carry definite momentum.

It is instructive to reformulate Eq. (7.42) in a number of different ways. Representing the δ-function as a time integral, $2\pi\delta(\omega) = \int dt \exp(+i\omega t)$, one obtains

$$\begin{aligned}
\mathcal{P}(q) &= \int dt \sum_\beta |\langle\beta|\hat\rho(\mathbf{q})|0\rangle|^2 e^{+it(\omega - \ _\beta)} \\
&= \int dt\, e^{+i\omega t} \sum_\beta \langle 0|e^{i(\hat H - \mu\hat N)t}\hat\rho(-\mathbf{q})e^{-i(\hat H-\mu\hat N)t}|\beta\rangle\langle\beta|\hat\rho(\mathbf{q})|0\rangle \\
&= \int dt\, e^{+i\omega t}\langle 0|e^{i(\hat H-\hat\mu N)t}\hat\rho(-\mathbf{q})e^{-i(\hat H-\mu\hat N)t}\hat\rho(\mathbf{q})|0\rangle = \int dt e^{+i\omega t}\langle 0|\hat\rho(-\mathbf{q},t)\hat\rho(\mathbf{q},0)|0\rangle.
\end{aligned}$$

This clearly illustrates the connection between the observable scattering rate and the microscopic characteristics of the system, i.e. the rate $\mathcal{P}(\mathbf{q},\omega)$ is a measure of the dynamical propagation of density modulations of wavelength $\mathbf{q}$ at time scales $\sim\omega^{-1}$.

To establish the connection to the previously developed apparatus of response functions, we introduce the abbreviation $\hat\rho(\mathbf{q})_{\alpha\beta} = \langle\alpha|\hat\rho(\mathbf{q})|\beta\rangle$ and reformulate Eq. (7.42) as

$$\begin{aligned}
\mathcal{P}(q) &= -2\ \mathrm{Im}\sum_\beta \frac{\rho(\mathbf{q})_{\beta 0}\rho(-\mathbf{q})_{0\beta}}{\omega^+ + \mathrm{fl}_{0\beta}} = -2\lim_{T\to 0}\ \mathrm{Im}\mathcal{Z}^{-1}\sum_{\alpha\beta}\frac{\rho(\mathbf{q})_{\beta\alpha}\rho(-\mathbf{q})_{\alpha\beta}e^{-\beta\ _\alpha}}{\omega^+ + \mathrm{fl}_{\alpha\beta}} \\
&= -2\lim_{T\to 0}\ \mathrm{Im}\mathcal{Z}^{-1}\sum_{\alpha\beta}\frac{\rho(\mathbf{q})_{\beta\alpha}\rho(-\mathbf{q})_{\alpha\beta}(e^{-\beta\ _\alpha} - e^{-\beta\ _\beta})}{\omega^+ + \mathrm{fl}_{\alpha\beta}} \\
&= -2\lim_{T\to 0}\ \mathrm{Im}C^+(\omega) = A(\mathbf{q},\omega),
\end{aligned}$$

where $A(\mathbf{q},\omega)$ denotes the spectral density function evaluated for the density operators $\hat X_1 = \hat\rho(\mathbf{q})$, $\hat X_2 = \hat\rho(-\mathbf{q})$. Here, we have made use of the fact that, for $T\to 0$, the Boltzmann weight $\exp(-\beta\mathrm{fl}_\alpha)$ projects onto the ground state. Similarly, for $\omega > 0$, the contribution $\exp(-\beta\mathrm{fl}_\beta)$ vanishes (exercise: why?).

We thus note that information about the scattering cross-sections is also carried by a retarded real time response function. More specifically:

> The inelastic scattering cross-section for momentum transfer $\mathbf{q}$ and energy exchange ω is a direct probe of the spectral density function $A(\mathbf{q},\omega)$.

Although the derivation above did not exactly follow the linear response scheme, it had the same weak coupling perturbative flavor. (The golden rule is a first-order perturbative approximation!) While we derived our formula for the particular case of a short-range density coupling, it is clear that a more general beam–target coupling mechanism would lead to an expression of the same architecture, i.e. a suitably defined retarded response function.

7.4 Electromagnetic linear response

In the previous two sections we have assembled everything needed to compute the response of physical systems to moderately weak perturbations. We have learned how to linearize the response in the strength of the generalized force and to extract real time dynamical

information from imaginary time data. In this section we will illustrate the functioning of this formalism on undoubtedly its most important application, the response to a general electromagnetic field.

The general setup of the problem is easily formulated: suppose a system of charged particles has been subjected to an electromagnetic signal represented through a scalar potential $\phi(\mathbf{r},t)$ and/or a vector potential $\mathbf{A}(\mathbf{r},t)$. To simplify the notation, let us represent the perturbation through a $(1+d)$-dimensional[24] potential $A^\mu(x)=(\phi(x),\mathbf{A}(x))$, where $x\equiv(t,\mathbf{r})$ is a $(1+d)$-dimensional space-time argument vector. The system will respond to this perturbation by a redistribution of charge, $\rho(x)\equiv\langle\hat{\rho}(x)\rangle$, and/or the onset of current flow $\mathbf{j}(x)\equiv\langle\hat{\mathbf{j}}(x)\rangle$. Confining charge and vectorial current into a $(1+d)$-dimensional generalized current vector $j^\mu=(\rho,\mathbf{j})$, our task is to identify the linear functional $j=K[A]+\mathcal{O}(A^2)$ relating the current to its driving potential. Written more explicitly,

$$j_\mu(x)=\int_{t'<t}dx'\;K_{\mu\nu}(x,x')A^\nu(x'), \tag{7.43}$$

where the condition $t'<t$ indicates that the response is retarded. To compute the elements of the response tensor, we proceed according to the general recipe constructed in the preceding sections: we first employ the general formalism to derive the imaginary-time response $K(\mathbf{r},\mathbf{r}';i\omega_n)$, and then continue to real frequencies, $i\omega_n\to\omega+i0$.

However, before formulating this programme in detail, let us derive two fundamental constraints to be fulfilled by the kernel K. Firstly, a gauge potential $A_\mu=\partial_\mu f$ (f is a function) cannot drive a physical current. Substituting this condition into Eq. (7.43), we find

$$0\stackrel{!}{=}\int_{t'<t}dx'\;K_{\mu\nu}(x,x')\partial^\nu f(x')=-\int_{t'<t}dx'\;(\partial^\nu_{x'}K_{\mu\nu}(x,x'))f(x').$$

Since f is arbitrary one may conclude that $0=K_{\mu\nu}\;\overleftarrow{\partial}^\nu$ where the arrow indicates that the derivative acts from the right. Secondly, current conservation demands $\partial^\mu j_\mu=0$ or, transcribed to Eq. (7.43), $0\stackrel{!}{=}\int_{t'<t}dx'\,\partial^\mu_x K_{\mu\nu}(x,x')A^\nu(x')$. Due to the arbitrariness of A_μ, this condition can only be generally valid if $\overrightarrow{\partial^\mu}\;K_{\mu\nu}=0$. Summarizing,

> Gauge invariance and particle number conservation demand the identity
> $$\overrightarrow{\partial^\mu}\;K_{\mu\nu}=K_{\mu\nu}\;\overleftarrow{\partial}^\nu=0.$$

We next turn to the derivation of the linear response kernel. Our starting point is an observation made already in Chapter 1 (and several times thereafter), namely the fact that

[24] To not unnecessarily exclude important applications of the formalism to effectively two- or one-dimensional problems, the dimensionality of space is left unspecified.

the coupling of matter to the classical electromagnetic field is described by the relation[25]

$$j_\mu = \frac{\delta S_c[A]}{\delta A_\mu}, \tag{7.44}$$

where the subscript "c" indicates that only the part of the action that couples matter to the field (but not the background action of the field) is differentiated. In this expression we are back to a Euclidean metric $v_\mu w_\mu \equiv v_0 w_0 + \mathbf{v}\cdot\mathbf{w}$ (on account of the definition, $j_0 \equiv i\rho$, $A_0 \equiv i\phi$ of imaginary time current and vector potential, respectively). The additional i appearing in this convention mirrors the i of the temporal component of the imaginary-time vector $(t, \mathbf{r}) \to (-i\tau, \mathbf{r})$. Notice, however, that we are merely changing conventions, i.e. both the imaginary- and the real-time action contain the invariant contribution $-\rho\phi + \mathbf{j}\cdot\mathbf{A}$. To keep the notation simple, we will not indicate the difference between imaginary-time and real-time vectors explicitly; the appropriate convention is determined by the context in which we are operating.

This appealingly simple structure (7.44) is all we need to write down a general expression for the linear response kernel. Comparison with Section 7.2.1 shows that $F = F' = A_\mu$, i.e. the generalized force, F', and the auxiliary "force" F used to generate the expectation value of $\hat{j}$ by differentiation are both given by A_μ. Equation (7.6) then tells us that

$$\boxed{K_{\mu\nu}(x,x') = \mathcal{Z}^{-1}\,\frac{\delta^2}{\delta A_\mu(x)\;\delta A_\nu(x')}\mathcal{Z}[A]\bigg|_{A=0}}, \tag{7.45}$$

which is one of the most important relations of microscopic response theory. Notice that, owing to the interchangeability of the two derivatives, $K_{\mu\nu}(x,x') = K_{\nu\mu}(x',x)$. This symmetry in turn implies that – an observation repeatedly made before – gauge invariance, $K_{\mu\nu}\,\partial_\nu = 0$, and particle number conservation, $\overrightarrow{\partial_\mu}\,K_{\mu\nu} = 0$, represent different sides of the same coin. Equation (7.45) is a very general, but also very formal, result. To give it some meaning, it is instructive to evaluate the two derivatives for a few specific functionals $\mathcal{Z}[A]$, as described in the next section.

Electromagnetic response of the microscopic theory

As a particularly important example, let us consider the microscopic action of a Fermi or Bose system in the presence of an electromagnetic field. Ignoring the coupling of the field to the spin degrees of freedom,

$$S[\bar\psi,\psi,A] = \int dx\;\bar\psi_\sigma\left(\partial_\tau + \phi + \frac{1}{2m}(-i\nabla - \mathbf{A})^2 - \mu + V_0\right)\psi_\sigma + S_{\rm int}[\bar\psi,\psi],$$

[25] You may ask yourself why we use the relation (a) $j_\mu = \delta_{A_\mu} S_c[A]$ instead of a direct representation of linear coupling (b) $S_c[A] = \int j_\mu A_\mu + \ldots$ The reason is that in some prominent cases – the microscopic theory of charged particles discussed in Section 7.4 being the most prominent example – the current $j_\mu = j_\mu[A]$ depends on A by itself. This means that A will enter the action *non-linearly* (viz. by a "diamagnetic term" $\sim A^2$) and this in turn implies that (a) ceases to be a faithful representation of the more general (b). However, our theory of linear response is based on derivative operations such as (b) anyway and the above complication does not pose a significant problem.

where V_0 denotes a (field-independent) potential. With $A_0 = i\phi$, $A_i = (\mathbf{A})_i$, and

$$\hat{j}_0^A = i\hat{\rho} = i\bar{\psi}_\sigma\psi_\sigma, \quad \hat{j}_i^A = (\hat{\mathbf{j}})_i = \frac{1}{2m}\bar{\psi}_\sigma(-i\,\partial_i + A_i)\psi_\sigma, \tag{7.46}$$

where $f\ \partial_i\ g \equiv f\partial_i g - (\partial_i f)g$, we have $\hat{j}_\mu^A = \frac{\delta}{\delta A_\mu}S[A]$ and the notation j^A hints at the important fact that the current itself depends on the vector potential. Application of Eq. (7.45) then gives

$$\begin{aligned} K_{\mu\nu}(x,x') &= \mathcal{Z}^{-1}\,\frac{\delta^2}{\delta A_\mu(x)\;\delta A_\nu(x')}\bigg|_{A=0}\int D(\bar{\psi},\psi)\;e^{-S[\bar{\psi},\psi,A]} \\ &= -\mathcal{Z}^{-1}\,\frac{\delta}{\delta A_\nu(x')}\bigg|_{A=0}\int D(\bar{\psi},\psi)\,\hat{j}_\mu^A(x)\,e^{-S[\bar{\psi},\psi,A]} \\ &= \langle -\delta(x-x')\delta_{\mu\nu}\,\partial_{A_\mu(x)}\hat{j}_\mu^A(x) + \hat{j}_\mu^A(x)\hat{j}_\nu^A(x')\rangle\Big|_{A=0}, \end{aligned}$$

where the angular brackets denote functional averaging. Setting $A = 0$, one obtains

$$\boxed{K_{\mu\nu}(x,x') = -\frac{\langle\hat{\rho}(x)\rangle}{m}\delta(x-x')\delta_{\mu\nu}(1-\delta_{\mu 0}) + \langle\hat{j}_\mu^p(x)\hat{j}_\nu^p(x')\rangle.} \tag{7.47}$$

The first term contributing to the response kernel is known as the **diamagnetic term**. Indeed, tracing back through the derivation, one discovers that this term originates from the diamagnetic contribution $\sim A^2$ to the Hamiltonian. Conversely, $\hat{j}^p \equiv \hat{j}\big|_{A=0}$ is called the paramagnetic contribution to the current operator. The functional expectation value $\sim \langle\hat{j}^p\hat{j}^p\rangle$ defines the **paramagnetic term**.

Notwithstanding its unappealing structure, Eq. (7.47) represents a strong result which encompasses virtually all aspects of electromagnetic linear response.[26] For example, the diagonal vectorial components $K_{ii}, i = 1, 2, \ldots, d$, of the response tensor describe the **longitudinal conductivity** of the system (see Section 7.4.1). In cases where a magnetic field is present, the off-diagonal components $K_{i\neq j}$ measure the **Hall conductivity**. The temporal components K_{00} describe the **density response** of the system, a feature that is of importance, for example, in the analysis of scattering data, etc.

Electromagnetic response of e ective theories

In cases where we are operating on a level beyond the microscopic description, i.e. within the framework of an effective low-energy theory, the structure of the response tensor may differ from Eq. (7.47). To identify the "effective" response tensor, we need to carry out a canonical two-step programme: (i) identify the coupling of the electromagnetic potential to the relevant degrees of freedom (in cases where one has not kept track of the field dependence from the very beginning, it usually suffices to minimally couple the field, i.e. to introduce the components A_μ so as to make the action gauge invariant); (ii) perform the two-fold derivative Eq. (7.45).

[26] Except for spin-related phenomena.

We illustrate the procedure on a familiar example, the **phase action of the BCS superconductor**,

$$S[\theta] = \int dx \, \left[\nu(\partial_\tau\theta)^2 + \frac{n_s}{2m}(\nabla\theta)^2\right]. \tag{7.48}$$

Under a gauge transformation induced by some function $f(x)$, $\partial_\mu\theta \to \partial_\mu\theta + \partial_\mu f$, i.e. the gauge invariant extension of the action reads (cf. Eq. (6.34)) $S[\theta, A] = \int dx \, [\nu(\partial_\tau\theta - \phi)^2 + \frac{n_s}{2m}(\nabla\theta - \mathbf{A})^2]$. Differentiating this result with respect to the components $\mathbf{A}_i$, one obtains

$$K_{ij}(x, x') = -\frac{n_s}{m}\left[\delta_{ij} - \frac{n_s}{m}\langle\partial_i\theta(x)\partial_j\theta(x')\rangle\right]. \tag{7.49}$$

EXERCISE Evaluate the correlator $\langle\partial_i\theta\,\partial_j\theta\rangle$ to show that the conductivity $\sigma_{ii}(\mathbf{q} = 0, \omega)$ diverges in the limit $\omega \to 0$. The **divergence of the conductivity** can be traced back to the fact that, in a superconductor, there is no cancellation between diamagnetic and paramagnetic responses. Compute the response of the system to a static magnetic field. Show that, in the London gauge $\cdot\,\mathbf{A} = 0$, current and vector potential are proportional to each other, $\mathbf{j} \propto \mathbf{A}$. Recall (cf. Section 6.4) that this result, in combination with the Maxwell equation $\times\,\mathbf{H} = 4\pi\mathbf{j}$, implies the **Meissner e ect**.

7.4.1 Longitudinal conductivity of the disordered electron gas

Equations (7.47) and (7.49) exemplify the structure of the response tensor after the master formula (7.45) has been applied. However, to obtain a concrete result for the conductivity, say, one must evaluate the two-($\langle\hat{\rho}\rangle$) or four-($\langle\hat{j}\hat{j}\rangle$) point correlation functions appearing in these expressions. Of course, the details of this last step of the program depend sensitively on the microscopic structure of the theory under consideration, i.e. no universally applicable computational recipe can be formulated. Notwithstanding these differences in details, a number of large-scale structural elements are recurrent in the mathematical analysis of the current–current correlation functions of microscopic response theory. To illustrate these common structures, let us consider an example that is of considerable importance in its own right, namely the **longitudinal AC conductivity of the electron gas**.

The AC conductivity is defined through the relation

$$\mathbf{j}(\omega) = \sigma(\omega)\mathbf{E}(\omega), \tag{7.50}$$

i.e. as the coefficient relating the current density to a homogeneous external field oscillating with frequency ω. In the absence of symmetry-breaking perturbations such as a strong magnetic field or system-intrinsic anisotropies, the current flow will be in line with the field gradient. This justifies the scalar, rather than a more complex tensorial *ansatz* for the conductivity in Eq. (7.50) (For a more complex situation, see Problem 7.6.4.)

INFO Before entering the details of the linear response calculation, it is instructive to recapitulate how the conductivity can be obtained from common sense reasoning. To this end, let us look at the world from the persective of an individual conduction electron. In the presence of an electric field, the electron will be subject to two different forces: the force of the field, $-e\mathbf{E}$, and a dissipative friction force $-\frac{m}{\tau}\mathbf{r}$ inhibiting its free acceleration (deviating from our convention,

$e = 1$, we temporarily reintroduce the electron charge). The damping rate is essentially set by the scattering rate off static impurities, viz. $1/\tau$. To a first approximation, the dynamics of the electron is thus described by the equation of motion $m\ddot{\mathbf{r}} = -e\mathbf{E}(t) - \frac{m}{\tau}\mathbf{r}$ or, in Fourier representation, $-im\omega\mathbf{v}(\omega) = e\mathbf{E}(\omega) - \frac{m}{\tau}\mathbf{v}(\omega)$. Solving for $\mathbf{v}$ one finds that the current density $\mathbf{j} = -ne\mathbf{v}$ (n is the particle density) is given by $\mathbf{j}(\omega) = \sigma(\omega)\mathbf{E}(\omega)$ with

$$\boxed{\sigma(\omega) = \frac{ne^2}{m}\frac{1}{\frac{1}{\tau} - i\omega}.} \tag{7.51}$$

In the limit $\omega \gg \tau^{-1}$, $\sigma(\omega) \simeq i\frac{ne^2}{m}\omega^{-1}$, i.e. the electron current is determined by the ballistic motion of the electrons in the electric force field. Conversely, in the DC limit $\omega \to 0$, one obtains the Drude formula $\sigma = \frac{ne^2\tau}{m}$, i.e. the field drives a steady current density whose value is limited by the amount of momentum relaxation.

Below we compute the conductivity under the simplifying assumption that Coulomb or other types of many-body interaction are negligible.[27] By contrast, the discussion of the Info block above shows that any meaningful analysis of the conductivity must take account of the presence of static disorder; without disorder, the field would make the electrons freely accelerate, i.e. there would be no such thing as a steady current flow in metals. Thus, what we should have in mind when we think about the conductivity is $\langle\sigma\rangle_V$, the conductivity averaged over all realizations of a microscopic disorder potential.[28] To obtain the conductivity, we will explore the current flow in response to a vector potential $\mathbf{A}$, where $\partial_t\mathbf{A} = -\mathbf{E}$ generates the electric field. Anticipating that, after averaging over impurities, the system will be effectively translationally invariant, the analysis is most economically carried out in Fourier space, i.e. we compute the expectation value $\mathbf{j}(\mathbf{q} \to 0, \omega)$ in response to a potential $\mathbf{A}(\mathbf{q} \to 0, \omega)$, where the limit $\mathbf{q} \to 0$ indicates that we are interested in a spatially homogeneous external field. Fourier transforming Eq. (7.47) in the difference of coordinates, $x - x'$ (cf. the remarks made in connection with Eq. (7.4)), one verifies that the appropriate response kernel is given by

$$K(q) = \frac{1}{L^d}\left(-\frac{1}{m}\langle\langle\hat{\rho}\rangle\rangle_V + \langle\langle\hat{j}^p_{i,q}\hat{j}^p_{i,-q}\rangle\rangle_V\right), \tag{7.52}$$

where the vectorial index i is arbitrary and the double brackets indicate the two-fold average over the quantum thermal distribution and the disorder potential. Also notice that the connection $\omega_m\mathbf{A}(q) = \mathbf{E}(q)$ implies

$$\sigma(\omega) = -\lim_{\mathbf{q}\to 0}\frac{1}{\omega_m}K(q)\bigg|_{i\omega_m\to\omega+i0}. \tag{7.53}$$

[27] Nonetheless, the calculation will still be fairly technical. If you find the Drude conductivity of the electron gas too elementary an observable to justify these efforts, please keep in mind that our prime motivation is methodological: technical operations very similar to those detailed here appear in practically every quantum response analysis.

[28] A good question to ask is whether the conductivity of any particular realization of a disordered metal will differ from the averaged conductivity, i.e. whether the conductivity is a "self-averaging" quantity. This leads one to the interesting problem of **conductance statistics**, a topic beyond the scope of the current text.

To process this expression, we substitute the Fourier transform of Eq. (7.46) (exercise),

$$\hat{\rho} = \sum_p \bar{\psi}_{\sigma,p}\psi_{\sigma,p}, \quad \hat{j}^p_{i,q} = \frac{1}{2m}\sum_p (2p+q)_i \bar{\psi}_{\sigma,p}\psi_{\sigma,p+q},$$

into (7.52) and apply Wick's theorem to compute the thermal expectation value. This leads to the expression

$$K(q) = -\frac{2T}{L^d}\sum_{n,\mathbf{p},\mathbf{p}'}\left(\frac{\delta_{\mathbf{p},\mathbf{p}'}}{m}\langle G_{n,\mathbf{p},\mathbf{p}}\rangle_V + \frac{(2p+q)_i(2p'+q)_i}{(2m)^2}\langle G_{n+m,\mathbf{p}+\mathbf{q},\mathbf{p}'+\mathbf{q}}G_{n,\mathbf{p},\mathbf{p}'}\rangle_V\right), \tag{7.54}$$

where the factor of two accounts for the spin summation (for simplicity we assume that the Hamiltonian is spin-independent), $G_{n,\mathbf{p},\mathbf{p}'} \equiv \langle \bar{\psi}_{n,\mathbf{p}}\psi_{n,\mathbf{p}'}\rangle$ is the thermal electron Green function for a particular realization of the disordered background, and the remaining bracket stands for the disorder average. (Notice that, before disorder averaging, the system lacks translational invariance, i.e. the single-particle Green function is not diagonal in momentum space.) A diagrammatic representation of the paramagnetic response kernel in terms of Green functions is shown in the upper part of the figure below, where the wavy lines denote the current operator and the dashed lines symbolically represent the scattering off the static impurity potential (cf. our discussion of the impurity scattering and Green functions in Section 6.5.)

To make further progress with this expression, we shall adopt an approximation that critical readers may find questionable: we will replace the average of the two-Green-function correlator by an impurity average of the individual Green functions, $\langle GG\rangle \to \langle G\rangle\langle G\rangle$.[29] In Section 6.5 it has been shown that these averaged Green functions are given by

$$\langle G_{n,\mathbf{p},\mathbf{p}'}\rangle = \delta_{\mathbf{p},\mathbf{p}'}G_p \equiv \frac{\delta_{\mathbf{p},\mathbf{p}'}}{i\omega_n - \xi_{\mathbf{p}} + \frac{i}{2\tau}\,\mathrm{sgn}\,\omega_n},$$

where τ defines the mean impurity scattering time. (Recall what has been said above about the meaning of the imaginary part of the Green function denominator as an effective inverse lifetime. In the present context, τ measures the time after which a particle with initial momentum $\mathbf{p}$ gets scattered into states of different momentum.) Substituting this result into Eq. (7.54), we obtain

$$K(q) = -\frac{2T}{L^d}\sum_p\left(\frac{1}{m}G_p + \frac{1}{(2m)^2}(2p+q)_i^2 G_{p+q}G_p\right). \tag{7.55}$$

[29] Readers who have navigated through the disorder section in Chapter 6 are invited to critically assess the validity of this approximation. The result of this analysis is that, for hard impurity scattering potentials, i.e. for impurity potentials $\langle \mathbf{p}|V|\mathbf{p}'\rangle$ = const. that scatter isotropically over the entire momentum shell, the approximation above becomes justifiable in the limit $\mathbf{q} \to 0$. To understand why, construct any diagram involving impurity lines connecting the two Green functions. You will notice that, in this case, the two fast momenta carried by the current operators are no longer locked to each other. The subsequent angular integration over these momentum vectors then leads to a vanishing of the diagram. The physical mechanism behind this vanishing is that, in a disordered medium, the velocity vector of an electron changes rapidly, i.e. a velocity–velocity (or current–current) correlation function is highly susceptible to large-angle impurity scattering.

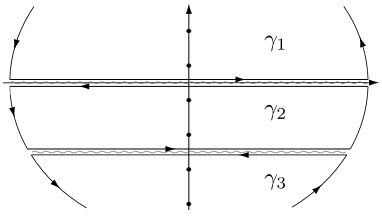

Looking at the structure of Eq. (7.54), one might be tempted to perform the frequency summation by one of the standard formulae. However, a moment's thought shows that this strategy will not work. The reason is that, in the present case, the extension of the Green function to the complex plane, $G_p = G_{\mathbf{p}}(z) = \left(z - \xi_{\mathbf{p}} + \frac{i}{2\tau}\,\mathrm{sgn\,Im}\,z\right)^{-1}$, has a cut along the real axis; this, in turn, means that the product $G_{\mathbf{p+q}}(z + i\omega_m)G_{\mathbf{p}}(z)$ has cuts at $\mathrm{Im}(z) = 0$ and $\mathrm{Im}(z + i\omega_m) = 0$ (see the figure). To circumvent this difficulty, we need to integrate over a contour that (a) encompasses all Matsubara frequencies and (b) avoids the cut lines. While there is no simple contour that does the job, a joint integration over the three contours $\gamma_{1,2,3}$ shown in the figure faithfully represents the Matsubara sum:

$$\sum_{\omega_n} G_p G_{p+q} = -\frac{\beta}{2\pi i} \oint\limits_{\gamma_1\ \gamma_2\ \gamma_3} dz\, n_{\mathrm{F}}(z) G_{\mathbf{p}}(z) G_{\mathbf{p+q}}(z + i\omega_m).$$

The three integrals contributing to the sum lead to very different results: as shown in the exercise below, the two integrals over the contours γ_1 and γ_3 cancel against the diamagnetic contribution to the response tensor, i.e. the first term in Eq. (7.55).

INFO To appreciate why the contribution from the contours γ_1 and γ_3 is unphysical, notice that, e.g.

$$\frac{\beta}{2\pi i} \oint\limits_{\gamma_1} dz\ n_{\mathrm{F}}(z) G_{\mathbf{p}}(z) G_{\mathbf{p+q}}(z + i\omega_m) = \frac{\beta}{2\pi i} \int_{-\infty}^{\infty} d\epsilon n_{\mathrm{F}}(\epsilon) G_{\mathbf{p}}(\epsilon + i0) G_{\mathbf{p+q}}(\epsilon + i\omega_m)$$
$$\overset{i\omega_m \to \omega + i0}{\longrightarrow} \frac{\beta}{2\pi i} \int_{-\infty}^{\infty} d\epsilon\ n_{\mathrm{F}}(\epsilon) G_{\mathbf{p}}(\epsilon + i0) G_{\mathbf{p+q}}(\epsilon + \omega + i0),$$

i.e. the integral extends over a product of two retarded single-particle Green functions. Now, remember that at the end of the day we want to compute the conductance, i.e. a quantity that resembles a transition probability (namely the probability for electrons propagating under the influence of an applied electric field). In quantum mechanics, probabilities $\sigma \sim GG^*$ appear as absolute squares of amplitudes, G. Indeed, we have seen before that the retarded Green function can be interpreted as a transition amplitude of quantum mechanical particles. We also saw that its complex conjugate, G^*, is an advanced Green function. Put differently, our admittedly very hand-waving argument indicates that the quantum dynamics of conduction should be described in terms of products of advanced and retarded Green functions. However, a product of two retarded (or two advanced) Green functions lacks an obvious physical interpretation. Indeed, these contributions cancel against the diamagnetic term.

We thus focus on the integral over γ_2:

$$\begin{aligned}
&\frac{\beta}{2\pi i}\oint_{\gamma_2} dz\; n_{\rm F}(z)G_{\mathbf{p}}(z)G_{\mathbf{p}+\mathbf{q}}(z+i\omega_m)\\
&\qquad=\frac{\beta}{2\pi i}\int_{-\infty}^{\infty} d\epsilon\; n_{\rm F}(\epsilon)\left[-G_{\mathbf{p}}(\epsilon-i0)G_{\mathbf{p}+\mathbf{q}}(\epsilon+i\omega_m)+G_{\mathbf{p}}(\epsilon-i\omega_m)G_{\mathbf{p}+\mathbf{q}}(\epsilon+i0)\right]\\
&\qquad\overset{i\omega_m\to\omega+i0}{\longrightarrow}\frac{\beta}{2\pi i}\int_{-\infty}^{\infty} d\epsilon\; n_{\rm F}(\epsilon)\left[-G_{\mathbf{p}}(\epsilon^-)G_{\mathbf{p}+\mathbf{q}}(\epsilon^++\omega)+G_{\mathbf{p}}(\epsilon^--\omega)G_{\mathbf{p}+\mathbf{q}}(\epsilon^+)\right]\\
&\qquad=-\frac{\beta}{2\pi i}\int_{-\infty}^{\infty} d\epsilon\;[n_{\rm F}(\epsilon)-n_{\rm F}(\epsilon+\omega)]G_{\mathbf{p}}(\epsilon^-)G_{\mathbf{p}+\mathbf{q}}(\epsilon^++\omega),
\end{aligned}$$

where, in the first equality, we have used the symmetry $n_{\rm F}(\epsilon+i\omega_m)=n_{\rm F}(\epsilon)$ of the distribution function under translation by bosonic frequencies. Substituting this result into Eq. (7.55) and (7.53), we arrive at the intermediate result

$$\boxed{\sigma(\omega)=\frac{1}{2\pi}\int_{-\infty}^{\infty} d\epsilon\;\frac{n_{\rm F}(\epsilon)-n_{\rm F}(\epsilon+\omega)}{\omega}\frac{2}{L^d m^2}\sum_{\mathbf{p}} p_i^2 G^-_{\mathbf{p}}(\epsilon)G^+_{\mathbf{p}}(\epsilon+\omega),} \tag{7.56}$$

where $G^{\pm}_{\mathbf{p}}(\epsilon)=\left(\epsilon-\xi_{\mathbf{p}}\pm\frac{i}{2\tau}\right)^{-1}$.

EXERCISE To complete our analysis, we need to understand better the **cancellation of the diamagnetic term** and, relatedly, the role played by the integration contours $\gamma_{1,3}$. We first write $K(q)=K(0)+[K(q)-K(0)]$ and observe that (i) the contribution of γ_2 discussed above sits solely in the finite q term, $K(q)-K(0)$ (the contour γ_2 collapses to zero at $q=0$), while (ii) the diamagnetic term and the contribution of the curves $\gamma_{1,3}$ are in $K(0)$. (Finite q-corrections to the contour integrals along $\gamma_{1,3}$ vanish due to the strong convergence of the integrands and the fact that all singularities lie on one side of the real axis: think about this point.) The cancellation of the diamagnetic term against the contribution of $\gamma_{1,3}$ thus amounts to showing $K(0)=0$.

Introducing the notation $G_{n,\ }\equiv G_p|_{\ \mathbf{p}=}$, show that

$$K(0)=-\frac{2T}{m}\sum_n\int d\epsilon\,\nu(\epsilon)\left(1+\frac{2\epsilon}{d}\partial\right)G_{n,\ },$$

where $\nu(\epsilon)=\frac{1}{L^d}\sum_{\mathbf{p}}\delta(\epsilon-\epsilon_{\mathbf{p}})$, and we used $\sum_{\mathbf{p}}F(\epsilon_{\mathbf{p}})p_i^2=\frac{2m}{d}\sum_{\mathbf{p}}F(\epsilon_{\mathbf{p}})\epsilon_{\mathbf{p}}$ by the isotropy of space. Integrating by parts (why do the contributions of the integration boundaries vanish?), and using the fact that $\nu(\epsilon)=\text{const.}\times\epsilon^{(d-2)/2}$, show that $K(0)=0$.

The analytical structure of this result actually reveals a number of important elements of the electron conduction process: an AC field of frequency ω creates electron–hole pairs of excitation energy ω. The phase volume accessible to these processes is measured by the ϵ-integral, weighted by the difference of two Fermi functions, i.e. Fermi statistics demands that the energy of the electron to be excited lies within a shell $[\mu-\omega,\mu]$ at the Fermi surface (see the figure below). The dynamics of the excited electron is described by a retarded Green function of energy $\epsilon+\omega$.

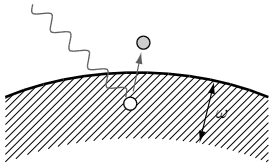

Conversely, the dynamics of the hole is described by the *advanced* Green function. Heuristically, this can be understood by noting that the advanced Green function describes the (fictitious) propagation of an electron backwards in time. However, an electron propagating in a chronologically reversed direction can be interpreted as a hole moving forward in time. Thus, the advanced electronic Green function effectively represents a descriptor of hole dynamics. That the product of two Green functions is weighted by two operators $\mathbf{p}_i/m$ reflects the fact that current transport essentially depends on the velocity of the electrons.

To perform the sum over $\mathbf{p}$ we note that, for a radially symmetric function $F(\xi_{\mathbf{p}})$,

$$\int d^d p\; p_i^2 F(\xi_{\mathbf{p}}) = \frac{1}{d}\int d^d p\; p^2 F(\xi_{\mathbf{p}}) = \frac{2m}{d}\int d\xi\; (\xi+\mu)\nu(\xi)F(\xi).$$

Identifying the function F with the product of our two Green functions, we obtain

$$\begin{aligned}\frac{2}{L^d}\sum_{\mathbf{p}} p_i^2 G_{\mathbf{p}}(\epsilon^-)G_{\mathbf{p}}(\epsilon^+ + \omega) &= \frac{4m}{(2\pi)^d d}\int_{-\mu}^{\infty} d\xi\; (\xi+\mu)\nu(\xi)G_\xi^-(\epsilon)G_\xi^+(\epsilon+\omega)\\ &\simeq \frac{4m\mu\nu}{(2\pi)^d d}\int_{-\infty}^{\infty} d\xi\; G_\xi^-(\epsilon)G_\xi^+(\epsilon+\omega) = \frac{1}{\frac{1}{\tau}-i\omega},\end{aligned}$$

where, in the third equality, we have used the fact that the Green functions are strongly peaked on scales $\tau^{-1} \ll \mu$ around $\xi = 0$ implying that, to a very good approximation, the ξ-integration can be extended to the entire real axis and the energy variation of the density of states $\nu(\xi)$ on the effective interval of integration is negligible. The last integral can be performed by elementary means or, more elegantly, by closing the ξ-integration contour in the upper or lower half plane and using the analytic structure of the Green functions. Substituting the result into our formula for $\sigma(\omega)$, and using the fact that $\int d\epsilon\; (n_{\rm F}(\epsilon) - n_{\rm F}(\epsilon+\omega))\omega^{-1} \simeq 1$, we arrive at the final result Eq. (7.51).

At this point it is rewarding to pause for a moment to look back at a number of large-scale structures of the analysis:

- ▷ On the microscopic level, the two-point function $\langle \hat{j}\hat{j}\rangle$ of current operators is represented in terms of a four-point function $\sim \langle \bar{\psi}\psi\bar{\psi}\psi\rangle$ of field operators. A moment's thought shows that **four-point correlation functions** generically appear as microscopic descriptors of the response functions of quantum single-particle operators (simply because, in second quantization, a single-particle operator maps onto a bilinear of field operators) and, therefore, of the vast majority of response functions.
- ▷ This observation implies a **hierarchy of correlation functions**. For example, in our non-interacting example, the retarded response correlation function was described in terms of a product of an advanced and a retarded microscopic single-particle correlation function.[30] This almost trivial observation is of some importance because it entails

[30] For interacting problems, the response functions no longer neatly split into a product of two single-particle Green functions. Instead, the four field operators describing the response functions can be connected by an arbitrarily complicated network of interaction vertices. However, ultimately, the propagators connecting this network are again the single-particle Green functions of the problem.

▷ a **separation of energy scales**. The argument $(\omega, \mathbf{q})$ of the response function is a measure of the frequency/momentum scale of the external perturbation. These parameters are to be distinguished from the argument $(\epsilon, \mathbf{p})$ of the single-particle propagators microscopically describing the response process. In many cases, the two sets of scales are parametrically different. For example, in the problem discussed above, $(\omega, \mathbf{q})$ is set by the resolution of an external electronic apparatus and, therefore, much slower than the frequency/momentum scale $(\epsilon, \mathbf{p})$ of electronic charge carriers at the Fermi surface. In these circumstances, the ratios ω/ϵ and $|\mathbf{q}|/|\mathbf{p}|$ define small expansion parameters which can be used in the approximate evaluation of the response kernel. (In other cases, e.g. spectroscopic analysis of microscopic single-particle excitations, it is essential that $(\omega, \mathbf{q})$ and $(\epsilon, \mathbf{p})$ be of the same order.)

7.5 Summary and outlook

This completes our preliminary survey of theory and application of correlation functions in many-body physics. We have seen that correlation functions, notably real-time retarded response functions, represent a principal interface between experiment and theory. The connection between these objects and experimental data – the latter represented through expectation values of certain operators – was established by a formalism known as linear response: assuming an experimentally imposed perturbation of a many-body system to be weak, its response can be analyzed within a controlled expansion scheme whose leading-order term is identified as a retarded correlation function.

A number of general properties of the response function – e.g. causality – could be identified from common sense reasoning. However, to develop a full understanding of this object, notably the connection between the imaginary time response function (the quantity produced by evaluation of the field integral) and its retarded real time counterpart (the quantity we are interested in), we had to go beyond that level. Indeed, we saw that the relation between various types of correlation function could be revealed by means of a powerful spectral representation that was simple, exact, and not dependent on any particular physical context (while not being particularly useful for practical computational purposes).

The structural elements developed early in the chapter were finally bundled into a powerful theory of electromagnetic linear response. We illustrated the application of this machinery on the example of the longitudinal conductivity of the electron gas and pointed out a number of computational elements common to most concrete microscopic linear response calculations.

In the next chapter we return to the intrinsic development of the theory. We become acquainted with the renormalization group, a versatile analytical tool designed to analyze correlation functions (and other objects of physical interest) within the vast space left open between straightforward perturbation theory at one end and the few available exact evaluation schemes at the other.

7.6 Problems

7.6.1 Orthogonality catastrophe

This problem describes a scenario realized frequently in condensed matter in which a spatially localized quasi-particle is immersed in a large host system (the latter described by some N-body ground state wavefunction). The resulting wavefunction, "single-particle state $\otimes$ N-particle ground state," turns out to be largely orthogonal to the true ground state of the now $(N+1)$-particle system. In practice, this means that it takes a very long time for the intruding particle to become accommodated to its new environment, a retardation mechanism known as the orthogonality catastrophe. Following Anderson's original line of argument we here explore the basic physical mechanism underlying the phenomenon.

In the thermodynamic limit, Anderson[31] has shown that the ground state $|\Psi'\rangle$ of a system in the presence of a local perturbation $V(\mathbf{r})$ is orthogonal to the ground state $|\Psi\rangle$ of the unperturbed system:

$$|\langle\Psi|\Psi'\rangle|^2 \overset{N\to\infty}{\longrightarrow} 0.$$

(Here, the local perturbation serves as a caricature of the interaction potential created by a new particle in the system.) This mechanism implies, for example, that transport coefficients measured in setups where a sample is connected to external leads at local contacts often determine a "contact resistance" (determined by the resistance of the sample to accommodate external charge carriers) rather than the bulk conduction properties of the system.

(a) Consider a system of non-interacting fermions. Show that the overlap between the many-particle ground states of the unperturbed system and of the perturbed system is bounded from above:

$$\tilde{\chi} \equiv |\langle\Psi|\Psi'\rangle|^2 < \chi = \exp\left[-\frac{1}{2}\sum_{\epsilon_n \;\; E_\mathrm{F},\epsilon_{m'}>E_\mathrm{F}} |\langle n|m'\rangle|^2\right] \equiv \exp[-\mathcal{I}],$$

where $|n\rangle$ and $|m'\rangle$ are single-particle states of the unperturbed and perturbed system, respectively, and E_F is the Fermi energy. To obtain this inequality, recall that the non-interacting many-particle states are Slater determinants. What is the overlap between ground states? To simplify the resulting expression, use the fact that $\det A \leq 1$ if A has normalized, but non-orthogonal rows. Here one may assume that, if the perturbation is small, $\sum_{\epsilon_{m'}>E_\mathrm{F}} |\langle n|m'\rangle|^2 \ll 1$ for $\epsilon_n \leq E_\mathrm{F}$.

(b) We next compute the exponent $\mathcal{I}$ for the particularly simple case of a spherically symmetric system of radius R. Focusing on the sector of lowest angular momentum $l = 0$, the unperturbed states are given by $\phi_n(r) = N_n \sin(k_n r)/k_n r$, where $k_n = \pi n/R$ and the normalization $N_n = k_n/\sqrt{2\pi R}$. The asymptotic profile of the perturbed wavefunctions can be approximated as $\phi'_n(r) = N_n \sin(k_n r + \delta_m(1 - r/R))/k_n r$, where δ is the

[31] P. W. Anderson, Infrared catastrophe in Fermi gases with local scattering potentials, *Phys. Rev. Lett.* **18** (1967), 1049–51.

s-wave scattering phase shift. Use this *ansatz* to compute first the overlap matrix A and then the exponent $\mathcal{I}$.

Answer:

(a) In the ground state, all single-particle levels with energies below the Fermi energy $E_{\rm F}$ are filled while all levels with higher energies are empty. Thus, the overlap of ground states is given by $\chi = \det A$, where $A_{nm} = \langle n|m'\rangle$ and $\epsilon_n, \epsilon_{m'} < E_{\rm F}$. Defining a row-normalized matrix $\tilde{A}$ by $\tilde{A}_{nm} \equiv A_{nm}/\mathcal{N}_n$ with $\mathcal{N}_n = \sqrt{\sum_m |\langle n|m'\rangle|^2}$, we conclude that $\chi = \det \tilde{A} \prod_n \mathcal{N}_n \leq \prod_n \mathcal{N}_n$. We next take the logarithm of this relation to obtain

$$\ln \chi \leq \sum_{\epsilon_n < E_{\rm F}} \ln\left(\mathcal{N}_n\right) = \frac{1}{2} \sum_{\epsilon_n < E_{\rm F}} \ln \sum_{\epsilon_{m'} < E_{\rm F}} |\langle n|m'\rangle|^2 \quad .$$

Using the closure relation $\sum_{m'} |m'\rangle\langle m'| = 1$ and expanding the logarithm in $x = \sum_{\epsilon_{m'} > E_{\rm F}} |\langle n|m'\rangle|^2 \ll 1$ we arrive at the approximation

$$\begin{aligned} \sum_{\epsilon_n < E_{\rm F}} \ln \sum_{\epsilon_{m'} < E_{\rm F}} |\langle n|m'\rangle|^2 &= \sum_{\epsilon_n < E_{\rm F}} \ln \; 1 - \sum_{\epsilon_{m'} > E_{\rm F}} |\langle n|m'\rangle|^2 \\ &\simeq - \sum_{\epsilon_n < E_{\rm F}, \epsilon_{m'} > E_{\rm F}} |\langle n|m'\rangle|^2 = -2\mathcal{I}. \end{aligned}$$

(b) The overlap matrix A is given by

$$\begin{aligned} A_{nm} = \langle n|m'\rangle &= 4\pi N_n N_m \int_0^R dr \; r^2 \frac{\sin(k_n r)}{k_n r} \frac{\sin\left(k_m r + \delta_m(1 - \frac{r}{R})\right)}{k_m r} \\ &\simeq \frac{2\pi N_n N_m}{k_n k_m} \sin\delta_m \frac{1}{k_n - k_m + \frac{\delta_m}{R}} = \frac{\sin\delta_m}{\pi(n-m) + \delta_m}. \end{aligned}$$

Performing the summation over wavenumbers n larger or smaller than the Fermi wave number $n_{\rm F} = k_{\rm F} R/\pi$ we obtain $\mathcal{I} = +\frac{1}{2\pi^2} \sum_{n<n_{\rm F}, m>n_{\rm F}} \frac{\sin^2\delta_m}{(n-m+\frac{\delta_m}{\pi})^2} \sim \sin^2\delta \ln M$, where $E_M = (\pi M/R)^2/(2m)$ is a cut-off energy at which the phase shift $\delta \equiv \delta_M$ has become negligibly small. Since E_M is some fixed (independent of the system size) energy scale, $M \sim E_M R^2 \sim N$ grows with the system size. Thus $\mathcal{I} \sim +\ln N$, which in turn implies that the overlap $|\langle\Psi|\Psi'\rangle|^2$ vanishes as some negative power of N.

7.6.2 RPA dielectric function

Much of the response of a system of charged fermions to an external electromagnetic perturbation is encoded in the dielectric function ϵ_q. While the dielectric function cannot be computed rigorously, the most common approximation scheme – asymptotically exact in the limit of the infinitely dense gas – is the RPA. It is the purpose of this problem to elaborate upon the various sporadic encounters with the RPA dielectric function we had in the text. Specifically, we will derive Eq. (7.35) and discuss the

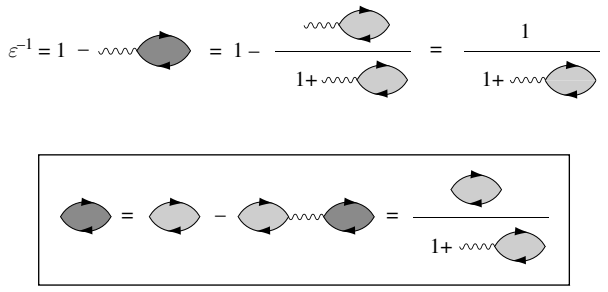

Figure 7.6 Representation of the dielectric function in terms of the full density–density correlation function (the dark-shaded bubble) and the interaction-irreducible density–density correlation function (light-shaded bubble).

generalization to a disordered electron gas. The problem is physically instructive and a good exercise in diagrammatic calculus.

(a) Derive Eq. (7.35). To this end, consider two infinitesimally weak (yet generally time-dependent) test charges immersed in a system of charged fermions. Omitting the self-interaction of the particles, determine the interaction correction to the free energy and use your result to compute the ratio between the vacuum and the actual interaction potential. Show that

$$\epsilon_q = \left(1 - \frac{TV_0(\mathbf{q})}{L^d}\langle \hat{n}_q \hat{n}_{-q}\rangle_{\mathrm{c}}\right)^{-1}, \tag{7.57}$$

where the subscript "c" indicates that only connected diagrams contribute. Analytic continuation to real frequencies obtains Eq. (7.35).

(b) Equation (7.57) represents a rigorous yet quite formal result for the dielectric function; it involves the exact density–density correlation function which is generally unknown. As a first step towards a more manageable expression, show that Eq. (7.35) is equivalent to

$$\epsilon_q = 1 + \frac{TV_0(\mathbf{q})}{L^d}\langle \hat{n}_q \hat{n}_{-q}\rangle_{\mathrm{irr}}, \tag{7.58}$$

where $\langle \hat{n}\hat{n}\rangle_{\mathrm{irr}}$ is the interaction-irreducible density–density response function, i.e. the sum of all diagrams that cannot be cut into two just by cutting one interaction line (i.e. $\langle \hat{n}\hat{n}\rangle_{\mathrm{irr}}$ is to the effective interaction what the self-energy is to the Green function). In order to show that Eq. (7.57) and (7.58) are equivalent, find a series expansion of $C(\mathbf{q}, i\omega_m)$ in terms of V_0 and $\Pi(\mathbf{q}, i\omega_m)$. The series is very similar to the RPA series. Note, however, that, in contrast to RPA, the bubble $\langle \hat{n}\hat{n}\rangle_{\mathrm{irr}}$ still contains interaction lines. A graphical representation might be helpful.

Answer:

(a) If we represent the two test charges with two charge distributions $\rho_{1,2}(q)$, the Coulomb interaction becomes $S_{\rm int} = \frac{T}{2L^d}\sum_q [\hat{n}_q + \rho_{1,q} + \rho_{2,q}] V_0(\mathbf{q}) [\hat{n}_{-q} + \rho_{1,-q} + \rho_{2,-q}]$. An expansion of the field integral (or, equivalently, the partition function) to lowest order in $\rho_{1,2}$ then produces the interaction contribution to the free energy,

$$F_{\rm int}[\rho_1, \rho_2] = -\frac{T^2}{L^d}\sum_q \rho_{1,q}\left[V_0(\mathbf{q}) - \frac{TV_0^2(\mathbf{q})}{L^d}\langle \hat{n}_{-q}\hat{n}_q\rangle_{\rm c}\right]\rho_{2,-q}.$$

The term in rectangular brackets determines the effective interaction potential $V_{\rm eff}(q)$. Remembering that $\epsilon_q = V_0(\mathbf{q})/V_{\rm eff}(q)$, we obtain Eq. (7.57).

(b) For a diagrammatic representation of the solution, see Fig. 7.6.

7.6.3 Electromagnetic response of a quantum dot

In Problem 6.7 we considered a model of quantum dots coupled by tunnel contacts to external leads. There, we derived an effective action for this system but did not say much about its actual physical behavior. As a first step towards a better understanding of the electromagnetic properties of small quantum dots, we here derive a formula elucidating the classical response of the system. In Problem 8.8.2, we then apply renormalization group methods to study how quantum fluctuations affect the low-temperature physics of the system. (Before addressing this problem, refamiliarize yourself with the derivation of the dissipative tunneling action in Problem 6.7.)

(a) Consider Eq. (6.67) for a quantum dot coupled to a lead. Assuming that a bias voltage $iU(\tau)$ between lead and dot has been applied, show that the argument of the dissipative action generalizes to $\phi(\tau) \to \phi(\tau) + \int_0^\tau d\tau'\, U(\tau')$. Focusing on the regime of high temperatures, expand the action to second order in ϕ (argue why, for high temperatures, anharmonic fluctuations of ϕ are small) and compute the 00-component of the linear response kernel, K_{00}. Analytically continue back to real frequencies and show that the current flowing across the tunnel barrier in response to a voltage $U(\omega)$ is given by

$$I(\omega) = \frac{U(\omega)}{\frac{2\pi}{g_T} - 2\frac{E_C}{i\omega}}. \tag{7.59}$$

(b) To understand the meaning of this result, notice that, classically, the dot is but a capacitor connected via a classical resistor to a voltage source. Apply Kirchhoff's laws to obtain the current–voltage characteristics of the classical system and compare with the result above.

Answer:

(a) Consider the action of the system at an intermediate stage, immediately after the fermions have been integrated out (cf. Eq. (6.68)). In the presence of a bias voltage, the "tr ln" contains a term $i(V+U)$, where V is the Hubbard–Stratonovich field decoupling the interaction. Removing the sum of these two fields by the same gauge transformation as used in the derivation of the dissipative action, the tunneling matrix elements acquire the phase factor specified above.

At second order in the expansion in ϕ, the action assumes the form

$$S^{(2)}[\phi,V]=\frac{1}{4E_CT}\sum_m\omega_m^2|\phi_m|^2+\frac{g_T}{4\pi T}\sum_m|\omega_m||\phi_m+U_m/i\omega_m|^2,$$

where the Fourier identity $|\omega_m|\leftrightarrow-\pi T\sin^{-2}(\pi T\tau)$ has been used. Differentiating twice with respect to U, we obtain

$$\begin{aligned}(K_{00})_m &= \mathcal{Z}^{-1}T\frac{\delta^2}{\delta U_m\delta U_{-m}}\mathcal{Z}[U]=-\frac{g_T}{2\pi|\omega_m|}\left(1-\frac{g_T|\omega_m|}{2\pi T}\langle\phi_m\phi_{-m}\rangle\right)\\ &= -\frac{g_T}{2\pi|\omega_m|}\left(1-\frac{g_T|\omega_m|}{2\pi T}\frac{1}{\frac{\omega_m^2}{2E_CT}+\frac{g_T|\omega_m|}{2\pi T}}\right)=-\frac{1}{\frac{2\pi|\omega_m|}{g_T}+2E_C}.\end{aligned}$$

The 00-element of the linear response tensor describes changes in the particle number[32] in response to an applied potential, $\delta N_m=(K_{00})_mU_m$. Noting that $i\partial_\tau\delta N=I$ is the current through the barrier, and substituting our result for K_{00}, we obtain $I_m=U_m\left(\frac{2\pi}{g_T}+\frac{2E_C}{|\omega_m|}\right)^{-1}$. Analytical continuation from positive imaginary frequencies $|\omega_m|\to-i\omega+0$ to real retarded frequencies gives Eq. (7.59).

(b) According to Kirchhoff's laws, the sum of all voltage drops in the system must equal zero, $0=U(\omega)+C^{-1}\delta N(\omega)-RI(\omega)$, where C and R denote the capacitance and resistivity, respectively. Using the fact that $\delta N=I/i\omega$, and solving for I, we readily obtain $I(\omega)=\frac{U(\omega)}{R-1/i\omega C}$, i.e. the current voltage characteristics of a classical RC-circuit. Identifications $R=2\pi/G_T$ and $C=1/2E_C$ bring us back to the formula derived microscopically above.

7.6.4 Hall conductivity

In this problem we derive microscopic expressions for the current response of a (generally disordered) electron gas in the presence of a perpendicular magnetic field. Our results will be the starting point for the analysis of the quantum Hall effect in the next chapter.

Consider a two-dimensional electron gas in the presence of a perpendicular magnetic field. The system is described by the Hamiltonian $\hat{H}=\frac{1}{2m}(\hat{\mathbf{p}}-\hat{\mathbf{A}})^2+\hat{V}$, where $\hat{V}$ is a one-particle

[32] Here, we notice that the factor of "volume" discriminating between particle number and density is contained in our definition of the source variables.

potential (disorder and/or boundary potential) and $\hat{\mathbf{A}} = \frac{B}{2}\hat{\mathbf{r}} \times \mathbf{e}_3$ is the vector potential of the external field. To compute the conductivity tensor, we start from the real-space[33] expression of (cf. Eq. (7.47) and (7.53)),

$$\sigma_{ij} = -\frac{1}{\omega_m L^2} \int d^2x \; d^2x' \left(\frac{2}{m} \delta_{ij} \delta(\mathbf{x} - \mathbf{x}') \langle \hat{\rho}_0(\mathbf{x}) \rangle + \langle \hat{j}_{m,i}(\mathbf{x}) \hat{j}_{-m,j}(\mathbf{x}') \rangle \right) \Big|_{i\omega_m \to +i0},$$

where $\hat{j}_i$ is defined in Eq. (7.46).[34] Using Wick's theorem to compute the expectation value of the current and density operators, we obtain

$$\begin{aligned} \sigma_{ij} \;\; = \;\; & \frac{1}{\omega_m} \frac{T}{L^2} \sum_n \int d^2x \; d^2x' \left(\frac{-2}{m} \delta_{ij} \delta(\mathbf{x} - \mathbf{x}') G_n(\mathbf{x}, \mathbf{x}) \right. \\ & \left. + (\hat{v}_i \hat{G}_{n+m})(\mathbf{x}, \mathbf{x}') (\hat{v}_j \hat{G}_n)(\mathbf{x}', \mathbf{x}) \right) \Big|_{i\omega_m \to +i0}, \end{aligned}$$

where $\hat{\mathbf{v}} = \frac{1}{m}(-i\nabla - \hat{\mathbf{A}})$ is the velocity operator and we have set the electron charge to unity. Anticipating the presence of cuts on the real energy axis, the frequency summation is split into three parts, $\sigma = \sigma^{--} + \sigma^{+-} + \sigma^{++}$, where $\sigma^{\pm\pm}$ denotes the contribution for which the frequency indices $n + m$ and n are positive or negative, respectively.

(a) Beginning with the diagonal contribution to the conductivity tensor, σ_{xx}, show that the paramagnetic contributions to $\sigma_{xx}^{--} + \sigma_{xx}^{++}$ cancel against the diamagnetic term. (Hint: Use the fact that for $n \cdot (n + m) > 0$ the product of two Green functions is short-range: $\langle G_{n+m} G_n \rangle_V = \langle G_{n+m} \rangle_V \langle G_n \rangle_V$, where, as usual, $\langle G \rangle_V$ decays on the scale of the mean free path (i.e. unlike the combination $G_{n<0} G_{n+m>0}$, no long-range quantum interference processes contribute to the product of two Green functions of identical signature). Due to this short-rangeness, we may approximate the position operator entering the definition of the current operator by a c-number valued vector whose value is set by spatial arguments $\mathbf{x} \simeq \mathbf{x}'$ of $G(\mathbf{x}, \mathbf{x}')$. Consequently, both $\hat{G}$ and $\hat{j}$ are diagonalized by the basis of momentum states.)

(b) Owing to the vanishing of σ_{xx}^{++} and σ_{xx}^{--}, the longitudinal contribution to the conductance tensor $\sigma_{xx} = \sigma_{xx}^{+-}$ is obtained by summation over the sector of mixed frequency signature. Show that

$$\sigma_{xx} \simeq \frac{1}{2\pi L^2} \int d^2x \; d^2x' \; (\hat{v}_x \hat{G}^+)(\mathbf{x}, \mathbf{x}') (\hat{v}_x \hat{G}^-)(\mathbf{x}', \mathbf{x}), \tag{7.60}$$

where $\hat{G}^\pm = (\mu \pm i/2\tau - \hat{H})^{-1}$.

(c) Turning to the Hall coefficients, we first note that (think why) $\sigma_{xy} = -\sigma_{yx}$ or $\sigma_{xy} = \frac{1}{2}\epsilon_{ij}\sigma_{ij}$. Using the simplifications listed in (a) and the identity $\hat{\mathbf{v}} = \frac{i}{m}[\hat{H}, \hat{\mathbf{x}}]$, show that $\sigma_{xy}^{++} + \sigma_{yx}^{--} \simeq \frac{i}{L^2} \partial_B \langle \hat{N} \rangle$, where $\hat{N}$ is the particle number operator. Convince yourself

[33] In view of the coordinate dependence of the vector potential, it is preferable to work in a real-space basis.

[34] Do not confuse the vector potential of the external magnetic field with the weak vector potential employed to probe the electromagnetic response of the system; the current operators in the conductivity formula above contain the former but not the latter.

that the region of mixed frequency signature contributes as in the longitudinal case, i.e. that the total **linear response Hall conductivity** is given by

$$\sigma_{xy} \simeq \frac{1}{4\pi L^2} \int d^2x\ d^2x'\ \epsilon_{ij} (\hat{v}_i \hat{G}^+)(\mathbf{x}, \mathbf{x}')(\hat{v}_j \hat{G}^-)(\mathbf{x}', \mathbf{x}) + \frac{i}{L^2} \partial_B \langle \hat{N} \rangle. \tag{7.61}$$

(d) In Chapter 9, we apply the linear response formulae derived above to a field-theoretical analysis of the quantum Hall effect, the physics of a two-dimensional electron gas subject to a strong perpendicular field. Our starting point will be the replicated partition sum $\mathcal{Z} = \int D(\psi, \bar{\psi})\ \exp(-S[\psi, \bar{\psi}])$, where

$$S[\psi, \bar{\psi}] = \int d^2x\ \bar{\psi}(\mathbf{x}) \left[i\delta\sigma_3 - \mu + \frac{1}{2m}(-i\nabla - \mathbf{A})^2 + V(\mathbf{x}) \right] \psi(\mathbf{x}),$$

and $\psi = \{\psi^{ar}\}$ is a $2R$-component field carrying a replica index $r = 1, \ldots, R$ and an index $a = +, -$ distinguishing between "retarded" and "advanced" field components. The Pauli matrix σ_3 acts in the space of a-indices, thus determining the imaginary offset of the inverse propagator in the action. To generate the linear response formulae derived above, we couple the action to a source: $\mathbf{A} \to \mathbf{A} + U^{-1}\nabla U$, where the matrix $U = \exp(i(x\kappa_x\sigma_1 + y\kappa_y\sigma_2) \otimes \mathcal{P}^{(1)})$ and $\mathcal{P}^{(1)} = \{\delta_{r1}\delta_{r'1}\}$ projects onto the first replica channel. Show that

$$\sigma_{xx} = \lim_{R\to 0} \frac{1}{4\pi L^2} \partial^2_{\kappa_x \kappa_x} \bigg|_{\kappa=0} \mathcal{Z}, \quad \sigma_{xy} = \lim_{R\to 0} \frac{1}{4\pi i L^2} \partial^2_{\kappa_x \kappa_y} \bigg|_{\kappa=0} \mathcal{Z}.$$

(Hint: You will encounter terms $\sim \langle \bar{\psi}\psi \rangle \sim \mathrm{Re}\ G^+$, which may be neglected.)

Answer:

(a) As with the previous analysis of the non-magnetic case,

$$\sigma^{++}_{xx} = \frac{1}{\omega_m} \frac{T}{L^2(2\pi)^2} \int d^2x\ d^2p \sum_{n>0} \left(\frac{2}{m} G^+_n(\mathbf{p}, \mathbf{x}) + v_x^2(\mathbf{p}, \mathbf{x})(G^+_n(\mathbf{p}, \mathbf{x}))^2 \right) \bigg|_{i\omega_m \to +i0},$$

where we made use of the simplifying approximations above, $\mathbf{v}(\mathbf{p}, \mathbf{x}) = (\mathbf{p} - \mathbf{A}(\mathbf{x}))/m$ (both $\mathbf{p}$ and $\mathbf{x}$ are vectors of c-numbers) and $G^+_n = (i\omega_n - m\mathbf{v}^2/2 + \mu + i/2\tau)^{-1}$. We may now shift $\mathbf{p} \to \mathbf{p} + \mathbf{A}$ to remove the spatial dependence of the integrand, use the identity $G^2 = +mp_x^{-1}\partial_{p_x} G$, and integrate by parts to conclude that $\sigma^{++}_{xx} = \sigma^{--}_{xx} = 0$.

(b) It is an instructive exercise to obtain the result by contour integration. Introduce a contour that, avoiding the cuts on the real axis, runs around the frequency interval $n(n+m) < 0$ and expand the product of Green functions to leading order in $i\omega_m$. Then take the DC limit. A simplified, yet less rigorous, derivation goes as follows. For low frequencies, $\omega_m < 1/\tau$, $\hat{G}_{n+m>0} \simeq \hat{G}^+$ and $\hat{G}_{n<0} \simeq \hat{G}^-$ are approximately independent of the frequency index. Noting that $\omega_m/(2\pi T)$ terms contribute to the frequency sum, we arrive at Eq. (7.60).

(c) Representing the frequency sums by a contour integral,

$$\begin{aligned}\sigma_{xy}^{++}+\sigma_{yx}^{--} &= -\frac{1}{4\pi i\omega_m L^2}\int d\epsilon\; n_{\rm F}(\epsilon)\int d^2x\; d^2x'\,\epsilon_{ij}\\ &\times\Big((\hat v_i\hat G)(\epsilon+i\omega_m,\mathbf{x},\mathbf{x}')(\hat v_j\hat G)(\epsilon+i0,\mathbf{x}',\mathbf{x})\\ &-(\hat v_i\hat G)\times(\epsilon-i0,\mathbf{x},\mathbf{x}')(\hat v_j\hat G)(\epsilon-i\omega_m,\mathbf{x}',\mathbf{x})\Big)_{i\omega_m\to+i0}.\end{aligned}$$

We next (i) use the identity $\hat{\mathbf{v}}=-i[\hat G,\hat{\mathbf{x}}]$, (ii) expand the Green functions to leading order in $i\omega_m$, and notice that the zeroth-order term in the expansion vanishes. This leads to the expansion

$$\begin{aligned}\sigma_{xy}^{++}+\sigma_{yx}^{--} &= \frac{1}{4\pi L^2}\int d\epsilon\; n_{\rm F}(\epsilon)\epsilon_{ij}\;{\rm tr}\left(\hat x_i\hat G(\epsilon+i0)\hat v_j\hat G(\epsilon+i0)-{\rm c.c.}\right)\\ &\simeq \frac{1}{2\pi L^2}\int d\epsilon\; n_{\rm F}(\epsilon)\partial_\epsilon\;{\rm tr}\left(\hat G(\epsilon+i0)\partial_B\hat H-{\rm c.c.}\right)\\ &= -\frac{i}{L^2}\int d\epsilon\; n_{\rm F}(\epsilon)\partial_\epsilon\;{\rm tr}\left(\delta(\epsilon-\hat H)\partial_B\hat H\right)\\ &= \frac{i}{L^2}\partial_B\int d\epsilon\; n_{\rm F}(\epsilon)\;{\rm tr}\left(\delta(\epsilon-\hat H)\right)=\frac{i}{L^2}\partial_B\langle\hat N\rangle,\end{aligned}$$

where in the second line we have used the approximate commutativity of the operators under the trace and the identity $\partial_B\hat H=\frac{1}{2}\epsilon_{ij}\hat v_i\hat x_j$.

(d) To simplify the notation, we will discuss the longitudinal and Hall conductances separately. To generate the *longitudinal conductance*, we need to expand the generating functional to second order in κ_x. Setting $\kappa_y=0$, we obtain $U^{-1}\nabla U=i\mathcal{P}^{(1)}\otimes\mathbf{e}_x\kappa_x$ and

$$S[\psi,\bar\psi]=S[\psi,\bar\psi]|_{\kappa=0}-i\kappa_x\int d^2x\,\bar\psi^1\sigma_1\hat v_x\psi^1-\kappa_x^2\int d^2x\,\bar\psi^1\psi^1.$$

Twofold differentiation with respect to κ_x then generates the expectation value

$$\begin{aligned}\lim_{R\to0}\frac{1}{L^2}\partial^2_{\kappa_x\kappa_x}\Big|_{\kappa=0}\mathcal{Z} &= \lim_{R\to0}\frac{1}{L^2}\quad-\left(\int d^2x\,\bar\psi^1\sigma_1\hat v_x\psi^1\right)^2+2\int d^2x\,\bar\psi^1\psi^1\\ &\to\frac{2}{L^2}\int d^2x\;d^2x'\;(\hat v_x\hat G^+)(\mathbf{x},\mathbf{x}')(\hat v_x\hat G^-)(\mathbf{x}',\mathbf{x})=4\pi\sigma_{xx},\end{aligned}$$

where in the second line we have noted that $\langle\bar\psi\mathcal{P}^{(1)}\psi\rangle\sim G^++G^-$ generates the real part of the Green function which we decided to omit. Turning to the *Hall conductivity*, an expansion up to order $\kappa_x\kappa_y$ gives

$$U^{-1}\nabla U=i\mathcal{P}^{(1)}\left(\kappa_x\sigma_1\mathbf{e}_x+\kappa_y\sigma_2\mathbf{e}_y+\kappa_x\kappa_y\sigma_3(x\mathbf{e}_y-y\mathbf{e}_x)\right).$$

Substituting this expression into the action, we obtain

$$\begin{aligned}S[\psi,\bar\psi] &= S[\psi,\bar\psi]|_{\kappa=0}-i\int d^2x\,\bar\psi^1(\sigma_1\kappa_x\hat v_x+\sigma_2\kappa_y\hat v_y)\psi^1\\ &-i\frac{\kappa_x\kappa_y}{2}\int d^2x\,\bar\psi^1\sigma_3(\{\hat v_y,\hat x\}-\{\hat v_x,\hat y\})\psi^1.\end{aligned}$$

Then applying the derivative, we obtain

$$\begin{aligned}\lim_{R\to 0}\frac{1}{L^2}\partial^2_{\kappa_x\kappa_y}\Big|_{\kappa=0}\mathcal{Z} = \lim_{R\to 0}\frac{1}{L^2}\quad &-\int d^2x\ \bar{\psi}^1\sigma_1\hat{v}_x\psi^1\int d^2x'\ \bar{\psi}^1\sigma_2\hat{v}_y\psi^1\\ &+\frac{i}{2}\int d^2x\ \bar{\psi}^1\sigma_3(\{\hat{v}_y,\hat{x}\}-\{\hat{v}_x,\hat{y}\})\psi^1\\ \to\frac{1}{L^2}\Big[&i\int d^2x\ d^2x'\ \epsilon_{ij}(\hat{v}_i\hat{G}^+)(\mathbf{x},\mathbf{x}')(\hat{v}_j\hat{G}^-)(\mathbf{x}',\mathbf{x})\\ &-4\int d^2x\ \epsilon_{ij}\hat{v}_i\hat{x}_j\ \mathrm{Im}\ G^+(\mathbf{x},\mathbf{x})\Big] = 4\pi i\sigma_{xy}.\end{aligned}$$

8

The renormalization group

The method of the renormalization group (RG) provides theorists with powerful and e cient tools to explore interacting theories, often in regimes where perturbation theory fails. Motivating our discussion with two introductory examples drawn from a classical and a quantum theory, we first become acquainted with the RG as a concept whereby nonlinear theories can be analyzed beyond the level of plain perturbation theory. With this background, we then proceed to discuss the idea and practice of RG methods in more rigorous and general terms, introducing the notion of scaling, dimensional analysis, and the connection to the general theory of phase transitions and critical phenomena. Finally, to conclude this chapter, we visit a number of concrete implementations of the RG program introduced and exemplified on a number of canonical applications.

In Chapter 5, ϕ^4-theory was introduced as an archetypal model of interacting continuum theories. Motivated by the existence of nonlinearities inherent in the model, a full perturbative scheme was developed, namely Wick contractions and their diagrammatic implementation. However, from a critical perspective, one may say that such perturbative approaches present only a limited understanding. Firstly, the validity of the ϕ^4-action as a useful model theory was left unjustified, i.e. the ϕ^4-continuum description was obtained as a gradient expansion of, in that case, a d-dimensional Ising model. But what controls the validity of the low-order expansion? Indeed, the same question could be applied to any one of the many continuum approximations we have performed throughout the first chapters of the text. Secondly, having identified a number of terms contributing to the perturbative expansion of the model (i.e. represented them in terms of momentum integrals over the non-interacting Green function), it rapidly became apparent that the expansion was seemingly uncontrolled: Those terms that were constructed explicitly (cf., e.g., Eq. (5.17) and the equation before) contained divergences at large momenta. We also saw that, in the transition region between the ferro- and the paramagnetic phase of the ϕ^4-theory, these integrals were prone to the build–up of infrared divergences. Worse still, we had to concede that we had no clue as to how to overcome these problems! Needless to say, such difficulties exemplified by the ϕ^4-model are endemic in field theory.

To better understand the origin and remedy of the problems identified above, we must develop some new ideas. To this end, it is helpful to remember that the central driving force of all of our efforts is the development of a better understanding of long-range characteristics. On the other hand, models such as ϕ^4 exhibit fluctuations on all length-scales, while it was the short-scale fluctuations that were responsible for the majority of difficulties. In

principle, we already know how to deal with situations of this kind: our aim should be an effective theory of long-range fluctuations realized by integrating over all short-range fluctuations. Indeed, this program has been exemplified already on numerous examples where some slow field was coupled to rapidly fluctuating microscopic fields, which were subsequently integrated out.

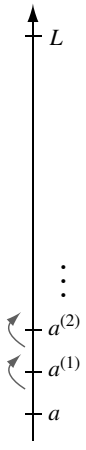

The problem with our current application is that the ϕ^4-theory is unaware of any clear-cut separation into "fast" and "slow" degrees of freedom. Rather, all fluctuations, ranging from the shortest scales (of the order of some microscopic cut-off, a, limiting the applicability of the theory) to the longest scales (of the order of, say, the system size, L) are treated on the same footing. However, to nonetheless implement the scheme of "integrating over fast modes to generate an effective action of the slow degrees of freedom," one must *declare* artificially a certain length scale $a^{(1)} \equiv ba > a$, as the scale separating "short-wavelength fluctuations" on scales $[a, a^{(1)}]$ from "long-wavelength fluctuations" on scales $[a^{(1)}, L]$. Having done so, one may proceed to integrate out the short-range fluctuations, thereby changing the action of the long-range degrees of freedom (see figure). Since the short-range action is by no means simpler than the action of the long-range degrees of freedom, this step will likely involve some approximation. Indeed, the integration procedure may lead to a number of conceivable scenarios. For example, it may corrupt the algebraic structure of the long-wavelength action, leaving us with a theory fundamentally different from the one with which we began. Alternatively, it may turn out that the effective action of the slow degrees of freedom is structurally similar to the original, in which case the entire effect of integrating over the fast fluctuations amounts to a changed set of coupling constants.

If the latter, the procedure is well motivated: we have arrived at a theory identical to the original but for (a) a different, or **renormalized**, set of coupling constants, and (b) an increased short-distance cut-off $a \to a^{(1)} = ba$. Evidently, one may then iterate this procedure; that is declare a new cut-off $a^{(2)} = ba^{(1)} = b^2 a$, integrate out fluctuations on length scales $[a^{(1)}, a^{(2)}]$, etc. Along with the recursive integration of more "layers of fluctuations," the coupling constants of the theory change, or "flow," until the cut-off $a^{(n)} \sim L$ has become comparable to the length scales in which we are interested. Remarkably, we will see that the renormalized set of coupling constants in fact encodes much of the important information about the long-range behavior of the theory.

Kenneth G. Wilson, 1936–

Recipient of the 1982 Nobel Prize in Physics, awarded for "discoveries he made in understanding how bulk matter undergoes phase transitions, i.e., sudden and profound structural changes resulting from variations in environmental conditions." Wilson's background ranges from elementary particle theory and condensed matter physics (critical phenomena and the Kondo problem) to quantum chemistry and computer science. (Image © The Nobel Foundation.)

The general line of reasoning above summarizes much of the thinking behind the renormalization group. Of course, the approach would be quite useless had we to perform each

and every recursion step $a^{(n-1)} \to a^{(n)}$ explicitly. However, the utility of the program relies on the recursive reproduction of the model at each step: a single step already encodes all the information about the renormalization properties of the model. Cast in abstract terms, the conceptual idea may sound obscure. Therefore, before developing a general and formal framework for the renormalization group scheme, we shall acquire some intuition for the approach by focusing on two specific applications which encapsulate the basic concepts.

INFO The **formulation of renormalization group ideas** has a long and varied history, reflecting, in part, the versatility and generality of the method.[1] Indeed, the advent of these ideas in the late 1960s and early 1970s marked the transition between two different "epochs." While hitherto researchers had focused primarily on the development and application of ever more-sophisticated perturbative techniques, the seventies remained under the spell of the renormalization program.

In the second half of the 1960s, ideas to recursively generate flows of coupling constants arose – apparently in independent developments – both in condensed matter and in particle physics. However, it took the insight of Kenneth Wilson to realize the full potential of the approach and to develop it into a widely applicable tool.[2] It is probably fair to say that Wilson's original formulation of the approach, and its later extension by others, led to revolutionary progress in condensed matter physics, particle physics, and general statistical mechanics. Perhaps no less important, the RG concept turned out to be one of the major driving forces behind the partial unification of these fields.

In fact, the (highly unfortunate) terminology of "renormalization group" discloses much of the historical origin of the approach. A widespread doctrine of late 1960s particle physics had been that, on a fundamental level, our world could be understood in terms of symmetries and their implementation through groups – the eight-fold way. In an attempt to absorb the newly developed RG approach into this general framework, it became dubbed the renormalization *group*. Of course, a linkage between group structures and renormalization methods would not have been drawn had it been utterly unjustified. Indeed, one may argue that the sequence of RG transformations outlined above defines the structure of a semigroup.[3] However, the connection between RG transformation and group algebraic structures is not only highly formal but also counterproductive. (It suggests a conceptual bond that simply is not there.) Besides, the group interpretation of the RG transformation is completely useless with regard to practical aspects.

To introduce the conceptual foundation of the renormalization group, we find it helpful to draw initially on classical theories, later turning our attention to addressing the effects

[1] A perspective on the development of the renormalization group can be found in the review article by M. E. Fisher, Renormalization group theory: its basis and formulation in statistical physics, *Rev. Mod. Phys.* **70** (1998), 653–81, or in the text by J. Cardy, *Scaling and Renormalization in Statistical Physics* (Cambridge University Press, 1996).

[2] See K. Wilson, The renormalization group: critical phenomena and the Kondo problem, *Rev. Mod. Phys.* **47** (1975), 773–840, still one of the best introductions to the approach!

[3] To this end, one should interpret an individual RG transformation as an abstract mapping between two actions: $S \overset{R}{\to} S'$, where S is the original action, S' the action with increased short-distance cut-off, and R the mapping between them. One may then notice that these transformations can be iterated, or "multiplied," $R \circ R'$. A moment's thought shows that the composition law obeys the defining conditions of a semigroup: there is a unit transformation (nothing is integrated out) and the iteration is associative. (We are dealing with a *semi*group because the RG transformation is irreversible, i.e. it does not have an inverse.)

of quantum fluctuations. Our first encounter with the renormalization group is, therefore, focused on the one-dimensional Ising model.

8.1 The one-dimensional Ising model

To illustrate the implementation of the RG program on a simple example (indeed the simplest of examples), let us consider the one-dimensional Ising model defined through the classical microscopic Hamiltonian

$$H = -J \sum_{i=1}^{N} S_i S_{i+1} - H_{\text{ext}} \sum_{i=1}^{N} S_i,$$

where $S_i = \pm 1$ denotes the (uniaxial) magnetization or spin of site i (periodic boundary conditions, $S_{N+1} = S_1$, imposed), and H_{ext} represents an external field. Throughout this section we will adhere to the discrete spin representation of the model, i.e. in contrast to Section 5.1, we will not map the model onto a continuum theory. However, this consideration does not impede our discussion of the RG program: One may simply regard $-\beta H[S]$ as a "functional" of the discrete "field" $\{S_i\}$, and all steps outlined above can be carried out without substantial modification.

8.1.1 Exact solution

The feature of the one-dimensional Ising model which makes it of pedagogical interest in the present context is that it admits an exact solution, i.e. all of its macroscopically observable properties can be computed in closed form. Both the exact solution of the model and its RG formulation rely on its **transfer matrix representation**. One may notice that the Boltzmann weight of the system can be factorized according to the relation

$$e^{-\beta H} = e^{\sum_{i=1}^{N} (K S_i S_{i+1} + h S_i)} = \prod_{i=1}^{N} T(S_i, S_{i+1}),$$

where, for notational convenience, we have introduced the dimensionless parameters $K \equiv \beta J > 0$ and $h = \beta H_{\text{ext}}$, and the weight is defined through the relation $T(S, S') = \exp[KSS' + \frac{h}{2}(S + S')]$. Defining a two-component matrix T with elements $T_{11} = T(1, 1)$, $T_{12} = T(1, -1)$, $T_{21} = T(-1, 1)$, and $T_{22} = T(-1, -1)$, one may confirm that the partition function of the system can be written as

$$\mathcal{Z} = \sum_{\{S_i\}} e^{-\beta H} = \sum_{\{S_i\}} \prod_{i=1}^{N} T(S_i, S_{i+1}) = \sum_{\{n_i\}} \prod_{i=1}^{N} T_{n_i n_{i+1}} = \operatorname{tr} T^N.$$

Thus, we have managed to represent the partition function as a trace of the Nth power of the two-dimensional "transfer" matrix T.[4] In this representation, the partition function

[4] The terminology "transfer matrix" originates in an interpretation of the Ising model as a fictitious dynamical process in which a state S_i is "transferred" to a state S_{i+1}, where the transition amplitude is given by $T(S_i, S_{i+1})$.

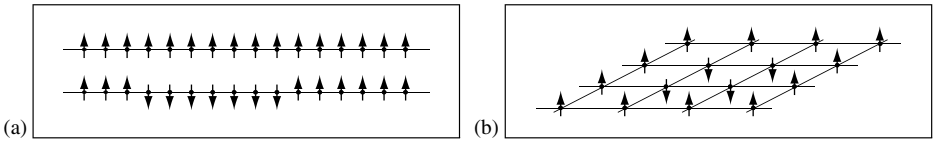

Figure 8.1 (a) On the absence of spontaneous symmetry breaking in the one-dimensional Ising model. No matter how low the temperature, the energy cost associated with the creation of a segment of flipped spins is outweighed by the entropy gain. (b) In higher dimensions, entropic factors no longer have the capacity to overpower the extensive growth of energy associated with the formation of mismatched regions.

may be presented in terms of the two eigenvalues, $\lambda_\pm = e^K[\cosh(h) \pm (\sinh^2(h) + e^{-4K})^{1/2}]$, of the transfer matrix

$$T = \begin{bmatrix} e^{K+h} & e^{-K} \\ e^{-K} & e^{K-h} \end{bmatrix},$$

as $\mathcal{Z} = \operatorname{tr} T^N = \lambda_+^N + \lambda_-^N$. Noting that $\lambda_+ > \lambda_-$, one may see that, in the thermodynamic limit $N \to \infty$, the contribution of the latter may be neglected, so that $\mathcal{Z} \overset{N\to\infty}{\longrightarrow} \lambda_+^N$. Restoring the original microscopic parameters, in the thermodynamic limit, one obtains the free energy

$$F \equiv -\frac{1}{\beta} \ln \mathcal{Z} = -N \left(J + T \ln \left[\cosh(\beta H_{\text{ext}}) + \sqrt{\sinh^2(\beta H_{\text{ext}}) + e^{-4\beta J}} \right] \right). \tag{8.1}$$

With this result, one can compute the magnetization M by differentiation with respect to the magnetic field. As a result one obtains the magnetization per spin,

$$m \equiv \frac{M}{N} = \frac{\sinh(\beta H_{\text{ext}})}{\sqrt{\sinh^2(\beta H_{\text{ext}}) + e^{-4\beta J}}}. \tag{8.2}$$

Two magnetization curves are shown in the figure at two non-zero temperatures. Notice that, while the magnetization curves grow ever more steeply with decreasing temperature, the system does not magnetize at any non-zero temperature in the absence of an external field, i.e., unlike its higher-dimensional descendants, the one-dimensional model does not display spontaneous symmetry breaking.

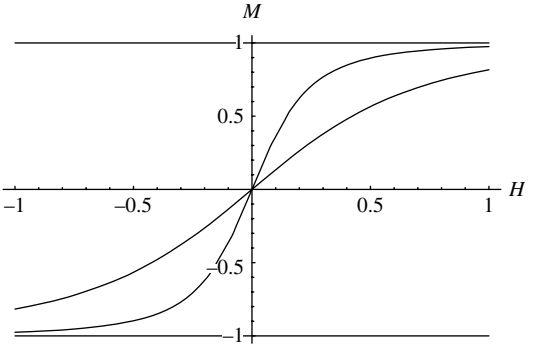

INFO There are many ways to understand the **absence of spontaneous symmetry breaking** in the one-dimensional Ising model (cf. our discussion of the connection with quantum mechanical tunneling in Section 3.3). Suppose that the system did exhibit a critical temperature T_c below which the system acquired long-range order with $\{S_i\} = 1$ or $\{S_i\} = -1$ (Fig. 8.1 (a)). Now, let us imagine that a segment of M consecutive spins were to flip. In doing so, they would incur an energetic cost of $\mathcal{O}(2J)$, i.e. the energy associated with the unfavorable spin alignment at

the two ends of the domain of reversed spins. However, there are some N different choices for placing the sector of M flipped spins, i.e. the energy loss is counteracted by an entropic factor of $\sim T \ln N$ (exercise). Thus, no matter how small T is, for large systems of large enough extent the *free* energy balance for domain creation is positive, implying that the system will be in a disordered phase at any non-zero temperature.

EXERCISE By enumerating the number of spin configurations with the same energy, obtain a formal expression for the classical partition function of a one-dimensional Ising model of length N with periodic boundary conditions. (Hint: Consider the number of domain wall configurations.) Making use of Stirling's approximation $\ln n! \simeq n(\ln n - 1)$, determine the temperature dependence of the correlation length (domain size) at low temperatures. Confirm that the system does not order at any finite temperature.

To what extent do these arguments carry over to **Ising systems of higher dimensionality**? Consider, for example, a two-dimensional variant of the model. Here the formation of a large connected region of M mismatched spins incurs an energy cost $U \sim M^{1/2}J$. To understand why, one may note that the energy cost is proportional to the length of the one-dimensional boundary that encloses a (circular) domain of reversed spins. However, the entropic gain still scales as $\sim k \ln N$. (Allowing for less symmetric domains, the energy/entropy balance becomes more subtle. Yet the qualitative conclusion remains robust.) Thus, for the two-dimensional system, $F \sim JM^{1/2} - T \ln N$. From this one can conclude that, over the range of temperatures for which this estimate is valid, no matter how small T, it is energetically unfavorable to flip a thermodynamic $M \sim N^{x>0}$ number of spins. One may, therefore, conclude that the $(d \geq 2)$-dimensional Ising model does exhibit a phase transition into an ordered low-temperature phase.

The phenomenon of spontaneous symmetry breaking occurs only in systems of sufficiently large dimensionality. The threshold dimension below which entropic mechanisms exclude spontaneous symmetry breaking is called the **lower critical dimension** d_c.

Our argument above indicates that the lower critical dimension of the Ising model and, more generally,

The lower critical dimension of systems with discrete symmetries is $d_c = 1$.

Pursuing this theme, let us complete the discussion by addressing the question of the lower critical dimension for systems with a **continuous symmetry** (e.g. the U(1) symmetry of the superfluid phase, the O(3)-symmetry of the Heisenberg ferromagnet, etc.). To address this question, one may proceed in a manner analogous to that used in the Ising system, i.e. let us assume that a critical temperature exists below which the system is ordered. Using, for concreteness, the language of magnetic phenomena, we might say that the system with two-component spin degrees of freedom acquires a state of uniform magnetization $\mathbf{S}(\mathbf{r}) = S\mathbf{e}_1$, where $\mathbf{e}_1$ denotes the unit vector in the, say, 1-direction. Expanding the Hamiltonian $\beta H[\mathbf{S}]$ in fluctuations around this configuration (and, for simplicity, taking a continuum limit), one obtains

$$S[\mathbf{S}] = \frac{cS^2}{2T} \int d^d r \, (\partial\theta)^2,$$

where $\theta(\mathbf{r})$ denotes the polar angle measuring fluctuations around the ordered state and c is a coupling constant. One may now explore the thermal (or, if appropriate, quantum thermal) expectation value $\langle S_1(\mathbf{r})\rangle$ of the 1-component of the spin variable anywhere in the system. Assuming that we are close to the ordered state, an expansion in θ gives $S_1(\mathbf{r}) = S\cos\theta = S(1-\frac{1}{2}\theta^2+\cdots)$. We now proceed to check whether the close-to-ordered assumption was actually legitimate. For this, we have to verify that, with $\langle S_1(\mathbf{r})\rangle = S - \frac{S}{2}\langle\theta^2(\mathbf{r})\rangle + \cdots$, the contribution associated with fluctuations is much smaller than the leading-order constant. Performing the Wick contraction with respect to the quadratic action, and switching to momentum space, one obtains

$$\langle S_1(\mathbf{r})\rangle \approx S \;\; 1 - \frac{T}{2cS^2}\sum_{\mathbf{q}}\frac{1}{q^2} \;\; \approx S \;\; 1 - \frac{T}{2cS^2}\left(\frac{L}{2\pi}\right)^d \int \frac{d^dq}{q^2} \quad .$$

Crucially, in dimensions $d \quad 2$, the integral is divergent. In the marginal case $d = 2$, $\int_{L^{-1}}^{a^{-1}} \frac{d^2q}{q^2} = \pi\ln(L/a)$, where we have used the fact that the momentum integral should be limited by a short- (long-) wavelength cutoff of the order of the inverse lattice spacing (the system size). In the thermodynamic limit, $L\to\infty$, the integral grows without bound, implying that the assumption of an ordered state was ill-founded no matter how small the temperature; the system is in a disordered state. Noting that nowhere did we rely on specifics of the spin system, we draw a conclusion known as the **Mermin–Wagner theorem:**

> The lower critical dimension of systems with broken continuous symmetries is $d = 2$.

Obviously, the divergence of the fluctuation integral is due to the fact that, for large wavelengths, and in low dimensions, the integration volume (alias the entropy) of fluctuations $\sim q^d$ scales more slowly to zero than the energy cost $\sim q^2$. That is, as in the Ising model case, the Mermin–Wagner theorem[5] can be understood as the statement of a competition of energy and entropy.[6]

8.1.2 Elements of scaling theory

Returning to the one-dimensional Ising model, we may note that Eq. (8.2) represents a full solution of the problem. We have explicitly obtained the magnetization as a function of the magnetic field and the microscopic coupling constant of the model. Other thermodynamic characteristics, such as the magnetic susceptibility $\chi = -\partial_H^2 F$, can be generated by further differentiation with respect to H and/or T. (Here, and henceforth, we drop the subscript "ext" from the definition of the external field, $H_{\rm ext}$, noting that it can always be discriminated from the Hamiltonian H by its context.) However, in the vast majority of physically interesting problems we will not be in possession of a closed analytical solution. This means that, before comparing the exact solution with the outcome of the RG program, we should reformulate the former in a universally applicable language, i.e. a code that can be used to

[5] N. D. Mermin and H. Wagner, Absence of ferromagnetism or antiferromagnetism in one- or two-dimensional isotropic Heisenberg models, *Phys. Rev. Lett.* **17** (1966), 1133–6.

[6] For completeness, we mention that the proof of the theorem (of which we gave a fairly abridged version here) in a subtle way relies on the fact that the symmetry in question is compact. For the (rare) class of systems with non-compact, e.g. hyperbolic, symmetries, the statement does not hold.

characterize the behavior of a model irrespective of the particular method by which this behavior has been analyzed.

This objective leads us back to the familiar notion of **correlation functions**. All models of physical interest display non-trivial fluctuation behavior on large length scales. Indeed, in the vicinity of critical points marking the position of continuous phase transitions, one expects the onset of critical fluctuations, i.e. the accumulation of fluctuations on *all* length scales. (For a precise formulation of the terminology, see the section on phase transitions and critical phenomena below.) One of the central working hypotheses of the theory of "critical phenomena" is that, in the vicinity of the critical points there is only one length scale of physical relevance, the **correlation length** ξ. Within the context of the Ising model (cf. our previous discussion on page 199), ξ is defined as the decay length of the correlation function,

$$C(\mathbf{r}_1 - \mathbf{r}_2) \equiv \langle S(\mathbf{r}_1)S(\mathbf{r}_2)\rangle - \langle S(\mathbf{r}_1)\rangle\langle S(\mathbf{r}_2)\rangle \sim \exp\left[-\frac{|\mathbf{r}_1 - \mathbf{r}_2|}{\xi}\right],$$

where we have switched to a continuum notation $S_i \to S(r)$, to emphasize the large-distance character of ξ. To relate this quantity to the thermodynamic characteristics, one may note that the magnetic susceptibility is given by

$$\chi = -\partial_H^2 F\,\big|_{H=0} = T\partial_H^2 \ln \mathcal{Z}\big|_{H=0} = \beta \int d^d r\, d^d r' \overbrace{\left(\langle S(\mathbf{r})S(\mathbf{r}')\rangle - \langle S(\mathbf{r})\rangle\langle S(\mathbf{r}')\rangle\right)}^{C(\mathbf{r}-\mathbf{r}')}. \qquad (8.3)$$

INFO In fact, this is yet another manifestation of the **fluctuation–dissipation theorem** discussed in the previous chapter. A dissipative quantity (in this case, the susceptibility) is determined by the fluctuation behavior of the system.

Comparison with the definition of the correlation function above identifies $\chi \sim \xi^d$, i.e., in the one-dimensional system, the magnetic susceptibility is directly proportional to the length scale determining the decay of correlations in the system. So far, we have not yet made use of the specific results obtained for the Ising models above. However, to actually determine the correlation length for our present example, we need only differentiate Eq. (8.2) once again with respect to H, to obtain

$$\xi \sim \chi \sim \partial_H|_{H=0}\, m \sim e^{2\beta J}, \qquad (8.4)$$

i.e. the correlation length exponentially increases in the limit $T \to 0$ on a scale set by the microscopic "stiffness constant", J. This result should not be too surprising: unlike its higher-dimensional counterparts, the one-dimensional Ising model does not display a finite-temperature phase transition between a ferro- and a paramagnetic phase. It is only in the limit $T \to 0$ that long-range correlations develop.

In the vicinity of a critical point, the diverging correlation length specifies the singular thermodynamic properties of the system. More specifically, all observables X of dimensionality [length]^{D_X} should obey the **scaling form**

$$X \sim \xi^{D_X} g_X,$$

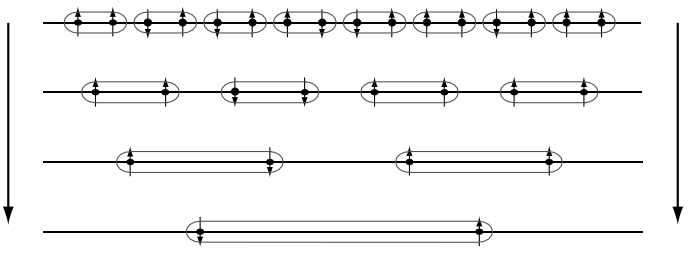

Figure 8.2 RG or block spin transformation of the Ising model illustrated for clusters of size $b = 2$. An r-fold iteration of the procedure reduces the degrees of freedom by a factor 2^r.

where g_X is a dimensionless function. Let us explore this concept on our present example. The "reduced free energy,"

$$f(T) \equiv \frac{F}{TL}, \tag{8.5}$$

has dimension L^{-1}. Noting that $N \sim L$, a straightforward low-temperature expansion of Eq. (8.1) indeed gives

$$f(T) - f(0) = \xi^{-1}\left(-1 - \frac{1}{2}\xi^2 h^2\right) \equiv \xi^{-1} g(\xi h), \tag{8.6}$$

where we have subtracted the infinite but inessential constant $f(0)$ and assumed that $1 \gg \xi^{-1} \gg h$. (The scaling form above actually suggests that the magnetic field has dimension L^{-1}, a prediction substantiated below.)

We have thus found that the correlation length of the one-dimensional Ising system diverges according to Eq. (8.4) upon approaching zero temperature, and that the free energy obeys the scaling law (8.6). Of course, this is only a fraction of the full information stored in the exact solution. However, the reduced set of data has the striking advantage that it is of general relevance. Indeed, we saw above that the correlation length is directly related to measurable properties of the system such as the magnetic susceptibility. Similarly, the output of experiments on systems with long-range correlations is commonly encoded in the language of scaling relations. In other words, we have extracted that part of the information contained in the exact solution that carries universal relevance and can be compared with the output of other approaches.

8.1.3 Kadanoff s block spin RG

With this background we are in a position to explore some of the conceptual foundations of the RG on a model application. According to the general scheme outlined at the beginning of the chapter, our aim is to devise an algorithm to recursively trace out parts of the short-scale fluctuations of the system and assess their influence on the remaining degrees of freedom.

Leo P. Kadanoff 1934-

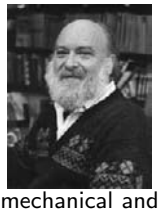

Theoretical physicist and applied mathematician who has contributed widely to research in the properties of matter, the development of urban areas, statistical models of physical systems, and the development of chaos in simple mechanical and fluid systems. He was instrumental in the development of the concepts of scale invariance and universality as they are applied to phase transitions.

Following the program outlined by Kadanoff's seminal work on the foundations of the RG, we will follow a strategy whereby this renormalization step may be effected by subdividing the spin chain into regular clusters of b neighboring spins (see Fig. 8.2). We may then proceed to sum over the 2^b sub-configurations of each cluster, thereby generating an effective functional describing the inter-cluster energy balance. While it is clear that this energy functional exists, a far less obvious question to ask is whether it will again have the form of an effective Ising spin system. Remarkably, the answer is affirmative: the Ising model is said to be "renormalizable." The structural reproduction of the model implies that we can think of each cluster as some kind of meta-Ising spin, or **block spin**. More importantly, it guarantees that the renormalization step qualifies for iteration: in a second RG step, b block spins are grouped to form a new cluster (now comprising b^2 of the microscopic spins) which are then traced out, etc. We next discuss how this algorithm is implemented in concrete terms.

Within the transfer matrix approach, a cluster of b spins is represented through b transfer matrices T. Taking the partial trace over its degrees of freedom amounts to passing from these b matrices to the product $T' = T^b$. (By construction of the approach, the internal index summation involved in taking the product amounts to tracing out the degrees of freedom of the cluster.) The transition from the original partition function $\mathcal{Z}$ to the new partition function $\mathcal{Z}'$ is defined through the relation

$$\mathcal{Z}_N(K,h) = \mathrm{tr}\, T^N = \mathrm{tr}\, (T^b)^{N/b} = \mathrm{tr}\, (T')^{N/b} = \mathcal{Z}_{N/b}(K',h'), \tag{8.7}$$

where the notation makes the parametric dependence of the partition function on the size of the system, N, and on the coupling constants K, h explicit. Notice that the equation above makes the highly non-trivial assumption that the reduced trace, $\mathrm{tr}\, (T')^{N/b}$, can again be expressed as an Ising partition function or, equivalently, that the effective transfer matrix T' has the same algebraic structure as the elementary matrices T.

To confirm the integrity of the transformation, one may explore the structure of the product matrices T' for the simplest case of $b = 2$ block spins. Introducing the abbreviations $u \equiv e^{-K}$, $v \equiv e^{-h}$, we have

$$T = \begin{bmatrix} e^{K+h} & e^{-K} \\ e^{-K} & e^{K-h} \end{bmatrix} = \begin{bmatrix} u^{-1}v^{-1} & u \\ u & u^{-1}v \end{bmatrix},$$

while the product takes the form

$$T' \equiv T^2 = \begin{bmatrix} u^2 + u^{-2}v^{-2} & v + v^{-1} \\ v + v^{-1} & u^2 + u^{-2}v^2 \end{bmatrix} \stackrel{!}{=} C \begin{bmatrix} u'^{-1}v'^{-1} & u' \\ u' & u'^{-1}v' \end{bmatrix}.$$

In the last equality we require that the new transfer matrix be of the same structure as the original. However, noting that this requirement will introduce three conditions (for the

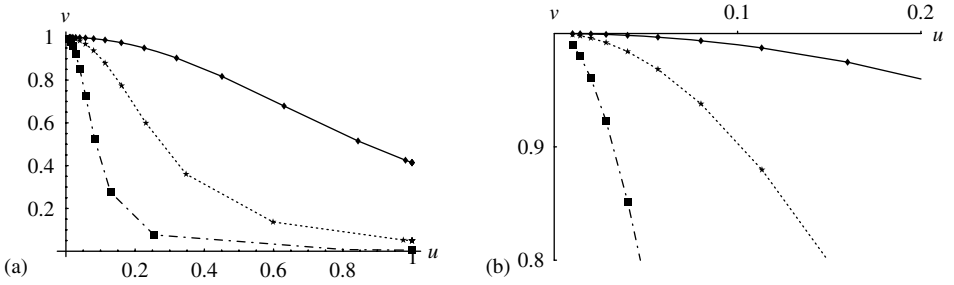

Figure 8.3 (a) The flow of coupling constants of the one-dimensional Ising model generated by iteration of the RG transformation. The three lines shown are for starting values $(u, v) = (0.01, 0.9999)(\blacklozenge)$, $(0.01, 0.999)(\star)$, and $(0.01, 0.99)(\blacksquare)$. (b) Magnification of the zero-temperature fixed point region.

three independent entries of the symmetric matrices T and T'), we are willing to tolerate the appearance of an overall multiplicative constant C.[7] Having introduced this new parameter, we have enough freedom to solve the three equations, from which one finds (exercise)

$$u' = \frac{\sqrt{v + v^{-1}}}{(u^4 + u^{-4} + v^2 + v^{-2})^{1/4}}, \quad v' = \frac{\sqrt{u^4 + v^2}}{\sqrt{u^4 + v^{-2}}}, \tag{8.8}$$

and $C = \sqrt{v + v^{-1}}(u^4 + u^{-4} + v^2 + v^{-2})^{1/4}$. As a corollary, we remark that the possibility of representing the new transfer matrix in the same algebraic structure as the old one implies that the transformed model again describes an Ising spin system (namely the spin system whose transfer matrix would be given by T'). However, the Hamiltonian βH of the new block spin system:

- ▷ is defined at a different temperature, magnetic field and exchange constant (as described by the new values of the coupling constants (u', v')) and
- ▷ describes fluctuations on length scales that are twice as large as in the original system. In particular, the short-distance cutoff has been doubled.

To make further progress, one may focus on the two relevant parameters u' and v' and observe that the result of the block spin transformation can be represented as a discrete map

$$\begin{bmatrix} u' \\ v' \end{bmatrix} = \begin{bmatrix} f_1(u, v) \\ f_2(u, v) \end{bmatrix},$$

where the functions $f_{1,2}$ are defined through Eq. (8.8). In Fig. 8.3 sequences of points generated by an iterative application of the map f are shown for different values of "initial conditions" (u_0, v_0). It is evident from the **RG trajectories** that the map f possesses two

[7] Taking the product of the new transfer matrices, we see that this constant appears in the partition function as $\mathcal{Z}' \sim C^{N/b}$, i.e. the free energy acquires an overall additive constant $F' \sim -\frac{NT}{b} \ln C$ which will be of no further significance.

disjoint sets of **fixed points**, i.e. points (u^*, v^*) that remain invariant under the application of the map f:

$$\begin{bmatrix} u^* \\ v^* \end{bmatrix} = \begin{bmatrix} f_1(u^*, v^*) \\ f_2(u^*, v^*) \end{bmatrix}.$$

Inspection of Eq. (8.8) shows that this is the case for (a) the point $(u^*, v^*) = (0, 1)$, and (b) the line $(u^*, v^*) = (1, v)$.

The set of fixed points represents the most important structural characteristic of an RG analysis. They organize the space of "flowing" coupling constants into sectors of qualitatively different behavior. In particular, one may note that, at a fixed point, all characteristics of the model, including its correlation length ξ, remain invariant. On the other hand, we noticed above that an RG step is tantamount to doubling the fundamental length scale of the system. Consistency requires that either $\xi = 0$ or $\xi = \infty$. In the present case, the line of fixed points is identified with $u = \exp[-\beta J] = 1$, i.e. $\beta = 0$. This is the limit of infinitely large temperatures, at which we expect the model to be in a state of maximal thermal disorder, that is $\xi = 0$. Besides the high-temperature fixed line, there is a zero-temperature fixed point $(u, v) = (\exp[-\beta J], \exp[-\beta h]) = (0, 1)$ implying $T \to 0$ and $h = 0$. Upon approaching zero temperature, the system is expected to order and to build up long-range correlations, $\xi \to \infty$.

Notice, however, an important difference between the high- and the low-temperature set of fixed points: while the former is an **attractive fixed point** in the sense that the RG trajectories approach it asymptotically, the latter is a **repulsive fixed point**. No matter how low the temperature at which we start, the RG flow will drive us into a regime of effectively higher temperature or lower ordering. (Of course, the physical temperature does not change under renormalization. All we are saying is that the block spin model behaves as an Ising model at a higher temperature than the original system.)

To explore the low-temperature phase of the system quantitatively, we may linearize the RG map in the vicinity of the $T = 0$ fixed point. That is, condensing the fixed point coordinates into a two-component vector, $\mathbf{x}^* \equiv (u^*, v^*)^T = (1, 0)^T$, and assuming that $\Delta\mathbf{x}$ parameterizes a small deviation from the fixed point, one may write $\mathbf{x}^* + \Delta\mathbf{x}' = \mathbf{f}(\mathbf{x}^* + \Delta\mathbf{x}) \approx \mathbf{f}(\mathbf{x}^*) + \partial_{\mathbf{x}}\mathbf{f} \cdot \Delta\mathbf{x} + \mathcal{O}(\Delta\mathbf{x}^2)$. Now, drawing on the invariance of the fixed point, $\mathbf{f}(\mathbf{x}^*) = \mathbf{x}^*$, we obtain the linearized map $\Delta\mathbf{x}' = \partial_{\mathbf{x}}\mathbf{f} \cdot \Delta\mathbf{x} + \mathcal{O}(\Delta\mathbf{x}^2)$. To explore the linearized mapping in more detail, it is convenient to introduce yet another pair of variables, namely $r \equiv u^4$, $s \equiv v^2$, whereupon the RG transformation becomes rational, $r' = \frac{2+s+s^{-1}}{r+r^{-1}+s+s^{-1}}$, $s' = \frac{r+s}{r+s^{-1}}$. Differentiating this map at $(r, s) = (1, 0)$, it is straightforward to show that

$$\begin{bmatrix} \Delta r' \\ \Delta s' \end{bmatrix} = \begin{bmatrix} 4 & \\ & 2 \end{bmatrix} \begin{bmatrix} \Delta r \\ \Delta s \end{bmatrix}.$$

Noting that a transformation with $b = 4$, say, is equivalent to a two-fold application of a $b = 2$ transformation, one may recast the relation above in the more general form

$$\begin{bmatrix} \Delta r' \\ \Delta s' \end{bmatrix} = \begin{bmatrix} b^2 & \\ & b \end{bmatrix} \begin{bmatrix} \Delta r \\ \Delta s \end{bmatrix}, \tag{8.9}$$

applicable to arbitrary b.

To make use of Eq. (8.9), let us once again consider the reduced free energy Eq. (8.5): $f(\Delta r, \Delta s) \equiv -N^{-1} \ln \mathcal{Z}_N(K(\Delta r), h(\Delta s)) \equiv -N^{-1} \ln \mathcal{Z}_N(\Delta r, \Delta s)$ and reformulate Eq. (8.7) according to

$$f(\Delta r, \Delta s) = -\frac{1}{N} \ln \mathcal{Z}_N(\Delta r, \Delta s) = -\frac{1}{N'b} \ln \mathcal{Z}_{N'}(\Delta r', \Delta s') = \frac{1}{b} f(b^2 \Delta r, b\Delta s).$$

This equation describes the "scaling" of the free energy density under block spin transformations (all in the linearizable low-temperature regime) or, equivalently, changes of the fundamental length scale at which we consider our model. The right-hand side of the equation describes how the model would look from a "blurred" perspective where all degrees of freedom on scales $< b$ have been comprised in a single structural unit.

Importantly, b is a free parameter without intrinsic significance; it can be set to any desired value. For example, we may find it convenient to look at our model at scales where $b^2 \Delta r = 1$. With this choice one obtains $f(\Delta r, \Delta s) = \Delta r^{1/2} f(1, \Delta s/\Delta r^{1/2}) \equiv \Delta r^{1/2} g(\Delta s/\Delta r^{1/2})$, where the dimensionless one-parameter function g is defined through the second equality. Finally, one can relate back to the physical parameters of the system:

$$\Delta r = r - 0 = r = u^4 = e^{-4K}, \quad \Delta s = s - 1 = v^2 - 1 = e^{-2h} - 1 \simeq -2h,$$

which brings us to the scaling relation

$$f = e^{-2K} g(e^{2K} h). \tag{8.10}$$

This is the scaling form predicted by the RG analysis. Notice that a non-trivial statement is being made. The *a priori* dependence of the free energy on two independent parameters K, h has been reduced to a one-parameter function, multiplied by an overall prefactor. Indeed, we expect on general grounds that (see the discussion of the previous section) the reduced free energy should scale with the inverse of the correlation length ξ, which in turn diverges upon approaching the zero-temperature fixed point. Comparing with Eq. (8.10), and noting that there are no reasons for the rescaled free energy $g(x) = f(1, x)$ to diverge by itself, we conclude that the divergence of ξ is driven by the prefactor, i.e. $\xi \sim e^{2K}$, in agreement with the result of the exact analysis. With this identification we obtain

$$f = \xi^{-1} g(\xi h),$$

i.e. the magnetic field appears in conjunction with the correlation length and we have reproduced the exact asymptotic Eq. (8.6).

Notice that there is no reason to be too irritated about the excessive appearance of vague proportionalities "$\sim$." As fixed points are approached, physical systems tend to build up all sorts of singular scales. The most fundamental of these is the correlation length, but the divergence of ξ usually entails singular behavior of other physical quantities. These singularities characterize much of the observable behavior of a system both theoretically and, in fact, experimentally. In the immediate vicinity of a fixed or transition point, all but the strongest driving forces of singular scaling are of secondary importance. Indeed, this is why we could, for example, conclude from Eq. (8.10) that $\xi \sim \exp(2K) \sim \exp(2\beta J)$. We know on general grounds that $f \sim \xi^{-1}$. On the other hand, (8.10) implies that the leading (i.e. exponential) driving force behind the divergence of that scaling factor must

reside in $\exp(2\beta J)$. This leads to the identification $\xi \sim \exp(2\beta J)$, where all other factors of proportionality are of secondary importance.

EXERCISE Apply the block spin RG procedure to the one-dimensional q-state Potts spin model $\beta H = -K \sum_{i=1}^{N} \delta_{s_i, s_{i+1}}$, where $s_i = (1, 2, \ldots, q)$. Identify all fixed points and note their stability.

In Section 8.3.3 below we discuss these scaling arguments from a more rigorous and general perspective. However, before doing so, let us exemplify an RG analysis of a second case study.

8.2 Dissipative quantum tunneling

Previously, we have explored the impact of the external environment on the quantum mechanical tunneling of a particle from a well. In particular, we have seen that, under a wide range of conditions, the influence of the environment can be captured by an ohmic contribution to the action, of the form $S_{\rm diss}[\theta] = \frac{1}{\pi T g} \sum_{\omega_n} |\omega_n||\theta_n|^2$, where the parameter g^{-1} characterizes the bare viscosity. Indeed, we have seen that a similar dissipative structure appears in a number of different settings, including the problem of impurity scattering in a quantum wire (see Problem 4.5). There, the dissipative term appeared as a result of integrating over the collective fluctuations of the bosonized field while pinning the field θ at the impurity.

In the following, we exploit an RG program to uncover the effect of dissipation on the facility to tunnel. To be concrete, let us assume that the quantum mechanical particle inhabits a periodic potential, $U(\theta) = c\cos\theta$. In this case, the quantum transition probability can be encapsulated by the quantum partition function $\mathcal{Z} = \int D\theta \, \exp(-S[\theta])$ where[8]

$$\boxed{S[\theta] = \frac{1}{4\pi T g} \sum_n |\omega_n||\theta_n|^2 + c \int d\tau \cos(\theta(\tau)).} \tag{8.11}$$

To explore the physical behavior of the system described by the effective action (8.11), we might decide to focus on a physical observable that would then be calculated by taking appropriate functional averages with respect to the effective action $S[\theta]$. However, we shall instead proceed in a somewhat more indirect manner: following the general philosophy outlined at the beginning of the chapter, we begin by arbitrarily subdividing the set of all fields $\{\theta\}$ into short- and long-wavelength degrees of freedom. For example, assuming that the maximum frequency up to which the effective bosonic theory of the problem applies is given by Λ, we might say that fluctuations on scales $\Lambda/b < |\omega_n| < \Lambda$ are "fast" ($b > 1$) while those with $|\omega_n| < \Lambda/b$ are "slow."

INFO Notice that this mechanism of subdivision of the degrees of freedom differs from that employed earlier. In the previous example, we carried out an RG transformation by integrating

[8] Here, taking the viscosity $1/g$ to be large, we have neglected the influence of the kinetic contribution $\int d\frac{m}{2}\dot{\theta}^2$, which serves only to regularize the UV behavior.

out field fluctuations on short scales in real space, i.e. we performed a **real space renormalization**. Here, we chose to integrate over a high-lying sector in frequency space. Alluding to the status of frequency as the $(d+1)$th component of a generalized momentum, this implementation of the RG transformation is called **momentum shell renormalization**. While the real space renormalization may seem more intuitive, it is usually less convenient to carry out analytically. (As regards numerical renormalization procedures, the situation is different.) It goes without saying that the net outcome of any RG strategy must not depend on the specific choice of the integration procedure.

Our first objective is to identify the effective action of the slow degrees of freedom after the fast fluctuations have been integrated out. To prepare this integration, it is useful to decompose a general field amplitude $\theta(\tau)$ into a slow contribution $\theta_{\rm s}(\tau)$ and its fast complementary $\theta_{\rm f}(\tau)$ part, that is $\theta(\tau) \equiv \theta_{\rm s}(\tau) + \theta_{\rm f}(\tau)$, where

$$\theta_{\rm s}(\tau) \equiv \sum_{\omega_n,{\rm s}} e^{-i\omega_n\tau}\theta_n \equiv \int_{\rm s} \frac{d\omega}{2\pi} e^{-i\omega\tau}\theta(\omega), \quad \theta_{\rm f}(\tau) \equiv \sum_{\omega_n,{\rm f}} e^{-i\omega_n\tau}\theta_n \equiv \int_{\rm f} \frac{d\omega}{2\pi} e^{-i\omega\tau}\theta(\omega). \tag{8.12}$$

Here we have introduced the abbreviations $\sum_{\omega_n,{\rm s}} \equiv \sum_{|\omega_n|<\Lambda/b}$ and $\sum_{\omega_n,{\rm f}} \equiv \sum_{\Lambda/b \ \ |\omega_n|<\Lambda}$. Anticipating that we shall be working at very low temperatures $T \ll \Lambda$, we note that one may represent the discrete frequency summations by integrals, $\int_{\rm s} d\omega \equiv \int_{|\omega|<\Lambda/b} d\omega$ and $\int_{\rm f} d\omega \equiv \int_{\Lambda/b \ \ |\omega|<\Lambda} d\omega$. (It is a good exercise to convince oneself of the legitimacy of this simplification at every step of the construction below. Also notice that, with the continuum fields, $\theta(\omega) = \theta_n/T$.)

On substituting into the continuum representation of the action (8.11),

$$S[\theta] = \frac{1}{4\pi g}\int_{|\omega|<\Lambda} \frac{d\omega}{2\pi}|\theta(\omega)|^2|\omega| + c\int d\tau\cos(\theta(\tau)), \tag{8.13}$$

one obtains $S[\theta_{\rm s},\theta_{\rm f}] = S_{\rm s}[\theta_{\rm s}] + S_{\rm f}[\theta_{\rm f}] + S_U[\theta_{\rm s},\theta_{\rm f}]$, where

$$S_{\rm s,f}[\theta_{\rm s,f}] = \frac{1}{4\pi g}\int_{\rm s,f} \frac{d\omega}{2\pi}|\theta(\omega)|^2|\omega|, \quad S_U[\theta_{\rm s},\theta_{\rm f}] = c\int d\tau\cos(\theta_{\rm s}(\tau)+\theta_{\rm f}(\tau)).$$

To proceed with this expression, we will resort to an approximation that is difficult to justify in advance. Defining $e^{-S_{\rm eff}[\theta_{\rm s}]} \equiv e^{-S_{\rm s}[\theta_{\rm s}]}\langle e^{-S_U[\theta_{\rm s},\theta_{\rm f}]}\rangle_{\rm f}$, where $\langle\cdots\rangle_{\rm f} \equiv \int D\theta_{\rm f} e^{-S_{\rm f}[\theta_{\rm f}]}(\cdots)$, and assuming that the coupling constant c is small, we approximate

$$e^{-S_{\rm eff}[\theta_{\rm s}]} = e^{-S_{\rm s}[\theta_{\rm s}]}\,\langle 1 - S_U[\theta_{\rm s},\theta_{\rm f}] + \cdots\rangle_{\rm f} \approx e^{-S_{\rm s}[\theta_{\rm s}]}e^{-\langle S_U[\theta_{\rm s},\theta_{\rm f}]\rangle_{\rm f}}. \tag{8.14}$$

That is, by assuming that the coupling constant c is in some sense small, we expand in c – which appears to be similar to our previous perturbative approaches – only to re-exponentiate it in the next step – a manipulation very different from plain perturbation theory. Evidently, the validity of this step is bound to small values of the coupling constant. However, before attempting a more qualified justification, let us tentatively accept the approximation above and explore its consequences.

Computing the average

$$\begin{aligned}\langle S_U[\theta_{\rm s},\theta_{\rm f}]\rangle_{\rm f} &= c\int D\theta_{\rm f}\, e^{-S_{\rm f}[\theta_{\rm f}]}\int d\tau\cos(\theta_{\rm f}(\tau)+\theta_{\rm s}(\tau))\\ &= \frac{c}{2}\int d\tau\, e^{i\theta_{\rm s}(\tau)}\int D\theta_{\rm f}\, e^{-\frac{1}{4\pi g}\int_{\rm f}\frac{d\omega}{2\pi}\theta(\omega)|\omega|\theta(-\omega)}e^{i\int_{\rm f}\frac{d\omega}{2\pi}e^{i\omega\tau}\theta(\omega)}+{\rm c.c.}\\ &= \frac{c}{2}\int d\tau\, e^{i\theta_{\rm s}(\tau)}e^{-\pi g\int_{\rm f}\frac{d\omega}{2\pi}|\omega|^{-1}}+{\rm c.c.}=c\int d\tau\cos(\theta_{\rm s})e^{-2\pi g\int_{\Lambda/b}^{\Lambda}\frac{d\omega}{2\pi\omega}}\\ &= c\int d\tau\cos(\theta_{\rm s})e^{-g\ln b}=cb^{-g}\int d\tau\cos(\theta_{\rm s}),\end{aligned}$$

We arrive at the remarkable conclusion that the effective action for the slow field,

$$S_{\rm eff}[\theta_{\rm s}]=\frac{1}{4\pi g}\int_{\rm s}\frac{d\omega}{2\pi}|\theta(\omega)|^2|\omega|+cb^{-g}\int d\tau\cos(\theta_{\rm s}),$$

is structurally identical to the action we started out from; in other words, we have seen that the action is renormalizable. Nonetheless, $S_{\rm eff}$ differs from the initial action S above in two important respects: firstly, the integration over the fast fields induces a change of the coupling constant of the perturbation; secondly, the new action takes values on field configurations that fluctuate only on scales $|\omega_n|<\Lambda/b$.

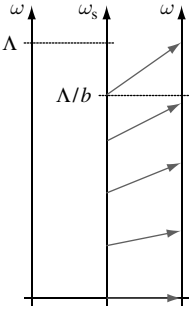

The next step of the RG program requires the comparison of the model before and after the integration over the fast fields. However, two model actions taking values on different sets of field configurations cannot be sensibly compared. Rather, one must effect a **rescaling** of the fundamental unit of frequency/time, $(\tau,\omega)\to(\tau',\omega')$, such that the transformed field $\theta_{\rm s}(\omega)\to\theta'(\omega')$ also fluctuates on all scales $|\omega'|<\Lambda$. We thus introduce a rescaled frequency variable according to

$$\omega'\equiv b\omega.$$

This change of variables engages a number of secondary transformations. In order to keep the dimensionless combination $\omega\tau$ relating time to frequency invariant, one must set $\tau'\equiv b^{-1}\tau$. As to the transformation of the field variable θ, there is some freedom (because θ is an integration variable that can be transformed arbitrarily). However, the Fourier representation Eq. (8.12) implies that, after the transformation of $\theta(\tau)$ has been fixed, the transformation of $\theta(\omega)$ follows from our previous rescaling of frequency/time. In order to keep the algebraic structure of the cosine operator invariant, we choose to define $\theta'(\tau')\equiv\theta_{\rm s}(\tau)$. Equation (8.12) then enforces the condition

$$\theta'(\omega')=b^{-1}\theta(\omega).$$

Substitution of the new variables $\omega',\tau',\theta'(\tau')$, and $\theta'(\omega')$ into the effective action then gives

$$S_{\rm eff}[\theta_s]=S'[\theta']\equiv\frac{1}{4\pi g}\int_{|\omega'|<\Lambda}\frac{d\omega'}{2\pi}|\theta'(\omega')|^2|\omega'|+cb^{1-g}\int d\tau'\cos(\theta'(\tau')).$$

Notice that the first contribution to the action remained invariant, save for the fact that the integration now extends over the full interval $|\omega'| < \Lambda$.

INFO In fact, one may note that, without any calculation, the transformation of the action under the rescaling of variables could have been anticipated from **dimensional analysis**: the definition $\omega' = b\omega$ implies that all contributions to the action of dimension [frequency]^d change by a factor b^{-d}. Since $\theta(\tau)$ is a dimensionless phase, we have $[\theta(\tau)] = 1$ while $[\theta(\omega)] = [\text{frequency}]^{-1}$. Thus, the first term of the action has dimension 1 and remains invariant. The second operator carries the dimension $[d\tau] = [\text{frequency}]^{-1}$ and, therefore, changes by a factor b.

We are now in a position to compare the effective actions $S[\theta]$ and $S'[\theta']$ before and after the integration over the fast modes. Obviously, the principal effect of the integration over fast modes is that the coupling constant of the periodic potential has changed according to the relation

$$c \to c(b) \equiv cb^{1-g}. \tag{8.15}$$

(However, do not forget a point that is implicit in the notation: the new action describes fluctuations on slower frequency scales or larger temporal scales. That this difference is not manifest in the notation is due to the fact that we chose to measure the "new" frequency continuum in rescaled variables $\omega' = b\omega$.)

This finding contains a preliminary answer to the question formulated above. To recapitulate, we asked how the presence of the dissipative term manifests itself in the facility to tunnel. We have found that an integration over short-scale fluctuations of the collective field θ alters the effective strength of the potential. (In the context of the quantum impurity problem in the wire, this change is a manifestation of the mutual influence of the Friedel scattering pattern and interactions in the electron gas. Indeed, it is apparent that in the non-interacting case, i.e. for $g = 1$ (cf. Eq. (4.52)), the coupling constant does not change. For repulsive (attractive) interactions, $g < 1$ ($g > 1$) the coupling increases (decreases) in accord with the qualitative picture formulated above.)

However, at this stage, our result merely indicates how the coupling constant changes after one RG step. Notably, Eq. (8.15) depends in a non-universal manner on how we choose to dissect the frequency spectrum (the parameter b). However, ideally, we would like to know the value of the coupling constant after all degrees of freedom down to a certain infrared cutoff scale $\omega_{\min}$ have been integrated out. (For example, the role of $\omega_{\min}$ might be taken by temperature, the oscillation frequency of an external perturbation, etc.) The general route towards obtaining this information is to iterate the RG step, i.e., setting $c \equiv c^{(0)}$ and $c' \equiv c^{(1)}$, explore the sequence of coupling constants $c^{(0)} \to c^{(1)} \to c^{(2)} \to \cdots$ In all that follows, it is convenient to think of this sequence as a kind of dynamical system. In each discrete "time step," the variable c changes according to $c \to c' = cb^{1-g} = ce^{\ln b(1-g)}$. Assuming that $b = 1 + \epsilon$ is very close to unity (which means that, in each step, only an asymptotically thin layer in frequency space is "shaven off"), we can encapsulate this information in the differential equation $\frac{c'-c}{\epsilon} \approx \frac{dc}{d\epsilon} \approx \frac{dc}{d\ln b} = c(1-g)$. The evolution equation

describing the flow of the coupling constant under an infinitesimal change of the control parameter,

$$\boxed{\frac{dc}{d\ln b} \equiv \beta(c) = c(1-g),} \tag{8.16}$$

is known as a **Gell-Mann–Low equation**. For historical reasons, the right-hand side of the equation is called the β**-function**.

Equation (8.16) makes the interpretation of the RG-generated change of the coupling constant as a dynamical system manifest. Thinking of the parameter $t \equiv \ln b$ as a "time coordinate," we can integrate the evolution equation to obtain[9] $c(t) = c(0)e^{(1-g)t}$, where $c(t=0) = c(b=1)$ has the status of the bare coupling constant of the theory. (Remember that, for $b = 1$, $\Lambda_{\rm eff} = \Lambda/b = \Lambda$, which is the level of the unrenormalized theory.)

Having inferred the RG flow, one may wonder at what "time" $t_{\max}$ should we stop the renormalization? What is the "real" value of the coupling constant? The answers to these questions are somewhat application-specific. For example, we might have coupled the system to an external perturbation of characteristic frequency ω_m. In that case, we might want to integrate out all degrees of freedom with frequency $\omega_{n>m}$ to then explore the effective low-energy theory at scales $\sim \omega_m$, i.e. we would set $\Lambda_{\rm eff} = \omega_m$, or $t = \ln(\Lambda/\omega_m)$. The effective theory would then look structurally identical to the microscopic model but with a renormalized coupling constant $c = c(0)(\Lambda/\omega_m)^{1-g} \propto \omega_m^{g-1}$. (Notice that both the bare constant $c(0)$ and the cutoff Λ depend in a non-universal manner on microscopic elements of the model. The use of the proportionality sign indicates that we are not, in general, interested in these details but rather focus on the dependence of the coupling constant on the low-energy scale ω_m.) Alternatively, we might want to integrate out all degrees of freedom down to the lowest frequency allowed by Matsubara frequency quantization, $\Lambda_{\rm eff} = 2\pi T$. In this case, $c \propto T^{g-1}$. For a system of finite extent L, we might argue that the spectrum of the modes $\theta(k)$ is quantized with $\omega_{\min} = \pi v/L$. In this case, the effective value of the coupling at the lowest frequencies would be $c \propto L^{1-g}$. Summarizing, the RG flow should be terminated at a low-energy scale determined by the specific problem under consideration.

Our results so far on the behavior of the coupling constant are summarized in the bottom part of the figure below. We have found that, for interaction parameters $g > 1\,(g < 1)$, the coupling constant c decreases (increases). The "non-interacting" case $g = 1$ defines a fixed line where the coupling strength does not change. However, at this stage, we must remember that the analysis was based on a spurious expansion of the action to first order in the impurity operator. This implies that, in the repulsive case, even if the initial value of the coupling constant was small, it will soon flow into a region where the perturbative RG analysis loses its meaning (indicated by a wavy line in the figure).

[9] Critical readers will notice that this result coincides with the change of the coupling constant obtained after the first RG step. This coincidence, however, is a consequence of the simple structure of the β-function in the present example. In more complicated cases, the change of the coupling constant after an infinitesimal RG step will structurally differ from the result obtained after following the RG flow all the way down to the IR cutoff. The concept of a β-function and its integration are therefore indispensable elements of the theory.

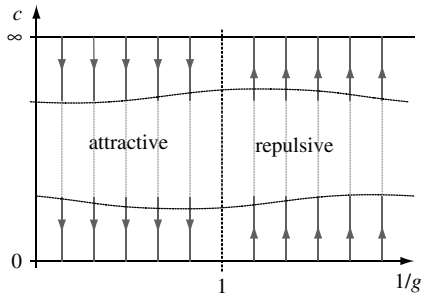

How do we know what happens after the coupling constant has disappeared into the forbidden zone? Remarkably, it turns out that, for the particular model in question, not only the regime of a weak potential but also the complementary case of an asymptotically large potential (the upper part of the figure) is amenable to analytical investigation. As a result of a strong coupling perturbative expansion (see Problem 8.8.1) one may show that the coupling constant flows to (away from) infinite coupling for repulsive (attractive) interactions. It is thus tempting to conjecture a globally increasing/decreasing flow continuously interpolating between the two asymptotic regimes. (Application of the machinery of conformal field theory to the problem has indeed shown this conjecture to be true.)

Therefore, when put together, we arrive at a remarkable conclusion. For $g > 1$, the strength of the potential flows to zero, implying that the asymptotic dependence at zero temperature is free: the particle can tunnel freely between minima of the potential. However, for $g < 1$, the coupling constant flows to infinity, implying that the particle becomes localized, confined to a minimum of the potential.

INFO Notwithstanding the limitation to small values of the coupling, we still have to discuss the **consistency of the fast field integration**, i.e. to show that the re-exponentiation of the potential operator after the averaging over fast fluctuations (see Eq. (8.14)) underlying the previous analysis is legitimate. According to Eq. (8.14), the functional average of the exponentiated action can effectively be replaced by the exponential of the averaged action, $\langle \exp(-S_c)\rangle \approx \exp(-\langle S_c\rangle)$. To explore the integrity of this assumption, let us explore the relevance of a typical correction. For example, an expansion of the exponent to second order in the potential operator would lead to expressions of the type

$$\left\langle c^2 \int d\tau\, d\tau'\, \cos(\theta_s(\tau) + \theta_f(\tau)) \cos(\theta_s(\tau') + \theta_f(\tau')) \right\rangle_c ,$$

where, here, we used the connected average $\langle \hat{A}\hat{B}\rangle_c \equiv \langle \hat{A}\hat{B}\rangle - \langle \hat{A}\rangle\langle \hat{B}\rangle$ since the square of the averaged action $\sim (\langle c \int d\cos(\theta)\rangle)^2$ is already included in our previous scheme. At first sight, this expression looks worrisome. By averaging over the fast field θ_f we are bound to generate a composite operator that depends in a non-local manner on two time arguments τ and τ'. Re-exponentiation of these objects would lead to an action much more complicated than the original.

However, before losing hope, let us have a closer inspection of the fast field average of the expression above. Representing the cos-functions as sums of exponentials, we are led to consider

expressions of the type

$$\begin{aligned}
&\left\langle \exp\left[\pm i(\theta_{\rm s}(\tau)+\theta_{\rm f}(\tau))\right]\exp\left[\pm i(\theta_{\rm s}(\tau')+\theta_{\rm f}(\tau'))\right]\right\rangle_{\rm c}\\
&\quad\propto\left\langle\exp\left[i\int_{\rm f}\frac{d\omega}{2\pi}\quad\pm e^{i\omega\tau}\pm e^{i\omega\tau'}\quad\theta(\omega)\right]\right\rangle-\left(\left\langle\exp\left[\pm i\int_{\rm f}\frac{d\omega}{2\pi}\,e^{i\omega\tau}\theta(\omega)\right]\right\rangle\right)^2\\
&\quad=\exp\left[-2\pi g\int_{\rm f}\frac{d\omega}{2\pi}\,|\omega|^{-1}\quad 1\pm\cos(\omega(\tau-\tau'))\quad\right]-\left(\exp\left[-\pi g\int_{\rm f}\frac{d\omega}{2\pi}\,|\omega|^{-1}\right]\right)^2\\
&\quad=b^{-2g}\left(\exp\quad\mp 4\pi g\int_{\Lambda/b}^{\Lambda}\frac{d\omega}{2\pi\omega}\,\cos(\omega(\tau-\tau'))\quad-1\right)\approx 0.
\end{aligned}$$

Here, the $\pm$ signs in the first line indicate the four different possible combinations of signs; in the second equality we have used our previous results on the integrals over the high-lying frequency shell; and in the crucial third equality, we have noticed that, typically, $(\tau-\tau')>b/\Lambda, 1/\Lambda$ such that the oscillatory term integrates to something close to zero and can be neglected in comparison with the constant.

The estimate above is limited to time arguments $|\tau-\tau'|\Lambda/b>1$ outside a narrow strip $|\tau-\tau'|\sim b/\Lambda$. To show that the contribution of composite operators from these domains is also negligible, we employ an argument that is symptomatic for RG analyses: consider the connected average

$$\begin{aligned}
&\left\langle c^2\int_{|\tau-\tau'|<b/\Lambda}d\tau\,d\tau'\,\cos(\theta_{\rm s}(\tau)+\theta_{\rm f}(\tau))\cos(\theta_{\rm s}(\tau')+\theta_{\rm f}(\tau'))\right\rangle_{\rm c}\\
&\qquad\propto b\int d\tau\,\left\langle\cos^2(\theta_{\rm s}(\tau))+\theta_{\rm f}(\tau)\right\rangle_{\rm c}\propto b^{-4g+1}\int d\tau\,\cos^2(\theta_{\rm s}(\tau))+\text{const.},
\end{aligned}$$

where the notation highlights the fact that the integration area is proportional to b, and we have used the fact that, for those narrow time windows, the field integration will be oblivious to the difference between $\theta(\tau)$ and $\theta(\tau')$. The second proportionality is obtained by averaging the integrand along the lines of our previous calculations.

After the rescaling of time and frequency to restore the old cutoff, the operator gets multiplied by another factor of b, i.e. the overall scaling factor is given by $b^{2(1-2g)}$. This factor tells us that the composite operator generated by higher-order cumulative expansion of the action is of less **operator relevance** than the contributions we are keeping. For values of the interaction $g\approx 1$ not too distant from unity, the relative value of the coupling constants of the anomalous operator ($\propto b^{2(1-2g)}$) and of the standard $\cos\theta$ contribution ($\propto b^{1-g}$) will scale to 0 as b is increased. A classification of operators according to their relevance under the RG transformation indeed forms the general basis for the limitation of low-energy actions to few contributions, namely those contributions that promise to be of strongest scaling relevance as larger and larger field fluctuations are probed. We will discuss this point more systematically in the next section.

Before leaving this section, let us make a few general observations about the renormalization procedure. We first notice that it would have been futile to attack the problem by the "plain" perturbation theory developed in Chapter 5. The reason is that the propagator of the $(0+1)$-dimensional effective theory, $|\omega|^{-1}$, leads to logarithmic divergences when integrated over unbounded frequency intervals, i.e. the present theory is again plagued by the UV/IR divergences observed above in different contexts. In Section 5.1 we had argued

that, in principle, a way to overcome these problems was to introduce a UV and, if needed, an IR cutoff into the theory. However, we soon dismissed this option because it seemed evident that it would lead to spurious non-universal cutoff dependences of physical results.

How do these observations relate to what we are doing presently? Obviously, the present[10] version of the RG procedure also relies on the introduction of a cutoff regularizing the logarithmic UV divergences mentioned above; apparently, the RG procedure shares a lot of structures with the perturbative approach. But, somehow, we managed to extract the information in which we were interested – the dependence of the potential strength on long-range system parameters – in a manner independent of the cutoff.[11] The key to obtaining this information was to introduce not one, but an entire hierarchy of cutoffs and to integrate over each of these domains recursively.

Now, a subtle and important point is that this procedure does not imply that the cutoff or, more generally, short-scale fluctuations of the model have silently made their way out of the theory. After all, the UV divergences mentioned before are manifestations of a large "phase volume" of field fluctuations that are likely to somehow affect the behavior of the system. To understand the "implicit" way through which these fluctuations enter our results, let us return to a remark made on page 425. There, we had noted that, upon scaling frequency/time, each operator changes according to its physical dimension. An operator carrying the dimension $[\text{time}]^d$ would acquire a scaling factor b^d. The scaling dimension of an operator predicted by its "physical" dimension is called the **naive scaling dimension**, the **canonical scaling dimension**, or, for obscure reasons, the **engineering dimension**.

The designations indicate, however, that these dimensions are not the last word on the actual scaling behavior of an operator. Indeed, the net result of the RG analysis was that our operator of interest, $\int d\tau \cos\theta$, an object of engineering dimension 1, changes according to b^{1-g}. The correction to the naive scaling dimension (presently, g) is called the **anomalous dimension** of an operator. Its origin lies in the (cutoff-dependent) phase volume of fluctuations co-determining the change of an operator during each RG step. Put differently, we can say that the cutoff Λ, by itself a quantity of dimension $[\text{time}]^{-1}$, acts as a "gray eminence" implicitly affecting the scaling behavior of an operator. The anomalous scaling dimensions of the theory effectively determine its long-range observable behavior and, therefore, represent quantities of prime interest.

8.3 Renormalization group: general theory

Having discussed two extended examples, we are in a position to attempt a reasonably general outline of the RG strategy. Suppose we are given a field theory defined through the

[10] Below we become acquainted with UV regularization procedures that are not based on introduction of a cutoff.

[11] One may object that the solutions of the β-functions given above actually *do* contain the bare cutoff, through an initial condition; they also depend on the bare coupling strength and, possibly, other "non-universal" parameters. However, that need not worry us: in most applications (both experimental and theoretical) one is interested not so much in the "absolute value" of physical observables (as these usually depend on unknown material parameters anyway) but rather in the way these observables change as a relevant control parameter is varied. The important feature found above is that the rate at which the effective potential strength varies with temperature, say, is largely universal and cutoff-independent.

action

$$S[\phi] \equiv \sum_{a=1}^{N} g_a \mathcal{O}_a[\phi],$$

where ϕ is some (generally multi-component) field, g_a are coupling constants and $\mathcal{O}_a[\phi]$ a certain set of operators. For concreteness, one may think of these operators as $\mathcal{O}_a = \int d^d x\, (\nabla\phi)^n \phi^m$, i.e. as space–time local operators involving powers of the field and its derivatives – although more general structures are conceivable.[12] By "renormalization of the theory," we refer to a scheme to derive a set of **Gell-Mann–Low equations** describing the change of the coupling constants $\{g_a\}$ as fast fluctuations of the theory are successively integrated out.

8.3.1 Gell-Mann–Low equations

There are a number of methodologically different procedures whereby the set of flow equations can be obtained from the microscopic theory. Here, we formulate this step in a language adjusted to applications in statistical field theory (as opposed to, say, particle physics). While there is considerable freedom in the actual implementation of the RG procedure, all methods share the feature that they proceed in a sequence of three more or less canonical steps.

I: Subdivision of the field manifold

In the first step, one may decompose the integration manifold $\{\phi\}$ into a sector to be integrated out, $\{\phi_{\rm f}\}$, and a complementary set, $\{\phi_{\rm s}\}$. For example:

- ▷ We may proceed according to a generalized **block spin scheme** and integrate over all degrees of freedom located within a certain structural unit in the base manifold $\{\mathbf{x}\}$. (This scheme is adjusted to lattice problems where $\{\mathbf{x}\} = \{\mathbf{x}_i\}$ is a discrete set of points. However, as pointed out above, even then it is difficult to implement analytically.)
- ▷ We could decide to integrate over a certain sector in momentum space. When this sector is defined to be a shell $\Lambda/b \leq |\mathbf{p}| < \Lambda$, one speaks of a **momentum shell integration**. Naturally, within this scheme, the theory will be explicitly cutoff-dependent at intermediate stages.
- ▷ Alternatively, we may decide to integrate over all high-lying degrees of freedom $\lambda^{-1} \leq |\mathbf{p}|$. In this case, we will of course encounter divergent integrals. An elegant way to handle these divergences is to apply **dimensional regularization**. Within this approach one formally generalizes from integer dimensions d to fractional values $d \pm \epsilon$. One motivation for doing so (for another, see below) is that, miraculously, the formal extension of the characteristic integrals appearing during the RG step to non-integer dimensions are finite. As long as one stays clear of the dangerous values $d =$ integer one can then safely monitor the

[12] In our previous example of the Luttinger liquid, there appeared an operator $\int (d\omega/2\pi)\theta(\omega)|\omega|\theta(-\omega)$. When represented in space-time, this operator is highly non-local.

dependence of the integrals on the IR cutoff λ^{-1}. For a good introduction to dimensional generalization we refer to the textbook by Ryder.[13]

▷ For a discussion of alternative schemes, such as the introduction of short-distance real space cutoffs underlying the so-called **operator product expansion**, we refer to the literature (see, e.g., the excellent text by Cardy.[1])

II: RG step

The second, and central, part of the program is to actually integrate over short–range fluctuations. As exemplified above, this step usually involves approximations. In most cases, one will proceed by a so-called **loop expansion**, i.e. one organizes the integration over the fast field $\phi_{\rm f}$ according to the number of independent momentum integrals – loops[14] – that occur after the appropriate contractions. Of course, this strategy makes sense only if we can guarantee that the contribution of loops of higher orders is in some sense small, a precondition that is, alas, often difficult to meet. At any rate, to engage loop numbers as an expansion parameter, we first need to understand the key role played by space-dimensionality in the present context. We return to this point in Section 8.4.

Following the procedure, an expansion over the fast degrees of freedom gives an action

$$S'[\phi_s] \equiv \sum_a g'_a \mathcal{O}'_a[\phi_s],$$

in which coupling constants of the remaining slow fields are altered. Notice that the integration over fast field fluctuations may (and usually does) lead to the generation of "new" operators, i.e. operators that have not been present in the bare action. In such cases one has to investigate whether the newly generated operators are "relevant" (see below) in their scaling behavior. If so, the appropriate way to proceed is to include these operators in the action from the very beginning (with an *a priori* undetermined coupling constant). One then verifies whether the augmented action represents a complete system, i.e. one that does not lead to the generation of operators beyond those that are already present. If necessary, one has to repeat this step until a closed system is obtained.

III: Rescaling

One next rescales frequency/momentum so that the rescaled field amplitude ϕ' fluctuates on the same scales as the original field ϕ, i.e. one sets

$$q \to bq, \quad \omega \to b^z \omega.$$

Here, the **frequency renormalization exponent** or **dynamical exponent** z may be unity, two, or sometimes a non-integer value, depending on the effective dispersion relating frequency and momentum. We finally note that the field ϕ, as an integration variable, may be rescaled arbitrarily. Using this freedom, we select a term in the action which we believe governs the behavior of the "free" theory – in a theory with elastic coupling this might,

[13] L. H. Ryder, *Quantum Field Theory* (Cambridge University Press, 1996).
[14] For the definition of loops, see Section 5.1.

for example, be the leading-order gradient operator $\sim \int d^d r (\nabla\phi)^2$ – and require that it be strictly invariant under the RG step. To this end we designate a dimension L^{d_ϕ} for the field, chosen so as to compensate for the factor b^x arising after the renormalization of the operator. The rescaling

$$\phi \to b^{d_\phi}\phi,$$

is known as **field renormalization**. It renders the "leading" operator in the action scale invariant.

As a result of all these manipulations, we obtain a renormalized action

$$S[\phi] = \sum_a g'_a \mathcal{O}_a[\phi],$$

which is entirely described by the set of changed coupling constants, i.e. the effect of the RG step is fully encapsulated in the mapping

$$\mathbf{g}' = \tilde{R}(\mathbf{g}),$$

relating the old value of the vector of coupling constants, $\mathbf{g} = \{g_a\}$, to the renormalized one, $\mathbf{g}' = \{g'_a\}$. By letting the control parameter, $\ell \equiv \ln b$, of the RG step assume infinitesimal values, one can make the difference between bare and renormalized coupling constants arbitrarily small. It is then natural to express the difference $\mathbf{g}' - \mathbf{g} = \tilde{R}(\mathbf{g}) - \mathbf{g}$ in the form of a **generalized β-function** or **Gell-Mann–Low equation**

$$\boxed{\frac{d\mathbf{g}}{d\ell} = R(\mathbf{g}),} \tag{8.17}$$

where the right-hand side is defined through the relation $R(\mathbf{g}) = \lim_{\ell\to 0} \ell^{-1}(\tilde{R}(\mathbf{g}) - \mathbf{g})$.

INFO As mentioned at the beginning of the section, the formulation of the RG step above is actually not the only one possible. For instance, in high-energy physics, **other renormalization schemes** appear to be more natural. In this area of physics, there is actually no reason to believe in the existence of a well-defined "bare" action with finite coupling constants. (Contrary to the situation in condensed matter physics, the bare action of quantum electrodynamics, say, is in principle inaccessible.) However, one may legitimately require that, after an integration over UV-divergent fluctuations, the "renormalized" coupling constants of the theory (which, in turn, determine observables such as the physical electron mass) are finite. One may then postulate that the bare coupling constants of the theory are actually infinite. The value of these infinities is fine-tuned so as to combine with the fluctuation-induced "infinities" to realize finite renormalized coupling constants. Alternatively, one may deliberately add extra operators, **counter-terms**, to the action which are designed so as to cancel divergences due to fluctuations. However, the net result of all these RG schemes (which are by and large equivalent) is a mapping describing the flow of the coupling constants upon variation of a control parameter.

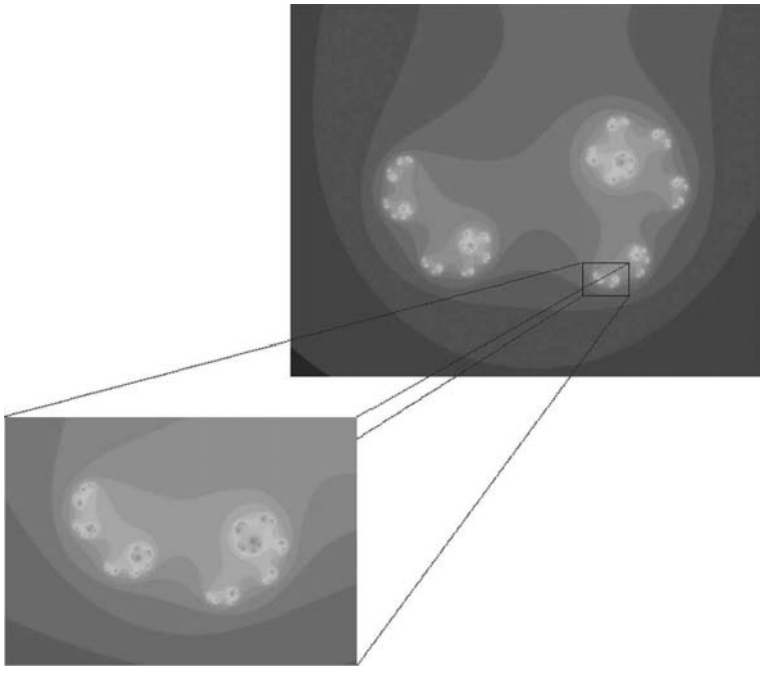

Figure 8.4 The fractal Julia set is self-similar in the sense that any sub-region of it contains the full information of the original set.

8.3.2 Analysis of the Gell-Mann–Low equation

The Gell-Mann–Low equation (8.17) represents the principal result of an RG analysis. Thinking of the control parameter ℓ as a kind of "flow parameter," one may identify this equation as a generalized dynamical system, namely the system describing the evolution of the effective coupling constants of a model upon changing length or time scales. As with any dynamical system, the prime structural characteristic of the set of equations (8.17) is the set of **fixed points**, i.e. the submanifold $\{\mathbf{g}^*\}$ of points in coupling constant space which are stationary under the flow: $R(\mathbf{g}^*) = 0$. Once the coupling constants are fine-tuned to a fixed point, the system no longer changes under subsequent RG transformations. In particular it remains invariant under the change of space/time scale associated with the transformation. Alluding to the fact that they look the same no matter how large a magnifying glass is used, systems with this property are referred to as **self-similar**. (For example, **fractals** such as the Julia set shown in Fig. 8.4 are paradigmatic examples of self-similar systems; the magnification of any sub-region of the fractal looks identical to the full system.)

Now, to each system, one can attribute at least one intrinsic length scale, namely the length ξ determining the exponential decay of field correlations. However, the existence of a finite, and pre-determined, intrinsic length scale clearly does not go together with invariance under scale transformations. We thus conclude that, at a fixed point, either $\xi = 0$ (not so interesting), or $\xi = \infty$. However, a diverging correlation length $\xi \to \infty$ is a hallmark of

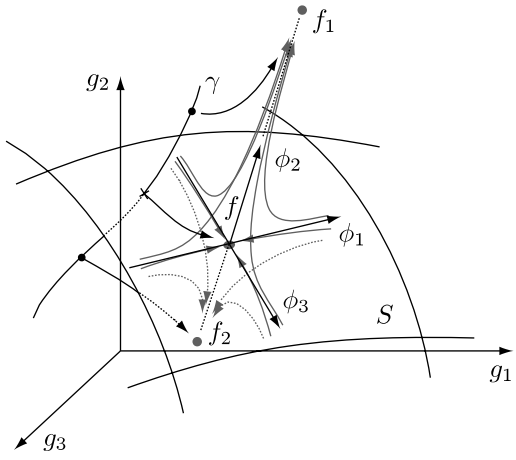

Figure 8.5 Showing the RG flow in the vicinity of a fixed point with two irrelevant (ϕ_1, ϕ_3) and one relevant (ϕ_2) scaling fields. The manifold S defined through the vanishing of the relevant field, $\phi_2 = 0$, is called a **critical surface**. On this submanifold, the RG flow is directed towards the fixed point f. Deviations off criticality make the system approach one of the stable fixed points f_1 and f_2.

a second-order phase transition. We thus tentatively identify fixed points of the RG flow as candidates for "transition points" of the physical system. (For a more comprehensive review of phase transitions and the critical phenomena accompanying them, see the Info block starting on page 436 below.) This being so, it is natural to pay special attention to the behavior of the flow in the immediate vicinity of the fixed-point manifolds. If the set of coupling constants, $\mathbf{g}$, is only close enough to a fixed point, $\mathbf{g}^*$, it will be sufficient to consider the linearized mapping

$$R(\mathbf{g}) \equiv R((\mathbf{g}-\mathbf{g}^*)+\mathbf{g}^*) \simeq W(\mathbf{g}-\mathbf{g}^*), \quad W_{ab} = \left.\frac{\partial R_a}{\partial g_b}\right|_{\mathbf{g}=\mathbf{g}^*}.$$

To explore the properties of flow, let us assume that we had managed to diagonalize the matrix W. Denoting the eigenvalues by $\lambda_\alpha, \alpha = 1, \ldots, N$, and the *left*-eigenvectors[15] by ϕ_α, we have

$$\phi_\alpha^T W = \phi_\alpha^T \lambda_\alpha.$$

The advantage of proceeding via the unconventional set of left-eigenvectors is that it allows us to conveniently express the flow of the physical coupling constants under renormalization. To this end, let v_α be the αth component of the vector $\mathbf{g}-\mathbf{g}^*$ when represented in the basis $\{\phi_\alpha\}$:

$$v_\alpha = \phi_\alpha^T(\mathbf{g}-\mathbf{g}^*).$$

[15] Since there is no reason for W being symmetric, the left- and right-eigenvectors may be different.

These components display a particularly simple behavior under renormalization:

$$\frac{dv_\alpha}{d\ell} = \phi_\alpha^T \frac{d}{d\ell}(\mathbf{g} - \mathbf{g}^*) = \phi_\alpha^T W(\mathbf{g} - \mathbf{g}^*) = \lambda_\alpha \phi_\alpha^T (\mathbf{g} - \mathbf{g}^*) = \lambda_\alpha v_\alpha .$$

Under renormalization, the coefficients v_α change by a mere scaling factor λ_α, wherefore they are called **scaling fields** – a somewhat unfortunate nomenclature. (The coefficients v_α are actually not fields but simply a set of ℓ-dependent coefficients, the vector of coupling constants when expressed in the basis of eigenvectors ϕ_α.) These equations are trivially integrated to obtain

$$\boxed{v_\alpha(\ell) \sim \exp(\ell \lambda_\alpha).}$$

This result suggests a discrimination between at least three different types of scaling fields:

- ▷ For $\lambda_\alpha > 0$ the flow is directed away from the critical point. The associated scaling field is said to be **relevant** (in the sense that it forcefully drives the system away from the critical region). In Fig. 8.5, v_2 is a relevant scaling field.
- ▷ In the complementary case, $\lambda_\alpha < 0$, the flow is attracted by the fixed point. Scaling fields with this property (v_1, v_3) are said to be **irrelevant**.[16]
- ▷ Finally, scaling fields which are invariant under the flow, $\lambda_\alpha = 0$, are termed **marginal**.[17]

The distinction of relevant/irrelevant/marginal scaling fields in turn implies a classification of different types of fixed points:

- ▷ Firstly, there are **stable fixed points**, i.e. fixed points whose scaling fields are all irrelevant or, at worst, marginal. These points define what we might call "stable phases of matter": when you release a system somewhere in the parameter space surrounding any of these attractors, it will scale towards the fixed point and eventually sit there. Or, expressed in more physical terms, looking at the problem at larger and larger scales will make it more and more resemble the infinitely correlated self-similar fixed-point configuration. (Recall the example of the high-temperature fixed line of the one-dimensional Ising model encountered earlier.) By construction, the fixed point is impervious to moderate variations in the microscopic morphology of the system, i.e. it genuinely represents what one might call a "state of matter."
- ▷ Complementary to stable fixed points, there are **unstable fixed points**. Here, all scaling fields are relevant (cf. the $T = 0$ fixed point of the 1-D Ising model). These fixed points represent the concept of a Platonic ideal: you can never get there and, even if you managed

[16] The terminology "irrelevant" indicates that a scaling field of negative dimension usually does not play much of a physical role. There are, however, exceptions to this rule. For instance, it may happen that the free energy of the system depends in a singular manner on an irrelevant scaling variable – in which case the variable is called **dangerously irrelevant**. Dangerously irrelevant scaling variables not only strongly affect the outcome of the theory, but also invalidate the applicability of a number of established concepts of RG theory (such as the scaling laws to be discussed below).

[17] A marginal scaling field corresponds to a direction in coupling constant space with vanishing partial derivative, $\partial_{\phi_\alpha} R|_{\mathbf{g}^*=0} = 0$. In this case, to obtain a refined picture, one sometimes considers the second-order derivative, $\partial^2_{\phi_\alpha} R|_{\mathbf{g}^*=0} \equiv 2x$. In the vicinity of the fixed point, the scaling field then behaves as $d\ v_\alpha = x v_\alpha^2$. For $x > 0$ ($x < 0$) the field has the status of a **marginally relevant (irrelevant)** scaling field. It is relevant (irrelevant) on account of the non-vanishing direction of the flow. However, it is also "marginal" because the speed of the flow decreases upon approaching the critical regime.

to approach it closely, the harsh conditions of reality will make you flow away from it. Although unstable fixed points do not correspond to realizable forms of matter, they are of importance inasmuch as they "orient" the global RG flow of the system.

▷ Finally, there is the **generic class of fixed points** with both relevant and irrelevant scaling fields. These points are of particular interest inasmuch as they can be associated with **phase transitions**. To understand this point, we first note that the r eigenvectors Φ_α associated with irrelevant scaling fields span the tangent space of an (r)-dimensional manifold known as the **critical surface**. (A schematic illustration for the case $r = 2$ is shown in Fig. 8.5.) This critical manifold forms the **basin of attraction** of the fixed point, i.e. whenever a set of physical coupling constants $\mathbf{g}$ is fine-tuned so that $\mathbf{g} \in S$, the expansion in terms of scaling fields contains only irrelevant contributions and the system will feel attracted to the fixed point as if it were a stable one.

However, the smallest deviation from the critical surface introduces a relevant component driving the system exponentially away from the fixed point. A sketch of the resulting flow is shown in Fig. 8.5 for the case of just one relevant scaling field. For example, in the case of the ferromagnetic phase transition – discussed in more detail in the next section – deviations from the critical temperature T_c are relevant. If we consider a system only slightly above or below T_c, it may initially (on intermediate length scales) appear to be critical. However, upon further increasing the scale, the relevant deviation will grow and drive the system away from criticality, either towards the stable high-temperature fixed point of the paramagnetic phase ($T > T_\mathrm{c}$) or towards the ferromagnetic low-temperature phase ($T < T_\mathrm{c}$).

This picture actually suggests that systems with generic fixed points typically possess complementary stable fixed points, i.e. fixed points towards which the flow is directed after it has left the critical region. We also notice that a scaling direction that is relevant at one fixed point (e.g. Φ_2 at the critical fixed point) may be irrelevant at others (Φ_2 at the high- and low-temperature fixed points).

INFO The discussion above suggests that the concept of renormalization is intimately linked to the **theory of phase transitions and critical phenomena**, the traditional platform for the development of the subject in the literature. In view of the existing wealth of literature (and acknowledging the fact that we are approaching the field from a more operational perspective), we shall not endeavor to present another "introduction to the theory of critical phenomena." Rather, we will summarize in a concise, but hopefully self-contained, manner, those few tenets and principles that are necessary to place the concept of renormalization into a larger physical context.

The most fundamental[18] signature of a phase transition is its **order parameter**, M, i.e., a quantity whose value unambiguously identifies the phase of the system. Examples from classical statistical mechanics include the magnetization for the ferromagnetic–paramagnetic transition, the density for the liquid–vapor transition, the order parameter amplitude for the BCS transition, etc. (However, to keep the terminology concrete, we shall mostly use the language of the ferromagnetic transition in the following.)

[18] Notice that there are transitions whose order parameter is actually unknown. A famous example is the **quantum Hall transition** discussed in more detail in Section 9.3.4.

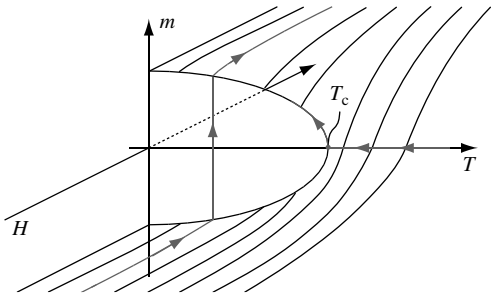

Figure 8.6 Phase diagram of the ferromagnetic transition. Tuning a magnetic field at fixed temperature $T < T_c$ through zero causes the magnetization to jump discontinuously: $[0, T_c]$ is a line of first-order transitions. This line terminates in the unique second-order transition point of the system, $(T = T_c, H = 0)$. Lowering the temperature at $H = 0$ causes the non-analytic, but continuous, development of a finite magnetization at $T < T_c$.

Transitions between different phases of matter fall into two large categories.[19] In **first-order** phase transitions the order parameter exhibits a discontinuous jump across the transition line while, in the complementary class of **second-order** transitions, the order parameter changes in a non-analytic but continuous manner. (The two cases are exemplified in Fig. 8.6 by the classical ferromagnet.)

The phenomenology of second-order transitions is generally richer than that of first-order transitions. As a thermodynamic state variable, the order parameter is coupled to a **conjugate field**, $H : M = -\partial_H F$, where F is the free energy. At a second-order transition, M changes non-analytically, which means that the second-order derivative, a **thermodynamic susceptibility**, $\chi = -\partial_H^2 F$, develops a singularity. Now, you may recall from the discussion of the fluctuation dissipation theorem that the susceptibility is intimately linked to the field fluctuation behavior of the system. More precisely, χ is proportional to the integral over the correlation function C determining the fluctuation behavior of the fields (cf. Eq. (8.3)). A divergence of the susceptibility implies the accumulation of infinitely long-range field fluctuations.

The divergence of the susceptibility goes hand in hand with non-analytic and/or singular behavior of all sorts of other physical quantities. In fact, an even stronger statement can be made. We have seen that, right at the transition/fixed point, the system is self-similar. This implies that the behavior of its various characteristics must be described by **power laws**. Referring for a more substantial discussion to Section 8.3.3 below, we here merely support this statement by a heuristic argument. Consider a function $f(t)$, where f is representative of an observable of interest and t is a control parameter (a scaling field) determining the distance to the transition point. In the immediate vicinity of the transition point, f is expected to "scale," i.e. under a change of the length scale $x \to x/b$, $t \to tb^{-D_t}$, the function f must, at most, change by a factor reflecting its own scaling dimension. $f(t) = b^{D_f} f(tb^{-D_t})$. (A more serious, structural change of the function would be in conflict with asymptotic self-similarity.) Mathematically speaking, this equation amounts to homogeneity of the function f, equivalently expressed by $f \sim t^{D_f/D_t}$.

[19] Readers absolutely unfamiliar with the thermodynamics of phase transitions may wish to consult the corresponding section of a textbook on statistical mechanics.

The set of different exponents characterizing the relevant power laws occurring in the vicinity of the transition are known as **critical exponents**. For at least four different reasons, the set of critical exponents represents the most important structural fingerprint of a transition:

1. They carry universal significance, i.e. we do not have to invent a set of critical exponents for each transition anew. (For example, the divergence of the correlation length, $\xi \sim |t|^{-}$, is characterized by a critical exponent commonly, and irrespective of the particular transition under consideration, denoted by ν.)
2. The set of critical exponents carries the same information as the set of exponents of the scaling fields, i.e. knowledge of the critical exponents is equivalent to the knowledge of the linear dynamical system characterizing the flow in the transition region. (In fact, the set of critical exponents overdetermines the scaling field exponents, i.e. it contains redundancy. For example, of the six critical exponents characterizing the magnetic transition, only two are independent. The others are interrelated by[20] **scaling laws** or **exponent identities** to be discussed below.
3. Critical exponents are fully universal; they are numbers depending, at most, on dimensionless characteristics such as the space-time dimensionality or number of components of the order parameter.
4. Perhaps most importantly, the critical exponents represent quantities that can be measured. In fact, their universality and structural importance make them quantities of prime experimental interest.

In the following, let us briefly enumerate the list of the most relevant exponents, α, β, γ, δ, η, ν, and z.[21] Although we shall again make use of the language of the magnetic transition, it is clear that (and, indeed, how) the definitions of most exponents generalize to other systems.

α: In the vicinity of the critical temperature, the **specific heat** $C = -T\partial_T^2 F$ scales as $C \sim |t|^{-\alpha}$, where $t = (T - T_c)/T_c$ measures the distance to the critical point. Note that, by virtue of this definition, a non-trivial statement has been made: although the phases above and below the transition are essentially different, the scaling exponents controlling the behavior of C are identical. The same applies to most other exponents listed below.

β: Approaching the transition temperature from below, the **magnetization** vanishes as $M \equiv -\partial_H F\big|_{H \;\; 0} \sim (-t)^{\beta}$.

γ: The **magnetic susceptibility** behaves as $\chi \equiv \partial_h M|_{h \;\; 0} \sim |t|^{-\gamma}$.

δ: At the critical temperature, $t = 0$, the **field dependence of the magnetization** is given by $M \sim |h|^{1/\delta}$.

ν: Upon approaching the transition point, the **correlation length** diverges as $\xi \sim |t|^{-}$.

η: This implies that the correlation function,

$$C(\mathbf{r}) \sim \begin{cases} \frac{1}{|\mathbf{r}|^{d-2+}}, & |\mathbf{r}| \ll \xi, \\ \exp[-|\mathbf{r}|/\xi], & |\mathbf{r}| \gg \xi, \end{cases}$$

crosses over from exponential to a power law scaling behaviour at the length scale ξ. To motivate the power, one may notice that $C \sim \langle\phi\phi\rangle$ carries twice the dimension of the field

[20] Unfortunately, the language used in the field of critical phenomena makes excessive use of the prefix "scaling."
[21] Historically, the exponents are drawn from the first six letters of the Greek alphabet. The exceptional designation of the last exponent, z, betrays the fact that quantum dynamical fluctuations were considered only later.

ϕ. The engineering dimension of the latter follows from the requirement that the gradient operator $\sim \int d^d r\,(\ \ \phi)^2$ be dimensionless: $[\phi] = L^{(2-d)/2}$, according to which $C(\mathbf{r})$ has canonical dimension L^{2-d}. The exponent η, commonly referred to as the **anomalous dimension** of the correlation function, measures the mismatch between the observed and the canonical dimension.

z: A quantum theory can, to a large extent, be viewed as a kind of classical theory in $d+1$ dimensions. The theory is "quantum critical" if the effective classical theory contains a critical point. In the vicinity of that point large fluctuations are observed in both the d spatial directions and the temporal "direction." However, the different physical origin of these dimensions manifests itself in the scaling being anisotropic. Denoting the correlation length in the temporal direction by τ, we define $\tau \sim \xi^z$, where deviations $z = 1$ in the **dynamical exponent** measure the degree of anisotropy.

Now, a moment's thought shows that, of the six classical exponents, only a few can be truly independent. Previously we have noted that, modulo irrelevant perturbations, the flow in the vicinity of a transition point is controlled by the relevant scaling fields. Referring for a more quantitative discussion to Section 8.4 below, we anticipate that, for the magnetic transition, the magnetic field will certainly represent a relevant perturbation (a fact readily expressed by the positivity of the exponent δ). Moreover, deviations from the critical temperature, $t = 0$, are also relevant.[22] However, for the magnetic transition, that exhausts the list; in the asymptotic vicinity of the transition, the flow is controlled by a two-dimensional dynamical system. This suggests that four constraining equations should reduce the set of six classical exponents to only two independent ones. Historically, these **scaling laws** were discovered one by one (at a time when the underlying connections to the system of "scaling fields" had not been fully appreciated). For the sake of reference, these constraint equations (along with the names of the people who discovered them) are listed below. In Section 8.3.3 below, we exemplify how the scaling laws can be transparently derived from the intrinsic structure of the theory.

Fisher	$\nu(2-\eta) = \gamma$
Rushbrooke	$\alpha + 2\beta + \gamma = 2$
Widom	$\beta(\delta - 1) = \gamma$
Josephson	$2 - \alpha = \nu d$

For practical purposes, we need only compute/measure two exponents – no matter which – to fully specify the scaling structure of the theory.

In the next section we discover that the dynamical system of scaling fields encapsulates practically all information about "critical" fluctuation phenomena accompanying a phase transition. However, for the moment, we shall restrict ourselves to the discussion of one more aspect of conceptual importance, namely **universality**. In fact, the majority of critical systems can be classified into a relatively small number of **universality classes**. Crudely speaking, leaving apart more esoteric classes of phase transitions there are $\mathcal{O}(10^1)$ fundamentally different types of flow recurrently appearing in practical applications. This has to

[22] If you find it difficult to think of temperature as a "coupling constant," remember that, in our derivation of the ϕ^4-model as the relevant theory of the magnetic transition, the coupling constant of the "mass operator" $r \int d^d r\, \phi^2$ turned out to be proportional to the reduced temperature $t = |T - T_c|/T_c$.

be compared with the near infinity of different physical systems that display critical phenomena. Why, then, is it that the plethora of all these transitions can be grouped into a very limited set of different universality classes? Remarkably, the origin of this universality can readily be understood from the concept of critical surfaces.

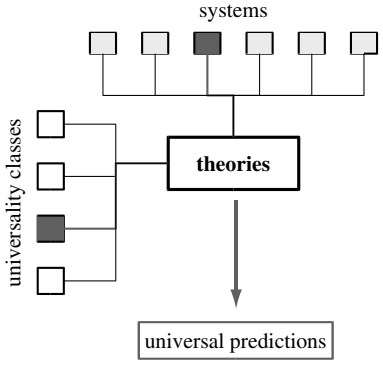

Imagine, then, an experimentalist exploring a system that is known to exhibit a phase transition. Motivated by the critical phenomena that accompany phase transitions, the available control parameters X_i (temperature, pressure, magnetic field, etc.) will be varied until the system begins to exhibit large fluctuations. On a theoretical level, the variation of the control parameters determines the initial values of the coupling constants of the model (as they functionally depend on the X_is through their connection to the microscopic Hamiltonian). In Fig. 8.5 the curve in coupling constant space defined in this way is indicated by γ. For microscopic parameters corresponding to a point above or below the critical manifold, the system asymptotically (i.e. when looked at at sufficiently large scales) falls into either the "high-" or the "low-temperature" regime (as indicated by the curves branching out from γ in Fig. 8.5). However, eventually the trajectory through parameter space will intersect the critical surface. For this particular set of coupling constants, the system is critical. As we look at it on larger and larger length scales, it will be attracted by the fixed point at S, i.e. it will display the universal behavior characteristic of this particular point. This is the origin of universality: variation of the system parameters in a different manner (or for that matter considering a second system with different material constants) will generate a different trajectory $g_\alpha(\{X_i\}) = \gamma'$. However, as long as this trajectory intersects with S, it is guaranteed that the critical behavior will exhibit the same universal characteristics (controlled by the unique fixed point).

In fact a more far-reaching statement can be made. Given that there is an infinity of systems exhibiting transition behavior (symbolically indicated by the row of boxes in the upper part of the figure above) while there is only a very limited set of universality classes (the set of boxes on the left), many systems of very different microscopic morphology must have the same universal behavior. More formally, different microscopic systems must map onto the same critical low-energy theory. Examples of these coincidences include (to mention but a few entries of an endless list) the equivalence of the disordered Luttinger liquid to a Josephson junction (cf. Problem 6.7), the equivalence of models of planar magnets (see Section 8.6 below) to two-dimensional classical Coulomb plasmas, and the equivalence of the liquid–gas transition to the ferromagnetic transition. (In all cases, "equivalence" means that the systems exhibit identical scaling behavior and, therefore, fall into the same universality class.) Further coincidences of this type will be encountered below.

8.3.3 Scaling theory

Previously, we have seen that the dynamical system of scaling fields encodes a wealth of information on the large-scale structure and on the phases of a physical system. However, we have not yet established a connection between the concept of renormalization and concrete (i.e. experimentally accessible) data. This is the subject of the present section. Imagine, then, that we had represented some observable of experimental interest, X, in the language of the functional integral. According to the discussion of the previous chapter this means that we have managed to express

$$X = \sum_{\mathbf{p}} C(p_i, g_\alpha),$$

as the sum over an n-point correlation function $C(p_i, g_\alpha) = \langle(\cdots)\phi\phi\cdots\phi\rangle_\phi$, where the (symbolic) notation indicates that C may depend both on the momentum scale at which it is evaluated (e.g. through the explicit momentum dependence of current operators, etc.) and on the coupling constants. The ellipsis $(\cdots)$ stand for optional algebraic elements entering the definition of the correlation function.

We next build on our assumption of renormalizability of the theory, i.e. we make use of the fact that we can evaluate C before or after an RG step; the result must be the same. On the other hand, the RG transformation will, of course, not leave the individual constituents entering the definition of C invariant; it will change coupling constants, g_α, the momenta p_i, and the field amplitudes ϕ according to the prescriptions formulated in the previous section. Expressed in a single formula,

$$\boxed{C(p_i, g_\alpha) = b^{nd_\phi} C(p_i b, g_\alpha b^{\lambda_\alpha}),} \tag{8.18}$$

where we have simplified the notation by assuming that the coupling constants themselves scale (for, otherwise, the matrix elements of a linear transformation mediating between the coupling constants and the scaling fields would appear). For notational convenience, let us also assume that the fixed point values of the coupling constants are specified in such a way that $\mathbf{g}^* = 0$. The factor b^{nd_ϕ} accounts for the explicit rescaling of the n fields entering the definition of C.

Notice that Eq. (8.18) presents a remarkable statement. Although the three different elements (ϕ, p_i, g_α) contributing to the correlation function change under the transformation in seemingly unrelated manners, the net result of the concerted rescaling is nil. Indeed, Eq. (8.18) serves as a starting point for the derivation of various relations of immediate practical relevance.

Scaling functions

Let us return to a principle already employed in connection with the one-dimensional Ising model. For concreteness, imagine that we are working under conditions where there is just a

single relevant scaling field g_1, while all $g_{\alpha>1}$ are irrelevant (or, for that matter, marginal). We can then write

$$\begin{aligned} C(p_i, g_1, g_\alpha) &= b^{nd_\phi} C(p_i b, g_1 b^{\lambda_1}, g_\alpha b^{\lambda_\alpha}) = g_1^{-nd_\phi/\lambda_1} C(p_i g_1^{-1/\lambda_1}, 1, g_\alpha g_1^{-\lambda_\alpha/\lambda_1}) \\ &\overset{g_1 \ll 1}{\approx} g_1^{-nd_\phi/\lambda_1} C(p_i g_1^{-1/\lambda_1}, 1, 0) \equiv g_1^{-nd_\phi/\lambda_1} F(p_i g_1^{-1/\lambda_1}). \end{aligned}$$

Here, we have used the freedom of arbitrarily choosing the parameter b to set $g_1 b^{\lambda_1} = 1$ while, in the third equality, we have assumed that we are sufficiently close to the transition that the dependence of C on irrelevant scaling fields is inessential. The function F defined through the relation

$$C(p_i, g_1) = g_1^{-nd_\phi/\lambda_1} F(p_i g_1^{-1/\lambda_1}), \tag{8.19}$$

is an example of a **scaling function**. Alternatively (for example, if C represents a thermodynamic observable or a global transport coefficient) we might be interested in the correlation function $C(g_1, g_\alpha) \equiv C(p_i = 0, g_1, g_\alpha)$ at zero external momentum $p_i = 0$. In this case, a typical question to ask would be the dependence of C on the most relevant *and* the second most relevant control parameter g_2 (where we leave unspecified whether g_2 is relevant, marginal, or irrelevant). Following the same logic as above, one obtains

$$C(g_1, g_2) = g_1^{-nd_\phi/\lambda_1} \tilde{F}(g_2 g_1^{-\lambda_2/\lambda_1}),$$

with some different scaling function $\tilde{F}$.

INFO As an example particularly relevant to the comparison between analytical theory and numerics, we note the concept of **finite-size scaling**. While analytical theories are most conveniently formulated in the thermodynamic limit, numerical simulations are carried out for systems of still very limited size. The need to compare theory and numerical simulations motivates the need to explicitly keep track of the system size under renormalization. Indeed, the system size L has dimension [length] and, therefore, gets rescaled as $L \to L/b$. Setting $L/b = 1$, we obtain a scaling function

$$G(g_\alpha, L) = L^{nd_\phi} F_{\rm fs}(g_\alpha L^{\ \alpha}),$$

with explicit system size dependence.

While the construction of any particular scaling function may be context-dependent, the principle behind the derivation is general: once the scaling behavior of a correlation function is known, the arbitrariness of the scaling parameter b can be used to reduce the number of independent variables by one. The reduced correlation function is called a scaling function. As with the response functions discussed in the previous chapter, scaling functions also represent a prime **interface between theory and experiment**. Experimentally, the measurement of an observable X in its dependence on a number of relevant system parameters, t and h say, results in a multi-parameter function $X(t, h)$. In fact, a better way to think about this object is as a set of one-dimensional functions $X_h(t)$ depending on a parameter h. (This is because, in experiment, one typically varies only a single control parameter, e.g. temperature at fixed magnetic field.) Scaling implies that all these functions collapse onto

a generic one-dimensional[23] profile, if only the data are plotted as a function of the relevant scaling parameter th^x.

This mechanism can be exploited in several different ways. For example, if there is not yet a theory of the transition phenomenon in question, an experimentalist may empirically identify the relevant scaling parameters and pose the explanation of the observed scaling exponent x – by construction a fully universal number – as a challenge to theorists.[24] Conversely, theorists may suggest a scaling exponent that can be put to the test by checking whether the experimental data collapse onto this exponent. Summarizing, one of the great virtues of the concept of scaling is that it condenses the information exchange between experiment and theory (and analytical theory and numerics for that matter) into a small set of universal numbers.

INFO For the sake of completeness we mention that, especially in the field theoretical community, the information encapsulated in the scale-dependent correlation functions is often represented in a different manner. Starting out from the relation

$$C(p_i, g_\alpha) = e^{n\ d_\phi} C(p_i e\ , g_\alpha(\ell)),$$

where we have set $b = e$, we can use the ℓ-independence of the left-hand side to write $0 = \frac{d}{d} e^{n\ d_\phi} C(p_i e\ , g_\alpha(\ell))$. (Notice that, here, we do not need to be in the asymptotic scaling regime, i.e., for the sake of the present construction, the ℓ-dependence of the coupling constants need not be explicitly exponential.) We next carry out the ℓ-differentiation to obtain

$$\boxed{n\ \ d_{\mathrm{e},\phi} + \frac{\eta}{2}\ \ + \partial\ + \beta_\alpha(g_\alpha)\partial_{g_\alpha}\ \ C(p_i e\ , g_\alpha(\ell)) = 0.} \tag{8.20}$$

Here, $d_{\mathrm{e},\phi}$ is the engineering dimension of the field ϕ and $\eta/2 = d_\phi - d_{\mathrm{e},\phi}$ its anomalous dimension (see the definition of η in the Info block starting on page 436). Further, the partial derivative ∂ acts on the explicit scale dependence of the momentum arguments (or any other explicitly scale-dependent argument for that matter). Finally, $\beta_\alpha(g_\alpha)$ is the β-function defined above. Equation (8.20) is known as a **renormalization group equation**. Both the RG equation and the scaling form that we used to derive it equivalently express the scaling behavior of the correlation function.

Scaling functions and critical exponents

Another important aspect of scaling theory is that it can be used to disclose relations between the seemingly independent[25] critical exponents of the theory. For the sake of concreteness, let us consider the case of the ferromagnetic transition, i.e. a transition we have previously characterized in terms of six critical exponents $\alpha, \ldots, \eta$ (see page 438). However, the flow in the vicinity of the magnetic fixed point is controlled by only two relevant scaling fields, the (reduced) temperature t and the reduced magnetic field $h \equiv H/T$. Neglecting

[23] For an n-dimensional data set, the collapse is to an $(n-1)$-dimensional functional set.

[24] Parenthetically, one may note that the empirical collapse of experimental data onto scaling functions requires a lot of skill. For example, if the data set consists of a number of functional "patches" of only limited overlap, it is quite "easy" to construct a scaling function of, in fact, almost any desired power law dependence. Data of this type tend to contain a lot of statistical uncertainty, which can easily lead to erroneous conclusions.

[25] After all, the critical exponents describe the behavior of quite different physical observables in the transition region.

irrelevant perturbations, we thus conclude that, under a renormalization group transformation, the reduced free energy $f = F/TL^d$ will behave as[26] $f(t,h) = b^{-d} f(tb^{y_t}, hb^{y_h})$. We next fix $tb^{y_t} = 1$ to reduce the number of independent variables to one:

$$\boxed{f(t,h) = t^{d/y_t} \tilde{f}(h/t^{y_h/y_t}).} \tag{8.21}$$

Containing the complete thermodynamic information, Eq. (8.21) is all that we need to compute the critical exponents. Indeed, comparing with the definitions summarized on page 438, it is straightforward to show that

$$\left.\begin{aligned} &\alpha = 2 - \frac{d}{y_t}, \quad \beta = \frac{d - y_h}{y_t}, \quad \gamma = \frac{2y_h - d}{y_t}, \\ &\delta = \frac{y_h}{d - y_h}, \quad \nu = \frac{1}{y_t}, \qquad \eta = 2 + d - 2y_h, \end{aligned}\right\} \tag{8.22}$$

from where follow the cross-relations summarized in the table on page 439 by direct comparison. These relations illustrate our previous assertion that, conceptually, the dimensions of the relevant scaling fields have a more fundamental status than the critical exponents.

EXERCISE Verify these statements. To obtain the fifth relation, the **hyperscaling relation**, notice that, under a change of scale, $\xi \to b\xi$. On the other hand, we know that $t \sim \xi^{-1/\ }$. The sixth relation is obtained from Eq. (8.3) by a substitution of the definition of the spatial profile of the correlation function in terms of the critical exponent η into the integral to obtain a relation between the critical exponents γ and η (Fisher's scaling law).

8.4 RG analysis of the ferromagnetic transition

In the previous section, we became acquainted with some fundamental elements of the structure of RG analyses, and their connection to the theory of critical phenomena. Being kept at a general and conceptual level, the discussion may have seemed somewhat abstract. Therefore, to elucidate the concepts introduced above, and to introduce some more elements of the RG, we turn now to a concrete application of the approach to the classical theory of the (uniaxial) ferromagnetic (or liquid–gas) transition. In Section 5.1, the ϕ^4-theory was identified as an effective low-energy model of the ferromagnetic system. However, beyond the mean-field, we have not yet applied the model to explore the universal characteristics of the transition. In the following, we shall see that RG methods, and only RG methods, can be applied to successfully understand much of the intriguing behavior displayed by the $(d > 2)$-dimensional Ising model in the vicinity of its phase transition.

[26] Here we have made use of the fact that the reduced free energy does not carry an anomalous dimension. By definition, the free energy $F = -T \ln \mathcal{Z}$ does not change under renormalization (which after all, merely amounts to representing the number $\mathcal{Z}$ through functional integrals of different space-time resolution). Thus, the scaling of the reduced free energy is entirely carried by the prefactor L^{-d}.

8.4.1 Preliminary dimensional analysis

The first question that we wish to address has a somewhat technical status: with what justification was the Ising model represented in terms of the model action[27]

$$S[\phi] = \int d^d r \left[\frac{r}{2}\phi^2 + \frac{1}{2}(\nabla\phi)^2 + \frac{\lambda}{4!}\phi^4 - h\phi \right], \tag{8.23}$$

i.e. why was it possible to neglect both higher powers and gradients of the field ϕ that are surely present in the exact reformulation of the Ising problem in terms of ϕ-variables? To rationalize the neglect of these terms, we proceed by dimensional analysis. Anticipating that the "real" dimensions carried by the operators in the action will be not too far from their engineering dimensions (see below), we begin by exploring the latter. We proceed along the lines of the general scheme outlined in the previous chapter and attribute a dimension of unity to the leading gradient term $\int(\nabla\phi)^2$ in the action. This entails the choice $[\phi] = L^{(2-d)/2}$, from where it is straightforward to attribute engineering dimensions to all other operators:

$$\left[\int \phi^2\right] = L^2, \quad \left[\int \phi^4\right] = L^{-d+4}, \quad \left[\int \phi^n\right] = L^{d+(2-d)n/2}, \quad \left[\int (\nabla^m\phi)^2\right] = L^{2(1-m)}.$$

These relations convey much about the potential significance of all structurally allowed operators:

- ▷ The engineering dimension of the non-gradient operator $\sim \phi^2$ is positive in all dimensions, indicating general relevance.
- ▷ The ϕ^4 operator is relevant (irrelevant) in dimensions $d < 4$ ($d > 4$). This suggests that for $d > 4$ a harmonic approximation ($\lambda = 0$) of the model should be reasonable. It also gives us a preliminary clue as to how we might want to approach the ϕ^4-model on a technical level: while for dimensions "much" smaller than $d = 4$ the interaction operator $\sim \phi^4$ is strongly relevant, the dimension $d = 4$ itself is borderline. This suggests that we analyze the model at $d = 4$, or maybe "close"[28] to $d = 4$ where the ϕ^4 operator is not yet that virulent, and then try to extrapolate to infer what happens at the "physical dimensions" of $d = 2$ and 3.
- ▷ Operators $\phi^{n>4}$ become relevant only in dimensions $d < (-1/n + 1/2)^{-1} < 4$. However, even below these threshold dimensions, operators of high powers in the field variable are much less relevant than the dominant non-harmonic operator $\int \phi^4$. This is the *a posteriori* justification for the neglect of $\phi^{n>4}$ operators in the derivation of the model.
- ▷ Similarly, operators with more than two gradients are generally irrelevant and can be neglected in all dimensions.
- ▷ In contrast, the operator $\int \phi$ coupling to the magnetic field carries dimension $1 + d/2$ and is therefore always strongly relevant.

[27] Generalizing our discussion from Section 5.1, we have incorporated a coupling to an external field. (Exercise: Recapitulate the construction of Section 5.1 to convince yourself that, to lowest order in an expansion in terms of ϕ, coupling the system to a magnetic field leads to the fourth term of Eq. (8.23). In case you are too impatient to do this: justify the structure of the term on physical grounds.)

[28] As we see shortly, the analysis of the problem is readily generalized to non-integer dimensions.

Dimensional analysis provides us with some valuable hints as to the importance of various operators appearing in the theory. It also indicates that, in the present context, dimension $d = 4$ might play a special role. Guided by this information, we now proceed to analyze the model in a sequence of steps of increasing sophistication.

8.4.2 Landau mean-field theory

Given an action of the form (8.23), the first thing one might try is a mean-field analysis. That is, assuming that our coupling constants r and λ are sufficiently large we might assume that the functional integral over ϕ is centered around solutions of the equation $\frac{\delta S[\phi]}{\delta \phi} = 0$, or

$$r\bar{\phi} + \frac{\lambda}{6}\bar{\phi}^3 - h = 0, \tag{8.24}$$

where we have used the fact that the low-energy mean-field configuration will be spatially constant. Just by inspecting the potential part of the field-free Lagrangian, $\frac{r}{2}\phi^2 + \frac{\lambda}{4!}\phi^4$, it is clear that, depending on the sign of r, the mean-field equation possesses two fundamentally different types of solution. For $r > 0$, the action has a global minimum at $\phi = 0$, implying that $\bar{\phi} = 0$ is the unique mean-field (see Fig. 8.7). Noticing that the amplitude of ϕ represents a measure of the magnetization of the system (which is clear from the way the ϕ^4-action was derived from the Ising model on page 196), we identify $r > 0$ as a phase of zero net magnetism, the **paramagnetic phase**.

In contrast, for $r < 0$, the action has two degenerate minima at non-zero values, $\bar{\phi} = \pm\phi_0 \equiv \pm(6|r|/\lambda)^{1/2}$ (see Fig. 8.7). The system then has to make a choice as to whether it wants to sit in the ground state configuration $\bar{\phi} = \phi_0$ or $\bar{\phi} = -\phi_0$. This is the state of spontaneous symmetry breaking indicative of the low-temperature **ferromagnetic phase**. (Notice that, upon the switching on of a small magnetic field, the degeneracy between the two ground states is lifted and the system will populate a state of predetermined magnetization, $\bar{\phi} = \pm\phi_0$, depending on the sign of h.)

The preliminary analysis above indicates that r has the status of a fundamental parameter tuning the system through the ferromagnetic transition. Indeed, the microscopic analysis in Section 5.1 had indicated that $r \sim T - T_c$ was a function of temperature that changed sign at some critical temperature T_c, the mean-field critical temperature of the transition. However, even if we did not know the microscopics, it would be clear that $r(T)$ is (i) *some*

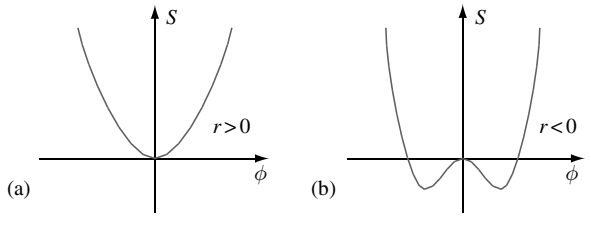

Figure 8.7 Action of the ϕ^4-theory evaluated on a constant field configuration above (a) and below (b) the critical point.

Table 8.1 *Critical exponents of the ferromagnetic transition obtained through di erent methods. Experimental exponents represent cumulative data from various three-dimensional ferromagnetic materials.*

Exponent	Experiment	Mean-field	Gaussian	ϵ^1	ϵ^5
α	0–0.14	0	1/2	1/6	0.109
β	0.32–0.39	1/2	1/4	1/3	0.327
γ	1.3–1.4	1	1	7/6	1.238
δ	4–5	3	5	4	4.786
ν	0.6–0.7		1/2	7/12	0.631
η	0.05		0	0	0.037

Source: Data taken from K. Huang, *Statistical Mechanics* (Wiley, 1987).

function of temperature which (ii) must have a zero at some temperature $T = T_c$ (otherwise there would be no transition to begin with). Therefore, in the vicinity of $T = T_c$, we can set $r \sim T - T_c$ as our prime measure of the distance to the critical point. (This observation is, in fact, in perfect agreement with our earlier observation that the operator $\int \phi^2$ coupled to r is relevant – see the discussion in Section 8.3.2.)

What can mean-field theory say about the prime descriptors of the transition, the **critical exponents**? Identifying the field amplitude ϕ (alias the magnetization) with the order parameter of the transition, and referring back to our list of exponents on page 438, the low-temperature profile is given by $|\bar{\phi}| = (12|r|/\lambda)^{1/2} \sim |t|^{1/2}$, implying that $\beta = 1/2$. The exponent γ is obtained by differentiating Eq. (8.24) with respect to h. With $\chi \sim \partial_h \phi$, it is then straightforward to verify that, on approaching the critical point from either side of the transition, $\chi \sim |t|^{-1}$, implying an exponent $\gamma = 1$. The action evaluated on the mean-field-configuration takes the form

$$\frac{S[\bar{\phi}]}{L^d} = \frac{r}{2}\bar{\phi}^2 + \frac{\lambda}{4!}\bar{\phi}^4 \sim \begin{cases} \lambda^{-1}t^2, & t < 0, \\ 0, & t > 0. \end{cases} \tag{8.25}$$

With the mean-field free energy $F = TS[\bar{\phi}]$ we find that the specific heat $C = -T^2\partial_T^2 F \sim \partial_t^2 S$ behaves as a step function at the transition point, implying $\alpha = 0$. Right at the critical temperature, $r = 0$, the mean-field magnetization depends on h as $\bar{\phi} \sim h^{1/3}$, implying that $\delta = 3$. Finally, the correlation length exponents ν, η cannot directly be computed from plain mean-field theory as they are tied to the spatial profile of fluctuating field configurations.

For the sake of later comparison, the mean-field critical exponents are summarized in Table 8.1. At first sight the differences between the experimentally observed exponents (second column) and the mean-field exponents (third column) do not look too dramatic – apparently the primitive mean-field approach pursued here fares reasonably favorably – which, in view of the accumulation of pronounced fluctuations at the critical point, should come as something of a surprise. On the other hand we must keep in mind that the exponents describe singular power laws in the transition region. In view of that, the difference between

1.3 and 1 does look quite significant. At any rate, we should try to refine our theoretical understanding of the transition and search for the source of the discrepancy with experiment.

8.4.3 Gaussian model

As a first improvement on the mean-field approximation, let us explore the effect of quadratic fluctuations around the constant field configuration $\bar{\phi}$. Approaching the transition point from above, we set $\bar{\phi} = 0$ and approximate the action through its quadratic expansion[29]

$$S[\phi] \approx \int d^d r \left[\frac{r}{2}\phi^2 + \frac{1}{2}(\nabla\phi)^2 - h\phi \right]. \tag{8.26}$$

In this form, one may effect the Gaussian integral over field fluctuations and evaluate the dependence of the free energy on the external parameters h and r. However, in anticipation of our analysis of the full problem below, we here pursue a slighly different, renormalization-group-oriented approach, i.e., pretending that we did not know how to do the Gaussian integral, we subject the quadratic action to a momentum shell RG analysis.

Proceeding along the lines of the canonical scheme, we split our field into fast and slow degrees of freedom $\phi = \phi_{\rm s} + \phi_{\rm f}$ resulting in the, now familiar, fragmentation of the action $S[\phi_{\rm s}, \phi_{\rm f}] = S_{\rm s}[\phi_{\rm s}] + S_{\rm f}[\phi_{\rm f}] + S_{\rm c}[\phi_{\rm s}, \phi_{\rm f}]$. However, the crucial simplification, characteristic of a Gaussian theory, is that the action $S_{\rm c}$ coupling fast and slow components vanishes (exercise), implying that the integration over the fast field merely leads to an inessential constant. The effect of the RG step on the action is then entirely contained in the rescaling of the slow action. According to our previous discussion, the scaling factors thus appearing are determined by the engineering dimensions of the operators appearing in the action, i.e. $r \to b^2 r$ and $h \to b^{d/2+1} h$. Using the fact that $r \sim t$ we can then readily write down the two relevant scaling dimensions of the problem, $y_t = 2$ and $y_h = d/2 + 1$. Comparison with Eq. (8.22) finally leads to the list of exponents,

$$\alpha = 2 - \frac{d}{2}, \quad \beta = \frac{d}{4} - \frac{1}{2}, \quad \gamma = 1, \quad \delta = \frac{d+2}{d-2}, \quad \nu = \frac{1}{2}, \quad \eta = 0.$$

Notice that the exponents now explicitly depend on the dimensionality of the system, a natural consequence of the fact that they describe the effect of spatial fluctuations. Table 8.1 contains the values of the exponents for a three-dimensional system. We cannot really say that the results are any better than those obtained by the mean-field analysis. Some exponents (e.g. δ) agree better with the experimental data, while others (e.g. α) are decidedly worse.

As a corollary to this section, we note that the Gaussian model possesses only one fixed point, namely $r = h = 0$, which in the context of ϕ^4-theory is called the **Gaussian fixed point**.

[29] The appearance of a linear term indicates that we are expanding not around the "true" mean-field, i.e. the exact solution of (8.24), but rather around the solution $\bar{\phi} = 0$ of the field-free system. However, in view of the fact that h has the status of an external perturbation, this choice of the reference configuration is quite natural.

8.4.4 Renormalization group analysis

In the present analysis of the model, we have not really touched upon its principal source of complexity, namely the effect of the "interaction operator" ϕ^4 on the fluctuation behavior of the field. It seems likely that the neglect of this term is responsible for the comparatively poor predictive power both of the straightforward mean-field analysis, and of the Gaussian model. Indeed, the dimensional analysis of Section 8.4.1 indicated that the ϕ^4 addition to the action becomes relevant below four dimensions. A more physical argument, to the same effect, is given in the Info block below.

Although the solution of the general problem posed by the action (8.23) still appears to be hopelessly difficult, there is one aspect we can turn to our advantage. While physical systems exist in integer dimensions $d = 1, \ldots, 4, \ldots$, there is actually no reason why we should not be allowed to evaluate our theory, i.e. the functional integral with action (8.23), in fractional dimensions. In the present context, this seemingly academic freedom turns out to be of concrete practical relevance. The point is that the nonlinear ϕ^4 operator was found to be marginal at $d = 4$ and relevant below. One may thus expect that, in dimensions $d = 4 - \epsilon$, $\epsilon \ll 1$, the operator is relevant but not that relevant, i.e. one may expect that, for sufficiently small deviations off the threshold dimension, four, the theory knows of an expansion parameter, somehow related to ϵ, which will enable us to control the interaction operator. Of course, at the end of the day, we will have to "analytically continue" to dimensions of interest, $\epsilon = 1$ or even $\epsilon = 2$, but, for the present, we will see what we can learn from a $d = 4 - \epsilon$ representation of the theory.

INFO Our previous analysis relied on the assumption that the field integration is tightly bound to the vicinity of the extrema of the action. But let us now ask under what conditions this assumption is actually justified. We should develop some intuition as to the relative importance of the mean-field content of the theory and of the **fluctuations around the mean-field**. While there are several ways to proceed with this program, we will focus on the analysis of the magnetic susceptibility. (At this point, we should warn the reader that the arguments formulated below, while technically straightforward, are conceptually involved. The critical contemplation of the logical steps of the construction is time well invested.) Firstly, let us recall the definition of the susceptibility,

$$\chi = -\partial_H^2 F \sim \int d^d r \, \langle \phi(\mathbf{r})\phi(0)\rangle_{\mathrm{c}} \sim G(\mathbf{k} = 0),$$

where we have used the fact that $\langle \phi(\mathbf{r})\phi(\mathbf{r}')\rangle = G(\mathbf{r}-\mathbf{r}')$ is the Green function of the model. Given this identification, we note that a formal criterion of the transition – divergent susceptibility! – is synonymous with a singularity of the zero-momentum Green function.

On the level of the Gaussian theory (see Eq. (8.26)) $G(\mathbf{k}) = (r + k^2)^{-1}$, i.e. $\chi \sim r^{-1}$. Anticipating troubling observations to come, we reiterate that the mean-field transition temperature is identified by the condition $r \sim t = 0$. Now, let us move on to explore corrections to the mean-field susceptibility on the level of a perturbative one-loop calculation. To this end, we recall that (if necessary, recapitulate the discussion of Section 5.1), due to the presence of the ϕ^4 operator, the Green function acquires a self-energy which, at the one-loop level, is given by $\Sigma = -\frac{1}{2}\sum_{\mathbf{k}'} \frac{1}{r+k'^2}$.

As a consequence, one can identify the susceptibility as

$$\chi^{-1} \sim \left(G(\mathbf{k}=0)\right)^{-1} = r - \Sigma = r + \frac{\lambda}{2}\sum_{\mathbf{k}'}\frac{1}{r+k'^2}.$$

A first observation to be made is that non-Gaussian fluctuations (physically: interactions between harmonic fluctuations around the mean-field amplitude) lower the transition amplitude, i.e., setting $r \sim T - T_{\rm c}$, it now takes a smaller temperature T to reach the critical point; in accord with the intuitive expectation that fluctuations tend to "disorder" the system. Frustratingly, one may also observe that the cutoff Λ is needed to prevent the "correction",

$$-\frac{\lambda}{2}\sum_{\mathbf{k}'}\frac{1}{r+k'^2} \sim \lambda\int^{\Lambda} d^dk'\frac{1}{r+k'^2},$$

from diverging in dimensions $d \geq 2$. To deal with this singularity, we have to realize that the effect of fluctuations is actually two-fold: the transition temperature gets shifted and the temperature dependence of the inverse susceptibility is apparently no longer simply linear (by virtue of the r-dependence of the integrand). The two effects can be disentangled by writing

$$\chi^{-1} = r + \frac{\lambda}{2}\left(\frac{L}{2\pi}\right)^d\int^{\Lambda} d^dk'\left(\frac{1}{r+k'^2} - \frac{1}{k'^2}\right) \approx r - \frac{\lambda r}{2}\left(\frac{L}{2\pi}\right)^d\int^{\Lambda}\frac{d^dk'}{(r+k'^2)k'^2}, \qquad (8.27)$$

where

$$r \equiv r + \frac{\lambda}{2}\left(\frac{L}{2\pi}\right)^d\int^{\Lambda}\frac{d^dk'}{k'^2},$$

represents the shifted transition temperature while the integral describing the deviation from the linear temperature dependence of the susceptibility is now UV-convergent in dimensions $d < 4$. Notice that in the second equality of Eq. (8.27) we have replaced the parameter r in the integrand by the modified parameter r. To the accuracy of a one-loop calculation, this manipulation is permissible.

Naively, it looks as if this sequence of manipulations has led to a catastrophe: the fluctuation-renormalized transition temperature appears to diverge as one sends the cutoff to infinity, clearly a nonsensical prediction! However, one may note that there was actually no justification for identifying the *physical* transition temperature through the parameter r in the first place. This identification was based on mean-field theory alone, i.e. an approach to the problem which neglected altogether the key effect of fluctuations. However, the bare parameter r appearing in the action carries as little "universal" meaning as the cutoff Λ, or any other microscopic system parameter for that matter!

Once we have acknowledged this interpretation, we should then identify the transition temperature through the singularity of the macroscopically observable properties (e.g. divergence of the susceptibility leads to the vanishing of the modified parameter r at the one-loop level) while the microscopic parameters carry no significance by themselves.

EXERCISE This interpretation closely parallels the philosophy of **renormalization in high-energy physics**. There, the bare parameters of the action are fundamentally undetermined, while the inverse of the Green function at zero external momentum represents a physical observable, e.g. the mass of the electron. Since the loop corrections to this physical quantity appear to be infinite (and the theory does not enjoy the luxury of the presence of a physically motivated cutoff), one postulates that the bare parameters of the action have been infinite by themselves. These singularities are deliberately adjusted so as to cancel the divergence of the

fluctuation corrections and to produce finite "physical" quantities. It is instructive to consult a textbook on renormalization in high-energy physics (such as Ryder[30]) to become acquainted with the functioning of this strategy, and with the enormous success it has had in the context of QED and other sub-branches of particle physics.

We now turn to the second effect of the fluctuation correction, namely the deviation from the linear temperature dependence, as described by the integral contribution to Eq. (8.27). On dimensional grounds, the integral depends on the parameter r as $\sim \lambda L^d r^{(d-4)/2}$. The (mean-field + quadratic fluctuations) approach to the problem breaks down when this contribution becomes more important than the leading-order contribution to the susceptibility, i.e. for dimensions $d \quad 4$. This observation is the essence of the so-called **Ginzburg criterion**. The criterion states that mean-field theory becomes inapplicable below the so-called **upper critical dimension** $d_c = 4$. While we have derived this statement for the particular case of the ϕ^4-model, it is clear that similar estimates can be performed for every nonlinear field theory, i.e. as with the lower critical dimension, the upper critical dimension also represents an important threshold separating the mean-field dominated $d > d_c$ from the fluctuation dominated $d < d_c$ behavior. Also notice that the analysis above conforms with our previous observation that the nonlinear ϕ^4 operator is relevant in dimensions $d < 4$. (Convince yourself that the two lines of argument reflect the same principle, namely the dependence of fluctuations on the accessible phase volume, as determined by the dimensionality of the system.)

Before proceeding to the details of the RG program, let us try to predict a number of general elements of the ϕ^4 phase diagram on dimensional grounds. We saw that in dimensions $d > 4$ the ϕ^4 operator is irrelevant and that the Gaussian model essentially dictates the behavior of the system. Specifically, for $d > 4$, the Gaussian fixed point $r = \lambda = h = 0$ is the only fixed point of the system. Below four dimensions, the ϕ^4 operator becomes relevant and the emergence of a richer fixed point structure may be expected. However, for $\epsilon = 4 - d$ sufficiently small, we also expect that, whatever new fixed points appear, they should be close to the Gaussian point. This means that we can conduct our search for new fixed points within a double expansion in ϵ, and the small deviation of the coupling constants r, λ, h around the Gaussian fixed point. (In fact, we will momentarily identify a third expansion parameter, namely the number of momentum loops appearing in fast-field integration.)

Step I

We next proceed to formulate the steps of the RG in detail. To keep things simple, the RG transformation will be carried out to lowest order in a triple expansion in ϵ, the coupling constants, and the number of momentum loops. The rationale behind the loop expansion can be best understood if we assume that the entire action[31] is multiplied by a large parameter (which, in the case of a quantum theory, might be $\hbar^{-1}$). The expansion in the number of loops is then equivalent to an expansion in the inverse of that parameter (for a quantum theory, an expansion away from the classical limit).

[30] L. H. Ryder, *Quantum Field Theory*, (Cambridge University Press, 1996).
[31] Before we rescaled the fields so as to make the leading-order coefficient equal to 1/2.

EXERCISE Verify this statement; to this end, notice that a diagram of nth order in perturbation theory in the ϕ^4 vertex contains a prefactor a^n involving the large parameter. On the other hand, each of the I internal lines, or propagators, contained by the diagrams contributes a factor a^{-1}, so that the overall power is a^{n-I}. Next relate the number of internal lines to the number L of loops. Notice that each line corresponds to a momentum summation. However, the number of independent summations is constrained by the n δ-functions carried by the vertices. Use this information to show that the overall power of the graph is a^{-L+1}, i.e. an expansion in L is equivalent to an expansion in the inverse of a.

Let us now decompose the action in the standard manner, setting $S[\phi_{\rm s},\phi_{\rm f}] = S_{\rm f}[\phi_{\rm f}] + S_{\rm s}[\phi_{\rm s}] + S_{\rm c}[\phi_{\rm s},\phi_{\rm f}]$, where

$$\begin{aligned} S_{\rm f}[\phi_{\rm f}] &= \int d^d r \left[\frac{r}{2}\phi_{\rm f}^2 + \frac{1}{2}(\nabla\phi_{\rm f})^2\right], \\ S_{\rm s}[\phi_{\rm s}] &= \int d^d r \left[\frac{r}{2}\phi_{\rm s}^2 + \frac{1}{2}(\nabla\phi_{\rm s})^2 + \frac{\lambda}{4!}\phi_{\rm s}^4 - h\phi_{\rm s}\right], \\ S_{\rm c}[\phi_{\rm s},\phi_{\rm f}] &= \frac{\lambda}{4}\int d^d r \phi_{\rm s}^2\phi_{\rm f}^2 + \cdots \end{aligned}$$

Several approximations related to the loop order of the expansion are already imposed at this level. We have neglected terms of $\mathcal{O}(\phi_{\rm f}^4)$ because their contraction leads to two loop diagrams. The same applies to terms of $\mathcal{O}(\phi_{\rm s}\phi_{\rm f}^3)$ (exercise). Terms of $\mathcal{O}(\phi_{\rm s}^3\phi_{\rm f})$ do not arise because the addition of a fast momentum and three slow momenta is incompatible with momentum conservation.

Steps II and III

To simplify the notation, let us rescale the momentum according to $\mathbf{q} \to \mathbf{q}/\Lambda$, implying that coordinates are measured in units of the inverse cutoff $\mathbf{r} \to \mathbf{r}\Lambda$. With the coupling constants rescaled according to their engineering dimensions, $r \to r\Lambda^2$, $\lambda \to \lambda\Lambda^{4-d}$, the action remains unchanged, while the fast and slow momenta are now integrated over the dimensionless intervals $|\mathbf{q}_{\rm s}| \in [0, b^{-1}]$ and $|\mathbf{q}_{\rm f}| \in [b^{-1}, 1]$, respectively. We next construct an effective action by integration over the fast field: $e^{-S_{\rm eff}[\phi_{\rm s}]} = e^{-S_{\rm s}[\phi_{\rm s}]}\left\langle e^{-S_{\rm c}[\phi_{\rm s},\phi_{\rm f}]}\right\rangle_{\rm f}$. In performing the average over fast fluctuations, $\langle\cdots\rangle_{\rm f}$, we shall (a) retain only contributions of one-loop order while (b) neglecting terms that lead to the appearance of $\phi_{\rm s}^{n>4}$ contributions in the action. (For example, the contraction $\langle\left(\int \phi_{\rm s}^2\phi_{\rm f}^2\right)^3\rangle$ would lead to such a term.) To this level of approximation, one obtains

$$e^{-S_{\rm eff}[\phi_{\rm s}]} = e^{-S_{\rm s}[\phi_{\rm s}]}\exp\left[-\langle S_{\rm c}[\phi_{\rm s},\phi_{\rm f}]\rangle_{\rm f} + \frac{1}{2}\left\langle S_{\rm c}[\phi_{\rm s},\phi_{\rm f}]^2\right\rangle_{\rm f}^{\rm c}\right],$$

where the superscript c denotes a connected average. (Exercise: It is instructive to check the consistency of this expansion for yourself.) The two diagrams corresponding to the contractions $\langle S_{\rm c}[\phi_{\rm s},\phi_{\rm f}]\rangle_{\rm f}$ and $\langle S_{\rm c}[\phi_{\rm s},\phi_{\rm f}]^2\rangle_{\rm f}^{\rm c}$ are shown in parts (a) and (b) of the figure below, respectively, where the external line segments indicate the passive $\phi_{\rm s}$ amplitudes.

According to the standard rules of perturbation theory, the first of the two diagrams, (a), evaluates to

$$\langle S_{\rm c}[\phi_{\rm s},\phi_{\rm f}]\rangle_{\rm f} = \frac{\lambda}{4}\int_{\rm f}\frac{d^dq'}{(2\pi)^d}\frac{1}{r+q'^2}\int_{\rm s}\frac{d^dq}{(2\pi)^d}\phi_{\rm s}(\mathbf{q})\phi_{\rm s}(-\mathbf{q}).$$

We now consider the summation over fast momenta appearing in this expression. Using the fact that we are in the near vicinity of the critical point and anticipating that we are interested in no more than the expansion of the β-function for small values of the coupling, we now expand the integrand to first order in r, $\int_{\rm f}\frac{d^dq}{(2\pi)^d}\frac{1}{r+q^2} = I_1 - rI_2$, where we have introduced the shorthand notation,

$$I_\alpha \equiv \int_{\rm f}\frac{d^dq}{(2\pi)^d}\frac{1}{q^{2\alpha}}. \tag{8.28}$$

These integrals are straightforwardly computed by switching to polar coordinates,

$$I_\alpha = \Omega_d\int_{b^{-1}}^1 dq\; q^{d-2\alpha-1} = \frac{\Omega_d}{d-2\alpha}(1-b^{2\alpha-d}),$$

where $\Omega_d = (2\pi^{d/2}/\Gamma(d/2))/(2\pi)^d$ denotes the volume of the d-dimensional unit sphere (measured in units of 2π). We thus find that, after the integration over fast modes, and the standard rescaling operation, $\mathbf{q}\to b\mathbf{q}, \phi\to b^{(d-2)/2}\phi$, the quadratic part of the action takes the form

$$S^{(2)}[\phi] = \frac{b^2}{2}\left[r + \frac{\lambda\Omega_d}{2(d-2)}(1-b^{2-d}) - \frac{r\lambda\Omega_d}{2(d-4)}(1-b^{4-d})\right]\int d^dr\,\phi^2. \tag{8.29}$$

Turning to the second diagram (b) in the figure, we notice that, owing to the presence of four external legs, its contribution will be proportional to $\phi_{\rm s}^4$. Further, momentum conservation implies that the momenta carried by the internal lines of the diagram will depend on both the fast "internal" momentum and the external momenta carried by the fields $\phi_{\rm s}$. However, we can simplify the analysis by neglecting the dependence on the latter from the outset. The reason is that the integration over the internal momentum followed by Taylor expansion in the slow momenta would generate expressions of the structure $F(\mathbf{q}_1,\mathbf{q}_2,\mathbf{q}_3)\phi(\mathbf{q}_1)\phi(\mathbf{q}_2)\phi(\mathbf{q}_3)\phi(-\mathbf{q}_1-\mathbf{q}_2-\mathbf{q}_3)$, where $\mathbf{q}_{1,2,3}$ represent slow momenta and F is some polynomial. Taking account of the small momenta would thus generate derivatives acting on an operator of fourth order in ϕ, a combination that we saw above is irrelevant.

(a) (b)

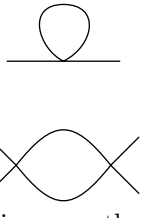

Neglecting the external momenta, diagram (b) leads to the result

$$\frac{1}{2}\langle S_{\rm c}[\phi_{\rm s},\phi_{\rm f}]^2\rangle_{\rm f} \simeq \frac{\lambda^2}{16}\int d^dr\,\phi_{\rm s}^4\int_{\rm f}\frac{d^dq}{(2\pi)^d}\frac{1}{(r+q^2)^2} = \frac{\lambda^2 I_2}{16}\int d^dr\,\phi_{\rm s}^4 + \mathcal{O}(\lambda^2 r).$$

Evaluating the integral and rescaling, we find that the quartic contribution to the renormalized action reads

$$S^{(4)}[\phi] = b^{4-d}\left(\frac{\lambda}{4!} - \frac{\lambda^2\Omega_d}{16}\frac{1-b^{4-d}}{d-4}\right)\int d^dr\,\phi^4.$$

Finally, there are no one-loop diagrams affecting the linear part of the action, i.e.

$$S^{(1)}[\phi] = hb^{d/2+1} \int d^d r\, \phi,$$

rescales according to its engineering dimension.

Combining everything, we find that, to one-loop order, the coupling constants scale according to the relations $r \to b^2(r + \frac{\lambda\Omega_d}{2(d-2)}(1-b^{2-d}) - \frac{r\lambda\Omega_d}{2(d-4)}(1-b^{4-d}))$, $\lambda \to b^{4-d}(\lambda - \frac{3}{2}\lambda^2\Omega_d \frac{1-b^{4-d}}{d-4})$, and $h \to hb^{d/2+1}$. We next set $d = 4-\epsilon$ and evaluate the right-hand sides of these expressions to leading order in ϵ. With $\Omega_{4-\epsilon} \approx \Omega_4 = \frac{1}{8\pi^2}$, we thus obtain

$$\begin{aligned} r &\to b^2\left(r + \frac{\lambda}{32\pi^2}(1-b^{-2}) - \frac{r\lambda}{16\pi^2}\ln b\right), \\ \lambda &\to (1+\epsilon\ln b)\left(\lambda - \frac{3\lambda^2}{16\pi^2}\ln b\right), \\ h &\to hb^{3-\epsilon/2}, \end{aligned}$$

which, setting $b = e^\ell$, lead to the **Gell-Mann–Low equations**:

$$\boxed{\begin{aligned} \frac{dr}{d\ell} &= 2r + \frac{\lambda}{16\pi^2} - \frac{r\lambda}{16\pi^2}, \\ \frac{d\lambda}{d\ell} &= \epsilon\lambda - \frac{3\lambda^2}{16\pi^2}, \\ \frac{dh}{d\ell} &= \frac{6-\epsilon}{2}h. \end{aligned}} \tag{8.30}$$

These equations clearly illustrate the meaning of the ϵ-expansion. According to the second equation, a perturbation away from the Gaussian fixed point will initially grow at a rate set by the engineering dimension ϵ. While, on the level of the classical, zero-loop theory, λ would grow indefinitely, the one-loop contribution $\sim \lambda^2$ stops the flow at a value $\lambda \sim \epsilon$.

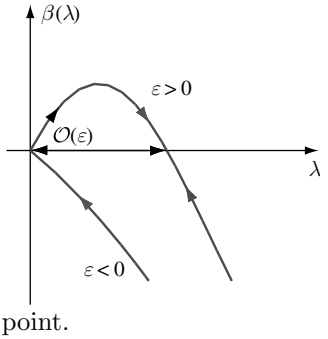

Equating the right-hand sides of Eq. (8.30) to zero (and temporarily ignoring the magnetic field), we indeed find that besides the Gaussian fixed point $(r_1^*, \lambda_1^*) = (0,0)$ a **non-trivial fixed point** $(r_2^*, \lambda_2^*) = (-\frac{1}{6}\epsilon, \frac{16\pi^2}{3}\epsilon)$ has appeared. Notice that, in accord with the schematic considerations made at the beginning of the section, the second fixed point is $\mathcal{O}(\epsilon)$ and coalesces with the Gaussian fixed point as ϵ is sent to zero. Plotting the β-function for the coupling constant λ (see figure), we further find that, for $\epsilon > 0$, λ is relevant around the Gaussian fixed point but irrelevant at the non-trivial fixed point.

To understand the full flow diagram of the system, one may linearize the β-function around both the Gaussian and the non-trivial fixed point. Denoting the linearized mappings by $W_{1,2}$, we find

$$W_1 = \begin{pmatrix} 2 & \frac{1}{16\pi^2} \\ 0 & \epsilon \end{pmatrix}, \quad W_2 = \begin{pmatrix} 2-\frac{1}{3}\epsilon & \frac{1+\epsilon/6}{16\pi^2} \\ 0 & -\epsilon \end{pmatrix}.$$

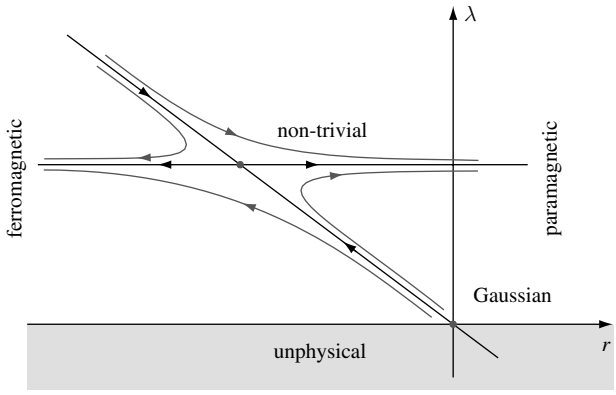

Figure 8.8 Phase diagram of the ϕ^4-model as obtained from the ϵ-expansion.

Figure 8.8 shows the flow in the vicinity of the two fixed points, as described by the matrices $W_{1,2}$ as well as the extrapolation to a global flow chart. Notice that the critical surface of the system – the straight line interpolating between the two fixed points – is tilted with respect to the $r \sim$ temperature axis of the phase diagram. This implies that it is not the physical temperature alone that decides whether the system will eventually wind up in the paramagnetic ($r \gg 0$) or ferromagnetic ($r \ll 0$) sector of the phase diagram. Rather one has to relate temperature ($\sim r$) to the strength of the nonlinearity ($\sim \lambda$) to decide on which side of the critical surface we are. For example, for strong enough λ, even a system with r initially negative may eventually flow towards the disordered phase. This type of behavior cannot be predicted from the mean-field analysis of the model (which would generally predict a ferromagnetic state for $r < 0$). Rather it represents a non-trivial effect of fluctuations. Finally notice that, while we can formally extend the flow into the lower portion of the diagram, $\lambda < 0$, this region is actually unphysical. The reason is that, for $\lambda < 0$, the action is fundamentally unstable and, in the absence of a sixth-order contribution, does not describe a physical system.

What are the critical exponents associated with the one-loop approximation? Of the two eigenvalues of W_2, $2 - \epsilon/3$ and $-\epsilon$, only the former is relevant. As with the Gaussian fixed point, it is tied to the scaling of the coupling constant, $r \sim t$, i.e. we have $y_t = 2 - \epsilon/3$ and, as before, $y_h = (d+2)/2 = (6-\epsilon)/2$. An expansion of the exponents summarized in Eq. (8.22) to first order in ϵ then yields the list

$$\alpha = \frac{\epsilon}{6}, \quad \beta = \frac{1}{2} - \frac{\epsilon}{6}, \quad \gamma = 1 + \frac{\epsilon}{6}, \quad \delta = 3 + \epsilon, \quad \nu = \frac{1}{2} + \frac{\epsilon}{12}, \quad \eta = 0.$$

If we are now reckless enough to extend the radius of the expansion to $\epsilon = 1$, i.e. $d = 3$, we obtain the fifth column of Table 8.1. Apparently the agreement with the experimental results has improved – even in spite of the fact that we have driven the ϵ-expansion well beyond its range of applicability! (For $\epsilon = 1$, terms of $\mathcal{O}(\epsilon^2)$ can, of course, no longer be neglected!)

How can one rationalize the **success of the ϵ-expansion**? Trusting in the principle that good theories tend to work well beyond their regime of applicability, we might simply speculate that nature seems to be sympathetic to the concept of renormalization and the loop expansion. Of course, a more qualified approach to the question is to explore what happens at higher order in the ϵ-expansion. Needless to say, the price to be paid for this ambition is that, at orders $\mathcal{O}(\epsilon^{n>1})$, the analysis indeed becomes laborious. Nonetheless, the success of the first-order expansion prompted researchers to drive the ϵ-expansion up to fifth order! The results of this analysis are summarized in the last column of Table 8.1. In view of the fact that we are still extending a series beyond its radius of convergence,[32] the level of agreement with the experimental data is striking. In fact, the exponents obtained by the ϵ-expansion even agree – to an accuracy better than one percent – with the exponents of the *two*-dimensional model,[33] i.e. for a situation where the "small" parameter ϵ has to be set to two.

However, it is important to stress that the ϵ-expansion is not just a computational tool for the calculation of exponents. On a more conceptual level, its merit is that it enables one to explore the phase diagram of nonlinear theories in a more or less controlled manner. In fact, the ϵ-expansion not only is useful in the study of field theories close to the upper critical dimension (i.e. close to the mean-field threshold) but can equally well be applied to the analysis of systems in the vicinity of the lower critical dimension. In the following section, we consider a problem of this type, i.e. we will apply an ϵ-expansion around $d = 2$ to detect the onset of global thermal disorder in models with continuous symmetries.

8.5 RG analysis of the nonlinear σ-model

The scalar field theory encapsulates a wide class of systems encompassing a single-component order parameter. However, throughout the text, we have encountered problems where the order parameter involves more than one component, e.g. the complex field associated with condensation phenomena, the matrix field associated with the quantum disordered metallic system, or the field theories involving spin. In such cases, one very often finds that the low-energy content of the theory involves a projection which imparts a constraint to the field integral. In the context of condensation phenomena, we saw that, at low temperatures, one can neglect the massive amplitude fluctuations of the order parameter, while the collective fluctuations of the phase mode impacted significantly on the low-energy properties of the system. In this case, the phase degree of freedom is constrained by its topology to lie on the unit circle. Similarly, if we neglect the "high-energy" physics of local moment formation, classical and quantum spin theories are constrained by the normalization of the local spin. When subjected to an auxiliary constraint, theories that are otherwise free are known as nonlinear σ-models. The aim of the present section is to apply methods of the RG to explore the critical properties of a general class of nonlinear

[32] Indeed, it is believed that we are dealing with a series that is only asymptotically convergent. That is, beyond a certain order of the expansion, the agreement with the "true" exponents will presumably become worse.

[33] The latter are known from the exact solution of the two-dimensional model, see L. Omsager, Crystal statistics I. A two-dimensional model with an order–disorder transition. *Phys. Rev.* **65** (1944), 117–49.

σ-models. Later, in the next section and in Chapter 9, we will consider the way topological considerations can impact on the nature of the system.

Let us then consider the nonlinear σ-model defined by the partition function $\mathcal{Z} = \int Dg\, e^{-S[g]}$, where

$$S[g] = \frac{1}{\lambda} \int d^d r \ \mathrm{tr}\left[\nabla g \nabla g^{-1}\right], \tag{8.31}$$

$g \in G$ takes values in some compact Lie group G and the integration $\int Dg = \prod_x \int d_\mu g(x)$ extends over the **Haar measure** $d_\mu g$ of G. (Later in this section, we will specialize to the case $G = \mathrm{O}(3)$ relevant to the case of the three-component spin models, the Heisenberg magnet. Other realizations of G will be met in the next chapter.)

INFO The **Haar measure** $d_\mu g$ of a compact Lie group G is a (uniquely specified) integration measure that is (a) unit normalized, i.e. $\int_G d_\mu g \cdot 1 = 1$, and (b) invariant under left and right multiplication by a fixed group element:

$$\int_G d_\mu g\, f(g) = \int_G d_\mu g\, f(gh^{-1}) = \int_G d_\mu g\, f(h^{-1}g)$$

for any $h \in G$. Upon translation of the integration variable $g \to hg$ or $g \to gh$, these equations assume the form $\int_G d_\mu(gh)\, f(g) = \int_G d_\mu g\, f(g) = \int_G d_\mu(hg)\, f(g)$. Holding for any f, this implies that $d_\mu(hg) = d_\mu g = d_\mu(gh)$, which tells us that the Haar measure assigns equal volume density to any point on the group manifold. Owing to this homogeneity property, integrations over groups are almost always performed with respect to the Haar measure. Details on the explicit construction of this measure can be found in textbooks on Lie group theory.[34]

Alexander M. Polyakov 1945–

He has made several important contributions to quantum field theory from non-abelian gauge theory to conformal field theory. His path integral formulation of string theory had profound and lasting impacts in the conceptual and mathematical understanding of the theory. He also played an important role in elucidating the conceptual framework behind renormalization independent of Kenneth Wilson's Nobel prize winning work. He formulated pioneering ideas in gauge/string duality long before the breakthrough of AdS/CFT using D-branes.

As we have seen above, the presence of a continuous symmetry identifies the lower critical dimension of the theory at $d_\mathrm{c} = 2$. At dimensions of d_c and below, massless Goldstone fluctuations of the field destroy long-range order at any non-zero temperature. However, in the range $2 < d < 4$, one expects an ordered phase to persist at low temperatures, while the critical characteristics of the phase in the vicinity of the transition are fluctuation dominated. For reasons that will become clear, in the following we develop an ϵ-expansion around the lower critical dimension to detect the fixed point structure of the model. (Such an ϵ-expansion was proposed in a seminal work

[34] See, e.g., J. Fuchs and C. Schweigert, *Symmetries, Lie Algebras and Representations, a Graduate Course for Physicists* (Cambridge University Press, 1997).

by Polyakov.[35]). However, before turning to the actual formulation of the RG analysis, we need to do a bit of preparatory work.

As usual, let us split the matrix fields g into "slow" and "fast" components. This is achieved by defining $g(\mathbf{r}) = g_{\rm s}(\mathbf{r})g_{\rm f}(\mathbf{r})$, where $g_{\rm s}(\mathbf{r})$ and $g_{\rm f}(\mathbf{r})$ have momentum components in the ranges $[0, \Lambda b^{-1}]$ and $[\Lambda b^{-1}, \Lambda]$, respectively. Substituting this decomposition into the action, one obtains $S[g_{\rm s}g_{\rm f}] = S[g_{\rm s}] + S[g_{\rm f}] + S_{\rm c}[g_{\rm s}, g_{\rm f}]$, where the coupling action

$$S_{\rm c}[g_{\rm s}, g_{\rm f}] = \frac{2}{\lambda} \int d^d r \ {\rm tr} \left[g_{\rm s}^{-1} \nabla g_{\rm s} g_{\rm f} \nabla g_{\rm f}^{-1} \right] . \tag{8.32}$$

In the next step, one must integrate over the fast field $g_{\rm f}$. Since, of course, this integration cannot be performed exactly, we will have to resort to an approximation scheme based on the loop expansion. Yet, before doing so, we need to provide a little more background information on field integration over group-valued variables in general.

8.5.1 Field integrals over groups

As with any other nonlinear integration space, to perform an integral over a group one first needs to introduce a set of suitable coordinates. Of course, with the choice of these variables one can exercise some freedom. However, in most applications, one will employ exponential coordinates, i.e. one may start out from $g = e^W$, where $W \in \mathcal{G}$ lives in the Lie algebra of the group, and then expand $W = i \sum_a \pi^a T^a$ in the Hermitian group generators.

INFO Recall that the **generators T^a of a Lie group** are M elements of the Lie algebra $\mathcal{G}$ specified by the following two conditions. (i) The set $\{T^a | a = 1, \ldots, M\}$ is a basis of $\mathcal{G}$.[36] (ii) The commutators translate to the relation $[T^a, T^b] = -if^{abc}T^c$, where the so-called **structure constants** f^{abc} encode the geometry of the group. For example, the structure constants of the three-dimensional ($M = 3$) groups SU(2) and O(3) are given by $f^{abc} = \epsilon^{abc}$, $a, b, c = 1, 2, 3$, where ϵ^{abc} is the antisymmetric tensor. For SU(2), the generators $T^a = \frac{1}{2}\sigma_a$ can be identified with (one half of) the Pauli matrices, for O(3) with the angular momentum operators familiar from quantum mechanics.

For later reference, we note that the generators of the group families ${\rm U}(N), {\rm SU}(N)$ and ${\rm O}(N)$ obey the **completeness relations**

$$\sum_{a=1}^{M} T^a_{ij} T^a_{kl} = \frac{1}{2}\delta_{il}\delta_{jk}, \quad {\rm U}(N), \tag{8.33}$$

$$\sum_{a=1}^{M} T^a_{ij} T^a_{kl} = \frac{1}{2}\delta_{il}\delta_{jk} - \frac{1}{2N}\delta_{ij}\delta_{kl}, \quad {\rm SU}(N), \tag{8.34}$$

$$\sum_{a=1}^{M} T^a_{ij} T^a_{kl} = \delta_{il}\delta_{jk} - \delta_{ik}\delta_{jl}, \quad {\rm O}(N). \tag{8.35}$$

[35] A. M. Polyakov, Interactions of Goldstone particles in two dimensions. Applications to ferromagnets and massive Yang–Mills fields, *Phys. Lett. B* **59** (1975), 79–81.

[36] The Lie algebra of an M-dimensional Lie group is a vector space, so it has a basis. The "vectors" of this space are realized by $(N \times N)$-dimensional matrices T_a.

(Here, the upper summation limits are set by $M = N^2$ for $G = \mathrm{U}(N)$, $M = N^2 - 1$ for $G = \mathrm{SU}(N)$, and $M = N(N-1)/2$ for $G = \mathrm{O}(N)$ – exercise: why?)

In general, the generators can be chosen so as to obey the normalization condition $\mathrm{tr}(T^a T^b) = c\delta^{ab}$, where c is a normalization constant. Interpreting $\langle W|W'\rangle \equiv \mathrm{tr}(WW')$ as a scalar product on the Lie algebra (exercise: convince yourself that $\langle\ |\ \rangle$ meets all the criteria required of a scalar product), the equation above tells us that the set $\{T_a\}$ forms an orthonormal basis. In the cases $\mathrm{U}(N), \mathrm{SU}(N)$ and $\mathrm{O}(N)$, consistency with the orthonormalization relation above enforces the normalization $c = 1/2, 1/2$, and 1, i.e.

$$\begin{aligned} \mathrm{tr}(T^a T^b) &= \frac{\delta^{ab}}{2}, \quad \mathrm{U}(N), \mathrm{SU}(N), \\ \mathrm{tr}(T^a T^b) &= \delta^{ab}, \quad \mathrm{O}(N). \end{aligned} \tag{8.36}$$

Integration over all N real coefficients π^a will cover the full group G. Yet there remains one non-trivial problem to be solved: we need to understand how to express the Haar measure $d_\mu g \to d\pi\, J(\pi)$ in terms of the new integration variables. Here, the "flat measure" $d\pi = \prod_a d\pi^a$ comprises the integration over all Lie algebra coefficients while the function $J(\pi)$ encapsulates both the geometry of the Haar measure and the Jacobian associated with the transformation $g \to \sum_a \pi^a T_a$. Referring for a more detailed discussion of the function J to text books on group theory, we here merely note that its Taylor expansion in π starts as $J(\pi) = 1 + \mathcal{O}(\pi^4)$ where the $\mathcal{O}(\pi^4)$ term will not play a role in the context of the one-loop analysis below. Thus, at the level of approximation discussed in this text, the integration measure of the fast-field components can be approximated by the "flat" measure $d\pi$.

Using the RG application above as an example, let us now discuss how integrals over fluctuations in the group space are performed in practice. Substitution of the expansion $g_\mathrm{f} = e^W = 1 + W + W^2/2 + \cdots$ into $S[g_\mathrm{f}]$ and $S_\mathrm{c}[g_\mathrm{f}, g_\mathrm{s}]$, gives a series of contributions $S = \sum_n S^{(n)}$ where $S^{(n)}$ is of nth order in the local field amplitudes W. As usual, we will organize our analysis around the fully solvable sector of the theory, i.e. the action quadratic in W. A straightforward substitution into $S[g_\mathrm{f}]$ gives

$$\begin{aligned} S^{(2)}[W] \quad &= \quad -\frac{1}{\lambda}\int d^d r\, \mathrm{tr}\,[\nabla W\, \nabla W] = \frac{1}{\lambda}\int d^d r\, \nabla\pi^a \nabla\pi^b\, \mathrm{tr}\left[T^a T^b\right] \\ &\overset{(8.36)}{=} \quad \frac{1}{\lambda}\int d^d r\, \nabla\pi^a \nabla\pi^a = \frac{1}{2}\sum_{\mathbf{p}\in f} \pi^a_{\mathbf{p}} \Pi^{-1}_{\mathbf{p}} \pi^a_{-\mathbf{p}}, \end{aligned}$$

where we have used the normalization condition (8.36), $\sum_{\mathbf{p}\in f}$ stands for a summation over the fast momentum sector and we have introduced $\Pi_{\mathbf{p}} \equiv \frac{\lambda}{2L^d p^2}$ as the propagator of the fast fields π^a.

Below, we engage integrals of the type $\langle \mathrm{tr}(F(W(\pi))\mathrm{tr}(G(W(\pi))\cdots\rangle_W$, where $F, G, \ldots$ are functions of the generators W and $\langle\cdots\rangle_\pi \equiv \mathcal{N}\int d\pi \exp(-S^{(2)}[\pi])(\cdots)$ denotes averaging over the quadratic action. These integrals may be evaluated with the help of Wick's theorem and the completeness relation (8.35). Wick's theorem states that we need to form all possible pairings of π-variables or, equivalently, W-matrices. Each pairing is of the form either $\langle \mathrm{tr}(AW)\mathrm{tr}(A'W)\rangle$ or $\langle \mathrm{tr}(AWA'W)\rangle$, where the matrices A and A' may contain W-

matrices themselves (however, when computing an individual pairing, these matrices are temporarily kept fixed). Specifically, for $G = \mathrm{O}(N)$ the Gaussian integrals give[37]

$$\begin{aligned}\langle \mathrm{tr}(AW_{\mathbf{p}})\mathrm{tr}(A'W_{\mathbf{p}'})\rangle_W &= -\langle \pi^a_{\mathbf{p}}\pi^{a'}_{\mathbf{p}'}\rangle_W \,\mathrm{tr}(AT^a)\mathrm{tr}(A'T^{a'}) \\ &= -\delta_{\mathbf{p},-\mathbf{p}'}\Pi_{\mathbf{p}}\,\mathrm{tr}(AT^a)\,\mathrm{tr}(A'T^a) \overset{(8.35)}{=} -\delta_{\mathbf{p},-\mathbf{p}'}\Pi_{\mathbf{p}}\left[\mathrm{tr}(AA') - \mathrm{tr}(AA'^T)\right], \\ \langle \mathrm{tr}(AW_{\mathbf{p}}A'W_{\mathbf{p}'})\rangle_W &= -\underset{W}{\pi^a_{\mathbf{p}}\pi^{a'}_{\mathbf{p}'}}\,\mathrm{tr}\,(AT^aA'T^{a'}) \\ &= -\delta_{\mathbf{p},-\mathbf{p}'}\Pi_{\mathbf{p}}\,\mathrm{tr}(AT^aA'T^a) \overset{(8.35)}{=} -\delta_{\mathbf{p},-\mathbf{p}'}\Pi_{\mathbf{p}}\left[\mathrm{tr}(A)\mathrm{tr}(A') - \mathrm{tr}(AA'^T)\right].\end{aligned}$$

Integrals over W-matrices are computed by applying these contraction rules until all possible pairings have been exhausted. Probably the best way to become acquainted with this procedure is to work through an example.

EXERCISE Consider the expression $X \equiv \big\langle \mathrm{tr}(A_{\mathbf{q},\mathbf{p}}W_{\mathbf{p}+\mathbf{q}}W_{-\mathbf{p}})\mathrm{tr}\;\; A'_{\mathbf{q}',\mathbf{p}'}W_{\mathbf{p}'+\mathbf{q}'}W_{-\mathbf{p}'}\;\big\rangle_W$, where $A, A' \in \mathrm{o}(N)$ belong to the Lie algebra of $\mathrm{O}(N)$ (which implies, in particular, that they are traceless). Show that the pair contraction of the first W-matrix with the second (the third and the fourth) vanishes due to the tracelessness of A and A'. Next perform the contractions $(1-4)(2-3)$ and $(1-3)(2-4)$ to obtain the result $X = (N-2)\;\;{}_{\mathbf{p}}\;\;{}_{\mathbf{p}+\mathbf{q}}\mathrm{tr}\left[A_{\mathbf{p},\mathbf{q}}\;\;A'_{-\mathbf{q},\mathbf{p}+\mathbf{q}} - A'_{-\mathbf{q},-\mathbf{p}}\;\right]$.

8.5.2 One-loop expansion

With this background, let us now return to the actual RG program for the $\mathrm{O}(N)$-model. As a first step, we need to identify all contractions that lead to no more than one fast momentum integration (one-loop order). Since the contraction of terms of $\mathcal{O}(W(x)^{n>4})$ will generate at least two fast integrations, it suffices [38] to consider the action $S[g_{\mathrm{s}}, W]$ at order W^2. Substitution of $g_{\mathrm{f}} = 1 + W + W^2/2$ into the action (8.32) gives

$$S^{(2)}_{\mathrm{c}}[g_{\mathrm{s}}, W] = \frac{1}{\lambda}\int d^dr\;\mathrm{tr}\,(\Phi_\mu[\nabla_\mu W, W]) \simeq -\frac{2iL^d}{\lambda}\sum_{\mathbf{q}}\sum_{\mathbf{p}\in\mathrm{f}} p_\mu\,\mathrm{tr}\,[\Phi_{\mu,-\mathbf{q}}W_{\mathbf{p}+\mathbf{q}}W_{-\mathbf{p}}],$$

where we have introduced the abbreviation $\Phi_\mu = g_{\mathrm{s}}^{-1}\partial_\mu g_{\mathrm{s}}$ and, in the last representation, neglected the small momentum in comparison with the fast, $2\mathbf{p}+\mathbf{q} \simeq 2\mathbf{p}$. To obtain all one-loop corrections, we have to expand the functional in powers of $S^{(2)}_{\mathrm{c}}[g_{\mathrm{s}}, W]$ and integrate over W. However, since each power of $S^{(2)}_{\mathrm{c}}$ comes with one derivative acting on a slow field, and terms of more than two such derivatives are irrelevant, it suffices to consider terms of order $\mathcal{O}((S^{(2)}_{\mathrm{c}})^2)$. To one-loop order, the RG step thus effects the replacement

$$S[g] \to S[g_{\mathrm{s}}] - \ln\left(1 + \frac{1}{2}\big\langle\left(S^{(2)}_{\mathrm{c}}[g_{\mathrm{s}}, W]\right)^2\big\rangle_W\right) \simeq S[g_{\mathrm{s}}] - \frac{1}{2}\big\langle\left(S^{(2)}_{\mathrm{c}}[g_{\mathrm{s}}, W]\right)^2\big\rangle_W.$$

[37] Although we are primarily interested in the case $N = 3$, it will be instructive to monitor the RG flow for general values of N.

[38] Convince yourself that contributions to the action of $\mathcal{O}(W^3)$ also do not contribute at the one-loop level. (A good way to do this is to invent some prototypical diagrammatic code that keeps track of the momentum flow.) As in our previous analysis of the ϕ^4-model, the expansion of $S[g_{\mathrm{s}}, W]$ to linear order in W vanishes. (Momentum conservation implies that it is not possible to integrate a single fast field against a single slow field.)

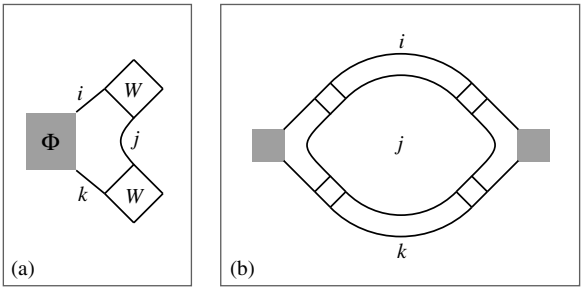

Figure 8.9 (a) Graphical visualization of the matrix vertex $\mathrm{tr}(\Phi W W)$. The line segments connecting the boxes represent the matrix indices. (b) One-loop diagram representing the contraction $\langle \mathrm{tr}(\Phi W W)\,\mathrm{tr}\,(\Phi W W)\rangle \to N\,\mathrm{tr}\,(\Phi\Phi)$. The factor of N stems from the free summation over the central index j.

Written more explicitly,

$$\Big\langle \Big(S_{\rm c}^{(2)}[g_{\rm s},W]\Big)^2\Big\rangle_W = \sum_{\mathbf{q},\mathbf{q}'}\sum_{\mathbf{p},\mathbf{p}'\in {\rm f}} \langle \mathrm{tr}(A_{\mathbf{q},\mathbf{p}}W_{\mathbf{p}+\mathbf{q}}W_{-\mathbf{p}})\mathrm{tr}(A_{\mathbf{q}',\mathbf{p}'}W_{\mathbf{p}'+\mathbf{q}'}W_{-\mathbf{p}'})\rangle_W,$$

where $A_{\mathbf{p},\mathbf{q}} = -\frac{2iL^d}{\lambda}p_\mu \Phi_{\mu,-\mathbf{q}}$, i.e. an expression of the type considered in the exercise above. Drawing on that analysis (see Fig. 8.9), one obtains

$$\begin{aligned}
\Big\langle \Big(S_{\rm c}^{(2)}[g_{\rm s},W]\Big)^2\Big\rangle_W &\simeq -\frac{8(N-2)L^{2d}}{\lambda^2}\sum_{\mathbf{p}\in{\rm f}}(\Pi_{\mathbf{p}})^2 p_\mu p_\nu \sum_{\mathbf{q}}\mathrm{tr}(\Phi_{\mu,\mathbf{q}}\,\Phi_{\nu,-\mathbf{q}})\\
&\simeq -2(N-2)\int \frac{d^dp}{(2\pi)^d}\frac{p_\mu p_\nu}{p^4}L^d\sum_{\mathbf{q}}\mathrm{tr}(\Phi_{\mu,\mathbf{q}}\Phi_{\nu,-\mathbf{q}})\\
&= -C\int d^dr\,\mathrm{tr}\,[\Phi_\mu\,\Phi_\mu] = C\int d^dr\,\mathrm{tr}\left[\nabla g_{\rm s}\nabla g_{\rm s}^{-1}\right] = C\lambda S[g_{\rm s}],
\end{aligned}$$

where the constant

$$\begin{aligned}
C &= \frac{2(N-2)}{d}\int\frac{d^dp}{(2\pi)^d}\frac{1}{p^2} = \frac{2(N-2)\Omega^d}{d(2\pi)^d}\int_{\Lambda/b}^{\Lambda} dp\; p^{d-3}\\
&= \frac{2(N-2)\Omega^d(\Lambda^{d-2}-(\Lambda/b)^{d-2})}{(2\pi)^d d(d-2)} \overset{d=2+\epsilon}{\simeq} \frac{(N-2)\ln b}{2\pi}.
\end{aligned}$$

Substituting this result back into the action, one obtains

$$S[g] \to \left(1-\frac{(N-2)\ln b\lambda}{4\pi}\right)S[g_s] \mapsto \left(1-\frac{(N-2)\ln b\lambda}{4\pi}\right)b^\epsilon S[g],$$

where in the second step we performed the rescaling of the momenta (i.e. we rescaled $q \to bq$, in such a way that the formerly "slow" momenta again take values up to the cutoff Λ, and noted that $\epsilon \equiv d-2$. As expected, the RG reproduces the action up to a global

scaling factor. Absorbing this factor in a renormalized coupling constant, $\lambda_{\rm r}$, we obtain $\lambda_{\rm r}^{-1} = \left(1 - \frac{(N-2)\ln b\lambda}{2\pi}\right) b^{\epsilon}\lambda^{-1}$, or

$$\lambda_{\rm r} = \left(1 - \frac{(N-2)\ln b\lambda}{4\pi}\right)^{-1} b^{-\epsilon}\lambda \simeq \ln b\lambda \left(\frac{(N-2)\lambda}{4\pi} - \epsilon\right) + \lambda.$$

Here, in the last equality, we have made use of the fact that both λ and ϵ are small.[39] Finally, differentiating this result one obtains the RG equation

$$\boxed{\frac{d\ln\lambda}{d\ln b} \simeq \frac{(N-2)\lambda}{4\pi} - \epsilon + \mathcal{O}(\lambda^2, \epsilon^2, \lambda\epsilon).} \tag{8.37}$$

The figure below shows the RG flow for generic ($N > 2$) group dimensions and different values of ϵ. As expected, for dimensions two and below, the coupling constant inexorably flows towards a phase with large λ where fluctuations are large (and our perturbative analysis loses its basis) – the "disordered" type of behavior pervasive in the physics of low-dimensional systems with continuous symmetries. However, for dimensions $d > 2$, the model exhibits a fixed point at finite coupling strength $\lambda_{\rm c} = 2\pi\epsilon/(N-2)$. Linearizing in the vicinity of the fixed point, one finds a thermal exponent $y_\lambda = \epsilon$ from which, making use of the scaling relations, one can deduce a correlation length exponent $\nu \approx 1/\epsilon$ and a heat capacity exponent $\alpha \approx 2 - 2/\epsilon$.

EXERCISE To complete the analysis of the O(3) model, one may explore the magnetic exponent. Introducing a magnetic field perturbation into the action, i.e. $h\int d^dr\,\mathrm{tr}\,[g + g^{-1}]$, show that, under renormalization, $h' = b^{y_h}h$, where $y_h = 1 + \frac{N-3}{2(N-2)} + \mathcal{O}(\epsilon^2)$. From this result, use the exponent identities to show that the correlation length exponent $\eta \approx \epsilon/(N-2)$.

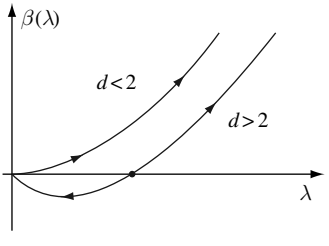

Notice that, for $d = 2$ and $N = 2$, the coupling constant does not renormalize. This is because, for O(2) – the abelian group of planar rotations – the action of the σ-model simplifies to $S = \frac{1}{\lambda}\int d^2r\,(\nabla\phi)^2$, where $\phi(\mathbf{r})$ is the field of local rotation angles. This is a free action which is not renormalized by small fluctuations. (However, in the following section, we see that the situation is not quite as simple as it seems. The O(2) model admits large fluctuations – vortex configurations of the angular field – which *do* have a non-trivial impact on its behavior. However, being topological in nature, these excitations are beyond the scope of our present analysis.)

[39] The smallness of λ is needed to justify the perturbative loop expansion. In the opposite regime $\lambda \gg 1$, the fields g fluctuate wildly and perturbative expansions are not an option.

EXERCISE Repeat the analysis above for the SU(N)-model. First derive the intermediate identities,

$$\begin{aligned}\langle \mathrm{tr}(AW_{\mathbf{p}})\mathrm{tr}(A'W_{\mathbf{p}'})\rangle_W &= -\delta_{\mathbf{p},-\mathbf{p}'}\frac{\mathbf{p}}{2}\left[\mathrm{tr}(AA') - \frac{1}{N}\mathrm{tr}(A)\mathrm{tr}(A')\right],\\ \langle \mathrm{tr}(AW_{\mathbf{p}}A'W_{\mathbf{p}'})\rangle_W &= -\delta_{\mathbf{p},-\mathbf{p}'}\frac{\mathbf{p}}{2}\left[\mathrm{tr}(A)\mathrm{tr}(A') - \frac{1}{N}\mathrm{tr}(AA')\right],\end{aligned}$$

where $\mathbf{q} = \lambda/L^d p^2$, and

$$p_\mu p_{\mu'}\langle \mathrm{tr}(\Phi_{\mu,\mathbf{q}}W_{\mathbf{p}+\mathbf{q}}W_{-\mathbf{p}})\mathrm{tr}(\Phi_{\mu',\mathbf{q}'}W_{\mathbf{p}'+\mathbf{q}'}W_{-\mathbf{p}'})\rangle_W = N\frac{\mathbf{p}\quad\mathbf{p}+\mathbf{q}}{4}p_\mu p_{\mu'}\mathrm{tr}(\Phi_{\mu,\mathbf{q}}\Phi_{\mu',-\mathbf{q}}).$$

Use these results to obtain the RG equation

$$\frac{d\ln\lambda}{d\ln b} \simeq \frac{N\lambda}{8\pi} - \epsilon + \mathcal{O}(\lambda^2, \epsilon^2, \lambda\epsilon). \tag{8.38}$$

Notice that the right-hand side of the SU($N = 2$) equation coincides with the right-hand side of the O($N = 3$) equation. This reflects the (local) isomorphism of the groups O(3) and SU(2).

8.6 Berezinskii–Kosterlitz–Thouless transition

The majority of theories discussed in earlier chapters were defined on essentially structureless target spaces – the real line, the complex plane, or, more generally, vector spaces of arbitrary dimensionality. Although we have encountered a number of models with more complex target manifolds (such as the superconductor, the Luttinger action with fields defined on the unit circle, and the nonlinear σ-model theories discussed in the previous section), the global geometric structure of the target space did not seem to play such an important role: the phase behavior of the O(N)-theory appears to differ little from an unconstrained N-component vector ϕ^4-theory. However, the large-scale geometry, or topology of the field manifold, may have a striking influence on the long-range behavior of a system, and it is one of the objectives of the present section to illustrate this phenomenon on a particular example. (A more comprehensive discussion of the role of geometry and topology in quantum field theory will be developed in the next chapter.)

Consider then a two-dimensional square lattice with a phase-like variable $\exp(i\theta_i) \in S_1$ defined on each of its sites i. Demanding that the Hamiltonian or action of the system be periodic in all θ_i and minimal on homogeneous field configurations, the most elementary action we can formulate reads

$$\boxed{S[\theta] = -J\sum_{\langle ij\rangle}\cos(\theta_i - \theta_j),} \tag{8.39}$$

where $\sum_{\langle ij\rangle}$ denotes the usual sum over nearest neighbor sites of a lattice. Equation (8.39) is known as the action of the **two-dimensional XY-model**. (Its incarnation as a continuum field theory is the U(1) version of the nonlinear σ-model discussed above.) To motivate the terminology, one may regard θ_i as an angle parameterizing the direction of a unimodular vector (a classical "spin") in the two-dimensional XY-plane. Indeed, the model Eq. (8.39)

can be viewed as a two-dimensional descendant of the classical Heisenberg model, i.e. as a model where the Heisenberg spin is confined to a two-dimensional plane (a condition in fact realized for a number of magnetic materials).

INFO Besides its natural occurrence in magnetism, the XY-model appears in many applications in condensed matter physics. By way of an example, we mention here the physics of granulated metals and the **Josephson junction array**.

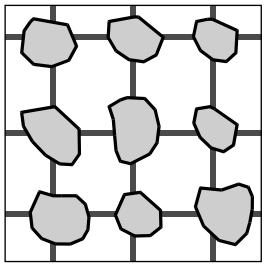

Imagine then a system of small metallic (or superconducting) islands (see figure), which are connected by poorly conducting tunneling barriers. (Arrays of this structure are believed to mimic the mesoscopic morphology of structurally disordered metals. However, they can also be manufactured artificially, with islands as small as several nanometers.) On a microscopic level, the state of the system is essentially determined by the number N_i of electronic charges populating each island i. However, unless the inter-grain tunneling conductance, $g_{\rm T}$, is small (i.e. $g_{\rm T} < e^2/h$, the fundamental quantum unit of conductance), temporal fluctuations of the charge degrees of freedom are vast. It is then more favorable to characterize the state of the system in terms of the variable canonically conjugate to the charge variable, i.e. the phase θ_i. (Remember that $[\theta_i, \hat{N}_j] = -i\delta_{ij}$ form a canonically conjugate pair.) The model action $S[\theta]$ then, of course, depends on the microscopic structure of the system. However, for the case of a superconductor array, in the classical limit (where temporal fluctuations of the phase field $\theta(\tau)$ are suppressed), and neglecting charging effects, the action collapses to that of the XY-action shown above. (Recapitulate the structure of the single-junction Josephson action discussed in Problem 6.7 to convince yourself that this is true.)

Amongst the class of classical spin models, the two-dimensional XY-model assumes a unique status – a fact already hinted at in consideration of the RG in the previous section. To understand why, it is helpful to explore the high- and low-temperature expansions of the theory. In the **high-temperature** phase, $J \to 0$, one may expect that the classical partition function for the lattice system can be developed as a series expansion in J,

$$\mathcal{Z} = \int_0^{2\pi} \prod_i \frac{d\theta_i}{2\pi} e^{-S[\theta_i]} = \int_0^{2\pi} \prod_i \frac{d\theta_i}{2\pi} \prod_{\langle ij \rangle} \left[1 + J\cos(\theta_i - \theta_j) + \mathcal{O}(J^2)\right].$$

Here each term in the product can be represented by a "bond" that connects neighboring sites i and j. To the lowest order in J, each bond on the lattice contributes a factor of either one or $J\cos(\theta_i - \theta_j)$. But, since $\int_0^{2\pi} d\theta_1 \cos(\theta_1 - \theta_2) = 0$, any graph with a single bond emanating from a site vanishes. On the other hand, a site at which two bonds meet yields a factor $\int_0^{2\pi} (d\theta_2/2\pi)\cos(\theta_1 - \theta_2)\cos(\theta_2 - \theta_3) = (1/2)\cos(\theta_1 - \theta_3)$. Therefore, in this way, the classical partition function can be presented as a closed "loop" expansion. Similarly, the high-temperature expansion can be used to estimate the spin–spin correlation function $\langle \mathbf{S}_0 \cdot \mathbf{S}_{\mathbf{r}} \rangle = \langle \cos(\theta_{\mathbf{r}} - \theta_0) \rangle$. To leading order, only those graphs that join sites 0 and $\mathbf{r}$ will survive, implying an exponential decay of the correlation function,

$$\langle \mathbf{S}_0 \cdot \mathbf{S}_{\mathbf{x}} \rangle \sim \left(\frac{J}{2}\right)^{|\mathbf{x}|} \sim \exp\left[-\frac{|\mathbf{x}|}{\xi}\right],$$

with a correlation length $\xi^{-1} = \ln(2/J)$. Conversely, in the **low-temperature** phase, where fluctuations of neighboring phases θ_i are strongly penalized, the lattice model can be safely replaced by the continuum theory $\frac{1}{2}\int d^2r\ J(\nabla\phi)^2$. Taking only harmonic fluctuations of the field $\phi(\mathbf{r})$, i.e. neglecting the topological constraint placed by the geometry, the spin–spin correlation function can be inferred from the rules of Gaussian integration, to wit $\langle \mathbf{S}(0)\cdot\mathbf{S}(\mathbf{r})\rangle = \mathrm{Re}\langle e^{i(\theta(0)-\theta(\mathbf{r}))}\rangle = e^{-\langle(\theta(0)-\theta(\mathbf{r}))^2\rangle/2}$. Since, in two dimensions, Gaussian fluctuations grow logarithmically, $\langle(\theta(0)-\theta(\mathbf{r}))^2\rangle/2 = \ln(|\mathbf{r}|/a)/2\pi J$, where a denotes a short-distance cutoff (e.g. the lattice spacing), one can infer a spin–spin correlation function that decays algebraically,

$$\langle \mathbf{S}(0)\cdot\mathbf{S}(\mathbf{r})\rangle \simeq \left(\frac{a}{|\mathbf{r}|}\right)^{\frac{1}{2\pi J}},$$

a phase of **quasi-long-range order**.

The distinction between the nature of the asymptotic decays allows for the possibility of a finite-temperature phase transition. However, these arguments are not specific to the XY-model: any continuous spin model will exhibit exponential decay of correlations at high temperature and, in two dimensions, a power law decay in a low-temperature Gaussian approximation. Now, formally, to establish that "Gaussian" behavior persists at low temperatures, one must prove that it is not modified by higher-order terms in the gradient expansion (including those induced by the nonlinear constraint, $\mathbf{S}_i^2 = 1$). However, while the results of the $(2+\epsilon)$-expansion of the U(N) theory show that the two-dimensional model flows to a disordered phase for $N > 2$ (in accord with the Mermin–Wagner theorem), for $N = 2$ the theory is non-committal. Indeed, in an extension of the perturbative RG to higher loop order, the β-function remains zero. So we are left with the question, is there indeed a phase transition that delineates between the high- and low-temperature asymptotics, and what is the mechanism by which the quasi-long-range order is destroyed at higher temperatures? Since the perturbative RG suggests that higher-order terms in the gradient expansion are not relevant, it is necessary to search for other relevant operators.

8.6.1 Vortices and the topological phase transition

The gradient expansion describes the energy cost of small deformations around the ground state, and applies to configurations that can be continuously deformed to the uniformly ordered state. In separate and seminal works,[40] Berezinskii, and Kosterlitz and Thouless, proposed that the disordering is facilitated by the "condensation" of topological defects or vortices. Since the angle describing the orientation of a spin is defined up to an integer multiple of 2π, it is possible to construct spin configurations in which the traversal of a closed path will see the angle rotate by $2\pi n$. The integer n defines a **topological charge** enclosed by the path. The discrete nature of the charge makes it impossible to find a continuous

[40] V. L. Berezinskii, Violation of long range order in one-dimensional and two-dimensional systems with a continuous symmetry group. I. Classical systems, *Sov. Phys. JETP* **32** (1971), 493–500; J. M. Kosterlitz and D. J. Thouless, Ordering, metastability, and phase transitions in two-dimensional systems, *J. Phys. C* **6** (1973), 1181–203.

deformation that returns the state to the uniformly ordered configuration in which the charge is zero. (More generally, topological defects arise in many models with a compact group describing the order parameter – e.g., a domain wall defect (e.g. an instanton) in a model with Z_2 symmetry, or a "skyrmion" configuration in an O(3) three-component spin Heisenberg ferromagnet; see the next chapter for a discussion of topological defects.)

David J. Thouless, 1934–
co-recipient with John Michael Kosterlitz of the 2000 Lars Onsager Prize "for the introduction of the theory of topological phase transitions, as well as their subsequent quantitative predictions by means of early and ingenious applications of the renormalization group, and advancing the understanding of electron localization and the behavior of spin glasses."

The elementary defect, known in the present context as a **vortex** configuration, has a unit "charge": in completing a circle centered on the defect, the orientation of the spin changes by $\pm 2\pi$ (see Fig. 8.10). If the radius r of the circle is sufficiently large, the variations in angle will be small and the underlying lattice structure of the spin model can be neglected. By symmetry $\nabla\theta$ has uniform magnitude and points along the azimuthal direction. The magnitude of the distortion can be obtained by integrating around a path that encloses the defect, $\oint \nabla\theta \cdot d\mathbf{l} = 2\pi n$, i.e. $\nabla\theta = \frac{n}{r}\hat{\mathbf{e}}_z \times \hat{\mathbf{e}}_r$, where $\hat{\mathbf{e}}_r$ and $\hat{\mathbf{e}}_z$ are unit vectors respectively in the plane and perpendicular to it. This continuum approximation fails close to the center (core) of the vortex where the lattice structure becomes important.

Although the defect-driven topological phase transition can be described within the framework of the RG (see below), the nature of the transition can be understood from a simpler and intuitive line of reasoning that one can find in the original paper by Kosterlitz and Thouless. The energy cost of a single vortex of charge n can be divided into contributions from the core region as well as from the relatively uniform distortions away from the center. The distinction between regions inside and outside the core is arbitrary (see below) and, for simplicity, we shall use a circle of radius a to distinguish the two, i.e. for a vortex of charge n, the associated action is given by

$$S_n = S_n^{\rm core}(a) + \frac{J}{2}\int_a d^2r\,(\nabla\theta)^2 = S_n^{\rm core}(a) + \pi J n^2 \ln\left(\frac{L}{a}\right).$$

The dominant contribution to the action arises from the region outside the core and diverges logarithmically with the system size L.[41] The large energy cost associated with the defects inhibits their spontaneous formation at low temperatures and protects the integrity of the quasi-long-range ordered phase. To explore the range over which vortices are suppressed, one may explore the partition function for a configuration with just a single vortex of unit

[41] Notice that, if the spin degrees of freedom have three components or more, the energy cost of a defect is only finite. Following the arguments below, one may reflect on the implications of this fact for the inability of topological defects to effect a topological transition in systems with $N > 2$.

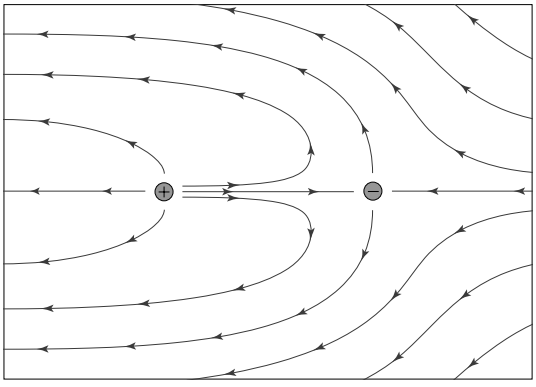

Figure 8.10 Spin configurations of the two-dimensional XY-model showing vortices of charge ± 1.

charge $n = 1$,

$$\mathcal{Z}_1 \approx \left(\frac{L}{a}\right)^2 \exp\left[-S_1^{\text{core}}(a) - \pi J \ln\left(\frac{L}{a}\right)\right]. \tag{8.40}$$

Here the factor of $(L/a)^2$ results from the configurational entropy associated with the range of possible vortex locations in an area of size L^2. The entropy and energy of a vortex both grow as $\ln L$, and the free energy is dominated by one or the other. At low temperatures (i.e. large J) the potential energy dominates over the entropy and $\mathcal{Z}_1$, a measure of the weight of configurations with a single vortex, vanishes. However, when $J < J_c = 2/\pi$, the entropic contribution overwhelms the potential and one may expect the spontaneous formation of vortices and a transition to the disordered phase.

In fact one might expect that this estimate of J_c represents only a lower bound for the stability of the system towards the condensation of topological defects. This is because pairs (dipoles) of defects may appear at larger couplings. Consider a pair of charges ± 1 separated by a distance d (see Fig. 8.10). Distortions far from the core $|\mathbf{r}| \gg d$ can be obtained by superposing those of the individual vortices, i.e. $\nabla\theta = \nabla\theta(\mathbf{r} + \mathbf{d}/2) - \nabla\theta(\mathbf{r} - \mathbf{d}/2) \approx \mathbf{d} \cdot \nabla(\hat{\mathbf{e}}_r \times \hat{\mathbf{e}}_z/|\mathbf{r}|) \sim d/|\mathbf{r}|^2$. Integrating this distortion, one may infer that the energy cost of the configuration is only finite, and hence dipoles appear with the appropriate Boltzmann weight at any non-zero temperature. The low-temperature phase should therefore be visualized as a "gas" of tightly bound dipoles, their density and size increasing with temperature. The high-temperature phase constitutes a plasma of unbound vortices.

To a large extent, the argument above conveys much of the phenomenology of the Berezinskii–Kosterlitz–Thouless (BKT) phase transition. However, one may justifiably question the impact of harmonic fluctuations and dipole interactions in suppressing or even destroying the transition. To explore these effects, one has to turn to a more rigorous line of reasoning. To do so, we will once again draw on the RG.

8.6.2 RG analysis of the BKT transition

To prepare for the application of the RG, we must first reorganize the action to emphasize the different channels of fluctuations. Fortunately, for the two-dimensional XY-model, the different channels (harmonic and topological) can be neatly separated. To understand why, it is helpful to draw an analogy, noting that the distortion field, $\mathbf{u} \equiv \nabla\theta$, is similar to the velocity of a fluid. In the absence of vorticity, the flow is potential, i.e. $\mathbf{u} = \mathbf{u}_0 = \nabla\phi$, and $\nabla \times \mathbf{u}_0 = 0$. The topological charge can be related to the vorticity $\nabla \times \mathbf{u}$ by noting that, for any closed path, $\oint d\mathbf{l} \cdot \mathbf{u} = \int d^2r\, \hat{\mathbf{e}}_z \cdot \nabla \times \mathbf{u}$, where the second integral is over the area enclosed by the path. Since the left-hand side is an integer multiple of 2π, one can set $\nabla \times \mathbf{u} = 2\pi\hat{\mathbf{e}}_z \sum_i n_i \delta^2(\mathbf{r} - \mathbf{r}_i)$, describing a collection of vortices of charge $\{n_i\}$ at locations $\{\mathbf{r}_i\}$. The solution to this equation can be obtained by setting $\mathbf{u} = \mathbf{u}_0 - \nabla \times (\hat{\mathbf{e}}_z\psi)$, leading to

$$\nabla \times \mathbf{u} = \hat{\mathbf{e}}_z \nabla^2\psi \Rightarrow \nabla^2\psi = 2\pi \sum_i n_i \delta^2(\mathbf{r} - \mathbf{r}_i). \tag{8.41}$$

Thus, the field ψ behaves as the potential due to a set of point charges $\{2\pi n_i\}$ while the solution, $\psi(\mathbf{r}) = \sum_i n_i \ln(|\mathbf{r} - \mathbf{r}_i|)$, is simply a superposition of the potentials. Any two-dimensional distortion can therefore be written as $\mathbf{u} = \mathbf{u}_0 + \mathbf{u}_1 = \nabla\phi - \nabla \times (\hat{\mathbf{e}}_z\psi)$, where $\mathbf{u}_0$ accommodates the harmonic field fluctuations while $\mathbf{u}_1$ includes the topological defects. The corresponding action, $S[\mathbf{u}] = \frac{1}{2}\int d^2r\ J\mathbf{u}^2$, can be decomposed as

$$S[\mathbf{u}] = \frac{J}{2}\int d^2r \left[(\nabla\phi)^2 - 2\nabla\phi \cdot \nabla \times (\hat{\mathbf{e}}_z\psi) + (\nabla \times \hat{\mathbf{e}}_z\psi)^2\right].$$

An integration by parts shows that the second term vanishes ($\nabla \cdot \nabla \times \mathbf{u} = 0$), while the third term can be simplified by noting that $\nabla\psi$ and $\nabla \times (\hat{\mathbf{e}}_z\psi)$ are orthogonal vectors of equal length. Hence, making use of Eq. (8.41), the action associated with the topological defects takes the form

$$S_{\rm t} \equiv \frac{J}{2}\int d^2r\ (\nabla \times \hat{\mathbf{e}}_z\psi)^2 = -\frac{J}{2}\int d^2r\ \psi\nabla^2\psi = -2\pi^2 J \sum_{ij} n_i n_j C(\mathbf{r}_i - \mathbf{r}_j),$$

where $C(\mathbf{x}) = \ln|\mathbf{x}|/2\pi$ is the two-dimensional Coulomb potential. Once again, the unphysical divergence of the potential for $i = j$ must be regularized by the core energy, whence

$$S_{\rm t} = \sum_i S^{\rm core}_{n_i} - 4\pi^2 J \sum_{i<j} n_i n_j C(\mathbf{r}_i - \mathbf{r}_j). \tag{8.42}$$

Conveniently, the configuration space of the XY-model can thus be partitioned into different topological regions: one set arises from the degrees of freedom associated with the charges, $\{n_i\}$, while the other reflects the harmonic spin-wave excitations associated with the field $\phi(\mathbf{r})$. The partition function of the lattice model is then approximately given by $\mathcal{Z} \approx \mathcal{Z}_{\rm s.w.}\mathcal{Z}_{\rm t}$ where

$$\mathcal{Z}_{\rm s.w.} = \int D\phi\, \exp\left[-\frac{J}{2}\int d^2r\ (\nabla\phi)^2\right], \quad \mathcal{Z}_{\rm t} = \sum_{N=0}^{\infty} \frac{1}{(N!)^2}\int \left(\prod_{i=1}^{2N} d^2r_i\right)\ e^{-S_{\rm t}},$$

and the r_i are dimensionless integration variables $r_i = x_i/a$ where x_i is the position of the vortex centre. (Exercise: Consider why the combinatorial factors $(N!)^2$ are needed to prevent overcounting of identical charge configurations.) To summarize, $\mathcal{Z}_{\rm t}$ describes a grand canonical ensemble of "charges" with a two-dimensional Coulomb interaction. In fact, our derivation of the action relied on an integration by parts. The surface integral that was neglected in the process in fact grows with the system size as $\ln L \sum_i n_i$. Therefore, one must impose on the field configurations contributing to $\mathcal{Z}_{\rm t}$ the constraint of overall charge neutrality. In the following, to simplify our analysis further, we will limit considerations to only elementary excitations with $n_i = \pm 1$.[42] Then, if we define the fugacity of the vortices as $y_0 \equiv \exp[-S^{\rm core}_{\pm 1}]$, the partition function

$$\boxed{\mathcal{Z}_{\rm t} = \sum_{N=0}^{\infty} \frac{y_0^{2N}}{(N!)^2} \int \left(\prod_{i=1}^{2N} d^2 r_i \right) \exp\left[4\pi^2 J \sum_{i<j} \sigma_i \sigma_j C(\mathbf{r}_i - \mathbf{r}_j) \right],} \tag{8.43}$$

reduces to that of a **neutral Coulomb plasma** of $2N$ unit charges $n_i = \pm 1$.

EXERCISE The low-temperature physics of many two-dimensional systems is effectively reduced to that of the XY-model or of the two-dimensional Coulomb plasma. For this reason, the equivalence XY-model $\Leftrightarrow$ Coulomb plasma demonstrated above represents an important result in its own right. In fact, there exists a third important system falling into this universality class: the **two-dimensional sine–Gordon model** defined by the action

$$\boxed{S[\theta] = \frac{c}{2} \int d^2 r \quad \theta \quad \theta + g \int d^2 r \cos(\theta),} \tag{8.44}$$

where θ is a real scalar field. To demonstrate its equivalence to the Coulomb gas model, expand the partition function in powers of g and show that

$$\mathcal{Z} = \sum_{N=0}^{\infty} \frac{y_0^{2N}}{(N!)^2} \prod_{i=1}^{2N} \int d^d r_i \left\langle \exp\left(i \sum_{i=1}^{2N} (-)^i \theta(\mathbf{r}_i) \right) \right\rangle,$$

where $y_0 = g/2$ and the angular brackets denote averaging over the free action. (To prove that positive and negative phases appear in equal numbers, consider the role of the integration over the zero mode $\theta(\mathbf{r}) = \text{const.}$) Using the fact that $\langle \theta(\mathbf{r}) \theta(\mathbf{r}') \rangle = C(|\mathbf{r} - \mathbf{r}'|)/c$, and neglecting the infinite self-interaction of the fields at coinciding points, show that the partition function becomes identical to Eq. (8.43) when $c = 1/8\pi^2 J$.

Since $\mathcal{Z}_{\rm s.w.}$ and $\mathcal{Z}_{\rm t}$ involve independent degrees of freedom, they can be treated separately. Further, as the Gaussian partition function $\mathcal{Z}_{\rm s.w.}$ is everywhere analytic, any phase transition of the XY-model must originate from the Coulomb gas. Now, as mentioned above, in the low-temperature phase, charges appear only as tightly bound dipole pairs while, at high temperatures, the dipoles dissociate, forming a plasma. The two phases can be distinguished

[42] A charge two vortex costs about as much energy as two unit-charge vortices. However, its entropy $\sim 2T \ln(L/a)$ is much lower than the entropy $\sim 4T \ln(L/a)$ of the two-vortex configuration. This is why vortices of high winding number are negligible in the low-temperature limit.

by examining the interaction between two external test charges at some large separation X. In the absence of internal charges, the two particles interact by the bare Coulomb interaction $C(X)$. The presence of internal charges provides a mechanism to screen the interaction, namely $C(X)/$, where is an effective dielectric constant. With this interpretation, the transition with increasing temperature (or increasing y_0) can be viewed as a transition from an insulating (dipolar) phase to a metallic (plasma) phase in which the external charges are completely screened and their effective interaction decays exponentially.

To quantify this picture, one can compute the effective interaction between two external charges at $\mathbf{r}$ and $\mathbf{r}'$ perturbatively in the fugacity y_0. To lowest order, the effects of screening can be incorporated by including configurations with only two internal charges (positioned at $\mathbf{s}$ and $\mathbf{s}'$). In this case, the effective interaction can be written as

$$e^{-S_{\text{eff.}}(\mathbf{r}-\mathbf{r}')} \equiv \langle e^{-4\pi^2 JC(\mathbf{r}-\mathbf{r}')}\rangle_{\text{t}} = \frac{\begin{array}{c}\mathbf{s}\qquad -\qquad \mathbf{s}'\\ (\mathbf{r}\quad -\quad \mathbf{r}') + y_0^2\int d^2s\, d^2s' \quad | \quad \times \quad | \quad + \mathcal{O}(y_0^4)\\ \mathbf{r}\qquad -\qquad \mathbf{r}'\end{array}}{1 + y_0^2 \int d^2s\, d^2s'\ (\mathbf{s} \quad - \quad \mathbf{s}') + \mathcal{O}(y_0^4)},$$

from which one obtains

$$\begin{aligned} &e^{-S_{\text{eff.}}(\mathbf{r}-\mathbf{r}')+4\pi^2 JC(\mathbf{r}-\mathbf{r}')} \\ &\quad = \frac{1 + y_0^2 \int d^2s\, d^2y'\, e^{-4\pi^2 JC(\mathbf{s}-\mathbf{s}')+4\pi^2 J[C(\mathbf{r}-\mathbf{s})-C(\mathbf{r}-\mathbf{s}')-C(\mathbf{r}'-\mathbf{s})+C(\mathbf{r}'-\mathbf{s}')]} + \mathcal{O}(y_0^4)}{1 + y_0^2 \int d^2s\, d^2s'\, e^{-4\pi^2 JC(\mathbf{s}-\mathbf{s}')} + \mathcal{O}(y_0^4)} \\ &\quad = 1 + y_0^2 \int d^2s\, d^2s'\, e^{-4\pi^2 JC(\mathbf{s}-\mathbf{s}')} \left(e^{4\pi^2 JD(\mathbf{r},\mathbf{r}',\mathbf{s},\mathbf{s}')} - 1\right) + \mathcal{O}(y_0^4). \end{aligned} \tag{8.45}$$

Here, $D(\mathbf{r},\mathbf{r}',\mathbf{s},\mathbf{s}') = C(\mathbf{r}-\mathbf{s}) - C(\mathbf{r}-\mathbf{s}') - C(\mathbf{r}'-\mathbf{s}) + C(\mathbf{r}'-\mathbf{s}')$ denotes the interaction between the internal and external dipoles, while the direct interaction $C(\mathbf{s}-\mathbf{s}')$ tends to keep the separation $\mathbf{x} = \mathbf{s}' - \mathbf{s}$ small. Defining the center of mass $\mathbf{X} = (\mathbf{s}+\mathbf{s}')/2$, we can change variables to $\mathbf{s} = \mathbf{X} - \mathbf{x}/2$ and $\mathbf{s}' = \mathbf{X} + \mathbf{x}/2$, and expand the dipole–dipole interaction in small $\mathbf{x}$ as $D(\mathbf{r},\mathbf{r}',\mathbf{s},\mathbf{s}') \simeq -\mathbf{x}\cdot\nabla_{\mathbf{X}} C(\mathbf{r}-\mathbf{X}) + \mathbf{x}\cdot\nabla_{\mathbf{X}} C(\mathbf{r}'-\mathbf{X}) + \mathcal{O}(x^3)$. To the same order

$$\begin{aligned} e^{4\pi^2 JD(\mathbf{r},\mathbf{r}',\mathbf{s},\mathbf{s}')} - 1 \simeq &-4\pi^2\, J\mathbf{x}\cdot\nabla_{\mathbf{X}}(C(\mathbf{r}-\mathbf{X}) - C(\mathbf{r}'-\mathbf{X})) \\ &+ 8\pi^4 J^2 [\mathbf{x}\cdot\nabla_{\mathbf{X}}(C(\mathbf{r}-\mathbf{X}) - C(\mathbf{r}'-\mathbf{X}))]^2 + \mathcal{O}(x^3). \end{aligned}$$

Substituting this expression into Eq. (8.45), and changing integration variables, one finds that the term linear in $\mathbf{x}$ integrates to zero while the angular average of $(\mathbf{x}\cdot\nabla_{\mathbf{X}} C)^2$ leads to $x^2(\nabla_{\mathbf{X}} C)^2/2$. Thus, to $\mathcal{O}(r^4)$, one obtains

$$\begin{aligned} e^{-S_{\text{eff}}(\mathbf{r}-\mathbf{r}')} &\simeq e^{-4\pi^2 JC(\mathbf{r}-\mathbf{r}')} \\ &\times \left[1 + y_0^2 \int (dx\, 2\pi\, x) e^{-4\pi^2 JC(x)} 8\pi J^2 \frac{x^2}{2} \int d^2X\, (\nabla_{\mathbf{X}}(C(\mathbf{r}-\mathbf{X}) - C(\mathbf{r}'-\mathbf{X})))^2\right]. \end{aligned}$$

Using the identity $\nabla^2 C(\mathbf{r}) = \delta^2(\mathbf{r})$, one may note that $\int d^2X\ [\nabla_{\mathbf{X}}(C(\mathbf{r}-\mathbf{X}) - C(\mathbf{r}'-\mathbf{X}))]^2 = 2(C(\mathbf{r}-\mathbf{r}') - C(0))$. Finally, absorbing the short-distance divergence into an appropriate

cutoff with $C(x) \to \ln(x/a)/2\pi$, one arrives at the expression

$$e^{-S_{\rm eff}(\mathbf{r}-\mathbf{r}')} = e^{-4\pi^2 J C(\mathbf{r}-\mathbf{r}')}\left[1 + 16\pi^5 J^2 y_0^2 C(\mathbf{r}-\mathbf{r}')\int_1^\infty dx\, x^3\, e^{-2\pi J \ln x} + \mathcal{O}(y_0^4)\right],$$

where the variable x has been rescaled to absorb the short distance cutoff. Exponentiating the second term, one obtains the effective interaction $S_{\rm eff}(\mathbf{r}-\mathbf{r}') \simeq 4\pi^2 J_{\rm eff} C(\mathbf{r}-\mathbf{r}')$, where

$$J_{\rm eff} = J - 4\pi^3 J^2 y_0^2 \int_1^\infty dx\, x^{3-2\pi J} + \mathcal{O}(y_0^4), \tag{8.46}$$

From this result, to leading order in y_0^2, one can infer the dielectric constant of the medium as $= J/J_{\rm eff}$. However, while the integral remains convergent at large x, the perturbative correction is small. The breakdown of the perturbation theory for $J < J_{\rm c} = 2/\pi$ occurs precisely at the point where the free energy of an isolated vortex changes sign. Indeed, this breakdown of the perturbation theory is reminiscent of that encountered in the ϕ^4-theory for $d < 4$. This being so, one may propose a reorganization of the perturbation series into a RG calculation for the parameters J and y_0.

The difficulty associated with the divergence at small J can be overcome by employing a **renormalization** procedure first used by José *et al.*[43] By breaking the integral in Eq. (8.46) into two parts, i.e. $\int_1^\infty \to \int_1^b + \int_b^\infty$, the non-singular short-distance contribution to the integral can be evaluated and incorporated into J. This procedure can be carried out order by order in y_0 even though the coefficient of y_0^2 is formally divergent. This leads to a new equation $J_{\rm eff}^{-1} = \widetilde{J}^{-1} + 4\pi^3 y_0^2 \int_b^\infty dx\, x^{3-2\pi J} + \mathcal{O}(y_0^4)$, where $\widetilde{J}^{-1} = J^{-1} + 4\pi^3 y_0^2 \int_1^b dx\, x^{3-2\pi J} + \mathcal{O}(y_0^4)$. The variables in the remaining integral can be rescaled ($x \to x/b$) to yield an equation for $J_{\rm eff}^{-1}$ equivalent to Eq. (8.46) but with shifted and rescaled parameters J and y_0:

$$J_{\rm eff}^{-1} = \widetilde{J}^{-1} + 4\pi^3 \widetilde{y}_0^2 \int_1^\infty dx\, x^{3-2\pi J} + \mathcal{O}(y_0^4),$$

where $\widetilde{y}_0 = b^{2-\pi J} y$. By choosing an infinitesimal renormalization, i.e. $b = e^\ell \approx 1 + \ell$, one obtains the differential recursion relations

$$\begin{aligned} \frac{dJ^{-1}}{d\ell} &= 4\pi^3 y_0^2 + \mathcal{O}(y_0^4), \\ \frac{dy_0}{d\ell} &= (2 - \pi J) y_0 + \mathcal{O}(y_0^3). \end{aligned} \tag{8.47}$$

From these equations, one may note that the (inverse) coupling constant J^{-1} increases monotonically with ℓ while the recursion relation for y_0 changes sign at $J_{\rm c}^{-1} = \pi/2$. At high temperatures, when J is small, y_0 is relevant, while at lower temperatures it becomes irrelevant. The RG flows, shown in Fig. 8.11(a), separate the parameter space into two regions. At low temperatures, and small y_0, flows terminate on a fixed line at $y_0 = 0$ and $J_{\rm eff} \geq 2/\pi$. This is the insulating phase, in which only dipoles of finite size occur (hence the vanishing of y_0 under coarse-graining). The strength of the effective interaction is given by the point on the fixed line at which the flow terminates. Flows that do not terminate on the

[43] J. V. José, L. P. Kadanoff, S. Kirkpatrick, and D. R. Nelson, Renormalization, vortices, and symmetry-breaking perturbations in the two-dimensional planar model, *Phys. Rev. B* **16** (1977), 1217–41.

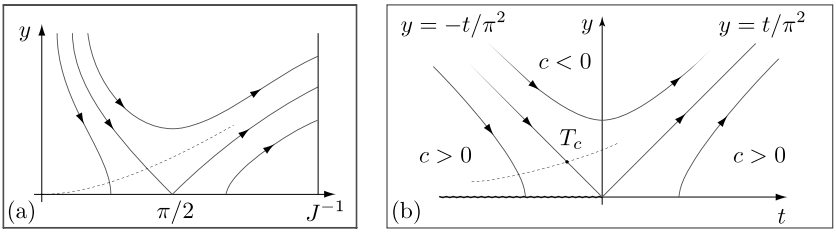

Figure 8.11 Schematic RG flow diagram for the XY-model. (a) Far from the critical point, and (b) close to the critical point.

fixed line asymptote to larger values of J^{-1} and y_0 where perturbation theory eventually breaks down. This is the signal of the high-temperature phase where vortices proliferate.

The critical trajectory that separates the two regions of the phase diagram flows to a fixed point at ($J_{\rm c}^{-1} = \pi/2$, $y_0 = 0$). To explore the critical behavior at the transition, one must expand the recursion relations in the vicinity of this point. Setting $t = J^{-1} - \pi/2$, to lowest order, Eq. (8.47) simplifies to

$$\begin{aligned} \frac{dt}{d\ell} &= 4\pi^3 y^2 + \mathcal{O}(ty^2, y^4), \\ \frac{dy}{d\ell} &= \frac{4}{\pi} ty + \mathcal{O}(t^2 y, y^3). \end{aligned}$$

In contrast to those discussed in previous sections, the recursion relations here are inherently nonlinear in the vicinity of the fixed point (see Fig. 8.11(b)), suggesting that the critical behavior is likely to be novel. To uncover the structure, one may note that $t^2 - \pi^4 y^2$ is a conserved quantity, i.e. the flow proceeds along hyperbolae characterized by different values of $c \equiv t^2 - \pi^4 y^2$. For $c < 0$, the focus of the hyperbola is along the y-axis, and the flows proceed to $(t, y) \to \infty$. Conversely, hyperbolae with $c > 0$ have foci along the t-axis, and have two branches in the half plane $y \geq 0$: the branches for $t < 0$ flow to the fixed line, while those in the $t > 0$ quadrant flow to infinity. The critical trajectory separating flows to zero and infinite y corresponds to $c = 0$, i.e. $t_{\rm c} = -\pi^2 y_{\rm c}$. Therefore, a small but finite fugacity y_0 reduces the critical temperature to $J_{\rm c}^{-1} = \pi/2 - \pi^2 y_0 + \mathcal{O}(y_0^2)$.

In terms of the original XY-model, the **low-temperature phase** is characterized by a line of fixed points with $J_{\rm eff} = \lim_{\ell\to\infty} J(\ell) \geq 2/\pi$. Here the phase correlations decay as a power law, i.e. $\langle \cos(\theta(\mathbf{r}) - \theta(0)) \rangle \sim 1/|\mathbf{r}|^\eta$, with $\eta = 1/2\pi J_{\rm eff} \leq 1/4$. Since the parameter c is negative in the low-temperature phase, and vanishes at the critical point, we can set $c = -b^2(T_{\rm c} - T)$ close to the transition. In other words, the trajectory of initial points tracks a line $(t(T), y(T))$. The resulting $c = t^2 - \pi^4 y^2 \propto (T_{\rm c} - T)$ is a linear measure of the proximity of the phase transition. Under renormalization, such trajectories flow to a fixed point at $y = 0$, and $t = -b\sqrt{T_{\rm c} - T}$. Thus, in the vicinity of the transition, the effective interaction parameter,

$$J_{\rm eff} = \frac{2}{\pi} - \frac{4}{\pi^2} \lim_{\ell\to\infty} t(\ell) = \frac{2}{\pi} + \frac{4b}{\pi^2}\sqrt{T_{\rm c} - T},$$

exhibits a square root singularity.

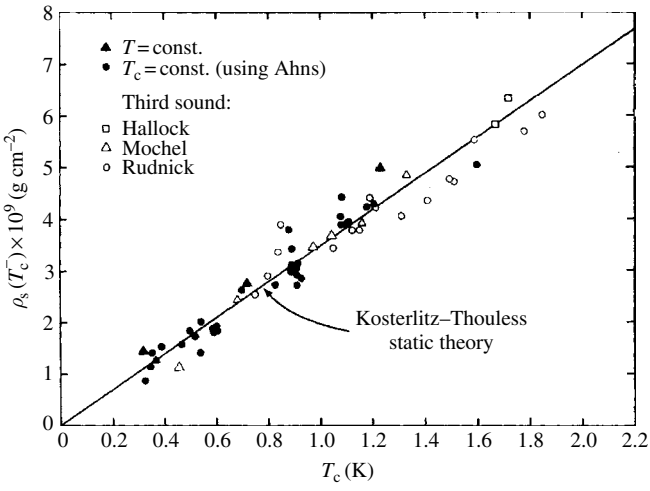

Figure 8.12 Measurement of the superfluid density $\rho_s(T_c)$ as a function of T_c. The approximate linearity $\rho_s \sim T_c$ demonstrates the universality of the stiffness constant J at the transition. (Reprinted with permission from D. J. Bishop and J. D. Reppy, Study of the superfluid transition in two-dimensional ^{4}He films, *Phys. Rev. Lett.* **40** (1978), p. 1727–30. Copyright (1978) by the American Physical Society.)

INFO The stiffness, J_{eff}, can be measured directly in **experiments on superfluid films**. As we have seen in Chapter 6, in the superfluid phase, the low temperature of neutral superfluids is described by a phase action with a stiffness $J = \beta\rho_s/m^2$ determined by the superfluid density of the system. The density ρ_s is measured by examining the changes in the inertia of a torsional oscillator; the superfluid fraction, ρ_s experiences no friction and does not oscillate.

Bishop and Reppy examined ρ_s for a variety of superfluid films (of different thickness, ^{4}He concentration, etc.) wrapped around a torsional cylinder. By inferring the effective stiffness J as a function of temperature, they found that, for all films, it undergoes a universal jump of $2/\pi$ at the transition while the behavior of J for $T < T_c$ was consistent with a square root singularity. They also observed (see Fig. 8.12) that the ratio $\rho_s(T_c)/T_c = J_c m^2 = 2m^2/\pi$ is a universal quantity independent of the material parameters of the film.

In the **high-temperature phase**, the correlations decay exponentially. In this phase the parameter $c = t^2 - \pi^4 y^2 = b^2(T - T_c)$ is positive all along the hyperbolic trajectory. Here the recursion relation $\frac{dt}{d\ell} = 4\pi^3 y^2 = \frac{4}{\pi}(t^2 + b^2(T - T_c))$ can be integrated to give

$$\frac{4}{\pi}\ell \simeq \frac{1}{b\sqrt{T - T_c}} \arctan\left(\frac{t}{b\sqrt{T - T_c}}\right).$$

The integration must be terminated when $t(\ell) \sim y(\ell) \sim 1$ since, beyond there, the perturbative calculation is invalid. This occurs for a value $\ell^* \approx \frac{\pi}{4b\sqrt{T-T_c}}\frac{\pi}{2}$, where we have used the fact that $\arctan(1/b\sqrt{T - T_c}) \approx \pi/2$. The resulting correlation length is given by

$$\xi \approx a e^{l^*} \approx a \exp\left[\frac{\pi^2}{8b\sqrt{T - T_c}}\right], \tag{8.48}$$

i.e. in contrast to the usual behavior described in previous sections, the divergence of the correlation length is not a power law, a consequence of the nonlinear nature of the recursion relations in the vicinity of the fixed point.

Finally, vortices occur in bound pairs for distances smaller than ξ while there can be an excess of vortices of one sign or the other at larger separations. The interactions between vortices at large distances can be obtained from the Debye–Hückel theory of polyelectrolytes. According to this theory, the free charges screen each other, leading to a screened Coulomb interaction $\exp(-x/\xi)C(x)$. On approaching the transition from the high-temperature side, the singular part of the free energy

$$f_{\text{sing}} \propto \xi^{-2} \propto \exp\left(-\frac{\pi^2}{4b\sqrt{T-T_{\text{c}}}}\right), \tag{8.49}$$

has only an essential singularity. All derivatives of this function are finite at T_{c}. Thus the predicted heat capacity is quite smooth at the transition. Numerical results based on the RG equations indicate a smooth maximum in the heat capacity at a temperature higher than T_{c} corresponding to the point at which the majority of dipoles unbind.

8.7 Summary and outlook

This concludes our preliminary introduction to the theory of the "renormalization group." It should be emphasized that our approach to the subject was biased in that it introduced the RG in a manner tailored to applications in quantum statistical physics; a more particle-physics-oriented introduction (see Ryder[13]) would have focused on the principal issues of renormalizability, different regularization schemes, renormalization through counter-terms and, of course, the many great triumphs renormalization group methods have had in QED and QCD. However, even with regard to statistical/condensed matter physics, our discussion has been far from complete (arguably the most serious omission being that of conformal symmetries – see the Info block below). We trust, however, that the discussion was substantial enough to convince the reader of the enormous power and versatility RG methods have in disclosing "deep" physical information and to motivate further exploration of the subject.

INFO While, for the most part, previous chapters were guided by symmetry principles, little has been said so far about the role of symmetries in connection with renormalization. At the same time it is quite obvious that, at a point of self-similarity, a physical system will have more symmetries than the ubiquitous global scale invariance: it will, at least, also be rotationally and translationally invariant: In fact, we expect these symmetries to be *local* symmetries, e.g. provided the system is described by a short-range effective theory, a local rescaling of coordinates $\mathbf{r} \to b(\mathbf{r})\mathbf{r}$ should not cause any effect; a point on which you might like to reflect.

More generally, we expect self-similar systems to be invariant under general **conformal mappings** $\mathbf{r} \to \mathbf{r}'(\mathbf{r})$, i.e. mappings that leave angles between vectors locally invariant. (In a more mathematical language, a mapping is conformal if it leaves the metric tensor $g_\mu\ (\mathbf{r})$ invariant, up to an optional scale factor, i.e. $g'_\mu\ (\mathbf{r}') = \ (\mathbf{r})g_\mu\ (\mathbf{r})$.) In general dimensions, the three classes of

transformations mentioned above, dilatations, rotations, and translations, essentially[44] exhaust the list of conformal mappings. It turns out, however, that the information gain due to the presence of these symmetries is rather restricted. However, a radically different situation arises in $d = 2$. Introducing complex coordinates, $z = z^0 + iz^1$, it can be shown[45] that every holomorphic mapping $z \to w(z)$ is automatically conformal. This means that two-dimensional systems at a fixed point are invariant under a vast group of symmetry operations. These symmetry conditions can be employed – the subject of **conformal field theory** – to obtain very far-reaching information about the behavior of correlation functions. In fact, it is customary in two-dimensional conformal field theory to characterize the behavior of a theory "indirectly," by the transformation characteristics of its correlation functions, rather than by specifying concrete microscopic actions. At any rate, a discussion of the foundations and applications of conformal field theory, and its ramifications in various branches of mathematical physics, is beyond the scope of the present text. For a very accessible first introduction to the subject we refer to Cardy.[1] Readers who want to learn more about the subject are referred to di Francesco *et al.*[46]

In Section 8.6 we saw the way large-scale topological defects render the physical behavior of a model, as seemingly innocuous as the two-dimensional XY-model, utterly non-trivial. Our observations made in connection with the XY-model exemplify a very general phenomenon: in physical systems admitting the formation of topologically stabilized excitations, a conspiracy of large-scale geometry-related structures and local fluctuations leads to intriguing physical effects. An introductory discussion of topological structures in quantum field theory, and of their ramifications in concrete physical phenomena, is the subject of the next chapter.

8.8 Problems

8.8.1 Dissipative quantum tunneling: strong potential limit

In Section 8.2, we considered a quantum particle subject to a periodic potential and a dissipative damping mechanism. A combination of perturbative methods and the renormalization group was applied to show that, for dissipation rates above a certain critical threshold, the external potential effectively grows. Eventually, however, the potential height will reach values at which a perturbative treatment is no longer valid. In this problem we explore the fate of the quantum particle in the high-potential limit. As a result, we obtain the upper portion of the flow diagram discussed in Section 8.2.

Let us consider the action (8.11) in the limit where the potential strength c is large in comparison with the high-frequency cutoff Λ of the theory. To explicitly implement the condition $\omega_n < \Lambda$, we add a "kinetic energy term" $S_{\rm kin}[\theta] = \frac{l^2 m}{2} \int d\tau\, \dot{\theta}^2$ to the action, where l is some fixed parameter of dimensionality [length]. The mass parameter is chosen such

[44] The so-called **special conformal transformation**, $\mathbf{r} \to \mathbf{r}/r^2$, also belongs to the family of conformal mappings.

[45] Under a change of coordinates, $z \to w$, the metric tensor changes according to $g^{\mu\nu} \to \frac{w^\mu}{z^\sigma} \frac{w^\nu}{z} g^\sigma$. It is straightforward to show (exercise) that the condition that the standard metric $g^{\mu\nu} = \delta^{\mu\nu}$ change only by a global factor is equivalent to the Cauchy–Riemann equations $\frac{w^1}{z^0} = -\frac{w^0}{z^1}$ and $\frac{w^0}{z^0} = -\frac{w^1}{z^1}$.

[46] P. di Francesco, P. Mathieu, and D. Sénéchal, *Conformal Field Theory* (Springer-Verlag, 1999).

that at the maximum value of the frequency, $\omega_n = \Lambda$, the kinetic energy term becomes of the same order as the dissipative term (i.e. for frequencies beyond Λ, the system is no longer effectively described by Eq. (8.11)): $ml^2 \sim 1/\Lambda g$. We are thus led to consider the imaginary time action

$$S[\theta] = \frac{1}{4\pi T g} \sum_{\omega_n} |\omega_n||\theta_n|^2 + \int d\tau \left[\frac{ml^2}{2} \dot{\theta}^2 + \cos(\theta(\tau)) \right],$$

describing a particle in a periodic potential and subject to a weak damping mechanism. Assuming the damping to be weak, we begin by exploring the solutions to the equations of motion of the undamped ($g = \infty$) problem. Varying the action, we obtain the equations of motion $ml^2 d_\tau^2 \bar{\theta} + \sin(\bar{\theta}) = 0$, i.e. the Newton equation of the mathematical pendulum. Although these equations can be solved in closed form, there is actually no need to do so. We need note only that extended periods where the classical particle rests at the maxima of the potential are interrupted by occasional events where it rolls through one of the potential minima (see the figure overleaf). Throughout, it will be convenient to characterize the profile of a general trajectory $\bar{\theta}$ in terms of its time-derivative $h = d_\tau \bar{\theta}$ (see the bottom part of the figure). For a function $\bar{\theta}$ containing n_+ instanton events and n_- anti-instanton events, $h(\tau) = \sum_{i=1}^{n} e_i f(\tau - \tau_i)$, where τ_i is the time of the event, $e_i = +1\,(-1)$ for an instanton (anti-instanton), $n = n_- + n_+$, and $f(\tau)$ is a function that is peaked around zero, has a width $\sim c$ and integrates to 2π: $\int_{-\infty}^{\infty} d\tau\, f(\tau) = h(\infty) - h(-\infty) = 2\pi$.

(a) Show that the action of a general instanton trajectory is given by

$$S[\bar{\theta}] = \frac{1}{4\pi T g} \sum_{\omega_m} \sum_{i,j=1}^{n} e_i e_j e^{i\omega_m(\tau_i - \tau_j)} \frac{|f_m|^2}{|\omega_m|} + n S_{\text{inst}},$$

where $S_{\text{inst.}}$ is the action of a single instanton event.

(b) Apply a Hubbard–Stratonovich transformation to bring the partition function to the form

$$\mathcal{Z} = \sum_n \sum_{\{e_i = \pm 1\}} e^{-n S_{\text{inst}}} \int Dq\, e^{-\frac{g}{4\pi T} \sum_m |q_m|^2 |\omega_m|} \frac{1}{n!} \prod_{i=1}^{n} \int d\tau_i\; e^{i \sum_{i=1}^{n} e_i q(\tau_i)},$$

where we have neglected the contribution from the fluctuation determinant. (Hint: Use the fact that, in the frequency range of interest, $f_m \simeq f_{m=0} = 2\pi T$.)

(c) Sum over all configurations of the "charges" e_i to obtain

$$\mathcal{Z} = \int Dq \exp\left(-\frac{g}{4\pi T} \sum_{\omega_m} |q_m|^2 |\omega_m| + \gamma \int d\tau \cos(q(\tau)) \right), \tag{8.50}$$

where $\gamma = 2e^{-S_{\text{inst}}}$. Intriguingly, we have arrived at a functional integral with an action structurally equivalent to our starting point (8.11). The "only" difference is a change in the coupling constants, $g \to g_{\text{dual}} \equiv \frac{1}{g}$ and $c \to \gamma = 2e^{-S_{\text{inst}}}$. In words: very large values of the potential c map onto a very small potential in the "dual problem"; dissipation strengths $g > 1$ map into $g_{\text{dual}} < 1$ and *vice versa*. Use this information to convince yourself of the validity of the upper portion of the flow diagram discussed in Section 8.2.

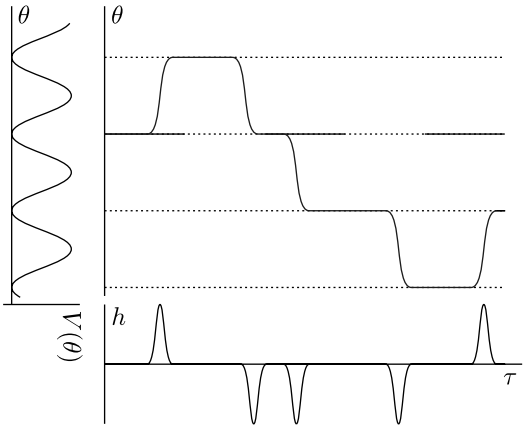

What we have achieved by the construction above is a **duality transformation**: a field theory subject to a strong potential (more generally, a field theory at strong interactions, or "strong coupling") has been mapped onto a weakly perturbed field theory (a theory at "weak coupling"). Duality transformations "boost" theories from one corner of their phase diagram into another and, therefore, establish links between sectors of the problem at hand that cannot be linked by perturbative means. This explains why the identification of its dual partners represents an important step in the analysis of any field theory. The problem above is special in that it is **self-dual**, i.e. the theory obtained after the transformation is structurally equivalent to the starting theory.

Answer:

(a) The result is obtained by substitution of $\bar{\theta}_m = -\frac{if_m}{\omega_m}\sum_i e_i e^{i\omega_m \tau_i}$ into the action.

(b) Substituting $q(\tau) = \sum_m e^{i\omega_m \tau} q_m$ into the Hubbard–Stratonovich transformed representation and performing the Gaussian integral over q_m, we arrive at

$$\mathcal{Z} = \sum_n \sum_{\{e_i = \pm 1\}} e^{-nS_{\rm inst}} \frac{1}{n!} \prod_{i=1}^{n} \int d\tau_i \; e^{-S[\bar{\theta}]},$$

i.e. the action of the previous line, integrated over all instanton coordinates and all "charge configurations" $\{e_i = \pm 1\}$.

(c) Starting from the representation derived in (b) and reorganizing terms, we obtain

$$\begin{aligned} \mathcal{Z} &= \int Dq\, e^{-\frac{g}{4\pi T}\sum_m |q_m|^2 |\omega_m|} \sum_n \frac{1}{n!} \left[e^{-S_{\rm inst.}} \sum_{e=\pm 1} \int d\tau\, e^{ieq(\tau)} \right]^n \\ &= \int Dq\, e^{-\frac{g}{4\pi T}\sum_m |q_m|^2 |\omega_m|} \sum_n \frac{1}{n!} \left[\gamma \int d\tau \cos(q(\tau) \right]^n . \end{aligned}$$

Resumming the exponential series, we obtain Eq. (8.50).

8.8.2 Quantum criticality

So far, we have focused predominantly on scaling and critical phenomena associated with a thermally induced phase transition. However, as we have seen in previous chapters, the quantum system affords the possibility of a phase transition driven by some external parameter even in the zero-temperature system. For example, a transition from the superconducting to the normal phase of a metal can be driven by an external magnetic field. Similarly, the transition between a paramagnetic and a ferro-

or anti-ferromagnetic itinerant electron phase can be driven by changing the strength of the effective interaction (through, e.g., external pressure). In both cases, the application of the external parameter leads to a substantial rearrangement of the ground state – a **quantum phase transition**. If this is continuous, as with a thermally induced transition, one can expect the appearance of characteristic critical phenomena analogous to, but potentially different from, the corresponding classical critical theory. The aim of the present problem is to explore the nature of the critical phenomena when the critical point is driven to zero temperature – a quantum critical point.

Motivated by the coherent state formulation of the quantum partition function of an interacting system, it is tempting to associate directly the quantum statistical mechanics of a d-dimensional system with the classical statistical mechanics of a $(d+1)$-dimensional system – the time coordinate would seem to just add one more dimension (albeit of finite extent β). However, in most applications, time and space enter the action in an anisotropic manner. As a result, one must consider scalings along the time and space directions separately. This provides for a rich variety of new phenomena associated with the quantum critical point. Although a general theoretical phenomenology of the quantum critical system was formulated by Hertz[47] soon after the development of the renormalization group method, it is only relatively recently that experimentalists have been able to access and explore in detail the quantum critical regime. Of these experimental developments, perhaps the most systematic has been in the exploration of metallic magnetism in the wide class of heavy fermion compounds. With this motivation in mind, let us then recall briefly our discussion of the Stoner transition in Problem 6.7.

INFO Without going into detail, we note that **heavy fermions** are compounds containing rare-earth elements such as Ce or Yb, or actinide elements such as U (examples including UBe_{13}, $CeCu_2Si_2$, and many more). Their inner shell conduction electrons often have effective masses several hundred times as large as that of bare electrons. As a consequence, the Fermi energy in heavy fermion materials is anomalously low (exercise). At low temperatures, many of these materials are magnetically ordered, others show strong paramagnetic behavior, and some display unconventional mechanisms of superconductivity.

Starting with the quantum partition function of the lattice Hubbard system, a field theory of the Stoner transition was derived. Specifically, it was shown that, after an appropriate rescaling of space and time, the quantum partition function of the interacting electron system could be presented as a functional field integral over a scalar magnetization field $m(x)$, weighted by the Euclidean time action[48]

$$S[m] = \frac{1}{2\beta V}\sum_q \left[\delta + \mathbf{q}^2 + \frac{|\omega_n|}{\Gamma_q}\right]|m_q|^2 + \frac{u}{4}\int dx\, m^4(x).$$

In the quantum critical system, the parameter δ measures the distance from the critical point while the Landau damping factor $\Gamma_q = \Gamma|\mathbf{q}|$ for the ferromagnetic transition and

[47] J. A. Hertz, Quantum critical phenomena, *Phys. Rev. B* **14** (1976), 1165–84.

[48] Here, to facilitate the RG, it is helpful to adopt the Fourier convention $m(x) = \frac{T}{L^d}\sum_q m_q e^{i(\mathbf{q}\cdot\mathbf{r}-\omega\tau)}$, $m_q = \int dx\, m(x) e^{-i(\mathbf{q}\cdot\mathbf{r}-\omega\tau)}$, where $dx \equiv \int d^dr \int_0^\beta d\tau$.

$\Gamma_q = \Gamma$, a constant, in the antiferromagnetic case. Finally, to regularize the theory, one may suppose that the momentum integration is cut off at the lattice scale $\Lambda = 1/a$. More generally, in the absence of an external magnetic field, one may consider a generalization from the scalar to a vectorial field $\mathbf{m}$. However, keeping our discussion simple, we focus on a system with uniaxial symmetry (such as a metamagnetic system[49]) where the field is scalar (uniaxial).

At the level of Landau mean-field theory, the magnetization field acquires a non-zero expectation value when $\delta < 0$. In the classical system, our analysis of the ϕ^4-theory (to which the present action collapses at high temperatures) has shown that, in dimensions $d \geq d_{\rm u} = 4$, the critical system is controlled by the Gaussian fixed point while in dimensions $1 > d > d_{\rm u}$ the critical properties are controlled by a new fixed point. Here, in the low-temperature system, one can expect the critical properties to be influenced by quantum dynamical fluctuations. Drawing on the seminal work of Hertz and, later, by Millis,[50] our aim here is to explore the ramifications of scaling in the quantum critical system.

(a) As a warm-up exercise, show that, up to a temperature-independent constant, the free energy of the **Gaussian theory** (i.e. $\delta > 0$, $u = 0$) takes the form

$$F_{\rm Gauss} = L^d \int \frac{d^d q}{(2\pi)^d} \int_0^{\Gamma_q} \frac{d\omega}{\pi} \coth\left(\frac{\omega\beta}{2}\right) \tan^{-1}\left(\frac{\omega/\Gamma_q}{\delta + \mathbf{q}^2}\right).$$

(Hint: Functional integration over the Gaussian field fluctuations leads to a formally divergent expression. To extract the finite δ-dependent contribution above, first differentiate, $\partial_\delta F$, to later regain the δ-sensitive part of F by integration, $\int d\delta\, \partial_\delta F$.)

(b) Although, as we have seen above, the free energy can be obtained directly from the functional integral, to guide our analysis of the non-Gaussian theory it is helpful to develop the RG on the Gaussian model first. Using the standard coarse-graining procedure,

$$m(q) = \begin{cases} m_{\rm s}(q), & 0 < |\mathbf{q}| < \Lambda/b, \\ m_{\rm f}(q), & \Lambda/b \leq |\mathbf{q}| < \Lambda, \end{cases}$$

show that the scaling exponent $y_\delta = 2$ and, from the temperature, identify the value of the dynamical exponent z for the ferromagnetic and antiferromagnetic models. Focusing on the Gaussian fixed point, show that the RG implies the scaling dimension $y_u = 4 - d - z$ from which one obtains the upper critical dimension $d_u = 4 - z$.

(c) To accommodate the effect of a general interaction U, one may make use of the perturbative RG expansion

$$\mathcal{Z} = \int Dm_{\rm s}\, e^{-S[m_{\rm s}]} \langle e^{-U[m_{\rm s}, m_{\rm f}]} \rangle_{\rm f},$$

[49] As derived in Problem 6.7, the Stoner transition takes place from a paramagnetic to a ferromagnetic phase. However, experimentally, one often finds that, while the paramagnetic phase is stable at zero external magnetic field, the magnetization can change abruptly at some non-zero field – a metamagnetic transition. The development of a Landau expansion of the action in the vicinity of the metamagnetic critical point leads to a theory with uniaxial symmetry.

[50] A. J. Millis, Effect of a non-zero temperature on quantum critical points in itinerant fermion systems, *Phys. Rev. B* **48** (1993), 7183–96.

where $U[m_{\rm s}, m_{\rm f}] = \frac{3u}{2}\int dx\, m_{\rm s}^2 m_{\rm f}^2$ and $\langle\cdots\rangle_{\rm f} = \int Dm_{\rm f} e^{-S^{(2)}[m_{\rm f}]}(\cdots)$ denotes averaging over the quadratic action of the fast field. Keeping terms to first order in the quartic interaction,[51] obtain the RG equations

$$\begin{aligned}\frac{dT(b)}{d\ln b} &= zT(b),\\ \frac{d\delta(b)}{d\ln b} &= 2\delta(b) + 12u(b) f^{(2)}[T(b)],\\ \frac{du(b)}{d\ln b} &= (4-d-z)u(b),\end{aligned}$$

where

$$f^{(2)}[T(b)] = \Lambda^d \Omega_d \Gamma_\Lambda \int_0^1 \frac{ds}{\pi}\left[\coth\left(\frac{s\Gamma_\Lambda\beta}{2}\right)\frac{s}{(\delta+\Lambda^2)^2+s^2} + z\coth\left(\frac{s^{z-2}\Gamma_\Lambda\beta}{2}\right)\frac{s^{d-3+z}}{(\delta+s^2\Lambda)^2+1}\right]$$

denotes a dimensionless integral function of the temperature and Ω_d is the surface of the d-dimensional unit ball divided by $(2\pi)^d$. (Hint: Notice that, for a given value of the cutoff Λ, the integration domain in frequency–momentum space is set by $|\omega| < \Gamma_q$, $|\mathbf{q}| \leq \Lambda$. This means that the "shell" of fast fluctuations obtained by a gradual lowering of the cutoff is of the form shown in the figure. Introduce the integration boundaries imposed on the fast-field integration after you have analytically continued to real frequencies.)

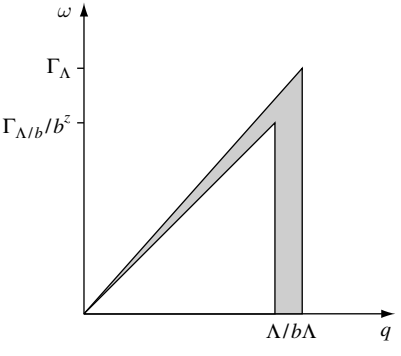

Already, from these differential recursion relations, one can recover much of the **phenomenology of the quantum critical system**. Integrating the last of the recursion relations, one finds that for $d + z \geq 4$, the interaction $u(b) = ub^{4-(d+z)}$ initially decreases under renormalization. Therefore, over at least some range of parameters, one may expect the theory to be controlled by the Gaussian fixed point $T^* = r^* = 0$. However, it is evident from the first of the scaling relations that the temperature increases under renormalization scaling as $T(b) = Tb^z$. Crucially, referring to the expression for $f^{(2)}[T(b)]$ (and, indeed, its higher-order descendants) – setting $\Lambda = \Gamma_\Lambda = 1$ for simplicity – one may see that the character of the renormalization changes when $T(b) \simeq 1$ (i.e. when $b \simeq b_0 = T^{-1/z}$). Here, the effect of the confinement in the Euclidean time direction begins to impact. Whether this scaling regime is reached depends on the physical bare parameters.

To stay within the scaling regime, we require $\delta(b) < 1$. Therefore, defining b_1: $\delta(b_1) = 1$, one may identify two regimes of behavior. Firstly, in a low-temperature regime where $1 \ll b_1 \ll b_0$, the system is characterized by quantum critical behavior controlled by the $T = 0$

[51] Comparing with the RG analysis of the standard ϕ^4-model in Section 8.4.4, consider which fluctuation effects are kept at this level of approximation and which are not.

fixed point. Here, approximating $f^{(2)}[T(b)] \simeq f^{(2)}[0]$, an integration of the scaling equation gives

$$\delta(b) = b^2 \left[\delta + \frac{12uf^{(2)}(0)}{z+d-2}\right] \equiv b^2 r,$$

the renormalization of δ recording the effect of quantum dynamical and spatial fluctuations on the critical point. Referred through b_1, this implies a "quantum critical regime" bounded by the inequality $T \ll r^{z/2}$.

However, if this inequality is reversed (i.e. $b_1 > b_0$), the scaling behavior must be separated into regimes where $b < b_0$ ($T(b) < 1$) and $b > b_0$ ($T(b) > 1$). Noting that, for $T(b) \gg 1$, $f^{(2)}[T(b)] \propto T(b)$, the recursion relations may be simplified (and, indeed, their nature elucidated) by defining $v(b) = u(b)T(b)$, whence they take a more familiar form,

$$\frac{d\delta(b)}{d\ln b} = 2\delta(b) + Cv(b), \quad \frac{dv(b)}{d\ln b} = (4-d)v(b),$$

with C relating the constant of proportionality. These are nothing but the differential recursion relations associated with the leading order of perturbation theory of the d-dimensional classical ϕ^4-theory with the familiar upper critical dimension $d_{\rm u} = 4$. Integrating these equations from b_0 to $b > b_0$, we obtain

$$\delta(b) = \left(\delta(b_0) - \frac{Cv(b_0)}{2-d}\right)\left(\frac{b}{b_0}\right)^2 + \frac{Cv(b_0)}{2-d}\left(\frac{b}{b_0}\right)^{4-d}, \quad v(b) = v(b_0)\left(\frac{b}{b_0}\right)^{4-d}.$$

To determine the initial values $(\delta, v)(b_0)$, we need to integrate the low-temperature ($b < b_0$, or $T(b) < 1$) scaling relations up to b_0. Setting $f^{(2)}(Te^{zx}) = f^{(2)}(0) + [f^{(2)}(Te^{zx}) - f^{(2)}(0)]$, the constant $f^{(2)}(0)$ recovers the result above while the term in rectangular brackets effects a temperature-dependent correction such that

$$\delta(b_0) = T^{-2/z}[r + BuT^{(d+z-2)/z}], \quad v(b_0) = uT^{(d+z-4)/z},$$

where $B = \frac{12}{z}\int_0^1 dT\, T^{[2-(d+2z)]/z}[f^{(2)}(T) - f^{(2)}(0)]$.

We now have to distinguish between two very different scenarios. (i) If the scaling is halted ($\delta(b) = 1$) while $v(b)$ remains small, the perturbative expansion remains valid. However, (ii) if $v(b)$ grows to order unity while $\delta(b)$ remains small, the scaling behavior moves into a region potentially controlled by non-Gaussian fluctuations. From the equations above, the condition for Gaussian behavior, i.e. $\delta(b) = 1$ and $v(b) \ll 1$, translates to the **Ginzburg criterion**

$$\frac{uT^{(d+z-3)/z}}{[r + (B+C)uT^{(d+z-2)/z}]^{1/2}} \ll 1.$$

From the same result, one can infer a **transition temperature**

$$T_{\rm c}(r<0, u) = \left[-\frac{r}{(B+C)u}\right]^{z/(d+z-2)}.$$

Notice that at the transition temperature we are always in regime (ii), i.e. a regime governed by strong non-Gaussian fluctuations. Gathered together, the results of this analysis are summarized in Fig. 8.13.

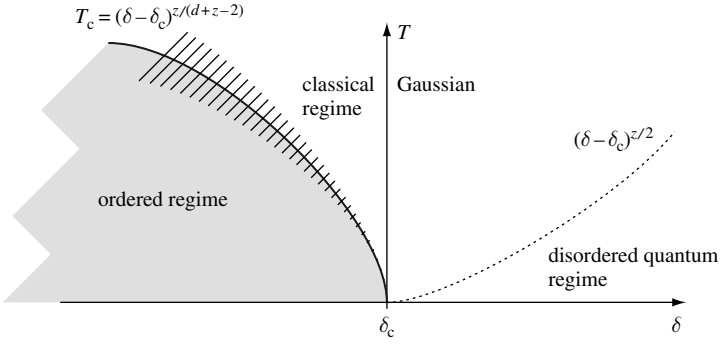

Figure 8.13 Phase diagram associated with a quantum critical point. The solid line denotes the locus of the transition temperature while the hatched area denotes the Ginzburg region where the scaling behavior is controlled by critical fluctuations.

INFO Although this completes our formal discussion of the renormalization properties of the quantum critical theory, it is instructive to question how these results can be translated to **experiment**. From the scaling behavior, one can infer directly a number of physical manifestations. Of these, the most straightforward relates to the temperature dependence of the magnetic susceptibility. Focusing on the classical Gaussian regime, in the disordered phase, we have seen that the mass scales as $\delta(b_0) = T^{-2/z}[r + BuT^{(d+z-2)/z}]$. The latter translates to a zero-field susceptibility

$$\chi(T) = \chi_0(r + BuT^{(d+z-2)/z}).$$

Once the bare temperature crosses into the disordered quantum regime, one expects the susceptibility to become temperature-independent.

Now, in the clean system, magnetic fluctuations present the dominant mechanism of low-temperature scattering. In this case, one can estimate their effect on the low-temperature resistivity. Referring to the literature, an estimate of the scattering rate based on the Born approximation gives

$$\frac{1}{2\tau} = -\text{Im}\ \Sigma^R(k_F, 0) \simeq g^2 \left(\frac{T}{v_F}\right)^3 \frac{1}{r + BuT^{(d+z-2)/z}},$$

where g denotes the coupling between the electrons and spin fluctuations. When the spin fluctuations dominate, one finds a resistivity $\rho(T) \sim T^{3-(d+z-2)/z}$ while, in the opposite regime, the contribution from electron–electron scattering dominates and one recovers the Fermi-liquid result $\rho(T) \sim T^2$.

Answer:

(a) For the Gaussian theory, integration over the fields $m(q)$ and subsequent differentiation with respect to δ gives the free energy density

$$\begin{aligned}\partial_\delta F_{\rm Gauss} &= L^d \int \frac{d^dq}{(2\pi)^d} T \sum_{\omega_n} \frac{1}{\delta + q^2 + \frac{|\omega_n|}{\Gamma_q}} = L^d \int \frac{d^dq}{(2\pi)^d} P \int_{-\Gamma_q}^{\Gamma_q} \frac{d\omega}{2\pi i} \frac{\tanh(\beta\epsilon/2)}{\delta + q^2 - i\frac{\omega}{\Gamma_q}} \\ &= -L^d \int \frac{d^dq}{(2\pi)^d} P \int_0^{\Gamma_q} \frac{d\omega}{\pi} \frac{\tanh(\beta\epsilon/2)\ \omega/\Gamma_q}{(\delta+q^2)^2 + (\omega/\Gamma_q)^2}.\end{aligned}$$

To arrive at the first integral, we have converted the sum over positive frequencies ω_n into a contour integral running parallel to the real axis, surrounding the pole at $\omega_m = 0$ along an infinitesimal semicircle in the upper complex half plane, and closing it at infinity through the upper complex half plane as usual. Noting that the infinitesimal integral around zero cancels against the contribution $\omega_m = 0$, the integral reduces to the principal value integral given above. (The integration is restricted to $|\omega| < \Gamma_q$ because outside this interval the low-frequency approximation of the polarization operator no longer applies.) Using the relation that $\partial_\delta \tan^{-1}\left(\frac{\omega/\Gamma_q}{\delta+q^2}\right) = -\frac{\omega/\Gamma_q}{(\delta+q^2)^2+(\omega/\Gamma_q)^2}$, we arrive at the required result.

(b) Since, at the level of the Gaussian theory, fast and slow fluctuations decouple, the effective action of the slow fields is given by

$$S[m_{\rm s}] = \frac{1}{2\beta} \int^{\Lambda/b} \frac{d^dq}{(2\pi)^d} \sum_{\omega_n} \left(\delta + \mathbf{q}^2 + \frac{|\omega_n|}{\Gamma_q}\right) |m_{\rm s}(q)|^2,$$

i.e. the original action with lowered cutoffs. (The presence of a cutoff in the frequency summation is implicit in the notation.) To restore the cutoffs to their original values, one must implement the rescaling $\mathbf{q}' = \mathbf{q}b, \omega_n' = b^z\omega_n$, where z denotes the dynamical exponent. Notice that the frequency scaling is tantamount to a redefinition of temperature, $T' = b^zT$. The final step of the RG involves the renormalization of the magnetization field, $m'(q') = m_{\rm s}(q')/y$. As a result, the action assumes the form

$$S[m] = -\frac{1}{2} \int^{\Lambda} \frac{d^dq'}{(2\pi)^d} T' \sum_{\omega_n'} \left(\delta + \mathbf{q}'^2 b^{-2} + \frac{|\omega_n'|b^z}{\Gamma_{q'/b}}\right) b^{-(d+z)} y^2 |m'(q')|^2.$$

Requiring that the gradient term remain invariant, one finds that $y = b^{(d+z+2)/2}$. Further, requiring that the damping term maintain the same form ensures that $(1/\Gamma_{q'/b}/b^z)b^{-(d+z)}y^2 = 1/\Gamma_{q'}$, fixing the dynamical exponent. In particular, for the ferromagnetic system ($\Gamma_q = \Gamma|\mathbf{q}|$), $z = 3$ while, for the antiferromagnetic system ($\Gamma_q = \Gamma$), $z = 2$. Finally, applied to the coefficient δ, invariance of the action requires $\delta' = y^2b^{-(d+z)}\delta = b^{y_\delta}\delta$ with $y_\delta = 2$. As expected, the Gaussian fixed point lies at $T^* = \delta^* = 0$ and has the fixed point action

$$S[m] = \frac{1}{2} \int^{\Lambda} \frac{d^dq}{(2\pi)^d} \frac{1}{2\pi} \int^{\Gamma_\Lambda} d\omega \left(\mathbf{q}^2 + \frac{|\omega_n|}{\Gamma_q}\right) |m(q)|^2,$$

where Γ_Λ sets the cutoff in frequency direction.

To identify the upper critical dimension, one must consider the effect of the quartic interactions. Firstly, applied to the gradient component of the fixed action $\int dx\ (\nabla m)^2$, the relation $m'(x') = m_{\rm s}(x')/\eta$ allows us to deduce the field renormalization $\eta = b^{(2-d-z)/2}$. Applied to the quartic interaction, the renormalization procedure leads to the relation

$$\frac{u}{4}\int dx\, m^4(x) \mapsto \frac{u}{4} b^{d+z}\eta^4 \int dx'\, m'^4(x'),$$

from which one obtains $u' = b^{4-d-z}u$. Therefore, in dimensions $d+z<4$ the interaction coefficient diminishes under renormalization and the properties of the system are governed by the mean-field exponents. Since the dynamical exponent $z = 2$ or 3, one finds that the majority of physical systems fall above the upper critical dimension and are controlled by the Gaussian fixed point.

(c) The first term in the u-expansion, $(3u/2)\int dx\, m_{\rm s}^2\langle m_{\rm f}^2\rangle$, gives rise to a renormalization of the coefficient δ. Evaluating this contribution, and expressing the frequency summation by a contour integral as in (a), we obtain

$$\langle m_{\rm f}^2\rangle = \frac{1}{\pi(2\pi)^d}\int_{\partial\Lambda} d^d q\, d\omega\, \coth\left(\frac{\omega\beta}{2}\right)\frac{\omega/\Gamma_q}{(\delta+\mathbf{q}^2)^2+(\omega/\Gamma_q)^2},$$

where the integral runs over the momentum shell $\partial\Lambda$ (see the figure on page 480). Taking each component of the integral in turn, one obtains

$$\langle m_{\rm f}^2\rangle = \left(\Lambda-\frac{\Lambda}{b}\right)\Lambda^{d-1}\Omega_d\int_0^{\Gamma_\Lambda}\frac{d\omega}{\pi}\coth\left(\frac{\omega\beta}{2}\right)\frac{\omega/\Gamma_\Lambda}{(\delta+\Lambda^2)^2+(\omega/\Gamma_\Lambda)^2} + \frac{1}{\pi}\int^{\Lambda}\frac{d^dq}{(2\pi)^d}\left(\Gamma_q-\frac{\Gamma_q}{b^z}\right)\coth\left(\frac{\Gamma_q\beta}{2}\right)\frac{1}{(\delta+\mathbf{q}^2)^2+1}.$$

Noting that $\Lambda(1-e^{-\ln b})\simeq\Lambda\ln b+\cdots$ and $\Lambda(1-e^{-z\ln b})\simeq\Lambda z\ln b+\cdots$, the latter can be expressed as $\langle m_{\rm f}^2\rangle = f^{(2)}[T(b)]\ln b$, where, applying the rescaling $s=\omega/\Gamma_\Lambda$ or $s=|\mathbf{q}|/\Lambda$ as appropriate, one obtains the required expression for $f^{(2)}[T(b)]$. Therefore, to first order in u, one obtains the scaling relation $\delta' = \delta(1+2\ln b)+12uf^{(2)}[T(b)]\ln b$. At first order in perturbation theory, the coupling constant u is not modified by fluctuation-induced corrections, i.e. u changes according to its engineering dimension, $u' = u(1+(4-d-z)\ln b)$. Similarly, $T' = b^zT$. Differentiating these expressions, we arrive at the required differential recursion relations.

8.8.3 RG analysis of the nonlinear σ-model II

Previously, we have argued that, below the lower critical dimension, Goldstone mode fluctuations become unbounded and induce a crossover of systems with spontaneously broken continuous symmetries into a "disordered" state. Technically, the long-distance fluctuation behavior of Goldstone modes is described by nonlinear σ-models with coset-space valued fields. In this problem, we apply RG methods to show that, at and below the dimension two, these models indeed flow towards a disordered phase.

Consider a situation where the symmetry of a model is broken from a "large" compact group G down to some subgroup H. On physical grounds, we expect that (i) the action of the associated Goldstone modes $g \in G/H$ is space(-time) rotationally invariant and starts at $\mathcal{O}$ (two derivative operators). By symmetry (Exercise: Think why!) (ii) the action must be invariant under *global* transformations by elements of the full symmetry group, $S[g] = S[\tilde{g}g]$, where $\tilde{g} \in G$ is constant. However, (iii) it must also be invariant under *local* transformations $S[g] = S[gh]$, where $h(x) \in H$ is a field taking values in the "small" group H. (This last condition simply states that g takes values in the (right) coset space G/H, i.e. is oblivious to (right) transformations $g \to gh$.)

How would one construct such an action in practice? An obvious recipe goes as follows. Take any reference ground state $|n_0\rangle$. (Think of $|n_0\rangle$ as an element of some vector space, e.g. a "spin up" state in a magnetic system.) Defining the symmetry transformed states $|n(\mathbf{x})\rangle = g(\mathbf{x})|n_0\rangle$, the unique G-invariant action is then given by $S[n] = c\int d^dx\,\langle\nabla n|\nabla n\rangle$. This action obviously meets all three criteria above. However, by making explicit reference to an arbitrarily chosen state ($|n_0\rangle$) it partially obscures the symmetries of the model. Thus, before turning to the RG formulation, let us briefly discuss an alternative, and more symmetry-oriented, formulation.

Let $\Lambda \in G$ be a group element that commutes with all $h \in H$, i.e. $h\Lambda h^{-1} = \Lambda$.[52] The set $\{Q = g\Lambda g^{-1} | g \in G\}$ is isomorphic to the coset space G/H (which is to say that two elements g and $g' = gh$ differing by an element of the small group are represented by the same Q). In the Q-language, the unique action meeting the criteria (i)–(iii) above (exercise: check!) is given by

$$S[Q] = \frac{1}{\lambda}\int d^dr\,\mathrm{tr}(\nabla Q\,\nabla Q).$$

Below, we will explore the long-range behavior of the field integral $\int DQ\exp(-S[Q])$, where DQ is the G invariant measure ($DQ = D(gQg^{-1})$) on the coset space.

INFO They being but **di erent representations of the same coset space** G/H it is, of course, always possible to explicitly relate the n- to the Q-representation. Consider, for example, the case $G = \mathrm{SU}(2)$, and $H = \mathrm{U}(1)$. Representing the group G through Euler angles (see Section 3.3), $g(\phi,\theta,\psi) = \exp(i\phi\hat{S}_3)\exp(i\theta\hat{S}_1)\exp(i\psi\hat{S}_3)$, define the (spin-coherent) states $|n(\phi,\theta)\rangle = g(\phi,\theta)|\ \rangle$, where $|\ \rangle$ is the state of maximal eigenvalue $S_3 = S$, and we noted that the ψ degree of freedom (spanning the small group) leaves $|S_3\rangle$ invariant (up to a phase) and can be omitted. In Section 3.3 we used this representation to identify the phase space of spin as the coset space $\mathrm{SU}(2)/\mathrm{U}(1)$, the 2 sphere. In the Q language, the same sphere is represented as $Q = g\sigma_3 g^{-1}$, where $\hat{S}_i = \sigma_i/2$ are identified with the Pauli matrices. Again, the ψ factor, commutative with σ_3, drops out. The integration measure $dQ = d\phi d\theta\sin\theta$ reduces to the invariant integration measure on the sphere.

[52] It being a subgroup of the (matrix-)group G, we can always find a representation wherein the group H is represented by block-diagonal matrices. In this representation, Λ will be a diagonal matrix that contains identical elements on all sub-blocks defining H.

(a) By way of example, let us consider the case $(G, H) = (\mathrm{SU}(2), \mathrm{U}(1))$, relevant to, e.g., the classical Heisenberg magnet.[53] Defining $g = g_\mathrm{s} g_\mathrm{f}$ where the fast field $g_\mathrm{f} = \exp(iW)$, $W = zE_{12} + \bar{z}E_{21}$, $z \in \mathbb{C}$ (explore the connection between this representation and the Euler angle representation above), and $\Phi_\mu \equiv g_\mathrm{s}^{-1}\partial_\mu g_\mathrm{s}$, show that the freedom to transform g_f by elements of the small group can be used to bring Φ_s to an off-diagonal form, $[\Phi_\mathrm{s}, \sigma_3]_+ = 0$. Show that the expansion of the action to second order ($\to$ one-loop order) in the fast generators W is given by $S[g_\mathrm{s}, W] = S[g_\mathrm{s}] + S_\mathrm{f}[z, \bar{z}] + S_\mathrm{fs}[g_\mathrm{s}, z, \bar{z}]$, where $S_\mathrm{f}[z, \bar{z}] = \frac{8}{\lambda}\int d^d r\, \nabla z \nabla \bar{z}$ and

$$S_\mathrm{fs}[g_\mathrm{s}, z, \bar{z}] = -\frac{8}{\lambda}\int d^d r\ \mathrm{tr}(\Phi_\mu(zE_{12} - \bar{z}E_{21})\Phi_\mu(zE_{12} - \bar{z}E_{21}) + \Phi_\mu\sigma_3\Phi_\mu\sigma_3 z\bar{z}).$$

(b) Integrate over the fields $z, \bar{z}$ to obtain the effective action $S[g_\mathrm{s}] = \frac{1}{\lambda_r}\int d^d r\ \mathrm{tr}(\nabla Q_\mathrm{s} \nabla Q_\mathrm{s})$, where λ_r is the renormalized coupling constant. Differentiate this constant with respect to the scaling parameter b to obtain the **RG equation of the σ-model on the 2-sphere**,

$$\frac{d\ln\lambda}{d\ln b} = \frac{\lambda}{8\pi} - \epsilon. \tag{8.51}$$

According to this equation, the coset σ-model behaves very much like its group-valued cousin explored in Section 8.5: at dimensions $d = 2$ and below it flows towards a disordered phase; at dimensions $d > 2$ there is a phase transition separating a disordered regime from an ordered phase.

Answer:

(a) Substituting $g = g_\mathrm{s} g_\mathrm{f}$ into the action and defining the shorthand notation $\Phi \equiv g_\mathrm{s}^{-1}\nabla g_\mathrm{s}$, we obtain $S[g_\mathrm{s}, g_\mathrm{f}] = \frac{1}{\lambda}\int d^d r\ \mathrm{tr}(\nabla^{[\Phi]} Q_\mathrm{f} \nabla^{[\Phi]} Q_\mathrm{f})$, where $Q_\mathrm{f} = g_\mathrm{f}\sigma_3 g_\mathrm{f}^{-1}$ and the "covariant derivative" $\nabla^{[\Phi]}Q = \nabla Q + [\Phi, Q]$. We next transform the integration variables $W \to hWh^{-1}$, where $h \in H$. (Notice that this really is a transformation of integration variables, i.e. the off-diagonal form of the generators is preserved.) This transformation induces a change $\nabla^{[\Phi]} \to \nabla^{[\Phi + h^{-1}\ \ h]}$ and we may choose h so as to remove the matrix-diagonal components of Φ. (Exercise: Explicitly construct a matrix h that does the job. Why can the matrix h be defined only locally and why does the absence of a globally defined h not matter in connection with a perturbative RG operation?)

[53] Below the transition temperature, the symmetry of the Heisenberg magnet is broken from full rotational symmetry, O(3), to rotations around the magnetization axis, O(2). Since $\mathrm{O}(3) \overset{\text{locally}}{\simeq} \mathrm{SU}(2)$, and $\mathrm{O}(2) \simeq \mathrm{U}(1)$, the example above covers the physics of the magnetic system. (We prefer to use the language of the unitary group, as it is somewhat easier to implement, technically.)

A straightforward expansion to second order in W, $Q_{\rm f} = \sigma_3(1 + 2iW - 2W^2 + \cdots)$, now leads to the expressions

$$\begin{aligned} S_{\rm f}[W] &= \frac{4}{\lambda}\int d^dr\ {\rm tr}(\partial_\mu W \partial_\mu W), \\ S[g_{\rm s}, W] &= -\frac{8}{\lambda}\int d^dr\, {\rm tr}(\Phi_\mu W\sigma_3\Phi_\mu W\sigma_3 + \Phi_\mu\sigma_3\Phi_\mu\sigma_3 W^2). \end{aligned} \tag{8.52}$$

Substituting the z-representation of the generators W, we arrive at the action given above.

(b) Every field Φ_μ contains a derivative acting on the slow field. Since we do not want to keep terms with more than two derivatives, the effective action is given by $S_{\rm eff}[g_{\rm s}] = S[g_{\rm s}] + \langle S^{(2)}[g_{\rm s}, z, \bar z]\rangle$. Switching to a momentum representation, $S_{\rm f}[z,\bar z] = \frac{8L^d}{\lambda}\sum_{\mathbf{p}\in{\rm f}} z_{\mathbf{p}}\bar z_{\mathbf{p}} p^2$, and doing the Gaussian integrals, we obtain

$$\langle S^{(2)}[g_{\rm s}, z, \bar z]\rangle = -\frac{I_1}{4}\int d^dr\, {\rm tr}([\Phi_\mu, \sigma_3]^2) = -\frac{I_1}{4}\int d^dr\, {\rm tr}(\nabla Q_{\rm s}\nabla Q_{\rm s}),$$

where the constant I_1 has been defined in Eq. (8.28). Substituting this result back into the effective action, we obtain

$$S_{\rm eff} = \left(\frac{1}{\lambda} - \frac{I_1}{4}\right)\int d^dr\, {\rm tr}(\nabla Q_{\rm s}\nabla Q_{\rm s}) = \frac{1}{\lambda_r}\int d^dr\, {\rm tr}(\nabla Q_{\rm s}\nabla Q_{\rm s}),$$

where we have rescaled momenta and $\lambda_{\rm r}^{-1} = [\lambda^{-1} - \Omega^d(1-b^{2-d})/4(d-2)]b^{d-2}$. Substituting $d = 2+\epsilon$ and expanding in ϵ, we obtain $\lambda_{\rm r} = \lambda\left(1 - \ln b\epsilon + \frac{\lambda}{8\pi}\ln b\right)$. Differentiating with respect to $\ln b$, we obtain the RG equation (8.51).

8.8.4 Scaling theory of the Anderson metal insulator transition

In Section 6.5 we derived the field theory of the disordered electron gas. Specifically, we showed that the low-energy physics of the system is governed by a phase of a spontaneously broken continuous symmetry. This being so we should expect $d = 2$ to be the "lower critical dimension" of the disordered electron gas. At and below $d = 2$ Goldstone mode fluctuations are likely to drive a nominally conducting system into a phase governed by unbounded Goldstone mode fluctuations – an insulator in fact. In higher dimensions the effect of fluctuations is comparatively weaker and metallic phases have a chance to prevail. In this problem we apply RG methods to obtain a semi-quantitative understanding of the Anderson transition between these two phases.

INFO Before turning to the technology, let us discuss the notion of **Anderson localization in metals** on a more qualitative level. Firstly, it is important to draw a distinction between qualitatively different mechanisms of localization. Consider a d-dimensional electron system in the presence of static disorder. Evidently, the lowest energy states in a disordered system will be dictated by "optimal fluctuations" of the random impurity potential. These "tail states" can be interpreted as bound states localized in regions where the potential is unusually low and uniform. Instead, here we are interested in the localization properties of states with energies greatly in excess of the typical magnitude of the impurity potential, i.e. $E_{\rm F}\tau \gg 1$. Here, the

mechanism of localization can derive only from the accumulation of interference corrections akin to the corrections discussed in Section 6.5 above.

According to its energy E, Anderson proposed[54] that a given state is either extended or localized depending on the degree of disorder. Following an argument due to Mott, it is also plausible that extended and localized states at the same energy do not coexist – in such circumstances, the admixture of the former due to arbitrarily small perturbations would lead to the delocalization of the latter. Moreover, it is natural that states at the band edge are more susceptible to the formation of bound or localized states. These considerations suggest a profile for the DoS in which the low-lying localized states are separated from higher-energy extended states by a **mobility edge**. The transition signaled by the mobility edge is known as the **Anderson transition**.

Following the pioneering work of Anderson, it was almost two decades before a consistent theory of localization emerged. Its basis was a simple yet powerful scaling hypothesis that followed naturally from a conjecture made by Edwards and Thouless:[55] the conductance $g(L)$ of a d-dimensional fragment of metal of size L^d ($L \gg \ell \gg \lambda_F$) is determined by the sensitivity of the single-particle energy levels inside the sample to changes in the boundary conditions. Building on this assumption, Abrahams et al. proposed[56] a **one-parameter scaling hypothesis of localization**. This hypothesis states that the conductance of a system of size bL is a function of $g(L)$ only: $g(bL) = f_b(g(L))$. The important point is that f_b does not explicitly depend on the system size L. Independent of Thouless' argument, this restriction can be made plausible by dimensional analysis: since g is dimensionless, the only way for the parameter L to appear in f is through a dimensionless ratio L/a, where a is some compensating scale of dimensionality [length]. This, however, would imply explicit dependence of the conductance on a microscopic reference scale, which conflicts with the presumption of universal scaling behavior.

Differentiation of the scaling form with respect to b gives the Gell–Mann–Low equation $\frac{d\ln g}{d\ln L} = \beta(g)$. The scaling function $\beta(g) \equiv f'(g)/g$ is universal, i.e. independent of the microscopic properties of the sample, such as the bare microscopic conductance and ℓ/λ_F. While these predictions still have to find a truly rigorous mathematical proof, they definitely represent an important milestone in phenomenology. Moreover, the scaling picture fits neatly into perturbative microscopic approaches to localization, such as the one discussed below. However, before turning to quantitative calculations, let us try to determine the profile of the β-function on qualitative grounds.

For an ohmic conductor, $g(L) \sim L^{d-2}$, implying that the scaling function takes a constant value $\beta = d-2$. On the other hand, deep in the insulating regime, where states are exponentially localized, $\beta(g) \sim \ln g$ (i.e. $g \sim e^{-L/\xi}$). A smooth interpolation between these limits (see Fig. 8.14) suggests that, below two dimensions, all states are localized, while, above, there is a critical conductance, g_*, marking a phase transition between a localized and a delocalized phase – the Anderson transition.

At the time when this scaling behavior was proposed, it was not yet known that the low-energy theory of the disordered electron gas was a nonlinear σ-model. However, with the benefit of hindsight, one may interpret the phenomenology outlined above as a ramification of the notorious

[54] P. W. Anderson, The absence of diffusion in certain random lattices, *Phys. Rev.* **109** (1958), 1492–505.
[55] J. T. Edwards and D. J. Thouless, Numerical studies of localization in disordered systems, *J. Phys. C* **5** (1972), 807–20.
[56] E. Abrahams, P. W. Anderson, D. C. Licciardello, and T. V. Ramakrishnan, Scaling theory of localization: absence of quantum diffusion in two dimensions, *Phys. Rev. Lett.* **42** (1979), 673–6.

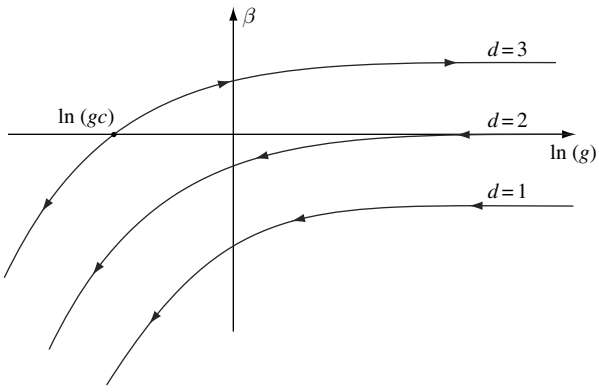

Figure 8.14 Scaling function of the dimensionless conductance, $\beta(g)$, in dimensions $d = 1, 2$, and 3. At large values of the conductance, the scaling function approaches the asymptote $\beta(g) \to d - 2$ corresponding to ohmic behavior. For very small values of conductance, the scaling function approaches $\beta(g) \to \ln g$, which is characteristic of insulating behavior. According to the weak localization expansion, a localization transition is predicted in dimensions greater than two.

scaling behavior displayed by these models. Below, we show that the one-loop β-function of the replica σ-model fully complies with the predictions of the one-parameter scaling theory.

(a) Recapitulate the construction of the replica nonlinear σ-model in Section 6.5. Convince yourself that, in order to explore the physical properties of a non-interacting disordered system, we actually do not need the full information contained in that model; the model introduced in Section 6.5 has been constructed to compute correlation functions $\langle \hat{G}_n \hat{G}_{n'} \rangle$ for arbitrary Matsubara frequencies ω_n and $\omega_{n'}$. However, sufficiently far-reaching information on the conduction behavior of a non-interacting system (cf. our discussion of linear response in Section 7.4) is contained in correlation functions $\sim \langle \hat{G}^+ \hat{G}^- \rangle$ involving the product of a retarded and an advanced Green function $\hat{G}^{\pm} = (E_{\rm F} \pm (\omega/2 + i0) - \hat{H})^{-1}$ at *fixed* energies $E_{\rm F} \pm \omega/2$. Retracing the derivation of the σ-model, convince yourself that correlation functions of this type can be obtained from the action Eq. (6.63), where the Q-matrices, $Q = g\Lambda g^{-1}$, are of dimension $4R$ (instead of $2RM$ as in the Matsubara case) and $\Lambda = \{\sigma_3 \delta_{\alpha\alpha'}\}$ assumes the role of the matrix $\Lambda = \{\mathrm{sgn}_{nn'} \delta_{\alpha\alpha'}\}$, i.e. the effectively infinite-dimensional space of Matsubara frequencies has been reduced to a two-component space discriminating between retarded and advanced Green functions. (Here, $\alpha = (a, \sigma)$ are $2R$-component indices comprising the replica index a and the two-component "time-reversal" index σ introduced in Section 6.5.)

(b) Focusing on the case of zero external frequency and introducing the abbreviation $\lambda^{-1} = \frac{\pi D \nu}{8}$, we wish to explore the scaling behavior of the action

$$S[Q] = \frac{1}{\lambda} \int d^d r \, \mathrm{tr} (\nabla Q)^2 .$$

To do so, we follow the same logic as in the previous problem: we decompose $Q = g_{\rm s} Q_{\rm f} g_{\rm s}^{-1}$ into fast and slow components and expand the former $Q_{\rm f} = \sigma_3 (1 + i2W - 2W^2 +$

$\cdots$). The matrices W anti-commute with σ_3, and live in the Lie algebra sp($4R$), i.e. they obey the condition $W = -\sigma_2^{\rm tr} W^T \sigma_2^{\rm tr}$ where the Pauli matrices act in time-reversal space. These two conditions are encapsulated in the representation (block structure in advanced/retarded space)

$$W = \begin{pmatrix} & B \\ B^\dagger & \end{pmatrix}, \quad B = -\sigma_2^{\rm tr} B^T \sigma_2^{\rm tr} \equiv -B^\tau, \tag{8.53}$$

where the matrices B are of dimension $2R$ and we have used the abbreviated notation $B^\tau \equiv \sigma_2^{\rm tr} B^T \sigma_2^{\rm tr}$. Substituting this representation into the action, we obtain $S[g_{\rm s}, W] = S[g_{\rm s}] + S_{\rm f}[W] + S_{\rm fs}[g_{\rm s}, W]$, where $S_{\rm f}$ and $S_{\rm fs}$ are given by Eq. (8.52).

Perform the Gaussian integrals over the matrices W. First show that $\langle B_{\mathbf{p}\alpha\beta} B^\dagger_{\mathbf{p}'\beta'\alpha'}\rangle = \frac{\lambda \delta_{\alpha\alpha'}\delta_{\beta\beta'}\delta_{\mathbf{q},\mathbf{q}'}}{16 L^d p^2}$. Use this result, and the symmetries of the B matrices, to verify the auxiliary identities

$$\begin{aligned} {\rm tr}(B_{\mathbf{p}} A B^\dagger_{\mathbf{p}'} A') &= \frac{\lambda}{16 L^d p^2} {\rm tr}(A)\,{\rm tr}(A'), & (8.54)\\ {\rm tr}(B_{\mathbf{p}} A B_{-\mathbf{p}'} A') &= \frac{\lambda}{16 L^d p^2}\, {\rm tr}(A A'^\tau). & (8.55) \end{aligned}$$

Use these relations to show that $\langle S[g_{\rm s}, W]\rangle = -\frac{I_1}{4}\int d^d r\, {\rm tr}(\nabla Q)^2$, where I_1 has been defined in Eq. (8.28). (Hint: Use the fact that $\Phi_\mu^\tau = -\Phi_\mu$ (exercise). Identify and neglect terms that vanish in the replica limit.) Adding this contribution to the core action $S[g_{\rm s}]$ we obtain the same renormalized coupling constant as in the previous problem. Thus, the **RG equation of the σ-model of disordered systems** (possessing spin rotation and time reversal invariance, to be precise) is again given by Eq. (8.51). In $2+\epsilon$ dimensions, the constant $\lambda \propto (D\nu)^{-1} \propto g^{-1}$ is proportional to the physical conductance and Eq. (8.51) describes the scaling of the latter. In accord with the phenomenological expectations summarized above, the scaling equation depends only on the conductance itself (one-parameter scaling) and predicts an (Anderson) transition point for $d > 2$. For further discussion of the scaling behavior of the replica σ-model and its ramifications in the physics of disordered systems we refer to, e.g., Efetov.[57]

Answer:

(a) Consider the Grassmann action $\int \bar\psi (E_{\rm F} + (\omega + i0)\sigma_3/2 - \hat H)\psi$, where $\psi = \{\psi^{\pm a}\}$ is a $2R$-component Grassmann field and σ_3 acts in the space of $\pm$-indices. By introducing suitably devised sources, this action can be employed to compute correlation functions involving an advanced and a retarded Green function. Recapitulating the derivation of the nonlinear σ-model, we notice that nothing changes except that the infinite vector of Matsubara frequencies $\hat\omega$ gets replaced by the two-dimensional matrix $(\omega + i0)\sigma_3/2$. Since the structure of the diagonal saddle-point, Λ, is solely determined by the sign of the

[57] K. B. Efetov, *Supersymmetry in Disorder and Chaos* (Cambridge University Press, 1996).

imaginary part of the frequency vector, $\Lambda = \{\mathrm{sgn}_{nn'}\delta_{aa'}\}$ gets replaced by $\Lambda = \{\sigma_3\delta_{aa'}\}$. The Q matrices reduce to $Q = g\Lambda g^{-1}$, where $g \in \mathrm{Sp}(4R)$.

(b) Switching to an index representation, $S[B, B^\dagger] = \frac{8L^d}{\lambda}\sum_{\alpha\alpha'} B_{\alpha\alpha'}B^\dagger_{\alpha'\alpha}$. From this representation, one might naively conclude that $\langle B_{\mathbf{q}\alpha\beta}B^\dagger_{\mathbf{q}'\beta'\alpha'}\rangle = \frac{\lambda}{8L^dq^2}\delta_{\alpha\alpha'}\delta_{\beta\beta'}\delta_{\mathbf{q},\mathbf{q}'}$ with a right-hand side twice as large as the correct result. However, thanks to the relation $B = -\sigma_2^{\mathrm{tr}}B^T\sigma_2^{\mathrm{tr}}$, the matrix elements of B and $B^\dagger$ are not independent complex variables. Using the symmetry relation (exercise), it is straightforward to show that all complex integration variables appear in pairs, i.e. the coupling constant effectively doubles. On the same basis, some matrix elements ($B_{a\sigma,a'\bar\sigma}$, where $\bar\sigma = (\sigma + 1 \bmod 2)$ turn out to be real rather than complex. In either case, the Gaussian integration obtains a result twice as small as for independent complex variables. This explains the factor $1/16$ in the given formula.

The auxiliary identity (8.54) readily follows by representing the trace as a sum over indices and using the Gaussian formula for the matrix indices above. To prove Eq. (8.55), we first need to relate the $\langle BB\rangle$ contraction to a $\langle BB^\dagger\rangle$ contraction:

$$\begin{aligned}
\langle \mathrm{tr}(B_{\mathbf{p}}AB_{-\mathbf{p}'}A')\rangle &= \langle \mathrm{tr}((\sigma_2^{\mathrm{tr}}A'B_{\mathbf{p}}A\sigma_2^{\mathrm{tr}})(\sigma_2^{\mathrm{tr}}B_{-\mathbf{p}'}\sigma_2^{\mathrm{tr}}))\rangle \\
&= \langle (\sigma_2^{\mathrm{tr}}A')_{\alpha\beta}B_{\mathbf{p}\beta\gamma}(A\sigma_2^{\mathrm{tr}})_{\gamma\delta}(\sigma_2^{\mathrm{tr}}B_{-\mathbf{p}'}\sigma_2^{\mathrm{tr}})_{\delta\alpha}\rangle \\
&= -\langle (\sigma_2^{\mathrm{tr}}A')_{\alpha\beta}B_{\mathbf{p},\beta\gamma}(A\sigma_2^{\mathrm{tr}})_{\gamma\delta}B^\dagger_{\mathbf{p}'\alpha\delta}\rangle = -\frac{\lambda}{16L^dp^2}(\sigma_2^{\mathrm{tr}}A')_{\alpha\beta}(A\sigma_2^{\mathrm{tr}})_{\alpha\beta} \\
&= -\frac{\lambda}{16L^dp^2}(\sigma_2^{\mathrm{tr}}A')_{\alpha\beta}(\sigma_2^{\mathrm{tr}}A^T)_{\beta\alpha} = \frac{\lambda}{16L^dp^2}\mathrm{tr}(AA'^\tau).
\end{aligned}$$

Using these contraction rules to compute the second term in Eq. (8.52), $\langle \mathrm{tr}(\Phi_\mu\sigma_3\Phi_\mu\sigma_3(BB^\dagger E_{11} + B^\dagger BE_{22}))\rangle \propto \mathrm{tr}(\mathbf{1}) \propto R$, we obtain an expression that vanishes in the replica limit. As for the first term, noting that $\Phi_\mu^\tau = \left(g_{\mathrm{s}}^{-1}\partial_\mu g_{\mathrm{s}}\right)^\tau = \partial_\mu g_{\mathrm{s}}^\tau g_{\mathrm{s}}^{-1\tau} = \partial_\mu g_{\mathrm{s}}^{-1}g_{\mathrm{s}} = -\Phi_\mu$ we obtain

$$\begin{aligned}
-\frac{8}{\lambda}\int d^dr\,\langle \mathrm{tr}(\Phi_\mu W\sigma_3\Phi_\mu W\sigma_3)\rangle &= -\frac{8}{\lambda}\int d^dr\,\langle \mathrm{tr}(\Phi_\mu(BE_{12} - B^\dagger E_{21}) \\
&\quad \times \Phi_\mu(BE_{12} - B^\dagger E_{21}))\rangle \\
\to -\frac{16}{\lambda}\int d^dr\,\langle \mathrm{tr}(\Phi_\mu BE_{12}\Phi_\mu BE_{12})\rangle &= I_1\int d^dr\ \mathrm{tr}(\Phi_\mu^{12}(\Phi_\mu^\tau)^{21}) \\
&= -\frac{I_1}{4}\int d^dr\ \mathrm{tr}([\Phi_\mu,\sigma_3][\Phi_\mu,\sigma_3]).
\end{aligned}$$

Here, the "$\to$" indicates that we are omitting terms that lead to traces of $\Phi^{ii} = 0$. We also note that, by virtue of the time reversal relation, contractions $\sim \langle BB\rangle$ and $\sim \langle B^\dagger B^\dagger\rangle$ lead to identical results. Expressing Φ_μ in terms of the original variables Q_{s}, we arrive at the formula above.

8.8.5 Kondo effect: poor man s scaling

In Problem 2.4 we saw that the low-energy properties of a metal, when it is coupled to a magnetic Anderson impurity, are encapsulated by an effective sd-Hamiltonian Eq. (2.51) involving itinerant carriers coupled to the spin of the magnetic impurity by an exchange coupling J. Applying a perturbative analysis, in Problem 5.5 we saw that the effect of the magnetic impurity fluctuations was to impart a contribution to the scattering rate which diverged at low temperatures – a phenomenon compatible with the observed increase in low-temperature resistivity. However, it being perturbative in character, little could be said about the effect of the magnetic impurity in the strong coupling regime. In the following, we will implement a perturbative RG scheme to monitor the flow of the coupling constant and explore the low-temperature properties of the Kondo impurity system.

Our starting point is the sd-Hamiltonian where, anticipating the capacity for anisotropy, we treat the bare components of the exchange coupling as independent parameters,

$$\hat{H}_{\rm sd} = \sum_{\mathbf{k}\sigma} \epsilon_{\mathbf{k}} c^\dagger_{\mathbf{k}\sigma} c_{\mathbf{k}\sigma} + \sum_{\mathbf{k}\mathbf{k}'} \left[J_z \hat{S}^z \left(c^\dagger_{\mathbf{k}\uparrow} c_{\mathbf{k}'\uparrow} - c^\dagger_{\mathbf{k}\downarrow} c_{\mathbf{k}'\downarrow} \right) + J_+ \hat{S}^+ c^\dagger_{\mathbf{k}\downarrow} c_{\mathbf{k}'\uparrow} + J_- \hat{S}^- c^\dagger_{\mathbf{k}\uparrow} c_{\mathbf{k}'\downarrow} \right]$$

where $\hat{\mathbf{S}}$ denotes the spin of the local moment formed by the d-electron system.

In the following, we will implement an adaptation of the RG procedure which monitors the effect of high-energy (fast) degrees of freedom on the low-energy (slow). Our analysis is taken from the original paper by Anderson.[58] (For a discussion of the generalization of the RG scheme and a much more lengthy discussion of the subject as a whole, we refer to the review by Hewson.[59]) To this end, let us divide the conduction band into high-lying electron/hole states that occupy an energy shell $D/b < |\epsilon_{\mathbf{k}}| < D$, where D denotes the bare bandwidth and $b > 1$, and the remaining states $0 < |\epsilon_{\mathbf{k}}| < D/b$. To eliminate the high-lying excitations that fall within the band edge, we may implement a general procedure that mirrors the one exploited in the construction of the sd-Hamiltonian from the Anderson model (Problem 2.4). Specifically, let us write the total wavefunction of the Hamiltonian $|\psi\rangle$ as the sum of terms $|\psi_0\rangle$, $|\psi_1\rangle$, and $|\psi_2\rangle$ where $|\psi_1\rangle$ describes the component in which there are no conduction electrons/holes in the upper/lower band edge, $|\psi_0\rangle$ has at least one hole in the lower band edge, and $|\psi_2\rangle$ has at least one electron in the upper band edge. Following the discussion in Problem 2.4, eliminating $|\psi_0\rangle$ and $|\psi_2\rangle$ from the Schrödinger equation $\sum_{n=0}^{2} \hat{H}_{mn}|\psi_n\rangle = E|\psi_m\rangle$, one obtains

$$\left[\hat{H}_{10} \frac{1}{E - \hat{H}_{00}} \hat{H}_{01} + \hat{H}_{11} + \hat{H}_{12} \frac{1}{E - \hat{H}_{22}} \hat{H}_{21} \right] |\psi_1\rangle = E|\psi_1\rangle.$$

(a) Taking into account the process that scatters a conduction electron into the upper band edge, show that the term

$$\hat{H}_{12} \frac{1}{E - \hat{H}_{22}} \hat{H}_{21} |\psi_1\rangle$$

[58] P. W. Anderson, A poor man's derivation of scaling laws for the Kondo problem, *J. Phys. C* **3** (1970), 2436–41.
[59] A. C. Hewson, *The Kondo Problem to Heavy Fermions* (Cambridge University Press, 1993).

is associated with eight possible contributions, which can be grouped in pairs. (You may find it helpful to enumerate these possibilities diagrammatically.) In particular, show that there exists a contribution

$$J_+J_-\sum_{\mathbf{k}'_{\rm s}\mathbf{k}_{\rm s}\mathbf{k}_{\rm f}}\hat{S}^-c^\dagger_{\mathbf{k}'_{\rm s}\uparrow}c_{\mathbf{k}_{\rm f}\downarrow}\frac{1}{E-\hat{H}_{22}}\hat{S}^+c^\dagger_{\mathbf{k}_{\rm f}\downarrow}c_{\mathbf{k}_{\rm s}\uparrow}|\psi_1\rangle,$$

where the wavevectors $\mathbf{k}_{\rm f}(\mathbf{k}_{\rm s})$ index states which lie within (outside) the band edge.

(b) Focusing on this contribution alone (for now), rearrange the operators to show that it takes the form

$$J_+J_-\sum_{\mathbf{k}'_{\rm s}\mathbf{k}_{\rm s}}\nu_0D(1-1/b)\hat{S}^-\hat{S}^+c^\dagger_{\mathbf{k}'_{\rm s}\uparrow}c_{\mathbf{k}_{\rm s}\uparrow}\frac{1}{E-D+\epsilon_{\mathbf{k}_{\rm s}}-\hat{H}_0},$$

where ν_0 denotes the (assumed constant) density of states at the band edge and $\hat{H}_0=\sum_{\mathbf{k}\sigma}\epsilon_{\mathbf{k}}c^\dagger_{\mathbf{k}\sigma}c_{\mathbf{k}\sigma}$ is the single-particle Hamiltonian of the band electrons. Now, measuring the energy with respect to the ground state of the non-interacting electron gas, $\hat{H}_0$ may be approximated by zero. Finally, noting that, for spin $S=1/2$, $\hat{S}^-\hat{S}^+=1/2-\hat{S}^z$, the contribution takes the form

$$J_+J_-\sum_{\mathbf{k}'_{\rm s}\mathbf{k}_{\rm s}}\nu_0D(1-1/b)(1/2-\hat{S}^z)c^\dagger_{\mathbf{k}'_{\rm s}\uparrow}c_{\mathbf{k}_{\rm s}\uparrow}\frac{1}{E-D+\epsilon_{\mathbf{k}_{\rm s}}}.$$

We leave it as an unanswered part of the exercise to confirm that the parallel contribution from the process in which a hole is created in the lower band edge leads to the expression

$$J_+J_-\sum_{\mathbf{k}'_{\rm s}\mathbf{k}_{\rm s}}\nu_0D(1-1/b)(1/2+\hat{S}^z)c_{\mathbf{k}'_{\rm s}\uparrow}c^\dagger_{\mathbf{k}_{\rm s}\uparrow}\frac{1}{E-D-\epsilon_{\mathbf{k}_{\rm s}}}.$$

(Try to use arguments based on particle/hole symmetry rather than developing a first principles analysis.) Following a similar procedure, one may confirm that the second class of spin conserving terms lead to the contributions

$$\frac{J_z^2}{4}\sum_{\mathbf{k}'_{\rm s}\mathbf{k}_{\rm s}\sigma}\nu_0D(1-1/b)c^\dagger_{\mathbf{k}'_{\rm s}\sigma}c_{\mathbf{k}_{\rm s}\sigma}\frac{1}{E-D+\epsilon_{\mathbf{k}_{\rm s}}},\quad \frac{J_z^2}{4}\sum_{\mathbf{k}'_{\rm s}\mathbf{k}_{\rm s}\sigma}\nu_0D(1-1/b)c_{\mathbf{k}'_{\rm s}\sigma}c^\dagger_{\mathbf{k}_{\rm s}\sigma}\frac{1}{E-D-\epsilon_{\mathbf{k}_{\rm s}}}.$$

This completes the analysis of contributions to the effective Hamiltonian for $|\psi_1\rangle$ which leave the electron and impurity spin unchanged. The four remaining contributions involve a spin flip. Following a similar procedure to the one outlined above, one may identify two further contributions

$$-\frac{J_zJ_+}{2}\sum_{\mathbf{k}'_{\rm s}\mathbf{k}_{\rm s}}\nu_0D(1-1/b)\hat{S}^+c^\dagger_{\mathbf{k}'_{\rm s}\downarrow}c_{\mathbf{k}_{\rm s}\uparrow}\frac{1}{E-D+\epsilon_{\mathbf{k}_{\rm s}}},$$

$$\frac{J_zJ_+}{2}\sum_{\mathbf{k}'_{\rm s}\mathbf{k}_{\rm s}}\nu_0D(1-1/b)\hat{S}^+c_{\mathbf{k}'_{\rm s}\uparrow}c^\dagger_{\mathbf{k}_{\rm s}\downarrow}\frac{1}{E-D-\epsilon_{\mathbf{k}_{\rm s}}},$$

where we have used the identity $\hat{S}^z\hat{S}^+=\hat{S}^+/2$. One may confirm that the corresponding terms with the order reversed generate an equal contribution.

When combined with terms from a spin-reversed process, altogether one finds that the components of the exchange constant become renormalized according to

$$\begin{aligned} J_\pm(b) &= J_\pm - J_z J_\pm \nu_0 D(1-1/b)\left(\frac{1}{E-D+\epsilon_{\mathbf{k}}}+\frac{1}{E-D-\epsilon_{\mathbf{k}'}}\right), \\ J_z(b) &= J_z - J_+ J_- \nu_0 D(1-1/b)\left(\frac{1}{E-D+\epsilon_{\mathbf{k}}}+\frac{1}{E-D-\epsilon_{\mathbf{k}'}}\right). \end{aligned}$$

Now, since we are interested in the renormalization of the low-energy properties, we may ignore E against D. Moreover, since the typical internal excitation energy $\epsilon_{\mathbf{k}} \ll D$, we may approximate these equations by the differential recursion relations

$$\frac{dJ_\pm}{d\ell} = 2\nu_0 J_z J_\pm, \quad \frac{dJ_z}{d\ell} = 2\nu_0 J_+ J_-,$$

where, as usual, $b = e^\ell$.

(c) Starting with these differential recursion relations, show that the scaling trajectory obeys the relation

$$J_z^2 - J_\pm^2 = \text{const.}$$

One may note that, on renormalization, the coupling constant J_z always increases. Therefore, in a ferromagnetic model $J_z < 0$ with bare coupling constants such that $|J_z| < J_\pm$, $J_\pm$ will scale to zero. Conversely, when the bare constants $|J_z| > J_\pm$, both J_z and $J_\pm$ flow to strong coupling where the perturbation theory breaks down.

For $J_z = J_\pm \equiv J > 0$, an integration of the scaling equations $dJ/d\ell = 2\nu_0 J^2$ gives

$$\frac{1}{J} - \frac{1}{J(\ell)} = 2\nu_0 \ell = 2\nu_0 \ln\left(\frac{D(\ell)}{D}\right).$$

Therefore, we may set

$$D\exp\left[-\frac{1}{\nu_0 J}\right] = D(\ell)\exp\left[-\frac{1}{\nu_0 J(\ell)}\right] \equiv T_{\mathrm{K}},$$

where T_{K} denotes the Kondo temperature.

Answer:

(a) Focusing on terms which scatter conduction electrons into the band edge, one may identify

$$\hat{H}_{21} = \sum_{\mathbf{k}_{\mathrm{s}},\mathbf{k}_{\mathrm{f}}} \left[J_z \hat{S}^z \left(c^\dagger_{\mathbf{k}_{\mathrm{f}}\uparrow} c_{\mathbf{k}_{\mathrm{s}}\uparrow} - c^\dagger_{\mathbf{k}_{\mathrm{f}}\downarrow} c_{\mathbf{k}_{\mathrm{s}}\downarrow} \right) + J_+ \hat{S}^+ c^\dagger_{\mathbf{k}_{\mathrm{f}}\downarrow} c_{\mathbf{k}_{\mathrm{s}}\uparrow} + J_- \hat{S}^- c^\dagger_{\mathbf{k}_{\mathrm{f}}\uparrow} c_{\mathbf{k}_{\mathrm{s}}\downarrow} \right],$$

where the wavevectors $\mathbf{k}_{\mathrm{f}}$ span the range of single-particle band energies $\epsilon_{\mathbf{k}}$ within the band edge while the components $\mathbf{k}_{\mathrm{s}}$ span the range of lower energies. Now, to evaluate the contribution of the term $\hat{H}_{21}(E - \hat{H}_{22})^{-1}\hat{H}_{21}$ to the effective Hamiltonian for $|\psi_1\rangle$ we must identify all processes that are closed. Since the action of the Hamiltonian must return us to the subspace in which the band edge states remain unoccupied, processes

involved in a virtual occupation of the band edge are constrained by the conservation of spin. From $\hat{H}_{12}\hat{H}_{21}$, one may identify eight allowed processes,

$$
\begin{aligned}
&(1)\ \ J_{-}\hat{S}^{-}c^{\dagger}_{\mathbf{k}'_{\mathrm{s}}\uparrow}c_{\mathbf{k}_{\mathrm{f}}\downarrow}\times J_{+}\hat{S}^{+}c^{\dagger}_{\mathbf{k}_{\mathrm{f}}\downarrow}c_{\mathbf{k}_{\mathrm{s}}\uparrow},\\
&(2)\ \ -J_{z}\hat{S}^{z}c^{\dagger}_{\mathbf{k}'_{\mathrm{s}}\downarrow}c_{\mathbf{k}_{\mathrm{f}}\downarrow}\times J_{+}\hat{S}^{+}c^{\dagger}_{\mathbf{k}_{\mathrm{f}}\downarrow}c_{\mathbf{k}_{\mathrm{s}}\uparrow},\\
&(3)\ \ J_{z}\hat{S}^{z}c^{\dagger}_{\mathbf{k}'_{\mathrm{s}}\uparrow}c_{\mathbf{k}_{\mathrm{f}}\uparrow}\times J_{-}\hat{S}^{-}c^{\dagger}_{\mathbf{k}_{\mathrm{f}}\uparrow}c_{\mathbf{k}_{\mathrm{s}}\downarrow},\\
&(4)\ \ J_{z}\hat{S}^{z}c^{\dagger}_{\mathbf{k}'_{\mathrm{s}}\uparrow}c_{\mathbf{k}_{\mathrm{f}}\uparrow}\times J_{z}\hat{S}^{z}c^{\dagger}_{\mathbf{k}_{\mathrm{f}}\uparrow}c_{\mathbf{k}_{\mathrm{s}}\uparrow},
\end{aligned}
$$

and the four counterparts related by symmetry. Of the four kinds of process, terms (2) and (3) involve a spin-flip process while terms (1) and (4) preserve the electron spin orientation. Each of these terms can be represented diagrammatically. When combined with the energy denominator, the particular contribution specified in the question corresponds to the first process (1).

(b) Since the band edge occupancy of the reference state $|\psi_1\rangle$ is zero, one can set

$$
\sum_{\mathbf{k}_{\mathrm{f}}} c^{\dagger}_{\mathbf{k}'_{\mathrm{s}}\uparrow}c_{\mathbf{k}_{\mathrm{f}}\downarrow}\frac{1}{E-\hat{H}_{22}}c^{\dagger}_{\mathbf{k}_{\mathrm{f}}\downarrow}c_{\mathbf{k}_{\mathrm{s}}\uparrow}|\psi_1\rangle = \nu_0 D(1-1/b)c^{\dagger}_{\mathbf{k}'_{\mathrm{s}}\uparrow}c_{\mathbf{k}_{\mathrm{s}}\uparrow}\frac{1}{E-D+\epsilon_{\mathbf{k}_{\mathrm{s}}}-\hat{H}_0},
$$

where $\hat{H}_0$ denotes the single-particle Hamiltonian of the band electrons, $\sum_{\mathbf{k}_{\mathrm{f}}} = \int_{D/b}^{D} d\epsilon\nu(\epsilon) \simeq \nu_0 D(1-1/b)$, and we have set $\epsilon_{\mathbf{k}_{\mathrm{f}}} \simeq D$. As a result, one obtains the required formula.

(c) Dividing the differential recursion relations, one obtains

$$
\frac{dJ_{\pm}}{dJ_z} = \frac{J_z}{J_{\pm}}.
$$

Integrating this equation, one obtains the required scaling trajectory.

9

Topology

x In this chapter we discuss low-energy theories with non-trivial forms of long-range order. We learn how to detect the presence of topologically non-trivial structures, and to understand their physical consequences. Topological terms (θ-terms, Wess–Zumino terms, and Chern–Simons terms) are introduced as contributions to the action, affecting the behavior of low-energy field theories through the topology of the underlying field configurations. Applications discussed in this chapter include persistent currents, quantum spin chains, and the quantum Hall effects.

In the preceding chapters we encountered a wide range of long-range orders, or, to put it more technically, different types of mean–fields. Reflecting the feature of (average) translational invariance, the large majority of these mean-fields turned out to be spatially homogeneous. However, there have also been a number of exceptions: under certain conditions, mean-field configurations with long-range[1] spatial textures are likely to form. One mechanism driving the formation of inhomogeneities is the perpetual competition of energy and entropy: being in conflict with the (average) translational invariance of extended systems, a spatially non-uniform mean-field is energetically costly. On the other hand, this very "disadvantage" implies a state of lowered degree of order, or higher entropy. (Remember, for example, instanton formation in the quantum double well: although energetically unfavorable, once it has been created it can occur at any "time," which brings about a huge entropic factor.) It then depends on the spatio-temporal extension of the system whether or not an entropic proliferation of mean-field textures is favorable.

A second mechanism behind the formation of inhomogeneities can be the topological structure of the order parameter field; does the mean-field accommodate solutions that simply cannot be continuously deformed back into a uniform state? The XY-model discussed at the end of the preceding chapter conveniently illustrates this principle: a vortex cannot be eliminated by any smooth deformation of the field. One might argue that this irreducibility is associated with the behavior of the core region of the vortex, where local order breaks down and the mean-field theoretical description simply does not apply (i.e. the vortex cannot be removed by manipulations of the phase field alone). However, an alternative, and more generally valid, explanation of the phenomenon is that a vortex represents a field configuration characterized by a non-vanishing winding number, i.e. an integer different from

[1] For example, sometimes a system may find it energetically favorable to develop a micro-texture optimally adjusted to the structure of the underlying Hamiltonian (a prominent example being charge density wave formation in one-dimensional systems). Yet even these structures exhibit a discrete translational invariance.

zero. But a non-vanishing integer cannot be continuously "deformed" to zero. (The vortex example also illustrates that the two principles of topology and entropic proliferation tend to cooperate. Once the energy necessary to form a mean-field of non-vanishing winding number has been invested, the system can benefit from the freedom to place the core region anywhere in the system.)

The remarks above touch upon but two of many interesting aspects of systems with topologically non-trivial order parameters. In the next section we employ a trivial example (namely a free particle on a ring) to set the stage for the discussion of further phenomena hinging on topological concepts. Specifically, we introduce the concept of a topological term, i.e. an operator which affects the low-energy behavior of a theory solely on the basis of the topology of its fields. Turning to the more systematic development of the theory, we then introduce homotopy as the key mathematical tool whereby fields can be topologically classified. This discussion provides the conceptual platform on which the rest of the chapter is based. It is followed by a discussion of different classes of topological terms (θ-terms, Wess–Zumino terms, Chern–Simons terms), along with a number of applications. It turns out that, whenever such terms are present in a theory, they tend to massively affect its long-range behavior. At the same time, topological terms are notoriously easy to overlook in "standard" schemes of distilling low-energy theories from their microscopic origins. For this reason, some emphasis is placed on purely operational aspects; i.e. tricks that prevent one from missing the presence of a topological term!

Before getting started, it is worthwhile emphasizing that we are about to plunge into a wide subject area that simply cannot be satisfactorily covered in a single chapter.[2] Consequently, our discussion is example–oriented and often regrettably superficial (with regard to both physical depth and, especially, mathematical structures). In fact, the aim of the present text is to demystify the subject of topology in field theory, to arouse the interest of readers and to motivate them to proceed to more profound and substantial discussions in the literature!

9.1 Example: particle on a ring

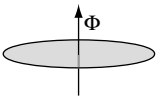

Consider the problem of a free quantum particle of charge e confined to one dimension and subject to periodic boundary conditions – a particle on a ring (see figure). To make the problem somewhat more interesting, let us assume that the ring is threaded by a magnetic flux Φ. Measuring the coordinate of the particle in terms of an angular variable $\phi \in [0, 2\pi]$, the free Hamiltonian of the system thus takes the form ($\hbar = e = c = 1$),

$$\hat{H} = \frac{1}{2}(-i\partial_\phi - A)^2, \tag{9.1}$$

[2] For an advanced text specifically targeted on topological considerations in physics, and the underlying mathematical structures, we refer to M. Nakahara, *Geometry, Topology and Physics* (IOP Publishing, 2003).

where $A = \Phi/\Phi_0$ denotes the vector potential corresponding to the magnetic field (exercise), and $\Phi_0 = hc/e = 2\pi$ represents the magnetic flux quantum. (Here, for notational simplicity, we have set the radius of the ring and the particle mass to unity.) Periodicity implies that we are working on a Hilbert space of wavefunctions ψ subject to the condition $\psi(0) = \psi(2\pi)$.

Of course, the problem defined by Eq. (9.1) is embarrassingly simple. One may readily verify that the eigenfunctions and spectrum of the Hamiltonian are given by

$$\psi_n(\phi) = \frac{1}{\sqrt{2\pi}} \exp(in\phi), \quad \epsilon_n = \frac{1}{2}\left(n - \frac{\Phi}{\Phi_0}\right)^2, \quad n \in \mathbb{Z}. \tag{9.2}$$

On the other hand, this very simplicity is somewhat deceptive;[3] we shall see in a moment that many of the concepts of topological quantum field theory find a preliminary realization in the problem above.

To explore these connections, let us reformulate the system in the language of the imaginary time path integral (cf. Problem 3.5):

$$\mathcal{Z} = \int\limits_{\phi(\beta)-\phi(0)\in 2\pi\mathbb{Z}} D\phi\, e^{-\int d\tau\, L(\phi,\dot\phi)}, \tag{9.3}$$

where the boundary condition $\phi(\beta) - \phi(0) \in 2\pi\mathbb{Z}$ expresses the fact that the phase is defined only up to integer multiples of 2π, and the Lagrangian is given by

$$L(\phi, \dot\phi) = \frac{1}{2}\dot\phi^2 - iA\dot\phi. \tag{9.4}$$

EXERCISE Verify by Legendre transformation that the Hamiltonian corresponding to this Lagrangian is given by Eq. (9.1). Obtain the spectrum Eq. (9.2) from the path integral, i.e. represent the partition function in the form $\mathcal{Z} = \sum_n \exp(-\beta\epsilon_n)$. (Hint: You may find the Hubbard–Stratonovich decoupling of the quadratic term useful.)

Suppose that we were unaware of the exact solution of the problem. Our canonical approach to controlling the integral would be to subject the theory to a saddle-point analysis. The saddle-point (alias Euler–Lagrange) equations of the action $S[\phi] = \int_0^\beta d\tau\, L(\phi, \dot\phi)$,

$$\frac{\delta S[\phi]}{\delta\phi(\tau)} = 0 \qquad \ddot\phi = 0,$$

have two interesting properties. (i) The vector potential does not enter the equations. On the other hand, we saw above that it *does* have a physical effect (the spectrum explicitly depends on A). We need to understand how these two seemingly contradictory observations can be reconciled with each other. (ii) There exists a whole family of solutions, $\phi_W(\tau) \equiv W 2\pi\tau/\beta$. The action of these configurations, $S[\phi_W]|_{A=0} = \frac{1}{2\beta}(2\pi W)^2$, varies discontinuously with W, i.e. by analogy with other cases where we found saddle-point

[3] Note that the literature is full of erroneous statements on even this simple system. The most frequent of these is that the periodic boundary conditions of the problem force the flux to be quantized in integer multiples of the flux quantum $\Phi = n\Phi_0$. This is, of course, incorrect. Even for non-integer Φ, the wavefunctions ϕ_n are perfectly periodic. The statement is probably triggered by flux-quantization in superconducting systems (a phenomenon that relies on energetic, and not topological, considerations).

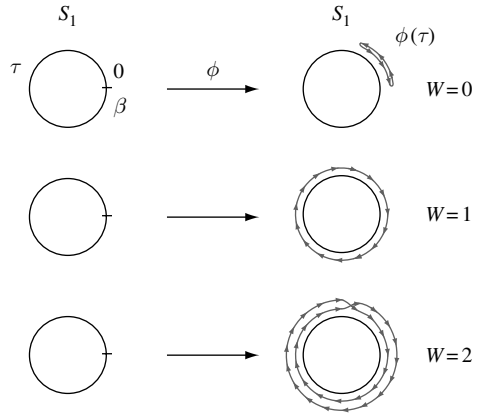

Figure 9.1 Showing mappings $\phi : S_1 \to S_1$ of different winding numbers.

configurations defined by an integer index (cf. instanton solutions in the quantum double well), we may expect the different solutions to be separated by huge energy barriers. However, the present problem is special insofar as, besides energy, there is a much more "profound" principle separating configurations of different W.

To understand this point, let us note that, mathematically, the field ϕ is a mapping

$$\begin{aligned} \phi : S_1 &\to S_1, \\ \tau &\mapsto \phi(\tau), \end{aligned}$$

from the unit circle S_1 (imaginary time with periodic boundary conditions[4]) into another circle (ϕ is a phase!). Mappings of this type can be assigned to a **winding number**, W, i.e. the number of times $\phi(\tau)$ winds around the unit circle as τ progresses from 0 to β: $\phi(\beta) - \phi(0) = 2\pi W$ (see Fig. 9.1).

Indeed, it is not possible to change W by a continuous deformation of ϕ. Since continuity is a paradigm implicit in field integration, the integration over all functions $\phi(\tau)$ can be organized as an integration over functions $\phi(\tau)$ of different winding numbers, or different **topological sectors**:

$$\mathcal{Z} = \sum_W \int\limits_{\phi(\beta)-\phi(0)=2\pi W} D\phi\, e^{-\int d\tau\, L(\phi,\dot\phi)} = \sum_W e^{2\pi i W A} \int\limits_{\phi(\beta)-\phi(0)=2\pi W} D\phi\, e^{-\frac{1}{2}\int d\tau\, \dot\phi^2}. \tag{9.5}$$

Here, we have noted that the A-dependent term in the action,

$$S_{\rm top}[\phi] \equiv iA \int_0^\beta d\tau\, \dot\phi = iA(\phi(\beta) - \phi(0)) = i2\pi W A,$$

involves only the index of the topological sector of ϕ. The representation (9.5) makes the topological aspects of the problem particularly transparent. Specifically, one may note that:

[4] Strictly speaking, imaginary time should be identified with a "circle" of circumference β. However, for our present purposes, all that matters is that the periodic boundary conditions render the interval $[0, \beta]$ isomorphic to a circle.

- ▷ The functional integral assumes the form of a sum of integrals over disjoint topological sectors.
- ▷ The contribution to the action, $S_{\rm top}$, is our first example of a topological term. (More precisely, it belongs to the class of " **-terms**.")
- ▷ Since $S_{\rm top}$ is sensitive only to the topological sector of a field contribution, it cannot affect the equations of motion. This is because these probe how the action responds to an infinitesimal variation of the field configuration, an operation that cannot change the winding number. (You may wish to ponder this point since it will be important.)
- ▷ However, the topological term does affect the outcome of the functional integration: it plays the role of a W-dependent "phase," weighting the contribution of different sectors.
- ▷ The fact that $S_{\rm top}$ knows only about the topological class of a field configuration implies that it is impervious to any changes in the metric of the base manifold of the theory (in our case, imaginary time). For example, we might decide to measure time in different units, i.e. $\tau \to \alpha\tau = \tau'$, where α is some scaling factor. This transformation leaves the topological term invariant.
- ▷ In particular, it remains form invariant under a change from imaginary to real time, $\tau \to -i\tau = t$. In both representations, $S_{\rm top}[\phi] = 2\pi i AW$ is purely imaginary. This, in fact, is a hallmark of topological terms; in both Euclidean and Minkowski space-time, their contribution to the action is always imaginary.

While formulated for the (almost trivial) example of the particle on the ring, all of these features generalize to much more involved settings. However, to discuss these generalizations in a sensible manner, we need to provide somewhat more mathematical background. This will be the subject of the next section.

INFO Owing to its simplicity, the system above frequently appears as an effective model in condensed matter physics. Examples we have encountered previously include the Josephson junction (where the presence of a condensate induces an additional cosine potential) and the physics of normal metal granules subject to strong charging (with the additional complication of dissipative damping of the ϕ-fluctuations). Here we briefly touch upon the physics of **persistent currents** as an example where the topological aspects of the problem play a particularly important role.

Consider then a ring-shaped conductor subject to a magnetic flux. According to a prediction by Byers and Yang[5] the magnetic field induces an equilibrium current

$$I(\Phi) = -\frac{\partial F(\Phi)}{\partial \Phi},$$

periodic in Φ with period Φ_0.

EXERCISE Remembering that a vector potential enters the free energy as $\sim \int d\mathbf{A} \cdot \mathbf{j}$, derive the Byers and Yang formula. Show that, at zero temperature, the persistent current flowing in a perfectly clean one-dimensional metal of non-interacting fermions assumes the form of a Φ_0-periodic sawtooth function, $I(\Phi) = \frac{2\pi v_{\rm F}}{L}[\Phi/\Phi_0]$, where $[x] = x - n$ and n is the largest integer smaller than x. (Hint: For zero temperature, the free energy of a non-interacting system of particles is equal to the sum of all single-particle energies up to the Fermi energy. Notice that the current is

[5] B. Byers and C. N. Yang, Theoretical considerations concerning quantized magnetic flux in superconducting cylinders, *Phys. Rev. Lett.* **7** (1961), 46–9.

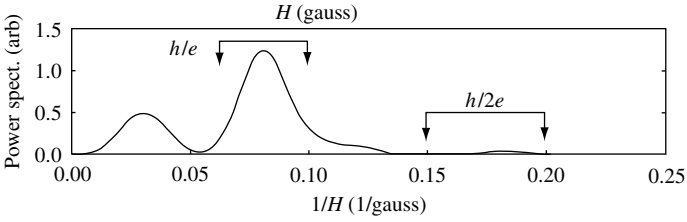

Figure 9.2 Power spectrum of the persistent current carried by a single gold loop (diameter $\mathcal{O}(1\,\mu\text{m})$, $L/\ell \sim 10$). The data shows a peak at h/e and a small satellite modulation at $h/2e$. The magnitude of the current is some two orders of magnitude larger than that predicted by theory. (Reprinted with permission from V. Chandrasekhar, R. A. Wells, M. J. Brady, *et al.* Magnetic response of a single, isolated gold loop, *Phys. Rev. Lett.* **67** (1991), 3578–81. Copyright (1991) by the American Physical Society.)

carried by the last occupied state, i.e. the currents $-\partial_\phi \epsilon_n$ carried by all levels beneath the Fermi energy cancel.)

For a long time it has been believed that this statement was largely academic since surely even a moderate concentration of impurities[6] would be sufficient to render the current undetectable. However, a simple consideration shows that this need not be the case: a gauge transformation $\psi(\phi) \to e^{iA\phi}\psi(\phi)$ removes A from the Hamiltonian while changing the boundary conditions to $\psi(0) = e^{2\pi i A}\psi(2\pi)$. In the gauge-transformed picture, the presence of the magnetic field thus amounts to a twist in the boundary conditions of the wavefunctions, and the persistent current is a measure of the sensitivity of the spectrum to this twist. Now, there is no reason to believe that a wavefunction in a disordered system should be less sensitive to its boundary conditions than that of a clean system.[7] Indeed, it is shown in Problem 9.7.1 that even rings of circumference $L \gg \ell$ may carry a sizeable persistent current.

In a series of beautiful experiments conducted in the early 1990s (see, e.g., Fig. 9.2), persistent currents in both "ballistic" ($L/\ell \sim 1$) and "dirty" ($L/\ell \sim 100$) environments were indeed observed experimentally. Frustratingly, the measured current appears to be some two orders of magnitude larger than the theories of non-interacting particles would predict. This disturbing discrepancy led to the formulation of a plethora of theories of persistent currents in interacting/disordered systems. However, to date, the discrepancy between theory and experiment remains unresolved.

[6] More precisely, it was believed that a sizeable current might only be observed if the circumference of the ring were smaller than the scattering mean free path. The artificial fabrication of rings of that quality requires semiconductor technology which was not available at the time. With regard to *molecular* rings, equilibrium currents had been predicted in the 1930s. However, the fields needed to drive currents in molecules ($\mathcal{O}(10^5\ \text{T})$) cannot be generated by the laboratory magnets currently available.

[7] What does diminish this sensitivity is mechanisms destroying the coherence of wavefunctions (thermal noise, etc.) and strong localization, i.e. a wavefunction confined to a finite portion of the ring will not sense changes in the boundary conditions. In fact, sensitivity with respect to changes in the boundary conditions has been used (largely by theorists) as a popular test for localization.

9.2 Homotopy

9.2.1 Generalities

To appreciate the generalization of the structures above to more complicated contexts, we need to introduce a few more mathematical concepts. In Chapter 1 (see page 6), we defined fields as mappings

$$\begin{aligned} \phi : M &\to T, \\ z &\mapsto \phi(z), \end{aligned}$$

from a "base manifold" M – usually $\mathbb{R}^d$ or a subset thereof – into some "target space" T. By now we have gained enough experience to determine what are the "most frequent" realizations of target spaces: indeed we have mostly been interested in the long-range behavior of Goldstone modes, i.e. long-range modes induced by a mechanism of symmetry breaking. In such cases (cf. page 257), $T = G/H$ will be a coset space obtained by dividing the symmetry group of the problem, G, by some subgroup $H \subset G$ stabilizing the mean-field around which the Goldstone modes fluctuate. Usually (but certainly not invariably) G will be one of the compact classical groups $\mathrm{U}(N)$, $\mathrm{O}(N)$, and $\mathrm{Sp}(N)$, and H some subgroup thereof.

INFO Why is the word "**topology**" so often deployed in this chapter? In the example above, the most relevant characteristic of a field configuration was its winding number, i.e. a quantity that does not change under any continuous deformation of a field, no matter how "large" is this deformation. More generally, in this chapter we are concerned with features of field theories that essentially rely on the concept of continuity, but do not involve the notion of "distance" or, more formally, of a metric.

The most general mathematical structure for which the notion of continuity can be defined is a **topological space**:[8] a mapping $\phi : X \to Y$ between two topological spaces is called **continuous** if, for any open set $U \subset Y$, the set $\phi^{-1}(U) \subset X$ is open in X. This definition is not tied to the existence of a metric.[9] This remark is not entirely academic: there are prominent physical spaces – the phase space of classical mechanics, for example – which do not possess a canonical metric but for which the notion of a continuous mapping certainly exists.

Although our discussion below does not rely on the in-depth mathematics of differential topology, the frequent use of the attribute "topological" emphasizes that what matters in this chapter is "continuity minus metric."

In fact, practical considerations also enable us to be a bit more specific as to the structure of the base manifold. Suppose our microscopic parent theory is defined on some simply connected manifold $M \subset \mathbb{R}^d$. As we shall be typically concerned with some kind of thermodynamic limit, M can be thought of as an "infinitely large" object. On the level of the low-energy theory of the system, this requires that "sensible" field configurations must

[8] As a reminder, let X be a set and $\mathcal{J} = \{Y_i \quad X | i \in I\}$ a collection of its subsets. The pair $(X, \mathcal{J})$ is called a topological space if and only if, (a) $\{\}, X \in \mathcal{J}$, (b) for $J \quad I$, $\quad_i \quad_J Y_i \in \mathcal{J}$, and, (c) for any finite subset $J \quad I$, $\quad_i \quad_J Y_i \in \mathcal{J}$. The elements of $\mathcal{J}$ are called **open subsets** of X.

[9] By contrast, in elementary mathematics courses, the continuity of a mapping ϕ is frequently defined via a metric, i.e. one relates the distance between two image points $\phi(x)$ and $\phi(y)$ to that between the arguments x and y.

approach a constant value on the boundary of M: i.e. $\phi|_{\partial M} = \text{const.}$ (lest the action become infinite).

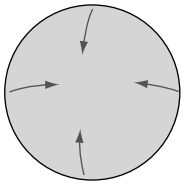

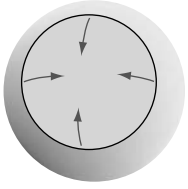

As far as our effective field theory is concerned, we may thus identify all boundary points with a single point at "infinity." Geometrically, this implies that M can be compactified to a large sphere (see the figure). However, as the radius of this sphere carries no significance (indeed, technically, it can be removed by a global rescaling of coordinates), we can, just the same, identify $M \simeq S^d$ with the d-dimensional unit sphere. The practical upshot of all of these considerations is that, in practice, we shall mostly be interested in fields

$$\begin{aligned} \phi : S^d &\to G/H, \\ z &\mapsto \phi(z), \end{aligned}$$

mapping a unit sphere into some coset space.

We now turn to the discussion of topological aspects of such mappings. By analogy to our discussion of the previous section (where we considered mappings $\phi : S^1 \to S^1 \simeq \mathrm{O}(2)$), let us consider two fields ϕ_1 and ϕ_2 as topologically equivalent if they can be continuously deformed into each other. Technically, this condition amounts to the existence of a continuous mapping (a **homotopy** in the language of mathematics)

$$\begin{aligned} \phi : S^d \times [0,1] &\to G/H, \\ (z,t) &\mapsto \hat{\phi}(z,t), \end{aligned}$$

such that $\hat{\phi}(\,.\,,0) = \phi_1$ and $\hat{\phi}_2(\,.\,,1) = \phi_2$. (Notice that $\hat{\phi}$ represents a mapping from $(d{+}1)$-dimensional space into G/H, a fact that will become important when we turn to the discussion of Wess–Zumino terms below.) We denote the **equivalence class** of all fields topologically equivalent to a given representative ϕ by $[\phi]$. (In the example discussed in the previous section, those equivalence classes would contain all fields of a given winding number.) The set of all topological equivalence classes $\{[\phi]\}$ of mappings $\phi : S^d \to T$ is called the ***d*-th homotopy group**, $\pi_d(T)$.

INFO Some readers might wonder in what sense $\pi_d(T)$ carries a group structure (rather than just being a set). To understand this point, it is convenient to deform our base manifold from a sphere to a d-dimensional unit cube $I^d = [0,1]^d$. As far as topology is concerned, this is a permissible operation, if and only if and only if we identify the boundary ∂I^d of the cube with a single point on the sphere. For example, it is convenient to choose this point to be the representative of the "infinitely large" boundary of our original base manifold. This choice requires that $\phi|_{\partial I^d} = \phi^* = \text{const.}$ be the constant field configuration approached at the "physical infinity".[10]

[10] The assumption of a unique asymptotic configuration ϕ^* is less of a restriction than it may seem; any (constant) boundary field ϕ can be converted to ϕ^* by a global transformation acting on the field (an operation that does not leave the equivalence class).

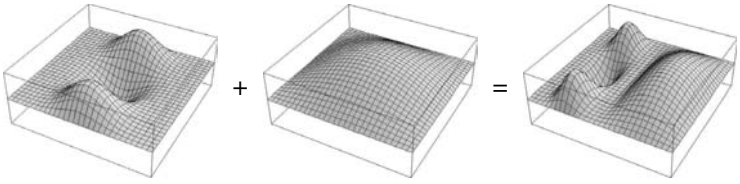

Figure 9.3 Concatenation of two two-dimensional fields into a single one.

The purpose of the cube construction is that it presents us with ways to glue two fields ϕ_1 and ϕ_2 together to form a new field $\phi_3 \equiv \phi_1 * \phi_2$ (see Fig. 9.3). For example, we might define

$$\phi_3(x_1, x_2, \ldots, x_d) = \begin{cases} \phi_1(2x_1, x_2, \ldots, x_d), & x_1 \in [0, 1/2], \\ \phi_2(2x_1 - 1, x_2, \ldots, x_d), & x_1 \in [1/2, 1]. \end{cases}$$

One might justly object that, due to its explicit coordinate dependence, this is not an acceptable mathematical definition. However, as far as our discussion of homotopy is concerned, this objection is immaterial. Indeed, we may define a group operation on $\pi_d(T)$ by

$$[\phi_1] * [\phi_2] \equiv [\phi_3]. \tag{9.6}$$

This definition is canonical in the sense that any other coordinate convention in our concatenation operation above would not leave the equivalence class of ϕ_3 (a point on which you might like to dwell). Similarly one may verify that "$*$" obeys all the criteria for a group mapping. In short, the very possibility to "concatenate" fields induces a well-defined group operation on the set of topological equivalence classes.

9.2.2 Examples of homotopies

The general group theoretical analysis of homotopies is a mathematical subject that reaches far beyond the scope of the present text. Here we restrict ourselves to the discussion of a few examples of practical interest. In simple cases, the homotopy group can be identified by common sense reasoning. For example, in the previous section we saw that mappings $S^1 \mapsto S^1$ can be classified in terms of winding numbers: $\pi_1(S^1) = \mathbb{Z}$. Similarly, it is clear that any mapping $S^1 \to S^2$ – a closed curve on the 2-sphere – is continuously contractible to a point: $\pi_1(S^2) = \emptyset$. The same applies, by definition, to any curve in a simply connected space. Prominent examples of such spaces are the higher-dimensional spheres $S^{d>1}$ and $\mathrm{SU}(N)$: $\pi_1(S^{d>1}) = \pi_1(\mathrm{SU}(N)) = \emptyset$. By contrast, the first homotopy groups of non-simply connected spaces are categorically non-trivial. For example, curves on the d-dimensional torus T^d are classified by (exercise: convince yourself of the veracity of this statement)

$$\pi_1(T^d) = \underbrace{\mathbb{Z} \times \cdots \times \mathbb{Z}}_{d}.$$

Turning to higher dimensions, it becomes more and more difficult to identify homotopy classes simply by invoking one's imagination. One of the last intuitively accessible examples is $\pi_2(S^2) = \mathbb{Z}$: maps of the 2-sphere into itself can be classified according to how often they

Table 9.1 *Homotopy groups of a number of frequently encountered mappings. A blank entry means that no general statements can be made.*

	S^1	S^2	$S^{d>2}$	T^d	SU(2)	SU(N)
$k=1$	$\mathbb{Z}$			$\underbrace{\mathbb{Z} \quad \cdots \quad \mathbb{Z}}_{d}$		
$k=2$		$\mathbb{Z}$				
$k>2$		[a]	$k<d$: $k=d$: $\mathbb{Z}$ $k>d$:		$\pi_3(\mathrm{SU}(2))=\mathbb{Z}$	

[a] But $\pi_3(S^2)=\mathbb{Z}$.

wrap around the sphere. This statement generalizes to $\pi_d(S^d)=\mathbb{Z}$, while $\pi_k(S^{d>k})=\emptyset$. Interestingly, the situation can be non-trivial for mappings $S^k \mapsto S^{d<k}$. For example, Hopf has shown that $\pi_3(S^2)=\mathbb{Z}$. For a summary of these, and a few more results, see Table 9.1.

Far from being complete, the list of examples in Table 9.1 fails to cover a number of homotopies of outstanding relevance. For example, in condensed matter physics (unlike particle physics where space and time are intertwined by relativistic covariance) we are typically confronted with a situation where time is separately compactified to a circle – imaginary time with periodic boundary conditions. On top of that, the finite-action arguments outlined above motivate a compactification of $\mathbb{R}^d \to S^d$ of real space to a d-dimensional sphere. This implies that, in quantum statistical field theory, one often encounters the base manifold $M \simeq S^1 \times S^d$ (instead of S^{d+1} as found in particle physics). Clearly the construction of homotopic groups $\pi(S^1 \times S^d, T)$ corresponding to mappings $S^1 \times S^d \to T$ is more complex than that involved in the definition of the group structures above. However, rather than dwelling on the near-endless field of homotopy theory, we now return to field theory and explore general implications of the homotopic classification scheme.[2]

9.3 -Terms

Returning to field theory considerations, let us address the question of what can be learned from the concepts introduced in the previous section. Each field $\phi : M \to T$ can be uniquely assigned to a certain homotopy class. Consequently, the functional integration defining a field theory can be organized as

$$\mathcal{Z} = \sum_{W \in G} \int D\phi_W \, e^{-S[\phi]},$$

where G is the homotopy group and $\int D\phi_W$ denotes integration over the homotopy class defined by a given element $W \in G$ – a "**topological sector**" of the theory. It may happen that the action of our field theory,

$$S[\phi] = S_0[\phi] + S_{\mathrm{top}}[\phi],$$

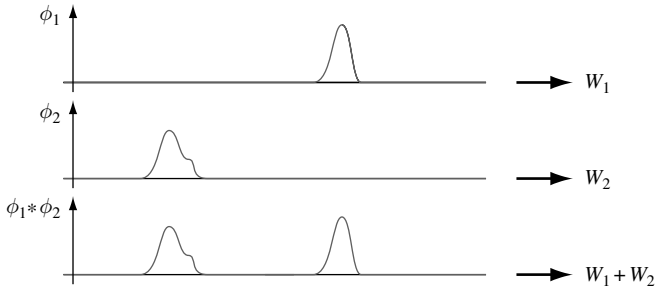

Figure 9.4 The combination of two fields with winding numbers W_1 and W_2 leads to a new field with winding number $W_1 + W_2$.

contains a **topological action** component: i.e. a contribution $S_{\rm top}[\phi] \equiv F(W)$ that depends only on the topological class of the field ϕ (which, for integer-valued W, is sometimes called the **topological charge** of the configuration). In such cases, one may pull the function $F(W)$ in front of the functional integral to write

$$\mathcal{Z} = \sum_{W \in G} e^{-F(W)} \int D\phi_W \, e^{-S_0[\phi]}. \tag{9.7}$$

In the following, we would like to understand in what way the topological action depends on the index W. This question can also be addressed by the type of reasoning ubiquitous in this chapter. Suppose we are given two fields ϕ_1 and ϕ_2 which are constant everywhere save for two well-localized regions of variation somewhere in space-time. Let us assume that the two regions where the fields vary are "infinitely" far away from each other (see Fig. 9.4). Now, suppose we had glued these fields together (e.g. by the prescription formulated in the previous section) to form a new field $\phi_1 * \phi_2$. The infinitely large separation of the two constituent fields implies that they are completely "uncorrelated," i.e. the action of the composite field $S[\phi_1 * \phi_2] = S[\phi_1] + S[\phi_2]$ is obtained simply by adding the actions of the constituents. In particular, $F(W_1 + W_2) = S_{\rm top}[\phi_1 * \phi_2] = S_{\rm top}[\phi_1] + S_{\rm top}[\phi_2] = F(W_1) + F(W_2)$, where in the first equality we have used the fact that the composite field has topological index $W_1 + W_2$.

The identity $F(W_1 + W_2) = F(W_1) + F(W_2)$ tells us that the topological action is linear in the topological index. For example, consider the simple (and at the same time most frequently encountered) case where $\pi(M, T) \simeq \mathbb{Z}$, i.e. $W_i \in \mathbb{Z}$ are just numbers. The linearity then uniquely determines the topological action,

$$F[W] = i\theta W,$$

up to a constant (which we choose to be real lest the action become ill-defined at large values of the topological charge).

These considerations tell us that the factor $\exp(-F[W]) = \exp(-i\theta W)$ weighing the different sectors assumes the form of a *phase*. Relatedly, the constant θ is usually referred to as a **topological angle**. (Since W is integer, θ is defined only mod 2π – an angular

variable.) For historical reasons[11] the topological action $S_{\rm top}$ is commonly referred to as a -**term**. Notwithstanding its simplicity, a drawback of this representation is that it explicitly relies on the decomposition of the field integral into a sum over distinct topological sectors. It would be much more desirable to work with a representation $S_{\rm top}[\phi]$ directly in terms of the field (rather than through its winding number). This would enable us to formulate the field integral more directly as $\int D\phi \exp(-S_0[\phi] - S_{\rm top}[\phi])$, without the necessity to explicitly sum over winding numbers.

Indeed, it is almost always possible to represent the topological action as an integral over a topological Lagrangian density,

$$S_{\rm top}[\phi] = \int d^d x \, \mathcal{L}_{\rm top}[\phi, \partial_\mu \phi].$$

Unfortunately, no canonical recipe for the construction of this representation exists. However, this is not as serious a problem as one might suspect. For one thing, the Lagrangian densities of the "usual suspects" of topologically non-trivial field theories are known. Conversely, it is usually straightforward to deduce whether or not a given term in the action is a θ-term in disguise. To illustrate these points, we next discuss the concept of a topological Lagrangian density on a few relevant examples.

In fact, we have already encountered the simplest representative of a θ-term in our analysis of the particle on a ring:

$$S_{\rm top}[\phi] \equiv i\theta \int_0^\beta \frac{d\tau}{2\pi} \dot{\phi} = iW\theta,$$

where $\theta = 2\pi A$ was proportional to the magnetic flux through the ring. We reiterate the key features of this term: it does not affect the equations of motion (a small distortion, or variation, of the field does not change its topological index, i.e. it leaves $S_{\rm top}$ invariant), and it is invariant under arbitrary coordinate reparameterizations $\tau \mapsto s = s(\tau)$. As a less simple example illustrating these features we now discuss a two-dimensional field theory.

9.3.1 A case study: $\pi_2(S^2)$

Consider a field theory in a two-dimensional compactified space with the two-sphere as a target manifold. Important examples falling into this category include the theory of quantum spin chains (see Section 9.3.3), the two-dimensional classical Heisenberg model, and the field theory of the integer quantum Hall effect (see Section 9.3.4). Technically, the fields of this theory are mappings

$$\begin{aligned} \mathbf{n} : S^2 &\to S^2, \\ \mathbf{x} &\mapsto \mathbf{n}(\mathbf{x}), \quad |\mathbf{n}| = 1, \end{aligned}$$

[11] One of the first major applications where terms of this type played a dominant role was 'tHooft's analysis of SU(2) gauge field instantons in $(3+1)$-dimensional compactified space-time. (G. 'tHooft, Magnetic monopoles in unified gauge theories, *Nucl. Phys.* **B79** (1974), 276–84.) There he systematically labeled the topological angle by θ; hence the name θ-term.

and the relevant homotopy group is $\pi_2(S^2) \simeq \mathbb{Z}$. Let us suppose that the topological action of this field theory is given by

$$S_{\rm top}[\mathbf{n}] = \frac{i\theta}{4\pi} \int dx_1\, dx_2\, \mathbf{n} \cdot (\partial_1 \mathbf{n} \times \partial_2 \mathbf{n}). \tag{9.8}$$

How does one verify an assertion of this type? A first condition for $S_{\rm top}$ to be of topological nature is an insensitivity to small variations of the field $\mathbf{n}$. Suppose then we vary $\mathbf{n}$ by a small amount, i.e. $\mathbf{n}(\mathbf{x}) \to \mathbf{n}(\mathbf{x}) + \epsilon^a(\mathbf{x}) R^a \mathbf{n}$, where the functions $\epsilon^a, a = 1, 2, 3$, are infinitesimal and R^a are the generators of rotations around the three coordinate axes. By integrating a few times by parts, it is straightforward to show that the variation of $S_{\rm top}$ assumes the form

$$\delta S_{\rm top}[\mathbf{n}] = \frac{3i\theta}{4\pi} \int dx_1\, dx_2\, \epsilon^a R^a \mathbf{n} \cdot (\partial_1 \mathbf{n} \times \partial_2 \mathbf{n}).$$

However, $R^a \mathbf{n}$ is perpendicular to $\mathbf{n}$ while (exercise) $(\partial_1 \mathbf{n} \times \partial_2 \mathbf{n})$ lies parallel, i.e. $\delta S_{\rm top} = 0$. (As a corollary we note that $S_{\rm top}$ will not affect the equations of motion.)

The invariance of $S_{\rm top}$ implies that we can evaluate its value on any convenient test field configuration $\mathbf{n}_0$; each field that can be reached by continuous deformation of $\mathbf{n}_0$ will have the same topological action. Consider, for example, the family of field configurations

$$\begin{aligned} \mathbf{n}^{(W)} :\ \mathbb{R}^2 &\to S^2, \\ (x_1, x_2) &\mapsto \left(\phi = W \tan^{-1}\left(\frac{x_2}{x_1}\right), \theta = 2 \tan^{-1}\left(\frac{a^2}{x_1^2 + x_2^2}\right)\right), \end{aligned}$$

where we used polar coordinates to parameterize $\mathbf{n}^{(W)}(\theta, \phi)$. For historical reasons,[12] these field configurations are commonly referred to as **skyrmions**. (Notice that the suffix "-on" indicates that we are dealing with highly stable [particle-like] excitations.)

A coarse visualization of the simplest skyrmion configuration, $\mathbf{n}^{(1)}$, is shown in the figure: a texture of unit vectors varying on a scale set by the parameter a. Skyrmions of higher winding numbers, $\mathbf{n}^{(W>1)}$, are difficult to visualize. However, it is straightforward to verify (by substitution of the unit vector $\mathbf{n}^{(W)}(\phi, \theta)$ into the integral (9.8)) that their topological charge is given by W. Equivalently, the topological action reads $S_{\rm top}[\phi^{(W)}] = i\theta W$.

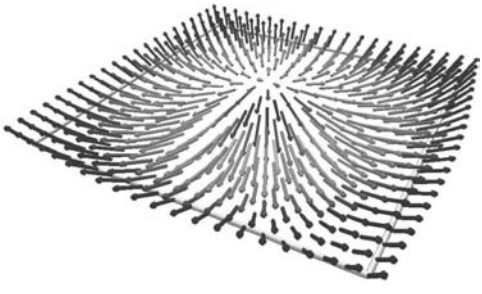

EXERCISE Verify these statements. Show that the topological charge is insensitive to coordinate changes on both the target and the base manifold. Try to invent other simple field configurations of non-vanishing topological charge.

INFO A word on **semantics**: depending on the context, topologically non-trivial field configurations are described as **solitons, instantons, skyrmions**, etc. While there seem to be no

[12] See T. H. R. Skyrme, A nonlinear field theory, *Proc. Roy. Soc. London A* **260** (1961), 127-38 where these excitations appeared in the context of an effective model of nuclear matter.

discernible systematics in this scheme, a rule of thumb is that topological excitations in dynamical quantum theories (i.e. theories where the base manifold represents space-time) are called "instantons." By contrast, "solitons" are topological solutions of classical equations of motions. However, this rule is also sometimes broken.

The ubiquitous presence of the suffix "-on" reflects a widespread tendency in physics to associate excitations that are protected from ordinary decay mechanisms (presently, by the presence of topological indices) with different kinds of "particles".

9.3.2 Functional integration and topological textures: generalities

How can our present understanding of topologically non-trival field configurations be extended to a working scheme of field integration? As we saw above, the different topological sectors of the theory essentially lead their "own lives." It is then an obvious idea to try to carry out the "canonical program" of field integration (analysis of mean-field configurations $\rightsquigarrow$ integration over fluctuations) in each sector separately. Our first step would thus be to seek solutions of the equation

$$\left.\frac{\delta S[\phi]}{\delta\phi}\right|_{\phi\in\phi_W} = \left.\frac{\delta S_0[\phi]}{\delta\phi}\right|_{\phi\in\phi_W} = 0. \tag{9.9}$$

(The later equality expresses the fact that the topological action does not change under field variation.) In our prototypical example of Section 9.1, the solutions of these equations were readily identified as $\phi_W(\tau) = 2\pi W\tau/\beta$. However, in general, finding solutions of Eq. (9.9) for $W \neq 0$ is a task more complicated than the analysis of the $W = 0$ mean-field. (This is because field configurations with $W \neq 0$ generally exhibit some non-trivial spatial variations, i.e. we cannot rely on the standard homogeneity assumptions.)

INFO However, there exists an elegant trick whereby the **identification of topologically non-trivial mean-field configurations** can sometimes be drastically simplified. Consider the expression

$$\begin{aligned} 0 \qquad & \frac{1}{2}\int d^2x\,(\partial_\mu \mathbf{n} + \epsilon_\mu\ \mathbf{n}\times\partial\ \mathbf{n})\cdot(\partial_\mu \mathbf{n} + \epsilon_\mu\ '\mathbf{n}\times\partial\ '\mathbf{n}) \\ = \quad & \int d^2x\,(\partial_\mu \mathbf{n}\cdot\partial_\mu \mathbf{n} + \epsilon_\mu\ \mathbf{n}\cdot(\partial_\mu \mathbf{n}\times\partial\ \mathbf{n}))\,, \end{aligned}$$

where the inequality simply expresses the fact that we are integrating a positive definite quantity. Now, we know that the second term in the latter integral yields just -8π times the topological charge, i.e.

$$W \qquad \frac{1}{8\pi}\int d^2x\,\partial_\mu \mathbf{n}\cdot\partial_\mu \mathbf{n} = S_0[\phi].$$

We thus conclude that W represents a lower bound for the action of field configurations of topological charge W. This limit is reached for extremal configurations

$$\partial_\mu \mathbf{n} + \epsilon_\mu\ \mathbf{n}\times\partial\ \mathbf{n} = 0, \tag{9.10}$$

on which the integral above vanishes. Since any continuous variation of these fields leads to a non-vanishing integral, they must be stationary field configurations. We have thus managed

to reduce the identification of stationary phase configurations to the solution of the *first*-order differential equation (9.10).

In passing we note that Eq. (9.10) is most elegantly solved by introducing complex coordinates $z \equiv x_1 + ix_2$ and representing $\mathbf{n}$ in terms of a stereographic projection:

$$n_1 + in_2 = \frac{2w}{1+|w|^2}, \quad n_3 = \frac{1-|w|^2}{1+|w|^2},$$

where $w \in \mathbb{C}$. Straightforward substitution then shows that Eq. (9.10) assumes the form $\partial_{\bar{z}} w(z) = 0$ (exercise). This means that any meromorphic function

$$w = \prod_{i=1}^{W} \frac{z-a_i}{z-b_i},$$

solves the equation. To understand the identification of the order of the product, W, with the topological charge, notice that the inverse $z(w)$ will be a W-valued function, i.e. W indeed measures the number of times the sphere (w-space) is covered by the compactified plane (z-space). (Exercise: Verify that, up to a different choice of the coordinate axes, the skyrmion $\phi^{(1)}$ above is one of these extremal configurations.)

As an attractive by-product, the scheme above automatically yields the action $S_0[\bar{\phi}] = W$ of the extremal configurations $\bar{\phi}$. A slightly modified variant of the same trick helps to find other topological mean-field configurations; e.g. the famous SU(2) instantons central to the analysis of θ-vacua in QCD (for a pedagogical discussion of this subject see, e.g. Ryder.[13]).

At this stage, the further course of action seems to be clear. We ought to compute the action of the mean-field solutions of a given topological index, and then integrate over fluctuations. In practice, however, things turn out to be not quite as straightforward. To understand what is going on, let us revisit a problem we discussed back in Chapter 3, namely the motion of a quantum particle in a steep periodic potential. The topological nature of that system follows from the fact that, (i) by virtue of the periodicity of the potential, $V(x) = V(x+a)$, we can identify the configuration space with a ring of periodicity a and, (ii) with exponentially large probability, at times $t \to \pm\infty$ the quantum particle will rest in any one of the minima

[13] L. H. Ryder, *Quantum Field Theory* (Cambridge University Press, 1996).

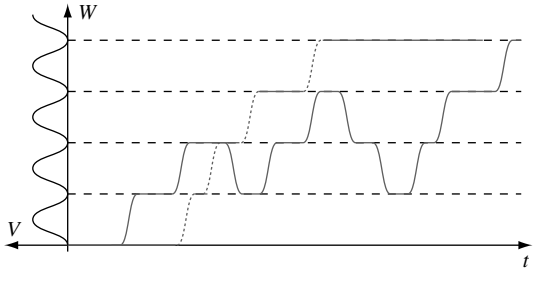

Figure 9.5 Snapshot of two typical field configurations of the U(1) model. Dashed: minimal field configuration with $W = 4$ instantons. Solid: field with 7 instantons and $7 - W = 3$ anti-instantons.

of the potential (see Fig. 9.5). This latter fact implies that the two points $t = \pm\infty$ forming the boundary of the base manifold can be identified (in analogy to our discussion of higher-dimensional compactification above). Within the path integral approach to the problem, we are thus integrating over mappings $S^1 \to S^1$; the spatial distance (in units of a) our particle traverses in the course of time translates to the winding number of the mappings.

This number is a topological invariant, i.e. it does not change under any continuous deformation of the path. However, what may well happen is that, on its way from the minimum at $x = 0$ to another one at $x = Wa$, the particle includes one or several detours (see Fig. 9.5). As is evident from the figure, any of those non-direct paths *can* be continuously deformed to a straight tunneling path $0 \to a \to 2a \to \cdots \to Wa$. To connect to the notions of topology, suppose that the individual tunneling events forming a path of total winding number W are widely separated in time. By analogy with our discussion in Section 9.2, we can then imagine the full path as the result of the superposition of $V \geq W$ single-instanton ($W = 1$) field configurations and $V-W$ anti-instantons ($W = -1$). The homotopic equivalence of a path with a non-vanishing number of anti-instantons to the direct path (no anti-instantons) amounts to the fact that an instanton and an anti-instanton annihilate, $1 + (-1) \to 0$, when their temporal coordinates approach each other; only the difference between the numbers of instantons and anti-instantons is a topological invariant.

For steep potentials, instantons and anti-instantons are widely separated in time, implying that correlations/annihilations are vanishingly improbable. For obvious reasons, such configurations are referred to as **dilute instanton gases**. However, for sufficiently shallow potentials, instantons begin to proliferate in number. The increase in the instanton "density" gives rise to correlation effects or "interactions" between the instantons. (Technically, the interaction of two nearby tunneling/anti-tunneling events no longer is just the sum of the two partial actions, but contains correlation terms.) Of course, these **instanton liquids** are much more difficult to describe than dilute instanton gases.

Clearly, these phenomena are not limited to the one-dimensional example above. For general $\pi(M, T) \simeq \mathbb{Z}$, instantons exist as "particles" ($W > 0$) and "anti-particles" ($W < 0$). Only the difference in the number of particles and anti-particles is a topological quantum number. The general plan of an instanton analysis will, therefore, typically take the following form:

- ▷ Solve mean-field equations – find the instantons/anti-instantons.
- ▷ Analyze the dilute instanton phase.
- ▷ Identify correlations between instantons and explore when the diluteness assumption breaks down.
- ▷ If possible, try to understand the physics of the correlated instanton system.

In Chapter 3, we exemplified this program on the U(1) example (albeit not emphasizing the underlying topology). A pedagogical discussion of the generalization to the S^2-instanton gas (skyrmions/anti-skyrmions) can be found in the text by Polyakov.[14] However, at this stage, we will not pursue further the complexities of the dense instanton systems. Rather

[14] A. M. Polyakov, *Gauge Fields and Strings* (Harwood, 1987).

we shall turn to the – long overdue – discussion of examples where S^2-instanton formation plays an important physical role.

9.3.3 Spin chains

In Section 2.2 we applied the Holstein–Primakoff transformation to explore the dispersion relation $\epsilon(\mathbf{p})$ of excitations in ferro- and antiferromagnetic spin systems. Within this approach we found that, for antiferromagnetic systems, the dynamics of long-wavelength spin-wave excitations is characterized by a linear dispersion relation

$$\epsilon(\mathbf{p}) \sim v_{\rm s}|\mathbf{p}|, \tag{9.11}$$

where $v_{\rm s}$ is the spin wave velocity. However, let us recall that this result was based on a crude semi-classical expansion valid only to leading order in $1/S$, where S is the magnitude of the spins. Yet, what happens when a $1/S$ expansion is seemingly unjustified? Do interaction processes between the elementary spin-waves significantly renormalize the observable excitation spectrum? At any rate, we are dealing with a "strong coupling problem" for which no obvious approximation scheme is in sight.

In situations like this it is usually a good idea to identify an exactly solvable reference system where the physics is known. In the present context, the $S = 1/2$ **antiferromagnetic spin chain** plays this role. Indeed, we have seen (in Problem 2.4[15]) that, at small wavevectors, the $S = 1/2$ antiferromagnet is equivalently described as a system of one-dimensional chiral fermions. We know that the excitations of the fermions (charge density waves) have a linear dispersion, i.e. they obey a one-dimensional variant of Eq. (9.11). This seems quite reassuring: both, $S \gg 1$ and the exactly solvable point $S = 1/2$ are characterized by a linear dispersion. It is then, perhaps, not too bold to speculate that, in the analytically inaccessible intermediate regime $S \simeq 1$, interactions will also not corrupt the linear dispersion of antiferromagnetic spin chains.

Surprisingly, though, this expectation does not conform with experimental observation. Neutron scattering experiments on one-dimensional spin 1/2 antiferromagnets have indeed shown that, in the vicinity of the Néel ordering wavevector $q = \pi/a$, the dispersion is linear. However, spin $S = 1$ chains show altogether different behavior! It turns out that these systems do not support low-energy magnetic excitations at all (see Fig. 9.6). More generally, the cumulative experimental finding is that antiferromagnetic chains of half-integer spin do support a relativistic low-energy excitation, while chains of integer spins are gapped.

[15] To be precise, in Problem 2.4 we applied a Jordan–Wigner transformation to represent the $S = 1/2$ chain in terms of a half-filled system of one-dimensional fermions. The fermion system contained an interaction term whose strength was determined by the anisotropy Δ of the magnetic correlations. In the XY-limit, $\Delta = 0$ (vanishing coupling of the z-components), the fermion system becomes free. (That is, both the fermion system and its equivalent partner, the spin system, support long-range excitations.) For general Δ, bosonization techniques can be applied to map the problem onto a two-dimensional sine–Gordon model. This model falls into the universality class of the two-dimensional (!) classical XY-model (cf. discussion on page 469). Translated back to the context of the spin chain, the RG flow behavior of the latter implies that, for values of the anisotropy all the way up to the Heisenberg limit $\Delta = 1$, the system remains in a gapless phase (the interaction stays irrelevant). For further discussion of the spin 1/2 chain we refer to A. O. Gogolin, A. A. Nersesyan, and A. M. Tsvelik, *Bosonization and Strongly Correlated Systems* (Cambridge University Press, 1998).

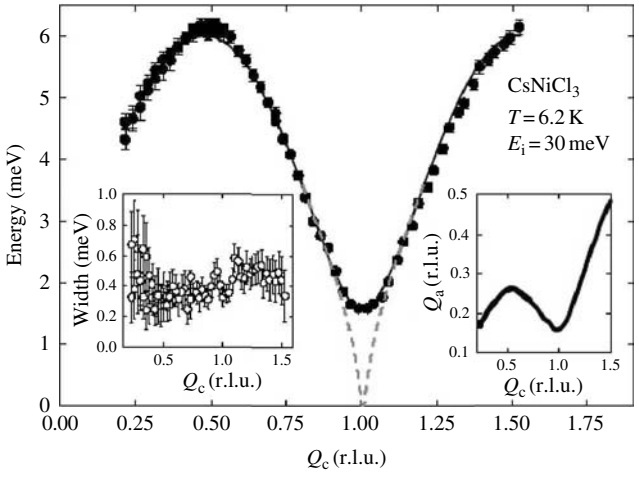

Figure 9.6 Neutron scattering data from the $S = 1$ compound $CsNiCl_3$. The main panel shows the excitation energy for wavevectors close to the antiferromagnetic nesting vector $Q_c = \pi$. In contrast to half integer spin systems, the spectrum is gapped. (Reprinted with permission from M. Kenzelmann, R. A. Cowley, W. J. L Buyers, *et al.*, Properties of Haldane excitations and multiparticle states in the antiferromagnetic spin-1 chain compound $CsNiCl_3$, *Phys. Rev. B* **66** (2002), 24407. Copyright (2002) by The American Physical Society.)

As a rule, physical phenomena depending on the parity of an integer quantum number (presently, $2S$ being even or odd) tend to be of topological origin. To understand why topology appears in the present context recall that, classically, the configuration space of a spin is a sphere (of radius S). The spin configuration of a spin chain is thus described by some mapping from $(1+1)$-dimensional space-time into the sphere. Compactification of space-time then leads to the mappings $S^2 \to S^2$ discussed above.

To substantiate this picture, let us start out from the quantum partition function of an isolated spin derived in Section 3.3:

$$\mathcal{Z}^{(1)} = \int D\mathbf{n}\, e^{iS\int_0^\beta d\tau\, \mathcal{L}_{\rm WZ}(\mathbf{n},\partial_\tau\mathbf{n})}, \quad \mathcal{L}_{\rm WZ}(\mathbf{n},\partial_\tau\mathbf{n}) = (1-\cos(\theta))\dot{\phi},$$

where the integration extends over all paths $\mathbf{n} : \tau \mapsto \mathbf{n}(\tau)$ and (ϕ, θ) are two angles parameterizing the unit vector $\mathbf{n}$.

INFO In the light of the discussion above, the action of this integral looks rather suspicious: it is purely imaginary and remains invariant under reparameterizations of time $\tau \mapsto \tau'(\tau)$ – both hallmarks of topological terms. Indeed, $\mathcal{L}_{\rm WZ}[\mathbf{n}, \partial_\tau\mathbf{n}]$ is the Lagrangian of a "**Wess-Zumino action**".[16] For the topological character of these actions, and their connection to the θ-terms discussed presently, see the next section.

[16] Notice that, from the point of view of a purist, the notation $\mathcal{L}_{\rm WZ}(\mathbf{n}, \partial_\tau\mathbf{n})$ is problematic. As discussed earlier, the Wess–Zumino action does not admit a globally coordinate invariant representation in terms of $\mathbf{n}$ and its derivatives. To formulate one, we have to deploy an explicit coordinate representation. For the underlying reason, see the next section.

The generalization of the $(0+1)$-dimensional path integral to a $(1+1)$-dimensional field integral of the spin chain is a good exercise in guessing effective actions. As a warm-up exercise, we begin our discussion with the **ferromagnetic spin chain**. The interaction between the neighboring spins is mediated by an operator

$$-J\hat{\mathbf{S}}_i \cdot \hat{\mathbf{S}}_{i+1} \longrightarrow -JS^2 \mathbf{n}_i \cdot \mathbf{n}_{i+1} \longrightarrow \frac{JS}{2}(\mathbf{n}_i - \mathbf{n}_{i+1})^2, \tag{9.12}$$

where J is the positive exchange constant, i labels the sites on the chain, and the first arrow maps to the representation $\hat{\mathbf{S}} \to S\mathbf{n}$ of the spin operators in the field integral language. In the second term we have noted that, up to irrelevant constants ($\mathbf{n}^2 = 1$), the interaction can be represented as a "discrete derivative." Adding to this interaction term the Wess–Zumino terms of the individual spins, we are led to the partition function $\mathcal{Z} = \int D\mathbf{n} \exp(-S[\mathbf{n}])$, with the effective action

$$S[\mathbf{n}] = \int d\tau \sum_i \left[\frac{JS^2}{2}(\mathbf{n}_i - \mathbf{n}_{i+1})^2 + iS\mathcal{L}_{\mathrm{WZ}}(\mathbf{n}_i, \partial_\tau \mathbf{n}_i) \right]. \tag{9.13}$$

Anticipating that, for a ferromagnetic system, the configuration $\{\mathbf{n}_i\}$ will typically be smooth, we may then take the continuum limit to arrive at the action

$$S_{\mathrm{ferro}}[\mathbf{n}] = a^{-1} \int d\tau\, dx \left[\frac{JS^2 a^2}{2}(\partial \mathbf{n})^2 + iS\mathcal{L}_{\mathrm{WZ}}(\mathbf{n}, \partial_\tau \mathbf{n}) \right], \tag{9.14}$$

where a denotes the lattice spacing. The action (9.14) does not contain a θ-term.

EXERCISE Derive the equations of motion of this action. Show that the mean-field dispersion of the ferromagnetic chain, $\omega \sim q^2$, is quadratic. (Hint: Recapitulate what we know about the variation of the Wess–Zumino term from Section 3.3.)

We now turn to the more interesting case of the **antiferromagnetic spin chain**. The exchange coupling is now negative, implying that the neighboring spins prefer antiparallel alignment. We thus start out from a configurational *ansatz*

$$\mathbf{n}_i = (-)^i \mathbf{n}'_i,$$

where $\mathbf{n}'$ is the antiferromagnetic order parameter field. To derive the antiferromagnetic analog of the continuum action (9.14), we ought to substitute this *ansatz* into Eq. (9.13) and perform a gradient expansion. However, rather than going through the technical details of this expansion (see e.g., Jackson[17]), we will here fix the structure of the action by qualitative reasoning. For one thing, we know that the system supports a wave-like mode. The minimal action consistent with the global rotational invariance of the model ($\mathbf{n} \to R\mathbf{n}$, where $R \in \mathrm{O}(3)$) and the presence of a wave-like mode is given by

$$S_0[\mathbf{n}] = \frac{S}{4} \int d\tau\, dx \left(\frac{1}{v_{\mathrm{s}}}(\partial_x \mathbf{n})^2 + v_{\mathrm{s}}(\partial_\tau \mathbf{n})^2 \right),$$

[17] J. D. Jackson, *Classical Electrodynamics* (Wiley, 1975).

where we have relabeled $\mathbf{n}' \to \mathbf{n}$ for notational simplicity and $v_s = 2aJS$ is the spin-wave velocity. Of course, the detailed structure of the coupling constants is beyond the scope of our present plausibility argument. However, what we *can* say is that the overall coupling constant must be proportional to a positive power of S. This is because, for large S, "interactions" between the elementary spin waves ought to become weak.

EXERCISE To show this, expand $\mathbf{n}$ around any preferential axis (e.g. by setting $\mathbf{n}_{1,2} \equiv r_{1,2}$, $\mathbf{n}_3 \equiv (1 - r_1^2 - r_2^2)^{1/2}$, $r_1^2 + r_2^2 \in [0,1]$). Expand the action in powers of r_i and show that, for large S, the contribution of anharmonic terms (spin-wave "interactions") becomes small.

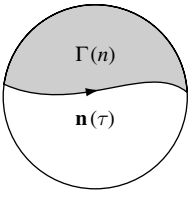

Rescaling variables, $\tau \to v_s^{-1/2}\tau \equiv x_0$, $x \to v_s^{1/2}x \equiv x_1$,

$$S_0[\mathbf{n}] \to \frac{1}{\lambda}\int d^2x\, \partial_{x_\mu}\mathbf{n}\cdot\partial_{x_\mu}\mathbf{n}, \quad \lambda = 4/S,$$

assumes the form of the action of the O(3) **nonlinear σ-model**.[18] However, as argued above, we expect the full action of the problem to contain not only a dynamical piece S_0 but also a θ-term. How can this be made plausible from the prototypical action (9.13)? We expect that, somehow, the θ-term must appear as a descendant of the Wess–Zumino action. In the ferromagnetic case, the Wess–Zumino actions of the spins basically added to give a contribution that was not a θ-term. However, in the present case, we are dealing with a staggered spin configuration that leaves room for more interesting things to happen. Let us first recall the interpretation of $iS\int_0^\tau d\mathcal{L}_{\rm WZ}(\mathbf{n}, \partial_\tau\mathbf{n})$ as the oriented area $\Gamma[\mathbf{n}]$ on the sphere swept out by the curve $\mathbf{n}(\tau)$ (see figure).

By an elementary geometrical consideration, $\Gamma[-\mathbf{n}] = 4\pi - \Gamma[\mathbf{n}] = -\Gamma[\mathbf{n}] \bmod 4\pi$. This implies that the continuum version of the Wess–Zumino action

$$S_{\rm top}[\mathbf{n}] = iS\sum_i (-)^i \int_0^\beta d\tau\, \mathcal{L}_{\rm WZ}(\mathbf{n}_i, \partial_\tau\mathbf{n}_i) = iS\sum_i (-)^i \Gamma[\mathbf{n}_i],$$

evaluated on a staggered configuration $(-)^i\mathbf{n}_i$ must contain a spatial derivative besides the temporal derivative inherent in $\mathcal{L}_{\rm WZ}$ (since for $\mathbf{n}_i = $ const. the factor $(-)^i$ would lead to a global cancellation). Indeed, the Wess–Zumino actions of two neighboring configurations $\mathbf{n}_{i+1}$ and $\mathbf{n}_i$ evaluate, respectively, to the areas bounded by the curves $\Gamma[\mathbf{n}_{i+1}]$ and $\Gamma[\mathbf{n}_i]$. For $|\mathbf{n}_{i+1} - \mathbf{n}_i|$ small, the area difference can be approximated by

$$\Gamma[\mathbf{n}_{i+1}] - \Gamma[\mathbf{n}_i] \simeq \int_0^\beta d\tau\, \mathbf{n}_i\cdot((\mathbf{n}_{i+1} - \mathbf{n}_i)\times\partial_\tau\mathbf{n}).$$

Summing over i and taking the continuum limit, we obtain (see figure)

$$S_{\rm top}[\mathbf{n}] = i\theta\int d\tau\, dx\, \mathbf{n}\cdot(\partial_x\mathbf{n}\times\partial_\tau\mathbf{n}), \quad \theta = \frac{S}{2}, \tag{9.15}$$

[18] Although the action above is commonly referred to as the action of the O(3)-model, a better terminology would be the (O(3)/O(2))-model. Indeed, the degrees of freedom of the theory span the 2-sphere $S^2 \simeq$ O(3)/O(2). Although the nonlinear σ-model on the sphere has to be distinguished from the σ-model on O(3) (cf. the discussion of Section 8.5 and Problem 8.8.3) we will follow the widespread convention to describe the model above as the O(3)-model.

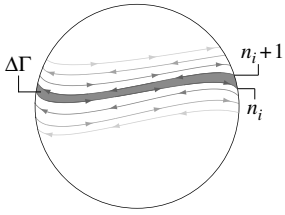

which we identify as our earlier representation of the θ-term. (Notice that the integral $\int d\tau\, dx$ really represents an integral over the sphere. This is because we agreed that, for $|\tau| \to \infty$ and/or $|x| \to \infty$, all trajectories approach a common reference point on S^2.)

Summarizing, we have obtained $S_0[\mathbf{n}] + S_{\rm top}[\mathbf{n}]$ as the effective action of the antiferromagnet. In Problem 8.8.3, we have seen that at large length scales a two-dimensional system described by the action $S_0[\mathbf{n}]$ flows into a disordered phase. But how will the presence of the topological term modify this behavior? To get some idea of what might happen, let us reformulate the partition function as a sum over disjoint topological sectors,

$$\mathcal{Z} = \sum_{W\in\mathbb{Z}} \int D\mathbf{n}_W\, e^{2\pi i S W} e^{-S_0[\mathbf{n}_W]}, \tag{9.16}$$

where $\mathbf{n}_W$ denotes field configurations of winding number W. Equation (9.16) provides a preliminary explanation for the observation of the half-integer/integer spin staggering phenomena mentioned above. For integer spin, $\exp(2\pi i S W) = 1$ and the topological term is not operational. By contrast, for half-integer spin, $\exp(2\pi i S W) = (-)^W$, i.e. consecutive topological sectors are weighted by alternating signs. Notice that the topological term is susceptible to the parity of $2S$ and nothing else. To understand heuristically the consequences of this feature we emphasize that, at the mean-field level (this stabilized by large S), the partition function is governed by a mode with linear dispersion. Quantum fluctuations around this configuration will alter its dispersion, potentially by the creation of an excitation gap. Now, in the integer case, these fluctuations additively ($\exp(-S_0) \in \mathbb{R}^+$) contribute to the partition function. For small S they may (and in fact do) totally mask the mean-field sector. By contrast, for half-integer spin, fluctuations contribute with alternating sign, thereby partially canceling each other; the mean-field sector has a better chance to survive. These observations form the basis of **Haldane's conjecture**,[19] according to which spin chains of integer S will flow into a disordered phase with no long-range excitations whilst, in chains of half integer spin, they remain in a gapless phase.

Reassuringly, the predictions born out of these rather abstract constructions are in full agreement with neutron scattering measurements of the dispersion of various quasi-one-dimensional magnets. But why should one, nonetheless, use the attribute "conjecture" (as opposed to, say, "theory")? The scenario above is based on a number of shaky suppositions. Most seriously, it is tacitly assumed that the σ-model will seamlessly scale into the strong coupling region without changing its form. (That the model remains form invariant under renormalization is a perturbative prediction which can be trusted only for $\lambda \ll 1$.) Indeed, a subsequent analysis by Affleck and Haldane[20] has shown that, *en route* to the strong coupling regime, much more drastic things happen. Specifically, the appropriate critical

[19] F. D.M. Haldane, Nonlinear field theory of large-spin Heisenberg antiferromagnets: semiclassically quantized solitons of the one-dimensional easy-axis Néel state, *Phys. Rev. Lett.* **50** (1983), 1153–6.

[20] I. Affleck and F. D. M. Haldane, Critical theory of quantum spin chains, *Phys. Rev. B* **36** (1987), 5291–300.

theory describing the behavior of half-integer chains at large length scales turns out to be not the O(3) nonlinear σ-model but rather a field theory with SU(2)-valued degrees of freedom. We discuss this theory in Section 9.4.4 after the concept of Wess–Zumino terms has been introduced.

Introducing another group of phenomena where mechanisms of topology are crucial, we now turn to a discussion of the quantum Hall effects (QHE). The QHE belongs here because (a) it is surely a compulsory part of any modern treatise on condensed matter phenomena, and (b) it is, in many respects, a topological phenomenon. On the other hand, our discussion will lead us somewhat astray inasmuch as it involves, necessarily, a review of experimental observation, the elementary quantum mechanics of electrons in the presence of strong magnetic fields, etc. Readers wishing to maintain a more streamlined discussion of topology in condensed matter field theory are therefore invited to skip the next section, and turn directly to the section on Wess–Zumino terms below.

9.3.4 Integer quantum Hall effect

In fact, it is quite misleading to talk about *the* quantum Hall effect: at the least, one should speak of the quantum Hall effect"s" – a spectrum of quite different phenomena, almost unparalleled in diversity and conceptual depth. To get a preliminary impression of the phenomena, observe the raw experimental data displayed in Fig. 9.7. The figure shows the Hall resistance $\rho_{xy} \equiv R_{\rm H}$ and the longitudinal resistance ρ_{xx} (the ragged curve in the bottom of the plot) of a two-dimensional electron gas as functions of a strong perpendicular magnetic field. Instead of a dull linearly increasing curve (the classical Hall resistance ρ_{xy}) or an approximate constant (the Drude resistance ρ_{xx}) one finds a profile that could hardly be more structured.

On close inspection of the data, one may notice a number of characteristic sub-structures: (1) Shubnikov–de Haas oscillations at small magnetic fields, followed by (2) the characteristic **quantum Hall plateaus** $\rho_{xy} = \nu^{-1} h/e^2$ at rational "filling fractions" (see below) $\nu \in \mathbb{Q}$ to which the effect owes its name. These are accompanied (3) by a dramatic **drop in the longitudinal resistance** ρ_{xx}. The functional form of the increase (4) from one plateau to the next is described by certain well-defined power laws as a function of temperature, indicative of a second-order phase transition – the zero-temperature **quantum Hall transition**. Barely visible, (5) a second generation of Shubnikov–de Haas oscillations is observed at $\nu = 1/2$. Finally, there appears much structure in the pattern of rationals ν for which plateaus are found. For example, for some low-lying rationals (such as $\nu = 1/4$) *no* plateau is formed. The set of rationals for which the effect occurs is known as the **quantum Hall hierarchy**.

These are but a few of the most striking observations gathered under the label quantum Hall effect. Undoubtedly, to account even superficially for all of these phenomena would present a task that is well beyond the scope of the present text. Rather, we will have to restrict ourselves to a brief (and, alas, painfully superficial) discussion of a number of conceptual basics. In the present section we shall focus on the discussion of the conductance plateaus observed at integer filling factors – the so-called **integer quantum Hall effect**

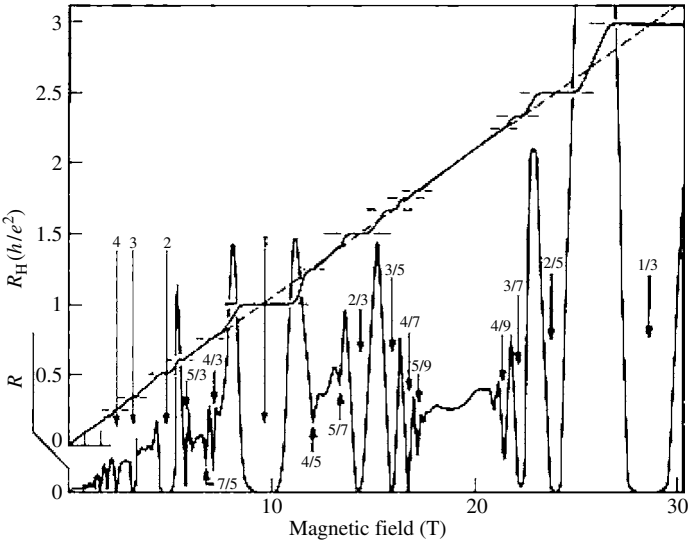

Figure 9.7 Hall conductance and longitudinal conductance of a two-dimensional electron gas as functions of a perpendicular magnetic field. For a discussion, see the main text. (Reprinted with permission from H. L. Störmer, D. C. Tsui, and A. C Gossard, The fractional quantum Hall effect, *Rev. Mod. Phys.* **71** (1999), S298–305. Copyright (1999) by the American Physical Society.)

(IQHE). The generalization to plateaus at rational filling fractions – which, curiously, hinges on altogether different physical concepts – is discussed in Section 9.5.1 below.

When specified in units of the conductance quantum e^2/h, the plateau conductance $\sigma_{xy} = \rho_{xy}^{-1}$ of the IQHE is an integer. By its very nature an integer cannot vary continuously (upon changing some physical control parameter). Indeed, more often than not, observables quantized in integer (or rational) units are linked to some topological origin. In the following, we will formulate two different "explanations" of the quantization phenomenon. The quotes indicate that, far from being rigorous, both lines of argument involve some degree of "bootstrap character": *assuming* that the effect is of topological nature, we feel free to subject the "real world" arrangement of a QHE experiment to all kinds of abuses (deformation of the sample boundaries, etc.) to then discover that, yes, the Hall conductance emerges as a topological invariant. The backbone of a more rigorous approach to the problem is discussed in Section 9.3.7 below.

9.3.5 Background information on the IQHE

Let us begin our discussion with a nutshell summary of the phenomenology of the IQHE. This is followed by a brief reminder of the phenomenology of Landau level quantization – formulated in a language that highlights the symmetries of the problem.

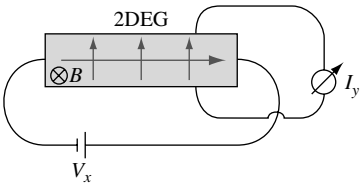

The QHE is observed in two-dimensional electron gases subject to a strong magnetic field. The prototypical setup of a QH experiment is shown in the figure. A voltage drop V_x applied across the sample induces a current I_x in the x-direction plus, by virtue of the Lorentz force, a Hall current I_y in the y-direction. The relation between I_x and I_y determines the Hall conductance. More precisely, the key quantities of interest are the entries σ_{xx} and σ_{xy} determining the conductance tensor

$$\sigma = \begin{pmatrix} \sigma_{xx} & \sigma_{xy} \\ -\sigma_{xy} & \sigma_{xx} \end{pmatrix},$$

which is defined as usual by $\mathbf{I} = \sigma\mathbf{V}$ where $\mathbf{I} = (I_x, I_y)^T$, $\mathbf{V} = (V_x, V_y)^T$ (note that, by symmetry, $\sigma_{xx} = \sigma_{yy}$). The inverse $\rho = \sigma^{-1}$ defines the resistance tensor $\mathbf{V} = \rho\mathbf{I}$. For a system of linear extension L, conduct*ance* g and conduct*ivity* σ are connected by the relation $g = \sigma L^{d-2}$. In two dimensions, the two quantities coincide. This implies that no device-geometry-dependent factors interfere when we pass from the basic quantity determined by the microscopic physics of the system (σ) to experimental observables (g); otherwise, no completely universal Hall conductance could possibly be observed. In the context of the QHE, it is truly important to keep the tensorial structure of σ and ρ in mind. For example, somewhat paradoxically, for $\sigma_{xy} \neq 0$, a vanishing of the longitudinal resistance ρ_{xx} implies a vanishing (as opposed to a divergence) of the longitudinal conductance σ_{xx}.

Within the context of the QHE, the natural unit for the strength of the applied magnetic field is the "**filling fraction**". This is defined as the ratio

$$\nu \equiv \frac{2\pi N l_0^2}{A}, \tag{9.17}$$

where N denotes the number of electrons in the system, A is the sample area and $l_0 = \sqrt{\Phi_0/2\pi|B|}$ the **magnetic length**, i.e. the external magnetic flux through the area l_0^2 is equal to (2π times) one flux quantum.[21]

Experimentally, one finds that (see the figure overleaf, courtesy of D. Leadley), for field strengths close to an integer filling fraction $\nu \in \mathbb{N}$, the Hall resistance is quantized, $\rho_{xy} = \nu^{-1}h/e^2$ to an accuracy of $\mathcal{O}(10^{-10})$.[22] At the same time, the longitudinal resistivity/conductivity drops by as much as 13 orders of magnitude. In passing we note that the rapid oscillations visible in the figure at small field strengths represent the familiar Shubnikov–de Haas oscillations.

[21] One may recall that the flux quantum is defined through the relation $\Phi_0 = h/e$. In our standard units $\hbar = e = c = 1$, $\Phi_0 = 2\pi$ and $l_0 = |B|^{-1/2}$.

[22] Due to the striking precision of the experimental data, the unit of electrical resistance is nowadays maintained as $h/e^2 = 25\,812.80\,\Omega$ through quantum Hall measurements.

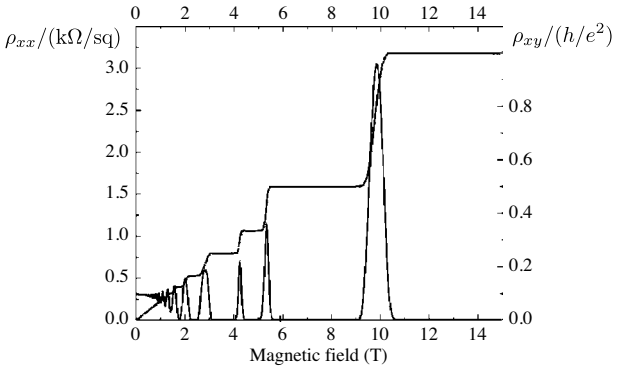

As a (presumed) topological phenomenon, we expect the quantization of the Hall conductance to be robust against sample imperfections and/or the presence of **static disorder**. What is more surprising is that the phenomenon, in fact, critically *relies* on the presence of disorder. To see this, let us for a moment assume that the opposite is true: we have a homogeneous electron gas accommodated by a translationally invariant device. We further assume the absence of external voltage gradients, $\mathbf{E} = 0$, so that no current is flowing in the system, $\mathbf{I} = 0$. Now suppose that we observe the system from a frame moving with velocity v in, say, the 1-direction. An experimentalist working in that frame would observe a current density $\mathbf{j} = -v\rho\mathbf{e}_1$, where ρ is the density of the electron gas. Further, the Lorentz covariance of electrodynamics implies that one would measure a finite electric field $\mathbf{E} = v\mathbf{e}_1 \times \mathbf{B} = -vB\mathbf{e}_2$, where $\mathbf{B} = B\mathbf{e}_3$ is the applied magnetic field. With $j_1 = \sigma_{12}E_2$, we obtain $\sigma_{12} = \rho B^{-1}$ for the Hall conductivity in the moving frame. Being independent of the boost velocity, v, this result holds in all moving frames, including the static frame, $v \to 0$. We conclude that, in any translationally invariant environment, the Hall conductivity is linearly related to the magnetic field.

Reciprocating the argument above, we see that the presence of (translational invariance breaking) disorder must be necessary for the observability of the QHE. In fact, we shall see in a moment that the effect is born out of a conspiracy of disorder induced localization and the phenomenon of **Landau level quantization**. However, before turning to the discussion of the combined effect of these two mechanisms, let us briefly recapitulate the formation of Landau levels in a clean two-dimensional electron gas subject to a magnetic field.

Let us temporarily consider a geometry where the electron gas assumes the form of a perfect disk.[23] To explore the quantum mechanics of this problem, we represent the in-plane vector potential in the so-called symmetric gauge, $A_i = (B/2)\epsilon_{ij}x_j$, $i = 1, 2$ (where the coordinates are measured with respect to the center of the disk), whereupon the free electron Hamiltonian, $\hat{H} = (\hat{\mathbf{p}} - \hat{\mathbf{A}})^2/(2m^*)$, assumes the form

$$\hat{H} = \frac{1}{2m^*}\left[\left(-i\partial_1 - \frac{x_2}{2l_0^2}\right)^2 + \left(-i\partial_2 + \frac{x_1}{2l_0^2}\right)^2\right]. \tag{9.18}$$

(To avoid confusion with the quantum number to appear shortly below, we designate the electron mass by m^*.) We wish to solve the Schrödinger equation $\hat{H}\psi_n = \epsilon_n\psi_n$. This task is greatly simplified by subjecting the eigenvalue problem to the similarity transformation

[23] Remember our fundamental working hypothesis whereby the quantization phenomena forming the QHE will not depend on details of the geometry.

$\hat{H} \to \hat{H}' = S\hat{H}S^{-1}$, $\psi_n \to \psi_n' = S\psi_n$, where $S = \exp\left[\frac{1}{4l_0^2}\left(x_1^2 + x_2^2\right)\right]$. The reason is that the transformed problem $\hat{H}'\psi_n' = \epsilon_n\psi_n'$ is governed by the effective Hamiltonian

$$\hat{H}' = \frac{1}{2m^*}\left[\left(-i\partial_1 + i\frac{1}{2l_0^2}(x_1 + ix_2)\right)^2 + \left(-i\partial_2 + \frac{1}{2l_0^2}(x_1 + ix_2)\right)^2\right],$$

i.e. an operator whose (vector) potential depends only on the linear combination $x_1 + ix_2$ rather than on two linearly independent coordinates x_1 and x_2. To benefit from this simplification, we may switch to complex coordinates, $z = x_1 + ix_2$, $\bar{z} = x_1 - ix_2$, in which the Hamiltonian assumes the form (exercise)

$$\hat{H}' = \frac{1}{2m^*}\left(-4\partial_z\partial_{\bar{z}} + 2\frac{z}{l_0^2}\partial_z + \frac{1}{l_0^2}\right).$$

This Hamiltonian possesses a family of eigenstates $\psi_n' \equiv z^n$ with eigenvalues $\epsilon_n = \frac{1}{m^* l_0^2}(n + 1/2) = \frac{B}{m^*}(n + 1/2)$. Undoing the similarity transform, one can conclude that the original Hamiltonian is diagonal on the states

$$\psi_n = z^n e^{-\frac{1}{4l_0^2}z\bar{z}}, \quad \epsilon_n = \omega_c(n + 1/2),$$

whose eigenvalues ϵ_n are the celebrated **Landau levels**. The Landau levels differ by integer multiples of the **cyclotron frequency** $\omega_c \equiv B/m^*$. On the other hand, we know that, for a system of linear extension L, there are of $\mathcal{O}(k_F L)^2$ states below the Fermi energy $k_F^2/2m^*$. This implies a typical level spacing $\sim 1/(m^* L)^2$ which is by a factor $\sim BL^2$ smaller than the spacing between Landau levels. Anticipating that the clean problem does not support energies other than ϵ_n, one can conclude that the Landau levels must be hugely degenerate: each of them hosting $BL^2 = (L/l_0)^2$ states.

To reveal the origin of the massive degeneracy of the Landau levels, we have to identify a symmetry of the Hamiltonian (9.18) or, equivalently, a set of linearly independent operators commuting with $\hat{H}$. In the present context, these are the "**magnetic translation operators**"

$$k = \partial_z - \frac{\bar{z}}{4l_0^2}, \quad \bar{k} = \partial_{\bar{z}} + \frac{z}{4l_0^2}, \quad \bar{k}\psi_n = 0.$$

(In the absence of a magnetic field $l_0 \to \infty$, these would be ordinary translation operators $\sim -i\partial_i$ transformed to complex coordinates; hence the name magnetic "translation" operators.) It is straightforward (exercise) to verify the following properties:

$$[\hat{H}, k] = [\hat{H}, \bar{k}] = 0, \quad [k, \bar{k}] = \frac{1}{2l_0^2}.$$

We next use these operators as generators for the creation of states degenerate with the reference states ψ_n. To this end, let us define

$$T = \exp\left[\frac{4\pi l_0^2}{L}k\right], \quad U = \exp\left[i\frac{2\pi l_0^2}{L}\bar{k}\right].$$

Using the commutation relations between k and $\bar{k}$, one may verify that these operators obey the relation

$$TU = UT\exp\left[4\pi^2 i\left(\frac{l_0}{L}\right)^2\right],$$

sometimes referred to as the **magnetic algebra**. We now have all elements to construct the entire set of states: the fact that $\bar{k}$ annihilates ψ_n implies that $U\psi_n = \psi_n$. Consider now the family of states

$$\psi_{n,m} \equiv \mathcal{N}_{n,m} T^m \psi_n, \tag{9.19}$$

where $\mathcal{N}_{n,m}$ is a normalization factor. Since $\hat{H}$ commutes with k (and therefore with T), $\psi_{n,m}$ form eigenstates with eigenenergy ϵ_n – they all populate the nth Landau level. However, we do not yet know whether $\psi_{n,m}$ actually form a set of linearly independent states. To prove their independence, one can employ Eq. (9.19) and $U\psi_n = \psi_n$ to show that $U\psi_{n,m} = \exp(-i4\pi^2 m(l_0/L)^2)\psi_{n,m}$. Therefore, as with Bloch states in a periodic potential, $\psi_{n,m}$ are eigenstates of a generalized translation operator. For $m = 1, \ldots, 2\pi(L/l_0)^2$, the corresponding eigenvalues are different, which proves that

$$\{\psi_{n,m} | 0 \leq m < 2\pi(L/l_0)^2\},$$

is a linearly independent set of eigenstates in the nth Landau level. The magnitude of this set $2\pi(L/l_0)^2$ coincides with our estimate of the degeneracy of the Landau levels above, i.e. we have succeeded in constructing a complete eigenbasis of the magnetic Hamiltonian.

9.3.6 IQHE as a topological phenomenon

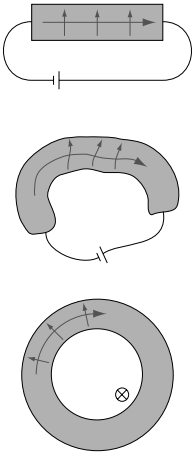

Shortly after the experimental discovery of the IQHE,[24] Laughlin presented an ingenious argument whereby the quantization of the Hall conductance could be explained under fairly general conditions.[25] Slightly later it became clear[26] that Laughlin's argument in fact implied a number of curious features of electrons subject to a magnetic field *and* static disorder. However, before turning to a more detailed discussion of Laughlin's ideas, and their subsequent refinement by Halperin, let us first outline the basic skeleton of the argument.

Given its complete universality, the quantization phenomenon must be insensitive to (continuous) deformations of the sample geometry. Using this freedom, Laughlin proposed to subject the basic quantum Hall geometry to the sequence of transformations indicated in the figure. From a "Hall bar" geometry we pass to an annular geometry of higher symmetry.

[24] K. von Klitzing, G. Dorda, and M. Pepper, New method for high-accuracy determination of the fine-structure constant based on quantized Hall resistance, *Phys. Rev. Lett.* **45** (1990), 494–7.

[25] R. B. Laughlin, Quantized Hall conductivity in two dimensions, *Phys. Rev. B* **23** (1981), 5632–3.

[26] See B. I. Halperin, Quantized Hall conductance, current-carrying edge states, and the existence of extended states in a two-dimensional disordered potential, *Phys. Rev. B* **25** (1982), 2185–90.

In the last step of the construction, the external bias voltage is replaced by the electromotive force generated by a weakly time-dependent flux through the annulus. Laughlin then suggested monitoring the fate of the system upon an adiabatic (i.e. infinitely slow) variation of the flux threading the annulus. Before discussing the response of the system in more detail, let us try to motivate this idea.

We know that, for specific values of the annular flux, namely integer multiples of a flux quantum $\phi = 2\pi n$, the Hamiltonian of the system is gauge equivalent to the Hamiltonian in the absence of flux. This is because an integer multiple of the flux quantum can be removed by the gauge transformation $\psi_a \to e^{in\theta}\psi_a$ acting on the wavefunctions of the system. (For non-integer fluxes, this transformation alters the boundary condition $\psi(r, 2\pi) = \psi(r, 0)$ and, therefore, the Hilbert space of the problem.)

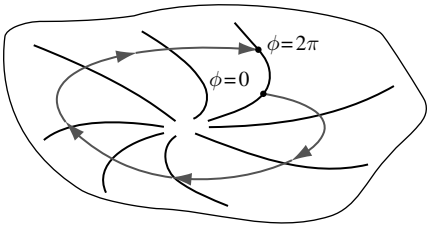

Now, let us see what happens as we gradually increase the flux from $\phi = 0$ to $\phi = 2\pi$. The situation is visualized in the figure where each line symbolically represents a basis of eigenstates of the Hamiltonian for a given value of the flux. Assuming that a gauge transformation has been applied to move the flux dependence of the problem to a change in the azimuthal boundary conditions (see our discussion in Section 9.1), the eigenstates for different values of the flux are truly distinct, i.e. as one increases the flux from $\phi = 0$, each state moves along a path "perpendicular" to the collective set of eigenstates, as shown schematically in the figure. Eventually, for $\phi = 2\pi$, we arrive back at the original $\phi = 0$ basis. (This follows from the fact that $\hat{H}|_{\phi=2\pi}$ can be mapped onto $\hat{H}|_{\phi=0}$ by a gauge transformation that does *not* alter the boundary conditions.) That, however, does not necessarily imply that individual basis states map onto themselves upon the completion of the path $\phi = 0 \to \phi = 2\pi$. I.e., while the set of eigenstates as a whole gets reproduced, permutations of individual states are consistent with the gauge invariance of the problem.

EXERCISE If this statement does not make much sense to you consider, as an example, a clean one-dimensional ring subject to a magnetic flux. Explore what happens to the eigenstates of $\hat{H} = \frac{1}{2m}(\hat{p} - A)$ as the flux is increased from 0 to 2π. Show that the non-invariance of individual states is compatible with the invariance of the global spectrum.

The non-invariance of individual states upon completion of a round trip back to a gauge-equivalent Hamiltonian is a phenomenon called **spectral flow**. The spectral flow of the eigenstates of our magnetic environment lies at the heart of Laughlin's argument. Specifically, we shall see that, upon the sending of a flux quantum through the ring, n states radially centered at the inner perimeter are pushed above the Fermi energy (n is the number of Landau levels below the Fermi energy). At the same time, n states at the outer perimeter sink below the Fermi energy. To regain thermal equilibrium, the system responds by transferring n electrons from the inner to the outer perimeter. This process takes place during the time t_0 it takes to adiabatically send the flux quantum through the system, i.e. the transverse current $I_2 = n/t_0$ (remember, $e = 1$). The electromotive force driving the process is $V_1 = \dot{\phi} = 2\pi/t_0$. The corresponding Hall conductance is therefore given by

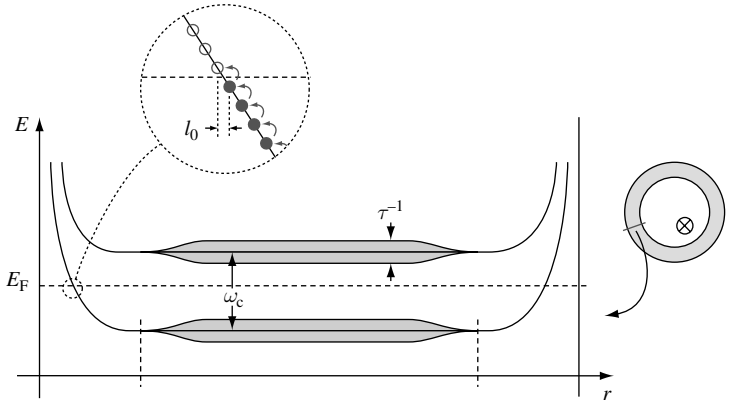

Figure 9.8 Energy levels of a quantum Hall annulus as functions of the radial coordinate. For a discussion, see the main text.

$\sigma_{12} = I_2/V_1 = n/2\pi$. Expressed in physical units, this can be cast in the form $\sigma_{12} = ne^2/h$ – the quantum Hall effect!

To substantiate this picture, let us consider a situation in which the Fermi level E_F is placed somewhere between the first and the second Landau level. For simplicity we shall also make the (artificial but physically immaterial, cf. Halperin's paper[26]) assumption that the disorder is confined to the inner regions of the sample. We require the disorder strength, as set by the inverse elastic scattering time, τ^{-1}, to be smaller than the separation between Landau levels, $\omega_c\tau \gg 1$. This condition is, in fact, necessary to prevent the Hall plateaus from becoming "washed out." As a result we obtain the level diagram shown in Fig. 9.8. The figure schematically shows the energies of the single-particle states as functions of the radial coordinate of the annular region. In the bulk of the annulus, disorder leads to a broadening of the Landau levels to energy bands of width τ^{-1}. At the outer/inner perimeter of the annulus, the confining potential pushes the levels energetically up. Crucially, this implies the presence of as many Fermi energy states – "**edge states**" – as there are occupied Landau levels (in our case, just one). These states, and not so much the bulk states buried deep below the Fermi energy, are likely to be the carriers of longitudinal currents in the system. As to the bulk states, let us presume that they are localized by disorder on a length scale ξ much smaller than the circumference $L_\parallel$ of the system. (Intriguingly, we shall soon see that this assumption leads to a contradiction.)

To explore the phenomenon of spectral flow in this environment, we need to turn to a refined description where individual levels are resolved. This is the subject of the following.

EXERCISE We wish to explore the radial structure of the states occupying the lowest Landau level. This task is most conveniently accomplished in a basis different from the set $\{\psi_{0,m}\}$ discussed above: revisit the construction on page 520 to show that all states $\phi_{0,m} \equiv \mathcal{N}_{0,m}\bar{z}^m \exp[-\frac{1}{4l_0^2} z\bar{z}]$ lie in the lowest Landau level. Switch to polar coordinates (r, θ) and verify that these states can be approximated as

$$\phi_{0,m}(r,\theta) \approx \mathcal{N}_{n,m} e^{-im} \; e^{-\frac{3}{4l_0^2}(r-r_m)^2}, \tag{9.20}$$

where r_m defines the area through which m flux quanta pass; $\pi r_m^2 B = mh/e$. Show that, for any reference angle θ_0, the azimuthal current carried by these states is given by

$$\begin{aligned} I_\parallel \equiv \frac{1}{m^*}\int_0^\infty dr \; \langle \hat{\mathbf{j}}_{(r,\ 0)} \rangle \cdot \mathbf{e} \qquad &= \frac{1}{m^*}\int_0^\infty dr \; |\phi_{0,m}|^2 \left(\frac{m}{r} - \frac{Br}{2}\right) \\ &\simeq \frac{B}{m^*}\int_0^\infty dr \; |\phi_{0,m}|^2 \, (r - r_m) \, . \end{aligned} \tag{9.21}$$

The wavefunctions $\phi_{0,m}(r,\theta)$ describe the system far away from its boundaries. They are symmetrically centered around r_m and carry angular momentum $L = m$. From Eq. (9.21) and the symmetry around the center coordinate r_m, we further conclude that the azimuthal current carried by these states vanishes, $I_\parallel = 0$. However, in the vicinity of the boundaries, this picture becomes perturbed. Firstly, the confining potential will push the states $\phi_{0,m}$ up in energy (see Fig. 9.8 where the circles represent the states centered at coordinates r_m close to the inner boundary of the annulus). Secondly, the boundary potential will render the states radially asymmetric, implying that the integral (9.21) no longer vanishes: azimuthal currents flow at the boundaries. The surface currents flowing at the inner/outer perimeter are opposite to each other.

We next discuss what happens as some weakly time-dependent flux $\tilde{\phi}$ is sent through the annulus to generate an electromotive force $E_\parallel = d_t\tilde{\phi}/r$. The vector potential generalized to the presence of the field $E_\parallel$ takes the form $\mathbf{A} = \frac{\phi(r)+\tilde{\phi}}{2r}\mathbf{e}_\theta$, where $\phi(r) = Br^2$. Referring for a more detailed discussion to Halperin's paper, we note that the flux $\tilde{\phi}$ adds to the background flux $\phi(r)$. As a consequence, the center coordinates $r_m(\phi + \tilde{\phi})$ "contract." Once a full flux quantum has been added to the system, $\tilde{\phi} = 2\pi$, the center coordinates have contracted by one unit, $r_m(\phi + 2\pi) = r_{m-1}(\phi)$, and the original set of levels (and therefore the spectrum of the system) is restored. However, the individual levels have changed – spectral flow: at the inner edge of the system, one occupied level has been pushed above the Fermi energy, at the outer edge one empty level dived below the Fermi energy (see Fig. 9.8). To repair this energy imbalance, the system will want to transfer one electron from the inner edge to the outer edge.

But how will it do that? Before the advent of the QHE, it had been common wisdom that the states of a two-dimensional electron gas in the presence of disorder (such as the states in the bulk of our annulus) are localized on a certain scale ξ. For $\xi/L_\parallel \gg 1$, these states would be completely oblivious to the presence of our driving flux $\tilde{\phi}$. This would imply that, as far as the action of $\tilde{\phi}$ is concerned, the inner and the outer edge of the system are decoupled. How, then, would the system know that it ought to transfer one electron between the edges. (After all, this transfer has to be mediated through the bulk.) The only way out of this dilemma is to courageously *postulate* (as Halperin did) that, notwithstanding the presence of disorder, there must be at least one **delocalized bulk state** below the Fermi energy. Subsequently, it was indeed found that the localization length diverges upon approaching the center of the Landau band. The delocalized states in the center of the band establish the contact between the edges and may act as conduits of electronic charge.

Laughlin's gauge argument hints at the topological nature of the QHE: independent of system-specific details, the addition of a flux quantum through the annulus transfers an integer charge across the system. This suggests that the effect should be understandable in terms of some kind of topological index lurking behind the mapping of a parameter space (presently, the amount of flux through the ring) into the Hilbert space of the problem. Subsequently, Avron and Seiler,[27] and Thouless, Kohmoto, Nightingale, and den Nijs[28] indeed succeeded in rigorously identifying the quantum Hall conductance as a topological invariant – the first Chern class of the $U(1)$ principal bundle over the two-dimensional torus. However, a satisfactory discussion of these ideas, for which we would need to introduce much more background in differential topology, would lead us too far astray. Instead, we shall head back to our prime subject, the discussion of topological concepts in low-energy field theories of condensed matter systems.

EXERCISE As preparation for the next section, refamiliarize yourself with the field theory approach to the disordered electron gas introduced in Section 6.5.

9.3.7 Field theory of the integer quantum Hall effect

Laughlin's gauge argument, and its subsequent refinement by others, helped to unravel many of the mysteries posed by the experimental discovery of the IQHE. Specifically it shed some light on the conspiracy of dissipationless edge currents, disorder induced localization of bulk states, and an exotic family of delocalized states in the formation of the effect. On the other hand, even with Laughlin's picture in store, we are still a long way from a more-than-schematic, quantitative understanding of the effect. A huge step towards a full microscopic theory of the IQHE – whose final structure still remains partly unknown – was taken by Pruisken when he adjusted the nonlinear σ-model of disordered fermion systems so as to account for the presence of a strong magnetic field. In the next two subsections, we will reconstruct Pruisken's field theory, and employ it to gain more insight into the long-range behavior of the quantum Hall system.

Pruisken s field theory: construction

As we have seen in earlier chapters of this book, much of the information about a non-interacting disordered electron system is contained in correlation functions involving the product of a retarded and an advanced single-particle Green function,

$$\langle \mathbf{x}_1 | \frac{1}{E_\mathrm{F} + \omega + i0 - \hat{H}} | \mathbf{x}_2 \rangle \langle \mathbf{x}_{2'} | \frac{1}{E_\mathrm{F} - \omega - i0 - \hat{H}} | \mathbf{x}_{1'} \rangle \Big\rangle_{\mathrm{dis}} .$$

Depending on the choice of coordinates and the energy argument ω, these functions describe the conductance of the system, the statistics of its spectrum and many other characteristics.

[27] J. E. Avron and R. Seiler, Quantization of the Hall conductance for general, multiparticle Schrödinger Hamiltonians, *Phys. Rev. Lett.* **54** (1985), 259–62.

[28] D. J. Thouless, M. Kohmoto, M. P. Nightingale, and M. den Nijs, Quantized Hall conductance in a two-dimensional periodic potential, *Phys. Rev. Lett.* **49** (1982), 405–8.

We have also seen that the long-range behavior (scales $L \gg \ell$, much larger than the elastic scattering mean free path, ℓ) of this correlation function can be extracted from a field theory whose action in $d = 2$ is of nonlinear σ-model type,[29]

$$S[Q] = \frac{\pi\nu}{4} \int d^2x \left[D \,\mathrm{tr}\,(\hat{\partial}_\mu Q \hat{\partial}_\mu Q) - 2\omega \,\mathrm{tr}\,(Q\sigma_3^{\mathrm{ar}}) \right]. \tag{9.22}$$

For later convenience, let us recapitulate a few key features of the field theory defined by Eq. (9.22).

- ▷ The matrix fields $Q^{aa',ss'}(\mathbf{x}) \sim \bar{\psi}^{as}(\mathbf{x})\psi^{a's'}(\mathbf{x})$ describe the behavior of a product of two fermion field amplitudes ψ^{as}. The dynamics of the latter is controlled by the advanced/retarded single-particle Green function, $\langle \bar{\psi}^{as}(\mathbf{x})\psi^{a's'}(\mathbf{x}')\rangle \sim (E_{\mathrm{F}} + s(\omega + i0) - \hat{H})^{-1}(\mathbf{x},\mathbf{x}')\delta^{ss'}\delta^{aa'}$. Here, the two-component index $s = +/-$, and $a = 1, \ldots, R$ refers to the replica index.
- ▷ The fields Q take values in the coset space $\mathrm{U}(2R)/(\mathrm{U}(R) \times \mathrm{U}(R))$.[30] A concrete representation is given by $Q = T\sigma_3^{\mathrm{ar}}T^{-1}$, where $T \in \mathrm{U}(2R)$ and σ_3^{ar} is a Pauli matrix in two-dimensional advanced/retarded (ar) space.
- ▷ For $\omega \to 0$ (the limit we will concentrate on throughout) the action above is invariant under two distinct symmetry transformations: global transformations $T \to gT$, where $g \in G \equiv \mathrm{U}(2R)$ is constant, and local transformations $T \to Th(\mathbf{x})$, where $h(\mathbf{x}) \in H \equiv \mathrm{U}(R) \times \mathrm{U}(R)$, i.e. the group of all matrices fulfilling the condition $[h(\mathbf{x}), \sigma_3^{\mathrm{ar}}] = 0$.
- ▷ The microscopic parent action from which Eq. (9.22) was derived was, in fact, rotationally invariant under the full group $\mathrm{U}(2R)$. That our fields Q live in a smaller coset space signals the fact that, in a metallic system, this symmetry is spontaneously broken: the Qs are the Goldstone modes associated with the breakdown of the symmetry from $\mathrm{U}(2R)$ to $\mathrm{U}(R) \times \mathrm{U}(R)$.
- ▷ Under a generalized[31] gauge transformation, $\psi \to e^{i\phi}\psi$, the Qs transform as $Q \to e^{-i\phi}Qe^{i\phi}$. Gauge invariance then implies that the operators $\hat{\partial}_\mu$ appearing in the effective action must be interpreted as covariant derivatives,

  $$\hat{\partial}_\mu = \partial_\mu - i[A_\mu, \,],$$

  where A_μ transforms as a non-abelian vector potential, $A_\mu \to e^{-i\phi}A_\mu e^{i\phi} - ie^{-i\phi}\partial_\mu e^{i\phi}$. (Notice, however, that the "physical vector potential" generating the perpendicular magnetic field $A_{\mathrm{phys}} \sim \delta^{ab}\delta^{ss'}$ is diagonal in replica and ar spaces and, therefore, does not enter the covariant derivative.)

In a series of famous papers, Pruisken[32] extended the formalism above so as to account for the effect of a strong magnetic field. It turned out that a key player in the action of that

[29] Here we are using the reduced variant of the model (see Problem 8.8.4) suitable to compute the product of a retarded and an advanced Green function.

[30] Due to the presumed presence of a massive magnetic field, time reversal symmetry is broken and the introduction of a "time-reversal space" unnecessary.

[31] By "generalized" we mean that ϕ can be a matrix in ar space as well as in replica space.

[32] For a review, see A. M. M. Pruisken, Field theory, scaling and the localization problem, in *The Quantum Hall E ect*, ed. R. E. Prange and S. M. Girvin (Springer-Verlag, 1987).

generalized field theory was a certain variant of a θ-term. As with many other examples before, there are two ways to obtain this action: one may generalize the derivation of the σ-model discussed in Section 6.5 for the presence of a strong magnetic field and derive the θ-term from first principles. For the details of this not entirely straightforward program we refer to the original papers. Alternatively, one may guess the structure of the generalized action on the basis of symmetry arguments and fix the coupling constants by running some consistency checks. It is this second strategy that we shall pursue shortly.

As discussed in Chapter 7, elements of the conductivity tensor $\sigma_{\mu\nu}$ can be obtained by a two-fold differentiation $\frac{\delta^2}{\delta A_\mu\, \delta A_\nu} Z[A]$ of the partition or generating function with respect to some generalized vector potential. Referring below for a more detailed discussion, all we shall aim for presently is to understand what kind of action is needed to produce a finite Hall conductivity $\sigma_{12} \sim \frac{\delta^2}{\delta A_1\, \delta A_2} Z[A]$. By symmetry, the mixed derivative computed on the field theory defined by Eq. (9.22) vanishes (a point that warrants some consideration). Rather, we have to look out for an operator comprising the two long derivatives $\hat\partial_1 Q$ and $\hat\partial_2 Q$ in a single local expression. For example, we might contemplate a term like $\int \mathrm{tr}(\hat\partial_1 Q\, \hat\partial_2 Q)$. This expression, however, is again not permitted by symmetry. The reason is that (unlike the rotationally invariant two-derivative operator in Eq. (9.22)) it is not form invariant under rotation of the coordinate axes (again something to think about). However, the next obvious choice,

$$S_{\mathrm{top}}[Q] = \theta\epsilon^{\mu\nu} \int d^2x\ \mathrm{tr}(Q\hat\partial_\mu Q \hat\partial_\nu Q), \tag{9.23}$$

does the job. For one thing, this term *is* rotationally invariant. Secondly, the definition of the long derivatives $\hat\partial_\mu$ implies that it contains terms linear in the combination $A_1 A_2$, from where we conclude that the (as yet undetermined) coupling constant θ must have something to do with the Hall conductivity.

To be somewhat more specific, let us draw on Problem 7.6.4 where it has been shown that a source-vector potential suitable for the calculation of the conductance takes the form $A_\mu = U^{-1}\partial_\mu U$ with $U = \exp(i(x_1\kappa_1\sigma_1^{\mathrm{ar}} + x_2\kappa_2\sigma_2^{\mathrm{ar}}) \otimes E_{11}^{\mathrm{r}})$ (here, E_{11}^{r} is a projector onto the first replica channel and κ_μ are numbers). With this choice,

$$\sigma_{11} = \lim_{R\to 0} \frac{1}{4\pi L^2}\, \partial^2_{\kappa_1\kappa_1}\big|_{\kappa=0}\, \mathcal{Z}, \quad \sigma_{12} = \lim_{R\to 0} \frac{1}{4\pi i L^2}\, \partial^2_{\kappa_1\kappa_2}\big|_{\kappa=0}\, \mathcal{Z}.$$

We also know that the conventional Drude theory of a weakly disordered metal is obtained by setting $Q = \sigma_3^{\mathrm{ar}}$. (Remember that fluctuations around the origin of the field space, σ_3^{ar}, describe mechanisms of localization, i.e. quantum effects beyond the Drude picture.) We next use this information to determine the coupling constants of the theory. To this end, we go to the Drude level (set $Q = \sigma_3^{\mathrm{ar}}$), substitute the source A_μ into our long derivatives, and evaluate the action. This leads to (exercise)

$$S[Q = \sigma_3^{\mathrm{ar}}] = 2\pi L^2 D\nu(\kappa_1^2 + \kappa_2^2) + 16 i L^2 \theta \kappa_1\kappa_2.$$

Evaluation of the derivatives above on $Z[A]|_{\mathrm{Drude}} \simeq \exp(-S[\sigma_3^{\mathrm{ar}}])$ then readily leads to the result $\sigma_{11}^0 = 2\pi D\nu$ for the longitudinal Drude conductance σ_{11}^0 (which we knew anyway),

and to the suspected identification $\theta = -\sigma_{12}^0/8$ of the coupling constant θ with the (Drude) Hall conductance. Summarizing, we obtain **Pruisken's action of the IQHE**,

$$S[Q] = \frac{1}{8}\int d^2x\, \left[\sigma_{11}\,\mathrm{tr}(\hat\partial_\mu Q\ \hat\partial_\mu Q) - \sigma_{12}\epsilon_{\mu\nu}\mathrm{tr}(Q\hat\partial_\mu Q\ \hat\partial_\nu Q)\right]. \tag{9.24}$$

What makes the identification $\theta \sim \sigma_{12}$ more interesting is that θ (and therefore the Hall conductance) actually plays the role of a topological angle; the second term in Eq. (9.24) is a topological term. That such a term might be present in our field theory follows from the fact that

$$\pi_2(\mathrm{U}(2R)/(\mathrm{U}(R)\times\mathrm{U}(R))) = \mathbb{Z}.$$

Unfortunately, we do not have the mathematical background to prove this result.[33] We can, however, make it plausible; and we can demonstrate that $S_{\rm top}$ above is a representation of the corresponding θ-term.

To this end, let us temporarily focus on a single replica channel ($a = 1$, say) and consider the field configuration

$$\begin{aligned}\tilde Q^{11}(\mathbf{x}) &= U(\mathbf{x})\sigma_3^{\rm ar}U^{-1}(\mathbf{x}) \equiv \mathbf{n}(\mathbf{x})\cdot\sigma^{\rm ar},\\ \tilde Q^{ab}(\mathbf{x}) &= \delta^{ab}\sigma_3^{\rm ar}, \quad a\neq 1,\end{aligned}$$

where $U(\mathbf{x}) \in \mathrm{U}(2)$. The second equality in the first line defines a unit vector $\mathbf{n}(\mathbf{x})$. It expresses the fact that the projection of the field space onto a single replica channel is isomorphic to S^2.[33] Evaluating $S_{\rm top}$ on this particular field configuration, it is straightforward to verify that $S_{\rm top}[\tilde Q] = i\frac{\sigma_{12}}{2}\int d^2x\,\mathbf{n}\cdot(\partial_1\mathbf{n}\times\partial_2\mathbf{n})$, an expression we identified earlier (see Eq. (9.8)) as the topological term of a two-dimensional field theory on the sphere. We can now generalize from our particular $\tilde Q$ to field configurations $Q = T(\mathbf{x})\tilde Q(\mathbf{x})T^{-1}(\mathbf{x})$ where $T(\mathbf{x}) \in \mathrm{U}(2R)$. However, using arguments similar to those employed in Section 9.3.1, one may convince oneself that small variations T will not change the value of the action $S_{\rm top}$. Indeed, $S_{\rm top}$ is the general θ-term on the coset space $\mathrm{U}(2r)/(\mathrm{U}(r)\times\mathrm{U}(r))$.

Pruisken s field theory: long-range physics

Now that we have "derived" the Pruisken action, the next question to ask is what to do with it. To begin with the bad news, the long-distance behavior of the model is still pretty much unknown and, in fact, a subject of ongoing research. (That this is the state of affairs some 20 years after its derivation signals the fact that we are dealing with a very rich field theory.) However, by investing one's physical insight in the quantum Hall problem (and with a little bit of good will) quite a few things about the model can, nonetheless, be said.

Suppose we were dealing with a system of annular geometry, similar to that discussed in the last section. Let us further assume that the Fermi energy lies in between the center of the nth and $(n+1)$th Landau bands, so that there are no delocalized states at $E_{\rm F}$. As discussed in the previous section, the bulk of the sample is then pretty much impervious to external

[33] Notice, however, that in the special case $R = 1$, $\mathrm{U}(2)/(\mathrm{U}(1)\times\mathrm{U}(1)) \cong \mathrm{SU}(2)/\mathrm{U}(1) \cong S^2$ is the 2–sphere. What is non-trivial here is the generalization of $\pi_2(\mathrm{U}(2)/(\mathrm{U}(1)\times\mathrm{U}(1))) = \pi_2(S^2) = \mathbb{Z}$ to general R.

perturbations, and the interesting Fermi-energy physics takes place at the boundaries (the inner and outer perimeters).

Indeed, it is possible to rewrite the topological action as a pure boundary operator. A straightforward application of Stokes' theorem[34] shows that

$$S_{\rm top}[T] = \frac{\sigma_{12}}{2}\int_{\partial M} d\mathbf{s}\cdot {\rm tr}(T\sigma_3^{\rm ar}\nabla T^{-1}), \tag{9.25}$$

where the integral runs over the boundary ∂M of the annulus. Notice, however, that Eq. (9.25) is not represented in terms of the fundamental degrees of freedom of the theory (the Qs) but rather relies on a particular "coordinate" representation ($Q = T\sigma_3^{\rm ar}T^{-1}$). As discussed in Section 9.4, this is not accidental but rather reflects a fundamental property of topological terms. For future reference, we also anticipate that the boundary descendant of the bulk θ-term Eq. (9.23) is an example of a **Wess–Zumino term**.

We next show that, under the conditions stated above, the boundary representation of the theory raises a consistency problem unless σ_{12} = integer. To appreciate the problem, recall that the bulk representation of the theory is invariant under local transformations $T(\mathbf{x}) \to T(\mathbf{x})h(\mathbf{x})$, where $h \in H = {\rm U}(R)\times{\rm U}(R)$. This follows trivially from the fact that its degrees of freedom $Q = T\sigma_3^{\rm ar}T^{-1} \to Th\sigma_3^{\rm ar}h^{-1}T^{-1} = Q$ are invariant. Now, under our present working conditions – Fermi energy in a mobility gap – there are no Q-field excitations in the bulk of the system (the Qs describe mobile Fermi energy excitations), and the theory reduces to two decoupled boundary theories which must be separately invariant. In this respect, the only contribution that may potentially cause trouble is the topological boundary contribution Eq. (9.25) (since it is not a functional of the invariant degree of freedom, Q). Indeed, let us consider the specific choice $h = \exp(i\sigma_3^{\rm ar}\theta)$, where θ is the azimuthal coordinate of the system. Focusing on the effect of this transformation at the inner perimeter, say, we obtain

$$\begin{aligned} S_{\rm top}[T] &= \frac{\sigma_{12}}{2}\int_0^{2\pi} d\theta\,{\rm tr}(T\sigma_3^{\rm ar}\partial_\theta T^{-1}) \to \frac{\sigma_{12}}{2}\int_0^{2\pi} d\theta\,{\rm tr}(Th\sigma_3^{\rm ar}\partial_\theta(h^{-1}T^{-1})) \\ &= S_{\rm top}[T] + \frac{R\sigma_{12}}{2}\int_0^{2\pi} d\theta\,{\rm tr}(\sigma_3^{\rm ar}h\partial_\theta(h^{-1})) = S_{\rm top}[T] + \frac{R\sigma_{12}}{2}\int_0^{2\pi} d\theta\,\partial_\theta\,{\rm tr}(\sigma_3^{\rm ar}\ln h^{-1}) \\ &= S_{\rm top}[T] + \frac{R\sigma_{12}}{2}{\rm tr}(\sigma_3^{\rm ar}\ln h^{-1})\Big|_0^{2\pi} = S_{\rm top}[T] - 2\pi i\sigma_{12}R. \end{aligned} \tag{9.26}$$

The invariance of the exponentiated (!) boundary action requires that $\exp(2\pi iR\sigma_{12}) \stackrel{!}{=} 1$, from which we conclude that $\sigma_{12} \stackrel{!}{=}$ integer. Summarizing, we have seen that, for Fermi energies in between two Landau band centers (that is, conditions where QH plateaus are experimentally observed), the intrinsic consistency of the theory requires quantization of the Hall conductance. A refined variant of such arguments (see Pruisken's aforementioned article) shows that the value of the conductance indeed coincides with the number of Landau levels below the Fermi energy. Notice also that the reasoning above is again "topological." This time, the key players are the winding numbers of the mappings $S^1 \to {\rm U}(1)\times{\rm U}(1)$ from

[34] For a review of the general form of Stokes' theorem, see Section 9.4.2 below.

the boundary manifold (topologically, a circle) into the projection of the local transformation group to a single replica channel (U(1) × U(1)).

EXERCISE As an exercise in group manipulations, extend the argument given above to more general transformations at the boundary. To this end, consider a general (but single-valued!) boundary transformation $h(\theta) \in H$ and show that we will not obtain information beyond the quantization criterion discussed above. Hint: Use the facts that $\mathrm{U}(r) = \mathrm{U}(1) \times \mathrm{SU}(r)$, and that $\forall R \in \mathrm{SU}(r) : 0 = \ln \det R = \mathrm{tr} \ln R$.

INFO The argument above focuses on the boundaries of the system. As a brief digression, let us show how the same information can be obtained from a **bulk picture**. In the bulk, all Fermi energy states are localized. Technically, this implies that the longitudinal conductance renormalizes to zero, $\sigma_{11} \overset{L \gg \xi}{\longrightarrow} 0$, where the notation is meant to indicate that, in a renormalization group sense, the conductance scales to zero on length scales $L \gg \xi$ much larger than the two-dimensional localization length. An alternative formulation of the same fact is to say that transformations $\psi(\mathbf{x}) \to T(\mathbf{x})\psi(\mathbf{x})$, where $T(\mathbf{x}) \in \mathrm{U}(2R)$ fluctuates on scales $\gg \xi$, must leave the theory invariant.[35] For $\sigma_{11} \to 0$, and frequency differences $\omega \to 0$, the non-topological sector of the action vanishes and is therefore trivially oblivious to fluctuations of the Qs. However, this is not the case with the topological action. No matter how slowly it fluctuates in space, a topologically non-trivial configuration $Q(\mathbf{x})$ will have topological action $S[Q] = 2\pi\sigma_{12}n$, where n is the corresponding winding number. The only way to make the theory generally impervious to Q-field fluctuations is to require $\sigma_{12} \overset{!}{=}$ integer – the bulk variant of the quantization criterion.

Quantum Hall transition

Having understood the basic quantization phenomenon, we might now ask what other features of the quantum Hall system can be extracted from the field theory approach. Given that the nonlinear σ-model arguably represents the most powerful approach to disordered electron systems in general, we might, for example, be ambitious enough to seek more information about the nature of the delocalized states expected to reside at the centers of the Landau bands. As we saw above, these states do play a vital role in the formation of the QHE. However, as long as they are deeply buried below the Fermi energy, they influence the system rather indirectly. We should expect them to become much more vivid as the Fermi energy sweeps through the center of a Landau band. Indeed, as $E_\mathrm{F} \to n\omega_\mathrm{c}$ approaches a band center, the system begins to build up long-ranged correlations. This is because the physics at the Fermi energy is now controlled by ever more extended, or delocalized, states. Formally, $E_\mathrm{F} \to (n+1/2)\omega_\mathrm{c}$ goes along with a diverging correlation length ξ, a phenomenon indicative of a second-order phase transition. Indeed, $E^* = (n+1/2)\omega_\mathrm{c}$ marks the position of a very peculiar (and still not fully understood) quantum phase transition, the **quantum Hall transition**.

[35] Indeed, we had argued earlier that metallic behavior goes along with a spontaneous breakdown of replica rotation symmetry. Our Qs are the Goldstone modes of this phenomenon. Conversely, localization is accompanied by a restoration of this symmetry; the Goldstone modes disappear and the theory will no longer respond to fluctuations of the Qs (or the Ts for that matter). Further, notice that we are now concentrating on the "large" transformation group of the model, $\mathrm{U}(2R)$, and not the "small" invariance group $\mathrm{U}(R) \times \mathrm{U}(R)$.

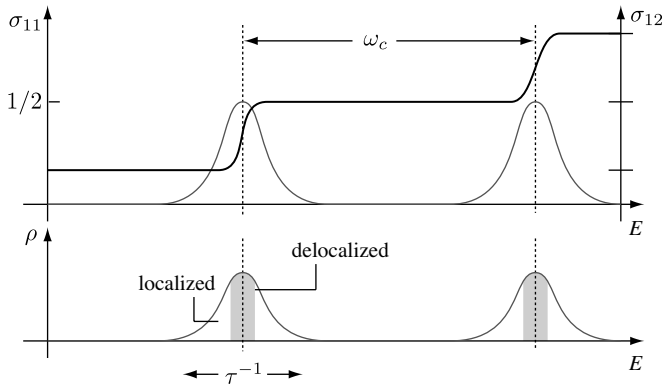

Figure 9.9 On the behavior of the longitudinal conductance, Hall conductance, and density of states, ρ, at the quantum Hall transition.

In Fig. 9.9, the behavior of the three most relevant players in the system, longitudinal conductance, Hall conductance, and density of states, is shown as functions of the Fermi energy. In the vicinity of the Landau band centers the system becomes critical. Right at a transition point, $E_{\rm F} \equiv E^*$, (a) the longitudinal conductance $\sigma_{11} = 1/2$, (b) the Hall conductance $\sigma_{12} = n+1/2$ is *half* integer, and (c) the correlation length ξ characterizing the spatial profile of wavefunctions at the Fermi energy has diverged. The latter implies that, for any system of finite size L, there is a whole range of energies around the critical value for which $\xi > L$. Within this energy range, the wavefunctions are effectively delocalized. Naturally, the width of the band of delocalized states shrinks upon increase of the system size and, in the thermodynamic limit, approaches zero. More precisely, upon approaching the band center, the correlation length diverges as

$$\xi \sim |E - E^*|^{-\nu},$$

where ν defines the correlation length exponent and we have introduced $\Delta E \equiv |E - E^*|$ as a relevant scaling variable. For a given system size, the width of the energy band, ΔE, of delocalized states is determined by the condition $L \sim \xi(\Delta E)$, or $\Delta E \sim L^{-1/\nu}$. The number of states within that window scales as $N \sim \frac{\Delta E}{\delta} \sim L^{-1/\nu+2}$, where $\delta \sim L^{-2}$ is the two-dimensional level spacing. Unfortunately, there is still no reliable analytical prediction for ν. (We shall see in a moment why this is so.) However, high-precision numerical analyses[36] have shown that $\xi = 2.35 \pm 0.08$. This implies that the number of states within the delocalized region diverges in the thermodynamic limit: even though the width of the delocalized energy window approaches zero, it hosts a continuum of extended states.

We shall next explore the extent to which these features can be understood from the **field theory approach**. To this end, let us imagine the partition function formally expanded in

[36] See, e.g., B. Huckestein, Scaling theory of the integer quantum Hall effect, *Rev. Mod. Phys.* **67** (1995), 357–96.

terms of the topological index of field configurations:

$$\mathcal{Z} = \sum_W e^{2\pi i W \sigma_{12}} \mathcal{Z}_W,$$

where $\mathcal{Z}_W$ is the partition function reduced to the sector of fields of winding number W, and $S_{\rm top} = 2\pi i W \sigma_{12}$ enters as a topological phase. In general, there is not much we can say about $\mathcal{Z}_W$, other than that it will be small: $|\mathcal{Z}_n| \overset{\sigma_{11}\gg 1}{\ll} 1$. Indeed, an estimate similar to the one employed on page 509 yields (exercise)

$$\begin{aligned} 0 &\leq \frac{1}{2}\int d^2x \,\mathrm{tr}\,[(\partial_\mu Q + i\epsilon_{\mu\nu} Q\partial_\nu Q)(\partial_\mu Q + i\epsilon_{\mu\lambda} Q\partial_\lambda Q)] \\ &= \int d^2x \,\mathrm{tr}\,[\partial_\mu Q\ \partial_\mu Q - i\epsilon_{\mu\nu} Q\ \partial_\mu Q\ \partial_\nu Q] = \int d^2x \,\mathrm{tr}(\partial_\mu Q\ \partial_\mu Q) - 16\pi W. \end{aligned}$$

From here, we conclude that the non-topological contribution to the action obeys the inequality

$$S_0[Q] = \frac{\sigma_{11}}{8}\int d^2x \,\mathrm{tr}(\hat\partial_\mu Q\ \hat\partial_\mu Q) \geq 2\pi W \sigma_{11},$$

and that $\mathcal{Z}_n \sim \exp(-2\pi W\sigma_{11})$ is weighted by a small "energetic" factor. We have had ample opportunity to see that such factors can, in principle, be compensated for by large "entropic" counterweights. However, Pruisken has shown that, in the present context, this does not happen.

Similarly, the functional expectation values for longitudinal and Hall conductance can be organized in an instanton series:

$$\sigma_{ij} = \sum_{W=0}^{\infty} e^{2\pi i W \sigma^0_{12}}\, C^{(W)}_{ij}(\sigma^0_{11}).$$

The coefficients $C^{(W)}_{ij}$ appearing in this series depend – in the exponentially sensitive way discussed above – on the longitudinal Drude conductance. Importantly, the right-hand side of the series depends on the Drude values σ^0_{ij} while the left-hand side sets the true renormalized conductance (i.e. the second-order derivative of the functional with respect to a generalized source-vector potential). There is not much more we can say about the structure of these series except for one important symmetry criterion: under a change of orientation of the coordinate system, σ_{12} changes sign while σ_{11} does not. Specifically,

$$\sigma_{12}(B) = -\sigma_{21}(B), \quad \sigma_{11}(B) = +\sigma_{22}(B),$$

which is an example of an **Onsager relation**. Consistency with these relations requires that the topological series be of the form

$$\begin{aligned} \sigma_{11} &= \sigma^0_{11} + \delta\sigma_{11} + \sum_{W=1}^{\infty} \cos(2\pi W\sigma^0_{12})\ a^{(W)}(\sigma^0_{11}), \\ \sigma_{12} &= \sigma^0_{12} + \sum_{W=1}^{\infty} \sin(2\pi W\sigma^0_{12})\ b^{(W)}(\sigma^0_{11}), \end{aligned} \tag{9.27}$$

where $a^{(W)}$ and $b^{(W)}$ are expansion coefficients. The notation emphasizes that, in the topologically trivial sector, $W = 0$, the longitudinal conductance may be subject to renormalization while σ_{12} remains unrenormalized.[37]

In view of these structures, let us now speculate a little on the **renormalization characteristics** of the model. Here, renormalization means, as usual, that we consider the outcome of the theory on ever increasing length scales. We have to keep in mind, however, that this program must be carried out for each topological sector separately: renormalization, i.e. the successive elimination of fast fluctuations, cannot change the topological index of a field configuration. On the same footing a topological angle (presently, the coefficient σ_{12}^0 of the topological term) should not renormalize, at least not in a conventional sense. (For the cautious formulation, see below.)

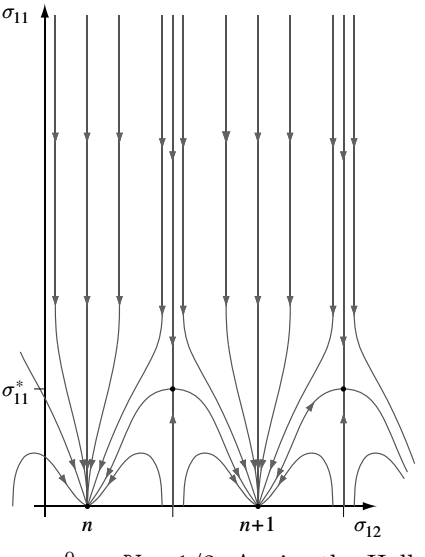

Consider, then, the flow $(\sigma_{12}(\lambda), \sigma_{11}(\lambda))$ in the two-dimensional parameter plane defined by longitudinal and Hall conductance as we increase a reference length scale λ. From Eq. (9.27) it follows that there are two families of lines on which σ_{12} does not renormalize: $\sigma_{12} = \sigma_{12}^0 \in \mathbb{N}$ and $\sigma_{12} = \sigma_{12}^0 \in \mathbb{N} + 1/2$. As to the first line, we do not expect any critical behavior in the vicinity of integer σ_{12}. (Remember that the quantum Hall transition is observed at $(\sigma_{12}, \sigma_{11}) = (\mathbb{N} + 1/2, 1/2)$.) Rather we expect that, in the vicinity of integer Hall conductances, the system behaves pretty much like an ordinary two-dimensional electron gas. This implies (cf. our discussion above) that the Goldstone modes become gapped, σ_{11} scales to 0 and σ_{12} scales to an integer value: for $(\sigma_{12}, \sigma_{11})$ close to a line $\sigma_{12} = n \in \mathbb{N}$, the system will flow towards the fixed point $(n, 0)$. A special situation arises for $\sigma_{12} = \sigma_{12}^0 \in \mathbb{N} + 1/2$. Again, the Hall conductance does not renormalize, but now we are sitting on a critical surface (namely, $E = E^*$, corresponding to half-integer Hall conductance). At the transition point, the correlation length has diverged and the system has become metallic. Accordingly we should expect the longitudinal conductance to scale towards a finite fixed point value σ_{11}^*. Indeed, experimentally, one observes $\sigma_{11}^* = \mathcal{O}(1)$ at the transition points. The two-parameter flow diagram discussed above was proposed in a seminal paper by Khmelnitskii.[38]

To theoretically understand the transition behavior, Pruisken and collaborators have derived renormalization group equations that take the lowest two topological sectors, $W =$

[37] Renormalization cannot change the prefactor of the topological term, σ_{12}^0. The contribution of the topologically trivial sector to the conductance is just this coefficient.

[38] D. E. Khmelnitskii, Quantization of Hall conductivity, *JETP Lett.* **38** (1983), 552–6.

0, 1, into account:

$$\begin{aligned}\beta_{11} &\equiv \frac{\partial\sigma_{11}}{\partial \ln L} = -\frac{1}{2\pi^2\sigma_{11}} - c\sigma_{11}e^{-2\pi\sigma_{11}}\cos(2\pi\sigma_{12}),\\ \beta_{12} &\equiv \frac{\partial\sigma_{12}}{\partial \ln L} = c\sigma_{11}e^{-2\pi\sigma_{11}}\sin(2\pi\sigma_{12}),\end{aligned} \tag{9.28}$$

where $c > 0$ is a numerical constant.[39] These equations indeed have a family of fixed points $(\sigma_{12}^*, \sigma_{11}^*)$, where $\sigma^* = \mathcal{O}(1)$ and $\sigma_{12}^* \in \mathbb{N} + 1/2$. In the vicinity of these points, σ_{12} (σ_{11}) is a relevant (irrelevant) scaling variable.

Summarizing, Pruisken's approach appears to predict a parameter flow as shown in the **two-parameter phase diagram** above. This diagram nicely conforms with experimental observations but, alas, there are some problems. For one thing, the interesting physics takes place in the vicinity of a fixed point value $\sigma_{11}^* = \mathcal{O}(1)$, well outside the regime of applicability of the σ-model as such. (Remember that the derivation of this hinges on $\sigma_{11} \gg 1$.) One may trust in the principle that "good" models (and Pruisken's model of the QHE certainly is good!) usually produce meaningful results even in parameter regimes where they no longer stand on safe ground. However, with the current problem, the chances are that this principle does not apply. Indeed, we have come across a very similar situation before: for large spin $S \gg 1$, an antiferromagnetic spin chain is described by an O(3) nonlinear σ-model. For topological angles $\theta = \pi$ (corresponding to half-integer spin) the model is critical and flows towards some strong coupling fixed point. The important observation now is that, in the vicinity of this point, the system is described no longer by an O(3) nonlinear σ-model but by an altogether different model: a field theory on the group manifold SU(2) with a topological term of Wess–Zumino–Witten type. Intriguingly, on its journey towards the strong coupling fixed point, the model manages to *enlarge* its field manifold from the coset space $\mathrm{O}(3)/\mathrm{O}(2) \simeq S^2$ of the O(3) nonlinear σ-model to the larger space $\mathrm{SU}(2) \overset{\text{locally}}{\simeq} \mathrm{O}(3)$ of the fixed point theory.

Now, when projected onto a single replica channel, Pruisken's $\sigma_{12} = 1/2$ theory indeed reduces to an O(3) nonlinear σ-model with topological angle $\theta = \pi$. It is, therefore, quite conceivable that, at strong coupling, the general model also flows towards a target model with a larger field manifold. Although nothing rigorous is known, a scenario to this effect has been outlined in the literature. At any rate, the applicability of Pruisken's RG equations in the vicinity of their fixed points remains questionable.

INFO There is one **other problem** which should not be swept under the carpet: as discussed above, the absence of Goldstone modes in the localized phase requires the coupling constant of the topological term to be integer. This coupling constant is set by the Drude conductance σ_{12}^0 and should not renormalize. In a way, we have to require that, for Fermi energies which lie between Landau levels, the Drude Hall conductance must already be integer, lest the theory run into a consistency problem. On the other hand, topological criteria do not require the physical conductance σ_{12} to be integer. This is exactly the opposite of our physical picture. We should

[39] One might have expected the topological angle σ_{12}^0, and not the physical conductance σ_{12}, as an argument of the transcendental functions (sine and cosine). For a discussion of why the physical conductance appears there, we refer to Pruisken's article (Pruisken, in *The Quantum Hall E ect*).

expect that for any value of the Drude conductance (away from $\mathbb{N} + 1/2$) the system will flow towards an integer value of the physical conductance. (This is the flow illustrated in the two-parameter flow diagram above.) Essentially, the problem boils down to the fact that the coupling constant of the topological term does not renormalize. (If it did, it should flow towards an integer value which could then justly be interpreted as the physical conductance.) To deal with this difficulty, Pruisken subjects the fields to a transformation $Q \to UQU^{-1}$, where U are the source fields introduced above, and then discusses the structure of the theory after the fields Q have been integrated out. This produces consistent results, but the procedure is highly implicit and, therefore, remains somewhat mysterious.

Summarizing, Pruisken's field theory microscopically explains many of the intriguing aspects of the quantum Hall effect. Notably, it elucidates the interplay of disorder scattering and topological mechanisms (spectral flow!) in the formation of the effect. Contrary to early expectations, though, it may well be that the actual quantum Hall transition lies outside the scope of the model. At any rate, a rigorous identification of the universality class of this transition, not to mention a quantitative calculation of its critical exponents, remains an open problem.

This concludes our discussion of θ-terms in condensed matter field theory. In our brief survey, we were unable to discuss one of the most exciting applications of θ-terms in field theory in *general*: 'tHooft's concept of θ-vacua, and its relevance to understanding some of the most intriguing observed features of matter – CP- and T-violation. (However, the energetic reader is strongly encouraged to turn to a textbook on theoretical particle physics to learn more of this subject.) Rather, we proceed now to discuss another large and important family of topological field theories.

9.4 Wess–Zumino terms

Almost every time that we met with a θ-term in the previous chapter, a field theory with a Wess–Zumino (WZ) term[40] was just around the corner. Yet most condensed matter physicists appear to be only vaguely familiar with the ideas behind WZ field theory (in contrast to, say, the much more widely appreciated concept of θ-terms). Perhaps the most important reason for this lack of appreciation is that the general meaning of a WZ term is difficult to grasp in the "traditional" languages familiar to condensed matter physicists. On the other hand, the relevant concepts become quite transparent once we venture to reformulate a few elements of field theory in the language of modern differential geometry. This reformulation will be the subject of the first half of this section. Not assuming any background knowledge, we begin with a crash course in differentiation on manifolds and exterior calculus. (Readers familiar with differential forms are invited to skip this introduction.) In Section 9.4.2 we

[40] As to the terminology of Wess–Zumino terms, there is no generally accepted convention. Historically, these topological terms first appeared in the work of Wess and Zumino. However, owing to Witten's seminal analysis of SU(N)-invariant chiral fermion systems (see below), they are often referred to as Wess–Zumino–Witten (WZW) terms. Yet another designation (especially popular in the Russian community) is Wess–Zumino–Novikov–Witten (WZNW) terms. Except for the discussion of SU(N)-symmetric systems below, we stick here to the short variant of WZ terms.

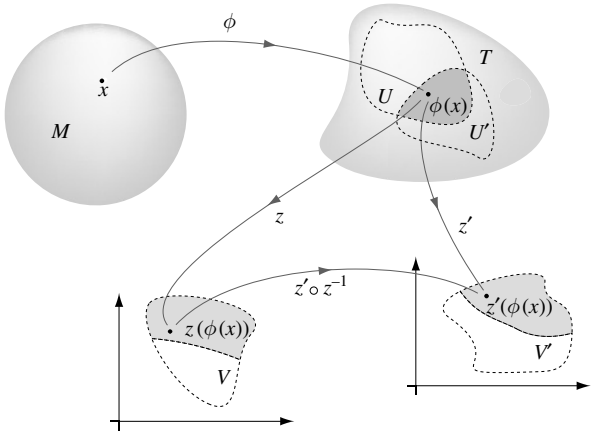

Figure 9.10 On the construction of coordinate representations of field manifolds. For a discussion, see the main text.

then explain the general ideas behind WZ field theory before we turn to the discussion of a number of interesting applications.

9.4.1 A crash-course in differential geometry

Figure 9.10 reiterates the mathematical backbone underlying most of our field theories: a field $\phi : M \to T, \mathbf{x} \mapsto \phi(\mathbf{x})$ is a mapping from a base-space M to a field space T. In practice, we mostly tend to nonchalantly identify field values $\phi \in T$ and their coordinate representations $\mathbf{z}(\phi) \in \mathbb{R}^n$ (n is the dimension of T). However, especially when it comes to the discussion of topological aspects, we must be very careful with such premature identifications. The point is that topologically non-trivial field spaces usually cannot be represented in terms of one globally defined system of coordinates. Take the sphere S^2 as an example. You may choose the standard representation in terms of two angles (θ, ϕ), a stereographic projection onto a single complex variable z, or any other parameterization. Inevitably, there will be regions on S^2 where the mapping "$S^2 \to$ coordinates" becomes ill-defined. One may object that this ambiguity, manifesting itself only at a set of "measure zero,"[41] cannot be of much practical significance. Yet, with regard to topology this is not the case.

Coordinate representations

Given the importance of these singularities in the context of topological field theory, it is pertinent this time to discuss the construction of proper coordinate representations with mathematical rigor: the basis of each coordinate system is formed by a system of open

[41] For example, in a system of polar coordinates, the problematic region is a *line* connecting the north and the south pole of the sphere.

subsets $U_i \subset T$ chosen so that the union $\bigcup_i U_i = T$ covers T.[42] One next defines coordinate mappings $z_i : U_i \to V_i \subset \mathbb{R}^n$ from the patches U_i onto some open subsets V_i of $\mathbb{R}^n$. The value $z_i(p) \in \mathbb{R}^n$ is a coordinate representation of the point $p \in T$. To make this representation unique, we require the z_is to have an inverse.

The central point is that, on our manifold, there will be non-vanishing overlaps $U_i \cap U_j \neq \{\}$, i.e. points $p \in T$ that have more than one coordinate representation (see Fig. 9.10). Ambiguities between the different systems are excluded by requiring that the maps $z_i \circ z_j^{-1} : z_j(U_i \cap U_j) \to z_i(U_i \cap U_j)$ be diffeomorphisms (invertible and differentiable). Conceptually, the functions $z_i \circ z_j^{-1}$ mediate the change between different coordinates. This being so, they must be as benign (differentiable) as possible. Notice, however, that it would be senseless to require the z_is themselves to be differentiable, simply because in general $T \not\subset \mathbb{R}^n$ and the notion of differentiability need not even exist on T.

In the jargon of differential geometry, the coordinate maps z_i are called **charts** of T while a fully covering collection $\{z_i\}$ is called an **atlas**. The existence of a proper atlas is, by definition, equivalent to the statement that T is a differentiable manifold.

Example Consider $T = S^1$, the unit circle. The one-dimensional manifold S^1 has a natural embedding into $\mathbb{R}^2 : S^1 = \{\mathbf{x} \in \mathbb{R}^2 | \mathbf{x}^2 = 1\}$. We need a minimum of two charts to cover S^1. For example, one may use

$$\begin{aligned} z^{-1} : (0, 2\pi) &\to S^1, \quad z^{-1}(\phi) = (\cos(\phi), \sin(\phi)), \\ z'^{-1} : (0, 2\pi) &\to S^1, \quad z'^{-1}(\phi) = (\cos(\phi + \pi), \sin(\phi + \pi)); \end{aligned}$$

z/z' cover all of S^1 except for the points $(1, 0)/(-1, 0)$.

Tangent space

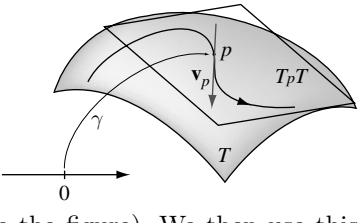

Having discussed the coordinate representations of (field) manifolds, we are now in a position to lift elements of standard calculus (differentiation, integration, etc.) from $\mathbb{R}^n$ to manifolds. (Later, we identify topological terms as integrals over certain differentials on T.) We begin by introducing the tangent space T_pT as a locally flat approximation to the manifold T at a point $p \in T$ (see the figure). We then use this planar approximation to describe how functions defined on T vary in the neighborhood of p. To construct the tangent space, consider a curve $\gamma : \mathbb{R} \to T$ with $\gamma(0) = p$. It is tempting (see the figure) to define a vector $\mathbf{v}_p$ tangent to T at p by setting $\mathbf{v}_p \stackrel{?}{\equiv} d_s\gamma(s)|_{s=0}$. However, this "definition" is problematic because, in general, $T \not\subset \mathbb{R}^m$, so that $\mathbf{v}_p$ is not a decent vector. Nonetheless, the idea above is not far from the truth. To make it suitable, let us consider some function $f \in \mathcal{C}(U)$ defined on an open neighborhood $U \ni p$. (Here, $\mathcal{C}(X)$

[42] Of course, one can exercise much freedom in the choice of the U_is. For example, for the sphere, one might define $U_{1,2}$ to be any two overlapping "caps" whose union covers T. Notice that overlaps are, in fact, unavoidable as we want to cover a compact set T by open subsets U_i.

denotes the space of smooth, real-valued functions defined on X.) We may then employ our curve γ to compute the directional derivative

$$\mathbf{v}_p^\gamma(f) \equiv d_s|_{s=0} f(\gamma(s)).$$

The notation on the right-hand side indicates that we have constructed a mapping that takes functions as arguments and produces a number.[43] We next define this mapping to be a **tangent vector** at point p. (Notice that the assignment "curve $\mapsto$ tangent vector" constructed in this way is not unique: two curves γ_1 and γ_2 tangent[44] to each other at p will produce the same directional derivative, $\mathbf{v}_p^{\gamma_1} = \mathbf{v}_p^{\gamma_2}$.) The set of all directional derivatives formed in this way defines the **tangent (vector) space** T_pT at point p.[45]

The definition of "vectors" given above may seem strange. (If you wait a while, its utility will become apparent!) However, given a coordinate function z we can meet the standard identification "vector $\leftrightarrow$ n-component object" familiar from linear algebra. This is achieved by writing

$$\mathbf{v}^\gamma(f) = d_s|_{s=0} f(z^{-1} \circ z \circ \gamma(s)) \equiv \sum_{i=1}^{n} \partial_i f \, v_i^\gamma,$$

where $\partial_i f \equiv \partial_i (f \circ z^{-1})$ is the ordinary partial derivative of the function $f \circ z^{-1} : V \subset \mathbb{R}^n \to \mathbb{R}$ and $v_i^\gamma \equiv d_s|_{s=0} z^i(\gamma(s))$. We define $v_i^\gamma \in \mathbb{R}$ to be the ith component of $\mathbf{v}^\gamma$ (in the coordinate representation defined by z). Notice that the **components of a tangent vector** v_i can alternatively be obtained as

$$\boxed{v_i = \mathbf{v}(z^i),}$$

i.e. as the directional derivative of the ith component of the coordinate function. (Here, we have simplified the notation by omitting the superscript reference to the curve γ.) Relatedly, a coordinate system induces a natural **basis of the tangent space**, T_p. This, is defined by

$$\boxed{\forall f \in \mathcal{C}(U)\colon \ \mathbf{e}_i(f) \equiv \partial_i f.}$$

Suppose that the reference point p is represented by two coordinate functions z and z'. It is then straightforward to verify (exercise!) that the components of the tangent vector transform as $v_i^\gamma = \sum_j \frac{\partial z^i}{\partial z'_j} v_j'^\gamma$.

EXERCISE Compute the basis vectors $\mathbf{e}$ and $\mathbf{e}'$ corresponding to the two charts forming the atlas of S^1 discussed on page 538. Show that $\mathbf{e} = \mathbf{e}' = \mathbf{e}_\phi$ where $\mathbf{e}_\phi$ is the azimuthal vector of a two-dimensional polar coordinate system, and the natural embedding of S^1 into $\mathbb{R}^2$ is understood.

[43] A purist might object that $\mathbf{v}_p^\gamma(f)$ is just what we had earlier defined to be a function*al*, so that we should use square brackets $[f]$ for the argument. However, following standard convention in differential geometry, we shall here stick to (f).

[44] In differential geometry, one uses this criterion to *de ne* the notion of tangency: two curves $\gamma_{1,2}$ through p are tangent to each other (with the same tangent velocity) if, for all functions f, $\mathbf{v}_p^{\gamma_1}(f) = \mathbf{v}_p^{\gamma_2}(f)$.

[45] Mathematically, T_pT is isomorphic to the space of all equivalence classes of curves through p, where two curves are called "equivalent" if they are tangent to each other.

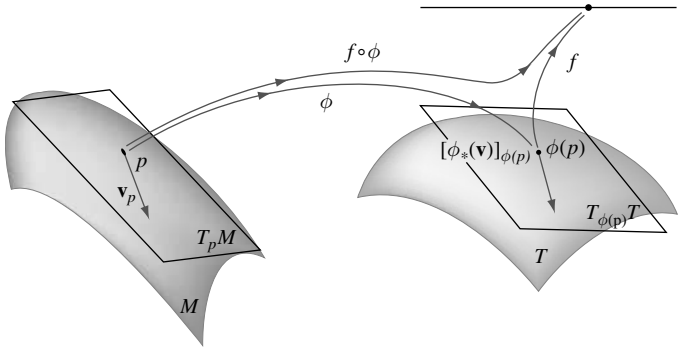

Figure 9.11 On the definition of the tangent mapping. For a discussion, see the main text.

The union $TT \equiv \bigcup_{p\in T} T_pT$ of all local tangent spaces is called the **tangent bundle** of the manifold T.[46] In fact, the tangent bundle is a differentiable manifold by itself. Its elements are given by $(p, \mathbf{v}_p) \in TT$, where $p \in T$ and $\mathbf{v}_p \in T_pT$. (The dimension of TT is given by $2n$, twice the dimension of T.) A mapping

$$\begin{aligned} \mathbf{v} : T &\rightarrow TT, \\ p &\mapsto (p, \mathbf{v}_p), \end{aligned}$$

smoothly assigning to each point of T a tangent vector is called a **vector field** on T.

Now, suppose we are given two manifolds M and T. (Later on, the role of M will be played by the base space of field theory, a differential manifold by itself.) Further, suppose that there is a mapping (the field!) $\phi : M \rightarrow T$. The definition of tangent spaces above then implies the existence of an induced mapping, the so-called **tangent mapping**,

$$\begin{aligned} \phi_* : TM &\rightarrow TT, \\ \mathbf{v} &\rightarrow \phi_*(\mathbf{v}). \end{aligned}$$

The image vector $(\phi_*(\mathbf{v}))_p$ is defined by setting $(\phi_*(\mathbf{v}))_p(f) \equiv \mathbf{v}_{\phi^{-1}(p)}(f \circ \phi)$, for any function defined in a neighborhood of $p \in T$ (see Fig. 9.11). Suppose we are given a system of coordinates w around $p \in M$ and z around $\phi(p) \in T$. It is then straightforward to show that the coordinate representation of the vector $(\phi_*(\mathbf{v}))_p$ is given by

$$\boxed{(\phi_*(\mathbf{v}))^i_p = \frac{\partial \phi^i}{\partial w^j}\, \mathbf{v}^j_{\phi^{-1}(p)},} \tag{9.29}$$

where $\phi^i = z^i(\phi)$ is a shorthand for the coordinate representation of ϕ. The formula above explains why the mapping ϕ_* is sometimes referred to as the differential of the mapping ϕ. It illustrates the general rule that everything taking place on the tangent spaces is a measure of local (or "infinitesimal") variations.

[46] The authors hate the double-T notation TT, too. However, the prefix T for tangent is a ubiquitous standard, and we want to keep emphasizing that the apparatus introduced here will be later applied to the target manifolds of field theory, T.

Di erential forms

A **1-form** ω_p is a linear mapping $\omega_p : T_pT \to \mathbb{R}$ (i.e. an element of the dual space of the vector space T_pT). Smoothly extending ω_p to a map ω globally defined on TT, we obtain a so-called **differential 1-form** (or, for brevity, just the 1-form). We will denote the space of 1-forms on T by $\Lambda^1(T)$. A number of important remarks on these definitions are in order:

▷ Most 1-forms that we shall encounter in practice are realized as **differentials of functions**: for $f \in \mathcal{C}(T)$ we define the differential df by

$$\boxed{df_p(\mathbf{v}_p) \equiv \mathbf{v}_p(f).}$$

(Exercise: Convince yourself that, for manifolds $T \subset \mathbb{R}^n$, this reduces to the standard definition of the differential with which you are familiar.)

▷ However, not every 1-form is a differential of a function. Consider, for example, the tangent basis of $T = S^1$ constructed in the exercise on page 539. Let us define a 1-form by setting $\omega(\mathbf{e}) = \omega(\mathbf{e}') = 1$, where the equality holds in the domain of overlap of the two charts. This 1-form cannot be represented as the differential of a single-valued function on S^1 (exercise: why?).

▷ Finally, let us make a formal remark: for reasons that will become clear in a moment, functions $f \in \mathcal{C}(T) \equiv \Lambda^0(T)$ are sometimes referred to as 0-**forms**. Technically, a 1-form is a mapping

$$\begin{aligned} \omega : TT &\to \Lambda^0(T), \\ \mathbf{v} &\to \omega(\mathbf{v}), \end{aligned}$$

that maps vector fields onto 0-forms. The value of the function $\omega(\mathbf{v})$ at a point p is given by $\omega(\mathbf{v})(p) = \omega_p(\mathbf{v}_p)$. Alternatively, we can say that the insertion of a vector field into a 1-form lowers the degree of the form from 1 down to 0.

Given a system of local coordinates, z, each 1-form can be represented as

$$\omega = f_i \, dz^i, \tag{9.30}$$

where the coefficient-functions are given by $f_i = \omega(\mathbf{e}_i)$ (a result that is instructive to check).

A 1-form maps a single vector field onto a function. However, to describe the geometric structure of a manifold (distances, surface and volume elements, etc.) we need mappings that take more than one vector field as input. Mappings of this type are called tensors and defined as follows: a **covariant tensor** of rank r is a multi-linear mapping

$$\begin{aligned} \omega : \underbrace{TT \times \cdots \times TT}_{r} &\to \Lambda^0(T), \\ (\mathbf{v}_1, \ldots, \mathbf{v}_r) &\mapsto \omega(\mathbf{v}_1, \ldots, \mathbf{v}_r). \end{aligned}$$

For example, some manifolds admit the definition of a **metric**. A metric g is a tensor of rank 2 that is positive ($\forall p \in T : g_p(\mathbf{v}_p, \mathbf{v}_p) > 0$) and non-degenerate ($\forall \mathbf{w}_p : g_p(\mathbf{v}_p, \mathbf{w}_p) = 0 \Rightarrow \mathbf{v}_p = 0$). A manifold with a metric is called a **Riemannian manifold**. We call $\sqrt{g_p(\mathbf{v}_p, \mathbf{v}_p)}$ the **length** of the tangent vector $\mathbf{v}_p$. For later reference, we note that, in a system of local

coordinates, g has the representation $g = g_{ij} dz^i \otimes dz^j$. Here, $g_{ij} = g(\mathbf{e}_i, \mathbf{e}_j)$ is the **metric tensor** of the manifold.

EXERCISE Show that, in polar coordinates (r, θ, ϕ), the standard metric of $\mathbb{R}^3$, $g = dx_1 \quad dx_1 + dx_2 \quad dx_2 + dx_3 \quad dx_3$, assumes the form

$$g = dr \quad dr + r^2 d\theta \quad d\theta + r^2 \sin^2\theta \; d\phi \quad d\phi. \tag{9.31}$$

However, by far most important in practical applications are tensors that are fully antisymmetric in their arguments: a p-**form** ω is a tensor that changes sign under odd permutations of its arguments: $\omega(\mathbf{v}_{S(1)}, \ldots, \mathbf{v}_{S(p)}) = \mathrm{sgn}(S)\omega(\mathbf{v}_1, \ldots, \mathbf{v}_p)$, where S is an element of the permutation group. The space of all p-forms on T is denoted by $\Lambda^p(T)$. Given a p-form ω and a q-form ξ we can produce a $(p+q)$-form $\omega \wedge \xi$ by the following rule:

$$\boxed{(\omega \wedge \xi)(\mathbf{v}_1, \ldots, \mathbf{v}_{p+q}) \equiv \frac{1}{p!q!} \sum_S \mathrm{sgn}(S)\, \omega(\mathbf{v}_{S(1)}, \ldots, \mathbf{v}_{S(p)})\, \xi(\mathbf{v}_{S(p+1)}, \ldots, \mathbf{v}_{S(p+q)}).}$$

The operation $\wedge : \Lambda^p(T) \times \Lambda^q(T) \to \Lambda^{p+q}(T)$ is called the **exterior product** of forms. (In passing we note that $\wedge$ defines the product of the **Grassmann algebra** $\Lambda(T) \equiv \bigoplus_{p=0}^{\infty} \Lambda^p(T)$ which we met already briefly in Section 4.1.)

EXERCISE Verify the following features: (a) $\omega \quad \omega = 0$ if $\omega \in \Lambda^p$ and p is odd, (b) $\omega \quad \xi = (-)^{pq} \xi \quad \omega$, and (c) $\omega \quad (\xi \quad \eta) = (\omega \quad \xi) \quad \eta$, permitting us to write just $\omega \quad \xi \quad \eta$ without brackets.

Given a coordinate function z, each p-form has the unique **coordinate representation**

$$\boxed{\omega = \frac{1}{p!} \omega_{i_1, \cdots, i_p} dz^{i_1} \wedge \cdots \wedge dz^{i_p},} \tag{9.32}$$

where $\omega_{i_1, \ldots, i_p} = \omega(\mathbf{e}_{i_1}, \ldots, \mathbf{e}_{i_p})$. To see this, notice that our definition of the exterior product above implies that $(df_1 \wedge \cdots \wedge df_p)(\mathbf{v}_1, \ldots, \mathbf{v}_p) = \sum_S \mathrm{sgn}(S)\, df_1(\mathbf{v}_{S(1)}) \cdots df_p(\mathbf{v}_{S(p)})$. Also notice that the coefficients $\omega_{i_1, \ldots, i_p}$ are antisymmetric under odd exchange of the indices i_j. This being so, Eq. (9.32) can alternatively be written as

$$\omega = \omega_{I_1, \ldots, I_p} dz^{I_1} \wedge \cdots \wedge dz^{I_p},$$

where, by convention, summations over capitalized indices are ordered, $I_1 < I_2 < \cdots < I_p$.

Above we have seen that, computing the differential of a 0-form $f \in \Lambda^0(T)$, we are led to a 1-form $df \in \Lambda^1(T)$. This principle can be generalized to forms of arbitrary degree: let us define the **exterior derivative** d by setting

$$\boxed{d\omega \equiv \partial_j \omega_{I_1, \ldots, I_p} dz^j \wedge dz^{I_1} \wedge \cdots \wedge dz^{I_p},} \tag{9.33}$$

where the coordinate representation Eq. (9.32) is understood. Obviously, $d\omega \in \Lambda^{p+1}(T)$, i.e. d can be interpreted as an operator on $\Lambda(T)$ that raises the degree of forms by one. However, mathematically inclined people will object that it is unclear whether Eq. (9.33), an equation based on a specific coordinate representation, really represents a proper definition (i.e., is

it clear that the same rule, applied to a different coordinate representation of ω, leads to the same form $d\omega$?). These worries are addressed in the following exercise.

EXERCISE Show that (a) the definition Eq. (9.33) does not depend on the choice of coordinates, (b) $d^2 = 0$, and (c) $d(\omega \quad \xi) = d\omega \quad \xi + (-)^p \omega \quad d\xi$, where p is the degree of ω.

In the following, two subspecies of differential forms will be of particular interest for us: we call a differential form $\omega \in \Lambda^p(T)$ **closed** if $d\omega = 0$. Conversely, ω is called **exact** if $\omega = d\xi$, i.e. if ω is obtained as the exterior derivative of some $(p-1)$-form ξ. Now, owing to the identity $d^2 = 0$, every exact form is closed. Yet not every closed form is exact.

EXERCISE Consider the 1-form ω on S^1 discussed on page 541. Since $\omega(\mathbf{e}) = \omega(\mathbf{e}') = 1$, ω has the local (i.e. restricted to individual charts) representation $\omega = d\phi$ or $\omega = d\phi'$. (The coordinates are those introduced on page 538.) Obviously, ω is closed. On the other hand, we have seen that there is no 0-form (function) f such that $\omega = df$; ω is not exact.

The classification of forms that are closed but not exact is a deep mathematical problem (the subject of **cohomology theory**). We shall return to this issue below when we discuss the geometry of topological terms. However, before doing so, we need to introduce one last concept of basic differential geometry. Previously, we have seen that a mapping $\phi : M \to T$ between two manifolds induced a mapping ϕ_* from the vector fields on M to those on T. In a very similar manner, ϕ gives rise to a mapping ϕ^* between forms on the two manifolds. This so-called **pullback** is defined by

$$\begin{aligned} \phi^* : \Lambda(T) &\to \Lambda(M), \\ \omega &\mapsto \phi^*(\omega) \equiv \omega \circ \phi_*. \end{aligned}$$

For example, for a 1-form $\omega \in \Lambda(T)$ and $\mathbf{v} \in TM$, we have $[\phi^*(\omega)](\mathbf{v}) = \omega(\phi_*(\mathbf{v}))$, etc. Notice that ϕ^* maps in a direction opposite to that of ϕ, hence the name "pullback."

In a system of local coordinates z and w on M and T, respectively, the components of the 1-form $\phi^*(\omega)$ are given by

$$\phi^*(\omega)_i = [\phi^*(\omega)](\mathbf{e}_i) = \omega(\phi_*(\mathbf{e}'_i)) \overset{(9.29)}{=} \omega\left(\frac{\partial \phi^k}{\partial z^i}\mathbf{e}_k\right) = \frac{\partial \phi^k}{\partial z^i}\omega_k,$$

where $\{\mathbf{e}'_i\}$ is a basis of T.

EXERCISE Check that the **coordinate representation of the pullback** of a p-form is given by

$$\phi^*(\omega)_{I_1,\ldots,I_p} = \det\left(\frac{\partial \phi^{J_1}, \ldots, \partial \phi^{J_p}}{\partial z^{I_1}, \ldots, \partial z^{I_p}}\right) \omega_{J_1,\ldots,J_p}.$$

Also verify the useful formula $\phi^*(\omega \quad \xi) = \phi^*\omega \quad \phi^*\xi$, and the commutativity $\phi^* \circ d = d \circ \phi^*$ of a pullback on an exterior derivative. (If you feel exhausted, just verify that $\phi^* d\omega = d(\phi^*\omega)$ holds when applied to forms $\omega \in \Lambda^{0,1}(T)$. The general proof proceeds along similar lines but is a bit more cumbersome.)

Indeed, the pullback of forms is a very important operation since it enables us to define ...

Integration on manifolds

Consider a **top-dimensional form** $\omega \in \Lambda^n(T)$, i.e. a form whose rank is equal to the dimensionality of T. To begin with, let us assume that $\mathrm{supp}(\omega) \subset U$ (i.e. $\omega_{p \notin U} = 0$), where $U \subset T$ is the domain of definition of a chart z. We then define the **integral** of ω over U as

$$\boxed{\int_U \omega \equiv \int_V z^{-1}\omega.} \tag{9.34}$$

To make this definition somewhat less abstract, notice that ω can be represented as

$$\omega = f dz_1 \wedge \cdots \wedge dz_n,$$

where f is a function on T (exercise: why?). The definition above then assumes the form

$$\int_U f(x) dz^1 \wedge \cdots \wedge dz^n = \int_V f(z) dz^1 \wedge \cdots \wedge dz^n \equiv \int_{V,\text{Riemann}} f(z) dz^1 \cdots dz^n.$$

Here, we have used the fact that $z^{-1}(f(x)dz^1 \wedge \cdots \wedge dz^n) = f(x(z))dz^1 \wedge \cdots \wedge dz^n$.[47] In the (crucial) second equality, we declare the integral over the product of forms $dz^1 \wedge \cdots \wedge dz^n$ in $V \subset \mathbb{R}^n$ to be the ordinary Riemann integral. This identification is meaningful because $(dz^1 \wedge \cdots \wedge dz^n)(\mathbf{v}_1, \ldots, \mathbf{v}_n)$ measures the volume of the parallelepiped spanned by the vectors $\mathbf{v}_1, \ldots, \mathbf{v}_n$ (in the standard metric of $\mathbb{R}^n$), i.e. it represents a sensible "volume element."[48]

To make the definition of the integral complete, we would have to discuss its extension to a **global integral over the manifold**. However, for practical reasons we shall not do so: for one thing, we are often enough dealing with manifolds T that admit a 1-chart atlas, in which case the definition above is sufficient. Only slightly worse is the situation where T can be covered by a single chart *except* for isolated singular points. (This is the case with, e.g., $T = S^1, S^2$ – exercise: why?) Since the integral is oblivious to "sets of measure 0," an integral over the domain of integration of such "nearly complete" charts is as good as an integral over all of T; again, the definition above does the job. In the rare cases where one is dealing with an unpleasant manifold which does not belong to the two species above, one has to work harder and split up the support of the integrand by means of a so-called "partition of unity." However, in view of the relative rarity of such cases, and the fact that they are dealt with in every textbook on differential geometry, we limit attention to the "local" definition above.

[47] Do not be confused by the appearance of the same symbols $dz^1 \wedge \cdots$ on both sides of the equations. On the left-hand side, dz^i is referring to the differential of the ith coordinate function $z^i : T \to \mathbb{R}$. On the right-hand side, $z^i : \mathbb{R}^n \to \mathbb{R}$ simply projects a vector onto its ith component.

[48] However, the discussion above sweeps one subtlety under the carpet: under a change of coordinates, $z \to w$, $\omega = f(z)dz^1 \wedge \cdots \wedge dz^n \to f(z(w)) \det(\partial z/\partial w)\ dw^1 \wedge \cdots \wedge dw^n$. Compatibility with the transition behavior of integration volume elements, $dz^1 \cdots dz^n \to |\det(\partial z/\partial W)|\, dw_1 \cdots dw_n$, requires $\det(\partial z/\partial W) > 0$. Coordinate systems with this property are said to have the same **orientation**. A manifold with an atlas of identically oriented charts is said to be **orientable**. (A prominent counterexample is presented by the Möbius strip.) The definition of the integral above implies that we have chosen a definite orientation.

For future reference, we remark that, if $\phi : T_1 \supset U_1 \to U_2 \subset T_2$ is a diffeomorphism between open subsets U_1 and U_2 of two manifolds T_1 and T_2, then

$$\int_{U_2} \omega = \int_{U_1} \phi^* \omega. \tag{9.35}$$

This is the generalization of the transformation law familiar from calculus to the integration on manifolds. (To understand this equation, notice that, if $z : U_2 \to V$ is a chart of U_2, then $z \circ \phi : U_1 \to V$ is one of U_1. The statement made by Eq. (9.35) then follows from Eq. (9.34).)

With the phalanx of definitions above, we are now – at last! – in a position to discuss the utility of differential forms in topological field theory.

9.4.2 From θ- to Wess–Zumino terms

In Section 9.3, we have seen that, more often than not, the topological phase associated with non-vanishing "winding numbers" could be given a representation in terms of an action S_{top}. However, no guidelines as to existence or non-existence of such representations have been given. We begin by discussing some principles behind the formulation of topological Lagrangian densities. This will bring us to a position where the connection to Wess–Zumino terms can be established.

The geometry of θ-terms

Let us first observe that most target manifolds T of topologically non-trivial field theories are Riemannian, i.e. come with a natural metric g. This may be the case because $T \subset \mathbb{R}^m$ is embedded into some $\mathbb{R}^m$ and inherits the natural metric of the latter (e.g. $S^2 \subset \mathbb{R}^3$, etc.); or because $T = G/H$ is a coset space of Lie groups[49] (a situation characteristic of problems with spontaneous symmetry breaking); or, indeed, for some other reason.

Most important is the fact that a metric g entails the existence of a canonical top-dimensional form ω on T. Here, the attribute "canonical" means the following: locally, each top-dimensional form can be represented as $\omega = f(z) dz^1 \wedge \cdots \wedge dz^n$, where $z^i, i = 1, \ldots, n$, are coordinate functions, n is the dimension of T, and f is some function. In general, the form of f depends on the choice of coordinates and cannot be globally specified. However, on a Riemannian manifold, a canonical n-form with coordinate-invariant definition exists. To see this, let $g_{ij} dz^i \otimes dz^j$ be the metric. Further, let us define

$$\omega = \sqrt{g} dz^1 \wedge \cdots \wedge dz^n, \tag{9.36}$$

where $g = \det\{g_{ij}\}$ is the determinant of the metric tensor. What makes ω special is that it has the same representation Eq. (9.36) in every coordinate system.[50]

[49] Remember that a Lie group is a manifold with the additional structure of a group. As shown in textbooks of group theory, the group structure induces a metric.

[50] To see this, recall that, under a change of coordinates $z \to W$, $dz^1 \wedge \cdots \wedge dz^n \to \det A^{-1}\, dw^1 \wedge \cdots \wedge dw^n$, where $A = (\partial w / \partial z)$. At the same time, $g_{ij} \to (A^T g A)_{ij}$, i.e. $g^{1/2} \to \det A g^{1/2}$. The two determinants cancel each other, so that ω remains form invariant.

The n-form ω is called the **volume element** of the manifold[51] and $V_T \equiv \int_T \omega$ is the volume of the (compact) Riemannian manifold T. Without loss of generality, we can set our unit of length so that $V_T = 1$.

EXERCISE For $d = 3$ and the metric Eq. (9.31), show that ω assumes the familiar form $\omega = \frac{1}{4\pi} r^2 \sin\theta \, dr \quad d\theta \quad d\phi$ proportional to the three-dimensional volume element in polar coordinates.

We now claim that, for base and field manifolds of equal dimensionality $\dim M = \dim T = d$,

$$\boxed{S_{\text{top}}[\phi] = i\theta \int_M \phi^* \omega,} \tag{9.37}$$

defines a **coordinate invariant representation of the -term**. To get warmed up to this abstract representation, we first note that $\phi^*\omega$ is a top-dimensional form on M, i.e. we really have something to integrate and the notation makes sense. Now, let us consider a trivial field configuration $\phi_0(x \in M) = \text{const}$. In this case, $\phi_0^*\omega = 0$ (exercise: why?) and $S_{\text{top}}[\phi_0] = 0$, as one should expect. Next, let us assume that $\phi = \phi_1$ is a diffeomorphic (1-1 and differentiable) covering of T. (The presumed existence of such a mapping amounts to the statement that we are dealing with a topologically non-trivial field theory.) In this case, the transformation law Eq. (9.35) holds and we get

$$S_{\text{top}}[\phi_1] = i\theta \int_M \phi_1^* \omega \overset{(9.35)}{=} i\theta \int_T \omega = 1 \times i\theta.$$

Now consider a mapping ϕ_n that covers T W times (i.e. every point $p \in T$ is the image of W points $x_{1,\ldots,W} \in M$). One can show that $S_{\text{top}}[\phi_W] = iW\theta$, i.e. S_{top} indeed counts the winding number of fields ϕ. Rather than giving the proof of this statement for general W, let us consider a simple example. Let $M = T = S^2$ and $\phi_W(\phi, \theta) = (W\phi, \theta)$.[52] Then, $\omega = \sin\theta \; d\theta \wedge d\phi$, and (check!) $\phi_W^*\omega = W \sin\theta \; d\theta \wedge d\phi$. We thus obtain $V_{S_2} = 4\pi$ and $i\theta \int_M \phi_W^*\omega = iW\theta$, in agreement with the general rule.

EXERCISE Let $n_i : S^2 \to \mathbb{R}, i = 1, 2, 3$, be the ith component of the unit vector defining a point $p \in S^2$. We consider the 2-form $\omega = \mathbf{n} \cdot (d\mathbf{n} \quad d\mathbf{n}) \equiv \epsilon^{ijk} n_i dn_j \quad dn_k$. Using the standard polar coordinate representation $n_i = n_i(\theta, \phi)$, show that ω can alternatively be represented as $\omega = \sin\theta \; d\theta \quad d\phi$, which is the familiar volume element on the sphere (upon choosing an orientation so that $z^{-1*}(d\theta \quad d\phi) = d\theta \, d\phi$). Considering a field $\mathbf{n} : (x, y) \mapsto \mathbf{n}(x, y)$ show that

$$\int_M \mathbf{n}^* \omega = \int_M \mathbf{n} \cdot (\partial_x \mathbf{n} \times \partial_y \mathbf{n}) dx \quad dy, \tag{9.38}$$

which we identify (again, for a definite orientation) with our earlier representation of the θ-term of a field theory with S^2-valued fields.

[51] To motivate this terminology, consider a basis in which the metric tensor $g_{ij} = g_i \delta_{ij}$ is diagonal. The volume spanned by the (mutually orthogonal) tangent vectors $\mathbf{e}_1, \ldots, \mathbf{e}_n$ is then simply given by the product of their lengths, i.e. by $\prod_{i=1}^{N} \sqrt{g}_i = \sqrt{g}$. This is precisely what we get when we evaluate $\omega(\mathbf{e}_1, \ldots, \mathbf{e}_n)$, i.e. the form ω measures the volume of the domain spanned by its arguments.

[52] Here we have adopted the usual abuse of notation; in principle we should write $(z \circ \phi_W \circ z'^{-1})(\phi, \theta) = (W\phi, \theta)$, where z and z' are polar coordinate charts on M and T respectively.

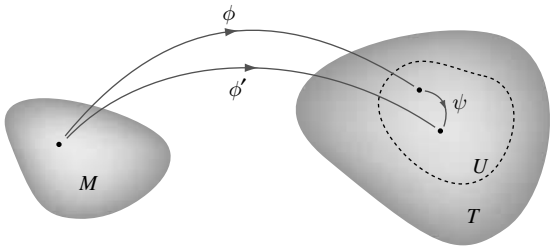

Figure 9.12 On the insensitivity of the integral representation Eq. (9.37) under field variations. For a discussion, see the main text.

The discussion above shows that, when evaluated on certain reference configurations ϕ_W, the integral Eq. (9.37) yields the winding number W. To complete the identification with our earlier representations of the θ-term, we have to show that Eq. (9.37) does not change under continuous distortions of ϕ_W (i.e. that it responds to the topological sector, and nothing else). Readers not content with our assertion that this is the case may wish to navigate through the following argument (which, as a byproduct, nicely illustrates the power of geometric methods in topological field theory).

INFO To show the invariance of Eq. (9.37) under continuous field deformations, let us consider two field configurations ϕ and ϕ' which can be continuously deformed into each other. More specifically, we set $\phi' = \psi \circ \phi$, where $\psi : T \to T$ is different from unity only inside the domain $U \supset T$ of some chart, see Fig. 9.12. (This is no serious restriction as, by iterative deformations of this type, any field configuration continuously deformable into ϕ can be reached.)

We then have

$$S_{\rm top}[\phi] - S_{\rm top}[\phi'] = i\theta \int_M (\phi^*\omega - (\psi\circ\phi)^*\omega) = i\theta \int_M \phi^*(\omega - \psi^*\omega).$$

Now $\omega - \psi^*\omega \in \Lambda^d(T)$ is a d-form on T, different from unity only locally (inside U). This implies its exactness, i.e. the existence of a representation $\omega - \psi^*\omega = d\kappa$, where $\kappa \in \Lambda^{d-1}(T)$.[53] We thus find

$$S_{\rm top}[\phi] - S_{\rm top}[\phi'] = i\theta \int_M \phi^* d\kappa = i\theta \int_M d(\phi^*\kappa) = i\theta \int_{\partial M} \phi^*\kappa = 0,$$

where, in the second equality, we have used the general commutativity of the exterior derivative and pullback and, in the third equality, Stokes' theorem (for a reminder, see below). In the fourth equality we have assumed that, on the boundary ∂M of the base manifold (physically, infinity), the fields $\phi|_{\partial M}$ approach a constant, so that $\phi^*\kappa = 0$.

The representation Eq. (9.37) sheds some light on the structure of θ-terms on Riemannian[54] field manifolds. However, this was, of course, not the only reason for maneuvering

[53] The reason is that, locally, $\omega - \psi^*\omega$ has a coordinate representation $\omega - \psi^*\omega = f dz_1 \wedge \cdots \wedge dz_n$. With the *ansatz* $\kappa = g dz_2 \wedge \cdots \wedge dz_n$, the equation $d\kappa = \omega - \psi^*\omega$ reduces to the differential equation $\partial_1 g = f$ (if the special role ascribed to the coordinate direction 1 is irritating, notice that κ is not uniquely defined; every $\kappa' = \kappa + \eta$ with a closed ($d\eta = 0$) form η will do the job just as well), defined on some open interval of x_1 (for fixed $x_2, \ldots, x_n$). This is an ordinary differential equation which can be solved.

[54] In fact, all we need to formulate the construction above is a canonical top-dimensional form, i.e. none of our arguments above actually relied on the fact that, in Riemannian geometry, this form happens to be the

through the geometric constructions above. Our prime reason for introducing the invariant formulation is that it contains the key to understanding the connection to Wess–Zumino terms.

The geometry of Wess–Zumino terms

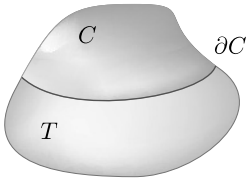

In this section, we discuss the general geometric principle common to all Wess–Zumino (WZ) terms. We then explore how our previous sporadic encounters with WZ field theories fit into this scheme and discuss a few more applications. Note that θ-terms appear in theories whose field manifold and base manifold are of equal dimensionality: $\dim M = \dim T$. In contrast, WZ terms are at home in field theories with $\dim M = \dim T - 1$.[55] How can a topological term be constructed that relies on this dimensional relation? As we shall see in a moment, the key to the answer lies in **Stokes' theorem**:

$$\boxed{\int_C d\omega = \int_{\partial C} \omega.} \tag{9.39}$$

Here, $C \subset M$ is a benign (smooth, orientable, etc.[56]) subset of a differentiable manifold M, ∂C is its boundary, and $d\omega \in \Lambda^n(M)$ is top-dimensional on M (see figure).

INFO The proof of Eq. (9.39) is beyond the scope of our present discussion and we have to refer to textbooks on differential geometry. Nonetheless, a few **remarks for readers not familiar with Stokes theorem** may be helpful. First note that ∂C is a manifold by itself, with $\dim \partial C = n-1$. Thus, ω is top-dimensional on ∂C and can be integrated. To gain some insight into the substance of Eq. (9.39) let us consider a few special cases. For example, let M be a three-dimensional manifold, $n = 3$. Consider the two-form $\omega = v_1 dx_2 \quad dx_3 + v_2 dx_3 \quad dx_1 + v_3 dx_1 \quad dx_2$ and interpret the coefficients $v_i = v_i(\mathbf{x})$ as the components of a three-dimensional vector field $\mathbf{v} = (v_1, v_2, v_3)$. With $d\omega = \operatorname{div} \mathbf{v}\, dx_1 \quad dx_2 \quad dx_3 \equiv \operatorname{div} \mathbf{v}\, dV$ and the identification $\omega = \mathbf{v} \cdot d\mathbf{S}$, where $d\mathbf{S}$ is the two-dimensional "surface element," we obtain the standard representation of **Gauss law**

$$\int_M dV \operatorname{div} \mathbf{v} = \int_{\partial M} d\mathbf{S} \cdot \mathbf{v}.$$

Similarly, let M be some two-dimensional surface, $n = 2$, and $\omega = v_1 dx_1 + v_2 dx_2 + v_3 dx_3$. Identifying the surface element as above, we then have $d\omega = \operatorname{curl} \mathbf{v} \cdot d\mathbf{S}$ and

$$\int_M d\mathbf{S} \cdot \operatorname{curl} \mathbf{v} = \int_{\partial M} d\mathbf{s} \cdot \mathbf{v},$$

where $\mathbf{v} \cdot d\mathbf{s} \equiv \omega$, $d\mathbf{s}$ is commonly known as a "line element," and $\int_{\partial M}$ is a line integral: this is called **Ampère s law**.

volume element. For example, some field theories with $\dim(T) = 2$ live on manifolds with a so-called symplectic structure (which is nothing but a skew-symmetric, non-degenerate 2-form). This form may then take over the role of our ω above and, in perfect analogy to our discussion above, gives rise to a topological Lagrangian density.

[55] More generally, WZ terms can be constructed if, in dimensions $\dim M + 1$, the manifold T possesses a closed differential form. (In the special case $\dim M + 1 = \dim T$, this form will be the volume form of T.)

[56] More precisely, C must be a so-called **chain** on M. However, for brevity, we shall keep the sloppy characterization above.

So suppose that we are dealing with a field theory defined on a d-dimensional base manifold M with $(d+1)$-dimensional target manifold T. Without (too much) loss of generality, we may think of $T = S^{d+1}$ and $M = S^d$ as unit spheres.

INFO Although we have seen that spheres frequently appear as target spaces in field theory, the statement above may seem to be too restrictive – for example, what about the many field theories with group-valued target manifolds? The rationale behind emphasizing spherical target manifolds lies in an important statement of homotopy theory: the integration spaces we encounter in field theories with continuous symmetries are usually embedded in some sufficiently large $\mathrm{U}(N)$. However, it can be shown that the topological structure of the group $\mathrm{U}(N \geq 2)$ essentially reduces to that of its subgroup $\mathrm{SU}(2) \subset \mathrm{U}(N)$, i.e. mappings into $\mathrm{U}(N)$ can be continuously deformed into mappings into $\mathrm{SU}(2)$. (If you find this difficult to visualize, consider a two-dimensional plane with a circular hole as an example. Any curve in the plane can be continuously deformed to a curve on the circle surrounding the hole. In this sense, the circle preempts the topological content of the plane. Similar reduction mechanisms exist for higher-dimensional manifolds.) However, $\mathrm{SU}(2) \simeq S^3$ is isomorphic to the 3-sphere. (Representing $\mathrm{SU}(2)$ as the group of matrices $g = x_0\sigma_0 + i\sum_{j=1}^3 x_j\sigma_j$, $x_\mu \in \mathbb{R}$, the condition $\det(g) = 1$ boils down to the relation $\sum_{\mu=0}^3 x_\mu^2 = 0$.) This argument shows that, as far as topology is concerned, the spaces $S^{1,2,3}$ basically exhaust the list of relevant target spaces.

As to the base manifold, the identification $M = S^d$ is motivated by the compactification scheme discussed in Section 9.3 above.

Notice that the target manifold $T = S^{d+1}$ is Riemannian and, therefore, comes with a canonical $(d+1)$-form ω.

Given these prerequisites, our strategy will be to utilize, as much as possible, our previous understanding of the geometry of the θ-term. To this end, let us interpret $\phi(M)$ as a d-dimensional submanifold in T. Further, let $\Gamma_+ \quad \phi(M)$ be a subset of T on which the T volume form $\omega = d\kappa_+$ can be represented as the exterior derivative of some d-form κ_+.

EXAMPLE In fact, we may even assume that $\Gamma_+ = S^{d+1} - \{p\}$ covers all of our sphere except for one point p. For example, on the 2-sphere S^2, the volume form $\omega = \sin\theta\, d\theta \quad d\phi$ is obtained from $\kappa_+ = (1-\cos\theta)d\phi$ as $\omega = d\kappa_+$ everywhere except for the south pole. Similarly, with $\kappa_- = -(1+\cos\theta)d\phi$, $\omega = d\kappa_-$ everywhere except for the north pole. Of course, the choice of the exclusion point is quite arbitrary. Notice, however, that there is no global representation $\omega = d\kappa$. If such a representation existed, $\mathrm{Vol}(T) = \int_T \omega = \int_T d\kappa = \int_{\partial T} \kappa = 0$, because T is boundaryless, i.e. the volume of the sphere would vanish.

We now dimensionally extend the field $\phi : M = S^d \to \Gamma_N \subset S^{d+1} = T$ to a mapping $\tilde{\phi} : S^{d+1}_{\mathrm{N}} \to S^{d+1}$ defined on the entire northern hemisphere, S^{d+1}_{N}, of S^{d+1}. This is achieved in a series of steps: firstly, identify $M = S^d$ as the equator of S^{d+1} (see Fig. 9.13). We then introduce a $(d+1)$-dimensional coordinate representation (s, x), $s \in [0,1]$, of S^{d+1}_{N}. These coordinates are defined in such a way that $(s = 1, x)$ parameterizes the equator $\simeq S^d = M$ while $\lim_{s\to 0}(s,x) = p_N$ is the north pole; otherwise, their choice is arbitrary. We finally extend our field to a mapping $\tilde{\phi} : S^{d+1}_{\mathrm{N}} \to \Gamma_N, (s,x) \to \tilde{\phi}(s,x)$. Apart from the obvious consistency condition $\tilde{\phi}(s=1,x) = \phi(x)$, the choice of this extension is, again, arbitrary.

Given this setup, let us define

$$\boxed{S_{\rm WZ}[\phi] = iC \int_{S^{d+1}_{\rm N}} \tilde{\phi}^* \omega,} \tag{9.40}$$

as a trial candidate of a topological action ($C = \text{const.}$). Constructed in manifest analogy to the θ-term Eq. (9.37), this expression is "topological" in nature (it is scale and reparameterization invariant, etc.). Nonetheless, the definition does not look quite trustworthy. Notably, we have written "$S_{\rm WZ}[\phi]$" while the right-hand side of the definition involves the extension $\tilde{\phi}$. To see that the integral is, in fact, independent of the particular choice of the extension, we use the fact that, on $\tilde{\phi}(S^{d+1}_{\rm N}) \subset \Gamma_N$, the volume form can be written as $\omega = d\kappa_N$. This implies

$$S_{\rm WZ}[\phi] = iC \int_{S^{d+1}_{\rm N}} \tilde{\phi}^* d\kappa_N = iC \int_{S^{d+1}_{\rm N}} d(\tilde{\phi}^* \kappa_{\rm N}) = iC \int_{M=S^d} \tilde{\phi}^* \kappa_{\rm N} = iC \int_M \phi^* \kappa_{\rm N}.$$

Here we have made use of (i), in the second equality, the commutativity of the pullback and exterior derivative, (ii) in the third equality, Stokes' theorem, and, (iii) in the crucial fourth equality, that the integral over $\partial S^{d+1}_{\rm N} = S^d = M$ depends only on the value of the boundary field $\tilde{\phi}(s = 1, x) = \phi(x)$. This proves the independence of the action $S_{\rm WZ}$ on the extension scheme. At the same time, we have obtained the alternative representation

$$\boxed{S_{\rm WZ}[\phi] = iC \int_M \phi^* \kappa_N,} \tag{9.41}$$

of the topological action. This form makes the independence of the action $S_{\rm WZ}$ of the field extension manifest. For this, however, a price has had to be paid: Eq. (9.41) involves the d-form $\kappa_{\rm N}$ which we saw is tied to a certain coordinate representation (owing to the absence of a global representation $\omega = d\kappa$) on the field manifold. In other words, the extension-independent representation Eq. (9.41) necessarily involves the choice of a specific coordinate system of the field.

INFO As an example, consider $M = S^1$ and $T = S^2$. Think of the latter as the space of unit-vectors $\mathbf{n}$. Our field is a mapping $\mathbf{n} : S^1 \to S^2, t \to \mathbf{n}(t)$, where $t \in [0, 1]$ and periodic boundary

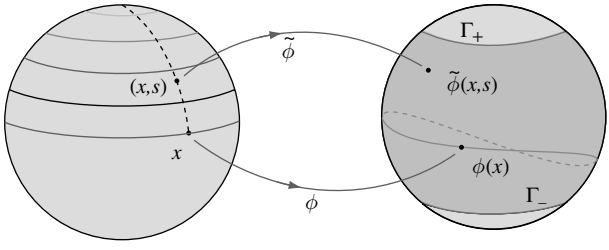

Figure 9.13 On the extension of a field theory defined on a d-dimensional base manifold $M \simeq S^d$ to a $(d + 1)$-dimensional theory.

conditions $\mathbf{n}(0) = \mathbf{n}(1)$ are understood. Extension to a field $\mathbf{n}(s,t)$ then allows us to represent the action $S_{\rm WZ}[\mathbf{n}]$ as (see Eq. (9.38))

$$S_{\rm WZ}[\mathbf{n}] = i\frac{C}{4\pi}\int_0^1 ds \int_0^1 dt\, \mathbf{n}\cdot(\partial_s\mathbf{n}\times\partial_t\mathbf{n}).$$

Now, except for the south pole, we can write the volume (or better to say area) form on S^2 as $\omega = d[(1-\cos\theta)d\phi]$. Then, using the fact that $\mathbf{n}^*[(1-\cos\theta)d\phi] = (1-\cos\theta(t))d\phi(t) = (1-\cos\theta(t))\partial_t\phi(t)dt$, we obtain the alternative representation

$$S_{\rm WZ}[\mathbf{n}] = i\frac{C}{4\pi}\int_0^1 dt\,(1-\cos\theta(t))\partial_t\phi(t). \tag{9.42}$$

Notice that this form explicitly uses the coordinate representation $\mathbf{n} \quad (\phi,\theta)$.

Equations (9.40) and (9.41) are two different representations of the **Wess–Zumino action**. As discussed above, both have their advantages and disadvantages – the need to artificially extend the field vs. lack of representation invariance – which is why they are used interchangeably in the literature.

Finally, we need to discuss one further important point; the value of the coupling constant C. As discussed above, the coupling constant of the θ-term, the topological angle, was quite arbitrary. This is not the case with the WZ term. In fact, we shall see that the constant C is subject to quantization conditions. To understand why, recall that above we have chosen the northern hemisphere $S^{d+1}_{\rm N}$ as the domain of integration of our extended field theory. Of course, the southern hemisphere $S^{d+1}_{\rm S}$ would have provided just as good a choice. In this case, we would have defined

$$S'_{\rm WZ}[\phi] \equiv -iC\int_{S^{d+1}_{\rm S}}\tilde{\phi}^*\omega,$$

where $\tilde{\phi}$ is a field extension to the southern hemisphere, and the extra minus sign takes care of the fact that the equator is the boundary of the oppositely oriented southern domain. Of course, our definition of the WZ action would be senseless if this ambiguity mattered. Therefore,

$$S_{\rm WZ}[\phi] - S'_{\rm WZ}[\phi] = iC\int_{S^{d+1}_{\rm S}}\tilde{\phi}^*\omega + iC\int_{S^{d+1}_{\rm N}}\tilde{\phi}^*\omega = iC\int_{S^{d+1}}\tilde{\phi}^*\omega = iCW,$$

where W is integer. At first sight, the non-vanishing of this expression looks worrysome. However, since the action appears in the exponent no harm is done as long as the difference is equal to (i times) an integer multiple of 2π, i.e. the the coupling constant C obeys the **quantization condition**[57]

$$\boxed{C = 2\pi k, \quad k\in\mathbb{Z}.} \tag{9.43}$$

The number k is called the **level** of the WZ theory. To summarize the main results of this section, we have found that:

[57] Recall that the volume form ω underlying the construction has been normalized in such a way that $\int_{S^{d+1}}\omega = 1$. For different choices of the normalization, the value of C will change accordingly.

▷ The WZ action is closely allied to the θ-term. It affords two different representations where:
▷ Equation (9.40) involves a dimensional extension of the field, while
▷ Equation (9.41) relies on an explicit coordinate representation of the field.
▷ The coupling constant of the WZ term is quantized according to Eq. (9.43).

Having discussed the structure and geometry of WZ theories, we now return to physics. Using a simple prototype system as an example, we begin by exploring how WZ terms enter low-energy theories of many-body quantum systems.

9.4.3 Example: magnetic moment coupled to fermions

Consider a single energy level ϵ of a spinful fermion system. (One may think, for example, of a discrete level of an atom.) Let us assume that fermions inhabiting the level are coupled to a classical magnetic moment $\mathbf{n}$. The coherent state action of this system is given by

$$S[\psi, \mathbf{n}] = \int_0^\beta d\tau\, \bar{\psi}(\partial_\tau + \xi + \gamma \mathbf{n} \cdot \sigma)\psi,$$

where γ is a coupling constant and, as usual, $\xi = \epsilon - \mu$. A complete specification of the problem would have to include a term $S[\mathbf{n}]$ controlling the dynamics of the uncoupled magnetic moment. However, for the purposes of the present discussion, it is sufficient to consider the moment–fermion coupling in isolation.

INFO Actions of this type appear as building blocks of larger systems. For example, once generalized to a *set* of levels ϵ_a, our model might describe a system of atomic shell electrons subject to **Hund s rule** coupling to a spin or orbital magnetic moment. Alternatively, the magnetic moment $\mathbf{n}$ might describe the Hubbard–Stratonovich decoupling of some electron–electron interaction in a spinful channel.

Integration over the fermion degrees of freedom brings us to the reduced action

$$S[\mathbf{n}] = -\mathrm{tr} \ln(\partial_\tau + \xi + \gamma \mathbf{n} \cdot \sigma).$$

To proceed, let us write $\mathbf{n} = R\mathbf{e}_3$, where $R \in \mathrm{SO}(3)$ is a rotation matrix, and then use the fact that a matrix $U \in \mathrm{SU}(2)$ can be found[58] such that

$$\mathbf{n} \cdot \sigma = (R\mathbf{e}_3) \cdot \sigma = U \sigma_3 U^{-1}. \tag{9.44}$$

For example, it is straightforward to verify that, with the standard polar representation, $\mathbf{n} = (\sin\theta\cos\phi, \sin\theta\sin\phi, \cos\theta)^T$, the choice

$$U = e^{-i\frac{\phi}{2}\sigma_3} e^{-i\frac{\theta}{2}\sigma_1} e^{-i\frac{\theta}{2}\sigma_3}, \tag{9.45}$$

[58] This is, in fact, just a concrete realization of the **correspondence between SU(2) and SO(3)** familiar from group theory.

will suffice. However, for the moment we shall not need an explicit representation of the rotation matrix. Rather, substituting the general expression Eq. (9.44) into the action, we obtain

$$\begin{aligned} S[\mathbf{n}] \to S[U] &= -\mathrm{tr}\ln(\partial_\tau + \xi + \gamma U\sigma_3 U^{-1}) = -\mathrm{tr}\ln(U^{-1}\partial_\tau U + \xi + \gamma\sigma_3) \\ &= -\mathrm{tr}\ln(\partial_\tau + \xi + \gamma\sigma_3 + U^{-1}\dot{U}), \end{aligned}$$

where, in the first equality, we have used the cyclic invariance of the trace and, in the last equality, we have defined $\partial_\tau U \equiv \dot{U}$. To proceed, we assume that the two energies $|\xi \pm \gamma| \gg T$ are well separated from the chemical potential, $|\epsilon \pm \gamma| \gg T$. We also assume that the frequency scales $\tilde{\omega}$ on which the fields $\mathbf{n} \leftrightarrow U$ vary are so slow that they do not change the occupation of the fermionic levels: $\tilde{\omega}/\gamma \ll 1$. In these circumstances, we may proceed by a straightforward expansion of the logarithm: $S[U] = \mathrm{tr}(\hat{G}\hat{U}^{-1}\dot{U}) + \mathcal{O}(\tilde{\omega}/\gamma)^2$, where $\hat{G} = (-\partial_\tau - \xi - \gamma\sigma_3)^{-1}$ and we have anticipated (check!) that higher-order terms of the expansion will be small in the parameter $\tilde{\omega}/\gamma$. Switching to a frequency representation,

$$\begin{aligned} S[U] &= \sum_n \mathrm{tr}(\hat{G}_n(\hat{U}^{-1}\dot{U})_{m=0}) = -\int d\tau\, \mathrm{tr}(n_{\mathrm{F}}(\xi + \gamma\sigma_3)U^{-1}\partial_\tau U) \\ &= -\int d\tau\, \mathrm{tr}\left(\left[n_{\mathrm{F}}(\xi + \gamma\sigma_3) - \frac{1}{2}\right] U^{-1}\partial_\tau U\right), \end{aligned}$$

where we have used the fact that the frequency sum of a fermionic Green function introduces the Fermi distribution function, n_{F}. In the last line, we have shifted n_{F} by $1/2$, which is permissible because $\mathrm{tr}(U^{-1}\dot{U})$ is a boundary term:

$$\int_0^\beta d\tau\, \mathrm{tr}(U^{-1}\dot{U}) = \int_0^\beta d\tau\ \partial_\tau\, \mathrm{tr}(\ln U) = \mathrm{tr}\ln(U)|_0^\beta = 0. \tag{9.46}$$

Now, if both levels are either occupied ($n_{\mathrm{F}}(\xi \pm \gamma) - 1/2 \approx 1/2$) or unoccupied ($n_{\mathrm{F}}(\xi \pm \gamma) - 1/2 \approx -1/2$), the action vanishes[59] since $\mathrm{tr}(\left[n_{\mathrm{F}}(\xi + \gamma\sigma_3) - \frac{1}{2}\right] U^{-1}\partial_\tau U) \propto \mathrm{tr}(U^{-1}\partial_\tau U)$ is again a boundary term.

Assuming, however, that $\xi + \gamma$ is empty while $\xi - \gamma$ is occupied we obtain

$$S[U]|_{\xi+\gamma \gg 0 \gg \xi-\gamma} \equiv S_{\mathrm{WZ}}[U] = -\frac{1}{2}\int_0^\beta d\tau\, \mathrm{tr}(\sigma_3 U^{-1}\dot{U}). \tag{9.47}$$

We now run a few tests on S_{WZ} to identify it as a topological term of Wess–Zumino type. For one thing, our base manifold $M \simeq S^1$ is one-dimensional and S_{WZ} involves a first-order derivative. This exemplifies the scale invariance characteristic of topological terms. The suspicion that S_{WZ} is topological is corroborated by the fact that it is purely imaginary. (The time-derivative acts on a unitary matrix, i.e. something like a generalized "phase" – for more details, see below.) But what type of topological term are we dealing with? To get an answer to this question, we first need to determine the dimensionality of the target manifold T. Clearly, $T \neq \mathrm{SU}(2)$ in spite of the fact that we are temporarily using $U \in \mathrm{SU}(2)$ for our

[59] Up to corrections of $\mathcal{O}(\exp(-|\xi \pm \gamma|/T))$ which, in any case, are beyond the scope of the first-order expansion of the "tr ln" above.

fields: our original theory was defined for $\mathbf{n} \in S^2$. Indeed, the representation Eq. (9.44) is invariant under the "gauge transformation" $U \to U \exp(i\psi\sigma_3)$. This means that the "true" field manifold is $\mathrm{SU}(2)/\mathrm{U}(1) \simeq S^2$ as one should expect. Now, $\dim S^2 = 2 = \dim M + 1$, so that S_{WZ} is likely to be a Wess–Zumino term.

Indeed, we observe that, under the gauge transformation above, $\mathrm{tr}(\sigma_3 U^{-1}\dot{U}) \to \mathrm{tr}(\sigma_3 U^{-1}\dot{U}) + 2i\dot{\psi}$, i.e. the topological density is not invariant. This indicates that we will not be able to find a coordinate-independent representation of S_{WZ} in terms of $\mathbf{n}$. As discussed in the previous chapter, the lack of parameterization invariance is a hallmark of WZ terms. (There is no need to worry, though, about the gauge invariance of the *theory*: the periodic boundary conditions imposed on U imply that $\psi(\beta) = \psi(0) + 2\pi n$, where n is some winding number. Under the gauge transformation, the action thus changes by $\delta S = -2\pi i n$, so that $\exp(-\delta S) = 1$ remains invariant.)

To present S_{WZ} in a less abstract form, we can substitute the angular representation Eq. (9.45) into Eq. (9.47). The straightforward evaluation of the derivative then gives

$$S_{\mathrm{WZ}}[\phi, \theta] = -\frac{i}{2} \int d\tau \; (1 - \cos\theta)\partial_\tau \phi. \tag{9.48}$$

We identify this expression as the coordinate representation Eq. (9.42) of the WZ term arising in theories with base S^1 and target S^2. Recall that S_{WZ} evaluates to $-i/2$ times the area swept out by the closed curve (ϕ, θ) on the sphere.

In fact, we have already met with the action Eq. (9.48) in Section 3.3 when we discussed the path integral of a single spin. That the core contribution to the action of that problem reappears here should not come as too much of a surprise: the classical magnetic moment $\propto \mathbf{n}$ "enslaves" the electron spin. In the limit of perfect alignment – realized under the conditions assumed above – we are left with the dynamics of a quantum spin whose dynamics are tied to that of $\mathbf{n}$. The resulting action therefore coincides with that of a free spin described by the unit vector $\mathbf{n}$.

In the literature, the action Eq. (9.48) is frequently referred to as the **Berry phase action**. To understand the rationale behind this terminology, let us briefly recall (see the Info block below) a few facts about the quantum mechanical Berry phase. Consider a quantum particle subject to the Hamiltonian $\hat{H}(x(t))$, where the D-component vector $x(t) \equiv \{x_i(t)\}$ parameterizes a weakly time-dependent contribution to $\hat{H}$. As shown by Berry, the dynamical phase acquired during the evolution of the particle can be expressed as $\exp(-i \int dt' \; \epsilon_0(t') + i\gamma(t))$, where $\epsilon_0(t)$ is the energy of the instantaneous ground state of $\hat{H}(t)$. The first contribution to the exponent is the usual dynamical phase of quantum evolution. (Here, it is assumed that the time-dependence of $\hat{H}$ is sufficiently weak for us to neglect transitions into excited levels; for a static Hamiltonian, this contribution reduces to

Sir Michael Berry 1941–

Theoretical physicist who has made groundbreaking contributions to the field of quantum nonlinear dynamics and optics. Berry introduced the concept of the Berry phase (or geometric phase as he himself prefers to call it) and explored its manifestations in various physical contexts. (Figure courtesy of Sir Michael Berry.)

the familiar phase $\epsilon_0 t$.) The second contribution, $\gamma(t)$, is of geometric origin, inasmuch as it depends on the path traced out by the vector x in parameter space, but not on dynamical details. (In particular, it is independent of the velocity at which the parameter path is traversed.) The **geometric phase** assumes a particularly simple form if the parameter dependence of $\hat{H}$ is periodic in time, $x(0) = x(t)$. In this case, $x(t)$ defines a closed curve and γ can be expressed as an integral over any surface in parameter space bounded by that curve. Specifically, for a spin S particle Zeeman-coupled to a weakly time-dependent magnetic field $\mathbf{B}(t) \equiv \mathbf{n}(t)B$ of constant magnitude, B,

$$\gamma = \frac{S}{2} \int d^2x \ \mathbf{n} \cdot \partial_1 \mathbf{n} \times \partial_2 \mathbf{n}, \tag{9.49}$$

is the area bounded by the curve $\mathbf{n}(t)$ on the 2-sphere (which, in this case, defines the parameter space). Comparison with Eq. (9.48) and the example discussed on page 538 indeed identifies the WZ-term as the Berry phase of the spin problem.[60]

INFO A brief reminder of the **Berry phase in quantum mechanics**: Consider a particle governed by a Hamiltonian $\hat{H}(x(t))$. It is assumed that the time-dependence of the parameter vector x is adiabatic, which means that a particle initially prepared in the ground state $|0(t=0)\rangle$ of the Hamiltonian $\hat{H}(x(0))$ will remain in the instantaneous ground state $|0(t)\rangle$ (i.e. the lowest eigenstate $\hat{H}(x(t))|0(t)\rangle = \epsilon(t)|0(t)\rangle$ of the operator $\hat{H}(x(t))$) throughout the entire observation time. (In practice, this means that the rate ω at which the parameters change in time must be much smaller than the excitation gap of the system.)

We are interested in computing the dynamical phase corresponding to the time evolution of $|0(t)\rangle$. To this end, let us represent the wavefunction of the particle as $|\psi(t)\rangle = e^{-i\phi(t)}|0(t)\rangle$ and consider the time-dependent Schrödinger equation

$$\hat{H}(x(t))|\psi(t)\rangle = i\partial_t|\psi(t)\rangle.$$

Substitution of the representation above and multiplication by $\langle 0(t)|$ then leads to the equation $\partial_t\phi = \epsilon(t) - i\langle 0(t)|\partial_t|0(t)\rangle$. Integrating over time and comparing with our discussion above, we are led to the identification $\gamma(t) = i\int_0^t dt' \ \langle 0(t')|\partial_{t'}|0(t')\rangle$ of the Berry phase (exercise: why is γ real?). Now, the instantaneous ground state inherits its time dependence from the parameters $x(t)$. We may thus write

$$\gamma(t) = i\int_0^t dt' \ \langle 0(x(t'))|\partial_{x_i(t')}|0(x(t'))\rangle \partial_t x_i(t') = i\int_{\mathrm{c}} dx \ \langle 0(x)|\partial_x|0(x)\rangle = i\int_{\mathrm{c}} \langle 0|d0\rangle.$$

Here, the second integral has to be interpreted as a line integral in parameter space. It is taken along a curve c which starts at $x(0)$, follows the evolution of the parameter vector, and ends at $x(t)$. Importantly, the line integral depends only on the choice of γ but not on the velocity at which this curve is traversed (the dynamics of the process). In this sense, we are dealing with a phase of geometric origin. The third integral representation above emphasizes the geometric

[60] In the discussion above, we considered a particle coupled to a weakly time-dependent magnetic moment – a canonical setup for the appearance of Berry phases. But why did the Berry phase/WZ-action also appear in our earlier discussion of a spin coupled to a fixed magnetic field? To answer this question, consider the world from the point of view of the spin. In the reference frame of the spin, the magnetic field is dynamical and a Berry phase term will be generated. Moreover, the area traced out by the field vector (i.e. the area determining the geometric phase) is equal to the area traced out by the spin (now we are back in the fixed-field reference frame) in its motion around the field axis.

nature of the phase even more strongly: for any value of x, we have a state $|0(x)\rangle$. We may then construct the differential 1-form $\langle 0(x)|d0(x)\rangle$.[61] The geometric phase is obtained by evaluating the integral of this form along the curve c.

The advantage of the third representation above is that it suggests yet another formulation of the geometric phase, at least in cases where a closed path in parameter space is traversed. For a closed loop c, application of Stokes' theorem gives

$$\boxed{\gamma = i \oint_c \langle 0|d0\rangle = i \int_S \langle d0| \quad |d0\rangle,} \tag{9.50}$$

where S may be any surface in parameter space that is bounded by γ. This last representation is aesthetic, and easy to memorize, but also a bit too compact to be of real computational use. To give it a more concrete meaning, we insert a spectral decomposition in terms of instantaneous eigenstates,

$$\gamma = i \int_S \sum_{m=0} \langle d0|m\rangle \quad \langle m|d0\rangle.$$

(Exercise: Why does the $m = 0$ term vanish, i.e. $\langle d0|0\rangle \quad \langle 0|d0\rangle = 0$? Hint: Make use of the fact that $d\langle 0|0\rangle = \langle d0|0\rangle + \langle 0|d0\rangle = 0$ and the skew-symmetry of the -product.) We now evaluate the equation $0 = \langle m|d[(\hat{H} - \epsilon_0)|0\rangle]$ to obtain $\langle m|d0\rangle = (\epsilon_0 - \epsilon_m)^{-1}\langle m|dH|0\rangle$ or

$$\boxed{\gamma = i \textstyle\int_S \sum_{m=0} \dfrac{\langle 0|dH|m\rangle \quad \langle m|dH|0\rangle}{(\epsilon_m - \epsilon_0)^2}.} \tag{9.51}$$

This is about as far as we get in general terms. We have established the geometric nature of the Berry phase. However, inasmuch as it requires explicit knowledge of the spectrum of $\hat{H}(x(t))$, the actual calculation of the phase remains a difficult problem.

There are cases, however, where the calculation of the geometric phase reduces to a straightforward surface integral in parameter space. One such **example** is provided by a spin subject to a weakly time-dependent magnetic field. Consider the Hamiltonian $\hat{H} = \mu \mathbf{n}(x) \cdot \sigma \equiv \mu U(x)\sigma_3 U^{-1}(x)$, where U is the rotation matrix introduced in Eq. (9.44). The $2S + 1$ instantaneous eigenstates of $\hat{H}$ are given by $U|S_3\rangle$, where $\sigma_3|S_3\rangle = S_3|S_3\rangle$ and $S_3 = -S, \ldots, S$ is the azimuthal spin quantum number. To compute the Berry phase, we can consider the first of the two representations in Eq. (9.50). Noting that the ground state is given by $|0\rangle = U|S_3 = -S\rangle$ (we assume that the magnetic moment $\gamma > 0$) and parameterizing the rotation matrix as in Eq. (9.45), one verifies that $\langle 0|d0\rangle = \langle -S|U^{-1}dU| - S\rangle = iS(1 - \cos\theta)d\phi$. We thus obtain $\gamma = S \int_c d\phi (1 - \cos\theta) = S \int dt\ (1 - \cos\theta)\phi$, which coincides (up to a Wick rotation $t \to -i\tau$, which we know does not affect topological terms) with the $S = 1/2$ WZ-action Eq. (9.48).

9.4.4 Spin chains: beyond the semi–classical limit

In Section 9.3.3, we began to explore the physics of one-dimensional spin chains. Much of our analysis was limited to the case $S \gg 1$, a semi-classical regime where quantum fluctuations

[61] Should you find the representation too abstract, choose any basis $\{|\lambda\rangle\}$ and write $\langle 0(x)|d0(x)\rangle \equiv \langle 0(x)|\lambda\rangle d\langle \lambda|0(x)\rangle$, where $d\langle \lambda|0(x)\rangle$ is the exterior derivative of the function $\langle \lambda|0(x)\rangle$.

are weak. In this limit, the spin chain is described by an O(3) nonlinear σ-model with a θ-term. This model, however, does not stay invariant under renormalization. It flows towards a "strong coupling" regime where fluctuations are large and the effective value of the spin (formally: the coupling constant of the gradient term in the model) becomes weak. Apart from the conjecture that, for half-integer/integer initial spin, the model flows towards an ordered/disordered phase with gapless/gapped excitations, there was nothing we could say about the large-distance behavior of the model (or about the physics of chains consisting of small spins $S = \mathcal{O}(1)$).

In this section, we invest quite some effort in developing a fresh attack on the physics of the small S spin chain. This is motivated in part by the enormous amount of recent experimental activity on quasi-one-dimensional spin compounds. ("Real" spin chains are often realized as structural sub-units of transition metal compounds. In these systems, the spin – which is carried by Hund's rule coupled inner shell electrons of transition metal atoms – may reach as high as 7/2.) Another, and more theory-related, motivation for our study is that the low-energy physics of the spin chain is governed by a fascinating interplay of different topologically non-trivial quantum field theories.

Following Affleck and Haldane,[62] the principal idea of our approach will be to exploit the equivalence of the antiferromagnetic spin chain to a one-dimensional Hubbard model at half filling.[63] The advantage gained by this digression is that the fermionic model is amenable to various analytical tools which (at least not in any known sense) do not apply to the spin-chain *per se*. We will find that the effective low-energy model describing the fermion system is the WZ field theory conjectured to be the fixed point theory of the σ-model in Section 9.3.3.

Fermion representation of the antiferromagnetic spin chain

Consider a one-dimensional chain of equidistant (spacing a) lattice sites i. Each site hosts n_c degenerate fermion states, or "orbitals." Consider a half-filled situation, i.e. on average, each orbital is occupied by a single spin-(1/2) fermion. We now introduce some dynamics so that the low-energy physics of the system is equal to that of an antiferromagnetic spin chain with spin $S = n_c/2$. (Notice that this construction is not quite as artificial as it may seem: the effective moments observed in "real" crystals are usually composite objects, composed of more than one elementary electron spin and stabilized by electron correlations.)

To align the n_c spins at each site, we introduce a strong ($U \gg T$) Hund's rule coupling

$$\begin{aligned}\hat{H}_{\rm int} &= -U \sum_i \hat{\mathbf{S}}_i \cdot \hat{\mathbf{S}}_i = -\frac{U}{4} \sum_i \left(\psi_{ia}^{\alpha\,\dagger} \sigma^{\alpha\beta} \psi_{ia}^{\beta} \right) \cdot \left(\psi_{ia'}^{\alpha'\,\dagger} \sigma^{\alpha'\beta'} \psi_{ia'}^{\beta'} \right) \\ &= \frac{U}{4} \sum_i \left[2 \left(\psi_{ia}^{\alpha\,\dagger} \psi_{ib}^{\alpha} - \delta_{ab} \right) \left(\psi_{ib}^{\beta\,\dagger} \psi_{ia}^{\beta} - \delta_{ba} \right) + \left(\psi_{ia}^{\alpha\,\dagger} \psi_{i\alpha}^{\alpha} - n_c \right)^2 \right] + \text{const.} \end{aligned} \tag{9.52}$$

[62] I. Affleck and F. D. M. Haldane, Critical theory of quantum spin chains, *Phys. Rev. B* **36** (1987), 5291–300.
[63] Recall that, for strong interaction, the one-dimensional Hubbard model maps onto the so-called $(t - J)$-model which (at half filling) reduces to the antiferromagnetic Heisenberg model (the spin chain).

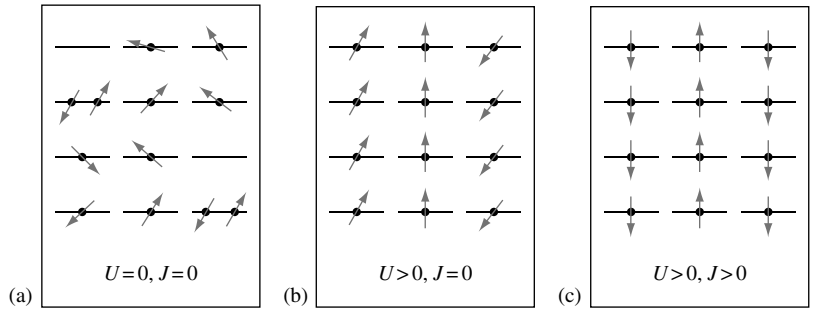

Figure 9.14 (a) A chain of sites, each containing n_c fermions on average. (b) A strong Hund's rule coupling maximizes the spin carried by each state to $S = n_c/2$. (c) Upon the switching on of a finite nearest neighbor hopping matrix element, the system becomes a spin S antiferromagnet.

Here, $a = 1, \ldots, n_c$ is the orbital index, α, β are spin indices, and, to get from the first to the second line, we have used the identity $\sigma^{\alpha\beta} \cdot \sigma^{\alpha'\beta'} = 2\delta^{\alpha\beta'}\delta^{\beta\alpha'} - \delta^{\alpha\beta}\delta^{\alpha'\beta'}$. Of special interest to our further discussion will be the last term in the second line. This Hubbard-type interaction tells us that each site favors a site occupancy of n_c electrons (i.e half-filled). Indeed, n_c electrons are needed to manufacture a net spin of maximum weight $S = n_c/2$ (see Fig. 9.14) and, thus, to optimize the Heisenberg interaction Eq. (9.52).

Let us now introduce a small amount of inter-site hopping:

$$\hat{H}_0 = -\frac{1}{2}(n_c JU)^{1/2} \sum_i \left[\psi_{ia}^{\alpha\,\dagger} \psi_{i+1a}^{\alpha} + \text{h.c} \right], \tag{9.53}$$

where the constant J determines the hopping strength. In the limit $J/U \to 0$, the half-filled system becomes equivalent to the spin S antiferromagnetic chain,

$$\hat{H} = \hat{H}_0 + \hat{H}_{\text{int}} \overset{\langle \hat{n}_i \rangle = n_c}{\longrightarrow} H_{\text{af}} = J \sum_i \hat{\mathbf{S}}_i \cdot \hat{\mathbf{S}}_{i+1} + \mathcal{O}(J/U). \tag{9.54}$$

The easiest way to see this is to recall the situation in the standard Hubbard model (the $n_c = 1$ variant of our present model) at half filling (cf. Section 2.2). There, virtual deviations from half filling led to an effective antiferromagnetic exchange coupling between the $S = 1/2$ spins carried by neighboring sites. The effective strength of this interaction was $J \sim t^2/U$, where t is the strength of the hopping term. Formally, the generalization of this mechanism to the case $n_c > 1$ can be shown, for example, by subjecting the Hamiltonian $\hat{H}$ to a canonical transformation eliminating the hopping term (all in complete analogy to the $n_c = 1$ canonical transformation discussed in Section 2.2).

We have, thus, established the equivalence between the strongly interacting $J \ll U$ fermion Hamiltonian and the spin chain. Now there comes a major conceptual jump – and admittedly one that is not backed up by quantitative reasoning: we postulate that the equivalence between the two systems pertains to the case $J > xU$, at least as far as the relevant long-range excitations are concerned. If this were not the case, there should be some kind of abrupt change (a phase transition) in the behavior of the system as the interaction

is increased. Although this scenario cannot be rigorously excluded, it seems unlikely to be taken too seriously.

Non-abelian bosonization

Let us, then, consider the low-energy physics of the weakly interacting ($J > U$) fermion system. In fact, we shall begin by considering the totally non-interacting case.[64] Switching from a lattice to a continuum description and linearizing around the two Fermi points (for details, see Section 2.2), we describe this prototypical system in terms of the action

$$S[\psi^\dagger, \psi] = \sum_{s=\pm 1} \int dx\, d\tau\, \psi_s^{\dagger r} \left(-isv_{\mathrm{F}}\partial_x + \partial_\tau\right) \psi_s^r = \int d^2x\; \bar{\psi}^r \not{\partial} \psi^r, \tag{9.55}$$

where $\psi_{s=\pm 1}$ are the left- and right-moving fermion fields. In the latter equality we have set $v_{\mathrm{F}} = 1$ and switched to the Dirac notation (for details, see Section 4.3), and $r = (a, \alpha) = 1, \ldots, 2n_{\mathrm{c}} \equiv N$ is a composite index comprising spin and orbital components of the fermion field. In previous chapters, we have seen that the one-component ($N = 1$) variant of this model could be equivalently described in terms of a free bosonic action,

$$S[\bar{\psi}, \psi] = \int d^2x\; \bar{\psi} \not{\partial} \psi \quad \leftrightarrow \quad S[\theta] = \frac{1}{2\pi} \int d^2x\; \partial_\mu \theta\; \partial_\mu \theta, \tag{9.56}$$

where the double arrow $\leftrightarrow$ indicates that all fermion operators $\mathcal{O}[\bar{\psi}, \psi]$ (currents, densities, etc.) can be expressed in terms of boson operators $\tilde{\mathcal{O}}[\phi]$, and correlation functions $\langle \mathcal{O}_1 \mathcal{O}_2 \cdots \rangle_\psi$ can be identically rewritten as $\langle \tilde{\mathcal{O}}_1 \tilde{\mathcal{O}}_2 \cdots \rangle_\phi$.

Edward Witten, 1951–
Mathematical physicist and string theorist. Awarded the 1990 Fields Medal for his ground breaking work in differential geometry. Witten contributed massively to the success of string theory. (Photo by Randall Hagadorn. Courtesy of the Institute of Advanced Study.)

To what extent does this picture survive generalization to the many-channel case? The answer to this question was given in a seminal paper by Witten. Witten found that[65]

> The free fermion action Eq. (9.55) can be equivalently described in terms of a two-dimensional nonlinear σ-model with a Wess–Zumino term.

More precisely, he showed that

$$S[\bar{\psi}, \psi] = \int d^2x\; \bar{\psi}^r \not{\partial} \psi^r \quad \leftrightarrow \quad S_{\mathrm{WZW}}[g] = \frac{1}{8\pi} \int_{S^2} d^2x\, \mathrm{tr}(\partial_\mu g \partial_\mu g^{-1}) + \Gamma\,[g], \tag{9.57}$$

[64] As in our previous discussion of the single-channel case, it will turn out that the inclusion of interactions is straightforward once the effective bosonic degrees of freedom have been identified.

[65] E. Witten, Nonabelian bosonization in two dimensions, *Commun. Math. Phys.* **92** (1984), 455–72.

where $g \in \mathrm{U}(N)$ and

$$\Gamma[g] = -\frac{i}{12\pi} \int_{B^3} d^3x \; \epsilon^{ijk} \, \mathrm{tr}(g^{-1}\partial_i g \, g^{-1}\partial_j g \, g^{-1}\partial_k g), \tag{9.58}$$

denotes the **WZ action**.[66] On the right-hand side of Eq. (9.57), two-dimensional space-time has been compactified to a 2-sphere S^2. This sphere is then understood as the boundary of a three-dimensional unit ball, B^3, which serves as the integration domain of the WZ functional. As in the one-component case, the double arrow in Eq. (9.57) implies equality of all correlation functions upon suitable identification of operators (see the Info block below).

Equation (9.58) is the multi-component or "non-abelian" generalization of the prototypical bosonization identity (9.56). To understand the connection between the two equations, consider the restriction of $\mathrm{U}(N)$ to its maximal abelian subgroup, i.e. the group of all diagonal matrices $g = \mathrm{diag}(e^{i2\theta^1}, \ldots, e^{i2\theta^N})$. Evaluated on such configurations, the WZ term vanishes (exercise: show this) while the gradient term,

$$S[\theta^r] = \sum_{r=1}^{N} \frac{1}{2\pi} \int d^2x \; (\partial_\mu \theta^r)^2, \tag{9.59}$$

collapses to the sum of N free boson actions. This is the description we would have obtained had we applied Eq. (9.56) to each of the N fermion components individually (which, after all, is a perfectly legitimate thing to do!). But what, then, is the advantage of the generalized variant of bosonization Eq. (9.57)? Referring for a more detailed discussion to the Info block below, we here merely note that the action Eq. (9.57) possesses a huge symmetry group: transformations $\psi_s \to g_s \psi_s, g_s \in \mathrm{U}(N)$, leave the action invariant, i.e. the symmetry group of the problem is given by $\mathrm{U}(N) \times \mathrm{U}(N)$. Suppose we had bosonized each fermion in the standard abelian manner, thus arriving at the action Eq. (9.59). We might now ask how the symmetries of the problem – which of course must survive a change of representation – act in the θ-language. Frustratingly, there is no answer to this question;[67] the symmetries are no longer manifestly present and there is no direct way to benefit from their existence. With the non-abelian generalization Eq. (9.57), this is not so. As we shall see in a moment, the symmetry group $\mathrm{U}(N) \times \mathrm{U}(N)$ acts on the g-degrees of freedom by left–right multiplication, $g \to g_+ g g_-^{-1}$.[68] In previous chapters we have emphasized time and again the tremendous importance of symmetries and the resulting conservation laws. Indeed it turns out that, in the present problem, the comparative complexity of the action Eq. (9.57) is far outweighed by the manifest presence of the symmetries.

[66] Deviating from our earlier conventions, we will denote the WZ-action by $\Gamma[g]$ throughout (instead of the notation $S_{\mathrm{WZ}}[g]$ used above). In doing so, we follow a standard literature convention. Also, the *full* action (including the gradient term) is commonly denoted by S_{WZW} (where the last "W" credits Witten's contribution to two-dimensional WZ field theory), and the resemblance between the two symbols S_{WZ} and S_{WZW} may cause confusion.

[67] One may object that a theory of free bosons is so simple that one need not care about the conservation laws introduced by symmetries. However, this argument is too shortsighted. It ignores the fact that most operators of interest are transcendental in the θs, i.e. the full theory is not quite as simple as Eq. (9.59) would suggest.

[68] This provides another explanation of why the θ-description is too narrow to accommodate the symmetry: a diagonal matrix g will not remain diagonal when acted upon by the transformation matrices.

INFO The proof of the bosonization identity (9.57) relies on an extension of the considerations summarized in Section 4.3 to the case of non-abelian symmetries. Although a detailed discussion of the construction (for which we refer to Witten's original, yet highly pedagogical, paper) would be beyond the scope of this text, let us briefly summarize some of the **principal ideas behind the method of non-abelian bosonization.**

Let us begin by recalling that, in the abelian case $N = 1$, we had two basic symmetries, $\psi_s \to g_s\psi_s$, where $g_s = \exp(i2\phi_s)$, ϕ_s are constant phases and $\psi_{s=\pm1}$ the left- and right-moving fermion fields. These symmetries express the independence of the left- and right-moving states or, equivalently, the chirality of the problem. A straightforward application of Noether's theorem (or, equivalently, a direct variation of the action) shows that the conservation laws induced by the chiral symmetry are $\partial_z\bar{j} = \partial_{\bar{z}}j = 0$, where $j = \psi_-^\dagger\psi_-$, $\bar{j} = \psi_+^\dagger\psi_+$ and we have introduced complex coordinates $z \equiv \frac{1}{\sqrt{2}}(x_0 + ix_1)$, $\partial_z = \frac{1}{\sqrt{2}}(\partial_0 - i\partial_1)$.[69]

In Section 4.3 we saw that, on the bosonic level, the chiral symmetries act as $\theta \to \theta + \phi_+ - \phi_-$. The conservation laws corresponding to these transformations read as $\partial_z\partial_{\bar{z}}\theta = 0$ (exercise: check this). At the same time we know that the transformation generated by ϕ_+ (ϕ_-) generates the conservation law $\partial_z\bar{j} = 0$ ($\partial_{\bar{z}}j = 0$). Comparison with the two equations above leads to the identification $\bar{j} = \psi_+^\dagger\psi_+ \quad -\frac{i}{\sqrt{2}\pi}\partial_{\bar{z}}\theta$ and $j = \psi_-^\dagger\psi_- \quad \frac{i}{\sqrt{2}\pi}\partial_z\theta$, where the factor of $i/\sqrt{2}\pi$ has been included to obtain consistency with the definition of the vectorial current $j_{v,0} = \rho \sim \partial_1\theta \sim j + \bar{j}$.[69]

We now reformulate these results in a manner amenable to generalization: introducing $g \equiv \exp(i2\theta) \in \mathrm{U}(1)$, the bosonic action of Eq. (9.56) assumes the form $S[g] = \frac{1}{8\pi}\int d^2x\, \partial_\mu g\ \partial_\mu g^{-1}$, while the symmetries now act by conjugation: $g \to g_+ g g_-^{-1}$. Here, $e^{i2\phi_\pm} \equiv g_\pm$. Finally, the conserved currents can be defined as

$$j = \frac{1}{\sqrt{8\pi}} g^{-1}\partial_z g, \quad \bar{j} = -\frac{1}{\sqrt{8\pi}}(\partial_{\bar{z}}g)g^{-1}. \tag{9.60}$$

At this stage, the ordering of the – abelian – factors g is of course arbitrary. However, this will change once we proceed to the multi-channel case. (Notice that the equations (9.60) are solved by $g = g_+(\bar{z})g_-(z)$, where the two independent factors g_+ and g_- describe the right/left-moving fermion states. This solution does not rely on the commutativity of the phases g and generalizes to the non-abelian case.)

For $N > 1$, the phases g_s generalize to two independent unitary matrices $g_\pm \in \mathrm{U}(N)$. The enlarged symmetry entails the conservation laws $\partial_z\partial_{\bar{z}}j^{rr'} = 0, r, r' = 1, \ldots, N$, where the currents are given by $j^{rr'} = \psi_+^{r\dagger}\psi_+^{r'}$ and $\bar{j}^{rr'} = \psi_-^{r\dagger}\psi_-^{r'}$.

EXERCISE To verify this last statement, consider the infinitesimal unitary transformation $U_s = \exp(i\eta W)$ and expand the action Eq. (9.55) to first order in the Hermitian generator matrices W.

What are the bosonic counterparts of these expressions? It is natural to generalize the phases $g \in \mathrm{U}(1)$ of the abelian case to unitary matrices $g \in \mathrm{U}(N)$. As before, the symmetry group will act by left–right-multiplication, i.e. $g \to g_+ g g_-^{-1}$ and we expect the conserved currents to be given by Eq. (9.60).[70]

[69] Throughout, it will be preferable to use this complex notation. Notice that the two conserved currents j and $\bar{j}$ are related to the components of the vectorial currents discussed in Section 4.3 by $j_{v0} \sim j + \bar{j}$ and $j_{v1} \sim \frac{1}{i}(j - \bar{j})$.

[70] Notice, however, that the currents are now matrices $j_s = \{j_s^{rr'}\}$ and that – unlike in the abelian case – the ordering of the matrices g on the right-hand side of the definition is crucial. The factors in Eq. (9.60) are ordered in such a way that $\partial_{\bar{z}}j = 0$ and $\partial_z\bar{j} = 0$ are compatible with each other.

We now need an action that (a) is invariant under the multiplicative action of the symmetry group and (b) for $N = 1$ reduces to $\int \partial_\mu g \partial_\mu g^{-1}$. An obvious candidate would be

$$S_0[g] = \frac{1}{8\pi} \int d^2x \, \mathrm{tr}(\partial_\mu g \partial_\mu g^{-1}). \tag{9.61}$$

Yet, for a number of reasons, Eq. (9.61) does not suffice. Firstly, for this action, the conservation laws derived from the symmetry of the problem, read $\partial_\mu (g^{-1}\partial_\mu g) = 0$, which is inconsistent with our result above, $\partial_{\bar z}(g^{-1}\partial_z g) = 0$. Secondly, we have seen in the previous chapter (cf. Section 8.5) that the nonlinear σ-model Eq. (9.61) renormalizes at large length scales to smaller values of the coupling constant. At the same time, it is supposed to describe the fermionic action (9.55), which obviously does not renormalize. This tells us that $S[g]$ alone does not suffice to establish the boson–fermion correspondence.

But let us now inspect the second term in the action proposed by Witten, the two-dimensional WZ functional. The first thing we have to understand is why the second term of the action indeed represents a WZ functional in the sense of the discussion of Section 9.4.2.[71] To construct a WZ term, we need a differential form ω on the target manifold that is closed, $d\omega = 0$, but only locally exact ($\omega = d\kappa$ only locally). In Problem 9.7.2 it is shown that, on a group-valued target manifold, these criteria are met by the form $\omega = \mathrm{tr}(g^{-1}dg \quad g^{-1}dg \quad g^{-1}dg)$. (Do not be confused by the notation. What it really means is $\omega = \sum_{ijklmno}((g^{-1})_{ij}dg_{jk} \quad (g^{-1})_{lm}dg_{mn} \quad (g^{-1})_{no}dg_{oi})$, where dg_{jk} is the differential form of the function g_{jk} assigning to each element $g \in \mathrm{U}(N)$ its matrix component g_{jk}.) The general theory developed in Section 9.4.2 then tells us that $iC\int_{B^3} g^*\omega$ is a WZ term where g is a smooth extension of the field $g : S^2 \to \mathrm{U}(N)$ to a field defined on the entire ball B^3. Expressed in terms of some coordinate functions (x_1, x_2, x_3) of B^3, this expression becomes identical to Eq. (9.58). (As to the quantization of the coupling constant, see Problem 9.7.2.) In passing we note that the WZ functional is manifestly invariant under the action of the chiral symmetry group, as is required by the general structure of the theory.

It is instructive to inspect the equations of motion obtained from the WZ term. In Problem 9.7.2 we show that, upon variation $g \to e^W g \simeq (1 + W)g$ and expansion to first order in W, we obtain

$$\Gamma[(1 + W)g] - \Gamma[g] = \frac{i}{4\pi} \int d^2x \, \epsilon_\mu \ \ \mathrm{tr}(W \partial_\mu g \partial \ g^{-1}) + \mathcal{O}(W^2). \tag{9.62}$$

A straightforward calculation shows that the variation of the gradient term S_0 is given by

$$S_0[(1 + W)g] - S_0[g] = -\frac{1}{8\pi} \int d^2x \, \mathrm{tr}(W(g\partial_\mu^2 g^{-1} - (\partial_\mu^2 g)g^{-1})) + \mathcal{O}(W^2).$$

Combining these two results, we obtain the equations of motion

$$-2i\epsilon_\mu \ \partial_\mu g \partial \ g^{-1} + g\partial_\mu^2 g^{-1} - (\partial_\mu^2 g)g^{-1} = 0.$$

A straightforward calculation shows that these equations are indeed equivalent to the relation $\partial_z \bar j \propto \partial_z((\partial_{\bar z} g)g^{-1}) = 0$.

Summarizing, we have succeeded in finding an action that (a) is manifestly chirally invariant and (b) produces the same conservation laws as the free fermion theory. Notice, however, that we have not "proven" the analogy Eq. (9.57); rather, our analysis was mostly based on drawing

[71] Notice that, in Section 9.4.2, we focused on the case $\dim T = \dim M + 1$. Presently, however, $\dim M = 2$ while $\dim T = \dim \mathrm{U}(N)$ can become arbitrarily large.

illustrative analogies to the one-dimensional case. (For a more rigorous discussion, we refer to Gogolin *et al.*[72])

We conclude our preliminary survey of non-abelian bosonization by noting two crucial differences to the abelian case:

In the abelian case, a free fermion action was mapped onto an equally free boson action. Being quadratic in the fields, the two theories manifestly do not renormalize. In the non-abelian case, the situation is different: although it is not obvious, the right–hand side of Eq. (9.57) – a highly nonlinear functional of the group-valued fields g – does not renormalize. For a proof of this feature we refer to Problem 9.7.3.

Above, we have seen that bilinears $\sim \psi_\pm^\dagger \psi_\pm$ composed of left- or right-moving fermions afford a representation in terms of the Bose fields. Without proof, we mention that even bilinears involving fermions of different chirality can be expressed in terms of bosonic fields:

$$\psi_+^{r\dagger} \psi_-^{r'} \sim g^{rr'}. \tag{9.63}$$

However, unlike in the abelian case (see Eq. (4.46)), no boson representation of individual fermion operators is known. This is quite unfortunate as it excludes the applicability of the formalism to several interesting fields of investigation, notably the physics of fermions in the presence of disorder.

In fact, the U(N) action introduced in Eq. (9.57) defines two independent field theories at once: every matrix $g \in \mathrm{U}(N)$ can be decomposed as $g = e^{i2\phi} g'$ into a matrix $g' \in \mathrm{SU}(N)$ and a phase factor $e^{i2N\phi} = \det(g) \in \mathrm{U}(1)$. Substituting this decomposition into the action, we obtain

$$S[g] = S[g'] + \frac{N}{2\pi} \int_{S^2} d^2x \, (\partial_\mu \phi)^2. \tag{9.64}$$

Equation (9.64) tells us that the action decomposes into a WZW action for an SU(N)-valued field variable and an independent second action for the phase degree of freedom. Recalling that the invariance of the action under a homogeneous phase (gauge) transformation corresponds to the conservation of electric charge, we identify the phase action as that of the collective charge degrees of freedom (the charge density waves), while the SU(N)-action describes the spin degrees of freedom.

Renormalization group "ow of the WZW model

The action (9.57) describes a free fermion fixed point, if not in an obvious manner. To understand better the behavior of the WZW model under renormalization, let us generalize the free fermion action by introducing an arbitrary coupling constant λ^{-1} in front of the gradient term. We thus consider the action

$$S = \frac{1}{\lambda} \int_{S^2} d^2x \, \mathrm{tr}(\partial_\mu g \, \partial_\mu g^{-1}) - \frac{i}{12\pi} \int_{B^3} d^3x \, \epsilon^{ijk} \mathrm{tr}(g^{-1}\partial_i g \, g^{-1}\partial_j g \, g^{-1}\partial_k g), \tag{9.65}$$

where $g \in \mathrm{SU}(N)$ (and the complementary U(1) action is trivially free). Except for the presence of the WZ term, the model defined by this action is equivalent to the SU(N) nonlinear σ-model studied in Section 8.5. However, the latter is known *not* to have a fixed

[72] A. O. Gogolin, A. A. Nersesyan, and A. M. Tsvelik, *Bosonization and Strongly Correlated Systems* (Cambridge University Press, 1998).

point at finite values of λ. This tells us that the WZ term must have a crucial impact on the RG flow. Suppose, then, we started renormalizing the model at small values of λ. In this regime, the gradient term dominantly suppresses field fluctuations and we expect the WZ term to be of little significance. Consequently, the RG flow will initially resemble that of the standard SU(N) model – towards larger values of λ. Eventually, however, λ and the coupling constant $i/12\pi$ of the WZ term will become of the same order. At this point, at last, the coupling constant will interfere with the flow. As we know that $\lambda = 8\pi$ defines a fixed point, we expect that it will simply truncate the flow of the coupling constant.

To confirm this expectation, we need to go through the RG program, at least to one-loop order. Fortunately, however, the RG analysis of the WZW model (see Problem 9.7.3) almost exactly parallels that of the standard SU(N) model. As a result, we can infer the scaling equation

$$\frac{d\lambda}{d\ln b} = \frac{N\lambda}{4\pi}\left[1 - \left(\frac{\lambda}{8\pi}\right)^2\right]. \tag{9.66}$$

This result confirms our qualitative expectation: the value $\lambda^* = 8\pi$ defines an (attractive) fixed point at which the upwards flow of λ comes to an end. Using the methods of conformal field theory, one can indeed show (see Witten's original paper[65]) that λ^* defines an exactly solvable reference point. (This is important additional information inasmuch as our one-loop analysis does not rigorously prove that λ^* is a fixed point.)

WZW model of interacting fermions

All we have accomplished so far is a highly complicated reformulation of the trivial free fermion problem. However, as we shall see in a moment, this exercise has been far from useless: as with the abelian case, it will turn out that the boson language is of unsurpassed efficiency when it comes to the discussion of particle interactions.

As usual, the most relevant particle interactions are mediated by certain four-fermion operators. Important constraints on the structure of these operators follow, once again, from the symmetries of the model. Above we have seen that the non-interacting model is invariant under transformations by $\mathrm{U}(2N_\mathrm{c}) \times \mathrm{U}(2N_\mathrm{c})$, where the first/second factor acts on spin and color indices of the left-/right-moving fermions. However, the Hubbard–type interaction Eq. (9.52) reduces this symmetry. Inspection of the interaction operator shows that chiral symmetry gets lost (i.e. only transformations that act identically on the left-/right-moving sector are permitted, $\mathrm{U}(2N_\mathrm{c}) \times \mathrm{U}(2N_\mathrm{c}) \to \mathrm{U}(2N_\mathrm{c})$), and the remaining $\mathrm{U}(2N_\mathrm{c}) \to \mathrm{U}(1) \times \mathrm{SU}(2) \times \mathrm{SU}(N_\mathrm{c})$ gets reduced to symmetry transformations that act on the charge/spin/color sector separately.

There are a number of continuum interaction operators that are compatible with the symmetries of the lattice system. Consider, for example, the bilinears $j^q_s \equiv \psi^{\dagger\alpha}_{sa}\psi^{\alpha}_{sa}$, $j^{s,i}_s \equiv \psi^{\dagger\alpha}_{sa}\sigma^{i,\alpha\beta}\psi^{\beta}_{sa}$ and $j^c_{s,j} \equiv \psi^{\dagger\alpha}_{sa}T_{aa'}\psi^{\alpha}_{sa'}$, where $T^j \in \mathrm{u}(N_c)$, $j = 1, \cdots, n_c^2 - 1$ are the generators of $\mathrm{U}(N_c)$ transformations, and $s = +/-$. These are the left-/right-moving components of the conserved currents $j^{q,s,c} = j^{q,s,c}_+ + j^{q,s,c}_-$, generated by U(1), SU(2), and SU(N_c)

transformations, respectively. As in the abelian case, interactions solely between left- or right-moving fermions are largely inessential. However, the operators

$$\lambda_q = j^q_+ j^q_-, \quad \lambda_s = \mathrm{tr}(j^s_+ j^s_-), \quad \lambda_c = \mathrm{tr}(j^c_+ j^c_-), \tag{9.67}$$

are physically relevant and compatible with the symmetries of the model. Another relevant player is the "**umklapp operator**" $\lambda_{\rm uk}(\psi^{\alpha\dagger}_{+a}\sigma_2^{\alpha\beta}\psi^{\dagger\beta}_{+a})\,(\psi^{\alpha'}_{-a'}\sigma_2^{\alpha'\beta'}\psi^{\beta'}_{-a'}) + \text{h.c.}$[73] For the discussion of a few more allowed interaction operators, we refer to the original reference of Affleck and Haldane.[62]

EXERCISE Show that the umklapp operator is invariant under the action of all three symmetry groups.

Expressed in terms of the continuum fields, the Hund's rules coupling Eq. (9.52) translates to a sum of the interaction operators listed above. The question we now have to answer is how these operators – which at sufficiently large strength will turn the free fermion model into the Heisenberg model in which we are interested – affect the long-distance dynamics of the model. Naturally, we shall address this question in the bosonized language developed in the previous section. As a warm-up to the case of arbitrary spin, we shall begin with the discussion of the colorless case, $N_{\rm c} = 1$, i.e. the **spin-1/2 chain**.

Writing $g = e^{i2\phi}g'$, where $g' \in \mathrm{SU}(2)$ acts on the spin indices, and using Eq. (9.60) for the bosonic representation of the currents, we obtain $j^q = -\frac{i}{\sqrt{2}\pi}\partial_z\phi$ and $j^s = \frac{1}{\sqrt{8}\pi}g'^{-1}\partial_z g'$ for the spin current. Reflecting its invariance under spin transformations, the bosonic representation of the umklapp operator reads $\sim \lambda_{\rm uk}\cos 4\phi$.

EXERCISE To obtain the bosonic representation of the umklapp operator, substitute Eq. (9.63) into its definition and obtain $\sim \lambda_{\rm uk}e^{i4\phi}\mathrm{tr}(g'\sigma_2 g'^T\sigma_2) + \text{h.c.} \sim \lambda_{\rm uk}\cos(4\phi)$. Here the last equality is best proven by using the representation $g' = \exp(i\mathbf{v}\cdot\sigma)$.

The action generalized for the presence of these interaction operators takes the form $S[\phi, g'] = S[\phi] + S[g']$, where

$$\begin{aligned} S[\phi] &= \frac{1}{2\pi}(1-\lambda_q)\int d^2x\left((\partial\phi)^2 + C\lambda_{\rm uk}\cos(\sqrt{4}\phi)\right), \\ S[g'] &= S_{\rm WZW}[g'] + \lambda_s\int d^2x\ \mathrm{tr}(\partial g'\partial g'^{-1}). \end{aligned} \tag{9.68}$$

Notably, the action still decouples into a spin and a charge sector (the separation of spin and charge characteristic of one-dimensional systems). Further, both $S[\phi]$ and $S[g']$ are old acquaintances: $S[\phi]$ is the action of the two-dimensional sine–Gordon model. In Section 8.6 we have seen that, for $\lambda_q < 0$ (repulsive interactions), it flows towards a phase with a mass gap. This flow is driven by the umklapp operator. What this tells us is that umklapp scattering leads to the presence of an excitation gap for charge density waves. This gap

[73] Recall that **umklapp scattering** is the scattering of two fermion states of opposite spin from one point of the Fermi surface ($\pm k_{\rm F}$) to the other ($k_{\rm F}$). At half filling, $k_{\rm F} = \pi/2a$, the momentum transferred in this process is of magnitude $2(\pi/2a - (-\pi/2a)) = 2\pi/a = G$, where $G = 2\pi/a$ is the reciprocal lattice vector. Since lattice momentum is conserved only up to multiples of G, umklapp scattering (at half filling) is a permissible process.

is nothing but the **Mott–Hubbard gap** present in the spectrum of interacting fermions at half filling. (Recall that the presence of umklapp processes is tied to the case of half filling.) Turning to the action $S[g']$, we note that the λ_s-perturbation merely renormalizes the coupling constant of the gradient term of $S_{\rm WZW}$, $1/8\pi \to (1/8\pi) + \lambda_s$. However, in the previous section, we have seen that this change does not alter the long-range behavior of the system: irrespective of the value of the coupling constant, the model will flow back towards the free fermion fixed point at $\lambda^* = 1/8\pi$.

Summarizing, we have found that the $N_{\rm c} = 1$ interacting fermion system builds up a Mott–Hubbard gap for its charge excitations while the spin excitations are described by a critical WZW theory. Now, our entire analysis was based on the presumed equivalence ($N_{\rm c} = 1$ interaction fermion system) $\quad$ ($S = 1/2$ Heisenberg chain). The existence of long-range excitations in the former then implies that the latter must be in an ordered phase (since a disordered phase would be *defined* by the absence of long-range excitations). This, however, is a result with which we are familiar.[74] The truly interesting question is what happens for larger values of the spin (i.e. larger values of $N_{\rm c}$).

At $N_{\rm c} > 1$, the structure of the theory gets significantly more involved. Referring for a more detailed analysis to the original paper by Affleck and Haldane,[62] we restrict ourselves here to a qualitative discussion of the most relevant aspects.

- ▷ Consider a matrix field $g' \in {\rm SU}(2) \times {\rm SU}(N_{\rm c})$.[75] Among the various interaction operators there is one that drives excitations of the color sector into a massive phase. This means that the soft excitations of the model can be parameterized as $g' = \hat{g} \times \mathbf{1}_{N_{\rm c}}$, where $\hat{g}$ acts in the spin sector. Substituting these configurations into the free fermion reference action, we obtain $S_{\rm WZW}[g'] = N_{\rm c} S_{\rm WZW}[\hat{g}]$, where the prefactor $N_{\rm c}$ arises from the tracing out of the color sector. Remembering our discussion of the quantization of the WZ coupling constant in Section 9.4.2, we identify this model as a **WZW model of level** $k = 2N_{\rm c}$.
- ▷ Among the plethora of conceivable perturbations of the critical theory, one operator family deserves special attention: ${\rm tr}(g^n)$, where $g \in {\rm SU}(2)$. (Here, we are writing g instead of $\hat{g}$ for notational simplicity and n is some integer.) For two reasons, these are interesting operators: firstly, they represent the most relevant perturbations of the theory (due to the absence of derivatives); secondly, they relate to an important discrete symmetry of the model. To understand why, let us return to the lattice version of the theory and consider the fermion representation of the spin operator $S_l^j = \psi_l^{\alpha\dagger} \sigma^{\alpha\beta} \psi_l^\beta$. Decomposing the fermion into left- and right-moving components, $\psi_l = e^{ik_{\rm F} l} \psi_+(x_l) + e^{-ik_{\rm F} l} \psi_-(x_l)$, where $x_l = la$, we obtain $S_l^j = \sum_s \psi_s^\dagger(x_l) \sigma^j \psi_s(x_l) + [(-)^l \psi_+(x_l)^\dagger \sigma^j \psi_-(x_l) + {\rm h.c.}] = {\rm tr}([c(j_+^s + j_-^s) + c'(-)^l (g + g^{-1})]\sigma^j)$, where c and c' are numerical constants. Here, we have used the relation $e^{ilk_f x} = e^{i(\pi/a)la} = (-)^l$ as well as the bosonization identity Eq. (9.63). The second term under the trace is of particular interest. It tells us that translation by one site, $l \to l + 1$, corresponds to a sign change of the field g. This observation can be read in different ways. For example, contributions to the action that are not invariant

[74] Recall that the $S = 1/2$ chain can be subjected to a Jordan–Wigner transformation whereupon it becomes a model of spinless interacting fermions. The existence of gapless excitations (charge density waves) thus proves the existence of long-range order in the spin chain.

[75] We will ignore the gapped charge sector throughout.

under $g \to -g$ explicitly break **translational invariance on the lattice**. Similarly, a ground state that is not sign invariant cannot be translationally invariant, etc.

▷ After these preparatory remarks, let us return to the discussion of the operators $\mathrm{tr}(g^n)$. As we are not interested in modeling situations where the Hamiltonian explicitly breaks translational invariance, only contributions with n even will be allowed. Physically, these operators correspond to products of n left-moving and n right-moving fermion states. In the case considered previously, $N_\mathrm{c} = 1$, there is only one such contribution, namely the backscattering operator discussed above. However, for $N_\mathrm{c} > 1$, terms $\mathrm{tr}(g^{2n\ \ N_\mathrm{c}})$ are physically allowed. Let us, then, consider the action $S[g] = N_\mathrm{c} S_\mathrm{WZW} + \lambda \int d^2x\ \mathrm{tr}(g^2)$.[76] Void of derivatives, the new contribution acts as a potential contribution to the action (although it is still invariant under the SU(2) symmetry transformation $g \to h^{-1}gh$). This being so, the physical behavior of the model crucially depends on the sign of the coupling constant λ.

▷ For $\lambda < 0$, the term $\lambda \int \mathrm{tr} g^2$ favors the mean-field configurations $\bar{g} = 1$ or $\bar{g} = -1$. Both ground states break the discrete sign inversion symmetry $g \to -g$ and, therefore, they cannot be translationally invariant. Before identifying the physical meaning of these ground states, let us briefly discuss the issue of fluctuations. Writing $g = e^{i\phi^j \sigma^j/2}\bar{g}$ and expanding to quadratic order in ϕ, we obtain a mass term $\frac{\lambda}{2} \int d^2x\ (\phi^j)^2$. This means that spin fluctuations around $\bar{g}$ are gapped. There is, indeed, one well known low-energy state of the spin chain that displays these features, the **dimer phase**. In this phase (see Fig. 9.15), spins at neighboring sites form spin singlets. Obviously, this state is not invariant under translation by one site (while translation by *two* sites is a symmetry). Further, there is no room for massless spin fluctuations, i.e. the system indeed shows an excitation gap.

▷ We next discuss the complementary case, $\lambda > 0$. In this case, configurations $\bar{g}$ with eigenvalues $(i, -i)$ are energetically favored. There is a continuous family of such states, namely $\bar{g} = \exp(i\pi \mathbf{n} \cdot \boldsymbol{\sigma}/2)$, where $|\mathbf{n}| = 1$. Again, these states break translational invariance $(g \to -g)$. However, they also break SU(2) symmetry $g \to hgh^{-1}$. This means that, unlike the dimerized case, the continuous spin rotation symmetry is spontaneously broken. Its breaking of both translational and spin rotational invariance identifies $\bar{g}$ as the **Néel state** of the chain.

▷ To describe the physics of the Goldstone modes corresponding to the symmetry broken state, we note that $h \exp(i\pi \mathbf{n} \cdot \boldsymbol{\sigma}) h^{-1} = \exp(i\pi \mathbf{n}' \cdot \boldsymbol{\sigma})$, where the unit vector $\mathbf{n}' = R\mathbf{n}$ and $R \in \mathrm{SO}(3)$ is a rotation matrix canonically corresponding to the SU(2)-matrix h.[77] Each $\mathbf{n}'$ defines a new ground state, i.e. we have identified the 2-sphere as the Goldstone mode manifold.

EXERCISE Try to guess what the action of the Goldstone modes might be!

To identify the Goldstone mode action, we substitute the soft field configurations $\exp(i\pi \mathbf{n}(x) \cdot \boldsymbol{\sigma}/2) = i\mathbf{n} \cdot \boldsymbol{\sigma}$ into the action. It is straightforward to verify that the gradient

[76] The operator $\mathrm{tr}(g^2)$ can be shown to be the most relevant of the family.

[77] To any element $h \in \mathrm{SU}(2)$, the prescription above assigns an element $R \in \mathrm{SO}(3)$. The correspondence is 2–1 and not 1–1 because both h and $-h$ map onto the same R.

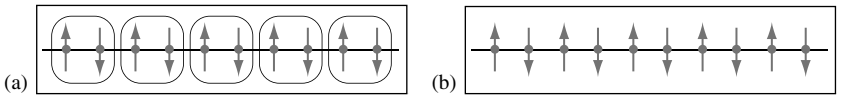

Figure 9.15 Dimerized phase of the spin chain (a) vs. Néel phase (b).

term of the WZW action simply becomes $S_0[i\mathbf{n}\cdot\boldsymbol{\sigma}] = \frac{N_c}{8\pi}\int d^2x\ (\partial\mathbf{n})^2$. As to the WZ functional, we show in Problem 9.7.2 that $N_c\Gamma[i\mathbf{n}\cdot\sigma] = \frac{N_c}{4}\int_{S^2}\mathbf{n}\cdot\partial_1\mathbf{n}\times\partial_2\mathbf{n} = \pi N_c S_{\rm top}[\mathbf{n}]$, i.e. the θ-term of the 2-sphere. Recalling that $N_c = 2S$, we conclude that, for large values of S (this is where the massive fluctuations around the Goldstone mode manifold can be neglected), the system is controlled by the action of the O(3) nonlinear σ-model with topological angle $2\pi S$,

$$S[\mathbf{n}] = \frac{1}{2\lambda}\int d^2x\ (\partial\mathbf{n})^2 + 2\pi S\, S_{\rm top}[\mathbf{n}], \tag{9.69}$$

the same $S[\mathbf{n}]$ identified earlier on semi-classical grounds as the low-energy action of the spin chain.

This is now a good point to pause and consider what we have obtained. At first sight, it seems as if nothing much has been achieved: as a result of a long series of derivations we have arrived back at the semi-classical representation of the chain, the σ-model. However, it turns out that it is the *interplay* between the WZW and the σ-model that enables us to really understand the physics of the problem. To see this, let us consider the $S = 1/2$ chain in the presence of a next-nearest neighbor ferromagnetic coupling – admittedly an artificial model but, for the sake of the present argument, this does not matter. One can show that the long-range physics of this system is described by the O(3)-model with topological angle $2\pi S = \pi$. On the other hand, we might have approached the problem via the WZW route discussed above. Within that context, the ferromagnetic perturbation turns out to be *irrelevant* (see Affleck and Haldane[62]), i.e. the long-range physics of the system is described by the critical free fermion WZW action. Comparing these two findings we can conclude that

> The O(3) nonlinear σ-model with topological angle $\pi \times$ (odd integer) is equivalent to the SU(2) WZW action at critical coupling,

(although no explicit field theoretical proof of this equivalence is known). This was the last missing piece of information needed to understand the long-range behavior of the spin chain. To summarize, we have found that (see Fig. 9.16) the antiferromagnetic spin S chain can be described in terms of a perturbed WZW action of level $k = 2S$. Depending on the sign of the most relevant perturbation $\sim \lambda\int\ {\rm tr}(g^2)$ (which is set by the material parameters of the problem), this model can be either in a globally gapped phase – the dimer phase of the chain – or in a Néel phase. The fluctuations superimposed on the Néel phase are described by an O(3) model with topological angle $2\pi S$. For integer spin, this model flows towards a strong coupling phase, i.e. the spin chain is in a disordered state. However, for S half-integer,

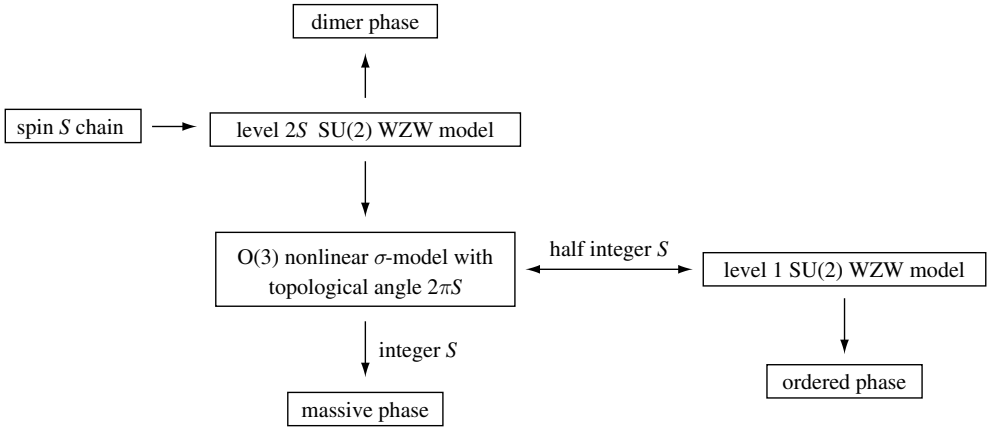

Figure 9.16 On the long-range physics of the antiferromagnetic spin chain. For a discussion, see the main text.

it becomes equivalent to the level 1 WZW model at criticality, implying ordered behavior of the chain.

Notice that none of the conclusions summarized above was established rigorously. More often than not we had to *trust* in the principle of adiabatic continuity, i.e. the belief that the physics of a system does not change qualitatively upon interpolating between the regime of weak interactions (where various approximation schemes work) to the regime of strong interactions (in which we are actually interested). Similarly, connections between different theories were constructed on the basis of symmetry arguments and indirect reasoning (rather than by "hard-boiled" calculations). In this way various pieces of evidence were pieced together to form a network that was intrinsically consistent and made physical sense. In recent years, this type of semi-quantitative research has become more and more prevalent in various areas of condensed matter physics. This development is driven by the increasing complexity of the questions and, relatedly, the absence of straightforward perturbative schemes. In the next section, we shall turn to another problem field where such "detective work" has been successful, the fractional quantum Hall effect.

9.5 Chern–Simons terms

As our third and last example of topological field theories with relevance to condensed matter physics, we now turn to the discussion of Chern–Simons (CS) theories. However, deviating from the strategy pursued in previous sections, this time we do not begin with a formal analysis of the underlying geometrical framework. Instead, we directly turn to a review of *the* master application of CS field theory in condensed matter physics, the fractional quantum Hall effect. It will then turn out that, once we have left the qualitative level and turned to the field integral description, we readily wind up in the basin of attraction of CS field theory.

9.5.1 Fractional quantum Hall effect (FQHE)

In Section 9.3.4 we interpreted the QHE as a topological phenomenon. Depending on the chosen perspective, the integer number setting the Hall conductance can be interpreted as the number of occupied edge channels or, more formally, as the number of instanton excitations in Pruisken's field theory. Both figures appear to be largely impervious to changes in the parameters of the system.

In essence, the basic mechanism behind the formation of integer-valued Hall conductance had been understood shortly after the discovery of the effect. It thus came as a surprise when Tsui *et al.*[78] discovered a sequence of plateaus at fractional values of the Hall conductance. More specifically, it turned out that:

- ▷ Fractional values $\sigma_{xy} = \nu \frac{e^2}{h}$, $\nu \equiv \frac{n}{m}$, of the Hall conductance are observed only in the purest samples. This indicates that, unlike with the integer effect, disorder does not stabilize the FQHE.
- ▷ Not every rational n/m qualifies as a plateau value. The most prominent plateaus are observed for the "principal sequence" $1/m$, where m is odd. More generally, plateaus have been observed for $\frac{n}{m} = \frac{p}{2sp+1}$, $s, p \in \mathbb{N}$.[79]
- ▷ Curiously, it has turned out that, at certain even-denominator fractions (formally, the limit $p \to \infty$ in the hierarchy) the system largely behaves as if no magnetic field were present at all! For instance, in the vicinity of $\nu = 1/2$, pronounced Shubnikov–de Haas oscillations (otherwise shown by Fermi liquids subject to a weak field) are observed.

At first sight, the coexistence of phenomena of that degree of complexity with the (seemingly so robust) integer QHE may cause some consternation. But, then, let us recall that we are considering an isolated Landau level at fractional filling! In other words, we are considering a hugely degenerate quantum state that is only partially populated. Within that environment, a macroscopic restructuring of the electron gas can be afforded at little cost (which will be set by "residual" mechanisms such as electron–electron interactions and/or disorder scattering). On the same footing, it is clear that perturbative expansions around any given trial ground state will be pretty fragile. (Perturbations enjoy a huge phase volume while "energy denominators" are small.)

Keeping these things in mind, it is perhaps no longer surprising that dramatic things happen in the fractionally filled Landau level. The considerations above suggest that elementary electrons – subject to the full strength of Coulomb interactions, at fully "quenched" kinetic energy – will hardly qualify as stable elementary excitations of the system. At the same time, the appearance of Fermi-liquid-like states at least for some filling fractions suggests that the dominant players in the game *are* elementary fermionic particles.

[78] D.C. Tsui, H.L. Stormer, and A.C. Gossard, Two-dimensional magnetotransport in the extreme quantum limit, *Phys. Rev. Lett.* **48** (1982), 1559–62.

[79] In fact, the two-parameter "hierarchy" defined by the right-hand side of this equation still is not general enough to account for all experimentally observed values. (The prominent exception is a fragile plateau at $\nu = 5/2$.) However, to explain these anomalous values of the Hall conductance, one has to keep track of the polarization of the electron spin, an extra level of complexity which we would here rather avoid.

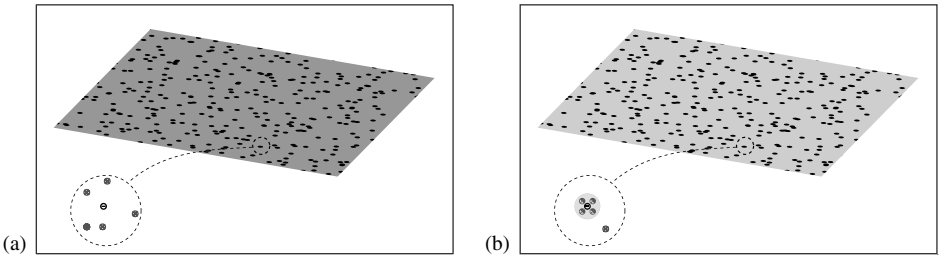

Figure 9.17 Illustrating the idea of the composite fermion approach. Imagine that an even number of flux quanta constituting the magnetic field get tied to the electrons in the system. The new composite particles ("electron + $(2n)$ flux quanta") continue to be fermions. They only see the remaining "free" flux quanta, i.e. a reduced external field (indicated by the lighter shading in part (b)).

Remarkably, it is not at all difficult[80] to conceive of a fermionic quasi-particle picture wherein – at least at a mean-field level – the plethora of phenomena above admits a straightforward explanation: imagine the external magnetic field as a large number N_ϕ of flux tubes piercing the plane of the two–dimensional electron gas (see Fig. 9.17). The ratio $\nu \equiv N/N_\phi$, where N denotes the number of electrons, defines the filling fraction of the system. Since we are working under "fractional" conditions, $0 < \nu < 1$, the number of flux quanta exceeds the number of charge carriers.[81] Now assume that, by some mechanism, each electron matches up with an even number of flux quanta to form a composite particle. (By way of example, consider $\nu = 1/3$, in which case there would be enough flux quanta around to let every electron pair with two flux tubes.) What can be said about the properties of these composite objects?

- ▷ Firstly, they would still be fermions. To understand why, recall that the statistics of particles can be probed by exchanging their position in space. However, our composite particles and the original electrons differ only in the presence of an even number of integer flux tubes. The flux tubes give rise to additional phase factors, so that our new particles are fermionic: one speaks of **composite fermions (CFs)**.
- ▷ The CFs see an effectively reduced external field. For example, for $\nu = 1/3$, each electron has absorbed two flux quanta. Thus, the residual field seen by the CFs is three times lower than the original field. In other words, the number of remaining flux quanta, $N_\phi - 2N = N$, is equal to the number of CFs. Forgetting for a moment about the origin of the composite particles, we are considering a large number N of (composite) fermions subject to N flux quanta, i.e. a situation where the *integer* QHE should arise. This picture suggests an interpretation of the FQHE as an IQHE of composite fermions.[82] In the specific case of a half-filled ($\nu = 1/2$)

[80] However, our discussion should not deceive the reader about the fact that the composite fermion picture represents the outgrowth of years of most intensive research!

[81] If $\nu > 1$, $\nu - [\nu]$, where $[\nu]$ is the largest integer smaller than ν, sets the filling fraction of the highest occupied Landau level and our discussion applies to that level.

[82] More generally, let us assume that every fermion binds $2s$ flux quanta to it. Further suppose that $N/(N_\phi - 2nN) = p$, i.e. that p Landau levels of the *residual* field are occupied. In this case, the CFs will also display the IQHE. This

band, $N_\phi - 2N = 0$, i.e. the CFs experience a mean-field of vanishing strength. This nicely conforms with the experimental observation of Fermi-liquid-like behavior (no QHE) close to half filling.

▷ We have seen in Section 9.3.4 that, when a flux quantum is adiabatically pushed through an annular quantum Hall geometry, an electron charge flows from the inner to the outer perimeter of the sample. In a way, the phase vortex created by the addition of the gauge flux leads to an expulsion of electronic charge. Similarly, the flux tubes involved in the construction of the CF picture effectively carry a positive charge ν. These "screen" the charge carried by the bare electron, so that the CF is not exposed to the full strength of the unit-charge Coulomb interaction.

In the history of the FQHE, the introduction of the CF picture by Jain[83] was preceded by a number of other important developments. Shortly after the experimental discovery of the effect, Laughlin[84] proposed a trial wavefunction which, in a close-to-optimal way,[85] minimizes the Coulomb repulsion between the quasi-particles in the lowest Landau level. Most of the concepts central to the subsequent introduction of the CF picture – fractionally charged quasi-particles, incompressibility of the QH state, the importance of correlations, etc. – have effectively been motivated by this trial wavefunction. Later, the theory of the (many-body) CF system was formulated in terms of a Chern–Simons type field theory.[86] This effective field theory has become the basis of many subsequent analyses of FQHE phenomena.

In this text, we shall turn the sequence of historical developments upside down: starting from a field theoretical description, we shall identify the CF degrees of freedom and then rediscover Laughlin's wavefunction. Once these structures are in place, the computation of the fractional Hall conductance will be little more than a straightforward exercise.

9.5.2 Chern–Simons field theory: construction

Consider the Hamiltonian of two-dimensional interacting electrons subject to a perpendicular magnetic field of strength B: $\hat{H} = \hat{H}_0 + \hat{H}_{\rm int}$ where

$$\begin{aligned} \hat{H}_0 &= \int d^2x\, a^\dagger(\mathbf{x}) \left[\frac{1}{2m}(-i\partial_{\mathbf{x}} + \mathbf{A}_{\rm ext})^2 + V(\mathbf{x}) \right] a(\mathbf{x}), \\ H_{\rm int} &= \frac{1}{2} \int d^2x\; d^2x'\; (\hat{\rho}(\mathbf{x}) - \hat{\rho}_0) V(\mathbf{x} - \mathbf{x}') (\hat{\rho}(\mathbf{x}') - \hat{\rho}_0). \end{aligned}$$

happens for filling fractions $\nu = N/N_\phi = p/(2sp+1)$. In essence, this simple picture explains the structure of the rationals where the FQHE is observed.

[83] J. K. Jain, Composite-fermion approach for the fractional quantum Hall effect, *Phys. Rev. Lett.* **63** (1989), 199–202.

[84] R. B. Laughlin, Anomalous quantum Hall effect: an incompressible quantum fluid with fractionally charged excitations, *Phys. Rev. Lett.* **50** (1983), 1395–8.

[85] For certain short-range correlated model interactions, the Laughlin wavefunction can even be shown to be an exact ground state, see F. D. M. Haldane, Fractional quantization of the Hall effect: a hierarchy of incompressible quantum fluid states, *Phys. Rev. Lett.* **51** (1983), 605–8.

[86] A. López and E. Fradkin, Fractional quantum Hall effect and Chern–Simons gauge theories, *Phys. Rev. B* **44** (1991), 5246–62.

Here, $\mathbf{A}_{\rm ext} = \frac{B_{\rm ext}}{2}(y,-x)^T$ is the vector potential of the external magnetic field (symmetric gauge), V is a single-particle potential created by the presence of, for example, impurities, and $\hat{H}_{\rm int}$ describes the particle interaction on the background of a constant counter-density ρ_0.

Singular gauge transformation

After our discussion in the previous section, we do not expect bare electrons to be a useful reference for the construction of a low-energy field theory. Certainly, it will be more promising to start out from composite fermions as discussed above. As we have seen, a CF is an electron with $2s$ integer flux tubes attached to it. Other fermions moving around the CF along a circular contour will acquire the winding phase $2s\phi$ indicative of the presence of $2s$ flux quanta. Within a first-quantized framework, these phase vortices can be attached[87] to the position of each fermion by virtue of the "gauge transformation"

$$\Psi(\mathbf{x}_1,\ldots,\mathbf{x}_N) \to \Psi(\mathbf{x}_1,\ldots,\mathbf{x}_N)\exp\left[-2is\sum_{i<j}\arg(\mathbf{x}_i-\mathbf{x}_j)\right], \tag{9.70}$$

where Ψ is the many-body wavefunction, and $\arg(\mathbf{x}) = \tan^{-1}(x_2/x_1)$ is the angle enclosed between $\mathbf{x}\in\mathbb{R}^2$ and the positive real axis. The transformation Eq. (9.70) becomes singular whenever two coordinates $\mathbf{x}_i \to \mathbf{x}_j$ approach each other, i.e. it does not represent an orthodox gauge transformation. In fact, the vector potential corresponding to the phase factor above, $\mathbf{a} = -2s\partial_{\mathbf{x}}\sum_i \arg(\mathbf{x}-\mathbf{x}_i) = -2s\sum_i \frac{(x_1-x_{i,1})\mathbf{e}_2-(x_2-x_{i,2})\mathbf{e}_1}{|\mathbf{x}-\mathbf{x}_i|^2}$, creates a perpendicular magnetic field[88] of strength

$$b = \epsilon^{ij}\partial_{\mathbf{x}_i}a_j = -4\pi s\sum_i \delta(\mathbf{x}-\mathbf{x}_i), \tag{9.71}$$

i.e. the field corresponding to $2sN$ flux tubes centered at the coordinates of the fermions. Summarizing, the singular gauge transformation above converts the N fermions into a system of CFs (fermions with $2s$ flux lines attached).

Derivation of the Chern–Simons action

Within the framework of the second quantization, the transformation Eq. (9.70) amounts to the replacement

$$a^\dagger(\mathbf{x}) \to a^\dagger(\mathbf{x})\exp\left[-2is\int d^2x' \arg\,(\mathbf{x}-\mathbf{x}')\hat{\rho}(\mathbf{x}')\right],$$

where, as usual, $\rho = a^\dagger a$.

EXERCISE Check that, with this definition, a quantum many-body wavefunction $|\ \rangle \equiv \prod_{i=1}^{N} a^\dagger{}_i|0\rangle$ transforms according to Eq. (9.70). (The index λ refers to the states $|\lambda\rangle$ of a suitably chosen single-particle basis [e.g. a basis of Landau states].)

[87] In fact, the attachment of these phases is *equivalent* to placing flux quanta at the winding center.
[88] This would, of course, not be possible for a non-singular gauge transformation.

Substituting the transformed operators into the Hamiltonian, one obtains

$$\hat{H}_0 \to \int d^2x\, a^\dagger(\mathbf{x}) \left[\frac{1}{2m}(-i\partial_{\mathbf{x}} + \hat{\mathbf{A}})^2 + V(\mathbf{x})\right] a(\mathbf{x}),$$

where $\hat{\mathbf{A}} = \mathbf{A}_{\rm ext} + \hat{\mathbf{a}}$ and

$$\hat{\mathbf{a}}(\mathbf{x}) = -2s \int d^2x'\ \frac{(x_1 - x_1')\mathbf{e}_2 - (x_2 - x_2')\mathbf{e}_1}{|\mathbf{x} - \mathbf{x}'|^2}\, \hat{\rho}(\mathbf{x}'). \tag{9.72}$$

At this stage it is convenient to switch to a real-time field integral representation. We thus introduce the partition function $\mathcal{Z} = \mathcal{N} \int D(\bar\psi, \psi)\, e^{iS[\bar\psi,\psi]}$, where the action $S[\bar\psi, \psi] = S_0[\bar\psi, \psi] + S_{\rm int}[\bar\psi, \psi]$, with

$$\begin{aligned} S_0[\bar\psi, \psi] &= \int dt\ d^2x\ \bar\psi \left[i\partial_t + \mu - \frac{1}{2m}(-i\partial_{\mathbf{x}} + \mathbf{A}[\bar\psi, \psi])^2 - V(\mathbf{x})\right] \psi, \\ S_{\rm int}[\bar\psi, \psi] &= -\frac{1}{2} \int dt \int d^2x\ d^2x'\ (\rho(\mathbf{x}) - \rho_0) V(\mathbf{x} - \mathbf{x}')(\rho(\mathbf{x}') - \rho_0), \end{aligned}$$

is obtained in the usual way by trading field operators for coherent state amplitudes (specifically, $\rho = \bar\psi\psi$ and $\mathbf{A}[\bar\psi, \psi] \equiv \hat{\mathbf{A}}_{(a,a^\dagger)\to(\psi,\bar\psi)}$). Thanks to the presence of the vector potential $A[\bar\psi, \psi]$, the kinetic energy operator has become a pretty unpleasant object, depending non-locally on up to six field amplitudes $\psi, \bar\psi$. To avoid this complication[89] let us shift the nonlinearities implied by the singular gauge transformation to some other place in the action. This can be achieved by promoting the vector potential to an integration variable whose value is set so as to generate the flux pattern: i.e. multiply the partition function by $1 = \mathcal{N} \int D\mathbf{a}_\perp \prod_{\mathbf{x},t} \delta\left(b(\mathbf{x}, t) + 4\pi s\rho(\mathbf{x}, t)\right)$, where $b = \epsilon^{ij}\partial_i a_{\perp,j}$ and the subscript " " indicates that the integration extends only over transversal configurations of the vector potential (that is, configurations obeying $\partial_i a_i = 0$).[90] As a result, we obtain the double functional integral,

$$\begin{aligned} \mathcal{Z} &= \mathcal{N} \int D(\bar\psi, \psi)\, D\mathbf{a}_\perp \prod_{\mathbf{x},t} \delta\left(b(\mathbf{x}, t) + 4\pi s\rho(\mathbf{x}, t)\right) \exp\left(-S[\bar\psi, \psi, \mathbf{a}_\perp]\right) \\ &= \mathcal{N} \int D(\bar\psi, \psi)\, D\mathbf{a}_\perp\, D\phi \exp\left(iS[\bar\psi, \psi, \mathbf{a}_\perp] - i \int d^2x\, dt\, \phi \left(\frac{b}{4\pi s} + \rho\right)\right) \\ &\equiv \mathcal{N} \int D(\bar\psi, \psi)\, D\mathbf{a}_\perp\, D\phi \exp\left(iS_{\rm CF}[\psi, \bar\psi, \mathbf{a}_\perp, \phi] + i\frac{\theta}{2} S_{\rm CS}[\mathbf{a}_\perp, \phi]\right), \end{aligned}$$

where we have introduced the common shorthand notation $\theta \equiv 1/2\pi s$, the action $S[\bar\psi, \psi, \mathbf{a}_\perp] \equiv S[\bar\psi, \psi]\big|_{\mathbf{A}[\bar\psi,\psi]\to\mathbf{A}_{\rm ext}+\mathbf{a}_\perp}$ is obtained by replacing the fixed vector potential

[89] Technically, it is not advisable to disturb the structure of the most basic operator of the theory.

[90] This latter condition is necessary because the δ-distribution does not fix the longitudinal, or gauge, freedoms of the potential. In two dimensions, the decomposition of the vector potential into longitudinal (φ) and transverse (θ) components is achieved by setting $a_i = \partial_i\varphi + \epsilon_{ij}\partial_j\theta$.

$\mathbf{a}[\bar\psi,\psi]$ by the integration variable $\mathbf{a}_\perp$,[91]

$$S_{\rm CF}[\psi,\bar\psi,a_\perp]=\int d^2x\ dt\,\bar\psi\left(i\partial_t+\mu-\phi+\frac{1}{2m}(-i\partial_{\mathbf{x}}+\mathbf{A})^2-V\right)\psi+S_{\rm int}[\bar\psi,\psi],\quad(9.73)$$

$$S_{\rm CS}[a_\perp]=-\int d^2x\ dt\,\phi\epsilon_{ij}\partial_i a_{\perp,j},\quad(9.74)$$

and $\mathbf{A}=\mathbf{A}_{\rm ext}+\mathbf{a}_\perp$. At this stage, we have fulfilled our intermediate goal; a field integral representation has been derived wherein particles are tightly bound to fluxes. There is, however, something unsatisfactory about the present representation of the theory: the way the variables $\mathbf{a}_\perp$ and ϕ enter the action (9.74) suggests an interpretation of the theory as one of fermions coupled to a $(2+1)$-dimensional electromagnetic gauge potential $a_\perp\equiv(\phi,\mathbf{a}_\perp)$. However, the action $S_{\rm CF}+S_{\rm CS}$ falls short of the two standard criteria any decent theory of electromagnetism should obey: (i) in its present representation, it has nothing to say about the longitudinal degrees of freedom $\mathbf{a}_\parallel$ of the vector potential and, relatedly, (ii) the contribution $S_{\rm CS}$ is not gauge invariant (which means that, using a covariant representation $x=\{x_\mu\}\equiv(x_0\equiv t,x_1,x_2)$, under a transformation $a_\mu\to a_\mu+\partial_\mu f$, $\mu=0,1,2$, it changes value).

We now claim that the action $S_{\rm CS}$ possesses a natural gauge-invariant extension, namely the well-studied **Chern–Simons action**[92]

$$\boxed{S_{\rm CS}[a]=-\int d^3x\ \epsilon_{\mu\nu\sigma}a_\mu\partial_\nu a_\sigma.}\quad(9.75)$$

Firstly, a straightforward integration by parts shows that $S_{\rm CS}$ is gauge invariant. Secondly, one verifies (exercise!) that, for a purely transverse configuration $a_\perp=(\phi,\partial_2\theta,-\partial_1\theta)$, $S_{\rm CS}[a_\perp]$ reduces to the form given in Eq. (9.74). Put differently, the prototypical action (9.74) is but the gauge-invariant Chern–Simons action evaluated in a particular gauge, namely the **Coulomb** or **radiation gauge** $a_\parallel=0$. The gauge-invariant extension of the theory is obtained by integration over all gauge sectors,

$$\mathcal{Z}=\mathcal{N}\int D(\bar\psi,\psi)\ Da\,\exp\left(iS_{\rm CF}[\bar\psi,\psi,a]+i\frac{\theta}{4}S_{\rm CS}[a]\right),\quad(9.76)$$

where

$$S_{\rm CF}[\psi,\bar\psi,a]=\int d^3x\,\bar\psi\left(i\partial_0+\mu-\phi+\frac{1}{2m}(-i\partial_{\mathbf{x}}+\mathbf{A}_{\rm ext}-\mathbf{a})^2-V\right)\psi+S_{\rm int}[\bar\psi,\psi],\quad(9.77)$$

[91] Notice that Eq. (9.72) is purely transversal, so that the replacement $\hat{\mathbf{a}}\to\mathbf{a}_\perp$ makes sense.
[92] Recall that space-time vectorial components are defined as $x_\mu=(x_0,x_1,x_2)$, while $\partial_\mu=(-\partial_0,\partial_1,\partial_2)$.

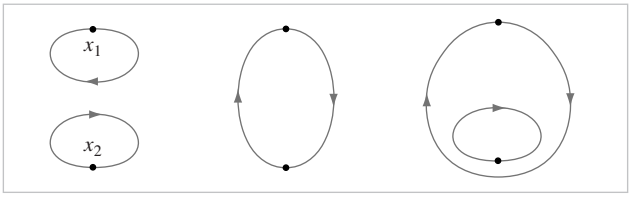

Figure 9.18 Different ways of realizing constructive particle exchange along transmutation paths.

is but the action (9.74) generalized to arbitrary gauge field configurations.[93] In the following we will investigate what information can be obtained from the functional integral Eq. (9.76) about the physical behavior of the FQH system.

Particle exchange in two dimensions

Before embarking on this program, it may be of interest to discuss a few general aspects of Chern–Simons field theory and **particle transmutation statistics**. In undergraduate quantum mechanics courses we learn to discriminate between particles with bosonic and fermionic statistics. On the formal level, the distinction between the two is met by considering the behavior of the wavefunction under an "exchange of particles," namely

$$\Psi(\ldots, x^1, \ldots, x^2, \ldots) = \pm\Psi(\ldots, x^2, \ldots, x^1, \ldots), \tag{9.78}$$

for bosons/fermions respectively. In fact, however, this definition should leave one with a certain feeling of uneasiness: what is actually meant by the phrase "exchange of particles"? Surely, the definition above does not imply a concrete physical prescription, i.e. strictly speaking it does not make sense.

To appreciate the fact that we are not just discussing a formal subtlety, let us try to give the exchange of particles a more physical meaning. (The construction below follows closely an argument from chapter I.2 of Wilczek.[94]) Consider two quantum particles occupying positions x^1, x^2 in a two-dimensional system. Suppose we were interested in computing the amplitude for these particles to re-occupy the positions x^1, x^2 after some time t. Clearly, these amplitudes receive two distinct contributions, (i) $x^1 \to x^1, x^2 \to x^2$ and (ii) $x^1 \to x^2, x^2 \to x^1$ where $x \to y$ denotes the single-particle amplitude for propagation from $x \to y$. Interpreting the second process as an operation of particle exchange, we are interested in identifying a fixed relative phase between (i) and (ii). Thinking about the total transition process in terms of a coherent double sum over single-particle paths, it is clear that contributions from (i) cannot be continuously deformed into those of type (ii). The path-sum falls into disconnected pieces, implying that there will be no variational (or classical) principles telling us about the relative phase. Yet, quantum mechanics itself provides us with

[93] As usual with gauge theories, the integral Eq. (9.76) must be interpreted in a qualified sense: the very fact that the action is gauge invariant implies that the integration over all the different gauge realizations yields the – infinite – volume of the gauge sector. To give the functional integral some meaning, a **gauge xing** contribution $S_{\text{fix}}[a]$ has to be added to the action, i.e. a contribution that restricts the integration to a specific reference gauge. Mostly, however, the presence of the gauge fixing action is not indicated explicitly.

[94] F. Wilczek, *Frictional Statistics and Anyons Superconductivity* (World Scientific Publishing, 1990).

an important clue: from the point of view of the first of the two particles, the net result of a (i)-process will be a rotation of particle 2 (around the position of particle 1) by an angle $\phi \in 2\pi\mathbb{Z}$. This is illustrated for $\phi = 0$ (left) and $\phi = 2\pi$ (right) in Fig. 9.18. Conversely, a (ii)-process corresponds to a rotation by $\phi \in (2\mathbb{Z}+1)\pi$. (For $\phi = \pi$, see the center of the figure.)

Now, let us suppose that the topologically distinct processes differ by some phase $\kappa(\phi)$. If we iterate transmutation processes, $(x^1, x^2) \stackrel{t}{\to} (x^2, x^1) \stackrel{t'}{\to} (x^1, x^2)$, the winding angles add while quantum mechanics requires that the topological phases multiply, $\kappa(\phi + \phi') = \kappa(\phi)\kappa(\phi')$, implying that $\kappa(\phi) = \exp(i\psi\phi)$, where $\psi \in [0, 2]$ is some parameter.[95]

Specifically, a single exchange operation $(x^1, x^2) \to (x^2, x^1)$ corresponds to a phase $e^{i\pi\psi}$. Let us compare this with the formal exchange definition above. According to Eq. (9.78), a twofold exchange, $(x^1, x^2) \to (x^2, x^1) \to (x^1, x^2)$, leaves the wavefunction unaltered. In contrast, even the most elementary "physical" exchange procedure corresponds to a winding angle $\phi = \pi$ and, therefore, to a topological phase $\exp(2\pi i\psi)$. Only for the special choices $\psi = 0$ (bosons) or $\psi = 1$ (fermions) do we recover the result of the formal exchange. For a beautiful (yet non-path-integral-oriented) extension of the arguments above to a physically meaningful exchange prescription for general N-particle systems we refer to the seminal paper of Leinaas and Myrheim.[96] Presently, all we need to appreciate is that a constructive exchange operation appears to leave more room for non-trivial (i.e. $\neq 1, -1$) transmutation statistics. Particles with $\psi \neq 0, 1$ have been dubbed **anyons**, where the "any" stands for "any exchange statistics." Skeptical readers may justly object that the overwhelming majority of particles observed in physics are of either bosonic or fermionic type. So where, then, does anyonic exchange statistics play a role? The short answer to this question is that our discussion above was critically tied to the two-dimensional system. In three or more dimensions, the winding angle ϕ is defined only mod 2π. For example, in the three-dimensional world, you might use the dimension perpendicular to the paper plane to contract the process shown in the right hand of Fig. 9.18, $\phi = 2\pi$, to a $\phi = 0$ type process. This forces ψ to be an integer, i.e. $\psi = 0$ (bosons) and $\psi = 1$ (fermions) simply exhaust the list of possible options:[97] in $d \neq 2$ anyons do not exist.[98] Yet, in various two-dimensional applications, anyonic excitations do play an important role. For example, a theoretical approach to the FQHE competing with the CF approach discussed in the text is based on composite *bosons*.[99] Although these are not anyons in the strict sense, here, too, the exchange statistics has been externally modified (in this case to manufacture bosons from fermions). Indeed, for a while, attempts were made to link anyons to the subject

[95] Since ϕ is a multiple of π, ψ is defined only mod 2.

[96] J. M. Leinaas and J. Myrheim, On the theory of identical particles, *Il Nuovo Cimento B* **37** (1977), 1–23.

[97] In $d = 1$, particles cannot be exchanged anyway, which accounts for the interchangeability of bosonic and fermionic modelings.

[98] Another argument can be developed to the same effect: according to the spin-statistics theorem, the exchange statistics of particles is intimately tied to the quantization of angular momentum. The latter, in turn, is a direct consequence of the SU(2) commutation relations $[\hat{J}_i, \hat{J}_j] = i\epsilon_{ijk}J_k$: the structure of the right-hand side fixes the dimension of the irreducible representations of SU(2) and, thereby, the particle statistics. Yet, when restricted to a two-dimensional world, the algebra of angular momentum becomes one-dimensional, i.e. abelian. The absence of angular momentum quantization then implies that the spin statistics theorem loses its meaning.

[99] S. C. Zhang, T. H. Hansson, and S. Kivelson, Effective field theory model for the fractional quantum Hall effect, *Phys. Rev. Lett.* **62** (1989), 82–5.

of high-temperature superconductivity.[100] Further, there is compelling evidence that the quasi-particle excitations in quasi-one-dimensional FQHE systems show fractional statistics, etc. Finally, field theories of anyons have been considered as prototypical model systems of matter fields coupled to massive gauge field excitations. These applications are motivation enough to briefly discuss the quantitative theoretical framework of anyon dynamics in two-dimensional systems.

Let us start out from the following functional setup:

$$\mathcal{Z} = \int Da\ D\phi\ \exp\left[iS_0[\phi] + i\int d^3x\, j_\mu^\uparrow a_\downarrow^\mu + \frac{i\theta}{4}S_{\rm CS}[a]\right],$$

where either $\int D\phi = \int D(\bar\psi,\psi)$ may stand for a coherent state field integral, or $\int D\phi = \int\prod_{i=1}^N D(\mathbf{x}^i,\dot{\mathbf{x}}^i)$ for a multiple path integral over the configuration space trajectories $\{\mathbf{x}^i\}$ of N particles. In the latter case (see the exercise below), $j(x) = \sum_{i=1}^N (1,\dot{\mathbf{x}}^i)\delta(\mathbf{x}-\mathbf{x}^i(t))$ is the current density carried by the world lines of N particles.

EXERCISE Subject the first-quantized many-particle Hamiltonian $\hat H = \sum_{i=1}^N(\frac{\hat{\mathbf{p}}^{i2}}{2m} + V(\hat{\mathbf{x}}^i))$ to the singular gauge transformation (9.70). Then construct a path integral representation for the transition amplitude $\langle\mathbf{x}^1,\dots,\mathbf{x}^N|\hat U(t)|\mathbf{y}^1,\dots,\mathbf{y}^N\rangle$. Show that the decoupling of the nonlinear gauge field contribution acquired by the Hamiltonian exactly parallels the field integral scheme discussed above. As before, the action contains the Chern–Simons contribution Eq. (9.75) and a current vector potential coupling. The latter is given by the canonical expression

$$\int dt\sum_i(-\phi(\mathbf{x}^i) + \mathbf{x}_i\cdot\mathbf{a}_i(\mathbf{x}^i)) \quad\equiv\quad \int dt\sum_i a_\mu(\mathbf{x}^i)j^\mu(\mathbf{x}^i,\mathbf{x}^i) \equiv \int d^3x\, a_\mu(x)j^\mu(x).$$

In the first line, $j(\mathbf{x}) \equiv (1,\mathbf{x})$ denotes the $(2+1)$-dimensional current carried by a point particle while, in the second line, $j(x) \equiv \sum_i(1,\mathbf{x}^i)\delta(\mathbf{x}-\mathbf{x}^i)$ represents the corresponding current density. (Upon space integration, $\int d^2x\, j^\mu(x) = \sum_i j^\mu(\mathbf{x}^i)$.)

We next employ the path integral variant to show that the statistical angle θ controls the transmutation statistics of the planar particle system. Let us consider a system of $N=2$ particles initially ($t=t_{\rm i}$) prepared to occupy the coordinates (y^1,y^2). We want to analyze the transition amplitude $\langle y^1,y^2|\hat U(t_{\rm f},t_{\rm i})|y^1,y^2\rangle$ to reoccupy the same state at a time $t_{\rm f}$. As in our qualitative construction above, the path integral describing this amplitude receives contributions from topologically distinct pairs of trajectories. (The world lines of two trajectories with winding angle $\phi=0$ (left) and $\phi=2\pi$ (right) are shown in the figure.)

To explore the impact of the statistical vector potential on the transition amplitude it is convenient to switch to an imaginary time formalism. Upon analytic continuation $t\to -i\tau$, $a_0\to ia_0$, the path integral for the two transition amplitudes assumes the form

$$\mathcal{Z} = \int D(\mathbf{x}^1,\mathbf{x}^2)\ \exp\left[-S_0[\phi] + \int d^3x\, j_\mu a_\mu - \frac{i\theta}{4}S_{\rm CS}\right],$$

[100] R. B. Laughlin, The relationship between high-temperature superconductivity and the fractional quantum Hall effect, *Science* **242** (1988), 525–33.

where $j_\mu = i\frac{\partial x_\mu(\tau)}{\partial\tau}\delta(\mathbf{x}-\mathbf{x}(\tau))$ is the $(2+1)$-dimensional imaginary time current. The most important consequence of the transition $t \to -i\tau \in -i[0,\beta]$ is that the initial and final points of our two space-time trajectories now have to be identified (the usual temporally periodic boundary conditions of the imaginary time formulation[101]). A glance at the figure shows that this leads to a pair of two closed world line curves which, for a winding angle $\phi = 2\pi n$, are n-fold intertwined.[102] Focusing on the two most elementary variants $\phi = 0$ and $\phi = 2\pi$, we next evaluate the Chern–Simons action on these trajectory pairs.

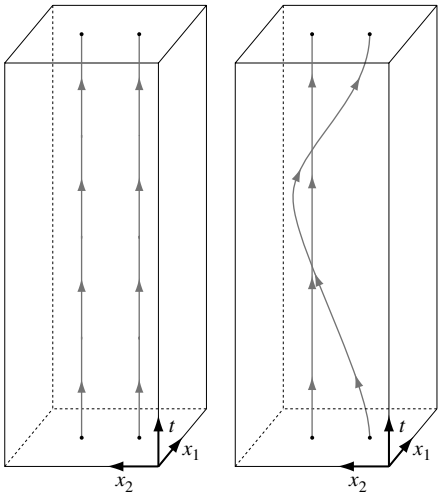

We begin by integrating out the statistical vector potential. For now, it will be convenient to perform this integration in the radiation gauge, $\partial_\mu a_\mu = 0$. (Remember that, to integrate over a gauge field, a specific gauge has to be chosen.) This gauge can be selected by adding a **gauge fixing** contribution $\alpha\int d^3x\,(\partial_\mu a_\mu)^2$ to the action. In the limit $\alpha\to\infty$, configurations with $\partial_\mu a_\mu$ no longer contribute to the integration and the gauge is effectively fixed. Equivalently, one may limit the integration from the outset so that only the two components of $a(q)$ perpendicular to q are integrated over. Either way, one finds (exercise) $\langle a_\mu(q)a_\nu(q')\rangle_a = \frac{2}{\theta}\frac{\epsilon_{\mu\nu\sigma}q_\sigma}{q^2}\delta_{q+q'}$, where $\langle\cdots\rangle_a$ denotes functional averaging over the (imaginary time) Chern–Simons action. Using this result, we obtain

$$\begin{aligned}
\mathcal{Z} &= \int D(\mathbf{x}^1,\mathbf{x}^2)\,\exp\left[-S_0[\phi]+\frac{1}{2}\int d^3x\;d^3x'\,j_\mu(x)j_\nu(x')\,\langle a_\mu(x)a_\nu(x')\rangle_a\right]\\
&= \int D(\mathbf{x}^1,\mathbf{x}^2)\,\exp\left[-S_0[\phi]+\frac{1}{2}\sum_{qq'}j_\mu(q)j_\nu(q')\,\langle a_\mu(q)a_\nu(q')\rangle_a\right]\\
&= \int D(\mathbf{x}^1,\mathbf{x}^2)\,\exp\left[-S_0[\phi]+\frac{\epsilon_{\mu\nu\sigma}}{\theta}\sum_q j_\mu(q)\frac{q_\sigma}{q^2}j_\nu(-q)\right].
\end{aligned}$$

Let us now try to understand the meaning of the last term in the action, the remnant of the Chern–Simons integration. In fact, this term will turn out to be a topological invariant which tells us about the degree of knotting of the two integration paths. To see this, let us define

$$\tilde{j}_\mu \equiv -ij_\mu = \partial_\tau\sum_{a=1,2}x^a_\mu(\tau)\delta(x_1-x^a_1(\tau))\delta(x_2-x^a_2(\tau)),$$

where $x=(\tau,x_1,x_2)$. Temporarily forgetting about the time-like origin of the first component, we may think of $\tilde{j}$ as the current vector field created by two loops in three-dimensional

[101] For the present, however, the parameter β does not carry any physical significance.
[102] For the moment, we do not consider odd multiples $\phi=(2n+1)\pi$ (corresponding to a particle *exchange*) since for $y^1\neq y^2$ these cases do not have a meaningful imaginary time extension.

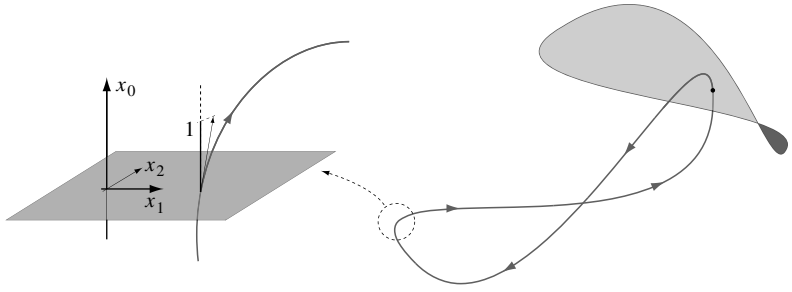

Figure 9.19 Two intertwined current loops in (2+1)-dimensional Euclidean space–time.

space, each carrying a current $I = 1$ of unit[103] strength (see Fig. 9.19). The key point now is that, according to **Ampère's law**, $b_\mu = -i\epsilon_{\mu\nu\sigma}\frac{q_\nu}{q^2}\tilde{j}_\sigma$ is the magnetic field created by a static[104] current distribution $\tilde{j}$. We may thus write the topological contribution to the action as

$$\begin{aligned} S_{\rm top}[x^1, x^2] &= -\frac{i}{\theta}\sum_{aa'}\int d^3x\, \tilde{j}^a_\mu(x) b^{a'}(x) = -\frac{i}{\theta}\sum_{aa'}\int d\tau\ \frac{dx^a(\tau)}{d\tau}\cdot b^{a'}(x) \\ &= -\frac{i}{\theta}\sum_{aa'}\oint_{\gamma^a} ds\cdot b^{a'} = -\frac{i}{\theta}\sum_{aa'}\int_{S^a} dS\cdot \mathrm{curl}\, b^{a'} = -\frac{i}{\theta}\sum_{aa'}\int_{S^a} dS\, \tilde{j}^{a'} \\ &= -\frac{2i}{\theta} I(\gamma^a, \gamma^{a'}). \end{aligned}$$

Here, γ^a is a shorthand for the curve $\{\tau, x^a_1, x^a_2\}$, and S^a a surface spanned by γ^a. The crucial last line states that the topological action is proportional to the current $I(\gamma^a, \gamma^{a'})$ flowing through the area spanned by loop a' due to the presence of loop a (see Fig. 9.19). Obviously, $I(\gamma^a, \gamma^a) = 0$. For $a \neq a'$, $I(\gamma^a, \gamma^{a'}) \in \mathbb{Z}$ is equal to the number of times γ^a pierces $S^{a'}$ or, in other words, the degree to which the two loops are intertwined.

Specifically, amplitudes where one of the particles encircles the other n times acquire a phase $\kappa(2\pi n) = e^{2\pi i n\psi}$, where $\psi = 1/(\pi\theta)$. We have thus found that the Chern–Simons action does the book-keeping of the anyonic exchange phases discussed qualitatively above. In fact, it is relatively straightforward to extend our present two-particle analysis to N particles, or to the fully-fledged formalism of the coherent state field integral. In the specific case of the Chern–Simons field theory of the FQHE, $\theta = (2\pi s)^{-1}$, i.e. fermions get transformed to (composite) fermions. In general, however, θ may be tuned so as to generate any form of exchange statistics.

[103] To compute the strength of the current, one may integrate $\tilde{j}$ over a space-like surface $x_0 = \tau = \text{const.}$ intersecting the loop (see Fig. 9.19). The integral gives $I = \int dx_1\, dx_2\, \tilde{j}_0(x) = \tilde{j}_0(\tau, x_1(\tau), x_2(\tau)) = 1$.

[104] Keep in mind that, in our present picture, the 0-direction of space no longer carries the significance of time.

9.5.3 Chern–Simons field theory II: analysis

Equation (9.76) defines an exact reformulation of the FQHE field integral in terms of a Chern–Simons action. Trusting that the CS gauge field degree of freedom is sufficiently benign, we now proceed to our familiar program "mean-field + fluctuations." We begin by subjecting the Coulomb interaction $S_{\rm int}$ to a Hubbard–Stratonovich transformation,

$$e^{iS_{\rm int}[\bar\psi,\psi]} = \int D\sigma\, e^{\frac{i}{2}\int d^3x\, d^3x'\, \sigma(x)[V^{-1}(\mathbf{x}-\mathbf{x}')\delta(x_0-x_0')]\sigma(x')+i\int d^3x\,(\hat\rho(x)-\rho_0)\sigma(x)},$$

where V^{-1} denotes the inverse of the interaction kernel. Integration over the – now Gaussian – CF degrees of freedom ψ then brings us to the partition function, $\mathcal{Z} = \mathcal{N}\int Da\; D\sigma\, e^{iS[a,\sigma]}$, where

$$S[a,\sigma] = -i\,\mathrm{tr}\ln\left[i\partial_0+\mu-\phi-\sigma+\frac{1}{2m}(-i\nabla+\mathbf{A})^2-V\right]-\rho_0\int d^3x\,\sigma(x)$$
$$+\frac{1}{2}\int d^3x\, d^3x'\,\sigma(x)V^{-1}(\mathbf{x}-\mathbf{x}')\delta(x_0-x_0')\sigma(x')+\frac{\theta}{4}S_{\rm CS}[a]. \tag{9.79}$$

Starting from this representation, we now subject the theory to a mean-field analysis.

Mean-field equations

Let us seek for solutions of the equations

$$\left.\frac{\delta S[a,\sigma]}{\delta a_\mu(x)}\right|_{\bar\sigma,\bar a} = \left.\frac{\delta S[a,\sigma]}{\delta\sigma(x)}\right|_{\bar\sigma,\bar a} = 0.$$

Explicitly performing the differentiation with respect to $a_0=\phi$, one may see that the first of these equations translates to the – by now familiar – form

$$\rho[\bar a,\bar\sigma] = \frac{1}{4\pi s}\bar b, \tag{9.80}$$

where $\rho[a,\sigma](x) = i(i\partial_0+\mu-\phi-\sigma+\frac{1}{2m}(-i\nabla+\mathbf{A})^2-V)^{-1}(x,x)$ denotes the local density of CFs, and the notation emphasizes the functional dependence of ρ on a and the Hubbard–Stratonovich potential σ. The differentiation with respect to the space-like components $\mathbf{a}$ does not yield independent new information; all it gives us is two relations expressing the compatibility of Eq. (9.80) with the continuity equation. Finally, differentiation with respect to σ gives

$$\sigma(x) = -\int d^2x'\, V(\mathbf{x}-\mathbf{x}')\;(\rho[\bar a,\bar\sigma](x')-\rho_0)|_{x_0'=x_0}\,. \tag{9.81}$$

This equation also affords a transparent interpretation: on the mean-field level the potential $\sim\int V\,[\rho-\rho_0]$ created by local density fluctuations compensates the interaction potential. In the absence of fluctuations of the external potential $V(\mathbf{x})$, Eq. (9.80) and (9.81) possess the obvious homogeneous solution

$$\rho[\bar a,0]=\rho_0=\text{const.},\quad \sigma=\phi=0,\quad \bar b = 4\pi s\rho_0 \qquad \mathbf{a} = 2s\nu\mathbf{A}_{\rm ext}.$$

The particle density is homogeneous, implying that no mean-field interaction σ is generated. The strength of the equally homogeneous CS mean-field $\bar b$ is set by the average density ρ of

composite fermions. As expected, the effective field seen by the CFs, $B = B_{\rm ext} - b$, turns out to be lower than that of the external magnetic field. Specifically, for a half-filled band, $\nu = 1/2$, $\rho_0 = B_{\rm ext}/4\pi$. In this case, CFs with two flux quanta attached, $s = 1$, experience a mean-field B of vanishing strength.

Now let us investigate the stability of the mean-field with respect to fluctuations. In many respects the N CFs behave like ordinary fermions subject to a perpendicular field of strength B. In particular, they will undergo a Landau quantization where, typically, the highest Landau level will be only partially occupied. Foreseeably, these generic configurations will be highly susceptible to all sorts of fluctuation effects (i.e. poor candidates for mean-field schemes): the massive degeneracy of the Landau levels leads to "small-energy denominators," so that even a slight perturbation/fluctuation may cause dramatic effects. We thus expect our present mean-field scheme to work only in the vicinity of filling fractions ν where an integer number p of CF Landau levels are fully occupied. These filling fractions are determined by the equation $\nu_{\rm eff} = p$ or $\Phi_{\rm eff} = 2\pi N/p$, where $\Phi_{\rm eff} = BL^2$ denotes the total effective flux piercing the system. Using the relation $B = B_{\rm ext} - b$ where $b = 4\pi s N L^{-2}$, it is straightforward to solve these equations to obtain

$$\nu = \frac{2\pi N}{B_{\rm ext} L^2} = \frac{p}{2sp+1},$$

in agreement with the experimental observation. Summarizing, the mean-field analysis of the Chern–Simons action confirms the basic expectation formulated on page 571 that

> the fractional QHE can be interpreted as an integer QHE of composite fermions.

INFO There is one more aspect of the theory that can be explored on the level of plain mean-field theory, namely the **charge of the composite fermions.** To this end, let us consider the functional expectation value of the operator

$$\mathcal{O}(x,x') \equiv \langle \bar\psi(x)\psi(x')\rangle\,.$$

The correlation function $\mathcal{O}$ describes the amplitude for creation of a CF at a space-time point x and its annihilation at x'. Let us regard this amplitude as the coherent sum over all paths γ connecting x and x'. Due to the presence of the external magnetic field, each such contribution acquires an Aharonov–Bohm phase $\phi_\gamma \equiv -q_{\rm eff} \int_\gamma dx_\mu\, A^\mu_{\rm ext}$, where the coefficient $q_{\rm eff}$ defines the effective charge of the particle. (As we shall see, the presence of the statistical field makes $q_{\rm eff}$ different from the bare electron value $q = 1$.) Performing the Gaussian integral over ψ, we represent $\mathcal{O}$ as

$$\begin{aligned}
\mathcal{O}(x,x') &= \left\langle \langle x|(i\partial_0 + \mu - \phi - \sigma + \frac{1}{2m}(-i\quad + \mathbf{A})^2 - V)^{-1}|x'\rangle \right\rangle_{a,\sigma} \\
&= \langle\langle \mathbf{x}|U(t,t')|\mathbf{x}'\rangle\rangle_{a,\sigma} \\
&= \left\langle \int_{\substack{x(t)=x\\ x(t')=x'}} Dx\, \exp\left[iS_0[x,\sigma] - i\int dt\ (\phi - \mathbf{A}\cdot\mathbf{x})\right]\right\rangle_{a,\sigma} \\
&\overset{\rm MF}{\approx} \text{const.} \times \int\limits_{\substack{x(t)=x\\ x(t')=x'}} Dx \exp\left[iS_0[x,0] - iq_{\rm eff}\int d\mathbf{x}\cdot\mathbf{A}_{\rm ext}\right].
\end{aligned}$$

In the first line, the angular brackets denote the functional averaging over the Chern–Simons action (a) and the interaction kernel (σ). Further, we have made use of the fact that the (retarded) real time Green function is equal to the time evolution operator U. The latter is represented as a *path* (as opposed to a "field") integral. The action of the path integral contains a field-independent contribution S_0, the coupling to the scalar field component ϕ, and the canonical coupling to the vector potential $\mathbf{A}$. Until now, all manipulations have been exact. In the crucial last line, we then evaluate the (a,σ)-integration in a mean-field approximation. Assuming that fluctuations (lumped into the "const." in front of the integral) will be small, this amounts to a substitution $(a,\sigma) \to (\bar{a},0)$ in the action. Using the fact that $\mathbf{a}_{\rm ext} = 2s\nu\mathbf{A}_{\rm ext}$, we arrive at the last line, where the coupling constant

$$q_{\rm eff} = 1 - 2s\nu = \frac{1}{1+2sp}, \tag{9.82}$$

is identified as the effective charge of the CF. The line of reasoning above tells us that CFs effectively carry **fractional charge**. The partial "screening" of the bare electron charge, $0 < q_{\rm eff} < 1$, is explained by the tendency of the phase vortices to expel electronic charge. In the specific case, $\nu = 1/2 \rightsquigarrow q_{\rm eff} = 0$, the electron charge becomes completely screened by $2s = 2$ vortices, a result that led some authors[105] to interpret the $\nu = 1/2$ FQHE as a dynamic phenomenon of **charge dipoles** – each comprising one electron ($q = 1$) and two vortices ("$q = -2 \times 1/2 = -1$").

Fluctuations

We now proceed to explore the role of quadratic fluctuations around the homogeneous mean-field. In particular:

- ▷ What does the field theory have to say about the electromagnetic response of the system?
- ▷ What else (beyond the fractional transmutation statistics) does it tell us about the microscopic features of the composite fermions?

To answer these questions, we do not have to go into much quantitative detail. Rather the ubiquitous condition of gauge invariance and the presence of an excitation gap (an integer number of CF Landau levels are fully occupied!) suffice to fix the structure of the quadratic action.

Shifting $a \to \bar{a} + a$ and $\sigma \to \bar{\sigma} + \sigma$, our goal is to expand the action to second order in the deviations (a,σ). Let us begin by considering the interaction field σ. A shift $a_0 = \phi \to \phi + \sigma$ removes σ from the "tr ln" component of the action and makes it reappear in the Chern–Simons action. More specifically, the Chern–Simons acquires a linear contribution[106] $S_{\rm CS}[a] \to S_{\rm CS}[a] - 2\int d^3x\, \sigma b$ so that the total σ-expansion of the action now reads

$$S[a,\sigma] = S[a] - \frac{\theta}{2}\int d^3x\, \sigma(x)b(x) + \frac{1}{2}\int d^3x\; d^3x'\, \sigma(x)V^{-1}(\mathbf{x}-\mathbf{x}')\delta(x_0 - x_0')\sigma(x').$$

[105] A. Stern, B. I. Halperin, F. von Oppen, and S. H. Simon, Half-filled Landau level as a Fermi liquid of dipolar quasiparticles, *Phys. Rev. B* **59** (1999), 12547–67.

[106] Here $b = \epsilon_{ij}\partial_i a_j$ describes the *uctuations* of the statistical magnetic field around its mean value $\bar{b}$.

After the straightforward Gaussian integration over σ we then obtain

$$S[a,\sigma] \xrightarrow{\int D\sigma} S[a] + \frac{1}{2}\int d^3x\; d^3x'\, b(x)V(\mathbf{x}-\mathbf{x}')\delta(x_0-x_0')b(x').$$

The physical interpretation of the induced term is obvious: in the CS theory, fluctuations of the particle density are tied to fluctuations of the statistical magnetic field. Accordingly, spatial inhomogeneities of the statistical magnetic field get penalized by an interaction contribution, as described by the second term above. However, as far as the two basic questions above are concerned, we may temporarily forget about this contribution (see, however, the concluding remarks below) and focus attention on the action $S[a]$.

Let us, then, consider the action $S[a,A'] \equiv S_{\rm CF}[\bar{a}+a+A'] + \frac{\theta}{4}S_{\rm CS}[\bar{a}+a]$, where

$$S_{\rm CF}[a] = -i\,\mathrm{tr}\ln\left(i\partial_0 + \mu - a_0 - \frac{1}{2m}(-i\nabla - \mathbf{a})^2 - V\right),$$

denotes the CF contribution to the action to which we have coupled a source potential A'. As usual, a two-fold differentiation with respect to elements of A' will later tell us about the relevant transport coefficients of the system. Next, we develop the formal expansion $S[a,A'] \equiv \sum_n S^{(n)}[a,A']$, where $S^{(n)}[a,A']$ is of total order n in a and A'. The zeroth-order term $S^{(0)}$ describes the CF system on the mean-field level and will not be of further interest to us. The first-order term $S^{(1)}$ does not contain a as we are expanding around a stationary configuration. Moreover, its A dependence $S^{(1)}[A] = iA_\mu\bar{j}^\mu$ is inessential because the mean-field CF density $\bar{j}^0$ is structureless and a mean-field current $\bar{\mathbf{j}} = 0$ does not flow. However, at the second-order level $S^{(2)}$, things start becoming more interesting. Formally, the second-order contribution can be represented as

$$S^{(2)}[a,A'] = \frac{1}{2}\int d^3x\; d^3x'\,(a+A')_\mu(x)K_{\mu\nu}(x,x')(a+A')_\nu(x') + \frac{\theta}{4}S_{\rm CS}[a], \tag{9.83}$$

where $K_{\mu\nu}(x,x') = \frac{\delta^2 S_{\rm CF}[a]}{\delta a_\mu(x)\delta a_\nu(x')}\Big|_{a=\bar{a}}$. By construction, K is but the linear response kernel discussed in Section 7.2. For the moment, all we need to recall about this object is that it (a) is gauge invariant, $\partial_\mu K^{\mu\nu} = K^{\mu\nu}\;\partial_\nu = 0$, (b) is generally short-range ($K(q)$ can be expanded in powers of q), and (c) contains information about both the polarizability of the medium and its conductivity.

Building on property (b), one can expand the second-order action in derivatives: $S^{(2)}[a,A'] = \sum_{l=0}^{\infty} S^{(2,l)}[a,A']$, where $S^{(2,l)}[a,A']$ is of lth order in derivatives (∂_0,∂_x) and, as usual, one may focus attention on the contribution with the least number of derivatives. As discussed before, no gauge-invariant zero derivative term $S^{(2,0)}$ can be constructed. However, with the contribution linear in the number of derivatives, $S^{(2,1)}$, the situation is more tricky. While in general there are no gauge invariant contributions of first order in $q \leftrightarrow -i\nabla$, terms nominally scaling as $|q|$ for $q \to 0$ exist. (For example, in systems with a non-vanishing longitudinal conductivity, the action takes the form $S^{(2,1)}[A'] \sim A'_\mu(q)\frac{q^\mu q^\nu - q^2}{Dq^2+i\omega}A'_\nu(-q)$, where D denotes the diffusion constant.) However, the system at hand is an insulator, so that no such term is present.

Yet, in two-dimensional systems, there exists one more gauge-invariant first-order derivative term, namely the notorious Chern–Simons term! Thus, we are led to the preliminary

identification $S^{(2,1)}[a,A'] = c\,S_{\rm CS}[a+A'] + \frac{\theta}{4}S_{\rm CS}[a]$, where the first contribution is obtained by a first-order gradient expansion of the CF action while the second contribution has been present from the outset. Of course, the coupling constant c remains to be determined. This can be done by explicit – and quite laborious – calculation or by the following more elegant construction: remembering that $S_{\rm CS}[a] = -\int d^3x\,\epsilon_{\mu\nu\sigma}a_\mu\partial_\nu a_\sigma = -i\sum_q \epsilon_{\mu\nu\sigma}a_\mu(q)q_\nu a_\sigma(-q)$, and comparing with Eq. (9.83), our findings so far translate to the relation

$$K_{\mu\nu}(q) = -i2c\,\epsilon_{\mu\sigma\nu}q_\sigma + \mathcal{O}(q^2). \tag{9.84}$$

INFO To fully describe the **electromagnetism of the statistical gauge field**, we should also include the second-order derivative contribution $S^{(2,2)}$ in our analysis: gauge-invariant contributions of second order are obtained as bilinears formed from elements of the field tensor $F_\mu = \partial_\mu a' - \partial a'_\mu$. These terms are then combined into an action $S^{(2,2)} = \frac{1}{2}\int d^3x\,(\epsilon\mathbf{e}'\cdot\mathbf{e}' + \chi b^2)$, where $e'_i = \partial_0 a'_i - \partial_i a'_0$ is the electric field derived from the gauge field a', and ϵ and χ are the electric and magnetic permeabilities, respectively. Physically, the action $S^{(2,2)}$ describes the electric and magnetic susceptibility of the (mean-field) CF medium to the presence of gauge field fluctuations. However, as far as our present objectives are concerned, these effects turn out to be of lesser relevance.

On the other hand, we know the conductivity of the system relates to the linear response kernel through the relation $\sigma^0_{12} = -i\lim_{q\to 0}\omega^{-1}K_{12}(\omega,\mathbf{q})$. For the present, we have to interpret $\sigma^0_{12} = \frac{p}{2\pi}$ as the quantized Hall conductivity carried by the CF system at the mean-field level. Comparison with Eq. (9.84) then leads to the identification $c = \sigma_{12}/2$, or

$$S^{(2,1)}[a,A'] = \frac{\sigma^0_{12}}{2}\,S_{\rm CS}[a+A'] + \frac{\theta}{4}S_{\rm CS}[a].$$

Of course, σ^0_{12} does not coincide with the actual Hall conductance σ_{12} carried by the system – within our present level of approximation, the latter is obtained by two-fold differentiation with respect to A' *after* the statistical gauge field has been integrated out. Now, there is a simple general formula telling us what happens to two *quadratic* actions (such as the Chern–Simons actions) upon integration over one half of the fields:

$$c_1 S[a+b] + c_2 S[a] \overset{\int Da}{\longrightarrow} \left(c_1^{-1} + c_2^{-1}\right)^{-1} S[b]. \tag{9.85}$$

EXERCISE Of course, Eq. (9.85) can be proven by straightforward Gaussian integration over a. A more elegant procedure is based on the fact that, for any *quadratic* action, $S[a,b] \overset{\int Da}{\longrightarrow} S[b,\bar{a}[b]]$, where $\bar{a}[b]$ is the solution of the mean-field equation $\delta_a S[a,b]\big|_{a=\bar{a}} = 0$. To make use of this identity, let us formally write $S[a] = a^T K a$, where K is a non-degenerate[107] operator kernel. Find the solution of the mean-field equations corresponding to the left-hand side of Eq. (9.85) and show that, upon substitution back into the action, we obtain the right-hand side. If you are critical, you may object that our CS actions are not, in fact, non-degenerate: when evaluated on

[107] Otherwise the field integration would create a headache!

a pure gauge configuration $a_\mu = \partial_\mu f$, they vanish. Nevertheless, you may convince yourself that Eq. (9.85) remains valid if the integration over a is performed in some fixed reference gauge.

When applied to our action $S^{(2,1)}$ above, the auxiliary identity Eq. (9.85) tells us that

$$S^{(2,1)}[a, A'] \stackrel{\int Da}{\longrightarrow} S_{\rm eff}[A'] \equiv \frac{\sigma_{12}}{2} S_{\rm CS}[A'],$$

where $\sigma_{12} \equiv (\frac{1}{\sigma^0_{12}} + \frac{2}{\theta})^{-1}$. The terminology "$\sigma_{12}$" is justified because, as seen above, the constant in front of a CS source action is but the **Hall conductance** of the system. Recalling that $\theta = 1/2\pi s$ and $\sigma^0_{12} = p/2\pi$, we find

$$\sigma_{12} = \frac{1}{2\pi} \frac{p}{1 + 2sp},$$

i.e. we confirm the expectation of fractional Hall quantization. Let us recall that this result is critically linked to the absence of a **longitudinal conductance** σ_{11}. In our analysis above, alluding to the striking analogies that exist between CFs and ordinary electrons in a magnetic field, we simply *postulated* $\sigma_{11} = 0$ at CF filling p. (Technically, this happened when we said that the CF "tr ln" does not support a longitudinal current–voltage relation.) However, one may note that the actual problem of **Anderson localization of CFs** has not yet been attacked on a truly microscopic level. What makes the problem so difficult is the massive inter-CF correlations induced by fluctuations of the statistical gauge field. In the absence of disorder, the full extent of this correlation mechanism does not yet become clear (at least not on the level of our simplistic "mean-field plus quadratic fluctuations" analysis). However, once external inhomogeneities are present, things instantly become more complicated. For example, a static impurity potential will be screened by an inhomogeneous CF distribution. This creates an accumulation of statistical flux that in turn acts as a scattering center of CFs, etc. Thus, we readily wind up with a full-blown problem "interaction + disorder + strong magnetic field" whose rigorous microscopic solution seems to be elusive. Nonetheless, all evidence suggests that eventually the CFs will be localized, so that the analogy (FQHE of fermions) $\leftrightarrow$ (IQHE of composite fermions) remains valid.

INFO As mentioned above, the field theory approach to the FQHE was preceded by a number of other developments. Perhaps most importantly, shortly after the experimental discovery of the effect, Laughlin proposed a trial wavefunction – nowadays generally referred to as **Laughlin s wavefunction**[108] – which did a fantastic job at explaining much of the phenomenology of the FQHE.

With the benefit of hindsight (!) it is not difficult to motivate the structure of the Laughlin wavefunctions from a few simple considerations. Consider a clean FQHE system at a filling fraction $\nu = 1/(2s+1)$ belonging to the principal series.[109] Any ground state many-body eigenfunction should (a) be built by superposition of single-particle states belonging to the lowest

[108] R. B. Laughlin, Anomalous quantum Hall effect: an incompressible quantum fluid with fractionally charged excitations, *Phys. Rev. Lett.* **50** (1983), 1395–8.

[109] For an extension to more complex fractions, see F. D. M. Haldane, Fractional quantization of the Hall effect: a hierarchy of incompressible quantum fluid states, *Phys. Rev. Lett.* **51** (1983), 605–8, and B. I. Halperin, Statistics of quasiparticles and the hierarchy of fractional quantized Hall states, *Phys. Rev. Lett.* **52** (1984), 1583–6.

Landau level, (b) optimally account for the effects of Coulomb repulsion (recall that the strongest player in the Hamiltonian, the kinetic energy, is completely degenerate), and (c) obey Fermi statistics.

As to (a), we have seen in Section 9.3.4 that any function of the form $\psi(z) = f(z)\exp(-|z|^2/(4l_0^2))$ automatically belongs to the lowest Landau level, provided that $f(z)$ is analytic.[110] So let us seek a many-body wavefunction of the form

$$= F(\{z_i - z_j\})e^{-\frac{1}{4l_0^2}\sum_i |z_i|^2},$$

where F must depend only on differences of coordinates (the translational invariance of the clean system). The antisymmetry of the wavefunction (c) requires that F is skew-symmetric under any exchange $z_i \quad z_j$. Also, (b) F should vanish whenever two coordinates approach each other. Taken together, (a)–(c) motivate the *ansatz*



Robert B. Laughlin 1950–
Theoretical condensed matter physicist. Laughlin was awarded one third of the 1998 Nobel Prsize for his groundbreaking contributions to the explanation of the FQHE. The complementary share went to the experimentalists **Horst L. Störmer** (1949–) and **Dan C. Tsui** (1939–) for the experimental discovery of the effect.

$$(z_1, \bar{z}_1, \ldots, z_N, \bar{z}_N) = \mathcal{N} \prod_{i<j} (z_i - z_j)^m e^{-\frac{1}{4l_0^2}\sum_i |z_i|^2} \tag{9.86}$$

with some *a priori* undetermined integer coefficient m. Equation (9.86) defines Laughlin's wavefunction. Notice its high degree of universality (except for the integer m, the trial wavefunction does not contain a single adjustable parameter!) and the simplicity of its structure. Nonetheless, the *ansatz* Eq. (9.86) offers a straightforward explanation of many observable features of the FQHE. Specifically, it can be shown that:

The integer m relates to the filling factor as $m = \nu^{-1} = 2s + 1$.
For certain types of short-range interaction, ψ is an exact ground state of the Hamiltonian. Numerical analyses have shown that, even for the long-range Coulomb interaction, ψ has a close to perfect overlap with the exact ground state.
Single-particle excitations superimposed on ψ are gapped and fractionally charged.
In fact, one may readily rewrite ψ in a way that suggests an interpretation in terms of composite fermions; simply factor out a power $(z_i - z_j)^{m-1}$ to obtain

$$\psi = \prod_{i<j} (z_i - z_j)^{2s} \psi\big|_{m=1}.$$

Here, $\psi_{m=1}$ is the wavefunction at an integer filling factor while the prefactor adds $2s$ winding phases to each particle coordinate. In other words, the prefactor converts fermions to composite fermions, so that ψ can be interpreted as a CF wavefunction at integer filling. Indeed, this anticipates the field theoretical picture constructed above.

[110] To be precise, in Section 9.3.4, we considered wavefunctions $\psi(z) = f(\bar{z})\exp(-|z|^2/(4l_0^2))$ with an anti-holomorphic prefactor. One can switch from one form to the other by inversion of the external field $B \to -B$. For notational simplicity, we shall use the analytic form throughout.

9.6 Summary and outlook

This concludes our introduction to topological quantum field theory.[111] We have seen the way "large-scale" geometric structures of quantum fields may lead to intriguing physical phenomena – phenomena, in fact, whose understanding required the application of the entire spectrum of field integral techniques developed earlier in this text. Once again, this chapter could provide no more than a very preliminary impression of the diversity of topology-related *quantum* phenomena in condensed matter physics. Given the rapid development of the field, we encourage readers motivated to deepen their knowledge in topological condensed matter field theory to turn to the original literature. (For an excellent particle-physics-oriented introduction we refer to Ryder.[13] A comprehensive discussion of topological textures in classical physics can be found in Efetov.[112])

9.7 Problems

9.7.1 Persistent current of a disordered ring

In the main text we have argued that, contrary to a long-standing belief, the presence of disorder does not conflict with the formation of persistent currents in normal metal rings. Here we support this assertion by a microscopic calculation.

Consider a quasi-one-dimensional ring of circumference $L \gg \ell$ and transverse extension $\lambda_F \ll L_\perp < \ell$, where ℓ is the mean free path. We assume that the ring is pierced by a magnetic flux . Using the fact that $L_\perp/L \ll 1$, variations in transverse direction of the vector potential $\mathbf{A}$ may be neglected, i.e. $\mathbf{A} = (\Phi/L)\mathbf{e}_\parallel$, where $\mathbf{e}_\parallel$ is the unit vector in the longitudinal direction and units $e = \hbar = 1$ are used. We are interested in the typical value $I_{\rm typ} \equiv \sqrt{\langle I^2\rangle}$ of the persistent current $I = -\partial_\Phi F$, where F is the flux-dependent free energy.[113] Assuming that the ring is metallic in the sense that its dimensionless conductance $g \gg 1$, we will be content with computing the first contribution to $I_{\rm typ}$ in an expansion in powers of g^{-1}. For notational simplicity, we assume the flux Φ to be measured in units of Φ_0 throughout.

(a) Represent $\langle I(\Phi_1)I(\Phi_2)\rangle$ as a correlation function of two non-interacting Green functions. Without going into quantitative detail, convince yourself that the dominant contribution to the correlation function is given by the sum of diagrams shown in Fig. 9.20, where the dots denote the operator $\left(-i\partial_\parallel - (\Phi/L)\right)/m \equiv -\hat{v}_\parallel$ and $\partial_\parallel$ is the derivative along the ring. Estimate the relative contributions of the four diagrams. (Hint: Recall the derivation of low-momentum diffusion modes in Section 6.5. Owing to the thinness of the ring, fluctuations of the diffuson/cooperon modes in the radial direction may safely be neglected.)

[111] Strictly speaking, the terminology "topological quantum field theory" is reserved for field theories whose behavior is *solely* determined by topological terms. However, we use it here in a more liberal sense to denote field theories where topological aspects play a significant role.

[112] K. B. Efetov, *Supersymmetry in Disorder and Chaos* (Cambridge University Press, 1996).

[113] In the presence of static disorder, the sign of I sensitively depends on the impurity configuration, i.e. $\langle I\rangle \ll I_{\rm typ}$ is much smaller than the typical value of the current for a fixed impurity configuration.

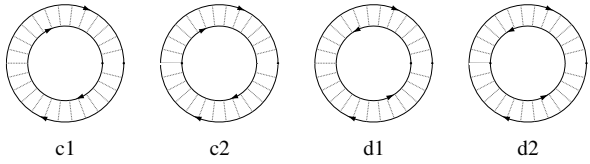

Figure 9.20 Four diagrams contributing at leading order to the correlation function $\langle I(\Phi_1)I(\Phi_2)\rangle$ of the persistent current in a disordered ring.

(b) To quantitatively compute the correlation function, we employ the formalism of the field integral. Using the fact that $F = -T\lim_{R\to 0}\frac{1}{R}(\mathcal{Z}^R - 1)$, construct a generalization of the nonlinear σ-model action $S[Q]$ suitable to compute the current correlation function. (Hint: Introduce a two-component index $t = 1, 2$ discriminating between the two currents, and derive the form of the vector potential by minimal substitution, cf. Eq. (6.64), i.e. by recalling that the flux dependence of the Hamiltonian may be formally removed by a gauge transformation.)

(c) As in Problem 8.8.4, introduce the parameterization $Q = e^{iW}\Lambda e^{-iW} = \Lambda(1 - 2iW - 2W^2 + \cdots)$, where the generators W are given in Eq. (8.53) (block structure in Matsubara space). Notice that $B = \{B^{nat\sigma,n'a't'\sigma'}\}$ are matrices in Matsubara (n), replica (a), current (t), and time-reversal (σ) spaces. Expand the action to second order in B. It is convenient to split $B = B_d + B_c$ into contributions diagonal and off-diagonal in time reversal space. Explore the symmetries of the constituent matrices $B_{d,c}$ and perform the Gaussian integrals. Show that

$$\langle I(\Phi_1)I(\Phi_2)\rangle \simeq \partial^2_{\Phi_1,\Phi_2}T^2 \sum_{q,\omega_n>0,\omega_{n'}<0} \Gamma_{q-(\Phi_1-\Phi_2)/L,nn'} + (\Phi_1 - \Phi_2 \to \Phi_1 + \Phi_2), \quad (9.87)$$

where $\Gamma_{qnn'} \equiv \frac{1}{2\pi\nu\tau}\left[Dq^2 + |\omega_n - \omega_{n'}|\right]^{-1}$ is the diffusion mode.

(d) The final step in the evaluation of the correlation function, the summation over $q, \omega_n, \omega_{n'}$, is a good exercise in executing tricky integrals (here defined as integrals which have to be simplified by physically motivated approximations).

EXERCISE Differentiate with respect to the flux before doing the frequency/momentum summations; identify four contributions corresponding to the diagrams above in Fig. 9.20.

What prevents the expression above from vanishing is the discreteness of the momentum sum; were we able to approximate the sum by an integral, a shift $q \to q + \Phi/L$ would remove the flux dependence of the integrand. The validity of an integral approximation in turn depends on the value of $|\omega|$. For $|\omega| > (2\pi)^2 D/L^2 \equiv E_c$ much larger than the magnitude of the lowest non-vanishing quantized q-mode (physically, the Thouless energy, i.e. the inverse time of diffusion around the ring), many modes contribute to the integral and a continuum approximation is valid. Thus, the dominant contribution to

the correlation function comes from frequencies $|\omega| < E_c$, for which the discreteness of the sum really matters.[114]

Carry out the sum over momenta by the methods otherwise employed in performing frequency summations. Approximate the subsequent sum over Matsubara frequencies $|\omega| < E_c$ by an integral. Show that, for small values of the flux, $I_{typ} \sim E_c \Phi(-\ln(\Phi))^{1/2}$. (Hint: Do not try to do the frequency integral rigorously; keeping the relevant information on board, simplify the integrand to obtain a manageable integral. As to the q-summation, use the freedom to do the flux derivatives before or after the summation to obtain a contour integral that is as simple as possible.)

The most important feature of this result is that it depends only algebraically on the disorder concentration, i.e. through $E_C \sim D \sim \tau$. In contrast, the long-standing yet erroneous expectation that impurity scattering destroys the phase coherence required to maintain a stable persistent current inevitably leads to the prediction $I_{typ} \sim \exp(-L/\ell)$. For experimentally "realistic" values $L/\ell = \mathcal{O}(10^2)$, the difference between the two results is dramatic. Irritatingly, the actually observed value of the current turns out to be roughly two orders of magnitude larger than our result above. Although the origin of this discrepancy is unknown, it is clear that it cannot be resolved within the framework of a non-interacting theory.

Answer:

(a) Using the fact that the free energy of a non-interacting Fermion system is given by $F = -T\sum_n \mathrm{tr}\ln(i\omega_n - \hat{H})$, where $\hat{H} = \frac{1}{2m}(\hat{\mathbf{p}} - \mathbf{A})^2 + \hat{V}$ and $\hat{V}$ represents the single-particle potential of the problem (the sum of disorder and confining potentials), we obtain $I(\Phi) = -T\sum_n \mathrm{tr}(\hat{G}_n \partial_\Phi \hat{H}) = \frac{T}{L}\sum_n \mathrm{tr}(\hat{G}_n \hat{v}_\parallel)$. Expanding the Green function in the impurity operator and constructing ladder diagrams at one-loop order, we identify the two cooperon (c1 and c2) and two diffuson (d1 and d2) diagrams in Fig. 9.20. Focusing on the cooperon sector, we note that the ladder diagram depends only on the sum $q-(\Phi_1+\Phi_2)/L$ of the fast momenta $\mathbf{p}-(\Phi_i/L)\mathbf{e}_\parallel$ carried by the Green functions.[115] More specifically, an individual cooperon ladder contributes a factor (see Section 6.5) $\sim \Gamma_{q-(\Phi_1+\Phi_2)/L,nn'} \equiv \frac{1}{2\pi\nu\tau}\left[D(q-(\Phi_1+\Phi_2)/L)^2 + |\omega_n - \omega_{n'}|\right]^{-1}$. Up to constants, the contribution of diagram c1 is thus given by $\Gamma_{q-(\Phi_1+\Phi_2)/L,nn'}$. Turning to diagram c2, we need to take into account the fact that the vector vertices $\sim v_\parallel$ indicated by the dots are now integrated independently over the fast momenta (because they are separated by impurity lines; recall the momentum structure of a ladder diagram). In the limit of zero momentum difference, $\mathbf{q} - (\Phi_1 + \Phi_2)/L \to 0$, the two Green function insertions carrying a dot vanish (think about it). This means that diagram c2 will be proportional

[114] This statement conforms with the expectation that the minimal time $t \sim \omega^{-1}$ required to sense the flux through a disordered ring is the diffusion time, i.e. the time for a quantum particle to traverse the ring at least once.

[115] Due to the thinness of the ring, fluctuations of the cooperon in the transverse direction are negligible, i.e. the momentum q is a scalar quantity measuring fluctuations in the longitudinal direction.

to $\sim (q-(\Phi_1+\Phi_2)/L)^2\Gamma^2_{q-(\Phi_1+\Phi_2)/L,nn'}$, where the factor Γ^2 accounts for the two ladders. The diffuson diagrams d1, d2 are obtained by replacing $\Phi_1+\Phi_2\to\Phi_1-\Phi_2$.

(b) Defining $\mathcal{Z}=\int D(\bar\psi,\psi)\exp(-S[\bar\psi,\psi])$ where

$$S[\bar\psi,\psi]=\int d^dr\ d\tau\ \bar\psi^{at}(\partial_\tau+\hat H(\mathbf{A}_t)-\mu)\psi^{at},$$

and $\mathbf{A}_t=(\Phi_t/L)\mathbf{e}_\parallel$, we have the representation $\langle I(\Phi_1)I(\Phi_2)\rangle=\lim_{R\to0}\frac{T^2}{R^2}\partial^2_{\Phi_1,\Phi_2}\mathcal{Z}$. All we need to do to deduce the structure of the low-energy action is to notice that the composite index (a,t) can be identified with a "replica index" of doubled dimension $2R$. Noting that the flux dependence of the Hamiltonian may be formally (i.e. at the price of changing boundary conditions) removed by the transformation $\psi\to e^{i\Phi_t r_\parallel}$, where $r_\parallel$ is the coordinate along the ring, and recalling the discussion above Eq. (6.64), we conclude that the action is given by $S[Q]=\frac{\pi\nu}{2}\int dr_\parallel\,\mathrm{tr}\left[\frac{D}{4}\left((\partial-i[A,])Q\right)^2-\hat\omega Q\right]$, where the vector potential $\mathbf{A}=\{\delta^{at,a't'}(\Phi_t/L)\}\otimes\sigma_3^{\rm tr}$.

(c) Using the symmetry relation $W=-\sigma_2^{\rm tr}W\sigma_2^{\rm tr}\Rightarrow B^T=-\sigma_2^{\rm tr}B^\dagger\sigma_2^{\rm tr}$, we verify that

$$B_{\rm d}=E^{\rm tr}_{11}b_{\rm d}-E^{\rm tr}_{22}b^*_{\rm d},\qquad B_{\rm c}=E^{\rm tr}_{12}b_{\rm c}+E^{\rm tr}_{21}b^*_{\rm c},$$

where $b_{\rm d,c}=\{b^{nat,n'a't'}_{\rm d,c}\}$ are complex matrices. Substituting this representation into the action and expanding to quadratic order, it is a straightforward matter to obtain

$$\begin{aligned}S^{(2)}[B,B^\dagger] &= \frac{L}{T\tau}\sum_{q,n>0,n'<0}\mathrm{tr}\left((b_{\rm d})^{tt'}_{nn'}\Gamma_{q-(\Phi_t-\Phi_{t'})/L,nn'}(b^\dagger_{\rm d})^{t't}_{n'n}\right)\\ &\quad+(b_{\rm d}\to b_{\rm c},\Phi_t-\Phi_{t'}\to\Phi_t+\Phi_{t'}).\end{aligned}$$

We finally integrate over the fields $b_{\rm d,c}$ and arrive at

$$\mathcal{Z}=\prod_{q,n>0,n'<0}\left(\Gamma_{q-(\Phi_1-\Phi_2)/L,nn'}\right)^{R^2}+(\Phi_1-\Phi_2\to\Phi_1+\Phi_2),$$

where the factor of R^2 counts the independent replica channels, constant factors $C^{R^2}\overset{R\to0}{\to}1$ have been omitted, and we also omitted those contributions to the integral that depend exclusively on Φ_1 or on Φ_2 (as they do not contribute to the two-fold derivative $\lim_{R\to0}R^{-2}\partial^2_{\Phi_1\Phi_2}$ [check!]). Differentiating with respect to the flux and sending $R\to0$, we obtain Eq. (9.87).

(d) Our strategy will be to do the momentum sum by contour integral methods. As it is not convenient to integrate over a function containing branch cuts (such as our logarithm), we do one of the flux derivatives, ∂_{Φ_1}, say, first. Focussing on the diffuson contribution, and introducing the shorthand notation $\Phi=\Phi_1-\Phi_2$, $|\omega|=|\omega_n-\omega'_n|$, we have

$$\begin{aligned}\partial_{\Phi_2}L^{-1}\sum_q\frac{D(q-\Phi/L)}{D(q-\Phi/L)^2+|\omega|} &= \partial_{\Phi_2}\frac{1}{4\pi i}\oint dz\coth(zL/2)\frac{D(-iz-\Phi/L)}{D(-iz-\Phi/L)^2+|\omega|}\\ &= -\frac{1}{2}\partial_{\Phi_2}\,\mathrm{Im}\coth([(|\omega|/E_{\rm c})^{1/2}+i\Phi]/2),\end{aligned}$$

where the integration contour is a circle at infinity avoiding the two poles of the integrand.[116] Notice that our result is 2π-periodic in the flux Φ, as it should be.

Turning to the frequency summation, we use the fact that $|\omega|/E_c < 1$ to approximate $\coth([(|\omega|/E_c)^{1/2} + i\Phi]/2) \simeq 2[(|\omega|/E_c)^{1/2} + i(\Phi \bmod 2\pi)]^{-1}$. This leads to the expression

$$\partial^2_{\Phi_1\Phi_2} T^2 \sum_{q,n,n'} \Theta(n)\Theta(-n')\Gamma_{q-\Phi/L,nn'} \simeq -\partial_{\Phi_2}(2\pi)^2 \operatorname{Im} \int_0^{E_c} d\omega \frac{\omega}{(|\omega|/E_c)^{1/2} + i\Phi}$$
$$= \partial_{\Phi_2}(2\pi E_c)^2 \Phi \int_0^1 dx \; \frac{x}{x+\Phi^2} = (2\pi E_c)^2 \partial_{\Phi_2}\left(\Phi - \Phi^3 \ln\left(\frac{\Phi^2+1}{\Phi^2}\right)\right).$$

For small values of the flux, the logarithm can be approximated as $-\ln(\Phi^2)$ and $\partial_{\Phi_2}\Phi^3 \ln(\Phi^2) \simeq 3\Phi^2 \ln(\Phi^2)$. Using this approximation and adding the cooperon contribution, we obtain

$$\langle I(\Phi_1) I(\Phi_2)\rangle \simeq -(2\pi E_c)^2 \left(3(\Phi_1-\Phi_2)^2 \ln((\Phi_1-\Phi_2)^2) - 3(\Phi_1+\Phi_2)^2 \ln((\Phi_1+\Phi_2)^2)\right).$$

Setting $\Phi_1 = \Phi_2$ we arrive at the required result.

9.7.2 Working with the $SU(N)$ Wess–Zumino term

In this problem, we develop some of the amazing mathematical features of the SU(N) WZ term Eq. (9.58). The problem also illustrates the superiority of the coordinate-free calculus of differential forms in topological quantum field theory. (Expressed in the standard languages of calculus, all formulae below become intolerably messy – not to mention the fact that the underlying structures are much more difficult to understand!)

(a) WZ terms generally originate from a closed (but only locally exact) differential form on the target manifold ω. Show that, on SU(N), the form $\omega = \mathrm{tr}(g^{-1}dg \wedge g^{-1}dg \wedge g^{-1}dg)$ is closed. (Why is it only locally exact? This question will be addressed in part (c) below.)

(b) Verify Eq. (9.61). Let us try to understand the **normalization of the WZW action**. To start with, let us recall a statement from group theory stated in the Info block on page 549: as far as topology is concerned, the subgroup SU(2) $\subset$ SU(N) preempts the structure of SU(N), i.e. without loss of generality, we may restrict our discussion to the SU(2) WZ action.

We next turn to the normalization of the WZW action. To start with, let us consider S^2 as the boundary of the northern hemisphere S^{3+} of the 3-sphere. We define the WZW term by integration over S^{3+}.[117] To parameterize S^{3+}, we introduce a third coordinate x_3 (in addition to the two coordinates (x_1, x_2) parameterizing S^2), such that $x_3 = 0$ defines the north pole and $x_3 = \pi/2$, the equatorial plane, S^2. For any field $g(x_1, x_2) \in$ SU(2), the WZW action then becomes $\Gamma^+[g] = i\mathcal{N} \int_0^{\pi/2} dx_3 \; \Gamma[g, x_3]$, where

[116] In spite of the weak convergence $\sim z^{-1}$ of the integrand at large values of z, it is permissible to do the integral in this manner: the second flux derivative implicitly levels the decay up to $\sim z^{-2}$.

[117] Topologically, this domain is equivalent to the three-dimensional unit ball B^3 used in the text (just as the northern hemisphere of the 2-sphere is topologically equivalent to the unit disk B^2).

$\Gamma[g,x_3] \equiv \int dx_1\ dx_2\ \epsilon^{\mu\nu\sigma}\,\mathrm{tr}(g^{-1}\partial_\mu g g^{-1}\partial_\nu g g^{-1}\partial_\sigma g)$, $\mu,\nu,\sigma = 1,2,3$, and $g(x_1,x_2,x_3)$ is a smooth extension of $g(x_1,x_2)$ from S^2 to S^{3+}. But, of course, it would have been just as good to take the southern hemisphere S^{3-} as our reference domain. To explore the consequences of this ambiguity, we extend the definition of the third coordinate in such a way that $x_3 = \pi$ corresponds to the south pole of S^3. In this case, the WZW action would assume the form $\Gamma^-[g] = -i\mathcal{N}\int_{\pi/2}^{\pi} dx_3, \Gamma\,[g,x_3]$, where $\Gamma[g,x_3]$ is defined as above (albeit for an extension $g(x_1,x_2,x_3<0)$.

For any reference field $g(x_1,x_2)$, the ambiguity,

$$\Gamma^+ - \Gamma^- = i\mathcal{N}\int_0^\pi dx^3 \int dx_1\ dx_2\ \epsilon^{\mu\nu\sigma}\mathrm{tr}(g^{-1}\partial_\mu g g^{-1}\partial_\nu g g^{-1}\partial_\sigma g) \stackrel{!}{=} 2\pi n,$$

must be an integer multiple of 2π.[118] Consider, thus, the field $g(x_1,x_2) \equiv i\mathbf{n}(x_1,x_2)\cdot\sigma$, where $\mathbf{n}(x_1,x_2)$ is a unit vector. As its extension into the northern/southern hemisphere, we choose $g(x_1,x_2,x_3) = \cos(x_3) + i\sin(x_3)g(x_1,x_2) = \exp(ix_3\mathbf{n}(x_1,x_2)\cdot\boldsymbol{\sigma}) \in \mathrm{SU}(2)$. This is an SU(2)**-instanton**, i.e. a mapping $S^3 \to \mathrm{SU}(2)$ that cannot be continuously deformed to the unit mapping.

(c) Show that $\Gamma^+[g] - \Gamma^-[g] = i\mathcal{N}24\pi^2 \times$ (integer), which enforces $\mathcal{N} = 1/12\pi$ as the normalization of the WZW action. As a corollary, we note that the form ω on which all of our discussion is based cannot be globally exact. (If it had been, Stokes' theorem would imply a vanishing of the integral over the boundary-less manifold S^3.)

(d) Show that, for the particular reference configuration considered in part (c), $g = i\mathbf{n}\cdot\boldsymbol{\sigma} \in \mathrm{SU}(2)$, the WZW action reduces to the θ-term for the unit-modular field $\mathbf{n} \in S^2$: $\Gamma[i\mathbf{n}\cdot\boldsymbol{\sigma}] = \pi S_{\mathrm{top}}[\mathbf{n}]$, where $S_{\mathrm{top}}[\mathbf{n}] = \frac{1}{4\pi}\int_{S^2} d^2x\ \mathbf{n}\cdot(\partial_1\mathbf{n}\times\partial_2\mathbf{n})$.

Answer:

(a) Using the fact that $g^{-1}dg\,g^{-1} = -dg^{-1}$ (why?) the form ω can be rewritten as $\omega = \mathrm{tr}(dg^{-1}\wedge dg\wedge dg^{-1}\,g)$, i.e. $d\omega = -\mathrm{tr}(dg^{-1}\wedge dg\wedge dg^{-1}\wedge dg)$. To show that this expression vanishes, one may make use of the fact that, for arbitrary matrix-valued forms, $\mathrm{tr}(\omega_1\wedge\omega_2) = (-)^{\deg(\omega_1)\deg(\omega_2)}\mathrm{tr}(\omega_2\wedge\omega_1)$.[119] Applied to $d\omega$, this yields $d\omega = +\,\mathrm{tr}(dg\wedge dg^{-1}\wedge dg\wedge dg^{-1}) = \mathrm{tr}(dg^{-1}\wedge dg\wedge dg^{-1}\wedge dg) = -d\omega$, where in the last step we applied the formula $g^{-1}dg = -dg^{-1}\,g$ to all derivatives.

[118] Geometrically, this is the integral of the differential 3-form $g^*\omega$ (i.e. the pullback of the SU(2) form ω by the field g to a form on S^3) over S^3.

[119] Proof: $\mathrm{tr}(\omega\wedge\eta) = \sum_{ij}\omega_{ij}\wedge\eta_{ji} = (-)^{\deg(\omega)\deg(\ )}\sum_{ij}\eta_{ji}\wedge\omega_{ij} = (-)^{\deg(\omega)\deg(\ )}\mathrm{tr}(\eta\wedge\omega)$.

(b) We want to explore what happens to the integral $\Gamma[g] = -\frac{i}{12\pi}\int_{B^3} g^*\omega$ upon variation $g \to e^W g \simeq (1+W)g$. Using the relation $g^{-1}dg \to g^{-1}dg + g^{-1}dW\, g$, we obtain

$$\begin{aligned}\Gamma[(1+W)g] - \Gamma[g] &\simeq -\frac{i}{4\pi}\int_{B^3} \mathrm{tr}(g^{-1}dW\, g \wedge g^{-1}dg \wedge g^{-1}dg) \\ &= \frac{i}{4\pi}\int_{B^3} \mathrm{tr}(dW \wedge dg \wedge dg^{-1}) = \frac{i}{4\pi}\int_{B^3} d\left[\mathrm{tr}(W \wedge dg \wedge dg^{-1})\right] \\ &= \frac{i}{4\pi}\int_{S^2} \mathrm{tr}(W \wedge dg \wedge dg^{-1}),\end{aligned}$$

where, in the last line, we have made use of Stokes' theorem.

(c) By an elementary rearrangement of fields,

$$\Gamma^+ - \Gamma^- = 3i\mathcal{N}\int_0^\pi dx_3 \int dx_1\, dx_2\, \epsilon^{ij}\mathrm{tr}(g\partial_3 g^{-1}\, \partial_i g\, \partial_j g^{-1}),$$

where the coordinates $i, j = 1, 2$. A straightforward calculation shows that $g\partial_3 g^{-1} = -i\mathbf{n}\cdot\boldsymbol{\sigma}$. Using the auxiliary identities $\partial_i g = i\sin(x_3)\partial_i \mathbf{n}\cdot\boldsymbol{\sigma}$ and $\mathrm{tr}(\mathbf{n}_1\cdot\boldsymbol{\sigma}\,\mathbf{n}_2\cdot\boldsymbol{\sigma}\,\mathbf{n}_3\cdot\boldsymbol{\sigma}) = 2i\mathbf{n}_1\cdot(\mathbf{n}_2\times\mathbf{n}_3)$, we thus obtain,

$$\begin{aligned}\Gamma^+ - \Gamma^- &= 6i\mathcal{N}\int_0^\pi dx_3 \sin^2(x_3)\int dx_1\, dx_2\, \epsilon^{ij}\mathbf{n}\cdot(\partial_i\mathbf{n}\times\partial_j\mathbf{n}) \\ &= 6i\pi\mathcal{N}\int dx_1 dx_2 \mathbf{n}\cdot(\partial_1\mathbf{n}\times\partial_2\mathbf{n}) = 24i\pi^2\times(\text{integer}),\end{aligned}$$

where the integer is the number of times the unit vector $\mathbf{n}$ wraps around the unit sphere.

(d) By analogy with the calculation performed in (c), we obtain $\Gamma^+[i\mathbf{n}\cdot\boldsymbol{\sigma}] = \Gamma^+ = 6i\pi\mathcal{N}\int dx_1\, dx_2\, \mathbf{n}\cdot(\partial_1\mathbf{n}\times\partial_2\mathbf{n}) = \pi S_{\mathrm{top}}[\mathbf{n}]$.

9.7.3 Renormalization group analysis of the $SU(N)$ Wess–Zumino model

Before embarking on this problem, it is helpful to recapitulate the RG analysis of the SU(N) nonlinear σ-model discussed in Section 8.5. We want to study the RG flow of the SU(N) WZW model, as specified by Eq. (9.65). As in our previous analyses of nonlinear σ-models, we can split a general field configuration $g = g_{\mathrm{s}}g_{\mathrm{f}}$ into a slow and a fast part, and expand the latter as $g_{\mathrm{f}} = 1 + W + W^2/2 + \cdots$, where $W \in$ su(N), i.e. W lives in the Lie algebra su(N) (the algebra of anti-Hermitian traceless matrices). To compute the one-loop RG equations, we need to expand the action to quadratic order in W and compute all contributions to the functional integral that contain (a) one fast momentum integration and (b) no more than two derivatives acting on a slow field.

(a) Show that the expansion of the action $S[g_{\mathrm{s}}g_{\mathrm{f}}]$ to second order in the generators takes the form $S[g_{\mathrm{f}}g_{\mathrm{s}}] = S[g_{\mathrm{s}}] + S[g_{\mathrm{s}}, W] + S^{(2)}[W]$, where

$$\begin{aligned}S^{(2)}[W] &= -\frac{1}{\lambda}\int_{S^2} d^2x\, \mathrm{tr}(\partial_\mu W \partial_\mu W), \\ S[g_{\mathrm{s}}, W] &= -\frac{1}{\lambda}\int_{S^2} d^2x\, \mathrm{tr}\left[\left(g_{\mathrm{s}}^{-1}\partial_\mu g_{\mathrm{s}} - \frac{i\lambda}{8\pi}\epsilon_{\mu\nu}g_{\mathrm{s}}^{-1}\partial_\nu g_{\mathrm{s}}\right)[\partial_\mu W, W]\right].\end{aligned} \tag{9.88}$$

(b) One-loop corrections to the action are obtained by expanding the functional to second order in $S^{(2)}[g_{\rm s}, W]$ and integrating over W: $S[g] \to S[g_{\rm s}] - \frac{1}{2}\langle S[g_{\rm s}, W]^2\rangle_W$. Use the results of Section 8.5 (in particular those derived in the exercises on page 463) to confirm that (i) only the gradient term of the action is renormalized and (ii) the RG equation for its coupling constant is given by Eq. (9.66).

Answer:

(a) The first line of Eq. (9.88) and the first term in the second line are obtained by substitution of $g_{\rm s}g_{\rm f}$ into the gradient term of the action (9.57) and expanding to second order in the generators W. The second term in $S[g_{\rm s}, W]$, a descendant of the WZ action, is best derived in the language of differential forms: substitution of $(g_{\rm s}g_{\rm f})^{-1}d(g_{\rm s}g_{\rm f}) = g_{\rm f}^{-1}(g_{\rm s}^{-1}dg_{\rm s} + (dg_{\rm f})g_{\rm f}^{-1})g_{\rm f}$ into the pullback $(g_{\rm s}g_{\rm f})^*\omega = {\rm tr}(g^{-1}dg \wedge g^{-1}dg \wedge g^{-1}dg)|_{g=g_{\rm s}g_{\rm f}}$ gives

$$\begin{aligned}(g_{\rm s}g_{\rm f})^*\omega &= g_{\rm s}^*(\omega) + \frac{3}{2}{\rm tr}(dg_{\rm s}^{-1} \wedge dg_{\rm s} \wedge [W, dW]) + 3{\rm tr}(dW \wedge dW \wedge g_{\rm s}^{-1}dg_{\rm s}) + \mathcal{O}(W^3)\\ &= g_{\rm s}^*(\omega) + \frac{3}{2}d\left[{\rm tr}([W, dW] \wedge g_{\rm s}^{-1}dg_{\rm s})\right] + \mathcal{O}(W^3).\end{aligned}$$

Application of Stokes' theorem thus leads to

$$\begin{aligned}\Gamma[g_{\rm s}g_{\rm f}] &= -\frac{i}{12\pi}\int_{B^3}(g_{\rm s}g_{\rm f})^*\omega = \Gamma[g_{\rm s}] - \frac{i}{8\pi}\int_{B^3} d\left[{\rm tr}([W, dW] \wedge g_{\rm s}^{-1}dg_{\rm s})\right] + \mathcal{O}(W^3)\\ &= \Gamma[g_{\rm s}] - \frac{i}{8\pi}\int_{S^2}{\rm tr}([W, dW] \wedge g_{\rm s}^{-1}dg_{\rm s}) + \mathcal{O}(W^3)\\ &= \Gamma[g_{\rm s}] - \frac{i}{8\pi}\int_{S^2} d^2x\epsilon_{\mu\nu}{\rm tr}([W, \partial_\mu W] \wedge g_{\rm s}^{-1}\partial_\nu g_{\rm s}) + \mathcal{O}(W^3),\end{aligned}$$

where the $\mathcal{O}(W^2)$ term appears as the second contribution to the action $S[g_{\rm s}, W]$.

(b) Defining $\Phi_\mu \equiv g_{\rm s}^{-1}(\partial_\mu + \frac{i\lambda}{8\pi}\epsilon_{\mu\nu}\partial_\nu)g_{\rm s}$, the action $S[g_{\rm s}, W]$ assumes the form $S[g_{\rm s}, W] = \frac{2iL^d}{\lambda}\sum_{pq} p_\mu {\rm tr}(\Phi_\mu\Phi_\mu)$. But for the difference in the definition of the field Φ, this is equal to the fast–slow action of the standard SU(N) model. Using the results derived in the exercises on page 463, we thus obtain

$$\begin{aligned}-\frac{1}{2}\langle S[g_{\rm s}, W]^2\rangle_W &= -\frac{N\ln b}{8\pi}\int d^2x\,{\rm tr}(\Phi_\mu\Phi_\mu)\\ &= -\frac{N\ln b}{8\pi}\left(1 - \left(\frac{\lambda}{8\pi}\right)^2\right)\int d^2x\,{\rm tr}(\partial g_{\rm s}\partial g_{\rm s}^{-1}).\end{aligned}$$

This result confirms that only the gradient term in the action is renormalized. By proceeding in direct analogy to the discussion of Section 8.5, it is a straightforward matter to derive the corresponding RG equation. The result is given by Eq. (9.66)

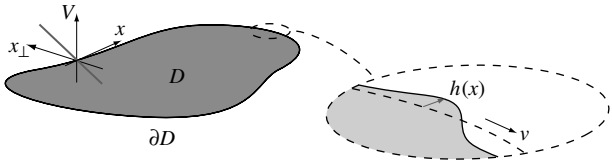

Figure 9.21 On the formation of surface wave excitations in an FQHE droplet. For an explanation, see the main text.

9.7.4 Fractional quantum Hall effect: physics at the edge

In Section 9.3.7 above, we have seen that the bulk physics of an integer quantum Hall system is intimately connected to that of its boundaries. These connections could be disclosed from both direct physical reasoning (the essence of the Laughlin–Halperin semi-phenomenological approach) and an analysis of the behavior of the microscopic theory under gauge transformations. Following the seminal work of Wen,[120] here we show that an equally close connection between bulk and boundaries exists for the FQHE. Again, we will be able to deduce the boundary physics by phenomenological, and by field-theory-oriented, reasoning.

Consider a finite FQHE system. For simplicity, we assume the system to be disc-shaped, although the details of the geometry will not be of relevance throughout. At the system boundaries, the two-dimensional electron gas is confined by a boundary potential V which we assume to be linear (see Fig. 9.21). In the first part of this problem, we want to describe the dynamics of edge excitations on phenomenological grounds. An important first observation is that the bulk system – presumed to sit at an FQHE plateau value – is in an "incompressible state." This follows from the fact that, for an integer number of composite fermion Landau levels, the system does not support gapless excitations: $\partial\mu/\partial_N \to \infty$. Now,[121] $\partial\mu/\partial_N \sim \kappa^{-1} \equiv -V(\partial P/\partial V)_N$ is proportional to the inverse compressibility, i.e. the lack of low-energy excitations implies an incompressible state. We should, therefore, think of our system as a rigid "liquid" rather than as a gas.

Given that the state is incompressible, the lowest-energy excitations of the system will be deformations of the boundary (similar to boundary distortions of a puddle of water). We may characterize these distortions by a surface density profile $\rho(x)$, where x parameterizes the boundary.[122]

(a) To derive the boundary action on phenomenological grounds, proceed in two steps. First derive the energy of a boundary distortion ρ. Second, argue why a distortion profile $\rho(x,t)$ propagates along the boundary at some constant velocity v. Derive an effective equation of motion for ρ and use it to determine the canonical momentum associated

[120] For a review, see X. G. Wen, Theory of the edge states in fractional quantum Hall effects, *Int. J. Mod. Phys.* **B6** (1992), 1711–62.

[121] G. Mahan, *Many Particle Physics* (Plenum Press, 1981).

[122] More precisely, the geometric shape of the system is described by some height function $h(x)$ (see Fig. 9.21). Using the fact that the constant charge density of the system (cf. Eq. (9.17)) is given by $\frac{\nu B}{2\pi} dx\, dx_\perp$, where $x_\perp$ is the coordinate perpendicular to the system boundary, $\rho(x)dx = \frac{\nu B}{2\pi}\int_0^{h(x)} dx_\perp\, dx = \frac{\nu B}{2\pi} h(x)dx$, i.e. the height profile is proportional to a density profile.

with the "displacement field" ϕ defined by $\partial_x \phi = 2\pi\rho$. Show that the Hamiltonian action of the displacement field is given by

$$S[\phi] = \frac{1}{4\pi\nu} \int dx\ d\tau \left(v(\partial_x \phi)^2 - i \partial_x \phi \partial_\tau \phi \right), \tag{9.89}$$

the action of a "**chiral Luttinger liquid**" – the terminology follows from the fact that Eq. (9.89) describes the uni-directional propagation of a density field. (The connection to the Luttinger liquid is made explicit by decomposing the coordinate–momentum pair describing one-dimensional charge density modes, $(\partial_x \phi, \theta)$, into left- and right-moving components, $\phi = \phi_{\rm L} + \phi_{\rm R}$, $\theta = \phi_{\rm L} - \phi_{\rm R}$. Substituting this representation into the action (4.49), the latter decomposes into a left- and a right-moving chiral action.) (Hint: A boundary distortion costs energy because of the presence of a voltage gradient. The presence of a constant drift follows, e.g. from the finiteness of the Hall conductivity. Also remember Eq. (9.17) for the density of a quantum Hall system.)

(b) We next derive the action from a complementary, bulk-oriented perspective. To this end, consider the CS action of the bulk system, Eq. (9.75). Throughout, it will be convenient (although not strictly necessary as one may translate all expressions back to the traditional representation) to use the language of differential forms. Interpreting a_μ as the coefficients of a differential 1-form, $a = a_\mu dx_\mu$, Eq. (9.75) assumes the compact form

$$S_{\rm CS}[a] = -\int_{D \times S^1} a \wedge da,$$

where the integral extends over the Cartesian product of the bulk of the system, D, and imaginary time S^1. Show that $S_{\rm CS}$ is gauge invariant *up to a boundary term*. To "cure" the gauge deficiency of the action, we adopt a gauge-fixing condition $a_0|_{\partial D} = 0$. Use this condition to integrate over the component a_0 in the entire system. Show that this integration leads to the global constraint $f_{ij} = 0$, where f_{ij} are the real-space components of the field strength tensor $f = da = \partial_\mu a_\nu dx_\mu \wedge dx_\nu$. This condition implies that the real-space component of the vector potential $\mathbf{a}$ can be represented as a pure gauge, $\mathbf{a} = \mathbf{d}\phi \equiv \partial_i \phi dx_i$, where we use the symbol $\mathbf{d}$ to denote the real space contribution to the exterior derivative. Plug this *ansatz* into the residual contribution to the action (after a_0 has been integrated out) to reduce the field strength tensor to the boundary action $S[\phi] = \int_{\partial B} dx \int d\tau\ \partial_x \phi \partial_\tau \phi$. Recalling that the CS action enters the theory as $\exp(\frac{i}{4\pi\nu} S_{\rm CS})$,[123] we conclude that the effective boundary action induced by the gauge non-invariance of $S_{\rm CS}$ reads

$$S_{\rm eff}[\phi] = -\frac{i}{4\pi\nu} \int_{\partial B} dx \int d\tau\ \partial_x \phi \partial_\tau \phi.$$

[123] To be precise, the coupling constant $1/4\pi\nu$ appeared after (a) the system had been coupled to an external vector potential, (b) the coupling between the statistical vector potential and the matter degrees of freedom had been taken into account, and (c) the statistical vector potential had been integrated out (see Section 9.5.3). Here we assume that all these steps are implied, i.e. we should think of a as an external electromagnetic field and $\frac{i}{4\pi\nu} S_{\rm CS}$ as the dominant (first-order derivative) contribution to its action.

(c) One may recognize $S_{\rm eff}[\phi]$ as the second contribution to the action (9.89). The obvious next question to ask is why we did not obtain the full action of the chiral Luttinger liquid. Indeed, it takes only a moment's thought to realize that a first principles derivation of the full boundary action from the bulk theory is out of the question. The point is that the missing contribution $\sim v(\partial_x\phi)^2$ depends on the boundary velocity, which in turn is determined by the steepness of the boundary potential. However, the bulk action does not know of the structure of the boundary. We can, however, employ a trick to infuse the required information on the system boundaries into the bulk theory. (Although this manipulation is fairly ad hoc, it shows, at least, that the bulk and the boundary theory are not inconsistent.) Indeed, the gauge-fixing condition employed in the construction above involves a lot of arbitrariness. For example, instead of $a_0 = 0$ the linear combination $a_0 + va_x = 0$ would have been just as good.

To explore the consequences of the new gauge-fixing condition, let us introduce a new set of coordinates, $\tilde{x} = x - vt$, $\tilde{t} = t$, and $\tilde{x}_\perp = x_\perp$. Recalling the transformation behavior of differential forms (see page 537) under coordinate changes, compute the components of the vector potential $a = \tilde{a}_\mu d\tilde{x}_\mu$. Show that the gauge fixing condition translates to $\tilde{a}_0 = 0$. We now benefit from the fact that we have expressed the CS term in a coordinate-invariant manner, i.e. it keeps the same form, no matter whether we express it in terms of the old or the new coordinates (a point on which to reflect!). However, in the new coordinates, the gauge-fixing condition assumes the same form $\tilde{a}_0$ as that considered in (b). This means that $S_{\rm CS}$ can be reduced to a boundary contribution, which, however, is expressed in new coordinates. Finally, translate back to the old coordinates to obtain the full chiral Luttinger action. The message to be taken home from this construction is that a boundary-gauge-fixing condition can be used to establish the equivalence between the boundary Luttinger and the bulk CS description of the system.

(d) Notwithstanding its innocuous appearance, the action (9.89) describes astonishingly rich physics. Referring for an in-depth discussion to the literature (see Wen's review article[120]), we here mention only a few of the characteristic features of the system described by Eq. (9.89). To establish contact with physically observable quantities, we first need to derive an expression for the electron operator $c^\dagger$ (the chiral analog of the fermion relation (4.46)). Arguing as in Section 4.3 above, we start from the observation that the creation of an electron goes along with the creation of a unit charge. Building on the connection between the displacement field and the charge operator, show that the chiral bosonic representation of the fermion operator will contain a piece

$$c^\dagger \sim e^{-i\nu^{-1}\phi}.$$

To complete the manufacturing of a fermion operator, we need to ensure that $c^\dagger$ obeys fermionic exchange statistics. Use the commutator relations of the field ϕ to show that

$$e^{i\nu^{-1}\phi(x)}e^{i\nu^{-1}\phi(x')} = e^{i\nu^{-1}\phi(x')}e^{i\nu^{-1}\phi(x)} \times e^{i\pi\nu^{-1}\mathrm{sgn}(x-x')}.$$

This means that $\exp(i\nu^{-1}\phi)$ describes a fermion provided that $\nu = 1/m$ belongs to the principal sequence.

INFO But what will happen for a general $\nu = n/m$? It is, in fact, not clear how to repair the *ansatz* above so as to generate **fermion statistics for general filling fractions**. Indeed, it turns out that the entire edge construction above is too narrow to describe the general case. We have seen in our discussion of the IQHE above that, in cases where $p > 1$ Landau levels are occupied, the edge hosts p edge channels. Similarly, an FQHE system with filling fraction $\nu = p/(2sp+1)$ (i.e. a system in which the composite fermions experience an effective $\nu = 1/p$ IQHE) will have p chiral edge channels circulating at its boundaries. However, the construction of this edge channel hierarchy is beyond the scope of the present text and we refer to the literature.

Notice that we may interpret $e^{i\nu^{-1}\phi} = (e^{i\phi})^{\nu^{-1}}$ as the ν^{-1}th power of the more elementary object $e^{i\phi}$. According to the construction above, $e^{i\phi}$ creates an entity of fractional charge $e \times \nu$. Also, the states created by $e^{i\phi}$ obey fractional exchange statistics. Comparing with our discussion in the main text, we identify $\exp(i\phi)$ as the creator of the boundary variant of the fractionally charged Laughlin quasi-particles.

Answer:

(a) Owing to the presence of an (approximately linear) confining potential $V = Ex_\perp$, a boundary distortion costs an energy (notation taken from footnote[122]) $H = \int dx \int_0^{h(x)} dx_\perp \sigma E x_\perp = \frac{\nu E B}{4\pi} \int dx\ h^2(x) = \frac{E}{4\pi\nu B} \int dx\ (\partial_x \phi)^2$.

To understand why the density profile propagates along the boundary, notice that the (confining) electric field E perpendicular to the boundary will generate a Hall current density $j \sim \sigma_{12} E = \sigma B^{-1} E$ tangential to the boundary. The total boundary current is obtained by integrating the current density from 0 to $h(x)$, i.e. $I \sim \rho E/B = \partial_x \phi E/2\pi B$. Integrating the continuity equation $\partial_t \rho = \partial_x j$ over x and substituting the identification of the current above, we obtain the equation of motion $\partial_t \phi = v \partial_x \phi$, where the velocity $v \sim E/B$ depends in a non-universal way on the boundary potential. This equation is solved by $\phi = \phi(x + vt)$, i.e. a uniformly propagating density distribution. Switching to momentum space, we may interpret $\dot{\phi}_k = \delta H/\delta \pi_k = vik\phi_k$ as an Hamiltonian equation of motion determining the momentum π conjugate to ϕ. Comparison[124] with $H = \frac{v}{2\pi\nu} \sum_k k^2 \phi_k \phi_{-k}$ leads to the identification $\pi_k = \frac{1}{2\pi\nu}(-ik)\phi_{-k}$, i.e. the strange looking prediction that the variable ϕ_k is canonically conjugate to its own derivative,

$$[\partial_x \phi(x), \phi(x')] = 2\pi i \nu \delta(x - x'). \tag{9.90}$$

Remembering that the Hamiltonian action of a system is given by $\int d\tau\ (H - i\pi \partial_\tau \phi)$, we arrive at the required result.

[124] Deviating from our standard conventions, we define the Fourier transform by $\phi_k = L^{-1/2} \int dx\ e^{ikx} \phi(x)$.

(b) Under a change of gauge, $a \to a + dg$, where g is a function, the CS action transforms as

$$\begin{aligned} S_{\rm CS}[a+dg] &= -\int_{D\times S^1} (a+dg)\wedge d(a+dg) = S_{\rm CS}[a] - \int_{D\times S^1} dg\wedge da \\ &= S_{\rm CS}[a] - \int_{\partial D\times S^1} dag, \end{aligned}$$

where we noticed that $dg \wedge da = d(gda)$ and applied Stokes, theorem. To remove the boundary gauge ambiguity, we need to fix a gauge at $\partial D \times S^1$, e.g. by setting $a_0|_{\partial D} = 0$. Decomposing $a = a_0 + \mathbf{a}$ and $d = \partial_0 d\tau + \partial_i dx_i \equiv d_0 + \mathbf{d}$ into temporal and real-space contributions, the action assumes the form

$$\begin{aligned} S_{\rm CS}[a_0,\mathbf{a}] &= -\int_{D\times S^1} (a_0+\mathbf{a})\wedge(d_0+\mathbf{d})(a_0+\mathbf{a}) \\ &= -\int_{D\times S^1} (a_0\wedge\mathbf{da} + \mathbf{a}\wedge d_0\mathbf{a} + \mathbf{a}\wedge\mathbf{d}a_0 + \mathbf{a}\wedge\mathbf{da}) \\ &= -\int_{D\times S^1} (2a_0\wedge\mathbf{da} + \mathbf{a}\wedge d_0\mathbf{a} + \mathbf{a}\wedge\mathbf{da}), \end{aligned}$$

where we have used the skew-symmetry of the exterior product and in the crucial second equality integrated by parts.[125] The boundary term corresponding to this integration vanishes due to the gauge-fixing condition $a_0|_{\partial D} = 0$. Linearly coupled to the action, the temporal component a_0 can be integrated out. As a result, we obtain a functional δ-distribution globally enforcing the constraint $da \equiv f = 0$, i.e. a vanishing of the spatial components of the field strength tensor. This in turn implies that $\mathbf{a}$ is a pure gauge, $\mathbf{a} = \mathbf{d}\phi$, where ϕ is some function. Substituting this representation into the action, we obtain $S[\phi] = -\int_{D\times S^1} \mathbf{d}\phi\wedge d_0\mathbf{d}\phi = -\int_{D\times S^1}\mathbf{d}(\mathbf{d}\phi\wedge d_0\phi) = -\int_{\partial D\times S^1}(\mathbf{d}\phi\wedge d_0\phi) = \int_{\partial D} dx\int d\tau\,\partial_x\phi\,\partial_\tau\phi$, where in the last step we switched back to conventional notation.

(c) Using the fact that $a = a_\mu dx_\mu = a_\mu(\partial x_\mu/\partial\tilde{x}_\nu)d\tilde{x}_\nu \equiv \tilde{a}_\nu d\tilde{x}_\nu$, and comparing coefficients, we obtain the identifications $\tilde{a}_x = a_x, \tilde{a}_{x_\perp} = a_{x_\perp}, \tilde{a}_0 = a_0 + v a_x$. "Form invariance" of the CS-action means that it does not matter whether we express it in terms of the old or the new coordinates:

$$S_{\rm CS}[a] = -\int (a_\mu dx_\mu)\wedge\left(dx_\nu\,\frac{\partial}{\partial x_\nu}\right)\wedge(a_\nu dx_\nu) = -\int(\tilde{a}_\mu d\tilde{x}_\mu)\wedge\left(d\tilde{x}_\nu\,\frac{\partial}{\partial\tilde{x}_\nu}\right)\wedge(\tilde{a}_\nu d\tilde{x}_\nu).$$

Focusing on the second representation (wherein $\tilde{a}_0|_{\partial D} = 0$), and repeating the analysis of (b), we obtain the real-time representation of the action $S_{\rm CS} = \int_{\partial D} d\tilde{x}\int d\tilde{t}\;\partial_{\tilde{x}}\phi\;\partial_{\tilde{t}}\phi$. Finally, using the fact that $\partial_x = \partial_{\tilde{x}}$ and $\partial_{\tilde{t}} = v\partial_x + \partial_t$, we arrive at $S_{\rm CS}[\phi] = \int_{\partial D} dx\int dt\,\left[v(\partial_x\phi)^2 + \partial_x\phi\;\partial_t\phi\right]$. Switching back to imaginary time and attaching the coupling constant, we obtain Eq. (9.89).

[125] That is, we have applied Stokes' theorem:

$$\int_{D\times S^1}\mathbf{a}\wedge\mathbf{d}a_0 = -\int_{D\times S^1}[\mathbf{d}(\mathbf{a}\wedge a_0) - \mathbf{da}\wedge a_0] = -\int_{D\times S^1}\mathbf{a}\wedge a_0 + \int_{D\times S^1}\mathbf{da}\wedge a_0 \overset{a_0|_{\partial D}=0}{=} \int_{D\times S^1}\mathbf{da}\wedge a_0.$$

(d) Since $\rho = \frac{1}{2\pi}\partial_x\phi$, the presence of a unit charge localized at x_0, $\rho(x) = \rho(x - x_0)$, amounts to the presence of a "kink" of height 2π in ϕ, i.e. $\phi(x) = 2\pi\theta(x - x_0)$. Now, according to Eq. (9.90), ϕ and $\partial_x\phi/2\pi\nu$ form a canonically conjugate pair. This implies that $U_d(x) \equiv \exp(-id\partial_x\phi/2\pi\nu)$ acts like a unit translation operator on ϕ: $U_d(x)\phi(x') = \phi(x') + d\delta(x - x')$. The unit-charge kink is generated by the action of $\int_{x_0}^{\infty} dx'\, U_{2\pi}(x') = \exp(-i\phi/\nu)$ on the field ϕ. Reformulating Eq. (9.90) as $[\phi(x), \phi(x')] = i\pi\nu\,\mathrm{sgn}(x - x')$, we find that

$$\begin{aligned} e^{i\nu^{-1}\phi(x)}e^{i\nu^{-1}\phi(x')} &= e^{i\nu^{-1}\phi(x')}\left(e^{-i\nu^{-1}\phi(x')}e^{i\nu^{-1}\phi(x)}e^{i\nu^{-1}\phi(x')}\right) \\ &= e^{i\nu^{-1}\phi(x')}\, e^{i\nu^{-1}\exp(-i\nu^{-1}[\phi(x'),\,])\phi(x)} \\ &= e^{i\nu^{-1}\phi(x')}e^{i\nu^{-1}\phi(x)} \times e^{i\pi\nu^{-1}\,\mathrm{sgn}(x-x')}. \end{aligned}$$

10

Nonequilibrium (classical)

This chapter provides an introduction to nonequilibrium statistical (field) theory. In the following, we introduce a spectrum of concepts central to the description of many particle systems out of statistical equilibrium. We will see that key elements of the theory – Langevin theory and the formalism of the Fokker–Planck equation – can be developed from the coherent framework of a path integral formalism. Applications discussed below include metastability, macroscopic quantum tunneling, driven diffusive lattices, and directed percolation. While the emphasis in this chapter is on *classical* nonequilibrium phenomena, the quantum theory of nonequilibrium systems will be discussed in the next chapter.

The world is a place full of nonequilibrium phenomena: an avalanche sliding down a sandpile, a traffic jam forming at rush hour, the dynamics of electrons inside a strongly voltage-biased electronic device, the turmoil of markets following an economic instability, the diffusion-limited reaction of chemical constituents and many others are examples of situations where a large number of correlated constituents evolves under "out-of-equilibrium" conditions. Statistical nonequilibrium physics is concerned with the identification and understanding of universal structures that characterise these phenomena. Notwithstanding the existence of powerful principles of unification, it is clear that a theory addressing the dazzling multitude of nonequilibrium phenomena must be multi-faceted. And indeed, nonequilibrium statistical physics is a strongly diversified field comprising many independent sub-disciplines. But this is not the only remarkable feature of this branch of physics. Considering the development of physics in, say, the last two decades, one may observe that nonequilibrium physics is a field of disproportionate growth. Occasionally one may get the impression that many particle theory as a whole is drifting towards the nonequilibrium!

INFO What does the attribute "**nonequilibrium**" actually define? Perhaps the most straightforward definition identifies it as the opposite of thermodynamic equilibrium, where the latter is defined by the following two conditions:[1]

> An equilibrium system is characterized by a unique set of extensive and intensive variables which do not change in time.
> After isolation of the system from its environment, all the variables remain unchanged.

The latter condition is necessary to distinguish equilibrium from stationary nonequilibrium states. For example, the particle distribution function of an electronic conductor subject to a

[1] W. Ebeling and I. M. Sokolov, *Statistical Thermodynamics and Stochastic Theory of Nonequilibrium Systems*, (World Scientific,2005).

strong time-independent voltage bias will be time-independent (first condition fulfilled), yet different from the equilibrium Gibbs distribution – a stationary nonequilibrium situation. However, after removal of the voltage carrying leads, or "environment," it will relax back to the Gibbs form (second condition violated).

The restrictiveness of the two conditions above vividly illustrates that thermodynamic equilibrium is a rare exception, a Platonic ideal scarcely realised in "real life."

What are the driving forces behind this development? For one thing, nonequilibrium statistical physics is a field of unusually high application potential. Many of the rapidly evolving interdisciplinary activities between physics and biology, or physics and the socio-economical sciences, expressly address nonequilibrium problems. But there is, of course, also intrinsic interest in the physics of nonequilibrium. For example, the response of an electronic device to shake-up by a sudden electromagnetic pulse evidently contains more structured information on its intrinsic dynamics than the (near equilibrium) linear response. The wealth of information encoded in the dynamics of strongly-driven many particle systems motivates the extension of existing (equilibrium) theories into the realm of nonequilibrium. Also, various many particle systems of interest are observed under nonequilibrium conditions (e.g. cold atom condensates), or intrinsically in a state of nonequilibrium (e.g. lasers). To understand the rich physical behavior of such systems, we need to develop a quantum theory of nonequilibrium phenomena.

From what has been said above, it should be clear that we will not be able to adequately introduce the full body of nonequilibrium statistical physics in this textbook; we really have to restrict ourselves to an absolute minimum of essentials. In the following we focus on areas of nonequilibrium statistical physics that are of relevance specifically to condensed matter physics. Interesting developments relevant to, say, the physics of biological or socio-economic systems are not covered. In line with the general philosophy of the book, the material is organized according to the conceptual structure of the theory (rather than by fields of application). We start by introducing elements of probability theory and stochastic processes, Langevin theory, the theory of noise, and the theory of the Fokker Planck equation. It will then be seen that various connections between these elements can be understood from the unifying field theoretical framework of the Martin–Siggia–Rose–Janssen–de Dominicis (MSRJD) field integral. We apply the MSRJD formalism to introduce elements of the theory of dynamic phase transitions. In the next chapter we then identify the MSRJD field integral as the classical limit of a more general theory, the Keldysh field integral of quantum nonequilibrium statistical mechanics.

INFO In this chapter, there is a lot of discussion about different types of "probability." For the convenience of the reader, a few **elements of probability theory** are summarized below. (This material need not be studied in a coherent fashion, and can be used as a glossary whenever necessary.)

Although we shall not enter a discussion of the foundations of probability theory, it may be worthwhile to note that the notion of "probability" is difficult to grasp. There exist different and, in fact, controversial definitions of what is meant by "the probability" of certain events. Here, we will sidestep these complications by assuming that the probabilities of certain basic events are *a priori* known (e.g. the probability of individual faces when throwing dice). The

task of probability theory then is to describe the probability of more complex, compound events (e.g. the probability of winning a certain game of dice). The probability P that a basic variable X take values $x_i, i = 1, \dots N$ (or continuous values $x \in [a, b]$), is described by the probability distribution,

$$\text{discrete:} \quad p_i \equiv P(X = x_i), \qquad p_i \geq 0, \qquad \sum_{i=1}^{N} p_i = 1,$$

$$\text{continuous:} \quad p(x)dx \equiv P(x < X < x + dx), \qquad p(x) \geq 0, \qquad \int_a^b p(x)\, dx = 1.$$

A variable whose defining properties are encapsulated in a probability distribution is called a **random variable**. To avoid discrete/continuous case distinctions, we may express the distribution of a discrete random variable in continuum form, $p(x)dx \equiv \sum_i \delta(x - x_i)dx$. Furthermore, we shall formulate our discussion for scalar random variables. The extension to multi-dimensional variables $\mathbf{X} \in \mathbb{R}^n$ should be obvious.

Expectation values of functions $f(X)$ depending on the random variable are defined as

$$\langle f(X) \rangle \equiv \int dx\, p(x) f(x).$$

Below we list a number of important examples of expectation values:

The **mean value** $\langle X \rangle \equiv \int dx\, p(x) x$ of the distribution and its **moments** $X_n \equiv \langle X^n \rangle \equiv \int dx\, p(x) x^n$. Notice that the moments of distributions need not necessarily exist. For example, the Lorentzian distribution $p(x) = \frac{1}{\pi} \frac{a}{a^2 + x^2}$ does not have moments at all.
The **cumulants**

$$\begin{aligned} \mu_1 &\equiv X_1, \\ \mu_2 &\equiv X_2 - X_1^2, \\ \mu_3 &\equiv X_3 - 3X_1X_2 + 2X_1^3, \\ \mu_4 &\equiv \dots, \end{aligned} \tag{10.1}$$

contain information about the degree of "correlation" in a probability distribution. They describe the way in which high moments differ from products of moments of lesser degree. A systematic way to define cumulants is by expansion of the cumulant generating function: $\ln\langle \exp(itX) \rangle = \sum_{i=1}^{\infty} \frac{(it)^n}{n!} \mu_n$. Exercise: Think about connections between cumulants and the connectedness of diagrams resulting from the expansion of free energies (symbolic notation) $F = -T \ln\langle \int D\phi \exp(-S[\phi]) \rangle$.
The probability distribution may be formally represented as the expectation value of a δ-distribution,

$$p(x) = \langle \delta(x - X) \rangle.$$

Far better than a useless tautology, this relation represents a vehicle to generate derived probability distributions: let $F(X)$ be some function and define $Y \equiv F(X)$. This is a new random variable which inherits its probability distribution $p(y)$ from $p(x)$. The connection between the two can be obtained as

$$p(y) = \langle \delta(y - Y) \rangle = \int dx\, p(x) \delta(y - F(x)) = p(x(y)) \left| \frac{\partial x}{\partial y} \right|_{x = x(y)},$$

where we assumed a unique functional relation $y = F(x)$. This relation may also be obtained by direct transformation of the probability *measure*, $p(x)dx = p(x(y))|\partial x/\partial y|dy \equiv p(y)dy$. In practice, however, the δ-representation is often more convenient to use.

The full set of information on a random variable is contained in the expectation value

$$g(t) \equiv \langle \exp(itX) \rangle. \tag{10.2}$$

From this **generating function**, all moments can be obtained by power series expansion and all cumulants by expansion of $\ln g(t)$:

$$g(t) = \sum_{n=0}^{\infty} \frac{(it)^n}{n!} X_n, \qquad \ln(g(t)) = \sum_{n=0}^{\infty} \frac{(it)^n}{n!} \mu_n.$$

The full probability distribution can be obtained (exercise) from the generating function by Fourier transformation,

$$p(x) = \int \frac{dt}{2\pi}\, e^{-itx} g(t).$$

For concreteness and later reference let us discuss a few distributions of outstanding importance. The **Gaussian distribution** is given by the familiar expression

$$p(x)dx = \frac{1}{\sqrt{2\pi\mu_2}} \exp\left(\frac{(x-\mu_1)^2}{2\mu_2}\right) dx. \tag{10.3}$$

Typically, it describes the probability of variables $x = \sum_{n=1}^{N} x_n$ that are obtained as the sum of a large number of elementary random variables, x_n, distributed according to some distribution p with first and second cumulant μ_1 and μ_2, respectively. In this case – the statement of the **central limit theorem**[2] – the probability of x is given by Eq. (10.3), with first and second cumulant $\mu_1 = N\mu_1$ and $\mu_2 = N\mu_2$, respectively. (All higher cumulants of the Gaussian distribution vanish. Exercise: verify this statement by showing that the generating function of the Gaussian distribution is again a Gaussian.) The ubiquity of additive random variables in nature explains the importance of Gaussians in natural sciences.

The **Poisson distribution** $p(m)$ describes the probability to observe m events in $n \gg 1$ trials when the events are mutually uncorrelated[3] and occur with low individual probability p. (As an example, consider the probability to count m cars passing a counter at a cross country road late at night in a time window of 100min when the passage probability per minute, $p = 0.05$.)

[2] The **proof of the central limit theorem** amounts to an instructive miniature version of the large N-expansion methods introduced in chapter 5.3:

$$\begin{aligned} p(x) = \langle \delta(x - \sum_{n=1}^{n} x_n) \rangle &= \prod_{n=1}^{N} dx_n\, p(x_n) \quad dk\, e^{ik(x_n - x)} \\ &= dk \exp \quad N \ln \quad dx\, p(x) e^{ikx} - ixk \quad = \quad dk \exp\left(N \ln g(k) - ixk\right) \\ &= dk \exp(N \;\; ik(\mu_1 - x/N) - k^2\mu_2/2 + \mathcal{O}(k^3)\;) \simeq \frac{1}{\sqrt{2\pi N\mu_2}} \exp \quad \frac{(x - N\mu_1)^2}{2N\mu_2} \quad , \end{aligned}$$

where in the first line we used the Fourier representation of the δ-function, g in the second line is the generating function of the distribution p, and in the crucial last equality we used the fact that anharmonic corrections to the quadratic k-exponent vanish in the large N limit.

[3] Two random variables X and Y are said to be **uncorrelated** if $\langle XY \rangle = \langle X \rangle \langle Y \rangle$. The correlation obviously vanishes if X and Y are **independent random variables**, i.e. if $p(x, y) = p_x(x)p_y(y)$. (The opposite conclusion, "lack of correlation $\to$ independence," is not valid in general.)

Assuming that the probability to observe the event in question at any individual trial is $p \ll 1$ while $n \gg m$, the Poisson distribution asymptotes to[4]

$$P(m) = \frac{(np)^m}{m!}\exp(-np). \tag{10.4}$$

The Poisson distribution has constant cumulants $\mu_l = np$. (Exercise: compute the generating function to prove this result.)

The **Lorentzian distribution** a.k.a. **Breit–Wigner distribution** or **Cauchy distribution** is defined by

$$p(x) = \frac{1}{\pi}\frac{a}{(x-x_0)^2 + a^2}. \tag{10.5}$$

In physics, the Lorentzian distribution describes the energy dependence of scattering resonances, (relatedly) the broadening of many particle spectral functions by interactions, the line shape distribution of damped electromagnetic modes, and many other phenomena governed by an interplay of driving/oscillation/damping. As mentioned above, its moments are undefined. Loosely speaking, the distribution is centered around x_0, has width a, and is exceptionally broad.

In probability theory one is often interested in computing the composite probability $p(x_2, x_1)$, from information about the probabilities $p_1(x_1)$ and $p_2(x_2)$ of elementary random variables X_1 and X_2. In this context, a natural question to ask is "what is the probability to obtain x_2 provided x_1 has been observed?" By definition, the answer is given by the **conditional probability**, $p(x_2|x_1)$. It is implicitly defined by

$$p(x_2, x_1) = p(x_2|x_1)p_1(x_1). \tag{10.6}$$

Summing over all possible realizations of the random variable X_2, we get the raw distribution of X_2, $\int dx_1\, p(x_2, x_1) = p(x_2)$, or

$$p(x_2) = \int dx_1\, p(x_2|x_1)p_1(x_1).$$

won't Considering the case where x_1 by itself is a composite random variable, $x_2 \to x_n$ and $x_1 \to (x_{n-1}, \ldots, x_1)$, we obtain an important generalization of Eq. (10.6). Iteration of the definition then leads to

$$p(x_n, \ldots, x_1) = p(x_n|x_{n-1}, \ldots, x_1)p(x_{n-1}|x_{n-2}, \ldots, x_1)\ldots p(x_2|x_1)p_1(x_1). \tag{10.7}$$

EXERCISE The **characteristic function** of a probability distribution $P(x)$ is defined as

$$g(t) = \langle e^{itX}\rangle = \int dx\, p(x)e^{itx}.$$

Compute the characteristic function for (a) the Gaussian distribution, $p(x) = \frac{1}{\sqrt{2\pi\sigma}}e^{-\frac{(x-x_0)^2}{2\sigma}}$, (b) the Lorentzian distribution, $p(x) = \frac{1}{\pi}\frac{a}{(x-x_0)^2+a^2}$, and (c) the Poisson distribution, $p(x) =$

[4] The probability to observe m successes is given by $P(m) = \binom{n}{m}(1-p)^{n-m}p^m$. For $n \gg 1$ and $p \ll 1$, $\binom{n}{m} \simeq n^m$ and $(1-p)^{n-m} \simeq (1-p)^n = (1-(np)/n)^n \simeq \exp(-np)$. Combining these estimates, we obtain the Poisson distribution. (Exercise: show that the derivation becomes exact in the limit $n \to \infty, p \to 0$ at fixed product np. Show that for $n \to \infty$ at fixed p the Gaussian distribution is obtained.)

$\frac{x}{x!}e^-$. Consider the distribution, $p(x) = \frac{1}{\pi}\frac{1}{\sqrt{x(1-x)}}$, for $x \in (0,1)$ and zero otherwise. Show that its characteristic function has the limiting behavior

$$g(t) \sim \frac{(1-i)(i+e^{it})}{\sqrt{2\pi t}} \quad \text{for} \quad t \to \infty.$$

10.1 Fundamental questions of (nonequilibrium) statistical mechanics

From the discussion above, it should be obvious that thermodynamic equilibrium represents an exception, rather than a rule. The one reason why many particle theory has focused historically on the description of (near-)equilibrium states is that the latter are so much easier to describe. In thermal equilibrium we know that the state of an N-particle system is governed by the thermal density operator $\mathcal{Z}^{-1}\exp(-\beta\hat{H})$. "All' that remains to be done is to compute physical observables from this distribution. However, in thermal nonequilibrium the distribution of the system in phase or Hilbert space is *apriori* unknown, a lack of knowledge that bears important consequences:

- ▷ Getting the relevant many particle distribution functions under control is an essential part of the theoretical challenge (and usually the first one to be addressed).
- ▷ Concepts which we tend to take for granted (the existence of a uniquely defined temperature, homogeneity of thermodynamic variables, etc.) need to be critically re-examined.
- ▷ There is no reason to hope that nonequilibrium statistical physics as a whole (whatever *that* is) will be nearly as universal as the equilibrium theory.

Imagine, then, a situation where no *apriori* information about the state of a many particle system is available. How can we compute the distribution of its states (classical or quantum)? Indeed, even the formulation of the problem that needs to be solved is not entirely obvious.

Ludwig Boltzmann 1844–1906

Austrian physicist famous for his pioneering contributions to statistical mechanics. Concepts such as Maxwell–Boltzmann statistics, the Boltzmann distribution, or the logarithmic connection between entropy and probability remain foundations of this field. Boltzmann was one of the most important supporters of early atomic theory, at a time when the reality of atoms was still controversial.

In principle, the state of a classical d-dimensional N-particle system can be represented by a point $\mathbf{X} \in \mathbb{R}^{2Nd}$ in $2Nd$ dimensional phase space. The full information about its dynamics, and all derived physical properties is then contained in some high-dimensional Hamiltonian equation of motion.

The above view is formally exact, but largely useless in practice. However, in the late nineteenth century, **Boltzmann** introduced an alternative picture which turned out to be much more powerful: Boltzmann suggested describing the system in terms of a "swarm" of N points in $2d$-dimensional phase space, rather than by a single point in an incredibly high dimensional space. This idea paved the way to a statistical formulation of the problem and may be considered as the starting point of statistical mechanics as an independent branch

of physics. Indeed, we may trade much of the excessive fine structure information encoded in the full coordinate data of the "swarm" by introducing a measure

$$f(\mathbf{x},t)d^dx,$$

where $\mathbf{x} = (\mathbf{q},\mathbf{p})$ is a point in phase space and the dimensionless function $f(\mathbf{x},t)$ is the (distribution of the) number of particles found at time t in the volume element $d^dx = \sum_{i=1}^{d} dq_i dp_i$ (see the figure), i.e. f is normalized according to

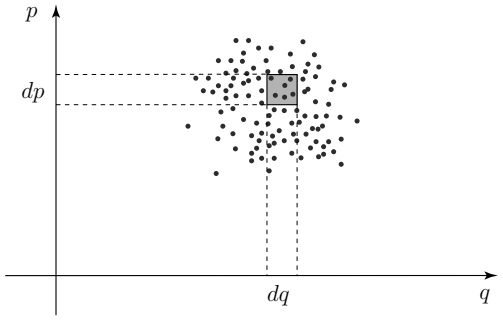

$$\int_\Gamma d^dx\, f(\mathbf{x}) = N,$$

where $\int_\Gamma$ is an integral over classical phase space. The function f is the prime information carrier of the theory. Average values of physical observables X can be calculated according to the relation,

$$\langle X\rangle = \int d^dx\, f(\mathbf{x},t)X(\mathbf{x}),$$

where $X(\mathbf{x})$ is the phase space function representing the observable. For example, the energy carried by the system is obtained as $E = \langle H\rangle = \int d^dx\, f(\mathbf{x},t)H(\mathbf{x})$, where $H(\mathbf{x})$ is the Hamiltonian, etc.

Since the state of the system is essentially described by its distribution function, we can reformulate the questions raised above as follows: How can we compute f for a given system if the Hamiltonian and an initial state $f(\,.\,,t)$ are specified? However, before addressing this problem in full, we should be able to answer two less ambitious questions: what is the equilibrium structure of f, and how does the system approach that equilibrium configuration if it is allowed to evolve unperturbed according to its own dynamics?

To begin, let us try to understand the (time-independent) **equilibrium form of the distribution function**, $f(\mathbf{x})$. Imagine a system prepared in some initial distribution. Think of the long-time density function $f(\mathbf{x}, t\to\infty)$ as a probabilistic object where averaging is over different initial conditions. We assume that the system is weakly interacting, or gaseous, in the sense that the dynamics is essentially of single particle type. Collisions between particles, $(\mathbf{x}_1,\mathbf{x}_2)\to(\mathbf{x}_1',\mathbf{x}_2')$ will serve as a mechanism of relaxation towards an equilibrium state by exchange of energy and momentum between individual particles. Under these conditions, it is safe to assume that the distribution of particles will be independent in the sense that the joint probability to observe particles at $\mathbf{x}_1$ and $\mathbf{x}_2$, respectively, $N^2p(\mathbf{x}_1,\mathbf{x}_2)$, factorizes into independent particle distributions $N^2p(\mathbf{x}_1,\mathbf{x}_2) = (Np(\mathbf{x}_1))\times(Np(\mathbf{x}_2)) \equiv f(\mathbf{x}_1)f(\mathbf{x}_2)$. By virtue of this assumption, the function f acquires the status of a statistical distribution, fully describing the state of the system.

EXERCISE Discuss: in what sense may this description become problematic once interactions become strong?

The fact that coordinate configurations $(\mathbf{x}_1, \mathbf{x}_2) \leftrightarrow (\mathbf{x}_1', \mathbf{x}_2')$ are coupled by an elementary scattering event implies conservation of probability, $f(\mathbf{x}_1, \mathbf{x}_2) = f(\mathbf{x}_1) f(\mathbf{x}_2) = f(\mathbf{x}_1') f(\mathbf{x}_2') = f(\mathbf{x}_1', \mathbf{x}_2')$. Assuming that $f(\mathbf{x}) = f(H(\mathbf{x})) \equiv f(\epsilon)$ is a function of energy, we conclude that probability conservation is compatible with energy conservation, $\epsilon_1 + \epsilon_2 = \epsilon_1' + \epsilon_2'$, if $\ln f(\epsilon) = a\epsilon + b$ is linear in energy. In this case, $f(\mathbf{x}_1) f(\mathbf{x}_2) = \exp(a(\epsilon_1 + \epsilon_2) + 2b) = \exp(a(\epsilon_1' + \epsilon_2') + 2b) = f(\mathbf{x}_1') f(\mathbf{x}_2')$ is indeed satisfied. To fix the constants a and b we require normalization of the partition function and employ the equipartition theorem, i.e. we use the fact that in thermodynamic equilibrium, the expectation value of the energy of each of the $2Nd$ degrees of freedom must equal $T/2$.[5] Normalization requires (exercise) $b = \ln N - \ln \int d^d x \exp(a\epsilon)$ and from the equipartition theorem we obtain

$$NdT \stackrel{!}{=} dN \frac{\int_\Gamma d^d x \, e^{aH(\mathbf{x})} H(\mathbf{x})}{\int_\Gamma d^d x \, e^{aH(\mathbf{x})}} = -\frac{Nd}{a} \Rightarrow a = -\frac{1}{T} = -\beta,$$

where, again, a quadratic Hamiltonian was assumed. We thus arrive at the conclusion:

$$\boxed{f(\mathbf{x}) = N \frac{e^{-\beta H(\mathbf{x})}}{\int_\Gamma dx \, e^{-\beta H(\mathbf{x})}},} \tag{10.8}$$

which is the famous **Maxwell–Boltzmann distribution**. Exercise: in what sense is Eq. (10.8) a direct descendant of the many particle Gibbs distribution?

The derivation above can tell us the form of the equilibrium distribution, but it is much too indirect to describe how equilibrium is actually approached. For that purpose we need to develop far more explicit ways to describe the dynamics of the distribution function. The construction of such theories is the subject of the next two sections.

10.2 Langevin theory

Imagine a situation where, at time $t = 0$, some initial distribution $f(\mathbf{x}, 0)$ has been prepared. We wish to understand its dynamics. Specifically, we wish to understand how the Maxwell–Boltzmann distribution is approached if the system is kept in isolation. It will also be of interest to explore deviations from equilibrium if the system is externally perturbed.

A purist might argue that phase space points $\mathbf{x} \stackrel{t}{\to} \mathbf{x}(t) = \exp(t\{H, \,.\,\})\mathbf{x}$ develop according to the deterministic time evolution of Hamiltonian dynamics. This view will lead to $f(\mathbf{x}, t) = f(\mathbf{x}(-t), 0)$, or $\partial_t f(\mathbf{x}, t) = \partial_s\big|_{s=0} f(\mathbf{x}, t+s) = -\partial_s\big|_{s=0} f(\mathbf{x}(s), t) = \{H, f(\mathbf{x}, t)\}$. Deterministic time evolution is thus described by the equation,

$$(\partial_t - \{H, \,.\,\})\, f(\mathbf{x}, t) = 0. \tag{10.9}$$

Now, this equation clearly does not capture the irreversible approach to equilibrium. What it neglects is that we are actually concerned with a many particle system. The presence of other particles will affect the dynamics in two different ways.

[5] Here we assume that, close to thermal equilibrium, the dynamics of each particle will be approximately oscillator-like, and energy comprises kinetic energy (d momentum degrees of freedom) and potential energy (d spatial degrees of freedom).

First, it will hinder the ballistic motion of individual particles and, in a coarse-grained perspective, will lead to **friction**. Second, repeated collisions with other particles will effectively act as a **fluctuating force**. As we shall see, these two mechanisms, dissipative friction and fluctuations are not independent. In thermal equilibrium they do, in fact, completely determine each other, a correlation we will identify as a manifestation of the fluctuation–dissipation theorem.

Paul Langevin 1872–1946

French physicist known who developed the concept of Langevin dynamics. He is also known for his modern interpretation of para- and diamagnetism in terms of the electron spin. Langevin was a devoted anti-fascist and lost his academic position under the Vichy regime. (Shortly before his death he was rehabilitated.)

In a seminal work [6] the French physicist Paul Langevin proposed to describe the concerted action of dissipation and fluctuation in terms of a stochastic generalization of Newton's equation, the celebrated **Langevin equation**,

$$\boxed{M d_t \mathbf{v} + m\gamma \mathbf{v} - \mathbf{F} = \quad (t),} \tag{10.10}$$

where $\mathbf{v}$ is the single particle velocity, $\mathbf{F} = -\partial_{\mathbf{q}} H$ a macroscopic force acting on the particles, γ a phenomenological friction coefficient, and a randomly fluctuating force describing the effect of erratic pair collisions. Langevin proposed to model the force in terms of a short-range correlated Gaussian random variable with zero mean, $\langle \xi_i(t) \rangle = 0$ and variance

$$\langle \xi_i(t) \xi_{i'}(t') \rangle = A \delta_{ii'} \delta(t - t'), \tag{10.11}$$

where $A > 0$ is a constant.

INFO The development of Langevin's theory was motivated by the phenomenon of **Brownian motion**. In 1827 the Scottish botanist, Robert Brown, observed[7] unceasing erratic motion of pollen particles in aqueous immersion. First qualitative explanations of the phenomenon in terms of random particle collisions appeared in the late nineteenth century. Langevin suggested Eq. (10.10) as an effective equation of motion controlling the dynamics of "mesoscopic" particles, subject to inter-particle collisions. The erratic nature of solutions of the Langevin equation – qualitatively consistent with Brownian motion – is illustrated in Fig. 10.1.

Before turning to the analysis of this equation, let us make a few general remarks:

▷ One of the important predictions of the theory is that, in thermal equilibrium, the friction coefficient, γ, and the fluctuation strength, A, are mutually dependent parameters: fluctuations and dissipative damping are twin effects – again, a manifestation of the **fluctuation-dissipation theorem**.

[6] P. Langevin, Sur la théorie du mouvement Brownien, *CR Hebd. Acad. Sci.* **146**, 530-3 (1908).
[7] The phenomenon had, in fact, been observed earlier by the Dutch physician Jan Ingenhousz in 1785.

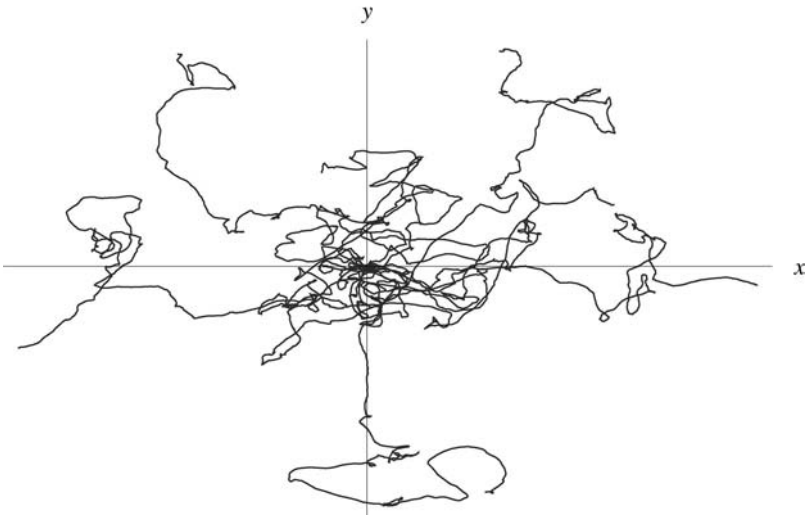

Figure 10.1 A few two-dimensional solutions of Eq. (10.10) for different fluctuation force configurations. The paths start at time $t = 0$ at $x = y = 0$. Qualitatively, they resemble the paths traced out by fictitious "Brownian particles".

- ▷ We may expect multiple particle collisions to cause effectively stochastic, or **diffusive motion** of individual particles. Indeed, we will identify the inverse A^{-1} as an effective measure of the diffusivity of the medium.
- ▷ A specific solution $\mathbf{q}(t)$ of the Langevin equation defines a realization of what is called a **stochastic process**. A stochastic process (cf. the more comprehensive discussion in Section 10.4 below) is described by a time-dependent random variable $X(t)$. Here, "random" means that no deterministic statements about the time dependence of X can be made. The best we can obtain is results on the *probability* distribution $P(X(t))$ of realizations of X. In the present context there are two alternatives: we may discuss the Langevin equation in terms of $\mathbf{v}[\ ]$, i.e. specific realizations of the velocity, randomly dependent on the realization . Suitable averages over will then lead to a statistical description of velocity distributions, etc. This is the strategy originally proposed by Langevin. Alternatively, we may aim to describe the velocity distribution $P[\mathbf{v}]$ directly in terms of certain statistical propositions. This latter strategy was proposed by Einstein in his famous work on Brownian dynamics (see below).

10.2.1 Fluctuation–Dissipation Theorem (FDT)

To discuss the connection between dissipation and fluctuation in an unperturbed system, we consider the Langevin equation in the absence of driving forces, $\mathbf{F} = 0$. Temporal Fourier transformation $\mathbf{v}(\omega) = \int dt \exp(i\omega t)\mathbf{v}(t)$, obtains the formal solution $\mathbf{v}(\omega) = \frac{1}{m(-i\omega+\gamma)}\ (\omega)$. According to this relation, the "induced" random variable $\mathbf{v}$ has zero mean, $\langle v_i(t)\rangle = 0$,

and second moment (exercise)

$$\langle v_i^2(t)\rangle = \frac{A}{m^2}\int_{-\infty}^{\infty}\frac{d\omega}{2\pi}\,\frac{1}{\omega^2+\gamma^2} = \frac{A}{2m^2\gamma}.$$

However, in thermal equilibrium, the equipartition theorem establishes a connection between the average kinetic energy per degree of freedom and temperature, $m\langle v_i^2\rangle/2 \stackrel{!}{=} T/2$. Comparison with the result above then leads to the **Einstein relation**,

$$A = 2m\gamma T, \tag{10.12}$$

i.e. in thermal equilibrium, the variance of environmental fluctuating forces is proportional to the strength of dissipative (frictional) forces, and to temperature.

INFO Let us briefly review **Einstein s derivation of Eq. (10.12)**. Einstein's approach is phenomenological but contains additional information inasmuch as it establishes a connection between the strength of fluctuation forces and the concept of diffusion. The basis of the argument is that, in a medium governed by frequent inter-particle collisions, the dynamics of individual particles will be **di usive**. Similarly, externally applied forces will cause **drift motion**, rather than free ballistic acceleration. The first postulate implies that a density gradient, ∂f, in the medium will lead to a diffusion current,

$$\boxed{\mathbf{j}_{\rm d} = -D \quad f,} \tag{10.13}$$

i.e. a current acting to restore a uniform density profile. Equation (10.13) is generally known as **Fick s (first) law**. Application of the continuity equation $d_t f = - \quad \cdot \mathbf{j}_{\rm d}$ then shows that $\partial_t f = D\Delta f$ (Fick's second law) implying that the dynamics is indeed diffusive.

The second postulate states that $\mathbf{j}_{\rm ext} = \gamma^{-1}m^{-1}f\mathbf{F}_{\rm ext}$, i.e. an external force generates a drift current proportional to the force, the density, and the inverse of the friction coefficient. (This formula may be obtained by dimensional analysis, or by consideration of the stationary configuration, $\partial_t\langle\mathbf{v}\rangle = 0$ obtained by averaging the Langevin equation (10.10).) In thermal equilibrium, diffusion current and external current must compensate each other, i.e. $\mathbf{j}_{\rm d} = -\mathbf{j}_{\rm ext}$, or $D \quad f = -f \quad V/m\gamma$, where we assumed that the force is generated by some potential, V. This equation for the density profile is solved by $f \sim \exp(-V/Dm\gamma)$. However, compatibility with the Maxwell–Boltzmann distribution (10.8) requires that $f \sim \exp(-V/T)$, or

$$\boxed{D = \frac{T}{m\gamma}.} \tag{10.14}$$

Equation (10.14) is the celebrated **Einstein relation**. Comparison with Eq. (10.12) finally leads to the identification,

$$A = \frac{2T^2}{D}, \tag{10.15}$$

i.e. the variance of the (microscopic) fluctuation forces in the medium is inversely proportional to its (macroscopic) diffusion constant.

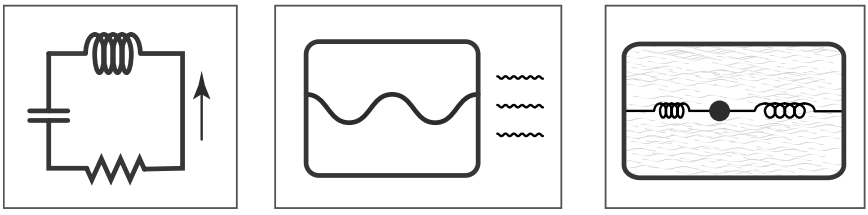

Figure 10.2 Three realizations of resonator modes subject to the interplay of fluctuations and dissipation. Left: RLC-electronic circuit; Middle: a resonator mode subject to radiation losses; Right: damped mechanical oscillator.

10.2.2 A brief compendium on noise

Our discussion above conveys the important message, that dissipation or friction are intimately linked to the presence of fluctuating forces. However, unlike the everyday phenomenon of friction, the corresponding fluctuation forces are usually less noticeable. The reason is that friction acts in a directed way (cf. the action of a brake), while the response caused by fluctuations tends to average out. Yet, there are important exceptions to this rule. For example, high amplification levels render the fluctuations, or noise caused by resistive elements in electronic circuits a quite noticeable (and usually unwelcome) side effect.

Figure 10.2 shows three prominent setups where the interplay of fluctuations and dissipation is operational: an electronic RLC-circuit, an electromagnetic cavity mode experiencing radiative losses, and a damped oscillator. All of these systems are characterised by idealized non-dissipative dynamics that is harmonic. The presence of dissipation (resistor/radiative losses/mechanical damping) generates fluctuations. In the case of the macroscopic mechanical oscillators, these fluctuations will be largely inconsequential. However in the first two systems they cause noticeable effects.

Johnson–Nyquist noise

Let us explore the situation in the example of the RLC-circuit. In this case, we are concerned with the charge Q transmitted through the circuit (from which current and voltage drop across the resistive element are obtained as $I = \dot{Q}$ and $U = R\dot{Q}$, respectively). In elementary courses, we learn that the dynamics of charge is governed by the equation,

$$Ld_t^2 Q + \frac{Q}{C} + Rd_t Q = U_{\text{ext}}, \tag{10.16}$$

where U_{ext} is the externally applied voltage. This is the equation of motion of a dissipatively damped oscillator. However, in view of our discussion above, we know that Eq. (10.16) neglects the effect of the fluctuations accompanying dissipation. A correct way to think about Eq. (10.16) is as an equation for the coordinate $\langle Q \rangle$, averaged over realizations of those fluctuations. A realization specific generalization of Eq. (10.16) compatible with the

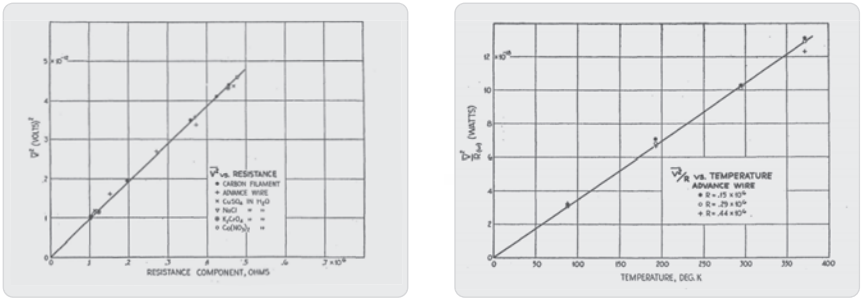

Figure 10.3 Left panel: Noise strength vs. resistance for wires made of different materials. Right panel: Noise strength vs. temperature for the "advanced wire". The two data sets display near-perfect linearity, in agreement with the theory of Johnson–Nyquist noise. Data taken from J. B. Johnson, Phys. Rev. **32**, 97-109 (1928).

fluctuation dissipation theorem is given by

$$Ld_t^2 Q + \frac{Q}{C} + Rd_t Q = U_{\rm ext} + U_{\rm jn}(t), \tag{10.17}$$

where the correlator of the noise term is given by

$$\langle U_{\rm jn}(t)\rangle = 0, \qquad \langle U_{\rm jn}(t)U_{\rm jn}(t')\rangle = 2TR\delta(t-t'). \tag{10.18}$$

The noise term in Eq. (10.17) can be interpreted as a time-dependent fluctuating voltage, additional to the external voltage. It is important to realize that this type of noise is an inevitable consequence of the presence of resistive elements in electronic circuits; it cannot be removed by "improving the quality" of the device.

The presence of a fluctuating voltage of strength $\langle |U_{\rm jn}(\omega)|^2\rangle = 2TR$ was experimentally discovered by Johnson[8] (cf. Fig. 10.3). Nyquist[9] explained the phenomenon in terms of the thermal equipartition of energy of electromagnetic oscillator modes. Reflecting this background, $U_{\rm jn}$ is alternatively denoted **Johnson noise**, **Nyquist noise**, **Johnson–Nyquist noise**, or just **thermal noise**.

INFO The **strength of the noise correlator** is fixed by slight modification of the arguments used in Section 10.2.1 above: Think of a non-resistive LC-circuit as an electronic realization of the harmonic oscillator. The $R = 0$, $U = 0$ variant of Eq. (10.17) is obtained by variation of the "Lagrangian" action

$$S = i\int dt\left(\frac{L}{2}Q^2 - \frac{1}{2C}Q^2\right),$$

[8] J. B. Johnson, Thermal agitation of electricity in conductors, *Phys. Rev.* **32**, 97-110 (1928).
[9] H. Nyquist, Thermal agitation of electric charge in conductors, *Phys. Rev.* **32**, 110-13 (1928).

where $LQ^2/2$ and $Q^2/2C$ represent the kinetic (inductive) and potential (capacitive) energy, respectively. We expect an interplay of fluctuation and dissipation to establish an energy balance compatible with the equipartition theorem,

$$\frac{L}{2}\langle Q^2\rangle = \frac{1}{2C}\langle Q^2\rangle = \frac{T}{2},$$

i.e. $T/2$ for both kinetic and potential energy. This energy balance should be established no matter how strong is the dissipation (R). In the absence of external biasing, $U_{\rm ext} = 0$, the temporal Fourier transform is given by

$$Q(\omega) = \frac{U_{\rm jn}(\omega)}{i\omega R - \omega^2 L + C^{-1}}.$$

Using Eq. (10.17) and (10.18), it is then straightforward to verify that

$$\frac{L}{2}\langle Q(t)^2\rangle = 2TR\frac{L}{2}\int \frac{d\omega}{2\pi}\frac{\omega^2}{\omega^2R^2 + (\omega^2 L - C^{-1})^2} = \frac{T}{2}.$$

Similar reasoning shows that $\frac{1}{2C}\langle Q^2\rangle = \frac{T}{2}$.

Although the voltage correlation Eq. (10.18) is consistent with the classical equipartition theorem, this very consistency generates an annoying problem: the second moment $\langle V_{\rm jn}(t)^2\rangle \propto \delta(0)$ diverges, i.e. our analysis makes the unphysical prediction that a voltmeter measuring noise amplitudes will detect voltage spikes of arbitrary strength. Equivalently, we are making the unphysical prediction that the noise fluctuates with constant intensity at arbitrarily high frequencies. (Expressed more formally, the **noise power**

$$S(U_{\rm jn},\omega) \equiv \lim_{T\to\infty}\frac{1}{T}\left|\int_{-T}^{T} dt\, U_{\rm jn}(t)e^{i\omega t}\right|^2 = RT, \tag{10.19}$$

which is a measure of the fluctuation intensity at characteristic frequency ω, remains constant.)

This problem disappears if we replace the classical fluctuation energy of the harmonic oscillator, $2\times\frac{T}{2} = T \to \omega(e^{\omega/T}-1)^{-1}$ by the energy of a quantum oscillator. (Exercise: explore this point.) For frequencies much larger than temperature, $\omega \gg T$, the mode does not store energy and the problem with the diverging noise amplitude disappears.[10]

Shot noise

Johnson noise is not the only "inevitable" source of noise. In electronic devices, the discreteness of charge quanta generates additional noise. A train of uncorrelated electrons running down a wire is an example of a Poisson process described in Section 10.4.2. The average number of electrons, n, passing through the wire in a time interval Δt (large in comparison to the mean passage time) defines the mean current,

$$\langle I\rangle = \frac{\langle n\rangle}{\Delta t}.$$

[10] Notice that the expression $\omega(e^{\omega/T}-1)^{-1}$ excludes the vacuum or zero-point energy, $\omega/2$. If the vacuum energy is kept in the energy balance, the problem with the divergence in the integrated noise power reappears. One may reason that the exclusion of the vacuum energy is justified because only physical *transitions* can participate in dissipative processes. For a more satisfactory picture, see below.

However, it is a characteristic feature of Poisson processes that the variance in the number of transmitted electrons $\mathrm{var}(n) = \langle n \rangle$, which means that the variance in the current,

$$\mathrm{var}(I) = \frac{1}{\Delta t} \langle I \rangle.$$

Although the signal-to-noise ratio $\langle I \rangle^2 / \mathrm{var}(I) = \Delta t \langle I \rangle$ increases with increasing observation times and increasing mean current strength, the discreteness of charge remains a principal source of noise. In a continuum model of charge transport this **shot noise**[11] can be modeled by addition of a suitable noise term to the right hand side of Eq. (10.16), in addition to the Johnson noise term. (In Section 11.6 of the next chapter we explore how this addition emerges in a microscopic construction.) Unlike Johnson noise, shot noise is independent of temperature and resistivity of the circuit. Both have in common that the noise power is largely independent of frequency.

Other sources of noise

A variety of physical processes produce noise. Empirically one finds that these sources of noise can add to an overall noise signal that is (a) non-universal in that it depends on all sorts of system-specific details and (b) strongly frequency dependent (unlike the "universal" sources of Johnson and shot noise). It is customary to denote noise signals with a power spectrum

$$S(\omega) \sim \omega^{-\alpha}, \qquad 0.5 < \alpha < 2,$$

as **$1/f$-noise** ("f," because in engineering it is customary to use f instead of ω for frequency). For further discussion of $1/f$-noise we refer to the literature.[12]

10.2.3 Fokker–Planck equation I

The network of connections revealed above and in Fig. 10.4 is of fundamental importance to statistical physics and deserves further investigation. To this end, we will adopt the second interpretation of the stochastic process $\mathbf{v}[\ ](t)$ advocated above and work in terms of a probability distribution $p(\mathbf{v}, t)$. Analysis of the effective equations controlling the probability distribution leads us straight to the concept of the Fokker–Planck equation, a dynamical equation whose importance to statistical physics can be compared to that of the Schrödinger equation to quantum mechanics.

EXERCISE Carefully think about the steps in the derivation below; it is exemplary of a general scheme to derive Fokker–Planck evolution equations in the theory of stochastic processes.

We wish to derive an equation controlling the evolution of the (conditional) probability $p(\mathbf{v}, t|\mathbf{v}_0, t_0)$ to observe a particle velocity $\mathbf{v}$ at time t provided we started out with velocity

[11] Shot noise was first observed in vacuum tubes, i.e. devices where electrons are "shot" from some cathode through empty space.

[12] For instance, see P. Dutta and P. M. Horn, Low-frequency fluctuations in solids: 1/f-noise, *Rev. Mod. Phys.* **53**, 497-516 (1981).

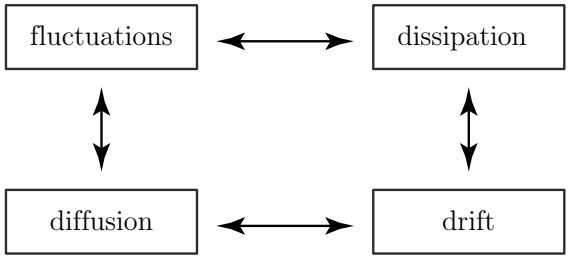

Figure 10.4 Different physical concepts revolving around the physics of the Langevin equation.

$\mathbf{v}_0$ at time $t_0 < t$. The evolution of the variable $\mathbf{v}$ is controlled by the Langevin equation (10.10), a first order differential equation in time. This means that the evolution $\mathbf{v}' \xrightarrow{\Delta t} \mathbf{v}$ from some initial configuration $\mathbf{v}'$ to $\mathbf{v}$ solely depends on the initial configuration $\mathbf{v}'$ (and, of course, on the specific realization of the random force,). However, it does *not* depend on the pre-history of the particle, i.e. the specific way in which it made it to the initial configuration $\mathbf{v}'$. (Exercise: consider why this is a specific feature of a first order differential equation.) This feature, implies the "convolution" property (again a statement to reflect upon),

$$p(\mathbf{v}, t|\mathbf{v}_0, t_0) = \int d^d v'\, p(\mathbf{v}, t|\mathbf{v}', t')p(\mathbf{v}', t'|\mathbf{v}_0, t_0), \tag{10.20}$$

where $t' \in [t_0, t]$ is arbitrary and the second factor under the integral is the probability to find $\mathbf{v}'$ at t' for initial data $(\mathbf{v}_0, t_0)$. Weighing by the conditional probability to move on to $\mathbf{v}$ and summing over all intermediate configurations, $\mathbf{v}'$, we obtain the total probability $(\mathbf{v}_0, t_0) \to (\mathbf{v}, t)$. Equation (10.20) is the defining property of a **Markovian process**, i.e. a process which is fully determined by one-step probabilities. (For a more systematic discussion, see Section 10.4.2 below.)

Evaluating Eq. (10.20) for the specific choice of time arguments $t \to t + \delta t$ and $t' \to t$, and suppressing the initial value argument $(\mathbf{v}_0, t_0)$ for notational simplicity, we obtain an equation for the incremental evolution of probability,

$$p(\mathbf{v}, t + \delta t) = \int d^d u\, w(\mathbf{v} - \mathbf{u}, t; \mathbf{u}, \delta t)p(\mathbf{v} - \mathbf{u}, t),$$

where we have introduced the notation

$$w(\mathbf{v}, t; \Delta\mathbf{v}, \Delta t) \equiv p(\mathbf{v} + \Delta\mathbf{v}, t + \Delta t|\mathbf{v}, t),$$

for the probability of "transitions" $(\mathbf{v}, t) \to (\mathbf{v} + \Delta\mathbf{v}, t + \Delta t)$. We next make use of the fact that, for diffusive motion, the "step width" $\mathbf{u}$ in a sufficiently small time window, δt, will be small in comparison to the length scales over which the probability distribution p changes considerably. It then makes sense to Taylor expand in the argument $\mathbf{v} - \mathbf{u}$ around $\mathbf{u}$, i.e. to expand in the underlined arguments in $w(\mathbf{v} - \underline{\mathbf{u}}, t; \mathbf{u}, \delta t)p(\mathbf{v} - \underline{\mathbf{u}}, t)$. It is important to appreciate that the legitimacy of this so called **Kramers–Moyal expansion** hinges on the

kinematics of the process. In cases where one-step transitions are over large distances (as is the case in, say, ballistic collisions in dilute gases) other procedures have to be applied. One of these alternative approaches, Boltzmann kinematic theory, is discussed in Section (10.3) below.

Performing the expansion, we obtain the infinite order differential equation,

$$p(\mathbf{v}, t+\delta t) = (\alpha^{(0)}p)(\mathbf{v},t) - \partial_{v_i}(\alpha_i^{(1)}p)(\mathbf{v},t) + \frac{1}{2}\partial^2_{v_i,v_j}(\alpha^{(2)}_{i,j}p)(\mathbf{v},t) + \ldots, \quad (10.21)$$

where

$$\alpha^{(0)}(\mathbf{v},t) = \int d^d u\, w(\mathbf{v},t;\mathbf{u},\delta t),$$
$$\alpha_i^{(1)}(\mathbf{v},t) = \int d^d u\, w(\mathbf{v},t;\mathbf{u},\delta t)\, u_i,$$
$$\alpha^{(2)}_{i,j}(\mathbf{v},t) = \int d^d u\, w(\mathbf{v},t;\mathbf{u},\delta t)\, u_i u_j.$$

To compute the coefficients, w, we use the fact that for sufficiently small δt, the Langevin equation assumes the approximate form

$$\mathbf{v}(t+\delta t) = \mathbf{v} - \delta t\gamma\mathbf{v} + \frac{\delta t}{m}\ \ (t).$$

The second and third term on the right–hand side tell us how the random variable $\mathbf{v}(t+\delta t)$ relates to the random variable , provided $\mathbf{v}(t) = \mathbf{v}$ was realized. This means that the transition probability is obtained as

$$w(\mathbf{v},t;\mathbf{u},\delta t) = p(\mathbf{v}+\mathbf{u}, t+\delta t|\mathbf{v},t) = \langle \delta(\mathbf{v}+\mathbf{u}-\mathbf{v}(t+\delta t))\rangle_\xi$$
$$= \langle \delta(\mathbf{u}+\delta t\gamma\mathbf{v} - \delta t\ \ (t)/m)\rangle_\xi\,.$$

Now, the functional distribution function controlling the fluctuation force is given by, $p([\ ]) = \mathcal{N}\int D\ \ \exp(-\frac{1}{2A}\int dt\,|\ \ (t)|^2) \to \mathcal{N}\int D\ \ \exp(-\frac{\delta t}{2A}\sum_t\ |\ \ (t)|^2)$ (cf. Eq. (10.11)), where $\mathcal{N}$ ensures normalization and in the second representation we used δt as our fundamental time step discretization. The distribution factorizes, and the probability to find at time t is given by

$$p(\ \ (t)) = \mathcal{N}\exp\left(-\frac{\delta t}{2A}|\ \ (t)|^2)\right).$$

Using this result, we get

$$w(\mathbf{v},t;\mathbf{u},\delta t) = \int d^d\xi\, p(\ \ )\,\delta(\mathbf{u}+\delta t\gamma\mathbf{v} - \delta t\ \ /m) = \mathcal{N}\exp\left(-\frac{m^2}{2A\delta t}|\mathbf{u}+\gamma\delta t\mathbf{v}|^2\right),$$

where $\mathcal{N} \to \mathcal{N}m/\delta t$ is a renormalized constant ensuring normalization of the probability, $\int d^d u\, w(\mathbf{v},t;\mathbf{u},\delta t) = 1$. With these results, it is straightforward to obtain the coefficients $\alpha^{(n)}$ as

$$\alpha^{(0)}(\mathbf{v},t) = 1, \qquad \alpha_i^{(1)}(\mathbf{v},t) = -\gamma\delta t v_i, \qquad \alpha^{(2)}_{i,j}(\mathbf{v},t) = \delta_{ij}\frac{2\delta t A}{m^2} + (\gamma\delta t)^2 v_i v_j.$$

Coefficients $\alpha^{(n>2)}(\mathbf{v},t) = \mathcal{O}(\delta t^2)$ are vanishingly small in the limit $\delta t \to 0$. Substitution of these results into Eq. (10.21), followed by first order expansion in δt leads to the **Fokker–Planck equation**,[13]

$$\boxed{\left(\partial_t - \partial_{v_i}\gamma v_i - \partial^2_{v_i v_i} D_v\right) p(\mathbf{v},t) = 0,} \tag{10.22}$$

where

$$D_v = \frac{A}{2m^2},$$

is the diffusion constant of *velocity*. In equilibrium, $D_v = T\gamma/m$ (cf. Eq. (10.15)), which is related to the particle diffusion constant (10.14) through the relation $D_v = \gamma^2 D$.

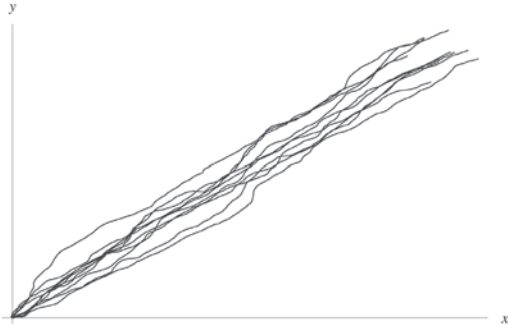

Eq. (10.22) is a partial second order differential equation for the probability distribution. It has to be solved with initial condition $p(\mathbf{v}, t = t_0) = \delta(\mathbf{v} - \mathbf{v}_0)$, i.e. Eq. (10.22) defines an initial value problem (much like the time-dependent Schrödinger equation in quantum mechanics). The second and third contribution to the Fokker–Planck operator describe the competition of drift and diffusion, respectively. The Fokker–Planck equation, thus, represents the "theory" behind the chain of connections shown in Fig. 10.4. Derived from the Langevin equation with its interplay of dissipation and fluctuation, it predicts diffusion and drift for the dominant transport mechanisms at large times. By way of example, the figure above shows a set of trajectories with a constant drift contribution but subject to different noise contributions leading to diffusion.

In the following, we discuss the dynamics described by Eq. (10.22) from a number of different perspectives. Specifically, we wish to understand the meaning of the diffusion and the drift term, the competition between the two, and at last, the approach to thermal equilibrium within the framework of Langevin theory.

▷ To understand the meaning of the drift term, consider the Langevin equation in the presence of a constant external driving force $\mathbf{F}$. Browsing through the steps in the derivation of the Fokker–Planck equation, one verifies that the essential[14] effect of this generalization is a shift $\alpha_i^{(1)} \to \delta t(-\gamma v_i + m^{-1}F_i)$ of the drift coefficient. The Fokker–Planck equation thus generalizes to $\left(\partial_t - \partial_{v_i}(\gamma v_i - m^{-1}F) - \partial^2_{v_i v_i} D_v\right) p(\mathbf{v},t) = 0$. Multiplying this equation by v_i, and integrating over velocity we obtain,

$$d_t\langle\mathbf{v}\rangle + \gamma\langle\mathbf{v}\rangle - m^{-1}\mathbf{F} = 0,$$

[13] Anticipating later generalizations to the case of $\mathbf{v}$-dependent coefficients, v, D_v, we place the latter to the right of the differential operators ∂_{v_i}.

[14] However, we also have to bear in mind that the presence of a constant external force drives the system out of equilibrium. (Switching off the force will change the state of the system, a criterion for a nonequilibrium situation.) This means that dissipation and fluctuation are no longer related to each other by the fluctuation–dissipation theorem.

a result that can equally be obtained by averaging the Langevin equation over noise. This equation describes the relaxation of the velocity expectation value to a stationary drift configuration $\langle \mathbf{v} \rangle \to \frac{1}{m\gamma}\mathbf{F}$. Identifying that expectation value with the force-induced drift current, we obtain $\mathbf{j}_{\rm d} = \mathbf{F}/m\gamma$, in agreement with the phenomenological reasoning above.

▷ The third term in Eq. (10.22) describes **diffusion**. The influence of the diffusion term on the dynamics is visualized in the figure above for the case of particles in two dimensions subject to a uniform driving force $\mathbf{F} = \text{const.} \times (2\mathbf{e}_x + \mathbf{e}_y)$. Diffusion leads to a stochastic spreading around the (deterministic) drift trajectory. The corresponding distribution $p(\mathbf{v})$ is predicted by the stationary long time limit of the Fokker–Planck equation, $(\partial_{v_i}(\gamma v_i - m^{-1}F_i) + D_v\partial^2_{v_i v_i})p(\mathbf{v}) = 0$, or

$$\left(\gamma v_i - m^{-1}F_i + D_v\partial_{v_i}\right) p(\mathbf{v}) = 0.$$

This is solved by $p(\mathbf{v}) \sim e^{-\frac{\gamma}{2D_v}|\mathbf{v}-\frac{1}{m\gamma}\mathbf{F}|^2}$, i.e. a "diffusion cloud" centered around the drift trajectory. At $\mathbf{F} = 0$, the diffusion constant $D_v = T\gamma/m$ assumes its equilibrium value and $p(\mathbf{v}) = e^{-\frac{m}{2T}|\mathbf{v}|^2}$ reduces to the **Maxwell–Boltzmann distribution**. We thus draw the important conclusion that

> in the absence of external driving, a conspiracy of diffusion and drift sends the system into a state of thermal equilibrium.

EXERCISE Our discussion above focused on the diffusive character of the *velocity* distribution, $p(\mathbf{v}, t)$. To describe the **di usive dynamics of the particle coordinates**, $\mathbf{q}$, let us consider a force-free ($\mathbf{F} = 0$) Langevin equation in the overdamped limit, $m\gamma d_t\mathbf{q} = \boldsymbol{\xi}$, i.e. a limit void of external forces where ballistic acceleration $\sim m d_t^2\mathbf{q}$ is negligible. Show that the Fokker–Planck equation for $p(\mathbf{q}, t)$ takes the form

$$(\partial_t - D\partial_q^2)p(\mathbf{q}, t) = 0, \tag{10.23}$$

where D is given by Eq. (10.14). This confirms the expectation that in thermal equilibrium the coordinate will perform drift-less diffusive motion whose level of agitation increases with temperature.

EXERCISE Imagine that the single particle dynamics is governed by *some* Hamiltonian $H(\mathbf{x})$ (as usual, $\mathbf{x} = (\mathbf{q}, \mathbf{p})$). Again, we model the influence of the environment by a combination of dissipation and fluctuation. This leads to the generalized phase space Langevin equation, $d_t\mathbf{q} = \frac{\partial H}{\partial \mathbf{p}}$, $d_t\mathbf{p} = -\frac{\partial H}{\partial \mathbf{q}} - \gamma\mathbf{p} + \boldsymbol{\xi}$. Show that the probability distribution $p(\mathbf{x}, t)$ is governed by the **phase space Fokker–Planck equation**,

$$d_t p(\mathbf{x}, t) = -\{H, p(\mathbf{x}, t)\} + \frac{\partial}{\partial \mathbf{p}}\left[\gamma\mathbf{p} + D_p\frac{\partial}{\partial \mathbf{p}}\right] p(\mathbf{x}, t), \tag{10.24}$$

where $D_p = m^2 D_v = T\gamma m$ is the diffusion constant of momentum. The second operator on the right–hand side describes the dissipation/fluctuation generalization of deterministic single particle dynamics (cf. Eq. (10.9)).

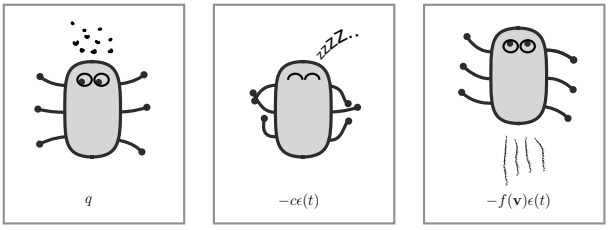

Figure 10.5 Schematic showing the "daily routine" of an amoeba. Left: energy intake at a rate q. Middle: dissipative energy losses due to basic metabolic activity, rate $-c\epsilon(t)$, where $\epsilon(t)$ is the instantaneous energy stored in the organism. Right: motion at a velocity $\mathbf{v}$ leads to an energy loss proportional to both, $\epsilon(t)$ and a velocity dependent loss function, $f(\mathbf{v})$.

10.2.4 Beyond equilibrium

We have seen how the Langevin equation describes the approach to equilibrium: dissipative energy losses and the intake of energy through fluctuations balance each other in a way to form an equilibrium configuration. However, the descriptive power of Langevin theory extends well-beyond the physics of equilibrium. Effective Langevin equations with dissipation/fluctuation imbalances can be employed to describe rather complex out-of-equilibrium phenomena in physics, life sciences, and socio-economics.

Active Brownian motion

By way of example, we here discuss the construction of a minimalistic model to describe the phenomenon of collective biological motion ("**swarming**"). Of course, we do not aim to describe the actual behavior of a concrete species. Rather, our objective is to formulate an as-simple-as-possible model of collective intake of energy and its conversion into kinematic action. For the formulation of more powerful models and a survey of the recent literature, we refer to Ebeling and Sokolov.[1]

Our strategy is to endow the Brownian "particles" (you may now think of them as amoebae or another not too complex animal) with a mechanism of self-propulsion. To this end, we imagine the particles endowed with an energy storage. The time-dependent energy level, $\epsilon(t)$, will (a) increase due to food intake at some rate, q, (b) decrease at rate $-c\epsilon(t)$ due to metabolic activity (notice the assumption that energy loss is the larger the larger the energy stored in the organism), and (c) decrease due to kinematic activity (see Fig. 10.5). We assume that motion leads to a loss at rate $-\epsilon(t)f(\mathbf{v})$, where $f(\mathbf{v}) \equiv \kappa\mathbf{v}^2$. The net change of the particle's energy is thus given by,

$$d_t\epsilon = q - c\epsilon - \kappa\mathbf{v}^2\epsilon.$$

We next assume that the kinematic energy loss is translated to a propelling force, $\mathbf{F}$. The form of that force $\mathbf{F} = \epsilon\kappa\mathbf{v}$ follows from the condition that the work per time interval done by the force $\mathbf{F}\cdot d\mathbf{r}/dt = \mathbf{F}\cdot\mathbf{v}$ must equal the kinematic energy loss, $\kappa\mathbf{v}^2\epsilon$, and the assumption that $\mathbf{F}$ $\mathbf{v}$.

The particle dynamics is then described by the generalized Langevin equation,

$$md_t\mathbf{v} + m\gamma\mathbf{v} = -\nabla U + \epsilon\kappa\mathbf{v} + \quad ,$$

where ∇U represents an external potential and γ the background friction coefficient. Further progress with this equation can be made if we assume that the population is in a balanced state in that the energy "depots" are kept at equal filling levels, on average: $d_t\epsilon = 0$, or

$$\epsilon = \frac{q}{c + \kappa\mathbf{v}^2}.$$

This condition can be used to replace ϵ in the Langevin equation and to obtain an effective Langevin equation governed by a mechanism of **activated friction**

$$md_t\mathbf{v} + m\gamma_{\rm eff}(\mathbf{v})\mathbf{v} = -\nabla U + \quad , \qquad \gamma_{\rm eff}(\mathbf{v}) = \gamma - \frac{q\kappa}{m(c + \kappa\mathbf{v}^2)}. \tag{10.25}$$

An interesting situation arises if the background friction is small in that $\gamma < \frac{\kappa q}{mc}$. Under this condition, the effective friction *vanishes* for finite velocities,[15]

$$|\mathbf{v}|^2 = v_0^2 \equiv \frac{\kappa q - mc\gamma}{m\kappa\gamma}.$$

The condition $|\mathbf{v}|^2 = v_0^2$ defines a sub-manifold in velocity space on which the dynamics becomes effectively Liouvillian, i.e. unhindered by friction. To understand how the particles arrange themselves around that manifold, we need to compute the velocity distribution function. Inspection of the derivation of the Fokker–Planck equation shows that the generalization to activated friction amounts to a mere replacement $\gamma \to \gamma_{\rm eff}(\mathbf{v})$ in Eq. (10.22). This means that the steady state probability distribution of the particles is determined by the equation, $(D_v\partial_{v_i} - \gamma_{\rm eff}(\mathbf{v})v_i)p(\mathbf{v}) = 0$. Integration of this equation leads to

$$p(\mathbf{v}) = \mathcal{N}\exp\left(-\frac{1}{2D_v}\left(\gamma|\mathbf{v}|^2 - \frac{q}{m}\ln(c + \kappa|\mathbf{v}|^2)\right)\right),$$

where $\mathcal{N}$ ensures normalization. In the absence of energy supply, $q = 0$, and the distribution reduces to the Maxwell–Boltzmann form. However, in general, $p(\mathbf{v})$ is far from equilibrium. The center of the distribution is determined by the condition $\partial_{|\mathbf{v}|^2}(\text{exponent}) = 0$ which is solved by $|\mathbf{v}|^2 = v_0^2$. We conclude that the frictionless manifold $|\mathbf{v}|^2 = v_0^2$ is attractive in that it defines the center of the distribution function. The sharpness of the distribution is determined by the inverse of the diffusion constant, i.e. the more noisy the Langevin equation, the less rigid the fixation of the condition $|\mathbf{v}|^2 = v_0^2$.

Swarms

The model above fixes the modulus of the velocity of individual particles. However, to describe more complex patterns of collective biological motion, we need to (a) think about mechanisms controlling the direction of velocity, and (b) correlate the motion of many

[15] In cases where the velocity $v_0^2 \ll c\kappa^{-1}$, the effective friction function $\gamma_{\rm eff}(\mathbf{v}) \simeq c + c'\mathbf{v}^2$ may be effectively linearized in the squared velocity. Activated friction profiles were employed by Rayleigh to describe the complex energy feedback of musical instruments. (J. W. S. Rayleigh, On the resultant of a large number of vibrations of the same pitch and of arbitrary phases, *Phil. Mag.* **10**, 73-8 (1880).)

particles to form collective entities. Crudely speaking, three prototypes of collective motion are frequently observed in nature: translational motion (a wandering herd of elephants), rotational motion (a school of fish), and uncorrelated motion (bacteria, etc.). Theorists are trying to mimic such types of collective dynamics by extended effective friction models. Referring for a more comprehensive discussion to chapter 12 of Ebeling and Sokolov.[1], we here restrict ourselves to a brief review of a few concepts relevant to this field.

One aim is to characterize a swarm of N particles in terms of a center coordinate $\sim \sum \mathbf{v}_i$ and relative motion. Often, the dynamics of the center is of limited concern. One may, then, decide to impose an external mean velocity $\mathbf{V}(t)$. The more interesting relative dynamics of the particles is governed by a combination of a one and a two-particle potential

$$U(\mathbf{q}_1, \ldots, \mathbf{q}_N) = \sum_{i=1}^{N} U^{(1)}(\mathbf{q}_i) + \sum_{i,j=1}^{N} U^{(2)}(\mathbf{q}_i, \mathbf{q}_j).$$

The interactions may be attractive (e.g. when one seeks to model motion of a school of fish in open water), or repulsive (insects in a confined geometry). Collective and relative dynamics are described by the set of equations

$$m d_t \mathbf{v}_i + m\gamma_{\text{eff}}(\mathbf{v}_i) + c(\mathbf{v}_i - \mathbf{V}(t)) = -\partial_{\mathbf{q}_i} U(\mathbf{q}_1, \ldots, \mathbf{q}_N) + \quad (t), \tag{10.26}$$

where the term $c(\mathbf{v}_i - \mathbf{V}(t)),\ c > 0$ drives the particle velocity towards the mean velocity of the swarm.

This is about as much as can be said in general. Approximation schemes employed to describe specific types of motion include approximate decoupling of the equations into an equation for the center coordinate and $N - 1$ equations for the relative coordinates, and mean field treatment of the pair interaction. For example, assuming that the mean field interaction potential is of the form, $U^{(2)} \sim \frac{c}{2}(\mathbf{q}_i - \mathbf{Q})^2$, where $\mathbf{Q}$ is the center of mass coordinate, the equations for the relative coordinates decouple into the form

$$m d_t \mathbf{v}'_i + m\gamma_{\text{eff}}(\mathbf{v}'_i) = -c\mathbf{q}'_i + \quad (t),$$

where the primes indicate relative coordinates, and we assumed that $|\mathbf{v}'_i| \gg \mathbf{V}$, so that the friction force depends dominantly on the relative velocity. The four-dimensional dynamics predicted by these equations converges to a limit cycle on the frictionless manifold $|\mathbf{v}'|^2 = v_0^2$ and with radius specified by $c|\mathbf{q}'|^2/2 = mv_0^2/2$ (equipartition of potential and kinetic energy). The dynamics of the many particle system then resembles the rotational motion of a swarm. For the discussion of other types of collective dynamics we refer to Ebeling and Sokolov.[1].

10.3 Boltzmann kinetic theory

Previously, we have explored the ways in which a sequence "Langevin dynamics → Fokker–Planck equation → distribution functions" leads to predictions on the macroscopic state of many particle systems, both in and out of equilibrium. A central step in the derivation of the Fokker–Planck equation was the Kramers–Moyal expansion, an expansion of the probability

of short time transitions $\mathbf{x} \stackrel{\delta t}{\to} \mathbf{x}'$ in the difference $\mathbf{x} - \mathbf{x}'$. The Kramers–Moyal expansion makes sense if, for sufficiently short δt, the hopping steps in phase space become small in comparison to the typical phase space coordinates themselves. More precisely, we assumed that the moments $\langle (\mathbf{x}' - \mathbf{x})^n \rangle$ of the conditional probability $p(\mathbf{x}', t + \delta t | \mathbf{x}, t)$ exist and scale with positive powers $\delta t^{p(n)}$. Only terms with $p(n) \leq 1$ (in the specific case of Gaussian distributed noise, the first two) enter the Fokker–Planck derivative operator. Put differently, the evolution of the probability distribution can be described in terms of a low order linear differential equation only if the nth moments of the transition probability are well behaved in that $p(n) > 1$ for all but the lowest ns. There are plenty of instances in many particle physics where this "locality principle" is violated. Below we derive an effective evolution equation that describes the dynamics of distribution functions under these circumstances.

10.3.1 Derivation of the Boltzmann equation

By way of an example, consider a gaseous system of particles in a container. In the infinitely dilute limit (where particle collisions can be neglected), the phase space coordinates of individual particles change according to Newtonian dynamics (cf. Eq. (10.9)). Specifically, the single particle energy ϵ is conserved, and (assuming the absence of smooth potential gradients) momentum is constrained to an energy shell $|\mathbf{p}|^2/2m = \epsilon$.

However, once interactions are taken into account, the rate at which the distribution $f(\mathbf{x}_1, t)$ changes gets influenced by particle collisions: losses occur when particles at phase space point $\mathbf{x}_2$ scatter off particles of the reference momentum $\mathbf{x}_1$ into final states $\mathbf{x}_1'$ and $\mathbf{x}_2'$ (cf. the figure). We denote the corresponding two-particle transition rate by $w(\mathbf{x}_1', \mathbf{x}_2'; \mathbf{x}_1, \mathbf{x}_2) d^d x_1' d^d x_2' d^d x_1 d^d x_2$, where the function w encapsulates kinematic constraints (energy and momentum conservation) of the collision. The $d_t f$ due to "out" processes then reads

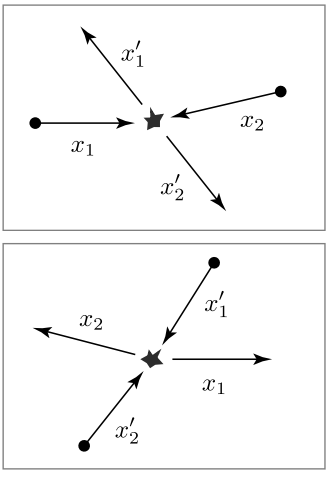

$$d_t f_1 \big|_{\text{out}} = \int d2\, d1'\, d2'\; w(1', 2'; 1, 2) f_1 f_2,$$

where we take into account the fact that the total transition rate depends linearly on the number of available collision partners in the two initial states, and introduce a (standard) notation wherein coordinate dependencies are indicated by numbers, $d^d x_1 \to d1$, $f(\mathbf{x}_1) \to f_1$, etc.

Gain occurs when particles get scattered into the reference state in collisions $(1', 2') \to (1, 2)$:

$$d_t f_1 \big|_{\text{in}} = \int d2\, d1'\, d2'\; w(1, 2; 1', 2') f_{1'} f_{2'}.$$

The total occupation change due to collisions $I[f] \equiv d_t f_1\big|_{\rm in} - d_t f_1\big|_{\rm out}$ is summed up in what is commonly called the collision integral,

$$I[f] = \int d2\, d1'\, d2'\ \left(w(1,2;1',2')f_{1'}f_{2'} - w(1',2';1,2)f_1 f_2\right). \tag{10.27}$$

Notice that the collision integral is a nonlinear functional of the distribution functions, i.e. we are facing up to a nonlinear theory.

The transition rates w are subject to certain symmetry relations which reflect time-reversal invariance and unitarity of the microscopic laws of physics. For example, **microreversibility** implies that a transition $(1,2) \to (1',2')$ must be as probable as the time-reversed process $(1'^T, 2'^T) \to (1^T, 2^T)$, where $1^T \equiv (\mathbf{q}_1, \mathbf{p}_1)^T = (\mathbf{q}_1, -\mathbf{p}_1)$ is the time-reverse of a phase space point, i.e.

$$w(1',2';1,2) = w(1^T, 2^T; 1'^T, 2'^T).$$

The consequences of unitarity are best exposed if we interpret the coefficients w as classical limits of quantum transition probabilities. Identifying $(1,2) \leftrightarrow |\mathrm{i}\rangle$ as a classical approximation to a (coherent) state in two particle Hilbert space,[16] and $(1',2') \leftrightarrow |\mathrm{f}\rangle$ as a final state, we have the identification,

$$w(1',2';1,2) \leftrightarrow |S_{\rm fi}|^2,$$

where $S_{\rm fi}$ is the scattering matrix. Unitarity means that $\sum_{\rm i} |S_{\rm fi}|^2 = \sum_{\rm i} |S_{\rm if}|^2 = 1$, or

$$\int d1' d2'\, w(1',2';1,2) = \int d1' d2'\, w(1,2;1',2').$$

Using this relation in the out-process, the **collision integral** can be transformed to

$$\boxed{I[f] = \int d2\, d1'\, d2'\ w(1,2;1',2')\left(f_{1'}f_{2'} - f_1 f_2\right).} \tag{10.28}$$

Adding $I[f] \equiv d_t f_1\big|_{\rm in} - d_t f_1\big|_{\rm out}$ as the many particle contribution to the changes in the distribution function to the right–hand side of Eq. (10.9), we obtain the celebrated **Boltzmann transport equation**,[17]

$$\boxed{\left(\partial_t - \{H,\ .\}\right) f(\mathbf{x},t) = I[f].} \tag{10.29}$$

10.3.2 Discussion of the Boltzmann equation

What is the Boltzmann equation (10.29) good for? First, it has been, and still is, a very powerful tool in applied many particle physics. Before the advent of the more powerful

[16] Here, we consider the particles as distinguishable, i.e. no (anti)symmetrization is implied.
[17] In the Russian literature, the Boltzmann equation is usually called the "**kinetic equation**."

techniques reviewed in previous chapters of this book, it used to be *the* principal tool to calculate physical observables in interacting many particle systems.[18] Even today, Boltzmann equation-based approaches often represent the most economic and straightforward route to understanding the physics of interacting many particle systems.

Second, the Boltzmann equation is of great conceptual value. Many of the principal questions raised in the beginning of the chapter have a relatively straightforward answer in terms of this equation. We first note (cf. the more schematic discussion before Eq. (10.8)) that the collision term vanishes in thermal equilibrium. In equilibrium, the distribution function is given by the Maxwell–Boltzmann distribution Eq. (10.8). Energy conservation in elastic collisions, $H(\mathbf{x}_1)+H(\mathbf{x}_2)=H(\mathbf{x}_1')+H(\mathbf{x}_2')$, means that $f_1 f_2 = f_{1'} f_{2'}$, i.e. vanishing of $I[f]$. In equilibrium the losses and gains due to many particle collisions compensate each other and $I[f]$ does not change the distribution. (Since $f(\mathbf{x}) = f(H(\mathbf{x}))$, the single particle dynamics conserves f as well, $\{H, f\} = 0$, i.e. the Maxwell–Boltzmann distribution is truly stationary under (10.29).)

The Boltzmann H-Theorem

However, it is not quite as easy to show that the collision term actually drives the distribution *towards* the thermal equilibrium configuration. The defining property of the thermal equilibrium is that it maximizes entropy, S. In equilibrium statistical mechanics, it is usually taken for granted (the second law of thermodynamics) that many body relaxation processes increase entropy, $d_t S \geq 0$, before the maximum of the equilibrium configuration is reached. However, a more general conceptual framework such as Boltzmann kinetic theory should be able to actually demonstrate the ways in which a microreversible theory leads to macroscopic irreversibility and entropy increase.

INFO In view of the comparative complexity of this problem, the collision term is sometimes linearized in what is called the **relaxation time approximation**. One effects the following replacement of the complicated nonlinear collision integral,

$$I[f] \longrightarrow -\frac{1}{\tau}(f - f_0), \tag{10.30}$$

where f_0 is the Maxwell–Boltzmann distribution. The linearized approximation then describes a tendency to approach equilibrium at a rate set by τ, a time scale interpreted as the mean collision time of interaction processes.

The manner in which interactions increase entropy was demonstrated by Boltzmann in a famous construction known as the **H-theorem**. (It is known as the H-theorem rather than

[18] For a detailed account of various applications and computational schemes revolving around the Boltzmann equation, see L.D. Landau and E. M. Lifshitz, *Course of Theoretical Physics, Vol 10 - Physical Kinetics*, (Butterworth-Heinemann, 1981).

the S-theorem because Boltzmann called entropy H.) Consider the information-theoretic definition of entropy[19] according to which $S = -\langle \ln(f/e) \rangle$, or

$$S = -\int d^d x\, f(\mathbf{x}, t) \ln(f(\mathbf{x}, t)/e).$$

The temporal change of S is then given by

$$d_t S = -\int d^d x\, \ln f\, \partial_t f = -\int d^d x\, \ln f\, [\{H, f\} + I[f]]\,.$$

Since the full phase space integral of any function is invariant under Hamiltonian flow (exercise: why?), we have $0 = \int d^d x\, \{H, f \ln(f/e)\} = \int d^d x\, \ln(f)\{H, f\}$, i.e. the change in entropy is entirely due to interactions.

To explore how interactions do the job, consider the collision integral in its prototypical variant Eq. (10.27). For an arbitrary function $\phi(\mathbf{x})$, and using the abbreviation $d\Gamma \equiv d1\, d2\, d1'\, d2'$, we have

$$\begin{aligned}\int d1\, \phi(1) I[f(1)] &= \int d\Gamma\, \phi(1)\, (w(1,2;1',2') f_{1'} f_{2'} - w(1',2';1,2) f_1 f_2) \\ &= \int d\Gamma\, (\phi(1) - \phi(1')) w(1,2;1',2') f_{1'} f_{2'} \\ &= \frac{1}{2} \int d\Gamma\, (\phi(1) + \phi(2) - \phi(1') - \phi(2')) w(1,2;1',2') f_{1'} f_{2'}, \quad (10.31)\end{aligned}$$

where in the first equality we relabeled coordinates $(1,2) \leftrightarrow (1',2')$ and the second equality is based on the symmetry $1 \leftrightarrow 2$ under exchange of the collision partners.

From this result, we can derive a few auxiliary identities. Setting $\phi = 1$, we conclude that the collision term vanishes upon integration,

$$0 = \int d\Gamma\, I[f] = \int d\Gamma\, w(1,2;1',2')(f_{1'} f_{2'} - f_1 f_2),$$

where the second representation Eq. (10.28) was used. Introducing the abbreviations

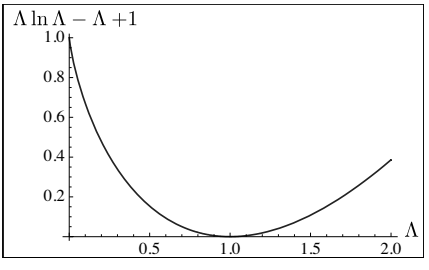

$$\Lambda \equiv \frac{f_{1'} f_{2'}}{f_1 f_2}, \qquad X \equiv w(1,2;1',2') f_1 f_2,$$

this can be written as $0 = \int d\Gamma\, X(\Lambda - 1)$. Setting $\phi = \ln \Lambda$, Eq. (10.31) yields $0 = \int d\Gamma\, X \Lambda \ln(\Lambda)$. Combination of these results finally leads to

$$d_t S = \frac{1}{2} \int d\Gamma\, X(\Lambda \ln \Lambda - \Lambda + 1).$$

[19] If you are not familiar with this definition, consult any advanced textbook on equilibrium statistical mechanics. Exercise: show that in thermal equilibrium, the above definition reduces to the standard definition of thermodynamics.

Now, the functions X and Λ are manifestly positive. For positive Λ, the combination $\Lambda \ln \Lambda - \Lambda + 1$ is positive as well (see the figure or, alternatively, try to prove it). This demonstrates that elastic particle collisions indeed increase the entropy of the system.

Mesoscopic evolution laws

The arguments used in the derivation of the H-theorem are useful to derive "mesoscopic' dynamical equations for observables of physical interest – densities, currents, and the like – i.e. equations that describe their behavior at length scales much larger than the collision mean free path $l = \tau v$ (where v is a typical particle velocity) yet smaller than macroscopic scales.

These equations must reflect the fundamental conservation laws of the system, the conservation of energy, particle number, momentum, etc. Now, interactions may change the energy or momentum of individual particles, but they will not change the total energy and momentum of a sufficiently large assembly of particles. To see this in quantitative terms, let $\delta\Gamma \equiv \delta V \quad \mathbb{R}^3$ be a thin slice in phase space containing phase space points in the small volume element δV at coordinate $\mathbf{q}$ and of arbitrary momentum $\mathbf{p} \in \mathbb{R}^3$. The average particle, energy, and momentum density, respectively, are then given by

$$\left.\begin{array}{c} \rho(\mathbf{q},t) \\ \epsilon(\mathbf{q},t) \\ (\mathbf{q},t) \end{array}\right\} = \delta V^{-1} \int_{\delta\Gamma} d^d x\, f(\mathbf{x},t) \left\{\begin{array}{l} 1 \\ H(\mathbf{x}) \\ \mathbf{p} \end{array}\right. .$$

It is now straightforward to prove that interactions do not change these values. To this end, let us assume that the coefficients w describe an elastic point interaction, i.e. an interaction local in space that respects energy and momentum conservation. In this case (exercise: think why), a restriction of Eq. (10.31) to the volume restricted phase space element $\delta\Gamma$ holds, i.e.

$$\int_{\delta\Gamma} d1\, \phi(1) I[f(1)] = \frac{1}{2} \int_{1\in\delta\Gamma} d\Gamma\, (\phi(1) + \phi(2) - \phi(1') - \phi(1')) w(1',2';1,2) f_{1'} f_{2'}.$$

Now, particle, energy, and momentum conservation mean that, in the particular cases $\phi = 1, \epsilon, \quad$, the linear combinations $\phi(1) + \phi(2) - \phi(1') - \phi(1')$ on the right–hand side of the equation vanish. We thus conclude

$$\int_{\delta\Gamma} d1\, I[f(1)] \left\{\begin{array}{l} 1 \\ H(\mathbf{x}) \\ \mathbf{p} \end{array}\right. = 0\,.$$

This identity is the key to the formal derivation of conserving transport equations. For example, changes in the particle density are obtained as

$$\begin{aligned} \partial_t \rho\, \delta V &= \int_{\delta\Gamma} d^d x\, \partial_t f = \int_{\delta\Gamma} d^d x\, \{H, f\} = \int_{\delta\Gamma} d^d x\, (\partial_{q_\alpha} H \partial_{p_\alpha} f - \partial_{p_\alpha} H \partial_{q_\alpha} f) \\ &\simeq \partial_{q_\alpha} H \int_{\delta\Gamma} d^d x\, \partial_{p_\alpha} f - \int_{\delta\Gamma} d^d x\, v_\alpha \partial_{q_\alpha} f \simeq 0 - \partial_{q_\alpha} j_\alpha, \end{aligned}$$

where $j_\alpha \equiv \delta V^{-1} \int_{\delta\Gamma} d^d x\, v_\alpha f$ is the α-component of the particle current density. We thus obtain the particle density continuity equation,

$$\partial_t \rho + \nabla \cdot \mathbf{j} = 0.$$

If you find this result trivial, keep in mind that it has been derived for arbitrary distribution functions, and under specific (if reasonably general) assumptions on the nature of the microscopic interactions. Particle number conservation as well as the energy and momentum conservation laws discussed in the exercise below impose important consistency constraints on the validity of the theory.

EXERCISE Show that, for a translationally invariant system, energy and momentum density obey the conservation laws

$$\partial_t \epsilon + \quad \cdot \mathbf{j} \;= 0, \qquad \partial_t \pi_a + \partial_{q_\beta} \quad _{\alpha\beta} = 0, \tag{10.32}$$

where $\mathbf{j} \equiv \delta V^{-1} \int_\delta d^d x\, f H \mathbf{v}$ and $\quad _{\alpha\beta} \equiv \delta V^{-1} \int_\delta d^d x\, f m v_\alpha v_\beta$ are the energy current density and the momentum current tensor respectively.

Beyond equilibrium: zero modes of the collision integral

As with Langevin theory, the full potential of the formalism becomes visible once we go beyond the level of thermal equilibrium. We have seen that the collision integral favours a Maxwell–Boltzmann distribution, $f(\mathbf{x}) = \mathcal{N}\exp(-\epsilon/T)$. Importantly, however, it is indiscriminate as to the value of temperature, or the normalization factor $\mathcal{N}$ (which determines the particle number). In fact, if it were left to the collision integral alone, *local* equilibrium configurations described by spatially varying profiles $T \to T(\mathbf{q})$, $\mathcal{N} \to \mathcal{N}(\mathbf{q})$ are perfectly balanced; all the collision integral requests is a logarithmically linear function of energy, $\sim \exp(\text{const.} \times \epsilon)$. What prevents strong local variations of temperature and normalization is the left–hand side of the Boltzmann equation, where Liouville flow builds up correlations across the system. Once the system is perturbed out of equilibrium (by application of a strong electric field, say, or by connection to two thermal reservoirs kept at different temperature), we may then expect a scenario wherein the collision integral aims to establish local thermal equilibrium, while the left hand side will try to compromise between the "cost" of spatial variations and the need to adjust to the conditions imposed by the external perturbation.

The quantitative description of such competitions is the subject of Boltzmann transport theory, a substantial field by itself (again, we refer to Landau and Lifshitz [18] for a very detailed exposure). In the following, we discuss a few basic elements of this theory and apply them to an example. To this end, let us imagine a system weakly perturbed out of equilibrium. We may then assume that its effective distribution function is of the form $f = f^0 + \ldots$, where f^0 is a Maxwell–Boltzmann distribution with uniform parameters and the ellipses represent a small deviation. The fact that f^0 depends on the phase space coordinates only through energy, $\epsilon(\mathbf{x}) \equiv H(\mathbf{x})$, suggests a representation

$$f(\mathbf{x}) = f^0(\epsilon) + \frac{\partial f^0}{\partial \epsilon}(\epsilon)\chi(\mathbf{x}) = f^0(\epsilon) - \frac{f^0(\epsilon)}{T}\chi(\mathbf{x}),$$

where χ describes deviations from equilibrium. Substituting this *ansatz* into the collision integral (10.28), and using the fact that $f_1^0 f_2^0 = f_{1'}^0 f_{2'}^0$, we obtain the linear integral operator

$$I[\chi] = -\frac{f_1^0}{T} \int d2\, d1'\, d2'\; w(1,2;1',2') f_2^0 \left(\chi_{1'} + \chi_{2'} - \chi_1 - \chi_2\right). \tag{10.33}$$

This operator has a number of manifest "zero modes": for

$$\chi(\mathbf{x}) = c(\mathbf{q}), \qquad \chi(\mathbf{x}) = c(\mathbf{q})\,\epsilon(\mathbf{p}), \qquad \chi(\mathbf{x}) = \mathbf{v}(\mathbf{q})\cdot\mathbf{p}, \tag{10.34}$$

with space-dependent $c(\mathbf{q}), \mathbf{v}(\mathbf{q})$,[20] we have $I[\chi] = 0$. These zero modes reflect the invariance of the collision integral under local variations of the equilibrium parameters. For example, a local change in the particle density can be described by $\mathcal{N} \to \mathcal{N}^0 + \delta\mathcal{N}(\mathbf{q})$. Linearity of the Maxwell–Boltzmann distribution function in δN then gives

$$f \to f^0 + \frac{\partial f^0}{\partial \mathcal{N}} \delta N(\mathbf{q}) = f^0 - \frac{f^0}{T} \frac{T\delta N(\mathbf{q})}{\mathcal{N}^0},$$

i.e. with the identification $c(\mathbf{q}) = T\delta N(\mathbf{q})/\mathcal{N}^0$, a variation as in the first equality of Eq. (10.34).

EXERCISE Extend this argument to show that the second zero mode corresponds to local changes in temperature, and the third reflects Gallilean invariance, i.e. invariance under Gallilean transformation to an inertial frame moving with velocity $\mathbf{v}(\mathbf{q})$. (Again, the locality of the collision integral entails that the boost velocity can be spatially varying.)

Example: thermal conductivity of a gas of particles

Even the linearized Boltzmann equation is a complicated integro-differential equation which is difficult to solve in generality. Often, however, it is possible to resort to certain simplifying approximations – of which the relaxation time approximation is one of the more popular – whereupon the Boltzmann equation becomes a highly efficient computational tool. In the following, we illustrate some of these ideas on the example of the thermal conductivity of a gas.

Suppose we have imposed a temperature gradient $T(\mathbf{q})$ on a gas of interacting particles. The gas will respond by the buildup of a heat current $\mathbf{j}_\epsilon$ (cf. Eq. (10.32)). For sufficiently weak temperature gradients, the current will depend linearly on ∇T, and we may define the **thermal conductivity**, κ, through the relation,

$$\mathbf{j}_\epsilon = -\kappa \nabla T. \tag{10.35}$$

In the following, we outline, how this coefficient may be obtained in a semi-phenomenological manner from the Boltzmann equation (for a more substantial discussion, cf. §7 of Landau and Lifshitz.[18]

If the temperature gradient is small, we may assume a distribution of the form

$$f(\mathbf{x}) = f^0(\mathbf{x}) + \frac{f^0(\mathbf{x})}{T(\mathbf{q})}\chi(\mathbf{x}),$$

[20] Here we assume that the energy conserved in elastic collisions is a function of momentum only, at least on the microscopic length scales relevant to the interaction processes.

where $f^0(\mathbf{x}) = \mathcal{N}\exp(-\epsilon(\mathbf{p})/T(\mathbf{q}))$ is a local Maxwell–Boltzmann distribution with spatially varying temperature, and χ accounts for the distortion of the system out of the local equilibrium described by f^0. Since χ describes a mere readjustment of the particle concentration, we have $\int d^dx\, f^0\chi = 0$. The heat current density carried by the system is given by (cf. Eq. (10.32)

$$\mathbf{j}_\epsilon = \frac{1}{T\delta V}\int_{\delta\Gamma} d^dx\, f^0\chi\epsilon\mathbf{v},$$

where we used the fact that the distribution f^0 does not support a current.

We next substitute the above *ansatz* in the Boltzmann equation and linearize: noting that deviations out of (local) equilibrium are driven by $\partial_\mathbf{q}T$, we anticipate that, to leading order, $\chi = \mathcal{O}(\partial_\mathbf{q}T)$. Terms of higher order in $\partial_\mathbf{q}T$ will be neglected which means that, on the left hand side of the Boltzmann equation, the zeroth order approximation $f \simeq f^0$ can be used. On the right hand side, we meet with the linearized collision integral $I[\chi]$. Assuming stationarity of the distribution, we thus obtain

$$-\{H, f^0\} = \mathbf{v}\cdot\partial_\mathbf{q}f^0 = \partial_T f^0\mathbf{v}\cdot\partial_\mathbf{q}T = \frac{f_0}{T}\frac{\epsilon}{T}\mathbf{v}\cdot\partial_\mathbf{q}T = I[\chi].$$

The linearity of $I[\chi]$ in χ suggests an *ansatz* $\chi = (\mathbf{v}\cdot\partial_\mathbf{q}T)g(\mathbf{p})$, where g is a scalar function. While the solution of the linear integral equation for g remains a formidable task, things get a lot simpler if we resort to the phenomenological relaxation time approximation Eq. (10.30),

$$I[\chi] = -\frac{f^0}{T}\frac{1}{\tau}(\mathbf{v}\cdot\partial_\mathbf{q}T)g(\mathbf{p}),$$

where τ is the characteristic time of relaxation processes in the medium. Substitution of this *ansatz* into the Boltzmann equation then readily leads to the solution

$$g(\mathbf{p}) = -\frac{\epsilon(\mathbf{p})\tau}{T}.$$

Substitution into the formula for the current then gives

$$\mathbf{j}_\epsilon = -\delta V^{-1}\int_{\delta\Gamma} d^dx\, f^0\left(\frac{\epsilon}{T}\right)^2\tau(\mathbf{v}\cdot\partial_\mathbf{q}T)\mathbf{v} = -\frac{\tau}{d}\int d^dp\, f^0\left(\frac{\epsilon}{T}\right)^2 v^2\partial_\mathbf{q}T,$$

which leads to the result

$$\kappa = \frac{\tau}{d}\int d^dp\, f^0\left(\frac{\epsilon}{T}\right)^2 v^2 \sim l\sqrt{\frac{T}{m}},$$

for the **thermal conductivity**. Here, $l = \tau\bar{v}$ is the collision mean free path, and we have made use of the fact that the mean velocity of particles scales as $\bar{v} \sim (T/m)^{1/2}$. (Typically, the mean free path depends only weakly on temperature.)

Although our discussion above focused on a specific example, it reflects a number of **general principles in Boltzmann transport theory**:

▷ In systems weakly perturbed out of equilibrium, it is convenient to use a representation $f = f^0 + \partial_\epsilon f^0\chi$ for the distribution function, where f^0 is a (local) Maxwell–Boltzmann distribution.

- ▷ Typically, the left–hand side of the Boltzmann equation contains the perturbing influences, while the right–hand side (the collision term) aims to drive the system back to equilibrium. This suggests...
- ▷ an expansion of the left–hand side to first order in the perturbations and to zeroth order in the distribution function. On the right–hand side we linearize the collision integral, using the fact that $I[f^0] = 0$.
- ▷ The expansion of the left–hand side then contains the perturbation in a form whose symmetries suggest a problem-adjusted *ansatz* for the correction, χ. Substitution of this *ansatz* produces an effective equation for the strength of the correction which can be solved, e.g., in a relaxation time approximation.

Programs of this type often provide an efficient route to results otherwise obtained by microscopic linear response theory. However, problems far removed from equilibrium call for a more tailored approach and no general schemes can be formulated.

10.4 Stochastic processes

In the previous sections we have introduced a few strategies to describe the approach to (as well as as departures from) thermal equilibrium. En route we have met with different realizations of stochastic dynamics, or "stochastic processes." Stochastic processes play a fundamental role in a whole spectrum of sciences, including the life sciences, engineering, socio-economic sciences, and many more. Equally important (for us as physicists) the languages in which stochastic processes are commonly described – the vocabulary includes "probability," "rate equations," "Markov approximations," etc. – are spoken by a large community of scientists, which is an ideal basis for interdisciplinary dialogue.

10.4.1 The notion of a stochastic process

A process describes the temporal evolution of a certain state. It can be described in terms of a sequence $\{a_i(t_i)\}$ where $t_i, i = 1, \ldots, n$ are the discrete times at which the states are recorded and $a_i(t_i)$ is a (generally multi-dimensional) state variable. A **stochastic process**[21] is one where the evolution $a_i(t_i) \to a_{i+1}(t_{i+1})$ involves elements of randomness. In the description of stochastic processes we then need to focus on the totality of all possible sequences $\{a_i(t_i)\}$ where each realization gets assigned a certain probability $p(a_n, t_n; \ldots; a_1, t_1)$. The probability function p carries the full information on the process, and this is the object we need to describe.

Before moving on, it is worthwhile to distinguish between a few general types of stochastic processes. We speak of a **stationary stochastic process** if p does not change under simultaneous translation $t_i \to t_i + t_0$, $i = 1, \ldots n$ of all time arguments, i.e. if the theory is, on average, translationally invariant. Using the notion of conditional probabilities

[21] For a state of the art introduction to theory and application of stochastic processes we refer to N.G. van Kampen, *Stochastic Processes in Physics and Chemistry*, (Elsevier,1992).

(cf. Eq. (10.7)), the joint probability function describing a stochastic process can be iteratively constructed as

$$p(a_n, t_n; \dots; a_1, t_1) = p(a_n, t_n | a_{n-1}, t_{n-1}; \dots; a_1, t_1) \\ \times p(a_{n-1}, t_{n-1} | a_{n-2}, t_{n-2}; \dots; a_1, t_1) \times \cdots \times p(a_2, t_2 | a_1, t_1) \times p(a_1, t_1).$$

The process is called **purely random** if the probabilities $p(a_j, t_j | a_{j-1}, t_{j-1}; \dots; a_1, t_1) = p(a_j, t_j)$ are independent of the history of events. In this case,

$$p(a_n, t_n; \dots; a_1, t_1) = \prod_{j=1}^{n} p(a_j, t_j),$$

is the product of n random numbers lacking intrinsic correlation. Evidently, purely random processes do not display very interesting dynamics. Next in the hierarchy of complexity are conditional probabilities for which

$$p(a_n, t_n | a_{n-1}, t_{n-1}; \dots; a_1, t_1) = p(a_n, t_n | a_{n-1}, t_{n-1}). \tag{10.36}$$

Processes of this type are called **Markov processes**. Markov processes enjoy an enormous spectrum of applications in statistical sciences, which is why they deserve a separate discussion.

10.4.2 Markov processes

In a Markov process, the passage to the state (a_{n+1}, t_{n+1}) depends on the current state (a_n, t_n), but not on the history that got us there, $(a_{n-1}, t_{n-1}; \dots)$. Put differently, a Markov process lacks memory.

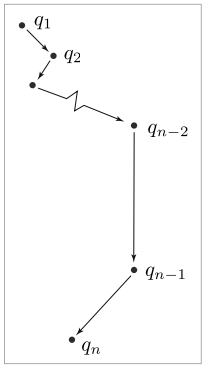

Markov processes owe their popularity to the fact that they optimally compromise between descriptive power and analytical tractability; if possible, one will try to (approximately) reduce a given process to an effective Markovian process. In doing so, it is important to keep in mind that[22] the Markovian property holds only in an approximate sense. In modeling a process, the update times $\Delta t = t_{n+1} - t_n$ have to be chosen long enough to eradicate the short time memory of a process, yet short enough not to loose relevant aspects of the dynamics. (For example, in the process of Brownian motion, Δt must be chosen to be much[23] larger than microscopic collision times.)

Whether or not a process assumes a Markovian form generally depends on the coordinates used. For example, in a process where a velocity-like variable evolves in a Markovian process,

[22] For a more substantial in-depth discussion, see van Kampen.[21]

[23] To understand the meaning of "much larger," suppose that $\Delta t = \mathcal{O}(\text{collision time})$. If at a given instant, t_n, the real space coordinate difference $|\mathbf{x}_n - \mathbf{x}_{n-1}|$ happens to be atypically large, we know that the velocity at t_n must have been high. It is then likely, that $|\mathbf{x}_{n+1} - \mathbf{x}_n|$ will also be large, i.e. the probability to reach $\mathbf{x}_{n+1}$ depends not just on the conditional probability $p(\mathbf{x}_{n+1}, t_{n+1} | \mathbf{x}_n, t)$, but also on the history of events before $(\mathbf{x}_n, t)$. Averaging over a large number of collisions is necessary to average out this memory effect.

the corresponding coordinates – the integrals of velocity over time – may store long time memory and, therefore, be non-Markovian. (To see this, imagine a process of Brownian motion represented in coordinate space, $q_1 \to q_2 \to \cdots \to q_{n-2} \to q_{n-1} \to q_n$, where the coordinates are recorded at equal time steps. If the spacing $|q_{n-1} - q_{n-2}|$ was exceptionally large, the particle will have high velocity. Chances then are that the next step $q_{n-1} \to q_n$ will also be large. In other words, the conditional probability $p(q_n|q_{n-1}, q_{n-2}, \dots) \neq p(q_n|q_{n-1})$ and the process is not Markovian. Exercise: consider why velocity is a variable with less memory.) For a given process one will naturally try to identify coordinates that make it as "Markovian" as possible.

Chapman–Kolmogorov relation and master equation

The Markovian nature of a process can be expressed in a manner alternative to Eq. (10.36). Consider the probability to observe a at t given initial data $(a_\mathrm{i}, t_\mathrm{i})$ and some intermediate event (a', t'), $p(a, t; a', t'; a_\mathrm{i}, t_\mathrm{i})$. From this object, the "transition probability" $p(a, t; a_\mathrm{i}, t_\mathrm{i})$ is obtained by integration over all realizations of the intermediate event,

$$p(a, t; a_i, t_i) = \int da'\, p(a, t; a', t'; a_\mathrm{i}, t_\mathrm{i}) = \int da'\, p(a, t|a', t'; a_\mathrm{i}, t_\mathrm{i}) \times p(a', t'; a_\mathrm{i}, t_\mathrm{i}),$$

where we have used Eq. (10.7). For a Markovian process, $p(a, t|a', t'; a_\mathrm{i}, t_\mathrm{i}) = p(a, t|a', t')$, this reduces to the **Chapman–Kolmogorov relation**

$$\boxed{p(a, t; a_\mathrm{i}, t_\mathrm{i}) = \int da'\, p(a, t|a', t') \times p(a', t'; a_\mathrm{i}, t_\mathrm{i}).} \tag{10.37}$$

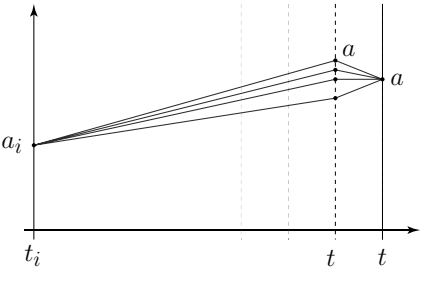

The usefulness of Eq. (10.37) becomes evident if we consider the case $|t - t'| \ll |t - t_\mathrm{i}|$. Eq. (10.37) then factorizes the description of the process into its three most relevant compounds, (a) our quantity of interest, i.e. the probability to get to a given we started at a_i, (b) the probability to reach an intermediate stage a' shortly before the final time, t, and (c) the short time transition probability $a' \xrightarrow{t-t'} a$ (see figure). This iterative, or "transfer matrix type" description of the process stands as the basis of most theories of Markovian dynamics.

To push this iterative approach somewhat further, consider what happens if $t - t' \equiv \delta t$ becomes (infinitesimally) small. To a very good approximation, $p(a, t|a', t - \delta t) \simeq \delta(a - a') + \mathcal{O}(\delta t)$ will then be stationary. The term of $\mathcal{O}(\delta t)$ comprises losses out of a' due to transition into some state a'', and input due to transition from a'. Denoting the probability of transitions $a_1 \xrightarrow{\delta t} a_2$ by $W(a_2|a_1)\delta t$, we may thus write

$$p(a, t|a', t - \delta t) = \left(1 - \delta t \int da''\, W(a''|a')\right) \delta(a - a') + \delta t\, W(a|a').$$

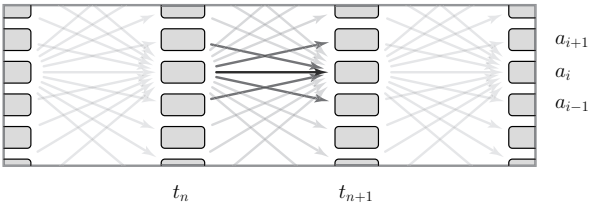

Figure 10.6 The evolution of Markovian probability, as described by the master equation: probability gain of states a_i (here considered as discrete entities, while the text uses continuum notation) due to in-processes is counteracted by loss due to out-processes. The sum over all feeds cancels, reflecting probability conservation.

Substituting this expression into Eq. (10.37), taking the limit $\delta t \to 0$ and suppressing the initial time argument for notational simplicity $p(a,t|a_i,t_i) = p(a,t)$, we then obtain the so-called **master equation**[24] (see Fig. 10.6).

$$\boxed{\partial_t p(a,t) = \int da' \, [W(a|a')p(a',t) - W(a'|a)p(a,t)] \, .} \tag{10.38}$$

Notice that the master equation conserves the total probability, i.e. $\partial_t \int da\, p(a,t) = 0$.

INFO In general, little can be said about the master equation. An important exception regards the master equation for physical systems that are closed and isolated in that no matter is exchanged with the outer world, and energy is conserved. The attribute "physical" means that we consider systems whose microscopic dynamics is governed by some Hamiltonian. At large time scales, the solution of the master equation will relax to a time-independent equilibrium distribution function $p_\mathrm{eq}(a)$, typically a Maxwell–Boltzmann distribution of the "energy" corresponding to the state a. We thus have, $0 = \int da' \, [W(a|a')p_\mathrm{eq}(a') - W(a'|a)p_\mathrm{eq}(a)]$. This equation should be interpreted as an effective sum rule obeyed by the transition matrix elements $W(a|a')$. Using the invariance of microscopic Hamiltonian dynamics under time-reversal, it can in fact be shown[24] that the above balance equation not only holds in an integral sense, but even for individual pairs (a,a'), i.e. $W(a|a')p_\mathrm{eq}(a') = W(a'|a)p_\mathrm{eq}(a)$, or

$$\boxed{\frac{W(a|a')}{W(a'|a)} = \frac{p_\mathrm{eq}(a)}{p_\mathrm{eq}(a')}.} \tag{10.39}$$

Equation (10.39) is known as the principle of **detailed balance**.

[24] The term "master equation" was coined in A. Nordsieck, W. E. Lamb, and G. E. Uhlenbeck, On the theory of cosmic-ray showers I: the furry model and the fluctuation problem, *Physica* **7**, 344-60 (1940), where a rate equation similar to Eq. (10.38) appeared as a fundamental equation of the theory.

The principle of detailed balance constrains the equilibrium behavior of systems containing different compounds (as represented by the state variables a). For example, it states that, in a solution containing several chemical agents, the equilibrium reaction rates will be such that the reaction rates $A \to B$ between any one *pair* of agents A and B exactly compensate for the back reaction rates $B \to A$.

EXERCISE **Kangaroo process:** Consider the master equation,

$$\partial_t p(a,t) = \int da' \left[W(a|a')p(a',t) - W(a'|a)p(a,t) \right],$$

with a factorizable transition matrix $W(a|a') = u(a)v(a')$. What is kangaroo-like for the above transition matrix? Solve the master equation with the help of the Laplace transform $p(a,z) = \int_0^\infty dt\, e^{izt} p(a,t)$. In a first step, show that the following relation holds

$$p(a,z) = \frac{p(a,t=0) + u(a)\sigma(z)}{-iz + v(a)/\tau},$$

where $1/\tau = \int da\, u(a)$ and $\sigma(z) = \int da\, v(a)p(a,z)$. Determine $\sigma(z)$ by substituting the expression for $p(a,z)$ and solving the resulting algebraic equation.

Kubo–Anderson process: Taking $v(a) \equiv v$, simplify the resulting equation for $p(a,z)$ and compute the inverse Laplace transform to obtain the time evolution of the distribution $p(a,t)$. Compare with the Ornstein–Uhlenbeck process (Problem 10.9.2).

Example: Gaussian process

Let us illustrate the general concepts introduced above on two important examples. Consider a **one-dimensional random walk**, i.e. a process wherein a particle performs random motion on a one-dimensional lattice (see figure). Setting the lattice spacing to unity, the state variable $a \equiv n \in \mathbb{Z}$ takes integer values, and our goal is to compute the probability $p(n,t|n_0,t_0)$. Defining the probability density for an individual left-turn (right-turn) as $q\,dt$ ($(1-q)\,dt$), the master equation assumes the form

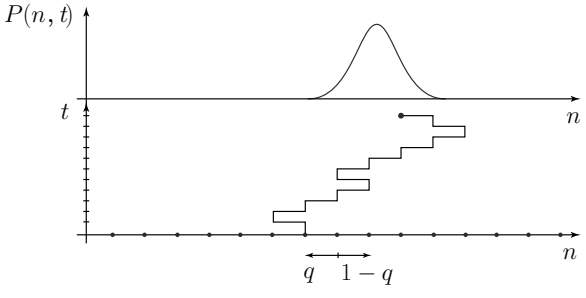

$$\partial_t p(n,t) = qp(n+1,t) + (1-q)p(n-1,t) - p(n,t).$$

Anticipating smoothness of the probability distribution we may convert this equation into a differential equation. To this end we assume (without altering the problem too much) that the process takes place on a lattice of N points subject to periodic boundary conditions. Defining the scaling variable $x = n/N \in [0,1]$ and a rescaled probability distribution $\tilde{p}(x)dx = p(Nx)dn = p(Nx)(dn/dx)dx \Rightarrow \tilde{p}(x) = Np(Nx)$, and Taylor expanding,

$\tilde{p}(x \pm 1/N) = \tilde{p}(x) \pm N^{-1}\partial_x \tilde{p}(x) + (1/2)N^{-2}\partial_x^2 \tilde{p}(x)$, the master equation assumes the form of a generalized diffusion equation (for notational simplicity, we write p instead of $\tilde{p}$),

$$\left(\partial_t + \gamma\partial_x - D\partial_x^2\right) p(x,t) = 0, \qquad p(x,t_0) = \delta(x - x_0),$$

with "drift coefficient" $\gamma = (1-2q)N^{-1}$, diffusion constant $D = 1/2N^2$, and initial point $x_0 = n_0/N$. This equation is solved by

$$p(x,t) = \int \frac{dk}{2\pi}\, e^{-(i\gamma k + Dk^2)t} e^{ik(x-x_0)} = \frac{1}{2(\pi D t)^{1/2}} e^{-\frac{(x-x_0-\gamma t)^2}{4Dt}},$$

or, in terms of the original variables,

$$p(n,t) = \frac{1}{(2\pi t)^{1/2}} \exp\left(-\frac{(n - n_0 - (1-2q)t)^2}{2t}\right).$$

(Exercise: consider how you would solve the structurally similar Schrödinger equation of a free particle.) General comments on Gaussian processes:

- ▷ Gaussian or "normal" distributions typically arise when large numbers of statistically-independent events add to form a composite random variable. (In cases where the composite variable is obtained by *multiplication* of elementary random variables, logarithmically normal distributions result.)
- ▷ The Gaussian form of the probability distribution is a manifestation of the central limit theorem: we may think of n as a random variable obtained by summing t elementary random variables ± 1 drawn from a bimodal distribution with probability $p(1) = 1 - q$ and $p(-1) = q$. According to the central limit theorem, the result will be a Gaussian distributed variable centered around the mean $t \times n_0 + (1-2q)t$ and variance $\sim \sqrt{t}$.
- ▷ Random processes whose distributions are Gaussian are generally called **Gaussian processes**. The example illustrates that Gaussian processes are typically the results of the addition of a large number of elementary random variables.

Example: Poisson process

Now consider a sequence of elementary events occurring in a manner uncorrelated in time (e.g. apples falling off a tree on an autumn day, signals of a Geiger counter exposed to weak radiation, etc.). The random variable of interest is the number, n, of events occurring in a certain time t (see figure). Assuming that the probability of an event to occur in a short time window dt is νdt, the master equation takes the form

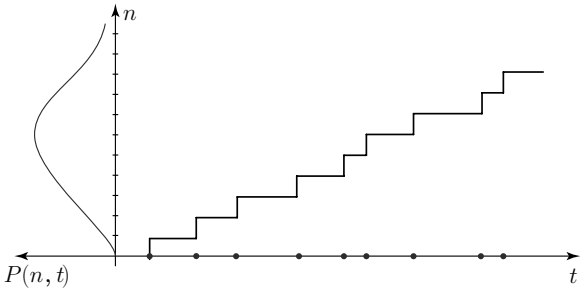

$$\partial_t p(n,t) = \nu p(n-1,t) - \nu p(n,t). \tag{10.40}$$

For definiteness, we assume that this equation has to be solved with the boundary condition $p(n, t = 0) = \delta_{n,n_0}$.

Again, we may approximately solve this equation by assuming smoothness of the distribution and Taylor expansion. However, this procedure is a little bit too coarse to resolve the specific statistics relating to the discreteness of events. (Exercise: solve the equation by Taylor expansion and compare with the results below.) In the following, we employ concepts borrowed from quantum mechanics to construct a more accurate solution. Later on, we see that specific aspects of stochastic processes – the dynamics of very rare events, to mention one example – afford a general description in terms of "quantum" theory. (The quotes are used here because, of course, there is no true $\hbar$ involved.)

We start by rewriting the equation as $\partial_t p(n,t) = \nu(\hat{E}_{-1} - 1)p(n,t)$, where $\hat{E}_m$ is the translation operator in discrete n-space, i.e. $\hat{E}_m f(n) \equiv f(n+m)$. Now, the translation operator affords a representation in terms of the "momentum" operator $\hat{\phi}$ conjugate to the "number operator" n: With $[\hat{\phi}, \hat{n}] = -i$, we have $\hat{E}_m = e^{im\hat{\phi}}$. In the "$n$-representation," the translation operator E_{-1} takes the form $\hat{E}_{-1} = \exp(-\partial_n)$. Its eigenfunctions are given by $f_k(n) = (2\pi)^{-1/2}\exp(ikn)$ with eigenvalue $\lambda_k = \exp(-ik)$. Finally, the initial configuration of the probability distribution affords the spectral representation $p(n,0) = \delta_{n,n_0} = \int_0^{2\pi} \frac{dk}{2\pi}\, e^{-ik(n-n_0)}$. By analogy with the solution of a quantum initial value problem, we may thus represent $p(n,t)$ as

$$p(n,t) = \int_0^{2\pi} \frac{dk}{2\pi}\, e^{-\nu t(e^{-ik}-1)} e^{ik(n-n_0)}.$$

Using the identity $\int_0^{2\pi} \frac{dk}{2\pi}\, e^{i\Delta nk} = \delta_{\Delta n,0}$, a straightforward Taylor expansion of the exponent obtains the result (exercise)

$$p(n,t) = \frac{(\nu t)^{n-n_0}}{(n-n_0)!} e^{-\nu t}. \tag{10.41}$$

- ▷ The process is described by a Poisson distribution (cf. Eq. (10.4) where $\nu t \leftrightarrow np$ represents the product of "attempts" ($t \leftrightarrow n$) and "success probability" ($\nu \leftrightarrow p$)), hence the name Poisson process.
- ▷ The first and second cumulant of the Poisson distribution are given by, respectively, $\mu_1 = \nu t$, $\mu_2 = \nu t$, i.e. centered around $\mu_1 = \nu t$, the width of the distribution is given by $\sim (\nu t)^{1/2}$.
- ▷ The variable t is a bookkeeping index, which need not necessarily be physical time. For example, the statistics of energy levels on the energy axis of integrable quantum systems is usually described by a Poisson distribution, which reflects the lack of inter-level correlations.

EXERCISE **One-step processes**: The master equation of a one-step process is given by

$$p_n = r_{n+1}p_{n+1} + s_{n-1}p_{n-1} - (r_n + s_n)p_n.$$

To solve the master equation it is useful to make use of the generating function $g(z,t) = \sum_{n=-\infty}^{\infty} z^n p_n(t)$, where $g(1,t) = 1$ reflects the conservation of probability. Show that for a given g, the probability follows from the inverse Mellin transform

$$p_n(t) = \frac{1}{2\pi i} \oint dz\, z^{-1-n} g(z,t), \tag{10.42}$$

where the integral is taken around a contour enclosing $z = 0$ (but no singularities of g.)
(a) **Symmetric random walk:** Consider the special case $r_n = s_n = 1$ with the initial condition $p_n(0) = \delta_{n,0}$. From the master equation, derive a differential equation for $g(z,t)$ and show that its solution is $g(z,t) = \exp((1/z + z - 2)t)$. Solve the integral (10.42) in the saddle-point approximation and show that the resulting behavior for large times $t \to \infty$ is diffusive, $p_n(t) \simeq e^{-n^2/4t}/\sqrt{4\pi t}$.
(b) **Furry process:** Consider the case $r_n = 0$ and $s_n = \gamma n$ with the initial condition $p_n(0) = \delta_{n,1}$. Determine $g(z,t)$. You can solve its partial differential equation with help of the method of characteristics. Using Eq. (10.42) show that the probabilities for $n > 0$ are given by $p_n(t) = e^{-\gamma t}(1 - e^{-\gamma t})^{n-1}$.
(c) **Population growth:** Consider the case $r_n = \alpha n$ and $s_n = \beta n$ with the initial condition $p_n(0) = \delta_{n,m}$. Show that the probability that the population dies out at time t is given by $p_0(t) = \left(\frac{\alpha(1-\epsilon)}{\beta-\alpha}\right)^m$, where $\epsilon = e^{(\alpha-\beta)t}$. Discuss the short and long time limits.

10.4.3 Fokker–Planck equation II

The master equation (10.38) is a linear integral equation for the probability density, p. It can be formally solved in terms of a spectral decomposition of the integral kernel $\{W(a|a')\}$ (exercise). However, in cases where $W(a|a')$ exhibits nontrivial dependence on the state variables a (which may be multi-dimensional!), an explicit eigenmode decomposition of p may be not attainable.[25] However, in many cases of practical interest:

- ▷ The integral kernel $W(a|a')$ decays rapidly as a function of the "distance" $|a - a'|$, i.e. for sufficiently short times δt, transitions between remote states are strongly suppressed. (Here, we assume that state space $\{a\}$ comes with a meaningful notion of distance, which usually is the case.)
- ▷ We may anticipate smoothness of the distribution $p(a)$ on the scales of variation of W.

Under these conditions, a **Kramers–Moyal expansion** can be applied to reduce the integral equation to the more benign form of a quasi-local equation (i.e. a differential equation). Repeating the sequence of steps carried out in Section 10.2.3, we change notation $W(a|a') = W_b(a')$, $b \equiv a - a'$, where $W_b(a')$ is the transition probability for $a' \to a' + b$. In this notation,

$$\partial_t p(a) = \int db\, [(W_b p)(a - b) - (W_{-b} p)(a)]\,.$$

[25] Although a numerical diagonalization of W may still be the most efficient route to obtain the (long time) profile of p.

Using the relation, $\int db\,(W_b(a) - W_{-b}(a)) = 0$, Taylor expansion of $(W_b p)(a-b)$ in b around a (the index in W_b remains passive!) obtains the series

$$\partial_t p(a,t) = \sum_{n=1}^{\infty} \frac{(-)^n}{n!} \partial_a^n \left(\alpha_n p\right)(a,t), \tag{10.43}$$

where the coefficients α_n are the moments of the transition probabilities,

$$\alpha_n(a) = \int db\, W_b(a) b^n. \tag{10.44}$$

The **Fokker–Planck approximation**

$$\partial_t p(a,t) = \left(-\partial_a \alpha_1(a) + \frac{1}{2}\partial_a^2 \alpha_2(a)\right) p(a,t), \tag{10.45}$$

with $\alpha_1 = \int db\, W_b(a) b$ and $\alpha_2 = \int db\, W_b(a) b^2$ assumes that all terms beyond $n = 2$ are negligible. As exemplified in Section 10.2.3 above:

- ▷ The first derivative, or **drift term** $\sim \partial_a \alpha_1 p$ is "deterministic" in that it describes the evolution of the *averaged* variable $\langle a \rangle$. Indeed,

$$\begin{aligned} \partial_t \langle a \rangle &= \int da\, a \partial_t p(a,t) \\ &= \int da\, a \left(-\partial_a \alpha_1(a) + \frac{1}{2}\partial_a^2 \alpha_2(a)\right) p(a,t) = \int da\, \alpha_1(a) p(a,t) = \langle \alpha_1 \rangle, \end{aligned}$$

  where, to prove this identity, we have applied an integration by parts.
- ▷ The second derivative, or **diffusion term** describes the diffusive spread of probability around the center of the distribution, $\langle a \rangle$.

In many cases, the Fokker–Planck approximation does an excellent job at describing the probability distributions of stochastic processes. However, as with any other approximation scheme, it is not perfect. Some care must be exercised, e.g. if one is asking questions about the **tails of probability distributions**, "rare event" regions where p has become small. In the next section, we discuss an example illustrating success and partial failure of the Fokker–Planck approximation in a very simple setting.

10.4.4 Quality of the Fokker–Planck approximation: an example

The Fokker–Planck approximation is routinely applied as a tool to explore analytically the dynamical evolution of probability distributions. It is therefore important to identify those situations where the approximation goes qualitatively wrong.

Empirically, large deviations between the predictions of the Fokker–Planck equation and results obtained by (numerical) iteration of the Master equation are frequently observed in the tails of the probability distribution. Often these tails carry information about "rare" events far from the typical behavior of the system. Such rare events can be of profound importance. For example, in cases where the master equation describes the epidemic proliferation of a virus, one will likely be interested in the probability of exceptionally persistent

infections. Equally, in a master equation modeling a nuclear chain reaction, the eventuality of an uncontrolled chain reaction, no matter how unlikely, will be of definite interest, etc.

In the following, we explore the shortcomings of the Fokker–Planck approximation for the familiar example of the Poisson process. In Section 10.4.2 we introduced the master equation of the Poisson process and obtained Eq. (10.41) for its rigorous solution. Now, let us see what we would have got instead had we subjected the master equation to a Kramers–Moyal expansion.

Introducing a scaled variable, $x = n/N, N \gg 1$, with associated continuum probability distribution $\tilde{p}(x,t)dx = p(n,t)dn \Rightarrow \tilde{p}(x,t) = p(xN,t)N$, we may subject the equation to a second order Kramers–Moyal expansion. For later reference, we note that this expansion amounts to second order expansion of the translation operator $\hat{E}^{-1} - 1 = e^{-\partial_x/N} - 1 \simeq -\frac{1}{N}\partial_x - \frac{1}{2N^2}\partial_x^2$. As a result, we obtain the Fokker–Planck equation

$$\left(\partial_t + \frac{\nu}{N}\partial_x - \frac{\nu}{2N^2}\partial_x^2\right)\tilde{p}(x,t) = 0,$$

with $p(x,0) = \delta(x)$. This equation is solved by $\tilde{p}(x,t) = N(\frac{1}{2\pi\nu t})^{1/2}\exp(-\frac{1}{2t\nu}(Nx - t\nu)^2)$ or, upon translating back to the original variable n,

$$p(n,t) = \left(\frac{1}{2\pi\nu t}\right)^{1/2} \exp\left[-\frac{1}{2t\nu}(n - t\nu)^2\right]. \tag{10.46}$$

This "Gaussian approximation" displays the two principal characteristics of the Poisson distribution, mean value νt and width $\sim (\nu t)^{1/2}$. However, in the tails of the distribution, the approximation is poor. This is illustrated in (the logarithmic representation of) the figure: At values of n about four times bigger than the mean value, in the far tails of the distribution, the Fokker–Planck prediction is by many orders of magnitude off the true result.

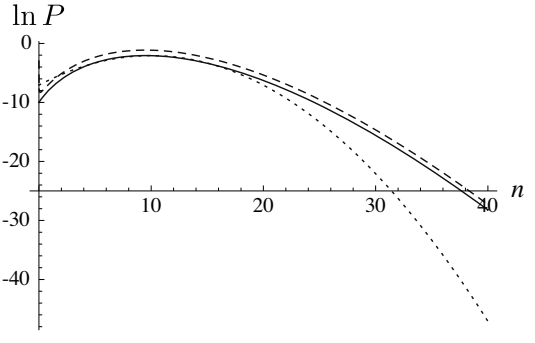

The origins of the this error can be traced to the second order expansion of the operator $\hat{E}_1 = e^{-\partial_x/N}$. Doing so, and replacing this operator by an effective long-range approximation wherein the "momentum operator" $-i\partial_x$ is considered small, we forget about the integer nature of the variable n. (Exercise: why?) To obtain a better result in the far tail regions, we ought to keep the integrity of this operator intact. This makes the theory more complicated. However, pushing the quantum analogy further, and thinking of $p(n,t) = p(n,t|0,0)$ as a "transition amplitude" we may turn the smallness of p to an advantage: using a path integral oriented language, and writing $p \sim \int \exp(-S)$ as the integral over an exponentiated "action", we know that $S \gg 1$ in the far tails. This suggests that semiclassical approximation schemes might be applicable. In the following, we formulate a semiclassical approach to the Poisson process, and demonstrate that it does an excellent job of describing the tail regions.

Defining the "Hamiltonian operator", $\hat{H} \equiv -\nu\left(e^{-i\hat{p}}-1\right)$, the master equation assumes the form of a Schrödinger equation for an imaginary time evolution operator,

$$(\partial_t + \hat{H})p(n,t) = 0, \qquad p(n,0) = \delta_{n,0}.$$

Here, we are working in the system of original variables n, instead of the rescaled coordinate x. This equation has the formal solution

$$p(n,t) = \langle n|e^{-t\hat{H}}|0\rangle = \int_{q(0)=0}^{q(t)=n} D(q,p)\, e^{\int_0^t dt\,(ip\dot{q}-H(p,q))},$$

where $\langle n|n'\rangle = \delta_{n,n'}$ is the scalar product in n-space, and in the second equality we switched to a path integral representation. To avoid the mixed appearance of real and imaginary terms in the exponent, we subject the integration over the momentum variable to a Wick-rotation, $p \to -ip$. In the new variables,

$$p(n,t) = \int_{q(0)=0}^{q(t)=n} D(q,p)\, e^{\int_0^t dt'\,(p\dot{q}-H(q,p))}, \qquad H(q,p) = -\nu\left(e^{-p}-1\right).$$

We evaluate this path integral in the crudest form of a stationary phase approximation,

$$p(n,t) \simeq e^{-S[q,p]}, \qquad S[q,p] = -\int_0^t dt'\,(p\dot{q} - H(q,p)),$$

where $(q,p)(t')$ are solutions of the extremal equations with the configuration space boundary conditions $q(0) = 0, q(t) = n$. Varying the action we obtain the equations of motion,

$$\begin{aligned} d_{t'}q &= \quad \partial_p H = \nu e^{-p}, \\ d_{t'}p &= -\partial_q H = 0. \end{aligned}$$

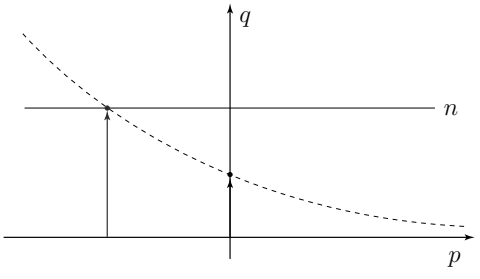

The solution of these equations reads

$$\begin{aligned} p(t') &= -\ln(n/\nu t), \\ q(t') &= n(t'/t). \end{aligned}$$

The conserved energy is given by $H = -n/t + \nu$. It is instructive to take a brief look at the "phase portrait" of these solutions shown in the figure above. Conservation of momentum means that the flow is parallel to the q-axis with velocity νe^{-p}. At $p = 0$, $q(t') = \nu t'$, which reflects the temporal evolution of the *mean* value $\langle n(t')\rangle$ of the Poisson process. The action corresponding to this mean trajectory vanishes, $S(q, p = 0) = 0$. Within the Hamiltonian approach it is possible to reach final configurations $q(t) = n(t)$ very different from $t\nu$. However, this comes at the price of a large action: the action of the solutions above is readily obtained as

$$S[q,p] = n\ln(n/\nu t) - n + \nu t.$$

(Notice that this action assumes its minimum value $S = 0$ at $n = \nu t$.) The stationary phase approximation to the probability distribution thus reads

$$p(n,t) \simeq e^{-(n\ln(n)-n)+n\ln(\nu t)-\nu t} = e^{-(\ln(n)-n)}(\nu t)^n e^{-\nu t} \simeq \frac{(\nu t)^n}{n!}e^{-\nu t},$$

where the last approximate equality is based on an "exponential" approximation to the Stirling formula, $n! \simeq \frac{1}{2}\ln(2\pi n)e^{n\ln n - n} \sim e^{n\ln n - n}$. The semiclassical approximation is shown in the figure on p.641, dashed. In the center of the distribution, where $S = 0$ and semiclassical approximations are problematic, the Fokker–Planck equation does a better job at approximating the Poisson distribution. However, in the tail regions, where $S \gg 1$, semiclassics works well! The quality of the result may be improved by including quadratic fluctuations around the mean field trajectory, which then leads to an improved variant of Stirling's approximation. However, to "exponential accuracy," the present approximation is sufficient.

The take home message of this exercise is that variational methods can be a powerful tool in the study of "rare events" in a stochastic process. Significant deviations from the Fokker–Planck approach are to be expected if the Hamiltonian of the process is not harmonic in momenta (which means that the corresponding "Schrödinger equation" differs from the second order Fokker–Planck equation) due to, e.g., discreteness of the agents participating in the process. However, even if the Fokker–Planck equation is valid, the semiclassical analysis can be a useful aid. The point is that the Fokker–Planck equation – mathematically similar to an imaginary time Schrödinger equation – usually defies rigorous analytical solution. Much as WKB-type semiclassics is useful in quantum mechanics, the "semiclassical" approximation to a Fokker–Planck equation can be an economic route to obtain information on large-action/rare-event statistics.

10.5 Field theory I: zero dimensional theories

In the previous sections, we have introduced basic elements of classical nonequilibrium theory. We have seen that nonequilibrium systems can be described (see Fig. 10.7) on:

- ▷ a **microscopic level**, i.e. in terms of microscopic Hamiltonians and their interactions,
- ▷ a **mesoscopic level**, where the microscopic transition rates are lumped into either a stochastic differential equation of Langevin type, or a master equation,
- ▷ a **continuum level**. In our discussion so far, the continuum description was formulated in terms of the Fokker–Planck equation, a second order partial differential equation in the state variables, and first order in time.

Both, from a formal and a conceptual point of view, the description of nonequilibrium phenomena in terms of differential (Langevin, Fokker–Planck) or integral (master) equations bears similarities to the Schrödinger approach to quantum mechanics. It requires comparatively little theoretical machinery, affords a lean and reasonably intuitive description of many physical phenomena, but also suffers from limitations. We had a first glimpse of the deficiencies of the Fokker–Planck approach when we explored the tail regions of the Poisson

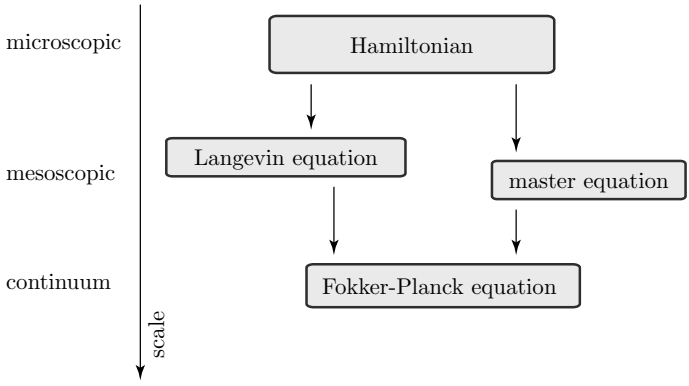

Figure 10.7 Showing the three levels of description of nonequilibrium systems.

process: To stay with the analogy above, the tails turned out to be described better in terms of a "path integral approach."

Generally speaking, much of what has been said in the introductory chapters of this text by way of motivation of path integral and field theory oriented approaches to genuine quantum systems carries over to the present context. Specifically:

- ▷ In the description of **rare events and large fluctuations**, variational approaches and the analysis of extremal action configurations may be a powerful alternative to the solution of the Fokker–Planck equation.
- ▷ So far, our discussion has been limited to statistical problems described in terms of only a few random variables – the analog of "zero dimensional" quantum problems. However, many applications of interest are described in terms of many spatially resolved random variables – think of a *field* $\{n(\mathbf{r}, t)\}$ describing the local population size in a problem of evolutionary ecology. Much as in quantum field theory, field integration techniques are the method of choice to explore the ensuing phenomena of collective dynamics, criticality, etc.
- ▷ The Langevin equations explored above have been linear equations, on account of the oscillator dynamics of the underlying non-dissipative dynamics. Extremal principles derived from effective path integral descriptions are an efficient method to explore the more interesting behavior shown by **nonlinear stochastic differential equations**.

In this section we introduce a number of field theoretical tools that have been designed to study the behavior of classical nonequilibrium systems. For the sake of clarity, (a) this section is devoted exclusively to the discussion of formalism. Applications are addressed in the follow-up section. Furthermore, (b) we introduce the field theory approaches in the simple setting of zero-dimensional problems, i.e. as $(0 + 1)$ dimensional path integrals. The extension to $(d + 1)$-dimensional field theories is discussed in Section 10.6.

10.5.1 Martin–Siggia–Rose–Janssen–de Dominicis approach

Let us begin our discussion by constructing a path integral reformulation of stochastic differential equations. A (first order) **stochastic differential equation** is an equation of the structure

$$\partial_t n + f(n) = \xi, \tag{10.47}$$

where $n = n(t)$ is a time-dependent random variable, $f = f(n(t))$ a function, and $\xi = \xi(t)$ a noise term. In some applications, $\xi = \xi(n, t)$ depends on n. However, here we restrict ourselves to the case of *linear* noise, where ξ does not depend on n.[26] For simplicity, we assume that the noise is Gaussian with correlator,

$$\langle \xi(t) \rangle_\xi = 0, \qquad \langle \xi(t)\xi(t') \rangle_\xi = A\delta(t - t'). \tag{10.48}$$

As a first step towards the construction of a path integral representation, we discretize time, $n(t) \to n_i, i = 1, \ldots, N$, according to

$$n_i - n_{i-1} + \Delta t \, [f(n_{i-1}) - \xi_{i-1}] = 0, \tag{10.49}$$

where Δt is the temporal discretization interval. Denoting a solution of the differential equation by $n[\xi]$, expectation values of observables $\langle \mathcal{O}[n] \rangle_\xi$ may then be formally represented as

$$\langle \mathcal{O}[n] \rangle_\xi = \int Dn \, \mathcal{O}[n] \, \langle \delta(n - n[\xi]) \rangle_\xi = \int Dn \, \mathcal{O}[n] \quad \left| \frac{\delta X}{\delta n} \right| \delta(X) \quad _\xi ,$$

where $Dn = \prod_i dn_i$ is the functional measure and $\delta(n - n[\xi]) = \prod_i \delta(n_i - n[\xi]_i)$. In the second equality, we have introduced a vector $X = \{X_i\}$, where $X_i \equiv n_i - n_{i-1} + \Delta t \, [f(n_{i-1}) - \xi_{i-1}]$ and $|\delta X / \delta n|$ is the (modulus) of the determinant of $\{\frac{\partial X_i}{\partial n_j}\}$. The advantage of the discretization chosen above is that $\delta X / \delta n$ is a triangular matrix with unit diagonal, i.e. the functional determinant equals unity. Thus, substituting the definition of X,

$$\langle \mathcal{O}[n] \rangle_\xi = \int Dn \, \mathcal{O}[n] \, \langle \delta(\partial_t n + f(n) - \xi) \rangle_\xi, \tag{10.50}$$

where $\partial_t n = \{n_i - n_{i-1}\}$ is shorthand for the lattice time derivative.

INFO The discretization leading to a unit functional determinant goes under the name **Ito discretization**. More general discretization schemes call for a treatment of the corresponding functional determinants. It is customary to represent these determinants in terms of Grassmann integrals. The resulting integrals jointly involve real integration variables (the functional representation of the δ-function), and Grassmann variables. Interestingly, these integrations are coupled by a symmetry principle known as BRS-symmetry. For further discussion of BRS symmetries in the context of stochastic differential equations, we refer to J. Zinn-Justin, *Quantum Field Theory and Critical Phenomena*, (Oxford University Press, 1993).

[26] For an application with nonlinear noise term, see Section 10.7.2 below.

Representing the δ-function in terms of a Fourier integral, and switching back to a continuum notation, we arrive at the functional integral representation

$$\langle \mathcal{O}[n] \rangle_\xi = \int D(n,\tilde{n})\, \mathcal{O}[n] \quad e^{i\int dt\, \tilde{n}(\partial_t n + f(n) - \xi)} \Big)_\xi ,$$

where the structure of the "action" suggests that the two fields n and $\tilde{n}$ are "canonically conjugate" to each other. We finally average over the noise to arrive at the celebrated **Martin–Siggia–Rose–Janssen–de Dominicis (MSRJD) functional integral**

$$\boxed{\langle \mathcal{O}[n] \rangle_\xi = \int D(n,\tilde{n})\, \mathcal{O}[n] \exp\left(\int dt\, \left[i\tilde{n}(\partial_t n + f(n)) - \frac{A}{2}\tilde{n}^2 \right] \right).} \tag{10.51}$$

Equivalently, we may use the path integral representation to compute the conditional probability $p(n,t|n_0,0)$ (just set $\mathcal{O}[n] = \delta(n - n(t))$) in terms of a path integral with "configuration space boundary conditions"

$$\boxed{p(n,t|n_0,0) = \int_{n(0)=n_0}^{n(t)=n} D(n,\tilde{n}) \exp\left(\int dt\, \left[i\tilde{n}(\partial_t n + f(n)) - \frac{A}{2}\tilde{n}^2 \right] \right).} \tag{10.52}$$

Before proceeding, let us make a few remarks on the structure of the path integrals (10.51) and (10.52):

- ▷ Introducing a new set of variables (q,p) through $(n,\tilde{n}) \equiv (q,-ip)$, Eq. (10.51) assumes the form of an imaginary time **phase space path integral**,

$$p(n,t|n_0,0) = \int_{q(0)=n_0}^{q(t)=n} D(q,p)\, e^{\int dt\, [p\dot{q} - H(q,p)]}, \qquad H(q,p) = -pf(q) - \frac{A}{2}p^2. \tag{10.53}$$

  It is important to keep in mind that the integration over p extends over the imaginary axis.
- ▷ The action of the path integral vanishes on the line $p = 0$. That line generally hosts a solution of the classical equations of motion. Varying the action we indeed find that $(q(t), p = 0)$, where $\dot{q} = -f(q)$ is a solution. Comparison with the Langevin equation shows that the dynamics describes the noise-averaged Langevin variable, $q(t) \leftrightarrow \langle n(t) \rangle$, if fluctuations are weak: $\partial_t \langle n \rangle = -\langle f(n) \rangle \simeq -f(\langle n \rangle)$.
- ▷ Although the Hamiltonian does not assume the "standard form" $H = T(p) + V(q)$, it is quadratic in momenta. We may thus integrate over p to obtain

$$p(n,t|n_0,0) = \int_{q(0)=n_0}^{q(t)=n} D(q)\, e^{-\frac{1}{2A}\int dt\, [\partial_t q + f(q)]^2}. \tag{10.54}$$

Multiplying out the square in the exponent, we arrive at a **Lagrangian variant** of the theory, the **Onsager–Machlup functional**[27]

$$p(n,t|n_0,0) = \int_{q(0)=n_0}^{q(t)=n} D(q)\, e^{-\int dt\, L(q,\dot{q})}, \qquad L(q,\dot{q}) = \frac{1}{2A}\dot{q}^2 + \dot{q}\frac{f(q)}{A} + \frac{f(q)^2}{2A}. \quad (10.55)$$

This is the Lagrangian of a one-dimensional point particle with "mass" $m = 1/A$ which is coupled to a velocity-dependent one-dimensional "vector potential" of strength $A(q) = f(q)/A$, and a potential $V(q) = f(q)^2/2A$.

We may interpret the Onsager–Machlup representation of the probability distribution as the formal analog of a Lagrangian path integral for a quantum time evolution operator. On general grounds, the **Schrödinger equation** corresponding to this formulation reads

$$\left(\partial_t - \frac{1}{2m}(\partial_q + A(q))^2 + V(q)\right)\phi(q,t) = \left(\partial_t - \frac{A}{2}\partial_q^2 - \partial_q f(q)\right)\phi(q,t) = 0,$$

where ϕ is the analog of a wave function. Specifically, the "time evolution operator" $p(n,t|n_0,0)$ is a solution of the initial value problem

$$\left(\partial_t - \frac{A}{2}\partial_q^2 - \partial_q f(q)\right)p(q,t)\Big|_{q=n} = 0, \qquad p(n,0) = \delta(n-n_0),$$

which is nothing but the Fokker–Planck description of the Langevin dynamics. We thus arrive at the important conclusion that

> the Fokker–Planck equation is the "Schrödinger equation" of the MSRJD path integral.

The discussion above is overly-concise in that (a) we are not explicit regarding sign factors and imaginary is. For instance, the "momentum" operator in our Schrödinger equation reads ∂_q instead of the conventional $-i\partial_q$, because the equation is derived from a theory with real exponent $-S[q]$, instead of $iS[q]$. More importantly, (b) we do not keep track of the order of derivatives (why $\partial_q f(q)$, instead of $f(q)\partial_q$?). To monitor the correct ordering, one needs to keep track of the properly Ito-discretized sequential ordering of operators in the action (an instructive if somewhat technical exercise).

INFO It may be instructive to observe the functioning of the concepts above on a miniature application. Consider a particle at rest in the bottom of a metastable potential configuration (see inset of Fig. 10.8). Thermal activation may help the particle in surmounting the potential barrier to settle in an overall more favourable true energy minimum. We know that the corresponding **thermal escape rates** are controlled by **Arrhenius factors**. The detailed computation of such rates is of importance in, say, the chemistry of thermally activated reactions. For a given potential landscape, the functional integrals above can be a powerful aid in analyzing the corresponding

[27] L. Onsager and S. Machlup, Fluctuations and irreversible processes, *Phys. Rev.* **91**, 1505-12 (1953).

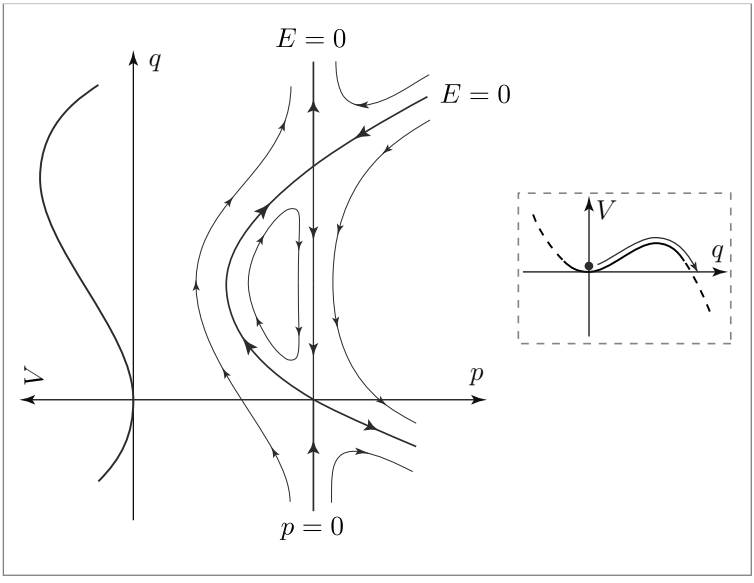

Figure 10.8 Inset: particle in a metastable potential well. Main figure: phase space portrait of the corresponding MSRJD functional. For a discussion, see main text.

escape kinematics. By way of example, here we discuss the emergence of Arrhenius activation factors from the functional integral formalism.

Assuming overdamped dynamics, the equation of motion of a point particle in the well is given by

$$\gamma q + \partial_q V(q) = \xi'(t),$$

where, by the fluctuation-dissipation theorem, $\langle \xi'(t)\xi'(t')\rangle = 2\gamma T\delta(t-t')$. Dividing by γ, we obtain a stochastic differential equation of the type Eq. (10.47), with the identification $q \quad n$, $f = \partial_q V$ and noise strength $A = 2T\gamma^{-1}$. Let us assume that thermal escape will be an unlikely event in the sense that $V/T \gg 1$, where ΔV is the difference between the local maximum of the metastable well and its minimum. We thus expect a small escape probability $p \sim \exp(-V/T)$. The largeness of the exponent $-\ln p \sim V/T \gg 1$ then suggests an evaluation of the path integral (10.53) by semiclassical methods. In its crudest form, semiclassics means that we evaluate the Hamiltonian path integral at its stationary points and neglect all fluctuation effects.

With $H(q,p) = -\frac{p}{\gamma}(\partial_q V(q) + Tp)$, the Hamiltonian equations of motion of the action (10.53) read

$$q = \quad \partial_p H(q,p) = -\frac{1}{\gamma}\partial_q V(q) - \frac{2T}{\gamma}p, \qquad p = -\partial_q H(q,p) = \frac{1}{\gamma}p\partial_q^2 V(q).$$

For the purposes of the present discussion, we do not need to solve these equations; it is sufficient to inspect the phase portrait of the Hamiltonian.

As we shall see, the topology of Hamiltonian flow in phase space is essentially determined by the zero energy contours $H(q,p) = 0$. The structure of the Hamiltonian implies that one of these curves is specified by $(q, p = 0)$. On the line $p = 0$, the equations of motion reduce to $\gamma q = -\partial_q V(q)$. This is drift motion down the potential gradient towards the local minimum. We

note that the point of the local potential maximum $q \equiv q^*$ defines an unstable point on that line, while $q = 0$ is stable. This observation entails two important consequences: (a) we expect that the equilibrium coordinates on the $p = 0$ line, 0 and q^*, must define points of origin of motion qualitatively different from downward drift $q^* \to 0$. Specifically, we expect the option of noise-activated reverse motion $0 \to q^*$. If so, the equilibrium points must be the terminal points of another $E = 0$ trajectory. Indeed, the equation $H(q, p) = 0$ possesses a second solution, $p = -T^{-1}\partial_q V$. At the potential extrema $\partial_q V = 0$, or $q = 0, q^*$, this curve intersects the $p = 0$ line, which means that $(q^*, 0)$ and $(0, 0)$ are terminal points of phase space *separatrices*. (Recall that the principle of non-crossing phase space curves requires that the motion along the separatrices takes infinite time. For example, you may convince yourself that in a strict mathematical sense, the downward drift trajectory $q^* \to 0$ has infinite passage time.) (b) The conservation of phase volume (Liouville's theorem) implies that the two phase space fixed points $(0, 0)$ and $(q^*, 0)$ are hyperbolic. This means that the point $(0, 0)$ (stable in coordinate direction) is unstable in momentum direction, while $(q^*, 0)$ (unstable in coordinate direction) is stable in momentum direction. Notice that the discussion above did not rest upon many specific characteristics of the escape problem. Indeed, the existence of $E = 0$ separatrices terminating in hyperbolic fixed points on the $p = 0$ line is a principle that carries over to many other "noise" phase portraits.

The separatrices largely determine the topology of phase flow, as exemplified in Fig. 10.8. Specifically, the separatrix $0 \to q^*$ accounts for the possibility of noise-assisted motion *against* the potential gradient. Within our semiclassical framework, the probability for this happening $p \sim \exp(-S)$ is proportional to the action accumulated along this trajectory. The latter is calculated as

$$S = -\int dt\,(p(q)q - H(q,p)) = \frac{1}{T}\int_0^{q^*} dq\,\partial_q V(q) = \frac{1}{T}(V(q^*) - V(0)) = \frac{\Delta V}{T},$$

where we have used $H(q, p) = 0$, and the defining equation of the separatrix. As expected, we obtain the Arrhenius weight as the dominant factor controlling the escape probability. Of course, much less heavy artillery is needed to arrive at just this result. However, as usual with functional approaches, the advantage of the above formalism is its extensibility to more complex problems.

10.5.2 Field integral representation of the master equation I

In order to avoid potential confusion with the momentum variable below, the notation for probability are capitalized in this section, $p \to P$.

By generalization of the ideas exemplified in Section 10.4.4 on the Poisson process, we can derive a path integral representation for the master equations describing Markovian stochastic processes. Unsurprisingly, this path integral turns out to be a close ally of the MSRJD functional integral above.

For simplicity, we consider a **one step master equation**, i.e. an equation where a discrete state variable n changes by no more than one unit ± 1 in each time step.[28] The

[28] The straightforward generalization to finite range equations leads to path integrals with more complicated actions. However, in many cases, the long time dynamics deriving from these integrals is qualitatively similar to the one of the single step process.

general form of a one step master equation reads

$$\partial_t P(n,t) = \Big[(\hat{E}_1 - 1)f_-(n) + (\hat{E}_{-1} - 1)f_+(n)\Big]\, P(n,t), \tag{10.56}$$

where $E_{\pm 1} f(n) \equiv f(n \pm 1)$ acts by unit translation. As in our example application in Section 10.4.4, it is useful to think of the probability distribution as the analog of a quantum time evolution operator $\hat{P}$ with "matrix elements" $P(n,t;n_0,t_0) \equiv P(n,t|n_0,0) \equiv P(n,t)$. Equation (10.56) then becomes an (imaginary time) evolution equation,

$$\Big(\partial_t + \hat{H}(\hat{q},\hat{p})\Big)\, \hat{P}(t) = 0, \qquad \hat{P}(0) = \mathbf{1}, \tag{10.57}$$

with the "Hamiltonian operator"

$$\hat{H}(\hat{q},\hat{p}) = -\left(e^{+i\hat{p}} - 1\right) f_-(\hat{q}) - \left(e^{-i\hat{p}} - 1\right) f_+(\hat{q}). \tag{10.58}$$

Here, it is understood that the eigenvalue spectrum of the "position operator," $\hat{q}$, will eventually be evaluated at discrete values n,[29] and $\hat{p}$ is canonically conjugate to $\hat{q}$. In the q representation, $\hat{p} = -i\partial_q$.

We proceed by representing the formal solution of Eq. (10.57) in terms of an imaginary time phase space path integral

$$P(n,t;n_0,t_0) = \langle n|e^{-t\hat{H}}|n_0\rangle = \int_{q(0)=n_0}^{q(t)=n} D(q,p)\, e^{\int dt\,(ip\dot{q} - H'(p,q))},$$

where $H'(q,p)$ is the classical Hamiltonian corresponding to the operator Eq. (10.58). If it were not for the imaginary unit multiplying the $p\dot{q}$-term, the action of the path integral would be structurally identical to a Hamiltonian action. We may remove that discrepancy by introducing a new momentum variable $p \to -ip$, whereupon the path integral assumes the form

$$P(n,t;n_0,t_0) = \int_{q(0)=n_0}^{q(t)=n} D(q,p)\, e^{\int dt\,(p\dot{q} - H(p,q))},$$
$$H(q,p) = -\left(e^{+p} - 1\right) f_-(q) - \left(e^{-p} - 1\right) f_+(q). \tag{10.59}$$

Here, $H(p,q) \equiv H'(q,-ip)$ is the Hamiltonian evaluated at the "Wick rotated" momentum.

At this stage it is instructive to make a few remarks on the structure of the path integral:

▷ It is important to remember that the integration over p extends over the imaginary axis.

▷ As with the path integral representation of Langevin dynamics Eq. (10.53), the action vanishes on the axis $p = 0$. Again, the line $p = 0$ accommodates a solution of the variational equations, $(q(t), p = 0)$, where $\dot{q} = f_+(q) - f_-(q)$. Comparison with $d_t\langle n\rangle =$

[29] One may worry that the initial condition of the operator $P(q = n, t; n_0, 0) = \delta(n - n_0)$ conflicts with the discrete condition $P(n,t|n_0,0) = \delta_{n,n_0}$. Should this ever become an issue, one may switch to the framework of quantum mechanics of operators with discrete eigenvalue spectra. However, the continuous variables used here are better suited to the formulation of path integral methods below.

$\langle f_+(n)\rangle - \langle f_-(n)\rangle \to f_+(\langle n\rangle) - f_-(\langle n\rangle)$ shows that this equation describes the dynamics of the fluctuationless theory, again in analogy with the Langevin theory.

▷ The Fokker–Planck approximation to the master equation is obtained by quadratic expansion of the Hamilton operator,

$$\hat{H} \simeq i\hat{p}(f_+(\hat{q}) - f_-(\hat{q})) + \frac{\hat{p}^2}{2}(f_-(\hat{q}) + f_+(\hat{q})).$$

Substituting into Eq. (10.57), we obtain

$$\left(\partial_t + \partial_q(f_+ - f_-)(q) - \frac{1}{2}\partial_q^2(f_- + f_+)(q)\right) P(q,t) = 0.$$

The functional integral Eq. (10.59) is strikingly similar to the MSRJD functional Eq. (10.53). The analogy becomes almost perfect if we replace the Hamiltonian of the former by the quadratic approximation above. Indeed, we may think of the discreteness of the state variables entering the master equation as a source of "noise." If we are only interested in structures Δq much larger than the "lattice spacing" $\Delta n = 1$, the expansion of the Hamiltonian operator may be restricted to the first two non-vanishing terms. If we keep only the first term $\sim \partial_q$, we obtain deterministic drift, $\dot{q} = (f_+ - f_-)(q)$ (as can be seen by integrating over p in Eq. (10.59)). The second term describes noise due to residual discreteness effects. This noise affects the time evolution of the probability distribution much like Langevin noise.

10.5.3 Doi–Peliti operator technique

Equation (10.59) is not the only field theory representation of the master equation. There exists another approach, the Doi–Peliti operator technique[30] which extensively draws upon the Fock space structures and coherent state field integration introduced in previous chapters. Although this technique can be introduced in rather general terms, it is tailored to situations where the weight functions f_- in Eq. (10.56) are low order polynomials in n.[31] By way of example, let us consider the case $f_+ = 0$, $f_- = \lambda n$. The resulting master equation,

$$\partial_t P(n,t) = \lambda(\hat{E}_1 - 1)nP(n,t),$$

describes extinction of a population whose individuals $A \xrightarrow{\lambda} 0$ perish at a constant rate λ.

To set the stage, let us identify an integer valued[32] configuration $\{n\}$ with a bosonic Fock space state $|n\rangle$ of occupation number, n. Next, let us introduce an algebra of Fock space operators through

$$a|n\rangle = |n-1\rangle, \qquad \bar{a}|n\rangle = (n+1)|n+1\rangle. \tag{10.60}$$

[30] M. Doi, Second quantization representation for classical many-particle system, *J. Phys. A* **9**, 1465-77 (1976); M. Doi, Stochastic theory of diffusion-controlled reaction, *J. Phys. A* **9**, 1479-95 (1976); L. Peliti, Path integral approach to birth-death processes on a lattice, *J. Physique* **46**, 1469-83 (1985).

[31] As with the formalism introduced in the previous section, the Doi–Peliti operator technique affords straightforward generalization to transitions further than $n \pm 1$, as well as to multi-component/multi-dimensional situations.

[32] The generalization to other discretization intervals as well as to multi-valued configurations should be obvious.

It is straightforward to verify that these operators obey canonical commutation relations, $[a, \bar{a}] = 1$, i.e. they are related to the standard operator algebra[33] used in second quantization by canonical transformation. The operators a and $\bar{a}$ can be used to represent the action of the linear operator on the right–hand side of Eq. (10.56) in terms of the second quantized Hamiltonian (exercise),

$$\hat{H} = -\lambda(\bar{a} - \bar{a}a). \tag{10.61}$$

With this definition, it is straightforward to verify that

$$P(n,t) \equiv \langle n|e^{-t\hat{H}}|n_0\rangle, \tag{10.62}$$

is a Fock space representation of the distribution function.

We next apply the techniques introduced in Chapter 4 to represent the matrix element above in terms of a coherent state field integral. Proceeding in the usual manner, we decompose the time interval into $N \gg 1$ steps, $e^{-t\hat{H}} = (e^{-\delta\hat{H}})^N$, $\delta = t/N$, note that the Hamiltonian Eq. (10.61) is properly normal ordered, and insert coherent state resolutions of the identity, id. $= \int d(\bar{\psi},\psi)\, e^{-\bar{\psi}\psi}|\psi\rangle\langle\psi|$, where the coherent states $|\psi\rangle$ obey the relations $a|\psi\rangle = \psi|\psi\rangle$, $\bar{a}|\psi\rangle = \partial_\psi|\psi\rangle$, $\langle\psi|\bar{a} = \langle\psi|\bar{\psi}$, $\langle\psi|a = \partial_{\bar{\psi}}\langle\psi|$. This leads to the representation

$$P(n,t) = \int D(\bar{\psi},\psi) e^{-\delta\sum_{n=0}^{N-1}\left[\delta^{-1}(\bar{\psi}_n - \bar{\psi}_{n+1})\psi_n + H(\bar{\psi}_{n+1},\psi_n)\right] + n\ln\psi_N + n_0\ln\bar{\psi}_0 - \ln n!}.$$

Here, $H(\bar{\psi},\psi) = -\lambda\bar{\psi}(1-\psi)$ is the coherent state representation of the (normal ordered) Hamiltonian and the last two terms in the action represent the boundary matrix elements

$$\begin{aligned} \langle n|\psi_N\rangle &= \psi_N^n = e^{n\ln\psi_N}, \\ \langle\psi_0|n_0\rangle &= \frac{1}{n!}\bar{\psi}_0^{n_0} = e^{n_0\ln\bar{\psi}_0 - \ln n_0!}. \end{aligned} \tag{10.63}$$

Switching to a continuum notation, we arrive at the **Doi–Peliti functional integral**

$$\boxed{P(n,t) = \int D(\bar{\psi},\psi) e^{-\int_0^t dt'\left[-\partial_{t'}\bar{\psi}\psi + H(\bar{\psi},\psi)\right] + n\ln\psi(t) + n_0\ln\bar{\psi}(0) - \ln n_0!}.} \tag{10.64}$$

The coherent state field integral Eq. (10.64) defines a representation of the probability distribution which is an alternative to the phase space path integral Eq. (10.59). But how do these two representations relate to each other? The answer can be found by comparing the respective Hamiltonians. For $f_+ = 0$ and $f_- = \lambda n$, the Hamiltonian Eq. (10.58) reduces to $\hat{H} = -\lambda(e^{\hat{p}} - 1)\hat{q}$, where we used the Wick rotated form of the momentum operator, $\hat{p} \to -i\hat{p}$. Comparison with Eq. (10.61) suggests the identification

$$\bar{a} = e^{\hat{p}}\hat{q}, \qquad a = e^{-\hat{p}}, \tag{10.65}$$

[33] The latter is defined by

$$a|n\rangle = n^{1/2}|n-1\rangle, \qquad a^\dagger|n\rangle = (n+1)^{1/2}|n+1\rangle.$$

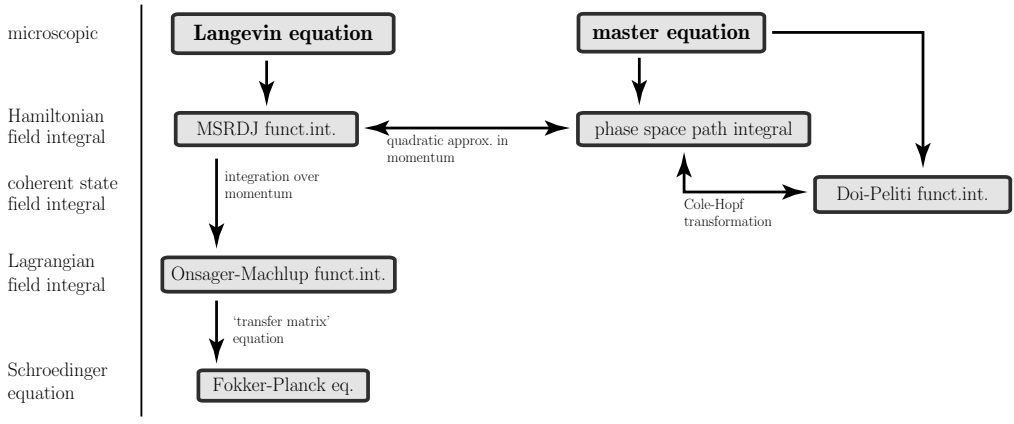

Figure 10.9 Summary of different field theory approaches to Langevin dynamics and stochastic processes.

which, up to a constant, leads to an identification of the two Hamiltonians. Eq. (10.65) is known as a **Cole–Hopf transformation**. It is straightforward to verify, that the Cole–Hopf transformation is canonical, i.e. the relation $[\hat{p}, \hat{q}] = 1$ is compatible with $[a, \bar{a}] = 1$. Substitution of the (coherent state version of the) transformation into the functional integral Eq. (10.64) transforms the "bulk contribution" to the action, $\int dt'(-(\partial_{t'}\bar{\psi})\psi + H(\bar{\psi}, \psi))$ into that of Eq. (10.59). A careful treatment of the boundary term generates the effective boundary condition $\int_{q(0)=n_0}^{q(t)=n}$.

EXERCISE Explicitly represent the coherent states above as exponentials of the operators $a, \bar{a}$ and verify the relations (10.63). Apply the Cole–Hopf transformation to the time-discretized representation of the functional integral to prove the above boundary identity in the large n-limit. Carefully avoid usage of the hermitian adjoint operation – the operator $\bar{a}$ is different from $a^\dagger$!

Summarizing, we have constructed two representations of $P(n, t)$ which are related by a Cole–Hopf transformation. Historically, the coherent state representation Eq. (10.64) was introduced prior to the path integral Eq. (10.59). (This is surprising inasmuch as Eq. (10.59) relies on a less formal construction.) It is probably not possible to decide categorically which of the two representations is the "better." At least for certain types of stochastic processes, the Doi–Peliti functional is controlled by a comparatively simple, if non-hermitian Hamiltonian operator. The price to be paid for this simplicity is that the integration variables ψ and $\bar{\psi}$ do not have a direct physical interpretation.

The network of different theories constructed in the previous sections is summarized in Fig. 10.9. So far, we have been focusing on the case of low-dimensional problems, where the state variable is a scalar or vectorial variable. In the next section, we upgrade the formalism to a genuine field theory describing multi-dimensional problems.

10.6 Field theory II: higher dimensions

Our aim in this section is to construct an effective field theory approach to higher dimensional systems showing dynamical or steady state nonequilibrium phenomena. To give the discussion some perspective, let us list a few categories of system we have in mind:

- ▷ **Interacting lattice particle systems**, i.e. systems of particles whose dynamics is governed by an interplay of single particle hopping and interactions. Important examples include **exclusion processes**, i.e. systems wherein a hardcore repulsion excludes multiple occupancy of lattice sites, and **driven diffusive lattice gases**, systems where a uniformly applied force stabilizes a steady state nonequilibrium configuration.
- ▷ **Reaction–diffusion systems**, i.e. lattice systems populated by particle species $A, B, \ldots$ which may undergo reactions. Setups of this type are common in the modeling of chemical reaction kinetics, the description of evolutionary or ecological dynamics, traffic simulation and many more. Thinking, for example, about a "fast" chemical reaction $A + B \to C$ in solution, the factor limiting the total reaction throughput may be the speed at which the chemicals diffuse through the reaction vessel. In this case, a combination of diffusion (conveniently modeled on a lattice) and local (on-site) reaction will be the minimal framework to describe the process. Important examples of particle reaction processes include birth $\emptyset \to A$, death $A \to \emptyset$, transmutation $A \to B$, death at contact, $A + B \to A$, etc.

Notice an important difference between the two categories above: while the particle number in interacting lattice systems is conserved, reaction–diffusion systems contain non-conserved particle species.

10.6.1 Basic notions of dynamical critical phenomena

What would be a good strategy to describe systems such as those listed above? On a fully microscopic level, the dynamics is governed by incredibly high dimensional equations of motion whose solution is out of the question. In practice we will, rather, turn to a description in terms of effective or coarse-grained variables. For example, in a system which may undergo a phase transition the order parameter field, $m(\mathbf{x})$, of the transition would be an obvious choice of an effective variable; in a reaction diffusion system one might think of the coarse-grained concentration variables $n_A(\mathbf{x}), n_B(\mathbf{x}), \ldots$ of the particle species, etc. For definiteness we will denote our effective variables by ϕ_a, $a = 1, \ldots, n$ throughout.

As in our "zero-dimensional" discussion in Section 10.2, the presence of microscopic "hidden degrees of freedom" affects the dynamics of the effective variables in two different ways: (i) a conspiracy of dissipative and macroscopic forces drives the effective variables towards local stationary configurations. However, (ii) we have observed that the presence of dissipative relaxation mechanisms is generally accompanied by microscopic stochastic fluctuations. Finally, (iii) for conserved effective variables, time-dependent changes, $\partial_t \phi$ must be consistent with a continuity relation $\partial_t \phi + \nabla \cdot \mathbf{j} = 0$, where $\mathbf{j}$ is some current field.

Before turning to the discussion of effective theories consistent with the principles (i)-(iii) above, it is worthwhile to formulate a set of good questions (observables) to ask. We are

interested in out of equilibrium systems wherein particle correlations generate collective or even critical phenomena. As usual in many particle physics, we aim to identify fixed points separating phases with distinct universal properties. One may then proceed to an analysis of power law correlations emerging in the vicinity of critical points. In the next section, we set the stage for these types of discussion by introducing a few elements of the theory of dynamical critical phenomena. This material follows closely a seminal review article[34] by Hohenberg and Halperin.

Consider a system with some second order (continuous) phase transition. We measure the distance to the transition point in terms of some relevant scaling field τ (e.g. $\tau = (T-T_c)/T_c$, where T is temperature, and T_c the critical temperature.). We denote the order parameter of the transition by ϕ. We assume that the order parameter is conjugate to a field h, in the sense that $\langle \phi_a \rangle = -\partial_h F[h]$, where $F[h]$ is a suitably chosen functional (in thermal equilibrium, the free energy of the system).

In the vicinity of a critical point, the system builds up long range correlation. For example, the instantaneous or static correlation function $C(\mathbf{x}) \equiv \langle \phi(\mathbf{x})\phi(0) \rangle$ is expected to show power law behavior

$$C(\mathbf{x}) = |\mathbf{x}|^{-(d-2+\eta)} Y(|\mathbf{x}|/\xi), \tag{10.66}$$

where $\xi \sim |\tau|^{-\nu}$ is the correlation length and Y a dimensionless scaling function. The correlation length is a measure for the characteristic length scales of order parameter fluctuations. Turning to dynamics, we anticipate that the corresponding **order parameter time scales** will increase as

$$\boxed{t(\tau) \sim \xi(\tau)^z \sim |\tau|^{-\nu z},} \tag{10.67}$$

where the **dynamical exponent** z depends on how the order parameter relaxes in large correlation volumes. The growth of the relevant time scales is a phenomenon known as **critical slowing down**. Equation (10.67) can be converted to a statement on the **dispersion of order parameter fluctuations**. The characteristic frequencies corresponding to Eq. (10.67), $\omega(\tau) \sim t(\tau)^{-1} \sim \tau^{\nu z}$, relate to the momenta $|\mathbf{q}| \sim \xi^{-1} \sim |\tau|^{\nu}$

$$\omega \sim |\mathbf{q}|^z f(|\mathbf{q}|\xi),$$

where f is a dimensionless function.

Turning to the temporal fluctuation behavior of the order parameter, imagine a situation where ϕ has been prepared in some initial state and is subsequently allowed to relax. It is reasonable to describe the relaxation profile by the scaling *ansatz*

$$\phi(t, \tau) = |\tau|^{\beta} g(t/t(\tau)),$$

where β is the order parameter exponent and g a dimensionless scaling function with asymptotics $g(x \to \infty) \to$ const. (relaxation towards the static value $(-\tau)^{\beta}$ below the transition point $\tau < 0$, and zero above). For short times, $t \to 0$, the relaxation process cannot be

[34] P. C. Hohenberg and B. I. Halperin, Theory of dynamic critical phenomena, *Rev. Mod. Phys.* **49**, 435-79 (1977).

susceptible to the full extension of the correlation volume, and $\phi(t,\tau)$ must be independent of τ. This leads to the condition $g(t/t(\tau)) \overset{t\to 0}{\sim} |\tau|^{-\beta}$, or

$$\phi(t) \sim t^{-\alpha}, \qquad \alpha = \beta/\nu z.$$

We next define two important correlation functions characterising the fluctuation/correlation behavior of the order parameter: The **dynamic susceptibility**, χ, is defined through the linear response relation

$$\langle \phi(q) \rangle \overset{h\to 0}{=} \chi(q) h(q), \tag{10.68}$$

where $q = (\mathbf{q}, \omega)$. Causality (i.e. the fact that $\phi(t)$ can depend only on $h(t' < t)$) means that $\chi(\omega)$ is an analytic function in the upper complex ω-plane. (Why was that?) The spatio-temporal fluctuation behavior of the order parameter is described by the **dynamical correlation function**,

$$C(x) \equiv \langle \phi(x)\phi(0) \rangle - \langle \phi(0) \rangle^2, \tag{10.69}$$

where $x = (\mathbf{x}, t)$. As we review in Section 10.6.4 below, the classical **fluctuation–dissipation theorem** now states that, in thermal equilibrium,

$$\boxed{C(\mathbf{q},\omega) = \frac{2T}{\omega}\chi(\mathbf{q},\omega).} \tag{10.70}$$

Violations of this relation will be an important tool to diagnose nonequilibrium conditions.

10.6.2 Field theories of finite dimensional Langevin systems

Armed with the definitions above, we are now in a position to formulate an effective field theory approach to dynamical phenomena. We imagine that the energy stored in a particular order parameter configuration is described by some energy functional $H[\phi]$. The question now is how to model the dynamics of the order parameter field. Following Hohenberg and Halperin (HH),[34] we argue that:

- ▷ In a model for a system with **non-conserved order parameter** (model A, according to the conventions of HH), the order parameter will relax to the minima of the energy functional, i.e. the equations of motion will contain a contribution

$$\partial_t \phi(\mathbf{x},t) = -D\frac{\delta H[\phi]}{\delta \phi(\mathbf{x},t)} + \ldots,$$

  where D is a characteristic relaxation constant.
- ▷ In contrast, in a system with conserved order parameter (HH's model B), the continuity equation $\partial_t \phi + \nabla \cdot \mathbf{j}$ has to be obeyed. We assume that the current acts to evade regions of increased energy, $\mathbf{j}(\mathbf{x},t) = -D\nabla \frac{\delta H[\phi]}{\delta \phi(\mathbf{x},t)} + \ldots$, where the ellipses represent fluctuating

contributions to the current to be discussed in a moment. (Exercise: consider the meaning of this definition.)[35] The continuity relation then assumes the form

$$\partial_t \phi(\mathbf{x},t) = D\Delta \frac{\delta H[\phi]}{\delta \phi(\mathbf{x},t)} + \dots .$$

The two evolution equations above can be subsumed as $\partial_t \phi(\mathbf{x},t) = D\Delta^n \frac{\delta H[\phi]}{\delta \phi(\mathbf{x},t)} + \dots$, where $n = 0, 1$ for models A and B, respectively. According to principle (ii) above, the relaxational character of the dynamics implies the presence of fluctuations. The full evolution equation, a **generalized Langevin equation**, thus reads as

$$\boxed{\partial_t \phi(\mathbf{x},t) = -D(-\Delta)^n \frac{\delta H[\phi]}{\delta \phi(\mathbf{x},t)} + \xi(\mathbf{x},t),} \tag{10.71}$$

where the noise is correlated as

$$\langle \xi(\mathbf{x},t)\xi(\mathbf{x}',t')\rangle = 2\delta(t-t')K(\mathbf{x}-\mathbf{x}') \equiv 2K(x-x'). \tag{10.72}$$

This correlator presumes that, on suitably chosen time scales, the noise can be modeled as Markovian. However, at this stage, not much can be said about the spatial correlation kernel K.

We finally note that correlation functions can be generated by addition of a "conjugate field" contribution to the Hamiltonian,

$$H[\phi] \to H[\phi] - \int d^d x\, \phi(\mathbf{x},t) h(\mathbf{x},t).$$

Functional averages $\langle \mathcal{O}[\phi]\rangle_\xi$ may now be computed by straightforward generalization of the $(0+1)$-dimensional functional (10.50):

$$\langle \mathcal{O}[\phi]\rangle_\xi = \int D\phi\, \mathcal{O}[\phi] \quad \prod_x \delta\left(\partial_t \phi(x) + D(-\Delta)^n \frac{\delta H[\phi]}{\delta \phi(x)} - \xi(x)\right)_\xi .$$

In practice, $F[\phi](\mathbf{x},t) = F(\phi(\mathbf{x},t), \partial_{\mathbf{x}}\phi(\mathbf{x},t), \dots)$ will be a local *function* of the field and its spatial derivatives. Representing the δ-constraint in terms of a Fourier integral over a "momentum field" ψ and integrating over the noise field we arrive at

$$\langle \mathcal{O}[\phi]\rangle_\xi = \int D(\phi,\psi)\, \mathcal{O}[\phi]\, e^{i\int dx\, \psi(x)\left(\partial_t\phi(x) + D(-\Delta)^n \frac{\delta H[\phi]}{\delta\phi(x)}\right) - \int dx dx'\, \psi(x) K(x-x')\psi(x')},$$

[35] Typically, the dominant contribution (in the sense of dimensional relevancy) to the Hamiltonian will be a quadratic form in the order parameter $H[\phi] = \frac{r}{2}\int d^d x\, \phi^2(\mathbf{x},t) + \dots$ In this case, the current reduces to $\mathbf{j} = -Dr \quad \phi + \dots$, which is a generalization of Fick's law.

where $\int dx \equiv \int d^dx dt$. A "Wick rotation" $\psi \to -i\psi$ finally brings us to the finite dimensional generalization of the **MSRJD–functional**

$$\boxed{\langle \mathcal{O}[\phi]\rangle_\xi = \int D(\phi,\psi)\, \mathcal{O}[\phi]\, e^{\int dx\, \psi(x)\left(\partial_t\phi(x) + D(-\Delta)^n \frac{\delta H[\phi]}{\delta\phi(x)}\right) + \int dx dx'\, \psi(x) K(x-x')\psi(x')}.} \tag{10.73}$$

As in the zero–dimensional cases above, we may integrate over the momentum field ψ to obtain the generalized **Onsager–Machlup functional**

$$\langle \mathcal{O}[\phi]\rangle_\xi = \int D\phi\, \mathcal{O}[\phi]\, e^{-\frac{1}{4}\int dx \left(\partial_t\phi(x) + D(-\Delta)^n \frac{\delta H[\phi]}{\delta\phi(x)}\right) K^{-1}(x-x') \left(\partial_t\phi(x') + D(-\Delta)^n \frac{\delta H[\phi]}{\delta\phi(x')}\right)}, \tag{10.74}$$

where K^{-1} is the inverse of the noise kernel.

INFO It is an instructive exercise to derive from Eq. (10.74) a **functional variant of the Fokker–Planck equation** – "functional" because the distribution function we are after, $P_t[\phi]$, is a functional of ϕ, and the partial derivatives $\partial_{n_i} P(n,t)$ appearing in the standard Fokker–Planck operator (cf. Eq. (10.22)) become functional derivatives. (To avoid the simultaneous appearance of rectangular and conventional brackets, we denote the time argument in $p_t[\phi]$ by an index.)

Our starting point is the Onsager–Machlup functional for the probability functional,

$$\begin{aligned} p_t[\phi] &\equiv \left\langle \prod_{\mathbf{x}} \delta(\phi(\mathbf{x}) - \phi(\mathbf{x},t)) \right\rangle \\ &= \int\limits_{\phi(\mathbf{x})=\phi(\mathbf{x},t)} D\phi\; e^{-\frac{1}{4}\int dx dx'\, (\partial_t\phi(x) - F[\phi](x)) K^{-1}(x-x') \left(\partial_t\phi(x') - F[\phi](x')\right)}, \end{aligned}$$

where we have introduced the abbreviation $F[\phi](x) \equiv -D(-\Delta)^n \frac{\delta H[\phi]}{\delta\phi(x)}$, and $\phi = \{\phi(\mathbf{x})\}$ is the argument of $p_t[\phi]$ while $\phi(\mathbf{x},t)$ is the $(d+1)$-dimensional integration variable.

As a first step towards the derivation of a Fokker–Planck equation, we switch back to a time discretized representation, $p_t \to p_l$, where $l = t/\delta$ is an integer counting variable and δ a small time increment. The Ito-time discretized Onsager–Machlup functional then reads as

$$p_l[\phi] = \int\limits_{\phi(\mathbf{x})=\phi_l(\mathbf{x})} D\phi\; e^{-\frac{\delta}{4}\sum_{k=0}^{l-1} \mathcal{O}[\phi_{k+1},\phi_k]}, \tag{10.75}$$

where $\mathcal{O}[\phi,\phi']$ is shorthand for

$$\mathcal{O}[\phi,\phi'] \equiv \int d^dx d^dx' \left(\frac{1}{\delta}(\phi-\phi') - F[\phi']\right)(\mathbf{x}) K^{-1}(\mathbf{x}-\mathbf{x}') \left(\frac{1}{\delta}(\phi-\phi') - F[\phi']\right)(\mathbf{x}').$$

We next have to realize that the integral over the first $l-1$ fields ϕ_k above defines the probability distribution p_{l-1}:

$$p_l[\phi] = \int D\phi_{l-1}\, e^{-\frac{\delta}{4}\mathcal{O}[\phi,\phi_{l-1}]}\, p_{l-1}[\phi_{l-1}] = \int D\mu\, e^{-\frac{\delta}{4}\mathcal{O}[\phi,\phi-\mu]}\, p_{l-1}[\phi-\mu],$$

where in the second equality we have renamed integration variables. Introducing the shorthand notation $\langle f|K|g\rangle \equiv \int d^dx d^dx'\, f(\mathbf{x}) K(\mathbf{x}-\mathbf{x}') g(\mathbf{x}')$, we next represent the operator $\mathcal{O}[\phi,\phi-\mu]$ as

$$\mathcal{O}[\phi,\phi-\mu] = \left.\frac{\mu}{\delta} - F[\phi-\mu]\right| K \left|\frac{\mu}{\delta} - F[\phi-\mu]\right. .$$

Using the abbreviation $\langle \dots \rangle \equiv \int D\mu\, e^{-\frac{1}{4\delta}\ \mu|K|\mu\rangle}(\dots)$, an expansion to leading order in δ – the structure of the Gaussian weight entails that each power of μ scales as $\delta^{1/2}$ – then obtains

$$\begin{aligned} p_l[\phi] = &\quad \left(1+\frac{1}{2}\langle\mu|K|F[\phi]\rangle - \frac{1}{2}\ \ \mu|K|\frac{\delta F[\phi]}{\delta\phi}\mu\ \ + \frac{1}{8}\left(\langle\mu|K|F[\phi]\rangle\right)^2 - \frac{\delta}{4}\langle F[\phi]|K|F[\phi]\rangle\right) \\ &\times\left(p_{l-1}[\phi] - \left\langle\frac{\delta p_{l-1}[\phi]}{\delta\phi}\Big|\mu\right\rangle + \frac{1}{2}\left\langle\mu\left|\frac{\delta^2 p_{l-1}[\phi]}{\delta\phi\delta\phi}\right|\mu\right\rangle\right) \\ = &\ p_{l-1}[\phi] - \delta\left\langle\frac{\delta p_{l-1}[\phi]}{\delta\phi}\Big|F[\phi]\right\rangle - \delta\left\langle 1\Big|\frac{\delta F[\phi]}{\delta\phi}\right\rangle p_{l-1}[\phi] - \frac{\delta}{4}\langle F[\phi]|K|F[\phi]\rangle p_{l-1}[\phi] \\ &+\frac{\delta}{4}\langle F[\phi]|K|F[\phi]\rangle p_{l-1}[\phi] + \delta\mathrm{tr}\left(K\frac{\delta^2 p_{l-1}[\phi]}{\delta\phi\delta\phi}\right). \end{aligned}$$

Here, $\frac{\delta p[\phi]}{\delta\phi\delta\phi} \equiv \frac{\delta p[\phi]}{\delta\phi(\mathbf{x})\delta\phi(\mathbf{x}')}$. Dividing by δ, taking the limit $\delta\to 0$, and switching back to a continuous time notation we obtain

$$\partial_t p_t[\phi] + \left\langle\frac{\delta p_t[\phi]}{\delta\phi}\Big|F[\phi]\right\rangle + \left\langle 1\Big|\frac{\delta F[\phi]}{\delta\phi}\right\rangle p_t[\phi] - \mathrm{tr}\left(K\frac{\delta^2 p_t[\phi]}{\delta\phi\delta\phi}\right) = 0,$$

or, in a coordinate resolved notation,

$$\boxed{\partial_t p_t[\phi] - D\int d^dx\frac{\delta}{\delta\phi(\mathbf{x})}\left((-\Delta)^n\frac{\delta H[\phi]}{\delta\phi(\mathbf{x})}p_t[\phi]\right) - \int d^dx d^dx'\, K(\mathbf{x}-\mathbf{x}')\frac{\delta^2 p_t[\phi]}{\delta\phi(\mathbf{x})\delta\phi(\mathbf{x}')} = 0.} \tag{10.76}$$

Equation (10.76) is a functional generalization of the **Fokker–Planck equation**. Roughly speaking, $(-\Delta)^n\delta H/\delta\phi$ replaces the "friction coefficient" of the finite dimensional equation, i.e. the instance that drives the distribution towards a relaxation equilibrium. The "diffusion term" is controlled by the correlation matrix of the noise.

So far, we have not specified the noise kernel, K. However, we expect that in equilibrium it relates in a definite way to the drift term – the fluctuation dissipation theorem. By "equilibrium" we mean a time-independent distribution of generalized Maxwell–Boltzmann type,

$$p_{\mathrm{eq}}[\phi] \equiv \mathcal{N}e^{-\frac{1}{T}H[\phi]}, \tag{10.77}$$

where $\mathcal{N}$ effects normalization. We now show that the condition that p_{eq} is a solution imposes a condition on the form of K. Substitution of Eq. (10.77) into (10.76) indeed obtains

$$\begin{aligned} &-D\int d^dx\left(\frac{\delta}{\delta\phi(\mathbf{x})}(-\Delta)^n\frac{\delta H[\phi]}{\delta\phi(\mathbf{x})}\right) + \frac{D}{T}\int d^dx(-\Delta)^n\frac{\delta H[\phi]}{\delta\phi(\mathbf{x})}\frac{\delta H[\phi]}{\delta\phi(\mathbf{x})} \\ &+\frac{1}{T}\int d^dx d^dx' K(\mathbf{x}-\mathbf{x}')\left[\left(\frac{\delta}{\delta\phi(\mathbf{x})}\frac{\delta H[\phi]}{\delta\phi(\mathbf{x}')}\right) - \frac{1}{T}\frac{\delta H[\phi]}{\delta\phi(\mathbf{x})}\frac{\delta H[\phi]}{\delta\phi(\mathbf{x}')}\right] = 0. \end{aligned}$$

This equation is solved provided that we declare that

$$K(\mathbf{x}-\mathbf{x}') = DT(-\Delta)^n\delta(\mathbf{x}-\mathbf{x}'). \tag{10.78}$$

Notice that for a Hamiltonian functional that is local in ϕ (think of $H[\phi] = \frac{1}{2}\int d^dx((\partial\phi)^2 + r\phi^2 + \dots)$) the functional derivatives appearing in the Fokker–Planck equation are singular (for example, $\frac{\delta^2}{\delta\phi(\mathbf{x})\delta\phi(\mathbf{x})}H[\phi] = -(\partial^2+r)\delta(0)$, etc.) and need regularization. However, for the purposes of our present discussion, a symbolic understanding of the derivatives is sufficient.

To conclude, let us summarize several "take home messages" implied by the construction above:

The concept of a Fokker–Planck equation affords a generalization to finite dimensional problems.
However, such an equation involves an infinite dimensional partial integro-differential equation which does not look very inviting.
We do not have to solve the equation explicitly to verify that the underlying generalized Langevin equation relaxes to a Maxwell–Boltzmann (or Gibbs) equilibrium configuration, provided that
the noise correlator is chosen appropriately.

Finally, it is worth noting that the strategy pursued above, i.e. the construction of an integral recursion equation in discrete time space (Eq. (10.75)), followed by a Taylor expansion in the incremental variables, reflects a general scheme for the derivation of transfer matrix type equations.

10.6.3 Field theory of finite dimensional stochastic processes

Problems in reaction kinetics or population dynamics are often encoded in terms of **master equations defined on a finite dimensional lattice**,

$$\partial_t p_t[n] = \sum_{n'} \left(W[n, n'] p_t[n'] - W[n', n] p_t[n] \right). \tag{10.79}$$

The notation $P_t[n]$ indicates that the distribution depends on the "function" $\{n_i\}$ where i is a lattice point and n_i a container variable comprising all relevant local information (the local concentrations $A_i, B_i, \ldots$ of chemicals, etc.). The transition rates, $W[n, n']$ depend, likewise, on lattice functions. In many applications, transition rates W describe a competition of diffusive spreading (a random walk on a lattice) and particle reactions. Systems of this kind are termed **reaction–diffusion systems**. Field theories for reaction–diffusion systems can be obtained by straightforward generalization of the $(0 + 1)$-dimensional techniques introduced in Sections 10.5.1 and Eq. (10.61).

By way of example, consider a pure extinction process, $A \xrightarrow{\lambda} \emptyset$ wherein a certain agent A perishes at a constant rate. Defining $n_i \equiv (\#$ of As at lattice site $i)$, we may then ask how the probability $p_t[n]$ evolves under the joint influence of annihilation and diffusive spreading. A field theory representation of this process can be obtained by generalization of the Doi–Peliti operator algebra,

$$\begin{aligned} a_i |\ldots, n_i, \ldots\rangle &= |\ldots, n_i - 1, \ldots\rangle, \\ \bar{a}_i |\ldots, n_i, \ldots\rangle &= (n_i + 1) |\ldots, n_i + 1, \ldots\rangle, \end{aligned} \tag{10.80}$$

where we represent the population $\{n_i\}$ in terms of a Fock space state. Again, the operator algebra obeys canonical commutation relations, $[a_i, \bar{a}_j] = \delta_{ij}$. A straightforward extension of our discussion of Section 10.5.3 shows that the Hamiltonian generating the stochastic process above is given by

$$\hat{H} = -D \sum_{ij} \bar{a}_i \Delta_{ij} a_j - \lambda \sum_i \bar{a}_i (1 - a_i), \tag{10.81}$$

where Δ_{ij} is the lattice Laplacian and D a diffusion constant. The corresponding coherent state field integral action then reads

$$S[\bar{\psi},\psi] = \int d^d x dt \left[\bar{\psi}(\partial_t - D\Delta)\psi - \lambda\bar{\psi}(1-\psi)\right], \tag{10.82}$$

where we have switched to a continuum notation.

EXERCISE We may also derive a field theory by generalization of the techniques introduced in Section 10.5.2. Derive the corresponding action and show that it relates to Eq. (10.82) by a Cole–Hopf transformation.

10.6.4 Fluctuation–dissipation theorem (revisited)

The field theories above represent our most general descriptions of non-equilibrium many particle systems. A question that frequently arises in applications is whether or not a given system is in thermal equilbrium. A straightforward answer to this question may be given as follows: compute the long time stationary probability distribution and check whether it is of Maxwell–Boltzmann form. This procedure is generally valid but can be unnecessarily cumbersome in practice. (You have to compute the stationary distribution first, and this can be hard.) Often, it is more efficient to check whether the fluctuation–dissipation theorem – a hallmark of equilibrium systems – is fulfilled. Now, we have encountered the FDT in many different forms and contexts. Given its practical importance, it is worthwhile to briefly summarize some of the more important incarnations. The last of these, a formulation of the FDT for a linear variant of MSRJD field theory, plays an important role in the applications below.

FDT I: Equilibrium linear response

In Chapter 7 we discussed the apparatus of linear response for equilibrium systems. We considered the expectation value of certain observables $\hat{X}(x)$[36] (with $x = (\mathbf{x}, t)$ as usual). Assuming that $\hat{X}$ is conjugate to a generalized "force," F, and that $X(x) \equiv \langle \hat{X}(x)\rangle = 0$ in an unbiased situation, we considered the linear relation

$$X(\omega) = \chi(\omega)F(\omega) + \mathcal{O}(F^2), \tag{10.83}$$

where $\chi(\omega)$ defines a **generalized susceptibility**. Equation (10.83) establishes a connection between a macroscopic force (F) and a macroscopic observable (X) in a "bath" containing a large number of microscopic degrees of freedom. In this sense, χ is a quantity probing "dissipative" physical processes. In Section 7.3 we showed that

$$\chi(\omega) = C^+(\omega) = -i\Theta(t)\langle[\hat{X}(t), \hat{X}(0)]\rangle,$$

where C^+ was the **retarded response function**. We then established a connection between C^+ and another correlation function, the **time ordered correlation function**,

$$C^T(t) \equiv -i\langle T_t \hat{X}(t)\hat{X}(0)\rangle,$$

[36] Chapter 7 was formulated for quantum theories, but that aspect will not be of relevance throughout.

which describes "fluctuations" of the observable X. Specifically, we found that (cf. Eq. (7.21))

$$\mathrm{Im}\, C^T(\omega) = \mathrm{Im}\, C^+(\omega) \coth(\beta\omega/2). \tag{10.84}$$

This is the **quantum fluctuation dissipation theorem**. We next wish to explore what happens to this relation in the classical limit.

In the **classical limit**, $\hat{X} \to X(\mathbf{x})$ becomes a function in phase space (formally, the Wigner transform of the operator $\hat{X}$. For more information on the Wigner transform, see Section 11.5.1), the time dependence, $\hat{X}(t) \to X(\mathbf{x}(t))$ resides in the classical time evolution of the argument, and the time ordering of operators involved in the definition of C^T becomes inessential. This means that the classical limit of the time ordered correlation function is given by

$$C^T_{\mathrm{cl}}(t) = \langle X(t)X(0)\rangle,$$

where

$$\langle X(t)X(0)\rangle \equiv \int_\Gamma d^d x\, \rho(\mathbf{x}) X((\mathbf{x}(t))X(\mathbf{x}).$$

It is not difficult to verify that the Fourier transform $C_{\mathrm{cl}}(\omega) = \mathrm{Im}\, C_{\mathrm{cl}}(\omega)$ is purely imaginary. Likewise, it can be shown that the retarded response function approaches the form $C^+ = \hbar C^+_{\mathrm{cl}}$ – note the extra "$\hbar$" – with

$$C^+_{\mathrm{cl}}(t) = \chi_{\mathrm{cl}}(t) = \Theta(t)\langle\{X(t), X(0)\}\rangle,$$

where the Poisson bracket replaces $(-(i/\hbar)$ times) the quantum commutator. (However, this expression is not too useful in applications. In practice, one will often try to obtain the linear response susceptibility by different means.)

EXERCISE The expressions above, Poisson brackets replacing commutators, etc., contain the "natural" classical counterparts of the quantum formulae. To actually verify their validity, employ the Wigner representation of the operator $\hat{X}$ (cf. Section 11.5.1) and then take the classical limit by leading order expansion in $\hbar$.

Finally, the Fourier argument ω in Eq. (10.84) has the dimension of a frequency. This means, that the bosonic distribution function must be understood as $\coth(\beta\hbar\omega/2) \overset{\hbar \ll T/\omega}{\longrightarrow} \frac{2T}{\hbar\omega}$. Combining everything, we obtain the **classical fluctuation dissipation theorem**

$$\boxed{C(\omega) = \frac{2T}{\omega}\mathrm{Im}\,\chi(\omega),} \tag{10.85}$$

where we removed the subscript "cl." In the theory of steady state phenomena, it is often useful to consider a static variant of the FDT. To this end, let us define the **equal time correlation function** as

$$C \equiv \int \frac{d\omega}{2\pi} C(\omega) = \langle X(0)X(0)\rangle.$$

The analytic properties of $C(\omega)$ and $\chi(\omega)$ (explore this point) then imply the **static version of the FDT**,

$$\boxed{C = T\chi(0).} \tag{10.86}$$

FDT II: linear Langevin equations

In Section 10.2.1 we discussed the FDT within the framework of linear Langevin theory. (Here "linear" means Langevin equations that are linear in the dynamical variable.) We saw that consistency with the equipartition law of equilibrium thermodynamics implies the presence of fluctuations in any dissipative medium. But how does this observation correlate with the linear response picture above?

To understand this connection, let us look at the Langevin oscillator equation

$$\ddot{q} + \omega_0^2 q + \gamma\dot{q} = \xi,$$

where ω_0 is the oscillator frequency and mass has been set to unity. The FDT as discussed in Section 10.2.1 requires that $\langle \xi(t)\xi(t')\rangle = 2\gamma T\delta(t-t')$. In Fourier space, this may be solved as

$$q(\omega) = \chi(\omega)\xi(\omega), \qquad \chi(\omega) = -\frac{1}{\omega^2 - \omega_0^2 + i\gamma\omega}. \tag{10.87}$$

The notation indicates, that the kernel χ can be interpreted as the **dynamical susceptibility** describing the response of the coordinate q to the "driving force" ξ. The point to appreciate here is that the dynamical susceptibility of a system describes both its response to fluctuations (as in Langevin theory) and the response to external driving (as in linear response theory).

The Fourier transform of the dynamical correlation function $C(t) = \langle q(t)q(0)\rangle$ reads as

$$C(\omega) = \frac{2\gamma T}{(\omega^2 - \omega_0^2)^2 + (\omega\gamma)^2} = \frac{2T}{\omega}\mathrm{Im}\,\chi(\omega), \tag{10.88}$$

where we have used the relation $\langle \xi(\omega)\xi(\omega')\rangle = 2\gamma T\delta(\omega+\omega')$. Comparing Eq. (10.88) and Eq. (10.87) we see that the general fluctuation dissipation theorem Eq. (10.85) and the two approaches "FDT from equipartition" and "FDT from linear response" describe different sides of the same coin.

FDT III: MSRJD field theory

In later sections, we explore the collective behavior of many particle systems by field theoretical methods. The FDT will turn out to be an important diagnostic tool to test whether a system is in equilibrium or not. Let us, then, explore how the FDT can be probed within the framework of field theory. To this end we consider the MSRJD functional Eq. (10.73) with noise correlator (10.78). While the FDT Eq. (10.85) is of general validity, we begin by considering linear (free) field theories. Assuming that the relaxation of ϕ is controlled by the quadratic Hamiltonian

$$H[\phi] = \int d^dx \left(\frac{1}{2}(\partial\phi)^2 + \frac{r}{2}\phi^2 - h\phi\right),$$

where the field h will be used to probe the linear response of the system, the corresponding MSRJD functional takes the form

$$\mathcal{Z} \equiv \int D(\phi,\psi)\, e^{\int dx\, [\psi(\partial_t\phi + D(-\Delta)^n(-\Delta\phi + r\phi - h)) + DT\psi(-\Delta)^n\psi]}.$$

Switching to momentum space and introducing a matrix notation,

$$\mathcal{Z} \equiv \int D(\phi,\psi) \exp\left(-S_0[\phi,\psi] - D\int dq\, \psi_q q^{2n} h_{-q}\right),$$
$$S_0[\phi,\psi] = -\frac{1}{2}\int dq\, (\phi,\psi)_{-q} \begin{pmatrix} 0 & (g^-)^{-1} \\ (g^+)^{-1} & 2DTq^{2n} \end{pmatrix}_q \begin{pmatrix} \phi \\ \psi \end{pmatrix}_q,$$

where $\int dq \equiv \int \frac{d^d k d\omega}{(2\pi)^{d+1}}$, $g_q^{\pm} \equiv \left(\mp i\omega + Dk^{2n}(k^2+r)\right)^{-1}$, and we are using an index notation g_q, instead of $g(q)$ for improved notational clarity.[37] Now, let us employ this functional to compute the dynamic susceptibility. Due to the evenness of S_0 in the fields, $\langle\phi\rangle_0 = 0$, where $\langle\ldots\rangle_0 \equiv \int D(\phi,\psi)\exp(-S_0[\phi,\psi])$. To leading order in the driving field, we thus obtain

$$\langle\phi_q\rangle \simeq D\int dq'\, \langle\phi_q\, q'^{2n}\, \psi_{-q'}\rangle h_{q'} = Dg_q^+ q^{2n} h_q \equiv \chi_q h_q.$$

This leads to the identification $\chi(q) = Dq^{2n} g_q^+$. On the other hand, the fluctuation correlation function is given by

$$C(q) = \int dq' \langle\phi_q\phi_{q'}\rangle_0 = 2DTq^{2n} g_q^+ g_q^- = \frac{2T}{\omega}\mathrm{Im}\chi_q,$$

consistent with the FDT. This consideration shows that the *free* equilibrium field theory conforms with the FDT. However, it is much more challenging to show that this compatibility pertains to the interacting case. In practical applications, one will want to verify (for example by perturbative methods, or by renormalized perturbation theory) that (a) the equilibrium theory does obey the FDT. One may then proceed to (b) detect deviations from equilibrium by violations of the FDT.

INFO In the theory of continuum systems, the correlation function $C(q) \equiv C(\mathbf{q},\omega) \equiv S(\mathbf{q},\omega)$ is often referred to as the **dynamic structure factor**. This notation alludes to the fact that the function $C(\mathbf{q},\omega)$ describes spatio-temporal fluctuations in the system at the characteristic length scale $|\mathbf{q}|^{-1}$ and time scale ω^{-1}. The FDT establishes a connection between the dynamic structure factor and the dynamic susceptibility. Likewise, the static version of the FDT Eq. (10.86) relates the **static structure factor** $C(\mathbf{q}) \equiv S(\mathbf{q})$ to the static susceptibility.

Finally, note that we may be confronted with a system that is kept at some predetermined noise level (possibly determined by the action of an underlying microscopic agent, or due to coupling to an external environment). One may then argue that an effective equilibrium emerges wherein the noise strength *determines* the effective temperature by way of the FDT condition.

[37] If you find the sign-difference between the retarded and the advanced Green function unfamiliar, keep in mind that we are considering irreversible dynamics. Compute the time representation of $g^{\pm}$ for the case $n = 0$, $r = 0$, to show that the sign properly distinguishes between retarded and advanced propagation.

10.7 Field theory III: applications

Having invested considerable effort into deriving various field theories of nonequilibrium systems, it is now time to apply the formalism. However, before doing so, let us identify a number of questions we may want to address:

- ▷ In Section 10.5.2 we assumed knowledge of a certain "Hamiltonian" $H[\phi]$ that drives the order parameter field ϕ to an equilibrium configuration. But how can such a Hamiltonian be motivated and constructed for concrete physical systems?
- ▷ What can field theory say about the different phases realized in and out of equilibrium?
- ▷ And what can be said about the transitions between these phases? The theories constructed above bear structural similarity to different equilibrium theories discussed earlier in the text. To what extent can concepts developed earlier for equilibrium systems (the notion of upper and lower critical dimension, mean field theory, renormalized theory of fluctuations, etc.) be generalized to the present context?
- ▷ How do critical correlations reflect in the dynamical behavior of a system?

These are but a few questions that can be asked. Rather than attempting to find general answers, we shall address some of these questions on two specific examples. Even so, our discussion will be rather superficial and can provide little more than a glimpse of the theory of nonequilibrium critical phenomena. (Some guides to further reading are given below.)

10.7.1 Driven diffusive lattice gases

Imagine yourself confronted with the following exercise: engineer a genuine many particle system (a system containing particle dynamics and interaction) that is (a) simple, (b) couples to an efficient mechanism driving an out-of-equilibrium situation, and (c) reduces to one of the "large" universality classes of physics in the equilibrium limit. It is actually not so easy to come up with a good answer.

One system that meets these criteria reasonably well is the **driven diffusive lattice gas** (see Fig. 10.10). As is indicated by the name, it involves a system of particles hopping on a lattice. The particles may hop from one site to the next at some rate t, and are subject to nearest neighbour repulsion as described by the Hamiltonian

$$H[n] \equiv J \sum_{\langle ij \rangle} n_i n_j. \tag{10.89}$$

Here $n_{i,j} \in \{0, 1\}$ reflecting that each site can be occupied by one particle at most. For simplicity we imagine periodic boundary conditions in all directions, i.e. the system lives on a d-dimensional torus.

We next allow the particles to hop between nearest neighbour lattice sites (subject to the condition of no more than single occupancy). This will render the system dynamical and allow it to settle in a configuration compromising between single particle dynamics and interactions. To see this more clearly, imagine the dynamics described in terms of a master equation. Interactions will influence transition rates in this equation, but not change the configurations by themselves. Above we have seen that the changes in the configurations

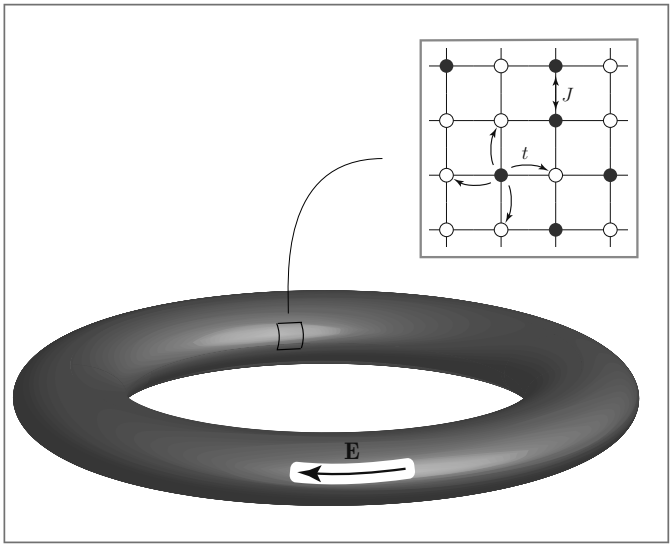

Figure 10.10 The driven diffusive lattice gas. A system of nearest neighbour interacting particles hopping on a lattice and subject to periodic boundary conditions. The system is driven by a constant force.

(presently caused by hopping) afford an interpretation in terms of Langevin dynamics.[38] This means, that we may think of the capacity to hop in terms of some effective thermal activation, or noise acting on the system. This noise will enable the gas to settle in an effective equilibrium configuration favoured by the interaction, at an effective temperature set by the hopping rates.

To drive the system out of equilibrium, we introduce a force acting uniformly along one of the directions of the torus. Moving against its action once around the torus (a closed loop) costs energy, i.e. the force is not conservative, and there is no corresponding potential. Rather, we may think about the force as an "electromotive" force due to piercing the torus by a time dependent magnetic field. The coupling to this "work reservoir" gives rise to a nonequilibrium situation. Lack of a conservative potential invalidates descriptions of the system in terms of a Hamiltonian; this is the ultimate motivation to describe it in terms of master equations and effective Langevin equations. In this language, the effect of the force will be a bias in the hopping rates along one of the toroidal directions.

An important preliminary conclusion to be drawn from this consideration is that the equilibrium physics of our system will fall into the **Ising universality class**. Indeed, we may introduce spin variables $S_i = 2n_i - 1 \in \{-1, 1\}$. Expressed in terms of the S_is the interaction Hamiltonian $H[S]$ assumes the form of an Ising Hamiltonian, where the sign of J determines whether the coupling is ferromagnetic or antiferromagnetic. In equilibrium,

[38] A quadratic approximation of the transition generators, the momenta conjugate to the occupation number variables, led to a quadratic contribution to the Hamiltonian action formally equivalent to the averaged noise term in the MSRJD functional.

the system will be described by a Gibbs distribution, $\sim \exp(-H[S]/T)$, at a temperature set by the hopping rates. Introduction of a finite bias is expected to cause departures from the Ising/ϕ^4-universality class.

Summarizing, the driven diffusive lattice gas conforms with the three principles above: it is relatively simple, contains nonequilibrium driving, and relates to the big Ising universality class. Sadly, there do not seem to be any direct experimental realizations of this system, although it may be argued that aspects of its behavior reflect in the physics of ionic conductors, microemulsions of charged particles, and DNA gel electrophoresis.[39]

Our theoretical approach to the system below is organized in a number of steps. After reviewing elements of its microscopic physics, we introduce a mesoscopic theory describing the approach to equilibrium in the unbiased case, as much as the principal effects of the driving mechanism. We expect the consequences of driving to be particularly strong if the system is tuned to its equilibrium transition point. Less evidently, however, it turns out that driving also causes remarkable phenomenological consequences *above* criticality (the "disordered" phase). In our analysis below, we first address the latter regime, and then turn towards the more ambitious study of criticality. It should be emphasized that, to date, many aspects of driven diffusive systems remain poorly understood, and there is lack of direct experimental data. In our discussion of the system, we thus have to draw more liberally than usual from a mix of field theoretical evidence, simulation data, and common sense reasoning. The material assembled below is a fragmentary excerpt from the text by Schmittmann and Zia.[39]

Microscopic formulation

Consider the master equation Eq. (10.79) for the evolution of the lattice gas population. In the absence of an external field, we have a Hamiltonian $H[n]$ assigning to each configuration n an energy. In equilibrium, the system will settle into a configuration described by the distribution,

$$p_{\rm eq}[n] \stackrel{\mathbf{E}=0}{=} \mathcal{N}\exp(-H[n]/T). \tag{10.90}$$

We do not have to specify the transition rates $W[n,n']$ explicitly to say that compatibility with Eq. (10.90) implies the **detailed balance relation**

$$\frac{W[n,n']}{W[n',n]} = \frac{p_{\rm eq}[n]}{p_{\rm eq}[n']} = e^{-\beta(H[n]-H[n'])}. \tag{10.91}$$

This relation is satisfied, e.g., by the choice $W[n,n'] = \text{const.} \times \exp(-\beta(H[n]-H[n'])/2)$. More generally, any $W[n,n'] \equiv f(\beta(H[n]-H[n']))$ with $f(x)/f(-x) = \exp(-x)$ will also do the job. In the presence of a driving field, we do not have a globally defined Hamiltonian any more. Locally, however, we may assign to a configuration n an "energy" that increases if we move against the field. Modeling the dynamics in terms of transitions $n \to n'$ that involve only local changes in the configuration, we may generalize according to

$$W[n,n'] \to f(\beta(H[n]-H[n']+kaE)),$$

[39] B. Schmittmann and R. K. P. Zia, *Statistical Mechanics of Driven Di usive Systems*, (Academic Press,1995).

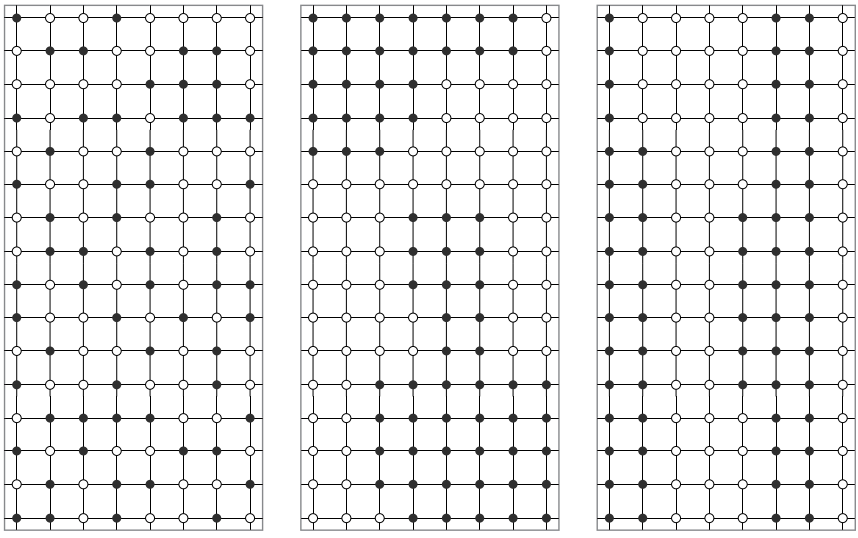

Figure 10.11 Three phases of the driven diffusive lattice gas. Left: disordered (unmagnetized) phase at high temperatures. Center: ordered (magnetized) islands at low temperatures and zero field. Right: ordered (magnetized) stripes at low temperatures in the presence of a driving field.

where a is the lattice spacing and k the number of steps particles have to climb against the direction of the field E to get from configuration n' to n.

Suppose we have modelled the system in terms of transition rules satisfying the above constraints. The corresponding master equation is the starting point for **computer simulations**. Given the lack of experimental data, and the relative unfamiliarity of the system, such simulations[40] have played an important role in guiding analytical work: not surprisingly, it has been confirmed that the field-free system falls into the Ising universality class. However, contrary to the standard Ising model, the total magnetization $\langle M \rangle \equiv \sum_i S_i \equiv 2 \sum_i n_i - N$ (N is the total number of lattice sites) is conserved in our system. This means that, above a critical temperature T_c, the system will be in a "disordered" phase, i.e. particles spread randomly across the lattice (see Fig. 10.11 left). Below T_c, we enter an ordered phase characterized by the presence of magnetized domains (particle clusters). The total area of spin up and spin down domains is determined by the concentration of particles in the system (Fig. 10.11 middle). A cursory inspection of numerical data may lead to the impression that above T_c, the application of a field has not much of an effect. We will see, however, that this is not the case. Finally, it has been found numerically that below T_c and for $\mathbf{E} \neq 0$, the magnetized areas arrange in stripes parallel to the field direction (see Fig. 10.11 right).

[40] S. Katz, J. L. Lebowitz, and H. Spohn, Nonequilibrium steady states of stochastic lattice gas models of fast ionic conductors, *J. Stat. Phys.* **34**, 497-537 (1984).

Below we try to explain aspects of these observations analytically. In principle, master equations based on the transition rates $W[n, n']$ may serve as a starting point towards the construction of an analytical theory, along the lines of our discussion in Section 10.6.3. However, the reduction of the resulting "microscopic field theory" to an effective long range theory will arguably be laborious. Instead, we will build our construction on a "mesoscopic formulation" wherein the dynamics of the site occupancy is described in coarse-grained terms.

Mesoscopic formulation

To provide coarse-grained description of the system, we describe its state in terms of its continuous magnetization $\phi(\mathbf{x}, t) \equiv \langle 2n(\mathbf{x}, t)\rangle - 1\rangle$, where $\langle \dots \rangle$ is symbolic for an average over many lattice sites. Let us consider the field free case first. We then know from our discussion in section 5.1, that the effective Hamiltonian governing the static profile of the magnetization variable in the absence of driving is the ϕ^4-functional,

$$H[\phi] = \frac{1}{2}\int d^d x \left((\partial\phi)^2 + r\phi^2 + \frac{u}{12}\phi^4\right). \tag{10.92}$$

This Hamiltonian will determine the form of the Langevin equation. Second, we know that magnetization is a "conserved quantity," $\int d^d x\, \phi = \text{const}$, by virtue of particle number conservation. Thus, our model belongs to class B in the classification of Section 10.6.2, and we may write down an effective Langevin equation of motion,

$$\partial_t \phi = D\Delta \frac{\delta H[\phi]}{\delta \phi} + \partial \cdot \xi = D\Delta\left(r\phi - \partial^2\phi + \frac{u}{6}\phi^3\right) + \partial \cdot \xi. \tag{10.93}$$

Here we have absorbed the derivatives appearing in the model B noise correlator Eq. (10.78) into the definition of a vectorial noise field $\langle \xi_i(x)\xi_{i'}(x')\rangle = 2A\delta_{ii'}\delta(x - x')$, and the constant A determines the effective equilibrium temperature as $A = DT$.

Let us now explore what happens once driving is switched on. As discussed above, the Hamiltonian cannot accommodate the **non-conservative driving field**. However, we may argue that the right–hand side of the Langevin equation represents the divergence of a current. An external field will cause a current that (i) is proportional to the field $\mathbf{E}$ in direction and strength, and (ii) vanishes if neither particles nor holes are present. This motivates the *ansatz*,

$$\mathbf{j} = 4n(1 - n)\mathbf{E} = (1 - \phi^2)\mathbf{E}, \tag{10.94}$$

where a constant of proportionality has been absorbed in a redefined $\mathbf{E}$. The addition of the divergence of this current to the right–hand side of Eq. (10.93) will generate the bare version of a generalized Langevin equation. However, we must keep in mind that the **strong anisotropy** introduced by the field will, by way of renormalization, render the effective parameters of the Langevin anisotropic as well. This motivates the more general anisotropic representation

$$\partial_t \phi = D\left[\left(r\hat{\partial}^2 - \alpha\partial^4 + \hat{r}\hat{\partial}^2 - \hat{\alpha}\hat{\partial}^4 - \beta\partial^2\hat{\partial}^2\right)\phi + E\partial\phi^2 + \frac{1}{3!}\left(u\partial^2 + \hat{u}\hat{\partial}^2\right)\phi^3\right] - \partial\xi - \hat{\partial}\cdot\hat{\xi}, \tag{10.95}$$

where quantities carrying a caret refer to the $d-1$ directions transverse to the field, and the various coefficients account for the possibility of anisotropic renormalization. Accordingly, the effective noise correlator takes the form

$$\begin{aligned}\langle \xi(x)\xi(x')\rangle &= 2A\delta(x-x'),\\ \langle \hat{\xi}_i(x)\hat{\xi}_{i'}(x')\rangle &= 2\hat{A}\delta_{ii'}\delta(x-x').\end{aligned} \tag{10.96}$$

The MSRJD functional of this equation (cf. Eq. (10.53)) is given by $\mathcal{Z} = \int D(\phi,\psi)\, e^{-S[\phi,\psi]}$, where

$$\begin{aligned}S[\phi,\psi] = \int dx \Big(\psi\Big(\partial_t\phi - D\Big[\Big(r\partial^2 - \alpha\partial^4 + \hat{r}\hat{\partial}^2 - \hat{\alpha}\hat{\partial}^4 - \beta\partial^2\hat{\partial}^2\Big)\phi \\ + E\partial\phi^2 + \frac{1}{3!}\Big(u\partial^2 + \hat{u}\hat{\partial}^2\Big)\phi^3\Big]\Big) + A(\partial\psi)^2 + \hat{A}(\hat{\partial}\psi)^2\Big).\end{aligned} \tag{10.97}$$

In the following sections we aim to extract some physical information from this seemingly formidable expression.

Above criticality: consequences of FDT violation

Let us consider the system at temperatures $T > T_c$ far above its ordering transition. Drawing upon our experience with equilibrium physics, we expect the system to be in a disordered state, void of any long range (power law) correlations. Remarkably, however, the physics of the driven system turns out to be different. We will see that the external field leads to long range correlations and critical phenomena even in the high temperature regime.

Following the standard logic in the theory of continuous phase transitions we assume that, for $T > T_c$, the intrinsic nonlinear terms (such as $\sim \psi\phi^3$) provide subleading contributions to the dynamics. Alluding to their low operator relevance, we will also neglect all terms containing more than two gradient operators. We thus consider the bare action

$$S[\phi,\psi] = \int dx\, \left(\psi\left(\partial_t\phi - D\left[r\Delta\phi + E\partial\phi^2\right]\right) - A\psi\Delta\psi\right),$$

where we have anticipated that the bare theory is isotropic, $A = \hat{A}$ and $r = \hat{r}$ and the driving term provides the only non-Gaussian contribution to the action. The importance of the driving term can be assessed by computing its engineering dimension. To this end, let us consider the effect of a rescaling $\mathbf{q} \to \mathbf{q}' \equiv \mathbf{q}b^{-1}$. Requiring that all Gaussian terms in the action remain scale invariant, we obtain the relations

$$\begin{aligned}\mathbf{q}' &= b^{-1}\mathbf{q}, \qquad t' \to b^{-2}t,\\ \phi' &= b^{\frac{d}{2}}\phi, \qquad \psi' = b^{\frac{d}{2}}\psi.\end{aligned}$$

Substituting the rescaled quantities into the action, we are led to the renormalization $E' = b^{-\frac{d}{2}+1}E$. Thus, the upper critical dimension of our nonlinearity is $d_c = 2$. Below $d = 2$, the driving term is relevant, at $d = 2$ it is marginal, and above irrelevant.

However, it would be premature to conclude that in dimensions $d > 2$, driving has no physical effects! To appreciate this point, imagine that on the short distance scales $|\mathbf{q}| \sim l$ where the renormalization process is started, our action is isotropic in that $r(l) = \hat{r}(l)$ and

$A(l) = \hat{A}(l)$. In the course of renormalization, the effective strength of E will diminish (exponentially, if $d > 2$). However, the residual $E(L)$ will also renormalize the coupling constants of the Gaussian model, and it will do so in an anisotropic manner.

EXERCISE Identify the interaction processes that cause the renormalization of the coupling constants. You may want to formulate the RG equations?

At large length scales, we thus have an effective Gaussian model, $E = 0$, which, however, is anisotropic. In other words, we have a **family of Gaussian fixed points**, each described by a free action

$$\begin{aligned} S[\phi,\psi] &= \int dx \, \left(\psi\left(\partial_t\phi - D\left(r\partial^2 + \hat{r}\hat{\partial}^2\right)\phi\right) + A(\partial\psi)^2 + \hat{A}(\hat{\partial}\psi)^2\right) \\ &= \frac{1}{2}\int dq\,(\phi,\psi)_{-q}\begin{pmatrix} & (g^-)^{-1} \\ (g^+)^{-1} & 2(Ak^2+\hat{A}\hat{k}^2)\end{pmatrix}_q \begin{pmatrix}\phi\\ \psi\end{pmatrix}_q, \end{aligned}$$

where $g_q^{\pm} = (\mp i\omega + D(rk^2 + \hat{r}\hat{k}^2))^{-1}$, and $q = (\mathbf{k},\omega)$ with $\mathbf{k} = (k,\hat{k})^T$. As we are going to show next, each of these actions exhibits "critical behavior" in that it generates anisotropic power law correlations in the system. Indeed, consider the dynamic structure factor

$$S(\mathbf{k},\omega) = \int dq' \,\langle\phi_q\phi_{q'}\rangle = 2(Ak^2 + \hat{A}\hat{k}^2)g_q^+ g_q^- = 2\frac{Ak^2+\hat{A}\hat{k}^2}{\omega^2 + D^2(rk^2+\hat{r}\hat{k}^2)^2}. \tag{10.98}$$

Integration over ω generates the **static structure factor**

$$S(\mathbf{k}) = \int \frac{d\omega}{2\pi} S(\mathbf{k},\omega) = \frac{1}{D}\frac{Ak^2+\hat{A}\hat{k}^2}{rk^2+\hat{r}\hat{k}^2}. \tag{10.99}$$

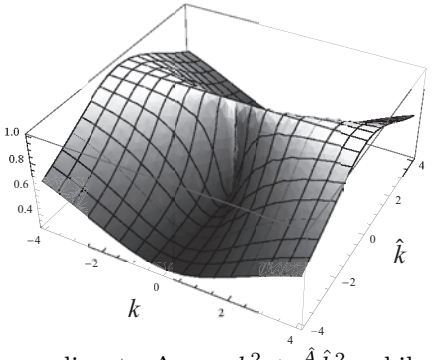

In equilibrium, the FDT enforces the fraction on the right hand side of this equation to equal unity. To appreciate this point, remember our discussion at the end of Section 10.6.2. We had seen that a (model B) system may relax to equilibrium if the noise correlator is weighted by a Laplace operator (cf. Eq. (10.78)) which compensates for the Laplace operator in Eq. (10.71). In the present context, both operators get renormalized to anisotropic second order differential operators. Specifically, the noise- or "fluctuation" Laplace operator gets renormalized according to $\Delta_f \to k^2 + \frac{\hat{A}}{A}\hat{k}^2$, while the "dissipation" operator becomes $\Delta_d \to k^2 + \frac{\hat{r}}{r}\hat{k}^2$. An equilibrium configuration at some effective temperature T_{eff} can be approached (cf. the construction above Eq. (10.78)), if and only if $\Delta_f \propto \Delta_d$. While this does not necessarily imply isotropy in space, a minimal requirement reads

$$w \equiv \frac{A\hat{r}}{\hat{A}r} = 1.$$

This condition entails $S(\mathbf{k}) = \text{const.}$. Equivalently, violation of the FDT condition $w = 1$ implies singular (albeit finite) behavior of the structure factor. The singularity can, e.g., be characterized by the ratio

$$R \equiv \frac{S(0, \hat{k} \to 0)}{S(k \to 0, 0)}.$$

The anisotropy singularity of the structure factor implies power law correlations in coordinate space. To see this, let us consider the case $d = 3$ for concreteness and compute the Fourier transform

$$\begin{aligned} S(\mathbf{x}) &\equiv \int \frac{d^3k}{(2\pi)^3} e^{i\mathbf{k}\cdot\mathbf{x}} S(\mathbf{k}) \propto \int d^3k\, e^{i(xk+\hat{\mathbf{x}}\cdot\hat{\mathbf{k}})} \frac{\frac{A}{\tilde{A}}k^2 + \hat{k}^2}{\frac{r}{\tilde{r}}k^2 + \hat{k}^2} \propto \int d^3k\, e^{i(\tilde{x}k+\hat{\mathbf{x}}\cdot\hat{\mathbf{k}})} \frac{wk^2 + \hat{k}^2}{|\mathbf{k}|^2} \\ &= -(w\partial_{\tilde{x}}^2 + \partial_{\hat{x}}^2) \int d^3k\, e^{i(\tilde{x}k+\hat{\mathbf{x}}\cdot\hat{\mathbf{k}})} \frac{1}{|\mathbf{k}|^2} \propto (w\partial_{\tilde{x}}^2 + \partial_{\hat{x}}^2) \frac{1}{(\tilde{x}^2 + \hat{x}^2)^{1/2}} \\ &= (w-1)\partial_{\tilde{x}}^2 \frac{1}{(\tilde{x}^2 + \hat{x}^2)^{1/2}} = (w-1) \frac{2\tilde{x}^2 - \hat{x}^2}{(\tilde{x}^2 + \hat{x}^2)^{5/2}}, \end{aligned}$$

where $\tilde{x} = (\hat{r}/r)x$ is a rescaled coordinate and in the third line we discarded a contribution $(\partial_{\tilde{x}}^2 + \partial_{\hat{x}}^2)\frac{1}{(\tilde{x}^2+\hat{x}^2)^{1/2}} \propto \delta(|\mathbf{x}|)$, because our effective theory holds only for large $|\mathbf{x}|$ anyway.

We thus come to the surprising conclusion that

> the high temperature ("disordered") phase of the system supports power law correlations in coordinate space.

These correlations reflect the presence of a line of inequivalent Gaussian fixed point theories.

INFO Can these power law correlations above criticality actually be **observed in real systems?** Anisotropies in the structure factor such as those shown in the figure above have actually been measured in uniaxial ferromagnets with dipolar interactions[41] However, these systems support long range correlations on the bare level, and it is not really clear whether they share a universality class with our short range Ising type benchmark model. However, singular behavior in correlation functions is definitely observable in Monte Carlo simulations[40] of the system.

It is also worth noting that the mechanisms whereby long range correlations were generated in our discussion above appear to be of rather general nature: to appreciate this point, consider the temporal decay of correlations in a diffusive environment $C(0,t) \sim t^{-d/2}$. The dynamical exponent of diffusive dynamics is given by $z = 2$. Power counting arguments would then suggest that $C(\mathbf{x}, t) \sim |\mathbf{x}|^{-d}$ at fixed t. However, in equilibrium statistical mechanics, we are more accustomed to *exponentially* decaying correlations (power law correlations indicating criticality being an exception).

Our discussion above signals, that the paradigm "no long range correlations away from criticality" may not have quite as generic a validity as is suggested by the theory of equilibrium. Rather, we saw that violations of the FDT may generate power law correlations far away from critical points.

[41] J. Skalyo, B.C. Frazer, and G. Shirane, Ferroelectric-mode motion in KD_2PO_4, *Phys. Rev. B* **1**, 278-86 (1970).

EXERCISE Retrace the discussion above for an isotropic system with conserved diffusive dynamics. Convince yourself that the FDT enforces vanishing of power law correlations in the correlation function.

Inasmuch as equilibrium (obedience to FDT) is an exception rather than the rule, we may expect that long range correlations in nature are of more frequent occurrence than what is implied by equilibrium statistical mechanics.

The system at criticality

At some critical T_c the system undergoes a transition into its ordered phase. Numerical analysis has shown that, in the presence of strong driving, this ordered phase contains stripes of uniform magnetization. The formation of stripes may be diagnosed by monitoring the behavior of the static structure factor upon changing the temperature. Specifically, we expect that: (i) the proximity to the phase transition point is characterized by some correlation length, ξ. (ii) At length scales larger than ξ, the structure factor will exhibit the $\sim |\mathbf{x}|^{-d}$ scaling discussed in the previous section. (iii) At length scales smaller than ξ we expect **anisotropic scaling**; correlations in the direction parallel to $\mathbf{E}$ will be qualitatively different from those in the transverse direction. In the following, we tune the system right into the critical point and explore its correlation behavior.

However, before doing so, we first have to *identify* the transition point. In equilibrium ϕ^4-theory, the transition occurs when the (renormalized) coefficient, of the quadratic term in the action $\sim \phi^2$ vanishes. Presently, however, we have two such terms, with coefficients r and $\hat{r}$, respectively. This raises the question whether the ordering transition occurs at (i) $r = 0$, $\hat{r} \neq 0$, or (ii) $r \neq 0$, $\hat{r} = 0$, or (iii) $r = \hat{r} = 0$. In the following, we go through a construction that self-consistently shows (ii) to be the correct variant.[42]

Let us *assume* that $r \neq 0$, $\hat{r} = 0$ characterizes the system at criticality. We begin by determining the engineering scaling dimensions of the various contributions to the action. Specifcially, we should like to identify the upper critical dimension, i.e. the dimension below which nonlinear terms become qualitatively important. To this end, let us use the freedom to independently scale $q, \hat{\mathbf{q}}, t, \phi, \psi$ in a manner to leave the dominant quadratic contributions to the action invariant. Defining the scale transformation

$$\begin{aligned} &\hat{\mathbf{q}} \to b\,\hat{\mathbf{q}}, \qquad q \to b^{\sigma} q, \qquad t \to b^{-z} t, \\ &\phi \to b^{d_\phi}\phi, \qquad \psi \to b^{d}\ \psi, \end{aligned} \tag{10.100}$$

[42] At first sight this claim may seem surprising. Since we expect ordering in the field direction, would not one expect the coefficient corresponding to *that* direction to vanish?

let us consider the scaling behavior of different contributions to the action Eq. (10.97),

$$\int dx \begin{cases} D & \psi\partial_t\phi \\ D & \psi\hat{\partial}^4\phi \\ Dr & \psi\partial^2\phi \\ \hat{A} & \psi\hat{\partial}^2\psi \\ A & \psi\partial^2\psi \\ DE & \psi\partial\phi^2 \\ Du & \psi\partial^2\phi^3 \\ D\hat{u} & \psi\hat{\partial}^2\phi^3 \end{cases} \to b^{\sigma+(d-1)+z} \int dx \begin{cases} b^{-(d_\phi+d\ )-z} & D & \psi\partial_t\phi \\ b^{-(d_\phi+d\ )-4} & D & \psi\hat{\partial}^4\phi \\ b^{-(d_\phi+d\ )-2\sigma} & Dr & \psi\partial^2\phi \\ b^{-2d\ -2} & \hat{A} & \psi\hat{\partial}^2\psi \\ b^{-2d\ -2\sigma} & A & \psi\partial^2\psi \\ b^{-(2d_\phi+d\ )-\sigma} & DE & \psi\partial\phi^2 \\ b^{-(3d_\phi+d\ )-2\sigma} & Du & \psi\partial^2\phi^3 \\ b^{-(3d_\phi+d\ )-2} & D\hat{u} & \psi\hat{\partial}^2\phi^3 \end{cases} . \quad (10.101)$$

We now choose the scaling dimensions d_ϕ, d_ψ, z, and σ so as to make the first four contributions to the list above scale invariant. This generates the conditions

$$z = 4, \qquad \sigma = 2, \qquad d_\psi = \frac{d+3}{2}, \qquad d_\phi = \frac{d-1}{2}. \quad (10.102)$$

With these values, we can estimate the engineering dimensions of the remaining terms. Specifically, we find that (a) the noise term $\propto A$ is strongly irrelevant in all dimensions, (b) the interaction term $\propto u$ is less relevant (by two dimensions) than the interaction term $\propto \hat{u}$, (c) the driving term $\propto E$ carries dimension $(5-d)/2$, and (d) the interaction term $\propto \hat{u}$ carries dimension $3-d$. Specifically, point (c) implies that **the model has upper critical dimension** $d_c = 5$. Notice that the high value of the upper critical dimension reflects the strongly intrusive role of the driving – below $d = 5$, the physics of the model becomes fluctuation dominated, earlier than in the equilibrium model with its $d_c = 4$. In addition, the driving term is more relevant than the interaction term $\propto \hat{u}$, which becomes relevant only below $d = 3$.

The estimate above suggests that we should drop the terms proportional to $A, u, \hat{u}$. We will thus model the critical system by the reduced effective action

$$\begin{aligned} S[\phi,\psi] &= \int dx\, D\Big(\psi\left(D^{-1}\partial_t - r\partial^2 + \hat{\partial}^4\right)\phi + E\partial\phi^2 + (\hat{\partial}\psi)^2\Big) \\ &= \frac{1}{2}\int dx\, \left[(\phi,\psi)\begin{pmatrix} & (g^-)^{-1} \\ (g^+)^{-1} & -2\hat{\partial}^2 \end{pmatrix}\begin{pmatrix}\phi\\ \psi\end{pmatrix} + DE\psi\partial\phi^2\right], \end{aligned} \quad (10.103)$$

where $g^\pm = (\pm\partial_t - Dr\partial^2 + D\hat{\partial}^4)^{-1}$, and we have absorbed the noise coefficient $\hat{A}$ in a rescaled field amplitude.

In the following, we aim to understand the build–up of anisotropies in the critical system at $d = 5-\epsilon$ dimensions. To understand the ramifications of scaling anisotropies, let us begin by computing the **Fourier transform of the static structure factor** – the spatial correlation function of the system – in a tree approximation. Comparing with Eq. (10.98) and (10.99), we obtain

$$S(\mathbf{k}) = \int d\omega\, S(\mathbf{k},\omega) = \int \frac{d\omega}{2\pi}\frac{2\hat{k}^2}{\omega^2 + D^2(\hat{r}\hat{k}^2 + \hat{k}^4)^2} = \frac{\hat{k}^2}{D(rk^2 + \hat{k}^4)},$$

and

$$S(\mathbf{x}) = \int \frac{d^d k}{(2\pi)^d}\, e^{i(kx+\hat{\mathbf{x}}\cdot\hat{\mathbf{k}})} S(\mathbf{k}) = \int \frac{d^d k}{(2\pi)^d}\, e^{i(kx+\hat{\mathbf{x}}\cdot\hat{\mathbf{k}})} \frac{\hat{k}^2}{D(rk^2+\hat{k}^4)}$$
$$\sim \int \frac{d^{d-1}\hat{k}}{(2\pi)^{d-1}}\, e^{-\hat{k}^2|x|r^{-1/2}+i\hat{\mathbf{x}}\cdot\hat{\mathbf{k}}} \sim |x|^{-\frac{d-1}{2}} e^{-\frac{x^2 r^{1/2}}{4|x|}}.$$

This expression provides an *a–posteriori* justification of our choice of "mass parameters" r and $\hat{r}$ at criticality. We have obtained a correlation function that decays as a power law in the longitudinal direction and exponentially in the transverse direction. This behavior conforms with the build–up of critical fluctuations in the longitudinal direction, while the transverse direction remains in a disordered state.

Perturbative RG

How will **critical fluctuations** effect this picture? In the following, we perform a rudimentary RG analysis to show that below the upper critical dimension $d_c = 5$, fluctuations conspire to strengthen the anisotropic character of the system. (For a full exposition of an RG analysis of this system, we refer to Schmittmann and Zia.[39]) As in Section 8.3, we aim to explore what happens as fast fluctuations successively get integrated out. To this end, we first introduce a graphical language representing the building blocks relevant to the perturbative RG (see the figure.)

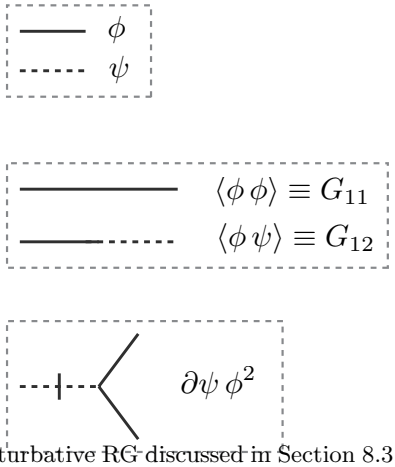

EXERCISE Refamiliarize yourself with the plan of the perturbative RG discussed in Section 8.3. Decompose the fields as $\phi = \phi_s + \phi_f$ into fast and slow sectors. To one loop order in the fast fields, explore the different diagrams contributing to the perturbative RG step. Specifically, convince yourself that no vertices other than those contained in the action Eq. (10.103) will be generated. Use power counting arguments to show that the one fast momentum integration becoming dangerous below $d = 5$ will act to renormalize the $\partial^2\phi\psi$ vertex.

The one diagram driving the renormalization of the theory is shown in the figure to the right. To explore the effect of this contribution, we divide the fields into fast and slow contributions. In view of the anisotropies inherent to the model, it is actually not so obvious how the space of coordinates $(q, \hat{\mathbf{q}}, \omega)$ is to be divided into a fast and a slow sector. On the other hand, the RG procedure should be insensitive to the detailed choice of an (infinitesimally thin) layer of fast modes. (As an exercise, check it by inventing schemes different from the one below.) We thus meet the technically convenient choice, fast: $\Lambda/b < |\hat{\mathbf{q}}| < \Lambda$, (q, ω) arbitrary, slow: $|\hat{\mathbf{q}}| < \Lambda/b$, (q, ω) arbitrary. Denoting the

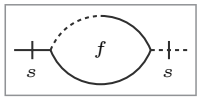

integration over the fast modes by $\int_f dq$, the diagram above renormalizes the coefficient r according to

$$\begin{aligned} r \to r + \text{const.} \times DE^2 \int_f dq\, G_{21}(q) G_{22}(q) &= r + \text{const.} \times DE^2 \int_f dq\, g_q^+ \hat{q}^2 (g^+ g^-)_q \\ &= r + \text{const.} \times DE^2 \int_f d^{d-1}\hat{q} \int dq d\omega \frac{\hat{q}^2}{(-i\omega + Drq^2 + D\hat{q}^4)^2 (i\omega + Drq^2 + D\hat{q}^4)} \\ &= r + \text{const.} \times \frac{E^2}{D} \int_f d^{d-1}\hat{q} \int dq\, \frac{\hat{q}^2}{(rq^2 + \hat{q}^4)^2} \simeq r + \frac{cE^2}{Dr^{1/2}} \ln b + \mathcal{O}(\epsilon^2), \end{aligned}$$

where $c = \mathcal{O}(1)$ is a numerical constant. At the one-loop level, the vertex $\propto E$ does not renormalize; its renormalization stems from the the rescaling of momenta following the RG step, $E \to b^{(5-d)/2} E = e^{\ln b \epsilon/2} E$. This latter rescaling does not change the r-term, as the field dimensions have been deliberately chosen so as to make this term (engineering) scale invariant. We thus obtain the two RG equations

$$\frac{dE}{d\ln b} = \frac{\epsilon}{2} E, \qquad \frac{dr}{d\ln b} = \frac{cE^2}{Dr^{1/2}}. \tag{10.104}$$

Substituting the solution of the first equation, $E = b^{\epsilon/2} E_0$ into the second, and solving the remaining ordinary differential equation, we obtain $r \sim b^{\frac{2}{3}}$. This fluctuation induced scaling needs to be taken into account in an updated variant of the determination of scaling dimensions. Accounting for the scaling of r in Eq. (10.101), we find that the anisotropy exponent changes according to

$$\sigma = 2 + \frac{\epsilon}{3}. \tag{10.105}$$

This result adds to our overall observation that **driving massively interferes with the physics of the system**. By way of summary, we have seen that:

- ▷ In the disordered regime above criticality, external driving leads to the formation of new macroscopic structures which manifest themselves in new types of power law correlation.
- ▷ The strongly invasive character of driving is also reflected in the increased value of the upper critical dimension, $4 \to 5$ (as compared to the equilibrium system).
- ▷ At criticality, driving causes fluctuations which superimpose to strengthen the anisotropy of the system, Eq. (10.105). Qualitatively, the fluctuations generate patterns that appear to be strongly aligned in the field direction.

For a deeper analysis of the system, and a discussion of its physics below criticality, we refer to a more comprehensive study of its scaling and renormalization behavior.[39].

10.7.2 Directed percolation

Amongst the different universality classes of equilibrium statistical mechanics, the ϕ^4- or Ising-class is the simplest. It owes its frequent occurrence in nature to the fact that its free energy function, a quartic polynomial of a real scalar variable, is the most basic one that leads to nontrivial critical behavior. In nonequilibrium statistical mechanics, the directed

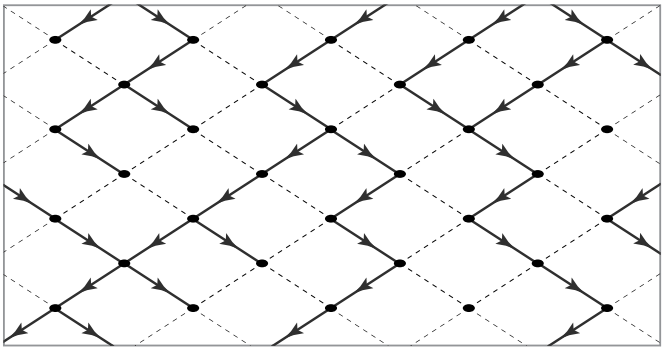

Figure 10.12 Cartoon of a directed percolation network with a given realization of open bonds, cf. ordinary, or **isotropic percolation**, where the network bonds are directionless.

percolation class plays a similarly paramount role. In this section, we try to understand the importance of this universality class to nonequilibrium statistical mechanics, and explore a few of its critical properties. However, before doing so, it is useful to briefly review directed percolation *perse*. (The material presented below is inspired by an excellent review by H. Hinrichsen.[43])

Directed Percolation: Phenomenology

The term "directed percolation" (DP) refers to a class of models that describe the spatially directed spreading of a substance through a medium – think, for example, of a liquid dispersing through porous rock under the influence of a gravitational force. Alternately, one may identify the driving direction with time, in which case directed percolation mimics, for example, the spreading of an epidemic, or related dynamical phenomena.

The directed percolation model (see Fig. 10.12) is defined on a d-dimensional hypercubic lattice. A certain "main diagonal" of the lattice is introduced as the identifier of a sense of direction. The links of the lattice are then chosen to be open or closed with probability p and $1-p$, respectively. Like its cousin, the undirected, or isotropic percolation model, this system exhibits a phase transition at a critical value of the connectivity probability, $p = p_c$, the **directed percolation phase transition** (see Fig. 10.13). The order parameter of this transition is the probability P_∞ that a randomly chosen site of the lattice is at the origin of an infinitely large connected cluster. At $p < p_c$, and using a language alluding to the liquid/porous rock application, the system is in a "dry phase." At $p > p_c$, it has become "wet."

Despite the simplicity of the model, the critical properties of the DP-transition are not fully understood. What can be said without any further calculation is that the critical value $p_c = p_c(d)$ will depend on dimensionality. (In one dimension, any broken bond will truncate the cluster, i.e. $p_c(1) = 1$; in infinite dimensions, the unlimited number of options to go

[43] H. Hinrichsen, Nonequilibrium critical phenomena and phase-transitions into absorbing states, *Adv. Phys.* **49**, 815-958 (2000).

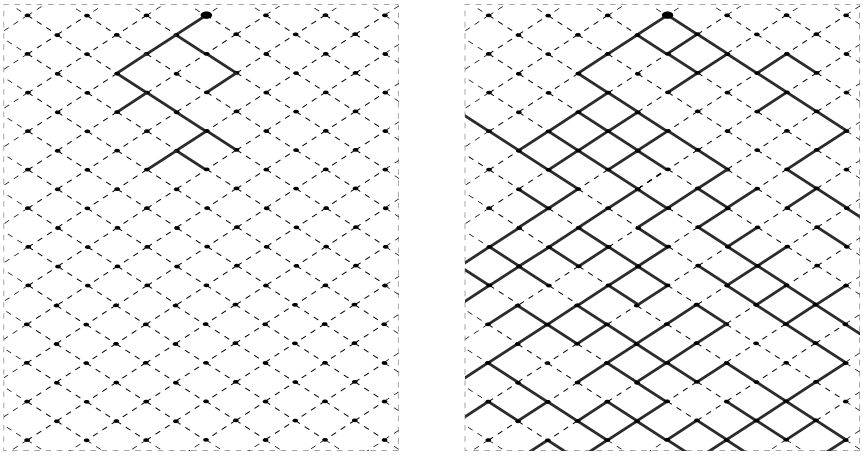

Figure 10.13 The two phases of a directed percolation network. Left, **dry phase**, wherein individual sites generate finite size clusters; right, **wet phase** with infinite size cluster generation.

from any lattice site implies $p_c(d \to \infty) \quad 0$.) Both, numerical analysis and field theory suggest that the corresponding critical exponents are complicated, and likely irrational.

What gives the understanding of the DP transition increased relevance is that many **reaction–diffusion processes** appear to fall into the DP universality class. To heuristically understand this connection, simply note that, upon interpreting the sense of direction as the flow of time, the elementary compounds of a cluster afford a natural interpretation in terms of "reactions," or diffusion (cf. Fig. 10.14). The generation update on the DP network need not be modeled simply by drawing bond connectivities according to some fixed probabilities; more sophisticated update rules can be invented to describe a large set of dynamical setups. Algorithms implementing such update rules are called **cellular automata**. Many such automata exhibit a phase transition between two "absorbing states" of the lattice, the empty state (above termed "dry") and the totally occupied state ("wet"). One of the theoretical challenges in this field is to understand the universal properties of such transitions, and specifically their connection to the basic DP universality class.

Below, we explore some of the universal properties of the DP transition by field theoretical methods. We also aim to understand the origins of the ubiquity of the DP class in reaction–diffusion kinetics.

Elements of scaling theory

Many physical properties of the DP transition can be conveniently described in terms of scaling laws. Introducing $\tau = p - p_c$ as a scaling field measuring the distance from the transition point, the correlation behavior of the system is characterized by a **correlation length** $\xi \sim \tau^{-\nu}$ in its "spatial directions," and a **correlation time** $t \sim \xi^z \sim \tau^{-\nu z}$ in the orienting direction. The transition as such can be probed in terms of two candidate order

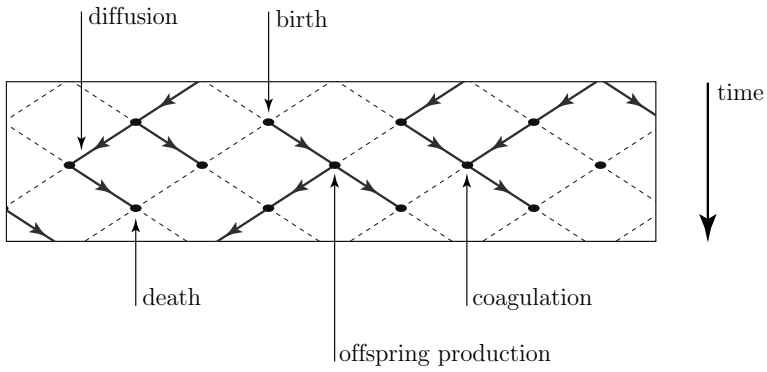

Figure 10.14 Dynamical interpretation of a DP network. Each row of sites represents a generation of particles. The generation dynamical update then involves diffusion, birth and death, coagulation and offspring creation.

parameters. The first is the **average number of active**, or wet sites,

$$\rho(t) \equiv N^{-1} \quad \sum_i s_i(t) \quad ,$$

where N is the total number of sites within one time layer, and $s_i = 1$ if site i is active, and zero otherwise. In the vicinity of the transition, ρ is expected to exhibit power law scaling, $\rho(t \to \infty) \equiv \rho \sim \tau^\delta, \tau < 0$. More generally, the critical time dependence of order parameter fluctuations is described by the *ansatz*

$$\rho(t) \sim |\tau|^\beta g(t/t(\tau)),$$

with the short time asymptotics (cf. the discussion of Section 10.6.1),

$$\rho(t) \sim t^{-\alpha}, \qquad \alpha = \beta/\nu z.$$

Another possible order parameter is the **infinite cluster size probability** P_∞ introduced above. We can generalize to a time-dependent quantity by declaring $P(t)$ to be the average probability that a cluster started at $t = 0$ is still active at time t. Since the "spatial" size of the cluster grows indefinitely with time, $P_\infty = P(t \to \infty)$. The scaling behavior of P is described by $P_\infty = \tau^{\beta'}$, $\tau < 0$, and

$$P(t) \sim |\tau|^{\beta'} g'(t/t(\tau)),$$

with short time limit $P(t) \sim t^{-\alpha'}$, $\alpha' = \beta'/\nu z$. The four exponents ν, z, β, β' describe the basic scaling behavior of the system. (For the elementary DP class, infinite cluster size probability and overall wetness are equivalent characteristics, $\beta = \beta'$. For general phase transitions between absorbing states, however, these quantities can be different.)

An important derived quantity, similar in nature to the pair correlation functions of many particle theories, is the **pair connectedness function** $C(\mathbf{x}, t)$. This function is defined as

the probability that an active site at $(0,0)$ is connected to the site at $(\mathbf{x},t)$ by an open path. The scaling hypothesis implies that

$$C(\mathbf{x},t) = t^{\theta-d/z} F(|\mathbf{x}|/t^{1/z}, \tau t^{1/\nu z}). \tag{10.106}$$

The dimension θ can be fixed by running a few consistency checks: the probability that $(\mathbf{x} \simeq 0, t)$ is connected to $(0,0)$ is proportional to both the probability of finding a cluster of temporal extension $P(t)$, and the density of active sites, $\rho(t)$. Here, the notation $\mathbf{x} \simeq 0$ means that the final point $\mathbf{x}$ should lie inside the "conical" cluster spreading out from 0, i.e. $C(0,t) \overset{t\to\infty}{\sim} \tau^{\beta+\beta'}$. On the other hand, the expected stationarity of $C(0, t \to \infty)$ requires that $F(0, \tau t^{1/\nu z}) \overset{!}{\sim} t^{-(\theta-d/z)}$, i.e. $F(0, \tau t^{1/\nu z}) \sim \tau^{-\nu z(\theta-d/z)}$. Comparing these two conditions, we obtain the identification $\tau^{-\nu z(\theta-d/z)} \overset{!}{\sim} \tau^{\beta+\beta'}$, or

$$\theta = \frac{1}{z}\left(-\frac{\beta+\beta'}{\nu} + d\right). \tag{10.107}$$

Equations (10.106) and (10.107) describe much of the correlation behavior of the cluster. Notice, however, that the argument leading to Eq. (10.107) relied on the cluster spreading "underneath" the initial point. However, in high dimensions, this condition may be violated, on account of the cluster spreading out in directions "orthogonal" to $|\mathbf{x}-0|$. Closer analysis shows that the validity of Eq. (10.107) is limited to dimensions below the upper critical dimension of the process.

For the discussion of scaling functions higher in the hierarchy, and describing features such as the average extension of clusters, their volume, etc., we refer to Hinrichsen.[43] In the next section, we discuss how field theoretical methods can be applied to describe the fluctuation behavior of the system and its critical exponents.

Field theory

Before analysing low energy field theories of the DP transition, we first have to construct one. On the face of it, it is not so obvious how to do this: we have not described DP in the language of master equations, nor by Langevin type evolution, so our standard recipes do not apply. Instead, we aim to construct a "dynamical mean field equation" of DP on phenomenological grounds. We then use this equation as input for the construction of a field theory, along the lines of Section 10.6.3.

The mean field equation we are going to construct operates on the mean density of active sites, $\rho(t)$. Adopting the dynamical interpretation of DP, $\rho(t)$ increases at a rate that is proportional to the probability of open bonds, p, the density $\rho(t)$ of active sites at time step $n-1$ that may act as germs of newly generated active sites, and the density of empty sites at time step n that may be converted to active sites. The density decreases at a rate proportional to the density of active sites at the previous time step, and the probability of closed bonds, $1-p$. Combining all these considerations, we are led to the equation $\partial_t \rho = c_1 p\rho(1-\rho) - c_2(1-p)\rho$, where $c_{1,2}$ are nonuniversal constants depending on the dimensionality of the system, and on the unit at which time is measured. We may always rescale density and time such that the equation assumes the form,

$$\partial_t \rho = (\lambda - 1)\rho - \lambda\rho^2. \tag{10.108}$$

The defining feature of this equation is that it possesses (a) a stationary configuration $\rho = 0$, and (b) a non-empty stationary state $\rho = \frac{\lambda-1}{\lambda}$, provided $\lambda > 1$. The critical value $\lambda_c = 1$ at which the non-empty "mean field" begins to emerge marks the position of the continuous DP transition. Notice the simplicity of the DP mean field equation. It explains the ubiquity of the DP class: alluding to the principle of universality, one may suspect that processes described by a rate equation free of constant terms generically exhibit a DP transition, provided that the first two terms $\sim \rho$ and $\sim \rho^2$ admit a non-zero solution.

Equation (10.108) fixes the **mean field critical exponents** of the system. Using the notation $\tau = \lambda - \lambda_c = \lambda - 1$ for the difference to the mean field critical point, near criticality $\rho \simeq \tau$, i.e. $\beta_{\rm mf} = 1$. In the dry phase, $\tau < 1$, the asymptotic temporal decay of the density is given by $\rho \sim \exp(-|\tau|t)$, which means that $-\nu z = 1$. However, lacking any spatial structure, mean field theory cannot say anything about ν (nor z) individually.

The mean field equation (10.108) can be upgraded to a spatially resolved rate equation by upgrading $\rho(t) \to \rho(\mathbf{x}, t) \equiv \rho(x)$ to a local density profile and adding a diffusion term:

$$\partial_t \rho = D\partial^2 \rho + \tau\rho - \lambda\rho^2. \tag{10.109}$$

Dimensional analysis shows that $\nu_{\rm mf} = 1/2$. In combination with the results above (which survive generalization to a local equation – exercise) we then have the mean field, or tree level prediction,

$$\beta_{\rm mf} = 1, \qquad \nu_{\rm mf} = 1/2, \qquad z_{\rm mf} = 2. \tag{10.110}$$

A field theory can now be constructed by interpreting Eq. (10.110) as a model A rate equation along the lines of our discussion of Section 10.6.2. To this end, we upgrade Eq. (10.109) to a noisy equation,

$$\partial_t \rho = D\partial^2 \rho + \tau\rho - \lambda\rho^2 + \xi,$$

where the noise is correlated as

$$\langle \xi(x) \rangle = 0, \qquad \langle \xi(x)\xi(x') \rangle = 2A\rho(x)\delta(x - x'). \tag{10.111}$$

The crucial feature here is the scaling $\xi \sim \sqrt{\rho}$. It reflects the assumption that the system self-generates noise through its active sites. This type of noise must vanish in the empty state, $\rho = 0$. Further, we are to interpret ξ as a coarse-grained variable sampling fluctuations in a large number of active sites. According to the central limit theorem, these fluctuations scale as $\sqrt{\rho}$, which explains the above correlation law. Generally, noise that scales with some power of the Langevin variable is termed **multiplicative noise**.

We next subject Eq. (10.110) to our standard treatment of Langevin equations, thus generating the **field theory representation of DP** partition function, $\mathcal{Z} = \int D(\phi, \psi)\, e^{-S[\phi,\psi]}$ where[44]

$$\boxed{S[\phi, \psi] = \int dx \, \left[\psi(\partial_t - D\partial^2 - \tau)\phi + \kappa\psi\phi(\phi - \psi) \right],} \tag{10.112}$$

[44] Curiously, the field theory Eq. (10.112) has a background in particle physics, where it is known as **Reggeon eld theory**, see M. Moshe, Recent developments in Reggeon field theory, *Phys. Rep.* **37**, 255-345 (1978) for a review.

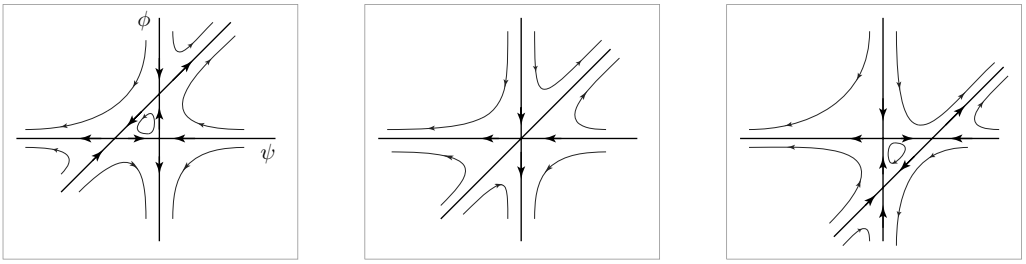

Figure 10.15 Three distinct phase portraits of directed percolation. Left: phase supporting a finite concentration of active sites, center: phase transition, right: empty state.

and $\kappa \equiv (A\lambda)^{1/2}$.(In deriving Eq. (10.112), we made use of the freedom to rescale fields so as to make the coefficients of the two nonlinear terms $\sim \phi\psi^2$ and $\sim \phi^2\psi$ equal.) We next explore (cf. Eqs. (10.100) and (10.101)) the behavior of the different terms in the action under the rescaling transformation

$$\begin{aligned} &\mathbf{x} \to \mathbf{x}/b, t \to t/b^z, \\ &\phi \to b^{d_\phi}\phi, \qquad \psi \to b^d \ \psi. \end{aligned} \tag{10.113}$$

Referring to the action (10.97), we have

$$\int dx \begin{cases} & \psi\partial_t\phi \\ D & \psi\partial^2\phi \\ \tau & \psi\phi \\ \lambda & \psi\phi^2 \\ A & \psi^2\phi \end{cases} \to b^{d+z} \int dx \begin{cases} b^{-(d_\phi+d\ )-z} & \psi\partial_t\phi \\ b^{-(d_\phi+d\ )-2} & D\ \psi\partial^2\phi \\ b^{-(d_\phi+d\ )} & \tau\ \psi\phi \\ b^{-(2d_\phi+d\ )} & \lambda\ \psi\phi^2 \\ b^{-(d_\phi+2d\ )} & A\ \psi^2\phi \end{cases} . \tag{10.114}$$

Choosing $z = 2$ and $d_\phi = d_\psi = d/2$, the first two contributions to the action become (tree level) scale invariant. The operator $\sim \tau\psi\phi$ measuring the distance off criticality is strongly relevant with dimension 2. Finally, the nonlinear operators $\sim \lambda\psi\phi^2$ and $\sim A\psi^2\phi$ carry dimension $4 - d$. This identifies the **upper critical dimension** of directed percolation as $d = 4$.

Before turning to the discussion of the role of fluctuations below $d = 4$, let us briefly recapitulate the mean field picture in the language of the effective field theory Eq. (10.112). As with the zero-dimensional problems discussed in Section 10.4, the phase structure of the system is essentially determined by the pattern of intersecting zero energy lines of the mean field Hamiltonian, $H = \psi\phi(\phi - \psi - \tau)$. Depending on the sign of τ, three distinct phases need to be distinguished (see Fig. 10.15). At $\tau > 0$, the system is in its **active phase**: on the fluctuationless manifold $\psi = 0$, the concentration variable ϕ is driven towards the stable configuration $\phi = \tau$. (Notice that only positive values of ϕ are physically meaningful.) At $\tau < 0$, the empty state $\phi = 0$ is stable, the **inactive phase**. The mean field **phase transition** between both phases happens at $\tau = 0$. The phase space picture of directed

percolation was introduced in Kamenev [45] as the basis for a far-reaching classification of phase transitions in reaction–diffusion systems. For further aspects of the utility of the Hamiltonian approach in this field, we refer to the original reference.

Perturbative RG

How will **fluctuations** alter this picture? Close to the upper critical dimension, in $d = 4-\epsilon$, renormalization group techniques can be applied to answer this question. Carrying out an RG analysis similar to that detailed in Section 10.7.1 (cf. Problem 10.9.4), one finds that the two coupling constants τ and κ flow according to the equations

$$\frac{d\tau}{d\ln b} = -DC\kappa^2 + \tau\left(2 - \frac{3}{4}C\kappa^2\right),$$
$$\frac{d\kappa}{d\ln b} = \kappa\left(\frac{\epsilon}{2} - \frac{3}{2}C\kappa^2\right), \tag{10.115}$$

where the constant $C = \frac{S_4}{(2\pi)^4 D^2}$ and S_4 is the area of the four dimensional unit-sphere. Within the above RG scheme, the diffusion constant, D, and the pre-factor of the frequency term ω are kept fixed. The dynamical exponent and the "field renormalization" $\phi \to \phi b^{-\frac{4-}{2}+}$ are given by, respectively,

$$z = 2 - \frac{C\kappa^2}{4}, \qquad \chi = \frac{C\kappa^2}{4}.$$

These equations possess a non-trivial fixed point at $\tau^* = \frac{D\epsilon}{6} + \mathcal{O}(\epsilon^2)$, $\kappa^* = \left(\frac{\epsilon}{3C}\right)^{1/2}$ which means that fluctuations shift the position of the DP transition to a non-vanishing value of τ. At the fixed point, $z = 2 - \epsilon/12$ and $\chi = \epsilon/12$. Linearization of the RG equations around the fixed point leads to

$$\frac{d\tilde{\tau}}{d\ln b} = \left(2 - \frac{\epsilon}{4}\right)\tilde{\tau} - \tilde{\kappa}CD\kappa^*\left(2 + \frac{\epsilon}{4}\right),$$
$$\frac{d\tilde{\kappa}}{d\ln b} = -\epsilon\tilde{\kappa},$$

where $\tau = \tau^* + \tilde{\tau}$ and $\kappa = \kappa^* + \tilde{\kappa}$. The linearized equations imply that the coupling constant $\tilde{\tau}$ is a relevant scaling field with $\tilde{\tau} \sim b^{2-\bar{4}}$. This result can in turn be used to determine the 1-loop **critical exponents**: the scaling $b^{-1} \sim \xi \sim \tilde{\tau}^{-\nu} \sim b^{-\nu(2-\bar{4})}$ leads to the identification $\nu = \frac{1}{2} + \frac{\epsilon}{16} + \mathcal{O}(\epsilon^2)$. The critical exponent β follows from the scaling relation $\tau^\beta \overset{!}{\sim} \langle\phi\rangle = b^{-\frac{4-}{2}+}\,\phi(\tau b^{2-\bar{4}})$. Setting $b \sim \tau^{-\frac{1}{2-\bar{4}}}$, we obtain the identification $\beta = 1 - \frac{\epsilon}{6} + \mathcal{O}(\epsilon^2)$. Summarizing, the 1-loop RG analysis generates the list of exponents

$$z = 2 - \frac{\epsilon}{12} + \mathcal{O}(\epsilon^2), \qquad \nu = \frac{1}{2} + \frac{\epsilon}{16} + \mathcal{O}(\epsilon^2), \qquad \beta = 1 - \frac{\epsilon}{6} + \mathcal{O}(\epsilon^2).$$

How do these values compare with reality? Numerical simulations for $(3+1)$-dimensional clusters[46] obtain $(z, \nu, \beta) = (1.90(1), 0.581(5), 0.81(1))$ which compares reasonably well with

[45] A. Kamenev, Classification of phase transitions in reaction–diffusion models, *Phys. Rev. E* **74**, 41101-17 (2006).
[46] I. Jensen, Critical behavior of the three-dimensional contact process, *Phys. Rev. E* **45**, R563-6 (1992).

the $\epsilon = 1$ extrapolation of the exponents above, $(z, \nu, \beta) = (1.92, 0.56, 0.83)$. A two-loop extension of the RG[47] leads to excellent agreement. However, in lower dimensions, the situation is decidedly worse. For example, in the extreme case of $(1+1)$-dimensional percolation clusters, the RG exponents are off the results of simulations by ca. 40%. Even so, the field theory analysis sheds light on the physical mechanisms generating critical behavior, and this is information that cannot be obtained from direct simulations.

10.8 Summary and Outlook

In this chapter, we have discussed foundations of nonequilibrium statistical mechanics, with emphasis put on later extensibility to quantum nonequilibrium theory. We have introduced the two major pathways to the description of nonequilibrium systems, Langevin dynamics and probabilistic formulations in terms of master equations. We saw that these two approaches afford a unified description in terms of functional integrals, the MSRJD formalism. Interpreting the latter as a Hamiltonian functional integral, we looked at its Lagrangian partner – the Onsager–Machlup functional – and recovered the Fokker–Planck equation as its dynamical equation (similarly to the Schrödinger equation being the dynamical equation of the quantum mechanical path integral). The arch stretching from the Langevin/master equations over the MSRJD–/Onsager–Machlup functional to the Fokker–Planck equation provides a powerful framework wherein many nonequilibrium phenomena can be studied in a unified setting. Specifically, the functional integral description suggested a variational approach (similar in nature to the WKB approach of quantum mechanics) to the description of large fluctuations: fluctuations in higher dimensional environments could be analyzed by concepts borrowed from the theory of critical phenomena, etc. In the next chapter, the focus is on another important aspect of the formalism, the interpretation of the MSRJD functional as the classical limit of a generalized quantum theory.

10.9 Problems

10.9.1 Wigner surmise

The problem of eigenvalue correlations of Hermitian matrices drawn from random distributions is a subject with a long history dating back to studies of resonances in atomic nuclei. The following problem concerns the distribution of level spacings in a canonical 2×2 random Hamiltonian. The result, known as the Wigner surmise, captures much of the behavior of the general expression for random matrices of arbitrary rank.

Consider a Hamiltonian $\mathcal{H}$ of the form of a 2×2 matrix parameterized as

$$\hat{H} = \begin{pmatrix} H_1 & \Delta \\ \Delta & H_2 \end{pmatrix}.$$

[47] J. B. Bronzan and J. W. Dash, Higher order epsilon terms in the renormalization group approach to Reggeon field theory, *Phys. Lett. B* **51**, 496498 (1974).

Suppose that the three real numbers H_1, H_2, and Δ are drawn from a Gaussian distribution $P(H_1, H_2, \Delta) \propto e^{-\frac{1}{2}\mathrm{tr}\,\hat{H}^2}$. Derive the joint distribution $P(E_1, E_2)$ of the two energy levels E_i, $i = 1, 2$, of the Hamiltonian $\hat{H}$. Using this, derive the Wigner surmise describing the distribution of the energy splitting $s = |E_1 - E_2|$, and show that it has the form

$$P(s) = c_1\, s\, e^{-c_2 s^2},$$

with some constants c_1 and c_2.

Answer:
The joint eigenvalue distribution is given by

$$P(E_+, E_-) \sim \int dH_1\, dH_2\, d\Delta\, \delta(E_+ - \lambda_+)\delta(E_- - \lambda_-)e^{-(E_+^2+E_-^2)/2}\,,$$

where $\lambda_\pm = \frac{H_1+H_2}{2} \pm (\Delta^2 + (\frac{H_1-H_2}{2})^2)^{1/2}$ denote the eigenvalues of the matrix $\mathcal{H}$ and we assumed $E_+ > E_-$ (in the opposite case, one has to interchange $\lambda_+ \leftrightarrow \lambda_-$). Integrating over $(H_1 + H_2)/2$ and setting $\delta H = H_1 - H_2$, one obtains $P(E_+, E_-) \sim \int d\delta H\, d\Delta\, \delta(E_+ - E_- - 2(\Delta^2 + \delta H^2)^{1/2})e^{-(E_+^2+E_-^2)/2}$. Finally, setting $r = (\Delta^2 + \delta H^2)^{1/2}$, and integrating over the "angular" variable, one obtains $P(E_+, E_-) \sim \int_0^\infty dr\, r\, \delta(E_+ - E_- - 2r)e^{-(E_+^2+E_-^2)/2} \sim (E_+ - E_-)e^{-(E_+^2+E_-^2)/2}$. From this result, we obtain the distribution

$$P(s) \sim \int_{E_+>E_-} dE_+\, dE_-\, P(E_+, E_-)\delta(E_+ - E_- - s) \sim s e^{-s^2/8}\,.$$

We therefore find that $c_2 = 1/8$, and $c_1 = 1/4$ is obtained from the normalisation condition. This result shows that the probability of finding a degeneracy is vanishing i.e. levels repel. As a further exercise, show that if $\mathcal{H}$ is a complex Hermitian, i.e. both real and imaginary parts of Δ are drawn from a Gaussian distribution, the probability distribution vanishes as $P(s) \sim s^2$ for small s.

10.9.2 Ornstein-Uhlenbeck process

The Ornstein-Uhlenbeck process[48] is the "harmonic oscillator" of nonequilibrium dynamics. It describes stochastic evolution in cases where the averaged dynamics of a Langevin particle is described by a linear first order differential equation. Realizations include the dynamics of a particle subject only to friction (but no "external forces"), or the dynamics of an overdamped particle in a harmonic external potential. Dissipative dynamics close to extremal potential points is often described by variants of this process.

(a) Consider a Brownian particle in 1d whose velocity is governed by the stochastic differential equation

$$\dot{v} + \gamma v = \frac{f(t)}{m}, \tag{10.116}$$

[48] G. E. Uhlenbeck and L. S. Ornstein, On the theory of Brownian motion, *Phys. Rev.* **36**, 823-41 (1930).

where f is a Langevin force, and $\langle f(t)f(t')\rangle = A\delta(t-t')$. Determine the general solution of Eq. (10.116) for the velocity with the initial condition $v(0) = v_0$, and calculate $\langle v(t)\rangle$ and $\langle v^2(t)\rangle$. Using the long-time limit of the latter, identify the coefficient A with the help of the equipartition theorem.

(b) Consider the time-dependent velocity distribution $p(v,t)$. It is governed by the Fokker–Planck equation

$$\left[\frac{\partial}{\partial t} + \frac{\partial}{\partial v}a_1(v) - \frac{1}{2}\frac{\partial^2}{\partial v^2}a_2(v)\right] p(v,t) = 0. \tag{10.117}$$

With the help of Eq. (10.117), derive equations for $\partial_t\langle v\rangle$ and $\partial_t\langle v^2\rangle$ and identify the coefficients a_1 and a_2, e.g., by using the results of part (a). Show that the corresponding Fokker–Planck equation for the generating function $g(k,t) = \int dv e^{-ikv}p(v,t)$ is given by

$$\left[\frac{\partial}{\partial t} + \gamma k\frac{\partial}{\partial k} + \frac{\gamma T}{m}k^2\right] g(k,t) = 0. \tag{10.118}$$

(c) The first order partial differential equation Eq. (10.118) can be solved for example with the method of characteristics. Show that a general solution is of the form

$$g(k,t) = e^{-\frac{T}{2m}k^2}\phi(ke^{-\gamma t}).$$

Determine the function ϕ from the initial condition $p(v,t=0) = \delta(v-v_0)$ and derive the distribution $p(v,t)$. Discuss the short and long-time limits of your result.

Answer:

(a) Formally, integrating the equation, one obtains the solution,

$$v(t) = e^{-\gamma t}\left[v_0 + \int_0^t dt'\,\frac{f(t')}{m}e^{\gamma t'}\right],$$

where $v_0 \equiv v(0)$. Then, averaging over the distribution for the Langevin force, since $\langle f\rangle = 0$, we have $\langle v(t)\rangle = v_0 e^{-\gamma t}$. Similarly, making use of the expression for the correlator, we have

$$\begin{aligned}\langle v^2(t)\rangle &= e^{-2\gamma t}\left[v_0^2 + \int_0^t dt'\,dt''\,\frac{\langle f(t')f(t'')\rangle}{m^2}e^{\gamma(t'+t'')}\right]\\ &= e^{-2\gamma t}\left[v_0^2 + \frac{A}{2\gamma m^2}(e^{2\gamma t}-1)\right].\end{aligned}$$

In the long time limit, $\langle v^2(t)\rangle = \frac{A}{2\gamma m^2} \overset{\text{FDT}}{=} \frac{T}{m}$, i.e. $A = 2\gamma mT$. Setting $\delta v(t) = v(t) - \langle v(t)\rangle$, one may further show that $\langle \delta v(t)\delta v(t')\rangle = \frac{T}{m}(e^{-\gamma|t-t'|} - e^{-\gamma(t+t')})$.

(b) Using the Fokker–Planck equation, we have

$$\partial_t\langle v\rangle = -\int dv v\partial_v(a_1P) + \int dv\frac{1}{2}v\partial_v^2(a_2P) = \int dv a_1P - \frac{1}{2}\int dv\,\partial_v(a_2P) = \langle a_1\rangle.$$

From this result, we obtain $a_1(v) = -\gamma v$. Similarly

$$\begin{aligned}\partial_t\langle v^2\rangle &= -\int dv v^2 \partial_v(a_1 P) + \int dv \frac{1}{2} v^2 \partial_v^2(a_2 P) \\ &= \int dv 2v a_1 P - \int dv v \partial_v(a_2 P) = \langle 2v a_1\rangle + \langle a_2\rangle.\end{aligned}$$

From part (a), we have $\partial_t\langle v^2\rangle = -2\gamma v_0^2 e^{-2\gamma t} + \frac{A}{m^2} e^{-2\gamma t}$. As a result, after a small amount of algebra, we find that $\langle a_2\rangle = \frac{2\gamma T}{m}$.

The derivation of Eq. (10.118) amounts to a straightforward substitution of the Fokker–Planck equation into the Fourier integral defining $g(k)$.

(c) Using the method of characteristics, from the left-hand side of the equation in (b), we have $-\gamma k dt + dk = 0$, i.e. $\frac{dk}{dt} = \gamma k$ and $k(t) = ce^{\gamma t}$. From the variation of g along the characteristic, $\frac{dg}{g} = -\frac{T}{m} k\, dk$, we obtain $g(k,t) = \text{const.} e^{-k_B T k^2/2m}$, i.e.

$$g(k,t) = e^{-k_B T k^2/2m} \phi(k e^{-\gamma t}).$$

With the initial condition, $g(k,0) = e^{-ikv_0}$, we have $\phi(k) = e^{-ikv_0} e^{k_B T k^2/2m}$. As a result, we obtain the solution

$$g(k,t) = \exp\left[-ikv_0 e^{-\gamma t} - \frac{T}{2m} k^2 (1 - e^{-2\gamma t})\right].$$

Taking the inverse transform, we thus obtain the probability distribution function,

$$p(v,t) = \left(\frac{2\pi T}{m}(1 - e^{-2\gamma t})\right)^{-1/2} \exp\left[-\frac{(v - v_0 e^{-\gamma t})^2}{2\frac{T}{m}(1 - e^{-2\gamma t})}\right].$$

In the limit $t \to 0$, $p(v,t) \simeq \sqrt{\frac{1}{2\pi D t}} \exp[-\frac{(v-v_0)^2}{4Dt}]$, with diffusion constant $D = \frac{T}{m}\gamma$. In the limit $t \to \infty$, $p(v,t) \simeq P^{\text{eq.}}(v) = \sqrt{\frac{m}{2\pi T}} \exp[-\frac{mv^2}{2T}]$.

10.9.3 Ornstein-Uhlenbeck process revisited

We here approach the Ornstein-Uhlenbeck process from the point of view of path integration. As with the harmonic oscillator in quantum mechanics, the path integral approach to the problem is cumbersome (as compared to a direct solution of the Fokker–Planck equation.) However, the path integral of the Ornstein-Uhlenbeck process frequently appears as an approximate integral describing quadratic fluctuations around the stationary points of more complex integrals (much like the harmonic oscillator integral describes quadratic fluctuations in quantum mechanical path integrals). For this reason, it is well invested time to study the integral approach to the Ornstein-Uhlenbeck process.

Once more, we write P instead of p to distinguish probability distributions from momenta p in phase space.

Consider the stochastic equation describing a particle in a harmonic potential with overdamped dynamics, $\dot{q} + \frac{\omega_0^2}{\gamma} q = \xi$ with $\langle \xi(t)\xi(t')\rangle = A\delta(t-t')$ where $A = 2T\frac{\omega_0^2}{\gamma^2}$. In the path integral representation, the probability distribution reads

$$P(q_f, t|q_i, 0) = \int_{q(t)=q_f, q(0)=q_i} D[q,p] e^{-S[q,p]},$$

where $S = -\int_0^t dt' \, (p\dot{q} - H)$, and $H = -\alpha pq - \frac{A}{2}p^2$ with $\alpha = \frac{\omega_0^2}{\gamma}$.

(a) Solve the Hamiltonian equations of motion and determine the corresponding classical action $S_{\rm cl}$.

(b) In order to go beyond the leading semiclassical approximation $P(q_f, t|q_i, 0) \sim e^{-S[q,p]}$, we need to determine the fluctuation determinant. In Section 3.2 we had seen that the fluctuation determinant of a path integral assumes the form (cf. Eq. 3.28)

$$\frac{1}{\sqrt{2\pi}} \sqrt{-\frac{\partial^2 S_{\rm cl}}{\partial q_i \partial q_f}}, \tag{10.119}$$

where the replacement $i \to -1$ of the pre-factor under the square root relates to the fact that we are now dealing with an imaginary time integral. However, the direct substitution of expression (10.119) for the fluctuation determinant would be premature: (10.119) applies to theories whose Hamiltonian is of "conventional" type, $\hat{H} = \hat{T} + \hat{U}$, where $\hat{T}$ and $\hat{U}$ are kinetic and potential energy, respectively. Interpreting q and p as operators with commutation relation $[p, q] = 1$, bring the Hamiltonian of the theory into this form. Show that this substitution changes the action to $S_{\rm cl} \to S_{\rm cl} - \frac{\alpha}{2}t$. (If you feel uncomfortable about the interpretation of the function H in terms of operators, derive the Fokker–Planck equation of the path integral, i.e. the analog of the Schrödinger equation. Re-arrange operators so as to make the Fokker–Planck operator manifestly hermitean. Then construct the path integral representation of that hermitean representation to arrive at the modified action stated above. Think why the alternative representation corresponds to a "mid-point" discretization scheme, different from the Itô representation used in the construction of the MSRJD functional.)

(c) Evaluate the determinant Eq. (10.119) to obtain the result

$$P(q_f, t|q_i, 0) = \left(\frac{2\alpha}{A}\right)^{1/2} \frac{e^{-\frac{\alpha}{A}\frac{(q_i - q_f e^{\alpha t})^2}{e^{2\alpha t}-1}}}{(1-e^{-2\alpha t})^{1/2}}.$$

Notice that the shift $-\alpha t/2$ we obtained as a result of the change in the discretization scheme cancels against a long-time divergent factor in the fluctuation determinant.

Answer:

(a) The classical equations of motion read

$$\dot{q} = \partial_p H = -\alpha q - Ap, \qquad \dot{p} = -\partial_q H = \alpha p,$$

with the solution $p(t) = p_0 e^{\alpha t}$ and $q(t) = ce^{-\alpha t} - \frac{Ap_0}{2\alpha} e^{\alpha t}$. From the boundary conditions, one finds $-\frac{Ap_0}{2\alpha} = \frac{q_i - q_f e^{\alpha t}}{1-e^{2\alpha t}}$ and $c = \frac{q_i - q_f e^{-\alpha t}}{1-e^{-2\alpha t}}$. Substituted into the classical action, after some algebra, one obtains

$$S_{\rm cl} = -\int_0^t dt' (p\dot{q} + \alpha pq + \frac{A}{2}p^2) = \frac{\alpha}{A} \frac{(q_i - q_f e^{\alpha t})^2}{e^{2\alpha t} - 1},$$

with $\alpha/A = \gamma/2T$. (You may check for consistency that $\partial S/\partial q_i = p_i$.)

(b) The form of the Hamiltonian used in the path integral is only correct for the Itô discretization. In order to apply the familiar techniques of quantum mechanics, we have to symmetrise the Hamiltonian by modifying the "vector potential" term,

$$H = -\alpha pq - \frac{A}{2}p^2 \to -\alpha \frac{pq + qp}{2} - \frac{\alpha}{2} - \frac{A}{2}p^2,$$

where the symbol "$\to$" designates a correspondence that would apply if the functions p in the Hamiltonian were to be interpreted as an operator $p = \partial_q$. This leads to an additional factor in the exponential which is linear in t, $S_{\rm cl} \to S_{\rm cl} - \frac{\alpha}{2}t$. More rigorously, we may observe that the full information on the path integral is stored in the Fokker–Planck equation

$$\left(\partial_t + \alpha \partial_q q + \frac{A}{2}\partial_q^2\right) P = 0.$$

The "Fokker–Planck" operator can be rewritten as

$$\frac{\alpha}{2}(\partial_q p + p\partial_q) + \frac{A}{2}\partial_q^2 + \frac{\alpha}{2} = \frac{A}{2}\left(\partial_q + \frac{\alpha}{A}q\right)^2 - \frac{\alpha^2}{2A}q^2 + \frac{\alpha}{2},$$

i.e. in a form resembling a harmonic oscillator Hamilton operator subject to a gauge potential $\alpha q/A$. If we now apply the standard rules of path integral construction in quantum mechanics (a mid-point discretization to properly deal with the gauge potential understood) to the new Fokker–Planck/Hamilton operator, we arrive at the imaginary time integral for our Hamiltonian function H (on the level of Hamiltonian functions, ordering is not an issue), shifted by the constant $\alpha t/2$. The appearance of this constant can be attributed to a change in the discretization scheme.

(c) A straightforward exercise in differentiation.

10.9.4 Directed percolation

This problem is of more technical nature. Within the framework provided by the field theory Eq. (10.112), we explore the role of fluctuations in directed percolation slightly below the upper critical dimension, $d = 4 - \epsilon$. This leads us to a set of RG equations, whose physical significance is discussed in the main text.

Phase transitions in the **directed percolation** universality class are described by the field theory Eq. (10.112). As with our previous examples, contractions of the fields ϕ, ψ w.r.t. the free action of the theory, $\kappa = 0$, generate a Green function,

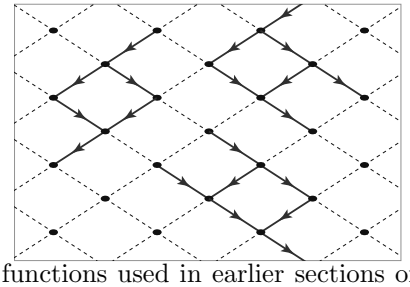

$$\langle \phi_q \psi_{q'} \rangle = g_q \delta_{q,-q'}, \qquad g_q^{-1} = -i\omega + Dk^2 - \tau, \tag{10.120}$$

where g_q relates to the advanced and retarded Green functions used in earlier sections of the text as $g_q \equiv g_q^+ = g_{-q}^-$, and $q \equiv (\omega, \mathbf{k})$ is the four-momentum.

(a) **Perturbation theory:** In order to become familiar with the structure of perturbation theory that treats the interaction κ as a small parameter, we consider the form of the perturbative corrections to the Green function and the vertex. Show that the Green function generalizes to $g^{-1} \to g^{-1} + \Sigma$, where, to lowest order in κ, the self-energy correction reads as

$$\Sigma_q = 2\kappa^2 \int \frac{d^d k'}{(2\pi)^d} \frac{1}{-i\omega + Dk'^2 + D(\mathbf{k} - \mathbf{k}')^2 - 2\tau}. \tag{10.121}$$

Show that the lowest order correction to the coupling constant $\kappa \to \kappa + \delta\kappa$ appears at third order and has the form,

$$\delta\kappa \simeq -2\kappa^3 \int \frac{d^d k'}{(2\pi)^d} \frac{1}{(Dk^2 - \tau)^2}. \tag{10.122}$$

Convince yourself that the diagrams contributing to the renormalization of κ and τ correspond to the "configuration space" processes exemplified by the figure above.

(b) **Renormalization group:** Consider the theory regularized with a hard cutoff Λ for the (spatial) momentum integral. We rescale (spatial) momentum by this cutoff $\mathbf{k} \to \mathbf{k}/\Lambda$ which means that the momentum integrals now extend over the support $|\mathbf{k}| \leq 1$ and all coupling constants are measured in units Λ^{d_x}, where d_x is the relevant engineering dimension.

Integrate out perturbatively the spatial fast modes within the momentum shell $(1, 1/b)$ with $0 < \ln b \ll 1$. Show that in spatial dimension $d = 4 - \epsilon$, this modifies the coupling constants in the following way,

$$\omega \to \omega \left(1 - \frac{x}{2} \ln b\right), \qquad D \to D \left(1 - \frac{x}{4} \ln b\right),$$
$$\tau \to \tau \left(1 - \left(\frac{D}{\tau} + 1\right) x \ln b\right), \qquad \kappa \to \kappa \left(1 - 2x \ln b\right),$$

where we introduced

$$x \equiv \frac{S_4}{(2\pi)^4} \left(\frac{\kappa}{D}\right)^2, \tag{10.123}$$

and S_4 is the area of the four-dimensional unit-sphere. Next, rescale coordinates and fields as $q \to q/b$, $\omega \to \omega/b^z$, $\phi \to \phi b^{-\frac{4-}{2}+}$. Choose the dynamical exponent z and the

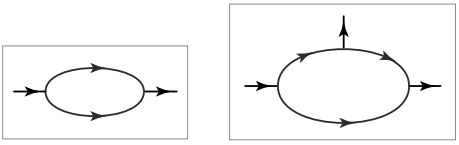

Figure 10.16 Skeleton structure of the two diagrams contributing to the renormalization of the propagator (left) and interaction vertex (right), respectively.

field renormalization exponent χ so as to make the diffusion constant D and the coefficient of frequency invariant under renormalization. Show that this condition generates the equations

$$z = 2 - \frac{x}{4}, \qquad \chi = \frac{x}{4}.$$

The "mass term" τ and the interaction constant κ flow according to Eq. 10.115. The meaning of these equations is discussed in the main text.

Answer:

(a) In Fourier basis, the interaction contribution to the action $S = S_0 + S_{\rm int}$ is given by

$$S_{\rm int}[\phi, \psi] = \kappa \int dq dq' \, \psi_q \phi_{q'} (\phi_{-q-q'} - \psi_{-q-q'}),$$

where the measure $dq = d\omega d^d k/(2\pi)^{d+1}$. Expanding the action to second order in κ, and applying the contraction rule Eq. (10.120), we obtain the self energy

$$\Sigma_q = -2\kappa^2 \int dq' \, (g_{q-q'} g_{q'} + g_{q+q'} g_{q'}).$$

The frequency integration $\int d\omega'$ over $g_{q+q'} q_{q'}$ vanishes because the integrand falls off as $\sim 1/\omega'^2$ and has no poles in the upper complex plane. Doing the contour integration over the remaining contribution, we readily obtain Eq. (10.121). The diagrammatic representation of this term is shown in Fig. 10.16, where the external field vertices (not contributing to the self energy) have been included for the sake of notational clarity.

To obtain the renormalisation of the coupling constant of the interaction, κ it is necessary to develop the third order of perturbation theory. The Wick contraction of these terms (up to the "external field vertices" entering the interaction operator, $\sim \psi\phi^2$ and $\sim \psi^2\phi$) obtains two one-loop diagrams. In one of these all Green functions have their poles on one side of the real axis, which implies vanishing upon frequency integration. The survivor diagram, whose graphical representation is shown in Fig. 10.16 has the analytic representation

$$\frac{(-1)^3}{3!} \langle S^3_{\rm int} \rangle \to -\frac{2^4 3}{3!} \kappa^3 \int dq dq' dq'' \, \phi_{q'} \psi_{q''} (-\phi_{q-q'-q''} + \psi_{q-q'-q''}) \int dp \, g_p^2 g_{-p},$$

where we neglected the "small" momenta q, q', q'' in the arguments of the "fast" Green functions g_p. The required renormalisation of $\delta\kappa$ thus reads $\delta\kappa = -(2\kappa)^3 \int dq\, g_q^2 g_{-q}$. Doing the integral over frequency, we obtain Eq. (10.122).

(b) Consider the contribution $\delta\Sigma$ to Eq. (10.121) due to the integration over the fast momentum layer $\int_f d^d k' \equiv \int_{1/b<|\mathbf{k}'|\ \ 1} d^d k'$. An expansion of the self energy in "small" corrections to the fast momenta obtains

$$\delta\Sigma_q \simeq -2\kappa^2 \left(\frac{I_{-2}}{2D} + \frac{(i\omega + 2\tau) I_{-4}}{(2D)^2} + \frac{k^2}{4D} \left(\frac{2}{d} - 1 \right) I_{-4} + \dots \right),$$

where we introduced $I_n \equiv \int_f \frac{d^d k'}{(2\pi)^d} k'^n$. Likewise, the fast momentum contribution to the coupling constant correction Eq. (10.122) reads

$$\delta\kappa \simeq -\frac{2\kappa^3}{D^2} I_{-4}.$$

In dimensions $4 - \epsilon$, we have $I_{-2} \simeq I_{-4} = \frac{S_4}{(2\pi)^4} \ln b$. Substituting this result into the fast-fluctuation induced change of the Green function, $g^{-1} \to g^{-1} - \delta\Sigma$, we obtain the required renormalization of coupling constants.

The re-scaling of coordinates and fields modifies the renormalization of coupling constants according to

$$\omega \to \omega \left(1 + \left(2\chi - \frac{x}{2} \right) \ln b \right), \qquad D \to D \left(1 + \left(2\chi + z - 2 - \frac{x}{4} \right) \ln b \right),$$
$$\tau \to \tau \left(1 + \left(2\chi + z - \frac{Dx}{\tau} - x \right) \ln b \right), \qquad \kappa \to \kappa \left(1 + \left(\frac{\epsilon}{2} + 3\chi + z - 2 - 2x \right) \ln b \right).$$

Invariance of the first two terms generates the required conditions on χ and z. We finally substitute χ and z into the remaining two equations to obtain the RG equations (10.115).

11

Nonequilibrium (quantum)

In the previous chapter we have seen that departures from equilibrium generate a plethora of new phenomena in statistical physics. While our discussion so far has been limited to classical phenomena, in this chapter we want to ask how quantum mechanics interferes with the conditions of nonequilibrium. Experience shows that, in some cases, nonequilibrium quantum systems can be understood in terms of reasonably straightforward quantization of their classical limits. In others, an interplay of quantum coherence and nonequilibrium driving leads to entirely new phenomena – such as lasing, a paradigm for a steady state nonequilibrium quantum system. At any rate, we have every reason to anticipate that quantum nonequilibrium physics will be as diverse and colourful as its classical counterpart.

Even minor departures from equilibrium call for a theoretical description entirely different from the 'Matsubara formalism' developed in earlier chapters of this book. The applicability of the latter is rigidly tied to the existence of a quantum grand canonical density operator, the hallmark of a many particle equilibrium system. But how then, can an functional theory of nonequilibrium quantum systems be developed? An obvious idea would be to once more go through the different elements of classical nonequilibrium theory developed in the previous chapter, and subject every one of them to an individual quantization scheme. Luckily, there are more efficient ways to achieve our goal: some decades ago, a many particle formalism suitable to describe nonequilibrium systems under the most general conditions[1] was introduced by Keldysh.[2] For a number of reasons, the **Keldysh formalism** will be the principal tool in our approach to quantum nonequilibrium physics: (i) it is highly flexible and can be applied to study the physics of practically any quantum system, in and out of equilibrium. (ii) Although the Keldysh technique was introduced in a pre-path integral era, it is tailor-made to functional integral formulations. (iii) The classical limit of that Keldysh field integral turns out to be the MSRJD functional integral extensively discussed in the previous chapter. In this sense, the Keldysh functional will be our 'theory of everything'; from it the entire body of nonequilibrium theory, both quantum and classical can be derived by reduction.

The discussion above motivates a strategy different from that pursued in our introductory discussion of nonequilibrium physics above. In a "top-down" approach, we begin by

[1] By "most general," we mean that the Keldysh formalism enjoys applicability independent of the distribution (operator) describing the state of the system under consideration.

[2] L. V. Keldysh, Diagram technique for nonequilibrium processes, *Sov. Phys. JETP* **20**, 1018-26 (1965).

a formal introduction of the Keldysh formalism. We alternatively interpret the theory as a generalization of the Matsubara formalism, and as a quantum extension of the MSRJD field integral. After these conceptual structures have been thoroughly introduced, we will turn to the discussion of applications.

INFO In reference to the stochastic aspects of classical nonequilibrium processes, we began the last chapter with a short treatise on probability. Quantum mechanics, on the other hand, is a theory that is *intrinsically* probabilistic; the most we can hope for is to obtain results on the **quantum probability** to measure certain values of observables. The theory of quantum nonequilibrium processes, therefore, involves two "layers" of stochasticity, quantum probability and the extrinsic stochasticity of nonequilibrium processes. As it is important not to confuse these two, we begin by asking what sort of probability distributions might suitably generalize the distributions employed in the previous, classical chapter.

To start, let us consider a classically deterministic system, prepared in a definite quantum state $|\ \rangle$. The (quantum) expectation value to measure a certain observable is then given by $(\hat{X}) \equiv \langle\ |\hat{X}|\ \rangle = \sum_n X_n |\ _n|^2$, where X_n is the nth eigenvalue of X (the generalization to a continuous spectrum is straightforward), $\ _n \equiv \langle n|\ \rangle$, and $|n\rangle$ is the nth eigenstate. We denote the quantum expectation value by ordinary brackets to distinguish it from the average over fluctuations below.

The equation above suggests an interpretation of $P_{\hat{X}}(x) \equiv \sum_n \delta(x - X_n)|\ _n|^2$ as a "quantum probability" distribution of the operator $\hat{X}$. This notation is suggestive in that it allows us to express the computation of quantum observables in formal analogy to the probabilistic formalism used in the previous chapter. For example, $(\hat{X}^n) = \int dx\, P_{\hat{X}}(x) x^n$, and $P_{\hat{X}}(x) = (\delta(x - \hat{X}))$, etc. While the quantity $P_{\hat{X}}$ underpins the probabilistic nature of quantum mechanics, its usefulness rapidly reaches its limits.[3]

For our present purposes, an alternative representation of quantum expectation values will prove more useful: the above expression may equivalently be written as $(\hat{X}) = \mathrm{tr}\,(\hat{\rho}_{|\ \rangle}\hat{X})$, where $\hat{\rho}_{|\ \rangle} \equiv |\ \rangle\langle\ |$ is a particular type of a quantum density operator, viz. a projector onto the one-dimensional space spanned by $|\ \rangle$. The alternative representation can be readily generalized to the – more realistic – situation where the state of the system is not known with certainty. In general, $\hat{\rho} = \sum_a p_a |\ _a\rangle\langle\ _a|$, where $\{|\ _a\rangle\}$ is a complete orthogonal set, and the positive coefficients p_a, $\sum_a p_a = 1$, represent the probability to find the system in state $|\ _a\rangle$. In a many particle system, the inevitable presence of fluctuations – cf. the principles discussed in the previous chapter – may render the coefficients p_a effectively random. These fluctuations may be externally imposed, or caused by integration over microscopic degrees of freedom of the system. Summarily denoting the average over fluctuations by $\langle \dots \rangle_{\mathrm{f}}$, we then have

$$\langle \hat{X} \rangle \equiv \langle (\hat{X}) \rangle_{\mathrm{f}} = \ \mathrm{tr}\,(\hat{\rho}\hat{X})\ _{\mathrm{f}} = \mathrm{tr}\,(\langle \hat{\rho} \rangle_{\mathrm{f}} \hat{X}) = \sum_a \langle p_a \rangle_{\mathrm{f}} \langle\ _a|\hat{X}|\ _a\rangle .$$

This representation illustrates the division of work between quantum and statistical fluctuations. In a canonical (basis-invariant) manner, all aspects of quantum mechanics – interference, wave coherence, etc. – are encapsulated in the mathematical properties of the density operator and

[3] The function P_X suggests deceptively that the basic information on the state of a system is stored in the (positive definite) probability $|\ _n|^2$. However, we know that the essence of quantum mechanics resides in wave function *amplitudes*. For example, it is not possible to unambiguously generalize the notion of P to that of a joint probability $P_{X,Y}(x, y)$ of two non-commutative operators. This means that positive definite probability distributions such as the one above will not suffice to describe quantum processes.

the trace operation. The statistics of fluctuations (both thermal, and externally imposed) is contained in the average over coefficients, $\langle \dots \rangle_{\rm f}$. We repeat that these latter fluctuations may effectively be generated by a quantum average (i.e. a trace operation) over microscopic degrees of freedom of the system.

The discussion above suggests the following transcription of the probabilistic elements of classical nonequilibrium mechanics into quantum mechanics: Notice that if and only if $\hat\rho$ is an

classical	quantum
variable X	hermitian operator $\hat X$
values of X, x	eigenvalues of $\hat X$, x
probability distribution p	density operator $\hat\rho$
moments $\langle X^n\rangle = \int dx\, p(x) x^n$	moments $\langle \hat X^n\rangle = \mathrm{tr}(\hat\rho \hat X^n)$

operator function of $\hat X$ (which will typically happen if $\hat X \equiv \hat H$ is energy), $\langle \hat X^n\rangle = \mathrm{tr}(\hat\rho \hat X^n) = \int dx\, \rho(x) x^n$, where $\rho(x)$ are the eigenvalues of $\rho(\hat X)$. In this particular case, we have a normalized ($\int dx\, \rho(x) = 1$) and positive quantum probability distribution. In general, however, quantum statistical mechanics cannot be described in terms of positive definite probability functions. Rather, the relevant information is stored in density operators, and it is these objects we need to understand.

11.1 Prelude: Quantum master equation

Before turning to the systematic construction of the Keldysh formalism, let us introduce a few elements of the quantum mechanics of nonequilibrium systems in more elementary terms. This discussion will get us acquainted with various "quick and dirty" routes to the description of nonequilibrium systems but will also motivate the construction of the more systematic theories below. (Readers wishing to proceed in a maximally streamlined manner may skip this discussion and directly turn to section 11.2.1.)

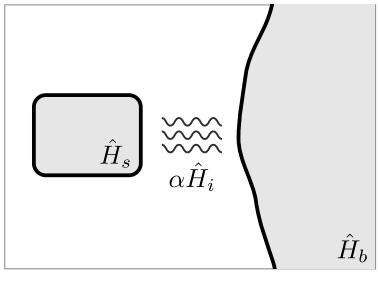

We consider the standard setup of a "system" coupled to a "bath" (cf. the figure.) The bath may alternatively be interpreted as a large system of external degrees of freedom (e.g. the oscillator modes of an external electromagnetic field), or in terms of microscopic internal degrees of freedom affecting the more macroscopic (but still quantum) dynamics of the degrees of freedom we consider to be the "system." By straightforward adaptation of the principles discussed in the previous chapter, we interpret the degrees of freedom of the bath as unobservable. Integration over these degrees of freedom produces an effective, and foreseeably irreversible dynamics of the system. Our immediate goal is the derivation of the equations of motion governing this effective dynamics.

11.1.1 Derivation of the master equation

Consider the density operator $\hat{\rho}$ describing the state of the total system in the product Hilbert space $\mathcal{H} \equiv \mathcal{H}_s \otimes \mathcal{H}_b$ of system (s) and bath (b). The reduced information in which we are interested is stored in the quantity $\hat{\rho}_s \equiv \mathrm{tr}_b(\hat{\rho}) : \mathcal{H}_s \to \mathcal{H}_s$, where tr_b denotes the trace ("integration") over the Hilbert space of the bath. The **reduced density matrix** $\hat{\rho}_s$ is a linear operator acting in the system Hilbert space $\mathcal{H}_s$. The dynamics of the full system is controlled by the Hamiltonian operator $\hat{H} \equiv \hat{H}_s + \hat{H}_b + \alpha \hat{H}_i$, where the coupling between system and bath, $\hat{H}_i$, is weighted by a dimensionless coupling constant α. We assume that, at some initial time $t = 0$ (a) the system and bath had been independent, and (b) that the bath was in a state of thermal equilibrium, $\hat{\rho}(0) = \hat{\rho}_s(0) \otimes \hat{\rho}_b^{\mathrm{eq}}$.

We now aim to formulate an equation of motion for the reduced density matrix. Reflecting the applied relevance of this problem, plenty of different strategies to achieve this goal have been formulated. Here, we derive the equation by a formally exact projector formalism,[4] and then compare to other approaches. The dynamics of the density operator is governed by the equation of motion

$$(\partial_t - \hat{L})\hat{\rho} = 0,$$

where $\hat{L} = \hat{L}_s + \hat{L}_b + \alpha \hat{L}_i$, and $\hat{L}_{s,b,i} \equiv -i[\hat{H}_{s,b,i}, \ ]$ are "quantum Liouville operators." We next introduce the projector

$$\mathcal{P} \equiv \hat{\rho}_b^{\mathrm{eq}} \, \mathrm{tr}_b(\, . \,),$$

where the trace operation acts on everything to the right, and unit normalization of $\hat{\rho}_b^{\mathrm{eq}}$ is assumed. (As an exercise, consider why this is a projector.) To simplify the derivation, we assume that the thermal trace of the interaction operator over $\mathcal{H}_b$ vanishes,[5] $\mathrm{tr}_b(\hat{\rho}_b^{\mathrm{eq}} \hat{H}_i) = 0$. Our projector thus obeys the equations,

$$\mathcal{P}\hat{L}_b = \hat{L}_b\mathcal{P} = 0, \qquad [\hat{L}_s, \mathcal{P}] = 0, \qquad \mathcal{P}\hat{L}_i\mathcal{P} = 0, \tag{11.1}$$

where the first follows from the cyclic invariance of the trace, the second should be obvious, and the third expresses the presumed vanishing of the interaction under the bath-trace. Introducing the complementary projector $\mathcal{Q} \equiv \mathrm{id} - \mathcal{P}$, and the shorthand notation $\hat{\rho}_P \equiv \mathcal{P}\hat{\rho}$, $\hat{\rho}_Q \equiv \mathcal{Q}\hat{\rho}$, the quantum Liouville equation may now be split into two,

$$\begin{aligned} \partial_t \hat{\rho}_P &= \hat{L}_s \hat{\rho}_P + \alpha \mathcal{P}\hat{L}_i \hat{\rho}_Q, \\ \partial_t \hat{\rho}_Q &= \mathcal{Q}\hat{L}\hat{\rho}_Q + \alpha \mathcal{Q}\hat{L}_i \hat{\rho}_P. \end{aligned} \tag{11.2}$$

The second of these equations is solved by (exercise)

$$\hat{\rho}_Q(t) = \alpha \int_0^t dt' \, e^{t' \mathcal{Q}\hat{L}\mathcal{Q}} \hat{L}_i \hat{\rho}_P(t - t').$$

[4] S. Nakajima, On quantum theory of transport phenomena: steady diffusion, *Prog. Theory. Phys.* **20**, 948-59 (1958); R. Zwanzig, Ensemble method in the theory of irreversibility, *J. Chem. Phys.* **33**, 1338-41 (1960).

[5] Should this condition not be met by the interaction under consideration, the term $\mathrm{tr}_b(\hat{\rho}_b^{\mathrm{eq}} \hat{H}_i) = 0$ can be interpreted as part of the *system* Hamiltonian operator.

Substitution of this result into the first equation obtains

$$\partial_t \hat{\rho}_P = \hat{L}_s \hat{\rho}_P + \alpha^2 \int_0^t dt' \, \mathcal{P}\hat{L}_i e^{t' \mathcal{Q}\hat{L}\mathcal{Q}} \hat{L}_i \hat{\rho}_P(t-t'), \tag{11.3}$$

or, employing the projector operation $\mathcal{P}$,

$$\boxed{\partial_t \hat{\rho}_s = \hat{L}_s \hat{\rho}_s + \alpha^2 \int_0^t dt' \quad \hat{L}_i e^{t' \mathcal{Q}\hat{L}\mathcal{Q}} \hat{L}_i \quad {}_b \, \hat{\rho}_s(t-t'),} \tag{11.4}$$

where $\langle \dots \rangle_b \equiv \mathrm{tr}_b((\dots)\hat{\rho}_b^{\mathrm{eq}})$.

Equation (11.4) is commonly denoted a **generalized master equation**. But in fact, the resemblance to a master equation is only formal. Rather, this equation (together with a complementary equation for $\hat{\rho}_Q$) is an exact reformulation of the full quantum theory; the complete information on quantum unitary time evolution resides in the time non-local memory kernel on the right hand side. In contrast, the master equation generally describes time-local (Markovian) and irreversible processes. To obtain a "true" master equation one may eliminate information in what effectively amounts to a Markovian approximation. Assuming that the time scales over which ρ_s changes are large in comparison to the relaxation times t' of the integral kernel, Eq. (11.4) reduces to a Markovian equation $\partial_t \hat{\rho}_s = (\hat{L}_s + \alpha^2 \hat{X})\hat{\rho}_s(t)$, where $\hat{X} \equiv \int_0^\infty dt' \, \langle \hat{L}_i e^{t' \mathcal{Q}\hat{L}\mathcal{Q}} \hat{L}_i \rangle_b$.

It is also customary to assume weak coupling, or small α, so that the α-dependence of the exponent can be neglected (a variant of a "Born approximation"). The resulting simplifications are best discussed in the language of the prototypical equation (11.3): defining $\hat{L}_0 \equiv \hat{L}_s + \hat{L}_b$, the integral kernel in that equation reduces to

$$\mathcal{P}\hat{L}_i e^{t' \mathcal{Q}\hat{L}_0 \mathcal{Q}} \hat{L}_i \, \hat{\rho}_P(t-t') = \mathcal{P}\hat{L}_i e^{t' \hat{L}_0} \hat{L}_i \, \hat{\rho}_P(t-t').$$

EXERCISE Use Eq. (11.1) above to verify this relation.

Further, defining $\hat{H}_0 = \hat{H}_s + \hat{H}_b$, and $\hat{O}(t) \equiv e^{it\hat{H}_0} \hat{O} e^{-it\hat{H}_0}$ for the interaction picture time representation of an operator $\hat{O}$, we have

$$\mathcal{P}\hat{L}_i e^{t' \hat{L}_0} \hat{L}_i \, \hat{\rho}_P(t-t') \simeq \mathcal{P}\hat{L}_i \hat{L}_i(-t') \, \hat{\rho}_P(t-t').$$

EXERCISE For an arbitrary operator $\hat{O}$, show that $e^{t\hat{L}_0}\hat{O} = \hat{O}(t)e^{t\hat{L}_0}$. The equality above is approximate because we neglect the action of $e^{t' \hat{L}_0}$ on the (slow) operator $\hat{\rho}_P$.

Using this result, we find that Eq. (11.4) reduces to the (Markovian) **quantum master equation**

$$\boxed{\partial_t \hat{\rho}_s = \left(\hat{L}_s + \alpha^2 \int_0^t dt' \quad \hat{L}_i(0) \hat{L}_i(-t') \quad {}_b \right) \hat{\rho}_s.} \tag{11.5}$$

11.1.2 Example: oscillator coupled to a bath

It is instructive to study the meaning of the master equation on a concrete example: consider a harmonic oscillator – the system – coupled to an assembly of other oscillators, the bath. We describe this setup in terms of the Hamiltonian $\hat{H} = \hat{H}_s + \hat{H}_b + \alpha\hat{H}_i$, where

$$\hat{H}_s = \epsilon\left(a^\dagger a + \frac{1}{2}\right), \qquad \hat{H}_b = \sum_k \omega_k \left(a_k^\dagger a_k + \frac{1}{2}\right), \qquad \hat{H}_i = \sum_k \left(c_k a_k^\dagger a + \text{h.c.}\right). \quad (11.6)$$

Using the fact that $a(t) = e^{-i\epsilon t}a$ and $a_k(t) = e^{-i\omega_k t}a_k$, it is straightforward to verify that

$$\begin{aligned}
\alpha^2 \int_0^t dt' \quad & \hat{L}_i(0)\hat{L}_i(-t') \quad {}_b\hat{\rho}_s = -\alpha^2 \sum_k |c_k|^2 \int_0^\infty dt' \\
& \times \Big(e^{-i(\omega_k-\epsilon)t'} \left(\langle\hat{n}_k\rangle \left(\hat{\rho}_s a a^\dagger - a^\dagger\hat{\rho}_s a\right) + \langle\hat{n}_k+1\rangle \left(a^\dagger a\hat{\rho}_s - a\hat{\rho}_s a^\dagger\right)\right) \\
& \quad e^{+i(\omega_k-\epsilon)t'} \left(\langle\hat{n}_k\rangle \left(a a^\dagger\hat{\rho}_s - a^\dagger\hat{\rho}_s a\right) + \langle\hat{n}_k+1\rangle \left(\hat{\rho}_s a^\dagger a - a\hat{\rho}_s a^\dagger\right)\right) \Big) \\
= \alpha^2\pi & \sum_k |c_k|^2 \delta(\epsilon-\omega_k) \\
& \times \left(\langle\hat{n}_k\rangle \left(2a^\dagger\hat{\rho}_s a - \hat{\rho}_s a a^\dagger - a a^\dagger\hat{\rho}_s\right) + \langle\hat{n}_k+1\rangle \left(2a\hat{\rho}_s a^\dagger - \hat{\rho}_s a^\dagger a - a^\dagger a\hat{\rho}_s\right)\right) \\
\simeq \pi\alpha^2 & |c_\epsilon|^2 \rho(\epsilon) \left(\langle\hat{n}_\epsilon\rangle \left(2a^\dagger\hat{\rho}_s a - \hat{\rho}_s a a^\dagger - a a^\dagger\hat{\rho}_s\right) + \langle\hat{n}_\epsilon+1\rangle \left(2a\hat{\rho}_s a^\dagger - \hat{\rho}_s a^\dagger a - a^\dagger a\hat{\rho}_s\right)\right).
\end{aligned}$$

Here, $\hat{n}_k = a_k^\dagger a_k$ is the number operator of the bath, and we have neglected the subscript 'b' in $\langle\ldots\rangle \equiv \langle\ldots\rangle_b$. In the fourth equality we introduced the spectral density of the bath, $\rho(\omega) \equiv \sum_k \delta(\omega-\omega_k)$, and we assumed that $c_k \equiv c_{\omega_k}$ and $\langle\hat{n}_k\rangle \equiv \langle\hat{n}_{\omega_k}\rangle$ depend only on the energy of the reference state.

EXERCISE In the second equality above we assumed that $[\hat{\rho}_s, a^\dagger a] = 0$. Verify that a relaxation of that assumption will lead to terms of the structure $\sim P\int d\omega \frac{|c_\omega|^2\ (\omega)}{\omega-} \langle\hat{n}_\omega\rangle [a^\dagger a, \hat{\rho}_s]$, where $P\int$ is the principal value integral. Interpret these expressions in terms of an **energy shift** of the oscillator energy due to virtual transitions into the bath.

Assuming once more commutativity of $\hat{\rho}_s$ with $\hat{n} \equiv a^\dagger a$, we have $\hat{L}_s\hat{\rho}_s = 0$ and thence

$$\begin{aligned}
\partial_t\rho_s = \pi\alpha^2|c_\epsilon|^2\rho(\epsilon) \big[& \langle\hat{n}_\epsilon\rangle \left(2a^\dagger\hat{\rho}_s a - \hat{\rho}_s a a^\dagger - a a^\dagger\hat{\rho}_s\right) \\
& + \langle\hat{n}_\epsilon+1\rangle \left(2a\hat{\rho}_s a^\dagger - \hat{\rho}_s a^\dagger a - a^\dagger a\hat{\rho}_s\right)\big]. \qquad (11.7)
\end{aligned}$$

But what is the meaning of this equation? In fact, it will be instructive to look at Eq. (11.7) from a number of different perspectives: the commutativity $[\hat{\rho}_s, \hat{n}] = 0$ implies that $\hat{\rho}_s = \hat{\rho}_s(\hat{n})$. Using commutator relations such as $a^\dagger\hat{\rho}_s(\hat{n}) = \hat{\rho}_s(\hat{n}-1)a^\dagger$, it is then straightforward to bring Eq. (11.7) into the form

$$\begin{aligned}
\partial_t\rho_s(\hat{n}) = 2\pi\alpha^2|c_\epsilon|^2\rho(\epsilon)\Big[& \underbrace{\langle\hat{n}_\epsilon\rangle \left(\hat{n}\hat{\rho}_s(\hat{n}-1) - (\hat{n}+1)\hat{\rho}(\hat{n})\right)}_{\text{absorption}} \\
& + \underbrace{\langle\hat{n}_\epsilon+1\rangle \left((\hat{n}+1)\hat{\rho}_s(\hat{n}+1) - \hat{n}\hat{\rho}_s(\hat{n})\right)}_{\text{emission}}\Big].
\end{aligned}$$

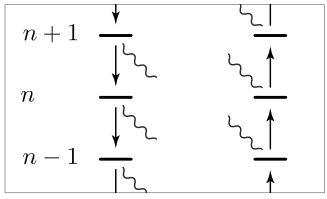

The right–hand side of this equation now affords a straightforward interpretation in terms of absorption and emission of bath bosons (see figure). The absorption term is proportional to the number of available bosons ($\langle\hat{n}_\epsilon\rangle$) resonant with the oscillator frequency, the golden rule transition rate, $\sim |c_\epsilon|^2\rho(\epsilon)$, and to the number of absorbing bosons (plus one). Importantly, the absorption process contributes to the right–hand side in a manner symptomatic of a master equation. The density operator (or better to say, the eigenvalue) $\hat{\rho}_s(n)$ increases due to an "in" process $\propto \hat{\rho}_s(\hat{n}-1)$ and it diminishes due to an "out" process $\propto \hat{\rho}_s(\hat{n})$. There is also an emission process wherein bath bosons are resonantly created from oscillator bosons. Emission, too, enters the master equation as a sum of an in and an out process.

A few more comments can be made on the structure of the master equation:

- ▷ The concerted appearance of in- and out- terms implies the conservation of the trace of the density operator (the quantum analogue of the conservation of probability): $\partial_t \mathrm{tr}(\hat{\rho}_s) = 0$ (exercise).
- ▷ Assume the bath is in equilibrium, $\langle\hat{n}_\epsilon\rangle = (\exp(\beta\epsilon)-1)^{-1}$. It is then straightforward to verify that the distribution $\hat{\rho}_s$ becomes stationary (the right–hand side of the master equation vanishes) on the equilibrium configuration

$$\hat{\rho}_s(\hat{n}) = \mathcal{Z}^{-1} e^{-\beta\epsilon\hat{n}},$$

  where $\mathcal{Z} = (1-e^{-\beta\epsilon})^{-1}$ is the normalizing partition function. Interaction with the bath "thermalizes" the system at a temperature set by the bath temperature. Notice that equilibration relies on the interplay of emission and absorption processes.
- ▷ It is worth noting that the in-terms (out-terms) in the master equation derive from the terms $\sim a^\dagger\hat{\rho}_s a$, etc. ($\sim \hat{\rho}_s a^\dagger a$, etc.) in the parent equation (11.7). To understand the heuristics behind this observation, recall that the interaction picture time evolution of the density operator is given by (symbolic notation throughout) $\hat{\rho}_s(t) = \hat{U}(t)\hat{\rho}_s(0)\hat{U}^\dagger(t)$, where $\hat{U}$ is the time evolution operator. We may visualize the time evolution described by these operators by two lines in "time space," one directed forward and one backward, cf. Fig. 11.1.

  If we now probe the incremental change of $\hat{\rho}_s$ in time, i.e. compare $\hat{\rho}_s(t+\Delta t)$ with $\hat{\rho}_s(t)$, we may linearly expand either $\hat{U}$ or $\hat{U}^\dagger$ in $\alpha\hat{H}_i$. This produces a factor $\alpha\hat{H}_i(t)$ acting either to the left or to the right of the time evolution operator, or an interaction Hamiltonian acting at the end of the forward or the backward time contour. However, to obtain a non-vanishing result, we need to expand to one more order. This gives a factor $\sim \alpha\int dt'\hat{H}_i(t')$ which, again, may act to the left or the right of the density operator, or on the forward or backward contour. All in all, we obtain four contributions, as visualized in Fig. 11.1. Now, the contributions where $\hat{H}_i$ acts on different time contours (a) are formally described by a density operator sandwiched between creation and annihilation operators, and (b) physically change the state of the system (c) alluding to diagrammatic language, they resemble 'vertex corrections" in a "two-particle propagator. These are the in-terms.

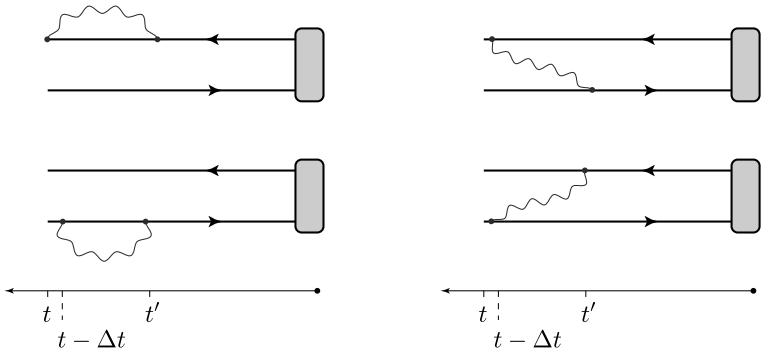

Figure 11.1 Evolution of the density operator (shaded box) along the double time contour. Left: out-processes ("self-energy corrections"), right: in-processes ("vertex corrections"). For the motivation for the "left" orientation of the time arrow, see below.

Conversely, the contributions where $\hat{H}_i$ acts twice on the same contour, (a) are described by pairs of operators acting on one side of the density operator, and (b) do not change the state of the system (more precisely, it is first changed at t' and then changed back at t.) (c) These out–terms resemble self-energy corrections in a two-particle propagator. Indeed, we have seen on various occasions that the (imaginary part) of a self-energy correction represents a decay rate, i.e. the rate of an "out-process."

It is worth pointing out that our discussion of the quantum master equation so far has been rather superficial (for a more substantial exposition, see Weiss,[6] van Kampen,[7] and Haake[8]). Its primary purpose was to motivate a number of concepts relevant to the physics of quantum nonequilibrium phenomena. We next turn to the construction of a field integral based theory which will enable us to describe nonequilibrium phenomena in a much broader setting.

11.2 Keldysh formalism: basics

11.2.1 The idea

Before venturing into the construction of the Keldysh nonequilibrium theory, let us first try to summarize what kind of theory we are after:

1. Previously, we have argued that the object generalizing the probability distributions which pervade the previous chapter is the quantum density operator $\hat{\rho}$. Expectation values of observables are evaluated by taking the traces of hermitian operators against the **dynamically evolved density operator**.

[6] U. Weiss, *Quantum Dissipative Systems*, (World Scientific Publishing, 1993).
[7] N.G. van Kampen, *Stochastic Processes in Physics and Chemistry*, (Elsevier,1992).
[8] F. Haake, *Quantum Signatures of Chaos* (Springer-Verlag, 2001).

2. That dynamics is described by the (adjoint action of the) quantum time evolution operator, $\hat{\rho} \to U(t)\hat{\rho}\hat{U}(t)^\dagger$. We may interpret $\hat{U}$ ($\hat{U}^\dagger$) as the descriptor of quantum time evolution forward (backward) in time. The notion of **chronological directedness** becomes manifest in the interaction-picture representation of the evolution operator $\hat{U}$ as a time ordered exponential $\hat{U} = T\exp(-i\int_0^t dt'\hat{H}_{\rm int}(t'))$. Conversely, we may generate $\hat{U}^\dagger$ by time ordering along a reversed temporal contour, $\hat{U}^\dagger = \tilde{T}\exp(-i\int_t^0 dt'\hat{H}_{\rm int}(t'))$, where $\tilde{T}$ puts operators to the left that are chronologically earlier.
3. In many applications we may safely assume that, at some **initial time** (set as $t = -t_0$ for definiteness) the system of interest was in a known state. For example, $\hat{\rho}(-t_0) = \exp(-\beta\hat{H})$ may have been an equilibrium distribution, or $\hat{\rho}(-t_0) = \hat{\rho}_s \otimes \hat{\rho}_b$ in the case of a composite involving a system coupled to a bath. It is assumed that the interactions/correlations/nonequilibrium conditions rendering the situation nontrivial are slowly switched on at some later time.
4. From our experience with classical probability theory, we know that it is convenient to work with **generating functions**. For instance, in equilibrium statistical mechanics, one might wish to compute the Maxwell–Boltzmann generating functional (symbolic notation) $G(h) \equiv \mathcal{Z}^{-1}\int\exp(-\beta(H - hX))$, where $\mathcal{Z} = \int\exp(-\beta H)$ is the partition function, $\int$ denotes an integration over all states of the system, H is the Hamiltonian and X an observable of interest. Differentiation with respect to the sources h generates moments of X and we have the normalization $G(0) = 1$.

   How can the concept of generating functions be generalized to the quantum nonequilibrium case? Generalization to "quantum" is relatively obvious: replace functions by operators, and integrals by traces. But what about "nonequilibrium"? From what has been said above, it should be evident that we need to endow some known quantum distribution $\hat{\rho}(0)$ with a sense of dynamics, in a manner that leads to a properly normalized, and generally time-dependent generating functional.

In the mid–1960s, Keldysh formulated a theory[2] that solved the problems alluded to above in one stroke.[9] At first sight, **Keldysh's conceptual ansatz** may look strange, if not downright silly: suppose we are given an initial density operator $\hat{\rho}$ which described our system at some time $t \equiv -t_0 \to -\infty$ in the distant past when the world was nice and easy – no interactions, stochastic fluctua-

Leonid. V. Keldysh 1931–

Former Director of the Lebedev Physical Institute, Moscow. Keldysh has made seminal contributions to solid state theory from the physics of electron–hole excitations in semiconductors to the development of techniques to explore quantum systems driven from equilibrium. Recipient of the Lenin Prize, Lomonosov Prize, and the Hewlett-Packard Prize.

[9] For earlier work in the same spirit, see J. Schwinger, Brownian motion of a quantum oscillator, *J. Math. Phys.* **2**, 407-32 (1961), L.P. Kadanoff and G. Baym, *Quantum Statistical Mechanics* (Benjamin, New York, 1962), R. P. Feynman and F. L. Vernon, The theory of a general quantum system interacting with a linear dissipative system, *Ann. Phys.* **24**, 118-73 1963.

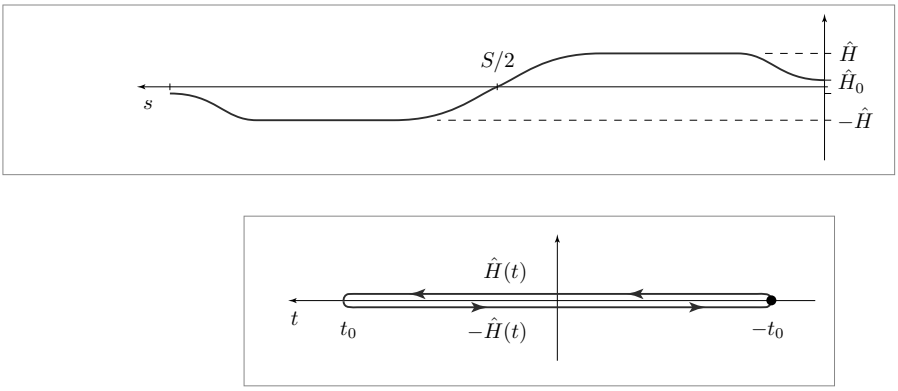

Figure 11.2 Top: parameter dependence of the system Hamiltonian along an "abstract" Keldysh contour. Bottom: embedding of the contour in the complex time plane.

tions, or similar complications. Our goal is to endow the density operator with a sense of dynamics. To this end, consider an abstract parameter interval, $[0, S]$. On this interval, we define an operator valued function $\hat{H}(s)$ according to the following rules: (i) $\hat{H}(0) = -\hat{H}(S) = \hat{H}_0$, where $\hat{H}_0$ is the "trivial" Hamiltonian operator governing the system at time $-t_0$. (ii) As s increases, the non-trivial elements of the dynamics are gradually (adiabatically) switched on (cf. Fig. 11.2) until the Hamiltonian has reached its full form $\hat{H}(s) = \hat{H}$. (iii) Upon approaching the center of the parameter interval, we let the Hamiltonian diminish down to $\hat{H}(S/2) = 0$. (iv) Beyond $s = S/2$, the profile of $\hat{H}$ is anti-symetrically continued, i.e. $\hat{H}(s) = -\hat{H}(S - s)$ for $s \in [S/2, S]$.

Now consider the unitary operator $\hat{U} \equiv T_s \exp(-i \int_0^S ds \hat{H}(s))$, where T_s orders along the s-contour. This operator is but a complicated representation of unity, $\hat{U} = \mathbf{1}$. Heuristically, the triviality of $\hat{U}$ follows from the fact that the dynamic "phases" $\sim \int ds \hat{H}(s)$ accumulated along the forward branch of the contour cancel against those from the backward branch. More formally, one may consider the generalization $\hat{U}(s_2, s_1) \equiv T_s \exp(-i \int_{s_1}^{s_2} ds \hat{H}(s))$ to arbitrary segments on the contour. These operators satisfy the composition law (proof is analogous to the one for conventional time ordered operators) $\hat{U}(s_1, s_2)\hat{U}(s_2, s_3) = \hat{U}(s_1, s_3)$, where $s_1 > s_2 > s_3$. Thus, $\hat{U} \equiv \hat{U}(S, 0) = \hat{U}(S, S/2)\hat{U}(S/2, 0)$. But $\hat{U}(S/2, 0) = \hat{U}(S, S/2)^{-1}$, by construction of the Hamiltonian. The equality $\hat{U} = \mathbf{1}$ trivially implies

$$\mathcal{Z} \equiv \mathrm{tr}(\hat{U}\hat{\rho}) = 1, \tag{11.8}$$

on account of the normalization of $\hat{\rho}$. We therefore have an object that is obtained by dynamical evolution (1) of a known initial density operator (3), is time ordered (2), and manifestly normalized (4). What is not clear, however, is what the "partition function" $\mathcal{Z}$ might be good for!

At the same time, the operator $\hat{U}\hat{\rho}$ is not too different from the objects studied in the previous section. There, we had considered dynamically evolved density operators $\hat{U}\hat{\rho}\hat{U}^\dagger$, $\hat{U} \equiv \hat{U}(t_0, -t_0)$. The trace over these operators, $\mathrm{tr}(\hat{U}\hat{\rho}\hat{U}^\dagger) = \mathrm{tr}(\hat{U}^\dagger\hat{U}\hat{\rho}) = \mathcal{Z}$ can be interpreted as a variant of the above partition function, where the curve $[0, S]$ is parameterized in terms of a time argument running from $-t_0$ to t_0 and back. Pictorially, (cf. Fig. 11.1), the trace operation can be visualized by a closure of the lines emanating from the initial density operator at a large time t_0.

To get a first hint at the usefulness of the closed contour construction, let us add a perturbation to $\hat{H}(s)$ that breaks the symmetry between the contours: we generalize $\hat{H}(s) \to \hat{H}(s)+a\delta(s-s_0)\hat{X}$, where $s_0 \in [0, S/2]$ is in the first half of the contour, a is a number, and $\hat{X}$ is some operator. Let $\hat{U}_{\rm int}$ be the time evolution operator in the "interaction representation" with respect to this perturbation. This representation is defined in perfect analogy to the interaction representation of conventional time-dependent quantum mechanics, only that the "time integrals" extend over the contour $[0, S]$, instead of over an interval on the real time axis. Specifically, $\hat{U}(a) = \hat{U}_0\hat{U}_{\rm int}(a) = \hat{U}_{\rm int}(a)$, where $\hat{U}_0 = \mathbf{1}$ is the unperturbed evolution operator, and $\hat{U}_{\rm int}(a) = \mathbf{1}+ia\int_0^S ds\delta(s-s_0)\hat{X}(s)+\mathcal{O}(a^2) = \mathbf{1}+ia\hat{X}(s_0)+\mathcal{O}(a^2)$, where $\hat{X}(s_0) = \hat{U}_0^\dagger(s_0,0)\hat{X}U_0(s_0,0)$. Insertion of this result into the trace leads to the result

$$-i\partial_a\Big|_{a=0}\mathrm{tr}(\hat{U}(a)\hat{\rho}) = \mathrm{tr}(\hat{U}_0^\dagger(s_0,0)\hat{X}\hat{U}(s_0,0)\hat{\rho}) = \mathrm{tr}(\hat{X}\hat{\rho}(s_0)),$$

where $\hat{\rho}(s_0) = \hat{U}(s_0,0)\hat{\rho}\hat{U}^\dagger(s_0,0)$ is the density operator evolved to s_0 and we omitted the subscript 0. Thus, differentiation of the density operator with respect to the source generates expectation values of operators in the dynamically evolved state of the system. Put differently, $\mathcal{Z}(a) \equiv \mathrm{tr}(\hat{\rho}\hat{U}(a))$ is a normalized ($\mathcal{Z}(0) = 1$) **generating function** for quantum expectation values of the operator $\hat{X}$ in the dynamical state of the system – which need not be in equilibrium. It thus appears that the closed time formalism efficiently addresses the points (1)-(4) listed above. This is the basic idea behind Keldysh's formalism.

11.2.2 Case study

As a first step towards the construction of a functional integral implementation of the Keldysh partition function, we consider a miniature quantum system containing only a single bosonic state of energy ω. In a rather natural way, the construction of the corresponding functional integral will introduce most concepts central to the Keldysh formalism, while the notation remains refreshingly simple.

Consider, then, the partition function

$$\mathcal{Z} \equiv \mathrm{tr}\left(T_\gamma e^{-i\int_\gamma dt\,\hat{H}(t)}\hat{\rho}_0\right), \tag{11.9}$$

where, setting $\mathcal{Z}_0 = (1-e^{-\beta(\omega-\mu)})^{-1}$,

$$\hat{\rho}_0 = \mathcal{Z}_0^{-1}\, e^{-\beta(\hat{H}-\mu\hat{N})}, \tag{11.10}$$

is the equilibrium density operator, $\hat{H} = \omega a^\dagger a$ the Hamiltonian operator and $\hat{N} = a^\dagger a$, as usual. The operator T_γ orders along the contour $\gamma : (t = 0) \to (t = T) \to (t = 0)$, and

we denote the initial (final) time of the theory by $t = 0$ ($t = T$) instead of the $t = -t_0$ ($t = t_0$) used in the previous section. Finally, the time-dependent Hamiltonian operator reads $\hat{H}(t) = \hat{H}\,\mathrm{sgn}(T - t)$, where we ignore the stages of adiabatic switching on and off alluded to in the previous section. (The straightforward generalization to a smoothly varying $\hat{H}(t)$ will render the notation slightly more complicated but is otherwise inconsequential.)

EXERCISE Show that

$$\langle\bar{\psi}|e^{ca^\dagger a}|\psi\rangle = e^{e^{c\,-}}\quad , \tag{11.11}$$

where $\langle\bar{\psi}|$ and $|\psi\rangle$ are boson coherent states. Hint: differentiate by c to derive a first order differential equation and use the uniqueness of its solution.

Let us now construct a coherent state field integral by the usual recipe – insertion of a large number $2N$ of coherent state resolutions of unity into a time-slice dissection of $\mathcal{Z}$. This leads to expressions of the form,

$$\langle\psi_N^-|\hat{U}_{-\epsilon}|\psi_{N-1}^-\rangle\langle\psi_{N-1}^-|\hat{U}_{-\epsilon}\ldots|\psi_1^-\rangle\langle\psi_1^-|\mathbf{1}|\psi_N^+\rangle\langle\psi_N^+|\hat{U}_\epsilon|\psi_{N-1}^+\rangle\langle\psi_{N-1}^+|\hat{U}_\epsilon\ldots|\psi_1^+\rangle\langle\psi_1^+|\hat{\rho}_0|\psi_N^-\rangle,$$

where $\epsilon = T/N$ and $\hat{U}_\epsilon = e^{-i\epsilon\hat{H}}$. The functional integral representation then becomes

$$\begin{aligned}\mathcal{Z} = \mathcal{Z}_0^{-1}\int D(\bar{\psi},\psi)\, e^{\sum_{j=2}^N\left(\bar{\psi}_j^+\left[\psi_{j-1}^+-\psi_j^+-i\epsilon\omega\psi_{j-1}^+\right]+\bar{\psi}_j^-\left[\psi_{j-1}^--\psi_j^-+i\epsilon\omega\psi_{j-1}^-\right]\right)}\\ \times\, e^{-\bar{\psi}_1^+\psi_1^+-\bar{\psi}_1^-\psi_1^-+\kappa\bar{\psi}_1^+\psi_N^-+\bar{\psi}_1^-\psi_N^+},\end{aligned} \tag{11.12}$$

where $\kappa \equiv \exp(-\beta(\omega - \mu))$. At this stage, we would normally take a continuum limit, $N \to \infty$ at fixed T. In the present context, however, it is rewarding to stay for a while with the discrete representation, and interpret the exponent of the functional integral as a bilinear form $i\bar{\psi}G^{-1}\psi$, with the $(2N) \times (2N)$ dimensional matrix kernel

$$G^{-1} = i\left[\begin{array}{cccc|cccc} 1 & & & & & & & -\kappa \\ -a_+ & 1 & & & & & & \\ & \ddots & \ddots & & & & & \\ & & -a_+ & 1 & & & & \\ \hline & & & -1 & 1 & & & \\ & & & & -a_- & \ddots & & \\ & & & & & \ddots & 1 & \\ & & & & & & -a_- & 1 \end{array}\right], \tag{11.13}$$

where $a_\pm \equiv 1 \mp i\epsilon\omega$. Let us explore a few properties of this matrix. First, it is straightforward to verify that

$$\det(-iG^{-1}) = 1 - \kappa(a_+a_-)^N.$$

EXERCISE Verify this result. Hint: use the identity det = exp tr ln. Expand the logarithm in powers of the difference from the unit matrix, $(-iG^{-1} - 1)$ (essentially the side-diagonal containing the coefficients $a_\pm$, plus the corner element κ). Take the trace and re-sum the series into another logarithm. Exponentiation leads to the result.

Taking the limit $N \to \infty$, we obtain

$$\det(-iG^{-1}) = 1-\kappa(1+(\epsilon\omega)^2)^N = 1-\kappa\left(1+\left(\frac{(T\omega)^2}{N^2}\right)\right)^N \overset{N\to\infty}{\longrightarrow} 1-\kappa = 1-e^{-\beta(\epsilon-\mu)} = \mathcal{Z}_0^{-1}.$$

Since $\mathcal{Z} = \mathcal{Z}_0^{-1}\det(-iG^{-1})^{-1}$, this result proves the **unit normalization** of the functional Keldysh partition function.

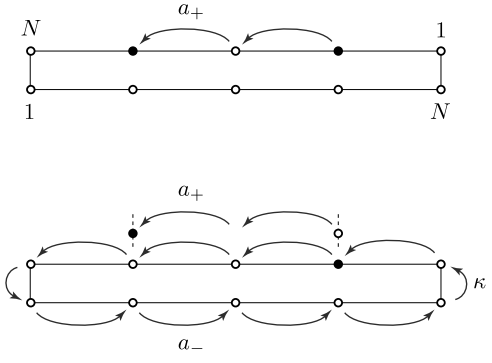

In later applications we will need to compute expectation values $\langle\bar\psi_i\psi_j\dots\psi_k\rangle$ by Wick's theorem. For this purpose, we need to know the elementary contractions

$$G^{CC'}_{ii'} = -i\langle\psi^C_i\bar\psi^{C'}_{i'}\rangle,$$

where $C, C' = \pm$. To this end, let us introduce the block decomposition $G^{-1} = \left(\begin{smallmatrix} M^{++} & M^{+-} \\ M^{-+} & M^{--}\end{smallmatrix}\right)$. It is a straightforward (and worthwhile) exercise to show that

$$\left[M^{CC}\right]^{-1}_{ij} = -i\Theta(i-j)a_\pm^{i-j},$$

where $\Theta(n) = 1$ if $n \geq 0$ and zero otherwise. We may now use the general formulae for the inversion of 2×2 block matrices to obtain $G^{++} = (M^{++} - \mathrm{fl}^{++})^{-1}$, where $\mathrm{fl}^{++} = M^{+-}(M^{--})^{-1}M^{-+}$. Substitution of $\mathrm{fl}^{++}_{ij} = i\delta_{i1}\delta_{jN}a_-^{N-1}\kappa$ into this formula followed by a straightforward series expansion in fl leads to the result

$$G^{++}_{ij} = -ia_+^{i-j}\left(\Theta(i-j) + \frac{\kappa(a_+a_-)^{N-1}}{1-\kappa(a_+a_-)^{N-1}}\right). \tag{11.14}$$

INFO This formula affords an **intuitive interpretation** (cf. the figure above). The matrix G^{++} is the amplitude for propagation between two discrete points j and i on the $+$-part of our closed time contour. To get from j to i we may either go directly, which is possible if $i > j$ (the time ordering). In this case, we pick up $i-j$ hopping amplitudes a_+. This is the first term in the equation. Alternatively, we may go via round-trips through the $-$-part of the contour. In this case, and no matter what the chronological ordering between i and j, we first go from j to N ($(N-j)$ amplitudes a_+), then proceed from 1 to N on the bottom part ($(N-1)$ amplitudes a_-) go back to the upper part (a factor κ), and finally make it from 1 to i ($(i-1)$ amplitudes a_+). This interprets the first order in κ contribution to the second term. Now, the going round can be repeated infinitely. Each additional round trip gives a factor $\kappa a_-^{N-1}a_+^{N-1}$. Summation over all these processes generates the denominator of the equation.

The other three propagator amplitudes can be computed in the same manner. Alternatively, one may just derive them by summing over all paths orbiting the closed contour. As a result

we obtain

$$G^{--}_{ij} = -ia_-^{i-j}\left(\Theta(i-j) + \frac{\kappa(a_-a_+)^{N-1}}{1-\kappa(a_-a_+)^{N-1}}\right),$$
$$G^{+-}_{ij} = -i\frac{\kappa a_-^{N-j}a_+^{i-1}}{1-\kappa(a_-a_+)^{N-1}},$$
$$G^{-+}_{ij} = -i\frac{a_+^{N-j}a_-^{i-1}}{1-\kappa(a_+a_-)^{N-1}}.$$

Now, let us take the continuum limit. To this end, we assign to lattice points on the upper/lower contour a time variable (cf. Fig. 11.2)

$$+ : t = i\epsilon,$$
$$- : t = (N-i)\epsilon. \tag{11.15}$$

Remembering that, in the large N limit, $(a_+a_-)^N \to 1$, and noting that

$$a_+^i \to e^{-i\omega t}, \qquad a_-^i \to e^{i\omega(T-t)},$$

we obtain the **propagators in a continuous time representation**

$$G^{++}_{tt'} = -ie^{-i\omega(t-t')}(\Theta(t-t') + n(\omega)),$$
$$G^{--}_{tt'} = -ie^{-i\omega(t-t')}(\Theta(t'-t) + n(\omega)),$$
$$G^{+-}_{tt'} = -ie^{-i\omega(t-t')}n(\omega),$$
$$G^{-+}_{tt'} = -ie^{-i\omega(t-t')}(1+n(\omega)), \tag{11.16}$$

where $n(\omega) = \kappa/(1-\kappa) = (e^{\beta(\omega-\mu)}-1)$ is the Bose distribution function.

INFO In the literature, it is customary to denote the Green functions by the alternative **notation** $G^{++} \equiv G^T$, $G^{--} \equiv G^{\tilde{T}}$, $G^{+-} \equiv G^<$, $G^{-+} \equiv G^>$. As, however, this notation is not particularly easy to memorize, and the Green functions above will soon be replaced by different functions, we here stick to the contour index notation.

11.2.3 Continuum field theory

Having derived the continuum propagators, let us now cast the action in Eq. (11.12) in a continuum form. Using Eq. (11.15), we obtain

$$\boxed{\mathcal{Z} = \mathcal{Z}_0^{-1}\int D(\bar\psi,\psi)\, e^{i\int_0^T dt\, \bar\psi\sigma_3(i\partial_t-\omega)\psi},} \tag{11.17}$$

where $\psi \equiv (\psi_+, \psi_-)^T$ is a two component field in contour space and σ_i are Pauli matrices in that space. Equation (11.17) is our first prototype of a **Keldysh functional integral.** Notice that the continuum representation of the action ignores the boundary terms in Eq. (11.12) and specifically the information stored in the initial density operator. The proper way to interpret the sloppiness of the compact (and customary) notation of Eq. (11.17) is

as follows: the field theory is defined by its correlation functions, or propagators. The latter must be computed with proper boundary conditions, that is, with reference to the boundary data stored in the density operator ρ_0, and the gluing procedure at temporal "infinity" $t = T$. Although we might encapsulate this information in a boundary contribution to the continuum action, the operationally safest way is by resorting to the discrete formulation above. Regardless, the result of such a calculation will be the set of Green functions (11.16). In other words, as long as we interpret these Green functions as the propagators of the action (11.17), the boundary conditions have been taken care of. (And of course, the propagators demonstrate that the upper and lower contour are *not* independent.)

One more thing to notice is that the Green function G contains a certain degree of **redundancy**. Inspection of Eq. (11.16) shows, for example, that $G^{++}+G^{--} = G^{+-}+G^{-+}$. Defining the linear transformation

$$U \equiv \frac{1}{\sqrt{2}} \begin{pmatrix} 1 & 1 \\ 1 & -1 \end{pmatrix}, \tag{11.18}$$

we obtain the alternative representation of the block Green function

$$\begin{aligned} G_{tt'} \to G'_{tt'} \equiv U G_{tt'} U^\dagger &= \frac{1}{2} \begin{pmatrix} 1 & 1 \\ 1 & -1 \end{pmatrix} \begin{pmatrix} G^{++} & G^{+-} \\ G^{-+} & G^{--} \end{pmatrix}_{tt'} \begin{pmatrix} 1 & 1 \\ 1 & -1 \end{pmatrix} \\ &= -ie^{-i\omega(t-t')} \begin{pmatrix} 1+2n(\omega) & \Theta(t-t') \\ -\Theta(t'-t) & 0 \end{pmatrix} \equiv \begin{pmatrix} G^K & G^+ \\ G^- & 0 \end{pmatrix}_{tt'}, \end{aligned} \tag{11.19}$$

where the three block Green functions are defined by[10]

$$\begin{aligned} G^+_{tt'} &\equiv -i\Theta(t-t')e^{-i\omega(t-t')}, \\ G^-_{tt'} &\equiv +i\Theta(t'-t)e^{-i\omega(t-t')}, \\ G^K_{tt'} &\equiv -i(1+2n(\omega))e^{-i\omega(t-t')}. \end{aligned} \tag{11.20}$$

The denotation $G^\pm$ indicates that we have met with the **retarded and advanced Green function** of quantum mechanics, i.e.

$$\begin{aligned} G^+_{t-t'} &= -i\Theta(t-t')\langle[a(t), a^\dagger(t')]\rangle, \\ G^-_{t-t'} &= +i\Theta(t'-t)\langle[a(t), a^\dagger(t')]\rangle, \end{aligned}$$

where $a(t) = e^{i\hat{H}t}ae^{-i\hat{H}t} = e^{-i\omega t}a$ are the Heisenberg evolved boson operators of our theory. The **Keldysh Green function**, G^K, is a new acquaintance. Notice that G^K, and only G^K, does the book–keeping of the initial distribution. We obtain a better understanding of the meaning of G^K as we proceed.

The correspondence $G^{CC'}_{tt'} = -i\langle\psi^C_t\bar{\psi}^{C'}_{t'}\rangle$ implies that $G'^{CC'}_{tt'} \equiv (UGU^\dagger)^{CC'}_{tt'} = -i\langle(U\psi)^C_t(\bar{\psi}U^\dagger)^{C'}_{t'}\rangle \equiv -i\langle\psi'^C_t\bar{\psi}'^{C'}_{t'}\rangle$. It is customary to denote the transformed fields as

$$\psi' = U\psi = \frac{1}{\sqrt{2}} \begin{pmatrix} \psi_+ + \psi_- \\ \psi_+ - \psi_- \end{pmatrix} \equiv \begin{pmatrix} \psi_c \\ \psi_q, \end{pmatrix}, \tag{11.21}$$

[10] Or, expressed in terms of the block Green functions, $G^\pm = G^{++} - G^\pm$ and $G^K = G^{++} + G^{--}$.

where ψ_c and ψ_q denote the **classical and quantum field**, respectively. To understand the origin of this notation, notice that the difference between classical and quantum dynamics is that the latter is governed by the product of two independent quantum amplitudes. It is *di erences* between these amplitudes which makes quantum dynamics distinct from classical. This motivates calling $(\psi_+ - \psi_-)/\sqrt{2}$ a quantum field and $(\psi_+ + \psi_-)/\sqrt{2}$ a classical field.

With $\psi = U^\dagger \psi'$ and $\bar{\psi} = \bar{\psi}' U$, and noting that $U\sigma_3 U^\dagger = \sigma_1$, the theory assumes the form $\mathcal{Z} = \mathcal{Z}_0^{-1} \int D(\bar{\psi}', \psi')\, e^{iS[\bar{\psi}', \psi']}$ where

$$S[\bar{\psi}', \psi'] \equiv \int dt\, (\bar{\psi}_c, \bar{\psi}_q) \begin{pmatrix} & i\partial_t - \omega \\ i\partial_t - \omega & \end{pmatrix} \begin{pmatrix} \psi_c \\ \psi_q \end{pmatrix}. \tag{11.22}$$

This representation has two undesirable and, in fact, interrelated aspects to it: (i) given that the action is purely imaginary, one may wonder whether the functional integral is properly convergent, and (ii) the action still does not contain explicit information on the initial distribution. These two deficiencies can be repaired in one sweep. We first notice that the temporal exponents in Eq. (11.19) must be understood as infinitesimally damped, $\exp(-it\omega) \to \exp(-it\omega - \delta|t|)$, $\delta > 0$. Fourier transformation of the Green functions then leads to

$$G^{\pm,K}(\epsilon) = \int_{-\infty}^{\infty} dt\, e^{i\epsilon t} G^{\pm,K}_{t,0}, \tag{11.23}$$

with

$$G \pm (\epsilon) = \frac{1}{\epsilon^\pm - \omega},$$
$$G^K(\epsilon) = -2\pi i F(\epsilon)\delta(\epsilon - \omega) = F(\epsilon)\left[G^+(\epsilon) - G^-(\epsilon)\right].$$

Here we have defined the function

$$F(\epsilon) \equiv 1 + 2n(\epsilon) = \coth\left(\frac{\epsilon - \mu}{2T}\right). \tag{11.24}$$

Notice that the temporal integration has been extended to infinity, in spite of the fact that we are living on a contour $[0, T]$ of finite duration. The rationale behind this extension is that the upper limit T must be chosen large enough that the finiteness of correlation times $\sim \delta^{-1}$ leads to finite decay before the end of the contour is reached, $T/\delta \gg 1$.

INFO Equation (11.23) suggests **two di erent representations of the Keldysh Green function**, both of which prove useful below. Noting that $\delta(\epsilon - \omega) \equiv \rho(\epsilon)$ is the single particle density of states of our one-level system, we may write

$$G^K(\epsilon) \equiv -2\pi i F(\epsilon)\rho(\epsilon). \tag{11.25}$$

Alternatively, we may notice that G^K is an anti-hermitian operator. (Exercise: trace back the origin of G^K to the basic propagators on the Keldysh contour to convince yourself that anti-hermiticity of G^K is a general feature, not dependent on the simplistic nature of our model.) Equation (11.23) then suggests the *ansatz*

$$\hat{G}^K \equiv \hat{G}^+ \hat{F} - \hat{F}\hat{G}^-, \tag{11.26}$$

where $\hat{G}^{\pm}$ are the resolvent operators of the theory and $\hat{F}$ is an hermitian operator. In the present context, insertion of the matrix elements $G^{\pm}_{tt'} = G^{\pm}_{t-t'}$ $G^{\pm}(\epsilon)$ and $F_{t-t'}$ $F(\epsilon)$ leads back to Eq. (11.23). In general, we have the block structure

$$\hat{G} = \begin{pmatrix} \hat{G}^K & \hat{G}^+ \\ \hat{G}^- & 0 \end{pmatrix} = \begin{pmatrix} \hat{G}^+\hat{F} - \hat{F}\hat{G}^- & \hat{G}^+ \\ \hat{G}^- & 0 \end{pmatrix}. \tag{11.27}$$

Inserting these Fourier transforms, we obtain the **energy representation of the action**,

$$\boxed{S[\psi_c, \psi_q] = \int \frac{d\epsilon}{2\pi} (\bar{\psi}_c, \bar{\psi}_q)_\epsilon \begin{pmatrix} (\hat{G}^-)^{-1} \\ (\hat{G}^+)^{-1} & \left[(\hat{G}^+)^{-1}\hat{F} - \hat{F}(\hat{G}^{-1})^{-1}\right] \end{pmatrix} \begin{pmatrix} \psi_c \\ \psi_q \end{pmatrix}_\epsilon,} \tag{11.28}$$

where the matrix kernel defines the inverse of the Green function (11.27). In the specific context of our toy model where $\hat{F}$ commutes with $\hat{G}^{\pm}$,

$$S[\psi_c, \psi_q] = \int \frac{d\epsilon}{2\pi} (\bar{\psi}_c, \bar{\psi}_q)_\epsilon \begin{pmatrix} \epsilon^- - \omega \\ \epsilon^+ - \omega & \left[2i\delta \coth\left(\frac{\epsilon-\mu}{2T}\right)\right] \end{pmatrix} \begin{pmatrix} \psi_c \\ \psi_q \end{pmatrix}_\epsilon. \tag{11.29}$$

This formula makes the full significance of the δ-broadening manifest:

- ▷ The action now contains explicit reference to the distribution function, and we have arrived at a self–contained representation.
- ▷ The functional integral is convergent. (Show that the imaginary part of the action is positive.)
- ▷ At first sight, keeping track of the infinitesimal δ may seem to be a book–keeping trick to get the distribution function into our description. Remember, however, that in physical systems, initially small convergence generating factors mostly get upgraded to finite "self energies." Similarly here. We will see that interactions will act to make the lower diagonal part of the inverse Green function finite. The upper diagonal part, however, will categorically remain zero.
- ▷ Mindful of the discussion in the previous chapter, one may feel reminded of the structure of the MSRJD action. This coincidence is, of course, not accidental. In a sense discussed below, Eq. (11.29) defines an elementary quantum generalization of an MSRJD functional theory.

11.2.4 Generalization

Before carrying on, it is useful to upgrade Eq. (11.29) to a functional field theory of generic interacting Bose systems. Nowhere in the derivation have we, in fact, made exclusive refer-

ence to the simplistic nature of the model system. This means that our prototypical field theory Eq. (11.17) affords the generalization, $\mathcal{Z} = \mathcal{Z}_0^{-1} \int D(\bar{\psi}, \psi)\, e^{iS_0[\bar{\psi},\psi]+iS_{\rm int}[\bar{\psi},\psi]}$, where

$$\begin{aligned} S_0[\bar{\psi},\psi] &\equiv \int dt d^d r \sum_C \bar{\psi}_C s_C (i\partial_t - \hat{H})\psi_C, \\ S_{\rm int}[\bar{\psi},\psi] &\equiv -\frac{1}{2}\int dt d^d r d^d r' \sum_C s_C\, (\bar{\psi}_C\psi_C)(\mathbf{r},t)\, V(\mathbf{r}-\mathbf{r}')\, (\bar{\psi}_C\psi_C)(\mathbf{r}',t), \end{aligned} \tag{11.30}$$

and s_C is a sign factor assuming the values $+1/-1$ on the upper/lower contour, respectively, $\psi = \{\psi_C(\mathbf{r},t)\}$, $\hat{H}$ is the single particle contribution and $V(\mathbf{r}-\mathbf{r}')$ represents a two-particle interaction.

We may now introduce **classical and quantum fields** through the transformation (11.21). Substitution of the transformed fields into the action leads to the representation

$$\begin{aligned} S_0[\bar{\psi},\psi] &\equiv \int dt d^d r\, (\bar{\psi}_c, \bar{\psi}_q) \begin{pmatrix} 0 & (\hat{G}^-)^{-1} \\ (\hat{G}^+)^{-1} & (\hat{G}^{-1})^K \end{pmatrix} \begin{pmatrix} \psi_c \\ \psi_q \end{pmatrix}, \\ S_{\rm int}[\bar{\psi},\psi] &\equiv -g \int dt d^d r\, \left(\bar{\psi}_c \bar{\psi}_q (\psi_c^2 + \psi_q^2) + \text{c.c.} \right), \end{aligned} \tag{11.31}$$

where, for notational simplicity, we assumed the interaction to be contact, $V(\mathbf{r}) = 2g\delta(\mathbf{r})$, $\hat{G}^{\pm} = (i\partial_t \pm i\delta - \hat{H})^{-1}$ are the retarded and the advanced Green functions, and

$$(\hat{G}^{-1})^K \equiv (\hat{G}^+)^{-1}\hat{F} - \hat{F}(\hat{G}^-)^{-1}, \tag{11.32}$$

is the Keldysh sector of the inverse of the Green function. Generalizing the discussion of the previous section, let us now interpret the meaning of the different constituents of this action.

Retarded and advanced Green function

The infinitesimal increments in Eq. (11.31) signify that the retarded and advanced Green functions obey the causality constraint $G^{\pm}(t,t') \propto \Theta(\pm(t-t'))$.[11] For a time-independent Hamiltonian,

$$\begin{aligned} G^{\pm}(t,t') &= G^{\pm}(t-t') = \mp i\Theta(\pm(t-t'))e^{-i\hat{H}(t-t')}, \\ G^{\pm}(\omega) &= \frac{1}{\omega \pm i\delta - \hat{H}}. \end{aligned} \tag{11.33}$$

If $\hat{H}$ contains explicit time-dependence, we need to include a time ordering procedure,

$$G^{\pm}(t,t') = \mp i\Theta(\pm(t-t'))T_{\pm}e^{-i\int_t^{t'} d\tilde{t}\, \hat{H}(\tilde{t})},$$

where $T_{\pm}$ time orders in chronological/anti-chronological direction. Finally, the Green functions obey the composition law $G^{\pm}(t,t') = G^{\pm}(t,t'')G^{\pm}(t'',t')$ and the limit behavior $G^+(t,t) + G^-(0,0) = 0$.

[11] In the discrete representation used in the previous chapter, causality emerged as a consequence of $(G^+)^{-1}$ being a matrix containing one side diagonal below the main diagonal. This meant that G^+ was a lower triangular matrix. Within the continuum formalism, we use imaginary increments to keep track of causality.

Keldysh Green function

First notice a subtlety in the notation: $(\hat{G}^{-1})^K$ is the Keldysh block of the inverse of the Green function, but *not* the inverse of the Keldysh Green function, $(\hat{G}^K)^{-1}$. As discussed in the previous section, the anti-hermiticity of $\hat{G}^K$ motivates the *ansatz* (11.32), with an *apriori* undetermined hermitian matrix F. This object plays a crucial role in the theory; it is responsible for the book–keeping on the state, or "distribution" of our system.

The task of determining $\hat{F}$ gets drastically simplified by the *ansatz*

$$\hat{F} = \{F(t,t')\},$$

depending on time arguments, but independent of the Hilbert space indices of the problem (**r** in our current continuum field theory).

INFO To **motivate this ansatz for** $\hat{F}$, we recall its origins in the non-interacting sector of the theory (cf. Eq. (11.25)) and interpret $\hat{F}$ as a generalized (quasi-)particle distribution function. As long as interactions and external time dependencies do not play a role, it is natural to assume that $\hat{F}(\epsilon) = \hat{F}(\epsilon, \hat{H})$ depends on the Hamiltonian of the system. The straightforward generalization of Eq. (11.25) to a higher dimensional Hilbert space $\hat{G}^K(\epsilon) = -2\pi i \hat{F}(\hat{H}, \epsilon)\delta(\epsilon - \hat{H})$ then suggests the eigenfunction representation $\hat{G}^K(\epsilon, \omega_a) = -2\pi i \hat{F}(\epsilon, \omega_a)\delta(\epsilon - \omega_a)$. The important point here is that the spectral δ-function locks the eigenenergies ω_a to the energy argument. Since $\hat{F}$ always appears in combination with the spectral function, dropping its Hilbert space index, $\hat{F}(\epsilon, \omega_a) = \hat{F}(\epsilon)$ does not imply a loss of information.

In a time-independent context, $F(t,t') = F(t-t')$ and the Fourier transform $F(\epsilon)$ signifies the occupation of quasi-particles at energy ϵ. (For instance, $F(\epsilon) = \coth(\epsilon T/2) = 1 + 2n(\epsilon)$ under equilibrium conditions, where $n(\epsilon)$ is the Bose distribution function.) In a time dependent environment, it is usually a good idea to represent F by its **Wigner transform**,

$$F(\epsilon, t) \equiv \int dt'\, e^{i\epsilon t'} F(t + t'/2, t - t'/2). \tag{11.34}$$

The function $F(\,.\,, t)$ then represents the instantaneous particle distribution function at time t (as an exercise, think why!).

We finally note that retarded, advanced, and Keldysh Green function are obtained by computing the correlator

$$\boxed{-i\langle \psi_\alpha(\mathbf{r}, t)\bar{\psi}_{\alpha'}(\mathbf{r}', t')\rangle = \begin{pmatrix} G^K & G^+ \\ G^- & 0 \end{pmatrix}_{\alpha\alpha'} (\mathbf{r}, t; \mathbf{r}', t').} \tag{11.35}$$

Interaction

There is not much we can say about the interaction vertex at this stage in generality. Notice, however, that the interaction vanishes for $\psi_q = 0$, which is a manifestation of the vanishing of the action of purely classical fields.[12] In later perturbative applications, it will

[12] The particular two body interaction considered here also vanishes on a pure quantum configuration. However, this vanishing does not reflect a general structure.

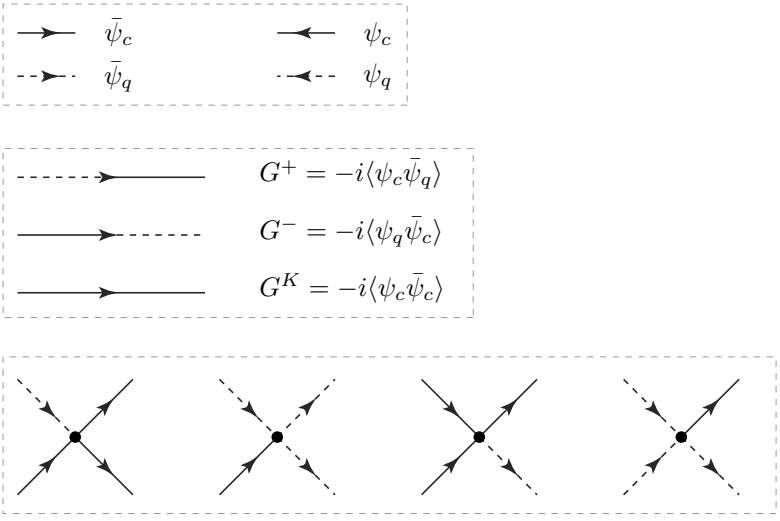

Figure 11.3 Building blocks of bosonic Keldysh diagrammatic perturbation theory. Top: field vertices, middle: propagators, bottom: interaction vertices.

be convenient to represent the interaction by a graphical code (see Fig. 11.3). Below we apply this language to explore the influence of interactions on the non-interacting sector of the theory.

11.2.5 Fluctuation dissipation theorem

In the case of thermal equilibrium, the Keldysh Green function is fully determined by the retarded and advanced Green functions, $\hat{G}^K = \hat{G}^+\hat{F} - \hat{F}\hat{G}^{-1}$. In thermal equilibrium, the commutativity of $\hat{F} = 1 + 2n = \coth(\epsilon/2T)$ with $\hat{G}^\pm$ implies

$$\hat{G}^K(\epsilon) = \coth\left(\frac{\epsilon}{2T}\right)(\hat{G}^+(\epsilon) - \hat{G}^-(\epsilon)). \tag{11.36}$$

The form of this dependence is reminiscent of the **quantum fluctuation dissipation theorem** reviewed in the previous chapter.

To make the connection to the FDT explicit, let us proceed as in Section 10.6.4 and discuss the correlation functions $\hat{G}^K$ and $\hat{G}^\pm$ in terms of their formal Lehmann representation. Beginning with the Keldysh Green function, we turn back to a representation in terms of contour fields and have

$$G^K(t,0) = -i\langle\psi_c(t)\bar{\psi}_c(0)\rangle = \frac{1}{2}\langle(\psi_+(t) + \psi_-(t))(\bar{\psi}_+(0) + \bar{\psi}_-(0))\rangle,$$

where we have omitted the Hilbert space indices of the fields for notational clarity. Now, interpret a correlation function

$$\langle\psi_C(t)\bar{\psi}_{C'}(0)\rangle \leftrightarrow \langle T_\gamma a_C(t)a^\dagger_{C'}(0)\rangle,$$

as the coherent state functional integral representation of a contour ordered operator expectation value. In the latter expression, the angular brackets represent the equilibrium thermal expectation value $\langle \dots \rangle = \mathrm{tr}((\dots)\hat{\rho}_0)$, and the combination (C,t) of the contour subscript and the time argument fixes the position of the operator on the closed time contour. We next employ the Heisenberg representation of the operators as

$$a_C(t) = e^{-i\int_{(C,t)}^{-t_0} dt\, \hat{H}(t)}\, a\, e^{-i\int_{-t_0}^{(C,t)} dt\, \hat{H}(t)},$$

where the time integrals in the exponents are along the time contour, and we have dropped the contour time ordering operator $T_\gamma e^{-i\int_{-t_0}^{(C,t)} dt\, \hat{H}(t)} = e^{-i\int_{-t_0}^{(C,t)} dt\, \hat{H}(t)}$, on account of the presumed time-independence of $\hat{H}$. (Exercise: Consider why this convention conforms with the definition of the coherent state field integral, and the contour conventions of the Keldysh approach in general.) If (C,t) lies on a later point on the contour than $(C',0)$, this representation yields

$$\langle a_C(t) a^\dagger_{C'}(0)\rangle = \quad e^{-i\int_{(C,t)}^{-t_0} dt\, \hat{H}(t)}\, a\, e^{-i\int_{(C',0)}^{(C,t)} dt\, \hat{H}(t)}\, a^\dagger\, e^{-i\int_{-t_0}^{(C',0)} dt\, \hat{H}(t)} \quad .$$

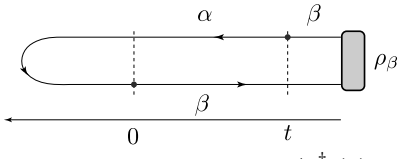

We may now insert complete sets of eigenfunctions of $\hat{H}$, $\{|\alpha\rangle\}$, to obtain the **Lehmann representation** of these expectation values. For example, for $C = +$, $C' = -$, $t < 0$, we obtain (cf. the figure)

$$\langle a^\dagger_-(0) a_+(t)\rangle = \mathcal{Z}_0^{-1} \rho_\beta |X_{\alpha\beta}|^2 e^{i\ \ _{\alpha\beta} t},$$

where $X_{\alpha\beta} \equiv \langle\alpha|a|\beta\rangle$, $\mathrm{fl}_\alpha = E_\alpha - \mu N_\alpha$, $\mathrm{fl}_{\alpha\beta} = \mathrm{fl}_\alpha - \mathrm{fl}_\beta$, the thermal weighting factor $\rho_\beta = e^{-\beta\ \ _\beta}$, and a summation over α, β is implied. Treating all other combinations in the same manner, we find

$$G^K(t,0) = -i\mathcal{Z}_0^{-1} |X_{\alpha\beta}|^2 e^{i\ \ _{\alpha\beta} t} (\rho_\alpha + \rho_\beta),$$

which Fourier transforms to

$$G^K(\epsilon) = -2\pi i \mathcal{Z}_0^{-1} |X_{\alpha\beta}|^2 \delta(\epsilon + \mathrm{fl}_{\alpha\beta})(\rho_\alpha + \rho_\beta).$$

Comparison with the expression above for the time ordered correlation function $G^T(t,0) = -i\langle T_t a(t) a^\dagger(0)\rangle$ leads us to the important conclusion,

$$G^K(\epsilon) = 2i \quad G^T(\epsilon). \tag{11.37}$$

The Keldysh Green function is equal to twice the imaginary part of the time ordered correlation function.

In a similar manner, the Lehmann representations of the Green functions $G^\pm$ can be analyzed to confirm that the latter conform with the general definition of retarded and advanced response functions. These identifications show that Eq. (11.37) is but a manifestation of the quantum fluctuation dissipation theorem.

11.2.6 Classical limit I

Readers who went through the previous chapter may have noticed the striking structural similarity between the Keldysh diagram language and the graphical code used in Section 10.5.1 to analyze the **MSRJD functional integral**. More generally, the block-triangular form of the Green functions, containing retarded and advanced blocks, in conjunction with distribution functions, is reminiscent of the structure of the MSRJD theory. In this section, we explore the classical limit of the theory within the framework of a stationary phase analysis. A more comprehensive discussion of the connection to MSRJD theory is given in Section 11.3.

Prior to taking semiclassical limits, we should let $\hbar$ re-enter the theory. Remembering the origin of the action as a contour integrated quantum phase, we set $iS \to \frac{i}{\hbar}S$. In the limit $\hbar \to 0$, the functional will then be governed by the stationary configurations of its action

$$\frac{\partial S[\psi_c, \psi_q]}{\partial \psi_q} = \frac{\partial S[\psi_c, \psi_q]}{\partial \psi_c} = 0. \tag{11.38}$$

These equations may have solutions for arbitrary (ψ_c, ψ_q) about which nothing much can be said in general terms. But there is always one that reflects the classical physics of the problem. Recalling that an expansion of the action in ψ_q starts at linear order (the purely classical action $S[\psi_c, 0] = 0$), we identify this **classical saddle point** by the equation,

$$\text{classical saddle point:} \quad \left.\frac{\partial S[\psi_c, \psi_q]}{\partial \psi_q}\right|_{\psi_q=0} = 0. \tag{11.39}$$

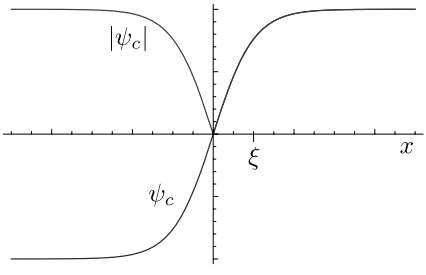

This saddle point is "classical" in that it is defined on the contour $\psi_q = \psi_+ - \psi_- = 0$, i.e. in a limit where the time evolution becomes classical. Specifically, for the interacting Bose action (11.30), the saddle point equation assumes the form

$$\left(i\partial_t - \hat{H} - V|\psi_c|^2\right)\psi_c = 0. \tag{11.40}$$

This is the celebrated **Gross–Pitaevskii equation**, a non-linear Schrödinger equation describing the classical physics of the evolution of a bosonic order parameter amplitude ψ_c in self–interaction with its own density $\sim |\psi_c|^2$.

INFO We may think of the **Gross–Pitaevskii equation (GPE)** as the time-dependent Ginzburg–Landau equation of the transition into a superfluid state. Alternatively, it may be interpreted as a nonlinear Schrödinger equation describing the wavefunction of a Bose–Einstein condensate. Inhomogeneous solutions of this equation describe collective excitations of the condensate field.

By way of example, let us consider the case of a one-dimensional spatially homogeneous system, $\hat{H} \to -\frac{(\hbar\partial_x)^2}{2m} - \mu$, where we have added a chemical potential term to $\hat{H}$. Passing to the "energy representation" of the equation, $i\hbar\partial_t \to E$,

$$\left(E + \frac{(\hbar\partial_x)^2}{2m} + \mu - V|\psi_c|^2\right)\psi_c = 0.$$

The solution of lowest energy, $E = 0$, is the spatially homogeneous condensate amplitude (cf. the discussion in Section 6.3)

$$|\psi_c|^2 = \frac{\mu}{V}.$$

However, the GPE also contains information on spatially inhomogeneous excitations of the condensate. For example, it is straightforward to verify that, for any x_0, the function

$$\psi_c \equiv \psi_0 \tanh\left(\frac{(x - x_0)}{\xi}\right), \tag{11.41}$$

solves the GPE (cf. the figure above.) Here, ψ_0 is a complex amplitude with $|\psi_0|^2 = \mu/g$, and $\xi \equiv \hbar/\sqrt{4m\mu}$ is the coherence length. The wave function (11.41) is called a **dark soliton**. The attribute "soliton" hints at the topological nature of the solution. The sign change at its origin x_0 means that the phase of the soliton changes by π. This jump cannot be removed by continuous deformation, and in this sense the soliton is a topological defect.

EXERCISE For a system with attractive interactions, $V < 0$, try to identify the **bright soliton**.

One may then expand around the "classical" saddle point to account for quantum and classical fluctuations. However, we find it more instructive to discuss these types of fluctuations in a slightly different context below.

This concludes our preliminary discussion of the generalities of the (bosonic) Keldysh formalism. Before carrying on, it may be worthwhile to recapitulate once more a few **structures of the theory**:

- ▷ We start at large negative times with a non-interacting system whose state is described by some initial distribution $\hat{F}_0$. In this non-interacting limit, the Keldysh sector of the inverse Green function, $(\hat{G}^{-1})^K$ is infinitesimally small, and related to the retarded and advanced sector by the FDT.
- ▷ As interactions are switched on, the system will aim to identify its new distribution. The initial proportionality of $(\hat{G}^{-1})^K$ to the initial imaginary damping terms $i\delta$ suggests that the Keldysh sector of the inverse Green function will no longer be infinitesimally small; the emergence of finite "self energies", $i\delta \to i\,\mathrm{Im}\,\Sigma$ will render it finite. Put differently, the self energies of the theory, and in particular the Keldysh component of the self-energy, are expected to contain essential information on the state of the system.

In the following, we explore the interaction-mediated formation of distribution functions on an instructive, and important example.

11.3 Particle coupled to an environment

Let us go back to the general paradigm formulated in Section 11.1.1, a quantum system coupled to a bath. For concreteness, we will assume the system to be a single quantum particle, while the bath is an ensemble of harmonic oscillators. In the particular case where the dynamics of the particle is harmonic, this gets us back to the oscillator–oscillator coupling studied in Section 11.1.2.

Keldysh theory of a quantum particle

Consider the quantum mechanics of a single point particle in one-dimensional space. In the distant past, we prepared the particle in some state (pure or mixed, it does not matter) and then let it evolve under the dynamics of its Hamiltonian operator $\hat{H} = \frac{\hat{p}^2}{2m} + V(\hat{q})$. This situation can be described by an obvious modification of our Keldysh functional theory. All we need to do is encapsulate the initial value information in a density operator $\hat{\rho}_0$, and replace the coherent state field integral by a Feynman path integral. As a result, we obtain the Keldysh partition function

$$\begin{aligned}\mathcal{Z}_s &= \mathcal{Z}_0^{-1} \int D(q,p)\, e^{i\sum_C s_C \int dt\,(p_C \partial_t q_C - H(q_C,p_C))} \\ &= \mathcal{Z}_0^{-1} \int Dq\, e^{i\sum_C s_C \int dt\,\left(\frac{m}{2}(\partial_t q_C)^2 - V(q_C)\right)} \\ &= \mathcal{Z}_0^{-1} \int Dq\, e^{i\int dt\,\left(m\partial_t q_q \partial_t q_c - V\left(\frac{1}{2}(q_c+q_q)\right)\right) + V\left(\frac{1}{2}(q_c-q_q)\right)\Big)}. \end{aligned} \tag{11.42}$$

To explore the **classical limit** of this expression, we re-introduce $\hbar$ as $iS \to i\hbar^{-1}S$. Alluding to the discussion of the quantum-nature of configuration differences $q_+ - q_- \sim q_q$ above, we also rescale $q_c \to \hbar q_c$. A first order expansion of the action in $q_c\hbar$ then identifies the $\hbar$-independent (classical) sector of the action

$$S_{\rm c}[q_c, q_q] \equiv \int dt\, q_q \left[-m\partial_t^2 q_c - \sqrt{2}\, V'\left(\frac{1}{\sqrt{2}} q_c\right)\right].$$

Integrating over the quantum component, we obtain the constraint $-m\partial_t^2 q_c - \sqrt{2}\,\partial_q V(q_c/\sqrt{2}) = 0$ or, upon rescaling coordinates $q_c/\sqrt{2} \equiv q$, **Newton's equations of motion**

$$m\partial_t^2 q = -\partial_q V(q). \tag{11.43}$$

But of course, the formalism can do much more than recover deterministic classical motion. This is seen the moment we couple the system to its bath:

Coupling to an oscillator bath

The bath as such is described by a partition function such as Eq. (11.31). Specifically, we assume the bath degrees of freedom to be non-interacting, $V = 0$, and oscillator-like, $\bar{\psi}\hat{H}\psi \equiv \sum_k \bar{\psi}_k\, \omega_k\, \psi_k$, with a wave-like dispersion $\omega_k \equiv c|k|$. Thus,

$$S_b[\bar{\psi}, \psi] \equiv \int \frac{d\omega}{2\pi} \sum_k \bar{\psi}_{k,\omega}\, \hat{G}^{-1}_{k,\omega}\, \psi_{k,\omega}, \tag{11.44}$$

with $\psi = (\psi_c, \psi_q)^T$, and the oscillator Green function,

$$\hat{G}^{-1}_{k,\omega} = \begin{pmatrix} 0 & \omega - i\delta - \omega_k \\ \omega + i\delta - \omega_k & [2i\delta \coth(\omega/2T)] \end{pmatrix}.$$

The coupling between system and bath is modelled by the action

$$\begin{aligned} S_{sb}[\bar{\psi}, \psi, q] &\equiv \int dt \sum_k \sum_C s_C q(t) \left(\gamma_k \psi_{C,k}(t) + \text{c.c.}\right) = \int dt \sum_k q(t)^T \sigma_1 \left(\gamma \psi_k(t) + \text{c.c.}\right) \\ &= \int \frac{d\omega}{2\pi} \sum_k \left(\gamma_k q^T_\omega \sigma_1 \psi_{k,-\omega} + \bar{\gamma}_k \bar{\psi}^T_{k,\omega} \sigma_1 q_{-\omega}\right), \end{aligned} \tag{11.45}$$

where $\gamma(k)$ is a set of complex coupling constants, and in the second line we switched to the Keldysh representation $q^T = (q_c, q_q)$.

Integration over oscillator modes

At this stage, the oscillators may be integrated out. Using the fact that $-i\langle \psi \bar{\psi}^T \rangle = \hat{G}$ (cf. Eq. (11.35)), we obtain the effective system action, $S_{\text{eff}} = S_s + S_{\text{diss}}$, where the **dissipative action** is given by

$$S_{\text{diss}}[q] = -\int \frac{d\omega}{2\pi} q^T_\omega \sigma_1 \left(\sum_k |\gamma_k|^2 \hat{G}_{k,\omega} \right) \sigma_1 q_{-\omega},$$

and the Green function has the form

$$\hat{G}_{k,\omega} = \begin{pmatrix} \left[-2\pi i \coth\left(\frac{\omega}{2T}\right) \delta(\omega - \omega_k)\right] & (\omega + i\delta - \omega_k)^{-1} \\ (\omega - i\delta - \omega_k)^{-1} & 0 \end{pmatrix}.$$

To make progress with this expression, we assume that the coupling constant exhibits power law dependence on $|k|$,

$$|\gamma_k| = \lambda |k|^\alpha,$$

where $\lambda > 0$ is a real coefficient. Noting that the Green function enters in a frequency-symmetrized form, $\sum_\omega q^T_\omega \hat{G}_\omega q_{-\omega} = \frac{1}{2} \sum_\omega q^T_\omega (\hat{G}_\omega + \hat{G}_{-\omega}) q_{-\omega}$, the summation over the k-modes then produces the expression (exercise)

$$S_{\text{diss}}[q] = \int \frac{d\omega}{2\pi} q^T_\omega \hat{K}_\omega q_\omega, \tag{11.46}$$

where the **dissipation kernel** $\hat{K}$ is given by

$$\hat{K}_\omega = \pi \nu \lambda^2 \left(\frac{\omega}{c}\right)^{2\alpha} \begin{pmatrix} 0 & -i \\ i & 2i \coth\left(\frac{\omega}{2T}\right) \end{pmatrix}. \tag{11.47}$$

Here we have introduced the density of modes, $\nu \equiv \sum_k \delta(\omega - \omega_k)$ and omitted a frequency-independent contribution to K (which can be absorbed in the chemical potential). We may think of $\hat{K}_\omega$ as a "self-energy" of the particle due to its coupling to the oscillator bath. The frequency dependence of K_ω signals that S_{diss} is a time-nonlocal contribution to the action.

The temporal profile of the dissipation kernel depends on the coupling γ. In the following, we concentrate on the case of **Ohmic dissipation**, where $\alpha = 1/2$ and

$$\hat{K}_\omega = g \begin{pmatrix} 0 & -i\omega \\ i\omega & 2i\omega \coth\left(\frac{\omega}{2T}\right) \end{pmatrix}, \tag{11.48}$$

with $g \equiv \frac{\pi\nu\lambda^2}{c}$.

INFO The power law $\alpha = 1/2$ is not quite as arbitrary as it may seem. Specifically, the choice $\gamma = i\lambda\,\mathrm{sgn}(k)\sqrt{|k|}$ describes the frequent situation of dissipation due to **coupling to an elastic medium**. To see this, recall the representation of the coherent state amplitudes in terms of oscillator coordinates and momenta,

$$\psi_k = \frac{1}{\sqrt{2}}\left(\sqrt{\omega_k}q_k + \frac{i}{\sqrt{\omega_k}}p_k\right).$$

Substitution into the coupling term generates the expression

$$\begin{aligned}\sum_k (\gamma_k\psi_k + \text{c.c.}) &\sim \sum_k \mathrm{sgn}\,(k)\sqrt{|k|}\left(i\left(\sqrt{\omega_k}q_k + \frac{i}{\sqrt{\omega_k}}p_k\right) + \text{c.c.}\right)\\ &\sim \sum_k ikq_k \sim \partial_x q(x)\big|_{x=0},\end{aligned}$$

where, noting that functions $q(x)$ and $p(x)$ are real, we have made use of the identities $\bar{q}_k = q_{-k}$ and $\bar{p}_k = p_{-k}$. The last term describes the local coupling of the system coordinate to the stress $\partial_x q(x)$ acting on an elastic string. In many dissipative environments, macroscopic degrees of freedom are coupled to approximately harmonic microscopic modes in this way. Prominent examples include the coupling of the electric field applied to a resistor to harmonic electromagnetic modes in the medium. This coupling (cf. our discussion of Johnson noise in the previous chapter) is responsible for the denotation "Ohmic" dissipation.

Langevin equation

We next explore the classical limit of the effective theory of the particle coupled to the bath. To this end, we let $\hbar$ enter at three different places in the functional,

$$\begin{aligned}&\text{(i)}: iS \to \frac{i}{\hbar}S,\\ &\text{(ii)}: \coth(\omega/2T) \to \coth(\omega\hbar/2T) \to \frac{2T}{\hbar\omega},\\ &\text{(iii)}: \psi_q \to \hbar\psi_q.\end{aligned} \tag{11.49}$$

In the semiclassical limit, and at fixed characteristic frequency ω, the "coth" can then be linearized as indicated in (ii). The extra power of $\hbar$ appearing in the denominator of this expression compensates for the additional power in $\hbar$ due to two factors q_q in the quantum–quantum sector of the action. Summarizing, the effective classical action is given by

$$S_\mathrm{c}[q_c, q_q] = \int dt\,\left[q_q\left(-m\partial_t^2 q_c - \sqrt{2}\,V'\left(\frac{1}{\sqrt{2}}q_c\right) - 2g\partial_t q_c\right) + 4iTgq_q^2\right].$$

This has the characteristic structure of an MSRJD action. Comparison with the discussion of MSRJD functionals in the previous chapter shows that the (scaled) quantum field $2gq_q$ plays a role identical to the MSRJD "momentum." Specifically, a "Langevin" equation[13] can be derived by Hubbard–Stratonovich decoupling of the q_c term:

$$S_c[q_c, q_q] \to S_c[q_c, q_q, \xi] = \int dt \left[q_q \left(-m\partial_t^2 q_c - \sqrt{2}\, V'\left(\frac{q_c}{\sqrt{2}}\right) - 2g\partial_t q_c + \sqrt{2}\xi \right) \right] + \frac{i}{8gT} \int dt\, \xi^2.$$

Introducing the rescaled variable $q = q_c/\sqrt{2}$ and integrating over q_q, we obtain the Langevin equation

$$m\partial_t^2 q + V'(q) + 2g\partial_t q = \xi, \tag{11.50}$$

where the noise correlator

$$\langle \xi(t)\xi(t') \rangle = 4Tg\delta(t - t'), \tag{11.51}$$

conforms with the FDT. To summarize, the coupling of the system to a bath renders the classical limit noisy. The effective equation of motion assumes the form of a Langevin equation, at a noise level that will drive the particle to an equilibrium distribution at the effective temperature of the bath.

INFO Notice that **the present theory solves a problem** that plagued the purely classical theory discussed in the previous chapter. Discussing dissipative damping of voltage fluctuations in a resistor network, we had seen that Johnson noise is problematic inasmuch as the white noise correlator $\langle \xi(t)\xi(t') \rangle = 2RT\delta(t - t')$ will predict singularly strong noise levels $\langle \xi(t)^2 \rangle$. We had cited the expectation that these singularities will be cut off if we take into account the fact that the actual coupling is to a bath of quantum, rather than classical oscillators.

This expectation is confirmed by our present theory. Comparison with Eq. (11.48) and the subsequent steps of the derivation shows that the frequency representation of the actual noise correlator reads

$$\langle \xi_\omega \xi_{\omega'} \rangle = \frac{g}{\pi} \delta(\omega + \omega') \omega \coth\left(\frac{\hbar\omega}{2T}\right).$$

In the classical limit $\hbar \to 0$, this reduces to the white noise limit $\frac{2Tg}{\pi\hbar}\delta(\omega + \omega')$, which Fourier transforms to Eq. (11.51). However, at large frequencies $\hbar\omega \gg T$, we obtain

$$\langle \xi_\omega \xi_{\omega'} \rangle \overset{\hbar\omega \gg T}{\longrightarrow} \frac{g}{\pi} \delta(\omega + \omega') |\omega|.$$

At first sight, it seems that the situation has become worse: the increase $\sim |\omega|$ implies ultraviolet behavior (short time correlations) even more malicious than in the white noise case. The resolution to this problem lies in a more careful interpretation of what is actually meant by the expression $\langle \xi_t \xi_{t'} \rangle$. The decomposition $\omega \coth \frac{\hbar\omega}{2T} \sim (1 + n(\omega)) + n(\omega)$ suggests that the voltage fluctuations are due to absorption from (n) and emission into $(n+1)$ the field of quantal resonator

[13] We put quotes around "Langevin" because the stochastic differential equations derived here contain second order time derivatives stemming from the acceleration terms in Newton's equations. (We are not working in the purely dissipative, overdamped limit.) The term "Langevin equation" is commonly reserved for first order equations, but this difference is of no relevance to the present discussion.

modes of the oscillator system. Specifically, there is response to its vacuum fluctuations (the "1" in $1+n$). At low temperatures, $T/\hbar\omega \to 0$, it is these fluctuations that cause our ultraviolet problems. On the other hand, it seems implausible that vacuum fluctuations will be probed in an actual measurement of noisy voltage fluctuations in a resistor. (The vacuum is a definite state, while the generation of fluctuations requires real transitions in the environment.) Closer inspection (cf. e.g., the pedagogical article G.B. Lesovik and R. Loosen, On the detection of finite-frequency current fluctuations, *JETP Lett.* **65**, 295-99 (1997)) shows that (i) the expression $\langle \xi_t \xi_{t'} \rangle \quad \frac{1}{2}\langle (\hat{V}_t \hat{V}_{t'} + \hat{V}_{t'} \hat{V}_t \rangle$ corresponds to a *symmetrized* correlation function of the quantum operators representing voltage fluctuations (exercise: to make this statement plausible, interpret $\langle \xi_t \xi_{t'} \rangle \sim G^K$ as a Keldysh correlation function and use the connection between G^K and time ordered correlation functions discussed in Section 11.2.4.) However, (ii) a concrete measurement will not correspond to this ordering. Specifically, it will not couple to the fluctuations of the vacuum. Once the vacuum contribution is removed, the ultraviolet problems disappear. For further discussion of this point, we refer to the literature.

This concludes our discussion of the backbones of Keldysh field theory. We have introduced its fundamental generating functional, discussed the meaning of the propagators, and exposed the connections to the classical theories discussed in the previous chapter. However, to make the picture complete, we need to introduce the fermion variant of the Keldysh functional. This will be as necessary as it is uninspiring. As one may expect, the formal differences from the bosonic theory amount to a few sign factors here and there. For this reason, we will try to keep the discussion as concise as possible and restrict ourselves to listing the main differences from the bosonic theory.

11.4 Fermion Keldysh theory (a list of changes)

11.4.1 Single level

As in the bosonic case, let us begin by considering a single level Hamiltonian $\hat{H} = \omega a^\dagger a$, where a and $a^\dagger$ are fermion operators. The definitions of the Keldysh partition function (11.9), and of the equilibrium density operator (11.10) remain unchanged, only that the normalizing factor is now given by $\mathcal{Z}_0 = 1 + e^{-\beta(\omega-\mu)}$. Again, we will want to represent the partition function in terms of (now fermionic) coherent states.

It is straightforward to verify that the auxiliary identity Eq. (11.11) generalizes to the fermionic case, which means that the discrete functional Eq. (11.12) remains as it is but for a sign change $\kappa \to -\kappa$. As in the construction of equilibrium (Matsubara) functionals, this change represents the sign we pick up when we sweep one of the $2N$ coherent state amplitude through all others, as we do in the construction of the functional integral. Consequently, the inverse of the discrete fermionic Green function is given by Eq. (11.13), again up to a sign change $\kappa \to -\kappa$. Up to this sign factor, all remaining formulae of the discrete discussion of Section 11.2.2 generalize to the fermionic case. Specifically, $\det(-iG^{-1}) \stackrel{N\to\infty}{\longrightarrow} 1 + \kappa = 1 + e^{-\beta(\omega-\mu)} = \mathcal{Z}_0$ which proves normalization of the functional integral. Taking the limit

$N \to \infty$, and switching to a continuum representation, we obtain the **fermionic Green functions**

$$\begin{aligned} G^{++}_{tt'} &= -ie^{-i\omega(t-t')}(\Theta(t-t') - n(\omega)), \\ G^{--}_{tt'} &= -ie^{-i\omega(t-t')}(\Theta(t'-t) - n(\omega)), \\ G^{+-}_{tt'} &= +ie^{-i\omega(t-t')}n(\omega), \\ G^{-+}_{tt'} &= -ie^{-i\omega(t-t')}(1-n(\omega)), \end{aligned} \tag{11.52}$$

where

$$n(\omega) = \frac{1}{1+e^{\beta(\omega-\mu)}},$$

is the Fermion distribution. (The global plus sign appearing in G^{+-} reflects the sign factor picked up upon passage of the terminal point of the contour.) We may now pass to a continuum representation of the functional integral whose unregularized form (no account for infinitesimal damping and boundary conditions) is given by the Grassmann version of Eq. (11.17). A glance at Eq. (11.52) shows that the redundancy in the theory which motivated the "Keldysh rotation" now assumes the form $G^{++} + G^{--} = G^{+-} + G^{-+}$. In the case of Grassmann variables, it is customary[14] to account for this redundancy by way of a field transformation slightly different from the bosonic Keldysh rotation above: using the independence of the Grassmann variables ψ and $\bar{\psi}$, we introduce new fields by

$$\begin{aligned} \psi_1 &\equiv \frac{1}{\sqrt{2}}(\psi_+ + \psi_-), & \psi_2 &\equiv \frac{1}{\sqrt{2}}(\psi_+ - \psi_-), \\ \bar{\psi}_1 &\equiv \frac{1}{\sqrt{2}}(\bar{\psi}_+ - \bar{\psi}_-), & \bar{\psi}_2 &\equiv \frac{1}{\sqrt{2}}(\bar{\psi}_+ + \bar{\psi}_-). \end{aligned} \tag{11.53}$$

Introducing the notation $\psi \equiv \binom{\psi_+}{\psi_-}$, $\psi' \equiv \binom{\psi_1}{\psi_2}$, $\bar{\psi} = (\bar{\psi}_+, \bar{\psi}_-)$, $\bar{\psi}' = (\bar{\psi}_1, \bar{\psi}_2)$, this assumes the form of a non-unitary transformation

$$\psi' \equiv U\psi, \qquad \bar{\psi}' \equiv \bar{\psi}\sigma_3 U^T,$$

where U has been defined in Eq. (11.18). (Due to the non-unitarity of the transformation, and the fact that Grassmann fields are never "classical," we do not speak of classical or quantum components.) The form of the above transformation is motivated by the transformed contraction rule

$$-i\langle\psi'\bar{\psi}'\rangle = U\langle\psi\bar{\psi}\rangle\sigma_3 U^T = U\hat{G}U^T\sigma_3 \equiv \hat{G}',$$

where $\hat{G} = \left(\begin{smallmatrix} \hat{G}^{++} & \hat{G}^{+-} \\ \hat{G}^{-+} & \hat{G}^{--} \end{smallmatrix}\right)$, and the transformed Green function assumes the form

$$\hat{G}' = \begin{pmatrix} \hat{G}^{+} & \hat{G}^{K} \\ & \hat{G}^{-} \end{pmatrix}, \tag{11.54}$$

[14] A. I. Larkin and Yu. N. Ovchinnikov, *Vortex motion in superconductors*, in Nonequilibrium Superconductivity, eds. D. N. Langenberg and A. I. Larkin, (Elsevier, 1986).

and the retarded, advanced, and Keldysh Green function are defined in analogy to Eq. (11.20),

$$\begin{aligned} G^{+}_{tt'} &\equiv -i\Theta(t-t')e^{-i\omega(t-t')}, \\ G^{-}_{tt'} &\equiv +i\Theta(t'-t)e^{-i\omega(t-t')}, \\ G^{K}_{tt'} &\equiv -i(1-2n(\omega))e^{-i\omega(t-t')}. \end{aligned} \tag{11.55}$$

As we will mostly work with the transformed Green function $\hat{G}'$, we omit the prime throughout, $\hat{G}' \to \hat{G}$.

11.4.2 Generalization

As with the bosonic theory, the form of the Green function Eq. (11.55) suggests the introduction of a fermionic distribution operator $\hat{F} = \{F(\epsilon)\}$, with

$$F(\epsilon) \equiv 1 - 2n(\epsilon). \tag{11.56}$$

Expressed as a Fourier transform, the Keldysh Green function then assumes the form

$$\hat{G}^{K} = \hat{G}^{+}\hat{F} - \hat{F}\hat{G}^{-}. \tag{11.57}$$

The generalization of the toy model above to a fully interacting theory is described by the Grassmann version of the functional Eq. (11.30). (The optional addition of spin-indices should be straightforward.) In contrast to the bosonic case, where mean field approaches to the native interacting theory lead to immediate results, most fermionic theories call for a Hubbard-Stratonovich decoupling of the interaction term. Prior to passing to the Keldysh rotated theory, we therefore introduce an auxiliary bosonic field to decouple the interaction as

$$\begin{aligned} e^{iS_{\rm int}[\bar{\psi},\psi]} = \int D\phi\, e^{-\frac{i}{2}\int dt d^d r d^d r' \sum_C s_C \phi_C(\mathbf{r},t) V^{-1}(\mathbf{r}-\mathbf{r}')\phi_C(\mathbf{r}',t)} \\ \times e^{+i\int dt d^d r \sum_C s_C \bar{\psi}_C(\mathbf{r},t)\phi_C(\mathbf{r},t)\psi_C(\mathbf{r},t)}. \end{aligned}$$

We may now implement the Keldysh rotation to arrive at the effective action $S[\bar{\psi},\psi,\phi] = S[\phi] + S[\bar{\psi},\psi] + S_{\rm int}[\bar{\psi},\psi,\phi]$, where

$$\begin{aligned} S[\phi] &= -i\int d^d r dt\, \phi_c(\mathbf{r},t) V^{-1}(\mathbf{r}-\mathbf{r}')\phi_q(\mathbf{r}',t), \\ S[\bar{\psi},\psi] &= \int d^d r dt\, \bar{\psi}\hat{G}_0^{-1}\psi, \\ S_{\rm int}[\bar{\psi},\psi,\phi] &= \frac{1}{\sqrt{2}}\int d^d r dt\, \bar{\psi}(\phi_c\sigma_0 + \phi_q\sigma_1)\psi. \end{aligned} \tag{11.58}$$

Here

$$\hat{G}_0^{-1} = \begin{pmatrix} (G_0^{+})^{-1} & (\hat{G}_0^{-1})^{K} \\ & (\hat{G}_0^{-})^{-1} \end{pmatrix}, \tag{11.59}$$

is the inverse of the free Green function[15] and $(\hat{G}_0^{\pm})^{-1} = (i\partial_t \pm i0 - \hat{H})$. We finally note that elements of the Green function are generated by the fermion variant of Eq. (11.35)

$$\boxed{-i\langle\psi_\alpha(\mathbf{r},t)\bar{\psi}_{\alpha'}(\mathbf{r}',t')\rangle = \begin{pmatrix} G^+ & G^K \\ 0 & G^- \end{pmatrix}_{\alpha\alpha'}(\mathbf{r},t;\mathbf{r}',t').} \tag{11.60}$$

11.5 Kinetic equation

The action Eq. (11.58) may serve as the starting point of numerous applications. Here, we restrict ourselves to the discussion of one interaction phenomenon that is particularly relevant to the central theme of the chapter: the interaction mediated **formation of effective particle distributions**. As a byproduct, we also introduce elements of Keldysh perturbation theory, and compare to the "equilibrium perturbation theory" discussed in earlier chapters. The concepts and techniques introduced in this section are very important and are routinely applied in the analysis of out of equilibrium quantum systems.

In carrying out the perturbative analysis, we are guided by two principles: first, we assume that the system (e.g. by way of high electron density) admits an effective RPA approach. Second, we think of the Hubbard–Stratonovich field, ϕ, as an independent, bosonic degree of freedom. That analogy becomes more substantial as we proceed and ϕ acquires its own dynamics. Specifically, the boson–fermion analogy suggests not to integrate over the fermion degrees of freedom just yet (which would be an option as a result of the quadratic nature of the action Eq. (11.58)), but to study boson and fermion propagators separately.

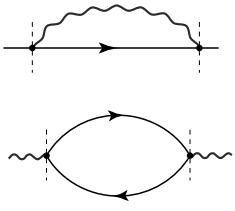

In Eq. (11.58), quasiparticles interact by the two-fermion one-boson interaction vertices contained in $S_{\rm int}$. Our intermediate goal will be to obtain the emerging boson and fermion self energies $\hat{\Sigma}_f$ and $\hat{\Sigma}_b$, respectively, in the RPA approximation, i.e. an approximation void of intersecting propagator lines. The topology of $\hat{\Sigma}_f$ is given by the first diagram shown in the figure, with external legs removed, and all propagators representing full propagators, with self–consistent account of the self energies. In a similar manner, $\hat{\Sigma}_b$ is obtained from the lower diagram. According to the general rules discussed above, the fermion self energies are obtained by contraction of interaction operators at fixed external field indices. Specifically, the fermion self-energy is defined as[16]

$$\int dxdx'\,\bar{\psi}'(x)\Sigma_f(x,x')\psi'(x') = -\frac{i}{2}\int dxdx'\bar{\psi}'(x)\quad\hat{\phi}(x)\psi(x)\bar{\psi}(x')\hat{\phi}(x')\quad\psi'(x'),$$

where $\hat{\phi} \equiv \phi_c\sigma_0 + \phi_q\sigma_1$ and we have switched to the space-time abbreviation $x \equiv (\mathbf{r},t)$. The self–consistency inherent to the RPA scheme requires that the contractions must be

[15] The off-diagonal block $(\hat{G}^{-1})^K$ is given by $(\hat{G}^{-1})^K = -(\hat{G}^+)^{-1}\hat{G}^K(\hat{G}^-)^{-1} = (\hat{G}^+)^{-1}\hat{F} - \hat{F}(\hat{G}^-)^{-1} = 2i\delta\hat{F}$, where the last identity holds if $\hat{F}$ commutes with $(\hat{G}^{\pm})^{-1}$.

[16] Should you feel uncertain about this result, it is worthwhile investing some time to recapitulate the perturbative construction of self energies.

interpreted to produce the full Green functions of the theory. Comparison of the two sides of the equation and usage of Eq. (11.60) leads to the identification,

$$\begin{aligned}\Sigma_f(x,x') &= -\frac{i}{2}\ \ \hat{\phi}(x)\psi(x)\bar{\psi}(x')\hat{\phi}(x')\ \ = -\frac{1}{2}\ \ \hat{\phi}(x)\hat{G}(x,x')\hat{\phi}(x') \\ &= -\frac{i}{2}\left(\hat{G}(x,x')D^K(x,x') + \hat{G}(x,x')\sigma_1 D^+(x,x') + \sigma_1\hat{G}(x,x')D^-(x,x')\right),\end{aligned}$$

where we have adopted the common convention to designate bosonic Green functions by $D^{+,-,K}$. Using this expression, the components of the self-energy operator

$$\hat{\Sigma}_f = \begin{pmatrix} \hat{\Sigma}_f^+ & \hat{\Sigma}_f^K \\ 0 & \hat{\Sigma}_f^- \end{pmatrix},$$

are identified as

$$\begin{aligned}\Sigma_f^{\pm}(x,x') &= -\frac{i}{2}\left(G^{\pm}(x,x')D^K(x,x') + G^K(x,x')D^{\pm}(x,x')\right) \qquad (11.61)\\ \Sigma_f^K(x,x') &= -\frac{i}{2}\left(G^K(x,x')D^K(x,x') + G^+(x,x')D^+(x,x') + G^-(x,x')D^-(x,x')\right) \\ &= -\frac{i}{2}\left(G^K(x,x')D^K(x,x') + (G^+(x,x') - G^-(x,x'))(D^+(x,x') - D^-(x,x'))\right),\end{aligned}$$

where we have made use of the fact that causality implies $G^+(x,x')D^-(x,x') = 0$, etc. Also notice that the causality of retarded and advanced Green functions, $D^{\pm}(x,x')G\ \ (x,x') = 0$, causes the vanishing of the lower right–hand block of the self-energy operator.

EXERCISE Show that the bosonic self-energy

$$\hat{\Sigma}_b = \begin{pmatrix} 0 & \hat{\Sigma}_b^- \\ \hat{\Sigma}_b^+ & \hat{\Sigma}_b^K \end{pmatrix},$$

is given by

$$\begin{aligned}\Sigma_b^{\pm}(x,x') &= -\frac{i}{2}\ \ G\ \ (x',x)G^K(x,x') + G^{\pm}(x,x')G^K(x',x)\ \ , \qquad (11.62)\\ \Sigma_b^K(x,x') &= -\frac{i}{2}\ \ G^K(x',x)G^K(x,x') + G^+(x',x)G^-(x,x') + G^-(x',x)G^+(x,x') \\ &= -\frac{i}{2}\ \ G^K(x',x)G^K(x,x') - (G^+ - G^-)(x',x)(G^+ - G^-)(x,x')\ \ .\end{aligned}$$

In the present context, where the boson field actually represents fluctuations in a scalar potential, we may think of the self-energy as an effective **polarization operator** screening field fluctuations.

11.5.1 Quasiclassical theory

We now have everything in place to address our main task, the computation of the fermion (or boson) distributions which develop in the interacting environment. The picture we should have in mind is that a system of fermions prepared in some initial distribution gets exposed to interactions. We wish to find out how the latter drive the system to a new state of equilibrium. The understanding of this mechanism is the basis for the description of out-of-equilibrium distributions forming, e.g. if the system is exposed to strong external fields.

Wigner transform

In a time-independent situation, all constituents of the theory depend only on time differences, Δt, and vary at time scales $\Delta t \sim \epsilon^{-1}$ comparable to their characteristic energies. In cases where systematic time-dependent changes occur (e.g. in response to the formation of a nonequilibrium initial state) on time scales $t \gg \Delta t$, it is convenient to pass to a Wigner transformed representation, $\hat{G}(t_1, t_2) \to G(\epsilon, t)$, where $t = (t_1 + t_2)/2$ and ϵ is conjugate to $\Delta t = t_1 - t_2$. Technically, the Wigner representation of an arbitrary operator $\hat{g} \equiv \{g(t, t')\}$ is defined by the transform

$$\begin{aligned} g(\epsilon, t) &\equiv \int d\Delta t\, e^{i\Delta t\epsilon} g(t + \Delta t/2, t - \Delta t/2), \\ g(t_1, t_2) &= \int \frac{d\epsilon}{2\pi}\, e^{-i(t_1 - t_2)\epsilon} g(\epsilon, t). \end{aligned} \tag{11.63}$$

In applications, we often need to know the Wigner representation of the product of two operators, $\hat{f}\hat{g}$. Using the definition above, it is straightforward to derive the **Moyal product** identity

$$\begin{aligned} (\hat{f}\hat{g})(\epsilon, t) &= e^{-\frac{i}{2}(\partial_{t_1}\partial_{\ 2} - \partial_{\ 1}\partial_{t_2})}\Big|_{\substack{1=\ 2=\\ t_1=t_2=t}} f(\epsilon_1, t_1) g(\epsilon_2, t_2) \\ &= f(\epsilon, t) g(\epsilon, t) - \frac{i}{2}\left(\partial_t f(\epsilon, t)\partial_\epsilon g(\epsilon, t) - \partial_\epsilon f(\epsilon, t)\partial_t g(\epsilon, t)\right) + \ldots \\ &= \left(fg - \frac{i}{2}\{f, g\} + \ldots\right)(\epsilon, t), \end{aligned} \tag{11.64}$$

where in the third line we have introduced the Poisson bracket

$$\{f, g\} = \partial_t f \partial_\epsilon g - \partial_\epsilon f \partial_t g. \tag{11.65}$$

The scope of the **Wigner transformation** actually extends beyond the temporal variables: in general, the distribution functions may exhibit explicit space dependence $\hat{F} \to \hat{F}(\mathbf{r})$. (This will occur, say, if a system is connected to two reservoirs kept at different temperatures, voltages, etc. In this case, gradients in the particle distributions may form.) We expect the characteristic scale of these variations to be much larger than the microscopic particle wavelengths. In this case, it is convenient to pass to the spatial Wigner transform, $\hat{G}(\mathbf{r}_1, \mathbf{r}_2) \to \hat{G}(\mathbf{r}, \mathbf{p})$, where $\mathbf{r} = (\mathbf{r}_1 + \mathbf{r}_2)/2$ and $\mathbf{p}$ is conjugate to $\Delta\mathbf{r} = \mathbf{r}_1 - \mathbf{r}_2$, i.e.

$$\begin{aligned} g(\mathbf{r}, \mathbf{p}) &\equiv \int d\Delta\mathbf{r}\, e^{-i\Delta\mathbf{r}\cdot\mathbf{p}} g(\mathbf{r} + \Delta\mathbf{r}/2, \mathbf{r} - \Delta\mathbf{r}/2), \\ g(\mathbf{r}_1, \mathbf{r}_2) &= \int \frac{d^d p}{(2\pi)^d}\, e^{i(\mathbf{r}_1 - \mathbf{r}_2)\cdot\mathbf{p}} g(\mathbf{r}, \mathbf{p}), \end{aligned} \tag{11.66}$$

where the different sign reflects the conventions standard in spatial and temporal Fourier transforms, respectively.

For later reference, a number of Wigner transform identities are summarized in table 11.1, where the spatial analogue of Eq. (11.65) is defined as $\{f, g\} = \partial_{\mathbf{r}} f \partial_{\mathbf{p}} g - \partial_{\mathbf{p}} f \partial_{\mathbf{r}} g$.

Table 11.1 *Wigner transform identities*

Temporal		Spatial	
Operator	Wigner representation	Operator	Wigner representation
$\hat{g}(\hat{t})$	$g(t)$	$\hat{g}(\hat{\mathbf{r}})$	$g(\mathbf{r})$
$\hat{g}(\hat{\epsilon}) = \hat{g}(i\partial_t)$	$g(\epsilon)$	$\hat{g}(\hat{\mathbf{p}}) = \hat{g}(-i\partial_{\mathbf{r}})$	$g(\mathbf{p})$
$[\hat{f}, \hat{g}]$	$-i\{f, g\} + \ldots$	$[\hat{f}, \hat{g}]$	$i\{f, g\} + \ldots$
$\mathrm{tr}(\hat{g})$	$\int \frac{d\ dt}{2\pi} g(\epsilon, t)$	$\mathrm{tr}(\hat{g})$	$\int \frac{d^d r d^d p}{(2\pi)^d} g(\mathbf{r}, \mathbf{p})$

In the following, it is convenient to bundle temporal and spatial transforms into a **spatio-temporal Wigner transform**,

$$g(x,p) \equiv \int d\Delta x\, e^{i\Delta x^T \eta p} g(x + \Delta x/2, x - \Delta x/2),$$
$$g(x_1, x_2) = \int dp\, e^{-i(x_1 - x_2)^T g p} g(x,p), \tag{11.67}$$

where $x = (t, \mathbf{x})^T = (x_1 + x_2)/2$, $p = (\epsilon, \mathbf{p})^T$, the Minkovski metric $\eta = \mathrm{diag}(1, -\mathbf{1}_d)$, and $dx \equiv dt d^d x$, $dp \equiv d\epsilon d^d p/(2\pi)^{d+1}$.

Derivation of the kinetic equation

We now set out to derive a differential equation describing the evolution of the distribution function. In view of the time scale separations alluded to above, it is convenient to formulate that equation in its Wigner representation. To this end, we consider the formal operator equation

$$\begin{pmatrix} \hat{\epsilon}^+ - \hat{H} - \Sigma_f^+ & -\Sigma_f^K \\ 0 & \hat{\epsilon}^- - \hat{H} - \Sigma_f^- \end{pmatrix} \begin{pmatrix} \hat{G}^+ & \hat{G}^K \\ 0 & \hat{G}^- \end{pmatrix} = \begin{pmatrix} \mathbf{1} & 0 \\ 0 & \mathbf{1} \end{pmatrix}.$$

Writing $\hat{G}^K = \hat{G}^+ \hat{F} - \hat{F}\hat{G}^-$, this matrix equation is equivalent to the set

$$(\hat{\epsilon} - \hat{H} - \hat{\Sigma}^\pm)\hat{G}^\pm = \mathbf{1}$$
$$(\hat{\epsilon} - \hat{H} - \hat{\Sigma}^+)(\hat{G}^+\hat{F} - \hat{F}\hat{G}^-) - \Sigma^K \hat{G}^- = 0.$$

Multiplying the second equation by $(\hat{G}^-)^{-1}$ and using the first equation, we obtain

$$\hat{F}(\hat{\epsilon} - \hat{H} - \hat{\Sigma}^-) - (\hat{\epsilon} - \hat{H} - \hat{\Sigma}^+)\hat{F} - \hat{\Sigma}^K = 0.$$

At this stage, it is convenient to pass to the Wigner transform. Making use of the identities summarized in table 11.1, we obtain the **kinetic equation**

$$\boxed{(\partial_t + \{H,\ \})\, F = i(\Sigma_f^K - (\Sigma_f^+ F - F\Sigma_f^-)) \equiv I_{\mathrm{col}}[F],} \tag{11.68}$$

where the equality is approximate in that higher order contributions to the Moyal product expansion have been neglected. In Eq. (11.68), $F = F(\epsilon, t, \mathbf{r}, \mathbf{p})$ is a function of spatial and temporal variables. The left–hand side of the kinetic equation describes the evolution of the distribution function F under the single particle dynamics.

The effect of particle interactions is encapsulated in the right–hand side, which defines the **collision term**. To lowest order in the Moyal expansion, the operator products appearing in the collision term may be understood as products of Wigner functions, $\Sigma_f^+ F \equiv \Sigma_f^+(\epsilon, t, \mathbf{r}, \mathbf{p}) F(\epsilon, t, \mathbf{r}, \mathbf{p})$, etc. As we will see in a moment, the term Σ^K $(\Sigma^+ F - F\Sigma^-)$ represents an **in-term** (**out-term**), i.e. an interaction-mediated gain (loss) of particle occupancy.

EXERCISE Compare the structure of the quantum kinetic equation to that of the classical Boltzmann equation discussed in Section 10.3. Try to anticipate the explicit structure of the collision term in our system of interacting electrons.

Collision term

So far, our discussion of the kinetic equation has been absolutely general; no reference to the specific mechanisms of self-energy generation has been made. To better understand the physics of the collision term, we now return to our example of interacting electrons.

EXERCISE Show that the Wigner transform of composite operators with space–time dependence $g(x, x')f(x, x')$ is obtained as

$$g(x, x')f(x, x') \to \int dp' g(x, p')f(x, p - p'). \tag{11.69}$$

Also show that

$$g(x, x')f(x', x) \to \int dp' g(x, p')f(x, p' - p). \tag{11.70}$$

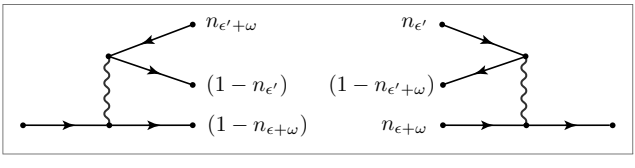

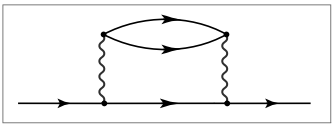

The collision term governs the rates of occupation number changes due to the collisions into and out of other states. This being so, we expect it to be determined by (a) the occupation numbers of the collision partners, and (b) the density of states participating in the interactions. We thus aim for a description in terms of occupation functions F or n_f, and **spectral functions** $A \equiv -2\,\mathrm{Im}\, G^+$. Finally, to expose the fermion propagators contained in the self-energy of the boson propagator $\hat{D}$, we will aim to express the latter in terms of $\hat{\Sigma}_b$. To this end, we note that the relation $\hat{D}^{-1} = \hat{V}^{-1}\sigma_1 - \hat{\Sigma}_b = \begin{pmatrix} 0 & \hat{V}^{-1} - \hat{\Sigma}_b^- \\ \hat{V}^{-1} - \hat{\Sigma}_b^+ & -\hat{\Sigma}_b^K \end{pmatrix}$ implies that

$$\hat{D}^{\pm} = (\hat{V}^{-1} - \hat{\Sigma}_b^{\pm})^{-1} = \hat{D}^+(\hat{V}^{-1} - \Sigma_b\,)\hat{D}^-,$$
$$\hat{D}^K = \hat{D}^+\hat{\Sigma}_b^K\hat{D}^-.$$

We now have everything we need to compute the quasiclassical representation of the collision term in Eq. (11.68):

$$
\begin{aligned}
I_{\rm col}[F](p) &\overset{(11.61),(11.69)}{=} \frac{1}{2}\int dq\Big[G^K(p+q)D^K(q) + (G^+ - G^-)(p+q)(D^+ - D^-)(q) \\
&\quad - \Big((G^+ - G^-)(p+q)D^K(q) + G^K(p+q)(D^+ - D^-)(q)\Big)F(p)\Big] \\
&\overset{(11.57)}{=} -\frac{i}{2}\int dq\, D^+(q)D^-(q)A(p+q) \\
&\qquad \times \Big[(F(p+q) - F(p))\Sigma_b^K(q) + (\Sigma_b^+ - \Sigma_b^-)(q)(1 - F(p+q)F(p))\Big] \\
&\overset{(11.62),(11.70)}{=} \frac{1}{4}\int dq dp'\, D^+(q)D^-(q)A(p+q)A(p'+q)A(p') \\
&\quad \times \Big[(F(p+q) - F(p))(1 - F(p'+q)F(p')) - (F(p'+q) - F(p'))(1 - F(p+q)F(p)\Big].
\end{aligned}
$$

We now assume that $F(p) = 1-2n_\epsilon$ depends only on energy, define the transition probability

$$
T(\epsilon,\epsilon',\omega) \equiv \int \frac{d^dp'}{(2\pi)^d}\frac{d^dq}{(2\pi)^d} D^+(q)D^-(q)A(p+q)A(p'+q)A(p'),
$$

and add and subtract a term $n_\epsilon n_{\epsilon+\omega}n_{\epsilon'}n_{\epsilon'+\omega}$ to arrive at the result

$$
I_{\rm col}[F](p) = \int d\omega d\epsilon'\, T(\epsilon,\epsilon';\omega)(n_\epsilon(1-n_{\epsilon+\omega})n_{\epsilon'+\omega}(1-n_{\epsilon'}) - (1-n_\epsilon)n_{\epsilon+\omega}(1-n_{\epsilon'+\omega})n_{\epsilon'}). \tag{11.71}
$$

Let us discuss the meaning of this expression:

- ▷ The structure of the collision term resembles that of the classical Boltzmann collision term discussed in Section 10.3. Quantum mechanics enters through the **Pauli blocking factors** $1 - n_\epsilon$, etc.
- ▷ Much as the collision term of Boltzmann theory was annihilated by the Maxwell–Boltzmann distribution, the collision term Eq. (11.71) vanishes on the **Fermi–Dirac equation**: interactions serve to install local equilibrium configurations, at a temperature T and chemical potential μ which remain *apriori* unspecified. Departures from equilibrium result from the competition between the left–hand side and the right–hand side of the kinetic equation. In many instances the system may end up in a compromise situation governed by a Fermi-Dirac distribution with spatially varying $T(\mathbf{q})$ and $\mu(\mathbf{q})$.
- ▷ Notice that the collision term vanishes in an approximation where the effects of screening in $\hat{D} \simeq \sigma_1\hat{V}$ are ignored (technically, by ignoring the RPA self-energy of the boson line). Diagrammatically, the building blocks $\hat{D}^+ - \hat{D}^- = \hat{D}^+(\hat{\Sigma}^+ - \hat{\Sigma}^-)\hat{D}^-$ and $\hat{D}^K = \hat{D}^+\hat{\Sigma}^K\hat{D}^-$ are described by the boson insertion to the self-energy diagram shown in the bottom part of the figure above. (Identify the two wavy lines with the self–consistent RPA $\hat{D}^R$ and $\hat{D}^A$, respectively, and the center bubble with the self-energy $\hat{\Sigma}$.) Heuristically, we may interpret this structure as the modulus square of the fundamental RPA **decay amplitudes** shown in the upper part of the figure: the out–term is due to the decay of a particle at energy ϵ into a particle hole excitation (energies ϵ' and $\epsilon' + \omega$, respectively) and a particle at energy $\epsilon + \omega$. This decay is mediated by the (now self–consistently screened) interaction

line at frequency ω. In an analogous manner, the collapse of a particle–hole excitation governs the "in" rate. These processes conserve energy and momentum, up to the smearing introduced by higher order decay processes. (Technically, the spectral functions A contain δ-distributions $\delta_\Sigma(\epsilon - \epsilon(\mathbf{p}))$, where the subscript Σ indicates their broadening by retarded self energies. As an exercise, consider how these self energies encapsulate the generation of higher order particle-hole decay processes, as described by the RPA approximation.)

11.6 A mesoscopic application

In the previous sections we have set up the essential machinery to study quantum systems beyond thermal equilibrium. We have understood how interaction effects aim to drive a system back to a (local) equilibrium configuration and how departures from that configuration can, in principle, be described. However, we have not yet explored the actual physical effects a nonequilibrium environment has on the quantum phenomenology of a system. Of course, this latter question has many facets to it and cannot be addressed in general terms. Rather, we focus on one specific aspect, and we study it within the framework of a concrete application: quantum mechanics is largely about the coherent propagation of matter waves, and the resulting interference phenomena. We know that coherence is averse to any kind of noisy fluctuations in environmental degrees of freedom. At the same time, noise is an inevitable companion of any coupling to a dissipative medium, and it is likely to increase if that coupling generates a nonequilibrium state.

In this section, we explore the formation of noise–levels in a quantum system coupled to a nonequilibrium environment, and its destructive influence on quantum coherence. Questions of this type are attracting a lot of current attention: advances in experimentation make it possible to explore the physics of nanoscopic systems that are strongly influenced by quantum interference phenomena – from ultracold atom physics, quantum information devices, and spintronics, to single molecule electronics, and beyond. At the same time, the very smallness of these systems implies that they are easily driven out of equilibrium, or are in an out of equilibrium state *per se*. Studying the influence of nonequilibrium noise on quantum coherence has, therefore, emerged as a mainstream topic.

11.6.1 Out-of-equilibrium quantum dot

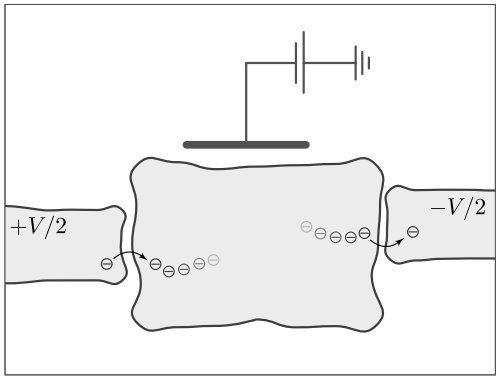

In this section,[17] we investigate the interplay between noise and coherence on a specific setup, the **out-of-equilibrium metallic quantum dot**. Consider a metallic or semiconducting island of mesoscopic size.[18] The island is connected by tunnel electrodes to two leads, which are kept at a voltage difference V. This voltage gradient will be the primary instance by which the system is driven out of equilibrium. Finally, we assume capacitive coupling to a gate electrode (indicated by the horizontal plate in the figure) which determines the electrostatically-preferred number of electrons on the dot.

We describe this system by the Hamiltonian $\hat{H} = \sum_{x=L,R}(\hat{H}_x + \hat{H}_{t,x}) + \hat{H}_d + \hat{H}_c$, where

$$\begin{aligned}
\hat{H}_x &= \sum_{ab} c^\dagger_{x,a} H_{x,ab} c_{x,b}, \\
\hat{H}_{t,x} &= \sum_{a\mu} c^\dagger_{x,a} T_{x,a\mu} d_\mu + \text{h.c.}, \\
\hat{H}_d &= \sum_{\mu\nu} d^\dagger_\mu H_{d,\mu\nu} d_\nu, \\
\hat{H}_c &= \frac{E_C}{2}\left(\sum_\mu d^\dagger_\mu d_\mu - N_0\right)^2 .
\end{aligned} \tag{11.72}$$

Here $c_{x=L/R,a}$ create fermions in state $|a\rangle$ of the left/right lead, respectively, d_μ creates fermions in state $|\mu\rangle$ of the dot, and $\hat{H}_x$ and $\hat{H}_d$ are the corresponding single-particle Hamiltonians. The operators $\hat{T}_{x=L/R}$ describe tunneling between the leads and the dot. Finally, E_C is the electrostatic charging energy on the dot, and N_0 defines its electrostatically-preferred charge. (Notice that N_0 need not be integer.) The voltage bias between the leads will be introduced momentarily through a chemical potential difference.

EXERCISE Recapitulate the discussion of the equilibrium physics of this system in Problems 6.7 and 6.7.

[17] This section is technical in nature. A few unanswered problems aimed at developing computational fluency in Keldysh field theory have been included in the text. (It is not necessary to tackle these problems at first reading.)

[18] By "mesoscopic," we mean that the temperature-dependent dephasing times over which quantum phase coherence is lost due to the interaction with environmental degrees of freedom exceed all time scales relevant to transport in the system. In practice, this means that we are studying systems of $\mathcal{O}(1\mu\text{m})$ or less at temperatures of $\mathcal{O}(10^{(1-2)}mK)$. System sizes/temperature ranges of this order are easily accessible to modern device technology.

Generalizing the theoretical formulation introduced in Problems 6.7 and 6.7, we next aim to derive a Keldysh theory of the nonequilibrium system. Our starting point is the fermion action $S[\bar\psi,\psi,V]\equiv\sum_{x=L,R}(S_x[\bar\psi_x,\psi_x]+S_{t,x}[\bar\psi_x,\psi_x,\bar\psi_d,\psi_d])+S_d[\bar\psi_d,\psi_d,V]+S_c[V]$, where

$$
\begin{aligned}
S_x[\bar\psi_x,\psi_x] &= \int dt\,\bar\psi_x \begin{pmatrix} i\partial_t+i\delta+E_F-\hat H_x & 2i\delta F_x \\ 0 & i\partial_t-i\delta+E_F-\hat H_x \end{pmatrix}\psi_x,\\
S_{t,x}[\bar\psi_x,\psi_x,\bar\psi_d,\psi_d] &= \int dt\,\left[\bar\psi_x\begin{pmatrix}\hat T_x & 0\\ 0 & \hat T_x\end{pmatrix}\psi_d+\bar\psi_d\begin{pmatrix}\hat T_x^\dagger & 0\\ 0 & \hat T_x^\dagger\end{pmatrix}\psi_x\right],\\
S_d[\bar\psi_d,\psi_d,V] &= \int dt\,\bar\psi_d \begin{pmatrix} i\partial_t+i\delta+E_F-\hat H_{0,d}-V_c & -V_q/2+2i\delta F_d \\ -V_q/2 & i\partial_t-i\delta+E_F-\hat H_{0,d}-V_c \end{pmatrix}\psi_d,\\
S_c[V] &= \int dt\,\left(\frac{1}{2E_C}V_cV_q+N_0V_q\right).
\end{aligned}
\tag{11.73}
$$

Here, the distribution functions

$$
F_{\substack{L\\R}} = \coth\left(\frac{\epsilon\pm V/2}{2T}\right), \tag{11.74}
$$

contain the information on the biasing of the system and $V_{c,d}$ are the classical and quantum components of a Hubbard-Stratonovich field decoupling the interaction.

EXERCISE Adapt the **Hubbard–Stratonovich transformation** introduced in Section 11.4.2 to the charging interaction in Eq. (11.72) to reproduce the action above. In Eq. (11.73), the Hubbard–Stratonovich classical and quantum fields V_c and V_d are defined as $V_c\equiv\frac{1}{2}(V_+ + V_-)$, $V_q\equiv V_+-V_-$, in terms of the fields $V_\pm$ decoupling the interaction on the contours. This differs by a factor of $\sqrt{2}$ from earlier conventions and facilitates the interpretation of V_c as a classical degree of freedom.

As with the equilibrium situation studied in Problem 6.7, it will be convenient to remove the fluctuating "voltage" V by a gauge transformation on the dot: introducing the change of variables, $\psi_d\to e^{-i\hat\phi}\psi_d$, $\bar\psi_d\to\bar\psi_d e^{i\hat\phi}$, where $\hat\phi=\phi_c+\phi_q\sigma_1/2$ and the phases are defined by $\partial_t\phi_{c,q}=V_{c,d}$, V disappears from the bulk action while the tunneling matrix becomes dynamical,[19]

$$
\hat T_x\to\hat T_x\,e^{-i\hat\phi}\equiv\tilde T_x.
$$

At this point, the fermions can be integrated out to generate the familiar "tr ln." The rest of the derivation then proceeds as in problem 6.7:

EXERCISE Adapt the derivation of Problem 6.7 to the present context: Expand the "tr ln" to second order in the tunneling matrix elements (recall what sort of assumptions may justify the second order truncation) to **generate the tunneling action**

$$
S_{\rm tun}[\phi]=i\sum_x{\rm tr}(\hat G_xT_x\hat G_dT_x^\dagger),
$$

[19] The gauge transformation also alters the distribution function F_d (exercise: how?).

Evaluate this expression under the following simplifying assumptions: (i) the Hamiltonian operators $\hat{H}_x$ and $\hat{H}_d$ are diagonal in the bases $|a\rangle$ and $|\mu\rangle$, respectively, (ii) in the range of relevant energies, the modulus $|T_{x,a\mu}|^2 \equiv |T_x|^2$ does not significantly depend on Hilbert space indices, and (iii) the spectral functions $\hat{A}_{x,d}(\epsilon) = -2\mathrm{Im}\,\hat{G}^+_{x,d}(\epsilon) = 2\pi\nu_{x,d}(\epsilon)$ are approximately energy independent. (Here $\nu_{x,d}$ are the single particle density of states of leads and dot, respectively.) Show that under these conditions, the tunneling action assumes the form Eq. (11.75). Hint: you may find it convenient to represent the Green functions as $\hat{G}^{\pm}(\epsilon) = \int \frac{d\ '}{2\pi} \frac{\hat{A}(\ ')}{\pm -\ '}$.

The derivation sketched in the formulation of the exercise above then leads to the **tunneling action**

$$S_{\rm tun}[\phi] = -\frac{i}{4}\sum_x g_x \mathrm{tr}(\Lambda_x e^{-i\hat{\phi}}\Lambda_d e^{i\hat{\phi}}), \tag{11.75}$$

where $\Lambda_{x,d}$ is a matrix with energy dependence,

$$\Lambda_{x,d} \equiv 2i\begin{pmatrix} g^+ & g^K_{x,d} \\ 0 & g^- \end{pmatrix}_\epsilon, \qquad g^K_{x,d} \equiv (g^+ - g^-)F_{x,d}, \tag{11.76}$$

the unit spectral density auxiliary "Green function" is defined by $g^{\pm} \equiv \int \frac{d\epsilon'}{2\pi}\frac{1}{\epsilon^{\pm}-\epsilon'}$, and

$$g_x \equiv 4\pi^2\nu_d\nu_x|T_x|^2, \tag{11.77}$$

defines the **tunneling conductance** between dot and lead $x = L/R$. Adding to this the phase representation of the **charging action** in Eq. (11.73),

$$S_c[\phi] = \int dt\left[\frac{1}{2E_C}\partial_t\phi_c\partial_t\phi_q + N_0\partial_t\phi_q\right], \tag{11.78}$$

we obtain a prototypical variant of the effective action in the phase representation, $S[\phi] = S_c[\phi] + S_{\rm tun}[\phi]$.

In the case of strong interactions, phase fluctuations are largely controlled by the tunneling action. Specifically, in nearly insulated dots, $g_x \ll 1$, the phases fluctuate wildly, and no longer represent suitable degrees of freedom. (Exercise: interpret this phenomenon in terms of the voltages $V_{c,q} = \partial_t\phi_{c,q}$; why do voltage fluctuations in the nearly decoupled dot become unimpeded?) As is usual in cases where a variable goes havoc, this limit is better described in terms of the canonically conjugate partner variable, which in the present context carries the significance of a **charge degree of freedom**, n. (Indeed, the dot charge will fluctuate only moderately in the limit of small g_x.)

Technically, the charge variable is introduced by a Hubbard–Stratonovich decoupling of the charging term. This leads to the **action in the phase-charge representation**,

$$\boxed{S[n,\phi] \equiv \int dt\,(n_c\partial_t\phi_q + n_q\partial_t\phi_c - 2E_c(n_c+N_0)n_q) + S_{\rm tun}[\phi].} \tag{11.79}$$

One may think of the above transformation as passing from a Lagrangian variant of the theory – one variable, ϕ, governed by an action with "velocity square" term $\dot{\phi}^2$ – to a Hamiltonian action $\int(n\dot{\phi} - H(n,\phi))$ defined in the phase space of variables (n,ϕ). Notice that the classical component n_c is conjugate to the quantum ϕ_q, and vice versa.

But what about **charge quantization**? We should expect charge in the isolated dot $g_x \to 0$ to be quantized to integer values, but our action above does not appear to know of this constraint. As in many other instances before, information on the quantization of n resides in the **boundary conditions** of its conjugate variable ϕ. So far, we have ignored these boundary conditions. But as we are dealing with phases, we should be alert and expect windings by multiples of 2π as ϕ_c and/or ϕ_q propagate along the Keldysh contour.

EXERCISE To explore the **topology of the phase field**, it is best to go back to the framework of the closed Keldysh contour $s \in [0, S]$. It is on this contour, where the Hubbard–Stratonovich field $\phi(s)$ is defined in the first place. Being a phase field, it is defined only up to multiples of 2π, i.e. we have the boundary conditions $\phi(S) = \phi(0) + 2\pi W$, where the integer W has to be summed over (cf. our discussion of functional integrals over S^1-valued fields in Chapter 3). Implement the condition above by the *ansatz*, $\phi(s) = \phi(s) + \frac{2\pi W}{2T}(s - T)$, where ϕ is periodic on the s-contour, and we assume the real time contour to be parameterized by $t \in [0, T]$. Show that this condition translates to an unconstrained field $\phi_c = \phi_c$, and to

$$\phi_q(t) = \phi_q(t) + \frac{2\pi W}{T}(t - T), \tag{11.80}$$

with Dirichlet conditions $\phi_q(0) = \phi_q(T) = 0$.

In the exercise above, it is shown that the information on phase windings resides in the quantum field, ϕ_q. Heuristically, quantization conditions for the field n may then be deduced as follows. Assuming that the winding number dependence of the tunneling action is negligible (the rationale being that in the limit $T \to \infty$ the W-contribution to Eq. (11.80) is a nearly constant phase shift which is likely to cancel out in a term probing the local tunneling dynamics), we observe that W enters the action through the contribution $2\pi W \frac{1}{T} \int_0^T dt\, n_c$. Summation over W then generates the condition $\frac{1}{T} \int_0^T dt\, n_c \in \mathbb{Z}$: the temporal average of classical charge on the dot is integer. But since the operators $\sim \exp(i\hat{\phi})$ in the action that change the charge do so in discrete steps, $n_c \to n_c \pm 1/2$, and the numbers of positive $(\exp(i\hat{\phi}))$ and negative $(\exp(-i\hat{\phi}))$ jumps are equal, this condition calls for an initial charge value $n_c(0) \in \mathbb{Z}$. In the course of time, this initial value may change, but it does so in integer steps, i.e. the classical charge $n_c(t)$ is quantized.

EXERCISE If you find the argument above too vague, you may derive **charge quantization in rigorous terms**. Do not ignore the W-dependence of the tunneling term. Rather, expand $\exp(iS)$ schematically to nth order in $S_{\rm tun}$. The winding numbers then enter as a pure phase $\exp(2\pi i F W)$, where F is an expression involving n_c, and the discrete set of times at which the phases of the tunneling terms are evaluated. Summation over W generates the quantization condition $F \in \mathbb{Z}$. Analyse F to show that this condition is equivalent to the initial value quantization $n_c(0) \in \mathbb{Z}$. In combination with the integer steps taken by the tunneling dynamics, this rigorously proves charge quantization.

In effect, we may account for the windings of the phase fields by limiting the integration path $n_c(t)$ to integer configurations, and thence forget about the winding numbers.

11.6.2 Dot distribution function

Hidden in the action (11.79) sits the distribution function of the dot (cf. Eq. (11.75) and (11.76)). In principle, we should think about the distribution function as an observable of the theory, a quantity that determines the distribution of the particles on the dot after all degrees of freedom (including the interaction) have been integrated out. However, the results of that integration actually depend on the dot distribution function, i.e. the rigorous determination of the latter poses a recursive problem whose solution is likely out of reach. In practice, one will rather work with a trial distribution, which should of course be reasonably close to the actual distribution.

In the present context, we will approximate F_d by the distribution function of the non-interacting dot. The rationale behind this *ansatz* is the assumption that the coupling to the leads will adjust an effective distribution on the dot, at time scales $\sim \nu|T|^2$, faster than the relaxation times due to interactions. The quality of such assumptions must of course be checked in retrospect.

Trial dot distribution function

But what will the distribution function on the dot, in the absence of interactions, look like? There are various ways to answer this question. Heuristically, one may argue that all single particle states on the dot will be occupied up to energy $-V/2$, i.e. up to the threshold energy above which the band of the right lead begins to dry up (cf. the figure.) At larger energies, states on the dot are hybridized with isoenergetic filled states in the left lead, and empty states in the right lead. These coupling mechanisms are mutually independent, and occur at a strength $g_{L,R}$, respectively. This suggests, that the distribution on the dot

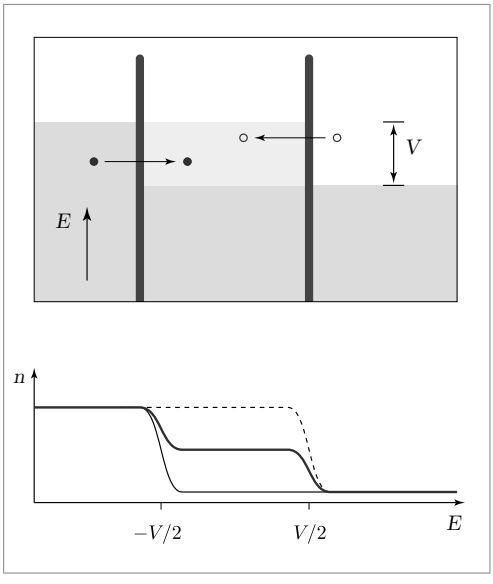

$$F_d = \frac{g_L F_L + g_R F_R}{g_L + g_R}, \qquad (11.81)$$

will be an additive superposition of the lead distributions. The corresponding distribution function $n_d = (-F_d + 1)/2$ assumes the form of a **double step distribution** (cf. the figure.)

EXERCISE Substantiate the argument above: To this end, consider the tunneling operators $\hat{T}_x$ as a "perturbation", and compute the corresponding self energies. Then consider the **kinetic equation** (11.68). For a stationary solution F, the left–hand side of the equation vanishes. Show that the vanishing of the right–hand side enforces the double step distribution.

Readers who feel comfortable enough with these ways of fixing the distribution function may advance to the next section. For the benefit of all others, we devote the rest of this section to showing how the (non-interacting) distribution function may be obtained directly from the effective action. To this end, we vary the tunneling action (11.75) in $\hat{\phi}$ and adjust Λ_d such that the non-interacting configuration $\hat{\phi} = 0$ is a stationary point. In the exercise below, we show the equivalence of this procedure to the kinetic equation approach above.

We need to determine Λ_d such that the linear expansion of the action in $\hat{\phi} = \phi_c + \phi_q\sigma_1$ vanishes. It is straightforward to verify that variations in ϕ_c vanish regardless of the distribution function. As for the quantum component, we generalize $\phi_q\sigma_1 \to \hat{\phi}_q \equiv \mathrm{Re}\,\phi_q\sigma_1 - \mathrm{Im}\,\phi_q\sigma_2$, which may be interpreted as a shift of the generator ϕ_q into the complex plane. It is then a straightforward exercise to verify that the variation of the action $\delta_{\bar{\phi}}S = 0$ generates equation (11.81). But what might be the logic behind this variational approach? The answer is given in the following exercise:

EXERCISE The distribution function on the dot can be found by solution of an appropriate kinetic equation, $(\hat{G}_0^{-1} - \Sigma)\hat{G} = \mathbf{1}$. In this exercise, we want to show that the component of this matrix equation relevant to the determination of F_d can be found by introduction of a suitable source. To this end, let us go back to the microscopic variant of the theory, Eq. (11.73), and generalize $i\delta\sigma_3 \to i\delta\, e^{i\hat{\phi}_q}\sigma_3 e^{-i\hat{\phi}_q}$ in the dot action, S_d. Verify that the expansion of the action to first order in $\bar{\phi}_q$ generates the Keldysh component of the kinetic equation. Under the assumption of constant spectral density (also underlying the derivation of the tunneling action), the vanishing of the linear variation becomes equivalent to the fulfilment of the kinetic equation. The stationary solution is given by Eq. (11.81).

For notational simplicity, we assume **contacts of equal transparency**,

$$g_L = g_R \equiv g,$$

throughout the rest of the section.

Tunneling action

We may use the result Eq. (11.81) to bring the tunneling action into a form more manageable than the abstract representation Eq. (11.75). To this end, let us introduce the notation

$$c \equiv e^{i\phi_c}\cos(\phi_q/2), \qquad s \equiv e^{i\phi_c}\sin(\phi_q/2).$$

We substitute $e^{i\hat{\phi}} = c + is\sigma_1$ and $e^{-i\hat{\phi}} = \bar{c} - i\bar{s}\sigma_1$ into Eq. (11.75) and obtain

$$\begin{aligned} S_{\mathrm{tun}}[\phi] &= 2g\int dtdt'\,(\bar{c}, -i\bar{s})_t \begin{pmatrix} 0 & \Sigma^- \\ \Sigma^+ & \Sigma^K \end{pmatrix}_{t,t'} \begin{pmatrix} c \\ is \end{pmatrix}_{t'} \\ &= 2g\int \frac{d\omega}{2\pi}\,(\bar{c}, -i\bar{s})_\omega \begin{pmatrix} 0 & \Sigma^- \\ \Sigma^+ & \Sigma^K \end{pmatrix}_{\omega} \begin{pmatrix} c \\ is \end{pmatrix}_{\omega}, \end{aligned} \tag{11.82}$$

where (notice the similarity to the self-energy of a boson coupled to fermions Eq. (11.62)),

$$\Sigma^{\pm}_{t-t'} = \frac{i}{2}\sum_x \left(g^{\pm}_{t-t'}g^K_{x,t'-t} + g^K_{d,t-t'}g_{t'-t}\right),$$
$$\Sigma^K_{t-t'} = \frac{i}{2}\sum_x \left(g^K_{x,t'-t}g^K_{d,t-t'} - (g^+ - g^-)_{t-t'}(g^+ - g^-)_{t'-t}\right).$$

Like so often, we focus on the damping contribution to the self energy, $\Sigma^+ - \Sigma^-$. Using $(g^+ - g^-)_\epsilon = -i$, we obtain

$$(\Sigma^+ - \Sigma^-)_\omega = \frac{i}{2}\sum_x \int \frac{d\epsilon}{2\pi}(F_{d,\epsilon} - F_{x,\epsilon-\omega}) = i\frac{\omega}{\pi}, \tag{11.83}$$
$$\Sigma^K_\omega = \frac{i}{2}\sum_x \int \frac{d\epsilon}{2\pi}(1 - F_{d,\epsilon}F_{x,\epsilon-\omega}) = \frac{i}{4\pi}\sum_{s=\pm1}(\omega F_b(\omega) + (\omega + sV)F_b(\omega + sV)),$$

where we used Eq. (11.74) and the relations, $\int \frac{d\epsilon}{2\pi}(F(\epsilon+\omega) - F(\epsilon)) = \frac{\omega}{\pi}$, $\int \frac{d\epsilon}{2\pi}(1 - F(\epsilon - \omega)F(\epsilon)) = \frac{\omega}{\pi}F_b(\omega)$, with $F(\epsilon) = \tanh(\epsilon/2T)$, and $F_b(\omega) = \coth(\omega/2T)$. Combining everything, we obtain

$$S_{\rm tun}[\phi] = \frac{g}{\pi}\int \frac{d\omega}{2\pi}(\bar{c}, -i\bar{s})_\omega \begin{pmatrix} 0 & -i\omega \\ i\omega & 2iK(\omega)\end{pmatrix}\begin{pmatrix} c \\ is\end{pmatrix}_\omega, \tag{11.84}$$

where $K(\omega) \equiv \frac{\omega}{2}F_b(\omega) + \frac{1}{4}\sum_{s=\pm1}(\omega + sV)F_b(\omega + sV)$. The action Eq. (11.79) with the tunneling contribution Eq. (11.84) is the basis of all our further discussion.

11.6.3 Observables

Before proceeding, we should choose an observable in terms of which the system's behavior will be described. While the system's total conductance (as opposed to the tunneling conductances of its individual dot-lead interfaces) might be the first option coming to one's mind, we here focus on the dot **tunneling density of states, (TDoS)**. The latter is defined as[20]

$$\nu(\epsilon) \equiv -\frac{1}{\pi}{\rm Im}\,{\rm tr}\,(\hat{G}^+(\epsilon)) = -\frac{1}{\pi}{\rm Im}\int dt\, e^{it\epsilon}{\rm tr}\,(\hat{G}^+(t)). \tag{11.85}$$

What makes the TDoS an interesting observable to consider?

▷ The **TDoS can be measured** by tunneling spectroscopy. See Fig. 11.4 for an example of local probes of the TDoS in a mesoscopic superconductor–normal–superconductor (SNS) wire. (Barely discernible in the figure is the straight normal wire, adjacent to a horseshoe shaped superconductor.) In this system, the TDoS is suppressed due to the superconductor proximity effect, the effect that a superconductor tends to induce pair correlations leading to a spectral gap in the adjacent normal metallic regions. The size of the gap as a function of voltage (energy) diminishes with the distance from the superconductor.

[20] The notation assumes a steady state configuration. In principle, $\nu(\epsilon, t)$ may be explicitly time dependent, via temporal changes in distribution functions.

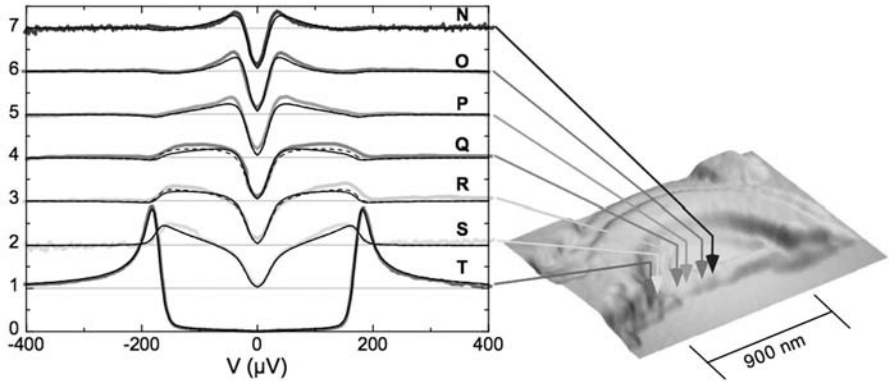

Figure 11.4 Tunneling density of states as a function of voltage (energy) in a mesoscopic SNS structure. The arrows mark the position where, in the normal wire, the TDoS was recorded. Figure taken from H. le Sueur, P. Joyez, H. Pothier, C. Urbina, and D. Esteve, Phase controlled superconducting proximity effect probed by tunneling spectroscopy, *Phys. Rev. Lett.* **100**, 197002-6 (2008).

▷ At the same time, the TDoS is an observable of considerable **conceptual interest**. As is obvious from its definition, the function $\nu(\epsilon)$ probes the amplitude of quasiparticle propagation in the system at time scales $t \sim \epsilon^{-1}$. This propagation amplitude comes with a quantum dynamical phase. Out of thermal equilibrium, we expect this quantum phase to be susceptible to all kinds of **nonequilibrium fluctuations**. In this sense, the TDoS is an observable very close to the central theme of this chapter.

More generally, the TDoS probes the general mechanism of the **orthogonality catastrophe** : the quantum state "bare quasiparticle plus unperturbed system" forming right after the tunneling event will typically be very different ("orthogonal") from the asymptotic stationary state in which the incoming particle has been accommodated into the system. The formation of that final state generally involves the re-adjustment of a large number of particles and may take much more time than, say, the tunneling process as such. This means that in strongly interacting systems, the TDoS is expected to show significant structure at small energy scales – the **zero bias anomaly**.

In fact, the **Coulomb blockade** discussed in Problem 6.7 can be viewed as an extreme manifestation of the zero bias anomaly: tunneling onto an isolated quantum dot creates a state that is energetically forbidden, or "sub-barrier," by an amount E_c. This means that the TDoS vanishes over an interval from $\epsilon = 0$ to $\epsilon = E_C$. (Recall that energy is measured from the Fermi energy.) Equivalently, we may say that tunneling processes onto the dot are limited to short duration $t \sim E_c^{-1}$. **Tunneling into a metallic system** leads to more intricate behavior. The tunneling process generates an initial charge distribution which is energetically unfavourable (sub-barrier). In the course of time, that initial distribution will relax in what typically will be a diffusive spreading process. The action associated

to that process weights the quasiparticle propagator and hence the TDoS. For example in a two-dimensional setting, the long time relaxation action diverges,[21] which implies singular behavior of the TDoS at low energies.

The open quantum dot discussed in this section forms a compromise between a closed dot and a bulk metallic system. Below we try to understand the TDoS of this system, and the ramifications of nonequilibrium fluctuations. However, before doing so, we first need to express $\nu(\epsilon)$ in terms of our effective degrees of freedom. Fortunately, this is a straightforward task. It turns out to be best to work in the representation of the theory prior to the Keldysh rotation. Comparison with the formulae in Section 11.4.1 shows that

$$\nu(\epsilon) = -\frac{1}{2\pi i}\int dt\, e^{i\epsilon t}\left(G^{-+}(t) - G^{+-}(t)\right).$$

To give the Green functions $G^{\pm}$ some meaning, we just need to note two things: in the presence of interactions $G^{-+}_{tt'} = -i\langle\psi^-_t\bar\psi^+_{t'}\rangle \to -ie^{i(\phi_-(t)-\phi_+(t'))}\langle\psi^-_t\bar\psi^+_{t'}\rangle = e^{i(\phi_-(t)-\phi_+(t'))}G^{-+}_{0,tt'}$, where G_0 is the non-interacting Green function. For a single level, its form is shown in Eq. (11.52). For our many level dot this generalizes to

$$\begin{aligned} G^{-+}_{0,tt'} &= -i\sum_\mu e^{-i\epsilon_\mu(t-t')}(1-n_d(\epsilon_\mu)) = -i\int d\epsilon\,\nu(\epsilon)e^{-i\epsilon(t-t')}(1-n_d(\epsilon)) \\ &\simeq -2\pi i\nu_d(1-n_d)(t-t'), \end{aligned}$$

where $n_d(t)$ is the Fourier transform of the function $n(\epsilon)$ and we assumed constant non-interacting density of states ν_d as before.[22] Combining this with the analogous construction for the Green function $G^{\pm}$, we obtain $\nu(\epsilon) = \nu_e(\epsilon) + \nu_h(\epsilon)$, where

$$\begin{aligned} \nu_e(\epsilon) &= \nu_d\,\mathrm{Re}\int dt\, e^{i\epsilon t}e^{i(\phi_-(t+\bar t)-\phi_+(\bar t))}(1-n_d)(t), \\ \nu_h(\epsilon) &= \nu_d\,\mathrm{Re}\int dt\, e^{i\epsilon t}e^{i(\phi_+(t+\bar t)-\phi_-(\bar t))}n_d(t). \end{aligned} \tag{11.86}$$

Here $\nu_{e,h}$ are to be interpreted as the contributions of electrons (holes) tunneling onto the dot, and $\bar t$ is an arbitrary reference time marking the beginning of the tunneling process. The hole contribution, ν_h, differs from ν_e in the replacement $(1-n_d) \to n_d$, and a sign change in the phase of the oscillatory exponential.

11.6.4 Open quantum dot

In this section, we study the TDoS at large values of the tunneling conductance, $g \gg 1$. In this limit, fluctuations of the phase ϕ are largely quenched. Conversely, the conjugate degree of freedom, the charge n, fluctuates strongly – the open quantum dot admits large variations of charges and currents. The discussion of the open system is rewarding in that

[21] L.S. Levitov and A. V. Shytov, Semiclassical theory of the Coulomb anomaly, *Pisma Zh. Eksp. Teor. Fiz.* **66**, 200-205 (1997) [JETP Lett. **66**, 214-221 (1997)].

[22] Notice that $(1-n_d)(t) = \delta(t) - n_d(t)$ is to be understood as the Fourier transform of $1-n_d(\epsilon)$.

it enables us to bridge between classical and quantum phenomena. On the one hand, the smallness of (quantum) fluctuations of the phase means that we stay close to the classical limit; in many respects, our system behaves like a classical RC-resistor unit, kept at voltage $\sim \dot{\phi}$. On the other hand, Eq. (11.86) demonstrates that the same phase determines the quantum mechanics of the observable ν. Indeed, we discover that the physics of the orthogonality catastrophe in the system can largely be understood in terms of classical voltage fluctuations.

At large g, the tunneling action may be expanded to second order in ϕ around its stationary configuration $\phi = 0$.[23] As a result of this expansion we obtain

$$S^{(2)}[\phi] = \frac{1}{2E_C}\int dt\, \partial_t\phi_c\partial_t\phi_q + \frac{g}{2\pi}\int \frac{d\epsilon}{2\pi}\,(\phi_c,\phi_q)_\omega \begin{pmatrix} 0 & -i\omega \\ i\omega & iK(\omega)\end{pmatrix}\begin{pmatrix}\phi_c\\ \phi_q\end{pmatrix}_\omega, \qquad (11.87)$$

where the kernel K is defined in Eq. (11.84) and we used the phase representation of the charging action Eq. (11.78). We have also neglected the N_0-contribution to the charging action, the formal reason being that for large g, topologically excited (finite winding numbers W) configurations of the phase field do not play a role. However, for $W = 0$, $N_0\int dt\,\partial_t\phi_q = 0$. (Exercise: what is the physical reason for the irrelevancy of the N_0-term in the widely open quantum dot?)

Except for the structure of the kernel K, this action is reminiscent of the standard MSRJD–actions describing dissipative classical systems. To understand the ramifications of this connection, we go one step backwards in the direction of classical physics and decouple the $\phi_q\phi_q$-term to obtain a Langevin-type system:

$$S[\phi,\xi] = \int dt\,\phi_q\left[\left(-\frac{1}{2E_C}\partial_t^2 - \frac{2g}{2\pi}\partial_t\right)\phi_c + \xi\right] + i\int\frac{d\omega}{2\pi}\xi_\omega\frac{\pi}{2gK(\omega)}\xi_{-\omega}. \qquad (11.88)$$

Classical resistor network

Integration over ϕ_q in Eq. (11.88) freezes the classical field to the configuration solving the equation

$$\left(\frac{1}{2E_C}\partial_t^2 + \frac{2g}{2\pi}\partial_t\right)\phi_c = \xi,$$

where the noise field ξ is correlated according to

$$\langle\xi(t)\xi(t')\rangle = \frac{g}{\pi}K(t-t'),$$

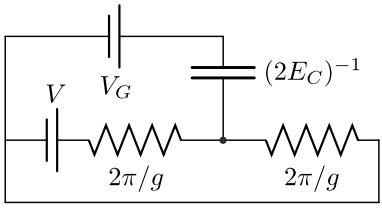

and $K(t) = \int\frac{d\omega}{2\pi}e^{-i\omega t}K(\omega)$ is the Fourier transform of the kernel K. This is the Langevin equation for voltage fluctuations on the classical resistor network equivalent to our quantum dot. The network is depicted in the figure where the central node represents the quantum dot, coupled by two resistors of resistance $R = g^{-1}$ to a bias voltage source. The dot is also

[23] Anharmonic fluctuations are suppressed in g^{-1}, but weakly singular in the infrared time scales of the theory. This indicates scaling of the coupling constants (g, E_c) of the theory, which, however, we do not discuss in this text.

coupled to a capacitor of capacitance $C = 1/2E_C$. That capacitor is kept at a gate voltage $V_G = N_0/C$ (which, however, we saw is irrelevant to the physics of the open dot).

To make the connection to classical circuit dynamics more explicit, we change notation in the Langevin equation above according to[24]

$$g = \frac{2\pi}{R}, \qquad E_C = \frac{1}{2C}, \qquad U = \partial_t \phi_c, \qquad \xi = C\eta.$$

The **Langevin equation describing voltage fluctuations** off the static value $V/2$ then assumes the form

$$\partial_t U + \gamma U = \eta, \tag{11.89}$$

where $\langle \eta(t)\eta(t')\rangle = \frac{\gamma}{C} K(t-t')$ and we have introduced the parameter $\gamma \equiv \frac{2}{RC}$. The **meaning of this equation** is not difficult to understand: in the absence of fluctuations, $\eta = 0$, the voltage on the dot relaxes to its stationary value, $V/2$, at the **RC-time scale** characteristic for a capacitive shunt. (The relaxation time scale is actually $2/RC$, because what matters is the resistance $R/2$ of a dot shunted by two parallel resistors.) In contrast to our previous studies of dissipative systems, the coupling to two distinct leads ("baths") implies that the voltage distribution on the dot cannot relax to an equilibrium configuration.

To explore this point, let us take a close look at the **fluctuation correlator**, K:

- ▷ In the **absence of biasing**, $V = 0$, and in the **classical limit** $(\hbar)\omega \to 0$, we have $K(\omega) = \omega \coth(\omega/2T) \overset{\omega\to 0}{\longrightarrow} 2T$, and $\langle \eta(t)\eta(t')\rangle = \frac{2T\gamma}{C}\delta(t-t')$. Comparison with our discussion of Langevin equations in the previous chapter then shows that the steady state distribution controlling the voltage on the dot takes the form

  $$P(V) = \mathcal{N}\, e^{-\frac{U^2 C}{2T}}.$$

  This is the **Maxwell–Boltzmann distribution** for a system with capacitive energy $U^2C/2$.
- ▷ Still assuming zero bias, $V = 0$, let us now explore the **zero temperature limit**. In this case, $K(\omega) = \omega \coth(\omega/2T) \overset{T\to 0}{\longrightarrow} |\omega|$. To understand the meaning of this limit, we may interpret the voltage fluctuations as due to the fluctuations of a large assembly of oscillators of arbitrary frequency ω. (In "reality" the fluctuations represent particle–hole excitations in the Fermi liquids constituting the system. However, for the sake of the argument, that concrete realization is not important.) In the classical limit $T \gg \omega$, each spectral component stores fluctuation energy T (the equipartition theorem), which explains the above classical correlator. However, in quantum mechanics, the energy reads $\omega(n(\omega)+1/2) = \frac{\omega}{2}\coth(\omega/2T)$. This means that at small temperatures T, it gets replaced by $|\omega|/2$. Also notice that for $\omega > 0$ the zero temperature energy is due to the factor $1/2$ in the energy balance: the observable fluctuations are due to vacuum oscillations of the quantum baths. As discussed in the previous chapter, the equilibrium oscillator fluctuations leading to the statistics above are called **Nyquist–Johnson noise**.

[24] The factor of 2π in the definition of R is explained as follows: g is the dimensionless conductance of the tunnel barriers. The physical conductance $G \equiv R^{-1} = ge^2/h = (g/2\pi)/\hbar$. In our units $e^2 = \hbar = 1$ and this reduces to $g = 2\pi/R$.

▷ We next consider the consequences of **finite biasing**, $V > 0$. For simplicity we keep the temperature at zero, $T = 0$. Inspection of Eq. (11.84) then reveals a crossover,

$$K(\omega) = \begin{array}{ll} |\omega|, & |\omega| \gg |V|, \\ \frac{1}{2}|V|, & |\omega| \ll |V|. \end{array}$$

The interpretation of this crossover is as follows: At large frequencies, $|\omega| \gg |V|$, noise is dominated by the equilibrium fluctuations of high frequency oscillator modes. However, at lower frequencies, we start sensing the distortion out of equilibrium, due to the biasing of the dot. The latter causes a finite mean current flow through the system. This in turn generates noise, which will be predominantly **shot noise**.

In the previous chapter we argued that if we define the current passing through an elementary resistor in a time window $[\bar{t}, \bar{t} + \Delta t]$ as $I_{\Delta t} = n/\Delta t$ in terms of the number of charges, n, passing through in a time Δt, the statistical variance of the current – incident charges assumed Poisson distributed – will be given by $\mathrm{var}(I_{\Delta t}) = \bar{I}/\Delta t$, where $\bar{I} = \langle I_{\Delta t} \rangle$ is the statistical average of the current. We may write the instantaneous current through the resistor as $I = \bar{I} + \delta I$, where $\langle \delta I(t) \delta I(t') \rangle = f \delta(t - t')$ describes short range correlated current fluctuations. Computing the variance,

$$\mathrm{var}(I_{\Delta t}) = \frac{1}{(\Delta t)^2} \int_{\bar{t}}^{\bar{t}+\Delta t} dt dt' \, \langle \delta I(t) \delta I(t') \rangle = \frac{f}{\Delta t},$$

we find that $f \equiv \bar{I}$ establishes compatibility to Poissonian shot noise.

We now relate these findings to the Langevin equation describing our more complex two-resistor system. To this end we rewrite the latter as

$$C d_t U = -\frac{2}{R} U + C\eta, \tag{11.90}$$

i.e. an equation that relates the rate of changes in the charge of the dot (left–hand side) to current flow (right–hand side). Specifically, $C\eta \equiv \delta I_L + \delta I_R$ is to be interpreted as the sum of current fluctuations through the left and right tunnel resistor. Each of the two contributions $I_x, x = L, R$ is expected to express Poissonian shot noise statistics, $\langle I_x(t) I_x(t') \rangle = \bar{I} \delta(t - t') = V/(2R) \delta(t - t')$. Compatibility with our considerations above then requires

$$\langle \eta(t) \eta(t') \rangle = \frac{1}{C^2} \left(\langle \delta I_L(t) \delta I_L(t') \rangle + \langle \delta I_R(t) \delta I_R(t') \rangle \right) = \frac{V}{RC^2} \delta(t - t'),$$

in agreement with Eq. (11.89) and $K(t - t') = (V/2)\delta(t - t')$: the noise in our system is obtained by superposition of the shot noise generated by the two resistive tunnel barriers.

INFO The analysis of noise levels in compounds comprising several elementary Poissonian noise sources plays an important role in **nonequilibrium mesoscopic physics**. It is customary to quantify the noise in a composite system by a parameter known as the **Fano factor**. The Fano factor relates the **DC-noise power** in the system,

$$S \equiv 2 \int dt \, \langle \delta I(0) \delta I(t) \rangle, \tag{11.91}$$

to the noise power, S_0, of an elementary resistor unit with Poissonian statistics,

$$F \equiv \frac{S}{S_0}. \tag{11.92}$$

Here δI is the fluctuation contribution to the current in the system. To make these definitions more concrete, consider the elementary RC-unit shown in Fig. 10.2, first at the absence of external biasing $V = 0$, and at temperature T. The Langevin equation controlling current flow in the system reads $Cd_tU = -R^{-1}U + \delta I$. The FDT requires that $\langle \delta I(t)\delta I(t')\rangle = \frac{2}{RT}$ which means that, in equilibrium, $S_{\rm eq} = 4T/R$. Now consider the complementary case of zero temperature, $T = 0$, but finite bias V across the resistor. In this case, the Poissonian statistics of charge transmission requires (cf. the discussion above) $\langle \delta I(t)\delta I(t')\rangle = \bar{I} = V/R$. This means that

$$S_0 = 2\bar{I} = \frac{2V}{R}.$$

What is the Fano factor of the double barrier quantum dot discussed above? We define $I = U/R$ as the current whose statistics we wish to characterize. Comparison with Eq. (11.90) shows that $\delta I = C\eta/2$. From this identification and Eq. (11.89) we find that, in equilibrium, the noise power $S = 2T/R$. This is the noise of a unit with total (series) resistance $R_{\rm tot} = 2R$. Out of equilibrium, the correlator $\langle \delta I(t)\delta I(0)\rangle = \frac{V}{4R}\delta(t-t')$ implies $S = V/2R = V/R_{\rm tot} = \bar{I} = S_0/2$, or $F = 1/2$. The system exhibits fluctuations lower than those of a single Poissonian resistor. The reason for this reduction is that the current fluctuations $\delta I = (\delta I_L + \delta I_R)/2$ are obtained by superposition of two statistically independent noise sources.

Zero bias anomaly

We next wish to explore the ramifications of the resistor voltage fluctuations in the quantum mechanics of the TDoS. To this end, consider the electron contribution ν_e to the density of states in Eq. (11.86). Using the fact that $\phi_c(t+\bar{t}) - \phi_c(\bar{t}) = \int_{\bar{t}}^{t+\bar{t}} dt'\, U(t')$, we can rewrite this expression as

$$\begin{aligned}\nu_e(\epsilon) &= \nu_d \,\mathrm{Re} \int dt\, e^{i\epsilon t} \quad e^{\frac{i}{2}\int_{\bar{t}}^{t+\bar{t}} dt'\, U(t')} e^{i(\phi_q(t+\bar{t})+\phi_q(\bar{t}))} \quad (1-n_d)(t) \\ &= \nu_d \,\mathrm{Re} \int dt\, e^{i\epsilon t} \quad e^{\frac{i}{2}\int_{\bar{t}}^{t+\bar{t}} dt'\, U\ (t')} \quad {}_{\eta}\,(1-n_d)(t)\end{aligned}$$

where $U[\eta]$ is the solution to the differential equation

$$(\partial_{t'} + \gamma)\, U_\eta(t') = \eta + \frac{1}{C}(\delta(t' - (\bar{t}+t)) + \delta(t'-t)).$$

Once more, this equation is easy to interpret. What is new in comparison to the Langevin equation (11.89) describing the source-free action is the presence of the two δ-functions on the right–hand side. These δ-functions reflect a unit-jump in the classical charge upon the entry of a particle (amplitude) in the dot. The voltage on the dot is thus driven by the superposition of the noise η, and the entry peaks. In response it relaxes, as described by the left–hand side of the Langevin equation. There is no reason to be puzzled by the appearance of two δ-functions; depending on the sign of t, only one of them contributes to the profile of U_η in the time window $[\bar{t}, \bar{t}+t]$ (or $[\bar{t}+t, \bar{t}]$ for negative t). The reason is that the time evolution of U is retarded, i.e. the equation describes the forward evolution of U in causal

response to driving sources. For example, for $t > 0$, only $\delta(t' - \bar{t})$ affects the evolution in the time window $[\bar{t}, \bar{t} + t]$.

We may interpret the phase $e^{\frac{i}{2}\int_{\bar{t}}^{t+\bar{t}} dt'\, U\ (t')}$ as the "Feynman propagator" of the tunneling amplitude. Our dot is largely structureless, i.e. the only contribution to the action of the particle is the fluctuating voltage U_η. To understand its effect, we need to average the phase over noise fluctuations. This is most efficiently done by substitution of the Fourier transform of U_η,

$$U_\eta(\omega) = \frac{\eta(\omega) + \frac{1}{C}\left(e^{i\omega(\bar{t}+t)} + e^{i\omega t}\right)}{-i\omega + \gamma},$$

and performing the Gaussian integral over $\eta(\omega)$ using

$$\langle \eta(\omega)\eta(\omega')\rangle = 2\pi\delta(\omega + \omega')\frac{\gamma}{C}K(\omega).$$

As a result of a straightforward but not particularly illuminating calculation, we then obtain

$$\nu_e(\epsilon) = \nu_d \,\mathrm{Re} \int dt\, e^{i\epsilon t} e^{-\frac{i}{2\gamma C}\,\mathrm{sgn}\,(t)\left(e^{-\gamma|t|}-1\right)} e^{-S(t)}(1 - n_d)(t),$$

where the noise action

$$S(t) = \frac{\gamma}{C}\int \frac{d\omega}{2\pi}\frac{1-\cos(\omega t)}{\omega^2\left(\omega^2+\gamma^2\right)}K(\omega), \tag{11.93}$$

and the oscillatory exponential describes the decay of the entry voltage peak on the RC-time scale. The integral form of $S(t)$ reflects the finite time interval over which the voltage fluctuations are monitored (the factor $\omega^{-2}(1-\cos(\omega t))$, the RC-retarded nature of the voltage response to fluctuations (the factor $((\omega^2+\gamma^2)^{-1})$, and the statistics of the fluctuations themselves, $K(\omega)$. The hole contribution, ν_h, differs from ν_e by a sign change in the oscillatory phase, and in the replacement $1 - n_d \to n_d$. Adding the two contributions and using the fact that, in the open limit, the largeness of the dimensionless parameter $\gamma C = 2/R \gg 1$ permits a linearization in the exponential phase, we obtain

$$\nu(\epsilon) = \nu_d\left(1 - \frac{1}{2\pi\gamma C}\sum_{\sigma=\pm}\int_0^\infty dt\,\frac{\cos((\epsilon+\sigma V/2)t)}{t}\left(1-e^{-\gamma t}\right)e^{-S(t)}\right), \tag{11.94}$$

where $\sum_\sigma e^{i\sigma V/2t}/(4\pi i t)$ is the Fourier transform of the dot distribution function Eq. (11.81) at zero temperature and equal barrier heights.

In the **unbiased limit**, $V = 0$, the noise action can be estimated as

$$S(t) \overset{V=0}{\simeq} \frac{1}{2\pi\gamma C}\ln\left(1+(\gamma t)^2\right).$$

This result states that at large time scales, a conspiracy of RC-relaxation and noise fluctuations leads to a logarithmically diverging action for particle tunneling processes. The consequences become evident once we substitute $S(t)$ into Eq. (11.94) for the tunneling

DoS. Noting that the factors $(1-e^{-\gamma|t|})$ and $\cos(\epsilon t)$ act as infrared and ultraviolet cutoffs, respectively, we obtain

$$\nu_\epsilon \simeq \nu_d \left(1-\frac{1}{\pi\gamma C}\int_{\gamma^{-1}}^{|\epsilon|^{-1}} \frac{dt}{t} e^{-S(t)}\right) \simeq \nu_d \left(1-\frac{1}{\pi\gamma C}\int_{\gamma^{-1}}^{|\epsilon|^{-1}} \frac{dt}{t} (\gamma t)^{\frac{1}{\pi\gamma C}} \simeq\right) = \nu_d (|\epsilon|/\gamma)^{\frac{1}{\pi\gamma C}},$$

or, using the definition of γ and R,

$$\nu(\epsilon) \overset{V=0,\epsilon\ll 1/RC}{\simeq} \nu_d \left(\frac{\pi C|\epsilon|}{g}\right)^{1/g}. \tag{11.95}$$

This is the celebrated **zero bias anomaly**. The accumulation of tunneling action at large time scales leads to a complete suppression of the tunneling DoS at small energies. Notice that the vanishing of the DoS at zero energy is a result of the weak accumulation of tunneling action, a phenomenon we may interpret as the long term maintenance of quantum coherence in the system.

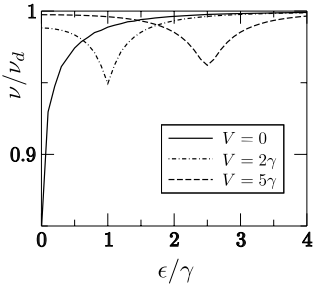

How will this picture change as we turn on a finite bias voltage to drive the system out of equilibrium? A glance at Eq. (11.94) shows that the voltage intervenes in two different ways: it splits the centre energy of the zero bias anomaly into two, $0 \to \pm V/2$. This reflects the shift in energy of the step distribution on the dot, relative to the Fermi distributions in the leads. Second, the voltage enhances the tunneling action. For example, at low energies, $\epsilon \ll V$, the action acquires a contribution $\propto (\gamma/C)\int_{t^{-1}}^{V} d\omega V/(\omega^2(\omega^2+\gamma^2)) \propto RV|t|$. This increases much more strongly, varying linearly in time, than the logarithmic increase we had in the equilibrium case. As a consequence, the coherent suppression of the DoS gets reduced and the zero bias anomaly peaks become less pronounced. In the figure above, the resulting profile for the DoS is shown for a few values of the bias voltage.

The discussion of this suppressive mechanism can be carried quite a bit further. For instance, the rounding of the zero bias anomaly peaks can be used as a means to define a **nonequilibrium dephasing rate**, or one may study the role of the voltage biasing in the complementary regime of low tunneling conductances $g \ll 1$ (where it turns out to be considerably less pronounced, cf. Problem 11.9.3). Here, however, we will not enter this more detailed discussion. Instead, and in view of the relatively technical character of this section, let us take a step back and summarize what we have found:

- ▷ The TDoS is a very "quantum mechanical observable." Its low energy profile is determined by long time matter wave coherence, as described by the appropriate Feynman path integral.
- ▷ Nonetheless, the TDoS is susceptible to classical fluctuations in the environment. The latter affect the classical action of the tunneling particle and, thus, the phase of the quantum mechanical propagator.
- ▷ In equilibrium and at zero temperature, these fluctuations (then, zero point fluctuations) do not prevent the build–up of long range coherence, a phenomenon that reflects, e.g., in

the build–up of the zero bias anomaly and a complete suppression of the TDoS. However, the installment of nonequilibrium conditions, even steady state nonequilibrium, goes along with increased noise levels, and this tends to suppress quantum coherence.

▷ Technically, the noise (Langevin noise η, in our above discussion) couples through a variable (voltage U_η) in a manner that encapsulates dynamical aspects of the system, and may involve system specific retardation effects. In the case study above, we did not introduce this coupling mechanism by postulation of an external bath. Rather, both the collective variable of interest (voltage), and the noise sources emerged out of one microscopically defined system. Such noise generation mechanisms are typical for interacting many particle systems that are projected onto the dynamics of a few collective variables.

11.7 Full counting statistics

Previously, we have seen that the statistics of currents may strongly affect the behavior of physical observables. It may also tell us about the internal structure of a system. For example, in the case study above, the noise level of currents (the Fano factor) signaled the presence of two tunneling barriers instead of just one. Statistical analysis of current fluctuations – both experimental and theoretical – has become a prominent tool of diagnostics to explore the microscopic nature of condensed matter systems through observable transport coefficients. The cumulative keyword for these types of analysis is **full counting statistics (FCS)**. In this section we introduce the notion of full counting statistics and apply it to elementary examples. A brief survey of more advanced applications is given in the end of the section.[25]

INFO The concept of full (photon) counting statistics was introduced in **quantum optics** (for a review, see e.g., L. Mandel and E. Wolf, *Optical Coherence and Quantum Optics* (Cambridge University Press, 1995).) Only much later have these ideas been transferred to the problem of transport in condensed matter (cf. L. S. Levitov and G. B. Lesovik, Charge distribution in quantum shot noise, *Pis ma Zh. Eksp. Teor. Fiz.* **58**, 225-30 (1993) [*JETP Lett.* **58**, 230-5 (1993)]). The ramifications of this concept are included in the brief review at the end of the section.

11.7.1 Generalities

Suppose we wish to characterize transport through a quantum system in terms of the charge transmitted in a time interval $[\bar{t}, \bar{t} + \Delta t]$,

$$\hat{N} \equiv \int_{\bar{t}}^{\bar{t}+\Delta t} dt\, \hat{I}(t), \tag{11.96}$$

[25] For more comprehensive reviews, see W. Belzig, *Full counting statistics in quantum contacts*, Proceedings of the Summer School/Conference on Functional Nanostructures, Karlsruhe, 2003; L.S. Levitov *The statistical theory of mesoscopic noise*, Quantum Noise in Mesoscopic Physics: Proceedings of the NATO Advanced Research Workshop, Delft, the Netherlands, 2002, and M. Kindermann and Yu. V. Nazarov, *Full counting statistics in electric circuits*, in: Quantum Noise in Mesoscopic Physics, ed. by Yu. V. Nazarov, Kluwer (Dordrecht), p.403 (2002).

where $\hat{I}$ is the operator measuring current flow through a section of the system. We may generate the expectation value of this operator by differentiation with respect to a suitably constructed source field. To this end, recall that the current density $\mathbf{j}(x)$, is obtained by differentiation of the action of the system with respect to its vector potential, $\mathbf{A}(x)$ (as usual $x \equiv (t, \mathbf{x})$ comprises space and time coordinates). Specifically, in the context of the Keldysh field theory

$$\mathbf{j}(x) = -i \frac{\delta}{\delta \mathbf{A}(x)}\Big|_{\mathbf{A}=0} \mathcal{Z}\left[\mathbf{A} \otimes \sigma_3/2\right],$$

where the notation $\mathcal{Z}[\mathbf{A} \otimes \sigma_3/2]$ indicates that the action is minimally coupled to a purely quantum vector potential (opposite signs on the two Keldysh contours). According to our general discussion of the Keldysh contour in Section 11.2.1, the coupling of $\mathbf{A}$ to σ_3 makes it a suitable source variable.[26] Building on this definition, we may introduce a **source variable for currents** by defining the vector potential,

$$\mathbf{A}(\mathbf{x}, t) = \chi(t)\mathbf{e}_\perp \int_S d^{d-1}x' \, \delta(\mathbf{x} - \mathbf{x}'), \tag{11.97}$$

where the surface integral confines the support of $\mathbf{A}$ to a planar section S of the system, $\mathbf{e}_\perp$ is normal to S (the generalization to curved sections is straightforward), and the definition of the **counting field**,

$$\chi(t) \equiv \chi \Theta(t - \bar{t})\Theta(\bar{t} + \Delta t - t),$$

implies a projection onto the counting time interval. Differentiation of $\mathcal{Z}[\mathbf{A} \otimes \sigma_3/2] \equiv \mathcal{Z}(\chi)$ with respect to the source parameter χ then generates the relation

$$-i \frac{\partial}{\partial \chi}\Big|_{\ =0} \mathcal{Z}(\chi) = \int_{\bar{t}}^{\bar{t}+\Delta t} \int_S dS \cdot \langle \mathbf{j}(\mathbf{x}, t) \rangle = \langle \hat{N} \rangle.$$

Further differentiation with respect to the source variable – and that is the prime advantage of the above construction – readily generates **moments of the current**:

$$\langle \hat{N}^n \rangle = (-i)^n \frac{\delta^n}{\delta \chi^n}\Big|_{\ =0} \mathcal{Z}(\chi). \tag{11.98}$$

This formula identifies $\mathcal{Z}(\chi)$ as the **moment generating function** and its logarithm

$$\ln g(\chi) \equiv \ln \mathcal{Z}(\chi),$$

as the **cumulant generating function**.

INFO Why would one want to know **moments higher than the second** of a current distribution? Suppose an experimentalist recorded the outcome of many runs of a charge transmission measurement. They might decide to communicate their results in a histogram "count number vs. events," i.e. data whose continuous idealization we interpret as a probability distribution. To a first approximation, the shape of this distribution is characterized by the first four cumulative moments, $\mu_{1,\ldots,4}$ (see Fig. 11.5):

[26] To be more accurate, in Section 11.2.1 we introduce a source on the upper Keldysh contour. The sign inverted source on the lower contour generates the same observable. Coupling to σ_3 adds the two contributions which are compensated for by the factor of 1/2 in the formula above.

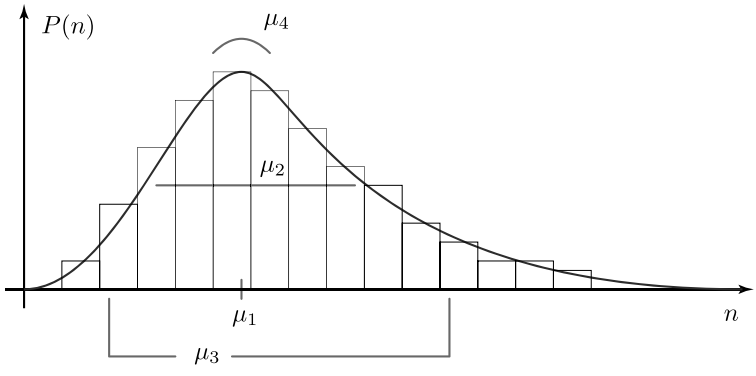

Figure 11.5 Hypothetical current distribution interpolating through an (equally hypothetical) discrete data set and its characterization in terms of mean, width, skewness, and kurtosis.

1. moment, μ_1: the **average**,
2. moment, μ_2: the **width**,
3. moment, μ_3: the **skewness** of the distribution,
4. moment, μ_4: the **kurtosis**. High kurtosis implies a sharply peaked distribution with fat tails. Low kurtosis indicates a mollified distribution, with broader shoulders.

The central limit theorem ensures that moments higher than the fourth are typically very small.

11.7.2 Realizations of current noise

In this section we introduce two frequently encountered realizations of noisy current distributions in a schematic manner. We then explore how these prototypical forms relate to the "real-life" example of our resistively shunted quantum dot.

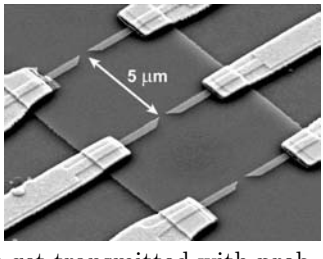

Quantum point contact: consider a "quantum point contact," i.e. an isolated scatterer embedded into a single-channel quantum conductor. This setup is not quite as academic as it may seem. By standard techniques of current device technology it is possible to manufacture few-channel quantum wires, and to introduce artificial imperfections or tunneling bridges (see the picture [courtesy of Nanocenter Basel] on the right for an example). Charge carriers which encounter the point contact get transmitted with probability T and reflected with probability $1-T$. This means that the probability to transmit n charges in N events is given by the **Bernoulli distribution**

$$p(n) = \left(\begin{array}{c} N \\ n \end{array} \right) T^n (1-T)^{N-n}.$$

The cumulant generating function of this distribution reads

$$g(\chi) \equiv \ln \sum_n e^{i\ \ n} p(n) = N \ln(1 + T(e^{i\ \ } - 1)).$$

A perfect single channel conductor has dimensionless conductance $g = e^2/h = 1/2\pi$ (in our usual units $e = \hbar = 1$). If the system is biased, $N = I\Delta t = V\Delta t/2\pi$ charges will be incoming, i.e. **the statistics of current in the quantum point contact** (at zero temperature[27]) is described by

$$\ln g(\chi) = \frac{V\Delta t}{2\pi} \ln(1 + T(e^{i\ \ } - 1)). \tag{11.99}$$

Ohmic resistor: in an Ohmic resistor the situation is different. Incidents of charge transmission are still uncorrelated, but we may not think of them as the result of a single scattering event. This suggests a description of charge transfer in terms of a Poisson distribution (cf. discussion on p.n 605),

$$p(n) = e^{-\nu} \frac{\nu^n}{n!} \longrightarrow \ln g(\chi) = \nu \left(e^{i\ \ } - 1\right). \tag{11.100}$$

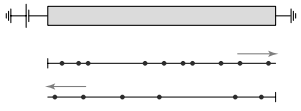

Bidirectional distribution: The current through a conductor connected to two terminals (for the generalization to multi–terminal geometries, see[25]) is generally obtained by additive superposition of two counter–propagating current flows (see figure). For simplicity, let us assume the two distributions $p_i(n_i)$, $i = 1, 2$ of counter-propagating charges to be statistically independent. The distribution $p(n)$ of the total number of transmitted charges, $n = n_1 - n_2$ can then be computed as follows:

$$\begin{aligned} p(n) &= \sum_{n_1 n_2} \delta_{n,n_1-n_2} p_1(n_1) p_2(n_2) \\ &= \sum_{n_1 n_2} \int \frac{d\chi}{2\pi} e^{-i\ \ (n-n_1+n_2)} \int \frac{d\chi_1}{2\pi} e^{-i\ \ _1 n_1} g(\chi_1) \int \frac{d\chi_2}{2\pi} e^{-i\ \ _2 n_2} g_2(\chi_2) \\ &= \int \frac{d\chi}{2\pi} e^{-i\ \ n} g_1(\chi) g_2(-\chi). \end{aligned}$$

This means that the generating function of the transmitted charge is the product $g(\chi) \equiv g_1(\chi) g_2(-\chi)$ of the partial distributions.

For example, in the case where the two constituent distributions are Poissonian, we find

$$\ln g(\chi) = \nu_1 \left(e^{i\ \ } - 1\right) + \nu_2 \left(e^{-i\ \ } - 1\right), \tag{11.101}$$

where ν_1 and ν_2 determine the average rates. These rates will typically be set by the applied voltage bias, barrier transparencies, temperature, and the like. In the following, we return to the biased quantum dot studied in previous sections and explore the relevance of the general structures discussed above to this physical example.

[27] For the generalization to finite temperatures, cf. Refs.[25].

11.7.3 Full counting statistics of the double barrier quantum dot

Let us now return to consider the quantum dot system introduced in Section 11.6.1. Our goal is to better understand the statistics of current flow. To this end, we will monitor the current through, say, the tunnel barriers connecting the dot to the left lead. The first thing we need is an appropriate counting field. Phenomenologically, we may argue that, in the presence of a vector potential $A\mathbf{e}_\perp$ normal to the lead axis, the tunneling matrix elements $T_{L,a\mu}$ utilized in Section 11.6.1 will generalize to $T_{L,a\mu} \to T_{L,a\mu}\exp(i\int dxA)$, where the integral runs over the transverse extension of the barrier. The definition Eq. (11.97) then means that the counting field couples to the tunneling matrix element on the Keldysh contour as

$$T_{L,a\mu} \to T_{L,a\mu}\exp(i\chi(t)\sigma_1/2).$$

Notice that, as with the quantum component of the interaction field, the counting field couples to the tunneling matrix element. This observation is sufficient to determine the coupling of the counting field to the effective action without much further calculation. For the sake of a more symmetric notation, let us define generalized matrix elements $T_{x,a\mu}\exp(i\chi_x(t)\sigma_1/2)$, $x = L, R$. (Later we will set $\chi_L \equiv \chi$, $\chi_R \equiv 0$.) The tunneling action Eq. (11.75) then assumes the form

$$S_{\rm tun}[\chi] = -\frac{i}{4}\sum_{x=L,R} g_x {\rm tr}\left(\Lambda_x(\chi_x)e^{-i\hat{\phi}}\Lambda_d e^{i\hat{\phi}}\right), \qquad \Lambda_x(\chi_x) \equiv e^{i\frac{\chi}{2}\sigma_1}\Lambda_x e^{-i\frac{\chi}{2}\sigma_1},$$

where we have generalized to barriers of different tunnel conductance, g_x. Following the logic of Section 11.6.2, our next step will be to determine the matrix Λ_d. As before, we do this by requiring stationarity under variations of ϕ. (Exercise: think why this condition is equivalent to the condition of zero stationary current flow onto/off the dot.) Variation of the action in the limit of vanishingly weak interaction, $\phi \simeq 0$, generates the condition

$$\left[\Lambda_d, \sum_x g_x\Lambda_x(\chi_x)\right] \stackrel{!}{=} 0. \tag{11.102}$$

Now, the transformations $\Lambda \to \exp(i\chi\sigma_1/2)\Lambda\exp(-i\chi\sigma_1/2)$ render the matrices $\Lambda_x(\chi_x)$ non-triangular. This means that stationary configurations Λ_d will in general no longer be of the form Eq. (11.76). However, the transformation by the counting field does not alter the "normalization condition," $\Lambda^2 = \sigma_0$ remains valid. It is straightforward to verify that the solution of Eq. (11.102) obeying this normalization is given by[28]

$$\Lambda_d = \frac{g_L\Lambda_L(\chi_L) + g_R\Lambda_R(\chi_R)}{\left(g_L^2 + g_R^2 + g_Lg_R[\Lambda_L(\chi_L), \Lambda_R(\chi_R)]_+\right)^{1/2}}.$$

(Notice that the matrix in the denominator commutes with the numerator, i.e. the relative ordering of numerator and denominator is not an issue. Also notice that in the limit $\chi = 0$,

[28] In computing this result, we approximate the diagonal elements of the matrices Λ in Eq. (11.76) by their imaginary parts, ± 1. Diligent readers may wish to trace the fate of the real parts and check that they regularize the superficially divergent constant C in Eq. (11.103) below.

the solution reduces to that discussed in Section 11.6.2.) Substitution of this configuration into the action leads to

$$S_{\rm tun}[\chi] = -\frac{i}{4}\,{\rm tr}\left(g_L^2 + g_R^2 + g_L g_R[\Lambda_L(\chi_L), \Lambda_R(\chi_R)]_+\right)^{1/2}.$$

Assuming that the inverse of the counting time window $(\Delta t)^{-1}$ is large in comparison to the energy scales relevant to the distribution functions, we will evaluate the trace over energy/time indices within the leading order Wigner approximation (cf. Section 11.5.1), ${\rm tr}(\dots) \to \int \frac{d\epsilon dt}{2\pi}(\dots)$, $F(\hat\epsilon) \to F(\epsilon)$, $\chi(\hat t) \to \chi(t)$, where $F(\epsilon)$ and $\chi(t)$ are ordinary functions of energy and time, respectively. As a result of a straightforward (if somewhat tedious) calculation, one finds that the matrix $[\Lambda_L(\chi_L), \Lambda_R(\chi_R)]$ is proportional to the unit matrix, and that the trace evaluates to

$$\begin{aligned} S_{\rm tun}[\chi] &= -\frac{i}{2}\int \frac{dtd\epsilon}{2\pi} \qquad (11.103)\\ &\times \left((g_L+g_R)^2 + 4g_Lg_R\left((e^{i(\ \ L-\ \ R)}-1)n_L(1-n_R) + (e^{i(\ \ R-\ \ L)}-1)n_R(1-n_L)\right)\right)^{\frac12}\\ &= -\frac{i\Delta t}{2}\int\frac{d\epsilon}{2\pi}\left((g_L+g_R)^2 + 4g_Lg_R\left((e^{i\ \ }-1)n_L(1-n_R) + (e^{-i\ \ }-1)n_R(1-n_L)\right)\right)^{\frac12} + C, \end{aligned}$$

where in the last equality we used $\chi_L(t) = \chi(t) = \chi\Theta(t-\bar t)\Theta(\bar t + \Delta t - t)$, and C is a constant. From this result we find the cumulant generating function $\ln g(\chi) \simeq \ln\exp(iS[\chi])$

$$\ln g(\chi) = \frac{\Delta t}{2}\int\frac{d\epsilon}{2\pi}\left((g_L+g_R)^2 + 4g_Lg_R\left((e^{i\ \ }-1)n_L(1-n_R) + (e^{-i\ \ }-1)n_R(1-n_L)\right)\right)^{\frac12}. \qquad (11.104)$$

Now, let us try to make sense of this expression. Comparison with Eq. (11.101) shows that $\ln g$ contains the generating functions of two Poisson distributions as building blocks. To explore the meaning of this result, let us first consider the limit of zero temperature and voltage bias V, $n_{L/R}(\epsilon) = \Theta((+/-)\frac{V}{2} - \epsilon)$. The generating function then reduces to

$$\ln g(\chi) = \frac{\Delta t V}{4\pi}\left((g_L+g_R)^2 + 4g_Lg_R\left((e^{i\ \ }-1)\right)\right)^{\frac12} + {\rm C}.$$

According to Eq. (11.98), the **first moment** of the transmitted charge through the system is given by

$$\langle\hat N\rangle = -i\partial_{\ \ =0}\ln g(\chi) = \frac{\Delta t V}{2\pi}\frac{g_Lg_R}{g_L+g_R}.$$

Comparison with the definition of the conductance, $G = \langle\hat I\rangle/V = \langle\hat N\rangle/V\Delta t$ gives $G = \frac{1}{2\pi}\frac{g_Lg_R}{(g_L+g_R)}$, which we recognize as the mean conductance of two tunnel conductances shunted in series (in units of the conductance quantum $e^2/h = 1/2\pi$.) Turning to **current statistics**, let us consider the limit $g_L \ll g_R$. We may then expand the square root to first order in the ratio g_L/g_R to obtain a bi-directional Poisson distribution Eq. (11.101), with (time–integrated) characteristic rates identified as

$$\nu_1 = \Delta t g_L\int\frac{d\epsilon}{2\pi}\,n_L(1-n_R), \qquad \nu_2 = \Delta t g_L\int\frac{d\epsilon}{2\pi}\,n_R(1-n_L).$$

These coefficients may be interpreted as the integrated rate at which filled states in the right lead scatter into empty states in the right lead, and vice versa. As one may expect, the statistics of the current is dominantly caused by the "bottleneck" in the system, i.e. the conductance of the weaker tunnel barrier, g_L. At finite temperature, $\nu_1 \simeq \Delta t g_L V/2\pi$, while $\nu_2 \simeq \exp(-V/T)\Delta t T/2\pi$ shows that thermal activation is necessary to push charges against the voltage gradient.

The second (cumulative) moment defines the **noise power** (cf. Eq. (11.91)),

$$S_0 = \frac{2}{\Delta t}\mathrm{var}\,(\hat{N}) = -\frac{2}{\Delta t}\partial^2\big|_{\ =0} \ln g[\chi] = \frac{2}{\Delta t}(\nu_1+\nu_2) = 2\frac{g_L}{2\pi}V\coth(V/2T).$$

This shows how the noise interpolates between equilibrium noise, $\langle \delta I(t)\delta I(t')\rangle \overset{V\to 0}{\sim} g_L T$ and the shot noise limit $\langle \delta I(t)\delta I(t')\rangle \overset{V\gg T}{\sim} g_L|V|$. In the more general case of barriers of comparable transparency, $g_L \simeq g_R$, the current statistics is more complicated and described by the full expression Eq. (11.104).

In principle, we might now include phase fluctuations to explore the interesting question as to how interaction effects will influence FCS. However, this topic[29] lies beyond the scope of the present text. Instead, let us conclude by briefly discussing a few more general aspects of full counting statistics.

11.7.4 General ramifications of FCS

Previously, we have introduced the concept of a counting field as a purely technical means to extract moments of observables from a Keldysh partition function. From a theoretical point of view, this has been an efficient procedure, but it is also somewhat naive: when we speak about moments of quantum observables, we inevitably enter the difficult territory of quantum measurement. First, we have to realize that, when talking about moments, what stands in the background is a repeated quantum measurement of observables. Second, in experiment, it is not the (fermion) current that is measured directly. Typically, it is fluctuations of secondary degrees of freedom, e.g. the bosonic modes of electromagnetic degrees of freedom coupling to the current that are detected. One thus needs to explore the connection between the original degrees of freedom (fermion current) and the **detector degrees of freedom**. These (deep) issues have been explored in the literature[25] and we here restrict ourselves to a very superficial discussion of some main ideas.

An elegant (if not particularly realistic) way to model the coupling to a detector degree of freedom is by coupling the fermion degrees of freedom to a spin. The precession of the **spin detector** then encapsulates information on the transmitted fermion charge. Curiously, this procedure exactly amounts to what we have been doing in introducing our Keldysh counting field, and this connection is worked out in the following

EXERCISE We here wish to explore in what sense our counting field, χ, effectively models a spin detector variable (cf. the review by Levitov[25] for an extended discussion). Consider a spin

[29] cf. D. A. Bagrets and Y. V. Nazarov, Full counting statistics of charge transfer in Coulomb blockade system, *Phys. Rev. B* **67**, 085316-32 (2003).

1/2 placed near our current carrying device and coupled to the latter through the Hamiltonian $\hat{H}_c = \int d^d r \mathbf{A} \cdot \mathbf{j} \sigma_z$, where $\mathbf{j}$ denotes the fermion current density operator, $\mathbf{A}$ is a vector potential mediating the coupling to the spin, and we assume that only the z-component of the latter is coupled. Now, let us assume that the spin has been prepared in some initial state, so that the measurement of the operator $\sigma_+ = (\sigma_x + i\sigma_y)/2$ would lead to the expectation value $\langle \sigma_+(0) \rangle_{\rm spin}$. The coupling to the fermion system makes the transverse spin components, probed by this expectation value precess. This precession is described by taking the expectation value at a later time, $\langle \sigma_+(t) \rangle_{\rm spin}$. Show that the coupling to the fermion system above implies

$$\langle \sigma_+(t) \rangle_{\rm spin} = \left\langle e^{i\hat{H}(+\mathbf{A})t} e^{-i\hat{H}(-\mathbf{A})t} \right\rangle_{\rm fermion} \langle \sigma_+(0) \rangle_{\rm spin},$$

where $\hat{H}(\mathbf{A})$ is the fermion Hamiltonian operator minimally coupled to the vector potential, $\mathbf{A}$. Express the fermion expectation value by a Keldysh partition function. The sign change in $\mathbf{A}$ relative to the contours then means that we have coupled the fermion system to a purely quantum vector potential, as we did in Section 11.7.1. Assuming that the spin-fermion coupling is local, i.e. that the vector potential is non-vanishing only in the immediate vicinity of a transverse section through the conductor, we arrive at a functional integral formally equivalent to the integral $\mathcal{Z}[\chi]$ employed above.

The assumption of a spin detector is artificial in two respects. First, currents are not normally measured by spins. Second the coupling of our system of interest to a detector will in general imply a "**back action**" of the latter on the former, and this will affect the current statistics. These aspects are discussed in the review by Kindermann and Nazarov cited above.[25] The authors argue that measurements on a (mesoscopic) device typically imply the embedding of the latter into a detector electromagnetic environment.

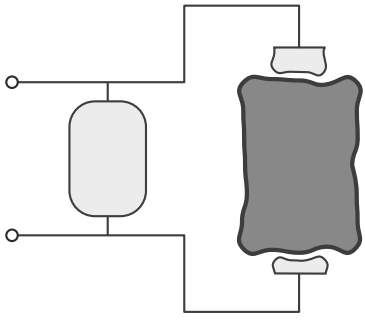

With reasonable generality, the detector environment may be modelled as a linear electromagnetic circuit (see figure), i.e. a system whose relevant degrees of freedom (currents, voltages, etc.) are controlled by some effective oscillator dynamics (cf. an LRC-circuit). The variables of the detector environment are linearly coupled to those of the mesoscopic device. (For example, the charge density on the latter may feel the potential fluctuations of the detector, etc.) One may then formulate an FCS functional for the composite system. Owing to their linearity, the degrees of freedom of the detector environment may be integrated out, and this leaves an effective functional in which the counting field and the primary variables of the mesoscopic device are coupled in a manner that will typically involve retardation effects. In this way, one has effectively described both a reasonably realistic readout procedure and, relatedly, the back action of the measurement device onto the microscopic system of interest. For further discussion of these issues we refer to the original literature.

11.8 Summary and outlook

In this final chapter of the book, we have introduced the Keldysh field theory as a modern – in spite of its formulation in the mid–60s – tool to describe quantum nonequilibrium phenomena. It must be conceded that the Keldysh formalism comes with a relatively steep learning curve. However, once one gets used to the concept of two counter propagating time contours, one realizes that Keldysh field theory provides an enormously powerful and, indeed, intuitive framework to approach quantum nonequilibrium phenomena. Practically all other theoretical nonequilibrium tools (at least those familiar to the authors of this text) can be recovered as restrictions of the Keldysh approach. Specifically, we have discussed the derivation of quantum master and quantum kinetic equations, the connection to equilibrium field theory, the classical limit (which neatly connects to the MSRJD formalism central to the previous chapter), nonequilibrium variants of diagrammatic perturbation theory, and various other aspects. However, notwithstanding its indisputable power, one should not get carried away and declare the Keldysh formalism the new master tool, superior to the equilibrium concepts discussed in earlier chapters of the book. The flexibility of Keldysh theory may come as a burden when one is actually carrying more information about a problem than that which is called for. In situations where one is at equilibrium, or close to it, there is no need to explicitly keep track of the (then known) distribution function, and the Matsubara formulation may be the more efficient option. However, at the time of writing of this book, quantum nonequilibrium problems are becoming more and more important, and this makes Keldysh theory an important concept in contemporary physics. At any rate, the best way for readers to proceed from here is to pick a nonequilibrium problem and conduct their own research!

11.9 Problems

11.9.1 Atom-field Hamiltonian

The "atom-field-Hamiltonian" is a simple model Hamiltonian of quantum optics. It reduces the interaction of atoms with electromagnetic field modes to a basic model of a two-level system ("the atom") coupled to an assembly of oscillator modes. The simplistic nature of this reduction notwithstanding, the atom-field Hamiltonian describes ample phenomenology, and it is a prominent model system of quantum optics. In this problem, we study the simplest variant of the system, the exactly solvable limit of the interaction with a single mode. The single mode limit describes fully coherent quantum phenomenology. We use it as a benchmark system to compare against the "incoherent" approximations underlying the quantum master equation of Section 11.1. In the follow up Problem 11.9.2 we then explore what happens upon generalization to multi-mode coupling.

Consider an atom exposed to electromagnetic radiation. Assuming that the field modes predominantly couple two atomic states $|a\rangle$ and $|b\rangle$ (see figure), and forgetting about the complications introduced by the polarization of the electromagnetic field, this setup may be described by the simple model Hamiltonian,

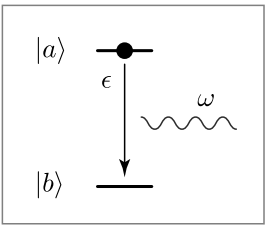

$$\hat{H} = \frac{\epsilon}{2}\sigma_3 + \sum_k \omega_k a_k^\dagger a_k + \sum_k \left(g_k \sigma_+ a_k + \bar{g}_k \sigma_- a_k^\dagger \right), \qquad (11.105)$$

where ϵ is the energy difference between the excited state, $|a\rangle$, and the lower state, $|b\rangle$, the Pauli matrices σ_i act in the two-dimensional Hilbert space defined by these states, and $\sigma_\pm = (\sigma_1 \pm i\sigma_2)/2$, as usual. This **atom-field Hamiltonian** describes excitation processes $|b\rangle \to |a\rangle$ by field quantum absorption (at coupling constants g_k), and the corresponding relaxation processes by quantum emission.

We may simplify the problem further by assuming that only a single mode of the electromagnetic field satisfies the resonance condition $\omega \simeq \epsilon$, that needs to be met to obtain significant conversion efficiency. This, then, leads to the **single mode Hamiltonian**

$$\hat{H} = \frac{\epsilon}{2}\sigma_3 + \omega a^\dagger a + g\left(\sigma_+ a + \sigma_- a^\dagger\right), \qquad (11.106)$$

where we have omitted the mode index "k" and gauged the coupling constant g so as to become real.

(a) Considering the atom as our "system," and the mode as a "bath," adapt the formalism introduced in Section 11.1 to derive an effective equation of motion for the reduced system density matrix, $\hat{\rho}_s$. In doing so, try to be critical concerning the approximate elements of the construction, notably the Markovian approximation. (Hint: you will be met with a singular effective coupling constant $\sim \delta(\epsilon - \omega)$. For the moment, do not worry about the regularization of this expression and treat it as a formal object.) Derive a closed expression for the diagonal elements of the reduced density operator $\rho_x \equiv \langle x|\hat{\rho}_s|x\rangle$, $x = a, b$ and verify that the stationary limit $\rho_{x,\infty} \equiv \rho_x(t \to \infty)$ obeys a **detailed balance** relation

$$\frac{\rho_{a,\infty}}{\rho_{b,\infty}} = \frac{\langle n \rangle}{\langle n+1 \rangle}, \qquad (11.107)$$

where n is the number of mode quanta and the expectation value is over the thermal distribution of the bath. Accordingly, the **population imbalance** between the levels approaches the limit

$$\Delta\rho \equiv \rho_{a,\infty} - \rho_{b,\infty} = -\frac{1}{2\langle n \rangle + 1}. \qquad (11.108)$$

Discuss the meaning of this expression. Is it really appropriate for the situation at hand? If not, where do you think the approximation involved in its derivation failed?

(b) Now, let us compare the predictions of the Markovian approximation to reality. To this end, solve the Schrödinger equation for the Hamiltonian above. (Hint: use the fact that the Hamiltonian couples only very few of the states $|x, n\rangle \equiv |x\rangle \otimes |n\rangle$, $x = a, b$, where $|n\rangle$ is an occupation eigenstate of the mode system. You will encounter a time dependent

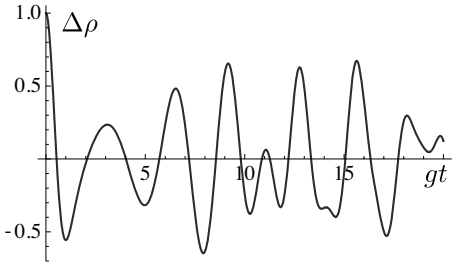

Figure 11.6 Imbalance between the population of the two atomic states as a function of dimensionless time gt. Notice the aperiodic changes in the population of the states and the absence of relaxation towards a ground state configuration $\Delta\rho = -1$.

Schrödinger equation that may be solved either by Fourier transform, or by educated guessing.) Interpreting $\rho_x \equiv \sum_n \langle x, n|x, n\rangle$ as the probability to find the system in state $|x\rangle$, compute the population imbalance and compare to the predictions of the Markovian approach Eq. (11.108). If you have access to a computer, you may find it instructive to plot the result for the time dependent imbalance for different values of temperature (presuming the mode distribution to be thermal), and frequency mismatch $\Delta = \epsilon - \omega$ as a function of the dimensionless time parameter gt. You will obtain patterns such as the one shown in Fig. 11.6.

(c) Discuss in qualitative terms the origin of the discrepancies between the two approaches. Why is the Markovian approximation not appropriate under the present circumstances, and why does the exact solution not predict relaxation of an initially occupied state $|a\rangle$ to the ground state, even at zero temperature.

Answer:

(a) In the interaction representation, $a(t) = e^{-i\omega t}a$, $\sigma_\pm(t) = e^{\pm i\epsilon t}\sigma_\pm$, the interaction Hamiltonian $\hat{H}_i \equiv g\left(\sigma_+ a + \sigma_- a^\dagger\right)$ reads

$$\hat{H}_i(t) = g\left(e^{i\Delta t}\sigma_+ a + e^{-i\Delta t}\sigma_- a^\dagger\right),$$

where we defined the **energy mismatch** $\Delta \equiv \epsilon - \omega$ between level splitting and mode frequency. Defining $\hat{L}_i = -i[\hat{H}_i, \ ]$, it is then straightforward to verify that Eq. (11.4) assumes the form

$$\partial_t \hat{\rho}_s = -g^2 \int^t dt'\, e^{+i\Delta t'} \left(+\langle n+1\rangle[\sigma_+, \sigma_-\hat{\rho}_s(t-t')] - \langle n\rangle[\sigma_+, \hat{\rho}_s(t-t')\sigma_-]\right)$$
$$- g^2 \int^t dt'\, e^{-i\Delta t'} \left(-\langle n+1\rangle[\sigma_-, \hat{\rho}_s(t-t')\sigma_+] + \langle n\rangle[\sigma_-, \sigma_+\hat{\rho}_s(t-t')]\right), \quad (11.109)$$

where the expectation value is over the mode distribution. Assume that at some initial time $t = 0$, the density operator had diagonal form,

$$\hat{\rho}_s = \rho_a P_+ + \rho_b P_-,$$

where $P_\pm$ are projectors onto the upper (a) or lower (b) state, and $\rho_{a,b}$, $\rho_a + \rho_b = 1$ are the probabilities of occupation of these states. It is straightforward to check that the evolution equation preserves the diagonal form. Adopting a Markovian approximation (but is it appropriate?) wherein the time dependence of $\hat{\rho}(s)$ under the integral above is considered negligible, the evolution equation for the coefficients $\rho_{a,b}$ takes the form of a **master equation**

$$\begin{aligned} \partial_t \rho_a &= \Gamma \left(\langle n \rangle \rho_b - \langle n+1 \rangle \rho_a \right), \\ \partial_t \rho_b &= \Gamma \left(\langle n+1 \rangle \rho_a - \langle n \rangle \rho_b \right), \end{aligned} \tag{11.110}$$

where the rate $\Gamma = 2\pi g \delta(\Delta)$ is singular at resonance. This equation predicts an (irreversible) approach to a stationary limit satisfying the detailed balance relation Eq. (11.107).

(b) It is evident that for any fixed $n \geq 0$ the Hamiltonian acts in the two-dimensional space spanned by the states $|a, n\rangle$ and $|b, n+1\rangle$. Specifically, $\hat{H}_i(t)|a, n\rangle = g e^{-i\Delta t}(n+1)^{1/2}|b, n+1\rangle$ and $\hat{H}_i(t)|b, n+1\rangle = g e^{+i\Delta t}(n+1)^{1/2}|a, n\rangle$. Introducing wavefunctions by $|\psi(t)\rangle = \psi_{a,n}(t)|a, n\rangle + \psi_{b,n+1}(t)|b, n+1\rangle$, the time dependent Schrödinger equation $i\partial_t \psi = \hat{H}_i(t)\psi$ assumes the form

$$\begin{aligned} i\partial_t \psi_{a,n} &= g e^{+i\Delta t}(n+1)^{1/2}\, \psi_{b,n+1}, \\ i\partial_t \psi_{b,n+1} &= g e^{-i\Delta t}(n+1)^{1/2}\, \psi_{a,n}. \end{aligned} \tag{11.111}$$

These equations are solved by (devise your own solution strategy, there are several)

$$\psi_{a,n}(t) = e^{+i\frac{\Delta}{2}t}\left(\psi_{a,n}(0)\cos(\Omega_n t) - i\frac{g(n+1)^{1/2}\psi_{b,n+1}(0) + \frac{\Delta}{2}\psi_{a,n}(0)}{\Omega_n}\sin(\Omega t) \right)$$

$$\psi_{b,n+1}(t) = e^{-i\frac{\Delta}{2}t}\left(\psi_{b,n+1}(0)\cos(\Omega_n t) - i\frac{g(n+1)^{1/2}\psi_{a,n}(0) - \frac{\Delta}{2}\psi_{b,n+1}(0)}{\Omega_n}\sin(\Omega t) \right),$$

where we introduced the abbreviation

$$\Omega_n \equiv \left(g^2(n+1) + \left(\frac{\Delta}{2}\right)^2 \right)^{1/2}.$$

Assuming for simplicity that the atom was initially in its excited state, we have $\psi_{b,n+1} = 0$ and $\psi_{a,n} = \sqrt{\rho_n}$, where ρ_n is the nth eigenvalue of the mode density operator (e.g., $\rho_n = \mathcal{Z}^{-1}\exp(-\beta\omega(n+1/2))$ if the mode distribution is thermal). The exact result for the population imbalance then reads

$$\Delta\rho = \sum_n \left(|\psi_{a,n}|^2 - |\psi_{b,n}|^2 \right) = \sum_n \rho_n \left(1 - \frac{2g^2(n+1)}{\Omega_n^2}\sin^2(\Omega_n t) \right).$$

This result is very different from the one obtained within the Markovian approach, Eq. (11.108): no stationary limit is approached. A short period of decay of the initial value $\Delta\rho(0) = 1$ merges into a pattern of irregular fluctuations – a result of a superposition of contributions of incommensurate frequencies (see Fig. 11.6). In quantum optics, the phenomenon of transient near-recoveries of the initial value is known as

collapse and revival while the fluctuations afford an interpretation as **Rabi oscillations**. Clearly, the oscillatory pattern is a result of maintained quantum coherence and reversibility of the dynamics, we do not observe a systematic decay of the upper state into the lower. Notice in particular that even at zero temperature the atom does not relax by emission of field quanta: at $T = 0$ only the $n = 0$ term (zero field quanta) contributes to the sum above. This leads to oscillatory behavior of the density operator in which the initial state is recovered at regular intervals $t \sim g$, but no relaxation. For further discussion of the fluctuation pattern we refer to Scully and Zubairy.[30] Here, our main conclusion is that the prediction of irreversible dynamics derived in (a) is evidently incorrect.

(c) The Markovian approximation fails because a single quantum oscillator mode does not behave as a bath. Indeed, the mode–atom coupling is strongest at resonance, $\Delta = 0$, when "system" and "bath" fluctuate at comparable time scales. Technically this means that the (Markovian) assumption of constancy of the time evolution operator under the integral Eq. (11.109) is not justified. The Markov approximation requires a short lived bath "memory," in the sense that bath correlation functions decay to zero at time scales much shorter than those at which the system density operator varies. This happens, e.g., if we couple to many modes instead of one (see the follow–up problem.) In this case, the analog of Eq. (11.108) contains many uncorrelated contributions, and the dynamics becomes effectively irreversible.[31]

11.9.2 Atom-field Hamiltonian II: Weisskopf–Wigner theory of spontaneous emission

(Attack this problem after 11.9.1.) In the previous problem, we saw that the coupling of an atom to a single electromagnetic mode does not lead to radiative relaxation. The relaxation processes ubiquitous in the physics of atomic radiation must, then, be a consequence of the presence of many field modes. In this problem, we study how the large phase space of the multi–mode system justifies an approximation that renders the dynamics of the atom-field system effectively irreversible and does describe relaxation by radiation. The theory derived here plays an important role as a building block of, e.g., laser theory.

(a) Consider the Hamiltonian Eq. (11.105) of a two-level atom coupled to a multi-mode field. Assuming zero temperature, derive the generalization of the Schrödinger equation (11.111) for the initial configuration $|a\rangle \otimes |0\rangle$ to the multi-mode case ($|0\rangle$ is the zero temperature photon vacuum). By formal integration of the second equation, convert the system to a single integro-differential equation. Assuming that $|g_k|^2 = g^2(\omega_k)$ depends only on the mode energy and that both the density of states of the bath modes and $g^2(\omega)$ change only negligibly over the inverse of the time scales at which the wave functions of

[30] M.O. Scully and M.S. Zubairy, *Quantum Optics*, (Cambridge University Press, 1997).

[31] Even then, it is not impossible that a rare accumulation of coherent contributions leads to an accidental population "revival" – after all, we are still dealing with unitary (reversible) dynamics. However, for sufficiently large numbers of contributing modes, such events are infinitely improbable, and an effectively irreversible approximation is justified.

the problem vary – the **Weisskopf–Wigner approximation** – derive an approximate solution of this equation.

(b) For arbitrary temperature and initial population, attack the multi-mode problem by generalization of the projector formalism applied in Problem 11.9.1 (a) to the single mode case and compare to the results of the Weisskopf–Wigner theory. Convince yourself that the approximation used there is equivalent to a Markovian approximation.

Answer:

(a) The initial state relevant to the description of an excited atom immersed into a zero temperature bath reads $|a\rangle \otimes |0\rangle$, where $|0\rangle$ is the vacuum of the bath system. The Hamiltonian couples this configuration to the states $|b\rangle \otimes a_k^\dagger |0\rangle$. Introducing a wave function by $\psi \equiv \psi_0 |a\rangle \otimes |0\rangle + \sum_k \psi_k |b\rangle \otimes a_k^\dagger |0\rangle$, the multi-mode generalization of the Schrödinger equation (11.111) reads

$$i\partial_t \psi_0 = \sum_k g_k e^{i\Delta_k t} \psi_k,$$
$$i\partial_t \psi_k = g_k e^{-i\Delta_k t} \psi_0,$$

where $\Delta_k = \epsilon - \omega_k$. We integrate the second equation and substitute the result into the first equation to arrive at

$$\partial_t \psi_0(t) = -\sum_k g_k^2 \int_0^t dt'\, e^{i\Delta_k (t-t')} \psi_0(t').$$

Introducing the **density of bath modes** $\rho(\omega) = \sum_k \delta(\omega - \omega_k)$, we obtain

$$\partial_t \psi_0(t) = -\int d\omega\, \rho(\omega) g(\omega) \int_0^t dt'\, e^{i(\epsilon-\omega)(t-t')} \psi_0(t') \simeq -2\pi\rho g^2 \psi_0(t),$$

where in the crucial second step we assumed approximate constancy of both $\rho(\omega) \simeq \rho$ and $g(\omega) \simeq g$ to evaluate the frequency integral as $\int d\omega\, e^{-i\omega(t-t')} = 2\pi\delta(t-t')$. The (irreversible) effective equation for ψ_0 is now trivially solved as[32]

$$\psi_0(t) = e^{-\pi\rho g^2 t}.$$

This means that the population imbalance between the two atomic levels

$$\Delta\rho \equiv |\psi_0|^2 - \sum_k |\psi_k|^2 = -1 + 2e^{-\Gamma t},$$

shows relaxation at the **golden rule decay rate**

$$\Gamma \equiv 2\pi\rho g^2. \tag{11.112}$$

[32] We count $\int_0^t dt' \delta(t-t') = 1/2$ since the δ-function lies at the boundaries of the integration domain.

(b) Comparing to the discussion in the previous problem, we verify that the multi-mode generalization of Eq. (11.109) reads

$$\begin{aligned}\partial_t \hat{\rho}_s = &- \int d\omega\, \rho(\omega) g^2(\omega) \int^t dt' \\ &\times \big[e^{+i(\epsilon-\omega)t'} \left(+\langle n(\omega)+1\rangle [\sigma_+, \sigma_- \hat{\rho}_s(t-t')] - \langle n(\omega)\rangle [\sigma_+, \hat{\rho}_s(t-t')\sigma_-] \right) \\ &\quad - e^{-i(\epsilon-\omega)t'} \left(-\langle n(\omega)+1\rangle [\sigma_-, \hat{\rho}_s(t-t')\sigma_+] + \langle n(\omega)\rangle [\sigma_-, \sigma_+ \hat{\rho}_s(t-t')] \right) \big],\end{aligned}$$

where $n(\omega)$ is the boson distribution function. However, unlike in the previous problem, we now have justification to assume near constancy of the density operator over the time scales at which the addition of uncorrelated bath contributions decays to zero. (Think why this is equivalent to the Weisskopf–Wigner assumption of frequency independent ρg^2.) Doing the integral, we obtain the master equation (11.110), where $\langle n\rangle = \langle n(\epsilon)\rangle$ is the mean number of bath quanta at the resonance energy and the decay rate is given by Eq. (11.112). Solution of this equation obtains the population imbalance

$$\Delta\rho(t) = \left(\Delta\rho(0) + \frac{1}{2\langle n\rangle + 1} \right) e^{-\Gamma(2n+1)t} - \frac{1}{2\langle n\rangle + 1}.$$

In the particular case of initial occupancy of $|a\rangle$, $\Delta\rho(0) = 1$ and zero temperature, $\langle n(\epsilon)\rangle = 0$, this reduces to the results obtained in (a).

Summarizing our results, we have found that in the multi-mode case the dynamics of the system becomes effectively irreversible. Technically, "multi-mode" means that we must be able to assume near constancy of the spectral density of bath modes over scales $\sim \Gamma$, i.e. the rate at which the density operator changes. Under this condition, the Markovian approximation (equivalent to the Weisskopf–Wigner approximation) becomes justified and the quantum master equation provides a convenient alternative to the direct solution of the Schrödinger equation.

11.9.3 Keldysh theory of the Coulomb blockade

(Recapitulate Section 11.6 before turning to this problem. If not stated otherwise, the notation of that section will be used throughout.) In this problem, we consider the out of equilibrium quantum dot discussed in Section 11.6 in a regime of near isolation from its environment ("leads"). Under these conditions, charge on the dot is quenched – the Coulomb blockade. We here discuss the dynamics of the formation of a Coulomb blockaded state, and its response to an external voltage bias.

In Problems 6.7 and 6.7 we considered an equilibrium quantum dot in a state of perfect or near isolation from its environment. At low temperatures, the dot admits only the integer quantum of charges that minimizes its capacitive energy. This Coulomb blockade manifests itself in the partition function of the isolated quantum dot,

$$\mathcal{Z} = \sum_n e^{-\frac{E_c}{T}(n-N_0)^2}, \tag{11.113}$$

where the optimal number of charges is determined by the parameter $N_0 \in \mathbb{R}$ (which may be set by changing external gate voltages) and E_c is the charging energy.

At first sight, it may appear strange that the Keldysh-description of even this simplest signature of the Coulomb blockade is far from trivial! To understand why this is so, recall that the dynamics on the Keldysh contour builds on the thermal distribution of a non-interacting theory, while the partition sum above describes the thermal state of an interacting system. We thus need to describe the passage between a non-interacting and an interacting equilibrium state. Naively, one might hope that the interpolation between the two states occurs as interactions are gradually switched on in the dynamical evolution along the Keldysh contour. But this is not so. The switching on of interactions results in an increase in energy of the N-particle sector of Fock space, however, the *distribution functions* controlling the occupation of single particle states are left un-altered (think about this point.) We need to include a mechanism of relaxation-by-interaction to effect the formation of a thermal state similar to that described by Eq. (11.113). Once the mechanism of thermalization has been understood, we can describe structures way beyond the partition function Eq. (11.113). For example, we may explore what happens to the Coulomb blockade when the system is biased out of equilibrium by external voltage, or we may explore the dynamics of the approach to equilibrium after a sudden change in the state of the system, etc.

But what, then, causes thermalization in the present context? It turns out that the most direct channel of relaxation is the coupling to the leads. Indeed, we have seen in Section 11.6.1 that the dot-lead coupling of the interacting systems reads (symbolic notation) $\bar\psi_d T e^{i\phi}\psi_x$, where ψ_d are the fermion fields of the dot, $\psi_{x=L,R}$, those of the leads, and $\dot\phi$ is the Hubbard–Stratonovich field of the interaction. This means that a quasiparticle entering the dot creates an excitation in the field ϕ (physically: a voltage fluctuation). That fluctuation may in turn create a particle-hole excitation (via the vertex $\bar\psi_x T^\dagger e^{-i\phi}\psi_d$) in the dot/lead system. We conclude that the coupling vertices provide a mechanism for the excitation of particle-hole pairs, and hence of relaxation in energy. Below we explore the formation of the Coulomb blockade out of these processes, and the generalization to a nonequilibrium state. To keep the discussion simple, we assume vanishing gate voltage $N_0 = 0$, and zero temperature $T = 0$ throughout. (Exercise: you may find it instructive to generalize to finite gate voltage and temperatures.)

(a) Our first step is purely technical: observing that at weak coupling to the external world, $g_T \ll 1$, fluctuations in the field ϕ are strong, we will trade the integration over ϕ for an integration over all charge states of the dot. (Recall that "charge" is the degree of freedom conjugate to the phase ϕ.) To this end, expand the action Eq. (11.79) in the tunneling action Eq. (11.82) and integrate over the phase degrees of freedom (hint: you may find it convenient to switch back to the contour variables $\phi_\pm$ before doing the integration, and mind the quantization condition $n_c(0) \in \mathbb{Z}$). to obtain the representation of the Keldysh partition function

$$\mathcal{Z} = \sum_{m=0}^{\infty} \frac{1}{m!}\left(-\frac{g}{2}\right)^m \sum_{\{\sigma\}} \int Dt\, e^{-iE_c \int dt\,(n_+^2(t) - n_-^2(t))} \prod_{k=1}^{m} L_{\sigma_{2k-1},\sigma_{2k}}(t_{2k-1} - t_{2k}), \tag{11.114}$$

where $\sum_{\{\sigma\}}$ is a sum over all sign configurations $\sigma \in \{-1,1\}^{2m}$, the integration measure $Dt = \prod_{k=1}^{2m} dt_k$ and the charge profiles

$$n_\sigma(t) = n + \sigma \sum_{k=1}^{2m} (-)^k \Theta(t - t_k) \delta_{\sigma_k,\sigma}. \tag{11.115}$$

Finally, the matrix elements of the kernel L are defined as

$$L_{\sigma\sigma'} = \frac{1}{4} \left(\sigma\sigma' \Sigma^K + \sigma \Sigma^+ + \sigma' \Sigma^- \right), \tag{11.116}$$

where the self energies $\Sigma^{K,\pm}$ have been introduced in Eq. (11.82).

This representation expresses the partition function as a sum over quasiparticle in- and out-tunneling events, connected by elements of the kernel L. We next need to make physical sense of this expansion.

(b) The temporal entanglement of tunneling events makes a closed computation of the partition function impossible. However, for sufficiently small values of the tunneling conductance, tunneling processes containing intersecting or nested "propagator lines" $L(t,t')$ are negligibly small. Estimate the temporal range of the propagator L to derive a criterion for the applicability of the **non-interacting blip approximation (NIBA)** wherein tunneling events occur in a strictly sequential manner (cf. the figure.)

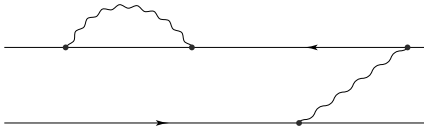

(c) The lack of entanglement of tunneling events in the NIBA makes the computation of the Keldysh partition function a lot easier. The basic picture now is that occasional charge tunneling events (so-called **blips** in the jargon of the field[33]) are interspersed into long periods of time wherein the charge contour profile stays in a diagonal state, $n_+ = n_- = n_{\rm cl} \equiv n$ ("**sojourns**.") During a blip, the quantum component $n_+ - n_- = n_{\rm q} \equiv \xi \in \{-1,0,1\}$ jumps to a value ± 1, depending on the configuration $(\sigma_{2k-1}, \sigma_{2k})$ of the tunneling event, and the sign of the time difference $t_{2k-1} - t_{2k}$ (see the figure below).

Building on this structure, and assuming zero biasing, $V = 0$, derive a master equation for the quantity $P(n,t) \equiv P(n,t|n_0,0)$, i.e. the probability that the system evolves into a charge state $(n_+,n_-) = (n,n)$ at time t, provided it started in (n_0,n_0) at $t = 0$. To this end, interpret $P(n,t)$ as the Keldysh field integral Eq. (11.114), subject to the constraint (cf. Eq. (11.115)) $n_\sigma(t) = n$ and $n_\sigma(0) = 0$. Relate $P(n,t)$ to $P(n',t-\delta t)$, where $\delta t \gg E_c^{-1}$ is much bigger than the typical duration of blips, yet smaller than the average spacing between blips, $\Delta t \ll (gE_c)^{-1}$.

[33] U. Weiss, *Quantum Dissipative Systems*, (World Scientific Publishing, 1993).

Apply a continuum approximation $(\Delta t)^{-1}(P(n,t) - P(n,t-\Delta t)) \simeq \partial_t P(n,t)$ to obtain the **master equation**

$$\partial_t P(n,t) = \Big[(\hat{E}_1 - 1)W_{n,n-1} + (\hat{E}_{-1} - 1)W_{n,n+1}\Big]P(n,t), \tag{11.117}$$

where $\hat{E}_{\pm 1} f(n) \equiv f(n \pm 1)$ are charge raising and lowering operators, the transition rates,

$$W_{n,n\pm 1} = \frac{g}{\pi} E_c(n, n \pm 1)\Theta(E_c(n, n \pm 1)),$$

and

$$E_c(n,n') \equiv E_c(n^2 - n'^2), \tag{11.118}$$

is the relative energy of different charging states.

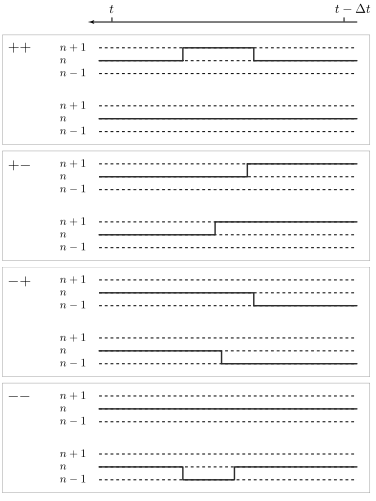

(d) Discuss the approach to a Coulomb blockaded state, as described by the master equation (11.117).

(e) Generalize to the case of finite bias voltage V. Will the ground state occupancy change?

Answer:

(a) Expressed in terms of the contour representation $\phi_c = (\phi_+ + \phi_-)/2$, $\phi_q = \phi_+ - \phi_-$, the charging contribution to the action $S_c = S\big|_{g=0}$ reads as

$$S_c[n,\phi] = \int dt\, \left(n_+ \partial_t \phi_+ - n_- \partial_t \phi_- - E_c(n_+^2 - n_-^2)\right),$$

where we have introduced

$$n_\pm = n_c \pm \frac{n_q}{2}.$$

The quantization condition on n_c translates to $n_+(0) = n_-(0) \in \mathbb{Z}$. The relative sign change between the first two terms tells us that the operator $e^{i\phi_+}$ raises the charge on the upper contour by one, $n_+ \to n_+ + 1$ while $e^{i\phi_-}$ lowers the charge on the lower contour by one, $n_- \to n_- - 1$. To make this action explicit, we first transform the tunneling action Eq. (11.84) to contour fields,

$$S_{\rm tun}[\phi] = \frac{g}{2} \int dt dt' \, (e^{-i\phi_+(t)}, e^{-i\phi_-(t)}) L(t-t') \begin{pmatrix} e^{i\phi_+(t')} \\ e^{i\phi_-(t')} \end{pmatrix},$$

where the matrix kernel $L = \{L_{\sigma\sigma'}\}$, $\sigma, \sigma' = \pm 1$ is defined in Eq. (11.116). We may now expand $\exp(iS_{\rm tun})$ in powers of the coupling constant to obtain the series

$$e^{iS_{\rm tun}[\phi]} = \sum_{m=0}^{\infty} \frac{1}{m!} \left(\frac{ig}{2}\right)^m \sum_{\{\sigma\}} \int Dt\, e^{i\sum_{k=1}^{2m} (-)^k \phi_{\sigma_k}(t_k)} \prod_{k=1}^{m} L_{\sigma_{2k-1},\sigma_{2k}}(t_{2k-1} - t_{2k}),$$

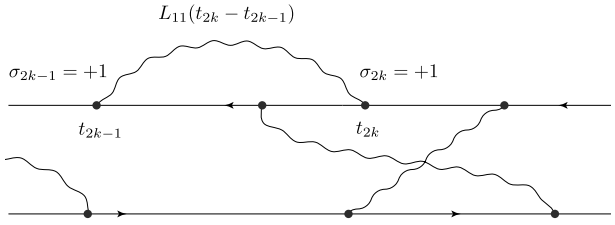

Figure 11.7 A configuration contributing to the expansion of the tunneling action: charge tunneling events at times $\ldots, t_{2k-1}, t_{2k}, \ldots$ are weighted by matrix elements of the dissipation kernel.

where $\sigma \in \{-1,1\}^{2m}$ are sign configurations and $Dt = \prod_{k=1}^{2m} dt_k$. The expansion weights in- and out-tunneling events at times t_{2k-1} and t_{2k}, respectively, with elements of the kernel L (cf. Fig. 11.7.) An interpretation in terms of charge tunneling is readily established by integration over the phase fields. Integrating the expansion above against the charging action S_c we obtain the constraint $\partial_t n_\sigma = \sigma \sum_{k=1}^{2m} (-)^k \delta(t-t_k)\delta_{\sigma_k,\sigma}$. Substitution of the solutions of this constraint Eq. (11.115) into the charging action we obtain the representation Eq. (11.114).

(b) Consider the kernel $L(\omega)$ at $V = 0$ (exercise: confirm that at finite V the temporal range of L shrinks below its $V = 0$ value. This means that at $V = 0$ we obtain the most conservative estimates for the validity of the NIBA). The scaling $L(\omega) \sim \omega$ (cf. Eq. (11.83)) implies $L(t) \sim t^{-2}$. This means that a charge tunneling event carries the statistical weight $\sim \int dt\, e^{\pm iE_c t} t^{-2} \sim E_C$. Its duration can be estimated as

$$\delta t \equiv \frac{\int dt\, e^{\pm iE_c t} t^{-2} t}{\int dt\, e^{\pm iE_c t} t^{-2}} \sim E_c^{-1}.$$

The total statistical weight of a tunneling event occurring somewhere in a time window of duration t_0 is then given by $\sim gE_C t_0$. This means that the average number of tunneling events in t_0 is

$$\langle m \rangle \simeq \frac{\sum_m \frac{m}{m!}(gE_C t_0)^m}{\sum_m \frac{1}{m!}(gE_C t_0)^m} = gE_C t_0.$$

The temporal spacing between events follows as $t_0/\langle m\rangle \sim (gE_c)^{-1}$, and this relates to the duration of the event as $t_0/\delta t \sim g^{-1}$: at low tunneling $g \ll 1$, the spacing between events exceeds their duration by far, and an approximation treating events in an uncorrelated sequential order becomes justified.

(c) For $E_c^{-1} \ll \Delta t \ll (gE_c)^{-1}$, the increment of P in the time window $[t-\Delta t, t]$ will be determined by zero or one blip processes:

$$P(n,t) \simeq P(n,-\Delta t) + \sum_{n'=n-1}^{n+1} C_{nn'} P(n', t-\Delta t),$$

where the coefficients $C_{nn'}$ are one-blip transition probabilities. An individual blip is characterized by its sign profile (σ, σ') (where the figure on p762 shows that the connection between the signs and the post-blip increment in classical charge is given by

$(+,+),(-,-) : n \to n$, $(+,-) : n \to n-1$, $(-,+) : n \to n+1$.), the center time of the blip $t_0 \in [t-\Delta t, t]$ and its duration, s. Comparison with Eq. (11.114) shows that, e.g.

$$C_{n,n-1} = \frac{ig\Delta t}{2}\int ds\, e^{iE_c(n-1,n)s} L_{-+}(s) = \frac{ig\Delta t}{2} L_{-+}(E_c(n-1,n))$$
$$= \frac{ig\Delta t}{2}(-\Sigma^K - \Sigma^+ + \Sigma^-)(E_c(n-1,n)) = \frac{g\Delta t}{\pi} E_c(n-1,n)\Theta(E_c(n-1,n)),$$

where the prefactor Δt results from the integration over the center time, and we introduced the relative charging energy Eq. (11.118). In an analogous manner, we obtain

$$C_{n,n+1} = \frac{g\Delta t}{\pi} E_c(n+1,n)\Theta(E_c(n+1,n)),$$
$$C_{nn} = \frac{g\Delta t}{\pi}\left(-E_c(n,n+1)\Theta(E_c(n,n+1)) - E_c(n,n-1)\Theta(E_c(n,n-1))\right),$$

where in computing C_{nn} it is important to keep in mind that $\Sigma^{\pm}(t) \propto \Theta(\pm t)$ carry retarded and advanced causality. Substituting this result into the evolution equation above, dividing by Δt and taking the continuum limit, we obtain the master equation (11.117).

(d) For our current parameter setting, $N_0 = 0$, $V = T = 0$, the charge state $n = 0$ defines the energetic ground state. The master equation describes relaxation to this state at rates const. $\times\, \Gamma$, where $\Gamma \equiv gE_c/\pi = 1/RC$ is inversely proportional to the RC-time of the system (the proportionality of these rates to g underpins the role of the lead-coupling as the source of relaxation) and the n-dependent constant prefactor increases with the distance off the ground state, $n = 0$.

To show the relaxation in more explicit terms, let us assume that the relaxation has progressed to a level where only the charge states $P_{-1,0,1}$ remain significantly populated. The restriction of the master equation to this sub-system reads

$$\partial_t P(0,t) = \Gamma(P(1,t) + P(-1,t)),$$
$$\partial_t P(\pm 1,t) = -\Gamma P(\pm 1,t),$$

which is solved by $P(\pm 1,t) = e^{-\Gamma t}P(\pm 1,0)$ and

$$P(0,t) = 1 - P(1,0) - P(-1,0) + \Gamma\int_0^t dt'\, e^{-\Gamma t'}(P(1,0) + P(-1,0)).$$

This solution describes the relaxation towards the state $P(n,t) \overset{t\to\infty}{\longrightarrow} \delta_{n,0}$.

(e) Finite voltages affect the theory through a redefined Keldysh self energy Σ^K. Comparison with Eq. (11.83) shows that

$$\Sigma^K(V) - \Sigma^K(0) = \frac{i}{2\pi}(V - |\omega|)\Theta(V - |\omega|).$$

The transition rates thus change to

$$W_{n,n\pm1} \to W_{n,n\pm1} + \frac{g}{4\pi}(V - |E_c(n\pm 1,n)|)\Theta(V \pm |E_c(n-1,n)|).$$

This change is easy to interpret: for voltages $|V| < |E_c(n \pm 1, n)|$ smaller than the charging energies, the transition rates of the unbiased problem remain unaltered. This means that the excess energy of external charge carriers $\sim V$ needs to exceed the charging energy to make charge transport through the dot possible; the Coulomb blockade is inert against moderate biasing.[34] At large voltages, $|V| \gg |E_c(n \pm 1, n)|$, the tunneling rates cross over to values $\sim gV/4\pi$. For these rates, different charging states become equally populated, at a rate $\sim gV$ set by the average current through the dot interfaces.

[34] Closer inspection shows that this statement is not entirely correct: the NIBA neglects tunneling processes of higher order in a g-expansion. Among these, there are some (so-called elastic **co-tunneling** processes) for which the extra power in g gets rewarded by a suppression in E_c that is only algebraic (as compared to the complete $\sim \exp(-E_c/T) \stackrel{T\to 0}{\longrightarrow} 0$ suppression of the direct tunneling processes considered here). Although the description of elastic co-tunneling goes well beyond the scope of this text, we note that its contribution is proportional to the mean single particle levels spacing, Δ, of the dot, i.e. the results above hold true in the double limit, $T, \Delta \to 0$.

Index